

Edited by **Malgorzata Kloc** • **Jacek Z. Kubiak**



Xenopus Development



WILEY Blackwell

www.Ebook777.com

***Xenopus* Development**

Xenopus Development

Edited by

Malgorzata Kloc

*Department of Surgery
Houston Methodist Research Institute
and Houston Methodist Hospital
Houston, TX, USA*

Jacek Z. Kubiak

*CNRS and University of Rennes 1,
Institute of Genetics & Development of Rennes (IGDR),
UMR 6290, Faculty of Medicine,
Rennes, France*

WILEY Blackwell

Copyright © 2014 by John Wiley & Sons, Inc. All rights reserved

Published by John Wiley & Sons, Inc., Hoboken, New Jersey
Published simultaneously in Canada

No part of this publication may be reproduced, stored in a retrieval system, or transmitted in any form or by any means, electronic, mechanical, photocopying, recording, scanning, or otherwise, except as permitted under Section 107 or 108 of the 1976 United States Copyright Act, without either the prior written permission of the Publisher, or authorization through payment of the appropriate per-copy fee to the Copyright Clearance Center, Inc., 222 Rosewood Drive, Danvers, MA 01923, (978) 750-8400, fax (978) 750-4470, or on the web at www.copyright.com. Requests to the Publisher for permission should be addressed to the Permissions Department, John Wiley & Sons, Inc., 111 River Street, Hoboken, NJ 07030, (201) 748-6011, fax (201) 748-6008, or online at <http://www.wiley.com/go/permission>.

Limit of Liability/Disclaimer of Warranty: While the publisher and author have used their best efforts in preparing this book, they make no representations or warranties with respect to the accuracy or completeness of the contents of this book and specifically disclaim any implied warranties of merchantability or fitness for a particular purpose.

No warranty may be created or extended by sales representatives or written sales materials. The advice and strategies contained herein may not be suitable for your situation. You should consult with a professional where appropriate. Neither the publisher nor author shall be liable for any loss of profit or any other commercial damages, including but not limited to special, incidental, consequential, or other damages.

For general information on our other products and services or for technical support, please contact our Customer Care Department within the United States at (800) 762-2974, outside the United States at (317) 572-3993 or fax (317) 572-4002.

Wiley also publishes its books in a variety of electronic formats. Some content that appears in print may not be available in electronic formats. For more information about Wiley products, visit our web site at www.wiley.com.

Library of Congress Cataloging-in-Publication Data:

Xenopus development / edited by Malgorzata Kloc, Jacek Z. Kubiak.
pages cm

Includes bibliographical references and index.

ISBN 978-1-118-49281-9 (hardback)

1. Xenopus laevis. 2. Xenopus–Larvae–Microbiology. 3. Microorganisms–Development. 4. Embryology.
I. Kloc, Malgorzata, editor of compilation. II. Kubiak, Jacek Z, editor of compilation.

QL668.E265X46 2014

597.8'654–dc23

2014000055

Printed in Malaysia

10 9 8 7 6 5 4 3 2 1

Contents

Contributors	vii	Section II Midblastula	
Preface	ix	Transition, Gastrulation,	
		and Neurulation	101
Section I Oocyte and			
Early Embryo	1	6 The <i>Xenopus</i> Embryo as a Model	
1 Transcription in the <i>Xenopus</i>		System to Study Asymmetric	
Oocyte Nucleus	3	Furrowing in Vertebrate	
<i>Joseph G. Gall</i>		Epithelial Cells	103
		<i>Jacek Z. Kubiak, Isabelle Chartrain,</i>	
		<i>& Jean-Pierre Tassan</i>	
2 RNA Localization during Oogenesis	16	7 Induction and Differentiation of	
in <i>Xenopus laevis</i>		the <i>Xenopus</i> Ciliated Embryonic	
<i>James O. Deshler</i>		Epidermis	112
		<i>Marie Cibois, Pierluigi Scerbo,</i>	
		<i>Virginie Thomé, Andrea Pasini,</i>	
		<i>& Laurent Kodjabachian</i>	
3 From Oocyte to Fertilizable Egg:	38	8 Wnt Signaling during Early <i>Xenopus</i>	
Regulated mRNA Translation and the		Development	130
Control of Maternal Gene Expression		<i>François Fagotto</i>	
<i>Chad E. Cragle & Angus M. MacNicol</i>			
4 Polarity of <i>Xenopus</i> Oocytes and Early	60	9 Neural Tube Closure in <i>Xenopus</i>	163
Embryos		<i>Hitoshi Morita, Makoto Suzuki,</i>	
<i>Malgorzata Kloc</i>		<i>& Naoto Ueno</i>	
5 Germ-Cell Specification in <i>Xenopus</i>	75		
<i>Mary Lou King</i>			

Section III Metamorphosis and Organogenesis	187	Section IV Novel Techniques and Approaches	309
10 Primordial Germ Cell Migration <i>Aliaksandr Dzementsei & Tomas Pieler</i>	189	16 Atomic Force Microscopy Imaging of <i>Xenopus laevis</i> Oocyte Plasma Membrane <i>Francesco Orsini</i>	311
11 Development of Gonads, Sex Determination, and Sex Reversal in <i>Xenopus</i> <i>Rafał P. Piprek & Jacek Z. Kubiak</i>	199	17 Size Scaling of Subcellular Organelles and Structures in <i>Xenopus laevis</i> and <i>Xenopus tropicalis</i> <i>Lisa J. Edens & Daniel L. Levy</i>	325
12 The <i>Xenopus</i> Pronephros: A Kidney Model Making Leaps toward Understanding Tubule Development <i>Rachel K. Miller, Moonsup Lee, & Pierre D. McCrea</i>	215	18 A Model for Retinal Regeneration in <i>Xenopus</i> <i>Masasuke Araki</i>	346
13 Development of Neural Tissues in <i>Xenopus laevis</i> <i>William A. Muñoz, Amy K. Sater, & Pierre D. McCrea</i>	239	19 The <i>Xenopus</i> Model for Regeneration Research <i>Ying Chen & Gufa Lin</i>	368
14 The Development of the Immune System in <i>Xenopus</i> <i>Louis Du Pasquier</i>	264	20 Genomics and Genome Engineering in <i>Xenopus</i> <i>Léna Vouillot, Aurore Thélie, Thibault Scalvenzi, & Nicolas Pollet</i>	383
15 Neural Regeneration in <i>Xenopus</i> Tadpoles during Metamorphosis <i>Mauricio Moreno, Karina Tapia, & Juan Larrain</i>	293	Index	403

Contributors

Masasuke Araki. Department of Biological Sciences, Developmental Neurobiology Laboratory, Nara Women's University, Nara, Japan.

Isabelle Chartrain. CNRS and University of Rennes 1, Institute of Genetics & Development of Rennes (IGDR), UMR 6290, Faculty of Medicine, Rennes, France.

Ying Chen. Stem Cell Institute, University of Minnesota, Minneapolis, MN.

Marie Cibois. Institute of Developmental Biology of Marseille, CNRS, Aix-Marseille Université, Marseille, France.

Chad E. Cragle. Department of Neurobiology and Developmental Sciences, University of Arkansas for Medical Sciences, Little Rock, AR.

James O. Deshler. Directorate for Biological Sciences, National Science Foundation, Arlington, VA.

Aliaksandr Dzementsei. Institute for Developmental Biochemistry, Göttingen, Germany.

Lisa J. Edens. Department of Molecular Biology, University of Wyoming, Laramie, WY.

François Fagotto. Department of Biology, McGill University, Montreal, Québec, Canada.

Joseph G. Gall. Department of Embryology, Carnegie Institution for Science, Baltimore, MD.

Mary Lou King. Department of Cell Biology, Miller School of Medicine, University of Miami, Miami, FL.

Malgorzata Kloc. Department of Surgery, Houston Methodist Research Institute and Houston Methodist Hospital, Houston, TX.

Laurent Kodjabachian. Institute of Developmental Biology of Marseille, CNRS, Aix-Marseille Université, Marseille, France.

Jacek Z. Kubiak. CNRS and University of Rennes 1, Institute of Genetics & Development of Rennes (IGDR), UMR 6290, Faculty of Medicine, Rennes, France.

Juan Larrain. Department of Cell and Molecular Biology, Centre for Aging and Regeneration, Millennium Nucleus in Regenerative Biology, Faculty of Biological Sciences, Pontificia Universidad Católica de Chile, Santiago, Chile.

Moonsup Lee. Department of Biochemistry and Molecular Biology, The University of Texas MD Anderson Cancer Center. Program in Genes and Development, The University of Texas Graduate School of Biomedical Sciences at Houston, Houston, TX.

Daniel L. Levy. Department of Molecular Biology, University of Wyoming, Laramie, WY.

Gufa Lin. Stem Cell Institute, University of Minnesota, Minneapolis, MN. School of Life

- Science and Technology, Tongji University, Shanghai, China.
- Angus M. MacNicol.** Department of Neurobiology and Developmental Sciences, University of Arkansas for Medical Sciences, Little Rock, AR.
- Pierre D. McCrea.** Department of Biochemistry and Molecular Biology, The University of Texas MD Anderson Cancer Center. Program in Genes and Development, The University of Texas Graduate School of Biomedical Sciences at Houston, Houston, TX.
- Rachel K. Miller.** Department of Biochemistry and Molecular Biology, The University of Texas MD Anderson Cancer Center. Department of Pediatrics, University of Texas Medical School at Houston, Houston, TX.
- Mauricio Moreno.** Department of Cell and Molecular Biology, Centre for Aging and Regeneration, Millennium Nucleus in Regenerative Biology, Faculty of Biological Sciences, Pontificia Universidad Católica de Chile, Santiago, Chile.
- Hitoshi Morita.** National Institute for Basic Biology, Okazaki, Japan. Institute of Science and Technology Austria, Klosterneuburg, Austria.
- William A. Muñoz.** Department of Biochemistry and Molecular Biology, The University of Texas MD Anderson Cancer Center, Houston, TX. Stowers Institute for Medical Research, Kansas City, MO.
- Francesco Orsini.** Physics Department, Università degli Studi di Milano, Milan, Italy.
- Andrea Pasini.** Institute of Developmental Biology of Marseille, CNRS, Aix-Marseille Université, Marseille, France.
- Louis Du Pasquier.** Zoology and Evolutionary Biology, University of Basel, Basel, Switzerland.
- Tomas Pieler.** Institute for Developmental Biochemistry, Göttingen, Germany.
- Rafał P. Piprek.** Department of Comparative Anatomy, Institute of Zoology, Jagiellonian University, Kraków, Poland.
- Nicolas Pollet.** CNRS, Institute of Systems and Synthetic Biology, Université d'Evry-Val-d'Essonne. Genopole, Centre d'Exploration et de Recherche Fonctionnelle Amphibiens Poissons, Evry, France.
- Amy K. Sater.** Department of Biology and Biochemistry, University of Houston, Houston, TX.
- Thibault Scalvenzi.** CNRS, Institute of Systems and Synthetic Biology, Université d'Evry-Val-d'Essonne, Evry, France.
- Pierluigi Scerbo.** Institute of Developmental Biology of Marseille, CNRS, Aix-Marseille Université, Marseille, France.
- Makoto Suzuki.** National Institute for Basic Biology, Okazaki, Japan.
- Jean-Pierre Tassan.** CNRS and University of Rennes 1, Institute of Genetics & Development of Rennes (IGDR), UMR 6290, Faculty of Medicine, Rennes, France.
- Karina Tapia.** Department of Cell and Molecular Biology, Centre for Aging and Regeneration, Millennium Nucleus in Regenerative Biology, Faculty of Biological Sciences, Pontificia Universidad Católica de Chile, Santiago, Chile.
- Aurore Thélie.** CNRS, Institute of Systems and Synthetic Biology, Université d'Evry-Val-d'Essonne, Evry, France.
- Virginie Thomé.** Institute of Developmental Biology of Marseille, CNRS, Aix-Marseille Université, Marseille, France.
- Naoto Ueno.** National Institute for Basic Biology, Okazaki, Japan.
- Léna Vouillot.** CNRS, Institute of Systems and Synthetic Biology, Université d'Evry-Val-d'Essonne, Evry, France.

Preface

The purpose of writing *Xenopus Development* was to provide a comprehensive review of the current knowledge on the most popular amphibian model in developmental biology. The pioneering research by John Gurdon on nuclear transfer and nuclear remodeling in *Xenopus laevis* was awarded the Nobel Prize in Medicine or Physiology in 2012. This is perhaps the first time that research on the *Xenopus* model has been recognized with the highest scientific award. Recent sequencing of the *Xenopus tropicalis* genome allows combining the classical developmental biology observations and experiments carried out on *X. laevis* with modern genetic and genomic studies of *X. tropicalis*. This is a unique situation in modern developmental biology, with two different but closely related species being used for different purposes and being studied using different approaches, thereby allowing the results to be automatically merged and easily extrapolated. Availability of these data sets will have an enormous impact on the general application of the *Xenopus* model system. At present, there are two *Xenopus* resource centers, one in the US and one in the UK, which offer training in the use of *Xenopus* as an experimental model system. Both the *X. laevis* and *X. tropicalis* models have the potential to be used more frequently in the future and will certainly deliver novel and exciting information in the field of developmental biology.

The book is divided into four parts: Section I – Oocyte and Early Embryo (Chapters 1–5); Section II – Midblastula Transition, Gastrulation, and Neurulation (Chapters 6–9); Section III – Metamorphosis and Organogenesis (Chapters 10–15); and Section IV – Novel Techniques and Approaches (Chapters 16–20). This arrangement allows presenting the novel discoveries in the field of *Xenopus* developmental biology in a systematic manner and focusing on the methodological aspects of *Xenopus* research. We are now witnessing an explosive development of novel methods, approaches, and techniques, which pave the way to explore new areas of research for scientific discoveries. Researchers in the field can benefit from these circumstances and make use of this unique opportunity.

Most importantly, we have managed to gather in this book outstanding contributors who have provided an excellent historical perspective as well as described the state of the art in the field of their expertise.

Last, but not least, there has not been a book dedicated to *Xenopus* since the 2000 Cold Spring Harbor Lab Press laboratory manual, and we hope that the current volume will fill this void successfully.

Malgorzata Kloc
Houston, USA
Jacek Z. Kubiak
Rennes, France

Section I

Oocyte and Early Embryo

- Chapter 1 Transcription in the *Xenopus* Oocyte Nucleus
- Chapter 2 RNA Localization during Oogenesis in *Xenopus laevis*
- Chapter 3 From Oocyte to Fertilizable Egg: Regulated mRNA Translation and the Control of Maternal Gene Expression
- Chapter 4 Polarity of *Xenopus* Oocytes and Early Embryos
- Chapter 5 Germ-Cell Specification in *Xenopus*

1

Transcription in the *Xenopus* Oocyte Nucleus

Joseph G. Gall

Department of Embryology, Carnegie Institution for Science, Baltimore, MD

Abstract: The mature oocyte of *Xenopus* is a gigantic cell with a diameter of 0.8mm in *Xenopus tropicalis* and 1.2mm in *Xenopus laevis*. It stores a large number of stable mRNAs for use during early development, all of which are transcribed by the giant lampbrush chromosomes inside the equally giant oocyte nucleus or germinal vesicle. The lampbrush chromosomes are specialized for an unusually high rate of transcription, but even so they require months to produce the enormous number of stable transcripts needed for early embryogenesis. Deep sequencing of oocyte mRNA reveals a wide variety of transcripts made by the lampbrush chromosomes during oogenesis.

Introduction

Oocytes of animals vary greatly in size, rate of growth, presence or absence of a quiescent stage, and association with supporting or nurse cells of various types (Davidson 1986; Voronina and Wessell 2003). These factors influence the nature of the transcription that takes place in the oocyte nucleus or germinal vesicle (GV). The *Xenopus* oocyte represents one extreme. Its oocyte grows to an enormous size, up to 1.2mm in *Xenopus laevis* and 0.8mm in *Xenopus tropicalis*, and there are no nurse cells (Figure 1.1). At their maximal size, the oocytes of *X. laevis* and *X. tropicalis* have volumes some 10^5 – 10^6 times that of a typical somatic cell. All of the transcripts

for this enormous cell must be synthesized by the single GV. The strategy used by the oocyte to accomplish this prodigious task involves three major components. First, the chromosomes in the GV transcribe at what is probably close to the theoretical maximum, giving rise to the remarkable lampbrush chromosomes (LBCs) (<http://projects.exeter.ac.uk/lampbrush/>), which will be a major focus of this chapter. Second, and equally importantly, transcription continues for several months during the long period of oocyte development. Finally, the transcripts produced by the GV and stored in the cytoplasm are unusually stable. Only by a combination of these three features is the *Xenopus* oocyte able to make and store

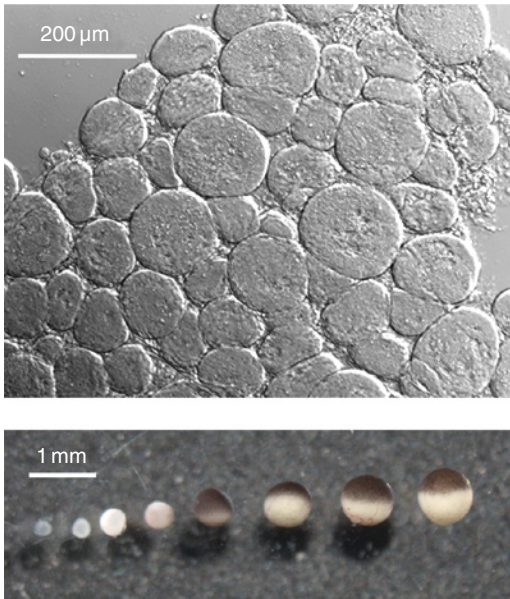


Figure 1.1 Oocytes of *X. tropicalis*. The top panel shows the range of oocyte sizes found in an ovary from an immature frog (3.5 cm snout to vent). At this stage, most oocytes have diameters under 100 μm . The lower panel shows oocytes of different sizes, obtained from the ovary of a mature female. Such ovaries also contain smaller oocytes like those shown in the upper panel. Photo courtesy of Zehra Nizami.

the transcripts needed for oogenesis and early embryogenesis.

LBCs similar to those of *Xenopus* are found in a wide range of organisms, both vertebrate and invertebrate (Callan 1986), and have even been described from a plant, the single-celled alga *Acetabularia* (Spring et al. 1975; Berger et al. 1994). It is worth emphasizing, however, that LBCs have been described only from large meiotic nuclei that provide transcripts to a large oocyte without help from nutritive cells. The situation can be very different in other organisms. For instance, the *Drosophila* oocyte is large but the GV is small and transcriptionally silent, or nearly so. In this case, there are no LBCs and transcripts are supplied to the growing oocyte by polyploid nurse cells (Spradling 1993). The example of *Drosophila* and other organisms with transcriptionally inactive GVs emphasizes the fact that LBCs are not *required* for meiosis or more generally for oogenesis (Gall 2012).

LBC structure: The standard model

Extensive studies on the LBCs of many organisms over the past 50–60 years have established what can be called the “standard model” of their physical structure. LBCs consist of four chromatids in the diplotene stage (G2) of the first meiotic division. Each chromatid is fundamentally a single, very long DNA double helix, which, if fully extended, would be centimeters in length (Callan and Macgregor 1958; Callan 1963; Gall 1963). The two homologues of each bivalent are independent of each other, except at the chiasmata, whose physical structure is almost completely obscure. It is the unique and variable association of sister chromatids that gives rise to the classic “lampbrush” condition. Specifically, there are condensed, transcriptionally *inactive* regions (chromomeres) along the major axis of each homologue, where sister chromatids are associated with each other. And there are transcriptionally *active* regions (loops) where sisters extend laterally from the axis independently of each other (Figure 1.2A and B). Each loop consists of one or more transcription units (TUs) that are visible at the light optical level as “thin-to-thick” regions, the thin end being where transcription initiates and the thick end where it terminates. The entire structure is visible primarily because the nascent RNA transcripts are associated with massive amounts of protein. These relationships are shown diagrammatically in Figure 1.3, variations of which have been published many times before (Gall 1956; Callan and Lloyd 1960; Hess 1971; Morgan 2002; Austin et al. 2009; Gaginskaya et al. 2009).

Chromomeres and loops

Beginning with the transcriptionally inactive axis of each homologue, we immediately run into unanswered structural issues. The more or less accepted view is that the axis consists of a series of DNA-rich chromomeres within which the sisters are tightly wound up in some fashion. They can be stained by various DNA-specific dyes, such as Feulgen or DAPI (Figure 1.2B and D). The chromomeres are separated by exceedingly delicate interchromomeric regions that are either invisible or barely

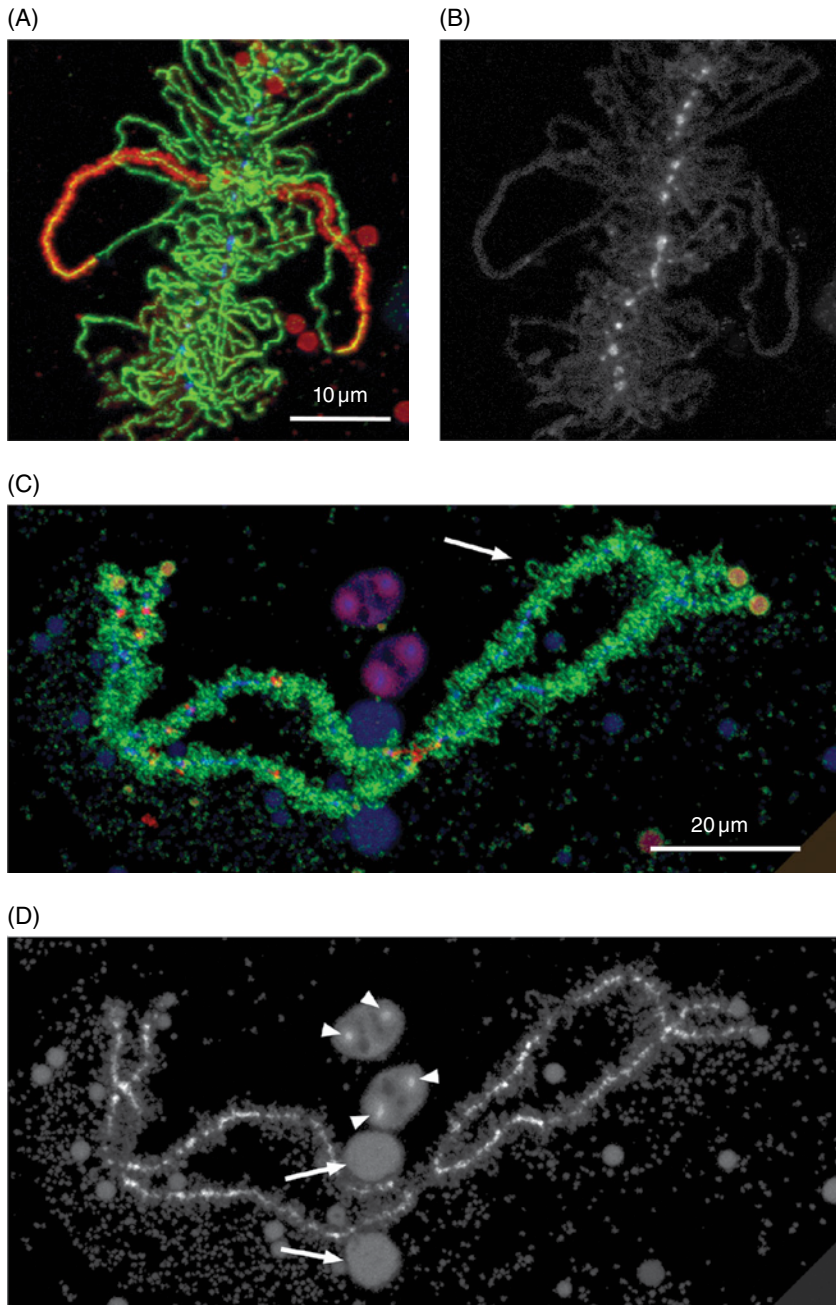


Figure 1.2 LBCs of the newt *Notophthalmus viridescens* (A and B) and *X. tropicalis* (C and D). (A) A short segment of an LBC stained with antibodies against pol II (green) and the RNA-binding protein CELF1 (red) (Morgan 2007). The axes of all loops appear as diffraction-limited green lines, because they are covered with closely spaced pol II molecules. One pair of sister chromatids is preferentially stained with CELF1, revealing the prominent thin-to-thick orientation of the associated loop matrix (RNP transcripts). (B) The same segment of LBC stained with the DNA-specific dye DAPI reveals the axis of transcriptionally inactive chromomeres. (C) Bivalent No. 2 of *X. tropicalis* stained with antibodies against pol II (green) and pol III (red). The vast majority of loops are transcribed by pol II. The loops of *X. tropicalis* are much shorter than those of the newt, and only a few are recognizable as loops in this image (arrow). (D) The same bivalent showing strong staining of the chromomere axes with DAPI. DAPI also reveals two amplified rDNA cores (arrowheads) in each of two extrachromosomal nucleoli. Regions of high protein concentration in the nucleoli also bind DAPI to a lesser extent. The same is true of two moderately stained structures near the middle of this bivalent (arrows), which represent loop pairs whose matrix has fused into a single large mass (lumpy loops). To see a color version of this figure; see Plate 1.

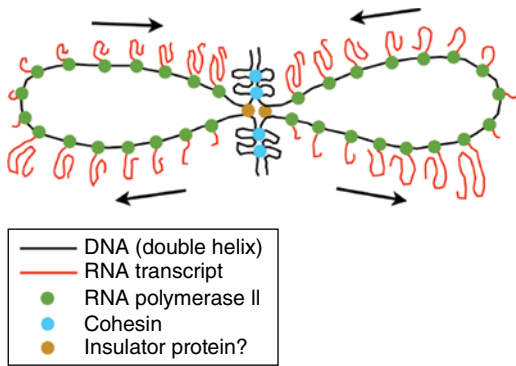


Figure 1.3 Highly stylized diagram of LBC structure. Transcriptionally active sister chromatids extend laterally from the main axis of the chromosome, which consists of regions where transcriptionally inactive sisters are closely paired and associated with cohesins (Austin et al. 2009). Loops can consist of one or more TUs, which may have either the same or opposite polarities on the same loop. RNA polymerase II molecules are packed closely along the DNA axis of each loop and elongating RNA transcripts are attached to them. The transcripts are associated with various proteins, including splicing factors (not shown here). It is not known what holds the bases of the loops together. One possibility is that insulators or similar molecules that define transcriptionally active regions of chromatin are involved. To see a color version of this figure; see Plate 2.

visible at the light optical level. By electron microscopy, these regions usually appear as a **single** fiber about 10nm in thickness (Tomlin and Callan 1951; Mott and Callan 1975). Although an analogy of the chromomeres and interchromomeric regions to the bands and interbands of polytene chromosomes is often made, this analogy breaks down when examined closely. Specifically, the number of chromomeres varies greatly during development of the oocyte, there being dozens of chromomeres in an amphibian or avian LBC at maximal extension, but a decreasing number as the chromosomes contract in length for the first meiotic division. It is possible to construct maps of individual chromosomes based on the chromomere pattern at maximal extension, as has been done for avian LBCs (Rodionov, Galkina, and Lukina in Schmid et al. 2005), but it is often difficult to recognize a reproducible chromomere pattern in amphibian LBCs, even between the

homologues of a given bivalent (Callan and Lloyd 1960). Macgregor (2012) discusses the “chromomere problem” in a recent essay.

To say that we are woefully ignorant about the internal structure of chromomeres is an understatement. The first question we might ask is whether sister chromatids are intimately paired inside the chromomere, as they are in the interchromomeric regions. Although we do not have an answer to that question, we can say definitively that a single chromatid **can** form either an entire LBC or part of one. The most direct evidence comes from LBCs that form when sperm heads are injected into a GV (Gall and Murphy 1998; Liu and Gall 2012). In such experiments, the single chromatids inside the sperm head are released within minutes and develop gradually into morphologically recognizable LBCs with transcriptionally active loops. Except that their loops are not paired, these LBCs are similar in overall organization to the normal LBCs in the same nucleus (Figure 1.4). A similar argument comes from the existence of “double-axis” regions of normal LBCs. Double-axis regions are segments of an LBC in which **sisters** are completely unpaired. Although rare, they are a regular feature of specific regions of certain chromosomes: one end of the shortest chromosome of *Triturus cristatus* (Callan and Lloyd 1960), near the middle of chromosome Nos. 8 and 9 of *X. laevis* (Figure A1.1), and roughly half of chromosome No. 10 of *X. tropicalis* (Figure A1.2). Although LBCs that consist of single chromatids, as well as the double-axis regions of otherwise typical LBCs, demonstrate that chromatids need not be paired to form typical “lampbrushes”, they do not directly address the organization of sister chromatids within the chromomeres of typical LBCs.

One structural issue on which there is no question is that sister chromatids form independent transcription loops. There is both observational and experimental evidence for this model, going back to Callan’s original stretching experiment (Callan 1957). Basically, Callan showed that an LBC chromosome “breaks” in a stereotypical and counterintuitive fashion when stretched between microneedles. Instead of breaking in the thinnest regions between the chromomeres, the chromosome doesn’t really break

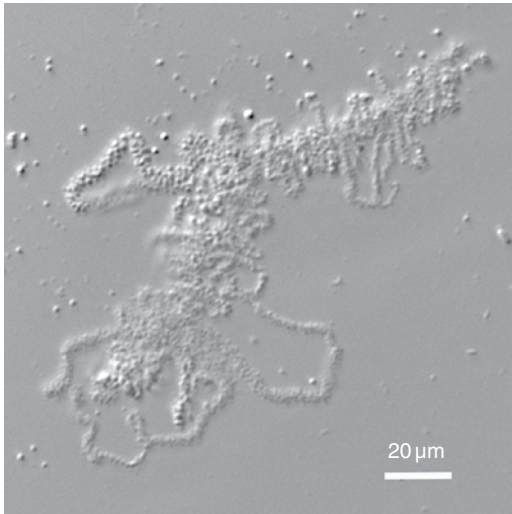


Figure 1.4 An LBC consisting of a single unpaired chromatid. This LBC was formed when a sperm head of *X. laevis* was injected into the GV of the newt *N. viridescens*. Individual chromatids derived from the sperm begin transcribing shortly after injection, eventually forming giant chromosomes similar to the endogenous LBCs. Because the *X. laevis* chromatids do not replicate in the GV, the LBCs formed from them consist of single chromatids and the transcription loops are unpaired.

at all. Instead, something happens at the bases of the loops such that a pair of loops, which originally extended laterally, comes to lie along the main axis of the chromosome. Such “double-loop bridges (dlb)” also occur when chromosomes are accidentally stretched during preparation for microscopical examination (Figure 1.5). Moreover, certain pairs of identifiable loops exist normally in the dlb configuration (Callan 1954; Callan and Lloyd 1960). An interesting example is found on chromosome No. 3 of *X. laevis* (Figure A1.1). Here, a prominent dlb near the centromere contains an unusually high concentration of the RNA-editing enzyme ADAR1 (Eckmann and Jantsch 1999).

Callan’s experiment provided what is arguably the single most important insight into the LBC structure: that each lateral loop is part of an extraordinarily long and continuous chromatid. Coupled with the demonstration that a loop contains one DNA double helix, whereas the main axis contains two helices, LBCs provided critical evidence

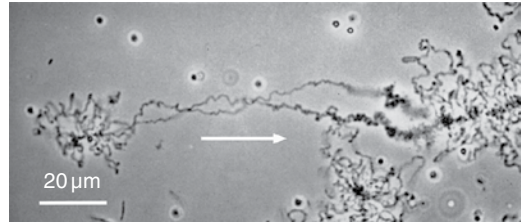


Figure 1.5 A dlb in a chromosome of the newt *N. viridescens*. Such bridges can be formed by stretching a chromosome with microneedles, but they also occur by accident when LBCs are prepared for microscopical examination. Note the polarity of the loops, which allows one to determine the direction of transcription (arrow) relative to the chromosome as a whole.

that the largest known chromosomes are not multistranded, but instead conform to the unimer hypothesis of chromosome structure (Gall 1963, 1981).

Transcription on LBC loops

The lateral loops are the most distinctive feature of LBCs and gave rise to the name “lampbrush”, which was coined by Rückert (1892) by analogy to the then familiar brushes used to clean soot from kerosene lamp chimneys. There is no question that the loops represent transcriptionally active regions of the chromosome, as opposed to the transcriptionally inactive chromomeres. The first hint came from the demonstration of RNase-sensitive staining in these regions (Gall 1954), followed by autoradiographic experiments showing that the loops incorporate RNA precursors such as adenine and uridine (Gall 1958; Gall and Callan 1962).

Well before there was detailed molecular evidence for transcription on the loops, the beautiful electron micrographs of Oscar Miller and his colleagues provided stunning images of TUs in amphibian oocytes at unprecedented resolution. Because “Miller spreads” involve disruption of the GV in distilled water, the overall organization of the chromosomes is lost. Nevertheless, it was abundantly evident that the (nonribosomal) “Christmas trees” were derived from the loops of LBCs (Miller and Hamkalo 1972; Hamkalo and Miller 1973; Scheer et al. 1976).

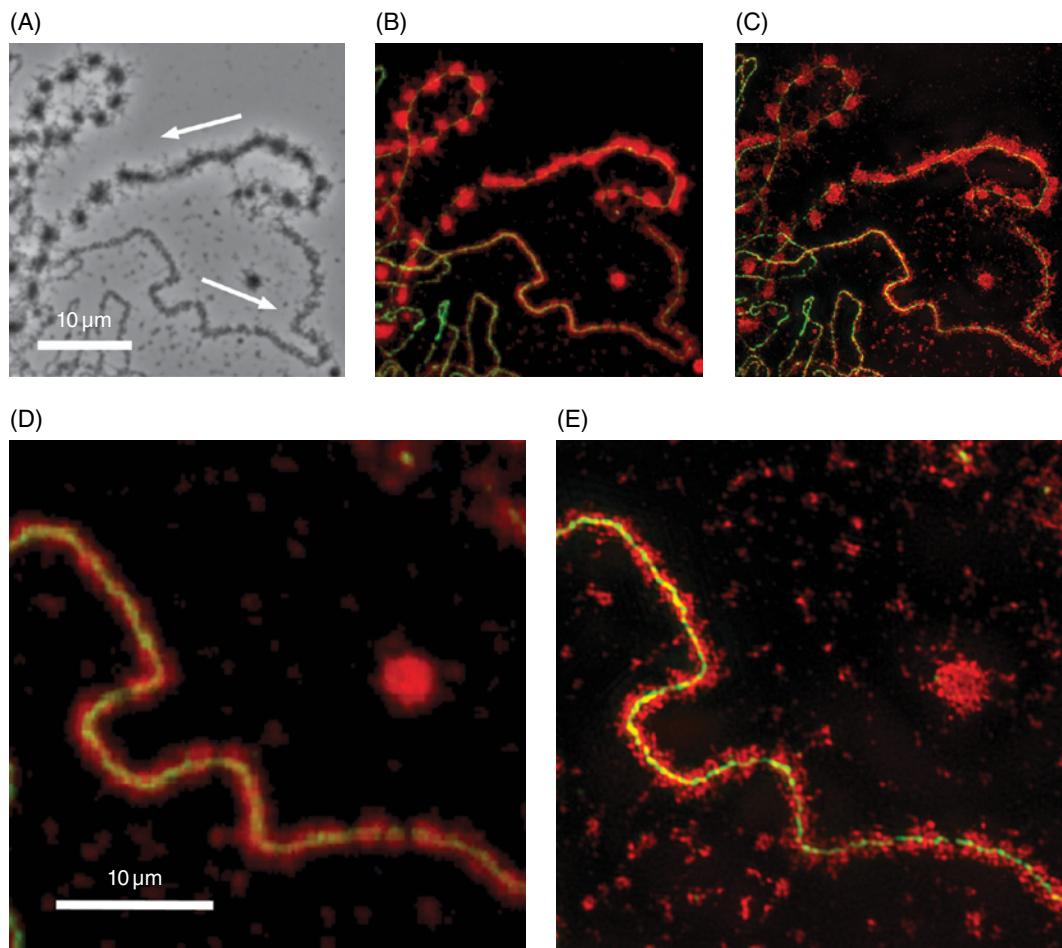


Figure 1.6 Images of a loop from the newt *N. viridescens*. (A) The entire loop imaged by phase contrast microscopy. The pronounced thin-to-thick polarity of the RNP matrix signifies the direction of transcription (arrows). (B) A confocal image of the same loop after immunostaining with mAb H14 against phosphorylated pol II (green) and mAb Y12 against symmetrical dimethylarginine, an epitope found on several splicing snRNPs (red). Green pol II stain is evident at the thin end of the loop but is obscured by the heavy mAb Y12 stain along most of the loop. (C) Image of the same loop taken by structured illumination superresolution microscopy. (D) Confocal image of the thin end of the loop at higher magnification. (E) The same loop imaged by structured illumination microscopy. Pol II now appears as a green line of nearly uniform width along the length of the loop. The red RNP matrix is resolved into a series of small particles about 50 nm in diameter. The superresolution images were taken on a DeltaVision OMX structured illumination microscope by Sidney Shaw and James Powers, Department of Biology, Indiana University. To see a color version of this figure, see Plate 3.

Immunofluorescent staining, especially when coupled with confocal or superresolution microscopy, now provides textbook images of active transcription on intact LBCs (Figures 1.2A, C, and 1.6). RNA polymerase II molecules form a diffraction-limited line along the axis of each loop, whereas ribonucleoprotein (RNP) transcripts appear as a massive coating around this axis. The thin-to-

thick organization of loops early suggested the direction of transcription, and in the case of the histone loops of the newt *Notophthalmus*, it was even possible to correlate the direction of transcription with the strand of DNA being transcribed (Stephenson et al. 1981). Multiple thin-to-thick regions within a single loop demonstrated that a one-to-one correlation between the loops and TUs is not possible.

Instead, a loop consists of one or more TUs, not necessarily oriented in the same direction (Scheer et al. 1976; Gall et al. 1983).

Interestingly, pol III transcription also occurs on loops. Because pol III transcripts are usually short, they do not form a matrix detectable by phase contrast or differential interference contrast microscopy. Nevertheless, pol III loops can be seen when they are immunostained with antibodies against pol III (Figure 1.2C). If the loops are extended, they appear as diffraction-limited lines; otherwise, they are seen as irregular masses of stain close to the chromosome axis (Figures A1.1 and A1.2) (Murphy et al. 2002). What are possibly pol III loops can also be recognized in electron micrographs by their very short transcripts (Scheer 1981).

It is not known what holds sister chromatids together at the bases of the loops. One would imagine this to be a protein or more likely a complex of proteins, but no one has been lucky enough to find an antibody that stains just the bases of the loops. Perhaps this hypothetical glue at the bases of the loops corresponds to the insulators that separate the functional units of the chromosome (Giles et al. 2010).

As just noted, a loop is not the same as a TU, since many loops contain multiple TUs. Moreover, a repeated gene locus can be represented by multiple loops, as is true for the histone gene loci of *Notophthalmus* (Diaz et al. 1981). There are other cases where loops of similar morphology occur not in pairs but in clusters, again suggesting a complex and variable relationship among TUs, loops, and the underlying genes or gene clusters.

Transcripts produced during oogenesis

Transcripts stored in the cytoplasm

Ribosomal RNA is the most abundant RNA present in the cytoplasm of the oocyte, and it occurs at about the same concentration as in cells of normal size (Brown and Littna 1964). In *X. laevis*, there are about 500–800 copies of the rDNA genes at a single nucleolus organizer (Wallace and Birnstiel 1966), a number

that is physically incapable of transcribing the total amount of rRNA produced during oogenesis. As shown a number of years ago, the genes coding for rRNA are amplified during the early stages of meiosis, giving rise to hundreds of transcriptionally active nucleoli (Figure 1.2D), which are physically separate from the LBCs (Peacock 1965; Miller 1966; Brown and Dawid 1968; Gall 1968; Perkowska et al. 1968). The 5S rRNA, which must be produced during oogenesis in equimolar amounts to the 18S and 28S rRNAs, is not generated from extrachromosomal copies. Instead, the *X. laevis* genome carries about 24,000 copies of a special oocyte-type 5S gene, which are transcribed specifically during oogenesis (Brown et al. 1971).

For protein-coding genes, the corresponding mRNAs are presumably all transcribed on the loops of the LBCs. It is beyond the scope of this chapter to consider the complexity of the mRNA stored in the cytoplasm, much of it for use during early embryogenesis, when transcription is shut down. The nature of this stored RNA has been the subject of investigation for many years; earlier studies are ably summarized in Davidson's text *Gene Activity in Early Development* (Davidson 1986). With the advent of deep sequencing, it is now possible to examine the totality of stored transcripts in great detail. A recently published study from John Gurdon's group detected cytoplasmic transcripts from over 11,000 genes of *X. tropicalis* (Simeoni et al. 2012), more than half of the 20,000 annotated genes in the genome (Hellsten et al. 2010). As shown by RT-PCR analysis for a selected subset, these transcripts range in abundance from more than 10^7 copies per oocyte to less than a few hundred. We have also examined transcripts from mature *X. tropicalis* oocytes and found a similar wide range of abundance (Gardner et al. 2012). These data revive – or rather continue – an old debate about LBC transcription: do LBCs simply transcribe a set of oocyte-specific genes at an unusually high rate, or do they transcribe most or all genes as part of specific germline reprogramming of the genome?

We have recently addressed a more limited question about oocyte transcription. Are there major changes in the relative abundance of transcripts stored in the oocyte during the course of oogenesis? To answer this question,

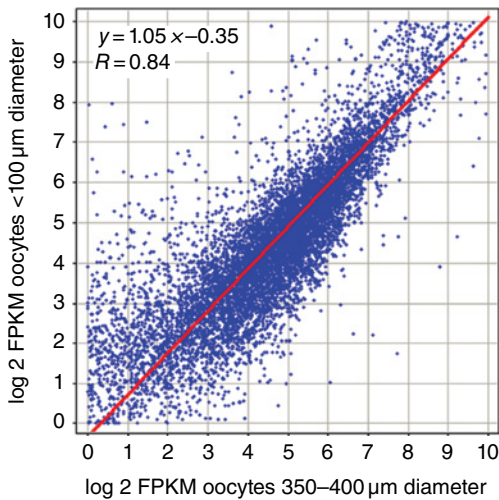


Figure 1.7 Similarity of transcriptomes from *X. tropicalis* oocytes less than 100 μm diameter and oocytes that have reached 350–400 μm diameter, approximately half their final size. Shown here are the log 2 FPKM scores for approximately 9700 different transcripts. The slope of approximately 1.0 and the high correlation ($R = 0.84$) show that transcripts are stored at similar relative concentrations from the earliest to midstages of oogenesis. Transcripts from fully mature oocytes are similar (not shown here).

we sequenced total oocyte RNA from *X. tropicalis* oocytes of different sizes, from less than 100 μm diameter to full-grown oocytes of about 800 μm (Figure 1.7). These data demonstrate three essential facts. First, from the beginning of oocyte development, the oocyte produces and stores transcripts from a wide variety of genes. Figure 1.7 shows data for approximately 9000 transcribed genes (specifically all genes with log 2 FPKM (fragments per kilobase per million reads) scores above 0). Second, these transcripts vary greatly in relative abundance, from transcripts that are just detectable at the read depth of our samples to some that are extremely abundant. Finally, the relative abundance of most transcripts changes very little during development of the oocyte, from well before the onset of yolk formation (oocytes about 100 μm diameter) all the way through until the mature oocyte.

Nascent transcripts on the LBCs

As just discussed, quantitative data are now available on the population of cytoplasmic

transcripts stored during oocyte development. These transcripts are produced by the LBCs and in this respect they give insight into the nature of LBC transcription. However, fundamental questions will remain until there is detailed information about the nascent transcripts themselves and the nature of their processing. In an attempt to gain such data, we carried out a deep sequence analysis of GV RNA from *X. tropicalis* oocytes (Gardner et al. 2012). To our surprise, we found that the bulk of GV RNA consists of stable intronic sequences (sisRNA) derived from the same set of genes whose transcripts are found in the cytoplasm. There is a rough correlation between the abundance of a given mRNA and the abundance of sisRNA from the same gene, although the absolute amount of mRNA is much greater (molar ratio roughly 100 : 1). For technical reasons, it was not possible to analyze sisRNA after GV breakdown by deep sequencing, but RT-PCR analysis of specific sequences demonstrated that sisRNA persists in the embryo until at least the blastula stage, at which time transcription resumes. At present, the functional significance of sisRNA is completely unknown.

We should not have been surprised that nascent transcripts were missing from our deep sequence data. Despite its enormous size, the GV of *X. tropicalis* contains only four sets of chromosomes with a total of 6–8 pg of genomic DNA (Gregory 2006). On the basis of incorporation data, Davidson earlier estimated that a *X. laevis* GV (with about twice the amount of genomic DNA as *X. tropicalis*) transcribes roughly 1.4 ng of chromosomal RNA per day. The total amount of RNA in nascent transcripts must be still smaller. Thus, even in a sample of RNA derived from several hundred GVs, the total amount of nascent transcripts will be no more than a few picograms, below the detection level in our experiments.

***In situ* hybridization of nascent transcripts on individual LBC loops**

Although global information about nascent transcripts must await the results of deep sequencing, specific transcripts have been investigated by *in situ* hybridization. The most complete analysis, carried out some

years ago, involved the histone gene clusters in the newt *Notophthalmus* (Diaz et al. 1981; Stephenson et al. 1981; Gall et al. 1983; Diaz and Gall 1985). The basic finding was that individual LBC loops contain one or more clusters of the five histone genes, the clusters being separated by extremely long tracts of a 221-bp repeated “satellite” DNA. *In situ* hybridization with probes specific for the histone genes and for the satellite DNA showed that most of the RNA on the loops is derived from the satellite DNA, presumably by read-through transcription from promoters in the histone gene clusters. Unfortunately, we do not have comparable data on other specific genes, although there is considerable evidence for transcription of repeated sequences on LBCs of other amphibians (Macgregor and Andrews 1977; Varley et al. 1980a, 1980b) and birds (Solovei et al. 1996; Deryusheva et al. 2007; Gaginskaya et al. 2009).

On the basis of this admittedly incomplete evidence, it is reasonable to suppose that the long length of LBC loops relative to the lengths of “ordinary” genes results at least in part from read-through transcription into downstream noncoding regions. The disparity between loop size and the length of genes, already an issue for the relatively modest-sized LBC loops of *Xenopus*, becomes even more problematic for the gigantic loops of salamander LBCs (Figures 1.2 and 1.6). Many loops in these organisms are 25–50 μm in length and some reach the almost unbelievable length of 1 mm. Because 1 μm of B-form DNA corresponds to about 3 kb, many loops (and hence TUs) of salamander LBCs must be hundreds of kb long. There is already convincing evidence for very long introns in some salamander genes (Casimir et al. 1988; Smith et al. 2009). Detailed analysis of a few highly transcribed genes in salamander (and *Xenopus*) LBCs by *in situ* hybridization would add greatly to our understanding of LBC structure and function during oogenesis. It may well turn out that the majority of RNA transcribed on LBCs consists of either intronic or downstream noncoding regions.

Appendix

The majority of LBC loops are similar in general morphology within a given organism, as exemplified by the relatively short loops of

anurans like *X. tropicalis* and the enormously longer loops of salamanders (Figure 1.2). As first shown in detail by Callan and Lloyd (1960) for the LBCs of the newt *Triturus*, it is possible to identify specific loops on the basis of their size and unique morphology of the RNP matrix. At present, we have almost no clue as to the functional significance of such differences among loops. It is possible to identify the transcripts being made on specific loops by correlating genetic maps and RNAseq data with fluorescent *in situ* hybridization analysis. To make such correlations easier, it is useful to have physical maps of the LBCs. Some years ago, we published relatively crude maps of the *X. laevis* LBCs, concentrating primarily on the distribution of the 5S and ribosomal RNA genes (Callan et al. 1988). In the interim, a good deal of additional mapping has been done, and updated maps are presented in Figure A1.1. More recently, *X. tropicalis* has become the favorite organism for sequence analysis, its major advantage being that it is a diploid species ($n=10$), whereas *X. laevis* is an allotetraploid ($n=18$). For that reason, it is useful to have LBC maps for this species as well. In Figure A1.2, we present our most current maps for *X. tropicalis*. Similar maps were recently published by Penrad-Mobayed et al. (2009). There are slight discrepancies in numbering between our maps and those of Penrad-Mobayed, resulting from the difficulty in determining relative lengths of the similarly sized chromosome. There are also discrepancies in numbering between both the LBC maps and the mitotic maps published earlier (Wells et al. 2011). These discrepancies will need to be resolved by *in situ* hybridization of specific sequences on the LBCs.

Acknowledgments

I thank the members of my laboratory for data and helpful discussions, especially Svetlana Deryusheva, Zehra Nizami, Jun Wei Pek, and Zheng'an Wu. Many of the ideas presented here were developed during conversations with Herbert Macgregor, Gary Morgan, and Michel Bellini. Special thanks go to Sidney Shaw and James Powers for help with super-resolution microscopy. The research reported in this publication was supported by the

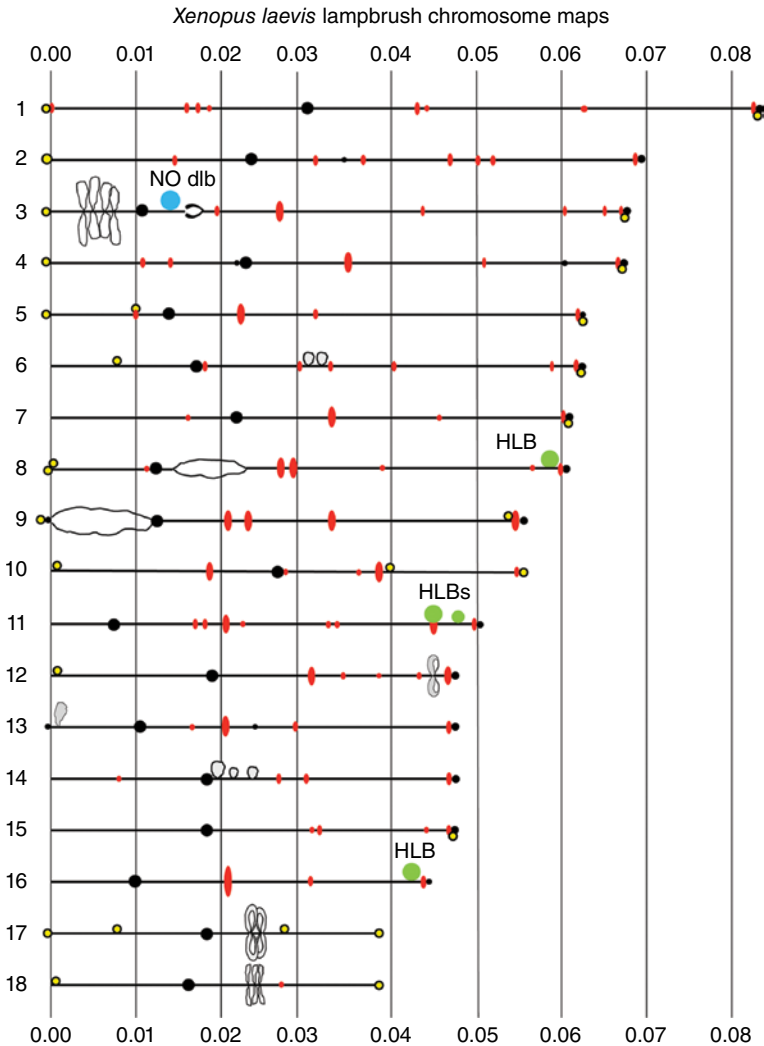


Figure A1.1 Cytological maps of the 18 LBCs of *X. laevis*, based on the analysis of 41 complete or nearly complete spread preparations. Lengths are given as fraction of the total length of all chromosomes. The numbering system is the same as that given in Murphy et al. (2002), differing slightly from the original maps in Callan et al. (1987). Centromere positions (large solid circles) were determined from a subset of 15 preparations in which the oocytes had been injected with a *myc*-tagged transcript of the centromere-specific protein CENP-C, and centromeres detected with an antibody against the tag. Pol III sites are shown as elongated ovals at positions described earlier in Murphy et al. (2002). Three chromosomes (Nos. 8, 11, and 16) bear histone locus bodies (HLB) at the histone gene loci (Callan et al. 1991). The nucleolus organizer is located near the centromere of chromosome No. 3 (Callan et al. 1988), although a nucleolus is only rarely seen at this locus. Oocyte-specific 5S genes are located at or near the end of the long arm of all chromosomes except Nos. 10, 17, and 18 (Callan et al. 1988). These regions are recognizable by the presence of a small terminal granule (solid circle) and pol III-labeled loops. Bodies identical in morphology and immunostaining properties to extrachromosomal speckles (B-snurposomes) are regularly seen at specific chromosome termini and at a few interstitial sites (small open circles). A dlb near the nucleolus organizer of chromosome No. 3 is associated with the RNA-editing enzyme ADAR1 (Eckmann and Jantsch 1999). Double-axis regions of unknown significance occur near the centromeres of chromosome Nos. 8 and 9.

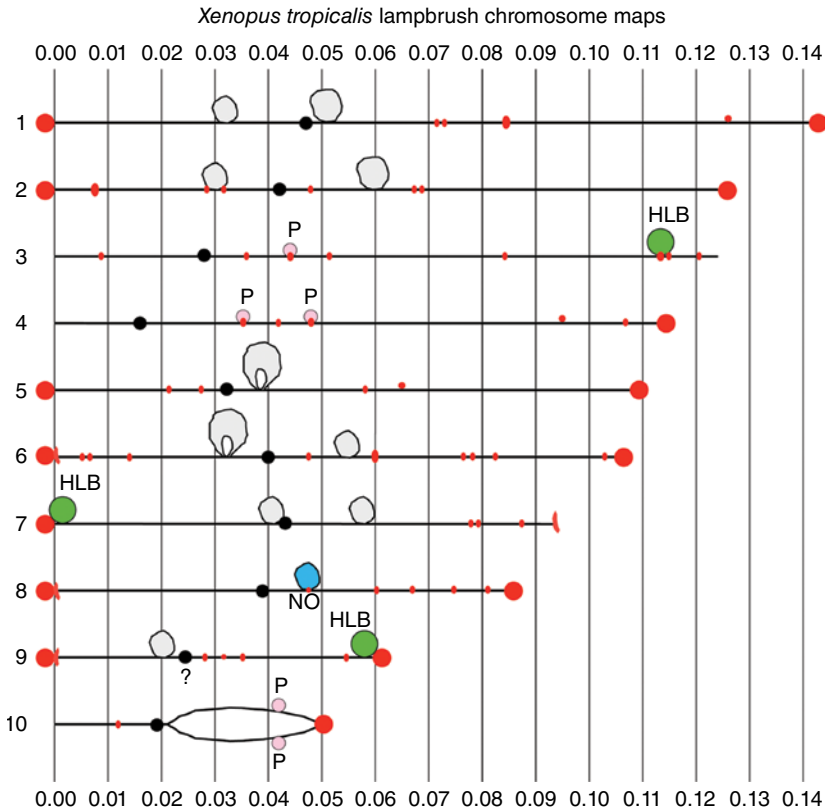


Figure A1.2 Cytological maps of the 10 LBCs of *X. tropicalis*, based on the analysis of 29 complete or nearly complete spread preparations. Lengths are given as fraction of the total length of all chromosomes. Centromere positions (large solid circles) were determined from a subset of 10 preparations in which the oocytes had been injected with a *myc*-tagged transcript of the centromere-specific protein CENP-C, and centromeres detected with an antibody against the tag. Terminal spheres of unknown nature are present on 15 of the 20 telomeres. These stain with an antibody against pol III, as do multiple internal sites (small solid circles). Four pol III sites on chromosome Nos 3, No. 4, and No. 10 frequently have pearls (P) associated with them (Nizami and Gall 2012). Three chromosomes (Nos. 3, 7, and 9) bear HLBs, presumably at the histone loci (not independently verified). The single nucleolus is located near the middle of chromosome No. 8, and the position of the nucleolus organizer (NO) has been verified by *in situ* hybridization. The large gray masses on several chromosomes are presumed to be “lumpy loops” as described originally by Callan in the newt *Triturus* (Callan and Lloyd 1960).

National Institute of General Medical Sciences of the National Institutes of Health under award number R01 GM33397. The content is solely the responsibility of the author and does not necessarily represent the official views of the National Institutes of Health. JGG is an American Cancer Society Professor of Developmental Genetics.

References

- Austin C, Novikova N, Guacci V, Bellini M (2009) Lampbrush chromosomes enable study of cohesin dynamics. *Chromosome Res* 17:165–184.
- Berger S, Menzel D, Traub P (1994) Chromosomal architecture in giant premeiotic nuclei of the green alga *Acetabularia*. *Protoplasma* 178:119–128.
- Brown DD, Littna E (1964) RNA synthesis during the development of *Xenopus laevis*, the South African clawed toad. *J Mol Biol* 8:669–687.
- Brown DD, Dawid IB (1968) Specific gene amplification in oocytes. *Science* 160:272–280.
- Brown DD, Wensink PC, Jordan E (1971) Purification and some characteristics of 5S DNA from *Xenopus laevis*. *Proc Natl Acad Sci U S A* 68:3175–3179.
- Callan HG (1954) Recent work on the structure of cell nuclei. in *Fine Structure of Cells: Symposium of the VIIIth Congress in Cell Biology*, Leiden 1954, International Union of Biological Sciences Publ, Series B, pp. 89–109. Noordhoff, Groningen.

- Callan HG (1957) The lampbrush chromosomes of *Sepia officinalis* L., *Anilocra physodes* L. and *Scyllium catulus* Cuv. and their structural relationship to the lampbrush chromosomes of amphibia. *Pubbl Staz Zool Napoli* 29:329–346.
- Callan HG (1963) The nature of lampbrush chromosomes. *Int Rev Cytol* 15:1–34.
- Callan HG (1986) Lampbrush Chromosomes. Springer-Verlag, Berlin.
- Callan HG, Macgregor HC (1958) Action of deoxyribonuclease on lampbrush chromosomes. *Nature (Lond)* 181:1479–1480.
- Callan HG, Lloyd L (1960) Lampbrush chromosomes of crested newts *Triturus cristatus* (Laurenti). *Philos Trans R Soc Lond B Biol Sci* 243:135–219.
- Callan HG, Gall JG, Berg CA (1987) The lampbrush chromosomes of *Xenopus laevis*: preparation, identification, and distribution of 5S DNA sequences. *Chromosoma (Berlin)* 95:236–250.
- Callan HG, Gall JG, Murphy C (1988) The distribution of oocyte 5S, somatic 5S and 18S + 28S rDNA sequences in the lampbrush chromosomes of *Xenopus laevis*. *Chromosoma (Berlin)* 97:43–54.
- Callan HG, Gall JG, Murphy C (1991) Histone genes are located at the sphere loci of *Xenopus* lampbrush chromosomes. *Chromosoma (Berlin)* 101:245–251.
- Casimir CM, Gates PB, Ross-Macdonald PB, Jackson JF, Patient RK, Brookes JP (1988) Structure and expression of a newt cardio-skeletal myosin gene. Implications for the C value paradox. *J Mol Biol* 202:287–296.
- Davidson EH (1986) Gene Activity in Early Development. Academic Press, Orlando.
- Deryusheva S, Krasikova A, Kulikova T, Gaginskaya E (2007) Tandem 41-bp repeats in chicken and Japanese quail genomes: FISH mapping and transcription analysis on lampbrush chromosomes. *Chromosoma* 116:519–530.
- Diaz MO, Gall JG (1985) Giant readthrough transcription units at the histone loci on lampbrush chromosomes of the newt *Notophthalmus*. *Chromosoma* 92:243–253.
- Diaz MO, Barsacchi-Pilone G, Mahon KA, Gall JG (1981) Transcripts from both strands of a satellite DNA occur on lampbrush chromosome loops of the newt *Notophthalmus*. *Cell* 24:649–659.
- Eckmann CR, Jantsch MF (1999) The RNA-editing enzyme ADAR1 is localized to the nascent ribonucleoprotein matrix on *Xenopus* lampbrush chromosomes but specifically associates with an atypical loop. *J Cell Biol* 144:603–615.
- Gaginskaya E, Kulikova T, Krasikova A (2009) Avian lampbrush chromosomes: a powerful tool for exploration of genome expression. *Cytogen Gen Res* 124:251–267.
- Gall JG (1954) Lampbrush chromosomes from oocyte nuclei of the newt. *J Morphol* 94:283–352.
- Gall JG (1956) On the submicroscopic structure of chromosomes. *Brookhaven Symp Biol* 8:17–32.
- Gall JG (1958) Chromosomal differentiation. in *A Symposium on the Chemical Basis of Development* (eds. WD McElroy, B Glass), pp. 103–135. Johns Hopkins Press, Baltimore.
- Gall JG (1963) Kinetics of deoxyribonuclease action on chromosomes. *Nature (Lond)* 198:36–38.
- Gall JG (1968) Differential synthesis of the genes for ribosomal RNA during amphibian oogenesis. *Proc Natl Acad Sci U S A* 60:553–560.
- Gall JG (1981) Chromosome structure and the C-value paradox. *J Cell Biol* 91:3s–14s.
- Gall JG (2012) Are lampbrush chromosomes unique to meiotic cells? *Chromosome Res* 20:905–909.
- Gall JG, Callan HG (1962) H³ uridine incorporation in lampbrush chromosomes. *Proc Natl Acad Sci U S A* 48:562–570.
- Gall JG, Murphy C (1998) Assembly of lampbrush chromosomes from sperm chromatin. *Mol Biol Cell* 9:733–747.
- Gall JG, Diaz MO, Stephenson EC, Mahon KA (1983) The transcription unit of lampbrush chromosomes. in *Gene Structure and Regulation in Development* (eds. S Subtelny, F Kafatos), pp. 137–146. Alan R. Liss, New York.
- Gardner EJ, Nizami ZF, Talbot CC, Jr., Gall JG (2012) Stable intronic sequence RNA (sisRNA), a new class of noncoding RNA from the oocyte nucleus of *Xenopus tropicalis*. *Genes Dev* 26:2550–2559.
- Giles KE, Gowher H, Ghirlando R, Jin C, Felsenfeld G (2010) Chromatin boundaries, insulators, and long-range interactions in the nucleus. *Cold Spring Harb Symp Quant Biol* 75:79–85.
- Gregory TR (2006) Animal Genome Size Database. <http://www.genomesize.com> (accessed on November 8, 2013).
- Hamkalo BA, Miller OL, Jr. (1973) Electron-microscopy of genetic activity. *Annu Rev Biochem* 42:379–396.
- Hellsten U, Harland RM, Gilchrist MJ, et al. (2010) The genome of the western clawed frog *Xenopus tropicalis*. *Science* 328:633–636.
- Hess O (1971) Lampenbürstchenchromosomen. in *Handbuch der allgemeinen Pathologie* (eds. H-W Altmann, F Büchner, H Cottier, et al.), pp. 215–281. Springer-Verlag, Berlin.
- Liu JL, Gall JG (2012) Induction of human lampbrush chromosomes. *Chromosome Res* 20:971–978.
- Macgregor HC (2012) Chromomeres revisited. *Chromosome Res* 20:911–924.
- Macgregor HC, Andrews C (1977) The arrangement and transcription of ‘middle repetitive’ DNA

- sequences on lampbrush chromosomes of *Triturus*. *Chromosoma* 63:109–126.
- Miller OL, Jr. (1966) Structure and composition of peripheral nucleoli of salamander oocytes. *J Natl Cancer Inst Monogr* 23:53–66.
- Miller OL, Jr., Hamkalo BA (1972) Visualization of RNA synthesis on chromosomes. *Int Rev Cytol* 33:1–25.
- Morgan GT (2002) Lampbrush chromosomes and associated bodies: new insights into principles of nuclear structure and function. *Chromosome Res* 10:177–200.
- Morgan GT (2007) Localized co-transcriptional recruitment of the multifunctional RNA-binding protein CELF1 by lampbrush chromosome transcription units. *Chromosome Res* 15:985–1000.
- Mott MR, Callan HG (1975) An electron-microscope study of the lampbrush chromosomes of the newt *Triturus cristatus*. *J Cell Sci* 17:241–261.
- Murphy C, Wang Z, Roeder RG, Gall JG (2002) RNA polymerase III in Cajal bodies and lampbrush chromosomes of the *Xenopus* oocyte nucleus. *Mol Biol Cell* 13:3466–3476.
- Nizami ZF, Gall JG (2012) Pearls are novel Cajal body-like structures in the *Xenopus* germinal vesicle that are dependent on RNA pol III transcription. *Chromosome Res* 20:953–969.
- Peacock WJ (1965) Chromosome replication. *J Natl Cancer Inst Monogr* 18:101–131.
- Penrad-Mobayed M, El Jamil A, Kanhoush R, Perrin C (2009) Working map of the lampbrush chromosomes of *Xenopus tropicalis*: a new tool for cytogenetic analyses. *Dev Dyn* 238:1492–1501.
- Perkowska E, Macgregor HC, Birnstiel ML (1968) Gene amplification in the oocyte nucleus of mutant and wild-type *Xenopus laevis*. *Nature (Lond)* 217:649–650.
- Rückert J (1892). Zur Entwicklungsgeschichte des Ovarialeies bei Selachiern. *Anat Anz* 7:107–158.
- Scheer U (1981) Identification of a novel class of tandemly repeated genes transcribed on lampbrush chromosomes of *Pleurodeles waltlii*. *J Cell Biol* 88:599–603.
- Scheer U, Franke WW, Trendelenburg MF, Spring H (1976) Classification of loops of lampbrush chromosomes according to the arrangement of transcriptional complexes. *J Cell Sci* 22:503–519.
- Schmid M, Nanda I, Hoehn H, et al. (2005) Second report on chicken genes and chromosomes 2005. *Cytogenet Genome Res* 109:415–479.
- Simeoni I, Gilchrist MJ, Garrett N, Armisen J, Gurdon JB (2012) Widespread transcription in an amphibian oocyte relates to its reprogramming activity on transplanted somatic nuclei. *Stem Cells Dev* 21:181–190.
- Smith JJ, Putta S, Zhu W, et al. (2009) Genic regions of a large salamander genome contain long introns and novel genes. *BMC Genomics* 10:19.
- Solovei IV, Joffe BI, Gaginskaya ER, Macgregor HC (1996) Transcription on lampbrush chromosomes of a centromerically localized highly repeated DNA in pigeon (*Columba*) relates to sequence arrangement. *Chromosome Res* 4:588–603.
- Spradling AC (1993) Developmental genetics of oogenesis. in *The Development of Drosophila melanogaster* (eds. M Bate, A Martinez-Arias), pp. 1–70. Cold Spring Harbor Laboratory Press, Cold Spring Harbor.
- Spring H, Scheer U, Franke WW, Trendelenburg MF (1975) Lampbrush-type chromosomes in the primary nucleus of the green alga *Acetabularia mediterranea*. *Chromosoma* 50:25–43.
- Stephenson EC, Erba HP, Gall JG (1981) Histone gene clusters of the newt *Notophthalmus* are separated by long tracts of satellite DNA. *Cell* 24: 639–647.
- Tomlin SG, Callan HG (1951) Preliminary account of an electron microscope study of chromosomes from newt oocytes. *Q J Microsc Sci* 92:221–224.
- Varley JM, Macgregor HC, Erba HP (1980a) Satellite DNA is transcribed on lampbrush chromosomes. *Nature (Lond)* 283:686–688.
- Varley JM, Macgregor HC, Nardi I, Andrews C, Erba HP (1980b) Cytological evidence of transcription of highly repeated DNA sequences during the lampbrush stage in *Triturus cristatus carnifex*. *Chromosoma* 80:289–307.
- Voronina E, Wessell GM (2003) The regulation of oocyte maturation. *Curr Top Dev Biol* 58:53–110.
- Wallace H, Birnstiel ML (1966) Ribosomal cistrons and the nucleolar organizer. *Biochim Biophys Acta* 114:296–310.
- Wells DE, Gutierrez L, Xu Z, et al. (2011) A genetic map of *Xenopus tropicalis*. *Dev Biol* 354:1–8.

2 RNA Localization during Oogenesis in *Xenopus laevis*

James O. Deshler

Directorate for Biological Sciences, National Science Foundation, Arlington, VA

Abstract: The polarized distribution of mRNA is a wide-spread mechanism for regulating cell differentiation and cell function. *Xenopus* oocytes have served as a wonderful model system to investigate the mechanism(s) underlying this process. Here, a summary of major findings in the *Xenopus* oocyte system is presented, and these findings are compared with findings in other species and cell types. A model is presented that suggests RNA localization elements form secondary structural elements comprised of distinct RNA strands from two or more localizing mRNA molecules. In this model, these intermolecular RNA structures play a role in recruiting critical proteins required for the localization process. Since this mechanism is likely to regulate the spatial expression patterns of thousands of proteins encoded in a single genome, future work should focus on advanced algorithm development to identify these and other types of nonprotein-coding RNA regulatory elements that play a major role in establishing diverse phenotypes from specific genotypes.

***Xenopus* oocytes as a model system for exploring RNA localization**

The generation of polarized distributions of specific RNAs, proteins, and subcellular organelles is a key step toward organizing a cell. This spatial and temporal aspect of regulation contributes significantly to cell type-specific functions in all organisms. The specific localization of distinct mRNAs is a widespread mechanism for generating polarity in both somatic and germ cells and has been studied extensively in highly polarized cells, such as oocytes, neurons, and

epithelial cells where the process of establishing mRNA polarity is most amenable to experimental investigation. The primary role for mRNA localization is to establish localized protein synthesis from distinct mRNAs at particular subcellular locations where proteins are required for specific cellular functions and exclude them from regions where they are not needed or may be deleterious. One example of this is the localized synthesis of proteins at neuronal synapses which can be hundreds of microns away from the nucleus in the cell bodies where mRNAs are synthesized. The local synthesis of distinct proteins at synapses

is thought to play a critical role in synaptic plasticity, long-term memory, as well as neurological disorders (Richter and Klann 2009; Liu-Yesucevitz et al. 2011).

Egg cells, like neuronal cells, also have a high degree of polarity and organization that is required to support the formation of an embryo as soon as fertilization occurs. These female germ cells of *Drosophila melanogaster* and *Xenopus laevis* have both been utilized extensively to investigate the mechanisms of RNA localization and the establishment of cell polarity because they are amenable to distinct types of experimental investigation. In both species, as in most animals, primordial germ cells are set aside early during embryogenesis as a source of stem cells that will differentiate into eggs or sperm in females or males, respectively. As primordial germ cells differentiate into oogonia and then oocytes in the ovary, they initiate meiosis, but arrest their cell cycle in the first meiotic prophase at which time they begin the process of oogenesis to form an egg. During oogenesis, these meiotic cells have the maximum copy number of each gene, and segments of genome that encode the ribosomal RNA genes are amplified to accommodate the high demand for protein synthesis in the growing oocytes. In *Xenopus*, this process takes 9–12 months but is on the order of just a few days in *Drosophila*. For a comparative description of this biological process in vertebrate and invertebrate animal models, including *Drosophila* and *Xenopus*, the reader is encouraged to read a review by Saffman and Lasko (1999). During oogenesis, oocytes accumulate yolk protein from the mother, but also generate highly organized patterns of mRNA localization and consequent protein expression. Sometimes the resulting polarized pattern of protein expression is visible to the naked eye. For example, fully grown *Xenopus* oocytes are over 1 mm in diameter and have pigment granules in the cortex of their animal hemisphere, making one half of the oocyte quite dark in appearance. Cells that acquired these pigment granules during early development migrate around the embryo, surrounding it completely later in development. The opposite hemisphere is referred to as the vegetal hemisphere. It has no pigment and appears light in color.

While arrested in the prophase of meiosis I, *Xenopus* oocytes progress through six characterized stages of growth, and a mixture of stage I–VI oocytes is present in the adult female ovary. Stage I oocytes are transparent and are 50–100 μm in diameter. As oocytes grow and accumulate yolk protein, they become opaque during stage II of oogenesis (100–450 μm diameter). Pigment granules form at the surface of the animal side of oocytes during the later stage III of oogenesis (450–600 μm diameter) and continue to increase in the animal hemisphere until the final stage VI of oogenesis (1200–1300 μm diameter) (Dumont 1972). Many RNAs have been discovered that localize to the vegetal pole and vegetal cortex of *Xenopus* oocytes. This process occurs primarily during stages I–III of oogenesis. Those RNAs that begin to localize in stage I oocytes, such as Xcat-2, first accumulate at a structure called the Balbiani body or mitochondrial cloud which is a large structure adjacent to one side of the nucleus and thus first defines the animal–vegetal axis of the growing oocyte (Figure 2.1). Some RNAs, such as Xcat-2, are targeted with somewhat more specificity to the germ plasm within the mitochondrial cloud, causing these RNAs to be segregated to primordial germ cells during early development (Kloc et al. 2000). The mitochondrial cloud, along with the associated early-pathway RNAs, migrates from its region near the nucleus of stage I oocytes to the vegetal cortex during stage II of oogenesis and remains at the vegetal pole through stage VI. RNAs that localize to the vegetal pole during the so-called “late pathway”, such as Vg1, are distributed throughout the cytoplasm of stage I oocytes and begin their localization during stage II at which point they localize to a wedge-shaped structure just behind the early-pathway RNAs at the vegetal pole (Figure 2.1). These RNAs continue to localize to the vegetal cortex during stages III and IV of oogenesis. By stage IV of oogenesis, most of the Vg1 is localized throughout the vegetal cortex, whereas early-pathway RNAs remain in the cortex at the vegetal pole. The two best-characterized late-pathway RNAs, Vg1 and VegT, encode proteins that act synergistically (Agius et al. 2000) to specify the mesoderm during early embryogenesis

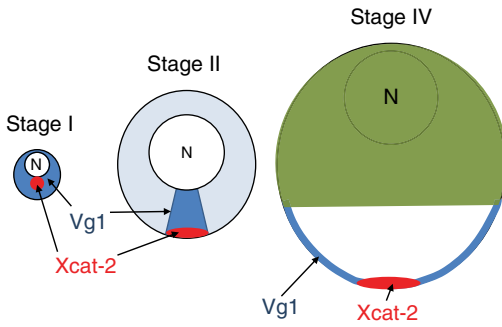


Figure 2.1 Distribution of early- and late-pathway RNAs in stage I–IV oocytes. On the left is a stage I oocyte showing the nucleus (N), the Vg1 mRNA distributed throughout the cytoplasm (blue), and the Xcat-2 localized to the Balbiani body or mitochondrial cloud adjacent to the nucleus (red). By stage II, the mitochondrial cloud and early-pathway RNAs have moved to the vegetal cortex, whereas late-pathway RNAs, such as Vg1 (blue), begin to localize to a wedge-shaped structure between the nucleus (N) and the early-pathway RNAs at the vegetal pole. A stage IV oocyte is shown on the right with a pigmented animal hemisphere at the top and Vg1 (blue) distributed through most of the vegetal cortex. Xcat-2 (red) and other early RNAs remain in the vegetal cortex but mostly at the vegetal pole. The oocytes are drawn to relative scale with the stage I oocyte being approximately 100 μm in diameter. The process of growing from a stage I to stage IV oocyte takes months in an adult female. For a comprehensive book of protocols and high-quality photos of different-staged oocytes, the reader is referred to volume 36 of *Methods in Cell Biology* (O’Keefe et al. 1991). To see a color version of this figure, see Plate 4.

(Kessler and Melton 1995; Joseph and Melton 1998; Zhang et al. 1998). Stage II oocytes are probably the best for studying the localization process because only at this stage will the early- and late-pathway injected exogenous RNAs adopt their relative localization patterns that most closely mimic their endogenous counterparts (Kloc et al. 1996) with only 18–36 h of culturing post injection. The molecular mechanism underlying this process of sorting and localizing mRNAs to the vegetal cortex will be the focus of this chapter.

In order to explore the mechanisms that mediate mRNA localization, it is important to consider the advantages and disadvantages of the various model systems employed to study the process. For example, a plethora of genetic manipulations are available in the *Drosophila*

system and have been used successfully to identify and characterize proteins required for mRNA localization and transport in *Drosophila* oocytes and embryos. Through an elegant application of molecular, genetic, and developmental approaches available only in *Drosophila*, it has been shown that ectopic mislocalization of a single posterior mRNA, *nanos*, to the anterior end of an oocyte is sufficient to generate an entire posterior body structure resulting in a bipolar embryo (Gavis and Lehmann 1992). This fascinating result demonstrates that the polarized distribution of just a single upstream factor can be sufficient to establish all downstream patterning of a developing embryo, at least in this system. Insights into both the importance and mechanism of mRNA localization gained from the *Drosophila* system have been enormous and are summarized in recent review articles (Becalska and Gavis 2009; Lasko 2011). One potential limitation of the *Drosophila* system, however, is that from an evolutionary perspective, the patterning observed in developing *Drosophila* embryos is highly derived, such that specific orthologous or homologous mRNA localization pathways in distantly related animals have not yet been identified in oocytes and may not exist, even though many of the core RNA binding proteins and molecular motors are shared between species. This is one reason investigators have studied mRNA localization in other models, such as *Xenopus* oocytes, where genetic manipulations are not possible, but in which other types of experimental approaches are available and have revealed key insights into the mRNA localization process of vertebrates. Important advantages of the *Xenopus* oocyte model system include the ability to prepare cellular extracts from individually staged oocytes, to prepare undiluted cytoplasmic extracts that maintain associations that are sensitive to dilution, to microinject known quantities of labeled and unlabeled RNAs for *in vivo* competition experiments, to perform live imaging of RNAs being localized, and to immunoprecipitate proteins and/or RNAs presumably associated with RNA localization complexes.

Previous reviews have described numerous mRNAs that become localized to the vegetal pole during stages I–IV of oogenesis in *Xenopus* (King et al. 2005; Kloc and Etkin

2005). In this review, I will focus on distinguishing features of and recent findings about the mRNA localization process that directs RNAs toward the vegetal pole of growing *Xenopus* oocytes. In addition, questions for future research in this system will be addressed with the expectation that further exploration into these areas will help to inform studies of the mRNA localization process in *Xenopus* as well as other species across the phylogenetic tree. A few RNAs have also been discovered that localize to the animal pole and appear to interact with some of the vegetal pathway localization factors (Snedden et al. 2013). However, little else is known about the mechanism of their localization, and they will not be discussed further in this chapter.

Cis-elements and the role of short repeated motifs

The first mRNA localization element (LE) to be mapped in *Xenopus* is located in a 340-nucleotide (nt) fragment of the approximately 1200-nt 3'-untranslated region (UTR) of the Vg1 mRNA (Mowry and Melton 1992). This fragment is both necessary and sufficient to localize to the vegetal pole when injected into stage III/IV oocytes and cultured for 2–3 days. This has turned out to be a trend in that mRNA LEs reside in the 3'-UTR of most localized mRNAs throughout various species. Subsequent characterization of the Vg1 LE showed that there were short five- to nine-nt interspersed perfect repeat sequences that seemed to be more important for localization (Deshler et al. 1997) than other regions of the Vg1 LE when subjected to a comprehensive deletion analysis (Gautreau et al. 1997). The biggest surprise resulting from these studies was that the deletion of the smallest repeat, UUCAC, repeated five times in the Vg1 LE, led to the biggest reduction in localization when compared to other repeated sequences that are longer or larger deletions of the LE that don't contain repeated motifs (Gautreau et al. 1997). Since the UUCAC motif and other short sequences are required for localization and serve as binding sites for proteins that were identified by their ability to bind specifically to RNA LEs, these RNA binding proteins

were also thought to be involved in the RNA localization process (Deshler et al. 1997, 1998). However, tandem arrays of these individual motifs fail to localize in isolation when injected into *Xenopus* oocytes (Deshler et al. 1998; Lewis et al. 2004), so it was postulated that combinations of motifs interact with a set of RNA binding proteins to form a ribonucleoprotein (RNP) complex that is competent to localize (Bubunencko et al. 2002; Lewis et al. 2004). This idea emerged through studies of the Vg1 and VegT mRNAs, both of which localize later in oogenesis than the so-called early-pathway RNAs, such as Xcat-2 or Xlsirt (Kloc and Etkin 1995).

The idea that a combination of distinct short RNA interspersed repeated sequence motifs interacts with their cognate RNA binding proteins to form a localization-competent RNP complex is a reasonable explanation for the role of these short motifs. However, this view became more complicated when a few early-pathway mRNAs were examined in detail. Xcat-2 is one of the best-characterized mRNAs that localizes to the mitochondrial cloud of early stage I oocytes before reaching the vegetal pole (Figure 2.1). Several groups have shown that when injected into later-stage oocytes, Xcat-2 is perfectly capable of localizing directly to the vegetal pole during the Vg1 or "late pathway" (Zhou and King 1996; Hudson and Woodland 1998; Allen et al. 2003), and *in vivo* competition assays show that the Xcat-2 LE competes for Vg1 localization factors more efficiently than the Vg1 LE does itself (Choo et al. 2005). Moreover, labeled Xcat-2 LE localizes much faster during later stages of oogenesis than the Vg1 LE (Choo et al. 2005), as does the Xlsirt early-pathway RNA when coinjected simultaneously with Vg1 into stage II oocytes (Kloc et al. 1996). These and other data, such as the fact that the Xcat-2 LE recruits Kinesin II (Betley et al. 2004), show quite convincingly that the Xcat-2 LE interacts extremely well with the Vg1 mRNA localization machinery and can utilize the late pathway even though endogenous Xcat-2 localizes much earlier than Vg1. Confusion arises from the discovery of a short motif, UGCAC, that is repeated six times in the approximately 230-nt Xcat-2 LE (Betley et al. 2002) and is absolutely required

for localization of the Xcat-2 LE at any stage. In addition, the UGCAC deletion mutant fails to compete for Vg1 localization machinery during the late pathway (Choo et al. 2005). Thus, from a functional sense, the UGCAC motif in the Xcat-2 LE is analogous to the UUCAC motif in the Vg1 LE. Furthermore, UGCAC and UUCAC motifs are at least partially interchangeable between the Xcat-2 and Vg1 LEs with regard to their ability to specify localization (Chang et al. 2004). A dilemma then arises when trying to explain why the UUCAC motif is a specific binding site for the Vg1 LE binding protein (Vera/Vg1RBP), whereas UGCAC is not (Deshler et al. 1998; Choo et al. 2005). This leads us to question the original interpretation of the correlation between UUCAC binding Vera/Vg1RBP and localization of vegetal RNAs, which inferred that UUCAC motifs promote localization by serving as binding sites for Vera/Vg1RBP (Deshler et al. 1998; Bubunenko et al. 2002; Kwon et al. 2002). In fact, recent work has shown that a dominant-negative RNA binding-deficient form of Vera/Vg1RBP fails to inhibit the localization of the Vg1 LE, suggesting that direct binding of Vera/Vg1RBP to the Vg1 LE RNA is not required for RNA localization of Vg1 (Rand and Yisraeli 2007). Together, these investigations raise the possibility that UUCAC motifs are more similar to UGCAC motifs and promote localization through some other mechanism yet to be identified. In fact, a situation such as this exists in the *Drosophila* field where 13 IMP binding motifs exist in the *oskar* 3'-UTR; IMP is a *Drosophila* homolog of Vera/Vg1RBP. In this system, the IMP binding sites are required for proper localization of *oskar* mRNA and for localization of the IMP protein with *oskar* at the posterior pole. Thus, IMP binding to the IMP binding motifs is required for its own localization to the posterior pole. However, IMP is not required for the localization of *oskar* to the posterior pole of *Drosophila* oocytes (Munro et al. 2006). Thus, IMP binding motifs must promote the localization of the *oskar* mRNA to the posterior pole through means other than serving as binding sites for the *Drosophila* Vera/Vg1RBP homolog, IMP.

Based on the findings just described, it is important to consider that UUCAC and IMP

binding sites are similar to UGCAC motifs and promote localization through a mechanism that does not require binding to Vera/Vg1RBP or IMP, respectively. What might such a mechanism be? Two scenarios seem most likely and are not mutually exclusive. In the first scenario, these motifs could simply be binding other RNA binding proteins that promote localization, but have not yet been detected using biochemical methods available in the *Xenopus* system. Along these lines, members of my laboratory spent a lot of time trying to identify RNA binding proteins that specifically recognize UGCAC motifs using a variety of biochemical methods in the hope of finding a new key factor required for the process. No such protein was ever identified. This is a negative result and consequently was never published.

Another possibility is that UUCAC, IMP binding sites, and/or UGCAC motifs are simply the building blocks or evolutionary signatures of higher-order RNA structures that promote localization through the interactions with localization machinery that recognizes secondary and/or tertiary RNA structures. Conceptually, this is an attractive scenario because it is known that the highly conserved double-stranded RNA binding protein Staufen is involved in the localization of RNAs to the vegetal cortex of *Xenopus* oocytes (Yoon and Mowry 2004). Staufen is required for the localization of mRNAs to both the anterior and posterior pole of *Drosophila* oocytes (St Johnston et al. 1991) and recognizes complex structures in the bicoid LE that consist of stem-loop structures and intermolecular base-pairing interactions that support the formation of dimers and/or multimers (Ferrandon et al. 1997). Thus, Staufen is a general RNA localization factor required for localization of multiple mRNAs to different locations in a cell, and it is known to recognize high-order RNA structures *in vivo* in a selective fashion in *Drosophila*. Even so, biochemical assays have failed to detect specific binding of Staufen protein to RNA localization sequences in any model system. Furthermore, specific Staufen binding sites and higher-order RNA structures required for localization have not been identified in vertebrates. Therefore, the identification of double-stranded segments of

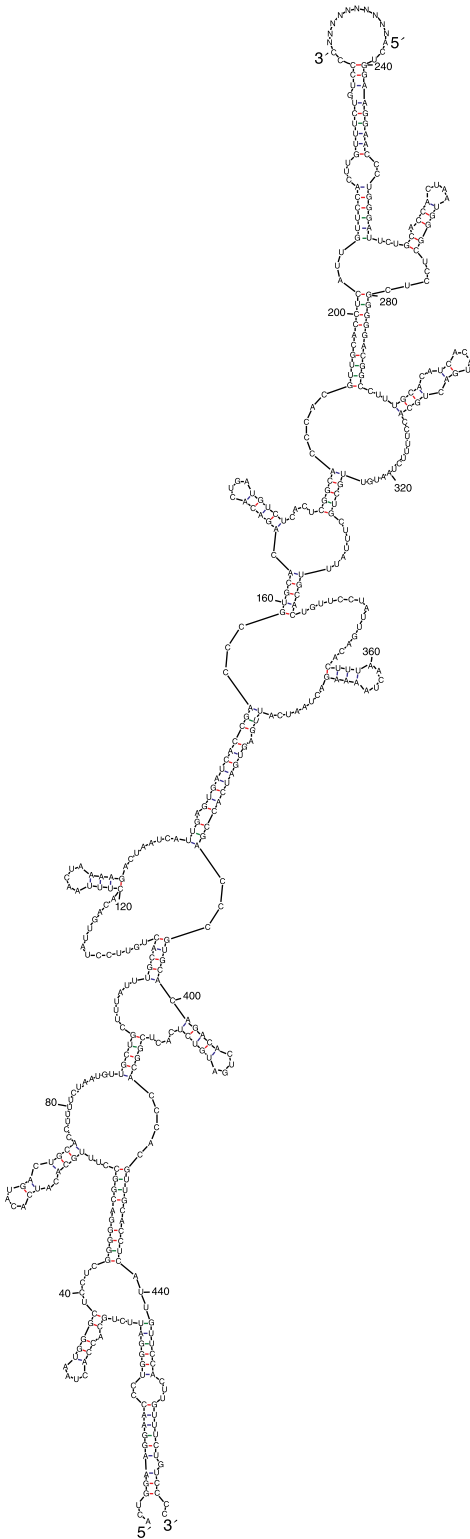
RNA LEs in the *Xenopus* system would represent an important step toward understanding how Staufen mediates RNA localization in these vertebrate cells.

The most effective *a priori* method for identifying RNA secondary structures that exist *in vivo* is to use phylogenetic comparisons of optimal (energetically most favorable) and suboptimal RNA secondary structures predicted for orthologous RNA sequences by RNA folding programs such as MFOLD. There is an approximately 90% chance that the biologically relevant RNA secondary structure for a single RNA sequence that forms *in vivo* will exist within the set of suboptimal structures that are within 10% of the free energy of the optimal structure predicted by MFOLD (Pace et al. 1989). Irrelevant secondary structures can generally be eliminated by comparing suboptimal structures predicted for two different, but orthologous, RNA sequences. Such an approach was used to identify the relatively complicated RNA secondary structure in the approximately 645-nt RNA LE of the *Drosophila* bicoid 3'-UTR (MacDonald 1990; Seeger and Kaufman 1990) which shows approximately 65% nt identity in alignments of *D. melanogaster* and *Drosophila pseudoobscura* bicoid sequences.

In an attempt to perform a similar analysis in the *Xenopus* system, I focused on the CAC-rich Xcat-2 LE (Betley et al. 2002) because it has extremely robust localization activity when compared to the Vg1 LE side by side (Choo et al. 2005), and it is much shorter, which limits the complexity of possible double-stranded RNA structures predicted through computational analysis. In addition, the Δ UGCAC localization-defective mutant is well characterized and could serve as a control for any structures emerging from this analysis. The sets of suboptimal structures predicted for the approximately 227 nt Xcat-2 RNA localization sequence of *X. laevis* or *Xenopus borealis* which show 89% nt identity when aligned to each other share no common secondary structural elements. One potential concern about this comparison was that too many common suboptimal structures would be identified given the high degree of sequence identity, making identification of the correct structure unlikely. Surprisingly, however, no

common optimal or suboptimal RNA secondary structures were found even though both share the six UGCAC motifs required for localization (Betley et al. 2002; Chang et al. 2004) in addition to their high overall nt identity (*X. borealis* actually has one additional UGCAC motif). Both MFOLD and PFOLD, designed to find secondary structures common to more than one sequence, were used in this analysis (data not shown).

As mentioned earlier, previous work has shown that intermolecular RNA base pairing that supports the dimerization and/or multimer formation of the bicoid RNA LE (Ferrandon et al. 1997) mediates its specific binding to Staufen protein *in vivo* (Wagner et al. 2001) which is required for localization of bicoid RNA (St Johnston et al. 1991). Even though no common secondary or "hairpin" structures in orthologous Xcat-2 sequences could be identified, it was still possible that dimerization domains could exist in the Xcat-2 localization sequence. To identify regions of the Xcat-2 LE that have the potential to form intermolecular RNA base pairs, two copies of the sequence were linked together in tandem and analyzed with MFOLD. This was done for the *X. laevis* and *X. borealis* sequences, and both showed the same basic result: their LEs are predicted to form extensive intermolecular base-pairing interactions (Figure 2.2). When one copy of the *X. laevis* and one copy of the *X. borealis* MCLE sequences are fused in tandem, the ability to form this intermolecular structure is lost, no matter which sequence is entered first into the folding program (data not shown). This finding suggests that as the *X. laevis* and *X. borealis* Xcat-2 genes evolved, their LEs maintained an ability to form dimers. The *X. laevis* region of intermolecular RNA base-pairing potential consists of 80 intermolecular base pairs and only 20 intramolecular base pairs. Importantly, the UGCAC localization-defective deletion mutant (Betley et al. 2002) is not predicted to form such extensive intermolecular base pairing (data not shown). This ability to form intermolecular stretches of double-stranded RNA was also observed when several ascidian CAC-rich RNA LEs were analyzed (data not shown). Strikingly, when the fastest or most efficient human CAC-rich RNA LE we have identified in humans (Syntaxin1B2) (Andken



et al. 2007) is analyzed in a similar fashion by MFOLD, it is also predicted to contain a significant intermolecular base-pairing region (data not shown). Together, these findings provide strong phylogenetic evidence for dimerization and/or multimerization domains within functional CAC-rich RNA LEs. A somewhat related analysis showed that the ability to form extended double-stranded stretches of RNA correlated with localization activity for the noncoding Xsirt RNA (Allen et al. 2003).

While the ability to form intermolecular dimers may be shared between the CAC-rich RNA LEs of Syntaxin1B2 and Xcat-2 and the bicoid RNA LE in *Drosophila*, there are major differences between the intermolecular interactions formed by bicoid and the vertebrate RNAs. Dimerization of bicoid is mediated by two discontinuous segments of only four or five base pairs via extremely dynamic RNA–RNA interactions (Ferrandon et al. 1997) referred to as RNA kissing reactions. RNA kissing is widely known to regulate a number of genetic processes (Eguchi et al. 1991; Gerhart et al. 1998) and can involve as few as two base pairs (Eguchi and Tomizawa 1991; Kim and Tinoco 2000). The stem-loop structures that have been proven through their evolutionary conservation position these kissing nt in the loop conformation that promotes the intermolecular pairing. The putative dimerization domains we have identified in vertebrate genes do not have conserved stem-loop structures and contain much more extensive intermolecular

Figure 2.2 Intermolecular base pairing potential of the Xcat-2 RNA LE. Two tandem copies of the Xcat-2 MCLE connected with 10 N were analyzed with MFOLD. The resulting structure is shown that has extensive intermolecular base-pairing potential that would support the formation of dimers or multimers *in vivo*. Evidence for this structure comes from the fact that mutations that reduce intermolecular base pairing impair localization but are rescued by compensatory mutations *in trans* (data not shown). For Xcat-2, nucleotides 403–610 were used, but we resequenced the DNA since a predicted restriction enzyme site from the NCBI sequence (Acc#X72340) was absent, and we identified a sequencing error that significantly affected the predicted extent of intermolecular base pairs. The sequence in this figure is the corrected sequence.

RNA–RNA interactions when compared to their intramolecular base-pairing potential and would presumably form more stable dimers or multimers than bicoid.

The most important aspect of this analysis is that it generated a molecular model that can be tested experimentally with some confidence in the likelihood that data would be generated that either support or negate the intermolecular base-pairing models in Figure 2.2. The general strategy for testing such a dimeric model *in vivo* is to make mutations that disrupt the base-pairing potential of the model dimer and then test whether such mutations reduce localization using a quantitative assay. It is important that such a mutation does not create strong alternative intra- or intermolecular structures because to generate convincing evidence in support of the model, a mutant that restores base pairing needs to be able to rescue localization. Therefore, when constructing such mutants it is essential to check the mutants using MFOLD or some other analogous program to insure that new stable structures are not created inadvertently that could prevent the rescuing mutations from forming the desired intermolecular base pairs. We tested the structure shown in Figure 2.2 using this strategy. The *Xenopus* oocyte system has been ideal for this because RNA localization assays can be extremely quantitative, detecting as little as a 10% change in localization efficiency. Mixtures of fluorescent mutant Xcat-2 LE RNAs and unlabeled compensatory or control RNAs can be made prior to injection. Our initial experiments show quite clearly that the double-stranded regions shown in Figure 2.2 are required for efficient localization *in vivo* (data not shown). Moreover, because of the way the experiments are done, unlabeled compensatory mutants rescue a labeled mutant RNA; the rescue has to be occurring in “*trans*”, demonstrating that the double-stranded regions of RNA shown in the model are indeed being formed by intermolecular RNA base pairs. Whether these intermolecular base pairs support the formation of dimers or multimers, however, will be difficult to determine experimentally, but the ratio of dimers to multimers may play a role in how localized RNAs ultimately become sorted and anchored to their final steady-state destinations

within a cell. These types of studies may begin to help us understand what the RNA substrates and binding sites are for the double-stranded RNA binding protein Staufen, which plays such a wide-ranging and ubiquitous role in mRNA trafficking, but for which no binding site required for cytoplasmic RNA localization has yet been identified in vertebrates. Consistent with this idea is that the Xcat-2 LE recruits endogenous Staufen when injected into early-staged oocytes (data not shown) as it also does Kinesin II (Betley et al. 2004).

When considering *cis*-elements and the role of small motifs that specify RNA localization, it is important to consider three general aspects of the motifs. First, there should be a statistical framework for understanding the likelihood of finding such motifs in randomized nt databases. This gives one a sense of the significance of the presence of such motifs. For example, when considering motifs such as the UUCAC motif first identified in the Vg1 LE, such a motif should be found by chance every 1024 nt (4^5) in random sequences. Therefore, every mRNA should have one to three of these motifs somewhere depending on its overall length. This is why we developed an algorithm for calculating the probabilities of every cluster of every repeated motif in a sequence called REPFIND (Betley et al. 2002) (<http://zlab.bu.edu/repfind/>). Using this program, we found that the predominant feature of most RNA sequences that localize to the vegetal cortex of *Xenopus* oocytes was a statistically significant clustering of short motifs that contain CAC, and that clusters of CAC motifs predicted precisely the regions of long 3'-UTRs that specify vegetal localization, such as the Xpat mRNA which has an approximately 3000-nt 3'-UTR (Figure 2.3); the Xpat LE has a region of its 3'-UTR with 10 UGCAC motifs in a approximately 550-nt region, whereas the rest of the 2.5 kb of this 3'-UTR has only two which would be expected by chance (Betley et al. 2002). Using such a statistical approach allows one to gain insights and develop conceptual frameworks for understanding these interesting noncoding elements before time-consuming mapping experiments are initiated, and incisive experiments can easily be designed to test the role of particular sequences that are over represented in RNA LEs.

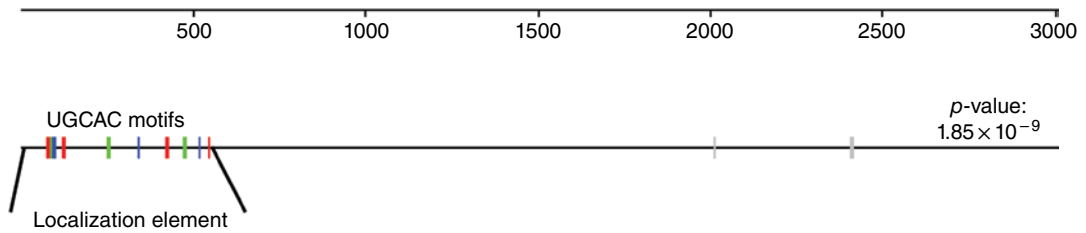


Figure 2.3 REPFIND output of the Xpat 3'-UTR. REPFIND was used to identify the most significant cluster of any repeat greater than 5 nt in length. The scale bar at the top represents the length of the 3'-UTR in nt. The colored bars represent UGCAC motifs (different colors are used to help visual counting only) considered in the calculated p -value shown at the right. The two grey bars to the right represent UGCAC motifs that were not included in the calculation. The p -value is the probability of finding this particular cluster. The first approximately 550-nt fragment localizes when injected into oocytes, whereas the remaining approximately 2.5-kb fragment does not (Betley et al. 2002). To see a color version of this figure, see Plate 5.

A second aspect of short motif clusters that should be considered is whether or not they have any predictive value. To be predictive however, one needs to be able to search entire genomes for sequence features that are unique to RNA LEs. For example, it is possible that CAC-motif clusters are common to other types of functional elements in genomes that have little to do with RNA localization. If this were the case, searching for genes that contain statistically significant CAC-motif clusters would frequently fail to identify RNA LEs unless additional screening criteria are superimposed on the predictive search being employed. A computational strategy has been developed that successfully identifies functional CAC-motif clusters across several mammalian species (Andken et al. 2007). In this approach, the REPFIND algorithm was used to generate a database of motif clusters and their respective p -values present in over approximately 60,000 vertebrate 3'-UTRs of the NIH Mammalian Gene Collection. This database was then searched for genes that have clusters of CAC motifs with p -values less than 10^{-4} . A statistical survey suggests that CAC-rich RNA LEs are present in about 10% of the genes in mammalian when compared to an analogous motif database that had its nt sequences randomized. When tested experimentally, four of these RNA sequences out of four tested localize to the vegetal pole of *Xenopus* (Andken et al. 2007). Two results are quite striking from this study and need to be emphasized. First, this is the only demonstration to our knowledge of

an *in silico* approach used to predict *a priori* functional RNA localization sequences from a genome-wide computational search of human 3'-UTRs. Second, these elements are functionally conserved in orthologous genes from species as distant as mouse and human even when alignment programs fail to detect any sequence homology in the orthologous 3'-UTR sequences; the rat and human Tub β 4 3' UTRs have no sequence homology using alignment algorithms, but both have conserved clusters of CAC-containing motifs and localize efficiently to the vegetal pole when injected into *Xenopus* oocytes. Previous work indicated that CAC-containing motifs are conserved and utilized for vegetal mRNA localization in ascidian eggs, suggesting that these elements arose early in the evolution of vertebrates (Betley et al. 2002). These more recent findings show that such elements have persisted in modern-day mammals including humans and play a major role in generating polarized distributions of proteins since they appear to be found in approximately 10% of the protein-coding genes. The continuation of these types of studies will lead to a better understanding of how the spatial cues for subcellular mRNA localization are distributed in genomes and across the phylogenetic tree.

Finally, when exploring the predictive value and the potential mechanistic role of small motifs implicated in RNA localization, it is critical to determine whether the motifs themselves are sufficient for localization. In fact, in at least one case, a short motif is sufficient for

localization in neurons (Huang et al. 2003). However, in the *Xenopus* system, it has become clear that most of the motifs are not sufficient for localization in isolation. This consideration of sufficiency has important implications for the mechanistic role played by the motifs, and as described earlier, it appears as though CAC-containing motifs may simply represent some sort of evolutionarily conserved building block or other type of signature for specifying higher-order RNA structures for interaction with double-stranded RNA binding factors, possibly Staufen. A similar analysis of other type of motifs has not yet been reported in the *Xenopus* system, but could possibly reveal new and important insights into the localization process.

Proteins, RNAs, and the endoplasmic reticulum

A number of proteins have been implicated in localizing RNAs to the vegetal pole of growing *Xenopus* oocytes, a few of which have already been mentioned. Many of these proteins were discovered through studies of the Vg1 mRNA which has been the most intensively investigated mRNA localized to the vegetal cortex. When considering these proteins, it is helpful to group them into one of three categories: (i) sequence-specific RNA binding proteins, (ii) RNP-associated proteins, and (iii) cytoskeletal proteins. Members of the first group contain putative RNA binding domains based on amino acid sequence analysis, and biochemical evidence or expression screening shows that they bind specifically to the Vg1 LE RNA sequence. UV cross-linking assays are commonly used in which a small piece of a radiolabeled LE RNA is transferred to the RNA binding protein upon exposure to UV light, demonstrating a direct binding event between the RNA the protein. In some cases, specific binding sites, such as the UUCAC motif that is bound by VgRBP/Vera described earlier, within the RNA LE have been identified. Another example is the VM1 motif (UUUCUA) thought to be involved in the localization of Vg1 and specifically bound by VgRBP60, an hnRNP-I-like protein (Cote et al. 1999).

Since RNA localization is likely to be a highly regulated cellular process that is exquisitely sensitive to the energy state of the cell (Heinrich and Deshler 2008), the specific binding of proteins to motifs *in vitro* suggests that such interactions may either promote or inhibit the localization process *in vivo*. In this regard, it is interesting to note that an excess of tandem UUCAC motifs injected into oocytes inhibits the localization of the Vg1 LE, whereas an excess of tandem UUUCUA (VM1) motifs stimulates localization, suggesting that these motifs titrate specific factors that promote or inhibit RNA localization, respectively, *in vivo* (Czaplinski and Mattaj 2006). However, such results need to be interpreted with caution since the tandem arrangement of the competing motifs in this experiment is much different than their natural interspersed configuration in the wild-type Vg1 LE sequence. As such, the tandem sequences may be creating novel structures that affect some other aspect of the cellular metabolism and possibly affect RNA localization indirectly in peculiar ways. Thus, additional approaches are required to determine if RNA binding proteins, such as Vera/Vg1RBP and VgRBP60, promote or negatively regulate the RNA localization process *in vivo*.

Elr-type proteins also bind specifically to several vegetal LEs presumably through their binding to AU-rich sequences, but deletion of these AU-rich *cis*-elements in one of the localized RNAs does not abolish localization (Claussen et al. 2011). Furthermore, overexpression of a wild-type Elr-type protein inhibits vegetal localization (Arthur et al. 2009). These findings suggest that Elr-type proteins are not likely to be involved in RNA localization *per se*, but possibly coordinate other aspects of regulation with the localization process. This scenario with the Elr-type proteins illustrates the potential difficulty in resolving the identity of core localization factors, whether regulatory or essential, from others that simply may coordinate localization with nuclear export, RNA stability, and/or translation.

Since genetic knockout experiments are not possible in *Xenopus*, other approaches are used to interfere with protein function for the purpose of eliciting roles for proteins in

the RNA localization process. However, these approaches do not work in some cases because maternal proteins are generally quite stable as oocytes grow and synthesize maternal factors during the 9–12 months required to build a healthy egg in the ovary. Consequently, techniques such as specific RNase H-dependent mRNA degradation directed by specific DNA oligonucleotides or inhibition of translation with morpholinos, which work well for functional studies during early embryogenesis, do little to reduce endogenous maternal proteins over the relatively short duration of a 1- or 2-day RNA localization experiment in oocytes. Therefore, investigators have relied on antibody inhibition studies and/or the expression of dominant-negative constructs to assess the role of RNA binding proteins *in vivo*. Of these, dominant-negative approaches are probably the best since specific antibodies directed to an RNA binding protein that negatively regulates RNA localization might actually inhibit, instead of activate, localization through steric or other biophysical artifacts that disrupt the localization process. To design a proper dominant-negative construct, careful consideration and experimentation need to be carried out to ensure that the dominant negative lacks critical activity needed by the endogenous protein but also interacts with the endogenous factor(s) in such a way as to block its function. Such an analysis has been done for the Vera/Vg1RBP protein, but has not yet been reported for VgRBP60. While no effect on localization was observed in the case of Vera/Vg1RBP, it is possible that the localization assays were not sufficiently quantitative to detect significant increases or decreases in the localization process since localization was assessed 4 days after injection (Rand and Yisraeli 2007). In this respect, it is important to ensure that one is in the linear range of their localization assay with respect to incubation times after RNA injection. Depending on the RNA, we and others have found that by 8–24 h after RNA injection, localization while not yet complete has proceeded sufficiently to quantify the degree of interference or enhancement (Yoon and Mowry 2004; Heinrich and Deshler 2008), but is not yet complete.

Prp is another RNA binding protein that binds directly and specifically to the Vg1 LE.

It was identified through screening an expression library with a radioactive Vg1 LE probe, but its precise binding sites within the Vg1 LE have not yet been identified nor has a functional analysis of this protein been performed in oocytes. The fact that it also interacts with components of the actin cytoskeleton suggests that it may be involved in anchoring vegetal RNAs at the cortex (Zhao et al. 2001). Likewise, a functional requirement for VgRBP60 has not been reported even though it binds the VM1 motif *in vitro* and associates with the Vg1 RNA *in vivo* (Kress et al. 2004).

The second class of proteins implicated in RNA localization to the vegetal cortex of *Xenopus* oocytes is that which consists of the Vg1 RNP-associated proteins. These are proteins that associate specifically with Vg1 RNP complexes, but do not bind specifically to the Vg1 RNA LE. 40LoVe is an example of this. It was identified originally using RNA affinity columns with Vg1 LE RNA as a substrate and shown to associate specifically with the Vg1 LE, but not other nonspecific RNA sequences. While 40LoVe does have the capability to bind RNA directly, it does so with little, if any, sequence specificity (Kroll et al. 2009). Instead, it binds specifically and directly to the sequence-specific RNA binding proteins VgRBP60 and Prp. Through these interactions, it also associates with Vg1RBP (Czaplinski and Mattaj 2006), but this interaction is sensitive to RNase treatment, indicating the association is indirect and requires RNA in the RNP complex. Finally, a role for 40LoVe in the localization process has been supported since 40LoVe-specific antibodies interfere with the localization of the Vg1 LE. However, since antibody inhibition experiments are subject to the caveats mentioned earlier, it is not absolutely clear whether 40LoVe stimulates or inhibits the localization of Vg1 under normal circumstances. Another example of an RNP-associated protein is *Xenopus* Staufen, or XStau. Staufen was cloned based on searches for *Xenopus* genes showing sequence homology to *Drosophila* Staufen (Allison et al. 2004; Yoon and Mowry 2004). By expressing a well-designed dominant-negative version of XStau to a concentration similar to that of endogenous XStau, localization of the Vg1 LE

was reduced by 75% under the conditions tested when compared to expressing the full-length wild-type form of XStau (Yoon and Mowry 2004). Since Staufen binds double-stranded RNA with little, if any, sequence specificity in isolation (St Johnston et al. 1992), it was proposed that Staufen, in combination with other sequence-specific RNA binding proteins, forms RNPs that are competent to localize and contain molecular motors (Yoon and Mowry 2004) required for their localization (see the following texts).

The third and final class of proteins to be considered for RNA localization is comprised of cytoskeleton components; this includes molecular motors and the cytoskeletal filaments themselves. The first evidence to suggest that the cytoskeleton was involved in the localization of Vg1 to the vegetal cortex utilized distinct drugs that specifically depolymerize either microtubules or actin filaments. This study suggested that microtubules are required to generate the polarized distribution of Vg1 in the vegetal hemisphere, while actin microfilaments are required for anchoring the Vg1 RNA to the vegetal cortex (Yisraeli et al. 1989). Biochemical studies suggested a role for intermediate filaments in anchoring the RNA at the cortex (Pondel and King 1988), but functional studies have not supported this (Klymkowsky et al. 1991). This early work in the field suggested that molecular motors that utilize microtubules are likely to play a major role in generating the polarized distribution of the Vg1 LE and transporting it to the vegetal cortex. More recently, a combination of antibody inhibition and dominant-negative approaches has implicated Kinesin II (Betley et al. 2004; Messitt et al. 2008), Kinesin I (Messitt et al. 2008), and Dynein (Gagnon et al. 2013) to be required for efficient RNA localization to the vegetal cortex of stage III using either Vg1 (Betley et al. 2004; Messitt et al. 2008; Gagnon et al. 2013) or Xcat-2 LEs (Betley et al. 2004) as reporter RNAs for localization. Interestingly, immunoprecipitation experiments show that Kinesin I and Kinesin II are associated in common RNP complexes containing Vg1, but not a nonspecific RNA, but this association is RNA-dependent as RNase treatment eliminates their coimmunoprecipitation. In addition, each

can rescue the specific inhibition of the other, indicating some overlapping redundancy in their function (Messitt et al. 2008). Together, these data have shown that microtubule-based motors indeed play a role in transporting RNAs to the vegetal cortex of growing stage III/IV oocytes, as was predicted.

In addition to the proteins previously described that form RNPs containing molecular motors responsible for transporting RNAs to the vegetal cortex, there have been two clear cases where the depletion of specific endogenous RNAs has also disrupted the localization of Vg1 to the vegetal cortex. The first case involved the depletion of Xlsirt RNAs which are localized prior to Vg1 mRNA. Xsirts are noncoding repetitive RNAs that utilize the early pathway. They are localized similarly to Xcat-2 (Figure 2.1), localizing first to the mitochondrial cloud of stage I oocytes prior to their gradual localization to the vegetal cortex in stage II oocytes (Kloc et al. 1993). In *Xenopus* oocytes, it is possible to cleave endogenous RNAs specifically with antisense DNA oligonucleotides; upon the DNA hybridizing to the target RNA, the resulting RNA-DNA duplexes are targeted as substrates for endogenous RNase H activity which cleaves the RNA leading to its degradation. Using this strategy, it was shown that depleting Xsirt RNAs in stage IV oocytes led to a release of Vg1 from the vegetal cortex, suggesting that Xsirts are involved in anchoring Vg1 at the vegetal cortex. Whether or not Xsirts are required for localization of the Vg1 LE to the cortex of stage III oocytes has not been reported and is not currently known. Likewise, similar experiments have shown that degradation of the VegT mRNA, but not reduction of the VegT protein, leads to the release of several RNAs from the vegetal cortex, including Vg1 (Heasman et al. 2001). We do not know how many RNAs have been tested in this fashion, but because this is a relatively small field, with just a handful of labs working on it, it is likely that these two RNAs are the only that have been tested in this way. If so, it would be interesting to determine whether the degradation of other localized RNAs has similar effects on the anchoring and/or the transport phase of other localized RNAs as well.

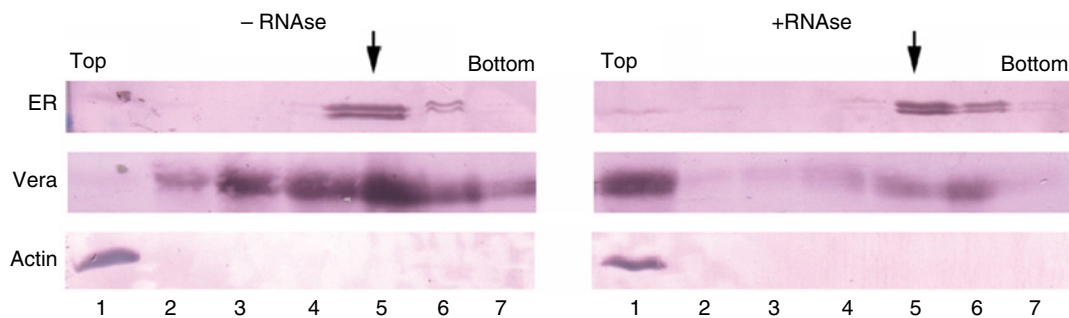


Figure 2.4 The association of Vera/Vg1RBP with the ER depends upon RNA. Concentrated cytoplasmic extracts were prepared from stage IV to VI oocytes and subjected to sucrose density gradient centrifugation as previously described (Deshler et al. 1997). Fractions were collected and analyzed by Western blotting using antibodies to TRAP α and actin to identify fractions that contain the ER and soluble proteins, respectively. An anti-Vera antibody shows that Vera cofractionates with ER membranes (left panel). The same experiment was repeated, but the extracts were first diluted about twofold with buffer and treated with RNase. As can be seen, Vera is released from the ER and sediments with soluble proteins. This indicates that Vera is associated with ER membranes through its association with RNAs and RNP particles in the undiluted extracts.

The endoplasmic reticulum (ER) has been implicated in the localization of mRNAs in plants (Choi et al. 2000), animals (Cohen 2005), and fungi (Schmid et al. 2006; Aronov et al. 2007). In *Xenopus* oocytes, the ER is a single and very large interconnected organelle that extends through all regions of the cytoplasm. The initial discovery that the ER is involved in mRNA localization again came through studies of the Vg1 mRNA somewhat serendipitously. Subcellular fractionation was being used to identify proteins that are cross-linked specifically to the Vg1 LE but also are associated with large particles in the hope of isolating and characterizing components of such particles. Since it was possible that such complexes might be sensitive to dilution levels routinely used to make cell extracts, a different approach was employed first to make undiluted cytoplasmic extracts. This is only possible in the *Xenopus* system and was originally developed to analyze mitosis in a cell-free system (Murray 1991). In this procedure, late-stage oocytes or eggs are crushed by centrifugation under conditions such that the undiluted cytoplasm collects in a single layer of a centrifuge tube and can be isolated with a syringe via side puncturing the tube. When the undiluted extracts were subjected to ultracentrifugation, it was found that Vera/Vg1RBP copurified with ER membranes either under flotation or sedimentation conditions; Vera stands for Vg1LE binding, ER-associated protein. If ext-

racts are diluted prior to sedimentation, Vera dissociates from the ER. Further experiments showed that both early-pathway RNAs (Kloc and Etkin 1998; Chang et al. 2004) and Vg1 itself (Deshler et al. 1997) colocalize to ER membranes in early- and later-stage oocytes, respectively, indicating that the ER is associated with all phases of RNA localization to the vegetal cortex of growing oocytes. Interestingly, when *Xenopus* oocytes extracts are minimally diluted such that Vera remains associated with ER membranes and then treated with RNase, Vera is released to soluble fractions (Figure 2.4). This establishes quite clearly that the interaction between Vera and ER membranes is not only sensitive to dilution, but is also indirect, occurring through its association with and binding to RNAs that must be targeted to the ER by some other mechanism. This mechanism may be distinct from the SRP and translation-dependent mechanism because RNA LEs associate with the ER and are noncoding RNA sequences that are not translated. In addition, others have accumulated evidence suggesting that an SRP-independent mechanism exists for targeting distinct sets of RNA to the ER (Pyhtila et al. 2008; Cui et al. 2012). From a biological perspective, it would be essential to have the ER associated with localized mRNAs in an SRP-independent fashion since many of them such as Vg1 encode secreted proteins, but are not translated until after localization occurs. Regardless of the mechanism, the role

the ER plays in the localization process, or vice versa, remains obscure.

Mechanism(s) for RNA localization to the vegetal cortex

Considerations

Early work showing two general classes of localized mRNAs at the vegetal cortex led investigators to propose that two distinct mechanisms existed for targeting RNAs to the vegetal cortex (Forristall et al. 1995; Kloc and Etkin 1995). Early-pathway RNAs (e.g., Xcat-2, Xlsirts, and Xwnt-11) were postulated to localize via a diffusion-entrapment mechanism in stage I oocytes. Since drugs that depolymerized microtubules disrupted Vg1 localization, but not the early-pathway RNAs, it was postulated that late-pathway RNAs utilize a microtubule-based motor system for localization during the late pathway in stage III/IV oocytes (Yisraeli and Melton 1988). Soon after the two pathways were proposed, features of the localization process were discovered that suggested they shared common elements. For example, localization of the Vg1 LE to the wedge-shaped structure of stage II oocytes was resistant to drugs that depolymerize microtubules, just as the early-pathway RNA localization process was in stage I oocytes (Kloc and Etkin 1998). In addition, all early-pathway RNAs localize efficiently during the late, Vg1 pathway. Moreover, the localization sequences for the two pathways turned out to have similar characteristics as previously described. Thus, it was beginning to become clear that a common set of factors participate in the localization of mRNAs to the mitochondrial cloud of stage I oocyte, the wedge and cortex of stage II oocytes, and the vegetal cortex of stage III oocytes.

Evidence showing that early- and late-pathway RNAs interact with common sequence-specific RNA binding proteins, RNP-associated proteins, and molecular motors has continued to grow in recent years. For example, purified Vera/Vg1RBP binds specifically to all four early-pathway RNA LEs tested with affinity similar to that for the Vg1 LE (Choo et al. 2005). In addition, Kinesin II which is required for

localization of the Vg1 or Xcat-2 LE during the late pathway (Betley et al. 2004) is also required for efficient localization of the Xcat-2 LE to the mitochondrial cloud of stage I oocytes (Heinrich and Deshler 2008). These and other data, including the fact that early- and late-pathway RNAs compete for common localization factors *in vivo* (Choo et al. 2005) and that the ER is involved in the early (Chang et al. 2004) as well as the late pathway (Deshler et al. 1997; Kloc and Etkin 1998), began to indicate that the early and late pathways have more in common with each other than originally believed.

Characterization of early-pathway RNAs revealed that a continuum exists along the animal-vegetal axis of stage I/II oocytes upon which different localized RNAs adopt distinct positions relative to each other. Double labeling *in situ* hybridization experiments showed clearly that Xcat-2, Xlsirt, and Xwnt-11 adopt three distinct positions along the animal-vegetal axis with little overlap between them; Xcat-2 is localized to the cortex first, followed by Xlsirt and then Xwnt-11 (Kloc and Etkin 1995). This sort of organization is consistent with a single, but regulated, mechanism for organizing RNAs along the vegetal axis in stage I/II and possibly later-staged oocytes. The question then becomes, how do these RNAs “know” where they are relative to each other in the growing oocyte?

The existence of a single, but regulated, mechanism for organizing mRNAs along a single axis of polarity is more compatible with the fact that RNA localization is much more common than it was originally thought to be in the field. A systematic *in situ* hybridization analysis in *Drosophila* showed that roughly 70% of mRNAs show some type of polarized distribution in early *Drosophila* embryos (Lecuyer et al. 2007) that mimics their protein expression patterns. In *Xenopus* and other vertebrates, a computational-experimental analysis of CAC-rich RNA LEs indicates that they reside in approximately 10% of protein-coding genes and that these elements function in neurons as well as oocytes (Andken et al. 2007). Thus, it now would be expected that a set of core localization factors, as well as gene-specific regulatory factors, exist for the RNA localization process as they do for transcription, splicing, mRNA decay, and translation.

The primary evidence in support of two mechanisms instead of one primary mechanism for RNA localization in stage I/II and stage III/IV *Xenopus* oocytes is based on the effects of drugs that depolymerize microtubules; these drugs do not disrupt localization in stage I/II oocytes (Kloc and Etkin 1995; Chang et al. 2004), whereas they have been reported to disrupt the localization of Vg1 mRNA in stage III/IV oocytes (Yisraeli et al. 1990). These findings contradict the fact that disrupting Kinesin II in stage I oocytes (Heinrich and Deshler 2008) or Dynein in stage II oocytes (Gagnon et al. 2013) impairs localization and transport dynamics of localizing RNAs, respectively. Moreover, early-pathway RNAs recruit and enrich Kinesin II to the mitochondrial cloud when injected into stage I oocytes (Heinrich and Deshler 2008). These paradoxical findings that microtubules do not play a role in stage I/II oocytes, but microtubule motors do, are difficult to explain. Heinrich and Deshler (2008) have argued that even though these drugs disrupt long microtubules, there remains an abundance of very short microtubules that might be sufficient to support the motor-dependent transport dynamics required for proper RNA localization. Another possibility is that Kinesin II and Dynein have roles in RNA localization that are independent of microtubules. This seems unlikely given that such roles are not generally known for these molecular motors. Therefore, when considering a hypothetical mechanism for RNA localization, we will assume that microtubules are involved in localizing RNAs in stage I/II as well as stage III/IV oocytes.

Assumptions

In order to conceptualize how RNA localization occurs, it will be assumed that the presumably hundreds to thousands of RNAs that are localized to the vegetal cortex share a common motor- and microtubule-dependent mechanism for their localization along the animal-vegetal axis throughout the first four stages of oogenesis. In this scenario, the precise RNA sequence of each RNA LE determines where it accumulates along the animal-vegetal axis through its association with core RNA

localization factors and the combined effects of its differential interactions with factors that positively or negatively regulate the localization process. The question then becomes, how exactly does this RNA localization process take place?

The process

As pre-mRNAs are transcribed in the nucleus, hnRNP proteins, splicing factors, polyadenylation factors, and nuclear export factors associate with the mRNA as it is being synthesized. Introns are spliced out at this time. The composition of each mRNA-protein complex determines how fast it will be exported from the nucleus, where it will go in the cytoplasm, and when it will be translated. The composition of such mRNPs is dynamic and regulated extensively by RNA helicases, such as DDX5/p68 (Zonta et al. 2013), which promotes extensive remodeling of the mRNP complexes throughout their lifetime in the nucleus and the cytoplasm. The RNA LEs that specify localization to the vegetal cortex of *Xenopus* oocytes are part of the mRNP complexes that are set up in the nucleus and ultimately specify where in the cytoplasm the mRNA will be transported and translated. In fact, a biochemical analysis of RNP complexes that form on the Vg1 LE shows that this RNP undergoes extensive remodeling as it transitions from the nucleus to the cytoplasm such that Vera/Vg1RBP and hnRNP I associate with it in the nucleus and cytoplasm, whereas Prpp and Staufien only become associated with the RNP complex when it reaches the cytoplasm (Kress et al. 2004) (Figure 2.5). While it is likely that RNA helicases also participate in the remodeling of RNPs involved in RNA localization, no specific RNA helicases have yet been identified for this process.

Once in the cytoplasm, Staufien, Prpp, and molecular motors associate with the RNPs and drive their localization to the mitochondrial cloud and vegetal cortex (Figure 2.5). One of the most exciting papers to be published in this field recently has revealed, through live imaging of RNA movement in stage II oocytes, that movement of the RNA in

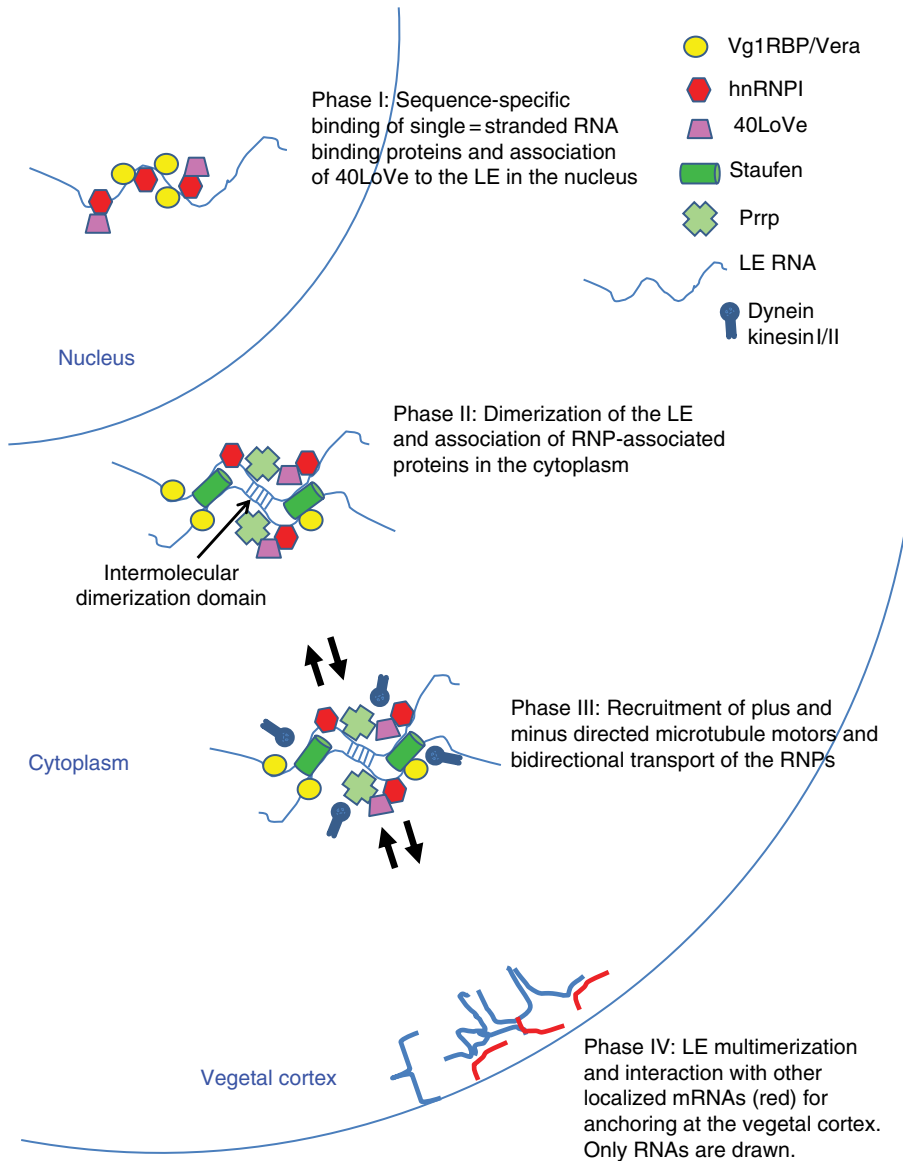


Figure 2.5 Four hypothetical phases to RNA localization in *Xenopus* oocytes. Features of the *cis*-elements that specify vegetal localization and the proteins involved in the localization process are described in the text. In this figure, sequence-specific RNA binding proteins and RNP-associated proteins, including the double-stranded RNA binding protein Staufen, are depicted as the indicated symbols at the upper right of the figure. A generic RNA LE that directs a particular mRNA to the vegetal cortex is shown as a squiggly line. During the first phase, the RNA is mostly single-stranded in the nucleus. Phases II and II occur throughout the cytoplasm, while the fourth phase, anchoring, occurs in the mitochondrial cloud of stage I oocytes (not depicted) or the vegetal cortex of stage II–IV oocytes. To see a color version of this figure, see Plate 6.

the vegetal region is bidirectional (Gagnon et al. 2013). These experiments involve photo-activation of RNA at a single point or column in the oocyte and then quantitating how much of the RNA moves back toward the nucleus

and how much toward the vegetal cortex. While movement of the RNA is clearly bidirectional, a 64% to 36% bias toward the vegetal cortex was detected in the cytoplasm in a region about half way between the nucleus

and the vegetal cortex. Interestingly, however, when the same experiment was performed closer to the vegetal cortex, directional bias was not detected and the RNA moved equally in both directions. These results were consistent with the fact that microtubules have mixed polarity in the vegetal region (Messitt et al. 2008) and provide for the first time a real-time view into the localization process. Measuring the bulk flow of RNA movement after photoactivation of a small fraction of injected RNA, it was determined that the net movement of Vg1 LE toward the vegetal cortex occurs at a rate of approximately $0.3 \mu\text{m/s}$. Since a low percentage of the RNA (3–5%) was determined to move at any given time, the time it takes for all of the RNA to become localized is relatively longer.

From the considerable work that has been carried out in the vegetal localization pathway, four major phases to the localization process will be described in a scenario to account conceptually for their movement toward the cortex, their sorting relative to each other along the animal–vegetal cortex, and their anchoring at the mitochondrial cloud or vegetal cortex (Figure 2.5). This is a working model based on the current knowledge summarized earlier. Much work will be required to validate, adjust, revise, and/or negate many aspects of it.

The first of the four phases of the localization process involves the binding of sequence-specific RNA binding proteins, such as Vera/Vg1RBP and hnRNP I (Kress et al. 2004), to single-stranded RNA binding sites or motifs in the LE shortly after it is transcribed in the nucleus (Figure 2.5). During this phase, the concentration and affinity of these factors may help determine the stage at which the RNA becomes localized by regulating when and how many molecular motors can gain access to the RNA once it is exported to the cytoplasm. Such a scenario could explain why the Vg1 LE localizes to the mitochondrial cloud when injected into the cytoplasm of stage I oocytes (Choo et al. 2005) as it may bypass much of phase I, whereas endogenous Vg1 undergoes phase I normally recruiting a high concentration of the sequence-specific RNA binding proteins and does not localize to the mitochondrial cloud. 40LoVe associates with

the RNP at this step through its direct interaction with hnRNP I (Kroll et al. 2009).

During the second phase of the localization of an LE RNP (Figure 2.5), the LE undergoes a conformational change in which it forms extensive intermolecular base pairs that support the binding of Staufén. Prpp also associates with the RNP at this stage (Kress et al. 2004). The amount of double-stranded RNA that forms may control the amount of Staufén that binds, or vice versa, leading to the recruitment of molecular motors that mediate the localization process in the third phase of the localization; Staufén is well known to be intimately associated with molecular motors involved in RNA transport in a number of systems (Kanai et al. 2004). It is during this second phase that distinct concentrations of plus end- and minus end-directed motors associate with the RNP to establish distinct localization rates for each distinct type of LE RNP. One possibility is that a high concentration of Vera/Vg1RBP and/or hnRNP I relative to Staufén could set up for relatively slow localization, whereas low Vg1RBP and high Staufén could lead to high localization rates. The evidence supporting this is that Staufén is required for localization, whereas Vera/Vg1RBP and or hnRNP I might serve as negative regulators of localization as described earlier. In a way, it could be that the sequence-specific RNA binding proteins are the dampers and the double-stranded nonspecific RNA binding protein Staufén is the throttle of the localization process in an analogous way that Rab proteins and Sec1 proteins act as the throttles and the dampers, respectively, for vesicle fusion with the plasma membrane (Rothman and Sollner 1997).

The third phase of the localization process (Figure 2.5) may be the most important when considering a continuum through which hundreds or thousands of distinct localized RNAs orient themselves along the animal–vegetal axis of growing oocytes relative to each other. What is most interesting is that in the one case where it has been examined, the movement of the Vg1 RNP is bidirectional with little, if any, bias of movement toward the vegetal cortex near the cortex (Gagnon et al. 2013). This suggests that biased movement may not be necessary for proper localization to occur. Imagine that each mRNA is forming dimers

with itself and multimers with itself and also continuously exploring its local environment with respect to other mRNAs, in order to adopt its correct position along the animal–vegetal axis. From two different studies, we know that the Vg1 LE interacts with at least two different RNAs, Xlsirt and VegT mRNA, either directly or indirectly and that this interaction is critical for its localization at the cortex (Kloc and Etkin 1994; Heasman et al. 2001). Thus, given that RNA helicases are omnipresent in cells and likely give each RNA the ability to explore which other RNAs are in its immediate surroundings, one could imagine that this exploration proceeds primarily in the dimeric configuration during phase II of localization until each RNA finds a position along the gradient such that its own local dimer concentration begins to increase relative to other RNAs at that position. This exploratory process would require high helicase activity and high levels of endogenous ATP, which is known to be essential and limiting for the localization process in oocytes (Heinrich and Deshler 2008).

The fourth phase involves the final sorting and “anchoring” of the LE RNP to its final destination in the oocyte (Figure 2.5). For Xcat-2, this happens in the mitochondrial cloud of stage I oocytes and Fluorescent Recovery After Photobleaching (FRAP) experiments show that indeed, the Xcat-2 LE required an extremely much longer time to recover its position in the mitochondrial cloud after photobleaching than it does in the cytoplasm (Chang et al. 2004). An important aspect of LEs that function in oocytes that has been noted previously is that the RNA sequences in the LEs that specify localization must be the same that specify anchoring since exhaustive mutational analyses have failed to identify specific motifs that disrupt anchoring but allow transport to occur normally. This combined with the fact that at least the Xcat-2 LE has the ability to form dimers/multimers that promote localization suggest that these same structures also mediate the anchoring process. So, during phase IV, it is proposed that the RNA dimers begin to concentrate at their final destination along the animal–vegetal axis. For Xcat-2, this would be the mitochondrial cloud of stage I oocytes or the vegetal cortex at the vegetal pole of later-stage oocytes. At these positions, the

local concentration of dimers would continue to increase, driving the formation of larger and larger multimers of the Xcat-2 LE sequence. As the structures grow, their size and mass would increase relative to the dimeric structures, and therefore, they would be much less motile than the dimer. Again, this would require helicase activity for remodeling of the RNP complexes in these locations. This model for anchoring is quite speculative, but given the lack of experimental evidence for any other mechanism for anchoring, it is plausible.

These four phases of the localization process are provided as a working model, for which many of the aspects can be tested in the future. Some aspects will be difficult or impossible to test with current technologies. For example, there is no way at the current time to distinguish between dimeric and multimeric RNA structures that might drive localization and anchoring, respectively, as proposed in phase III and phase IV. However, as imaging and other technologies continue to improve at their currently fast rate, such methods may become available sooner than one might expect. Likewise, the precise role for distinct molecular motors may be quite difficult to determine experimentally. Current results with only three molecular motors suggest that there may be overlapping and partially redundant functions in the RNA localization process (Messitt et al. 2008; Gagnon et al. 2013) as there are in mitosis where a systematic analysis of the 25 Kinesins and Dynein shows functional redundancy and alternative pathways are required for that process (Goshima and Vale 2003). Hopefully, the next 10 years will be as informative as the last decade and will continue to surprise us with unexpected insights into this mechanism that provides so much of the phenotypic diversity around us by generating hundreds to thousands of protein gradients that work together inside of cells, helping each type carry out its unique and specialized function.

Looking toward the future

One of the most unexpected findings in this field in the last decade is that hundreds to thousands of mRNA are predicted to contain

RNA localization signals that coordinate their relative concentrations along the animal–vegetal axis. This organization along a single axis in the egg poises the egg to undergo a cortical rotation upon fertilization that sets up both the anterior–posterior and dorsal–ventral axes of the tadpole prior to the first cell division of the embryo. To establish such a high degree of organization in the egg, each RNA molecule, through the formation of specialized RNPs, coordinates multiple microtubule motors so that the concentration of each mRNA is precisely determined across the oocyte. This organization of a large population of mRNAs along the animal–vegetal axis, combined with coordinated translational control, sets up the myriad of protein gradients that ultimately define the gene expression networks and patterns of cellular differentiation that drive the development of the embryo. The existence of new technologies and more quantitative assays, combined with a larger repertoire of localized RNAs, makes this an exciting time for the field, and more surprises are likely to come soon.

Some of the more interesting findings and implications from the *Xenopus* oocyte system are likely to have profound effects in the field of Neurobiology as well as Developmental Biology. This is because many of the core RNA localization factors that have been described in this chapter are conserved in neurons and, possibly more importantly, the *cis*-acting RNA localization signals that function in the *Xenopus* oocyte system also function in mammalian neurons (Andken et al. 2007). Thus, lessons learned in the *Xenopus* oocyte system are likely to provide major insights into how the nervous system forms during development and functions at the molecular and cellular level in adults. For example, recent work has identified over 5000 transcripts that are associated with *Aplysia* synapses, and this set of transcripts is referred to as the “synaptic transcriptome” (Puthanveetil et al. 2013). It will be interesting to apply the computational, biochemical, and molecular genetic approaches developed in the *Xenopus* system to determine how many of the 5000 transcripts might be using a pathway similar to the animal–vegetal pathway in *Xenopus* oocytes.

Two general points have emerged from work in *Drosophila* and also hold true in other

model systems. First, absolute quantitation of the degree of “polarity” or mRNA “localization” using imaging alone can be difficult since the tight localization of just a small percentage of a distinct transcript can appear highly polarized to the naked eye. An example is the *nanos* mRNA, which “looks” highly localized. However, only 4% of the *nanos* mRNA is localized to the posterior pole of the *Drosophila* oocyte; the other 96% is found diffused throughout the cytoplasm. Yet, because only the 4% that is localized is translated into NANOS protein, a gradient is established that is both necessary and sufficient to initiate the gene expression patterns that specify half of the embryo. Thus, quantitative approaches will need to be developed to model the mechanisms that establish RNA polarity as well as the gene expression patterns that provide the basis for development, neuronal, and other cell type-specific functions.

The scientific community and governments have invested huge amounts of resources, generating thousands of genome sequences all around the world. The amount of genomic data that is now available to individual investigators is astounding and will continue to grow. Undoubtedly, gene prediction algorithms will improve, and we will have a fairly complete understanding of where the protein-coding genes are in the genome and in what tissues they are expressed. However, the question of how their expression is controlled at the subcellular level will require advanced algorithm development that relies little on sequence alignments, but instead focuses on sequence composition and the potential to form higher-order RNA structures. The RNA localization field has only scratched the surface of such approaches to date, and establishing a fundamental understanding of the genetic information that encodes spatial information in the genome will require major efforts in this area. The *Xenopus* oocyte system will be ideal for continuing to predict, validate, and explore the genetic information that specifies where proteins are made in cells. This is fundamental to all of biology and key to understanding how genotypes lead to complex phenotypes. In a sense, the genetic information that specifies where proteins are made in cells can be thought of

being analogous to a global positioning system (“GPS”) of the cell. Understanding this type of information in the genome, in the long run, is also likely to help us understand how species with similar genomes show large amounts of phenotypic diversity.

References

- Agius, E., Oelgeschlager, M., Wessely, O., Kemp, C., and De Robertis, E. M. (2000). Endodermal nodal-related signals and mesoderm induction in *Xenopus*. *Development* 127, 1173–1183.
- Allen, L., Kloc, M., and Etkin, L. D. (2003). Identification and characterization of the Xlsirt cis-acting RNA localization element. *Differentiation* 71, 311–321.
- Allison, R., Czaplinski, K., Git, A., et al. (2004). Two distinct Staufen isoforms in *Xenopus* are vegetally localized during oogenesis. *RNA* 10, 1751–1763.
- Andken, B. B., Lim, I., Benson, G., et al. (2007). 3'-UTR SIRF: a database for identifying clusters of short interspersed repeats in 3' untranslated regions. *BMC Bioinf* 8, 274.
- Aronov, S., Gelin-Licht, R., Zipor, G., Haim, L., Safran, E., and Gerst, J. E. (2007). mRNAs encoding polarity and exocytosis factors are cotransported with the cortical endoplasmic reticulum to the incipient bud in *Saccharomyces cerevisiae*. *Mol Cell Biol* 27, 3441–3455.
- Arthur, P. K., Claussen, M., Koch, S., Tarbashevich, K., Jahn, O., and Pieler, T. (2009). Participation of *Xenopus* Elr-type proteins in vegetal mRNA localization during oogenesis. *J Biol Chem* 284, 19982–19992.
- Becalska, A. N. and Gavis, E. R. (2009). Lighting up mRNA localization in *Drosophila* oogenesis. *Development* 136, 2493–2503.
- Betley, J. N., Frith, M. C., Graber, J. H., Choo, S., and Deshler, J. O. (2002). A ubiquitous and conserved signal for RNA localization in chordates. *Curr Biol* 12, 1756–1761.
- Betley, J. N., Heinrich, B., Vernos, I., Sartet, C., Prodon, F., and Deshler, J. O. (2004). Kinesin II mediates Vg1 mRNA transport in *Xenopus* oocytes. *Curr Biol* 14, 219–224.
- Bubunenko, M., Kress, T. L., Vempati, U. D., Mowry, K. L., and King, M. L. (2002). A consensus RNA signal that directs germ layer determinants to the vegetal cortex of *Xenopus* oocytes. *Dev Biol* 248, 82–92.
- Chang, P., Torres, J., Lewis, R. A., Mowry, K. L., Houlston, E., and King, M. L. (2004). Localization of RNAs to the mitochondrial cloud in *Xenopus* oocytes through entrapment and association with endoplasmic reticulum. *Mol Biol Cell* 15, 4669–4681.
- Choi, S. B., Wang, C., Muench, D. G., et al. (2000). Messenger RNA targeting of rice seed storage proteins to specific ER subdomains. *Nature* 407, 765–767.
- Choo, S., Heinrich, B., Betley, J. N., Chen, Z., and Deshler, J. O. (2005). Evidence for common machinery utilized by the early and late RNA localization pathways in *Xenopus* oocytes. *Dev Biol* 278, 103–117.
- Claussen, M., Tarbashevich, K., and Pieler, T. (2011). Functional dissection of the RNA signal sequence responsible for vegetal localization of XGrip2.1 mRNA in *Xenopus* oocytes. *RNA Biol* 8, 873–882.
- Cohen, R. S. (2005). The role of membranes and membrane trafficking in RNA localization. *Biol Cell* 97, 5–18.
- Cote, C. A., Gautreau, D., Denegre, J. M., Kress, T. L., Terry, N. A., and Mowry, K. L. (1999). A *Xenopus* protein related to hnRNP I has a role in cytoplasmic RNA localization. *Mol Cell* 4, 431–437.
- Cui, X. A., Zhang, H., and Palazzo, A. F. (2012). p180 promotes the ribosome-independent localization of a subset of mRNA to the endoplasmic reticulum. *PLoS Biol* 10, e1001336.
- Czaplinski, K. and Mattaj, I. W. (2006). 40LoVe interacts with Vg1RBP/Vera and hnRNP I in binding the Vg1-localization element. *RNA* 12, 213–222.
- Deshler, J. O., Highett, M. I., and Schnapp, B. J. (1997). Localization of *Xenopus* Vg1 mRNA by Vera protein and the endoplasmic reticulum [see comments]. *Science* 276, 1128–1131.
- Deshler, J. O., Highett, M. I., Abramson, A., and Schnapp, B. J. (1998). A highly conserved RNA-binding protein for cytoplasmic mRNA localization in vertebrates. *Curr Biol* 8, 489–496.
- Dumont, J. N. (1972). Oogenesis in *Xenopus laevis* (Daudin). I. Stages of oocyte development in laboratory maintained animals. *J Morphol* 136, 153–179.
- Eguchi, Y. and Tomizawa, J. (1991). Complexes formed by complementary RNA stem-loops. Their formations, structures and interaction with Cole1 Rom protein. *J Mol Biol* 220, 831–842.
- Eguchi, Y., Itoh, T., and Tomizawa, J. (1991). Antisense RNA. *Annu Rev Biochem* 60, 631–652.
- Ferrandon, D., Koch, I., Westhof, E., and Nusslein-Volhard, C. (1997). RNA-RNA interaction is required for the formation of specific bicoid mRNA 3' UTR-STAUEN ribonucleoprotein particles. *EMBO J* 16, 1751–1758.
- Forristall, C., Pondel, M., Chen, L., and King, M. L. (1995). Patterns of localization and cytoskeletal association of two vegetally localized RNAs, Vg1 and Xcat-2. *Development* 121, 201–208.

- Gagnon, J. A., Kreiling, J. A., Powrie, E. A., Wood, T. R., and Mowry, K. L. (2013). Directional transport is mediated by a Dynein-dependent step in an RNA localization pathway. *PLoS Biol* 11, e1001551.
- Gautreau, D., Cote, C. A., and Mowry, K. L. (1997). Two copies of a subelement from the Vg1 RNA localization sequence are sufficient to direct vegetal localization in *Xenopus* oocytes. *Development* 124, 5013–5020.
- Gavis, E. R. and Lehmann, R. (1992). Localization of nanos RNA controls embryonic polarity. *Cell* 71, 301–313.
- Gerhart, E., Wagner, H., and Brantl, S. (1998). Kissing and RNA stability in antisense control of plasmid replication. *Trends Biochem Sci* 23, 451–454.
- Goshima, G. and Vale, R. D. (2003). The roles of microtubule-based motor proteins in mitosis: comprehensive RNAi analysis in the *Drosophila* S2 cell line. *J Cell Biol* 162, 1003–1016.
- Heasman, J., Wessely, O., Langland, R., Craig, E. J., and Kessler, D. S. (2001). Vegetal localization of maternal mRNAs is disrupted by VegT depletion. *Dev Biol* 240, 377–386.
- Heinrich, B. and Deshler, J. O. (2008). RNA localization to the Balbiani body in *Xenopus* oocytes is regulated by the energy state of the cell and facilitated by kinesin II. *RNA* 15, 524–536.
- Huang, Y. S., Carson, J. H., Barbarese, E., and Richter, J. D. (2003). Facilitation of dendritic mRNA transport by CPEB. *Genes Dev* 17, 638–653.
- Hudson, C. and Woodland, H. R. (1998). Xpat, a gene expressed specifically in germ plasm and primordial germ cells of *Xenopus laevis*. *Mech Dev* 73, 159–168.
- Joseph, E. M. and Melton, D. A. (1998). Mutant Vg1 ligands disrupt endoderm and mesoderm formation in *Xenopus* embryos. *Development* 125, 2677–2685.
- Kanai, Y., Dohmae, N., and Hirokawa, N. (2004). Kinesin transports RNA: isolation and characterization of an RNA-transporting granule. *Neuron* 43, 513–525.
- Kessler, D. S. and Melton, D. A. (1995). Induction of dorsal mesoderm by soluble, mature Vg1 protein. *Development* 121, 2155–2164.
- Kim, C. H. and Tinoco, I., Jr. (2000). A retroviral RNA kissing complex containing only two G.C base pairs. *Proc Natl Acad Sci U S A* 97, 9396–9401.
- King, M. L., Messitt, T. J., and Mowry, K. L. (2005). Putting RNAs in the right place at the right time: RNA localization in the frog oocyte. *Biol Cell* 97, 19–33.
- Kloc, M. and Etkin, L. D. (1994). Delocalization of Vg1 mRNA from the vegetal cortex in *Xenopus* oocytes after destruction of Xsirt RNA. *Science* 265, 1101–1103.
- Kloc, M. and Etkin, L. D. (1995). Two distinct pathways for the localization of RNAs at the vegetal cortex in *Xenopus* oocytes. *Development* 121, 287–297.
- Kloc, M. and Etkin, L. D. (1998). Apparent continuity between the messenger transport organizer and late RNA localization pathways during oogenesis in *Xenopus*. *Mech Dev* 73, 95–106.
- Kloc, M. and Etkin, L. D. (2005). RNA localization mechanisms in oocytes. *J Cell Sci* 118, 269–282.
- Kloc, M., Spohr, G., and Etkin, L. D. (1993). Translocation of repetitive RNA sequences with the germ plasm in *Xenopus* oocytes. *Science* 262, 1712–1714.
- Kloc, M., Larabell, C., and Etkin, L. D. (1996). Elaboration of the messenger transport organizer pathway for localization of RNA to the vegetal cortex of *Xenopus* oocytes. *Dev Biol* 180, 119–130.
- Kloc, M., Bilinski, S., Pui-Yee Chan, A., and Etkin, L. D. (2000). The targeting of Xcat2 mRNA to the germinal granules depends on a cis-acting germinal granule localization element within the 3'UTR. *Dev Biol* 217, 221–229.
- Klymkowsky, M. W., Maynell, L. A., and Nislow, C. (1991). Cytokeratin phosphorylation, cytoskeleton filament severing and the solubilization of the maternal mRNA Vg1. *J Cell Biol* 114, 787–797.
- Kress, T. L., Yoon, Y. J., and Mowry, K. L. (2004). Nuclear RNP complex assembly initiates cytoplasmic RNA localization. *J Cell Biol* 165, 203–211.
- Kroll, T. T., Swenson, L. B., Hartland, E. I., Snedden, D. D., Goodson, H. V., and Huber, P. W. (2009). Interactions of 40LoVe within the ribonucleoprotein complex that forms on the localization element of *Xenopus* Vg1 mRNA. *Mech Dev* 126, 523–538.
- Kwon, S., Abramson, T., Munro, T. P., John, C. M., Kohrmann, M., and Schnapp, B. J. (2002). UUCAC and Vera dependent localization of VegT RNA in *Xenopus* oocytes. *Curr Biol* 12, 558–564.
- Lasko, P. (2011). Posttranscriptional regulation in *Drosophila* oocytes and early embryos. *Wiley Interdiscip Rev RNA* 2, 408–416.
- Lecuyer, E., Yoshida, H., Parthasarathy, N., et al. (2007). Global analysis of mRNA localization reveals a prominent role in organizing cellular architecture and function. *Cell* 131, 174–187.
- Lewis, R. A., Kress, T. L., Cote, C. A., Gautreau, D., Rokop, M. E., and Mowry, K. L. (2004). Conserved and clustered RNA recognition sequences are a critical feature of signals directing RNA localization in *Xenopus* oocytes. *Mech Dev* 121, 101–109.
- Liu-Yesucevitz, L., Bassell, G. J., Gitler, A. D., et al. (2011). Local RNA translation at the synapse and in disease. *J Neurosci* 31, 16086–16093.
- MacDonald, P. M. (1990). bicoid mRNA localization signal: phylogenetic conservation of function and RNA secondary structure. *Development* 110, 161–171.

- Messitt, T. J., Gagnon, J. A., Kreiling, J. A., Pratt, C. A., Yoon, Y. J., and Mowry, K. L. (2008). Multiple kinesin motors coordinate cytoplasmic RNA transport on a subpopulation of microtubules in *Xenopus* oocytes. *Dev Cell* 15, 426–436.
- Mowry, K. L. and Melton, D. A. (1992). Vegetal messenger RNA localization directed by a 340-nt RNA sequence element in *Xenopus* oocytes. *Science* 255, 991–994.
- Munro, T. P., Kwon, S., Schnapp, B. J., and St Johnston, D. (2006). A repeated IMP-binding motif controls oskar mRNA translation and anchoring independently of *Drosophila melanogaster* IMP. *J Cell Biol* 172, 577–588.
- Murray, A. W. (1991). *Methods in Cell Biology*, Vol 36 (San Diego, CA: Academic Press, Inc.).
- O'Keefe, H. P., Melton, D. A., Ferreira, B., and Kintner, C. (1991). In situ hybridization. *Methods Cell Biol* 36, 443–463.
- Pace, N. R., Smith, D. K., Olsen, G. J., and James, B. D. (1989). Phylogenetic comparative analysis and the secondary structure of ribonuclease P RNA – a review. *Gene* 82, 65–75.
- Pondel, M. D. and King, M. L. (1988). Localized maternal mRNA related to transforming growth factor beta mRNA is concentrated in a cytokeratin-enriched fraction from *Xenopus* oocytes. *Proc Natl Acad Sci U S A* 85, 7612–7616.
- Puthanveetil, S. V., Antonov, I., Kalachikov, S., et al. (2013). A strategy to capture and characterize the synaptic transcriptome. *Proc Natl Acad Sci U S A* 110, 7464–7469.
- Pyhtila, B., Zheng, T., Lager, P. J., Keene, J. D., Reedy, M. C., and Nicchitta, C. V. (2008). Signal sequence- and translation-independent mRNA localization to the endoplasmic reticulum. *RNA* 14, 445–453.
- Rand, K. and Yisraeli, J. K. (2007). Vg1 RNA localization in oocytes in the absence of xVICKZ3 RNA-binding activity. *Differentiation* 75, 566–574.
- Richter, J. D. and Klann, E. (2009). Making synaptic plasticity and memory last: mechanisms of translational regulation. *Genes Dev* 23, 1–11.
- Rothman, J. E. and Sollner, T. H. (1997). Throttles and dampers: controlling the engine of membrane fusion. *Science* 276, 1212–1213.
- Saffman, E. E. and Lasko, P. (1999). Germline development in vertebrates and invertebrates. *Cell Mol Life Sci* 55, 1141–1163.
- Schmid, M., Jaedicke, A., Du, T. G., and Jansen, R. P. (2006). Coordination of endoplasmic reticulum and mRNA localization to the yeast bud. *Curr Biol* 16, 1538–1543.
- Seeger, M. A. and Kaufman, T. C. (1990). Molecular analysis of the bicoid gene from *Drosophila pseudoobscura*: identification of conserved domains within coding and noncoding regions of the bicoid mRNA. *EMBO J* 9, 2977–2987.
- Snedden, D. D., Bertke, M. M., Vernon, D., and Huber, P. W. (2013). RNA localization in *Xenopus* oocytes uses a core group of trans-acting factors irrespective of destination. *RNA* 19, 889–895.
- St Johnston, D., Beuchle, D., and Nusslein-Volhard, C. (1991). Staufen, a gene required to localize maternal RNAs in the *Drosophila* egg. *Cell* 66, 51–63.
- St Johnston, D., Brown, N. H., Gall, J. G., and Jantsch, M. (1992). A conserved double-stranded RNA-binding domain. *Proc Natl Acad Sci U S A* 89, 10979–10983.
- Wagner, C., Palacios, I., Jaeger, L., et al. (2001). Dimerization of the 3'UTR of bicoid mRNA involves a two-step mechanism. *J Mol Biol* 313, 511–524.
- Yisraeli, J. K. and Melton, D. A. (1988). The maternal mRNA Vg1 is correctly localized following injection into *Xenopus* oocytes. *Nature* 336, 592–595.
- Yisraeli, J. K., Sokol, S., and Melton, D. A. (1989). The process of localizing a maternal messenger RNA in *Xenopus* oocytes. *Development* 107, 31–36.
- Yisraeli, J. K., Sokol, S., and Melton, D. A. (1990). A two-step model for the localization of maternal mRNA in *Xenopus* oocytes: involvement of microtubules and microfilaments in the translocation and anchoring of Vg1 mRNA. *Development* 108, 289–298.
- Yoon, Y. J. and Mowry, K. L. (2004). *Xenopus* Staufen is a component of a ribonucleoprotein complex containing Vg1 RNA and kinesin. *Development* 131, 3035–3045.
- Zhang, J., Houston, D. W., King, M. L., Payne, C., Wylie, C., and Heasman, J. (1998). The role of maternal Vegt in establishing the primary germ layers in *Xenopus* embryos. *Cell* 94, 515–524.
- Zhao, W. M., Jiang, C., Kroll, T. T., and Huber, P. W. (2001). A proline-rich protein binds to the localization element of *Xenopus* Vg1 mRNA and to ligands involved in actin polymerization. *EMBO J* 20, 2315–2325.
- Zhou, Y. and King, M. L. (1996). RNA transport to the vegetal cortex of *Xenopus* oocytes. *Dev Biol* 179, 173–183.
- Zonta, E., Bittencourt, D., Samaan, S., Germann, S., Dutertre, M., and Auboeuf, D. (2013). The RNA helicase DDX5/p68 is a key factor promoting c-fos expression at different levels from transcription to mRNA export. *Nucleic Acids Res* 41, 554–564.

3 From Oocyte to Fertilizable Egg: Regulated mRNA Translation and the Control of Maternal Gene Expression

Chad E. Cragle & Angus M. MacNicol

Department of Neurobiology and Developmental Sciences, University of Arkansas for Medical Sciences, Little Rock, AR

Abstract: Growing evidence indicates a critical role for posttranscriptional mechanisms for regulation of gene expression in a variety of developmental transitions as well as for control of adult somatic cell function. A predominant regulatory paradigm is selective control of messenger RNA (mRNA) translation. Significant advances have provided unparalleled insight into the diverse mRNA translational control processes that govern early development and cell cycle progression. At the forefront of these new insights is work analyzing oocyte maturation in the frog *Xenopus laevis*. We will review general concepts underlying mRNA translational regulation and highlight recent advances characterizing RNA binding proteins (RBP) and their target sequences in the control of oocyte growth and maturation. In particular, we will discuss the characterization of bifunctional elements, which can switch from repression to activation in response to changes in cellular signaling. We will consider the increasing number of mRNA 3' untranslated regions (UTRs) containing multiple distinct elements with unique properties and the emerging issue of understanding the functional integration of translational control mechanisms. Finally, we will discuss the elucidation of nested feedback loops that drive and regulate sequential maternal mRNA translational control programs. These new advances indicate that regulated mRNA translation is likely to be much more complex than originally anticipated. The *Xenopus* oocyte is proving invaluable in the search for common underlying principles that guide mRNA translational control, that are applicable not only to oogenesis and maturation, but also to control of gene expression in somatic cells.

Mechanisms of mRNA translational control: Global versus selective targeting

The primary point of regulation in control of messenger RNA (mRNA) translation occurs at initiation. Assembly of a functional ribosome onto an mRNA is a complex, multistep

process. Two important regulated steps include the binding and formation of the 5' cap complex, eIF4F, and recruitment of the small ribosomal subunit as part of a 43S preinitiation complex (Figure 3.1). Formation of both the cap complex and the preinitiation complex, specifically the ternary complex (the initiator methionine-charged tRNA_i, the

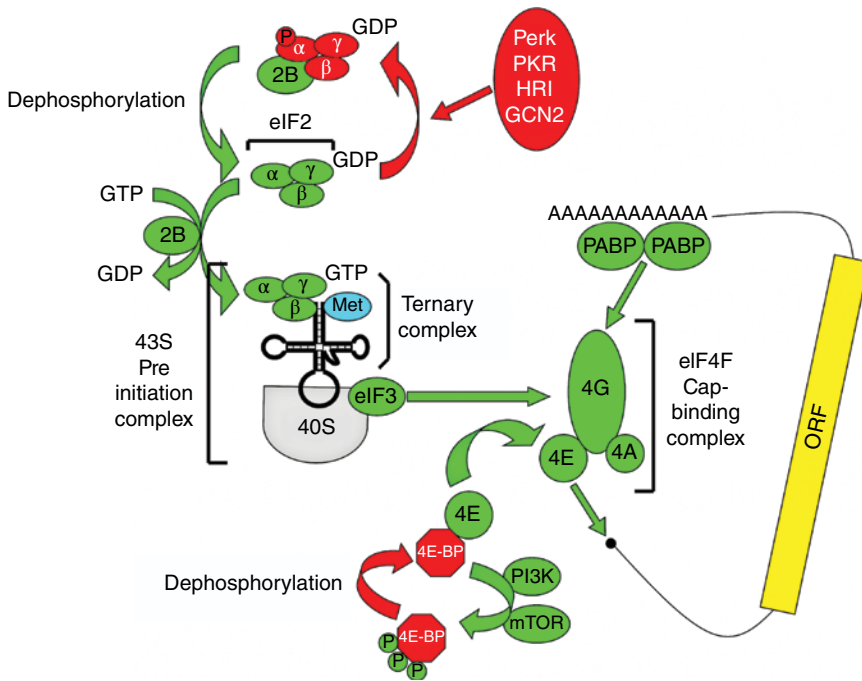


Figure 3.1 Translation initiation. Translation initiation in eukaryotes is a complex, multistep process. Of central importance is the formation of two major complexes: the 43S preinitiation complex and the eIF4F cap-binding complex. Formation of both complexes can be regulated to control gene expression. ORF, open reading frame; PABP, poly[A] binding protein; eIF, eukaryotic initiation factor; Met, methionine; PI3K, phosphoinositide 3-kinase; mTOR, mammalian target of rapamycin; 4E-BP, eIF4E binding protein; GTP, guanine triphosphate; GDP, guanine diphosphate; PERK, PRK-like ER kinase; PKR, protein kinase double-stranded RNA dependent; GCN2, general control nonderepressible-2; HRI, heme-regulated inhibitor. To see a color version of this figure, see Plate 7.

initiation factor eIF2, and GTP), is regulated (Dever 2002).

In the case of the cap complex, the cap-binding protein eIF4E interacts with the guanylyl 5' cap structure of the mRNA and recruits a large multifunctional protein eIF4G and the RNA helicase eIF4A (Gingras et al. 1999). Additional accessory factors that may influence eIF4A function can also be recruited (Rogers et al. 2001). Opposing assembly of the cap complex are a family of eIF4E binding proteins (4E-BPs) that block the formation of the cap complex by acting as competitive inhibitors of the eIF4E–eIF4G interaction (Haghighat et al. 1995; Pause et al. 1994). By preventing eIF4E–eIF4G interaction, the 43S preinitiation complex cannot be recruited to initiate translation since recruitment requires interaction of eIF3 on the preinitiation complex with eIF4G bound to the 5' cap (Lamphear et al. 1995). Interaction of 4E-BPs with eIF4E is

reversible; phosphorylation of 4E-BP on several distinct sites is primed by mammalian target of rapamycin (mTOR) signaling and additional phosphorylation by PI3 kinase-dependent pathways (Gingras et al. 2001). Phosphorylation of 4E-BPs renders them unable to interact with eIF4E and, as a consequence, prevents their inhibitory action on 5' cap-dependent translational initiation. Generally, this mechanism of inhibition is considered to act globally to dampen the initiation of all capped mRNAs in the cell, although there appears to be particular inhibitory sensitivity of mRNAs with long, structured 5' UTRs (D'Ambrogio et al. 2013; Koromilas et al. 1992). Additionally, targeting of cap complex assembly has been co-opted by regulatory factors that bind to specific mRNAs to allow selective regulation of a subset of the cellular mRNA population (Richter and Sonenberg 2005).

In addition to regulated formation of the cap complex, the ability to load the initiator methionine tRNA on the small 40S ribosomal subunit *via* the ternary complex (eIF2.GTP.tRNA_i^{Met}) is controlled by a family of kinases that target the α -subunit of eIF2 (Dever 2002). In response to various cellular stress (e.g., unfolded proteins, double-stranded RNA, low heme, or amino acid starvation), activation of the appropriate stress responder kinase (PERK, PKR, HRI, or GCN2, respectively) results in phosphorylation of serine 51 on the eIF2 α -subunit (Donnelly et al. 2013). eIF2 is a trimeric protein with inherent GTPase activity and phosphorylation of the α -subunit traps the eIF2 trimeric protein in a GDP-bound state that is unable to bind methionine-charged tRNA_i (Siekierka et al. 1982). The phosphorylated complex also sequesters eIF2B which normally functions as a guanine nucleotide (nt) exchange factor for eIF2 to reconstitute eIF2.GTP from eIF2.GDP (Rowlands et al. 1988). The inability to bind to the initiator tRNA and sequestration of eIF2B attenuate initiation by preventing the formation of functional 43S preinitiation complexes.

In addition to translational control mechanisms that affect general 5' cap-dependent initiation, select subsets of mRNAs may be coordinately regulated without affecting general mRNA translation. A priority for such regulated subsets of mRNAs is some distinguishing feature that "marks" them as candidates for selective regulation. The predominant feature of select mRNA translational regulation is the presence of one or more regulatory elements that identify it uniquely for regulation. A diverse array of regulatory elements has been discovered and includes upstream open reading frames/start codons (Meijer and Thomas 2002), internal ribosome entry sites (Komar et al. 2012), RNA secondary structures (see succeeding text), and binding sequences for regulatory proteins (see succeeding text). These regulatory elements are generally found within either the 5' or 3' UTRs of the mRNA, although some mRNAs possess regulatory elements within the coding region (Kuwako et al. 2010; Luo et al. 2011). The functions of these regulatory elements can vary considerably, from controlling formation of initiation complexes to enforcing subcellular localization and/or control of poly[A] tail

length. In somatic cells, mRNA stability can also be regulated, but this appears to be a less prominent mechanism of translational control during oogenesis (Zhang et al. 1999).

Sequestration of maternal mRNA contributes to control of gene expression during *Xenopus* oogenesis

Growth of oocytes during oogenesis provides a means to stockpile essential mRNAs that will be required for oocyte maturation and early embryonic development, periods during which gene transcription is actively suppressed. mRNAs are found in close association with numerous protein factors. In fact, the assembly of proteins onto a nascent mRNA begins even before transcription concludes (Aguilera 2005; Giorgi and Moore 2007). Such mRNA-protein complexes are referred to as mRNA ribonucleoprotein particles (mRNPs). The protein factors present on the mRNA direct its fate, including localization and sequestration within the cell. Sequestered mRNPs can be held translationally repressed until the proper stimulus induces activation and translation. Indeed, factors found as components of mRNPs have been demonstrated to reversibly repress translation *in vitro* (Richter and Smith 1984). This reversible sequestration and repression allows proper temporal and spatial synthesis of critical factors necessary for meiotic cell cycle progression and early embryonic cell divisions. A host of *Xenopus* mRNA binding proteins have been found to mediate sequestration and repression of mRNAs (Table 3.1), most of which have mammalian counterparts, suggesting evolutionarily conserved roles in mRNA translational regulation.

One common component of mRNPs is the RNA helicase DDX6/Xp54 (Ladomery et al. 1997). DDX6 is a member of the DEAD-box RNA helicase family and has a demonstrated role in nuclear assembly and shuttling of mRNPs for storage (Smillie and Sommerville 2002). Another abundant member of non-translating mRNPs is the cold-shock domain protein FRGY2 (p60/mRNP4) (Dearsly et al. 1985; Tafuri and Wolffe 1993). In *Xenopus* oocytes, overexpression of FRGY2 causes silencing of mRNA (Bouvet and Wolffe 1994),

Table 3.1 RBP influence the fate of an mRNA.

Protein	Cytoplasmic function	Binds	Reference
eIF4E	Binds 5' cap, translational initiation	5' Cap	Sonenberg (2008)
eIF4E1b	Binds 5' cap, translational repression	5' Cap	Minshall et al. (2007)
DDX6/Xp54	mRNP assembly/export/stability, mRNA unwinding	Likely ssRNA	Ladomery et al. (1997); Smillie and Sommerville (2002)
FRGY2/mRNP4	mRNP storage and repression	AACAUC/ssRNA	Bouvet and Wolffe (1994); Tafuri and Wolffe (1993)
RAP55	mRNP storage and repression	Oligo(U)	Tanaka et al. (2006)
hnRNP1	mRNA localization	VLE ("VM1"-YYUCU)	Cote et al. (1999)
Vg1RBP/vera	mRNA localization	VLE ("E2"-A/U,YCAC)	Elisha et al. (1995)
Staufen	mRNA localization	mRNA stem-loops	Yoon and Mowry (2004)
40LoVe	mRNA localization	VLE	Czaplinski et al. (2005); Czaplinski and Mattaj (2006)
VgRBP71	RNA cleavage; translation activation	VLE	Kolev and Huber (2003)
ElrA/ElrB	Translational repression	ARE	Colegrove-Otero et al. (2005)
SLBP1	Activates histone mRNA translation	Histone mRNA stem-loop	Sanchez and Marzluff (2002)
SLBP2	Represses histone mRNA translation	Histone mRNA stem-loop	Sanchez and Marzluff (2002)
Argonaute	Translational repression	miRNA-guided	Lund et al. (2011); Wilczynska et al. (2009)
Musashi 1	Translational activation	MBE	Charlesworth et al. (2006)
Musashi 2	Translational activation	MBE	Arumugam et al. (2010)
Zar2	Translational repression/activation	TCS	Charlesworth et al. (2012)
CPEB1	Translational repression/activation	CPE	Hake and Richter (1994)
CPEB4	Translational activation	CPE?	Huang et al. (2006); Igea and Mendez (2010)
Pumilio1	Translational repression	PBE	Nakahata et al. (2001)
Pumilio2	Translational repression	PBE	Padmanabhan and Richter (2006)
DAZL	Translational activation	GUUC (polyU with G/C)	Collier et al. (2005)
CPSF (complex)	Directs polyadenylation	AAUAAA	Dickson et al. (1999)
ePAB	Protects poly[A] tail, enhances translational activation	Poly[A]	Voeltz et al. (2001); Wilkie et al. (2005)

mRNAs are subject to extensive regulation. RBP recognize and associate with an mRNA through various binding sequences or structures and can then recruit cofactors. Through the formation of complex mRNPs, the cell can regulate the timing, duration, extent, and localization of the expression of any or all transcripts.

and injection of antibodies targeting FRGY2 family proteins relieves translational inhibition (Braddock et al. 1994). Interestingly, FRGY2 possesses separate mRNA binding activity in the N-terminus and C-terminus. The N-terminus contains the cold-shock domain, which contains a sequence-specific RNA Recognition Motif (RRM), while the C-terminus shows no sequence selectivity (Bouvet et al. 1995). It is the C-terminal binding activity that mediates translational repression (Matsumoto et al. 1996). Recently, RAP55, a member of the Scd6 family, has been shown to also be an important component of DDX6/FRGY2 mRNA storage particles. RAP55 was shown to co-occupy the same mRNAs as FRGY2, associate directly with DDX6/Xp54, and repress mRNA translation *in vitro* (Tanaka et al. 2006).

Localization and translational control

One of the most well-studied examples of mRNA localization in the oocyte is that of the Vg1 mRNA. A member of the TGF β family, Vg1, is important for induction of mesoderm and left–right asymmetry in the early embryo (Weeks and Melton 1987b). The RNA is detectable early in developing oocytes at stages (Dumont 1972) I and II. By stage IV, the Vg1 mRNA has become localized to the vegetal pole. The protein becomes detectable at this time, reaches maximal levels by stage VI, and is maintained until the gastrula stage of the embryo (Dale et al. 1989; Tannahill and Melton 1989). Localization of the mRNA requires an element in the 3' UTR known as the Vg1 localization element (VLE) (Mowry and Melton 1992). The VLE is bound by a host of proteins including hnRNP1, Vg1RBP/vera, 40LoVe, and Staufen (Cote et al. 1999; Czaplinski et al. 2005; Elisha et al. 1995; Yoon and Mowry 2004). The motor proteins Kinesin-1 and Kinesin-2 are thought to transport the mRNA along microtubules to the vegetal pole (Betley et al. 2004; Messitt et al. 2008). Anchoring of the Vg1 mRNA within the vegetal pole requires intact microfilaments (Yisraeli et al. 1990).

Repression of the Vg1 mRNA is dependent on a 250-nt sequence downstream of the VLE

known as the Vg1 translational element (VTE) (Otero et al. 2001; Wilhelm et al. 2000). The ELAV family proteins ElrA and ElrB bind the VTE. ElrB is thought to be primarily responsible for Vg1 repression because its expression is maximal in stages I and II and minimal by stage IV when Vg1 mRNA begins to be expressed, while ElrA is expressed minimally while Vg1 is repressed and maximally when Vg1 is expressed (Colegrove-Otero et al. 2005). To release Vg1 mRNA from repression, another protein called VgRBP71 binds the 3' end of the VLE and stimulates cleavage at an adjacent polyadenylation element, releasing the VTE and relieving repression of the mRNA (Kolev and Huber 2003).

Other vegetally localized mRNAs have been discovered. *Xenopus* Nanos1 (also known as Xcat2) is an RNA binding protein (RBP) similar to *Drosophila* nanos (Mosquera et al. 1993). Like Vg1, the Nanos1 mRNA is localized to the vegetal pole and is initially held translationally repressed. However, the mechanisms of localization and repression are quite distinct from those of Vg1. Localization occurs very early during oocyte development with the Nanos1 mRNA found within the mitochondrial cloud, a region of mitochondrial proliferation near the nucleus, in stage I oocytes. By stage II, the cloud material has localized to the cortex of the presumptive vegetal pole and the Nanos1 mRNA has been packaged into the germ plasma, comprising mRNA granules surrounded by mitochondria (Forristall et al. 1995). Repression of the Nanos1 mRNA is accomplished by a secondary structure that forms within the open reading frame, immediately downstream of the AUG start codon. Interestingly, this structural element represses translation by sterically blocking the recognition of the start codon by the 43S ribosome complex (Forristall et al. 1995; Luo et al. 2011).

In addition to vegetally localized mRNAs, several mRNAs localize to the animal pole. These include An1 which encodes a ubiquitin-like protein (Linnen et al. 1993) and An2 which encodes the α -subunit of the mitochondrial ATPase (Weeks and Melton 1987a). Whether these animal pole-localized mRNAs are also subject to translational regulation is an important goal for future studies.

Regulation of mRNA translation by structural elements

In addition to the nanos1 mRNA, the translation of replication-dependent histone mRNAs is also regulated by a structural element, specifically a noncanonical 3' end structure. Unlike many mRNAs found in *Xenopus* oocytes, as well as many other metazoans, histone mRNAs are not polyadenylated but rather possess a highly conserved 3' stem-loop structure (Harris et al. 1991; Marzluff 1992; Pandey and Marzluff 1987). The stem-loop appears to serve a function analogous to a poly[A] tail (Sanchez and Marzluff 2002; Sun et al. 1992). The histone stem-loop is bound by two stem-loop binding proteins (SLBPs) in *Xenopus* oocytes (Wang et al. 1999). Both SLBP1 and SLBP2 share a central RNA binding domain, but have very little similarity throughout the rest of the protein (Wang et al. 1999). SLBP2 has been shown to be expressed and active during early oogenesis and is degraded during maturation of stage VI oocytes, while SLBP1 is expressed throughout development and becomes most active during late oogenesis and early embryonic development (Wang et al. 1999). SLBP2 has been demonstrated to mask the translation of transcripts containing the histone stem-loop when overexpressed, while SLBP1 has been shown to stimulate translation (Sanchez and Marzluff 2002). Thus, an exchange of binding factors associating with the same 3' UTR element likely activates the translation of histone mRNA during oocyte maturation.

Small RNA-mediated translational control components

Another interesting method of translation regulation is targeting of mRNAs by microRNAs (miRNAs). These small RNA fragments, 20–30 nts in length, function as guides for the recognition of target mRNAs by RNA-induced silencing complexes (RISC) which contain, amongst others, members of the Argonaute protein family. Regulation may be accomplished by a number of pathways including RNA cleavage or deadenylation (Pratt and MacRae 2009). miRNA regulation has been

demonstrated to play an important role in translational regulation in the *Xenopus* embryo following resumption of transcription (Lund et al. 2009). It has not been demonstrated if miRNA regulation plays a part in the regulation of translation during oogenesis. However, miRNAs have been demonstrated to be present in the oocyte at all stages (Armisen et al. 2009; Watanabe et al. 2005), as have Argonaute proteins, although possibly at limiting abundance (Lund et al. 2011; Wilczynska et al. 2009). Further work will be required to establish the role and contribution of small noncoding RNAs to translational regulation in the oocyte.

Control of mRNA translation by regulated changes in poly[A] tail length

During maturation of stage VI oocytes, transcription is suppressed and remains attenuated until reactivation of the zygotic genome in the developing postfertilization embryo (Davidson 1986; Newport and Kirschner 1982). Thus, maturation of the oocyte to a fertilizable egg and subsequent early embryonic development after fertilization is critically dependent upon regulated mRNA translation of preexisting oocyte mRNA populations to control the synthesis of proteins necessary to mediate the correct temporal progression through meiosis and early embryonic mitotic cell cycles. Regulation of the length of mRNA poly[A] tails is a predominant mechanism to control translation in the latter phases of oogenesis and during maturation of oocytes to a fertilizable egg (Richter and Lasko 2011). To date, three regulatory elements have been identified that modulate poly[A] tail length during progesterone-stimulated maturation of stage VI oocytes (Table 3.2). These are the cytoplasmic polyadenylation element (CPE) (Fox et al. 1989; McGrew et al. 1989), the Musashi binding element (MBE, formerly referred to as a polyadenylation response element [PRE]) (Charlesworth et al. 2002), and the translational control sequence (TCS) (Wang et al. 2008). Each element in turn is recognized and bound by a sequence-specific RBP, namely, CPE-binding protein 1 (CPEB1) for the CPE (Hake and Richter 1994), Musashi1 or

Table 3.2 Summary of regulatory elements controlling mRNA translational recruitment during oocyte maturation.

Element	Sequence motif	RBP	Examples of target mRNA	Does the element mediate repression?	Timing of derepression or activation	Positional dependence for function	Comments
PBE	UGUANAUA*	Pumilio1, Pumilio2	Cyclin B1, Ringo	Yes	Derepression: immediate (<1 h after stimulus)	N.D.†	Progesterone-stimulated derepression can be masked by other repressor elements in same 3' UTR
MBE	RU ₁₋₃ AGU* or GUAG	Musashi1, Musashi2	Mos, cyclin B5, Musashi1 (Nrp1A/B)	No	Activation: early (<GVBD)	N.D.†	Acts dominantly to non-Hex overlap CPEs in same UTR. Early activation is suppressed by a Hex overlap CPE in same UTR
TCS	WUURUCU*	Zar2, Zar1?	Wee1, Pcm1	Yes	Activation: early (<GVBD)	N.D.†	May not direct activation if 3' of Hex. † Early activation is suppressed by a Hex overlap CPE
CPE	U ₄ A ₁₋₃ U	CPEB1, CPEB4?	Cyclin B1, Wee1, cyclin A1, cyclin B2	Yes	Activation: late (≥GVBD)	<100 nt from the Hex, not overlapping the Hex	Cyclin B/CDK-independent activation, but can be overridden by a Hex overlap CPE in the same UTR
CPE (nonconsensus)	U ₄ ACU, U ₄ AAGU, or U ₄ CAU	CPEB1	Cyclin B1	Yes	Activation: late (≥GVBD)	<100 nt from the Hex, not overlapping the Hex	Requires a second CPE or a PBE nearby in the same UTR
Polyadenylation hexanucleotide overlap CPE	U ₄ A ₂₋₃ UAAA	CPEB1, CPEB4?	Cyclin B1, cyclin A1	Yes	Activation: late (≥GVBD)	Overlapping the Hex	Cyclin B/CDK-dependent activation and acts dominantly to all elements listed earlier

Relevant properties of the Pumilio2 binding element (PBE), the MBE, the TCS, and the CPE are listed. Timing of progesterone-stimulated mRNA translation is defined as early if it occurs prior to GVBD and late if it occurs at or after GVBD.

*Single-letter code: N = A or C or G or T, R = A or G, W = A or T.

†The precise distance from, or the orientation relative to, the hexanucleotide polyadenylation signal (Hex) has not yet been determined. However, for the mRNA 3' UTRs where the function of these elements has been characterized, they lie <100 nt from the Hex.

*Although present 3' to the Hex in the Mos mRNA, the TCS does not contribute to early activation. See main text for further discussion.

Source: Adapted from MacNicol and MacNicol (2010).

Musashi2 for the MBE (Arumugam et al. 2010; Charlesworth et al. 2006), and Zygotic arrest 2 (Zar2) for the TCS (Charlesworth et al. 2012). While sharing some similarities in function, each factor possesses unique attributes.

CPE-dependent mRNA translational regulation

CPEs are bifunctional (Table 3.2) by virtue of the fact they can exert repression in immature oocytes and subsequently switch to activators of target mRNA translation in stage VI oocytes stimulated with progesterone (Richter 2007). A significant advance towards understanding the molecular basis of this functional switch in activity was the original cloning and characterization of the CPE-binding protein, CPEB1 (Hake and Richter 1994). It turned out to be the founding member of an evolutionarily conserved family of proteins, with representation in a broad range of species including *Caenorhabditis elegans* (Luitjens et al. 2000), *Drosophila* (Lantz et al. 1992), clam (Walker et al. 1999), zebrafish (Bally-Cuif et al. 1998), mice (Gebauer and Richter 1996), and humans (Welk et al. 2001). CPEB1-related proteins have also been reported in vertebrates (CPEB2, CPEB3, and CPEB4) (Kurihara et al. 2003; Theis et al. 2003). It is not entirely clear if these related proteins bind CPEs with low affinity or if they have alternate sequence-specific targets (Huang et al. 2006; Igea and Mendez 2010; Novoa et al. 2010).

Classical biochemical approaches helped to elucidate the identity of CPEB1 coassociated factors necessary for repression and activation. CPE-directed repression may be achieved by one of four potential mechanisms. First, CPEB1 was reported to interact with Maskin to mediate CPE-dependent repression of target mRNAs *via* the ability of Maskin to also interact with eIF4E and preclude eIF4E–eIF4G interaction (Stebbins-Boaz et al. 1999). As a consequence, Maskin is proposed to act as a CPE-tethered 4E-BP to prevent initiation complex assembly on CPE-containing mRNAs. This paradigm of interdicting eIF4E–eIF4G interaction via 3' UTR binding protein coupling to an eIF4E binding protein has been reported in both invertebrate and vertebrate

species (Richter and Sonenberg 2005). In the second mechanism, CPEB1 controls the tail length of target mRNAs through interaction with the evolutionarily conserved noncanonical poly[A] polymerase germline development 2 (GLD2) and the deadenylase poly[A]-specific ribonuclease (PARN) (Barnard et al. 2004). GLD2 does not possess inherent RNA binding activity and work in *C. elegans* demonstrated that GLD2 required interaction with the sequence-specific 3' UTR regulatory factor GLD3 to be guided to target mRNAs to mediate cytoplasmic polyadenylation (Wang et al. 2002). The *Xenopus* GLD2 ortholog binds to CPEB1 in immature oocytes. This observation seemed somewhat counterintuitive as CPE-containing target mRNAs generally have short poly[A] tails in immature oocytes and suggested that GLD2 activity must be attenuated in this cellular context. Indeed, PARN also binds to CPEB1 in immature oocytes and is thought to oppose the action of GLD2 to maintain the short poly[A] tail of CPE-containing mRNAs (Kim and Richter 2006). Although primarily considered to be nuclear, a proportion of the PARN protein was found to be cytoplasmic, consistent with a role in controlling the length of CPE-regulated mRNAs (Kim and Richter 2006). The third repressive mechanism involves CPEB1 interaction with 4E-T (an eIF4E binding protein that can mediate the transport of eIF4E into the nucleus) and eIF4E1b (an eIF4E isoform with weak cap-binding activity) (Minshall et al. 2007). Since eIF4E1b interacts with 4E-T rather than eIF4G, CPE-containing mRNAs are thus translationally repressed. In addition to eIF4E1b and 4E-T, CPEB1 was also shown to be part of a large complex with other proteins implicated in mRNP-mediated storage and translational repression including DDX6, Pat1, and RAP55. Since these are also components of germinal granules, neuronal granules, and processing bodies (P-bodies), it suggests CPEB1 interacts with a large repression complex where some components are shared with other cellular processes (Minshall et al. 2007; Standart and Minshall 2008). In the fourth mechanism, CPEB1 has been shown to interact with cytoplasmic CstF-77 (cleavage stimulatory factor 77) along with eIF4E, cytoplasmic polyadenylation specificity factor

(CPSF), and GLD2 (Rouget et al. 2006) to exert translational repression. Temporally, the potential to form these specific CPEB1 repressor complexes appears to be differentially restricted. Maskin and PARN are predominantly expressed from stage IV onwards, limiting formation of their respective CPEB1 complexes to the latter part of oogenesis, whereas CPEB1, CstF-77, 4E-T, eIF4E1b, DDX6, Pat1, and RAP55 are expressed throughout oogenesis (Minshall et al. 2007).

In response to progesterone, the CPEB1 repressor complexes may be remodeled to permit polyadenylation and translation of target mRNAs. First and foremost, CPEB1 undergoes maturation-promoting factor (MPF, cyclin B/cyclin-dependent kinase [CDK])-dependent phosphorylation and partial degradation after germinal vesicle breakdown (GVBD), resulting in loss of approximately 75% of the total CPEB1 population (Mendez et al. 2002; Reverte et al. 2001). In addition, progesterone-dependent signaling pathways result in dissociation of Maskin and eIF4E at or after GVBD to allow translational initiation of CPE-regulated mRNAs (Barnard et al. 2005; Cao and Richter 2002; Stebbins-Boaz et al. 1999). For GLD2 complexes, phosphorylation of CPEB1 on serine 174 (S174) leads to dissociation of PARN, resulting in the unopposed action of GLD2 to mediate polyadenylation and translational activation of CPE-regulated mRNAs (Kim and Richter 2006). For the 4E-T/eIF4E1b repressor complexes, a number of changes occur in response to progesterone including phosphorylation of 4E-T, degradation of Pat1, and a switch in p54-eIF4E1b interactions from being RNA independent to RNA dependent. To date, remodeling of the CstF-77 repressor complex has not been directly addressed. It is interesting to note that during the characterization of 4E-T/eIF4E1b repressor complexes, the Standart group did not detect CPEB1 interaction with Maskin or PARN (Minshall et al. 2007). This observation suggests that Maskin and/or PARN may form mutually exclusive repressor complexes distinct from those containing 4E-T and eIF4E1b. A provocative area for future study will be to determine if different CPE-containing mRNAs reside in separate inhibitory complexes, and if so, the mechanism of such differential sequestration.

CPE-independent mRNA translational regulation

Although CPEs are commonly found in the 3' UTR of many regulated mRNAs, polyadenylation of a number of early class mRNAs has been shown to be CPE independent (Charlesworth et al. 2004). The early class mRNA encoding the *Mos* proto-oncogene contains a CPE in the 3' UTR, and the molecular characterization of *Mos* mRNA translational regulation has proven to be a critical experimental model to unravel the complexity of CPE-independent and CPE-dependent regulatory mechanisms governing the temporal order of mRNA translation during *Xenopus* oocyte maturation. Antisense DNA oligonucleotide cleavage of the endogenous *Mos* mRNA 3' UTR to release the terminal 126 nts (including the CPE and polyadenylation hexanucleotide) was shown to block *Mos* mRNA translation as well as oocyte maturation (Sheets et al. 1995). Subsequent rescue with prosthetic RNA encoding the missing terminal 3' UTR sequence reconstituted the progesterone-dependent translation of the *Mos* mRNA and oocyte maturation, demonstrating the importance of progesterone-stimulated cytoplasmic polyadenylation for *Mos* mRNA translational activation (Sheets et al. 1995). However, the specific requirement for the CPE was not definitively shown. Indeed, when tested directly, a mutational disruption of the *Mos* CPE did not prevent early polyadenylation prior to GVBD (Charlesworth et al. 2002). This finding clearly indicated that a CPE-independent mechanism must contribute to early *Mos* translational control and that the element responsible must also reside within the terminal 126-nt region of the 3' UTR. The required element was shown to be upstream of and partially overlap the CPE and was initially designated a PRE (Charlesworth et al. 2002). The regulatory element was subsequently shown to bind specifically to the stem cell fate regulatory factor Musashi and was redesignated an MBE (Charlesworth et al. 2006). The MBE has a general consensus (G/A)UAG (Imai et al. 2001; Ohyama et al. 2012) and is present in a number of early class mRNAs (Arumugam et al. 2010, 2012a; Charlesworth et al. 2006).

The MBE directs early class progesterone-dependent mRNA polyadenylation and translational activation, but, unlike the CPE, does not appear to exert repression in immature stage VI oocytes (Arumugam et al. 2012a). The presence of Musashi protein in immature stage VI oocytes suggested that Musashi must undergo a functional switch in response to progesterone to promote MBE-dependent early class polyadenylation and translational activation. Indeed, activation of Musashi1 requires phosphorylation on two evolutionarily conserved sites in the C-terminal region of the protein (Arumugam et al. 2012b). Mutational disruption of these sites abrogates the ability of Musashi1 to mediate MBE-dependent polyadenylation and translational activation. Phosphorylation of Musashi1 is initially dependent upon Ringo/CDK activity and is subsequently augmented by MAP kinase signaling (Arumugam et al. 2012b). Since progesterone-stimulated MAP kinase activation is downstream of Mos, and Mos synthesis is dependent on Musashi function, augmentation of the initial Ringo/CDK trigger signal by MAP kinase establishes a positive feedback amplification loop to promote and sustain early class mRNA polyadenylation prior to GVBD (Arumugam et al. 2012b). The mechanism by which phosphorylated Musashi1 recruits and/or facilitates the activity of polyadenylation and translational initiation complexes has not yet been established.

The TCS was first identified in the CPE-dependent, late class Wee1 mRNA. Mutational disruption of the CPEs in the Wee1 3' UTR generated the surprising result of directing early class mRNA polyadenylation and translation prior to GVBD, rather than simply abolishing all polyadenylation as expected (Charlesworth et al. 2000). The region conferring this cryptic early polyadenylation and translational control was delineated and found to contain two tandem repeats of a seven-nt TCS element (Wang et al. 2008). The TCS, like the CPE, was shown to be bifunctional and was able to exert repression in stage VI immature oocytes. A bioinformatics search identified the mRNA encoding pericentriolar material-1 (Pcm1) as containing TCS, but not CPE, elements in the 3' UTR. The two Pcm1

TCS elements contributed to both repression in immature stage VI oocytes and early class mRNA polyadenylation and translational activation in response to progesterone stimulation (Wang et al. 2008). More recently, the TCS binding protein has been identified as Zygote Arrest 2 (Zar2) (Charlesworth et al. 2012). Zar2, like the founding family member, Zar1, are zinc finger-containing proteins. Mouse studies have revealed a critical role for Zar1 and Zar2 in the oocyte-to-embryo transition, where Zar1 was required for activation of zygotic gene transcription and cell cycle progression past the one-cell stage, while Zar2 was implicated in RNA processing and cell cycle progression past the two-cell stage (Hu et al. 2010; Wu et al. 2003). In the *Xenopus* oocyte, Zar2 is a sequence-specific RBP and functions to repress target mRNA translation in immature stage VI oocytes (Charlesworth et al. 2012). Zar2 has also been implicated in *Xenopus* embryonic epidermal cell fate determination (Nakajima et al. 2009), although it is not known if this is mediated *via* TCS-dependent mRNA translational control. Although sharing a highly conserved C-terminal RNA binding domain, it remains to be determined if Zar1 also exerts sequence-specific mRNA translational control. The mechanisms of Zar2-mediated translational control and the cofactors necessary for this process have not yet been elucidated.

Xenopus Pumilio1 and Pumilio2 (Pum1 and Pum2, respectively) are members of an evolutionarily conserved family of sequence-specific RBP (the PUF proteins) that regulate a number of developmental processes (Wickens et al. 2002). In *Xenopus*, the Pumilio proteins have been implicated in the translational control of the mRNAs encoding Ringo, an atypical activator of cyclin-dependent kinase 1 and cyclin-dependent kinase 2 (CDK1 and CDK2), and cyclin B1 (Cao et al. 2010; Nakahata et al. 2001, 2003; Ota et al. 2011; Padmanabhan and Richter 2006). The Ringo mRNA is translationally repressed in stage VI immature oocytes, and this repression was shown to require a Pumilio binding element (PBE) in the 3' UTR and interaction of Pum2 with the 5' cap structure of the Ringo mRNA (Cao et al. 2010; Padmanabhan and Richter 2006). Pum2 also associates with the mRNA translational control

protein Deleted for Azoospermia-like (DAZL) and with the embryonic form of poly[A] binding protein (ePAB), the predominant poly[A] binding protein expressed in oocytes (Padmanabhan and Richter 2006). Upon progesterone stimulation, Pum2 dissociates from the Ringo 3' UTR, while DAZL and ePAB are thought to promote Ringo mRNA translation. It has not been determined if Pumilio1-mediated repression is mechanistically similar to Pumilio2. Interestingly, the proposed cap-binding/repression domain was shown by another group to not mediate repression in *Drosophila*, but rather to inhibit repression (Weidmann and Goldstrohm 2012). Further work will be required to elucidate the molecular mechanisms controlling this potentially context-dependent bifunctional domain. To date, it does not appear that Ringo mRNA translational activation requires polyadenylation, and so, Ringo appears to be a founding member of an "immediate early", polyadenylation-independent class mRNA. In addition to regulating Ringo mRNA translation independently of CPE function, PBEs appear to function cooperatively with consensus or nonconsensus CPE elements to stabilize CPEB1 interaction and promote repression in immature oocytes and translational activation in response to progesterone (Pique et al. 2008).

In the absence of elements to promote progesterone-dependent cytoplasmic polyadenylation, housekeeping mRNAs are deadenylated and translationally silenced after GVBD (Wormington et al. 1996). However, it was recently demonstrated that a subset of mRNA species undergo progesterone-dependent cytoplasmic polyadenylation followed by selective deadenylation after GVBD, directed by AU-rich element (ARE) function (Belloc and Mendez 2008). Specifically, progesterone stimulates the polyadenylation and translation of the mRNA encoding C3H-4, an ARE binding protein. Synthesis of C3H-4 then attenuates the length of the poly[A] tail of the ARE-containing, cytoplasmically polyadenylated *Emi1*, *Emi2*, and *cyclin E* mRNAs after GVBD. This sequential polyadenylation and selective deadenylation has been proposed to ensure orderly progression through the distinct phases of meiosis (Belloc and Mendez 2008).

Given the complexity of the emerging picture of maternal mRNA translational control, it seems likely that additional regulatory sequences will be identified that contribute to regulation and mRNA-specific subcellular localization during oogenesis. As a case in point, although the *Pcm-1* mRNA was subject to TCS-dependent regulation, one or more as yet uncharacterized repression elements are also present in the *Pcm-1* 3' UTR (Wang et al. 2008).

Temporal control of maternal mRNA translation during meiotic maturation

Distinct mRNAs are translationally activated at distinct times in a strict order in response to progesterone stimulation (MacNicol and MacNicol 2010). Certain mRNAs are polyadenylated and translated early in maturation, prior to GVBD, while others were polyadenylated coincident with GVBD or after completion of GVBD. This polyadenylation behavior led to the designation of "early class" (polyadenylation occurring prior to GVBD) and "late class" (polyadenylation occurring at or after GVBD) maternal mRNAs (Ballantyne et al. 1997). This strict temporal regulation ensures that the correct proteins are synthesized in the correct phase of the cell cycle. For example, early *Mos* mRNA translation ensures normal progression through meiosis (Dupre et al. 2002; Sagata et al. 1988; Sheets et al. 1995). By contrast, translation of the CDK inhibitory kinase *Wee1* must occur after GVBD and MPF activation as *Wee1* and MPF activities are mutually antagonistic (McGowan and Russell 1993; Mueller et al. 1995; Parker and Piwnicka-Worms 1992). Indeed, precocious *Wee1* translation and activity prior to GVBD prevents meiotic progression and GVBD (Howard et al. 1999; Murakami and Vande Woude 1998; Nakajo et al. 2000). Thus, to avoid attenuation of MPF-dependent GVBD and entry into Meiosis 1, *Wee1* synthesis must occur after activation of MPF and GVBD such that *Wee1* is now synthesized in an inhibitory (active MPF) environment and accumulates in an inactive form for subsequent use in the first postfertilization mitotic cycle (Murakami et al. 1999).

Many mRNA 3' UTRs possess multiple distinct elements, empowering their selective temporal regulation and permitting fine-tuning of the duration and absolute levels of translation. Such finesse over the translation of mRNAs likely ensures the correct temporal accumulation of regulatory proteins with functional thresholds to permit orderly cell cycle progression in response to progesterone-stimulated oocyte maturation. The presence of multiple distinct mRNA regulatory elements complicates the interpretation of the individual contribution of each element to translational control, and not surprisingly, the molecular basis for the temporal control of early and late class polyadenylation-dependent mRNAs has proven to be a contentious issue. Two models have been proposed and their relative merits have been recently reviewed (MacNicol and MacNicol 2010; Villalba et al. 2011). In brief, one model posits a "CPE-combinatorial code" (Pique et al. 2008). In this model, the sequence and position of the CPEs relative to the polyadenylation hexanucleotide and neighboring PBEs within a 3' UTR direct the temporal control of target mRNAs such as *Mos* (early class), cyclin B5 (early class), and cyclin B1 (late class). However, while an attractively simple model, several reports contradict the underlying conclusions. Although the early class *Mos* mRNA 3' UTR contains a CPE, mutational disruption of CPE does not prevent early polyadenylation prior to GVBD (Charlesworth et al. 2002). Further, the CPEs in the cyclin B5 are not sufficient to mediate early polyadenylation (Arumugam et al. 2010). In both circumstances, it is important to point out that the CPEs are functional, but rather than directing early pre-GVBD polyadenylation, they direct late polyadenylation after oocyte GVBD.

The alternative model posits that distinct regulatory elements control early **versus** late polyadenylation (MacNicol and MacNicol 2010). Supporting this mechanism, an MBE is present in both the *Mos* and cyclin B5 3' UTRs and is necessary and sufficient for early polyadenylation and translational activation (Arumugam et al. 2010; Charlesworth et al. 2002). Further, the use of DNA antisense oligonucleotides to attenuate endogenous Musashi function prevented progesterone-dependent progression to GVBD as well as

both early and late class mRNA polyadenylation and translation (Arumugam et al. 2010). Rescue of the antisense phenotype and correct order of mRNA translational recruitment could be accomplished by ectopic Musashi expression but not by an RNA binding mutant of Musashi or ectopic CPEB1 expression (Arumugam et al. 2010). These findings position Musashi-dependent mRNA translational control upstream of CPEB1-dependent mRNA translation and are consistent with a dependence of the late class mRNAs on the prior polyadenylation and translational activation of early class mRNAs (Ballantyne et al. 1997). A complicating issue of this model, however, is that some late class mRNAs also possess MBEs (Charlesworth et al. 2006). Clearly, either positional considerations render MBEs ineffective in certain contexts and/or some functional integration must occur between MBEs and CPEs to establish *cis* dominance.

3' UTR regulatory element *cis* dominance

One defining feature of certain late class mRNAs is a CPE that overlaps the polyadenylation hexanucleotide sequence (Charlesworth et al. 2004; Tung et al. 2007). It has been proposed that when bound by CPEB1, this CPE configuration sterically hinders the recruitment of the CPSF complex to the polyadenylation hexanucleotide and attenuates mRNA polyadenylation until such time as the CPEB1 protein is degraded (Mendez et al. 2002). Since CPEB1 degradation is downstream of MPF phosphorylation, this event occurs at or after GVBD and so enforces late class mRNA translational regulation. Interestingly, the late class cyclin A1 mRNA contains a single hexanucleotide overlapping CPE. It was initially unclear how degradation of CPEB1 can be reconciled with CPE-dependent late class cyclin A1 polyadenylation after GVBD (Ballantyne et al. 1997; de Moor and Richter 1997; Sheets et al. 1994). However, a recent study suggests that CPEB1-dependent translational control stimulates accumulation of the CPEB4 protein, which can functionally substitute for CPEB1 and drive CPE-dependent mRNA translation after GVBD

(Igea and Mende 2010). A critical feature of this model is that the CPEB4 protein is regulated by distinct signaling pathways after GVBD and is not degraded by MPF.

Although the cyclin B1 and Wee1 mRNA 3' UTRs contain early class regulatory elements (MBE and TCS, respectively), the parent mRNAs are regulated in a late class CPE-dependent manner. It seems likely that suppression of early class regulatory function is a consequence of recruitment of CPEB1 to a polyadenylation hexanucleotide overlapping CPE that acts in *cis* to override the MBE and TCS. Consistent with this hypothesis, altering the MBE-dependent early class cyclin B5 3' UTR to position a CPE to overlap the polyadenylation hexanucleotide renders the polyadenylation of the mutant 3' UTR late class and dependent upon MPF activity (Pique et al. 2008). Similarly,

deletion of CPE function in the Wee1 3' UTR converts the polyadenylation and translational activation behavior from a late class to an early class mRNA (Wang et al. 2008). As more mRNAs are demonstrated to contain distinct regulatory elements, it will be a priority to understand how recruited mRNA translational regulatory complexes functionally integrate to exert a coordinated biological output.

A sequential hierarchy of translational control factors governs temporal recruitment of mRNAs during oocyte maturation

Taken together, the available data indicate that a sequential and interdependent hierarchy of distinct mRNA translational control

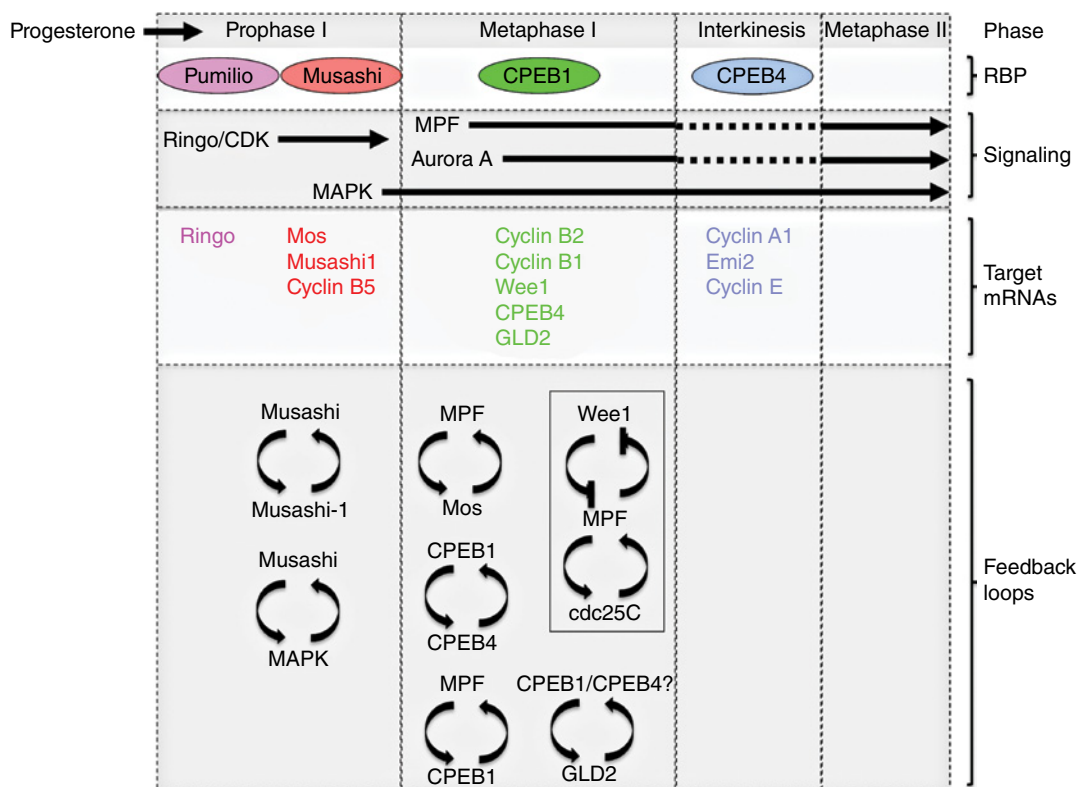


Figure 3.2 A series of positive feedback loops mediate amplification of a weak progesterone “trigger” signal to trigger activation of MPF. The sequential action of specific RBP regulates the ordered activation of signal transduction pathways and temporal recruitment of maternal mRNAs during meiotic cell cycle progression. A number of nested positive feedback loops contribute to the amplification of the initial progesterone stimulus and all-or-none transition through the cell cycle. For the purposes of focus on mRNA translational control and clarity, a number of negative feedback loops have been omitted. See text for details. To see a color version of this figure, see Plate 8.

factors governs the temporal recruitment of maternal mRNAs and progression through the oocyte meiotic cell cycle (Figure 3.2). Initial progesterone signaling stimulates dissociation of Pumilio from the Ringo mRNA, resulting in immediate early synthesis of Ringo and activation of Ringo/CDK. Active Ringo/CDK can phosphorylate and oppose the CDK inhibitor Myt1 (Ruiz et al. 2008) as well as mediate phosphorylation and activation of Musashi1 (Arumugam et al. 2012b). Musashi activation results in polyadenylation and activation of a number of early class mRNAs, including both the endogenous Musashi1 mRNA and the Mos mRNA (Arumugam et al. 2012a; Charlesworth et al. 2006). Translation of Mos leads in turn to activation of MAP kinase signaling and a number of downstream effects including priming of CPEB1 for activation, inhibition of Myt1, and phosphorylation and activation of Musashi (Arumugam et al. 2012b; Keady et al. 2007; Palmer et al. 1998; Peter et al. 2002). Thus, Musashi1 activates a translational control positive feedback loop to reinforce the initially weak progesterone “trigger” signaling pathway. CPEB1 activation was originally demonstrated to be a target of Aurora A kinase-mediated phosphorylation of S174 based on *in vitro* kinase and overexpression analyses (Mendez et al. 2000). While it has become popular in the literature to see diagrams positioning Aurora A upstream of CPEB1 *prior* to GVBD, this practice is misleading as the available evidence does not support this schema. Indeed, direct assessment of Aurora A function indicates that it becomes activated *after* GVBD (Castro et al. 2003; Frank-Vaillant et al. 2000; Maton et al. 2003; Pascreau et al. 2008) and that it is not required for CPEB1 S174 phosphorylation prior to GVBD (Keady et al. 2007). The identity of the kinase that mediates pre-GVBD CPEB1 S174 phosphorylation after a prior MAP kinase-dependent phosphorylation and priming event remains to be determined. Irrespective of the exact mechanism, full CPEB1 activation and CPE-dependent polyadenylation occur downstream of Musashi1 function in response to progesterone. In contrast to Musashi and CPEB1, activation of early class TCS-regulated mRNAs is less well understood. Moreover, the epistasis between TCS- and MBE-dependent translational activation has not

been characterized and is an important area for future study.

In addition to the linear progression of sequential mRNA translational programs, the “all-or-none” cell fate transition from an immature to a mature oocyte (Ferrell and Machleder 1998) involves a number of nested, positive feedback loops. These positive reinforcements act both at the level of signaling component activation and mRNA translational regulation (Figure 3.2). Examples of positive feedback signaling loops include MPF feedback stabilization of the Mos protein, MPF feedback inhibition of Wee1, and stimulation of Cdc25C (Karaiskou et al. 1998; Mueller et al. 1995; Nebreda et al. 1995). Examples of signaling feedback loops that impinge on mRNA translation include MAP kinase stimulation of Musashi to induce Mos mRNA polyadenylation (Arumugam et al. 2012b; Howard et al. 1999) and MPF-dependent degradation of CPEB1 to induce CPE-dependent cyclin B1 mRNA translation (Mendez et al. 2002). Feedback loops involving mRNA translational components include potential GLD2-mediated polyadenylation of the GLD2 mRNA *via* CPEB1-directed translational control (Rouhana and Wickens 2007), CPEB1-directed translation of CPEB4 to ensure maintenance of CPE-directed translation after GVBD (Igea and Mendez 2010), as well as the recently described Musashi1-mediated polyadenylation and translational control of Musashi1 mRNA translation (Arumugam et al. 2012a).

Future perspectives

Although considerable insight has been shed on the role and regulation of maternal mRNAs during oogenesis and maturation of fertilizable eggs, a number of important questions remain unresolved. First and foremost, the models for temporal control of mRNA translation in response to progesterone have been built from analysis of a very small cohort of characterized target mRNAs (approximately 30). More robust analyses on a genome-wide scale must be undertaken to provide definitive insight into the role, recruitment, and interdependence of separate coregulated mRNA populations (regulons; Keene 2007). Characterization of the global array of mRNA

translational regulation may reveal novel mRNAs controlling cell cycle progression or novel functions for proteins not hitherto implicated in meiotic control. Such detailed studies would also provide unparalleled insight into regulatory element interactions in *cis*, since mRNA 3' UTRs with multiple distinct regulatory elements are likely to represent the norm rather than the exception. Indeed, 10 of the best characterized maturation-regulated *Xenopus* maternal mRNAs all contain multiple regulatory elements, some of which possess opposing regulatory functions during early phases of maturation (MacNicol and MacNicol 2010). At this juncture, little is known about the cofactors necessary for Musashi or Zar2 to mediate translational control. It will be very informative to determine if these RNA-specific binding proteins interact with unique cellular components dedicated to their function only or if any of the coassociated components are also shared with CPEB1 or Pumilio. Given that some of the CPEB1 repressor complex proteins are also components of P-bodies and neuronal and germinal granules (Standart and Minshall 2008), we hypothesize that shared components between distinct RBP could provide a critical bridging activity to enforce the functional integration (possibly via steric hindrance or competition for a limiting component) necessary to orchestrate the extent and timing of translation of target mRNAs containing multiple distinct regulatory elements.

Beyond the oocyte

The lessons learned from analyses of regulated mRNA translation in *Xenopus* oocytes may have broad application to the control of post-fertilization mitotic cell cycles and indeed to the regulation of adult somatic cell function in general. For example, CPEB1 is implicated in the regulation of somatic cell growth, senescence, and malignancy as well as localized neuronal mRNA translation important for synaptic plasticity, learning, and memory (D'Ambrogio et al. 2013; Richter 2010). Many of the control mechanisms characterized in oocytes have been shown to be applicable to CPEB1-dependent control in somatic cells (Hodgman

et al. 2001; Huang et al. 2002; Udagawa et al. 2012). Similarly, Musashi function is implicated in maintaining stem cell self-renewal through repressor function, but some target mRNAs (e.g., p21, a CDK inhibitor [Battelli et al. 2006]) must be derepressed to facilitate differentiation in response to extracellular cues (Erhardt and Pittman 1998; Hughes et al. 2000; Yan and Ziff 1995). An extracellular-dependent switch in Musashi function from a repressor to an activator of target mRNA translation occurs during neural stem cell differentiation (MacNicol et al. 2011) and involves regulated phosphorylation on the conserved C-terminal residues (MacNicol et al. 2013), reflecting the mechanism of progesterone-dependent Musashi translational activation observed during oocyte maturation (Arumugam et al. 2012b). In somatic cells, growing evidence suggests that CPEB1 and Musashi can be present in the nucleus as well as the cytoplasm and may undergo regulated subcellular relocalization (Ernault-Lange et al. 2009; Kaneko and Chiba 2009; Lin et al. 2010; MacNicol et al. 2008; Okano et al. 2002; Rouget et al. 2006; Sakaguchi et al. 2004; Sugiyama-Nakagiri et al. 2006). The nuclear localization of these proteins appears to exert functional cellular consequences as both CPEB1 and Musashi exert control of gene expression in the nucleus, by influencing alternative splicing and miRNA biogenesis (Bava et al. 2013; Cuadrado et al. 2002; Kawahara et al. 2011; Lin et al. 2010). Thus, an important new area for future investigation will be to further examine the role of mRNA translational control factors in regulation of nuclear gene expression (e.g., transcription, alternative polyadenylation, miRNA function, or mRNA export) in addition to their well-documented roles in the cytoplasm.

In sum, the oocyte has provided a wealth of information and in many cases initial mechanistic insights into the molecular underpinnings of regulated mRNA translational control. Further insights into the role, assembly, integration, and regulation of mRNA translational control factors in oogenesis and maturation are likely to provide detailed molecular frameworks and novel insights for understanding the control of gene expression in both germ and somatic cells of vertebrate species, including humans.

Acknowledgments

The work in the MacNicol laboratory was supported by NIH grant RO1 HD35688 and intramural funding support from the UAMS College of Medicine Research Council. We thank Dr M.C. MacNicol for critical reading of the manuscript.

References

- Aguilera A (2005) Cotranscriptional mRNP assembly: from the DNA to the nuclear pore. *Curr Opin Cell Biol* **17**: 242–250.
- Armisen J, Gilchrist MJ, Wilczynska A, Standart N, Miska EA (2009) Abundant and dynamically expressed miRNAs, piRNAs, and other small RNAs in the vertebrate *Xenopus* tropicalis. *Genome Res* **19**: 1766–1775.
- Arumugam K, Wang Y, Hardy LL, MacNicol MC, MacNicol AM (2010) Enforcing temporal control of maternal mRNA translation during oocyte cell cycle progression. *EMBO J* **29**: 387–397.
- Arumugam K, MacNicol MC, MacNicol A (2012a) Autoregulation of Musashi1 mRNA translation during *Xenopus* oocyte maturation. *Mol Reprod Dev* **79**: 553–563.
- Arumugam K, MacNicol MC, Wang Y, et al. (2012b) Ringo/CDK and MAP kinase regulate the activity of the cell fate determinant Musashi to promote cell cycle re-entry in *Xenopus* oocytes. *J Biol Chem* **287**: 10639–10649.
- Ballantyne S, Daniel DLJ, Wickens M (1997) A dependent pathway of cytoplasmic polyadenylation reactions linked to cell cycle control by c-mos and CDK1 activation. *Mol Biol Cell* **8**: 1633–1648.
- Bally-Cuif L, Schatz WJ, Ho RK (1998) Characterization of the zebrafish Orb/CPEB-related RNA binding protein and localization of maternal components in the zebrafish oocyte. *Mech Dev* **77**: 31–47.
- Barnard DC, Ryan K, Manley JL, Richter JD (2004) Symplekin and xGLD-2 are required for CPEB-mediated cytoplasmic polyadenylation. *Cell* **119**: 641–651.
- Barnard DC, Cao Q, Richter JD (2005) Differential phosphorylation controls Maskin association with eukaryotic translation initiation factor 4E and localization on the mitotic apparatus. *Mol Cell Biol* **25**: 7605–7615.
- Battelli C, Nikopoulos GN, Mitchell JG, Verdi JM (2006) The RNA-binding protein Musashi-1 regulates neural development through the translational repression of p21(WAF-1). *Mol Cell Neurosci* **31**: 85–96.
- Bava FA, Eliscovich C, Ferreira PG, et al. (2013) CPEB1 coordinates alternative 3′-UTR formation with translational regulation. *Nature* **495**: 121–125.
- Belloc E, Mendez R (2008) A deadenylation negative feedback mechanism governs meiotic metaphase arrest. *Nature* **452**: 1017–1021.
- Betley JN, Heinrich B, Vernos I, Sardet C, Prodon F, Deshler JO (2004) Kinesin II mediates Vg1 mRNA transport in *Xenopus* oocytes. *Curr Biol* **14**: 219–224.
- Bouvet P, Wolffe AP (1994) A role for transcription and FRGY2 in masking maternal mRNA within *Xenopus* oocytes. *Cell* **77**: 931–941.
- Bouvet P, Matsumoto K, Wolffe AP (1995) Sequence-specific RNA recognition by the *Xenopus* Y-box proteins. An essential role for the cold shock domain. *J Biol Chem* **270**: 28297–28303.
- Braddock M, Muckenthaler M, White MR, et al. (1994) Intron-less RNA injected into the nucleus of *Xenopus* oocytes accesses a regulated translation control pathway. *Nucleic Acids Res* **22**: 5255–5264.
- Cao Q, Richter JD (2002) Dissolution of the maskin-eIF4E complex by cytoplasmic polyadenylation and poly(A)-binding protein controls cyclin B1 mRNA translation and oocyte maturation. *EMBO J* **21**: 3852–3862.
- Cao Q, Padmanabhan K, Richter JD (2010) Pumilio 2 controls translation by competing with eIF4E for 7-methyl guanosine cap recognition. *RNA* **16**: 221–227.
- Castro A, Mandart E, Lorca T, Galas S (2003) Involvement of Aurora A kinase during meiosis I-II transition in *Xenopus* oocytes. *J Biol Chem* **278**: 2236–2241.
- Charlesworth A, Welk J, MacNicol A (2000) The temporal control of Wee1 mRNA translation during *Xenopus* oocyte maturation is regulated by cytoplasmic polyadenylation elements within the 3′ untranslated region. *Dev Biol* **227**: 706–719.
- Charlesworth A, Ridge JA, King LA, MacNicol MC, MacNicol AM (2002) A novel regulatory element determines the timing of Mos mRNA translation during *Xenopus* oocyte maturation. *EMBO J* **21**: 2798–2806.
- Charlesworth A, Cox LL, MacNicol AM (2004) Cytoplasmic polyadenylation element (CPE)- and CPE-binding protein (CPEB)-independent mechanisms regulate early class maternal mRNA translational activation in *xenopus* oocytes. *J Biol Chem* **279**: 17650–17659.
- Charlesworth A, Wilczynska A, Thampi P, Cox LL, MacNicol AM (2006) Musashi regulates the temporal order of mRNA translation during *Xenopus* oocyte maturation. *EMBO J* **25**: 2792–2801.

- Charlesworth A, Yamamoto TM, Cook JM, et al. (2012) *Xenopus laevis* zygote arrest 2 (zar2) encodes a zinc finger RNA-binding protein that binds to the translational control sequence in the maternal Wee1 mRNA and regulates translation. *Dev Biol* **369**: 177–190.
- Colegrove-Otero LJ, Devaux A, Standart N (2005) The *Xenopus* ELAV protein ElrB represses Vg1 mRNA translation during oogenesis. *Mol Cell Biol* **25**: 9028–9039.
- Collier B, Gorgoni B, Loveridge C, Cooke HJ, Gray NK (2005) The DAZL family proteins are PABP-binding proteins that regulate translation in germ cells. *EMBO J* **24**: 2656–2666.
- Cote CA, Gautreau D, Denegre JM, Kress TL, Terry NA, Mowry KL (1999) A *Xenopus* protein related to hnRNP I has a role in cytoplasmic RNA localization. *Mol Cell* **4**: 431–437.
- Cuadrado A, Garcia-Fernandez LF, Imai T, Okano H, Munoz A (2002) Regulation of tau RNA maturation by thyroid hormone is mediated by the neural RNA-binding protein musashi-1. *Mol Cell Neurosci* **20**: 198–210.
- Czaplinski K, Mattaj IW (2006) 40LoVe interacts with Vg1RBP/Vera and hnRNP I in binding the Vg1-localization element. *RNA* **12**: 213–222.
- Czaplinski K, Kocher T, Schelder M, Segref A, Wilm M, Mattaj IW (2005) Identification of 40LoVe, a *Xenopus* hnRNP D family protein involved in localizing a TGF-beta-related mRNA during oogenesis. *Dev Cell* **8**: 505–515.
- Dale L, Matthews G, Tabe L, Colman A (1989) Developmental expression of the protein product of Vg1, a localized maternal mRNA in the frog *Xenopus laevis*. *EMBO J* **8**: 1057–1065.
- D'Ambrogio A, Nagaoka K, Richter JD (2013) Translational control of cell growth and malignancy by the CPEBs. *Nat Rev* **13**: 283–290.
- Davidson E (1986) *Gene Activity in Early Development*, 3rd edn. Academic Press, New York.
- de Moor CH, Richter JD (1997) The Mos pathway regulates cytoplasmic polyadenylation in *Xenopus* oocytes. *Mol Cell Biol* **17**: 6419–6426.
- Dearsly AL, Johnson RM, Barrett P, Sommerville J (1985) Identification of a 60-kDa phosphoprotein that binds stored messenger RNA of *Xenopus* oocytes. *Eur J Biochem/FEBS* **150**: 95–103.
- Dever TE (2002) Gene-specific regulation by general translation factors. *Cell* **108**: 545–556.
- Dickson KS, Bilger A, Ballantyne S, Wickens MP (1999) The cleavage and polyadenylation specificity factor in *Xenopus laevis* oocytes is a cytoplasmic factor involved in regulated polyadenylation. *Mol Cell Biol* **19**: 5707–5717.
- Donnelly N, Gorman AM, Gupta S, Samali A (2013) The eIF2alpha kinases: their structures and functions. *Cell Mol Life Sci* **70**: 3493–3511.
- Dumont JN (1972) Oogenesis in *Xenopus laevis* (Daudin). I. Stages of oocyte development in laboratory maintained animals. *J Morphol* **136**: 153–179.
- Dupre A, Jessus C, Ozon R, Haccard O (2002) Mos is not required for the initiation of meiotic maturation in *Xenopus* oocytes. *EMBO J* **21**: 4026–4036.
- Elisha Z, Havin L, Ringel I, Yisraeli JK (1995) Vg1 RNA binding protein mediates the association of Vg1 RNA with microtubules in *Xenopus* oocytes. *EMBO J* **14**: 5109–5114.
- Erhardt JA, Pittman RN (1998) Ectopic p21WAF1 expression induces differentiation-specific cell cycle changes in PC12 cells characteristic of nerve growth factor treatment. *J Biol Chem* **273**: 23517–23523.
- Ernault-Lange M, Wilczynska A, Harper M, et al. (2009) Nucleocytoplasmic traffic of CPEB1 and accumulation in Crm1 nucleolar bodies. *Mol Biol Cell* **20**: 176–187.
- Ferrell JE, Jr, Machleder EM (1998) The biochemical basis of an all-or-none cell fate switch in *Xenopus* oocytes. *Science* **280**: 895–898.
- Forristall C, Pondel M, Chen L, King ML (1995) Patterns of localization and cytoskeletal association of two vegetally localized RNAs, Vg1 and Xcat-2. *Development* **121**: 201–208.
- Fox CA, Sheets MD, Wickens MP (1989) Poly(A) addition during maturation of frog oocytes: distinct nuclear and cytoplasmic activities and regulation by the sequence UUUUUUAU. *Genes Dev* **3**: 2151–2162.
- Frank-Vaillant M, Haccard O, Thibier C, et al. (2000) Progesterone regulates the accumulation and the activation of Eg2 kinase in *Xenopus* oocytes. *J Cell Sci* **113** (Pt 7): 1127–1138.
- Gebauer F, Richter JD (1996) Mouse cytoplasmic polyadenylation element binding protein: an evolutionarily conserved protein that interacts with the cytoplasmic polyadenylation elements of c-mos mRNA. *Proc Natl Acad Sci U S A* **93**: 14602–14607.
- Gingras AC, Raught B, Sonenberg N (1999) eIF4 initiation factors: effectors of mRNA recruitment to ribosomes and regulators of translation. *Annu Rev Biochem* **68**: 913–963.
- Gingras AC, Raught B, Sonenberg N (2001) Regulation of translation initiation by FRAP/mTOR. *Genes Dev* **15**: 807–826.
- Giorgi C, Moore MJ (2007) The nuclear nurture and cytoplasmic nature of localized mRNPs. *Semin Cell Dev Biol* **18**: 186–193.
- Haghighat A, Mader S, Pause A, Sonenberg N (1995) Repression of cap-dependent translation by 4E-binding protein 1: competition with p220 for binding to eukaryotic initiation factor-4E. *EMBO J* **14**: 5701–5709.

- Hake LE, Richter JD (1994) CPEB is a specificity factor that mediates cytoplasmic polyadenylation during *Xenopus* oocyte maturation. *Cell* **79**: 617–627.
- Harris ME, Bohni R, Schneiderman MH, et al. (1991) Regulation of histone mRNA in the unperturbed cell cycle: evidence suggesting control at two posttranscriptional steps. *Mol Cell Biol* **11**: 2416–2424.
- Hodgman R, Tay J, Mendez R, Richter JD (2001) CPEB phosphorylation and cytoplasmic polyadenylation are catalyzed by the kinase IAK1/Eg2 in maturing mouse oocytes. *Development* **128**: 2815–2822.
- Howard EL, Charlesworth A, Welk J, MacNicol AM (1999) The mitogen-activated protein kinase signaling pathway stimulates mos mRNA cytoplasmic polyadenylation during *Xenopus* oocyte maturation. *Mol Cell Biol* **19**: 1990–1999.
- Hu J, Wang F, Zhu X, Yuan Y, Ding M, Gao S (2010) Mouse ZAR1-like (XM_359149) colocalizes with mRNA processing components and its dominant-negative mutant caused two-cell-stage embryonic arrest. *Dev Dyn* **239**: 407–424.
- Huang YS, Jung MY, Sarkissian M, Richter JD (2002) N-methyl-D-aspartate receptor signaling results in Aurora kinase-catalyzed CPEB phosphorylation and alpha CaMKII mRNA polyadenylation at synapses. *EMBO J* **21**: 2139–2148.
- Huang YS, Kan MC, Lin CL, Richter JD (2006) CPEB3 and CPEB4 in neurons: analysis of RNA-binding specificity and translational control of AMPA receptor GluR2 mRNA. *EMBO J* **25**: 4865–4876.
- Hughes AL, Gollapudi L, Sladek TL, Neet KE (2000) Mediation of nerve growth factor-driven cell cycle arrest in PC12 cells by p53. Simultaneous differentiation and proliferation subsequent to p53 functional inactivation. *J Biol Chem* **275**: 37829–37837.
- Igea A, Mendez R (2010) Meiosis requires a translational positive loop where CPEB1 ensues its replacement by CPEB4. *EMBO J* **29**: 2182–2193.
- Imai T, Tokunaga A, Yoshida T, et al. (2001) The neural RNA-binding protein Musashi1 translationally regulates mammalian numb gene expression by interacting with its mRNA. *Mol Cell Biol* **21**: 3888–3900.
- Kaneko J, Chiba C (2009) Immunohistochemical analysis of Musashi-1 expression during retinal regeneration of adult newt. *Neurosci Lett* **450**: 252–257.
- Karaiskou A, Cayla X, Haccard O, Jessus C, Ozon R (1998) MPF amplification in *Xenopus* oocyte extracts depends on a two-step activation of cdc25 phosphatase. *Exp Cell Res* **244**: 491–500.
- Kawahara H, Okada Y, Imai T, Iwanami A, Mischel PS, Okano H (2011) Musashi1 cooperates in abnormal cell lineage protein 28 (Lin28)-mediated let-7 family microRNA biogenesis in early neural differentiation. *J Biol Chem* **286**: 16121–16130.
- Keady BT, Kuo P, Martinez SE, Yuan L, Hake LE (2007) MAPK interacts with XGef and is required for CPEB activation during meiosis in *Xenopus* oocytes. *J Cell Sci* **120**: 1093–1103.
- Keene JD (2007) RNA regulons: coordination of post-transcriptional events. *Nat Rev Genet* **8**: 533–543.
- Kim JH, Richter JD (2006) Opposing polymerase-deadenylase activities regulate cytoplasmic polyadenylation. *Mol Cell* **24**: 173–183.
- Kolev NG, Huber PW (2003) VgRBP71 stimulates cleavage at a polyadenylation signal in Vg1 mRNA, resulting in the removal of a cis-acting element that represses translation. *Mol Cell* **11**: 745–755.
- Komar AA, Mazumder B, Merrick WC (2012) A new framework for understanding IRES-mediated translation. *Gene* **502**: 75–86.
- Koromilas AE, Lazaris-Karatzas A, Sonenberg N (1992) mRNAs containing extensive secondary structure in their 5' non-coding region translate efficiently in cells overexpressing initiation factor eIF-4E. *EMBO J* **11**: 4153–4158.
- Kurihara Y, Tokuriki M, Myojin R, et al. (2003) CPEB2, a novel putative translational regulator in mouse haploid germ cells. *Biol Reprod* **69**: 261–268.
- Kuwako K, Kakumoto K, Imai T, et al. (2010) Neural RNA-binding protein Musashi1 controls midline crossing of precerebellar neurons through post-transcriptional regulation of Robo3/Rig-1 expression. *Neuron* **67**: 407–421.
- Ladomery M, Wade E, Sommerville J (1997) Xp54, the *Xenopus* homologue of human RNA helicase p54, is an integral component of stored mRNP particles in oocytes. *Nucleic Acids Res* **25**: 965–973.
- Lamphear BJ, Kirchweger R, Skern T, Rhoads RE (1995) Mapping of functional domains in eukaryotic protein synthesis initiation factor 4G (eIF4G) with picornaviral proteases. Implications for cap-dependent and cap-independent translational initiation. *J Biol Chem* **270**: 21975–21983.
- Lantz V, Ambrosio L, Schedl P (1992) The *Drosophila* orb gene is predicted to encode sex-specific germline RNA-binding proteins and has localized transcripts in ovaries and early embryos. *Development* **115**: 75–88.
- Lin CL, Evans V, Shen S, Xing Y, Richter JD (2010) The nuclear experience of CPEB: implications for RNA processing and translational control. *RNA* **16**: 338–348.

- Linnen JM, Bailey CP, Weeks DL (1993) Two related localized mRNAs from *Xenopus laevis* encode ubiquitin-like fusion proteins. *Gene* **128**: 181–188.
- Luitjens C, Gallegos M, Kraemer B, Kimble J, Wickens M (2000) CPEB proteins control two key steps in spermatogenesis in *C. elegans*. *Genes Dev* **14**: 2596–2609.
- Lund E, Liu M, Hartley RS, Sheets MD, Dahlberg JE (2009) Deadenylation of maternal mRNAs mediated by miR-427 in *Xenopus laevis* embryos. *RNA* **15**: 2351–2363.
- Lund E, Sheets MD, Imboden SB, Dahlberg JE (2011) Limiting Ago protein restricts RNAi and microRNA biogenesis during early development in *Xenopus laevis*. *Genes Dev* **25**: 1121–1131.
- Luo X, Nerlick S, An W, King ML (2011) *Xenopus* germline nanos1 is translationally repressed by a novel structure-based mechanism. *Development* **138**: 589–598.
- MacNicol MC, MacNicol AM (2010) Developmental timing of mRNA translation—integration of distinct regulatory elements. *Mol Reprod Dev* **77**: 662–669.
- MacNicol AM, Wilczynska A, MacNicol MC (2008) Function and regulation of the mammalian Musashi mRNA translational regulator. *Biochem Soc Trans* **36**: 528–530.
- MacNicol MC, Cragle CE, MacNicol AM (2011) Context-dependent regulation of Musashi-mediated mRNA translation and cell cycle regulation. *Cell Cycle* **10**: 39–44.
- MacNicol AM, Hardy LL, MacNicol MC (2013) Neural stem and progenitor cell fate transitions require regulation of Musashi1 function (submitted).
- Marzluff WF (1992) Histone 3' ends: essential and regulatory functions. *Gene Express* **2**: 93–97.
- Maton G, Thibier C, Castro A, Lorca T, Prigent C, Jessus C (2003) Cdc2-Cyclin B triggers H3 kinase activation of aurora-A in *xenopus* oocytes. *J Biol Chem* **278**: 21439–21449.
- Matsumoto K, Meric F, Wolffe AP (1996) Translational repression dependent on the interaction of the *Xenopus* Y-box protein FRGY2 with mRNA. Role of the cold shock domain, tail domain, and selective RNA sequence recognition. *J Biol Chem* **271**: 22706–22712.
- McGowan CH, Russell P (1993) Human Wee1 kinase inhibits cell division by phosphorylating p34cdc2 exclusively on Tyr15. *EMBO J* **12**: 75–85.
- McGrew LL, Dworkin-Rastl E, Dworkin MB, Richter JD (1989) Poly(A) elongation during *Xenopus* oocyte maturation is required for translational recruitment and is mediated by a short sequence element. *Genes Dev* **3**: 803–815.
- Meijer HA, Thomas AA (2002) Control of eukaryotic protein synthesis by upstream open reading frames in the 5'-untranslated region of an mRNA. *Biochem J* **367**: 1–11.
- Mendez R, Hake LE, Andresson T, Littlepage LE, Ruderman JV, Richter JD (2000) Phosphorylation of CPE binding factor by Eg2 regulates translation of c-mos mRNA. *Nature* **404**: 302–307.
- Mendez R, Barnard D, Richter JD (2002) Differential mRNA translation and meiotic progression require Cdc2-mediated CPEB destruction. *EMBO J* **21**: 1833–1844.
- Messitt TJ, Gagnon JA, Kreiling JA, Pratt CA, Yoon YJ, Mowry KL (2008) Multiple kinesin motors coordinate cytoplasmic RNA transport on a subpopulation of microtubules in *Xenopus* oocytes. *Dev Cell* **15**: 426–436.
- Minshall N, Reiter MH, Weil D, Standart N (2007) CPEB interacts with an ovary-specific eIF4E and 4E-T in early *Xenopus* oocytes. *J Biol Chem* **282**: 37389–37401.
- Mosquera L, Forristall C, Zhou Y, King ML (1993) A mRNA localized to the vegetal cortex of *Xenopus* oocytes encodes a protein with a nanos-like zinc finger domain. *Development* **117**: 377–386.
- Mowry KL, Melton DA (1992) Vegetal messenger RNA localization directed by a 340-nt RNA sequence element in *Xenopus* oocytes. *Science* **255**: 991–994.
- Mueller PR, Coleman TR, Dunphy WG (1995) Cell cycle regulation of a *Xenopus* Wee1-like kinase. *Mol Biol Cell* **6**: 119–134.
- Murakami MS, Vande Woude GF (1998) Analysis of the early embryonic cell cycles of *Xenopus*; regulation of cell cycle length by *Xe-wee1* and *Mos*. *Development* **125**: 237–248.
- Murakami MS, Copeland TD, Vande Woude GF (1999) *Mos* positively regulates *Xe-Wee1* to lengthen the first mitotic cell cycle of *Xenopus*. *Genes Dev* **13**: 620–631.
- Nakahata S, Katsu Y, Mita K, Inoue K, Nagahama Y, Yamashita M (2001) Biochemical identification of *Xenopus* Pumilio as a sequence-specific cyclin B1 mRNA-binding protein that physically interacts with a Nanos homolog, *Xcat-2*, and a cytoplasmic polyadenylation element-binding protein. *J Biol Chem* **276**: 20945–20953.
- Nakahata S, Kotani T, Mita K, et al. (2003) Involvement of *Xenopus* Pumilio in the translational regulation that is specific to cyclin B1 mRNA during oocyte maturation. *Mech Dev* **120**: 865–880.
- Nakajima Y, Okamoto H, Kubo T (2009) Expression cloning of *Xenopus* zygote arrest 2 (*Xzar2*) as a novel epidermalization-promoting factor in early embryos of *Xenopus laevis*. *Genes Cells* **14**: 583–595.

- Nakajo N, Yoshitome S, Iwashita J, et al. (2000) Absence of *wee1* ensures the meiotic cell cycle in *xenopus* oocytes. *Genes Dev* **14**: 328–338.
- Nebreda AR, Gannon JV, Hunt T (1995) Newly synthesized protein(s) must associate with p34cdc2 to activate MAP kinase and MPF during progesterone-induced maturation of *Xenopus* oocytes. *EMBO J* **14**: 5597–5607.
- Newport J, Kirschner M (1982) A major developmental transition in early *Xenopus* embryos: I. characterization and timing of cellular changes at the midblastula stage. *Cell* **30**: 675–686.
- Novoa I, Gallego J, Ferreira PG, Mendez R (2010) Mitotic cell-cycle progression is regulated by CPEB1 and CPEB4-dependent translational control. *Nat Cell Biol* **12**: 447–456.
- Ohyama T, Nagata T, Tsuda K, et al. (2012) Structure of Musashi1 in a complex with target RNA: the role of aromatic stacking interactions. *Nucleic Acids Res* **40**: 3218–3231.
- Okano H, Imai T, Okabe M (2002) Musashi: a translational regulator of cell fate. *J Cell Sci* **115**: 1355–1359.
- Ota R, Kotani T, Yamashita M (2011) Biochemical characterization of Pumilio1 and Pumilio2 in *Xenopus* oocytes. *J Biol Chem* **286**: 2853–2863.
- Otero LJ, Devaux A, Standart N (2001) A 250-nucleotide UA-rich element in the 3' untranslated region of *Xenopus laevis* Vg1 mRNA represses translation both in vivo and in vitro. *RNA* **7**: 1753–1767.
- Padmanabhan K, Richter JD (2006) Regulated Pumilio-2 binding controls RINGO/Spy mRNA translation and CPEB activation. *Genes Dev* **20**: 199–209.
- Palmer A, Gavin A-C, Nebreda AR (1998) A link between MAP kinase and p34cdc2/cyclin B during oocyte maturation: p90rsk phosphorylates and inactivates the p34cdc2 inhibitory kinase Myt1. *EMBO J* **17**: 5037–5047.
- Pandey NB, Marzluff WF (1987) The stem-loop structure at the 3' end of histone mRNA is necessary and sufficient for regulation of histone mRNA stability. *Mol Cell Biol* **7**: 4557–4559.
- Parker LL, Piwnica-Worms H (1992) Inactivation of the p34cdc2-cyclin B complex by the human WEE1 tyrosine kinase. *Science* **257**: 1955–1957.
- Pascreau G, Delcrois JG, Morin N, Prigent C, Arlot-Bonnemains Y (2008) Aurora-A kinase Ser349 phosphorylation is required during *Xenopus laevis* oocyte maturation. *Dev Biol* **317**: 523–530.
- Pause A, Belsham GJ, Gingras AC, et al. (1994) Insulin-dependent stimulation of protein synthesis by phosphorylation of a regulator of 5'-cap function. *Nature* **371**: 762–767.
- Peter M, Labbe JC, Doree M, Mandart E (2002) A new role for Mos in *Xenopus* oocyte maturation: targeting Myt1 independently of MAPK. *Development* **129**: 2129–2139.
- Pique M, Lopez JM, Foissac S, Guigo R, Mendez R (2008) A combinatorial code for CPE-mediated translational control. *Cell* **132**: 434–448.
- Pratt AJ, MacRae IJ (2009) The RNA-induced silencing complex: a versatile gene-silencing machine. *J Biol Chem* **284**: 17897–17901.
- Reverte CG, Ahearn MD, Hake LE (2001) CPEB degradation during *Xenopus* oocyte maturation requires a PEST domain and the 26S proteasome. *Dev Biol* **231**: 447–458.
- Richter JD (2007) CPEB: a life in translation. *Trends Biochem Sci* **32**: 279–285.
- Richter JD (2010) Translational control of synaptic plasticity. *Biochem Soc Trans* **38**: 1527–1530.
- Richter JD, Lasko P (2011) Translational control in oocyte development. *Cold Spring Harbor Perspect Biol* **3**: a002758.
- Richter JD, Smith LD (1984) Reversible inhibition of translation by *Xenopus* oocyte-specific proteins. *Nature* **309**: 378–380.
- Richter JD, Sonenberg N (2005) Regulation of cap-dependent translation by eIF4E inhibitory proteins. *Nature* **433**: 477–480.
- Rogers GW, Jr, Richter NJ, Lima WF, Merrick WC (2001) Modulation of the helicase activity of eIF4A by eIF4B, eIF4H, and eIF4F. *J Biol Chem* **276**: 30914–30922.
- Rouget C, Papin C, Mandart E (2006) Cytoplasmic CstF-77 protein belongs to a masking complex with cytoplasmic polyadenylation element-binding protein in *Xenopus* oocytes. *J Biol Chem* **281**: 28687–28698.
- Rouhana L, Wickens M (2007) Autoregulation of GLD-2 cytoplasmic poly(A) polymerase. *RNA* **13**: 188–199.
- Rowlands AG, Panniers R, Henshaw EC (1988) The catalytic mechanism of guanine nucleotide exchange factor action and competitive inhibition by phosphorylated eukaryotic initiation factor 2. *J Biol Chem* **263**: 5526–5533.
- Ruiz EJ, Hunt T, Nebreda AR (2008) Meiotic inactivation of *Xenopus* Myt1 by CDK/XRINGO, but not CDK/cyclin, via site-specific phosphorylation. *Mol Cell* **32**: 210–220.
- Sagata N, Oskarsson M, Copeland T, Brumbaugh J, Vande Woude GF (1988) Function of c-mos proto-oncogene product in meiotic maturation in *Xenopus* oocytes. *Nature* **335**: 519–525.
- Sakaguchi H, Yaoi T, Suzuki T, Okano H, Hisa Y, Fushiki S (2004) Spatiotemporal patterns of Musashi1 expression during inner ear development. *Neuroreport* **15**: 997–1001.

- Sanchez R, Marzluff WF (2002) The stem-loop binding protein is required for efficient translation of histone mRNA in vivo and in vitro. *Mol Cell Biol* **22**: 7093–7104.
- Sheets MD, Fox CA, Hunt T, Vande Woude G, Wickens M (1994) The 3'-untranslated regions of c-mos and cyclin mRNAs stimulate translation by regulating cytoplasmic polyadenylation. *Genes Dev* **8**: 926–938.
- Sheets MD, Wu M, Wickens M (1995) Polyadenylation of c-mos mRNA as a control point in *Xenopus* meiotic maturation. *Nature* **374**: 511–516.
- Siekierka J, Mauser L, Ochoa S (1982) Mechanism of polypeptide chain initiation in eukaryotes and its control by phosphorylation of the alpha subunit of initiation factor 2. *Proc Natl Acad Sci U S A* **79**: 2537–2540.
- Smillie DA, Sommerville J (2002) RNA helicase p54 (DDX6) is a shuttling protein involved in nuclear assembly of stored mRNP particles. *J Cell Sci* **115**: 395–407.
- Sonenberg N (2008) eIF4E, the mRNA cap-binding protein: from basic discovery to translational research. *Biochem Cell Biol* **86**: 178–183.
- Standart N, Minshall N (2008) Translational control in early development: CPEB, P-bodies and germinal granules. *Biochem Soc Trans* **36**: 671–676.
- Stebbins-Boaz B, Cao Q, de Moor C, Mendez R, Richter JD (1999) Maskin is a CPEB-associated factor that transiently interacts with eIF-4E. *Mol Cell* **4**: 1017–1027.
- Sugiyama-Nakagiri Y, Akiyama M, Shibata S, Okano H, Shimizu H (2006) Expression of RNA-binding protein Musashi in hair follicle development and hair cycle progression. *Am J Pathol* **168**: 80–92.
- Sun J, Pilch DR, Marzluff WF (1992) The histone mRNA 3' end is required for localization of histone mRNA to polyribosomes. *Nucleic Acids Res* **20**: 6057–6066.
- Tafari SR, Wolffe AP (1993) Selective recruitment of masked maternal mRNA from messenger ribonucleoprotein particles containing FRGY2 (mRNP4). *J Biol Chem* **268**: 24255–24261.
- Tanaka KJ, Ogawa K, Takagi M, Imamoto N, Matsumoto K, Tsujimoto M (2006) RAP55, a cytoplasmic mRNP component, represses translation in *Xenopus* oocytes. *J Biol Chem* **281**: 40096–40106.
- Tannahill D, Melton DA (1989) Localized synthesis of the Vg1 protein during early *Xenopus* development. *Development* **106**: 775–785.
- Theis M, Si K, Kandel ER (2003) Two previously undescribed members of the mouse CPEB family of genes and their inducible expression in the principal cell layers of the hippocampus. *Proc Natl Acad Sci U S A* **100**: 9602–9607.
- Tung JJ, Padmanabhan K, Hansen DV, Richter JD, Jackson PK (2007) Translational unmasking of Emi2 directs cytostatic factor arrest in meiosis II. *Cell Cycle* **6**: 725–731.
- Udagawa T, Swanger SA, Takeuchi K, et al. (2012) Bidirectional control of mRNA translation and synaptic plasticity by the cytoplasmic polyadenylation complex. *Mol Cell* **47**: 253–266.
- Villalba A, Coll O, Gebauer F (2011) Cytoplasmic polyadenylation and translational control. *Curr Opin Genet Dev* **21**: 452–457.
- Voeltz GK, Ongkasuwan J, Standart N, Steitz JA (2001) A novel embryonic poly(A) binding protein, ePAB, regulates mRNA deadenylation in *Xenopus* egg extracts. *Genes Dev* **15**: 774–788.
- Walker J, Minshall N, Hake L, Richter J, Standart N (1999) The clam 3' UTR masking element-binding protein p82 is a member of the CPEB family. *RNA* **5**: 14–26.
- Wang ZF, Ingledue TC, Dominski Z, Sanchez R, Marzluff WF (1999) Two *Xenopus* proteins that bind the 3' end of histone mRNA: implications for translational control of histone synthesis during oogenesis. *Mol Cell Biol* **19**: 835–845.
- Wang L, Eckmann CR, Kadyk LC, Wickens M, Kimble J (2002) A regulatory cytoplasmic poly(A) polymerase in *Caenorhabditis elegans*. *Nature* **419**: 312–316.
- Wang YY, Charlesworth A, Byrd SM, Gregerson R, MacNicol MC, MacNicol AM (2008) A novel mRNA 3' untranslated region translational control sequence regulates *Xenopus* Wee1 mRNA translation. *Dev Biol* **317**: 454–466.
- Watanabe T, Takeda A, Mise K et al. (2005) Stage-specific expression of microRNAs during *Xenopus* development. *FEBS Lett* **579**: 318–324.
- Weeks DL, Melton DA (1987a) A maternal mRNA localized to the animal pole of *Xenopus* eggs encodes a subunit of mitochondrial ATPase. *Proc Natl Acad Sci U S A* **84**: 2798–2802.
- Weeks DL, Melton DA (1987b) A maternal mRNA localized to the vegetal hemisphere in *Xenopus* eggs codes for a growth factor related to TGF-beta. *Cell* **51**: 861–867.
- Weidmann CA, Goldstrohm AC (2012) Drosophila Pumilio protein contains multiple autonomous repression domains that regulate mRNAs independently of Nanos and brain tumor. *Mol Cell Biol* **32**: 527–540.
- Welk J, Charlesworth A, Smith GD, MacNicol AM (2001) Identification of the gene encoding human cytoplasmic polyadenylation element binding protein. *Gene* **263**: 113–121.

- Wickens M, Bernstein DS, Kimble J, Parker R (2002) A PUF family portrait: 3'UTR regulation as a way of life. *Trends Genet* **18**: 150–157.
- Wilczynska A, Minshall N, Armisen J, Miska EA, Standart N (2009) Two Piwi proteins, Xiwi and Xili, are expressed in the *Xenopus* female germline. *RNA* **15**: 337–345.
- Wilhelm JE, Vale RD, Hegde RS (2000) Coordinate control of translation and localization of Vg1 mRNA in *Xenopus* oocytes. *Proc Natl Acad Sci U S A* **97**: 13132–13137.
- Wilkie GS, Gautier P, Lawson D, Gray NK (2005) Embryonic poly(A)-binding protein stimulates translation in germ cells. *Mol Cell Biol* **25**: 2060–2071.
- Wormington M, Searfoss AM, Hurney CA (1996) Overexpression of poly(A) binding protein prevents maturation-specific deadenylation and translational inactivation in *Xenopus* oocytes. *EMBO J* **15**: 900–909.
- Wu X, Viveiros MM, Eppig JJ, Bai Y, Fitzpatrick SL, Matzuk MM (2003) Zygote arrest 1 (Zar1) is a novel maternal-effect gene critical for the oocyte-to-embryo transition. *Nat Genet* **33**: 187–191.
- Yan G, Ziff EB (1995) NGF regulates the PC12 cell cycle machinery through specific inhibition of the Cdk kinases and induction of cyclin D1. *J Neurosci* **15**: 6200–6212.
- Yisraeli JK, Sokol S, Melton DA (1990) A two-step model for the localization of maternal mRNA in *Xenopus* oocytes: involvement of microtubules and microfilaments in the translocation and anchoring of Vg1 mRNA. *Development* **108**: 289–298.
- Yoon YJ, Mowry KL (2004) *Xenopus* Staufen is a component of a ribonucleoprotein complex containing Vg1 RNA and kinesin. *Development* **131**: 3035–3045.
- Zhang S, Williams CJ, Wormington M, Stevens A, Peltz SW (1999) Monitoring mRNA decapping activity. *Methods* **17**: 46–51.

4

Polarity of *Xenopus* Oocytes and Early Embryos

Malgorzata Kloc

Department of Surgery, Houston Methodist Research Institute and Houston Methodist Hospital, Houston, TX

Abstract: The *Xenopus* oocyte/egg contains maternal information (factors) stored in the form of RNAs and proteins, which are necessary and sufficient for cell proliferation after fertilization and early development of the embryo. A large subpopulation of these maternal molecules has a polarized distribution along the animal–vegetal (A–V) axis within the oocyte cytoplasm. Polarity along the A–V axis develops during the elaborate process of oogenesis. It is maintained during egg maturation, fertilization, and subsequent cortical rotation and is required for the developmental transformation of the animal hemisphere into the ectodermal fate (future epidermis and neural cells), the vegetal hemisphere into the endodermal fate (gut) and the germ cell fate, and the marginal zone between into the mesodermal fate (muscle, bone, and blood). In this review, we will describe the factors, mechanisms, developmental functions, and consequences of *Xenopus* oocyte/egg polarity.

Oocyte polarity and embryonic axes

The animal body plan is determined by embryonic axes that are established prior to and soon after fertilization (Prodon et al. 2004; Heasman 2006). In *Xenopus*, the first axis to develop, during oogenesis, is the animal–vegetal (A–V) axis of the egg and cleaving embryo that specifies the developmental fate of the three primary germ layers, the ectoderm, endoderm, and mesoderm, in the embryo. The ectoderm (which differentiates to form the epidermis and the nervous system) will develop from the animal hemisphere, the

endoderm (which differentiates to form the gut and the lung epithelium) and primordial germ cells (PGCs) will develop from the vegetal hemisphere, and the mesoderm (which differentiates to form the muscle, blood, and bone) will develop from the equatorial or marginal zone (located between the animal and vegetal zones) when induced by signals emanating from the vegetal hemisphere and, partially, by maternal determinants localized to the vegetal hemisphere (Dale and Slack 1987; Gard 1995; Stennard et al. 1996; Zhang and King 1996; Heasman 1997; King et al. 1999; Kofron et al. 1999). In addition to germ layer

specification, the A–V axis also specifies the prospective dorsal side of the embryo because the vegetal hemisphere of the egg contains dorsal determinants. Shortly after fertilization, the egg cortex rotates 30° relative to the underlying cytoplasm (Vincent and Gerhart 1987; Gerhart et al. 1989). Cortical rotation translocates vegetally located determinants and dorsalizing activity toward the equatorial/marginal layer of the cytoplasm. This process subsequently activates the dorsal program, establishes the presumptive dorsal side of the embryo, and establishes the dorsal–ventral (D–V) embryonic axis, which ultimately dictates the orientation of the anterior–posterior (A–P) axis (Elinson and Holowacz 1995; Kageura 1997; Weaver and Kimelman 2004; Tao et al. 2005). Interestingly, not only the D–V axis-determining process but also the chiral properties of the egg cortex are linked to the emergence of the left–right (L–R) axis that influences the morphological asymmetries of the heart and other internal organs (see section “Maternal determination of planar and basolateral polarity and L–R asymmetry” and Danilchik et al. 2006).

Development of A–V polarity during oogenesis

In *Xenopus laevis*, formation of oocytes occurs within the ovary of stage 62–66 postmetamorphic, sexually differentiated froglets. Similar to many other vertebrates and invertebrates, the *Xenopus* oocyte is the product of four synchronous mitotic divisions of a single precursor cell (cystoblast), resulting in the formation of a cyst (nest/cluster) of 16 clonal oogonial cells (cystocysts) interconnected by intercellular bridges or ring canals (Figure 4.1) (Koch and King 1969; Mahowald 1971; Pepling et al. 1999, reviewed by de Cuevas et al. 1997; Kloc et al. 2004a). Although the importance of maintaining these intercellular bridges is not fully understood, they most likely facilitate the exchange of developmentally important molecules and mitochondria between the cells of the cyst (Fawcett et al. 1959; Gondos and Zamboni 1969; Mahowald 1971; Buning 1994; Cox and Spradling 2003, 2006; Kloc et al. 2004a, reviewed by King et al. 1982; de Cuevas

et al. 1997; Pepling et al. 1999; Deng and Lin 2001). After the completion of the last (fourth) mitotic division, all of the oogonia within the cysts (Figure 4.1), still interconnected by cytoplasmic bridges, synchronously enter prophase of the first meiotic division and become oocytes.

The oocytes progress through the leptotene, zygotene, and early pachytene phases of the first meiotic prophase in complete synchrony. In late pachytene, the invading prefollicular cells rupture the bridges and separate individual oocytes, which subsequently develop asynchronously (Al-Mukhtar and Webb 1971; Coggins 1973; Tourte et al. 1981; Hausen and Riebesell 1991; Kloc et al. 2004a). The first sign of polarity, which is detectable by the invariable location of centrioles with respect to the cytoplasmic bridge, is already visible in the oogonia following the first mitotic division within the cyst (two cell cyst; Figure 4.1) (Kloc et al. 2004a). This polarity is maintained during the consecutive oogonial divisions and subsequent growth of the oocyte and foreshadows the polarity along the A–V axis of the full-grown (stage VI) *Xenopus* oocyte. Therefore, the position of the cytoplasmic bridge and centrioles designates the position of the vegetal hemisphere in the full-grown oocyte (Kloc et al. 2004a). Light and electron microscopy analysis and three-dimensional reconstructions of a developing ovarian cyst in *Xenopus* showed that the pair of centrioles, which in all oogonia are consistently positioned polarly, i.e., in the vicinity of the cytoplasmic bridges, organizes the formation of the premitochondrial cloud (PMC) that precedes the mitochondrial cloud (Balbiani body [Bb]; Figure 4.2) that is consistently vegetally located in the oocytes (Figures 4.1, 4.2, and 4.3) (Heasman et al. 1984; Kloc et al. 2004a, b). In addition to the centrally located centrioles, the PMC contains multiple mitochondria and mitochondrial (intermitochondrial) cement that is the precursor of the germ cell determinant, the germinal granules (Kloc et al. 2004a, b). Interestingly, during the oogonial divisions, the mitochondrial cement does not disperse but remains attached to the mitochondria, and together, they segregate toward the spindle poles (Kloc et al. 2004a). After separating from

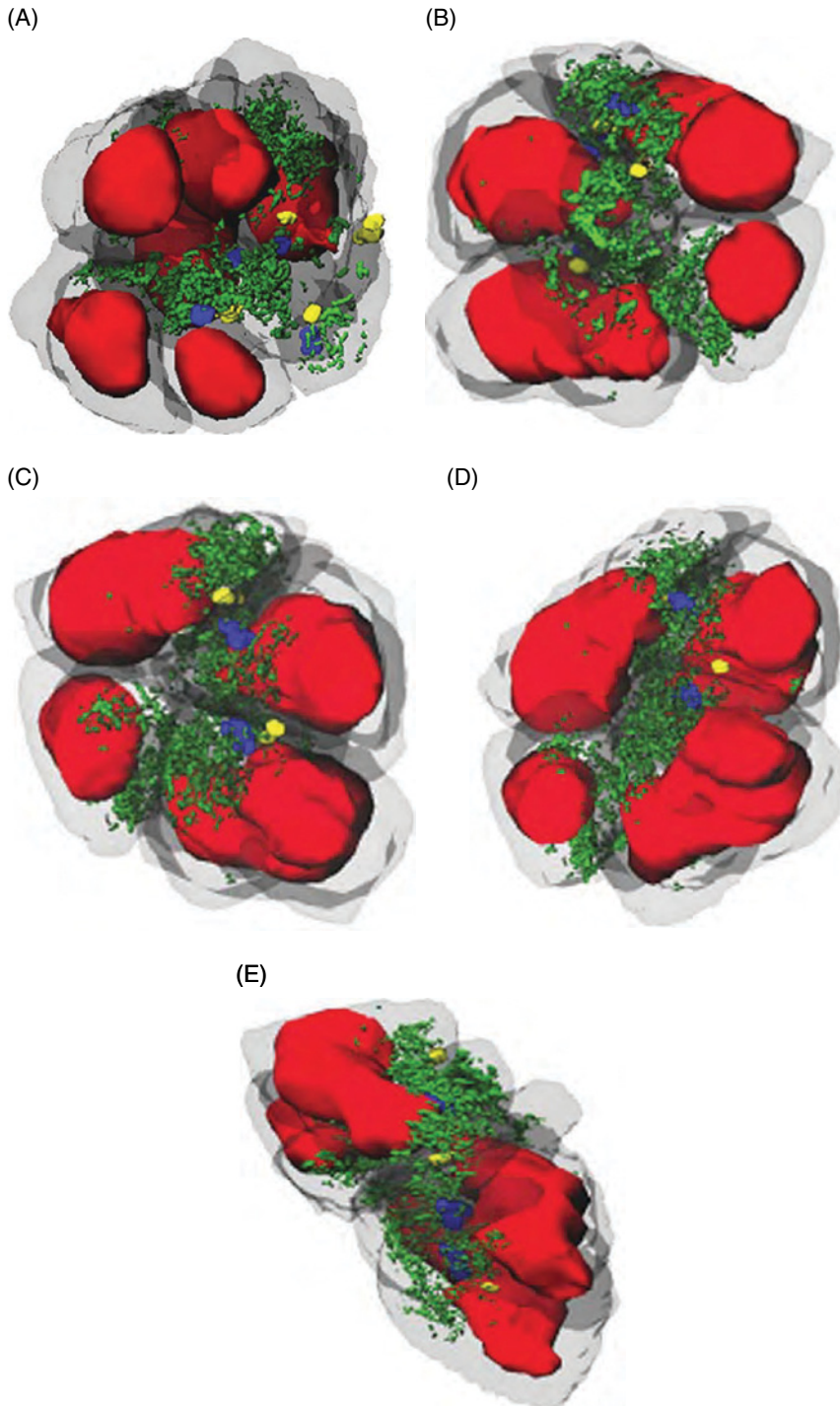


Figure 4.1 Three-dimensional reconstruction of interphase cysts. Two different eight-cell cysts with six nuclei visible. Cyst 1 (A) and four different views of cyst 2 (B–E). Cytoplasm is gray, nuclei are red, mitochondria of PMC are green, centrioles are blue, and ring canals are yellow. In cyst 1, five ring canals and four centrioles near the PMC and ring canals are visible. Spatial relationships between mitochondria, centrioles, and ring canals are visible in all reconstructions. Also note the constant distance ($2\ \mu\text{m}$) between the centrioles and ring canals in all cystocytes (see text). PMC, ring canals, and centrioles face each other and are located centripetally in “the rosette” conformation (see text). These reconstructions were from 38 serial ultrathin sections similar to the section shown in Figure 1B in Kloc et al. (2004a). Reprinted from Kloc et al. (2002) © with permission from Elsevier. To see a color version of this figure, see Plate 9.

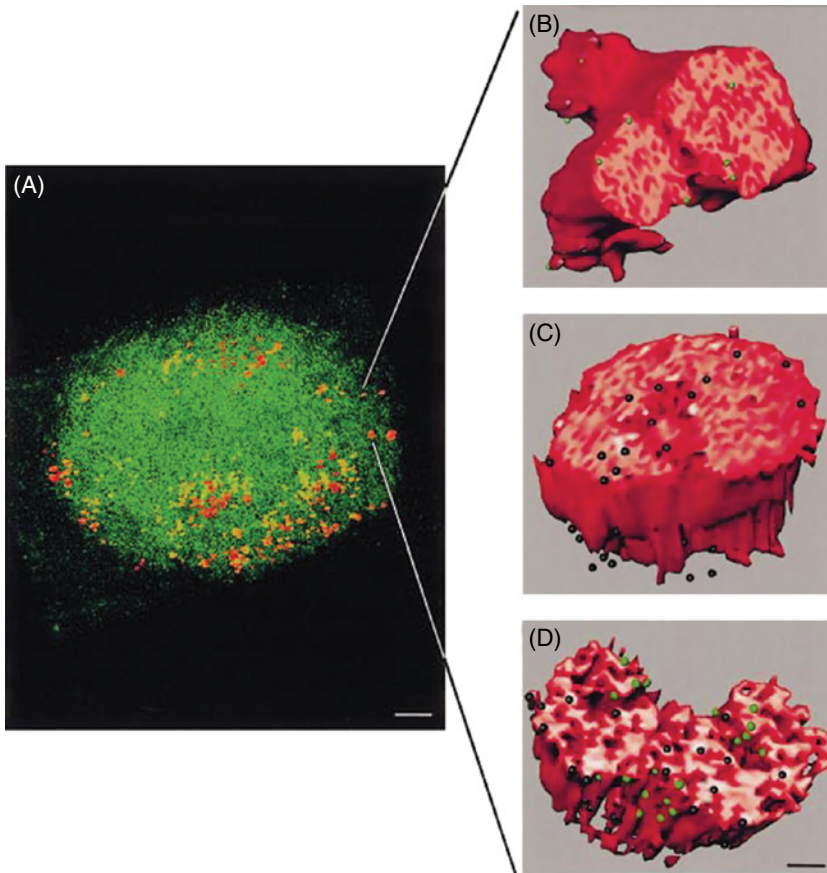


Figure 4.2 Three-dimensional ultrastructural reconstruction of mitochondrial cloud and germinal granules in stage I oocyte. (A) The mitochondrial cloud was reconstructed from 21 serial electron microscopy (EM) sections. The cloud is a sphere composed of thousands of mitochondria (green speckles) and germinal granules (red spheres). Germinal granules are concentrated in the form of a ring in the METRO region that is the part of the cloud facing the vegetal pole and are excluded from the center of the cloud. The oocyte nucleus, not visible in the picture, is above, and the vegetal pole of the oocyte is below the plane of the picture. (B and D) The half sections of three germinal granules from a mitochondrial cloud similar to the one shown in (A). The images were reconstructed from four serial sections of oocytes hybridized *in situ* with Xpat (B and D) and Xcat2 (C and D) antisense RNA probes. The Xpat RNA (green dots) is predominantly on the granule periphery with a small portion localized internally, while the majority of Xcat2 (black dots) is sequestered internally in the granule. For better clarity of the image, the original silver-enhanced gold label was replaced (using proper logarithm and computational programs; see Materials and Methods in Kloc et al. 2002) with uniform-sized dots. The bar is equal to 4.5 μm in (A) and 250 nm in (B–D). Reprinted from Kloc et al. (2004) © with permission from Elsevier. To see a color version of this figure, see Plate 10.

the cysts, the stage I oocytes are strikingly asymmetrical and polar; the nucleus is located in the animal hemisphere and the mitochondrial cloud in the vegetal hemisphere. At this stage, the mitochondrial cloud contains approximately half a million mitochondria and germinal granules, which are located at the vegetal tip of the cloud (Figure 4.2) (Kloc et al. 1996, 1998, 2001a, b, 2004a, b).

Subsequently, the oocytes (stages II–VI) enter the vitellogenic stage of growth that adds another element to the A–V polarity, unequal distribution of yolk platelets and (in the wild-type frog) pigment. During oocyte growth, the mitochondrial cloud fragments and transports mitochondria and germinal granules toward the vegetal pole (Figure 4.3). In full-grown stage VI oocytes, the heavily

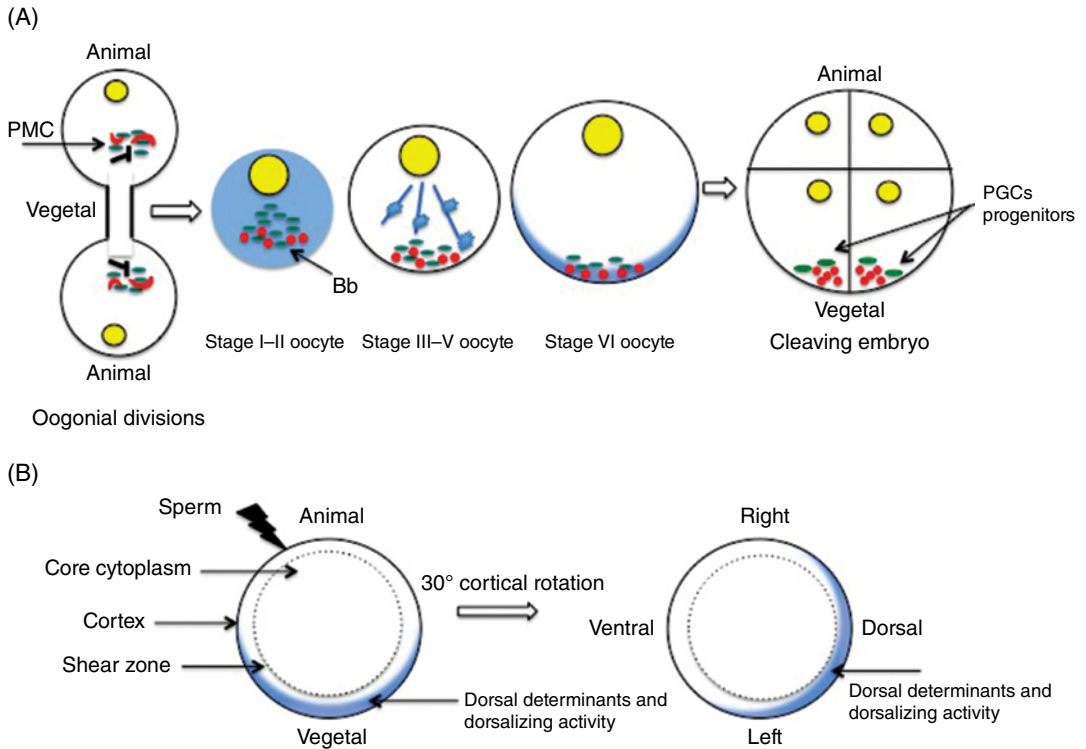


Figure 4.3 Polarity and axes formation during oogenesis, fertilization, and early cleavage. (A) During oogonial divisions, the PMC (the aggregate of mitochondria and mitochondrial cement containing various early pathway-localized RNAs) is located around the centrioles (black rods), which in all oogonia are invariably facing the cytoplasmic bridges that mark the presumptive vegetal pole of the oocyte. There are four synchronous oogonial divisions (for simplicity, only the first division is shown here) resulting in the formation of a nest of 16 oocytes connected by cytoplasmic bridges. During early (stage I to II) oogenesis, the early pathway-localized RNAs and germinal granules are concentrated at the vegetal tip of the mitochondrial cloud (Bb) that is always facing the vegetal pole of the oocyte. In contrast, at this stage of oogenesis, the late pathway RNAs, such as Vg1, are dispersed within the ooplasm. Between stages III and V of oogenesis, fragmentation of the mitochondrial cloud delivers germinal granules and early pathway RNAs to the vegetal cortex, while the late pathway RNAs (shown as clouds) are vegetally mobilized via microtubules (shown as rods). In full-grown stage VI oocytes, germinal granules and their resident early pathway RNAs are anchored at the vegetal cortex, and the late pathway RNAs are concentrated in the vegetal hemisphere. During cleavage, germinal granules and their resident RNAs segregate to vegetal blastomeres, which are the progenitors of PGCs. (B) After fertilization, the *Xenopus* egg contains a dense central cytoplasm surrounded by a shear zone of less dense cytoplasm containing the vegetally localized late pathway RNAs and dorsaling activity (shown as crescent). The cortex rotates 30° relative to the core cytoplasm, displacing dorsal determinants and dorsaling activity toward the presumptive dorsal region where they interact (see Weaver and Kimelman, 2004, for review) to specify the dorsal part of the embryo. The D–V axis-determining process acts in conjunction with the chiral properties of the egg cortex to form the L–R axis (see Danilchik et al. 2006).

pigmented animal hemisphere contains the nucleus and very small amounts of small yolk platelets, and the nonpigmented (or slightly pigmented) vegetal hemisphere contains the majority of the yolk and the germinal granules anchored via cytokeratin filaments (Kloc et al. 2001a, b, 2002, 2005, 2007) and actin meshwork (Alarcón and Elinson 2001) at the cortex of the vegetal pole.

Vegetal hemisphere maternal factors

In *Xenopus*, zygotic transcription of mRNAs begins only after the 12 cell divisions during the midblastula transition (MBT). Thus, early development completely relies on the maternal transcripts and proteins accumulated in the oocyte. The *Xenopus* stage VI oocyte contains approximately 10,000 maternal transcripts.

Recently, comprehensive microarray analysis of RNAs isolated from the vegetal cortices of *Xenopus* oocytes indicates that at least 275, approximately 2–3% of the total maternal transcripts, are vegetally localized (Cuykendall and Houston 2010). The identified vegetally localized RNAs present in *Xenopus* oocytes can be divided into three distinct groups based on the mode of localization and function: (i) RNAs localized in early oogenesis (pre-stage I to stage II oocytes) in the Bb and transported to the vegetal cortex via the messenger transport organizer (METRO) pathway; the majority of these RNAs are involved in germ plasm function, germ cell development, and migration (Figure 4.3) (Kloc et al. 1996, 1998; Kloc and Etkin 2005). (ii) RNAs involved in the patterning of embryonic germ layers (King et al. 1999, 2005; Kloc et al. 2002), which are localized later in oogenesis via microtubules and cytoskeletal motors (Figure 4.3) (Betley et al. 2004; King et al. 2005; Bullock et al. 2006; Bullock 2007; Messitt et al. 2008; Gagnon and Mowry 2010; Singer 2008). (iii) RNAs that share features of both METRO and late pathway localization and function and are referred to as intermediate transport pathway RNAs (Chan et al. 1999; Zearfoss et al. 2004). Further description of RNAs localized in *Xenopus* oocytes can be found in Chapters 2 (by J. Deshler) and 5 (by M. L. King) of this volume.

The following RNAs have been identified in these three groups.

Early pathway-localized RNAs

Nanos-like gene, *nanos1* (previously called *xcat2*), is a translational repressor believed to repress endoderm fate mRNAs in PGCs before they exit the endoderm (Lai et al. 2011). *Dazl*, a germ cell-specific translational regulator, is involved in the migration and differentiation of PGCs (Houston and King 2000) and, due to homology with zebrafish *Dazl*, is predicted to relieve miRNA-mediated repression of germline mRNAs by controlling poly(A) tail length (Takeda et al. 2009). *DEADSouth* encodes a DDX25 DEAD-box RNA helicase and is required for proper distribution of germ plasm in dividing PGCs during gastrulation

(Yamaguchi et al. 2012). *Xpat* mRNA and protein are localized to the germ plasm. The *Xpat* protein plays a role in germ plasm formation, and its ectopic expression induces the formation of germ plasm-like structures that are able to recruit mitochondria, which are the common components of naturally occurring germ plasm (Hudson and Woodland 1998; Machado et al. 2005). *Germes* encodes a protein that interacts with dynein light chain motor, organizes the germ plasm, and regulates germ plasm function (Berekelya et al. 2003, 2007). *Xotx1* is a homeobox gene related to the *Drosophila* gene orthodenticle that is involved in head development in the embryo (Andreazzoli et al. 1997; Pannese et al. 2000). *Hermes* encodes an RNA-binding protein that degrades within a few hours during oocyte maturation, and it functions during oocyte maturation to regulate the cleavage of specific vegetally derived cell lineages (Zearfoss et al. 2004). In addition, Song et al. (2007) showed that the *Hermes* protein negatively regulates at least three target mRNAs: *Ringo/Spy*, *Xcat2*, and *Mos*. *Ringo/Spy* and *Mos* are known to function in oocyte maturation, whereas *Ringo/Spy* and *Xcat2* mRNA colocalize with *Hermes* in the germ plasm, suggesting that *Hermes* functions in both oocyte maturation and germ cell development. *Wnt11* and *trim36*, which encode a ubiquitin ligase of the Tripartite motif-containing (Trim) family, are localized to the germ plasm and are required for the formation of the embryonic dorsal axis (Tao et al. 2005; Cuykendall and Houston 2009). *Xnif* encodes the neuron-specific *Xenopus* intermediate filament protein (Claussen et al. 2004). *Xcad2* encodes an organizer-specific homeobox transcription factor (Sindelka et al. 2010). *Grip2* mRNA, localized to the germ plasm, encodes a conserved PDZ-domain protein that functions in PGC development and migration (Claussen et al. 2011). *Exd2*, a novel exonuclease domain encoding mRNA of unknown function, was recently identified to be localized to the germ plasm (Cuykendall and Houston 2010). The same authors also identified a subpopulation of localized mRNAs encoding growth factor receptors such as *fgfr2*, *igfr1b*, and members of the bone morphogenetic protein (BMP) signaling pathway, *alk2*, *tob2*, and *madh2*/

smad7, which suggests a role for maternal growth factor signaling in oogenesis or early development (Cuykendall and Houston 2010). Interestingly, the group of early METRO pathway-localized RNAs also contains non-coding RNAs, of unknown function, such as *X. laevis* short interspersed repeat transcripts Xlsirts (Kloc et al. 1993) and germ plasm-transcribed locus 1 (gptl1) (Cuykendall and Houston 2010).

Late pathway-localized RNAs

Vg1 (TGF-beta family member); VegT (T-box transcription factor); Otx1 (orthodenticle homeobox) (reviewed by King et al. 2005; Kloc and Etkin 2005, and the chapters by M. L. King (Chapter 5) and J. Deshler (Chapter 2) in this volume); Xvelo1, function unknown (Claussen and Pieler 2004); Eg6, related to ascidian maternal mRNA posterior end mark-5 (PEM-5); and Spire, a *Drosophila* protein required to establish D-V and A-P axes of polarity and recently described as an actin nucleation factor (Le Goff et al. 2006) are all vegetally localized mRNAs. Eg6 mRNA is vegetally localized in the egg and at the posterior vegetal end of developing embryos; its protein may act in actin nucleation (Le Goff et al. 2006). The late pathway-localized transcripts localize via microtubules and molecular motors (Messitt et al. 2008). Various vegetally localized proteins, which facilitate transport and/or vegetal cortex anchoring of these mRNAs, have been identified. The Staufen protein, XStau1, is concentrated in the vegetal cortical region of the oocyte and is partially colocalized with the subcortical endoplasmic reticulum (ER). Staufen proteins are phosphorylated during oocyte maturation, which coincides with the release of localized mRNAs such as Vg1 from their cortical location. These findings suggest that Staufen proteins are involved in anchoring these RNAs to specific ER-rich domains in the vegetal cortex (Allison et al. 2004). Arthur et al. (2009) identified *Xenopus* Elr-type proteins, homologs of Hu/ELAV proteins, as novel components of the vegetal mRNA localization machinery. *Xenopus* Elr-type proteins

bind to the vegetal localization elements (VLEs) of mRNAs, and they form complexes with Staufen and Vera (Vg1RBP; Git and Standart 2002).

Intermediate pathway-localized RNAs

Fatvg/adipophilin (adfp) encodes a vesicular trafficking protein (Chan et al. 1999, 2001, 2007). Fatvg loss of function stabilizes the dorsalizing factor β -catenin at the vegetal pole and inhibits the proper localization of germ cell determinants. This is coincident with the inhibition of cortical rotation and abnormal aggregation in the germ plasm (Chan et al. 2007). Dead end (dnd) encodes an RNA-binding protein and is required for the dorsal migration of PGCs (Horvay et al. 2006). Centroid mRNA encoding a DEAD-box RNA helicase is present in the germ plasm at the surface of germinal granules, suggesting that centroid is involved in the regulation of germ plasm-stored mRNPs and/or germ plasm function (Kloc and Chan 2007).

Vegetal cortex

The cortex of a full-grown stage VI *Xenopus* oocyte contains a complex network of cytokeratin and actin filament cytoskeleton (Elinson et al. 1993; Forristall et al. 1995; Alarcon and Elinson 2001; Heasman et al. 2001; Kloc et al. 2002, 2005, 2007; Clarke and Allan 2003), which gradually increases in intricacy during oogenesis (Kloc et al. 2005). The cytokeratin and actin filaments of the vegetal cortex have a very unique role; they anchor vegetally localized RNAs and germinal granules in their proper location (King et al. 1999; Houston and King 2000; Kloc et al. 2002, 2005; Kloc 2009). Experimentally disrupting the integrity of this cytoskeletal network displaces vegetally localized mRNAs and causes abnormal fusion of germinal granules that lead to their aberrant segregation during cleavage, which in turn reduces or causes the complete disappearance of PGCs in the embryo (Kloc et al. 2005, 2007). Surprisingly, the integrity of the actin and

cytokeratin network in the vegetal cortex of the *Xenopus* oocyte depends on the structural function of several coding and noncoding RNAs. Using an antisense deoxynucleotide depletion method, Kloc (2009), Kloc et al. (2005), and Chan et al. (1999, 2001, 2007) showed that VegT and Fatvg mRNAs and noncoding Xsirts RNA are necessary for the integrity of cytokeratin and actin in the vegetal cortex. The removal of VegT mRNA and Xsirts results in the collapse of the cytokeratin network; release and delocalization of Veg, Wnt11, and Bicaudal-C mRNAs from the oocyte cortex; and fusion of the germinal granules (Kloc and Etkin 1994; Heasman et al. 2001; Kloc et al. 2005, 2007). Interestingly, the injection of exogenous (synthetic) VegT RNA into VegT RNA-depleted oocytes is able to rescue the collapse of the cytokeratin network and reconstitute the cytokeratin network (Kloc et al. 2005). Control experiments using anti-VegT morpholino oligonucleotides (which block translation but leave mRNA intact) reconfirmed that the structural function of VegT mRNA depends on the mRNA itself and does not involve VegT protein (Heasman et al. 2001; Kloc et al. 2005). In addition, depletion of another localized coding RNA, Fatvg mRNA (Chan et al. 1999, 2001, 2007), also results in dramatic changes causing the hyperpolymerization of not only cytokeratin but also actin filaments (Kloc 2009). This, in turn, affects the distribution of germinal granules and disrupts the normal formation of germ cells in the embryos (Chan et al. 2001, 2007). Recent studies showed that VegTm RNA contains cytokeratin polymerization and depolymerization signals (Kloc et al. 2011a). Using the molecular beacons technology (Bratu et al. 2003), Kloc et al. (2005) showed that Xsirts, VegT, and Fatvg RNAs are integrated into the cytoskeleton and have unique localization patterns on cytokeratin filaments. All of these findings demonstrate a novel structural role for localized coding and noncoding RNAs in the organization of cytokeratin and actin cytoskeleton in the vegetal cortex of the *Xenopus* oocyte (Kloc 2008, 2009; Dobrzynski et al. 2011; Kloc et al. 2011b).

Animal hemisphere maternal factors

There is a plethora of mRNAs and proteins localized in the animal hemisphere of *Xenopus* oocytes (Mowry and Cote 1999; Sindelka et al. 2008). It is generally believed that animal localization in the oocyte predicts the localization and function of these molecules in animal blastomeres or even during gastrulation, where they participate in the embryonic germ layer and D–V axis specification (Cao et al. 2007; Imbrie et al. 2012), cell polarity (Ossipova et al. 2002), and cell signaling (Christian et al. 1991). The timing of animal localization and spatial distribution within the animal hemisphere differs widely between different factors. Some factors such as CK2 α transcript (encoding a kinase modulating Wnt/ β -catenin signaling during dorsal axis specification) are localized early in oocyte development (Imbrie et al. 2012), whereas others such as Xbub3 (a homolog of the human mitotic checkpoint gene hBub3), Xoom (encoding a membrane protein), Pabp (encoding poly(A) binding protein), and ets-1 and ets-2 (encoding transcription factors) are localized during later stages of oogenesis (Schroeder and Yost 1996; Meyer et al. 1997; Goto and Kinoshita 1999; Hasegawa et al. 1999) or such as XG β 1 (an mRNA coding for a transducing protein) only in a mature oocyte (Devic et al. 1996). Certain factors, such as An3 (encoding an ATP-dependent RNA helicase) (Gururajan et al. 1994; Gururajan and Weeks 1997), are ubiquitously distributed within the cytoplasm of the entire animal hemisphere, and some are temporarily or permanently restricted to the perinuclear region (Xbub3) (Goto and Kinoshita 1999) or the animal subcortical layer (ets-1 and ets-2) (Meyer et al. 1997) of the oocyte. In some instances, both the transcript and its protein are animally located (Xoom) (Hasegawa et al. 1999, 2001), and in other cases (XIP3R mRNA encoding an IP3 receptor) (Kume et al. 1993), only the protein is restricted to the animal pole of the oocyte. This temporal and spatial variability suggests the presence and involvement of diverse, and still unknown, mechanisms responsible for animal localization of different molecules. For a long time, it was commonly believed that the

localization of molecules at the animal pole is passive and occurs through a default mechanism, i.e., accumulating at the vegetal pole yolk pushes molecules toward the comparatively “yolk-less” animal pole. However, the different animal localization patterns of different molecules and the experimental results on CK2 α mRNA, which indicate that its animal localization requires both the coding and 3' UTRs (Imbrie et al. 2012), suggest the involvement of active transport. The presence of CK2 α mRNA localization signals in the coding and noncoding region contrasts the localization signals used by vegetally localized RNAs that are restricted to the 3' UTR sequences (Chan et al. 1999; Shahbadian and Chartrand 2012; and the Chapters 2 and 5 by M. L. King and J. Deshler in this volume). Further studies are needed to establish if the localization signals present in CK2 α mRNA are shared by other anally localized transcripts.

Historically, the majority of published data on the localization of various vegetally or anally localized RNAs and proteins in *Xenopus* oocytes have been acquired from *in situ* hybridization and immunostaining analyses on whole or sectioned oocytes or through analysis of expression levels in the cytoplasm isolated from the animal or vegetal part of the oocyte. These data indicate that there is a precise distribution of these factors in their prospective (animal or vegetal) hemispheres. However, recently, Sindelka et al. (2008) used a more sophisticated method of subcellular expression profiling and quantification of mRNA within a single *Xenopus* oocyte. They used real-time PCR tomography to assess the polar distribution of 18 known RNAs, which were previously found to be vegetally or anally localized by *in situ* hybridization. They dissected each oocyte into thirty-five 30 μ m sections (containing approximately 75 ng of total RNA per section) and assessed the level of the studied RNAs in each section. This analysis showed that extreme polarization, where RNAs are categorically located at either pole, of both animal and vegetal genes visualized by *in situ* hybridization techniques does not apply to all RNAs. However, there was a distinct bias and all “animal” RNAs were preferentially located at the animal hemisphere and

“vegetal” RNAs at the vegetal hemisphere; some of the RNAs formed variably steep gradient distributions along the A–V axis, which was undetectable by *in situ* hybridization. These authors note that using even thinner (10 μ m) slices would enable higher resolution and more accurate profiles of localized RNA distribution within the oocytes.

Asymmetry of inorganic maternal factors

In addition to polar distribution of RNAs and proteins, there is also distinct asymmetry in the distribution of inorganic compounds, such as various ions and metals, in the *Xenopus* oocyte. For example Ca-activated chloride (Cl) channels are highly enriched in the animal hemisphere of the oocyte (Machaca and Hartzell 1998). Although the exact physiological function of asymmetrical distribution of these channels is not known, their preferential concentration at the animal pole and their activation during fertilization (see references in Busa et al. 1985) may play a role in cortical granule exocytosis to block polyspermy. Various metals are also asymmetrically distributed. Metals that form the active sites of redox sensors, enzymes, and transcription factors are indispensable for normal cell function. Recently, Popescu et al. (2007) used highly sophisticated X-ray synchrotron fluorescence analysis to demonstrate that the animal pole of a stage VI *Xenopus* oocyte is highly enriched in iron, zinc, and copper, and this finding suggests that the animal pole may serve as a metal reservoir for the developing embryo.

Maternal determination of planar and basolateral polarity and L–R asymmetry

All multicellular organisms have two types of cell polarity. Planar cell polarity (PCP) describes the polarization of a field of cells within the plane of a cell sheet and also the orientation of organelles and specialized structures such as cilia or pseudopodia within these cells, with respect to the body axis (Jones and Chen 2007; Vladar et al. 2009). Apical basolateral polarity (ABP) refers to the specification and positioning

of structures and organelles at the basolateral and apical surfaces and membranes of the individual cells (Goldstein and Macara 2007). Although PCP and ABP refer to the polarization of cells within multicellular entities such as differentiated tissues and developing cell layers in the embryos, recent studies indicate that the *Xenopus* oocyte itself has basolateral polarity and contains factors that define PCP/ABP in the cells of the developing embryo, beginning at fertilization or early cleavage (Cha et al. 2011; Mohanty and Gupta 2012). Recent studies on electrochemical gradients showed that ouabain-sensitive Na^+ , K^+ -ATPase (the enzyme responsible for maintenance of the electrochemical gradient) activity is confined to the animal hemisphere of stage VI oocytes, resulting in the polarization of the oocyte oolemma (Mohanty and Gupta 2012) and formation of a basolateral-equivalent domain in fully differentiated epithelial cells. Na^+ , K^+ -ATPase is gradually downregulated during oocyte maturation, suggesting that this enzyme plays a role in the maintenance of the germinal vesicle (GV) in stage VI oocytes and chromosomal condensation following GVBD (Mohanty and Gupta 2012). A study on maternal planar cell polarity core protein Van Gogh (Vangl2) and serine/threonine kinase atypical PKC (aPKC), an apical-basal complex component, showed that Vangl2 is concentrated in subcortical islands at the animal pole where it interacts with the post-Golgi vesicle protein v-SNARE, vesicle-associated membrane protein 1 (VAMP1), and acetylated microtubules in stage VI *Xenopus* oocytes (Cha et al. 2011). These authors also showed that aPKC interacts with Vangl2 to establish oocyte microtubule architecture and apical-basal membrane polarity in the mature oocyte and early embryo, which are required for the asymmetrical distribution and function of maternal D/V determinants VegT and Wnt11. The authors believe that Vangl2 and aPKC are part of the same network of interactions that influence the cytoarchitecture of the egg via both the stable microtubule network and the vesicle trafficking system (Cha et al. 2011).

In *Xenopus*, the site of sperm entry during fertilization dictates the D-V and L-R body plan with respect to the A-V axis of the egg (Figure 4.3) (Weaver and Kimelman 2004;

Danilchik et al. 2006). The embryonic plane of bilateral symmetry and the future left and right sides of the embryo can be identified after the establishment of the dorsal midline following fertilization and cortical rotation. Cortical rotation moves vegetally located maternal determinants and dorsalizing activity to the side opposite sperm entry toward the equatorial zone of the egg (Figure 4.3) (Weaver and Kimelman 2004), which locally suppresses the degradation of β -catenin and activates the transcription of dorsal and anterior genes (Rowning et al. 1997; Miller et al. 1999).

Although the majority of processes responsible for the establishment of L-R asymmetry are switched on and act during embryogenesis, the maternally inherited, microfilament-dependent innate organization of the *Xenopus* egg cortex provides directional cue for the distribution of maternal components of the L-R pathway, plays a role in axis determination during the first cell cycle, and is the early indicator of prospective L-R asymmetry (Danilchik et al. 2006). Using the 2,3-butanedione monoxime (BDM) inhibitor that affects the actin cortex and influences the intracellular concentration of Ca^{2+} to interfere with cytokinesis in cleaving *Xenopus* embryos and parthenogenetically activated eggs, Danilchik et al. (2006) showed that BDM causes a dramatic large-scale torsion, with the animal cortex shearing in an exclusively counterclockwise direction past the vegetal cortex, and promotes the development of long actin fibers in a shear zone parallel to the equator. The authors believe that the consistent chiral BDM response and the randomized L-R orientation of tadpole organs resulting from the disruption of cortical actin during the first cell cycle indicate that a maternally inherited, microfilament-dependent organization within the egg cortex plays an early role in the L-R axis determination during the first cell cycle (Danilchik et al. 2006). Another fascinating mechanism for the establishment of L-R asymmetry and common for all model vertebrate organisms studied to date relies on the beating and sensory functions of embryonic cilia in directing the nodal flow of the morphogens (Kramer-Zucker et al. 2005; Okada et al. 2005; Schweickert et al. 2007; Babu and

Roy 2013). For many decades, cilia, which are microtubule-based projections present in majority of eukaryotic cells, had been considered either a strictly sensory (immotile primary cilia) or mechanical and mindless wavers (motile cilia) used to generate cell movement or fluid flow in the lumen of various organs. However, recent studies indicate that the combination of sensory and motile functions of the motile cilia may be responsible for the establishment of asymmetrical gene expression and ultimately the sidedness of the vertebrate embryo (reviewed by Babu and Roy 2013). It remains to be seen how in *Xenopus* this mechanism, which operates during early embryogenesis, concurs with the maternally imposed determination of the L–R axis.

Conclusions

The *Xenopus* model system became an invaluable tool for the study of cell polarity and patterning during oogenesis and development. Some of the pathways and mechanisms operating in *Xenopus* are shared among many different species, while some are unique and have been specifically acquired or adjusted to fit *Xenopus*-specific developmental requirements. Further comparison of these processes between different model systems will shed light on their intraspecific uniqueness and interspecific similarities.

References

- Alarcón VB, Elinson RP. 2001. RNA anchoring in the vegetal cortex of the *Xenopus* oocyte. *J Cell Sci.* 114(Pt 9):1731–41.
- Allison R, Czaplinski K, Git A, et al. 2004. Two distinct Staufen isoforms in *Xenopus* are vegetally localized during oogenesis. *RNA.* 10(11):1751–63.
- Al-Mukhtar KAK, Webb AC. 1971. An ultrastructural study of primordial germ cells, oogonia and early oocytes in *Xenopus laevis*. *J Embryol Exp Morphol.* 26:195–217.
- Andreazzoli M, Pannese M, Boncinelli E. 1997. Activating and repressing signals in head development: the role of *Xotx1* and *Xotx2*. *Development.* 124(9):1733–43.
- Arthur PK, Claussen M, Koch S, Tarbashevich K, Jahn O, Pieler T. 2009. Participation of *Xenopus* Elr-type proteins in vegetal mRNA localization during oogenesis. *J Biol Chem.* 284(30):19982–92.
- Babu D, Roy S. 2013. Left-right asymmetry: cilia stir up new surprises in the node. *Open Biol.* 3:130052.
- Berekelya LA, Ponomarev MB, Luchinskaya NN, Belyavsky AV. 2003. *Xenopus* Germes encodes a novel germ plasm-associated transcript. *Gene Expr Patterns.* 3(4):521–4.
- Berekelya LA, Mikryukov AA, Luchinskaya NN, Ponomarev MB, Woodland HR, Belyavsky AV. 2007. The protein encoded by the germ plasm RNA Germes associates with dynein light chains and functions in *Xenopus* germline development. *Differentiation.* 75(6):546–58.
- Betley JN, Heinrich B, Vernos I, Sardet C, Prodon F, Deshler JO. 2004. Kinesin II mediates Vg1 mRNA transport in *Xenopus* oocytes. *Curr Biol.* 14(3):219–24.
- Bratu DP, Cha BJ, Mhlanga MM, Kramer FR, Tyagi S. 2003. Visualizing the distribution and transport of mRNAs in living cells. *Proc Natl Acad Sci U S A.* 100(23):13308–13.
- Bullock SL. 2007. Translocation of mRNAs by molecular motors: think complex? *Sem Cell Dev Biol.* 18:194–201.
- Bullock SL, Nicol A, Gross SP, Zicha D. 2006. Guidance of bidirectional motor complexes by mRNA cargoes through control of dynein number and activity. *Curr Biol.* 16:1447–52.
- Buning J. 1994. *The Insect Ovary: Ultrastructure, Previtellogenic Growth and Evolution.* Chapman & Hall, New York. 400 pp.
- Busa WB, Ferguson JE, Joseph SK, Williamson JR, Nuccitelli R. 1985. Activation of frog (*Xenopus laevis*) eggs by inositol trisphosphate. *J Cell Biol.* 101:677–82.
- Cao Y, Siegel D, Donow C, et al. 2007. POU-V factors antagonize maternal VegT activity and beta-Catenin signaling in *Xenopus* embryos. *EMBO J.* 26:2942–54.
- Cha SW, Tadjuidje E, Wylie C, Heasman J. 2011. The roles of maternal Vangl2 and aPKC in *Xenopus* oocyte and embryo patterning. *Development.* 138(18):3989–4000.
- Chan AP, Kloc M, Etkin LD. 1999. *fatvg* encodes a new localized RNA that uses a 25-nucleotide element (FVLE1) to localize to the vegetal cortex of *Xenopus* oocytes. *Development.* 126(22):4943–53.
- Chan AP, Kloc M, Bilinski S, Etkin LD. 2001. The vegetally localized mRNA *fatvg* is associated with the germ plasm in the early embryo and is later expressed in the fat body. *Mech Dev.* 100(1):137–40.
- Chan AP, Kloc M, Larabell CA, LeGros M, Etkin LD. 2007. The maternally localized RNA *fatvg* is required for cortical rotation and germ cell formation. *Mech Dev.* 124(5):350–63.

- Christian JL, Gavin BJ, McMahon AP, Moon RT. 1991. Isolation of cDNAs partially encoding four *Xenopus* Wnt-1/int-1-related proteins and characterization of their transient expression during embryonic development. *Dev Biol.* 143:230–4.
- Clarke EJ, Allan VJ. 2003. Cytokeratin intermediate filament organisation and dynamics in the vegetal cortex of living *Xenopus laevis* oocytes and eggs. *Cell Motil Cytoskeleton.* 56(1):13–26.
- Claussen M, Pieler T. 2004. Xvelo1 uses a novel 75-nucleotide signal sequence that drives vegetal localization along the late pathway in *Xenopus* oocytes. *Dev Biol.* 266(2):270–84.
- Claussen M, Horvay K, Pieler T. 2004. Evidence for overlapping, but not identical, protein machineries operating in vegetal RNA localization along early and late pathways in *Xenopus* oocytes. *Development.* 131(17):4263–73.
- Claussen M, Tarbashevich K, Pieler T. 2011. Functional dissection of the RNA signal sequence responsible for vegetal localization of XGrip2.1 mRNA in *Xenopus* oocytes. *RNA Biol.* 8(5):873–82.
- Coggins LW. 1973. An ultrastructural and radioautographic study of early oogenesis in the toad *Xenopus laevis*. *J Cell Sci.* 12:71–93.
- Cox RT, Spradling AC. 2003. A Balbiani body and the fusome mediate mitochondrial inheritance during *Drosophila* oogenesis. *Development.* 130(8):1579–90.
- Cox RT, Spradling AC. 2006. Milton controls the early acquisition of mitochondria by *Drosophila* oocytes. *Development.* 133(17):3371–7.
- de Cuevas M, Lilly MA, Spradling AC. 1997. Germline cyst formation in *Drosophila*. *Annu Rev Genet.* 31:405–28.
- Cuykendall TN, Houston DW. 2009. Vegetally localized *Xenopus* trim36 regulates cortical rotation and dorsal axis formation. *Development.* 136(18):3057–65.
- Cuykendall TN, Houston DW. 2010. Identification of germ plasm-associated transcripts by microarray analysis of *Xenopus* vegetal cortex RNA. *Dev Dyn.* 239(6):1838–48.
- Dale L, Slack JM. 1987. Regional specification within the mesoderm of early embryos of *Xenopus laevis*. *Development.* 100(2):279–95.
- Danilchik MV, Brown EE, Riepert K. 2006. Intrinsic chiral properties of the *Xenopus* egg cortex: an early indicator of left-right asymmetry? *Development.* 133(22):4517–26.
- Deng W, Lin H. 2001. Asymmetric germ cell division and oocyte determination during *Drosophila* oogenesis. *Int Rev Cytol.* 203:93–138.
- Devic E, Paquereau L, Rizzoti K, et al. 1996. The mRNA encoding a beta subunit of heterotrimeric GTP-binding proteins is localized to the animal pole of *Xenopus laevis* oocyte and embryos. *Mech Dev.* 59:141–51.
- Dobrzyński M, Bernatowicz P, Kloc M, Kubiak JZ. 2011. Evolution of bet-hedging mechanisms in cell cycle and embryo development stimulated by weak linkage of stochastic processes. *Results Probl Cell Differ.* 53:11–30.
- Elinson RP, Holowacz T. 1995. Specifying the dorso-anterior axis in frogs: 70 years since Spemann and Mangold. *Curr Top Dev Biol.* 30:253–85. Review.
- Elinson RP, King ML, Forristall C. 1993. Isolated vegetal cortex from *Xenopus* oocytes selectively retains localized mRNAs. *Dev Biol.* 160(2):554–62.
- Fawcett DW, Ito S, Slautterback D. 1959. The occurrence of intercellular bridges in groups of cells exhibiting synchronous differentiation. *Biophys Biochem Cytol.* 5:453–60.
- Forristall C, Pondel M, Chen L, King ML. 1995. Patterns of localization and cytoskeletal association of two vegetally localized RNAs, Vg1 and Xcat-2. *Development.* 121(1):201–8.
- Gagnon JA, Mowry KL. 2010. Visualizing RNA localization in *Xenopus* oocytes. *J Vis Exp.* 14(35):1704.
- Gard DL. 1995. Axis formation during amphibian oogenesis: reevaluating the role of the cytoskeleton. *Curr Top Dev Biol.* 30:215–52. Review.
- Gerhart J, Danilchik M, Doniach T, Roberts S, Rowning B, Stewart R. 1989. Cortical rotation of the *Xenopus* egg: consequences for the anteroposterior pattern of embryonic dorsal development. *Development.* 107 Suppl:37–51. Review.
- Git A, Standart N. 2002. The KH domains of *Xenopus* Vg1RBP mediate RNA binding and self-association. *RNA.* 8(10):1319–33.
- Goldstein B, Macara IG. 2007. The PAR proteins: fundamental players in animal cell polarization. *Dev Cell.* 13(5):609–22.
- Gondos B, Zamboni L. 1969. Ovarian development: the functional importance of germ cell interconnections. *Fertil Steril.* 20:176–82.
- Goto T, Kinoshita T. 1999. Maternal transcripts of mitotic checkpoint gene, Xbub3, are accumulated in the animal blastomeres of *Xenopus* early embryo. *DNA Cell Biol.* 18:227–34.
- Gururajan R, Weeks DL. 1997. An3 protein encoded by a localized maternal mRNA in *Xenopus laevis* is an ATPase with substrate-specific RNA helicase activity. *Biochim Biophys Acta.* 1350(2):169–82.
- Gururajan R, Mathews L, Longo FJ, Weeks DL. 1994. An3 mRNA encodes an RNA helicase that colocalizes with nucleoli in *Xenopus* oocytes in a stage-specific manner. *Proc Natl Acad Sci U S A.* 91(6):2056–60.
- Hasegawa K, Shiraishi T, Kinoshita T. 1999. Xoom: a novel oocyte membrane protein maternally

- expressed and involved in the gastrulation movement of *Xenopus* embryos. *Int J Dev Biol.* 43:479–85.
- Hasegawa K, Sakurai N, Kinoshita T. 2001. Xoom is maternally stored and functions as a transmembrane protein for gastrulation movement in *Xenopus* embryos. *Dev Growth Differ.* 43(1): 25–31.
- Hausen P, Riebesell M. 1991. *The Early Development of Xenopus laevis. An Atlas of the Histology.* Springer-Verlag, Berlin.
- Heasman J. 1997. Patterning the *Xenopus* blastula. *Development.* 124(21):4179–91. Review.
- Heasman J. 2006. Maternal determinants of embryonic cell fate. *Semin Cell Dev Biol.* 17:93–8. Review.
- Heasman J, Quarmby J, Wylie CC. 1984. The mitochondrial cloud of *Xenopus* oocytes: the source of germinal granule material. *Dev Biol.* 105:458–69.
- Heasman J, Wessely O, Langland R, Craig EJ, Kessler DS. 2001. Vegetal localization of maternal mRNAs is disrupted by VegT depletion. *Dev Biol.* 240(2):377–86.
- Horvay K, Claussen M, Katzer M, Landgrebe J, Pieler T. 2006. *Xenopus* Dead end mRNA is a localized maternal determinant that serves a conserved function in germ cell development. *Dev Biol.* 291(1):1–11.
- Houston DW, King ML. 2000. A critical role for Xdazl, a germ plasm-localized RNA, in the differentiation of primordial germ cells in *Xenopus*. *Development.* 127(3):447–56.
- Hudson C, Woodland HR. 1998. Xpat, a gene expressed specifically in germ plasm and primordial germ cells of *Xenopus laevis*. *Mech Dev.* 73(2):159–68.
- Imbrie GA, Wu H, Seldin DC, Dominguez I. 2012. Asymmetric localization of Ck2 α during *Xenopus* oogenesis. *Human Genet Embryol.* 54:001.
- Jones C, Chen P. 2007. Planar cell polarity signaling in vertebrates. *Bioessays.* 29(2):120–32. Review.
- Kageura H. 1997. Activation of dorsal development by contact between the cortical dorsal determinant and the equatorial core cytoplasm in eggs of *Xenopus laevis*. *Development.* 124(8):1543–51.
- King RC, Cassidy JD, Rousset A. 1982. The formation of clones of interconnected cells during gametogenesis in insects. In: King RC, Akai H (Eds.), *Insect Ultrastructure*, vol. 1. Plenum, New York, pp. 3–31.
- King ML, Zhou Y, Bubunenko M. 1999. Polarizing genetic information in the egg: RNA localization in the frog oocyte. *Bioessays.* 21(7):546–57. Review.
- King ML, Messitt TJ, Mowry KL. 2005. Putting RNAs in the right place at the right time: RNA localization in the frog oocyte. *Biol Cell.* 97(1): 19–33. Review.
- Kloc M. 2008. Emerging novel functions of RNAs, and binary phenotype? *Dev Biol.* 317(2):401–4. Review.
- Kloc M. 2009. Teachings from the egg: new and unexpected functions of RNAs. *Mol Reprod Dev.* 76(10):922–32. Review.
- Kloc M, Etkin LD. 1994. Delocalization of Vg1 mRNA from the vegetal cortex in *Xenopus* oocytes after destruction of Xlsirt RNA. *Science.* 265(5175):1101–3.
- Kloc M, Etkin LD. 2005. RNA localization mechanisms in oocytes. *J Cell Sci.* 118(Pt 2):269–82. Review.
- Kloc M, Chan AP. 2007. Centroid, a novel putative DEAD-box RNA helicase maternal mRNA, is localized in the mitochondrial cloud in *Xenopus laevis* oocytes. *Int J Dev Biol.* 51(8):701–6.
- Kloc M, Spohr G, Etkin LD. 1993. Translocation of repetitive RNA sequences with the germ plasm in *Xenopus* oocytes. *Science.* 262(5140):1712–4.
- Kloc M, Larabell C, Etkin LD. 1996. Elaboration of the messenger transport organizer pathway (METRO) for localization of RNA to the vegetal cortex of *Xenopus* oocytes. *Dev Biol.* 180:119–30.
- Kloc M, Larabell C, Chan AP-Y, Etkin LD. 1998. Contribution of METRO pathway localized molecules to the organization of the germ cell lineage. *Mech Dev.* 75:81–93.
- Kloc M, Bilinski S, Chan AP-Y, Allen LH, Zearfoss NR, Etkin LD. 2001a. RNA localization and germ cell determination in *Xenopus*. *Int Rev Cytol.* 203:63–91.
- Kloc M, Bilinski S, Chan A, Etkin LD. 2001b. Mitochondrial ribosomal RNA in the germinal granules in *Xenopus* embryos—Revisited. *Differentiation.* 67:80–3.
- Kloc M, Dougherty MT, Bilinski S, et al. 2002. Three-dimensional ultrastructural analysis of RNA distribution within germinal granules of *Xenopus*. *Dev Biol.* 241:79–93.
- Kloc M, Bilinski S, Dougherty MT, Brey EM, Etkin LD. 2004a. Formation, architecture and polarity of female germline cyst in *Xenopus*. *Dev Biol.* 266(1):43–61.
- Kloc M, Bilinski S, Etkin LD. 2004b. The Balbiani body and germ cell determinants: 150 years later. *Curr Top Dev Biol.* 59:1–36. Review.
- Kloc M, Wilk K, Vargas D, Shirato Y, Bilinski S, Etkin LD. 2005. Potential structural role of non-coding and coding RNAs in the organization of the cytoskeleton at the vegetal cortex of *Xenopus* oocytes. *Development.* 132(15):3445–57.
- Kloc M, Bilinski S, Dougherty MT. 2007. Organization of cytokeratin cytoskeleton and germ plasm in the vegetal cortex of *Xenopus laevis* oocytes depends on coding and non-coding RNAs: three-dimensional and ultrastructural analysis. *Exp Cell Res.* 313(8):1639–51.

- Kloc M, Dallaire P, Reunov A, Major F. 2011a. Structural messenger RNA contains cyto keratin polymerization and depolymerization signals. *Cell Tissue Res.* 346(2):209–22.
- Kloc M, Foreman V, Reddy SA. 2011b. Binary function of mRNA. *Biochimie.* 93(11):1955–61. Review.
- Koch EA, King RC. 1969. Further studies on the ring canal system of the ovarian cystocytes of *Drosophila melanogaster*. *Z Zellforsch Mikrosk Anat.* 102:129–52.
- Kofron M, Demel T, Xanthos J, et al. 1999. Mesoderm induction in *Xenopus* is a zygotic event regulated by maternal VegT via TGFbeta growth factors. *Development.* 126(24):5759–70.
- Kramer-Zucker AG, Olale F, Haycraft CJ, Yoder BK, Schier AF, Drummond IA. 2005. Cilia-driven fluid flow in the zebrafish pronephros, brain and Kupffer's vesicle is required for normal organogenesis. *Development.* 132:1907–21.
- Kume S, Muto A, Aruga J, et al. 1993. The *Xenopus* IP3 receptor: structure, function, and localization in oocytes and eggs. *Cell.* 73(3):555–70.
- Lai F, Zhou Y, Luo X, Fox J, King ML. 2011. Nanos1 functions as a translational repressor in the *Xenopus* germline. *Mech Dev.* 128(1-2):153–63.
- Le Goff C, Laurent V, Le Bon K, et al. 2006. pEg6, a spire family member, is a maternal gene encoding a vegetally localized mRNA in *Xenopus* embryos. *Biol Cell.* 98(12):697–708.
- Machaca K, Hartzell HC. 1998. Asymmetrical distribution of Ca-activated Cl channels in *Xenopus* oocytes. *Biophys J.* 74:1286–95.
- Machado RJ, Moore W, Hames R, et al. 2005. *Xenopus* Xpat protein is a major component of germ plasm and may function in its organisation and positioning. *Dev Biol.* 287(2):289–300.
- Mahowald AP. 1971. The formation of ring canals by cell furrows in *Drosophila*. *Z Zellforsch.* 118:162–7.
- Messitt TJ, Gagnon JA, Kreiling JA, Pratt CA, Yoon YJ, Mowry KL. 2008. Multiple kinesin motors coordinate cytoplasmic RNA transport on a subpopulation of microtubules in *Xenopus* oocytes. *Dev Cell.* 15(3):426–36.
- Meyer D, Durliat M, Senan F, et al. 1997. Ets-1 and Ets-2 proto-oncogenes exhibit differential and restricted expression patterns during *Xenopus laevis* oogenesis and embryogenesis. *Int J Dev Biol.* 41:607–20.
- Miller JR, Rowning BA, Larabell CA, Yang-Snyder JA, Bates RL, Moon RT. 1999. Establishment of the dorsal-ventral axis in *Xenopus* embryos coincides with the dorsal enrichment of dishevelled that is dependent on cortical rotation. *J Cell Biol.* 146:427–37.
- Mohanty BK, Gupta BL. 2012. A marked animal-vegetal polarity in the localization of Na(+),K(+)-ATPase activity and its down-regulation following progesterone-induced maturation. *Mol Reprod Dev.* 79(2):138–60.
- Mowry KL, Cote CA. 1999. RNA sorting in *Xenopus* oocytes and embryos. *FASEB J.* (3):435–45. Review.
- Okada Y, Takeda S, Tanaka Y, Belmonte J-C, Hirokawa N. 2005. Mechanism of nodal flow: a conserved symmetry breaking event in left-right axis determination. *Cell.* 121:633–44.
- Ossipova O, He X, Green J. 2002. Molecular cloning and developmental expression of Par-1/MARK homologues XPar-1A and XPar-1B from *Xenopus laevis*. *Mech Dev.* 119(Suppl 1):S143–8.
- Pannese M, Cagliani R, Pardini CL, Boncinelli E. 2000. Xotx1 maternal transcripts are vegetally localized in *Xenopus laevis* oocytes. *Mech Dev.* 90(1):111–4.
- Pepling ME, De Cuevas M, Spradling AC. 1999. Germline cysts: a conserved phase of germ cell development. *Trends Cell Biol.* 9:257–62.
- Popescu BF, Belak ZR, Ignatyev K, Ovsenek N, Nichol H. 2007. Asymmetric distribution of metals in the *Xenopus laevis* oocyte: a synchrotron X-ray fluorescence microprobe study. *Biochem Cell Biol.* 85(5):537–42.
- Prodon F, Pruliere G, Chenevert J, Sardet C. 2004. Establishment and expression of embryonic axes: comparisons between different model organisms. *Med Sci.* 20:526–38.
- Rowning BA, Wells J, Wu M, Gerhart JC, Moon RT, Larabell CA. 1997. Microtubule-mediated transport of organelles and localization of beta-catenin to the future dorsal side of *Xenopus* eggs. *Proc Natl Acad Sci U S A.* 94:1224–9.
- Schroeder KE, Yost HJ. 1996. *Xenopus* poly (A) binding protein maternal RNA is localized during oogenesis and associated with large complexes in blastula. *Dev Genet.* 19:268–76.
- Schweickert A, Weber T, Beyer T, et al. 2007. Cilia-driven leftward flow determines laterality in *Xenopus*. *Curr Biol.* 17:60–6.
- Shahbadian K, Chartrand P. 2012. Control of cytoplasmic mRNA localization. *Cell Mol Life Sci.* 69(4):535–52.
- Sindelka R, Jonák J, Hands R, Bustin SA, Kubista M. 2008. Intracellular expression profiles measured by real-time PCR tomography in the *Xenopus laevis* oocyte. *Nucleic Acids Res.* 36(2):387–92.
- Sindelka R, Sidova M, Svec D, Kubista M. 2010. Spatial expression profiles in the *Xenopus laevis* oocytes measured with qPCR tomography. *Methods.* 51(1):87–91.
- Singer RH. 2008. Highways for mRNA transport. *Cell.* 134(5):722–3.
- Song HW, Cauffman K, Chan AP, et al. 2007. Hermes RNA-binding protein targets RNAs-encoding proteins involved in meiotic maturation.

- tion, early cleavage, and germline development. *Differentiation*. 75(6):519–28.
- Stennard F, Carnac G, Gurdon JB. 1996. The *Xenopus* T-box gene, Antipodean, encodes a vegetally localised maternal mRNA and can trigger mesoderm formation. *Development*. 122(12):4179–88.
- Takeda Y, Mishima Y, Fujiwara T, Sakamoto H, Inoue K. 2009. DAZL relieves miRNA-mediated repression of germline mRNAs by controlling poly(A) tail length in zebrafish. *PLoS One*. 4(10):e7513.
- Tao Q, Yokota C, Puck H, et al. 2005. Maternal wnt11 activates the canonical wnt signaling pathway required for axis formation in *Xenopus* embryos. *Cell*. 120(6):857–71.
- Tourte M, Mignotte F, Mounlou J-C. 1981. Organization and replication activity of the mitochondrial mass of oogonia and precvitellogenic oocytes in *Xenopus laevis*. *Dev Growth Differ*. 23:9–21.
- Vincent JP, Gerhart JC. 1987. Subcortical rotation in *Xenopus* eggs: an early step in embryonic axis specification. *Dev Biol*. 123(2):526–39.
- Vladar EK, Antic D, Axelrod JD. 2009. Planar cell polarity signaling: the developing cell's compass. *Cold Spring Harb Perspect Biol*. 1(3):a002964. Review.
- Weaver C, Kimelman D. 2004. Move it or lose it: axis specification in *Xenopus*. *Development*. 131(15):3491–9. Review.
- Yamaguchi Y, Taguchi A, Watanabe K, Orii H. 2012. DEADSouth protein localizes to germ plasm and is required for the development of primordial germ cells in *Xenopus laevis*. *Biol Open*. 2:191–9.
- Zearfoss NR, Chan AP, Wu CF, Kloc M, Etkin LD. 2004. Hermes is a localized factor regulating cleavage of vegetal blastomeres in *Xenopus laevis*. *Dev Biol*. 267(1):60–71.
- Zhang J, King ML. 1996. *Xenopus* VegT RNA is localized to the vegetal cortex during oogenesis and encodes a novel T-box transcription factor involved in mesodermal patterning. *Development*. 122(12):4119–29.

5

Germ-Cell Specification in *Xenopus*

Mary Lou King

Department of Cell Biology, Miller School of Medicine, University of Miami, Miami, FL

Abstract: Primordial germ cells (PGCs) represent the only precursor stem cell population that normally gives rise to the gametes. For this reason, PGCs have been called the “stem cells of the species” and are prime examples of a normal totipotent state (Wylie, 1999. *Cell* 96 (2): 165–174). PGCs represent a remarkable lineage that will differentiate into highly specialized cells, either oocytes or sperm, yet also retain the ability to generate a complete new individual. Thus, a fundamental question in developmental and stem cell biology is how PGCs differentiate while retaining the potential for totipotency in contrast to somatic cells that become fate-restricted. In this chapter, we will review what is known about how *Xenopus* sets aside its germ-cell lineage.

Background

PGCs are formed early in development, before organogenesis and at a distance from the future gonads. Two general mechanisms have evolved in metazoans for producing PGCs. The ancestral approach is believed to require cell signaling and involve inductive interactions (Extavour and Akam 2003). In metazoans that go through an embryonic stage, this critical event occurs after the primary germ layers have been formed and includes mammals and urodelan amphibians. In mammals, PGCs arise from a pool of pluripotent cells in the epiblast after receiving BMP signals from extraembryonic tissues during

gastrulation (Saitou and Yamaji 2012). Germline cells can also be formed autonomously through the inheritance of a specialized ooplasm, the germ plasm that contains germ-cell determinants. Ultrastructurally, germ plasm appears similar across all species and includes large accumulations of maternal mitochondria, endoplasmic reticulum (ER), and unique electron-dense granules (reviewed by Kloc et al. 2004a,b). Within the germ plasm are found RNAs and proteins unique to it. In a poorly understood process, these components, including germline determinants (RNAs and proteins), assemble during oogenesis to create germ plasm. Model systems including *Caenorhabditis elegans*, *Drosophila*,

zebrafish, and *Xenopus* form their germline in this fashion (reviewed by Saffman and Lasko 1999).

Formation of the *Xenopus* germline

Xenopus germ plasm is assembled in early previtellogenic oocytes within a discrete membraneless structure called the Balbiani body or mitochondrial cloud (MC) (summarized in Figure 5.1A and B) (Kloc et al. 2001a,b, 2004a,b). The MC is a large structure, 30–40 μm in diameter, closely opposed to the nucleus. It contains the maternal stockpile of mitochondria that will be used later by the embryo (Tourte et al. 1991). Germ plasm comprises approximately a third of the MC and contains granulofibrillar material (GFM), which is the precursor of germinal granules (GG) and hundreds of GG embedded in a matrix also densely packed with smooth ER, mitochondria, Golgi complexes, numerous vesicles, and lipid droplets (Al-Mukhtar and Webb 1971; Chang et al. 2004; Heasman et al. 1984). The densely packed ER within the germ plasm appears to provide docking sites for RNAs (Chang et al. 2004).

Germ plasm is asymmetrically assembled at the tip of the MC closest to the future vegetal pole, a region sometimes called METRO for messenger transport organizer. RNAs, GFM, and GG remain within the cloud as it fragments and descends into the vegetal subcortical region during Dumont oocyte stages II/III (Wilk et al. 2005). The movement of germ plasm RNAs to the vegetal pole is referred to as the early or METRO pathway to distinguish it from the microtubule-dependent late pathway involved in localizing somatic cell determinants (Forristall et al. 1995; Kloc and Etkin 1995). By the end of oogenesis, both germ plasm and maternal RNAs responsible for endoderm/mesoderm specification and dorsal/ventral patterning are found within the vegetal subcortex in overlapping but distinct domains (Elinson et al. 1993; reviewed by Kloc et al. 2001a,b; Pratt and Mowry 2013).

As the fertilized egg divides, germ plasm gradually coalesces into larger yolk-free pools at the vegetal pole that can be seen in the

32-cell stage embryo (Figures 5.1A and 5.2E) (Savage and Danilchik 1993). During early cleavage stages, the germ plasm passes asymmetrically into only one daughter cell, resulting in four to six presumptive PGCs (pPGCs). In pPGCs, germ plasm is found closely apposed to the plasma membrane on one side. This cellular distribution facilitates the asymmetric passage of germ plasm into only one mitotic partner and keeps it concentrated within a few cells. The non-germ plasm-bearing blastomere remains fated to the endoderm. During gastrulation, the germ plasm moves, by a microtubule-based mechanism, to a perinuclear location (Taguchi et al. 2012). Subsequent divisions distribute the germ plasm into both daughter cells, now termed PGCs, as at this point the germline is separated from the surrounding endoderm cell lineages. Therefore, the germ-cell lineage is not separated from somatic lineages until gastrulation. Within the endoderm, PGCs undergo approximately three rounds of divisions at discrete time points (gastrulation stages 10–12, tail bud stages 22–24, late tail bud stages 37–39) and not in synchrony with the faster cell-cycle times of endoderm cells (staging according to Dziadek and Dixon 1977; Nieuwkoop and Faber 1967). By the swimming tadpole stage, there are between 20 and 50 PGCs (Kamimura et al. 1980; Whittington and Dixon 1975).

In all animals, PGCs migrate from the site of their formation and into the presumptive gonads where they will form mature gametes. Four stages of PGC locomotion have been described for *Xenopus*: clustering (stage 24) within the posterior endoderm, dispersing laterally (stage 28), directionally migrating dorsally (stage 33/34), and reaggregating (stage 41) before migrating into the dorsal mesentery (Figure 5.1A) (Terayama et al. 2013). What initiates these different programs of PGC behavior remains unknown. Are they autonomously regulated or do they depend on signals from the endoderm? At least the early movements appear to be autonomously programmed as they can occur in cultured PGCs (Terayama et al. 2013). The SDF-1/CXCR4 chemokine signaling system is likely involved in directional migration as SDF-1 is expressed in the dorsal mesentery and CXCR4

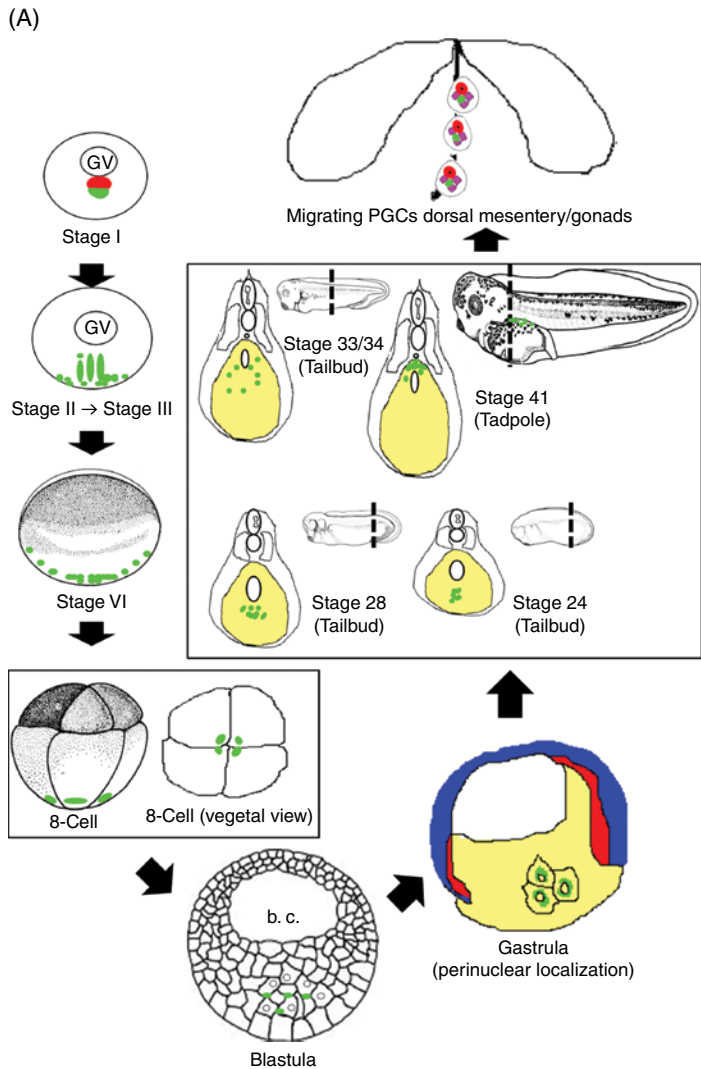


Figure 5.1 Schematic of germline formation in *Xenopus laevis*. (A) Stage I oocyte: germ plasm (green) assembles in MC (red) in close association with the germinal vesicle (GV). Stage II/III oocyte: MC fragments and moves toward the vegetal cortex. Stage VI: germ plasm within the vegetal cortical area. Eight-cell embryo: germ plasm is inherited by vegetal blastomeres shown from the lateral and vegetal pole perspective. Blastula: germ plasm lies near the plasma membrane of four to six cells, the pPGCs. Gastrulation: germ plasm translocates by a microtubule-based mechanism to a perinuclear position. The germline (PGCs) is now segregated from endoderm lineage (yellow, endoderm; red, mesoderm; blue, ectoderm). Tail bud stages 24–34: PGCs begin migration steps clustering, dispersing laterally, directionally migrating dorsally, and, at tadpole 41, reaggregating at the dorsal tip of the endoderm (adapted from Figure 1e'–h' in Terayama K, Kataoka K, Morichika K, Orii H, Watanabe K, Mochii M. Developmental regulation of locomotive activity in *Xenopus* primordial germ cells. *Dev Growth Differ* 2013;55(2):217–228.) Tadpole: PGCs migrate along the dorsal mesentery to reach the presumptive gonads. (B) Tadpole: PGCs enter somatic gonads where they pass through a mitotic proliferative stage (germ stem cell, cystoblast). Female germline cyst formation: at some point, cystoblast will undergo incomplete cytokinesis, remaining connected through four divisions (M1–M4) by cytoplasmic bridges (ring canals) to form the germline cyst. Note the polarity that is maintained throughout the divisions. Mitochondrial aggregate, the synaptonemal complex, the centriole, the ring canal, and the fusome that likely indicate the future vegetal pole of the oocyte. Primary oocyte: oogonia enter meiosis and transition into primary oocyte within cyst. During prophase, follicle cells move between oocytes and the interconnections are lost. Pre-stage I oocyte: mitochondria aggregates surround the nucleus (GV) with the aggregate containing the centriole becoming the major site of germ plasm formation. Stage I oocyte: mature MC with germ plasm assembled toward the vegetal pole. Germ plasm or PGCs (green), mitochondria (red), centriole (black dot), nucleus (purple), nuage (light blue), synaptonemal complex (black bars), ring canal (black line), and fusome (black triangle). (Adapted from Figs. 8 and 10 in Kloc M, Bilinski S, Dougherty MT, Brey EM, Etkin LD. Formation, architecture and polarity of female germline cyst in *Xenopus*. *Dev Biol* 2004a;266(1):43–61.) (All staging is according to the Normal Table of *Xenopus laevis* (Nieuwkoop and Faber 1967) (Daudin), Amsterdam: North-Holland Publishing Co.) To see a color version of this figure, see Plate 11.

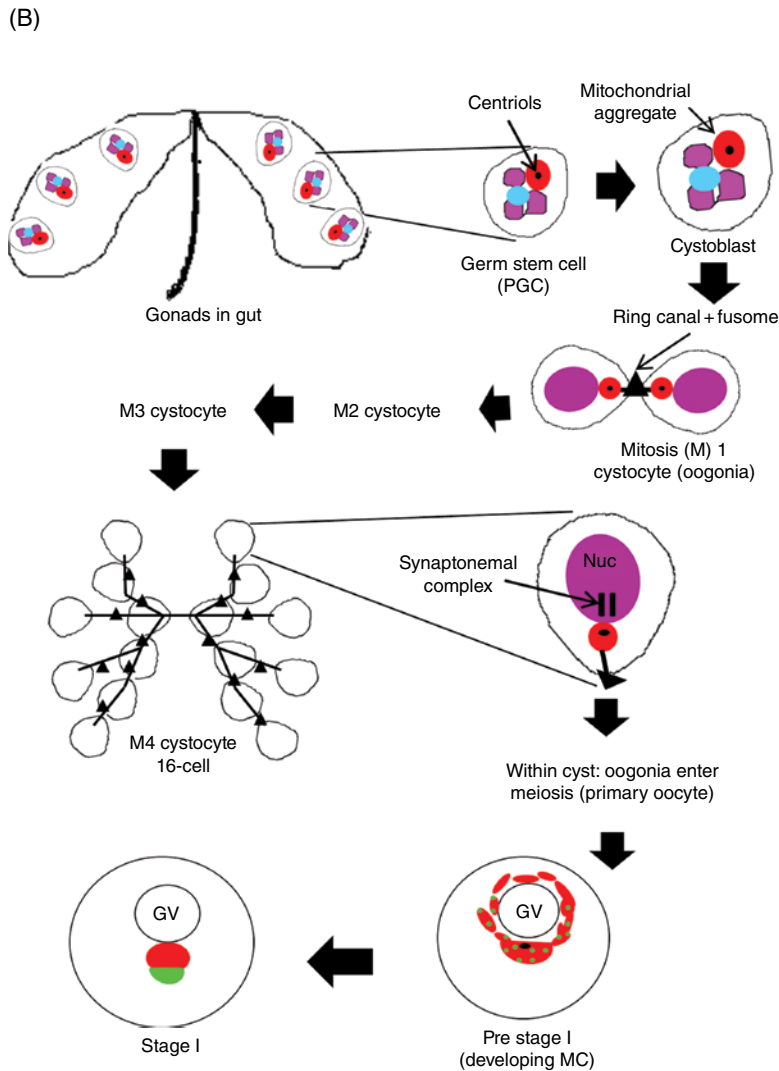


Figure 5.1 (continued)

is expressed on the surface of PGCs (Takeuchi et al. 2010). PGCs leave the endoderm and migrate along the dorsal mesentery until they reach the presumptive gonadal ridge (tadpole stages 44–49).

PGCs transmigrate into the indifferent gonad during stages 48–52, passing between the epithelia cells (Figure 5.1B). At this stage, PGCs appear essentially as they did at the postgastrula stages but without yolk platelets. They are distinguished from somatic cells by their large size (17 μm), diffuse chromatin, large nucleoli, highly lobulated nucleus, many small vesicles, and the perinuclear cluster of mitochondria. Once within the gonad, PGCs

transition into mitotically active oogonia or spermatogonia depending on how the somatic gonad has differentiated. Somatic gonads are sexually determined based on the level of estradiol present, with higher levels supporting testis formation (stage 56; Villalpando and Merchant-Larios 1990). For the remainder of the review, only female germ-cell development will be discussed.

The number of divisions gonadal PGCs undergo before becoming primary oogonia (cystoblast) remains unknown (Kloc et al. 2004a,b). The adult *Xenopus* ovary continuously produces oocytes and does so for years. It follows that such activity must

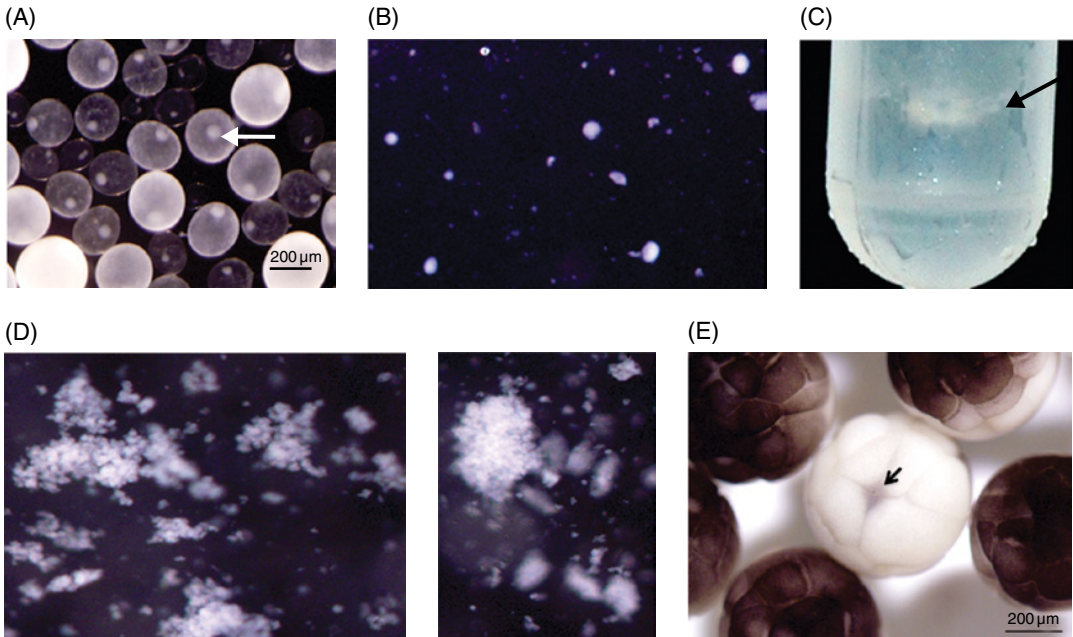


Figure 5.2 Isolation of MC with germ plasma. (A) Isolated stage I/II oocytes with MC. (B) Lysed oocytes with free MC. (C and D) MC material taken from Percoll gradient. This material was run on an SDS gel and used for mass spectrometry (see text and Table 5.2).

be supported by a germ stem cell population, likely found at the tip of the ovarian lobes. However, the exact relationship between PGCs and adult ovarian germ stem cells remains unclear. In newly metamorphosed froglets (stages 62–65), primary oogonia (cystoblasts) divide, giving rise to secondary oogonia (cystocytes). Cystocytes undergo four incomplete mitotic divisions, giving rise to 16 cells, all interconnected by ring canals. These events are summarized in Figure 5.1B and are based on elegant work by Kloc et al., (2004a, b). After four divisions, cystocytes enter meiotic prophase and transition into being primary oocytes. Oocytes remain interconnected by ring canals, developing synchronously until late pachytene when follicular cells come to cover individual oocytes, separating them. Oocytes remain in diplotene of first meiotic prophase for the remainder of oogenesis.

Similar to studies in *Drosophila*, ultrastructural analysis of the *Xenopus* germline has documented the presence of electron-dense granular material, in one form or another, at each developmental stage (reviewed by Al-Mukhtar and Webb 1971; Eddy 1975; Kloc et al. 2004a,b). This material is commonly

referred to as nuage (French for cloud) and is believed to give rise ultimately to the GG found in oocytes and PGCs. Based on structural similarities and developmental timing, Heasman et al. (1984) argued that GFM is derived from nuage material within the MC. In gonadal PGCs and oogonia through Dumont stage I oocytes, nuage-looking material is observed within the nucleus as well as passing through nuclear pores into the cytoplasm where aggregates of mitochondria are found. These mitochondria become embedded in the nuage material, now called mitochondrial cement. It is tempting to speculate that such an intimate association between nuage material and mitochondria reflects the passage between the two of molecular components or signals required for germ-cell specification. Kloc et al. (2004a,b) have proposed a model in which the mitochondrial cement gives rise to GFM and GFM to mature GG within the MC. GG are present in mature oocytes and are detected in PGCs until they migrate along the dorsal mesentery. Once inside the somatic gonads, PGCs now contain nuage. Thus, GG material appears in germ cells of all types: in oogonia, it appears as perinuclear nuage; in pre-vitellogenic oocytes, it appears in the MC as

GFM and GG; and in mature oocytes, eggs, and embryos, it appears as GG. Little has been learned about the functional significance these morphological changes reflect.

Is germ plasm both required and sufficient to form the *Xenopus* germline?

In classic studies, Nieuwkoop and Faber (1956) described “cytoplasmic inclusions” or germ plasm at the vegetal pole of *Xenopus* eggs and early embryos that segregated exclusively into the germline. Both loss- and gain-of-function experiments supported the conclusion that germ plasm was necessary for PGC formation (Nieuwkoop and Sutasurya 1976; Smith 1966; Wakahara 1977, 1978). However, studies by Wylie et al. (1985a,b) attempted to answer this question more directly by following the fate of germ plasm-bearing vegetal pole blastomeres labeled with TRITC (isothiocyanate derivative of Rhodamine) and transferred to nonendodermal locations. In their assay, germ plasm-containing blastomeres or migrating PGCs did not form germ cells, but adopted somatic cell fates dictated by their new environment (Wylie et al. 1985a,b). These results suggested that unlike *Drosophila* (Ephrussi and Lehmann 1992), the anuran germ plasm, although required, was not sufficient to form PGCs. In the same cell transplantation assay, vegetal blastomeres became restricted to the endoderm fate by the gastrula stage, suggesting that totipotency was lost in non-germ plasm-containing cells but retained in PGCs at this time (Wylie et al. 1987). Interestingly, PGC nuclei were found capable of supporting full development upon transfer to an enucleated egg, while endoderm nuclei could not (Smith 1965). Together, these results suggested that, in the presence of germ plasm, nuclei in PGCs remained totipotent.

What remained unclear was why PGCs retain totipotency in the endoderm but differentiate when placed in other regions of the embryo. Recently, this question was resolved with compelling evidence that shows *Xenopus* germ plasm is both required and sufficient to specify PGCs. Tada et al. (2012) used an enhanced green fluorescent protein (EGFP)

gene fused to a mitochondrial transport signal to preferentially label mitochondria-rich germ plasm. Two types of assays were done: (1) the labeled germ plasm was injected directly into animal pole cells and (2) germ plasm-bearing cells were placed in ectopic positions within the animal hemisphere of unlabeled embryos. The injected germ plasm behaved normally, moving to a perinuclear position at the correct stage and retaining germ plasm-specific RNAs such as *Xpat*, *nanos*, and *Xdazl*. However, these ectopic PGCs could only migrate to the genital ridges if they were transplanted back into the endoderm. Importantly, these PGCs formed from animal pole blastomeres could give rise to functional gametes. Thus, the germ plasm contains the determinants for the germline that are capable of acting autonomously to give rise to functional gametes. When Tada et al. (2012) duplicated the Wylie experiment with the EGFP label, they were able to detect labeled cells within the gonads. The simplest explanation for the difference in results is that TRITC did not persist long enough to detect the originally labeled cells within the gonads. Thus, the autonomous determinant nature of germ plasm is conserved from invertebrates to vertebrates.

Molecular components of germ plasm

Efforts have focused on determining the molecular identity and function of the germ plasm components with the goal of understanding the genetic program specifying germline totipotent identity. RNAs highly concentrated at the vegetal pole were found enriched in an oocyte cyokeratin fraction and led to the first molecular cloning of *Xenopus* germ plasm RNAs (Houston et al. 1998; MacArthur et al. 2000; Mosquera et al. 1993; Pondel and King 1988; Zhang and King 1996). More recently, microarray analysis of RNA from isolated vegetal cortices has yielded over a hundred candidates (Claussen et al. 2011; Cuykendall and Houston 2010). Some of these have now been confirmed by *in situ* hybridization as being specifically localized in the MC and later in oocyte germ plasm islands or embryonic germ plasm. These include *DeadSouth*, *Xdazl*, *Hermes*, *Germes*, *Dead-end*, and *Xpat* (Berekelya et al. 2003; Houston and

Table 5.1 Germ plasm RNAs.

RNA	Function	Gene ID (references)
Nanos/Xcat2	Translational repression of endoderm fate, zinc finger RNA-binding protein	xcat2 (Lai et al. 2011)
DeadSouth	Dead-box RNA-dependant helicase	deadsouth (MacArthur et al. 2000)
Xdazl	RNA-binding protein, PGC specification, gametogenesis, translation initiation	xdazl (Collier et al. 2005; Houston et al. 1998)
Xpat	Vegetal association and localization of exogenous transcripts, mitochondria recruitment	xpat (Hudson et al. 1997; Machado et al. 2005)
Grip2	Glutamate receptor-interacting protein 2, PGC anterior/posterior migration	xGRIP2 (Kaneshiro et al. 2007; Tarbashevich et al. 2007)
Germes	Two leucine zipper motifs with an EF-hand domain, organization and function of germ plasm	germes (Berekelya et al. 2003)
Centroid	Dead-box RNA helicase related	centroid (Kloc and Chan 2007)
Fatvg	Vesicle association, dorsal ventral axis specification, maintenance of cortical rotation	fatvg (Chan et al. 2007)
KIF13B	Polarization and directional migration	xKIF13B (Tarbashevich et al. 2011)
Otx1	Homeobox protein	xotx1 (Pannese et al. 2000)
RTN3.1 reticulon	ER association	xRTN3 (Park et al. 2005)
Xlsirts	Noncoding RNA, organizer of GG, maintenance of cytokeratin	xlsirts (Kloc et al. 2007a,b)
Xwnt11	Fibrillar network association of germ plasm, dorsal-ventral axis	xwnt11 (Kloc et al. 1998, 2002a,b)
Fingers	Zinc finger, unknown function	(Kloc et al. 2002,b)
XFACS/ACSL	Long-chain acyl-CoA synthetase, meiotic arrest	acsl1b (Wang et al. 2012)
Mitochondrially encoded large rRNA	Unknown function	mtlrRNA (Kloc et al. 2002a,b)
Mitochondrially encoded small rRNA	Unknown function	mtsrRNA (Kloc et al. 2002a,b)

King 2000a; MacArthur et al. 2000; Weidinger et al. 2003; Zearfoss et al. 2004) and are listed in Table 5.1. mRNAs encoding RNA-binding proteins include the zinc finger protein Nanos; RRM containing RNAs *Xdazl*, *dead-end*, and *hermes*; and helicases *DeadSouth* and *Centroid*. Other RNAs encode proteins involved in RNA metabolism and include *exd2*, a 3'-5' germ plasm exonuclease (Cuykendall and Houston 2010; Kloc et al. 2013). These RNAs support the underlining importance of posttranscriptional regulation in the future germline. Other functional groupings that can

be deduced are those involved in microtubule transport and/or PGC migration (*trim36*, *Grip2*, *germe* RNAs) and scaffolding components that facilitate and preserve the specific germ plasm population of proteins and RNAs. These would include *Xpat*, unique to the *Xenopus* taxon, presumptive long non-coding RNAs (lncRNAs) *Xlsirts*, and *gpt11* (Cuykendall and Houston 2010; Kloc et al. 1993, 2013; Zearfoss et al. 2003). The germline has been characterized as being immortal because, unlike somatic cells, the lineage is continuous from generation to generation.

One expectation, then, is that the germ plasm will contain gene pathway(s) that regulate apoptosis. The ER component reticulon (*rtn3.1*), the multipass membrane protein, is highly enriched as a germ plasm RNA and may be involved in regulating apoptosis (Cuykendall and Houston 2010; Park et al. 2005). Finally, the cell-signaling factor *Wnt11*, essential in dorsal specification, is found within the germ plasm. What role *Wnt 11* may play in the germline, if any, remains to be determined.

piRNAs ensure the genomic integrity of eggs and sperm, protecting the germ-cell DNA from the double-stranded breaks and insertional mutagenesis caused by active transposons (Houwing et al. 2007). Although hundreds of piRNAs have been identified in *Xenopus* oocytes, whether they are localized within the germ plasm has not been determined. Only two lncRNAs have been identified to date. However, with the recent technical advances in RNAseq, others will certainly be found in the near future.

In general, germ plasm RNAs that are translationally repressed during oogenesis are unlikely to play a role in germline determination or to participate in germ plasm assembly, as these events occur during oogenesis. Understandably, protein analysis has typically lagged behind RNA analyses, but is essential to complete the picture of germline specification. To date, only some 20 proteins have been identified and confirmed immunologically as being within the germ plasm (Bilinski et al. 2004; Kloc et al. 2004a,b). These proteins and their known or predicted functions are summarized in Table 5.2. These functions include repressing translation, antitransposon activity, GG assembly and maintenance, cell-cycle regulation, and RNA transport/localization. Interestingly, no transcription factors have been identified thus far, although at least one must be present to initiate the PGC gene program at neurula (Venkatarama et al. 2010).

Xpat is a major component of the germ plasm matrix, both as an RNA and a protein (Hudson and Woodland 1998; Machado et al. 2005). Oocyte-injected GFP-*Xpat* RNA translates into protein capable of localizing to the vegetal pole by a microtubule-dependent mechanism. Importantly, *Xpat* can assemble into structures

that visually resemble germ plasm islands and, like germ plasm, incorporate mitochondria. It is not found outside the *Xenopus* taxon and may be the functional equivalent of oskar in *Drosophila*, recruiting germ plasm components (Machado et al. 2005). No known functional domains have been identified within *Xpat* and thus its role remains somewhat enigmatic. Interestingly, *Xpat* has a nuclear presence and, lacking a recognizable nuclear localization signal (NLS), likely associates with other components to be transported there.

The *DeadSouth* helicase is translated sometime during oogenesis (M. L. King, unpublished observations). Although *Xdazl* RNA is an early MC germ plasm component, its protein is not detected within the germ plasm until early blastula stages and then continuously in migrating PGCs and oogonia (Houston and King 2000a,b; Mita and Yamashita 2000). However, *Xdazl* protein is found in oocyte cytoplasm where it plays a role promoting the translation of specific RNAs (Padmanabhan and Richter 2006). The *Xenopus* Vasa homolog XVLG1 is present within nuage and mitochondrial cement, but unlike *Drosophila* Vasa, it is not found within GG (Bilinski et al. 2004).

Recently, we have isolated enriched samples of MC and have begun characterizing the proteome by mass spectrometry (Figure 5.2). As expected, we found XVLG1 (Vasa) as well as other proteins previously confirmed in *Xenopus* by immunocytochemistry or by their germ plasm localization in other species (proteins with asterisk in Tables 5.2 and 5.3). What remains unclear is how germ plasm components work together to ensure the totipotent and immortal characteristics of the germline (Tada et al. 2012; Wakahara 1978; Wylie 1999). At least five important activities in *Xenopus* PGCs are required to both protect them from somatic differentiation and to initiate the germline-specific gene expression programs: (1) long-term storage of germline determinants during oogenesis, (2) repression of existing maternal messages encoding somatic determinants, (3) activation of sequestered maternal germline mRNAs, (4) transient genome-wide suppression of mRNA transcription at the MBT (midblastula transition) to ensure that somatic differentiation programs

Table 5.2 Germ plasm proteins.

Protein	Location	Function
Spectrin	MC, mitochondrial aggregate, primary MC, oogonia, oocytes, germ plasm (Kloc et al. 1998); fusome (Kloc et al. 2004a,b)	Structural/signaling, germline cyst formation (Kloc et al. 2004a,b)
Gamma tubulin	Germ plasm, MC	Structural/cytoskeleton (Kloc and Etkin 1998)
Vimentin*	Germ plasm in oocytes and early embryos	Structural/cytoskeleton (Torpey et al., 1990)
Cytokeratin*	Germ plasm	Structural/cytoskeleton (Gard et al. 1997)
EF-1 α *	MC	Nucleotide-binding protein (Viel et al 1990)
Vasa*	Nuage, mitochondrial cement. (Vasa excluded from MC?) (Ikenishi and Tanaka 2000; Kloc et al. 2004a,b)	Translational regulator (Luo 2011) (?)
Sm Proteins*	Nuage, mitochondrial cement, MC, Cajal bodies	Nuclear-MC RNA transport, GG formation (Bilinski et al. 2004)
Xpat	Germ plasm, MC, oocytes (all stages), embryos to at least stage 40	Germ plasm matrix formation (Machado et al. 2005)
Xpiwi	Germ plasm, microtubules (MT), meiotic spindles	RNA localization in oocytes; translation, involved in destruction of transposable elements; immunoprecipitates nanos RNA; interacts with Tudor in the absence of RNA (Lau et al. 2009)
Xdazl	Ooplasm, PGC germ plasm from stage 7 to migration to stage 52, oogonia (Mita and Yamashita 2000). The RNA, but not the protein, is detected in the MC	RNA-binding protein required for PGC differentiation and migration (Houston and King 2000a,b)
Xpix1	Germ plasm, MC, centrosome, MT-associated centrioles	MT-associated adaptor proteins (Hames et al. 2008)
Xpix2	MT during mitosis	
Bcl-x(L)	Germ plasm region, not exclusively	Antiapoptosis (Kloc et al. 2007a,b)
Hermes*	Germ plasm in oocytes, MC, associated with nanos RNA	RRM RNA-binding protein; forms RNP particles with nanos, ringo/spy and mos (Zearfoss et al. 2004)
Fatvg	Associated with oocyte lipid droplets, germ plasm	Cortical rotation; increases uptake of long-chain fatty acids. Possible role in the formation or stabilization of lipid storage droplets (possible homolog of adipose differentiation-related protein (ADRP)) (Chan et al. 2007)
Dead-end	Germ plasm; vegetal subcortex of oocyte, late pathway (Horvay et al. 2006)	Microtubule array formation, RNA localization (binds trim36 to the vegetal cortex) (Mei et al. 2013)
KIF13B	Kinesin for PGCs	Directed cell migration of PGCs (Tarbashevich et al 2011)
Xtr (Tudor)*	Germ plasm, PGCs	Localization and translation of germ plasm RNAs in association with piwi, MT assembly and karyokinesis (Hiyoshi et al. 2005)
GRP94	MC (mass spectrometry data)	Possible chaperone protein in ER. Inductive role in immunity (?)

*indicates protein identified by mass spec in germ plasm samples.

?indicates hypothesized function.

Table 5.3 Proteins in common with P-bodies and GG.

Protein	Function	Organism	References
Dhh1/RCK/p54*	Decapping activator, translational regulator	Xl	Smillie and Sommerville (2002)
RAP55	Decapping activator	Xl	Tanaka et al. (2006)
Pat1*	Decapping activator	Xl	Eulalio et al. (2007a,b,c); Marnef et al. (2012)
Dcp2/1	Decapping enzyme/coactivator	Xl	Eulalio et al. (2007a,b,c)
XRN	Exoribonuclease	Mouse	Kotaja et al. (2006a,b)
CPEB*	Translational regulator	Xl	Racki and Richter (2006); Standart and Minshall (2008)
eIF4E	Translation initiation factor that binds cap	Xl	Eulalio et al. (2007a,b,c)
4E-T	eIF4E-binding protein, translational regulation	Xl	Standart and Minshall (2008)
PABP*	Poly(A)-binding protein	Ce	Navarro and Blackwell (2005)
Staufen	Double-stranded RNA-binding protein, mRNA localization	Xl	Allison et al. (2004)
Sm/Lsm proteins*	Spliceosomal complex protein	Xl	Bilinski et al. (2004)
Argonaute	Gene silencing and RNAi pathway	Xl	Wilczynska et al. (2009)

* indicates protein identified by mass spec in germ plasm samples.

remain inactive when zygotic transcription is initiated in the rest of the embryo, and (5) transcriptional activation of PGC-specific genes at neurula after degradation of maternally inherited somatic determinants. In the succeeding text, we review what we have learned about each of these essential activities.

Repression of germline determinants during oogenesis

The germ plasm mode of germline determination has the inherent problem of preserving determinants synthesized quite early during oogenesis for months until embryogenesis when they are required to function. However, the protein/RNA components of these sequestered germline RNAs as well as the mechanism of repression remain to be characterized (reviewed by Houston and King 2000a,b; Kloc et al. 2001a,b, 2002a,b; Schisa 2012; Voronina et al. 2011). Ultrastructural studies have traced nuage-looking material from within the nucleus through nuclear pores and into larger aggregations of RNP-like material and GG (Bilinski et al. 2004; Kloc et al. 2001a,b, 2002a,b, 2004a,b). GG are commonly believed to be sites for the long-term storage of untranslated maternal mRNAs (Cuykendall and Houston

2010; Noble et al. 2008; Standart and Minshall 2008). In general, RNAs within GG appear to be inaccessible to ribosomes and cytoplasmic translation activating/mRNA decay signals (Kloc et al. 2001a,b; Eulalio et al. 2007a,b,c).

Kloc et al. (2002a,b, 2004a,b) have mapped the location of 11 germline RNAs and two proteins within the germ plasm forming region using three-dimensional reconstruction of EM serial sections after *in situ* hybridizations or immunostaining (Tables 5.1 and 5.2). Surprisingly, they found that most RNAs were associated with the germ plasm matrix, not with GG. Only the *nanos* RNA is sequestered within GG where it associates with the RNA-binding protein Hermes (Kloc et al. 2002a,b; Song et al. 2007). Hermes protein does not colocalize with other germ plasm RNAs, further suggesting that *nanos* repression occurs by a different mechanism from that of other *Xenopus* germline RNAs. Based on the ability of Hermes to form homodimers, one model has proposed that Hermes facilitates oligomerization of *nanos* RNA into granules (Song et al. 2007).

Another likely GG component is Xiwi, one of two Piwi proteins found in *Xenopus* early oocytes. It was detected in large complexes and coimmunoprecipitated with *nanos* RNA from egg extracts (Lau et al. 2009; Minshall et al. 2007). Piwi proteins are also identified as

components of the GG in many different species, suggesting a conserved role in the survival of the germline (Faehnle and Joshua-Tor 2007). Xiwi1 also appears to be a nucleocytoplasmic protein, with putative nuclear localization and export signals. It may accompany *nanos* RNA from the nucleus along with Sm proteins also localized to nuage and thought to play a role in germ plasm RNA transport (Bilinski et al. 2004; Lau et al. 2009). Xiwi was also found to associate with repressive translational regulators (cytoplasmic polyadenylation element-binding protein (CPEB) and the helicase Xp54) in an RNA-dependent manner. However, there is no evidence that Xiwi has repressor activity or interacts significantly with the cap-binding complex as described for piwi proteins in other species (Lau et al. 2009; Minshall et al. 2007). *Xenopus* Tudor (Xtr), a plural Tudor domain-containing protein, was also found in the germ plasm. It can interact with Vasa, Piwi, and Sm proteins, pointing to a role in translational regulation of maternal mRNAs (Golam Mostafa et al. 2009). Many of these proteins are also components of P-bodies, a cytoplasmic site involved in mRNA repression/decay in eukaryotes (Table 5.3) (Eulalio et al. 2007a,b,c; Parker and Sheth 2007).

How are germ plasm RNAs repressed outside of the GG? The answer might be in just the same way as other oocyte-stored mRNAs are repressed. Large ribonucleoprotein (RNP) complexes are abundant in early oocytes. They contain the RNA-binding proteins CPEB, RAP55B, Pat1 P100 family member, the helicase Xp54, 4E-T, and an ovary-specific eIF4E1b. All of these proteins interact with each other to repress translation (Minshall et al. 2007, 2009). In fact, Xp54 and RAP55 proteins are found in the *Xenopus* MC and in mouse germ-cell cysts (Ladomery et al. 1997; Racki and Richter 2006). Consistent with the CPEB-repressive complex operating in the germline, adult female CPEB knockout mice were sterile and had only vestigial ovaries devoid of oocytes (Racki and Richter 2006).

Some germ plasm mRNAs are translated during oogenesis while others are not. If RNAs within the germ plasm matrix were in CPEB-repressive RNP particles, one would anticipate that these particles would be more easily activated for translation during oogenesis, while

the GG components serve for long-term storage. In fact, *Xdazl*, *DeadSouth*, *Xpat*, and *Dnd* are each translated during oogenesis and all found in the matrix or associated with the periphery of the GG. Are there different kinds of RNP particles in the germ plasm matrix? Do these dictate when the RNAs will be active? The assembly of GG as well as the identity, regulation, and interaction of the germ plasm matrix components remains an active area of investigation.

Activation of sequestered maternal germline mRNAs

Little is known about how and when germline RNAs transition from repressed RNPs to translating mRNAs. The known components of GG and germ plasm matrix suggest that they are sites of protected untranslated RNAs, but RNAs primed for translation once embryogenesis is initiated. During maturation, several components of the early-formed repressive RNPs undergo modification, including phosphorylation (CPEB, 4E-T) and proteolysis (Pat1, CPEB) (Minshall et al. 2007). It seems likely that similar events will occur within the germ plasm at the developmental transition points marked by ovulation and fertilization. For example, the GG component *Hermes* is degraded at maturation. Shortly thereafter, postfertilization, GG undergo dynamic morphological changes (Kloc et al. 2002a,b). These changes would expose the granule-associated messages to the translational machinery in a temporally regulated manner, facilitating sequential translational activation. Consistent with these observations, *nanos* RNA is translated soon after fertilization and accumulates exclusively within the germ plasm (Lai et al. 2011; Luo et al. 2011).

NANOS

Recently, more has been learned about how *nanos* RNA is translationally activated in *Xenopus*. Although *nanos* RNA is detected in forming germ plasm early in oogenesis, it is not translated until after fertilization. Nanos protein persists until PGCs leave the endoderm at late tail bud stages (Lai et al. 2011; Luo et al. 2011; MacArthur et al. 1999). Thus,

Nanos1 protein is expressed in endodermal PGCs but not after they enter the dorsal mesentery (Lai et al. 2011; Luo et al. 2011; Mosquera et al. 1993; Zhou and King 1996a,b). Unlike other mRNAs, oocyte-injected *nanos1* RNA translates very poorly if at all. Apparently, sequestration of *nanos* RNA within GG is not the only mechanism for its repression. Surprisingly, a secondary structural element was discovered four nucleotides (nt) downstream of the AUG start site (Luo et al. 2011). This 90-nt translational control element (TCE) was required and sufficient to confer repression. Unlike other paradigms for *nanos* repression, this structure alone could block initiation events by preventing the 43S ribosomal subunit from binding (D'Agostino et al. 2006; Gavis et al. 1996; Kalifa et al. 2006). Importantly, repression could be relieved by simply inserting a small number of in-frame nucleotides, sufficient to allow ribosome entry, before the TCE. Oocyte extracts and wheat germ *in vitro* translation systems mimic *nanos* repression and offer powerful tools in which to identify the components of *nanos* RNA activation. Adding embryo extract to either of these repressed *in vitro* systems relieves *nanos* repression, consistent with the expectation of a developmentally regulated activator. RNase treatment did not inhibit activation, ruling out RNA as the activator.

What is the mechanism for *nanos* translational activation? Two stem-loops comprise the TCE and have a predicted free energy of -17 and -56 kcal/mol, respectively, more than sufficient to block ribosomal scanning (Kozak 1986). It follows that the activator will have helicase-like activity sufficient to disrupt the TCE. We tested the known germline helicases DeadSouth, Centroid, and Vasa as well as eIF4F (Jaramillo et al. 1990) and the unwinding RNA-editing enzyme originally discovered in *Xenopus* embryos (Bass and Weintraub 1988). None of these was sufficient to activate *nanos* translation. However, the RNA-binding protein Dead-end (Dnd1) was able to partially relieve repression when tested in experiments *in vivo* (Luo 2011). Dnd1 has ATPase activity, binds *nanos* RNA directly, and may act as a helicase (Horvay et al. 2006; Luo 2011; Weidinger et al. 2003; Youngren et al. 2005). Fertilization events likely trigger the activity of

proteins like germ plasm Dead-end (Mei et al. 2013), DeadSouth, and Vasa within the germ plasm. Vasa helicase plays a positive role in translation and although not found within *Xenopus* GG, is a germ plasm component (Buchan and Parker 2009; Raz 2000) (Table 5.2). These components might act together to bind *nanos* RNA and melt the TCE sufficiently to allow ribosome entry. Ribosomal binding and subsequent translocation of the mRNA through the P site generates sufficient force to disrupt the TCE completely, allowing translation (Takyar et al. 2005). Dnd1 protein recognizes and binds to the uridine-rich regions (URRs) in the 3' UTR of RNAs including *Xenopus trim36* and zebrafish *nanos* (Kedde et al. 2007; Mei et al. 2013). Unlike zebrafish, *Xenopus nanos* RNA does not contain any U-rich regions. It remains to be determined where Dnd1 does bind or whether the *nanos* 3' UTR is required (Luo 2011; Luo et al. 2011). The role Vasa may play in activating the translation of *Xenopus* germ plasm RNAs remains unclear. In *Drosophila*, Vasa has been linked to *nanos* translation. It will be important to determine if this relationship is preserved evolutionarily.

RNA structural inhibition of *nanos* translation provides a robust means of regulating its activity. The TCE is intrinsic to the message and independent of the proper localization of the RNA or the proper expression/stability of a repressor over the long duration of oogenesis. Whether *nanos* will offer insights into how other germline RNAs are translationally regulated remains to be seen, but it might explain why there are so many germ plasm helicases.

Dead-end (Dnd1)

Dnd1 is a conserved RNA-binding protein normally expressed in the germ cells of vertebrates and not found in lower species (Asaoka-Taguchi et al. 1999; Dalby and Glover 1993; Fox et al. 2005; Suzuki et al. 2010). *Dnd1* RNA follows a late *Vg1*-like localization pathway to the vegetal cortex (Horvay et al. 2006). There, Dnd1 protein is required to anchor the localized *trim36* RNA, whose encoded protein promotes the microtubule assembly essential for dorsal specification (Mei et al. 2013). Somatic *Dnd1* mRNA is degraded through an miRNA-18-mediated pathway and becomes

restricted to the germ plasm during embryogenesis. Thus, germline RNAs that encode proteins with multiple functions like Dnd1 may be localized late with somatic cell determinants becoming restricted to the germline after fertilization (Horvay et al. 2006). Fatvg RNA actually uses both the early and late pathways and has dual functions as well (Chan et al. 1999, 2001, 2007).

By the one-cell stage, Dnd1 RNA and protein have accumulated within the germ plasm and by the eight-cell stage, Dnd1 is highly enriched there. Knockdown of Dnd1 during embryogenesis resulted in a loss of PGCs in zebrafish and *Xenopus* (Horvay et al. 2006; Weidinger et al. 2003). Therefore, Dnd1 activity is required for germline maintenance and survival. The Dnd1 loss-of-function phenotype is similar to that of *nanos*, further supporting a model where Dnd1 is required for *nanos* translation.

Studies in zebrafish have revealed yet another later function for Dnd1 in counteracting the miRNA-mediated RNA degradation (Chen et al. 2010; Kedde et al. 2007; Mickoleit et al. 2011). Zebrafish Dnd1 was shown to block the 430/427/302 family of miRNAs in the germ plasm that target repression of *nanos* and TDRD7 (Tudor domain-containing 7) (Behm-Ansmant et al. 2006; Wu et al. 2007). In *Xenopus*, miRNAs mediate the rapid deadenylation of maternal mRNAs after MBT as well. Interestingly, Elr-type proteins synergize with *Xenopus* Dnd protein during embryogenesis to protect *Dnd1* RNA itself from miRNA degradation (Koebernick et al. 2010). *Xenopus* Elr-type proteins are found in isolated MC germ plasm (Figure 5.2) (M. L. King, unpublished observations) and are also part of the vegetal localization complex. Clearly, Dnd has many and divergent functions in both the soma and germline as an RNA-binding protein. How Dnd itself is translationally activated in the germline remains to be determined.

Xdazl

Xdazl RNA is localized within the MC germ plasm and is transported with it to the vegetal pole. *Xdazl* protein is first detected within the germ plasm at early blastula stages, well after *nanos* and *Dnd* are translated (Chang et al. 2004; Houston and King 2000a,b). However,

oocytes also contain *Xdazl* protein outside the germ plasm. The source of ooplasmic *Xdazl* protein is unclear, but it forms a complex with the embryonic poly(A)-binding protein (ePAB), sequence-specific RNA-binding protein Pumilio2, and RINGO/Spy mRNA (Collier et al. 2005; Moore et al. 2003; Voeltz et al. 2001). Following the induction of maturation, Pumilio dissociates not only from RINGO/Spy mRNA but also from *Xdazl* and ePAB and RINGO/Spy mRNA is translated.

What represses and then activates *Xdazl* translation within the germ plasm during cleavage stages remains unknown. All current evidence suggests that *Dazl* mediates its germline functions by promoting translation of specific RNAs (Brook et al. 2009; Collier et al. 2005; Reynolds et al. 2007). In an analogous fashion to that described earlier, *Xdazl* may recruit PABP to specific germline mRNAs and promote polyadenylation and translation. Both human and *Xenopus* *Dazl* have also been shown to interact with Pumilio (Fox et al. 2005; Padmanabhan and Richter 2006). Zebrafish *Dazl* and mouse *Dazl* have their own RNA consensus binding sites (Fox et al. 2005; Maegawa et al. 2002; Reynolds et al. 2005), but whether they require PUM for specific mRNA binding is not known. *Xdazl* may also prevent germline-specific maternal RNAs from miRNA-mediated degradation. Interestingly, *dazl*^{-/-} murine embryonic stem cells do not express pluripotency genes such as Oct-4, or PGC markers such as Nanos and PUM. The basis for these deficiencies is unknown.

To understand the molecular basis for *Xdazl* function in the germline, the mRNAs targeted by *Xdazl* for activation must be identified and validated. Only two *bona fide* mRNA targets whose translation is regulated by *Dazl* have been identified, and both were discovered in mouse testis: mouse vasa homolog (*Mvh*) and synaptonemal complex protein 3 (*SYCP3*) (Reynolds et al. 2005, 2007). All confirmed (or even suggested) *dazl* RNA targets encode products that regulate meiosis. The identity of these RNAs, therefore, is not helpful in explaining the role of *Dazl* in maintaining PGC fate or pluripotency (Haston et al. 2009). In fact, no RNA targets of *Dazl* have been positively confirmed in vertebrate oocytes or

in PGCs, a hindrance to understanding how *Dazl* functions as a translational regulator to promote germline fate.

Repression of existing maternal messages encoding somatic determinants

As previously discussed, maternal RNAs encoding determinants for both the germline and endoderm/mesoderm (e.g., the transcription factor *VegT*) and dorsal/ventral patterning (e.g., *Xwnt-11/trim36*) are localized to the oocyte's vegetal pole. As the fertilized egg divides, the germ plasm is asymmetrically segregated into only a few cells, while localized somatic RNAs are activated for translation and are passively transmitted to all vegetal cells, including PGCs (King et al. 2005; Lai et al. 2012; Venkatarama et al. 2010). Thus, well before zygotic gene transcription begins 12 divisions later at the MBT (~4000 cells), determinants are available to initiate somatic gene expression programs in PGCs (Venkatarama et al. 2010). Despite the presence of these somatic determinants, PGCs do not activate the endoderm gene expression program (Casey et al. 1999; Hudson et al. 1997). Instead, they remain competent to form all cell types. Thus, translational repression of maternal somatic determinants is key to preserving PGC identity.

Nanos and Pumilio: Germline translational repressors

Genetic and biochemical studies identified the conserved RNA-binding proteins Nanos and Pumilio as key regulators in such repression (Lai et al. 2012, 2011; Wreden et al. 1997; Wharton and Struhl 1991; reviewed by Lai and King 2013). We identified *Xcat2* as a *nanos* family member that is expressed in the *Xenopus* germline (Houston and King 2000a,b; Mosquera et al. 1993). Nanos1, homologous to human and mouse Nanos1, was shown to function as a translational repressor in standard tethered function assays (Lai et al. 2011). *Xenopus* Nanos1 is uncommonly small at only 128 amino acids in comparison with other Nanos family members of over 200 amino acids. Two evolutionarily conserved CCHC

zinc fingers are located in the C-terminus and are diagnostic for Nanos homologs. A region of 14 amino acids in the N-terminus is also conserved, present in hydra as well as humans, but surprisingly, not found in *Drosophila* or *C. elegans* (Lai et al. 2011; Mochizuki et al. 2000). Deletion of the 14-amino-acid sequence from Nanos resulted in the loss of repressive activity in the tethered function assays (Lai et al. 2011). Ectopic expression of Nanos within oocytes did not affect maturation or early cleavage stages, but caused severe gastrulation defects and, at lower levels of lethality, incomplete neural tube closure. These are likely to be gain-of-function phenotypes. Deletion of the 14-amino-acid region was sufficient to prevent abnormal development, providing compelling evidence for the importance of this conserved region in Nanos function (Lai et al. 2011; Luo et al. 2011).

Nanos1 can repress capped and polyadenylated RNAs but also represses RNAs without caps or poly(A) tails (Lai et al. 2011). Nanos1 appears capable of repressing translation by several different mechanisms which likely depends on what RNA is being repressed. *Xenopus* Nanos, like *Drosophila* Nanos, associates with cyclin B1 RNA *in vivo*, indicating that this target is evolutionarily conserved. Nanos1 protein is expressed in PGCs after fertilization and until PGCs prepare to migrate from the endoderm (Lai et al. 2011). Thus, Nanos protects PGC identity by repression only during their time within the endoderm.

Loss-of-function studies revealed that *Xenopus* Nanos1 is required to prevent endoderm gene expression and cell death in PGCs (Lai et al. 2011). To understand the molecular basis for both the gain-of-function and loss-of-function phenotypes, the mRNAs targeted by Nanos1 for repression must be identified and validated. Surprisingly, although general screens for the relevant target mRNAs have been carried out with Nanos and Pumilio (Fox et al. 2005; Suzuki et al. 2008, 2010), only five authentic Nanos targets have been confirmed: (1) the cell-cycle regulator *cyclin B1*, a target in frogs and flies (Asaoka-Taguchi et al. 1999; Dalby and Glover 1993; Kadyrova et al. 2007; Lai et al. 2011); (2) the *Drosophila* *hid/skl* promoter of apoptosis, which provides the

molecular link between *nanos* mutants and cell death (Hayashi et al. 2004; Sato et al. 2007); (3, 4) the somatic determinants *hunchback* (Wreden et al. 1997) and *bicoid* (Wharton and Struhl 1991); and (5) *C. elegans Fem-3*, which regulates sex determination (Ahringer and Kimble 1991; Zhang et al. 1997).

Although Nanos can bind RNA, it does so only weakly and with little sequence specificity. Correct selection of the mRNA for repression requires binding of Pumilio (PUM). In general, the known RNA targets for Nanos repression contain at least one conserved 8-nt sequence in their 3' UTRs (UGUANAUA). Pumilio specifically binds this sequence (Pum; Jaruzelska et al. 2003; Lai et al. 2012; Murata and Wharton 1995; Wang et al. 2009; Wharton et al. 1998; Zamore et al. 1997; Zhang et al. 1997); hence, it is called the Pumilio Binding Element (PBE, formerly Nanos Response Element). Although Nanos activity mediates repression, PUM selects the RNA target (but see Weidmann and Goldstrohm 2012). If Nanos is tethered to the RNA reporter, Pumilio is not required for repression (Lai et al. 2011). To what degree this observation can be generalized to other *in vivo* targets is not known. Recently, the structure of the conserved Nanos zinc finger region has been solved and shown to be required for RNA binding, although binding is not sequence specific with this protein fragment (Hashimoto et al. 2010). Two Pumilio family proteins have been characterized in *Xenopus* oocytes that differ significantly in their N-terminal regions, while their RNA-binding domains are virtually identical and are expected to bind to the same set of RNAs (Ota et al. 2011). PUM has many targets, associates with proteins other than Nanos, including *Xdazl* (Fox et al. 2005; Padmanabhan and Richter 2006), and is part of complexes in both somatic and germ cells. Thus, the challenge is to identify PGC RNAs that bind PUM, but which require either Nanos for repression or *Xdazl* for activation. Recently, a set of RNAs involved in meiosis and repressed by Nanos2 has been identified in mouse male gonads by immunoprecipitation with a Nanos antibody (Suzuki et al. 2008, 2010; note that mouse has three *nanos* genes and *Xenopus* only one). Interestingly, the Nanos2-interacting proteins identified in this study include the

CCR4–NOT deadenylation complex. These findings suggest that Nanos represses the expression of these RNAs and leads to their degradation.

Nanos-depleted PGCs transcribe endoderm-specific genes including *Xsox17* and *Bix4* and enter apoptosis while still within the endodermal mass (Lai et al. 2012; see the details in “Activation of sequestered maternal germline mRNAs”). *Xsox17* and *Bix4* are direct downstream targets of the maternal endoderm determinant and transcription factor *VegT*. *VegT* RNA is within the germ plasm and its 3' UTR contains a PBE. Therefore, *VegT* RNA seemed like an excellent candidate for Nanos/Pumilio repression. Pumilio was found to specifically bind *VegT* RNA *in vitro* and repress *VegT* translation within PGCs *in vivo* but only in the presence of Nanos (Lai et al. 2012). *VegT* RNA was significantly more stable in PGCs lacking Nanos1 than in wild-type PGCs. Nanos2 in the male mouse germline has been found to interact with the deadenylase complex (Suzuki et al. 2010) and this mechanism may account for the *VegT* RNA degradation in PGCs in the presence of Nanos1 (Lai et al. 2012).

Transient genome-wide suppression of mRNA transcription at the MBT

In 1976, Zalokar made an important observation that in *Drosophila* embryos, the nuclei of somatic cells but not germline cells were transcriptionally active. On the basis of these and related studies in *C. elegans* (Seydoux and Fire 1994), Williamson and Lehmann (1996) proposed that PGCs may not activate zygotic transcription at the time somatic cell nuclei do. RNA polymerase II transcription requires that the carboxyterminal domain (CTD) is phosphorylated on serine 5 for initiation events and on serine 2 for elongation events. PGCs were found to lack these phosphorylation events and were transcriptionally repressed. PIE-1 in *C. elegans* segregates with the germ-cell lineage and was found to be required for transcriptional repression (Seydoux et al. 1996). Although no homologs for *pie-1* have been found, an attractive model emerged from this work that is instructive.

Zhang et al. (2003) proposed that PIE-1 mimics the CTD substrate but cannot be phosphorylated, thus blocking the interaction between the CTD kinase (cyclinT/cdk9) and the authentic CTD substrate. A more fundamental question is, does totipotency depend on Ser2 not being phosphorylated? Is CTD-Ser2 the site of regulation? Ghosh and Seydoux (2008) reported that PIE-1 blocked cyclinT/cdk9 by competitive inhibition using a CTD-like motif as the model proposed. Surprisingly, blocking serine 2 phosphorylation was not essential for either transcriptional repression or specification of the germline. Blocking both CTD P-Ser5 and CTD P-Ser2, however, was essential for both transcriptional repression and germline specification. Thus, both transcriptional initiation and elongation steps have to be repressed. Different domains within PIE-1 accomplish these two tasks. In *Drosophila*, it is a small protein called Pgc that interacts with cyclinT/cdk9 and inhibits its recruitment to chromatin in PGCs (Hanyu-Nakamura et al. 2008). Again, there is no vertebrate counterpoint to Pgc, but the target, cyclinT/cdk9, is the same.

Do similar events occur in vertebrate germ cells? In *Xenopus* PGCs, transcription is globally repressed for 10 hours beyond when somatic cells become transcriptionally active (Venkatarama et al. 2010). Repression coincided with the failure of the cdk9–cyclinT complex to phosphorylate Ser2 in the CTD of RNA PolIII. However, unlike the germline in *C. elegans*, PGCs always expressed phosphorylated CTD P-Ser5. As expected, CTD P-Ser2 was evident at neurula stages when PGC transcripts were first detected (Venkataraman et al. 2004; Venkatarama et al. 2010). Thus, the elongation step of transcription appeared blocked in *Xenopus* PGCs, but the reason why remains unclear. Interestingly, PGCs lacking Nanos in *D. melanogaster*, *C. elegans*, and *Xenopus* prematurely initiate RNA PolIII transcription, inappropriately express somatic genes, and do not survive (Asaoka et al. 1998; Casey et al. 1999; Deshpande et al. 1999, 2005; Hayashi et al. 2004; Hudson et al. 1997; Kusz et al. 2009; Lai et al. 2012; Maegawa et al. 2002; Mosquera et al. 1993; Venkatarama et al. 2010; Wang and Lehmann 1991). In *Xenopus* PGCs lacking Nanos, *VegT* RNA is not repressed

and transcription occurs prematurely at MBT, resulting in the expression of endoderm-specific genes. In *C. elegans* and *Drosophila*, *nanos* mutants display a similar phenotype, suggesting that Nanos translationally represses an essential player of transcription or has a nuclear function independent of its function as a translational repressor (Asaoka et al. 1998; Deshpande et al. 1999, 2005).

In experiments designed to examine how *nanos* RNA was repressed in *Xenopus* (Luo et al. 2011), we found that myc-tagged Nanos accumulated within nuclei of all cells where it was expressed. We asked if endogenous Nanos could be immunologically detected in PGC nuclei at any stage, and although suggestive, the results were not convincing and require further analysis (Lai et al. 2011). Interestingly, human NANOS3 is strongly expressed within germ-cell nuclei where it colocalized with chromosomes. Colocalization with chromosomes is reminiscent of how *Drosophila* Pgc colocalizes with chromatin and blocks transcription in PGCs (Hanyu-Nakamura et al. 2008).

We addressed whether Nanos has transcriptional repressive activity by injecting a CMV-firefly luciferase plasmid into *Xenopus* one-cell embryos along with the control *Renilla* mRNA. Myc-*nanos* mRNA was coinjected into half the embryos. RT-PCR analysis showed that while the control *Renilla* RNA was stable, firefly transcripts were not detected in embryos expressing Nanos, but were on the control side. Further, repressive activity required myc-Nanos to be nuclear as a mutation within a conserved domain required for myc-*nanos* nuclear entry failed to repress (X. Luo and M. L. King, unpublished observations). An important area for future investigation is to understand why *nanos* mutants fail to repress transcription in PGCs. Is the mechanism based on the ability of Nanos to translationally repress or does it have a more direct function as suggested by its nuclear localization? In summary, inhibition of cyclinT/cdk9 appears to be a common mechanism during germ-cell specification in widely different organisms including *C. elegans*, *Drosophila*, and *Xenopus*. However, a mechanistic connection between *nanos* and transcriptional repression remains to be established in any system.

Do chromatin modifications play a role in *Xenopus* PGC specification?

Seydoux and Braun (2006) have suggested that totipotency is maintained in germ cells in part because of a unique chromatin composition. Unlike *Drosophila* and mouse, *Xenopus* represses transcription in PGCs in the context of a permissive rather than restrictive chromatin structure (Venkatarama et al. 2010). However, there is a change, at least at the level of RNA expression, in the H1 histone variants. These variants are involved in the formation of higher-order chromatin structures and can modulate the accessibility of regulatory proteins, chromatin-remodeling factors, and histone modification enzymes to target sites. Although much attention has been focused on the core histone modifications, little is known about the linker histone variants in PGCs or stem cells in general. Unexpectedly, the earliest epigenetic difference between endoderm and PGCs is in the nature of the histone 1 linker protein (Venkatarama et al. 2010). H1c mRNA, encoding a more restrictive linker variant (Saeki et al. 2005), replaces oocyte B4 and is prominent in the endoderm. PGCs completely lack both B4 and H1c mRNAs, leaving open the question of what H1 linker variant replaces B4 in PGCs. The C-terminal domain of H1 histone variants has a major role in chromatin condensation and higher-order structures. It is not surprising that PGCs would require a different H1 variant from differentiating somatic cells to maintain their potential for totipotency. H1c downregulation and replacement with a PGC-specific H1 variant may be an important step in preserving the germline.

Transcriptional activation of PGC-specific genes at neurula after degradation of maternally inherited somatic determinants

In *Xenopus*, Oct91 is the functional homolog of mammalian Oct4, the factor required to preserve totipotency in the germline (Cao et al. 2006; Morrison and Brickman 2006). Oct91 is a pivotal regulatory factor in preserving pluripotency in somatic cells before gastrulation.

Oct91 expression comes on *de novo* at neurula stage 14 in PGCs as these cells acquire transcriptional competence (Venkatarama et al. 2010). Thus, Oct91 is one of the first genes activated zygotically in PGCs. It follows that the transcription factor(s) required for its activity must be of maternal origin and likely a germ plasm component. An ongoing question is, what are the *cis*- and *trans*-acting regulatory factors governing Oct91 expression in PGCs?

Oct91 expression at the MBT is a cell-autonomous event and not the result of cell signaling (Frank and Harland 1992; Kloc et al. 2001a,b). At stage 14, Oct91 expression is lost or is waning in somatic cells now committed to germ layer-specific fates, while Oct91 is zygotically activated in PGCs. Thus, Oct91 expression declines in somatic cells as they acquire germ layer identity during gastrulation.

Morpholino depletion of Oct91 results in the premature expression of germ layer-specific genes such as *Xsox17* (Morrison and Brickman 2006). Thus, Oct91 acts to maintain multipotency by suppressing commitment during germ layer specification in somatic cells. In preliminary loss-of-function studies, PGCs lacking Oct91 underwent apoptosis by stage 25 as indicated by TUNEL staining. One explanation for these results could be that PGCs now ectopically express transcription factors regulating somatic cell fates and, eventually undergo a cellular crisis that triggers apoptosis. Alternatively, Oct91 could be a survival factor blocking pathways leading to apoptosis. Without Oct91, PGCs automatically enter apoptosis. Oct91 downregulates *xDR-M1*, a member of the death receptor family and a protein abundant in the ovary (Tamura et al. 2004). Does knockdown of Oct91 cause an increase in *xDR-M1* levels in PGCs?

Although much has been learned about mouse Oct4 gene networks in embryonic stem cells, little is known about how it is activated in the germline or what it regulates in PGCs, a significant deficiency in our understanding. Recently, the basal vertebrate ventral homeobox (*ventxs*) and mammalian Nanog factors were found to be structurally and functionally related (Scerbo et al. 2012). Interestingly, *ventx1/2* inactivation leads to loss of Oct91 and

to premature differentiation of blastula cells (Scerbo et al. 2012). Perhaps a related gene to *ventx1/2* will play a role in preserving Oct91 in the germline.

In order to gain insight into gene pathways regulated by Oct91, we carried out a microarray analysis by overexpressing Oct91 in the embryo. Overexpression of Oct91 resulted in prolonging uncommitted fates (Cao et al. 2006; Morrison and Brickman 2006), and thus, we reasoned that upregulated genes should provide clues as to Oct91 targets that preserve an uncommitted state in PGCs. Importantly, we found that *Dead-end* (*Dnd1*) expression increased over 10-fold in response to Oct91. In *Xenopus*, miRNA-427 mediates the rapid deadenylation of maternal mRNAs after MBT and *Dnd1* protects the germline from this degradation event (Kadyrova et al. 2007). The putative regulatory regions of the *Dead-end* gene contain 11 consensus Oct91 binding sites, strongly suggesting that *Dnd1* is a direct target of Oct91. Taken together, our preliminary findings suggest a direct link between Oct91 and the repression of miRNA-427 in the germline through *Dnd1*. We hypothesize that *Xenopus* Oct91 maintains maternal germline-specific RNAs by directly upregulating *Dnd1* in PGCs. Clearly there is much more research to be done to elucidate the mechanism of transcriptional activation in PGCs.

Concluding remarks

Germ cells are the only cell population that can pass genetic information to the offspring. Thus, maintenance of germline fate is one of the most critical events during embryo development. Significantly, abnormal PGCs that fail to undergo apoptosis are known to be the major cause of testicular germ-cell tumors, the most common cancer affecting young men. In the mouse, the *ter* mutation in the *Dnd* gene causes testicular cancer. How is apoptosis normally triggered in abnormal PGCs and why does its failure result in tumors? These are questions important to reproductive and stem cell biology as well as the cancer field.

Investigation into the function of small non-coding RNAs (piRNAs) as well as lncRNAs is

a new field undergoing rapid development. piRNAs are known to function in transposon silencing and to protect the integrity of the genome. Their function in translational repression and/or degradation of specific messages is also well known. The cooperation of piRNAs and germline components in regulating the translation of specific RNAs is becoming an exciting area of research. How do RNA-binding proteins target specific germline RNAs and effect structural changes that either conceal or expose RNAs to miRNA degradation? lncRNAs appear to play a role as enhancers, transcriptionally activating cell type-specific genes. Are there germline-specific lncRNAs other than *Xenopus* Xsirts? Are they involved in activating the unique gene expression program in PGCs? Answers to these questions will have a significant impact on our understanding of how genetic programs network to promote totipotency and immortality in the germline.

Acknowledgments

The author wishes to thank Dawn Owens for assembling Table 5.1 and creating Figure 5.1, Dr. Karen Newman for Table 5.2, and Dr. Tristan Aguero for Figure 5.2. The author also gratefully acknowledges the grant support from NIH that made her research and this review possible.

References

- Ahringer, J. and Kimble, J. 1991. Control of the sperm-oocyte switch in *Caenorhabditis elegans* hermaphrodites by the fem-3 3' untranslated region. *Nature* 349 (6307): 346–348.
- Allison, R., K. Czaplinski, A. Git, et al. 2004. Two Distinct Staufen Isoforms in *Xenopus* are Vegetally Localized during Oogenesis. *RNA (New York, N.Y.)* 10 (11): 1751–1763.
- Al-Mukhtar, K. A. and A. C. Webb. 1971. An Ultrastructural Study of Primordial Germ Cells, Oogonia and Early Oocytes in *Xenopus Laevis*. *Journal of Embryology and Experimental Morphology* 26 (2): 195–217.
- Asaoka, M., H. Sano, Y. Obara, and S. Kobayashi. 1998. Maternal Nanos Regulates Zygotic Gene Expression in Germline Progenitors of *Drosophila*

- Melanogaster. *Mechanisms of Development* 78 (1–2): 153–158.
- Asaoka-Taguchi, M., M. Yamada, A. Nakamura, K. Hanyu, and S. Kobayashi. 1999. Maternal Pumilio Acts Together with Nanos in Germline Development in *Drosophila* Embryos. *Nature Cell Biology* 1 (7): 431–437.
- Bass, B. L. and H. Weintraub. 1988. An Unwinding Activity that Covalently Modifies its Double-Stranded RNA Substrate. *Cell* 55 (6): 1089–1098.
- Behm-Ansmant, I., J. Rehwinkel, and E. Izaurralde. 2006. MicroRNAs Silence Gene Expression by Repressing Protein Expression and/or by Promoting mRNA Decay. *Cold Spring Harbor Symposia on Quantitative Biology* 71: 523–530.
- Berekelya, L. A., M. B. Ponomarev, N. N. Luchinskaya, and A. V. Belyavsky. 2003. *Xenopus Germes* Encodes a Novel Germ Plasm-Associated Transcript. *Gene Expression Patterns: GEP* 3 (4): 521–524.
- Bilinski, S. M., M. K. Jaglarz, B. Szymanska, L. D. Etkin, and M. Kloc. 2004. Sm Proteins, the Constituents of the Spliceosome, Are Components of Nuage and Mitochondrial Cement in *Xenopus* Oocytes. *Experimental Cell Research* 299 (1): 171–178.
- Brook, M., J. W. Smith, and N. K. Gray. 2009. The DAZL and PABP Families: RNA-Binding Proteins with Interrelated Roles in Translational Control in Oocytes. *Reproduction (Cambridge, England)* 137 (4): 595–617.
- Buchan, J. R. and R. Parker. 2009. Eukaryotic Stress Granules: The Ins and Outs of Translation. *Molecular Cell* 36 (6): 932–941.
- Cao, Y., D. Siegel, and W. Knochel. 2006. *Xenopus* POU Factors of Subclass V Inhibit activin/nodal Signaling during Gastrulation. *Mechanisms of Development* 123 (8): 614–625.
- Casey, E. S., M. Tada, L. Fairclough, C. C. Wylie, J. Heasman, and J. C. Smith. 1999. *Bix4* is Activated Directly by *VegT* and Mediates Endoderm Formation in *Xenopus* Development. *Development (Cambridge, England)* 126 (19): 4193–4200.
- Chan, A. P., M. Kloc, and L. D. Etkin. 1999. *Fatvg* Encodes a New Localized RNA that Uses a 25-Nucleotide Element (FVLE1) to Localize to the Vegetal Cortex of *Xenopus* Oocytes. *Development (Cambridge, England)* 126 (22): 4943–4953.
- Chan, A. P., M. Kloc, S. Bilinski, and L. D. Etkin. 2001. The Vegetally Localized mRNA *Fatvg* is Associated with the Germ Plasm in the Early Embryo and is Later Expressed in the Fat Body. *Mechanisms of Development* 100 (1): 137–140.
- Chan, A. P., M. Kloc, C. A. Larabell, M. LeGros, and L. D. Etkin. 2007. The Maternally Localized RNA *Fatvg* is Required for Cortical Rotation and Germ Cell Formation. *Mechanisms of Development* 124 (5): 350–363.
- Chang, P., J. Torres, R. A. Lewis, K. L. Mowry, E. Houliston, and M. L. King. 2004. Localization of RNAs to the Mitochondrial Cloud in *Xenopus* Oocytes through Entrapment and Association with Endoplasmic Reticulum. *Molecular Biology of the Cell* 15 (10): 4669–4681.
- Chen, S., M. Zeng, H. Sun, et al. 2010. Zebrafish Dnd Protein Binds to 3'UTR of Geminin mRNA and Regulates its Expression. *BMB Reports* 43 (6): 438–444.
- Claussen, M., K. Tarbashevich, and T. Pieler. 2011. Functional Dissection of the RNA Signal Sequence Responsible for Vegetal Localization of *XGrip2.1* mRNA in *Xenopus* Oocytes. *RNA Biology* 8 (5): 873–882.
- Collier, B., B. Gorgoni, C. Loveridge, H. J. Cooke, and N. K. Gray. 2005. The DAZL Family Proteins are PABP-Binding Proteins that Regulate Translation in Germ Cells. *The EMBO Journal* 24 (14): 2656–2666.
- Cuykendall, T. N. and D. W. Houston. 2010. Identification of Germ Plasm-Associated Transcripts by Microarray Analysis of *Xenopus* Vegetal Cortex RNA. *Developmental Dynamics: An Official Publication of the American Association of Anatomists* 239 (6): 1838–1848.
- D'Agostino, I., C. Merritt, P. L. Chen, G. Seydoux, and K. Subramaniam. 2006. Translational Repression Restricts Expression of the *C. Elegans* Nanos Homolog NOS-2 to the Embryonic Germline. *Developmental Biology* 292 (1): 244–252.
- Dalby, B. and D. M. Glover. 1993. Discrete Sequence Elements Control Posterior Pole Accumulation and Translational Repression of Maternal Cyclin B RNA in *Drosophila*. *The EMBO Journal* 12 (3): 1219–1227.
- Deshpande, G., G. Calhoun, J. L. Yanowitz, and P. D. Schedl. 1999. Novel Functions of Nanos in Downregulating Mitosis and Transcription during the Development of the *Drosophila* Germline. *Cell* 99 (3): 271–281.
- Deshpande, G., G. Calhoun, T. M. Jinks, A. D. Polydorides, and P. Schedl. 2005. Nanos Downregulates Transcription and Modulates CTD Phosphorylation in the Soma of Early *Drosophila* Embryos. *Mechanisms of Development* 122 (5): 645–657.
- Dziadek, M. and K. E. Dixon. 1977. An Autoradiographic Analysis of Nucleic Acid Synthesis in the Presumptive Primordial Germ Cells of *Xenopus Laevis*. *Journal of Embryology and Experimental Morphology* 37 (1): 13–31.
- Eddy, E. M. 1975. Germ Plasm and the Differentiation of the Germ Cell Line. *International Review of Cytology* 43: 229–280.

- Elinson, R. P., M. L. King, and C. Forristall. 1993. Isolated Vegetal Cortex from *Xenopus* Oocytes Selectively Retains Localized mRNAs. *Developmental Biology* 160 (2): 554–562.
- Ephrussi, A. and R. Lehmann. 1992. Induction of Germ Cell Formation by Oskar. *Nature* 358 (6385): 387–392.
- Eulalio, A., I. Behm-Ansmant, and E. Izaurralde. 2007a. P Bodies: At the Crossroads of Post-Transcriptional Pathways. *Nature Reviews. Molecular Cell Biology* 8 (1): 9–22.
- Eulalio, A., I. Behm-Ansmant, D. Schweizer, and E. Izaurralde. 2007b. P-Body Formation Is a Consequence, Not the Cause, of RNA-Mediated Gene Silencing. *Molecular and Cellular Biology* 27 (11): 3970–3981.
- Eulalio, A., J. Rehwinkel, M. Stricker, et al. 2007c. Target-Specific Requirements for Enhancers of Decapping in miRNA-Mediated Gene Silencing. *Genes & Development* 21 (20): 2558–2570.
- Extavour, C. G. and M. Akam. 2003. Mechanisms of Germ Cell Specification Across the Metazoans: Epigenesis and Preformation. *Development (Cambridge, England)* 130 (24): 5869–5884.
- Faehle, C. R. and L. Joshua-Tor. 2007. Argonautes Confront New Small RNAs. *Current Opinion in Chemical Biology* 11 (5): 569–577.
- Forristall, C., M. Pondel, L. Chen, and M. L. King. 1995. Patterns of Localization and Cytoskeletal Association of Two Vegetally Localized RNAs, *Vg1* and *Xcat-2*. *Development (Cambridge, England)* 121 (1): 201–208.
- Fox, M., J. Urano, and R. A. Reijo Pera. 2005. Identification and Characterization of RNA Sequences to Which Human PUMILIO-2 (PUM2) and Deleted in Azoospermia-Like (DAZL) Bind. *Genomics* 85 (1): 92–105.
- Frank, D. and R. M. Harland. 1992. Localized Expression of a *Xenopus* POU Gene Depends on Cell-Autonomous Transcriptional Activation and Induction-Dependent Inactivation. *Development (Cambridge, England)* 115 (2): 439–448.
- Gard, D. L., B. J. Cha, and E. King. 1997. The Organization and Animal-Vegetal Asymmetry of Cytokeratin Filaments in Stage VI *Xenopus* Oocytes Is Dependent upon F-Actin and Microtubules. *Developmental Biology* 184 (1): 95–114.
- Gavis, E. R., L. Lunsford, S. E. Bergsten, and R. Lehmann. 1996. A Conserved 90 Nucleotide Element Mediates Translational Repression of Nanos RNA. *Development (Cambridge, England)* 122 (9): 2791–2800.
- Ghosh, D. and G. Seydoux. 2008. Inhibition of Transcription by the Caenorhabditis Elegans Germline Protein PIE-1: Genetic Evidence for Distinct Mechanisms Targeting Initiation and Elongation. *Genetics* 178 (1): 235–243.
- Golam Mostafa, M., T. Sugimoto, M. Hiyoshi, et al. 2009. Xtr, a Plural Tudor Domain-Containing Protein, Coexists with FRGY2 Both in Cytoplasmic mRNP Particle and Germ Plasm in *Xenopus* Embryo: Its Possible Role in Translational Regulation of Maternal mRNAs. *Development, Growth & Differentiation* 51 (6): 595–605.
- Hames, R. S., R. Hames, S. L. Prosser, et al. 2008. Pix1 and Pix2 are Novel WD40 Microtubule-Associated Proteins that Colocalize with Mitochondria in *Xenopus* Germ Plasm and Centrosomes in Human Cells. *Experimental Cell Research* 314 (3): 574–589.
- Hanyu-Nakamura, K., H. Sonobe-Nojima, A. Tanigawa, P. Lasko, and A. Nakamura. 2008. *Drosophila* Pgc Protein Inhibits P-TEFb Recruitment to Chromatin in Primordial Germ Cells. *Nature* 451 (7179): 730–733.
- Hashimoto, H., K. Hara, A. Hishiki, et al. 2010. Crystal structure of zinc-finger domain of Nanos and its functional implications. *EMBO Reports* 11 (11): 848–853.
- Haston, K. M., J. Y. Tung, and R. A. Reijo Pera. 2009. Dazl Functions in Maintenance of Pluripotency and Genetic and Epigenetic Programs of Differentiation in Mouse Primordial Germ Cells In Vivo and In Vitro. *PLoS One* 4 (5): e5654.
- Hayashi, Y., M. Hayashi, and S. Kobayashi. 2004. Nanos Suppresses Somatic Cell Fate in *Drosophila* Germ Line. *Proceedings of the National Academy of Sciences of the United States of America* 101 (28): 10338–10342.
- Heasman, J., J. Quarmby, and C. C. Wylie. 1984. The Mitochondrial Cloud of *Xenopus* Oocytes: The Source of Germinal Granule Material. *Developmental Biology* 105 (2): 458–469.
- Hiyoshi, M., N. Nakajo, S. Abe, and K. Takamune. 2005. Involvement of Xtr (*Xenopus* Tudor Repeat) in Microtubule Assembly Around Nucleus and Karyokinesis during Cleavage in *Xenopus* Laevis. *Development, Growth & Differentiation* 47 (2): 109–117.
- Horvay, K., M. Claussen, M. Katzer, J. Landgrebe, and T. Pieler. 2006. *Xenopus* Dead End mRNA Is a Localized Maternal Determinant that Serves a Conserved Function in Germ Cell Development. *Developmental Biology* 291 (1): 1–11.
- Houston, D. W. and M. L. King. 2000a. A Critical Role for *Xdazl*, a Germ Plasm-Localized RNA, in the Differentiation of Primordial Germ Cells in *Xenopus*. *Development (Cambridge, England)* 127 (3): 447–456.
- Houston, D. W. and M. L. King. 2000b. Germ Plasm and Molecular Determinants of Germ Cell Fate. *Current Topics in Developmental Biology* 50: 155–181.
- Houston, D. W., J. Zhang, J. Z. Maines, S. A. Wasserman, and M. L. King. 1998. A *Xenopus*

- DAZ-Like Gene Encodes an RNA Component of Germ Plasm and Is a Functional Homologue of *Drosophila* Boule. *Development (Cambridge, England)* 125 (2): 171–180.
- Houwing, S., Kamminga, L. M., Berezikov, E., et al. 2007. A Role for Piwi and piRNAs in Germ Cell Maintenance and Transposon Silencing in Zebrafish. *Cell* 129:69–82.
- Hudson, C. and H. R. Woodland. 1998. *Xpat*, a Gene Expressed Specifically in Germ Plasm and Primordial Germ Cells of *Xenopus* Laevis. *Mechanisms of Development* 73 (2): 159–168.
- Hudson, C., D. Clements, R. V. Friday, D. Stott, and H. R. Woodland. 1997. *Xsox17alpha* and -Beta Mediate Endoderm Formation in *Xenopus*. *Cell* 91 (3): 397–405.
- Ikenishi, K. and T. S. Tanaka. 2000. Spatio-Temporal Expression of *Xenopus* Vasa Homolog, XVLG1, in Oocytes and Embryos: The Presence of XVLG1 RNA in Somatic Cells as Well as Germline Cells. *Development, Growth & Differentiation* 42 (2): 95–103.
- Jaramillo, M., K. Browning, T. E. Dever, et al. 1990. Translation Initiation Factors that Function as RNA Helicases from Mammals, Plants and Yeast. *Biochimica Et Biophysica Acta* 1050 (1–3): 134–139.
- Jaruzelska, J., M. Kotecki, K. Kusz, A. Spik, M. Firpo, and R. A. Reijo Pera. 2003. Conservation of a Pumilio-Nanos Complex from *Drosophila* Germ Plasm to Human Germ Cells. *Development Genes and Evolution* 213 (3): 120–126.
- Kadyrova, L. Y., Y. Habara, T. H. Lee, and R. P. Wharton. 2007. Translational Control of Maternal Cyclin B mRNA by Nanos in the *Drosophila* Germline. *Development (Cambridge, England)* 134 (8): 1519–1527.
- Kalifa, Y., T. Huang, L. N. Rosen, S. Chatterjee, and E. R. Gavis. 2006. Glorund, a *Drosophila* hnRNP F/H Homolog, Is an Ovarian Repressor of Nanos Translation. *Developmental Cell* 10 (3): 291–301.
- Kamimura, M., M. Kotani, and K. Yamagata. 1980. The Migration of Presumptive Primordial Germ Cells through the Endodermal Cell Mass in *Xenopus* Laevis: A Light and Electron Microscopic Study. *Journal of Embryology and Experimental Morphology* 59: 1–17.
- Kaneshiro, K., M. Miyauchi, Y. Tanigawa, K. Ikenishi, and T. Komiyama. 2007. The mRNA Coding for *Xenopus* Glutamate Receptor Interacting Protein 2 (XGRIP2) Is Maternally Transcribed, Transported through the Late Pathway and Localized to the Germ Plasm. *Biochemical and Biophysical Research Communications* 355 (4): 902–906.
- Kedde, M., M. J. Strasser, B. Boldajipour, et al. 2007. RNA-Binding Protein Dnd1 Inhibits microRNA Access to Target mRNA. *Cell* 131 (7): 1273–1286.
- King, M. L., T. J. Messitt, and K. L. Mowry. 2005. Putting RNAs in the Right Place at the Right Time: RNA Localization in the Frog Oocyte. *Biology of the Cell/Under the Auspices of the European Cell Biology Organization* 97 (1): 19–33.
- Kloc, M. and L. D. Etkin. 1995. Two Distinct Pathways for the Localization of RNAs at the Vegetal Cortex in *Xenopus* Oocytes. *Development (Cambridge, England)* 121 (2): 287–297.
- Kloc, M. and L. D. Etkin. 1998. Apparent Continuity between the Messenger Transport Organizer and Late RNA Localization Pathways during Oogenesis in *Xenopus*. *Mechanisms of Development* 73 (1): 95–106.
- Kloc, M. and A. P. Chan. 2007. *Centroid*, a Novel Putative DEAD-Box RNA Helicase Maternal mRNA, Is Localized in the Mitochondrial Cloud in *Xenopus* Laevis Oocytes. *The International Journal of Developmental Biology* 51 (8): 701–706.
- Kloc, M., G. Spohr, and L. D. Etkin. 1993. Translocation of Repetitive RNA Sequences with the Germ Plasm in *Xenopus* Oocytes. *Science (New York, N.Y.)* 262 (5140): 1712–1714.
- Kloc, M., C. Larabell, A. P. Chan, and L. D. Etkin. 1998. Contribution of METRO Pathway Localized Molecules to the Organization of the Germ Cell Lineage. *Mechanisms of Development* 75 (1–2): 81–93.
- Kloc, M., S. Bilinski, A. P. Chan, L. H. Allen, N. R. Zearfoss, and L. D. Etkin. 2001a. RNA Localization and Germ Cell Determination in *Xenopus*. *International Review of Cytology* 203: 63–91.
- Kloc, M., S. Bilinski, A. P. Chan, and L. D. Etkin. 2001b. Mitochondrial Ribosomal RNA in the Germinal Granules in *Xenopus* Embryos Revisited. *Differentiation; Research in Biological Diversity* 67 (3): 80–83.
- Kloc, M., M. T. Dougherty, S. Bilinski, et al. 2002a. Three-Dimensional Ultrastructural Analysis of RNA Distribution within Germinal Granules of *Xenopus*. *Developmental Biology* 241 (1): 79–93.
- Kloc, M., N. R. Zearfoss, and L. D. Etkin. 2002b. Mechanisms of Subcellular mRNA Localization. *Cell* 108 (4): 533–544.
- Kloc, M., S. Bilinski, M. T. Dougherty, E. M. Brey, and L. D. Etkin. 2004a. Formation, Architecture and Polarity of Female Germline Cyst in *Xenopus*. *Developmental Biology* 266 (1): 43–61.
- Kloc, M., S. Bilinski, and L. D. Etkin. 2004b. The Balbiani Body and Germ Cell Determinants: 150 Years Later. *Current Topics in Developmental Biology* 59: 1–36.
- Kloc, M., S. Bilinski, and M. T. Dougherty. 2007a. Organization of Cytokeratin Cytoskeleton and Germ Plasm in the Vegetal Cortex of *Xenopus* Laevis Oocytes Depends on Coding and Non-Coding RNAs: Three-Dimensional and

- Ultrastructural Analysis. *Experimental Cell Research* 313 (8): 1639–1651.
- Kloc, M., Y. Shirato, S. Bilinski, L. W. Browder, and J. Johnston. 2007b. Differential Subcellular Sequestration of Proapoptotic and Antiapoptotic Proteins and Colocalization of Bcl-x(L) with the Germ Plasm, in *Xenopus* Laevis Oocytes. *Genesis (New York, N.Y.: 2000)* 45 (8): 523–531.
- Kloc, M., M. Jaglarz, M. Dougherty, M. D. Stewart, L. Nel-Themaat, and S. Bilinski. 2008. Mouse Early Oocytes Are Transiently Polar: Three-Dimensional and Ultrastructural Analysis. *Experimental Cell Research* 314 (17): 3245–3254.
- Kloc, M., R. M. Ghobrial, and J. Z. Kubiak. 2013. *Recent Advances in the Understanding of Germ Cell-Specific Organelles and Their Functions. In Recent Advances in Germ Cells Research*, Aubry Perrote Ed.
- Koebernick, K., J. Loeber, P. K. Arthur, K. Tarbashevich, and T. Pieler. 2010. Elr-Type Proteins Protect *Xenopus* Dead End mRNA from miR-18-Mediated Clearance in the Soma. *Proceedings of the National Academy of Sciences of the United States of America* 107 (37): 16148–16153.
- Kotaja, N., S. N. Bhattacharyya, L. Jaskiewicz, et al. 2006a. The Chromatoid Body of Male Germ Cells: Similarity with Processing Bodies and Presence of Dicer and microRNA Pathway Components. *Proceedings of the National Academy of Sciences of the United States of America* 103 (8): 2647–2652.
- Kotaja, N., H. Lin, M. Parvinen, and P. Sassone-Corsi. 2006b. Interplay of PIWI/Argonaute Protein MIWI and Kinesin KIF17b in Chromatoid Bodies of Male Germ Cells. *Journal of Cell Science* 119 (Pt 13): 2819–2825.
- Kozak, M. 1986. Influences of mRNA Secondary Structure on Initiation by Eukaryotic Ribosomes. *Proceedings of the National Academy of Sciences of the United States of America* 83 (9): 2850–2854.
- Kusz, K. M., L. Tomczyk, M. Sajek, et al. 2009. The Highly Conserved NANOS2 Protein: Testis-Specific Expression and Significance for the Human Male Reproduction. *Molecular Human Reproduction* 15 (3): 165–171.
- Ladomery, M., E. Wade, and J. Sommerville. 1997. Xp54, the *Xenopus* Homologue of Human RNA Helicase p54, Is an Integral Component of Stored mRNP Particles in Oocytes. *Nucleic Acids Research* 25, 965–973.
- Lai, F. and M. L. King. 2013. Repressive Translational Control in Germ Cells. *Molecular Reproduction and Development* 80 (8): 665–676.
- Lai, F., Y. Zhou, X. Luo, J. Fox, and M. L. King. 2011. Nanos1 Functions as a Translational Repressor in the *Xenopus* Germline. *Mechanisms of Development* 128 (1–2): 153–163.
- Lai, F., A. Singh, and M. L. King. 2012. *Xenopus* Nanos1 Is Required to Prevent Endoderm Gene Expression and Apoptosis in Primordial Germ Cells. *Development (Cambridge, England)* 139 (8): 1476–1486.
- Lau, N. C., T. Ohsumi, M. Borowsky, R. E. Kingston, and M. D. Blower. 2009. Systematic and Single Cell Analysis of *Xenopus* Piwi-Interacting RNAs and Xiwi. *The EMBO Journal* 28 (19): 2945–2958.
- Luo, X. 2011. *Translational Control of Maternal Nanos1 and VegT in Xenopus Germ Line*. Doctoral Thesis, University of Miami School of Medicine.
- Luo, X., S. Nerlick, W. An, and M. L. King. 2011. *Xenopus* Germline nanos1 Is Translationally Repressed by a Novel Structure-Based Mechanism. *Development (Cambridge, England)* 138 (3): 589–598.
- MacArthur, H., M. Bubunenko, D. W. Houston, and M. L. King. 1999. Xcat2 RNA is a Translationally Sequestered Germ Plasm Component in *Xenopus*. *Mechanisms of Development* 84 (1–2): 75–88.
- MacArthur, H., D. W. Houston, M. Bubunenko, L. Mosquera, and M. L. King. 2000. DEADSouth Is a Germ Plasm Specific DEAD-Box RNA Helicase in *Xenopus* Related to eIF4A. *Mechanisms of Development* 95 (1–2): 291–295.
- Machado, R. J., W. Moore, R. Hames, et al. 2005. *Xenopus* Xpat Protein Is a Major Component of Germ Plasm and May Function in Its Organisation and Positioning. *Developmental Biology* 287 (2): 289–300.
- Maegawa, S., M. Yamashita, K. Yasuda, and K. Inoue. 2002. Zebrafish DAZ-Like Protein Controls Translation Via the Sequence 'GUUC'. *Genes to Cells: Devoted to Molecular & Cellular Mechanisms* 7 (9): 971–984.
- Mei, W., Z. Jin, F. Lai, et al. 2013. Maternal Dead-End1 Is Required for Vegetal Cortical Microtubule Assembly during *Xenopus* Axis Specification. *Development (Cambridge, England)* 140: 11.
- Mickoleit, M., T. U. Banisch, and E. Raz. 2011. Regulation of Hub mRNA Stability and Translation by miR430 and the Dead End Protein Promotes Preferential Expression in Zebrafish Primordial Germ Cells. *Developmental Dynamics: An Official Publication of the American Association of Anatomists* 240 (3): 695–703.
- Minshall, N., M. H. Reiter, D. Weil, and N. Standart. 2007. CPEB Interacts with an Ovary-Specific eIF4E and 4E-T in Early *Xenopus* Oocytes. *The Journal of Biological Chemistry* 282 (52): 37389–37401.
- Minshall, N., M. Kress, D. Weil, and N. Standart. 2009. Role of p54 RNA helicase activity and its C-terminal domain in translational repression, P-body localization and assembly. *Molecular Biology of the Cell* 20 (9): 2464–2472.

- Mita, K. and M. Yamashita. 2000. Expression of *Xenopus* Daz-Like Protein during Gametogenesis and Embryogenesis. *Mechanisms of Development* 94 (1–2): 251–255.
- Mochizuki, K., H. Sano, S. Kobayashi, C. Nishimiya-Fujisawa, and T. Fujisawa. 2000. Expression and Evolutionary Conservation of Nanos-Related Genes in Hydra. *Development Genes and Evolution* 210 (12): 591–602.
- Moore, F. L., J. Jaruzelska, M. S. Fox, et al. 2003. Human Pumilio-2 Is Expressed in Embryonic Stem Cells and Germ Cells and Interacts with DAZ (Deleted in AZoospermia) and DAZ-Like Proteins. *Proceedings of the National Academy of Sciences of the United States of America* 100 (2): 538–543.
- Morrison, G. M. and J. M. Brickman. 2006. Conserved Roles for Oct4 Homologues in Maintaining Multipotency during Early Vertebrate Development. *Development (Cambridge, England)* 133 (10): 2011–2022.
- Mosquera, L., C. Forristall, Y. Zhou, and M. L. King. 1993. A mRNA Localized to the Vegetal Cortex of *Xenopus* Oocytes Encodes a Protein with a Nanos-Like Zinc Finger Domain. *Development (Cambridge, England)* 117 (1): 377–386.
- Murata, Y. and R. P. Wharton. 1995. Binding of Pumilio to Maternal Hunchback mRNA Is Required for Posterior Patterning in *Drosophila* Embryos. *Cell* 80 (5): 747–756.
- Navarro, R. E. and T. K. Blackwell. 2005. Requirement for P Granules and Meiosis for Accumulation of the Germline RNA Helicase CGH-1. *Genesis (New York, N.Y.: 2000)* 42 (3): 172–180.
- Nieuwkoop, P. D. and Faber, J. (1956). *Normal Table of Xenopus laevis (Daudin)*, 1st ed. Amsterdam: North-Holland Publishing Co.
- Nieuwkoop, P. D. and Faber, J. 1967. *Normal Table of Xenopus laevis (Daudin)*. Amsterdam: North-Holland Publishing Co.
- Nieuwkoop, P. D. and L. A. Sutasurya. 1976. Embryological Evidence for a Possible Polyphyletic Origin of the Recent Amphibians. *Journal of Embryology and Experimental Morphology* 35 (1): 159–167.
- Noble, S. L., B. L. Allen, L. K. Goh, K. Nordick, and T. C. Evans. 2008. Maternal mRNAs Are Regulated by Diverse P Body-Related mRNP Granules during Early *Caenorhabditis Elegans* Development. *The Journal of Cell Biology* 182 (3): 559–572.
- Ota, R., T. Kotani, and M. Yamashita. 2011. Biochemical Characterization of Pumilio1 and Pumilio2 in *Xenopus* Oocytes. *The Journal of Biological Chemistry* 286 (4): 2853–2863.
- Padmanabhan, K. and J. D. Richter. 2006. Regulated Pumilio-2 Binding Controls RINGO/Spy mRNA Translation and CPEB Activation. *Genes & Development* 20 (2): 199–209.
- Pannese, M., R. Cagliani, C. L. Pardini, and E. Boncinelli. 2000. Xotx1 Maternal Transcripts Are Vegetally Localized in *Xenopus Laevis* Oocytes. *Mechanisms of Development* 90 (1): 111–114.
- Park, E. C., S. Shim, and J. K. Han. 2005. Identification and Expression of XRTN2 and XRTN3 during *Xenopus* Development. *Developmental Dynamics: An Official Publication of the American Association of Anatomists* 233 (1): 240–247.
- Parker, R. and U. Sheth. 2007. P Bodies and the Control of mRNA Translation and Degradation. *Molecular Cell* 25 (5): 635–646.
- Pondel, M. D. and M. L. King. 1988. Localized Maternal mRNA Related to Transforming Growth Factor Beta mRNA Is Concentrated in a Cytokeratin-Enriched Fraction from *Xenopus* Oocytes. *Proceedings of the National Academy of Sciences of the United States of America* 85 (20): 7612–7616.
- Pratt, C. A. and K. L. Mowry. 2013. Taking a Cellular Road-Trip: mRNA Transport and Anchoring. *Current Opinion in Cell Biology* 25 (1): 99–106.
- Racki, W. J. and J. D. Richter. 2006. CPEB Controls Oocyte Growth and Follicle Development in the Mouse. *Development (Cambridge, England)* 133 (22): 4527–4537.
- Raz, E. 2000. The Function and Regulation of Vasa-Like Genes in Germ-Cell Development. *Genome Biology* 1 (3): REVIEWS1017.
- Reynolds, N., B. Collier, K. Maratou, et al. 2005. Dazl Binds In Vivo to Specific Transcripts and Can Regulate the Pre-Meiotic Translation of Mvh in Germ Cells. *Human Molecular Genetics* 14 (24): 3899–3909.
- Reynolds, N., B. Collier, V. Bingham, N. K. Gray, and H. J. Cooke. 2007. Translation of the Synaptonemal Complex Component Sycp3 Is Enhanced in Vivo by the Germ Cell Specific Regulator Dazl. *RNA (New York, N.Y.)* 13 (7): 974–981.
- Saeki, H., K. Ohsumi, H. Aihara, et al. 2005. Linker Histone Variants Control Chromatin Dynamics during Early Embryogenesis. *Proceedings of the National Academy of Sciences of the United States of America* 102 (16): 5697–5702.
- Saffman, E. E. and P. Lasko. 1999. Germline Development in Vertebrates and Invertebrates. *Cellular and Molecular Life Sciences: CMLS* 55 (8–9): 1141–1163.
- Saitou, M. and M. Yamaji. 2012. Primordial Germ Cells in Mice. *Cold Spring Harbor Perspectives in Biology* 4 (11): a008375.
- Sato, K., Y. Hayashi, Y. Ninomiya, et al. 2007. Maternal Nanos Represses hid/skl-Dependent Apoptosis to Maintain the Germ Line in *Drosophila* Embryos. *Proceedings of the National*

- Academy of Sciences of the United States of America* 104 (18): 7455–7460.
- Savage, R. M. and M. V. Danilchik. 1993. Dynamics of Germ Plasm Localization and Its Inhibition by Ultraviolet Irradiation in Early Cleavage *Xenopus* Embryos. *Developmental Biology* 157 (2): 371–382.
- Scerbo, P., F. Girardot, C. Vivien, et al. 2012. Ventx Factors Function as Nanog-Like Guardians of Developmental Potential in *Xenopus*. *PLoS One* 7 (5): e36855.
- Schisa, J. A. 2012. New Insights into the Regulation of RNP Granule Assembly in Oocytes. *International Review of Cell and Molecular Biology* 295: 233–289.
- Seydoux, G. and A. Fire. 1994. Soma-Germline Asymmetry in the Distributions of Embryonic RNAs in *Caenorhabditis Elegans*. *Development (Cambridge, England)* 120 (10): 2823–2834.
- Seydoux, G. and R. E. Braun. 2006. Pathway to Totipotency: Lessons from Germ Cells. *Cell* 127 (5): 891–904.
- Seydoux, G., C. C. Mello, J. Pettitt, W. B. Wood, J. R. Priess, and A. Fire. 1996. Repression of Gene Expression in the Embryonic Germ Lineage of *C. Elegans*. *Nature* 382 (6593): 713–716.
- Smillie, D. A. and J. Sommerville. 2002. RNA Helicase p54 (DDX6) Is a Shuttling Protein Involved in Nuclear Assembly of Stored mRNP Particles. *Journal of Cell Science* 115 (Pt 2): 395–407.
- Smith, L. D. 1965. Transplantation of the Nuclei of Primordial Germ Cells into Enucleated Eggs of *Rana Pipiens*. *Proceedings of the National Academy of Sciences of the United States of America* 54 (1): 101–107.
- Smith, L. D. 1966. The Role of a “Germinal Plasm” in the Formation of Primordial Germ Cells in *Rana Pipiens*. *Developmental Biology* 14 (2): 330–347.
- Song, H. W., K. Cauffman, A. P. Chan, et al. 2007. *Hermes* RNA-Binding Protein Targets RNAs-Encoding Proteins Involved in Meiotic Maturation, Early Cleavage, and Germline Development. *Differentiation; Research in Biological Diversity* 75 (6): 519–528.
- Standart, N. and N. Minshall. 2008. Translational Control in Early Development: CPEB, P-Bodies and Germinal Granules. *Biochemical Society Transactions* 36 (Pt 4): 671–676.
- Suzuki, H., M. Tsuda, M. Kiso, and Y. Saga. 2008. Nanos3 Maintains the Germ Cell Lineage in the Mouse by Suppressing both Bax-Dependent and -Independent Apoptotic Pathways. *Developmental Biology* 318 (1): 133–142.
- Suzuki, A., K. Igarashi, K. Aisaki, J. Kanno, and Y. Saga. 2010. NANOS2 Interacts with the CCR4-NOT Deadenylation Complex and Leads to Suppression of Specific RNAs. *Proceedings of the National Academy of Sciences of the United States of America* 107 (8): 3594–3599.
- Tada, H., M. Mochii, H. Orii, and K. Watanabe. 2012. Ectopic Formation of Primordial Germ Cells by Transplantation of the Germ Plasm: Direct Evidence for Germ Cell Determinant in *Xenopus*. *Developmental Biology* 371 (1): 86–93.
- Taguchi, A., M. Takii, M. Motoishi, H. Orii, M. Mochii, and K. Watanabe. 2012. Analysis of Localization and Reorganization of Germ Plasm in *Xenopus* Transgenic Line with Fluorescence-Labeled Mitochondria. *Development, Growth & Differentiation* 54 (8): 767–776.
- Takeuchi, T., Y. Tanigawa, R. Minamide, K. Ikenishi, and T. Komiya. 2010. Analysis of SDF-1/CXCR4 Signaling in Primordial Germ Cell Migration and Survival or Differentiation in *Xenopus* Laevis. *Mechanisms of Development* 127 (1–2): 146–158.
- Takyar, S., R. P. Hickerson, and H. F. Noller. 2005. mRNA Helicase Activity of the Ribosome. *Cell* 120 (1): 49–58.
- Tamura, K., T. Noyama, Y. H. Ishizawa, N. Takamatsu, T. Shiba, and M. Ito. 2004. *Xenopus* Death Receptor-M1 and -M2, New Members of the Tumor Necrosis Factor Receptor Superfamily, Trigger Apoptotic Signaling by Differential Mechanisms. *The Journal of Biological Chemistry* 279 (9): 7629–7635.
- Tanaka, K. J., K. Ogawa, M. Takagi, N. Imamoto, K. Matsumoto, and M. Tsujimoto. 2006. RAP55, a Cytoplasmic mRNP Component, Represses Translation in *Xenopus* Oocytes. *The Journal of Biological Chemistry* 281 (52): 40096–40106.
- Tarbashevich, K., K. Koebnick, and T. Pieler. 2007. XGRIP2.1 Is Encoded by a Vegetally Localizing, Maternal mRNA and Functions in Germ Cell Development and Anteroposterior PGC Positioning in *Xenopus* Laevis. *Developmental Biology* 311 (2): 554–565.
- Tarbashevich, K., A. Dzementsei, and T. Pieler. 2011. A Novel Function for KIF13B in Germ Cell Migration. *Developmental Biology* 349 (2): 169–178.
- Terayama, K., K. Kataoka, K. Morichika, H. Orii, K. Watanabe, and M. Mochii. 2013. Developmental Regulation of Locomotive Activity in *Xenopus* Primordial Germ Cells. *Development, Growth & Differentiation* 55 (2): 217–228.
- Torpey, N. P., J. Heasman, and C. C. Wylie. 1990. Identification of Vimentin and Novel Vimentin-Related Proteins in *Xenopus* Oocytes and Early Embryos. *Development (Cambridge, England)* 110 (4): 1185–1195.
- Tourte, M., C. Besse, and J. C. Mounolou. 1991. Cytochemical Evidence of an Organized Microtubular Cytoskeleton in *Xenopus* Laevis

- Oocytes: Involvement in the Segregation of Mitochondrial Populations. *Molecular Reproduction and Development* 30 (4): 353–359.
- Venkatarama, T., F. Lai, X. Luo, Y. Zhou, K. Newman, and M. L. King. 2010. Repression of Zygotic Gene Expression in the *Xenopus* Germline. *Development (Cambridge, England)* 137 (4): 651–660.
- Venkataraman, T., E. Dancausse, and M. L. King. 2004. PCR-Based Cloning and Differential Screening of RNAs from *Xenopus* Primordial Germ Cells: Cloning Uniquely Expressed RNAs from Rare Cells. *Methods in Molecular Biology (Clifton, N.J.)* 254: 67–78.
- Viel, A., M. J. Armand, J. C. Callen, A. Gomez De Gracia, H. Denis, and M. le Maire. 1990. Elongation Factor 1 Alpha (EF-1 Alpha) Is Concentrated in the Balbiani Body and Accumulates Coordinately with the Ribosomes during Oogenesis of *Xenopus Laevis*. *Developmental Biology* 141 (2): 270–278.
- Villalpando, I. and H. Merchant-Larios. 1990. Determination of the Sensitive Stages for Gonadal Sex-Reversal in *Xenopus Laevis* Tadpoles. *The International Journal of Developmental Biology* 34 (2): 281–285.
- Voeltz, G. K., J. Ongkasuwan, N. Standart, and J. A. Steitz. 2001. A Novel Embryonic Poly(A) Binding Protein, ePAB, Regulates mRNA Deadenylation in *Xenopus* Egg Extracts. *Genes & Development* 15 (6): 774–788.
- Voronina, E., G. Seydoux, P. Sassone-Corsi, and I. Nagamori. 2011. RNA Granules in Germ Cells. *Cold Spring Harbor Perspectives in Biology* 3 (12): a002774.
- Wakahara, M. 1977. Partial Characterization of “Primordial Germ Cell-Forming Activity” Localized in Vegetal Pole Cytoplasm in Anuran Eggs. *Journal of Embryology and Experimental Morphology* 39: 221–233.
- Wakahara, M. 1978. Induction of Supernumerary Primordial Germ Cells by Injecting Vegetal Pole Cytoplasm into *Xenopus* Eggs. *Journal of Experimental Zoology* 203 (1): 159–164.
- Wang, C. and R. Lehmann. 1991. Nanos Is the Localized Posterior Determinant in *Drosophila*. *Cell* 66 (4): 637–647.
- Wang, Y., L. Opperman, M. Wickens, and T. M. Hall. 2009. Structural Basis for Specific Recognition of Multiple mRNA Targets by a PUF Regulatory Protein. *Proceedings of the National Academy of Sciences of the United States of America* 106 (48): 20186–20191.
- Wang, H. W., J. S. Fang, X. Kuang, et al. 2012. Activity of Long-Chain Acyl-CoA Synthetase Is Required for Maintaining Meiotic Arrest in *Xenopus Laevis*. *Biology of Reproduction* 87 (3): 74.
- Weidinger, G., J. Stebler, K. Slanchev, et al. 2003. Dead End, a Novel Vertebrate Germ Plasm Component, Is Required for Zebrafish Primordial Germ Cell Migration and Survival. *Current Biology: CB* 13 (16): 1429–1434.
- Weidmann, C. A. and A. C. Goldstrohm. 2012. *Drosophila* Pumilio Protein Contains Multiple Autonomous Repression Domains that Regulate mRNAs Independently of Nanos and Brain Tumor. *Molecular and Cellular Biology* 32 (2): 527–540.
- Wharton, R. P. and G. Struhl. 1991. RNA Regulatory Elements Mediate Control of *Drosophila* Body Pattern by the Posterior Morphogen Nanos. *Cell* 67 (5): 955–967.
- Wharton, R. P., J. Sonoda, T. Lee, M. Patterson, and Y. Murata. 1998. The Pumilio RNA-Binding Domain Is Also a Translational Regulator. *Molecular Cell* 1 (6): 863–872.
- Whittington, P. M. and K. E. Dixon. 1975. Quantitative Studies of Germ Plasm and Germ Cells during Early Embryogenesis of *Xenopus Laevis*. *Journal of Embryology and Experimental Morphology* 33 (1): 57–74.
- Wilczynska, A., N. Minshall, J. Armisen, E. A. Miska, and N. Standart. 2009. Two Piwi Proteins, Xiwi and Xili, Are Expressed in the *Xenopus* Female Germline. *RNA (New York, N.Y.)* 15 (2): 337–345.
- Wilk, K., S. Bilinski, M. T. Dougherty, and M. Kloc. 2005. Delivery of Germinal Granules and Localized RNAs Via the Messenger Transport Organizer Pathway to the Vegetal Cortex of *Xenopus* Oocytes Occurs through Directional Expansion of the Mitochondrial Cloud. *The International Journal of Developmental Biology* 49 (1): 17–21.
- Williamson, A. and R. Lehmann. 1996. Germ Cell Development in *Drosophila*. *Annual Review of Cell and Developmental Biology* 12: 365–391.
- Wreden, C., A. C. Verrotti, J. A. Schisa, M. E. Lieberfarb, and S. Strickland. 1997. Nanos and Pumilio Establish Embryonic Polarity in *Drosophila* by Promoting Posterior Deadenylation of Hunchback mRNA. *Development (Cambridge, England)* 124 (15): 3015–3023.
- Wu, C. F., C. Delsert, S. Faure, et al. 2007. Tumorhead Distribution to Cytoplasmic Membrane of Neural Plate Cells Is Positively Regulated by *Xenopus* p21-Activated Kinase 1 (X-PAK1). *Developmental Biology* 308 (1): 169–186.
- Wylie, C. 1999. Germ Cells. *Cell* 96 (2): 165–174.
- Wylie, C. C., D. Brown, S. F. Godsave, J. Quarmbay, and J. Heasman. 1985a. The Cytoskeleton of *Xenopus* Oocytes and Its Role in Development. *Journal of Embryology and Experimental Morphology* 89 (Suppl): 1–15.
- Wylie, C. C., S. Holwill, M. O’Driscoll, A. Snape, and J. Heasman. 1985b. Germ Plasm and Germ Cell

- Determination in *Xenopus Laevis* as Studied by Cell Transplantation Analysis. *Cold Spring Harbor Symposia on Quantitative Biology* 50: 37–43.
- Wylie, C. C., A. Snape, J. Heasman, and J. C. Smith. 1987. Vegetal Pole Cells and Commitment to Form Endoderm in *Xenopus Laevis*. *Developmental Biology* 119 (2): 496–502.
- Youngren, K. K., D. Coveney, X. Peng, et al. 2005. The Ter Mutation in the Dead End Gene Causes Germ Cell Loss and Testicular Germ Cell Tumours. *Nature* 435 (7040): 360–364.
- Zamore, P. D., J. R. Williamson, and R. Lehmann. 1997. The Pumilio Protein Binds RNA through a Conserved Domain that Defines a New Class of RNA-Binding Proteins. *RNA (New York, N.Y.)* 3 (12): 1421–1433.
- Zearfoss, N. R., A. P. Chan, M. Kloc, L. H. Allen, and L. D. Etkin. 2003. Identification of New Xlirt Family Members in the *Xenopus Laevis* Oocyte. *Mechanisms of Development* 120 (4): 503–509.
- Zearfoss, N. R., A. P. Chan, C. F. Wu, M. Kloc, and L. D. Etkin. 2004. *Hermes* Is a Localized Factor Regulating Cleavage of Vegetal Blastomeres in *Xenopus Laevis*. *Developmental Biology* 267 (1): 60–71.
- Zhang, J. and M. L. King. 1996. *Xenopus* VegT RNA Is Localized to the Vegetal Cortex during Oogenesis and Encodes a Novel T-Box Transcription Factor Involved in Mesodermal Patterning. *Development (Cambridge, England)* 122 (12): 4119–4129.
- Zhang, B., M. Gallegos, A. Puoti, et al. 1997. A Conserved RNA-Binding Protein that Regulates Sexual Fates in the *C. elegans* Hermaphrodite Germ Line. *Nature* 390 (6659): 477–484.
- Zhang, F., M. Barboric, T. K. Blackwell, and B. M. Peterlin. 2003. A model of repression: CTD analogs and PIE-1 inhibit transcriptional elongation by P-TEFb. *Genes & Development* 17 (6): 748–758.
- Zhou, Y. and M. L. King. 1996a. Localization of Xcat-2 RNA, a Putative Germ Plasm Component, to the Mitochondrial Cloud in *Xenopus* Stage I Oocytes. *Development (Cambridge, England)* 122 (9): 2947–2953.
- Zhou, Y. and M. L. King. 1996b. RNA Transport to the Vegetal Cortex of *Xenopus* Oocytes. *Developmental Biology* 179 (1): 173–183.

Section II

Midblastula Transition, Gastrulation, and Neurulation

- Chapter 6 The *Xenopus* Embryo as a Model System to Study Asymmetric Furrowing in Vertebrate Epithelial Cells
- Chapter 7 Induction and Differentiation of the *Xenopus* Ciliated Embryonic Epidermis
- Chapter 8 Wnt Signaling during Early *Xenopus* Development
- Chapter 9 Neural Tube Closure in *Xenopus*

6

The *Xenopus* Embryo as a Model System to Study Asymmetric Furrowing in Vertebrate Epithelial Cells

Jacek Z. Kubiak, Isabelle Chartrain, & Jean-Pierre Tassan

CNRS and University of Rennes 1, Institute of Genetics & Development of Rennes (IGDR), UMR 6290, Faculty of Medicine, Rennes, France

Abstract: Cell division, the process by which one mother cell delivers two distinct daughter cells, is highly sophisticated. Spectacular progress has been made toward the understanding of the molecular mechanisms of this process. Cells dividing in a tissue are subjected to various internal and external constraints. In addition, embryonic cells must adapt to the developmental features and coordinate their divisions with the developmental program. Recently, we established that the mode of cell division is modified in epithelial cells of *Xenopus* embryos at different stages of development. In the epithelium of the gastrula, the cytokinetic furrow ingresses asymmetrically. However, in earlier stages of development, the furrow ingresses downward, while later the direction of membrane ingression proceeds upward. Here, we discuss how the asymmetric furrowing is regulated and how this particular mode of cell division participates in embryo development. We also discuss the advantage of early *Xenopus* embryos for studying the mechanism of division in vertebrate cells.

Introduction

Asymmetric cell division produces daughter cells with distinct sizes and fates (Knoblich 2008 and Figure 6.1A). This mode of cell division is responsible for cell diversification during development and generation of a complex organism from a single cell: the fertilized egg. Hence, asymmetric cell division is a fundamental process during development. It is also a key process for cell renewal in adult tissue. Therefore, it plays a major role not only

in embryo development but also in the post-natal life of organisms. For these reasons, molecular mechanisms governing asymmetric cell division are actively studied in a wide variety of model organisms.

A far less well studied, and therefore less understood, is the asymmetric furrowing (Figure 6.1B). Asymmetric furrowing denotes the fact that instead of ingressing the cell plasma membrane all around the cell midzone in an isoconcentric manner, the cytokinetic furrowing proceeds unequally or unilaterally,

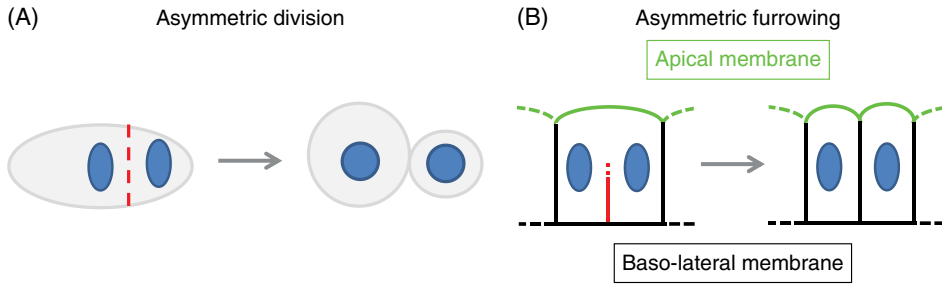


Figure 6.1 Asymmetric division vs. asymmetric furrowing. (A) Asymmetric division is achieved here by displacement of the cytokinetic apparatus, including the mitotic chromosomes (ovals). The division plane (dashed line) is not centered but laterally displaced. Consequently, the mother cell divides into two daughter cells of different sizes and fates. (B) Asymmetric furrowing in a polarized cell presenting an apical and a basolateral membrane. The division plane is centered and the two daughter cells will inherit similar size and fate. The cytokinetic furrow (dashed line) progresses asymmetrically: it starts to ingress basolaterally and progresses toward the apical membrane.

giving rise to an asymmetric furrow. This type of cell partitioning preserves epithelium integrity.

We have recently shown, by studying the role of the cell cycle-regulated protein kinase MELK (Maternal Embryonic Leucine zipper Kinase) during the early *Xenopus* development, that this kinase is involved in the process of asymmetric furrowing and that an inversion of furrow ingression occurs between late blastula and early gastrula stages. We thus focus on the role of the MELK protein kinase as well as the differential regulation of several well-characterized cytokinetic proteins during early development in *Xenopus* embryos.

MELK is a cell cycle-regulated kinase involved in development and cancer

MELK (Heyer et al. 1997), also known as pEg3 in *Xenopus* (Blot et al. 2002; Davezac et al. 2002), is a cell cycle-dependent protein kinase present during the early development of *Xenopus* embryo. MELK is involved in a variety of functions including cell cycle (Davezac et al. 2002), cell proliferation (Nakano et al. 2005), apoptosis (Lin et al. 2007; Jung et al. 2008), and RNA processing (Vulsteke et al. 2004). In normal and cancerous human and *Xenopus* cell lines, MELK expression is specific for cells engaged in cell division. It becomes strongly reduced upon cell cycle exit and falls down to undetectable levels in differentiated cells (Blot et al. 2002, Badouel et al. 2010). This

finding is particularly interesting since MELK expression is dramatically increased in a large spectrum of cancers (Gray et al. 2005; Marie et al. 2008; Nakano et al. 2008). Moreover, a high level of MELK mRNA correlates with malignancy grade in brain tumors (Marie et al. 2008; Nakano et al. 2008) and is associated with poor prognosis in breast cancer (Pickard et al. 2009). Thus, MELK is not only involved in normal embryo development but is also a marker for tumorigenesis.

In *Xenopus* oocytes and embryos, MELK is coded by a maternal mRNA (Paris and Philippe 1990). The protein is already present in the fully grown oocyte and its levels increase about 2.5-fold during oocyte maturation (Blot et al. 2002). This behavior strengthens a potentially important role of MELK in oocyte maturation and embryo development, which depend on maternal genetic information. During the first embryonic cell cycle, MELK levels are transiently decreased by about twofolds through an abrupt degradation. In cleaving embryos, MELK levels are similar to those observed in the egg and remain unchanged during early development. Both MELK phosphorylation/dephosphorylation and the catalytic activity are tightly controlled during oocyte maturation and early embryonic cleavage (Blot et al. 2002; Badouel et al. 2006). Importantly, we have shown that MELK regulation identified in the *Xenopus* embryo model, including its expression, phosphorylation, and catalytic activity, is conserved in human cells (Davezac et al. 2002; Badouel et al. 2010). Such intricate regulation

suggested that MELK could play an important function during the cleavage period that follows fertilization in *Xenopus*. We have recently shown that perturbing MELK expression, by either knockdown before fertilization or overexpression of this protein following fertilization, leads to abortive cell divisions in embryos, indicating that MELK is involved in cytokinesis.

MELK in *Xenopus laevis* embryo cytokinesis

From the first embryonic division up to the blastula stage, the endogenous MELK (Figure 6.2), as well as other essential cytokinetic proteins including actin, myosin heavy chain (MHC), the small RhoA GTPase, and anillin, accumulate in a narrow band at the equatorial cortex shortly before cells start their cytokineses (Bement et al. 2005; Le Page et al. 2011). This band ultimately corresponds to the cytokinetic furrow. Similarly to the discrete zone of active RhoA, MELK and anillin dynamically accumulate into the equatorial band. Importantly, MELK also accumulates at the cell periphery in a cell cycle-independent but cell–cell contact-dependent manner (Tassan 2011; Chartrain et al. 2013). We called this subpopulation *iMELK* for interphasic MELK. At present, the function of this MELK subpopulation remains unknown, but its constant presence at the cell borders suggests that it plays a role during interphase in maintaining correct cell–cell contacts and/or regulating mechanical forces at the cell cortex. The *iMELK* subpopulation is more concentrated at the apical junctional complexes than in the basal part of the cell border. Thus, its localization at this site appears highly correlated with cell polarity.

We have further shown that MELK copurifies with anillin (Le Page et al. 2011). Anillin is an essential cytokinesis component which stabilizes the division furrow (Hickson and O’Farrell 2008). Studies utilizing diverse organisms showed that anillin interacts with several molecules involved in cytokinesis, including actin (Field and Alberts 1995), MHC (Straight et al. 2005), RhoA (Piekny and Glotzer 2008), and MgcRacGAP (D’avino et al. 2008; Gregory et al. 2008). During cytokinesis,

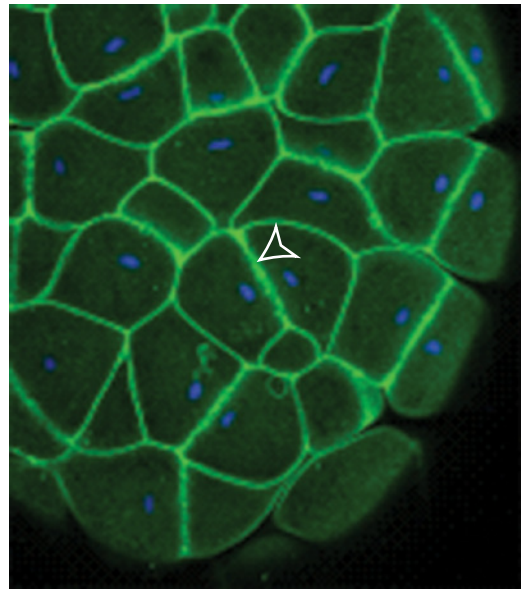


Figure 6.2 Localization of MELK in a *Xenopus* blastula stage embryo. MELK (green) is localized at cell–cell contacts. In dividing cells, MELK is also concentrated at the division site (empty arrowhead) between mitotic chromosomes. DNA is in blue. To see a color version of this figure, see Plate 12.

cell membrane ingression is mediated by an actomyosin-based contractile ring, the assembly and constriction of which are orchestrated by the small GTPase RhoA. Thus, anillin is considered to be a scaffold, which brings together several cytokinesis regulators associated with the force generator: the actomyosin ring located at the cytokinesis furrow. In *Xenopus* embryos, the fact that MELK, anillin, actin, MHC, and active RhoA concentrate in the equatorial band is consistent with a model in which all those proteins form a common large complex at the cell division site (Le Page et al. 2011). Overexpression of active MELK, but not a catalytically inactive mutant, induces cytokinesis defects. Although the cause of this effect is not fully understood at the molecular level, MELK overexpression was shown to impair active RhoA accumulation at the division site (Le Page et al. 2011). This might provide potential explanation for the cytokinesis defect induced by MELK overexpression.

The nature of the equatorial band observed in cleaving cells of the early embryos is at

present unknown. It may play a role of a specialized structure which concentrates several cytokinesis molecules in rapidly dividing large blastomeres of early embryos. In large blastula cells, some molecules including anillin, actin, MHC, RhoA, and MELK appear to be specifically recruited at the cell division furrow. Thus, cytokinetic proteins may contribute to potentiate the furrow constriction rate during cytokinesis. In particular, we proposed that MELK might be specifically involved in sustained cytokinesis in such large embryonic cells potentially requiring the action of higher mechanical forces to invaginate the plasma membrane. The decrease in MELK concentration at the equatorial cortex is correlated with the midblastula transition (MBT) and the diminution of cell sizes and potential requirement of lower forces. Thus, smaller cells may require less MELK and also other cytokinetic regulators. Altogether, these data indicate that profound modifications in the mode of cytokinesis occur during the pre-MBT period of embryo development.

In gastrula embryo, cells still accumulate anillin at the apical equatorial cortex (Figure 6.3A). In contrast to blastula stage, MELK (Figure 6.3B), actin, and MHC do not concentrate at this specific site. In epithelial cells of gastrula embryos, which constitute the embryo external cell layer, the division furrow progresses starting from the basolateral side toward the apical membrane. A drastic change in the direction of the furrowing occurs between late blastula and gastrula stages. The reason for this modification of the direction of ingression during development is yet unknown, but it could be related to the diminution of the size of cells.

Asymmetric furrowing is a mode of cytokinesis conserved throughout evolution

The asymmetric furrowing occurs in diverse model organisms ranging from worm to mouse. The fact that asymmetric furrowing is widely encountered suggests that this mode of cytokinesis may play an important role. Herein, readers will find few examples of reported cases of asymmetric furrowing

chosen to illustrate how widespread this specific mode of cell division is in the animal kingdom and what roles it may play in embryo development and adult organisms.

Asymmetric division is a general mode of cell division during embryonic development. In the worm *Caenorhabditis elegans*, the asymmetric furrowing occurs already during the first embryonic division (Audhya et al. 2005). In this organism, division occurs in two sequential steps with two separate sites of membrane invagination. First, a primary furrow ingresses, starting from one side of the embryo. When it reaches the proximity of the central mitotic spindle between the separating chromosomes, a transition occurs and it slows down its progression while the second ingression starts from the opposite side of the embryo. It is important to note that the mitotic spindle is centrally positioned in the one-cell *C. elegans* embryo. Further studies have shown that the two cytokinetic proteins anillin and septin are necessary for asymmetric furrowing in the *C. elegans* embryo (Maddox et al. 2007).

In the invertebrate ascidian embryo at the 16-cell stage, a displacement of the mitotic spindle induces asymmetric cell divisions, which are at the origin of the two small specialized cells called germ cell precursors. It was shown that in the particular cell-type pair B5.2 cells (in ascidian nomenclature), the division furrow ingresses asymmetrically from the apical membrane toward the basolateral membrane (Prodon et al. 2010). Thus, this mode of cell division in ascidian embryo appears similar to the asymmetric cytokinesis occurring in *Xenopus* embryo at the blastula stage. It was further shown in the ascidian embryo that the cell-cell contact inhibits the asymmetric furrowing; the furrowing becomes symmetric in isolated blastomeres (Prodon et al. 2010). Interestingly, it was also found that, unusually, the furrowing is initiated on the most distant side of the mitotic spindle midzone. According to the current model of cytokinesis, the spindle midzone stimulates the actomyosin-driven contraction of the cleavage furrow. Therefore, it will be particularly interesting to determine the molecular mechanisms, which regulate furrowing initiation distantly from the central spindle.

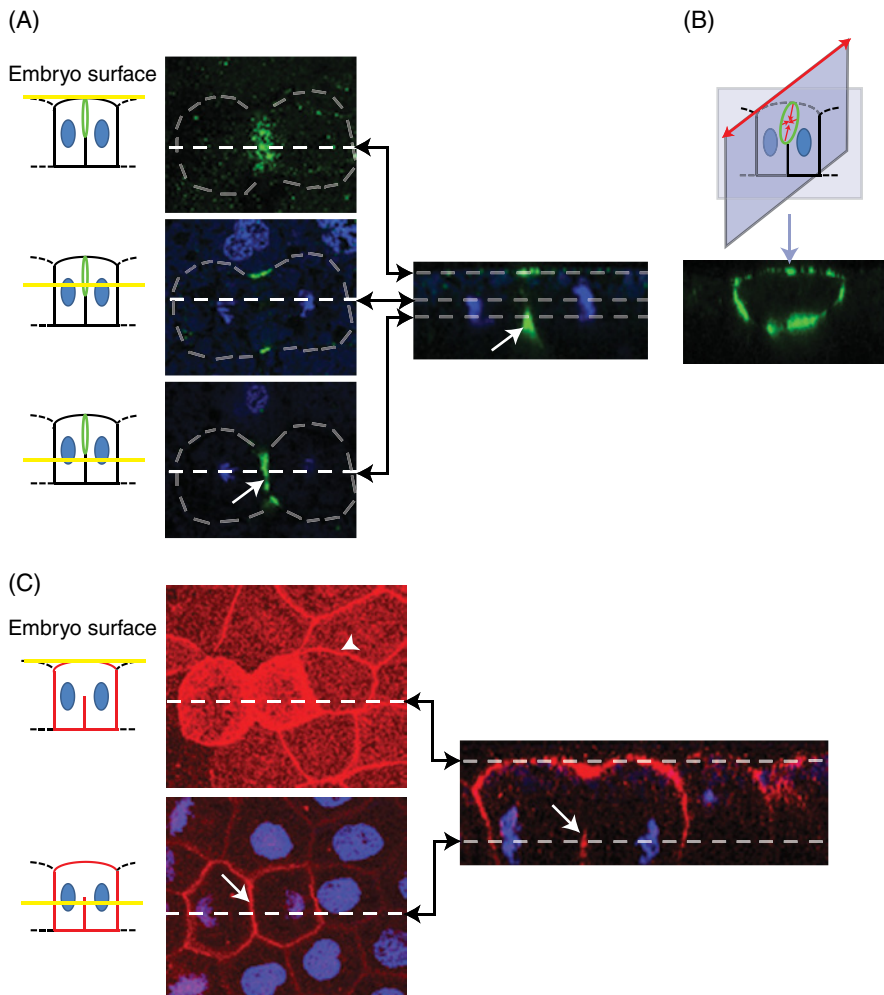


Figure 6.3 Localization of anillin and MELK in dividing gastrula stage embryo. (A) Localization of anillin (green) in the epithelium of a gastrula stage embryo. Diagrams on the left: yellow lines mark the confocal planes relative to the embryo surface. Grey dashed lines were drawn to indicate the limits of the dividing cell. White dashed line symbolizes the plane used for orthogonal projection of the confocal planes shown on the right. The green circle corresponds to the closing cytokinetic furrow. The arrow points to the asymmetric cytokinetic furrow. (B) Anillin localizes as a ring between the two daughter cells as shown on the orthogonal projection of the confocal planes. (C) Localization of MELK (red) in the epithelium of a gastrula stage embryo. Diagrams on the left: yellow lines mark the confocal planes relative to the embryo surface. White dashed line symbolizes the plane used for orthogonal projection of the confocal planes shown on the right. In interphase cells, MELK is localized at the apical junctional complexes (white arrow). In cells undergoing cytokinesis, MELK is localized all around the cell cortex as shown by the orthogonal projection. To see a color version of this figure, see Plate 13.

It will also be important to determine in ascidians whether during later embryo development cytokinesis progresses from the basal toward the apical membrane. This could indicate that a transition, as the one we described in *Xenopus*, occurs also in ascidian embryos.

Importantly, asymmetric furrowing is not restricted to embryos. Indeed, it was also

observed in adult tissue and polarized cells cultured *in vitro*. Asymmetric furrowing in rat pancreas was described already 40 years ago using electron microscopy (Pictet et al. 1972). This study shows that the asymmetric furrow progresses from the basal side toward the apical membrane in these pancreatic polarized cells. Another electron microscopy analysis of

mouse small intestine also shows that asymmetric furrowing occurs in epithelial cells situated in intestinal crypts (Jinguji and Ishikawa 1992). In this case, the furrow also forms at the basolateral membrane and progresses toward the apical membrane. The fact that asymmetric furrow ingression occurs in adult tissues of vertebrate organisms suggests that it is a potentially important and broadly executed mode of cytokinesis. Another example of asymmetric furrowing is the one occurring in MDCK cells cultured *in vitro*. When MDCK cells become confluent, they stop dividing to become differentiated and polarized. However, there is a short time window during which cells are confluent but still can tighten against each other, and consequently, some cells that are already polarized undergo cell division. This event occurs at a low frequency as the mitotic index in a confluent cell culture is very low. Nevertheless, it was shown that *in vitro* cultured MDCK cells at this stage also divide by asymmetric furrowing (Reinsch and Karsenti 1994). Also in this case, the asymmetric furrowing progresses in the basal to the apical direction.

The most spectacular example of asymmetric furrowing is the one occurring during oocyte maturation. In mouse oocyte, the polar body extrusion corresponds to a combination of an asymmetric division and asymmetric furrowing. During meiosis I and meiosis II, the mitotic spindle is positioned closely to the oocyte plasma membrane (oolemma), and during the two meiotic divisions, one chromosome set is expelled from the oocyte and forms the polar body (the small cell a few micrometers in diameter), and the second chromosome set remains in the oocyte (60–80 μm), conserving majority of the cytoplasm. Therefore, these particular cytokineses during meiotic divisions are remarkable examples of highly asymmetric division linked to the asymmetric positioning of the mitotic apparatus. Specifically during meiosis II, when initially the mitotic spindle is positioned parallel to the oolemma, cytokinesis is initiated at a single side at the oocyte cortex, leading to a unilateral furrowing on the closest side to the mitotic spindle (Ibanez et al. 2005; Wang et al. 2011). Then the meiotic spindle rotates, a bilateral furrow forms, and cytokinesis completes. It was proposed that the meiotic spindle induces furrowing only at

a very close distance from the oolemma, which could explain the biphasic induction of the furrowing being initially unilateral and later becoming bilateral.

What is the rationale for the occurrence of the asymmetric furrowing during cytokinesis? A commonly accepted and reasonable explanation for asymmetric furrowing in polarized cells, proposed for epithelial cells, is that this mechanism allows preserving the tissue integrity. Indeed, it has been shown that epithelial cells remain polarized and retain cellular junctions during their division (Baker and Garrod 1993). Importantly, they keep their apical junctional complexes, including, in vertebrates, the tight and adherens junctions. The correlation between the existence of apically positioned junctions (adherens only in invertebrates and adherens plus tight junctions in vertebrates) and the direction in which the furrow progresses in epithelial cells (from the basal to the apical membrane) leads us to propose the following hypothesis: apically positioned junctions could orient the furrow ingression from the basolateral membrane toward the apical membrane and simultaneously could prevent the furrowing in the opposite direction. Although the presence of apically positioned junctional complexes could explain why the furrowing progresses in an orientated manner, it does not explain, however, how the unilateral furrowing is initiated. Cell–cell contacts may inhibit symmetric furrowing, leading to an asymmetric furrow as shown in the ascidian embryo (Prodon et al. 2010). However, in the case of *C. elegans* one-cell embryo, which cleaves via asymmetric furrowing, no cell–cell contacts are present. Therefore, the regulation by lateral contact inhibition cannot be involved in this cleavage. Despite this, the case of *C. elegans* one-cell embryo is not an exception, but rather constitutes a rule in the mode of cytokinesis progression in one-cell embryos. Notably, in *Xenopus* one-cell embryo, the cleavage furrow is initiated at the animal pole, rapidly expands circumferentially toward the vegetal pole, then slows down, and finally completes at the animal pole. In the latter case, the asymmetric furrowing is certainly related to the stable polarization of the embryo already established during oogenesis.

Taken together, the studies performed in diverse model organisms revealed common characteristics of the asymmetric furrowing and allowed to draw several conclusions: (i) asymmetric furrowing is a highly conserved mode of cytokinesis; (ii) it occurs *in vivo* in both embryos and adult tissues; (iii) asymmetric furrowing occurs also in single cells, as in the case of the worm one-cell embryo and the mouse oocyte; (iv) it occurs in polarized cells; (v) in adult tissues and embryos at a certain developmental stage (*Xenopus*), the cytokinetic furrow ingresses in a conserved orientation from the basolateral to the apical membrane; and (vi) the opposite orientation, from the apical toward the basolateral membrane, appears restricted to early embryos as in *Xenopus* and ascidians.

The *Xenopus* embryo as a model system to analyze asymmetric furrowing

Xenopus embryo presents several advantages to study asymmetric furrowing in vertebrates. Obviously, to study asymmetric furrowing, polarized cells must divide, and it is much easier to study this phenomenon when these cell divisions are frequent, which is the case of the *Xenopus* embryo. In a pre-MBT embryo, blastomeres are already polarized and meta-synchronous cell divisions occur every 30 min. Although the rhythm of cell division slows down after MBT, in the gastrula embryo, epithelial cells still divide frequently. The mitotic index is about 10% in a gastrula (Saka and Smith 2001). Altogether, this creates a favorable model to follow cytokinesis in general. In addition, in gastrula, almost all of the cell divisions occur in the plane of the epithelium (Chalmers et al. 2003), and therefore, the cytokinetic furrow is perpendicular to the epithelial surface of the embryo. This situation is particularly favorable for imaging the asymmetric furrowing since it does not require spatial reorientation of the sample. As epithelial cells are at the embryo surface, and not embedded within the embryo such as in the pancreas or in the small intestine, the analysis of the asymmetric furrowing in living cells becomes a particularly easy task. Moreover, methods of live imaging in *Xenopus* embryos based on confocal

microscopy and fluorescent protein expression have been spectacularly improved within the last decade. Like in adult mammalian tissues, in gastrula embryos, furrowing occurs from the basal side toward the apical membrane. The fact that the furrowing orientation is conserved between gastrula embryo and adult mammalian tissue suggests that mechanisms that regulate asymmetric furrowing might also be conserved. Therefore, we propose that the *Xenopus* gastrula embryo could be a suitable model system to study this particular mode of cytokinesis. In addition, *Xenopus* embryo could be used to study the transition which occurs between the blastula and gastrula stages and therefore to identify how the inversion of the ingression is regulated. Methods allowing modification of gene expression in *Xenopus* embryo such as antisense morpholinos can be applied. The newly developed transcription activator-like effector nucleases (Talen) method, which has recently been shown to be successfully applied to *Xenopus* embryos (Lei et al. 2012), should improve genetic manipulations and will be helpful to dissect asymmetric furrowing at the molecular level.

Conclusions

Because in *Xenopus* embryo epithelial cells are external and not embedded as in mammalian adult tissues and also actively divide, the embryo offers a remarkably favorable model to analyze the dynamics and regulation of asymmetric furrowing. Therefore, we propose the *Xenopus* embryo as a model system for studying this particular mode of cytokinesis in vertebrates. We would like to stress that the advantages of using *Xenopus* embryo make this organism a favorable model to analyze not only asymmetric furrowing but also division of polarized cells and diverse aspects of epithelium homeostasis in vertebrates.

Acknowledgments

The work of the authors was supported by the Ligue Départementale contre le Cancer (22 et 35), the ARC, INCa, ANR KinBioFret, and CNRS.

References

- Audhya, A., Hyndman, F., McLeod, I. X., et al. 2005. A complex containing the Sm protein CAR-1 and the RNA helicase CGH-1 is required for embryonic cytokinesis in *Caenorhabditis elegans*. *J Cell Biol* 171(2): 267–79.
- Badouel, C., Korner, R., Frank-Vaillant, M., Couturier, A., Nigg, E. A. and Tassan, J. P. 2006. M-phase MELK activity is regulated by MPF and MAPK. *Cell Cycle* 5(8): 883–9.
- Badouel, C., Chartrain, I., Blot, J. and Tassan, J. P. 2010. Maternal embryonic leucine zipper kinase is stabilized in mitosis by phosphorylation and is partially degraded upon mitotic exit. *Exp Cell Res* 316(13): 2166–73.
- Baker, J. and Garrod, D. 1993. Epithelial cells retain junctions during mitosis. *J Cell Sci* 104(Pt 2): 415–25.
- Bement, W. M., Benink, H. A. and von Dassow, G. 2005. A microtubule-dependent zone of active RhoA during cleavage plane specification. *J Cell Biol* 170(1): 91–101.
- Blot, J., Chartrain, I., Roghi, C., Philippe, M. and Tassan, J.-P. 2002. Cell cycle regulation of pEg3, a new *Xenopus* protein kinase of the KIN1/PAR-1/MARK family. *Dev Biol* 241(2): 327–38.
- Chalmers, A. D., Strauss, B. and Papalopulu, N. 2003. Oriented cell divisions asymmetrically segregate aPKC and generate cell fate diversity in the early *Xenopus* embryo. *Development* 130(12): 2657–68.
- Chartrain, I., Le Page, Y., Körner, R., Kubiak, J. Z. and Tassan, J. P. 2013. Localization of MELK at the apical junctional complex is regulated by RACK1 in epithelial cells of *Xenopus* embryo. *Biology Open* 2(10): 1037–1048.
- Davezac, N., Baldin, V., Blot, J., Ducommun, B. and Tassan, J. P. 2002. Human pEg3 kinase associates with and phosphorylates CDC25B phosphatase: a potential role for pEg3 in cell cycle regulation. *Oncogene* 21(50): 7630–41.
- D'Avino, P. P., Takeda, T., Capalbo, L., et al. 2008. Interaction between Anillin and RacGAP50C connects the actomyosin contractile ring with spindle microtubules at the cell division site. *J Cell Sci* 121(Pt 8): 1151–8.
- Field, C. M. and Alberts, B. M. 1995. Anillin, a contractile ring protein that cycles from the nucleus to the cell cortex. *J Cell Biol* 131(1): 165–78.
- Gray, D., Jubbs, A. M., Hogue, D., et al. 2005. Maternal embryonic leucine zipper kinase/murine protein serine-threonine kinase 38 is a promising therapeutic target for multiple cancers. *Cancer Res* 65(21): 9751–61.
- Gregory, S. L., Ebrahimi, S., Milverton, J., Jones, W. M., Bejsovec, A. and Saint, R. 2008. Cell division requires a direct link between microtubule-bound RacGAP and Anillin in the contractile ring. *Curr Biol* 18(1): 25–9.
- Heyer, B. S., Warsowe, J., Solter, D., Knowles, B. B. and Ackerman, S. L. 1997. New member of the Snf1/AMPK kinase family, Melk, is expressed in the mouse egg and preimplantation embryo. *Mol Reprod Dev* 47(2): 148–56.
- Hickson, G. R. and O'Farrell, P. H. 2008. Anillin: a pivotal organizer of the cytokinetic machinery. *Biochem Soc Trans* 36(Pt 3): 439–41.
- Ibanez, E., Albertini, D. F. and Overstrom, E. W. 2005. Effect of genetic background and activating stimulus on the timing of meiotic cell cycle progression in parthenogenetically activated mouse oocytes. *Reproduction* 129(1): 27–38.
- Jinguji, Y. and Ishikawa, H. 1992. Electron microscopic observations on the maintenance of the tight junction during cell division in the epithelium of the mouse small intestine. *Cell Struct Funct* 17(1): 27–37.
- Jung, H., Seong, H. A. and Ha, H. 2008. Murine protein serine/threonine kinase 38 activates apoptosis signal-regulating kinase 1 via Thr 838 phosphorylation. *J Biol Chem* 283(50): 34541–53.
- Knoblich, J. A. 2008. Mechanisms of asymmetric stem cell division. *Cell* 132(4): 583–97.
- Le Page, Y., Chartrain, I., Badouel, C. and Tassan, J. P. 2011. A functional analysis of MELK in cell division reveals a transition in the mode of cytokinesis during *Xenopus* development. *J Cell Sci* 124(Pt 6): 958–68.
- Lei, Y., Guo, X., Liu, Y., et al. 2012. Efficient targeted gene disruption in *Xenopus* embryos using engineered transcription activator-like effector nucleases (TALENs). *Proc Natl Acad Sci U S A* 109(43): 17484–9.
- Lin, M. L., Park, J. H., Nishidate, T., Nakamura, Y. and Katagiri, T. 2007. Involvement of maternal embryonic leucine zipper kinase (MELK) in mammary carcinogenesis through interaction with Bcl-G, a pro-apoptotic member of the Bcl-2 family. *Breast Cancer Res* 9(1): R17.
- Maddox, A. S., Lewellyn, L., Desai, A. and Oegema, K. 2007. Anillin and the septins promote asymmetric ingression of the cytokinetic furrow. *Dev Cell* 12(5): 827–35.
- Marie, S. K., Okamoto, O. K., Uno, M., et al. 2008. Maternal embryonic leucine zipper kinase transcript abundance correlates with malignancy grade in human astrocytomas. *Int J Cancer* 122(4): 807–15.
- Nakano, I., Paucar, A. A., Bajpai, R., et al. 2005. Maternal embryonic leucine zipper kinase (MELK)

- regulates multipotent neural progenitor proliferation. *J Cell Biol* 170(3): 413–27.
- Nakano, I., Masterman-Smith, M., Saigusa, K., et al. 2008. Maternal embryonic leucine zipper kinase is a key regulator of the proliferation of malignant brain tumors, including brain tumor stem cells. *J Neurosci Res* 86(1): 48–60.
- Paris, J. and Philippe, M. 1990. Poly(A) metabolism and polysomal recruitment of maternal mRNAs during early *Xenopus* development. *Dev Biol* 140(1): 221–4.
- Pickard, M. R., Green, A. R., Ellis, I. O., et al. 2009. Dysregulated expression of Fau and MELK is associated with poor prognosis in breast cancer. *Breast Cancer Res* 11(4): R60.
- Pictet, R. L., Clark, W. R., Williams, R. H. and Rutter, W. J. 1972. An ultrastructural analysis of the developing embryonic pancreas. *Dev Biol* 29(4): 436–67.
- Piekny, A. J. and Glotzer, M. 2008. Anillin is a scaffold protein that links RhoA, actin, and myosin during cytokinesis. *Curr Biol* 18(1): 30–6.
- Prodon, F., Chenevert, J., Hebras, C., et al. 2010. A. Dual mechanism controls asymmetric spindle position in ascidian germ cell precursors. *Development* 137(2):2011–21.
- Reinsch, S. and Karsenti, E. 1994. Orientation of spindle axis and distribution of plasma membrane proteins during cell division in polarized MDCKII cells. *J Cell Biol* 126(6): 1509–26.
- Saka, Y. and Smith, J. C. 2001. Spatial and temporal patterns of cell division during early *Xenopus* embryogenesis. *Dev Biol* 229(2): 307–18.
- Straight, A. F., Field, C. M. and Mitchison, T. J. 2005. Anillin binds nonmuscle myosin II and regulates the contractile ring. *Mol Biol Cell* 16(1): 193–201.
- Tassan, J. P. 2011. Cortical localization of maternal embryonic leucine zipper kinase (MELK) implicated in cytokinesis in early *xenopus* embryos. *Commun Integr Biol* 4(4): 483–5.
- Vulsteke, V., Beullens, M., Boudrez, A., et al. 2004. Inhibition of spliceosome assembly by the cell cycle-regulated protein kinase MELK and involvement of splicing factor NIPP1. *J Biol Chem* 279(10): 8642–7.
- Wang, Q., Racowsky, C. and Deng, M. 2011. Mechanism of the chromosome-induced polar body extrusion in mouse eggs. *Cell Div* 6: 17.

7 Induction and Differentiation of the *Xenopus* Ciliated Embryonic Epidermis

Marie Cibois, Pierluigi Scerbo, Virginie Thomé, Andrea Pasini, & Laurent Kodjabachian

Institute of Developmental Biology of Marseille, CNRS, Aix-Marseille Université, Marseille, France

Abstract: In this chapter, we shall focus on the cellular and molecular mechanisms that control the development of the *Xenopus* embryonic ciliated epidermis, a question that received little attention in comparison to mesoderm or neural development. We shall review the events that transform the pluripotent cells of the animal blastula hemisphere into nonneural ectodermal progenitors that subsequently differentiate into the four major cell types of the premetamorphic epidermis. The focus will be put on the biogenesis of multiciliated cells, which can be studied in the *Xenopus* embryonic epidermis more easily and more deeply than in any other model. We shall demonstrate how working on the frog embryonic epidermis may continue to yield basic as well as biomedically relevant knowledge in the fields of signaling, cell and tissue polarity, and ciliogenesis.

Introduction

In vertebrates, the epidermis is the largest organ and one of the major interfaces between the body and the surrounding environment. It acts as a protection against temperature changes, irradiation, dehydration, shocks, pollutants and pathogens; hosts several sensory receptors; excretes wastes; and, in small aquatic organisms, mediates the exchanges of respiratory gases. Characterizing the cellular and molecular mechanisms that underlie and control the development of vertebrate epidermis is of greatest relevance in the fields of evolutionary biology, physiology, and medicine.

The developmental history, histology, and function of the epidermis in anuran amphibians reflect their peculiar life cycle, with a strictly aquatic larval phase and an adult capable of living on land. Thus, during anuran metamorphosis, the embryonic and larval epidermis, consisting of a simple epithelium adapted to life in an aquatic medium, is progressively replaced by a complex multilayered structure suitable to the more variable terrestrial environment. This metamorphic transition is supposed to have arisen about 360 million years ago, when the ancestors of modern-day amphibians diverged from lobe-finned fishes, and a better understanding

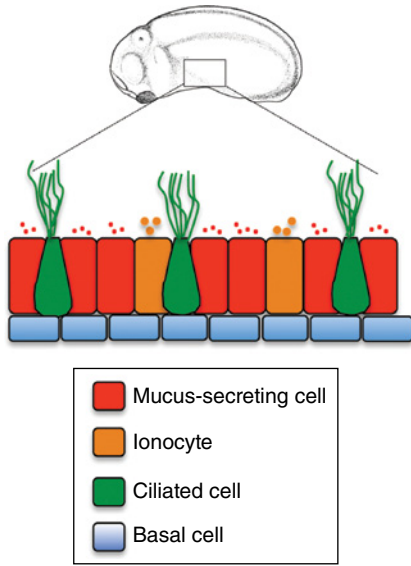


Figure 7.1 Cellular composition of the mature *Xenopus* embryonic epidermis. At the tail bud stage, the epidermis exhibits its final aspect. MCCs (green) and ionocytes (brown) are inserted in the superficial epithelial layer among mucus-secreting cells (red). Cells in the inner layer (blue) display a flattened morphology and rest on a basal lamina (not represented). Note the production of small secretory vesicles by mucus-secreting cells and of larger vesicles by ionocytes. To see a color version of this figure, see Plate 14.

of the underlying cellular and molecular mechanisms could in turn shed light on the evolutionary adaptation of tetrapods to the terrestrial life.

The mature embryonic *Xenopus* ectoderm consists of a simple bilayered tissue (Figure 7.1). The outer layer is a mucociliary epithelium composed of mucus-secreting goblet cells, among which are found regularly spaced multiciliated cells (MCCs) and scattered ionocytes, involved in the regulation of ionic homeostasis. The inner layer contains noncohesive cells that are progenitors for the larval and postmetamorphic epidermis. Although the precise function of epidermal MCCs is unclear, their biology can be best addressed in this tissue as they are exposed at the surface of 1-day-old embryos, a fairly unique feature in vertebrates (Hayes et al. 2007; Werner and Mitchell 2012). The embryonic ectoderm subsequently develops into a larval epidermis, consisting of an outer layer

of apical cells and an inner layer containing larval basal cells and keratin-positive skein cells, separated from the acellular collagen-rich primary connective tissue by a collagen lamella (Yoshizato 2007). Intriguingly, ciliated cells are no longer visible in the mature larval skin, which poses the question of their physiological role in the embryo and of their fate in the larva. In the course of metamorphosis, adult basal cells emerge, which will constitute the proliferating precursors of the multilayered adult epidermis. The multilayered organization of the adult *Xenopus* epidermis is analogous to that of the amniote epidermis, with a basal proliferative compartment consisting of cells in the basal and spinous layers, overlain by the progressively more differentiated cells of the granular and cornified layers.

In *Xenopus*, morphological observations can be combined with methods to manipulate gene function and imaging techniques, thus making this organism a very amenable experimental model for studying the developmental history, physiology, and pathophysiology of epidermis in vertebrates. As an example, it has been recently shown that in *Xenopus*, the morpholino oligonucleotide-mediated inactivation of PYCR1, a gene associated with the human skin disease autosomal recessive cutis laxa, leads to epidermal abnormalities, thus stressing the conservation of the molecular mechanisms that control the epidermal development across the tetrapod phylum (Reversade et al. 2009). In addition, the histological features of *Xenopus* epidermis at early developmental stages can also provide useful model systems for the study of amniote nonepidermal epithelia. This is shown, for example, by the structural and molecular analogies uncovered between the ciliated frog epidermis and the mucociliary epithelium lining the human airways (Hayes et al. 2007). Likewise, the presence of ionocytes in the frog embryonic epidermis may help understanding the biology of transporting epithelia such as the mammalian kidney, which contains cells of the same type (Dubaisi and Papalopulu 2011; Quigley et al. 2011).

Finally, it is worth noting that the epidermis of anuran amphibians constitutes both the main entry point and one of the target organs for the parasitic chytrid fungus *Batrachochytrium*

dendrobatidis, the agent of chytridiomycosis, an emerging disease, which appears to be among the causes of the current worldwide collapse in wild anuran populations (Voyles et al. 2009). Understanding the development and physiology of *Xenopus* epidermis will undoubtedly provide clues to the mechanisms controlling susceptibility and resistance to fungal and bacterial infections in other anurans.

Nonneural ectoderm specification

Understanding the ontogeny of the epidermal mucociliary epithelium requires tracing back its origin from the time when germ layers are individualized. The epidermis derives from the nonneural ectoderm, which is itself specified in two steps. First, the ectoderm is set apart from the mesoderm and endoderm. Second, the ectoderm is partitioned into neural and nonneural anlage. In this section, we shall review the key mechanisms controlling these transitions.

Decades of research on the *Xenopus* embryo have revealed that it undergoes both mosaic and regulative development. Thus, the endoderm is positioned in the vegetal hemisphere of the egg through the action of the maternal determinant VegT, a T-box transcription factor (Zhang et al. 1998) (Figure 7.2). VegT cell autonomously activates the expression of several transcription factors that play a conserved role in vertebrate endoderm specification, including *sox17*, *mixer*, *bix*, and *gata* genes (Xanthos et al. 2001). In contrast, the mesoderm, which forms in the equatorial region of the blastula, results from induction by TGF- β superfamily ligands, such as *Xenopus* Nodal-related 5 (*Xnr5*), *Xnr6*, and *Derrière*, that are activated by VegT (Sun et al. 1999; Takahashi et al. 2000; Luxardi et al. 2010; Skirkanich et al. 2011) (Figure 7.2). The same ligands also relay the action of VegT to reinforce the endodermal identity of vegetal blastula cells (Kofron et al. 1999; Yasuo and Lemaire 1999). Members of the FGF family also play key roles in mesoderm induction as they control the competence of embryonic cells to respond to TGF- β ligands and directly activate the transcription of key mesodermal effectors such as *Xbra* (Isaacs et al. 1994; Cornell et al. 1995) (Figure 7.2). The endoderm and mesoderm germ layers are also patterned in the early

blastula through the action of the maternal Wnt11/ β -catenin pathway that establishes the dorsal-ventral and anterior-posterior axes (Tao et al. 2005) (Figure 7.2). In particular, β -catenin synergizes with VegT to enhance the expression of *Xnr* genes in the presumptive Spemann's organizer territory (Agius et al. 2000; Takahashi et al. 2000). In turn, the organizer patterns all germ layers during the course of gastrulation (De Robertis et al. 2000).

The emerging picture regarding ectoderm specification suggests that it occurs by default through the action of factors that oppose the endoderm and mesoderm fate adoption by animal pole cells. Through this action, such factors contribute to maintain the developmental potential of embryonic cells that remain competent to adopt virtually any fate until midgastrula stage (Snape et al. 1987; Wylie et al. 1987). This potential was revealed in the transplantation assays, whereby single blastula animal cells can colonize all somatic tissues in a host embryo (Snape et al. 1987), and in the animal cap assay that was used to induce ectodermal, mesodermal, or endodermal derived fates through exposition to various cocktails of growth factors (Hemmati-Brivanlou and Melton 1994; Okabayashi and Asashima 2003). Since animal blastomeres can adopt any but the germ cell identity, they are considered somatically pluripotent. Multiple maternal and zygotic factors collaborate to maintain the uncommitted ectoderm. They are all enriched in the animal hemisphere and somehow involved in inhibiting the mesendodermal genetic program. For instance, the maternal transcriptional regulator *Zic2* is required to repress the expression of the mesendoderm inducers *Xnrs* in the animal hemisphere (Houston and Wylie 2005). Similarly, the maternal secreted BMP/TGF- β inhibitor *Coco* (Bell et al. 2003) and the maternal Smad4 ubiquitin ligase *Ectodermin* (Dupont et al. 2005) prevent the mesoderm from forming in the animal territory through repression of the TGF- β signal transduction.

Additional key regulators of pluripotency include maternal Oct-25 and Oct-60, as well as zygotic Oct-91, three members of the *Pou5f1* family of homeodomain transcription factors (Figure 7.2). Oct-25 and Oct-60 maintain the developmental potential of animal cells by

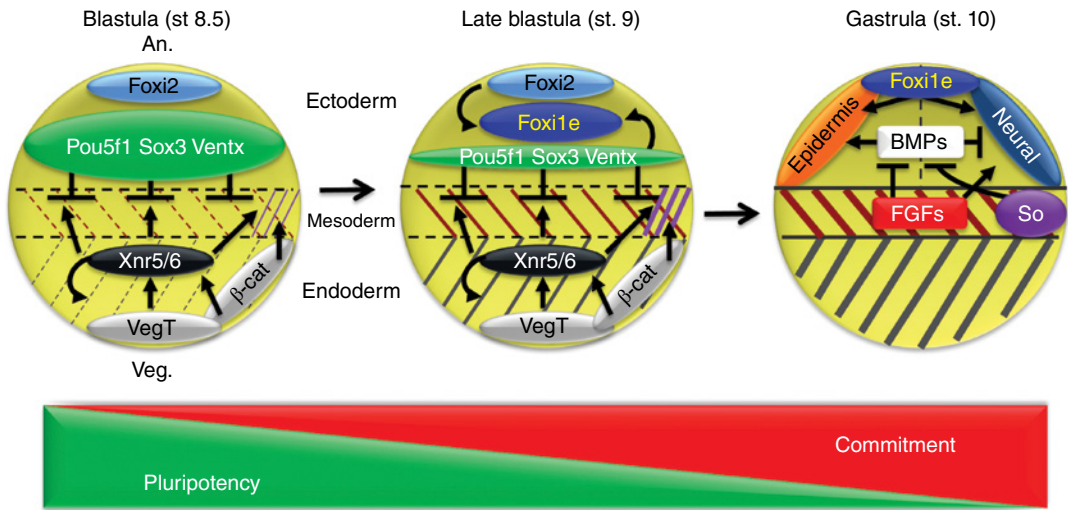


Figure 7.2 Molecular control of germ-layer positioning and transition from pluripotent to committed states of animal cells. At the MBT (st. 8.5), the maternal determinants VegT and β -catenin in the vegetal hemisphere and Foxi2 in the animal hemisphere contribute to position endoderm and ectoderm, respectively. VegT induces endodermal regulators directly and through Nodal-related proteins Xnr5 and 6. Nodal signaling also induces mesoderm fates in equatorial cells. Pluripotency regulators that include Pou5f1, Sox3, and Ventx antagonize VegT, β -catenin, and Nodals to prevent mesendoderm induction in animal cells. They also activate together with Foxi2 the ectoderm regulator Foxi1e that in turn authorizes the neural and epidermal programs to unfold. The choice between these two programs is controlled by the BMP genetic system that receives multiple regulatory inputs, particularly from antagonists produced by Spemann's organizer and by FGF/ERK signals. Note that cellular commitment is progressive over time and is linked to the depletion of pluripotency regulators. Only a selection of the known key players is represented for simplicity. Please refer to the text for a more complete description.

counteracting β -catenin and VegT transcriptional activity (Cao et al. 2006; Abu-Remaileh et al. 2010; Cao et al. 2010). Oct-91, which is expressed from midblastula transition (MBT) to late gastrulation, can maintain the cells of the animal pole in an uncommitted state when they are exposed to the mesoderm inducer FGF (Henig et al. 1998). When all three *Pou5f1* genes are knocked down, premature and increased differentiation of embryonic cells occur, as revealed by enhanced endoderm, mesoderm, and neural gene expression (Morrison and Brickman 2006). Many works have established that *Pou5f1* family members encode conserved regulators of uncommitted cell state, from fishes to mammals (Onichtchouk 2012). In mammalian embryonic stem (ES) cells, Pou5f1, best known as Oct-4, belongs to a now famous triad of transcription factors that collectively maintain pluripotency and prevent differentiation. Oct-4 partners are the SoxB1 family member Sox2 and the homeodomain factor Nanog (Chambers and

Tomlinson 2009). Key features of the Oct-4/Sox2/Nanog network are direct physical interactions, reciprocal regulations, and the capacity to directly repress the expression of prodifferentiation genes. In *Xenopus*, animal SoxB1 factors from maternal origin, such as Sox3, also maintain cells in an uncommitted state through transcriptional repression of mesendoderm inducers like Xnr5 (Zhang et al. 2004) (Figure 7.2). In contrast, *Nanog* is absent from the *Xenopus* genome. However, a recent line of work has suggested that the related homeodomain-containing *Ventx* genes may represent *Nanog* counterparts in *Xenopus*, as they prevent premature differentiation of embryonic cells and are bound and regulated by Pou5f1 (Cao et al. 2004; Scerbo et al. 2012) (Figure 7.2). Interestingly, whereas *Ventx* genes are absent from the mouse genome, *Ventx2* is present in human and is expressed in ES cells, where it is engaged in a positive regulatory loop with Oct-4 (Chia et al. 2010). Strikingly, axial patterning defects in *Ventx*

morphants – *Xenopus* embryos injected with Ventx antisense morpholino-modified oligonucleotides (MOs) – can be rescued by mouse *Nanog* mRNA injection (Scerbo et al. 2012). Similarly, pluripotency and self-renewal of mouse *Oct-4*-mutant ES cells can be rescued by the expression of *Xenopus Pou5f1* genes (Morrison and Brickman 2006). Thus, pluripotency in vertebrate cells appears to be regulated by a conserved network of transcription factors, making *Xenopus* animal blastula cells a valuable paradigm to further dissect this key biological property *in vivo*.

Maintenance of the pluripotent state of animal pole cells is permissive for ectoderm specification at the blastula to gastrula transition. Recent reports have started to highlight the prominent roles played by FoxI2 and FoxI1e, two members of the FoxI subclass of forkhead DNA binding proteins, in this phenomenon (Figure 7.2). FoxI2 is a maternally inherited determinant localized in animal pole cells, where it acts as a transcriptional activator required for ectoderm specification (Cha et al. 2012). Unlike pluripotency factor depletion, FoxI2 knockdown prevents ectoderm specification but does not cause mesendoderm expansion, suggesting that this factor controls the transition of animal cells from their initial pluripotent state towards the ectoderm fate. Among the ectoderm-specific genes under the control of FoxI2, *foxi1e* (also called *xema*) (Suri et al. 2005; Mir et al. 2007) and *lim5* (also called *lhx5*) have been the best characterized.

Foxi1e is a zygotic gene expressed dynamically in blastula animal cells, which appears to integrate multiple inputs, including direct transcriptional activation by maternal FoxI2 and repression by VegT (Suri et al. 2005; Mir et al. 2008; Cha et al. 2012). When ectopically expressed in vegetal endodermal cells, FoxI1e represses endodermal genes such as *sox17* and activates ectodermal markers such as the neural gene *Sox2*, the epidermal genes *ap2a* and *epidermal cytokeratin*, and the neural crest marker *Slug* (Mir et al. 2007). Conversely, *foxi1e* knockdown severely impairs ectoderm specification, as revealed by the loss of the aforementioned markers, without mesendoderm gene expansion in animal territories (Figure 7.2). At the tail bud stage, embryos

depleted of FoxI1e display anomalies both in neural tissue, with a clear reduction of central nervous system, and in epidermal tissue, where ciliated cells and ionocytes do not form (Mir et al. 2007; Dubaissi and Papalopulu 2011; Quigley et al. 2011). Thus, FoxI1e is the only described factor that is necessary and sufficient to induce all ectoderm-derived tissues, downstream of the maternal determinants VegT and FoxI2 that partition the blastula embryo into three germ layers.

Intriguingly, animal cells depleted of FoxI1e tend to dissociate from the ectodermal layer, consistent with a loss of identity and a change in their pattern of adhesion. The same phenotype is observed in embryos depleted of the ectoderm-specific LIM-homeodomain protein Lim5, although ectoderm patterning is unaffected (Houston and Wylie 2003). Lim5 ectopic expression in endoderm cells alters cell sorting, but unlike FoxI1e, it does not prevent endoderm formation, suggesting that it specifically controls a morphogenetic program in the ectoderm.

The earlier paragraphs described our current understanding of how animal cells are kept pluripotent and become fated to adopt ectodermal fates at the onset of gastrulation. The next step in the formation of the epidermis is the partitioning of the late blastula/early gastrula ectoderm into neural and nonneural territories. This step is particularly well understood, thanks to the intense research efforts spent over the last two decades to understand how the neural anlage is established, a process named neural induction. It is now very clear that the central mechanism for neural specification consists of the repression of bone morphogenetic protein (BMP) signaling (Munoz-Sanjuan and Brivanlou 2002; Stern 2005) (Figure 7.2). This repression is achieved at multiple levels: BMP gene expression is repressed by Wnt/ β -catenin activity in Spemann's organizer (Baker et al. 1999); the organizer secretes BMP antagonists such as Chordin, Noggin, Follistatin, and Cerberus (Piccolo et al. 1996; Zimmerman et al. 1996; Fainsod et al. 1997; Piccolo et al. 1999); the mesoderm produces FGF ligands that inhibit the BMP Smad1 transducer via ERK-dependent phosphorylation (Kuroda et al. 2005). However, our

laboratory also showed that FGF signaling plays a prominent BMP-independent role in neural induction, through direct transcriptional activation of early neural genes such as *zic3* and *foxD5* (Delaune et al. 2005; Marchal et al. 2009) (Figure 7.2). Work on other species showed that BMP and FGF pathways are also central to neural specification, with variable degrees of implication (Streit et al. 2000; Bertrand et al. 2003; Ying et al. 2003). If BMP inhibition is important for neural specification, this is because BMP activity is chiefly responsible for nonneural ectoderm specification (Figure 7.2). Thus, *in vivo* assays have shown that BMP activation is sufficient to transform neural into epidermal progenitors, whereas BMP inhibition is sufficient to transform epidermal into neural progenitors (Suzuki et al. 1997; Delaune et al. 2005; Chang and Harland 2007; Marchal et al. 2009). In conclusion, the ectoderm is divided into neural and nonneural territories at early gastrula stages through a tug of war between BMP agonist and antagonist molecules, all linked into a single self-regulating network active across the entire embryonic field (De Robertis 2006). Following its specification by BMP signaling, the nonneural anlage will give rise to the mature embryonic ciliated epidermis through another series of steps that are described in the next section.

Ontogeny of the mucociliary epithelium

A process of four steps

The development of the mature epidermis can be divided into four steps that span the first day of life of the larva (Figure 7.3). (i) During cleavage and blastula stages, asymmetric divisions lead to the formation of two distinct layers of cells in the ectoderm. (ii) During gastrulation, the precursors of the ciliated cells and of the ionocytes, as well as the basal cells, are specified in the inner layer of the nonneural ectoderm, whereas precursors of the mucus-secreting cells are specified in the outer layer. (iii) During neurulation, ionocytes and ciliated cells intercalate into the outer layer. (iv) Once in their final position, cells of the outer layer fully differentiate, whereas internal cells remain in a progenitor state.

Formation of two ectodermal layers

The formation of two molecularly distinct cellular layers throughout the ectoderm involves asymmetric divisions of cells overlying the blastocoelic cavity (Figure 7.3). As early as the 64-cell stage and throughout blastula stages, some of the superficial animal cells divide along the apical–basal axis, producing internal daughter cells (Chalmers et al. 2003). No particular spatial pattern of such vertical divisions has been detected, although they occur with constant frequencies between individual embryos. The mechanism that controls the orientation of these divisions remains unknown, but a correlation with cell shape has been noticed (Chalmers et al. 2003). Vertical divisions give rise to an outer polarized layer of cells displaying atypical protein kinase C (aPKC) on their apical surface and to an inner layer of nonpolarized cells (Chalmers et al. 2003). Cells from the outer layer form a true epithelium equipped with tight junctions that are likely positioned through the mutual antagonism between aPKC and LGL2 and PAR1, for which tagged forms were found localized at the basolateral membrane (Chalmers et al. 2005; Ossipova et al. 2007). In functional assays, PAR1 proved necessary and sufficient for ciliated cell fate adoption, whereas aPKC had the opposite effect (Ossipova et al. 2007). Although the localization of the endogenous PAR1 protein has not been reported, it is probably inherited by inner cells, following vertical divisions. Altogether, those works illustrated how apical–basal polarity is linked to cell fate determination through the activity of the aPKC/PAR1 genetic system (Figure 7.3).

Cell fate specification within the nonneural ectoderm

Cell fate determination in the *Xenopus* embryonic epidermis has so far been mainly linked to the Notch signaling pathway and the lateral inhibition mechanism (Figure 7.3). In this system, a cell expressing a Notch ligand (Delta or Serrate) adopts a certain fate and represses that fate in its immediate neighbors, where it activates the Notch receptor (Bray 2006). In the case of the *Xenopus* embryonic epidermis, transcripts of the Delta1 ligand are first expressed in ciliated cell precursors

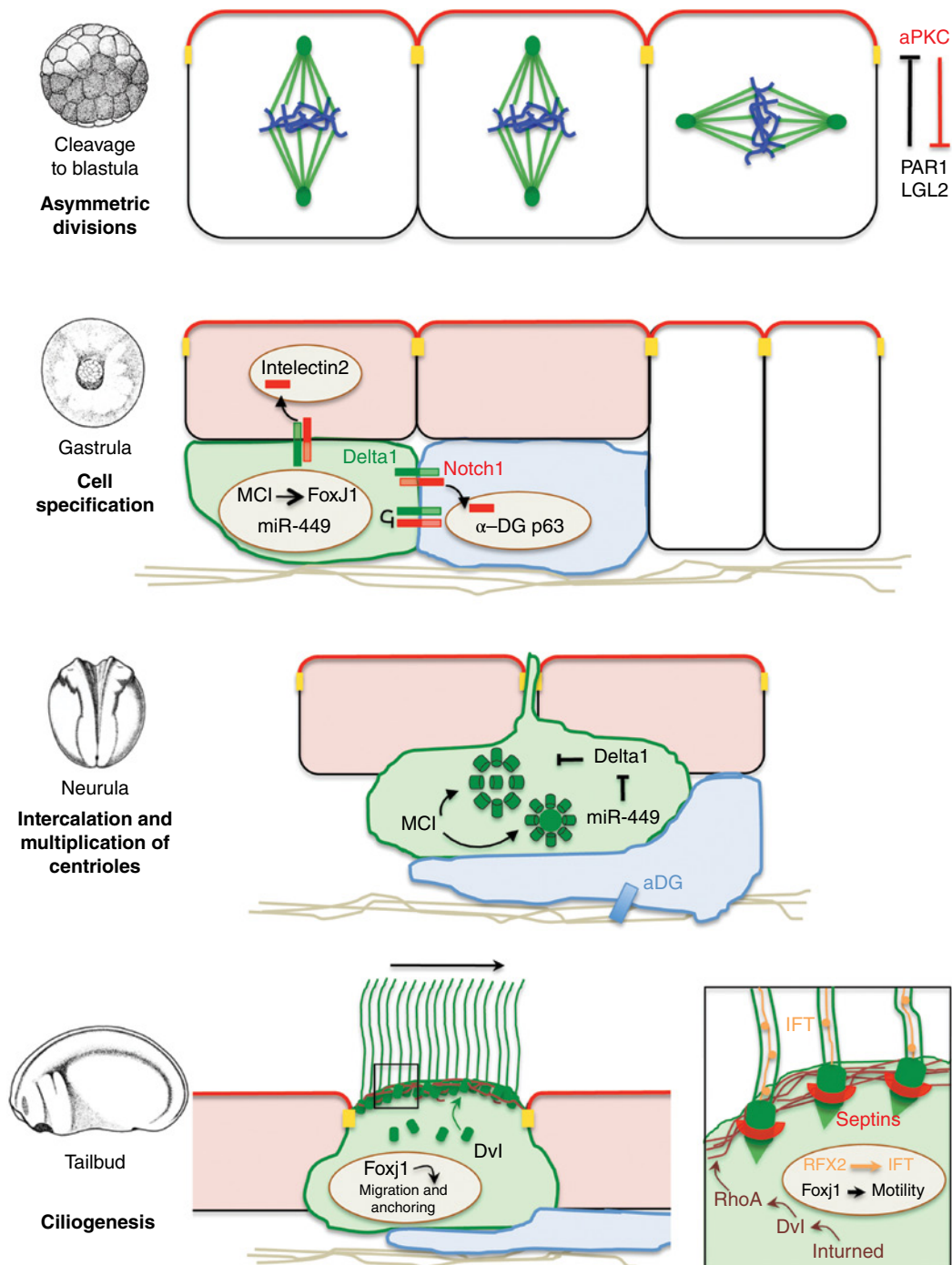


Figure 7.3 The four steps of MCC biogenesis. **Step 1.** From cleavage to blastula stages, divisions along the apical–basal axis generate distinct daughter cells, through asymmetric segregation of maternal determinants; outer cells inherit the apical protein aPKC, which opposes basolateral factors PAR1 and LGL2 to position tight junctions; inner cells do not inherit aPKC and remain loosely packed. **Step 2.** During gastrulation, CCPs are born in the inner epidermal layer. They express Delta1, which activates the Notch1 receptor both in neighboring inner cells that go on to express the markers α -DG and P63 and in outer cells that in turn express the goblet marker Intelectin2. CCPs express the transcription factors MCI and FoxJ1, as well as the microRNA miR-449. Note that in CCPs, Delta1 appears to inhibit Notch1 in *cis*. **Step 3.** During neurulation, CCPs go through two key events, radial intercalation and centrioles multiplication. Intercalation involves two steps: first, CCPs wedge in between the basal domain of outer cells and send protrusions apically. Second, CCPs migrate apically through vertices formed between three or more

(CCPs) and slightly later in ionocyte precursors (our unpublished data). Consistent with Delta1 distribution, both ciliated cells and ionocytes are selected by lateral inhibition. Thus, Notch pathway activation downstream of the receptor causes the suppression of both cell types, whereas Notch pathway inhibition induces supernumerary CCPs and ionocytes (Deblandre et al. 1999; Stubbs et al. 2006; Hayes et al. 2007; Quigley et al. 2011). One oddity, however, is that Delta1 overexpression does not stimulate lateral inhibition. Instead, it induces supernumerary CCPs, consistent with the idea that *cis*-inhibition of Notch by coexpressed Delta1 predominates in the epidermis (Deblandre et al. 1999; Marcet et al. 2011).

Interestingly, the Notch signaling system appears to be an immediate-early target of PAR1, although the precise outcome of this interaction in the epidermis remains to be fully characterized. On the one hand, PAR1 overexpression in epidermis leads to the localization of tagged Delta1 in cytoplasmic vesicles, a subcellular localization usually observed in Delta-positive signal-sending cells (Ossipova et al. 2007). On the other hand, in the *Xenopus* neural plate, PAR1 was shown to phosphorylate and cause the degradation of Mind Bomb, an E3 ubiquitin ligase necessary for signaling by Delta, thus suppressing lateral inhibition and favoring neuronal differentiation (Ossipova et al. 2009). In the epidermis, coexpression of PAR1 and Delta1 boosts CCP specification (Ossipova et al. 2007). Whether this reflects reduced lateral inhibition or increased *cis*-inhibition remains an interesting question to be addressed.

The central role of Notch signaling has offered an entry point into the genetic program

activated in the various epidermal cell populations. Thus, transcriptomic screens in embryos with challenged Notch pathway activity have identified key regulators of ciliated and ionocyte cell fates. The most compelling example comes from the recent identification of the gene encoding the nuclear factor Multicilin (MCI), which is activated following Notch pathway inhibition (Stubbs et al. 2012) (Figure 7.3). As its name indicates, this conserved gene encodes the first transcriptional regulator, which is necessary and sufficient for MCC differentiation in *Xenopus* embryonic epidermis, as well as in mouse airway epithelial cultures. MCI directly activates the expression of FoxJ1, a key conserved regulator of motile ciliogenesis (Stubbs et al. 2008; Yu et al. 2008), suggesting that MCI sits at the top of the genetic pathway regulating MCC differentiation (Figure 7.3). The precise mechanism of action of MCI remains to be determined, as it does not appear to activate transcription through sequence-specific DNA binding but rather through recruitment of additional factors via its coiled-coil and carboxy-terminal domains (Stubbs et al. 2012).

Another interesting target of Notch pathway inhibition is *FoxI1e*. Beside its role in ectoderm specification, FoxI1e acts at gastrula stages as an activator of ionocyte-specific genes, including proton pump subunits and ion channels (Dubaiissi and Papalopulu 2011; Quigley et al. 2011). Interestingly, mammalian FoxI1 controls a similar genetic program in proton-secreting cells within transporting epithelia, such as the kidney, suggesting that the *Xenopus* embryonic epidermis may help to model certain diseases affecting pH homeostasis.

outer cells. Centriole multiplication is required to produce dozens of BBs necessary for ciliary growth. Two pathways may be mobilized downstream of MCI: the centriole-dependent duplication pathway and the acentriolar pathway that implicates deuterosomes. This early step of CCP differentiation requires inhibition of Delta1 expression by miR-449. Note that nonintercalating cells make contact with the basal lamina that supports the bilayered epidermis, which allows the interaction of α -DG with extracellular matrix components. **Step 4.** At tail bud stages, ciliogenesis proceeds through the migration and anchoring of BBs at the apical cortex of the cell, a process under the control of FoxJ1 and PCP components, such as Dvl. PCP factors are also important for the assembly of a cortical actin web necessary for BB anchoring. Finally, cilium elongation can occur through the control of IFT machinery by RFX2, while FoxJ1 controls the expression of motility factors, such as Dynein arms. Septins act as gatekeepers to control the flow of molecules towards the base of the cilium. Rostrocaudal ciliary beating is coordinated between independent MCCs and within each MCC by PCP signaling that fine-tunes the rotation of BBs. Only a selection of the known key players is represented for simplicity. Please refer to the text for a more complete description.

Notch activation is important for the specification of nonintercalating inner epidermal cells or basal cells. Among the genes activated by Notch in basal cells, α -Dystroglycan (α -DG) encodes a transmembrane protein necessary for basement membrane formation and CCP intercalation (Sirour et al. 2011) (Figure 7.3). The same study also identified P63 as a positive target of Notch signaling in basal cells. Interestingly, in mammals, P63 controls the stem cell potential of basal cells in stratified epithelia, including those in airways (Rock et al. 2009). However, the role of P63 in basal cells of the *Xenopus* embryonic epidermis remains to be investigated.

Prior to intercalation of inner cells, all cells of the outer layer are fated to become mucus secretory cells. Our unpublished data suggest that Notch pathway activation by Delta1 is required for goblet cell fate adoption.

In conclusion, cell fate allocation in the developing *Xenopus* epidermis is largely controlled by Notch pathway deployment. However, it is more than likely that prominent roles are also played by additional signaling systems, such as the BMP pathway that is still active in the nonneural ectoderm when fate choices are made (Schohl and Fagotto 2002). Likewise, we surmise that additional transcription factors may play important regulatory roles. For instance, the HMG-box transcription factor Sox17 was shown to enhance FoxJ1 expression in mouse respiratory epithelium (Park et al. 2006a). In *Xenopus*, Sox7 is expressed in ciliated cells and could participate to their proper differentiation (Fawcett and Klymkowsky 2004).

The intercalation process

In 1992, Drysdale and Elinson showed that approximately half of the cells from the inner layer intercalate into the outer layer during neurulation of the embryo (Drysdale and Elinson 1992). Half of this population corresponds to CCPs and the other half corresponds to ionocyte progenitors. A more recent study showed that both CCPs and ionocyte progenitors, also described as intercalating nonciliated cells or INCs, intercalate into the outer layer in two steps (Stubbs et al. 2006) (Figure 7.3). They first wedge at the base of

outer layer cells and send protrusions upwards, although tight junctions in the surface layer remain intact. In a second step, they intercalate into vertices – sites where three or more outer layer cells are apposed – and thus reach the surface of the epidermis. During the whole process of intercalation, the superficial layer remains rather static, with very few cell divisions and no significant rearrangements (Stubbs et al. 2006). Thus, CCPs and INCs take the same route to the surface, although CCPs appear to do it first. However, physical rules may operate that dictate the final pattern of distribution of CCPs and INCs in the superficial layer. Such rules are revealed in cases of decreased Notch activity, which causes more ciliated cell and ionocyte progenitors to form in the inner layer (Stubbs et al. 2006). Whereas only one CCP can intercalate in a given vertex, two or more INCs can wedge in and emerge at the surface. Consequently, the spacing pattern of ciliated cells is preserved even when their number is increased, whereas several ionocytes can reside next to each other or around ciliated cells. As INCs are much smaller than CCPs, they are the favorite to win the competition for intercalation slots when the inner layer is crowded. Supernumerary CCPs may eventually intercalate at later stages when growth of the embryonic epidermis provides unoccupied vertices. Thus, CCP intercalation appears to be constrained by self-exclusion at vertices, by competition with INCs, and by the number of insertion sites imposed by the outer layer geometry.

From a molecular point of view, little is known about the key regulators and effectors of CCP and INC intercalation. Unexpectedly, the cell surface receptor α -DG, which is expressed by nonintercalating inner layer cells, is required for CCP intercalation (Sirour et al. 2011). Whether α -DG also plays a role in INC intercalation has not been addressed. α -DG is necessary for the assembly of the basement membrane on which the epidermis rests and for cadherin-mediated cell adhesion. Moreover, α -DG appears to control P63 expression in basal cells downstream of Notch. Whether α -DG participates in intercalation through its role in signaling or via its capacity to maintain a proper extracellular

matrix remains to be addressed. A recent study reported that Rab11, which encodes a factor necessary for vesicular trafficking, is expressed in CCPs and required for their intercalation in the superficial layer (Kim et al. 2012). Quite interestingly, Rab11-deficient CCPs displayed apical–basal polarity but remained stuck below the surface layer. However, the axis of polarity was randomly aligned with respect to the plane of the epithelium, suggesting that properly oriented polarization of CCPs during the wedging phase is critical for successful intercalation.

Thus, inner cell intercalation is a complex process regulated by multiple intrinsic and extrinsic physical and biochemical parameters. However, this apparent complexity may efficiently be deconstructed as the developing epidermis can easily be manipulated and imaged live.

Cellular differentiation in the outer epidermal layer

After inner cell intercalation, differentiation within the outer layer can resume. However, our current understanding of this last step in the production of the mature mucociliary epithelium is very incomplete, as is its actual biological role. For instance, how the secretory activity of goblet cells is controlled and what is the precise chemical composition of the secreted mucus remains poorly described, although specific lectins seem to contribute significantly (Nagata 2005). Likewise, although the various cell types derived from INCs have started to be described, it is unclear whether they all have been uncovered and what precise function they each play (Dubaissi and Papalopulu 2011; Quigley et al. 2011). More focus has been put on analyzing MCC differentiation, as a result of an increasing interest in ciliogenesis and related human diseases. The next section will discuss at length how MCCs are formed.

Emergence of the multiciliated phenotype

Ciliogenesis is a complex process mobilizing several hundreds of distinct proteins.

Additional complexity is coming with the differentiation into MCCs, which requires a dramatic reorganization of the microtubular network and a 20-fold increase of the apical cell membrane to accommodate dozens of cilia. Multiciliogenesis occurs after permanent cell cycle exit, followed by multiplication, migration, and anchoring of centrioles at the apical surface to form basal bodies (BBs), which then serve as scaffolds for axonemal growth and cilium elongation (Dawe et al. 2007) (Figure 7.3).

In somatic cells, a pair of orthogonally arranged centrioles embedded into a fibrous matrix of pericentriolar material composes the centrosome, the main microtubule-organizing center of animal cells. Two modes of centriole formation have been described through ultrastructural studies (Loncarek and Khodjakov 2009). In the so-called centriole-dependent duplication pathway, daughter centrioles are copied from mother centrioles. The second pathway is said to be acentriolar and involves *de novo* centriole synthesis from nonmicrotubule-containing structures called deuterosomes, found in the vicinity of the existing centrosomes. In cycling cells, the acentriolar pathway is suppressed as long as one mature centriole is present. In contrast, the two modes of centriole multiplication coexist in MCCs (Hagiwara et al. 2004) (Figure 7.3). Contrary to dividing cells, up to eight centrioles can form around the mother centriole in MCCs. However, the bulk of newly made centrioles in MCCs appears as rosettes around the deuterosomes, through totally enigmatic mechanisms. Ultrastructural studies have described deuterosomes as electron-dense spheroid structures, but the question of their origin and molecular nature remains unanswered. They contain proteins such as PCM-1 and p195 that are also associated with centrioles and BBs (Kubo et al. 1999; Hagiwara et al. 2000). Strikingly, however, the field still awaits the identification of the first deuterosome-specific marker. This may come in *Xenopus*, as the nuclear factor MCI was shown to stimulate the acentriolar pathway, probably through the activation of genes encoding deuterosome components and regulators (Stubbs et al. 2012). Ultrastructural studies have suggested that centriole multiplication is underway

when CCPs initiate their intercalation (Billett and Gould 1971). The transcription factor FoxJ1 is absolutely required for motile ciliogenesis in monociliated, as well as in multiciliated, cells (Stubbs et al. 2008; Yu et al. 2008). However, unlike MCI, FoxJ1 ectopic expression in *Xenopus* embryonic epidermis can only trigger the emergence of one or two motile cilia. Thus, FoxJ1 is unlikely to take part in centriole multiplication in MCCs, and additional regulators may act downstream of MCI to initiate this process. Interestingly, it was shown that the locus lying next to MCI on the genome of several vertebrates, including *Xenopus* and man, plays a key role in MCC biology (Marcet et al. 2011). This locus contains a gene called *cdc20b*, which codes for a protein of unknown function that decorates BBs in human airway MCCs. Furthermore, the second intron of *cdc20b* contains a triplet of microRNAs of the miR-449 family, which are specifically expressed in CCPs and are required for their differentiation in both *Xenopus* epidermis and human airway epithelial cultures. Thus, centriole multiplication and ciliogenesis do not occur in CCPs exposed to antisense miR-449 molecules. These microRNAs target and repress the Notch signaling pathway. More specifically in *Xenopus*, miR-449 clear Delta1 transcripts, allowing CCPs to proceed through differentiation (Figure 7.3). Delta1 is the key target of miR-449 in CCPs, as MO-mediated protection of Delta1 transcripts or Delta1 overexpression blocks CCP differentiation (Marcet et al. 2011). Future work should address the possible interactions between MCI and *cdc20b*/miR-449. In summary, this newly discovered genomic locus yields key conserved regulators of MCC biology, and further analyses may shed light on the poorly understood deuterosome-dependent mode of centriole multiplication (Figure 7.3).

Once they are multiplied, BBs migrate to the apical membrane and acquire specific features that distinguish them from centrosomal centrioles (Figure 7.3). In particular, they possess a ciliary rootlet, which extends into the cytoplasm and provides structural support to the cilium, a basal foot important for cilium orientation, and transitional fibers that help anchoring the BB to the membrane (Dawe et al. 2007; Kobayashi and Dynlacht 2011).

BBs are docked in a subcortical actin network lying beneath the apical membrane of MCCs (Pan et al. 2007). In *Xenopus* MCCs as well as in mouse primary airway cultures, it has been shown that FoxJ1 expression correlates with the formation of this actin web (Pan et al. 2007; Stubbs et al. 2008). In mouse, FoxJ1 expression is required for the activation of RhoA, which in turn triggers the remodeling of the actin cytoskeleton (Pan et al. 2007). Multiple studies showed a role of FoxJ1 for the localization of ezrin, a protein linked to the BB (Huang et al. 2003; Gomperts et al. 2004; Pan et al. 2007). In *Xenopus*, FoxJ1 controls apical actin network formation and BB docking, although its link to RhoA has not been reported (Stubbs et al. 2008). Among the multiple targets of *Xenopus* FoxJ1 uncovered by microarray analyses, cilia motility components such as Dynein arms predominate (Figure 7.3).

The correct orientation of BBs determines the orientation of the cilia and thus is essential for their proper beating as further detailed in the next section. A large body of work on *Xenopus* has revealed that the planar cell polarity (PCP) genetic system plays essential roles in ciliogenesis, particularly in BB docking and orientation (Werner and Mitchell 2012). The core PCP protein Dishevelled (Dvl) promotes fusion of BBs to apically targeted vesicles, a step required for BB docking at the cell surface (Park et al. 2008). Depletion of the downstream PCP effector Inturned also prevents apical docking of BBs (Park et al. 2006b). Dvl and Inturned morphants show MCCs with fewer and misshapen cilia, associated to defects in the apical actin web. Both Dvl and Inturned proteins are required for apical localization as well as activation of RhoA and cytoskeleton remodeling (Figure 7.3).

Axonemal growth and cilium elongation proceed through the addition of ciliary components carried by cytoplasmic vesicles towards apically docked BBs. This late step in ciliogenesis also mobilizes PCP proteins. Unlike Dvl and Inturned, the downstream PCP effector Fuzzy is not required for BB docking but for apical targeting of secretory vesicles towards docked BBs (Gray et al. 2009). Consequently, Fuzzy depletion causes absent or shorter cilia (Park et al. 2006b). Another PCP effector called Fritz intervenes yet at a

later stage, through the apical localization of Septin proteins that form a ring at the base of both primary and motile cilia (Kim et al. 2010). MCCs devoid of Fritz or Septins display short or absent cilia. As Septins are known to form diffusion barriers, it has been proposed that they regulate the protein composition of ciliary membranes. Additional non-PCP players have been shown to be required for ciliary growth. Among them, RFX2 belongs to the RFX transcription factor family, which is involved in ciliogenesis in both proto- and deuterostomians. RFX2 is necessary for both motile and primary cilia construction in *Xenopus* embryos (Chung et al. 2012). It is required for the expression of multiple ciliary genes, including some coding IntraFlagellar Transport (IFT) proteins and TTC25, which encodes a novel factor present both at the BB and the axoneme and required for cilia elongation (Hayes et al. 2007; Chung et al. 2012) (Figure 7.3). Whether RFX2 also participates in BB biogenesis has not been addressed. Recently, it was reported that midbody proteins that are normally involved in cytokinesis may also participate in ciliary growth (Smith et al. 2011). Among them PRC1, MLKP-1, INCENP, and Centriolin are located at the ciliary rootlet in *Xenopus* epidermal MCCs. During cytokinesis, these proteins are involved in exocyst-mediated vesicular trafficking at the cytokinetic furrow. Midbody proteins could play a similar role in vesicular trafficking at the BB to help cilium construction.

On the function of the ciliated epidermis

In this last section, we shall concentrate on observations made at the tissue level that highlight the cellular interactions controlling mucociliary epithelium construction and function.

The terminal differentiation program of MCCs appears to be autonomously controlled as revealed by the conversion of non-CCP ectoderm cells into MCCs by the sole MCI expression. However, the cellular environment of MCCs does impinge on their differentiation as revealed by ciliogenesis defects of FoxI1e morphant embryos, which lack ionocytes (Dubaiissi and Papalopulu

2011). This unexpected influence of ionocytes on MCCs illustrates the importance of analyzing cellular differentiation *in vivo*.

MCCs are only transiently present on the surface of the epidermis of amphibian embryos. Kessel et al. (1974) have shown, using scanning electron microscopy, that in *Rana pipiens* cilia progressively regress and that MCCs start to exhibit secretory vesicles. This apparent transdifferentiation has been confirmed in *Xenopus*, whereby some MCCs in tadpoles express both acetylated tubulin and a marker of goblet cells (Nishikawa et al. 1992). This observation is interesting within the context of the known conversion of ciliated into goblet cells in certain respiratory diseases, a phenomenon called mucous metaplasia that contributes to the worsening of symptoms in patients (Curran and Cohn 2010). This conversion is a natural phenomenon in the tadpole epidermis, offering the possibility to identify strategies to control it. The discontinuous presence of ciliated cells at the surface of the epidermis poses the question of their physiological role. Through their beating activity they are expected to produce a flow of water at the surface of the embryo. It has been proposed that this is important to replenish oxygenated water and favor oxygen uptake through the embryonic skin before hatching (Mueller and Seymour 2011). Alternatively, coordinated ciliary beating may be necessary to spread mucus and generate a protective layer before an efficient immune response is mounted in the tadpole. However, this latter possibility has never been directly evaluated.

Whatever its precise physiological role might be, the fluid flow generated by MCCs can easily be visualized and measured *in vivo* in normal and manipulated conditions. It is robust and runs from the anterior to the posterior of the embryo (Figure 7.3). In order to produce directional flow, MCCs must be polarized relative to each other within the epithelium, and individual cilia must be polarized relative to each other within a given cell. The direction of ciliary beating is instructed by BB rotational polarity at the base of each cilium. Individual cilia orientation can be visualized through confocal analysis of asymmetric distribution of BB constituents (centriole and rootlet), and functionally evaluated through measurement

of local fluid flow. Elegant grafting experiments have shown that the orientation of MCCs within the plane of the epidermis is set soon after gastrulation, before their final differentiation (Mitchell et al. 2009). The core PCP proteins Frizzled 3 (Fz3) and Vangl2 control the planar orientation of individual MCCs within the epidermis (Mitchell et al. 2009). Thus, clonal analysis revealed that MCCs orient their beating towards outer nonciliated cells with high Vangl2 and low Fz3 protein amounts. The key mediator of the polarity cue provided by Fz3 to each MCC is the cytosolic Dvl protein, which was found enriched at the BBs (Park et al. 2008). Depletion of Dvl causes cell-autonomous defects in BB rotational polarity and impairs flow production (Park et al. 2008). In summary, a satisfactory framework for the deployment of PCP players has started to be assembled, although direct evidence of polarized distribution of endogenous core PCP proteins is still missing.

In addition to the PCP genetic system, the flow itself can also impact on motile cilia polarity, although the precise mechanical reactions involved have not been described (Mitchell et al. 2007). The emerging model is that MCCs acquire initial polarity in response to PCP cues delivered by the neighboring outer cells, which only weakly bias individual cilia orientation. This initial bias translates into a weak directional flow that helps refining cilia orientation. This positive feedback loop gradually strengthens the flow and improves cilia orientation, until a vigorous directional flow is produced.

Perspectives and outstanding questions

Although the recent years have witnessed a remarkable improvement of our knowledge of the molecular and cellular mechanisms that underlie and control the development of the *Xenopus* ciliated embryonic epidermis, a large number of fascinating and challenging questions still lie ahead. With the growing list of molecules (transcription factors, signaling pathway components, PCP proteins, and – as the latest addition – noncoding RNAs) involved in the establishment of the ciliated

epithelium, it will become crucial to gain a clear understanding of the contribution of each factor, or combination of interacting factors, to the genesis of the different cell types and to the several distinct steps of the organogenetic process. For instance, it is remarkable that the Delta/Notch pathway is required for the selection of two distinct cell types, the MCCs and the ionocytes. Our data suggest that this is linked to the sequential expression of one single Delta ligand, first by the precursors of the MCC, then by those of the ionocytes. The molecular mechanisms of such a sequential selection process (modulation of the physical interaction between Delta and Notch, cyclic or cumulative expression of Notch targets, presence of cell-autonomous predisposition factors) are still unknown, and their elucidation in this particular context is likely to contribute to the wider understanding of the Notch pathway logic. As a particularly fitting example, our recent finding that the terminal differentiation of *Xenopus* MCCs is dependent on silencing of the Delta/Notch pathway by miR-449 has revealed a hitherto unknown mechanism to control the Notch pathway activity, which also plays a role in human physiology. Moreover, the frog embryonic epidermis may represent a model of choice to elucidate *in vivo* the poorly understood mechanism of Notch *cis*-inhibition by coexpressed ligands.

Despite its apparent histological simplicity, much remains to be understood also concerning the details of the cellular and tissular organization of the *Xenopus* ciliated epidermis. The recent description of two distinct subpopulations of ionocytes highlights the need for a thorough molecular, morphological, and functional classification of the several constituent cell types, which in turn may lead to the identification of new molecular factors involved in their genesis. In particular, it will be interesting to understand if the mechanisms which control the selection of the different epidermal cell types interact with the factors regulating the global anteroposterior and dorsoventral patterning of the epidermis to establish regionally restricted, discrete cellular subpopulations of each main cell type. Another question still awaiting investigation is the mutual interdependence of the different cell types during the various steps of

multiciliated epithelium organogenesis, as stressed, for example, by the ciliary defects observed in embryos lacking properly differentiated ionocytes. Efforts are also needed to reveal in live embryos the physical and molecular parameters of CCP and ionocyte intercalation. At a slightly later developmental stage, one major unresolved question concerns the molecular mechanisms of centriole multiplication in differentiating MCCs.

Quite surprisingly, many aspects of the actual physiological function of the different cellular components of the *Xenopus* multiciliated epidermis still remain obscure. The presence of multiple distinct subpopulations of ionocytes raises the possibility that each one of them is devoted to controlling the homeostasis of a particular solute or class of solutes. Even the function of the most iconic and representative cells of the epidermis, the MCCs, is at present unclear, and they have been alternatively proposed to be necessary for maintaining a flow of oxygenated water around the embryo or for homogeneously distributing the mucus produced by the goblet cells (which in turn could represent either a hydrodynamic lubricant or a barrier against bacterial and fungal infections). Whatever the function of MCCs might turn out to be, it is very likely to require the tight temporal and spatial coordination of ciliary beating across the entire embryonic epidermis. Whether this is regulated by mechanisms intrinsic to the epidermis (e.g., gap junction-mediated electrical coupling across the epidermis) or is under the control of external factors (e.g., innervation of groups or rows of MCCs by neurons of the central or peripheral nervous system) is unknown. Finally, our knowledge is very limited regarding the physiological significance and the governing mechanisms of processes that take place at later stages of development, such as the transdifferentiation of MCCs into goblet cells or the progressive conversion of the embryonic bilayered epithelium into the larval and juvenile stratified epidermis.

Concluding remarks

Due to its accessibility, the *Xenopus* embryonic epidermis has emerged as what is

probably the best model to study ciliated epithelia biology in an integrated context. However, the investigators wishing to tackle the generation and function of this tissue are faced with much more complex challenges than the misleading simplicity of this organ might imply. Luckily, they are also armed with a growing arsenal of tools, some of which, such as the photocontrollable MOs, tissue-targeted electroporation, and genome engineering technologies, hold the promise to substantially broaden and deepen our understanding of developmental processes at molecular, cellular, and whole-tissue levels.

References

- Abu-Remaileh M, Gerson A, Farago M, et al. (2010) Oct-3/4 regulates stem cell identity and cell fate decisions by modulating Wnt/beta-catenin signalling. *The EMBO Journal* **29**: 3236–3248.
- Agius E, Oelgeschlager M, Wessely O, Kemp C, De Robertis EM (2000) Endodermal nodal-related signals and mesoderm induction in *Xenopus*. *Development (Cambridge, England)* **127**: 1173–1183.
- Baker JC, Beddington RS, Harland RM (1999) Wnt signaling in *Xenopus* embryos inhibits bmp4 expression and activates neural development. *Genes & Development* **13**: 3149–3159.
- Bell E, Munoz-Sanjuan I, Altmann CR, Vonica A, Brivanlou AH (2003) Cell fate specification and competence by Coco, a maternal BMP, TGFbeta and Wnt inhibitor. *Development (Cambridge, England)* **130**: 1381–1389.
- Bertrand V, Hudson C, Caillol D, Popovici C, Lemaire P (2003) Neural tissue in ascidian embryos is induced by FGF9/16/20, acting via a combination of maternal GATA and Ets transcription factors. *Cell* **115**: 615–627.
- Billett FS, Gould RP (1971) Fine structural changes in the differentiating epidermis of *Xenopus laevis* embryos. *Journal of Anatomy* **108**: 465–480.
- Bray SJ (2006) Notch signalling: a simple pathway becomes complex. *Nature Reviews* **7**: 678–689.
- Cao Y, Knochel S, Donow C, Miethe J, Kaufmann E, Knochel W (2004) The POU factor Oct-25 regulates the Xvent-2B gene and counteracts terminal differentiation in *Xenopus* embryos. *The Journal of Biological Chemistry* **279**: 43735–43743.
- Cao Y, Siegel D, Knochel W (2006) *Xenopus* POU factors of subclass V inhibit activin/nodal signaling during gastrulation. *Mechanisms of Development* **123**: 614–625.

- Cao Y, Oswald F, Wacker SA, Bundschu K, Knochel W (2010) Reversal of *Xenopus* Oct25 function by disruption of the POU domain structure. *The Journal of Biological Chemistry* **285**: 8408–8421.
- Cha SW, McAdams M, Kormish J, Wylie C, Kofron M (2012) Foxi2 is an anially localized maternal mRNA in *Xenopus*, and an activator of the zygotic ectoderm activator Foxi1e. *PLoS One* **7**: e41782.
- Chalmers AD, Strauss B, Papalopulu N (2003) Oriented cell divisions asymmetrically segregate aPKC and generate cell fate diversity in the early *Xenopus* embryo. *Development (Cambridge, England)* **130**: 2657–2668.
- Chalmers AD, Pambos M, Mason J, Lang S, Wylie C, Papalopulu N (2005) aPKC, Crumbs3 and Lgl2 control apical polarity in early vertebrate development. *Development (Cambridge, England)* **132**: 977–986.
- Chambers I, Tomlinson SR (2009) The transcriptional foundation of pluripotency. *Development (Cambridge, England)* **136**: 2311–2322.
- Chang C, Harland RM (2007) Neural induction requires continued suppression of both Smad1 and Smad2 signals during gastrulation. *Development (Cambridge, England)* **134**: 3861–3872.
- Chia NY, Chan YS, Feng B, et al. (2010) A genome-wide RNAi screen reveals determinants of human embryonic stem cell identity. *Nature* **468**: 316–320.
- Chung MI, Peyrot SM, LeBoeuf S, et al. (2012) RFX2 is broadly required for ciliogenesis during vertebrate development. *Developmental Biology* **363**: 155–165.
- Cornell RA, Musci TJ, Kimelman D (1995) FGF is a prospective competence factor for early activin-type signals in *Xenopus* mesoderm induction. *Development (Cambridge, England)* **121**: 2429–2437.
- Curran DR, Cohn L (2010) Advances in mucous cell metaplasia: a plug for mucus as a therapeutic focus in chronic airway disease. *American Journal of Respiratory Cell and Molecular Biology* **42**: 268–275.
- Dawe HR, Farr H, Gull K (2007) Centriole/basal body morphogenesis and migration during ciliogenesis in animal cells. *Journal of Cell Science* **120**: 7–15.
- De Robertis EM (2006) Spemann's organizer and self-regulation in amphibian embryos. *Nature Reviews* **7**: 296–302.
- De Robertis EM, Larrain J, Oelgeschlager M, Wessely O (2000) The establishment of Spemann's organizer and patterning of the vertebrate embryo. *Nature Reviews Genetics* **1**: 171–181.
- Deblandre GA, Wettstein DA, Koyano-Nakagawa N, Kintner C (1999) A two-step mechanism generates the spacing pattern of the ciliated cells in the skin of *Xenopus* embryos. *Development (Cambridge, England)* **126**: 4715–4728.
- Delaune E, Lemaire P, Kodjabachian L (2005) Neural induction in *Xenopus* requires early FGF signalling in addition to BMP inhibition. *Development (Cambridge, England)* **132**: 299–310.
- Drysdale T, Elinson R (1992) Cell migration and induction in the development of the surface ectodermal pattern of the *Xenopus laevis* tadpole. *Development, Growth & Differentiation* **34**: 51–59.
- Dubaissi E, Papalopulu N (2011) Embryonic frog epidermis: a model for the study of cell-cell interactions in the development of mucociliary disease. *Disease Models & Mechanisms* **4**: 179–192.
- Dupont S, Zacchigna L, Cordenonsi M, et al. (2005) Germ-layer specification and control of cell growth by Ectoderm, a Smad4 ubiquitin ligase. *Cell* **121**: 87–99.
- Fainsod A, Deissler K, Yelin R, et al. (1997) The dorsalizing and neural inducing gene follistatin is an antagonist of BMP-4. *Mechanisms of Development* **63**: 39–50.
- Fawcett SR, Klymkowsky MW (2004) Embryonic expression of *Xenopus laevis* SOX7. *Gene Expression Patterns* **4**: 29–33.
- Gomperts BN, Gong-Cooper X, Hackett BP (2004) Foxj1 regulates basal body anchoring to the cytoskeleton of ciliated pulmonary epithelial cells. *Journal of Cell Science* **117**: 1329–1337.
- Gray RS, Abitua PB, Wlodarczyk BJ, et al (2009) The planar cell polarity effector Fuz is essential for targeted membrane trafficking, ciliogenesis and mouse embryonic development. *Nature Cell Biology* **11**: 1225–1232.
- Hagiwara H, Ohwada N, Aoki T, Takata K (2000) Ciliogenesis and ciliary abnormalities. *Medical Electron Microscopy: Official Journal of the Clinical Electron Microscopy Society of Japan* **33**: 109–114.
- Hagiwara H, Ohwada N, Takata K (2004) Cell biology of normal and abnormal ciliogenesis in the ciliated epithelium. *International Review of Cytology* **234**: 101–141.
- Hayes JM, Kim SK, Abitua PB, et al (2007) Identification of novel ciliogenesis factors using a new in vivo model for mucociliary epithelial development. *Developmental Biology* **312**: 115–130.
- Hemmati-Brivanlou A, Melton DA (1994) Inhibition of activin receptor signaling promotes neuralization in *Xenopus*. *Cell* **77**: 273–281.
- Henig C, Elias S, Frank D (1998) A POU protein regulates mesodermal competence to FGF in *Xenopus*. *Mechanisms of Development* **71**: 131–142.
- Houston DW, Wylie C (2003) The *Xenopus* LIM-homeodomain protein Xlim5 regulates the differential adhesion properties of early ectoderm cells. *Development (Cambridge, England)* **130**: 2695–2704.
- Houston DW, Wylie C (2005) Maternal *Xenopus* Zic2 negatively regulates Nodal-related gene

- expression during anteroposterior patterning. *Development (Cambridge, England)* **132**: 4845–4855.
- Huang T, You Y, Spoor MS, et al. (2003) Foxj1 is required for apical localization of ezrin in airway epithelial cells. *Journal of Cell Science* **116**: 4935–4945.
- Isaacs HV, Pownall ME, Slack JM (1994) eFGF regulates Xbra expression during *Xenopus* gastrulation. *The EMBO Journal* **13**: 4469–4481.
- Kessel RG, Beams HW, Shih CY (1974) The origin, distribution and disappearance of surface cilia during embryonic development of *Rana pipiens* as revealed by scanning electron microscopy. *The American Journal of Anatomy* **141**: 341–359.
- Kim SK, Shindo A, Park TJ, et al. (2010) Planar cell polarity acts through septins to control collective cell movement and ciliogenesis. *Science* **329**: 1337–1340.
- Kim K, Lake BB, Haremak T, Weinstein DC, Sokol SY (2012) Rab11 regulates planar polarity and migratory behavior of multiciliated cells in *Xenopus* embryonic epidermis. *Developmental Dynamics* **241**: 1385–1395.
- Kobayashi T, Dynlacht BD (2011) Regulating the transition from centriole to basal body. *The Journal of Cell Biology* **193**: 435–444.
- Kofron M, Demel T, Xanthos J, et al. (1999) Mesoderm induction in *Xenopus* is a zygotic event regulated by maternal VegT via TGFbeta growth factors. *Development (Cambridge, England)* **126**: 5759–5770.
- Kubo A, Sasaki H, Yuba-Kubo A, Tsukita S, Shiina N (1999) Centriolar satellites: molecular characterization, ATP-dependent movement toward centrioles and possible involvement in ciliogenesis. *The Journal of Cell Biology* **147**: 969–980.
- Kuroda H, Fuentealba L, Ikeda A, Reversade B, De Robertis EM (2005) Default neural induction: neuralization of dissociated *Xenopus* cells is mediated by Ras/MAPK activation. *Genes & Development* **19**: 1022–1027.
- Loncerek J, Khodjakov A (2009) Ab ovo or de novo? Mechanisms of centriole duplication. *Molecules and Cells* **27**: 135–142.
- Luxardi G, Marchal L, Thome V, Kodjabachian L (2010) Distinct *Xenopus* Nodal ligands sequentially induce mesendoderm and control gastrulation movements in parallel to the Wnt/PCP pathway. *Development (Cambridge, England)* **137**: 417–426.
- Marcet B, Chevalier B, Luxardi G, et al. (2011) Control of vertebrate multiciliogenesis by miR-449 through direct repression of the Delta/Notch pathway. *Nature Cell Biology* **13**: 693–699.
- Marchal L, Luxardi G, Thome V, Kodjabachian L (2009) BMP inhibition initiates neural induction via FGF signaling and Zic genes. *Proceedings of the National Academy of Sciences of the United States of America* **106**: 17437–17442.
- Mir A, Kofron M, Zorn AM, et al. (2007) FoxI1e activates ectoderm formation and controls cell position in the *Xenopus* blastula. *Development (Cambridge, England)* **134**: 779–788.
- Mir A, Kofron M, Heasman J, et al. (2008) Long- and short-range signals control the dynamic expression of an animal hemisphere-specific gene in *Xenopus*. *Developmental Biology* **315**: 161–172.
- Mitchell B, Jacobs R, Li J, Chien S, Kintner C (2007) A positive feedback mechanism governs the polarity and motion of motile cilia. *Nature* **447**: 97–101.
- Mitchell B, Stubbs JL, Huisman F, Taborek P, Yu C, Kintner C (2009) The PCP pathway instructs the planar orientation of ciliated cells in the *Xenopus* larval skin. *Current Biology* **19**: 924–929.
- Morrison GM, Brickman JM (2006) Conserved roles for Oct4 homologues in maintaining multipotency during early vertebrate development. *Development (Cambridge, England)* **133**: 2011–2022.
- Mueller CA, Seymour RS (2011) The importance of perivitelline fluid convection to oxygen uptake of *Pseudophryne bibronii* eggs. *Physiological and Biochemical Zoology: PBZ* **84**: 299–305.
- Munoz-Sanjuan I, Brivanlou AH (2002) Neural induction, the default model and embryonic stem cells. *Nature Reviews Neuroscience* **3**: 271–280.
- Nagata S (2005) Isolation, characterization, and extra-embryonic secretion of the *Xenopus laevis* embryonic epidermal lectin, XEEL. *Glycobiology* **15**: 281–290.
- Nishikawa S, Hirata J, Sasaki F (1992) Fate of ciliated epidermal cells during early development of *Xenopus laevis* using whole-mount immunostaining with an antibody against chondroitin 6-sulfate proteoglycan and anti-tubulin: trans-differentiation or metaplasia of amphibian epidermis. *Histochemistry* **98**: 355–358.
- Okabayashi K, Asashima M (2003) Tissue generation from amphibian animal caps. *Current Opinion in Genetics & Development* **13**: 502–507.
- Onichtchouk D (2012) Pou5f1/oct4 in pluripotency control: insights from zebrafish. *Genesis* **50**: 75–85.
- Ossipova O, Tabler J, Green JB, Sokol SY (2007) PAR1 specifies ciliated cells in vertebrate ectoderm downstream of aPKC. *Development (Cambridge, England)* **134**: 4297–4306.
- Ossipova O, Ezan J, Sokol SY (2009) PAR-1 phosphorylates mind bomb to promote vertebrate neurogenesis. *Developmental Cell* **17**: 222–233.
- Pan J, You Y, Huang T, Brody SL (2007) RhoA-mediated apical actin enrichment is required for ciliogenesis and promoted by Foxj1. *Journal of Cell Science* **120**: 1868–1876.

- Park KS, Wells JM, Zorn AM, Wert SE, Whitsett JA (2006a) Sox17 influences the differentiation of respiratory epithelial cells. *Developmental Biology* **294**: 192–202.
- Park TJ, Haigo SL, Wallingford JB (2006b) Ciliogenesis defects in embryos lacking inturmed or fuzzy function are associated with failure of planar cell polarity and Hedgehog signaling. *Nature Genetics* **38**: 303–311.
- Park TJ, Mitchell BJ, Abitua PB, Kintner C, Wallingford JB (2008) Dishevelled controls apical docking and planar polarization of basal bodies in ciliated epithelial cells. *Nature Genetics* **40**: 871–879.
- Piccolo S, Sasai Y, Lu B, De Robertis EM (1996) Dorsoventral patterning in *Xenopus*: inhibition of ventral signals by direct binding of chordin to BMP-4. *Cell* **86**: 589–598.
- Piccolo S, Agius E, Leyns L, et al. (1999) The head inducer Cerberus is a multifunctional antagonist of Nodal, BMP and Wnt signals. *Nature* **397**: 707–710.
- Quigley IK, Stubbs JL, Kintner C (2011) Specification of ion transport cells in the *Xenopus* larval skin. *Development (Cambridge, England)* **138**: 705–714.
- Reversade B, Escande-Beillard N, Dimopoulou A, et al. (2009) Mutations in PYCR1 cause cutis laxa with progeroid features. *Nature Genetics* **41**: 1016–1021.
- Rock JR, Onaitis MW, Rawlins EL, et al. (2009) Basal cells as stem cells of the mouse trachea and human airway epithelium. *Proceedings of the National Academy of Sciences of the United States of America* **106**: 12771–12775.
- Scerbo P, Girardot F, Vivien C, et al. (2012) Ventx factors function as Nanog-like guardians of developmental potential in *Xenopus*. *PLoS One* **7**: e36855.
- Schohl A, Fagotto F (2002) Beta-catenin, MAPK and Smad signaling during early *Xenopus* development. *Development (Cambridge, England)* **129**: 37–52.
- Sirour C, Hidalgo M, Bello V, Buisson N, Darribere T, Moreau N (2011) Dystroglycan is involved in skin morphogenesis downstream of the Notch signaling pathway. *Molecular Biology of the Cell* **22**: 2957–2969.
- Skirkanich J, Luxardi G, Yang J, Kodjabachian L, Klein PS (2011) An essential role for transcription before the MBT in *Xenopus laevis*. *Developmental Biology* **357**: 478–491.
- Smith KR, Kieserman EK, Wang PI, et al. (2011) A role for central spindle proteins in cilia structure and function. *Cytoskeleton (Hoboken)* **68**: 112–124.
- Snape A, Wylie CC, Smith JC, Heasman J (1987) Changes in states of commitment of single animal pole blastomeres of *Xenopus laevis*. *Developmental Biology* **119**: 503–510.
- Stern CD (2005) Neural induction: old problem, new findings, yet more questions. *Development (Cambridge, England)* **132**: 2007–2021.
- Streit A, Berliner AJ, Papanayotou C, Sirulnik A, Stern CD (2000) Initiation of neural induction by FGF signalling before gastrulation. *Nature* **406**: 74–78.
- Stubbs JL, Davidson L, Keller R, Kintner C (2006) Radial intercalation of ciliated cells during *Xenopus* skin development. *Development (Cambridge, England)* **133**: 2507–2515.
- Stubbs JL, Oishi I, Izpisua Belmonte JC, Kintner C (2008) The forkhead protein Foxj1 specifies node-like cilia in *Xenopus* and zebrafish embryos. *Nature Genetics* **40**: 1454–1460.
- Stubbs JL, Vladar EK, Axelrod JD, Kintner C (2012) Multicilin promotes centriole assembly and ciliogenesis during multiciliate cell differentiation. *Nature Cell Biology* **14**: 140–147.
- Sun BI, Bush SM, Collins-Racie LA, et al. (1999) *derriere*: a TGF-beta family member required for posterior development in *Xenopus*. *Development (Cambridge, England)* **126**: 1467–1482.
- Suri C, Harekaki T, Weinstein DC (2005) *Xema*, a foxi-class gene expressed in the gastrula stage *Xenopus* ectoderm, is required for the suppression of mesendoderm. *Development (Cambridge, England)* **132**: 2733–2742.
- Suzuki A, Kaneko E, Ueno N, Hemmati-Brivanlou A (1997) Regulation of epidermal induction by BMP2 and BMP7 signaling. *Developmental Biology* **189**: 112–122.
- Takahashi S, Yokota C, Takano K, et al. (2000) Two novel nodal-related genes initiate early inductive events in *Xenopus* Nieuwkoop center. *Development (Cambridge, England)* **127**: 5319–5329.
- Tao Q, Yokota C, Puck H, et al. (2005) Maternal *wnt11* activates the canonical *wnt* signaling pathway required for axis formation in *Xenopus* embryos. *Cell* **120**: 857–871.
- Voyles J, Young S, Berger L, et al. (2009) Pathogenesis of chytridiomycosis, a cause of catastrophic amphibian declines. *Science* **326**: 582–585.
- Werner ME, Mitchell BJ (2012) Understanding ciliated epithelia: the power of *Xenopus*. *Genesis* **50**: 176–185.
- Wylie CC, Snape A, Heasman J, Smith JC (1987) Vegetal pole cells and commitment to form endoderm in *Xenopus laevis*. *Developmental Biology* **119**: 496–502.
- Xanthos JB, Kofron M, Wylie C, Heasman J (2001) Maternal VegT is the initiator of a molecular network specifying endoderm in *Xenopus laevis*. *Development (Cambridge, England)* **128**: 167–180.
- Yasuo H, Lemaire P (1999) A two-step model for the fate determination of presumptive endodermal blastomeres in *Xenopus* embryos. *Current Biology* **9**: 869–879.
- Ying QL, Stavridis M, Griffiths D, Li M, Smith A (2003) Conversion of embryonic stem cells into neuroectodermal precursors in adherent monoculture. *Nature Biotechnology* **21**: 183–186.

- Yoshizato K (2007) Molecular mechanism and evolutionary significance of epithelial-mesenchymal interactions in the body- and tail-dependent metamorphic transformation of anuran larval skin. *International Review of Cytology* **260**: 213–260.
- Yu X, Ng CP, Habacher H, Roy S (2008) Foxj1 transcription factors are master regulators of the motile ciliogenic program. *Nature Genetics* **40**: 1445–1453.
- Zhang J, Houston DW, King ML, Payne C, Wylie C, Heasman J (1998) The role of maternal VegT in establishing the primary germ layers in *Xenopus* embryos. *Cell* **94**: 515–524.
- Zhang C, Basta T, Hernandez-Lagunas L, et al. (2004) Repression of nodal expression by maternal B1-type SOXs regulates germ layer formation in *Xenopus* and zebrafish. *Developmental Biology* **273**: 23–37.
- Zimmerman LB, De Jesus-Escobar JM, Harland RM (1996) The Spemann organizer signal noggin binds and inactivates bone morphogenetic protein 4. *Cell* **86**: 599–606.

8

Wnt Signaling during Early *Xenopus* Development

François Fagotto

Department of Biology, McGill University, Montreal, Québec, Canada

Abstract: *Xenopus* is arguably the vertebrate model where the role of Wnt in early development has been most comprehensively studied. It has also served and still serves as a unique *in vivo* test tube to dissect the various branches of the Wnt pathway. This chapter represents an attempt to synthesize the large body of knowledge that has accumulated over the past two decades, focusing primarily on the fundamental role of Wnt signaling in the establishment of the basic body plan.

Introduction

Wnts constitute a family of secreted growth factors that control a large number of developmental processes. Wnt signaling impacts on gene regulation as well as on other cellular processes, such as cell polarization and reorganization of the actin cytoskeleton. Intracellular activities are classically separated into the “canonical” pathway, which utilizes β -catenin as signal transducer, and the “noncanonical” pathways.

One of the most famous phenomena in developmental biology’s role is the “dorsalizing” activity that produces the Spemann Organizer, this astonishing inducing center capable on its own to direct the whole body organization. The allocation of this activity to the Wnt pathway represented a key achieve-

ment of molecular developmental biology. The early *Xenopus* embryo still remains today a powerful live “test tube” to dissect the pathway, due to the ease and rapidity to manipulate it, the high sensitivity of the phenotypes, the vast range of embryological, cellular, and biochemical assays that can be performed in this model, and the large amount of knowledge accumulated.

Many excellent reviews have been published on Wnts and the downstream signaling cascades. I will adopt here a more developmental angle: I will try to present an overview of the various developmental Wnt functions in the early *Xenopus* embryo, built by piecing together the various information about Wnt expression, Wnt signal activities, and functional data. I will devote a significant part of this chapter to the earliest processes, in

particular to the maternal activity that determines the dorsoventral axis of the embryo and to the cross-talk with other pathways that builds the early patterning network before gastrulation, since an update on these processes is quite timely. I will also summarize the subsequent zygotic activities that pattern the mesoderm and the neuroderm, as well as the noncanonical functions, including the control of convergence–extension. Some of the many other activities identified at later stages of development will also be mentioned.

I start with some general comments concerning the different branches of the pathway, about their definition and pending issues.

Wnt “canonical” and “noncanonical” pathways: Complexity and uncertainties

It was realized very early on that only about half of Wnt ligands could activate β -catenin in cancer cell lines and in vertebrate embryo models, while the other half failed to do so – and in some cases seemed even to inhibit the pathway. The capacity to specifically trigger the “canonical” pathway or not was then naturally attributed to the ligands themselves. The distinction between the two pathways seemed relatively straightforward: The canonical pathway led to stabilization of β -catenin, which could then enter the nucleus and regulate gene transcription; as for those Wnts which could not activate β -catenin, such as Wnt5a and Wnt11, it was found that they played a role in morphogenetic movements, in particular into the process of convergence–extension during gastrulation. With the identification of receptors and intracellular components, the pathways were further defined based on their molecular downstream outputs: Besides the canonical pathway, at least two noncanonical pathways were described in vertebrates. One of them was considered to be equivalent to the so-called planar-cell-polarity pathway (PCP) in *Drosophila* and functioned in particular in convergence–extension, while a second pathway was involved in tissue separation and implicated G proteins, Calcium, and PKC. Until recently, the noncanonical pathways were mostly studied for their

ability to regulate cytoskeleton organization and cell motility, but more recently started to be also examined for their specific effects on gene expression (reviewed in Hikasa and Sokol 2013).

What defined these pathways and how were they specifically activated? This question kept many labs busy for several years. All pathways used members of the Frizzled (Fz) family of receptors, and all required homologues of *Drosophila* Dishevelled downstream of Fz (note that vertebrates express three closely related Dishevelled homologues Dvl1–3, with Dvl2 and Dvl3 involved in the early *Xenopus* embryo, which I generically called Dishevelled, abbreviated Dsh). In addition to the aforementioned Wnt subgroups, it was thought that different Fz may also be specialized for one of the other pathways. The discovery of Wnt coreceptors seemed to provide the final answer for specificity: LRP5/6 would activate the canonical pathway, Ryk/Ror2 the noncanonical pathways (Figure 8.1, reviewed in Niehrs 2012).

While this categorization looked satisfactorily coherent, recent data have revealed a much more complex situation, and the separation of the three pathways is currently rather blurred (Figure 8.1, multiple arrows and dashed arrows). In addition, a recent assay critically reconsidered the definition PCP pathway in vertebrates and proposed to distinguish an actual strict homologue of the *Drosophila* PCP pathway from a distinct Wnt-Fz-Daam-RhoGTPase/JNK pathway (Lapebie, Borchiellini et al. 2011), a proposal which I personally approve (Figure 8.1). I explain here how previous confusing results were eventually satisfactorily solved and present a few observations that exemplify the current uncertainties in the field, including key experiments performed in the early *Xenopus* embryo that forced us to question previously accepted paradigms.

Lessons from the Wnt5a/Wnt11 case

As soon as Wnts were found to be potent inducers of a secondary body axis, faithfully mimicking Spemann organizer transplants, a search was launched for endogenous maternal Wnts that would constitute the actual endogenous dorsaling activity. As explained later in

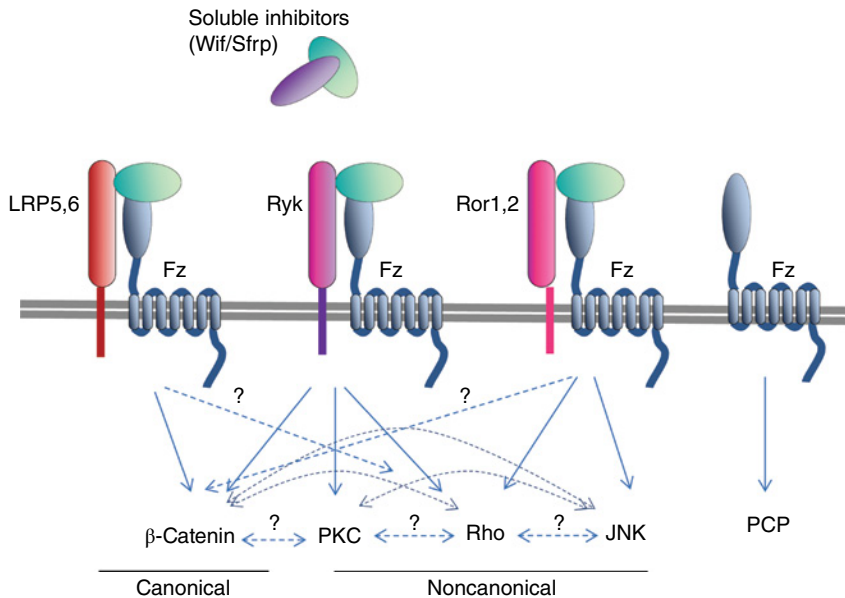


Figure 8.1 Major branches of Wnt signaling. Solid arrows represent established connections, dashed arrows and question marks indicate hypothetical connections awaiting experimental validation. In addition to the so-called canonical, which utilizes β -catenin as signal transducer, Wnts can activate several noncanonical pathways. Following the recent suggestion by Houlston and colleagues (Lapebie et al. 2011), we set the classical planar cell polarity pathway (PCP) aside. PKC, Rho, and JNK are typically involved in other branches of the pathway. The conditions that favor one or the other branch are poorly understood. One potential specificity factor is the formation of heterodimer between Frizzled receptor (Fz) and different coreceptors, including LRP6 for β -catenin activation, Ryk and Ror1,2 for noncanonical branches. Several other potential coreceptors have been identified, not depicted here. Heterodimerization however does not fully account for specific activation, since both Ryk and Ror1,2 appear to be able to activate more than one branch. Note also that the many components are shared by the various pathways, which suggest large overlaps/cross-talks. A series of regulatory mechanisms have been identified, including by soluble inhibitors that directly compete for Wnt-receptors binding, such as members of the Wnt-inhibitor factor (Wif) or soluble Frizzled-related protein, Sfrp, families. Other regulations include systems involving soluble regulators interacting with additional transmembrane proteins that regulate receptor stability (Kremen/Dickkopf, ZNRF3/R-spondins).

more detail, this activity was known to stabilize β -catenin, to be localized vegetally in the egg, and to move to the prospective dorsal region after fertilization. A few Wnts belonging to the “canonical” category were detected in the early embryo (Table 8.1), but they were all expressed at low levels, and none showed the expected localization. Wnt11, however, was a potentially exciting candidate, because its mRNA was vegetally localized in the unfertilized egg, as predicted for the “dorsal determinant” (Ku and Melton 1993). The functional results were however “disappointing”, since Wnt11 failed to induce the beautiful secondary axes readily obtained with Wnt1 or Wnt8. It did in fact induce tiny secondary structures (Ku and Melton 1993), which was clearly indicative of some canonical activity, but the phenotype was very modest and Wnt11 was classified among

those ligands that could not activate β -catenin. Note that He and colleagues (He, Saint-Jeannet et al. 1997) had shown that Wnt5a, a Wnt11 relative, could activate the canonical pathway if given the opportunity to interact with the appropriate Fz receptor, suggesting that the categories may not be strict. These results were however largely ignored for the next years, Wnt11 was kept in its category, and its capacity to induce a rudiment of an axis was forgotten.

Another path had indeed drawn most of the attention. It all started with the observation that Wnt5a induced gastrulation defects, which was initially interpreted as a sign of inhibition of the normal pathway (Torres, Yang-Snyder et al. 1996), and led to the notion that another Wnt pathway existed, which was called the “non-canonical” pathway. This new Wnt pathway was characterized by its sensitivity to G protein

Table 8.1 Maternal and zygotic Wnts during early *Xenopus* development.

<i>Maternal Wnts</i>				
Wnt	Expression			References
Wnt5a	Ubiquitous Persists during gastrula			Moon et al. (1993) Cha et al. (2008)
Wnt6	Animal, dorsal (gastrula)			Lavery et al. (2008a)
Wnt8b	Animal			Cui, Brown et al. (1995)
Wnt11	Vegetal → Dorsal Persists during gastrula			Ku and Melton (1993) Cha et al. (2008)
Wnt2,7B	Not analyzed			Landesman et al. (2002), Chang and Hemmati-Brivanlou (1998)
<i>Zygotic Wnts</i>				
Wnt	Start expression	Expression	MO phenotype	References
Wnt1	Late gastrula	Midbrain boundary		Wolda et al. (1993)
Wnt2	Late neurula	Mesoderm to anterior gut endoderm	Endoderm organogenesis	Landesman et al. (2002); Garriock et al. (2007)
Wnt3	Late neurula	Midbrain		Garriock, Warkman et al. (2007)
Wnt3a	Gastrula	Paraxial mesoderm, posterior neural, lateral margins of the neural plate	Neural patterning	McGrew et al. (1997) Elkouby et al. (2010); Fonar et al. (2011)
Wnt4	Neurula	Brain, neural tube, pronephros	Pronephros tubulogenesis	Saulnier et al. (2002)
Wnt5a	Gastrula	Endomesoderm circumblastoporal collar	Convergence extension	Shibata et al. (2005) see text
Wnt6	Tailbud	Epithelial tissues, developing organs	Heart, eye, intermediate mesoderm, somites, gut, pigment cells, tail fin.	Lavery et al. (2008a, b)
Wnt7b	Gastrula	Ectoderm + mesoderm		Chang and Hemmati-Brivanlou (1998); Zhang et al. (2011)
Wnt8	Early gastrula	Ventrolateral mesoderm, endoderm	Mesoderm patterning	Lemaire and Gurdon (1994)
Wnt8b	Late gastrula	Anterior neural ectoderm		Cui et al. (1995) Zhang et al. (2011)
Wnt9a	Tailbud	Pronephros		Garriock et al. (2007)
Wnt9b	Tailbud	Epidermal ectoderm overlying brachial arch		Garriock et al. (2007)
Wnt10a	Early neurula	Non-neural ectoderm		Garriock et al. (2007)

(Continued)

Table 8.1 (cont'd)

Zygotic Wnts				
Wnt	Start expression	Expression	MO phenotype	References
Wnt11	Early gastrula	Mesoderm, highest dorsal (maternal?)	Convergence extension Neural crests	Ku and Melton (1993) Pandur et al. (2002); De Calisto et al. (2005)
	Tailbud	Somites and 1st brachial arch	Heart	
Wnt11R	Late Gastrula	Neuroectoderm	Neural crests	Garriock et al. (2005); Ossipova and Sokol (2011)
		Heart	Heart	
Wnt16	Tailbud	Hypochord and eye		Garriock et al. (2005)

The main patterns of expression are presented. References were selected when possible for the most precise and/or complete expression data. Systematic analyses of Wnt expression at late stages can be found in (Garriock et al. 2007; Zhang et al. 2011).

inhibitors and stimulation of intracellular calcium release (studied in Zebrafish) (Slusarski et al. 1997a, b; Ishitani et al. 2003; Sheldahl et al. 2003; Veeman et al. 2003). Note that, rather awkwardly, “canonical” Wnts were never tested in parallel, neither for G proteins nor calcium activation, these features being assumed to be unique to the “noncanonical” pathway. We now know that G proteins are also involved in the β -catenin branch (Katanaev et al. 2005; Liu et al. 2005b; Stemmler et al. 2006), and thus presumably, calcium release must also occur.

In parallel, Wnt5a and Wnt11 gain- and loss-of-function showed effects on convergence extension in both Zebrafish and *Xenopus* (Heisenberg et al. 2000; Tada and Smith 2000). By analogy with the PCP pathway in *Drosophila*, it was hypothesized that the polarized organization of mesoderm cells required for convergence–extension was also controlled by a similar pathway. This was supported by many experiments that systematically examined the vertebrate homologues of the *Drosophila* PCP components (e.g., Strabismus/VanGogh, Flamingo, Prickle, see Table 8.2). Thus, Wnt5a and Wnt11 seemed to control two noncanonical pathways, and their “ β -catenin-independent” activity was found to be involved in a series of developmental processes (see Tables 8.2 and 8.3).

What happened in the meantime to the mysterious dorsal determinant? Various hypotheses had been emitted (see later), with little experimental confirmation. None of them included

Wnt11, until Heasman and colleagues decided to attack the problem frontally: They depleted the maternal mRNA using the oocyte transfer method and obtained an unambiguous answer – in the absence of maternal Wnt11, the embryos failed to build dorsal structures (Tao et al. 2005). Thus, more than 10 years later after its discovery, Wnt11 was finally given its true status of dorsal determinant! Heasman and colleagues went on to dissect the process in a series of beautiful experiments. They demonstrated that Wnt11 acts via LRP6, thus the classical canonical pathway (Kofron et al. 2007). Furthermore, they found that Wnt11 functions as a heterodimer with Wnt5a. Wnt5a is itself more evenly distributed throughout the embryo (Figure 8.2A), and the dorsalizing activity is formed only in the region where both expressions overlap (Cha et al. 2008). In retrospect, their experiments provided an obvious explanation for the failure to induce an ectopic axis by Wnt11 overexpression, as well as for the impression that Wnt5a and Wnt11 “inhibited” the canonical pathway: This inhibition was indeed most likely an artifact due to overexpressing only one component of the heterodimer, a common issue when dealing with stoichiometric protein complexes. The results obtained by Heasman and coworkers have now provided a crystal clear answer to the old mystery of vertebrate axis determination. They also give us a sense of the challenges ahead in terms of deciphering Wnt-receptor specificity and the control of the

Table 8.2 Depletions of maternal components.

Gene	Phenotype	References
Wnt11/5a	Ventralized+CE	Tao et al. (2005); Kofron et al. (2007); Cha et al. (2008, 2009)
LRP6	Ventralized	Kofron et al. (2007)
Fz7	Ventralized	Sumanas et al. (2000)
PP2A-B56e	Ventralized	Yang et al. (2003)
Dvl2,3	CE	Tadjuidje et al. (2011)
β -catenin	Ventralized	Heasman et al. (1994); Wylie et al. (1996)
Axin	Hyperdorsalized	Kofron et al. (2001)
GBP	Ventralized	Yost et al. (1998)
JNK	Hyperdorsalized	Liao et al. (2006)
TCF3	Hyperdorsalized	Houston et al. (2002)
TCF1	Dorsal side partially ventralized Ventral side partially dorsalized	Standley et al. (2006)
TCF4	Ventralized	Standley et al. (2006)
Pyrogopus	Ventralized	Belenkaya et al. (2002)
Ryk	CE	Kim et al. (2008)
Vangl2	Oocyte polarity	Cha et al. (2011)
Dkk1	Ventralized+CE	Cha et al. (2008)
aPKC	Oocyte polarity	Cha et al. (2011)

Compilation of maternal depletion through oocyte transfer protocol. CE, convergence extension phenotype.

different branches of the pathway. This enterprise will indeed require the systematic analysis of different combinations of Wnt homo- and heterodimers together with various combinations of receptors (Fz-LRP5/6 pairs with and without Ror/Ryk, etc.). We are also told, but this is not a real surprise, that levels matter, thus everything will need to be added at the appropriate dose. Similar careful and comprehensive approaches will have to be applied to the other issues, such as regulation by soluble agonists/antagonists, and to intracellular regulation, an even more daunting challenge.

Wnt-receptor specificity

One possible mechanism for selection of a particular pathway could reside in the Wnt-Fz interactions, but based on structural data, these interactions do not seem to provide sufficient

specificity (Janda et al. 2012). It was also thought that different Fz were specialized. Fz7 for instance seemed a good candidate to specifically trigger the “calcium-PKC” noncanonical pathway in the *Xenopus* gastrula (Medina et al. 2000; Winklbauer et al. 2001). Yet, Fz7 is without any possible doubt also required for the maternal β -catenin pathway (Sumanas et al. 2000; Tao et al. 2005; Kofron et al. 2007; Cha et al. 2008). Participation of the coreceptors LRP5/6 appeared to be even a better mechanism to switch to the canonical pathway: LRP5/6 can indeed directly interact with Axin, thus providing a satisfactory specific mechanism to regulate β -catenin (Bilic et al. 2007). Over these past years, the number of surface proteins interacting with Wnts has increased quite dramatically (reviewed by Niehrs 2012), and the newly arrived coreceptors Ror2/Ryk were perfect candidates to take care of the noncanonical branch of the pathway (Hikasa and Sokol 2013). This gave hope that combinations of Fz and

Table 8.3 Morpholino depletions and other interferences.

	Gene	Reagent	Branch	Phenotypes / comments	References
Intracellular	β -Catenin	MO	MD	Ventralization	Heasman et al. (2000)
	Axin MO	MO	ZV	Ventralization	Schneider et al. (2012); Tahinci et al. (2007)
	GSK3	DN, LiCl (ci)	MD	Dorsalization	Pierce and Kimelman (1995)
	CK1 ϵ	DN, MO, CK1-7 (ci)	CE	No effect on MD	Peters et al. (1999); Tsai et al. (2007)
	CK1 γ	MO	ZV	Dorsalization	Davidson et al. (2005)
	CK1+CK2	MO	NC	Wnt-Rac1 not Wnt-Ror2-cdc42	Bryja et al. (2008)
	TCF1,TCF3	MO	Meso Ind	Loss of Xbra, mesoderm defects	Liu et al. (2005a)
	TCF1, LEF1	MO, DN	ZV	Meso patterning defects, Loss of MyoD	Roel et al. (2002); Liu et al. (2005a)
	TCF4	MO		No effect on early development	Liu et al. (2005a)
	JNK	MO	MD	Dorsalization	Liao et al. (2006)
	JNK	MO	CE		Yamanaka et al. (2002)
	Dsh	MO	CE		Djiane et al. (2000)
	Dsh	Xdd1(Δ PDZ/DHR)	ZV+CE		Wallingford et al. (2000)
	Dsh	Δ DEP, Δ PDZ	CE	No effect on β -catenin	Wallingford et al. (2000)
	RIPK4	MO	ZV	Neural anterior defects, Phosphorylates Dsh	Huang et al. (2013)
	Diversin	MO		Defects in cilia basal bodies	Yasunaga et al. (2011)
	Pygopus 2 α	MO	ZV	Inhib midbrain Engrailed2	Lake and Kao (2003)
	Amer1/WTX	MO		Blocks Wnt-induced dorsalization	Major et al. (2007)
	Amer2	MO	CE		Pfister et al. (2012)
	Amer2	MO	ZV	Wnt activation Neural tissue	Major et al. (2007)
	Dapper	MO		Partial Ventralization	Cheyette et al. (2002)
	Par1A	MO	DM	Ventralization	Ossipova et al. (2005)
	Par1B	MO	CE		Ossipova et al. (2005)
	β -arrestin	MO	DM	Dorsalization	Bryja et al. (2007)
	β -arrestin-2	MO, DN	CE		Kim et al. (2008)

Table 8.3 (cont'd)

	Gene	Reagent	Branch	Phenotypes / comments	References
Wnt ligands	Prickle	MO	CE		Takeuchi et al. (2003)
	WGEF	MO	CE	RhoGEF	Tanegashima et al. (2008)
	DP1	MO	ZV	Neural defects – Dual positive/negative regulator	Kim et al. (2012)
	Xldax	MO	ZV	Posteriorized, neural spec. inhibitor	Michiue et al. (2004)
	Wnt8	MO, DN	ZV	Ventral reduction, loss of MyoD	Hoppler et al. (1996); Rana et al. (2006)
	Wnt5a	MO	CE(Ror2)	Inhibition of constriction	Schambony and Wedlich (2007)
	Wnt11	MO	CE(Rho)	Inhibition of elongation	Tada and Smith (2000); Schambony and Wedlich (2007)
Receptors, co-receptors, surface proteins	Fz2	MO	*	Bent axis	Rana et al. (2006)
	Fz6	MO	*	Shorter axis	Rana et al. (2006)
	Fz7	MO	MD	Ventralization	Sumanas et al. (2000)
	Fz7	MO	NC	Tissue separation	Winklbauer et al. (2001)
	Fz7	MO	CE		Medina et al. (2000); Rana et al. (2006)
	Fz8	MO	(*)	Involution defects	Rana et al. (2006)
	LRP5/6	MO	CE		Bryja et al. (2009)
	LRP6	MO	CE		Tahinci et al. (2007)
	Ror2	MO, DN	CE		Hikasa et al. (2002); Schambony and Wedlich (2007)
	Ryk	MO	CE		Kim et al. (2008)
	Strabismus/	MO	CE		Darken et al. (2002); Park and Moon (2002)
	VanGogh				
	Flamingo	MO		Bent axis	Rana et al. (2006)
LGR4/5	MO	CE	G protein-coupled receptor	Glinka et al. (2011)	
Knypek	MO	MD+CE	Glypican	Caneparo et al. (2007)	
APCDD1	MO	ZV	Posteriorized, Inhibitor, binds Wnt+LRP5	Shimomura et al. (2010)	
Secreted agonists/ antagonists	Sizzled	MO	ZV	Expansion ventral posterior mesoderm + blood islands	Collavin and Kirschner (2003)

(Continued)

Table 8.3 (cont'd)

Gene	Reagent	Branch	Phenotypes / comments	References
Dkk1	MO	ZV		del Barco Barrantes et al. (2003)
Kremen	MO	ZV	Defect anterior neural	Davidson et al. (2002)
Crescent	MO	CE		Shibata et al. (2005)
sFRP5	MO		Endoderm organogenesis	Damianitsch et al. (2009)
R-spondin2	MO	ZV	Required for myogenesis	Kazanskaya et al. (2004)
R-spondin3	MO	CE		Glinka et al. (2011)

Compilation of interference with components of the Wnt pathway through embryonic manipulations (injection in early embryo or inhibitor treatment). MO, morpholino oligonucleotide; dn, dominant negative construct; ci, chemical inhibitor. Affected branches of the pathway are categorized as follows: MD, maternal dorsalizing, canonical; ZV, zygotic ventralizing, canonical; NC, non-canonical; CE, non-canonical, convergence extension; MesInd, Mesoderm induction.

*Noncharacterized, phenotype reported from a screen.

coreceptors would account for stimulation of particular pathways. While this is probably part of the explanation, the situation is clearly complex: some combinations can activate more than one pathway, and, reciprocally, there are several possibilities to activate each pathway (Niehrs 2012). Again, studies in *Xenopus* have largely contributed to question hasty assumptions: Both LRP6 and Ryk were eventually found to function in multiple branches, with LRP6 also controlling the PCP pathway during convergence extension (Tahinci et al. 2007) and Ryk activating β -catenin (Lu et al. 2004; Berndt et al. 2011; Niehrs 2012). A more comprehensive biochemical/structural analysis of Wnt-receptor interactions has been hampered by the fact that Wnts are very difficult proteins to work with and further complicated by the need to account for simultaneous binding to coreceptors (MacDonald and He 2012). It seems likely however that the system must be rather described as an integrated network: Particular signal outputs are being preferentially – but not exclusively – activated by different combinations of Wnts – including heterodimers – receptors and coreceptors (van Amerongen and Nusse 2009; Niehrs 2012). Note that the dosage of each component may be as determinant as

the identity of the partners. For instance, Wnt5a binding to Ror2 and Fz stimulates the noncanonical pathway, but there is also evidence that its binding to Ror2 alone may antagonize the canonical pathway (Mikels and Nusse 2006). It is conceivable that this latter inhibitory reaction may result from a partial and unbalanced reaction produced by an excess of Wnt5a relative to Wnt11, a reasoning that may apply to most Wnt–Wnt and Wnt–receptor/coreceptor interactions. Such situations may not be restricted to artificial experimental conditions, but could be physiologically relevant: For instance, the fact that maternal Wnt5a and Wnt11 are expressed in different patterns (Table 8.1 and Figure 8.2A) could create a mosaic of different activities. This complexity has also important consequences for the interpretation of loss-of-function experiments, since removing one component, whether ligand or receptor, may well shift the system to a different type of output.

Specificity of intracellular components

The different pathways triggered by Wnts are generally considered to diverge downstream of Dsh. As mentioned previously, the canonical

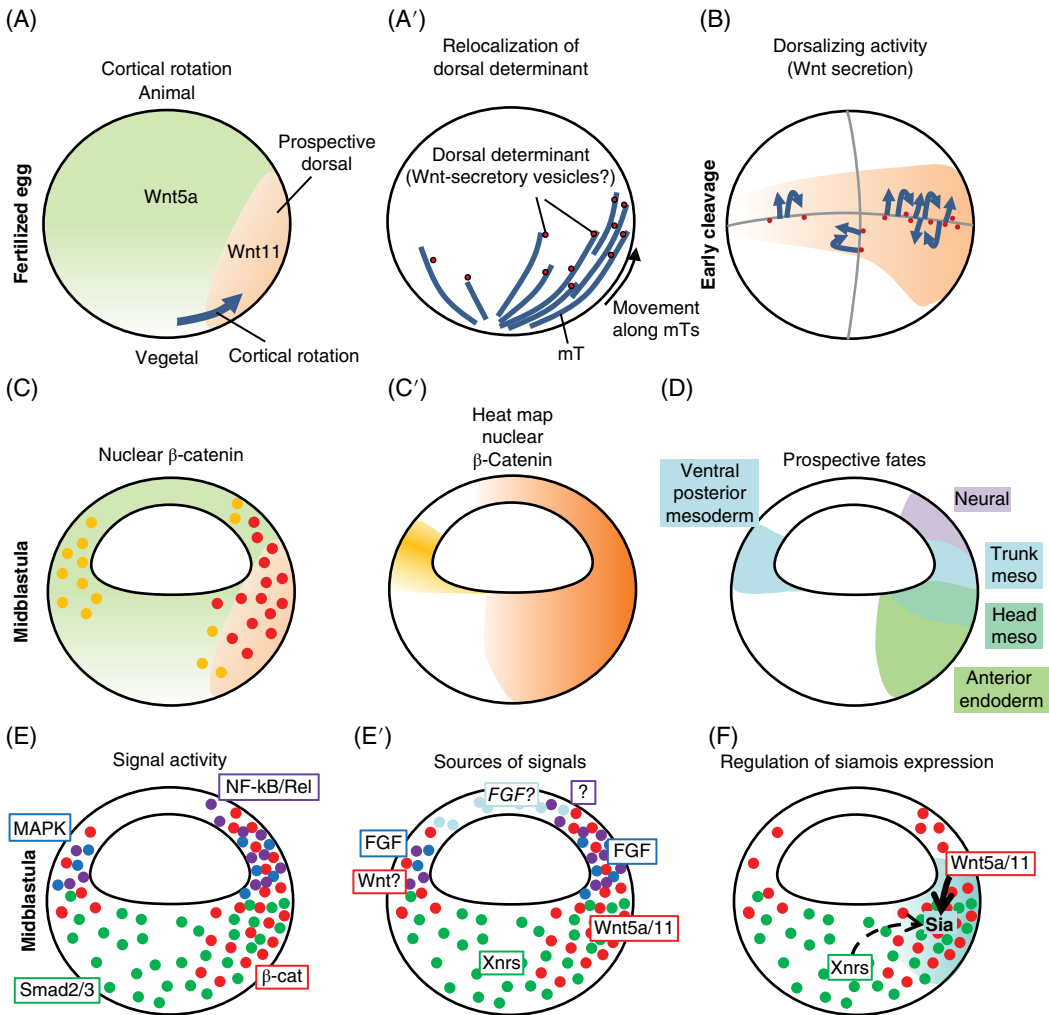


Figure 8.2 Maternal Wnt- β -catenin. (A) Distribution of Wnt ligands in the fertilized embryo. Two major maternal ligands are present in the *Xenopus* egg: Wnt11 mRNA is vegetally localized in the oocyte. After fertilization, Wnt11 protein is relocalized to the side opposite to sperm entry, due to a movement of the egg cortex called cortical rotation (Schroeder et al. 1999). Wnt5a mRNA is not localized. The shallow gradient represents the default distribution common to most *Xenopus* transcripts, with lower levels in the yolk-rich vegetal pole. (A') Cortical rotation of maternal dorsal determinant. Relocalization of the dorsal determinant has been shown to depend on microtubules. A subpopulation of microtubules is organized in parallel arrays on the prospective dorsal side, and vesicles have been observed to move toward the equator (Houlston 1994). These vesicles most likely transport Wnt11, either ready to be secreted, or possibly already interacting with its receptors Fz7 and LRP6. Note that the global microtubule distribution has not yet been established. The sparser tracks of microtubules on the ventral side represent a hypothetical broader gradient of upward relocalization yielding to a graded Wnt11 distribution around the equator (panel B), which would explain the presence of nuclear β -catenin all around the equator in the blastula (panel C, see Schohl and Fagotto 2002, 2003). (B) Hypothetical activation of the early maternal Wnt pathway. The β -catenin-activating determinant is here assumed to consist of Wnt11-containing secretory vesicles. Several lines of evidence indicate that the pathway is already activated at early cleavage stages, presumably through both paracrine and autocrine signaling (arrows). (C) Nuclear β -catenin localization (dots) in the early blastula. The diagram compares Wnt5a/Wnt11 distribution (after cortical rotation) and nuclear β -catenin localization in the blastula, is based on Schohl and Fagotto (2002). (C') Corresponding heat map of predicted β -catenin signaling activity. (D) Prospective regions under the influence of maternal Wnt- β -catenin signaling. Maternal β -catenin takes part in the determination of several different regions that correspond to the future neuroderm, trunk and head mesoderm, and anterior mesoderm. (E) Distribution of the four major inducing signals in the *Xenopus* blastula. Nuclear activated MAPK, Smad2 and β -catenin distributions have been established by Schohl and Fagotto (2002). NF κ B/Rel activity has been detected using a reporter gene (Armstrong et al. 2012). (E') Correspondence between nuclear signals and soluble ligands. A maternal FGF contribution has been suspected but not demonstrated (light blue). However, most of the FGF activity is probably due to early zygotic FGF ligands induced by maternal β -catenin and Xnrs (dark blue). Indirect evidence argues that the NF κ B/Rel pathway is controlled by maternal extracellular ligands (Armstrong et al. 1998). (F-F'') Interplay between the four signaling pathways. (F) Siamois (and closely related Twin) account for the transcriptional dorsalizing activity. They are direct targets of maternal β -catenin, with also a contribution from Xnr/Smad2 signaling.

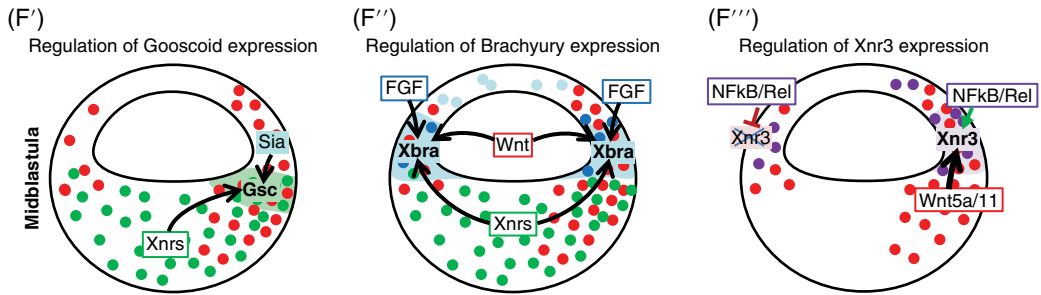


Figure 8.2 (continued) (F') Head mesoderm transcription factor Goosecois (*Gsc*) is activated by the joined activities of Siamois and *Xnrs*. (F'') Posterior and ventral mesoderm induction (*Xbra*) requires cooperation of Wnt, *Xnr* and FGF signaling. Note that the animal and vegetal boundaries of *Xbra* expression are further constrained by additional mechanisms (reviewed in Heasman 2006) (F''') *Xnr3* is an active component of the dorsalizing center, required in particular for formation of the neuroderm. *Xnr3* is a direct target of Wnt- β -catenin and NFkB/Rel pathways. Note the repressive action of ventral NFkB/Rel (Armstrong et al. 1998). To see a color version of this figure, see Plate 15.

pathway operates by regulating β -catenin degradation by the Axin complex, the PCP pathway has been classically defined (in vertebrates) by the activation of RhoGTPases and JNK, and the second noncanonical pathway by requirement for trimeric G proteins, Calcium release, and PKC activation. Here are a few examples that do not quite fit with this simple description: (i) G proteins also participate to the canonical pathway (Katanaev et al. 2005; Liu et al. 2005b; Stemmler et al. 2006; Schneider et al. 2012). (ii) β -catenin activity is also regulated by Rac and JNK, downstream of Wnt stimulation (Liao et al. 2006; Wu et al. 2008). (iii) Axin is well known to activate JNK (Zhang et al. 1999; Zhang et al. 2002). (iv) PKCs are not only involved in tissue separation, but also in convergence–extension, thus in the “PCP” pathway (Kinoshita et al. 2003), and can also influence the canonical pathway by phosphorylating β -catenin (Gwak et al. 2006). (v) Finally, RhoGTPases seem also to act not only along the “vertebrate PCP” pathway, but also downstream of the PKC pathway (e.g., Medina et al. 2004). Many additional aspects of these signaling cascades remain unclear, and again, as for the ligands/receptors/coreceptors interactions, the intracellular reactions may also form a network rather than linear pathways. I prefer to call them “branches” of the Wnt pathway, and considering the current difficulty to cleanly distinguish or even determine the number of branches, I will adopt here a simple conservative classification in two branches,

one β -catenin-dependent “canonical” and the second β -catenin-independent (“noncanonical”) (Table 8.3). Processes that involve specific components such as Strabismus/VanGogh will be classified as bona fide PCP-dependent (Lapebie et al. 2011). Table 8.2 contains a list of most of the components implicated in Wnt signaling that have been tested in *Xenopus*. The role of each component is described in terms of developmental process, e.g., maternal axis determination, convergence extension, without distinguishing at the molecular level between PCP or other noncanonical outputs.

Major processes regulated by Wnts during early *Xenopus* development

Cortical rotation and maternal Wnt signaling

Establishment of the dorsalizing center

Nieuwkoop (Nieuwkoop 1969) discovered the existence of very early-inducing signals responsible for mesoderm patterning: Vegetal explants dissected from the prospective dorsal or ventral side were able to induce respectively dorsal or ventral mesoderm in naïve ectoderm. We now know that the dorsal mesoderm requires at least two signals: (i) A general mesoderm-inducing signal is generated throughout the entire vegetal hemisphere, due to two maternal vegetally localized

Box 8.1 Early *Xenopus* patterning: Definitions

Dorsoventral and anterior–posterior axes: The initial asymmetry produced by cortical rotation is conventionally named dorso-ventral axis, but its geometrical relationship with the final dorsoventral and anterior–posterior axis is more complex, due to gastrulation movements. See Heasman (2006) for a clear description of the process and definition of the different prospective regions.

Organizer: Spemann showed that the blastopore lip of the early gastrula embryo grafted on the ventral side was able to generate a second entire body structure. The grafted cells participated to all types of dorsal structures, but also recruited neighboring ventral cells, indicating emission of inducing signals. The lip is since called the Spemann Organizer, or Organizer. Note however that evidence has accumulated for ability of different dorsal regions to specify preferentially different parts of the future dorsal body structures, which has led to the notion of different “regional organizers”. The original Spemann Organizer would thus correspond to the prospective head organizer, characterized in particular by the expression of Goosecoid, although experimentally its inducing capacities are sufficient to build a whole dorsal axis.

Dorsalizing center: This term is generically used to define the early activity, spread dorsally with its center positioned subequatorially, that is responsible for the dorsalization of all three germ layers. This activity is due to maternal Wnt- β -catenin signaling, which cooperates with mesoderm and endoderm-inducing Xnr signals to determine from vegetal to animal the anterior endoderm, the dorsal mesoderm, and the neuroderm. The neuroderm was originally thought to be induced by the mesoderm during gastrulation, but contribution from an early direct induction by maternal β -catenin has been shown.

mRNAs. One codes for Veg1, a secreted growth factor of the TGF β -family, the second for a transcription factor of the T-box family, called VegT. VegT activates zygotic expression of several other TGF β -like factors, most prominently nodal-related proteins (Xnrs), but also Derrière and Activin B (reviewed in Heasman 2006). All these factors combined activate transcriptional programs that specify endoderm and mesoderm (Wardle and Smith 2006). As we will see next, the actual picture is more complex. In particular, Xnrs are also targets of Wnt signaling. (ii) The second input is a “dorsalizing” activity (see Box 8.1 for some basic definitions of early *Xenopus* patterning). This activity is not restricted to the vegetal cell mass: It is roughly centered subequatorially and spreads quite high up into the animal hemisphere. A series of experimental manipulations, including direct cytoplasmic transfer by microsuction and microinjection, demonstrated that the dorsalizing activity is initially located at the vegetal pole of the unfertilized egg. Fertilization causes a process called cortical rotation, during which the

“dorsal determinant” is translocated upward on the side opposite to sperm entry (Figure 8.2A). This movement relies on parallel oriented microtubules (Figure 8.2B) (Houliston 1994). Microtubule depolymerization (UV-irradiation of the vegetal pole, incubation in heavy water D₂O, cold, or nocodazole treatment, Scharf and Gerhart 1980; Scharf et al. 1989; Houliston 1994) prevents migration of the determinant, which remains at the vegetal pole. Inhibition of cortical rotation leads to fully “ventralized” embryos that lack all anterior and dorsal structures. Normal embryos can be rescued by reinjection of vegetal cytoplasmic material on the side of a ventralized embryo (Yuge et al. 1990; Holowacz and Elinson 1993). The same result can also be achieved simply by tilting the egg: Gravity is apparently sufficient to generate an artificial cortical rotation (Scharf and Gerhart 1980). The dorsal determinant can be even physically “fragmented”, a common artifact of shaking embryos undergoing cortical rotation, which can produce embryos with perfectly duplicated dorsal axis similar to Spemann’s specimens.

Molecular nature of the dorsal determinant

The dorsalizing activity is clearly related to Wnt- β -catenin signaling: Ectopic activation of the pathway, at any level of the cascade, can induce a secondary axis and can also rescue a normal axis in ventralized embryos (e.g., Christian et al. 1991; Funayama et al. 1995; Yost et al. 1996). Furthermore, inhibition of the pathway, for example by depletion of β -catenin (Heasman et al. 1994; Wylie et al. 1996) or Axin overexpression (Zeng et al. 1997), abolishes formation of the Organizer and produces ventralized embryos. Finally, maternal depletion of Wnt11 and other upstream components of the pathway abrogate the dorsal activity (Table 8.2 and references therein).

However, the actual nature of the maternally localized determinant has been a matter of debate and remains unclear. A direct biochemical investigation has been so far hampered by the fact that the activity present in the egg cortical material could be only preserved when immediately reinjected in an embryo, but was lost upon transfer in a tube (Yuge et al. 1990). Microscopically, cortical rotation was accompanied by migration of a subpopulation of subcortical vesicles in the expected animal dorsal direction, which led to the speculation that the determinant was membrane-associated (Rowning et al. 1997). Exogenous GFP-tagged Dishevelled and GBP, which can bind a kinesin, were both found to move along the cortical microtubules during cortical rotation (Miller et al. 1999; Weaver et al. 2003). However, direct evidence for their involvement under physiological conditions is missing. As mentioned earlier, Wnt11 is the most likely candidate – it is vegetally located in the oocyte and relocalized dorsally after cortical rotation, and mRNA depletion in the oocyte abolishes the dorsalizing activity (Tao et al. 2005). The extreme sensitivity of mRNA to degradation by RNases may explain past failed attempts to isolate an active determinant.

Activation of maternal β -catenin

The effect of the maternal Wnt pathway is mediated by transcription of zygotic target genes (Lemaire et al. 1995; Heasman 2006). Zygotic transcription classically starts precisely

at the end of the cleavage stage, when the rhythm of cell divisions slows down and a proper G1 phase appears. However, this “midblastula transition” appears less sharply defined than originally thought. Indeed, some zygotic transcripts are detected very early, in fact as early as the 256-cell stage for two targets of the Wnt pathway, Xnr5 and 6 (Yang et al. 2002). This result sets the latest limit for the start of the Wnt activity. How long is it supposed to last? It appears that the embryo remains competent to respond to Wnt signaling to induce a dorsalizing center until the mid- to late blastula, but becomes then refractory (Kodjabachian and Lemaire 2001).

One of the most direct evidence for activation of the pathway is *in situ* detection of nuclear β -catenin. β -Catenin can be definitely seen in nuclei of the early blastula, and even at low levels during cleavage stages (Larabell et al. 1997; Schneider et al. 1996; Schöhl and Fagotto 2002). A slight difference in Dsh-positive dots in the early cleaving embryo has been reported, which was proposed to be the first sign of dorsal pathway activation (Miller et al. 1999). Unfortunately, these results have not been reproduced, and the specificity of the signal remains uncertain. A variety of results were used to attempt to further define the actual timing of pathway activation. While an artificial dorsalizing activity could be easily created by expression of Wnts or any downstream activator of the pathway, inhibition of the endogenous activity was much more restricted: β -catenin depletion was effective only during the first cleavages (Heasman et al. 2000); efficient inhibition was obtained by overexpressing components of the Axin destruction complex (Axin, GSK3), but attempts to block the pathway more upstream, i.e. at the level of Wnt ligands, Fz receptors, or Dsh failed (e.g., Hoppler et al. 1996; Sokol 1996). One of the initial hypotheses to explain these differences was that the pathway was activated at an intracellular step, which would inhibit the Axin complex without a requirement for Wnt ligand or receptor activity. The issue has now been largely, although not fully, solved by a series of experiments that used the experiments using depletion in oocytes (Kofron et al. 2001; Tao et al. 2005; Standley et al. 2006; Kofron et al. 2007; Cha et al. 2008,

2009; Tadjuidje et al. 2011). Thus, a classical activation by Wnts ligands is sufficient to account for the process, without need to include a hypothetical noncanonical cytoplasmic activation mechanism.

Largely thanks to the work of Heasman and colleagues, the maternal pathway can be tentatively described as follows (Figure 8.2A and B): At fertilization, Wnt5a is expressed throughout the embryo, while Wnt11 mRNA is sequestered by the vegetal pole. Wnt11 gets relocated to a broad dorsal region (Figure 8.2A), where Wnt5a/Wnt11 heterodimers can form. They activate, already during cleavage stages (Figure 8.2B), the receptors LRP6 and Fz7, both also maternally expressed in the whole embryo (Table 8.1). A canonical cascade is generated that inhibits the Axin complex, leading to early accumulation and nuclear localization of β -catenin (Figure 8.2C) and its interaction with TCF transcription factors. Three of these factors, TCF1, TCF3, and TCF4, are expressed maternally, which appear to play partially redundant/additive roles (Table 8.2). They generally have a bimodal function, i.e. they act as repressors in the absence of β -catenin and as activators when associated with it, but isoforms showed some differences in terms of activation in the dorsal side versus repression on the ventral side (Roel et al. 2002; Houston et al. 2002; Standley et al. 2006; Liu et al. 2005a). Several targets are controlled by the pathway, most prominently *Siamois* and its brother *Twin*, and *Xnr3*. These components constitute the core of the dorsalizing center and are crucial to turn on the complex program that creates the Organizer (Lemaire et al. 1995; Lustig et al. 1996; Brannon et al. 1997; Laurent et al. 1997; De Robertis et al. 2000; Ishibashi et al. 2008; Hikasa and Sokol 2013).

Early patterning downstream of maternal β -catenin: Cross-talks and regionalization

The action of Wnt- β -catenin signaling on early patterning cannot be presented without introducing the extensive cross-talk with other signaling pathways that occur in the blastula embryo. We will see that some of these interactions are well established, others still only partially characterized.

Complexity of early gene regulation

A preliminary comment is here required to warn about the intrinsic complexity of such circuits. This had not been always fully appreciated, which contributed to keep the description of early patterning quite confusing for many years. The first level of complexity comes from the multiple inputs that control each gene expression. Consistently, all genes examined so far in the early embryo appear to be activated by at least two pathways. In the simplest cases, regulation occurs directly at the level of the promoter regulatory sequences, which include binding sites for two or more transducers. One may predict that under normal conditions, expression is controlled by a combination of inputs, resulting in graded responses depending on absolute as well as relative strengths of each input. Experimentally, however, transcription can be often obtained by activation of a single pathway: One input may indeed bypass requirement for a second signal when artificially pushed, or low endogenous levels of the second signal may be sufficient to fulfill at least part of the requirement. This experimental **artefact** has been invaluable for the dissection of the pathways (imagine the challenge if all target genes would absolutely need a minimum of two inputs!), but it has also produced plenty of confusing data. The second related complication comes from the fact that the signals active in the blastula can also turn on transcription of other secreted factors, which will in turn activate other targets. As we will see, maternal dorsalizing and mesoderm-inducing factors partly operate through such relay mechanisms.

Setting of the four major pathways

Despite these challenges, the current knowledge has reached a quite acceptable state of refinement, allowing elaboration of a coherent description of early patterning. The situation can be summarized as follows (Figure 8.2E). Four pathways are active in the blastula, which I will call by their respective nuclear transducer: (i) β -catenin (red dots), (ii) Smad2 (green dots), (iii) MAPK (blue dots), and (iv) NF κ B/Rel (purple dots). Note that a

fifth BMP-Smad1 pathway appears during late blastula stages, It is not included in this description, because it participates mostly in the second round of zygotic patterning. I will first present the major factors that control the four pathways. I will expand on the fourth pathway, which has been only recently described. I will then summarize the main interactions between the pathways and present selected examples of classical genes that are controlled by these combined inputs.

- (1) β -Catenin: We saw that β -catenin is activated by maternal Wnt5a/11 and that the activity is centered in the dorsal sub-equatorial region, but spreads also anteriorly and equatorially all around the prospective mesoderm.
- (2) Smad2 signaling is activated by multiple TGF β factors, including maternally localized Veg1 and zygotic nodal-related proteins Xnr1,2,4,5,6, Activin and Derriere. The activity covers the whole vegetal hemisphere, but is strongest on the dorsal side (Figure 8.2E). Xnr proteins are direct targets of VegT (Xnr3 being an exception, see later). VegT is a T-box transcription factor, which is maternally expressed in the vegetal region. It accounts for most of the Smad2 activation pattern (Figure 8.2E) and is required for mesoderm and endoderm induction (Zhang et al. 1998; Kofron et al. 1999). Xnrs are also targets of β -catenin signaling, which explains the increased Smad2 activity in the dorsal side (Agius et al. 2000; Schohl and Fagotto 2003). Note that the earliest Smad2 pattern is not vegetal but equatorial (again highest on the dorsal side) (Schohl and Fagotto 2002), similar to β -catenin distribution, which denotes a predominant role of maternal β -catenin in the early phase of Xnr expression (discussed in Schohl and Fagotto 2003).
- (3) In the early embryo, MAPK is mainly under the control of FGF signaling (Tannahill et al. 1992; Christen and Slack 1999). Activated P-MAPK concentrates in an equatorial ring, which coincides with the known expression of FGF-dependent mesodermal markers, such as Xbra and eomesodermin (Schohl and

Fagotto 2003). The sources of early FGF are still incompletely defined. There has been some evidence for the maternal FGF activity, but direct confirmation is missing. What is better established is the early transcription of FGF ligands under the control of maternal β -catenin (Figures 8.2F and 8.3A) (Schohl and Fagotto 2003). This pathway explains well the striking parallel between the temporal and spatial patterns of β -catenin and MAPK activations. An additional input comes from early β -catenin-dependent Xnrs on the dorsal side, which in turn also activates FGF expression (Schohl and Fagotto 2003) (Figure 8.3A).

- (4) NF κ B/Rel signaling came as the last and rather unexpected contributor to early patterning (Armstrong et al. 1998; Armstrong et al. 2012, #1746). Interfering with NF κ B activity by expression of a transdominant form of the NF- κ B inhibitor I κ B α resulted in partial inhibition of dorsal axis formation (Armstrong et al. 2012). The phenotype was explained at the molecular level by a dramatic loss of expression of a subset of Organizer markers, including the direct β -catenin/TCF target Xnr3. Other targets such as Siamois were however not affected. Analysis of the Xnr3 promoter revealed closely apposed TCF and NF- κ B binding sites, and NF κ B isoforms were found to directly interact with β -catenin *in vitro* and *in vivo* (Armstrong et al. 2012). The use of reporter genes lacking one of the other binding sites showed that β -catenin/TCF-dependent transcription was partially asymmetric, but still significant in the ventral marginal region, consistent with the presence of nuclear β -catenin, while the NF κ B activity was exclusively detected in the dorsal animal region. These results explain well the more animal localization of Xnr3 compared to other Organizer genes and its important role for induction and development of tissues specifically derived from this region, i.e. neuroderm (Wessely et al. 2001) and trunk mesoderm (Yokota et al. 2003). The involvement of this pathway in axis specification

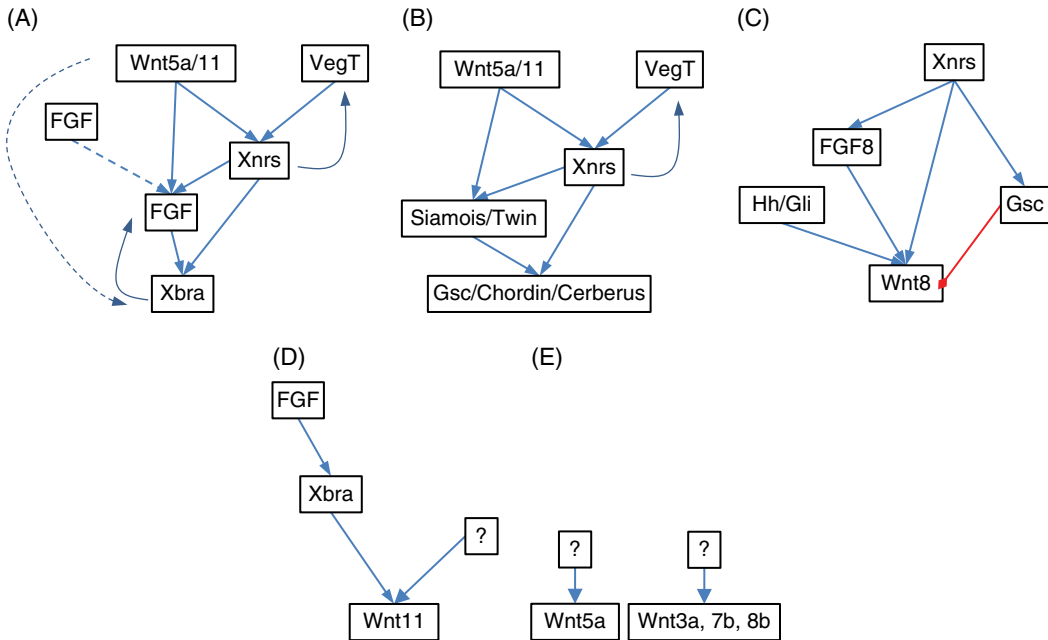


Figure 8.3 Regulatory circuits involving early Wnt signaling. (A) Posterior-ventral mesoderm induction (Xbra): The network is controlled by maternal Wnts and VegT (and possibly FGF). Xnrs expression is activated by both VegT and Wnts. FGF expression is induced by Wnts and Xnrs, and at later during gastrulation by a positive feedback loop with its target Xbra. Xbra is controlled directly by FGF and Xnrs, and probably also Wnt. Additional inhibitory controls of Xbra, e.g., by Gsc, are not shown. (B) Induction of dorsal anterior mesoderm. Siamois/Twin and Xnrs induce the major dorsal components responsible for patterning of gastrula (Spemann organizer), including the transcription factor Gsc and soluble inhibitors of BMP, Xnr and Wnt pathways, such as Chordin and Cerberus. (C) Control of zygotic Wnt8 expression (ventral-lateral mesoderm) in the gastrula by zygotic Xnrs and FGFs (Heasman 2006). Hedgehog signaling, now also active, also contributes (Mullor et al. 2001), while Gsc repressed Wnt8 in the dorsal side (Yao and Kessler 2001). (D) Expression of zygotic Wnt11 is controlled by Xbra (Tada and Smith 2000). (E) Transcriptional regulation of other Wnts expressed in the *Xenopus* gastrula is not known.

is very satisfying from an evolutionary point of view, since the homologous Toll-Dorsal pathway is well known to control establishment of the dorsoventral axis in *Drosophila* (Stathopoulos and Levine 2002).

A fascinating mystery that remains unresolved is the origin of the NF κ B signal. In *Drosophila*, the pathway is triggered by an extracellular proteolytic cascade that leads to activation of the Toll ligand Spätzle. In *Xenopus*, it was shown that the activity also depends on the MyD88-dependent Toll-like receptor/IL1-receptor (TLR/IL1-R). Expression of a dominant active form of *Drosophila* Easter, the protease upstream of Spätzle, was able to rescue an axis in ventral-

ized embryos, indicating quite provocatively that a Spätzle homologue must be expressed in the early embryo (Armstrong et al. 1998). Identification of *Xenopus* homologues of Easter, Spätzle, and Toll would be certainly an important step to complete the description of early patterning.

Interactions between the pathways

If one tries to summarize the core of the signaling network active in the pregastrula embryo, one realizes that it is largely controlled by maternal Wnt- β -catenin and VegT, with a minor contribution of vegetal Vg1, of animal-dorsal NF κ B/Rel and possibly of animal FGFs. These simple prelocalized cues produce a pattern largely based on

combinations of signals. The result is a mosaic of partially overlapping signals (Figure 8.2E), which leads to a complex landscape of gene expression (Figure 8.2D). Two of the interactive circuits are presented in Figure 8.3A and B, and selected synergistic regulation of classical markers of early patterning are shown in Figure 8.2F–F". One sees in particular that equatorial and dorsal signals are reinforced by two mechanisms, activation of *Xnrs* by Wnt- β -catenin and of FGF-MAPK by Wnt- β -catenin and *Xnrs*-Smad2. The former is important to directly strengthen the core of the dorsalizing center (*Siamois* expression, Figure 8.2F) as well as for activation of anterior endoderm genes (not shown, see Wardle and Smith 2006; Zorn and Wells 2007). β -Catenin further controls different regions of the dorsal mesoderm, i.e., head mesoderm (*Gooseoid*, or *Gsc*), trunk mesoderm (*Brachury* or *Xbra*). *Gsc* pattern can be explained by the combined influence of high dorsal Wnt- β -catenin and *Xnr*-Smad2 (Figure 8.2F', 3B). *Xbra* expression requires the conjunction of Wnt- β -catenin, *Xnr*-Smad2, and FGF-MAPK (Figure 8.2F"), the latter controlled by the former (Figure 8.3A). Finally, *Xnr3* is induced in the animal region of the dorsalizing center by Wnt- β -catenin and NF κ B/Rel signals (Figure 8.2F"). Note that I present here a much simplified description of the situation, since additional cross-talks modulate directly and indirectly these patterns.

More than dorsal: Equatorial maternal β -catenin signaling and early mesoderm induction

Our systematic mapping of nuclear β -catenin revealed that at the blastula stage, it did not only accumulate dorsally, as predicted, but also all around the equator (Schohl and Fagotto 2002) (Figure 8.2C). Even more surprising, the ventral signal was resistant to inhibition of transcription by α -amanitin and thus was all generated by a maternal signal (Schohl and Fagotto 2003). We demonstrated that the whole pool, dorsal and ventral, was required for the earliest phase of expression of the classical mesoderm markers *Xbra* and *eomesodermin* (Schohl and Fagotto 2003). As mentioned before and illustrated in Figure 8.3A, the action is largely indirect, via

stimulation of FGF expression, although β -catenin is also known to activate *Xbra* directly, at least at later zygotic stages (Vonica and Gumbiner 2002), consistent with other embryos (Yamaguchi et al. 1999). Thus, maternal Wnt- β -catenin appears to fulfill two different functions (Schohl and Fagotto 2003): Low levels seem to be sufficient to synergize with low *Xnrs* levels and/or maternal FGFs to induce ventral (*Xbra*, Figure 8.2F") or general (*eomesodermin*, not shown) mesoderm genes, while at higher levels, it activates dorsal genes such as *Siamois* and *Xnr3* (Figure 8.2F).

Wnt canonical signaling and patterning of the gastrula

Several Wnts are expressed in the gastrula (Figure 8.4), and both canonical and non-canonical branches play crucial roles during gastrulation.

The function of canonical Wnt signaling during gastrulation can largely be as two processes (Figure 8.4): (i) dorsoventral patterning of the mesoderm and (ii) anterior-posterior patterning of the neuroderm.

- (1) Mesoderm patterning depends on several signals, including a global dorsoventral polarization built based on ventrally secreted BMP ligands and dorsal extracellular inhibitors (De Robertis 2009). In addition, zygotic Wnt8 contributes specifically to mesoderm patterning, by stimulating expression of muscle-specific genes, such as *MyoD*, in the paraxial/presomitic mesoderm, and repressing expression of notochord genes (Hikasa and Sokol 2013). Thus, ectopic activation of zygotic Wnt/ β -catenin on the dorsal side confers somitic fate and reduces or even abolishes the notochord, while on the contrary, inhibition of the pathway causes a reduction of myogenic presomitic mesoderm. The pathway is regulated by several factors: Wnt8 is expressed throughout the ventrolateral mesoderm (and endoderm) (Figure 8.4), but its action is sharply limited in the dorsal (especially anterior) region by secreted Wnt inhibitors (Figure 8.4). Note however that this dorsal "window" of low Wnt signaling is open only

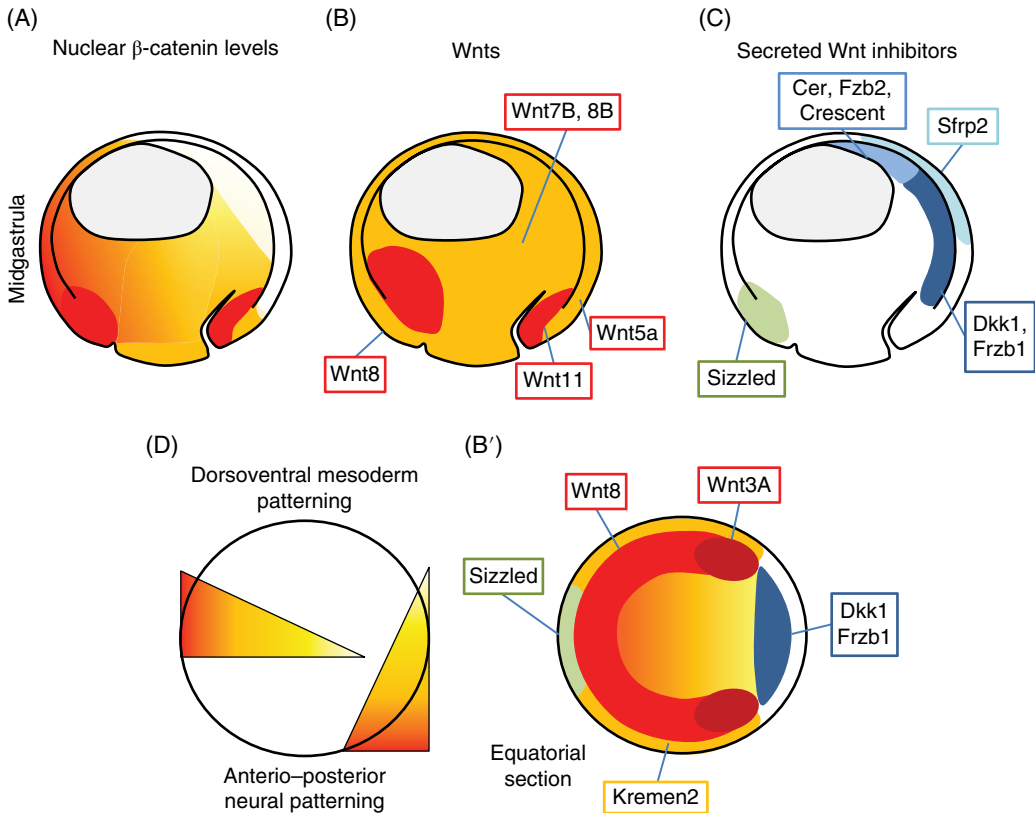


Figure 8.4 Wnt- β -catenin signaling in the *Xenopus* gastrula. The diagrams depict β -catenin signaling (A) (Schohl and Fagotto 2002) and the contribution of various Wnts (B, B', red-orange) and Wnt secreted inhibitors (C, B', blue-green), inferred from published *in situ* hybridization (summarized in Table 1, see Xenbase; Bouwmeester et al. 1996; Salic et al. 1997; Wang et al. 1997; Bradley et al. 2000; Pera and De Robertis 2000; Mao and Niehrs 2003; Hassler et al. 2007). (D) Two major sources of Wnts control β -catenin signaling during gastrulation (Heasman 2006; Hikasa and Sokol 2013): (A) ventro-lateral Wnt8 is involved in mesoderm patterning and is required in particular for expression of the myogenic MyoD in the paraxial mesoderm. A dorsal posterior source, probably due to a combination of Wnt3A, expressed in the paraxial mesoderm, and Wnt5a/Wnt11, expressed in the blastopore lip, provides a posteriorizing signal that patterns the neuroderm. A large number of soluble antagonists are secreted in the dorsal side, mostly by the anterior and trunk mesoderm. Their function is required for development of head and dorsal structures. An additional Wnt inhibitor, Sizzled, is expressed in the most ventral side and moderated there the action of Wnt8. Wnt8 activity is reinforced on the lateral sides by the agonist Kremen2. To see a color version of this figure, see Plate 16.

briefly at early gastrula stages (Schohl and Fagotto 2002), implying that most of the axial/paraxial patterning occurs over a short period of time, quite some time before the time of actual involution of the trunk mesoderm. During the rest of gastrulation, the blastopore lip is on the contrary the center of an intense β -catenin activity (Figure 8.4 and later). Note that in addition to the dorsoanterior source of Wnt inhibitors, a secreted frizzled-like inhibitor called sizzled is also expressed in

the most ventral region (Figure 8.4) (Salic et al. 1997), which prevents unwanted ventral expansion of somitic mesoderm.

- (2) The strong posterior Wnt/ β -catenin activity localized at the blastopore lip starting at the midgastrula (Figure 8.4) is likely to be produced by Wnt3a, with the possible contribution of Wnt5a and Wnt11. Experimental evidence is still lacking for any of the ligands. Its function is however quite well established, as it plays a major role in neural patterning by serving as the

posteriorizing activity (Ulloa and Marti 2010). Similar to mesoderm patterning, secreted inhibitors expressed in the mesoderm and the anterior region of the neurodem (Figure 8.4) are essential to build the proper gradient of Wnt activity. A recent study has discovered an additional intracellular mechanism that seems to both sharpen and stabilize the gradient at the level of β -catenin transcriptional activity (Kim et al. 2012).

Noncanonical pathway(s) and convergence extension

The first phase of mesoderm involution concerns the anterior or prechordal mesoderm, which spreads on the inner surface of the ectoderm and migrates toward the animal pole, i.e. anteriorly. Toward the end of gastrulation, it is the turn of the dorsal posterior (chordal, or trunk) mesoderm to involute. As soon as it enters the embryo, the dorsal-most region, the prospective notochord, is separated from the two paraxial regions, which become the presomitic mesoderm. The two tissues undergo in parallel and massive cell rearrangement, called convergence–extension, which transforms them into compact elongated structures. Mesoderm cells undergoing convergence–extension are characterized by an elongated shape and produce protrusions at both ends, reason why they are named **bipolar**. These bipolar cells are all aligned roughly perpendicular to the anterior–posterior axis of the embryo, which is also the direction of involution of the mesoderm.

The characteristic changes in cell shape and the resulting movements are controlled by noncanonical Wnt signaling involving Frizzled and Dsh. In *Drosophila*, several morphogenetic events such as formation of cuticle bristles in the epidermis and orientation of photoreceptors in the ommatidia also require polarized reorganization of the actin cytoskeleton, in a process called planar cell polarity (PCP) that also depends on Frizzled and Dsh. A parallel was thus made, and it was proposed that convergence–extension in vertebrates was similarly controlled by a noncanonical Wnt-PCP pathway. Consistent with this hypothesis,

involvement of typical PCP components, such as VanGogh/Strabismus in convergence–extension was clearly demonstrated (Darken et al. 2002; Park and Moon 2002; Takeuchi et al. 2003). Note that despite intense efforts over the past 10 years, the molecular mechanisms are still poorly understood. In *Drosophila*, it does not appear to require Wnt ligands, suggesting a ligand-independent function of Fz. In *Xenopus* and other vertebrates, convergence extension appeared to require regulation of RhoGTPases and JNK downstream of Wnt/Fz, and these components were incorporated into the “vertebrate” PCP pathway. Note however that Wnts are not required for *Drosophila* PCP. Note also that convergence–extension in *Drosophila* does not appear to be controlled by the PCP pathway. There is similarly no evidence for a direct link between VanGogh/Strabismus, Flamingo or Prickled and Rho, Rac or JNK in vertebrates. As mentioned earlier, Houliston and colleagues have recently suggested that there are probably two different pathways, one corresponding to the actual PCP, the other being a noncanonical pathway (with possibly several branches, see Figure 8.1) regulating, among other targets, the actin cytoskeleton (Lapebie et al. 2011).

In any case, mesodermal convergence–extension in *Xenopus* depends on Wnt5a and Wnt11, on Fz7 (and probably Fz8, Rana et al. 2006) and coreceptors Ryk and Ror2 (Table 3, Tada and Smith 2000; Cha et al. 2008; Hikasa et al. 2002; Schambony and Wedlich 2007; Kraft et al. 2012). Note that the pathway largely relies on maternal Wnt5a and Wnt11 (Cha et al. 2008), which is relatively surprising, as one used to consider that most processes were zygotic past the late blastula stage. Note also that both inhibition and overactivation of the PCP pathway lead roughly to the same overall defects, indicating that the right balance is required to build a correct cell polarity (Wallingford 2012). As mentioned earlier, loss-of-function experiments in the early embryo have shown that several key components are shared with the β -catenin branch involved in embryo patterning, including the two Wnts, Fz7, and LRP6 (Kofron et al. 2007; Cha et al. 2008). Finally, some data suggest that distinct branches may be dissected, e.g., one inputting on Rac1/JNK and one on Rho (Bryja et al. 2008).

The neuroderm also undergoes convergence–extension, which, although different from the mesoderm process in terms of cell orientation and behavior (Keller et al. 1992; Elul et al. 1997; Wallingford and Harland 2001), also relies on the PCP pathway (Wallingford 2012). Finally, PCP signaling is also controlling ciliogenesis. *Xenopus* epidermis produces beautiful multiciliated cells that are particularly favorable for investigation of the underlying molecular and cellular mechanisms (Wallingford 2012).

Wnt signaling and ectoderm–mesoderm separation

Another important morphogenetic process is the formation of boundaries that prevent cell mixing between newly formed embryonic tissues. Ectoderm–mesoderm separation has been intensively studied in *Xenopus* (Winklbauer et al. 2001; Medina et al. 2004; Winklbauer and Luu 2008; Winklbauer 2009; Rohani et al. 2011). Expression of Fz7 in the mesoderm has been shown to be required for correct separation (Winklbauer et al. 2001). It was proposed to control a Calcium/PKC-type pathway and was shown indeed to involve Dsh, G proteins, and PKC (Winklbauer et al. 2001). This pathway was further shown to interact with the protocadherin P APC (Medina et al. 2004). Note that Wnt5a/Wnt11 stimulate the pathway when ectopically expressed, but direct evidence for their requirement is still currently missing. Note also that many components that have been implicated in this process are also involved in convergence extension, including Fz7, Dsh, G proteins, Rho, and APC. It has been proposed that convergence–extension and tissue separation are controlled by overlapping yet distinct branches of the Wnt pathway (Medina et al. 2004). One alternative explanation is that the reactions downstream of Fz7 constitute a single pathway with multiple molecular outputs, which is primarily devoted to provide specific cellular properties, in particular the right cortical contractility, to mesoderm cells. These properties would be required for convergence–extension, but would also impact on tissue separation, because this

process is heavily dependent on cortex contractility. In other words, manipulations that affect the pathway may indirectly induce tissue mixing, for example by lowering the basal level of myosin activity in mesoderm cells (Fagotto 2013).

Wnt signaling at postgastrula stages

Wnt signaling in the neurula

Neural crest cells constitute another fascinating model intensively studied in *Xenopus*. This cell population forms precisely at the boundary between neuroderm and ectoderm, and different groups will then migrate along precise tracks to populate a variety of regions of the embryo. Excellent reviews are available on this subject (e.g., Stuhlmiller and Garcia-Castro 2012; Theveneau and Mayor 2012). Here, I will only mention that both canonical and noncanonical pathways are involved in both the induction of neural crest cells and their migration (Table 8.2). Noncanonical signaling is specifically required to allow the groups of cells to migrate directionally (Theveneau and Mayor 2012).

The midbrain–hindbrain boundary is another example where, according to other vertebrate models, Wnt/ β -catenin signaling is also involved. It controls there a well-known Wnt target, engrailed, conserved from *Drosophila* to mammals. Little has been done on this process in *Xenopus*.

Otherwise, the pattern of β -catenin activation indicates that the ventral Wnt8-dependent activity decays during the early neurula stages, while the posterior Wnt3a-dependent activity remains active longer (Figure 8.5). Furthermore, the trunk neuroderm also shows activation in the late neurula, which may correspond to involvement of Wnt signaling in dorsoventral patterning of the future neural tube, also studied in other vertebrates (Ulloa and Marti 2010).

Wnts and organogenesis

Wnt signaling participates in a large number of cases of induction, patterning, and morphogenesis of organs. We have

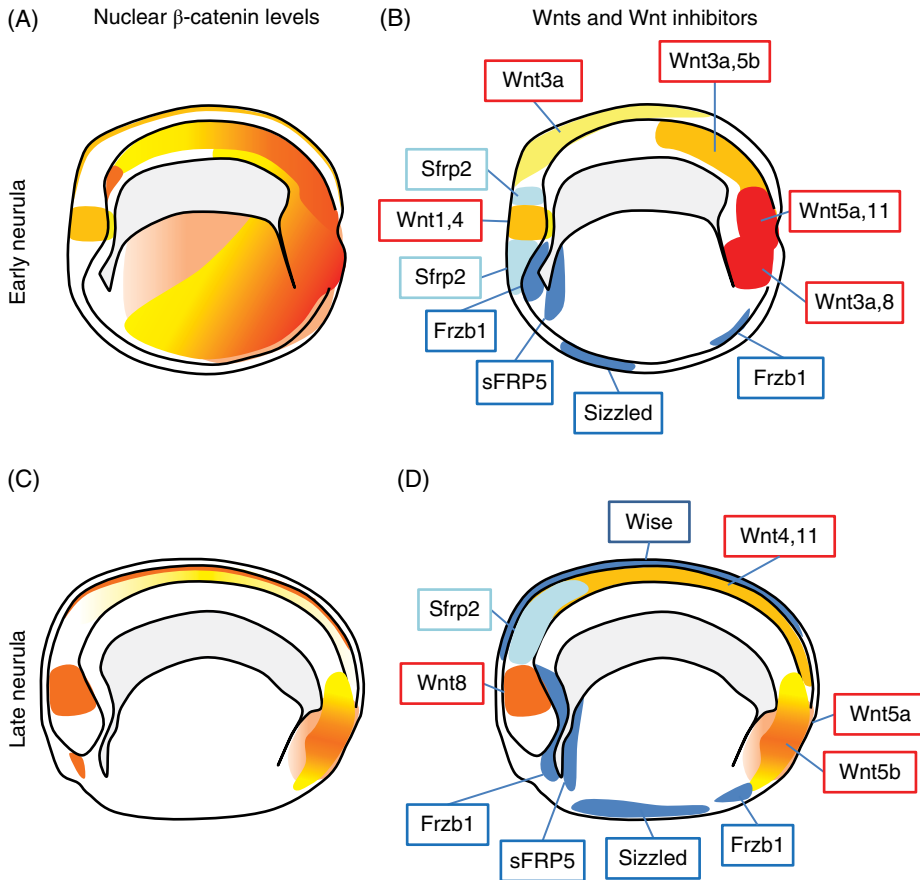


Figure 8.5 Wnt- β -catenin signaling in the *Xenopus* neurula. β -Catenin nuclear localization (A and C) and Wnt and Wnt inhibitor expression (B and D). Most of the β -catenin activity seems to be explainable by the published Wnts and Wnt inhibitors (summarized in Table 1, see Xenbase; Wang et al. 1997; Bradley et al. 2000; Pera and De Robertis 2000; Pilcher and Krieg 2002; Bell et al. 2003; Itasaki et al. 2003; Mao and Niehrs 2003), although direct systematic studies are lacking for most of the cases. To see a color version of this figure, see Plate 17.

compiled published examples in Table 8.4. The list is likely to be very incomplete. Indeed, studies usually focus on one particular organ and on a particular Wnt ligand and rarely mention additional phenotypes, even though one single Wnt generally controls several processes. One should also be prudent in inferring a specific role of a given Wnt to a particular organ formation based on loss-of-function phenotypes, keeping in mind that it is not always straightforward to distinguish a direct action on one of these late processes versus an earlier step in patterning and/or determination.

Xenopus as model to study the Wnt pathway: Manipulations and phenotypes

With now in mind the various processes that depend on Wnt signaling, one may better appreciate the possible applications of *Xenopus* for the study of this pathway. I present in Figure 8.6 an overview of the simple manipulations that can be performed on the endogenous canonical Wnt pathway and of those that ectopically activate it. These diagrams also emphasize the fact that not all manipulations can successfully target the early maternal pathways: Any upstream step (Dsh and upstream) has proven resistant to multiple strategies that were tried to inhibit the

Table 8.4 Wnt signaling in postgastrula developmental processes.

Tissue/organ	Branch	Wnt	Fz	Other regulators	Activ/inhib	Localized expression	Remarks	References
Midbrain boundary				PP2A-B56	A			Yang et al. (2003)
NCC induction	β cat		Fz7	Kremen 2	A			Wu et al. (2005); Abu-Elmagd et al. (2006); Hassler et al. (2007)
NCC induction	NC	Wnt11 Wnt11R	Fz7, Ror2	Dsh Par1	A	Wnt11, Fz7		De Calisto et al. (2005); Ossipova and Sokol (2011)
NCC migration	β cat		Fz3		A			Deardorff et al. (2001); Yanfeng et al. (2003); Hong et al. (2008); Stevenston et al. (2009)
NCC migration	NC				A		Contact inhibition	Carmona-Fontaine et al. (2008); Matthews et al. (2008)
Pronephros	β cat				A			Lyons, Miller et al. (2009); McCoy et al. (2011)
Pronephros induction	NC	Wnt11 Wnt11b			A	Yes		Tetelin and Jones (2010)
Pronephros	NC				I			McCoy et al. (2011)
Pronephros patterning, tubulogenesis	NC	Wnt4		Daam1	A	Yes		Saulnier et al. (2002); Naylor and Jones (2009); Miller et al. (2011)
Otic placode		Wnt1, Wnt8	Fz3 Fz7		A	Yes		Park and Saint-jeannet (2008)
Otic placode	NC	Wnt5a	Ror2		A	Yes	Placode boundary	Jung et al. (2011)
Optic tectum	β cat	XWnt-1 XWnt-3A				Yes		Lim et al. (2010)
Eye	NC	Wnt4			A	Yes		Wan et al. (2010); Maurus et al. (2005)

(Continued)

Table 8.4 (cont'd)

Tissue/organ	Branch	Wnt	Fz	Other regulators	Activ/inhib	Localized expression	Remarks	References
Retina	β cat		Fz5		A		Neural fate	Van Raay et al. (2005)
Sensory neurons	β cat		Fz10		A			Garcia-Morales et al. (2009)
Foregut	β cat			sFrp5	I	Yes	Fate	Li, Rankin et al. (2008)
	NC						Epithelization	
Cardiac field	β cat				I			Martin et al. (2010)
Heart	β cat	Wnt6			I	Yes	Limits size	Lavery et al. (2008b)
Heart	NC	Wnt11			A	Yes		Pandur et al. (2002)
Heart	NC	Wnt11R			A	Yes		Garrick et al. (2005)
Heart	β cat			IGFBP-4	I			Zhu et al. (2008)
Haematopoietic lineage	β cat	Wnt4			I	Yes		Tran et al. (2010)
Angioblast and vascular development	β cat			Rspodin3	A	Yes		Kazanskaya et al. (2008)
Liver	β cat	Wnt11		sFrp5	I	Yes		McLin et al. (2007)
Lung		Wnt5			A	Yes		Yin et al. (2010)
		Wnt7b						
Lung		Wif1			I	Yes		Yin, Winata et al. (2010)
Mouth opening	β cat			Frzb1, Crescent	A	Yes		Dickinson and Sive (2009)
Tail regeneration	β cat				A			Lin and Slack (2008)

Compilation of various post-gastrula processes, where Wnt signaling has been implicated. In each case, the branch of the pathway is indicated (β cat, canonical; NC, non-canonical), as well as, when available, the upstream gene targeted by loss-of-function (depletion). *AVI* stand for activator/inhibitor for the particular process.

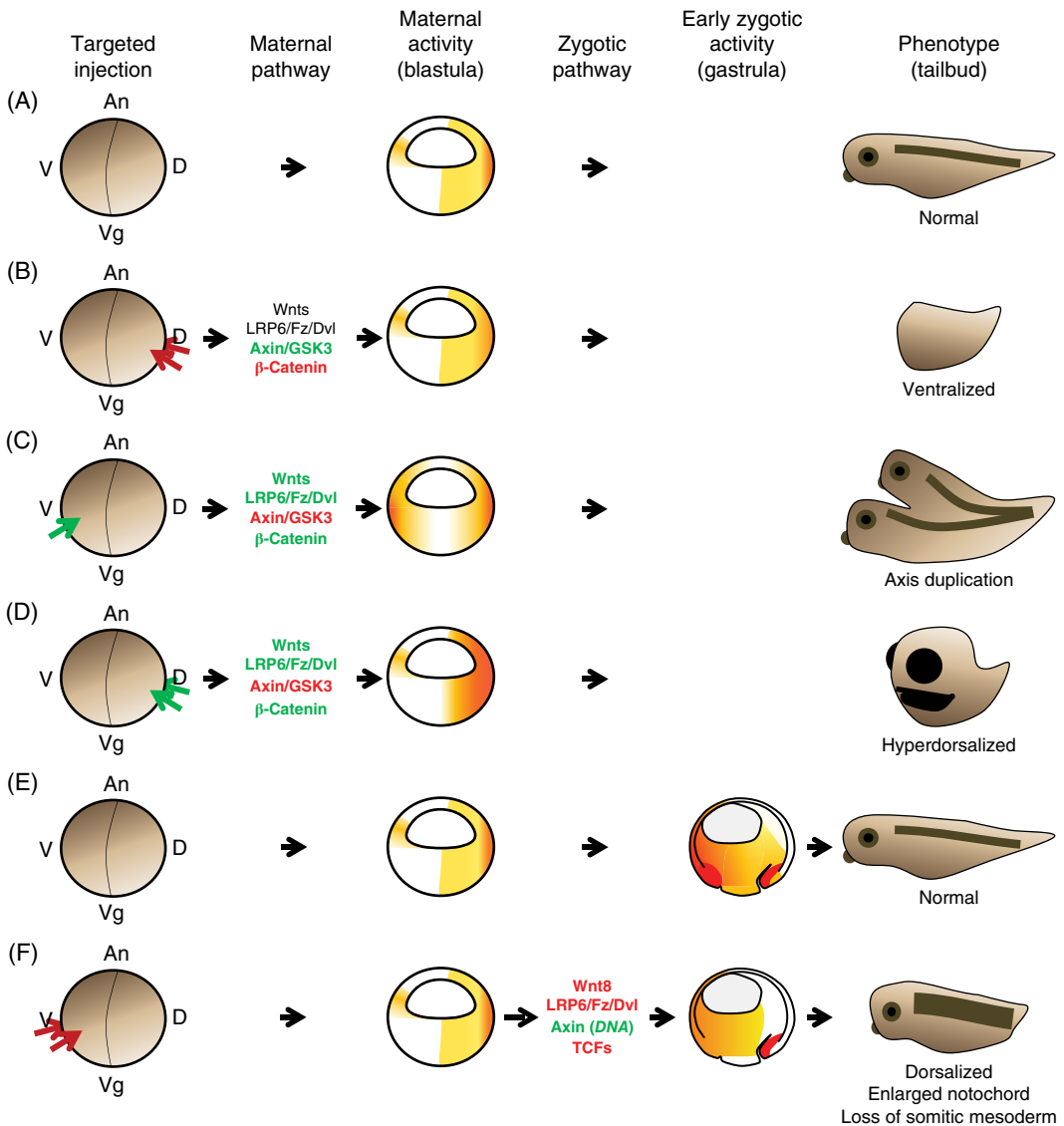


Figure 8.6 Major experimental interference strategies and corresponding phenotypes. (A) Normal maternal β -catenin signaling. (B) Endogenous maternal Wnt- β -catenin signaling can be blocked by dorsal injection of inhibitory reagents (red, e.g., β -catenin MO, Heasman et al. 2000, or dominant negative TCF3, Molenaar et al. 1996), or overexpression of negative regulators (green, such as Axin, Zeng et al. 1997). The resulting phenotype is a ventralized embryo. The severity of the phenotype ranges from reduction of anterior structures (cement gland, eyes) to complete loss of anterior and dorsal structures. The pathway cannot be inhibited by targeting upstream components of the pathway (black, e.g., Dsh). Interference with these upstream steps requires manipulations (depletion) in the oocytes (Tao et al. 2005; Kofron et al. 2007; Tadjuidje et al. 2011). (C) Ectopic activation in the ventral side produces embryos with duplicated anterior/dorsal structures (siamese twins). Manipulations include expression/overexpression of any positive regulator (green, e.g., Wnts, Smith and Harland 1991), or interference with negative regulators (red, e.g., dominant negative GSK3, Pierce and Kimelman 1995). Note that while dominant negative Axin forms injected as mRNA readily block maternal signaling (Fagotto et al. 1999), Axin MO fail to do so, presumably because maternal Axin is sufficiently stable (Schneider et al. 2012). (D) Similar manipulations on the dorsal side produce hyperdorsalized embryos, with large heads and reduced tail. (E) Normal maternal and zygotic β -catenin signaling. (F–G) Injections of reagents interfering with upstream components, such as Wnt inhibitors (Glinka et al. 1998) or dominant negative Wnt constructs (Hoppler et al. 1996) do not interfere with the maternal dorsalizing signal, but affect zygotic signals. (F) Ventral injections perturb mesoderm patterning, leading to axial defects (enlarged notochord and reduced or absent somites).

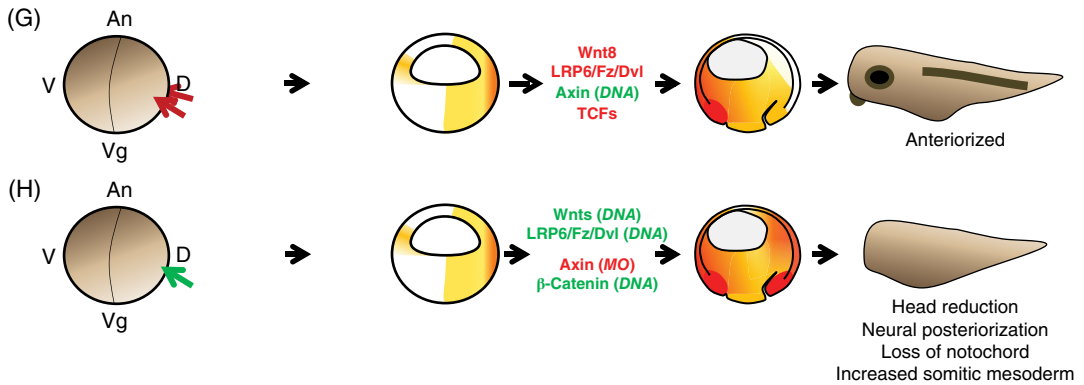


Figure 8.6 (continued) (G) Dorsal manipulations affect neural patterning (anteriorization). The same phenotypes are observed when with a positive components (e.g., β -catenin-Engrailed repressor, Montross et al. 2000) by injection of plasmid DNA. Because zygotically transcribed constructs only reach significant levels of expression in the late blastula/early gastrula, they do not affect maternal patterning. (H) Zygotic activation of the pathway can be similarly achieved by injection of plasmid DNA coding for example for Wnts, Wnt receptors, Dsh or β -catenin. The phenotypes include reduction in head structures and general posteriorization of the neural tube, decrease or loss of notochord and expansion of the somitic mesoderm. Axin depletion by morpholino injections is another example leading to the same phenotype (Schneider et al. 2012). To see a color version of this figure, see Plate 18.

pathway in the embryo. This is probably partly due to the fact the corresponding reaction takes place too early during development. For instance, inhibition of Wnt11 translation will have no effect, since Wnt11 seems to be already translated in the early embryo. In addition, some components may simply be stable, and inhibition of translation will not deplete them. In those cases, depletion in the oocyte is the only suitable method. This approach is beautifully effective and gives unambiguous results, but is unfortunately technically quite demanding (Heasman 2002).

It is important also to keep in mind that in those cases where the maternal pathway is resilient to interference, the interfering reagent is likely to affect the zygotic pathways, first of all the mesoderm ventralizing and the neuroderm posteriorizing canonical pathways (Figure 8.6). For several constructs, including Fz and Dishevelled, convergence–extension and ectoderm separation are two additional processes that will be equally affected. Figure 8.6 shows that injection of plasmid DNA is a simple and efficient method to target early zygotic signals without interfering with maternal dorsoventral patterning. To conclude, I wish that the complexity of the pathways

may be kept in mind when analyzing a process and/or a particular component: Clean specific functional and biochemical assays are essential to obtain unambiguous results. Hopefully, specificity for a given reaction/branch will be validated more systematically in the future, for instance by comparing different inputs (Wnts) and different outputs (e.g., β -catenin, PKC, JNK).

References

- Abu-Elmagd, M., C. Garcia-Morales, G. N. Wheeler (2006). Frizzled7 mediates canonical Wnt signaling in neural crest induction. *Developmental biology* **298**(1): 285–298.
- Agius, E., M. Oelgeschlager, O. Wessely, C. Kemp, E. M. De Robertis (2000). Endodermal Nodal-related signals and mesoderm induction in *Xenopus*. *Development* **127**(6): 1173–1183.
- Armstrong, N. J., H. Steinbeisser, C. Prothmann, R. DeLotto, R. A. Rupp (1998). Conserved Spatzle/Toll signaling in dorsoventral patterning of *Xenopus* embryos. *Mechanisms of development* **71**(1–2): 99–105.
- Armstrong, N. J., F. Fagotto, C. Prothmann, R. A. Rupp (2012). Maternal Wnt/beta-catenin signaling coactivates transcription through NF-kappaB binding sites during *Xenopus* axis formation. *PLoS one* **7**(5): e36136.

- Belenkaya, T. Y., C. Han, H. J. Standley, et al. (2002). *pygopus* Encodes a nuclear protein essential for wingless/Wnt signaling. *Development* **129**(17): 4089–4101.
- Bell, E., I. Munoz-Sanjuan, C. R. Altmann, A. Vonica, A. H. Brivanlou (2003). Cell fate specification and competence by Coco, a maternal BMP, TGFbeta and Wnt inhibitor. *Development* **130**(7): 1381–1389.
- Berndt, J. D., A. Aoyagi, P. Yang, J. N. Anastas, L. Tang, R. T. Moon (2011). Mindbomb 1, an E3 ubiquitin ligase, forms a complex with RYK to activate Wnt/beta-catenin signaling. *The journal of cell biology* **194**(5): 737–750.
- Bilic, J., Y. L. Huang, G. Davidson, et al. (2007). Wnt induces LRP6 signalosomes and promotes dishevelled-dependent LRP6 phosphorylation. *Science* **316**(5831): 1619–1622.
- Bouwmeester, T., S. Kim, Y. Sasai, B. Lu, E. M. De Robertis (1996). Cerberus is a head-inducing secreted factor expressed in the anterior endoderm of Spemann's organizer. *Nature* **382**(6592): 595–601.
- Bradley, L., B. Sun, L. Collins-Racie, E. LaVallie, J. McCoy, H. Sive (2000). Different activities of the frizzled-related proteins *frzb2* and *sizzled2* during *Xenopus* anteroposterior patterning. *Developmental biology* **227**(1): 118–132.
- Brannon, M., M. Gomperts, L. Sumoy, R. T. Moon, D. D. Kimelman (1997). A beta-catenin/XTcf-3 complex binds to the siamois promoter to regulate dorsal axis specification in *Xenopus*. *Genes & development* **11**(18): 2359–2370.
- Bryja, V., D. Gradl, A. Schambony, E. Arenas, G. Schulte (2007). Beta-arrestin is a necessary component of Wnt/beta-catenin signaling in vitro and in vivo. *Proceedings of the National Academy of Sciences of the United States of America* **104**(16): 6690–6695.
- Bryja, V., A. Schambony, L. Cajanek, I. Dominguez, E. Arenas, G. Schulte (2008). Beta-arrestin and casein kinase 1/2 define distinct branches of non-canonical WNT signalling pathways. *EMBO reports* **9**(12): 1244–1250.
- Bryja, V., E. R. Andersson, A. Schambony, et al. (2009). The extracellular domain of *Lrp5/6* inhibits noncanonical Wnt signaling in vivo. *Molecular biology of the cell* **20**(3): 924–936.
- Caneparo, L., Y. L. Huang, N. Staudt, et al. (2007). Dickkopf-1 regulates gastrulation movements by coordinated modulation of Wnt/beta catenin and Wnt/PCP activities, through interaction with the Dally-like homolog Knypek. *Genes & development* **21**(4): 465–480.
- Carmona-Fontaine, C., H. K. Matthews, S. Kuriyama, et al. (2008). Contact inhibition of locomotion in vivo controls neural crest directional migration. *Nature* **456**: 957–961.
- Cha, S. W., E. Tadjuidje, Q. Tao, C. Wylie, J. Heasman (2008). Wnt5a and Wnt11 interact in a maternal Dkk1-regulated fashion to activate both canonical and non-canonical signaling in *Xenopus* axis formation. *Development* **135**(22): 3719–3729.
- Cha, S. W., E. Tadjuidje, J. White, et al. (2009). Wnt11/5a complex formation caused by tyrosine sulfation increases canonical signaling activity. *Current biology* **19**(18): 1573–1580.
- Cha, S. W., E. Tadjuidje, C. Wylie, J. Heasman (2011). The roles of maternal Vangl2 and aPKC in *Xenopus* oocyte and embryo patterning. *Development* **138**(18): 3989–4000.
- Chang, C. and A. Hemmati-Brivanlou (1998). Neural crest induction by Xwnt7B in *Xenopus*. *Developmental biology* **194**(1): 129–134.
- Cheyette, B. N., J. S. Waxman, J. R. Miller, et al. (2002). Dapper, a Dishevelled-associated antagonist of beta-catenin and JNK signaling, is required for notochord formation. *Developmental cell* **2**(4): 449–461.
- Christen, B. and J. Slack (1999). Spatial response to fibroblast growth factor signalling in *Xenopus* embryos. *Development* **126**: 119–125.
- Christian, J. L., J. A. McMahon, A. P. McMahon, R. T. Moon (1991). Xwnt-8, a *Xenopus* Wnt-1/int-1-related gene responsive to mesoderm- inducing growth factors, may play a role in ventral mesodermal patterning during embryogenesis. *Development* **111**(4): 1045–1055.
- Collavin, L. and M. W. Kirschner (2003). The secreted Frizzled-related protein Sizzled functions as a negative feedback regulator of extreme ventral mesoderm. *Development* **130**(4): 805–816.
- Cui, Y., J. D. Brown, R. T. Moon, J. L. Christian (1995). Xwnt-8b: a maternally expressed *Xenopus* Wnt gene with a potential role in establishing the dorsoventral axis. *Development* **121**(7): 2177–2186.
- Damianitsch, K., J. Melchert, T. Pieler (2009). XsFRP5 modulates endodermal organogenesis in *Xenopus laevis*. *Developmental biology* **329**(2): 327–337.
- Darken, R. S., A. M. Scola, A. S. Rakeman, G. Das, M. Mlodzik, P. Wilson (2002). The planar polarity gene *strabismus* regulates convergent extension movements in *Xenopus*. *EMBO journal* **21**(5): 976–985.
- Davidson, G., B. Mao, I. del Barco Barrantas, C. Niehrs (2002). Kremen proteins interact with Dickkopf1 to regulate anteroposterior CNS patterning. *Development* **129**(24): 5587–5596.
- Davidson, G., W. Wu, J. Shen, et al. (2005). Casein kinase 1 gamma couples Wnt receptor activation to cytoplasmic signal transduction. *Nature* **438**: 867–872.
- Deardorff, M. A., C. Tan, J. P. Saint-Jeannet, P. S. Klein (2001). A role for frizzled 3 in neural crest development. *Development* **128**(19): 3655–3663.
- De Calisto, J., C. Araya, L. Marchant, C. F. Riaz, R. Mayor (2005). Essential role of non-canonical Wnt signalling in neural crest migration. *Development* **132**(11): 2587–2597.

- De Robertis, E. M. (2009). Spemann's organizer and the self-regulation of embryonic fields. *Mechanisms of development* **126**(11–12): 925–941.
- De Robertis, E. M., J. Larrain, M. Oelgeschlager, O. Wessely (2000). The establishment of the Spemann's organizer and patterning of the vertebrate embryo. *Nature reviews genetics* **1**: 171–181.
- del Barco Barrantes, I., G. Davidson, H. J. Grone, H. Westphal, C. Niehrs (2003). Dkk1 and noggin cooperate in mammalian head induction. *Genes & development* **17**(18): 2239–2244.
- Dickinson, A. J. and H. L. Sive (2009). The Wnt antagonists Frzb-1 and Crescent locally regulate basement membrane dissolution in the developing primary mouth. *Development* **136**(7): 1071–1081.
- Djiane, A., J. Riou, M. Umbhauer, J. Boucaut, D. Shi (2000). Role of frizzled 7 in the regulation of convergent extension movements during gastrulation in *Xenopus laevis*. *Development* **127**(14): 3091–3100.
- Elkouby, Y. M., S. Elias, E. S. Casey, et al. (2010). Mesodermal Wnt signaling organizes the neural plate via Meis3. *Development* **137**(9): 1531–1541.
- Elul, T., M. A. Koehl, R. Keller (1997). Cellular mechanism underlying neural convergent extension in *Xenopus laevis* embryos. *Developmental biology* **191**(2): 243–258.
- Fagotto, F. (2013). The cellular basis of tissue separation. *Development* (in press).
- Fagotto, F., E. Jho, L. Zeng, et al. (1999). Domains of axin involved in protein-protein interactions, Wnt pathway inhibition, and intracellular localization. *Journal of cell biology* **145**(4): 741–756.
- Fonar, Y., Y. E. Gutkovich, H. Root, et al. (2011). Focal adhesion kinase protein regulates Wnt3a gene expression to control cell fate specification in the developing neural plate. *Molecular biology of the cell* **22**(13): 2409–2421.
- Funayama, N., F. Fagotto, P. McCrea, B. M. Gumbiner (1995). Embryonic axis induction by the armadillo repeat domain of β -catenin: evidence for intracellular signaling. *Journal cell biology* **128**: 959–968.
- Garcia-Morales, C., C. H. Liu, M. Abu-Elmaq, M. K. Hajihosseini, G. N. Wheeler (2009). Frizzled-10 promotes sensory neuron development in *Xenopus* embryos. *Developmental biology* **335**(1): 143–155.
- Garriock, R. J., S. L. D'Agostino, K. C. Pilcher, P. A. Kreig (2005). Wnt11-R, a protein closely related to mammalian Wnt11, is required for heart morphogenesis in *Xenopus*. *Developmental biology* **279**(1): 179–192.
- Garriock, R. J., A. S. Warkman, S. M. Meadows, S. L. D'Agostino, P. A. Kreig (2007). Census of vertebrate Wnt genes: isolation and developmental expression of *Xenopus* Wnt2, Wnt3, Wnt9a, Wnt9b, Wnt10a, and Wnt16. *Developmental dynamics* **236**(5): 1249–1258.
- Glinka, A., W. Wu, H. Delius, A. P. Monaghan, C. Blumenstock, C. Niehrs (1998). "Dickkopf-1 is a member of a new family of secreted proteins and functions in head induction." *Nature* **391**(6665): 357–362.
- Glinka, A., C. Dolde, N. Kirsch, et al. (2011). LGR4 and LGR5 are R-spondin receptors mediating Wnt/beta-catenin and Wnt/PCP signalling. *EMBO reports* **12**(10): 1055–1061.
- Gwak, J., M. Cho, S. J. Gong, et al. (2006). Protein-kinase-C-mediated beta-catenin phosphorylation negatively regulates the Wnt/beta-catenin pathway. *Journal of cell science* **119**(Pt 22): 4702–4709.
- Hassler, C., C. M. Cruciat, Y. L. Huang, S. Kuriyama, R. Mayor, C. Niehrs (2007). Kremen is required for neural crest induction in *Xenopus* and promotes LRP6-mediated Wnt signaling. *Development* **134**(23): 4255–4263.
- He, X., J. P. Saint-Jeannet, Y. Wang, J. Nathans, I. Dawid, H. Varmus (1997). A member of the Frizzled protein family mediating axis induction by Wnt-5A. *Science* **275**(5306): 1652–1654.
- Heasman, J. (2002). Morpholino oligos: making sense of antisense? *Developmental biology* **243**: 209–214.
- Heasman, J. (2006). Patterning the early *Xenopus* embryo. *Development* **133**(7): 1205–1217.
- Heasman, J., A. Crawford, K. Goldstone, et al. (1994). Overexpression of cadherins and underexpression of β -catenin inhibit dorsal mesoderm induction in early *Xenopus* embryos. *Cell* **79**: 791–803.
- Heasman, J., M. Kofron, C. Wylie (2000). Beta-catenin signaling activity dissected in the early *Xenopus* embryo: a novel antisense approach. *Developmental biology* **222**(1): 124–134.
- Heisenberg, C. P., M. Tada, G. J. Rauch, et al. (2000). Silberblick/Wnt11 mediates convergent extension movements during zebrafish gastrulation. *Nature* **405**(6782): 76–81.
- Hikasa, H., M. Shibata, I. Hiratani, M. Taira (2002). The *Xenopus* receptor tyrosine kinase Xror2 modulates morphogenetic movements of the axial mesoderm and neuroectoderm via Wnt signaling. *Development* **129**(22): 5227–5239.
- Hikasa, H. and S. Y. Sokol (2013). Wnt signaling in vertebrate axis specification. *Cold Spring Harbor perspectives in biology* **5**(1): a007955.
- Holowacz, T. and R. P. Elinson (1993). Cortical cytoplasm, which induces dorsal axis formation in *Xenopus*, is inactivated by UV irradiation of the oocyte. *Development* **119**(1): 277–285.
- Hong, C. S., B. Y. Park, J. P. Saint-Jeannet (2008). Fgf8a induces neural crest indirectly through the activation of Wnt8 in the paraxial mesoderm. *Development* **135**(23): 3903–3910.

- Hoppler, S., J. D. Brown, R. T. Moon (1996). Expression of a dominant-negative Wnt blocks induction of MyoD in *Xenopus* embryos. *Genes & development* **10**(21): 2805–2817.
- Houliston, E. (1994). Microtubule translocation and polymerisation during cortical rotation in *Xenopus* eggs. *Development* **120**: 1213–1220.
- Houston, D. W., M. Kofron, E. Resnik, et al. (2002). Repression of organizer genes in dorsal and ventral *Xenopus* cells mediated by maternal XTcf3. *Development* **129**(17): 4015–4025.
- Huang, X., J. C. McGann, B. Y. Liu, et al. (2013). Phosphorylation of Dishevelled by protein kinase RIPK4 regulates Wnt signaling. *Science* **339**(6126): 1441–1445.
- Ishibashi, H., N. Matsumura, H. Hanafusa, K. Matsumoto, E. M. De Robertis, H. Kuroda (2008). Expression of Siamois and Twin in the blastula Chordin/Noggin signaling center is required for brain formation in *Xenopus laevis* embryos. *Mechanisms of development* **125**(1–2): 58–66.
- Ishitani, T., S. Kishida, J. Hyodo-Miura, et al. (2003). The TAK1-NLK mitogen-activated protein kinase cascade functions in the Wnt-5a/Ca(2+) pathway to antagonize Wnt/beta-catenin signaling. *Molecular and cellular biology* **23**(1): 131–139.
- Itasaki, N., C. M. Jones, S. Mercurio, A. Rowe, P. M. Domingos, J. C. Smith, R. Krumlauf (2003). Wise, a context-dependent activator and inhibitor of Wnt signalling. *Development* **130**(18): 4295–4305.
- Janda, C. Y., D. Waghray, A. M. Levin, C. Thomas, K. C. Garcia (2012). Structural basis of Wnt recognition by Frizzled. *Science* **337**(6090): 59–64.
- Jung, B., A. Kohler, A. Schambony, D. Wedlich (2011). PAPC and the Wnt5a/Ror2 pathway control the invagination of the otic placode in *Xenopus*. *BMC developmental biology* **11**: 36.
- Katanaev, V. L., R. Ponzelli, M. Semeriva, A. Tomilinson (2005). Trimeric G protein-dependent frizzled signaling in *Drosophila*. *Cell* **120**: 111–122.
- Kazanskaya, O., A. Glinka, I. del Barco Barrantes, P. Stanek, C. Niehrs, W. Wu (2004). R-Spondin2 is a secreted activator of Wnt/beta-catenin signaling and is required for *Xenopus* myogenesis. *Developmental cell* **7**(4): 525–534.
- Kazanskaya, O., B. Ohkawara, M. Heroult, et al. (2008). The Wnt signaling regulator R-spondin 3 promotes angioblast and vascular development. *Development* **135**(22): 3655–3664.
- Keller, R., J. Shih, A. Sater (1992). The cellular basis of the convergence and extension of the *Xenopus* neural plate. *Developmental dynamics: an official publication of the American Association of Anatomists* **193**(3): 199–217.
- Kim, G. H., J. H. Her, J. K. Han (2008). Ryk cooperates with Frizzled 7 to promote Wnt11-mediated endocytosis and is essential for *Xenopus laevis* convergent extension movements. *Journal of cell biology* **182**(6): 1073–1082.
- Kim, W. T., H. Kim, V. L. Katanaev, et al. (2012). Dual functions of DP1 promote biphasic Wnt-on and Wnt-off states during anteroposterior neural patterning. *EMBO journal* **31**(16): 3384–3397.
- Kinoshita, N., H. Iioka, A. Miyakoshi, N. Ueno (2003). PKCδ is essential for Dishevelled function in a noncanonical Wnt pathway that regulates *Xenopus* convergent extension movements. *Genes & development* **17**: 1663–1676.
- Kodjabachian, L. and P. Lemaire (2001). Siamois functions in the early blastula to induce Spemann's organizer. *Mechanisms of development* **108**(1–2): 71–79.
- Kofron, M., T. Deel, J. Xanthos, et al. (1999). "Mesoderm induction in *Xenopus* is a zygotic event regulated by maternal VegT via TGFβ growth factors." *Development* **126**: 5759–5770.
- Kofron, M., P. Klein, F. Zhang, et al. (2001). "The role of maternal axin in patterning the *Xenopus* embryo." *Developmental biology* **237**(1): 183–201.
- Kofron, M., B. Birsoy, D. Houston, Q. Tao, C. Wylie, J. Heasman (2007). Wnt11/beta-catenin signaling in both oocytes and early embryos acts through LRP6-mediated regulation of axin. *Development* **134**(3): 503–513.
- Kraft, B., C. D. Berger, V. Wallkamm, H. Steinbeisser, D. Wedlich (2012). Wnt-11 and Fz7 reduce cell adhesion in convergent extension by sequestration of PAPC and C-cadherin. *The journal of cell biology* **198**(4): 695–709.
- Ku, M. and D. A. Melton (1993). Xwnt-11: a maternally expressed *Xenopus* wnt gene. *Development* **119**(4): 1161–1173.
- Lake, B. B. and K. R. Kao (2003). Pygopus is required for embryonic brain patterning in *Xenopus*. *Developmental biology* **261**(1): 132–148.
- Landesman, Y., D. A. Goodenough, D. L. Paul (2002). Xwnt-2 (Xwnt-2b) is maternally expressed in *Xenopus* oocytes and embryos. *Biochimica et biophysica acta* **1576**(3): 265–268.
- Lapebie, P., C. Borchiellini, E. Houliston (2011). Dissecting the PCP pathway: one or more pathways?: Does a separate Wnt-Fz-Rho pathway drive morphogenesis? *BioEssays* **33**(10): 759–768.
- Larabell, C. A., M. Torres, B. A. Rowning, et al. (1997). Establishment of the dorso-ventral axis in *Xenopus* embryos is presaged by early asymmetries in beta-catenin that are modulated by the Wnt signaling pathway. *Journal of cell biology* **136**(5): 1123–1136.
- Laurent, M. N., I. L. Blitz, C. Hashimoto, U. Rothbacher, K. W. Cho (1997). The *Xenopus*

- homeobox gene twin mediates Wnt induction of gooseoid in establishment of Spemann's organizer. *Development* **124**(23): 4905–4916.
- Lavery, D. L., I. R. Davenport, Y. D. Turnbull, G. N. Wheeler, S. Hoppler (2008a). Wnt6 expression in epidermis and epithelial tissues during *Xenopus* organogenesis. *Developmental dynamics: an official publication of the American Association of Anatomists* **237**(3): 768–779.
- Lavery, D. L., J. Martin, Y. D. Turnbull, S. Hoppler (2008b). Wnt6 signaling regulates heart muscle development during organogenesis. *Developmental biology* **323**(2): 177–188.
- Lemaire, P. and J. B. Gurdon (1994). "A role for cytoplasmic determinants in mesoderm patterning: cell- autonomous activation of the gooseoid and Xwnt-8 genes along the dorsoventral axis of early *Xenopus* embryos." *Development* **120**(5): 1191–1199.
- Lemaire, P., N. Garrett, J. B. Gurdon (1995). Expression cloning of Siamois, a *Xenopus* homeobox gene expressed in dorsal-vegetal cells of blastulae and able to induce a complete secondary axis. *Cell* **81**(1): 85–94.
- Li, Y., S. A. Rankin, D. Sinner, A. P. Kenny, P. A. Krieg, A. M. Zorn (2008). Sfrp5 coordinates foregut specification and morphogenesis by antagonizing both canonical and noncanonical Wnt11 signaling. *Genes & development* **22**(21): 3050–3063.
- Liao, G., Q. Tao, M. Kofron, et al. (2006). Jun NH2-terminal kinase (JNK) prevents nuclear beta-catenin accumulation and regulates axis formation in *Xenopus* embryos. *Proceedings of the National Academy of Sciences of the United States of America* **103**(44): 16313–16318.
- Lim, B. K., S. J. Cho, G. Sumbre, M. M. Poo (2010). Region-specific contribution of ephrin-B and Wnt signaling to receptive field plasticity in developing optic tectum. *Neuron* **65**(6): 899–911.
- Lin, G. and J. M. Slack (2008). Requirement for Wnt and FGF signaling in *Xenopus* tadpole tail regeneration. *Developmental biology* **316**(2): 323–335.
- Liu, F., O. van den Broek, O. Destree, S. Hoppler (2005a). Distinct roles for *Xenopus* Tcf/Lef genes in mediating specific responses to Wnt/beta-catenin signalling in mesoderm development. *Development* **132**(24): 5375–5385.
- Liu, X., J. S. Rubin, A. R. Kimmel (2005b). Rapid, Wnt-Induced changes in GSK3beta associations that regulate beta-catenin stabilization are mediated by Galpha proteins. *Current biology* **15**: 1989–1997.
- Lu, W., V. Yamamoto, B. Ortega, D. Baltimore (2004). Mammalian Ryk is a Wnt coreceptor required for stimulation of neurite outgrowth. *Cell* **119**(1): 97–108.
- Lustig, K. D., K. Kroll, E. Sun, R. Ramos, H. Elmendorf, M. W. Kirschner (1996). A *Xenopus* nodal-related gene that acts in synergy with noggin to induce complete secondary axis and notochord formation. *Development* **122**(10): 3275–3282.
- Lyons, J. P., R. K. Miller, X. Zhou, et al. (2009). Requirement of Wnt/beta-catenin signaling in pronephric kidney development. *Mechanisms of development* **126**(3–4): 142–159.
- MacDonald, B. T. and X. He (2012). Frizzled and LRP5/6 receptors for Wnt/beta-catenin signaling. *Cold Spring Harbor perspectives in biology* **4**(12): a007880.
- Major, M. B., N. D. Camp, J. D. Berndt, et al. (2007). Wilms tumor suppressor WTX negatively regulates WNT/beta-catenin signaling. *Science* **316**(5827): 1043–1046.
- Mao, B. and C. Niehrs (2003). Kremen2 modulates Dickkopf2 activity during Wnt/LRP6 signaling. *Gene* **302**(1–2): 179–183.
- Martin, J., B. A. Afouda, S. Hoppler (2010). Wnt/beta-catenin signalling regulates cardiomyogenesis via GATA transcription factors. *Journal of anatomy* **216**(1): 92–107.
- Matthews, H. K., F. Broders-Bondon, J. P. Thiery, R. Mayor (2008). Wnt11r is required for cranial neural crest migration. *Developmental dynamics: an official publication of the American Association of Anatomists* **237**(11): 3404–3409.
- Maurus, D., C. Heligon, A. Burger-Schwarzler, A. W. Brandli, M. Kuhl M (2005). Noncanonical Wnt-4 signaling and EAF2 are required for eye development in *Xenopus laevis*. *EMBO journal* **24**(6): 1181–1191.
- McCoy, K. E., X. Zhou, P. D. Vize (2011). Non-canonical wnt signals antagonize and canonical wnt signals promote cell proliferation in early kidney development. *Developmental dynamics: an official publication of the American Association of Anatomists* **240**(6): 1558–1566.
- McGrew, L. L., S. Hoppler, R. T. Moon (1997). Wnt and FGF pathways cooperatively pattern antero-posterior neural ectoderm in *Xenopus*. *Mechanisms of development* **69**(1–2): 105–114.
- McLin, V. A., S. A. Rankin, A. M. Zorn (2007). Repression of Wnt/beta-catenin signaling in the anterior endoderm is essential for liver and pancreas development. *Development* **134**(12): 2207–2217.
- Medina, A., W. Reintsch, H. Steinbeisser (2000). *Xenopus* frizzled 7 can act in canonical and non-canonical Wnt signaling pathways: implications on early patterning and morphogenesis. *Mechanisms of development* **92**: 227–237.
- Medina, A., R. K. Swain, K. M. Kuerner, H. Steinbeisser (2004). *Xenopus* paraxial protocad-

- herin has signaling functions and is involved in tissue separation. *EMBO journal* **23**(16): 3249–3258.
- Michiue, T., A. Fukui, A. Yukita, et al. (2004). XIdax, an inhibitor of the canonical Wnt pathway, is required for anterior neural structure formation in *Xenopus*. *Developmental dynamics: an official publication of the American Association of Anatomists* **230**(1): 79–90.
- Mikels, A. J. and R. Nusse (2006). Purified Wnt5a protein activates or inhibits b-Catenin–TCF Signaling depending on receptor context. *PLoS biology* **4**: 0570–0582.
- Miller, J. R., B. A. Rowning, C. A. Larabell, J. A. Yang-Snyder, R. L. Bates, R. T. Moon (1999). Establishment of the dorsal-ventral axis in *Xenopus* embryos coincides with the dorsal enrichment of dishevelled that is dependent on cortical rotation. *The journal of cell biology* **146**(2): 427–437.
- Miller, R. K., S. G. Canny, C. W. Jang, et al. (2011). Pronephric tubulogenesis requires Daam1-mediated planar cell polarity signaling. *Journal of the American Society of Nephrology: JASN* **22**(9): 1654–1664.
- Molenaar, M., M. van de Wetering, M. Oosterwegel, et al. (1996). XTcf-3 transcription factor mediates β -catenin-induced axis formation in *Xenopus* embryos. *Cell* **86**: 391–399.
- Montross, W. T., H. Ji, P. D. McCrea (2000). A beta-catenin/engrailed chimera selectively suppresses Wnt signaling. *Journal of cell science* **113** (Pt 10): 1759–1770.
- Moon, R. T., R. M. Campbell, J. L. Christian, L. L. McGrew, J. Shih, S. Fraser (1993). Xwnt-5A: a maternal Wnt that affects morphogenetic movements after overexpression in embryos of *Xenopus laevis*. *Development* **119**(1): 97–111.
- Mullor, J. L., N. Dahmane, T. Sun, A. Ruiz i Altaba (2001). Wnt signals are targets and mediators of Gli function. *Current biology: CB* **11**(10): 769–773.
- Naylor, R. W. and E. A. Jones (2009). Notch activates Wnt-4 signalling to control medio-lateral patterning of the pronephros. *Development* **136**(21): 3585–3595.
- Niehrs, C. (2012). The complex world of WNT receptor signalling. *Nature reviews. Molecular cell biology* **13**(12): 767–779.
- Nieuwkoop, P. D. (1969). The formation of mesoderm in Urodelean amphibians. I. Induction by the endoderm. *Wilhelm Roux' Archiv fur Entwicklungsmechanik der Organismen* **162**: 341–373.
- Ossipova, O., S. Dhawan, S. Sokol, J. B. Green (2005). Distinct PAR-1 proteins function in different branches of Wnt signaling during vertebrate development. *Developmental cell* **8**(6): 829–841.
- Ossipova, O. and S. Y. Sokol (2011). Neural crest specification by noncanonical Wnt signaling and PAR-1. *Development* **138**(24): 5441–5450.
- Pandur, P., M. Lasche, L. M. Eisenberg, M. Kuhl (2002). Wnt-11 activation of a non-canonical Wnt signalling pathway is required for cardiogenesis. *Nature* **418**(6898): 636–641.
- Park, M. and R. T. Moon (2002). “The planar cell-polarity gene *sbm* regulates cell behaviour and cell fate in vertebrate embryos.” *Nature cell biology* **4**(1): 20–25.
- Park, B. Y. and J. P. Saint-Jeannet (2008). Hindbrain-derived Wnt and Fgf signals cooperate to specify the otic placode in *Xenopus*. *Developmental biology* **324**(1): 108–121.
- Pera, E. M. and E. M. De Robertis (2000). A direct screen for secreted proteins in *Xenopus* embryos identifies distinct activities for the Wnt antagonists Crescent and Frzb-1. *Mechanisms of development* **96**(2): 183–195.
- Peters, J. M., R. M. McKay, J. P. McKay, J. M. Graff (1999). Casein kinase I transduces Wnt signals. *Nature* **401**(6751): 345–350.
- Pfister, A. S., M. V. Hadjihannas, W. Rohrig, A. Schambony, J. Behrens (2012). Amer2 protein interacts with EB1 protein and adenomatous polyposis coli (APC) and controls microtubule stability and cell migration. *The Journal of biological chemistry* **287**(42): 35333–35340.
- Pierce, S. B. and D. Kimelman (1995). Regulation of Spemann organizer formation by the intracellular kinase Xgsk-3. *Development* **121**(3): 755–765.
- Pilcher, K. E. and P. A. Krieg (2002). Expression of the Wnt inhibitor, sFRP5, in the gut endoderm of *Xenopus*. *Gene expression patterns: GEP* **2**(3–4): 369–372.
- Rana, A. A., C. Collart, M. J. Gilchrist, J. C. Smith (2006). Defining synphenotype groups in *Xenopus tropicalis* by use of antisense morpholino oligonucleotides. *PLoS genetics* **2**(11): e193.
- Roel, G., F. S. Hamilton, Y. Gent, A. A. Bain, O. Destree, S. Hoppler (2002). Lef-1 and Tcf-3 transcription factors mediate tissue e-specific Wnt signaling during *Xenopus* development. *Current biology: CB* **12**(22): 1941–1945.
- Rohani, N., L. Canty, O. Luu, F. Fagotto, R. Winklbauer (2011). EphrinB/EphB signaling controls embryonic germ layer separation by contact-induced cell detachment. *PLoS Biology* **9**(3): e1000597.
- Rowning, B. A., J. Wells, M. Wu, J. C. Gerhart, R. T. Moon, C. A. Larabell (1997). Microtubule-mediated transport of organelles and localization of beta-catenin to the future dorsal side of *Xenopus* eggs. *Proceedings of the National Academy of Sciences of the United States of America* **94**(4): 1224–1229.

- Salic, A. N., K. L. Kroll, L. M. Evans, M. W. Kirschner (1997). Sizzled: a secreted Xwnt8 antagonist expressed in the ventral marginal zone of *Xenopus* embryos. *Development* **124**(23): 4739–4748.
- Saulnier, D. M., H. Ghanbari, A. W. Brandli (2002). Essential function of Wnt-4 for tubulogenesis in the *Xenopus* pronephric kidney. *Developmental biology* **248**(1): 13–28.
- Schambony, A. and D. Wedlich (2007). Wnt-5A/Ror2 regulate expression of XPAPC through an alternative noncanonical signaling pathway. *Developmental cell* **12**(5): 779–792.
- Scharf, S. R. and J. C. Gerhart (1980). Determination of the dorsal-ventral axis in eggs of *Xenopus laevis*: complete rescue of uv-impaired eggs by oblique orientation before first cleavage. *Developmental biology* **79**(1): 181–198.
- Scharf, S. R., B. Rowning, M. Wu, J. C. Gerhart (1989). Hyperdorsoanterior embryos from *Xenopus* eggs treated with D2O. *Developmental biology* **134**(1): 175–188.
- Schneider, S., H. Steinbeisser, R. M. Warga, P. Hausen (1996). “ β -catenin translocation into nuclei demarcates the dorsalizing centers in frog and fish embryos.” *Mechanisms of Development* **57**: 191–198.
- Schneider, P. N., D. C. Slusarski, D. W. Houston (2012). Differential role of Axin RGS domain function in Wnt signaling during anteroposterior patterning and maternal axis formation. *PloS one* **7**(9): e44096.
- Schohl, A. and F. Fagotto (2002). Beta-catenin, MAPK and Smad signaling during early *Xenopus* development. *Development* **129**: 37–52.
- Schohl, A. and F. Fagotto (2003). A role for maternal beta-catenin in early mesoderm induction in *Xenopus*. *EMBO journal* **22**(13): 3303–3313.
- Schroeder, K. E., M. L. Condic, L. M. Eisenberg, H. J. Yost (1999). Spatially regulated translation in embryos: asymmetric expression of maternal Wnt-11 along the dorsal-ventral axis in *Xenopus*. *Developmental biology* **214**(2): 288–297.
- Sheldahl, L. C., D. C. Slusarski, P. Pandur, J. R. Miller, M. Kuhl, R. T. Moon (2003). Dishevelled activates Ca²⁺ flux, PKC, and CamKII in vertebrate embryos. *The journal of cell biology* **161**(4): 769–777.
- Shibata, M., M. Itoh, H. Hikasa, S. Taira, M. Taira (2005). Role of crescent in convergent extension movements by modulating Wnt signaling in early *Xenopus* embryogenesis. *Mechanisms of development* **122**(12): 1322–1339.
- Shimomura, Y., D. Agalliu, A. Vonica, et al. (2010). APCDD1 is a novel Wnt inhibitor mutated in hereditary hypotrichosis simplex. *Nature* **464**(7291): 1043–1047.
- Slusarski, D. C., V. G. Corces, R. T. Moon (1997a). Interaction of Wnt and a Frizzled homologue triggers G-protein-linked phosphatidylinositol signalling. *Nature* **390**(6658): 410–413.
- Slusarski, D. C., J. Yang-Snyder, W. B. Blusa, R. T. Moon (1997b). Modulation of embryonic intracellular Ca²⁺ signaling by Wnt-5A. *Developmental biology* **182**(1): 114–120.
- Smith, W. C. and R. M. Harland (1991). Injected Xwnt-8 RNA acts early in *Xenopus* embryos to promote formation of a vegetal dorsalizing center. *Cell* **67**(4): 753–765.
- Sokol, S. Y. (1996). Analysis of Dishevelled signaling pathways during *Xenopus* development. *Current biology* **6**(11): 1456–1467.
- Standley, H. J., O. Destree, M. Kofron, C. Wylie, J. Heasman (2006). Maternal XTcf1 and XTcf4 have distinct roles in regulating Wnt target genes. *Developmental biology* **289**(2): 318–328.
- Stathopoulos, A. and M. Levine (2002). Dorsal gradient networks in the *Drosophila* embryo. *Developmental biology* **246**(1): 57–67.
- Stemmler, L. N., T. A. Fields, P. J. Casey (2006). The regulator of G protein signaling domain of Axin selectively interacts with G α 12 but not G α 13. *Molecular pharmacology* **70**: 1461–1468.
- Steventon, B., C. Araya, C. Linker, S. Kuriyama, R. Mayor (2009). Differential requirements of BMP and Wnt signalling during gastrulation and neurulation define two steps in neural crest induction. *Development* **136**(5): 771–779.
- Stuhlmiller, T. J. and M. I. Garcia-Castro (2012). Current perspectives of the signaling pathways directing neural crest induction. *Cellular and molecular life sciences: CMLS* **69**(22): 3715–3737.
- Sumanas, S., P. Strege, J. Heasman, S. C. Ekker (2000). The putative wnt receptor *Xenopus* frizzled-7 functions upstream of beta-catenin in vertebrate dorsoventral mesoderm patterning. *Development* **127**(9): 1981–1990.
- Tada, M. and J. C. Smith (2000). Xwnt11 is a target of *Xenopus* Brachyury: regulation of gastrulation movements via Dishevelled, but not through the canonical Wnt pathway. *Development* **127**(10): 2227–2238.
- Tadjudje, E., S. W. Cha, M. Louza, C. Wylie, J. Heasman (2011). The functions of maternal Dishevelled 2 and 3 in the early *Xenopus* embryo. *Developmental dynamics: an official publication of the American Association of Anatomists* **240**(7): 1727–1736.
- Tahinci, E., C. A. Thorne, J. L. Franklin, et al. (2007). Lrp6 is required for convergent extension during *Xenopus* gastrulation. *Development* **134**(22): 4095–4106.

- Takeuchi, M., J. Nakabayashi, T. Sakaguchi, et al. (2003). The prickle-related gene in vertebrates is essential for gastrulation cell movements. *Current biology*: CB **13**(8): 674–679.
- Tanegashima, K., H. Zhao, I. B. Dawid (2008). WGEF activates Rho in the Wnt-PCP pathway and controls convergent extension in *Xenopus* gastrulation. *EMBO journal* **27**(4): 606–617.
- Tannahill, D., H. V. Isaacs, M. J. Close, G. Peters, J. M. Slack (1992). Developmental expression of the *Xenopus* int-2 (FGF-3) gene: activation by mesodermal and neural induction. *Development* **115**: 695–702.
- Tao, Q., C. Yokota, H. Puck, et al. (2005). Maternal Wnt11 activates the canonical Wnt signaling pathway required for axis formation in *Xenopus* embryos. *Cell* **120**: 857–871.
- Tetelin, S. and E. A. Jones (2010). *Xenopus* Wnt11b is identified as a potential pronephric inducer. *Developmental dynamics: an official publication of the American Association of Anatomists* **239**(1): 148–159.
- Theveneau, E. and R. Mayor (2012). Neural crest delamination and migration: from epithelium-to-mesenchyme transition to collective cell migration. *Developmental biology* **366**(1): 34–54.
- Torres, M. A., J. A. Yang-Snyder, S. M. Purcell, A. A. DeMarais, L. L. McGrew, R. T. Moon (1996). Activities of the Wnt-1 class of secreted signaling factors are antagonized by the Wnt-5A class and by a dominant negative cadherin in early *Xenopus* development. *Journal of cell biology* **133**(5): 1123–1137.
- Tran, H. T., B. Sekkali, G. Van Imschoot, S. Janssens, K. Vleminckx (2010). Wnt/beta-catenin signaling is involved in the induction and maintenance of primitive hematopoiesis in the vertebrate embryo. *Proceedings of the National Academy of Sciences of the United States of America* **107**(37): 16160–16165.
- Tsai, I. C., J. D. Amack, Z. H. Gao, V. Band, H. J. Yost, D. M. Virshup (2007). A Wnt-CKI ν arepsilon-Rap1 pathway regulates gastrulation by modulating SIPA1L1, a Rap GTPase activating protein. *Developmental cell* **12**(3): 335–347.
- Ulloa, F. and E. Marti (2010). Wnt won the war: antagonistic role of Wnt over Shh controls dorsoventral patterning of the vertebrate neural tube. *Developmental dynamics: an official publication of the American Association of Anatomists* **239**(1): 69–76.
- van Amerongen, R. and R. Nusse (2009). Towards an integrated view of Wnt signaling in development. *Development* **136**(19): 3205–3214.
- Van Raay, T. J., K. B. Moore, I. Iordanova, et al. (2005). Frizzled 5 signaling governs the neural potential of progenitors in the developing *Xenopus* retina. *Neuron* **46**(1): 23–36.
- Veeman, M. T., J. D. Axelrod, R. T. Moon (2003). A second canon: functions and mechanisms of beta-Catenin-independent Wnt signaling. *Developmental cell* **5**: 367–377.
- Vonica, A. and B. M. Gumbiner (2002). Zygotic Wnt activity is required for Brachyury expression in the early *Xenopus laevis* embryo. *Developmental biology* **250**(1): 112–127.
- Wallingford, J. B. (2012). Planar cell polarity and the developmental control of cell behavior in vertebrate embryos. *Annual review of cell and developmental biology* **28**: 627–653.
- Wallingford, J. B. and R. M. Harland (2001). *Xenopus* Dishevelled signaling regulates both neural and mesodermal convergent extension: parallel forces elongating the body axis. *Development* **128**(13): 2581–2592.
- Wallingford, J. B., B. A. Rowning, K. M. Vogeli, U. Rothbacher, S. E. Frasser, R. M. Harland (2000). Dishevelled controls cell polarity during *Xenopus* gastrulation. *Nature* **405**(6782): 81–85.
- Wan, X., W. Ji, X. Mei, et al. (2010). Negative feedback regulation of Wnt4 signaling by EAF1 and EAF2/U19. *PloS one* **5**(2): e9118.
- Wang, S., M. Krinks, M. Moos, Jr. (1997). Frzb-1, an antagonist of Wnt-1 and Wnt-8, does not block signaling by Wnts -3A, -5A, or -11. *Biochemical and Biophysical Research Communications* **236**(2): 502–504.
- Wardle, F. C. and J. C. Smith (2006). Transcriptional regulation of mesendoderm formation in *Xenopus*. *Seminars in cell & developmental biology* **17**(1): 99–109.
- Weaver, C., G. H. Farr, 3rd, W. Pan, et al. (2003). GBP binds kinesin light chain and translocates during cortical rotation in *Xenopus* eggs. *Development* **130**(22): 5425–5436.
- Wessely, O., E. Agius, M. Oelgeschlager, E. M. Pera, E. M. De Robertis (2001). Neural induction in the absence of mesoderm: beta-catenin-dependent expression of secreted BMP antagonists at the blastula stage in *Xenopus*. *Developmental biology* **234**(1): 161–173.
- Winklbauer, R. (2009). Cell adhesion in amphibian gastrulation. *International review of cell and molecular biology* **278**: 215–275.
- Winklbauer, R. and O. Luu (2008). Frizzled-7-dependent tissue separation in the *Xenopus* gastrula. *Methods in molecular biology* **469**: 485–492.
- Winklbauer, R., A. Medina, R. K. Swain, H. Steinbeisser (2001). Frizzled-7 signalling controls tissue separation during *Xenopus* gastrulation. *Nature* **413**(6858): 856–860.

- Wolda, S. L., C. J. Moody, R. T. Moon (1993). Overlapping expression of Xwnt-3A and Xwnt-1 in neural tissue of *Xenopus laevis* embryos. *Developmental biology* **155**(1): 46–57.
- Wu, J., J. Yang, P. S. Klein (2005). Neural crest induction by the canonical Wnt pathway can be dissociated from anterior-posterior neural patterning in *Xenopus*. *Developmental biology* **279**(1): 220–232.
- Wu, X., X. Tu, K. S. Joeng, M. J. Hilton, D. A. Williams, F. Long (2008). Rac1 activation controls nuclear localization of beta-catenin during canonical Wnt signaling. *Cell* **133**(2): 340–353.
- Wylie, C., M. Kofron, C. Payne, et al. (1996). Maternal beta-catenin establishes a 'dorsal signal' in early *Xenopus* embryos. *Development* **122**(10): 2987–2996.
- Yamaguchi, T. P., S. Takada, Y. Yoshikawa, N. Wu, A. P. McMahon (1999). T (Brachyury) is a direct target of Wnt3a during paraxial mesoderm specification. *Genes & development* **13**(24): 3185–3190.
- Yamanaka, H., T. Moriguchi, N. Masuyama, et al. (2002). JNK functions in the non-canonical Wnt pathway to regulate convergent extension movements in vertebrates. *EMBO reports* **3**(1): 69–75.
- Yanfeng, W., J. P. Saint-Jeannet, P. S. Klein (2003). Wnt-frizzled signaling in the induction and differentiation of the neural crest. *BioEssays* **25**(4): 317–325.
- Yang, J., J. Wu, C. Tan, P. S. Klein (2003). PP2A:B56epsilon is required for Wnt/beta-catenin signaling during embryonic development. *Development* **130**(23): 5569–5578.
- Yao, J. and D. S. Kessler (2001). Goosecoid promotes head organizer activity by direct repression of Xwnt8 in Spemann's organizer. *Development* **128**(15): 2975–2987.
- Yasunaga, T., K. Itoh, S. Y. Sokol (2011). Regulation of basal body and ciliary functions by Diversin. *Mechanisms of development* **128**(7–10): 376–386.
- Yin, A., C. L. Winata, S. Korzh, V. Korzh, Z. Gong (2010). Expression of components of Wnt and Hedgehog pathways in different tissue layers during lung development in *Xenopus laevis*. *Gene expression patterns* **10**(7–8): 338–344.
- Yokota, C., M. Kofron, M. Zuck, et al. (2003). A novel role for a nodal-related protein; Xnr3 regulates convergent extension movements via the FGF receptor. *Development* **130**(10): 2199–2212.
- Yost, C., M. Torres, J. R. Miller, E. Huang, D. Kimelman, R. T. Moon (1996). "The axis-inducing activity, stability, and subcellular distribution of beta-catenin is regulated in *Xenopus* embryos by glycogen synthase kinase 3." *Genes & development* **10**(12): 1443–1454.
- Yost, C., G. H. Farr, 3rd, S. B. Pierce, D. M. Ferkey, M. M. Chen, D. Kimelman (1998). GBP, an inhibitor of GSK-3, is implicated in *Xenopus* development and oncogenesis. *Cell* **93**(6): 1031–1041.
- Yuge, M., Y. Kobayakawa, M. Fujisue, K. Yamana (1990). A cytoplasmic determinant for dorsal axis formation in an early embryo of *Xenopus laevis*. *Development* **110**(4): 1051–1056.
- Zeng, L., F. Fagotto, T. Zhang, et al. (1997). The mouse Fused locus encodes Axin, an inhibitor of the Wnt signaling pathway that regulates embryonic axis formation. *Cell* **90**(1): 181–192.
- Zhang, J., D. W. Houston, M. L. King, C. Payne, C. Wylie, J. Heasman (1998). "The role of maternal VegT in establishing the primary germ layers in *Xenopus* embryos [see comments]." *Cell* **94**(4): 515–524.
- Zhang, Y., S. Y. Neo, X. Wang, J. Han, S. C. Lin (1999). "Axin forms a complex with MEKK1 and activates c-Jun NH(2)-terminal kinase/stress-activated protein kinase through domains distinct from Wnt signaling." *Journal of biological chemistry* **274**: 35247–35254.
- Zhang, Y., W.-J. Qiu, S. C. Chan, J. Han, X. He, S. C. Lin (2002). Casein Kinase I and Casein Kinase II differentially regulate Axin function in Wnt and JNK pathways. *Journal of Biological Chemistry* **277**: 17706–17712.
- Zhang, B., U. Tran, O. Wessely (2011). "Expression of Wnt signaling components during *Xenopus* pronephros development." *PloS one* **6**(10): e26533.
- Zhu, W., I. Shiojima, Y. Ito, et al. (2008). IGFBP-4 is an inhibitor of canonical Wnt signalling required for cardiogenesis. *Nature* **454**(7202): 345–349.
- Zorn, A. M. and J. M. Wells (2007). Molecular basis of vertebrate endoderm development. *International review of cytology* **259**: 49–111.

9

Neural Tube Closure in *Xenopus*

Hitoshi Morita*, Makoto Suzuki, & Naoto Ueno

National Institute for Basic Biology, Okazaki, Japan

*Present address: Institute of Science and Technology Austria
Klosterneuburg, Austria

Abstract: The neural tube is the primordium that gives rise to brain and spinal cord in the central nervous system and thus its morphogenesis is thought to be one of the most important developmental events. In *Xenopus laevis*, it has been shown that there are at least two independent mechanisms to achieve the tube formation from a sheet of the neuroepithelial cells. One is a cell autonomous process apical constriction, the cell morphogenesis that minimizes the apical surface of the neuroepithelial cells at the hinge points and facilitates bending of the cell sheet. The other is the external force of nonneural ectoderm generated by the migration of the deep epithelial cell layer together with the superficial layer toward the midline that assists the closure movement. In this review, molecular and cellular mechanisms for neural tube morphogenesis are discussed.

Introduction

The neural tube is the anlage of the central nervous system (CNS). It eventually forms the brain and spinal cord, after becoming patterned along its anterior–posterior and dorsal–ventral axes. As in other amniotes including humans, neural tube formation in *Xenopus* involves dynamic tissue remodeling from a sheet of neuroepithelium to a tube-like structure (Smith and Schoenwolf 1997). Elucidation of the molecular and cellular mechanisms underlying this critical process has long attracted developmental biologists. In addition, improper neural tube closure

is implicated in congenital malformations known as neural tube defects (NTDs) (Copp and Greene 2010), which occur in 1 in 1000–2000 live births. Therefore, understanding the morphogenesis of *Xenopus* neural tube closure may clarify the cellular pathogenesis of NTDs and thus have significant medical impact. Due to the ease with which the entire process can be observed in cultured *Xenopus* embryos (Wallingford 2010), studies using this animal have contributed great mechanistic insight into the cellular processes underlying neural tube formation.

The formation of the CNS begins with neural induction, which directs undifferentiated

ectoderm residing in the animal hemisphere that would otherwise give rise to epidermis to become neural tissue. Neural induction occurs during gastrulation by the influence of involuting dorsal mesoderm, from which so-called “neural inducers” are emanated (De Robertis and Kuroda 2004; see also Chapter 13 by William Munoz et al.). After neural induction, the epithelial cells become neuralized; in this process, the cells express a variety of neural-specific genes that cause them to follow the neural fate. Subsequently, along with the elongation of the embryo proper, the neural plate undergoes a dynamic morphogenetic process known as “convergence and extension” or “convergent extension”, which involves the concomitant lengthening and narrowing of the plate (Keller et al. 2008b). At the same time, two-folds of neural ectoderm arise parallel to the anterior–posterior axis at the border with

the nonneural ectoderm; these folds gradually approach the dorsal midline and eventually fuse to close the tube (Figure 9.1). For the neural plate to adopt a tube-like structure, it needs to bend (for neural plate bending in the mouse, see Ybot-Gonzalez and Copp 1999). Morphogenetic processes called “cell elongation” and “apical constriction”, in which cells undergo cell-body elongation and minimization of the apical surface, respectively, are known to trigger the bending of the plate (Suzuki et al. 2012). Therefore, for neural tube closure to be completed properly, a series of cellular events needs to occur in a spatiotemporally controlled manner.

In this chapter, we focus on this dynamic yet incompletely understood morphogenesis of the neural tube, highlighting what is currently known about the molecular and cellular mechanisms.

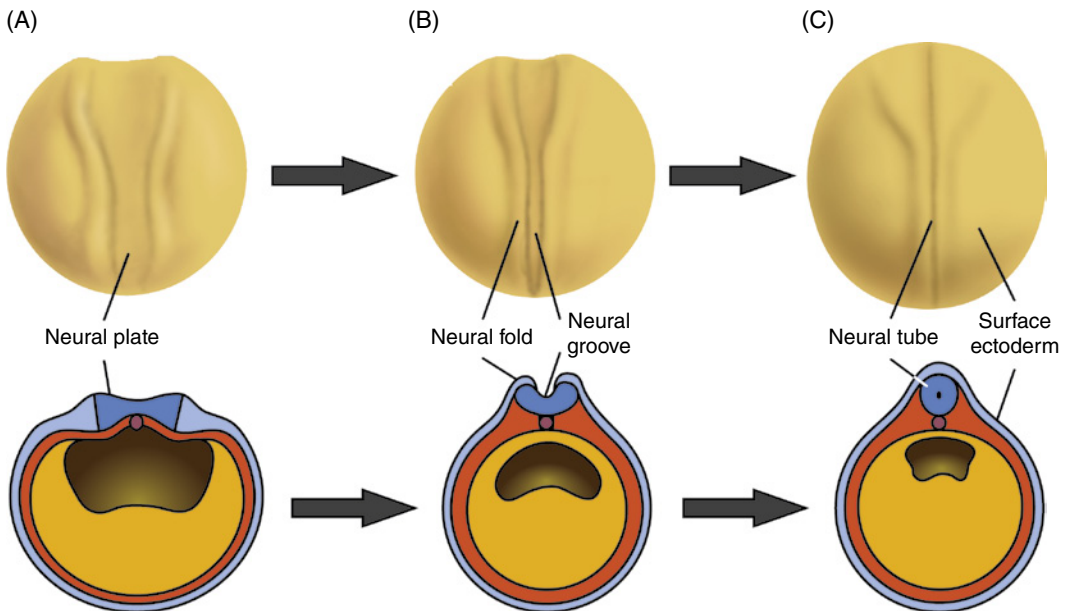


Figure 9.1 *Xenopus* neural tube formation. Dorsal views (Top) and transverse sections (Bottom) of generalized amphibian embryos in early (A), middle (B), and late (C) neurulae. (A) By the end of gastrulation, a flat neural plate (blue) is formed as a thickening of the ectoderm on the dorsal surface of the embryo. (B) The lateral borders of the neural plate rise to form the neural folds. As development proceeds, the neural folds continue to rise, and the neural plate bends to form the neural groove. (C) The edges of the neural folds eventually meet at the dorsal midline, where they fuse to form a hollow structure, the neural tube, positioned beneath the overlying surface ectoderm (light blue). To see a color version of this figure, see Plate 19.

Narrowing and elongation of the neural plate

During gastrulation, like the axial mesoderm, the posterior neural tissues including the presumptive hind brain and spinal cord undergo convergent extension cell movements consisting of mediolateral narrowing (convergence)

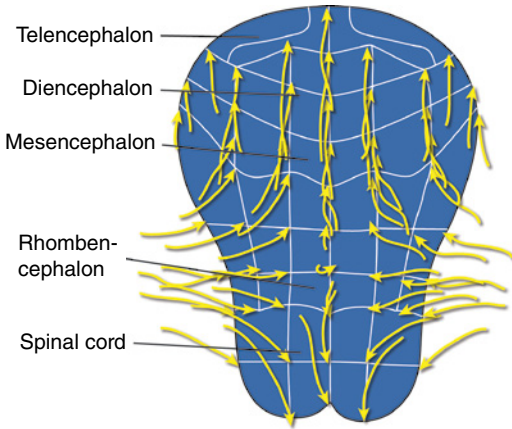


Figure 9.2 Conversion and extension in the neural plate. Cell movements of the neural plate recorded by time-lapse imaging of stage 11.5–15 *Xenopus* embryos and projected onto the fate map of the stage 15 neural plate (Eagleson and Harris 1990). Modified from Keller, R., Shih, J. and Sater, A. 1992. The cellular basis of the convergence and extension of the *Xenopus* neural plate. *Dev. Dyn.* 193:199–217.

and anteroposterior lengthening (extension) of the neural plate (Keller et al. 1992; Elul and Keller 2000) (Figures 9.2 and 9.3). This planar cell rearrangement within the neural plate is a prerequisite for neural tube closure. A failure in convergent extension in the neural plate results in incomplete neural tube closure, which results in NTDs, such as rachischisis and spina bifida in humans (Copp and Bernfield 1994). Similar phenotypes that may result from common cellular defects are recognized in other vertebrates, such as mouse and *Xenopus* (Ueno and Greene 2003; Wallingford 2005). In the following section, the cellular mechanism of convergent extension in the neural plate is discussed and compared with that of the axial mesoderm, which occurs in coordination with that in the neural plate.

Cell rearrangement during neural convergent extension

What cellular dynamics enables the rearrangement of cells in the neural plate? The *Xenopus* neural ectoderm consists of two cell layers: the superficial epithelial cells and the deep cells that underlie them and have a mesenchymal character. It is generally thought that the behavior of the neural deep cells plays a critical role in neural convergent extension.

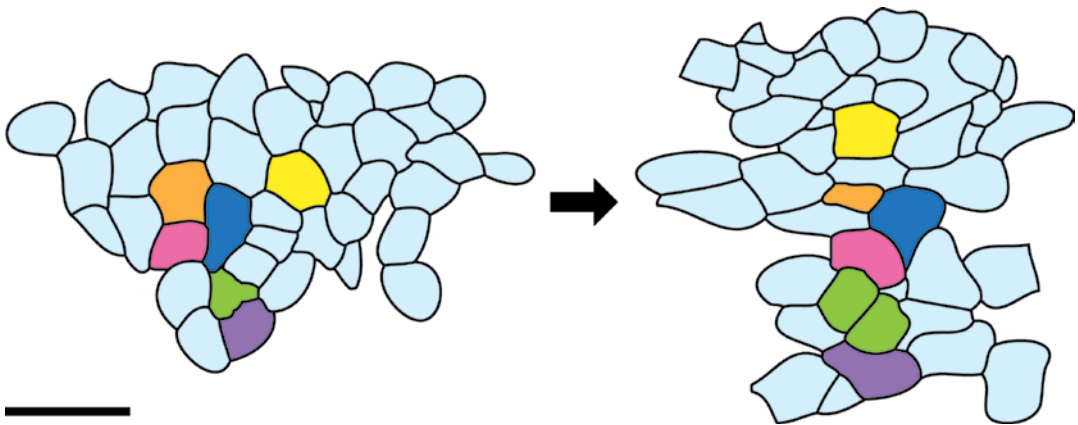


Figure 9.3 Cell rearrangement during convergent extension. Illustration based on video recordings showing that cell rearrangements occur as a result of mediolateral cell intercalation during convergent extension from stage 11.5 (left) to 17 (right). Modified from Elul, T. and Keller, R. 2000. Monopolar protrusive activity: a new morphogenic cell behavior in the neural plate dependent on vertical interactions with the mesoderm in *Xenopus*. *Dev. Biol.* 224:3–19. Scale bar indicate 40 μ m. To see a color version of this figure, see Plate 20.

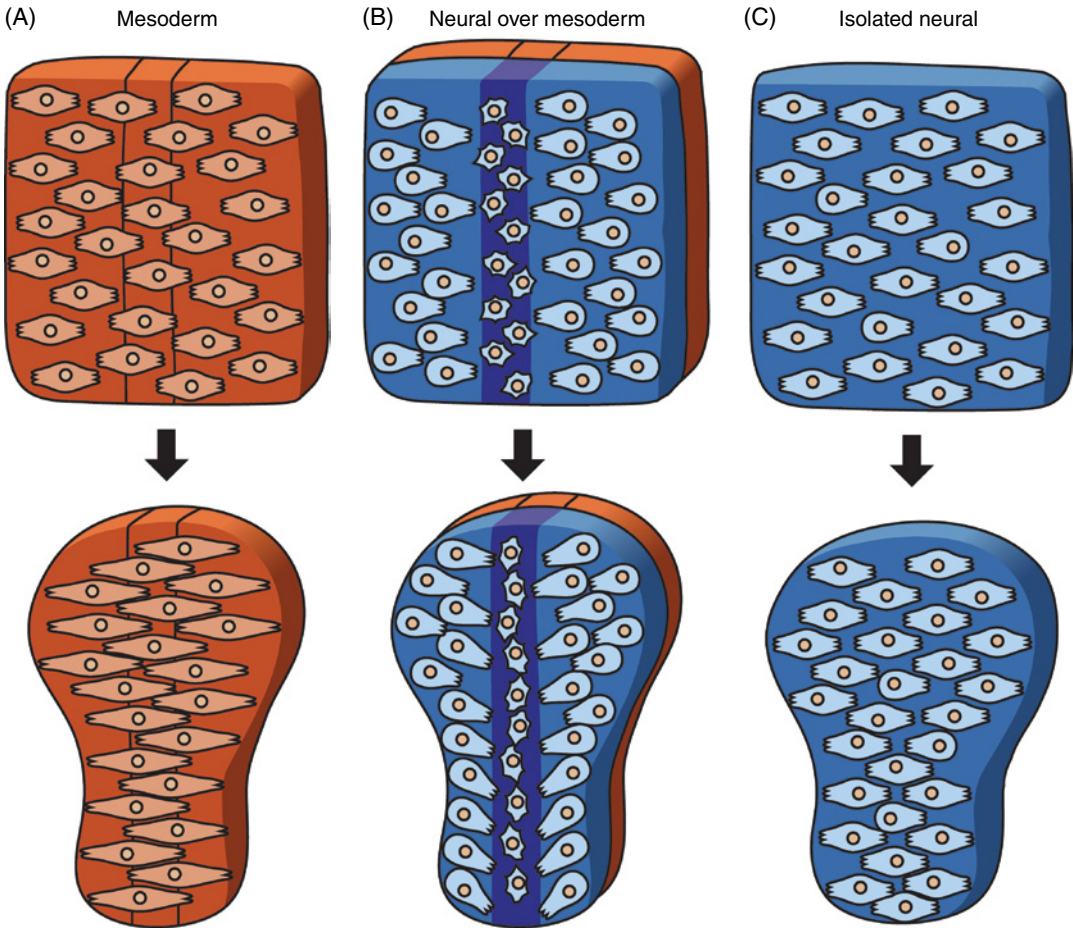


Figure 9.4 Convergent extension in mesoderm and neural explants. Cell morphology and polarity in isolated dorsal mesoderm (Shih and Keller, 1992) (A), neural-over-mesoderm (Elul and Keller, 2000) (B), and posterior neural ectoderm (Elul et al., 1997) explants (C). Red, mesoderm; blue, posterior neural tissue. In B, dark blue indicates the notoplate. Modified from Wallingford, J. B. and Harland, R. M. 2001. *Xenopus* Dishevelled signaling regulates both neural and mesodermal convergent extension: parallel forces elongating the body axis. *Development* 128:2581–2592. To see a color version of this figure, see Plate 21.

The tissue mechanics of the convergent extension cell movements is best understood in the dorsal mesoderm that forms the notochord (Domingo and Keller 1995; Wallingford et al. 2002). During gastrulation, these dorsal mesoderm cells display a spindle-like cell shape, suggesting that this change in cell morphology is critical for tissue remodeling. However, the neural deep cells do not undergo a similar cell-shape change and appear to contribute little to narrowing and elongation. In addition, time-lapse imaging of neural deep-cell explants showed that oriented cell division is not a major driving force for the

narrowing and elongation, as it is in the dorsal mesoderm; instead this force is created by mediolateral cell intercalation (Elul et al. 1997) (Figure 9.3).

The mediolaterally biased formation of lamellipodia, which are stable, mediolaterally oriented, bipolar protrusions seen in the mesoderm (Figure 9.4A), was proposed to supply the force for pulling the mesoderm cells toward each other (Brodland 2006), thereby narrowing the tissue (Figure 9.4A). However, the neural deep cells with the underlying mesoderm form protrusions only episodically, particularly in the lateral region (Figure 9.4B),

and these protrusions are medially oriented and monopolar, highlighting the tissue specificity of this mechanism. In fact, isolated neural cell explants lacking the apposed mesoderm autonomously converge mediolaterally and elongate anteroposteriorly (Elul et al. 1997) (Figure 9.4C), suggesting that signals in the neural deep cells are sufficient to promote convergent extension. Notably, neural cells in explants that lack mesoderm intercalate using bipolar, instead of monopolar, mediolaterally oriented lamellipodia (Elul et al. 1997), suggesting that the bipolar mode of intercalation represents a latent mechanism in the neural plate (Keller et al. 2000).

Role of the notoplate in establishing the mediolateral polarity

In the presence of mesoderm, the neural plate cells display two types of behavior: the cells lateral to the notoplate show monopolar, medially directed motility, whereas those in the medial region (notoplate) show randomly oriented motility (Figure 9.4B). What signals contribute to the behaviors of deep cells that cause this mediolateral patterning? Elul and Keller (2000) investigated the role of the mesoderm underlying the neural deep cells by comparing the cell behaviors in deep-cell explants that either included mesoderm or lacked it and found that the mesoderm plays a critical role in patterning the deep-cell behavior. In the presence of mesoderm, the neural deep cells exhibit medially oriented cell motility that is well correlated with medially biased cell protrusive activity and motility. In contrast, in the absence of underlying mesoderm, all the deep neural cells exhibit mediolateral cell motility, suggesting that the mesoderm underlying the neural deep cells not only induces neural genes in the neural plate but also confers the monopolarity that drives the medially oriented motility in the neural plate lateral to the notoplate. This mesodermal influence affects the cell intercalation and exchange of neighboring cells as seen in the neural cell-only explants, in which the medially oriented cell motility is compromised, resulting in inefficient convergent extension (Elul and Keller 2000).

These observations suggested that vertical signals from the notochord, which is the dorsal-most mesoderm, direct the notoplate, which resides above the notochord, to release soluble factors that guide neural plate cells to crawl medially. To test this possibility, Ezin et al. (2003) investigated the role of the dorsal structures (i.e., the notochord and notoplate), in the cell-movement patterning required for convergent extension of the neural plate. In the presence of dorsal mesoderm underlying the deep neural plate, the lateral neural plate cells displayed a monopolar, medially directed protrusive activity. In contrast, in the absence of the underlying dorsal mesoderm, neural plate explants showed a bipolar, mediolaterally directed protrusive activity. These explants were still in contact with somitic mesoderm underlying the neural plate, which apparently could not maintain the monopolar and medially biased protrusive activity. Importantly, these authors also demonstrated that placing ectopic midline cells in contact with the lateral edge of the explants restored the monopolar protrusive activity over the entire extent of these midline-less explants. Based on these observations, the authors postulated that two signals govern the cell behaviors in the neural plate: one causes cell polarization across the entire neural plate and the other orients the polarized cells toward the midline (Ezin et al. 2003). In other words, even though the neural plate adopts a unique mode of cell behavior in which the cell movement is monopolar and medially oriented as an additional level of regulation, a common mechanism for bipolarization underlies the convergent extension of two distinct tissues, the neural plate and the mesoderm.

Planar cell polarity signaling in neural tube closure

What molecular signals confer bipolarity throughout the neural plate? As in the dorsal mesoderm, planar cell polarity (PCP) signals are thought to be essential. As introduced in Chapter 8 by Fagotto, the noncanonical Wnt pathway plays a dominant role in establishing PCP in various tissues across species (Jones and Chen 2007). In this section, this pathway

will be referred to as the “Wnt/PCP pathway”. The requirement for the Wnt/PCP pathway in the convergent extension of dorsal mesoderm has been extensively studied, and in *Xenopus*, the disruption of this signaling pathway by knocking down its components causes broadening of the axial mesoderm and NTDs, including spina bifida (Wallingford 2012).

To examine whether Wnt/PCP also controls convergent extension in the neural plate, mutants of a Wnt/PCP signaling component, *Xenopus* Dishevelled (Xdsh), were expressed in neural tissues (Wallingford and Harland 2001). Xdsh- Δ PDZ/D2 (Xdsh-D2) (Wallingford et al. 2000) and Xdsh- Δ DEP (D6) (Rothbacher et al. 2000) are potent and selective inhibitors of the convergent extension in *Xenopus* mesoderm but do not inhibit canonical Wnt signaling, which mainly regulates cell differentiation through the nuclear translocation of β -catenin (MacDonald et al. 2009). When the mRNA of these inhibitors was injected into the dorsal animal blastomeres at the eight-cell stage or when an animal cap explant expressing Xdsh-D2 was grafted to stage 11.5 embryos from which the neural ectoderm was removed, most of the embryos manifested NTDs without affecting neural cell differentiation. The finding that inhibiting the Wnt/PCP pathway exclusively in the neural plate disrupts neural tube closure without bifurcation of the notochord suggests that Wnt/PCP signaling within the neural plate plays a critical role in its closure, independent of mesoderm convergent extension.

In addition, the Wnt/PCP pathway is required to achieve neural convergent extension as shown using Xdsh-D2 and another antagonist of the pathway, Xdd1 (Sokol 1996), in Keller sandwich explants (Wallingford et al. 2000; Sive et al. 2007). These findings demonstrated that the Wnt/PCP pathway mediated by Xdsh signaling controls the convergent extension in both the dorsal mesoderm and the posterior neural ectoderm of *Xenopus*. Consistent with this finding, several Wnt/PCP components were identified as causative genes for mouse mutants displaying NTDs (Juriloff and Harris 2012). Although the cellular pathogenesis for these mutant phenotypes have not been clarified, in the mouse, which has a single layer of neural plate cells, it

is suspected that polarity defects of the protrusive activity of the neural cells' basal side lead to improper morphogenesis of the neural tube. In fact, in *Xenopus*, Xdsh is known to be involved in controlling both the polarity and the stability of cell protrusions in the mesoderm (Wallingford et al. 2000). In addition, the Wnt/PCP pathway may be required for remodeling of the adherens junctions (AJs) of the neural cells of amniotes, as was recently shown in chick (Nishimura et al. 2012).

In summary, *Xenopus* appears to have co-opted the Wnt/PCP pathway to establish the PCP that confers bidirectional motility on the entire neural plate, in addition to the dorsal mesoderm, and other layers of regulation have been added to the neural plate to control the unidirectional (medial) motility.

Cell-shape changes causing neural tube morphogenesis

In addition to the neural deep cells, whose dynamic planar behavior in the narrowing and elongation of the neural plate was described in the previous section, the superficial neuroepithelial cells show a dramatic shape change during neural tube closure. Prior to neurulation, the neuroepithelial cells are cuboidal (Figure 9.5A). In the early neurula stage, the cells start to elongate along the apicobasal axis and become columnar (Schroeder 1970; Burnside 1971; Schoenwolf and Franks 1984) (Figure 9.5Ab). The volume of the neuroepithelial cells remains relatively constant, and the apical and basal surface areas decrease to a similar extent during this phase (Burnside 1973). The cell apices are then constricted and minimized, causing the columnar cells to adopt a wedge shape (Figure 9.5Ac). These movements are called cell elongation and apical constriction, respectively, and their coordinated actions generate the main physical force that causes the neural plate to bend (Glaser 1914; Karfunkel 1974) (Figure 9.5B). In *Xenopus*, cell elongation and apical constriction overlap considerably in time (Lee et al. 2007a), whereas in amniotes, the neuroepithelial cells elongate fully prior to apical constriction (Schoenwolf and Franks 1984).

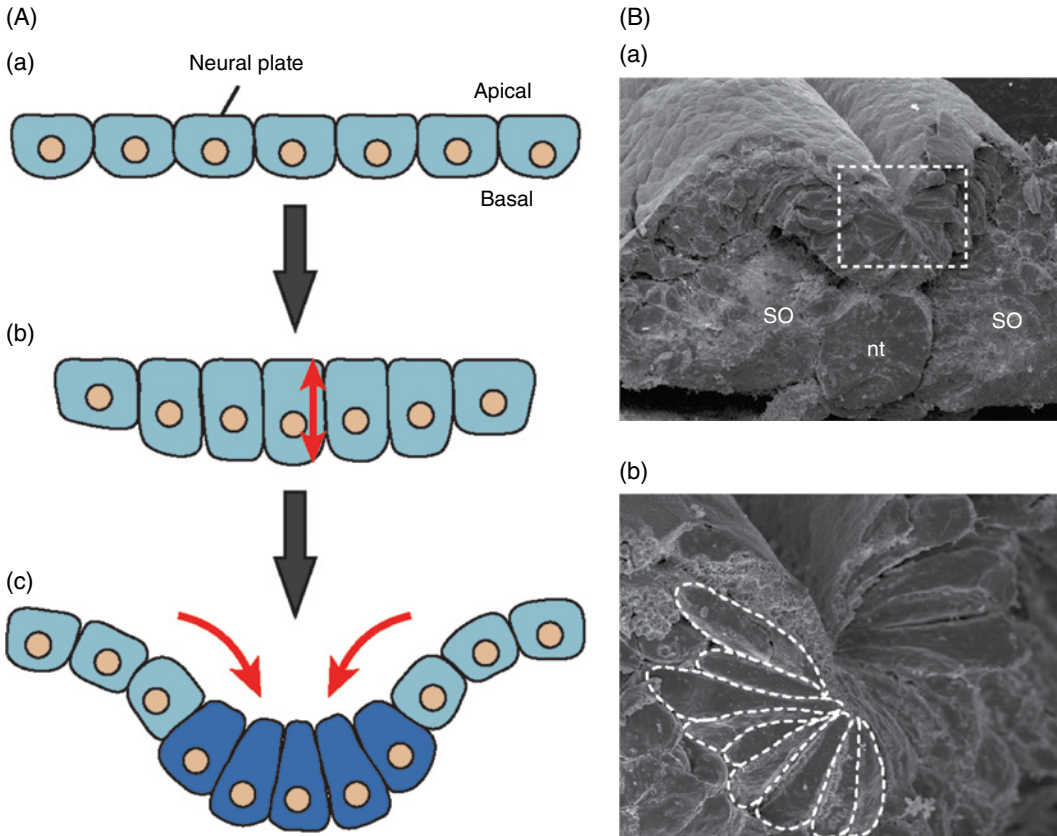


Figure 9.5 Cell-shape changes that contribute to neural plate bending and tube closure. (A) The process of cell-shape change. (a) Prior to neurulation, the neuroepithelial cells are cuboidal. (b) Cell elongation. The neuroepithelial cells first elongate along the apicobasal axis to become columnar. (c) Apical constriction. After cell elongation starts, the cell apices are constricted and minimized, causing the cells to assume a wedge or bottle-like shape from the columnar one. Apical constriction generates the main physical force that causes the neural plate to bend and form the neural tube. (B) Scanning electron micrographs of a transverse slice through the anterior spinal level of a stage 17 (middle neurula) *Xenopus laevis* embryo. Rectangular area in (a) is enlarged in (b). Dashed lines in (b) indicate the outlines of neuroepithelial cells undergoing cell elongation and apical constriction. nt, notochord; so, somite.

In the following sections, we describe the distributions and roles of two cytoskeletal components, actin filaments (F-actin) and microtubules, in apical constriction and cell elongation, respectively. We will then summarize the current understanding about the intracellular and cell adhesion proteins that directly modulate the cytoskeletal organization involved in the cell-shape changes during neural tube closure.

Apical constriction and actomyosin

Apical constriction is a basic strategy by which multicellular organisms form three-

dimensional structures from simple epithelial layers (Quintin et al. 2008). This cellular movement generally occurs through the contraction of cytoskeletal elements, particularly F-actin and nonmuscle myosin II (NMII). F-actin is composed of monomeric actin and is a major cytoskeletal component. NMII is a molecular motor that binds F-actin and is composed of two heavy chains, two essential light chains, and two regulatory light chains (MLC) (Quintin et al. 2008). The phosphorylation of MLC increases the motor activity of NMII, which in turn generates a contractile force between F-actin filaments. In neuroepithelial cells, as well as other epithelial cells,

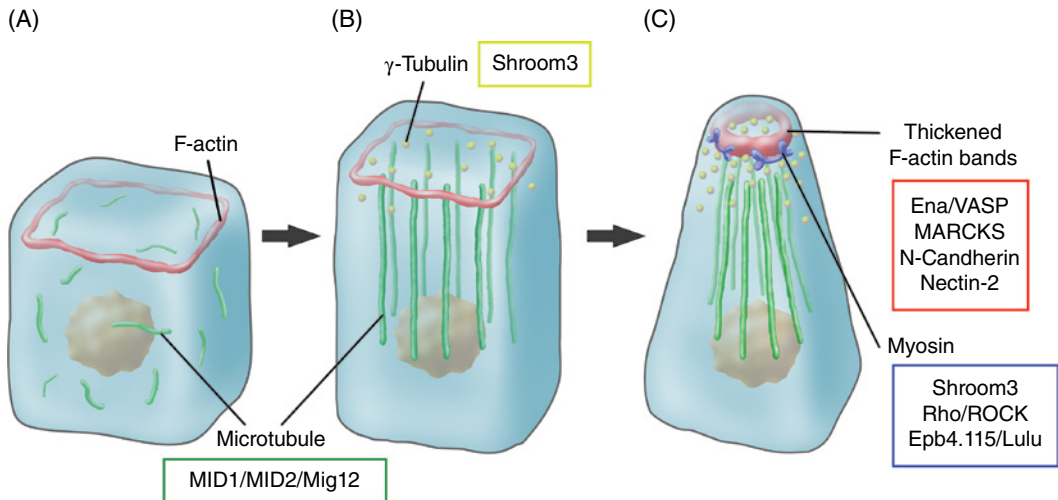


Figure 9.6 Distribution of actomyosin and microtubule cytoskeletal components during cell-shape change. (A) In the cuboidal neuroepithelial cells prior to neurulation, actin filaments (thin circular band) exist at the apical junction, and microtubules (filamentous structure) are diffusely distributed in the cytoplasm. (B) During cell elongation, noncentrosomal γ -tubulin particles (small globular shape) are distributed apically. Noncentrosomal microtubules polymerize and assemble parallel to the apicobasal axis. (C) During apical constriction, the actin filament bands become thickened. Nonmuscle myosin II (double Y shape structure on the circular actin) actively slides and generates a contractile force along the apical actin filaments as the cell apices become increasingly constricted. Intracellular and transmembrane proteins that regulate each type of cytoskeletal component are listed in boxes.

there are circular bands of F-actin at the adherens junctions (AJs) (Figure 9.6B), and these bands become thickened during apical constriction (Baker and Schroeder 1967; Schroeder 1970; Burnside 1971; Karfunkel 1971). NMII is also apically localized, overlapping with F-actin (Lee and Nagele 1985; Rolo et al. 2009). The disruption of F-actin by cytochalasin, or of NMII by blebbistatin or antisense MO, prevents the cells from constricting their apices and becoming wedge-shaped, resulting in severe defects in neural tube closure (Karfunkel 1972; Linville and Shepard 1972; Kinoshita et al. 2008; Rolo et al. 2009). Thus, F-actin and the contractile activity of NMII appear to act as purse strings, drawing string to constrict the apex of each cell. The molecular mechanisms of apical constriction in the neural plate have been investigated extensively in the last decade. These studies revealed that the Rho GTPase pathway is an essential regulator of the F-actin and NMII activities in apical constriction. Actin-binding and cell-cell adhesion proteins have also been shown to participate in this process.

Rho is a member of the Rho family of small GTPases, which are key regulators of actin

cytoskeleton organization and are required for diverse cellular functions, including cell-shape changes (Jaffe and Hall 2005). In particular, Rho activates NMII's phosphorylation via ROCK1 and ROCK2, major kinases that phosphorylate MLC (Quintin et al. 2008). In neuroepithelial cells, Rho and ROCK1 accumulate at the AJs (Kinoshita et al. 2008; Nishimura and Takeichi 2008). Inhibiting Rho or the ROCKs in chick embryos causes reductions in apical F-actin and phosphorylated MLC (pMLC) and leads to failed neural tube closure (Wei et al. 2001; Kinoshita et al. 2008). Conversely, in MDCK cells, apically targeted, constitutively active Rho induces apical constriction (Plageman et al. 2011a). This Rho-mediated apical constriction is dependent on ROCKs and NMII, indicating that apically localized, active Rho is required and sufficient for NMII-mediated apical constriction.

How is Rho's activity regulated? One of the major modulators of Rho function in the neural plate is the Shroom3 protein (Hildebrand and Soriano 1999). Shroom3 has a PDZ (PSD-95/Dgl/ZO-1) domain in its N-terminus, two Apx/Shrm domains (ASD1 and ASD2) in its central and C-terminal regions, and

putative EVH1- and PDZ-binding sites (Hagens et al. 2006). Shroom3 directly binds to F-actin via its central ASD1-containing region (Hildebrand and Soriano 1999) and is localized to AJs (Hildebrand 2005). In *shroom3* mutant mice and knockdown *Xenopus* and chick embryos, apical constriction is inhibited, in association with reduced apical F-actin and pMLC (Hildebrand and Soriano 1999; Haigo et al. 2003; Nishimura and Takeichi 2008). Conversely, ectopic Shroom3 induces apical constriction as well as apical F-actin and pMLC in the *Xenopus* animal cap and MDCK cells (Haigo et al. 2003; Hildebrand 2005). Interestingly, Shroom3 physically interacts with the central regions of ROCKs via ASD2 (Nishimura and Takeichi 2008). In the chick neural plate, disrupting this interaction causes reduced apical ROCK1 and pMLC, and failed neural tube closure (Nishimura and Takeichi 2008). Moreover, constitutively active RhoA targeted to the basolateral domain recruits Shroom3 to the basal end of MDCK cells (Plageman et al. 2011a). These findings indicated how the interactions between RhoA/ROCK and Shroom3 occur: the apically localized active RhoA recruits Shroom3, and Shroom3 further recruits ROCK1 to the apical side to phosphorylate MLC, resulting in apical constriction.

As discussed in “Narrowing and elongation of the neural plate”, the Wnt/PCP pathway regulates the convergent extension of the neural plate, which occurs by medial cell intercalation. Moreover, this pathway also controls apical constriction and hence neural plate bending by regulating Rho (Kinoshita et al. 2008; Nishimura et al. 2012). In the chick neural plate, F-actin, pMLC, and ROCK1 are preferentially localized to AJs that are oriented toward the mediolateral axis as multicellular cables, suggesting that anisotropic apical constriction occurs in a planar-polarizing manner (Nishimura et al. 2012). Interestingly, the Wnt/PCP core components Dishevelled 2 and Celsr1 and a Rho guanine nucleotide exchange factor PDZ-RhoGEF are also distributed to the AJs in a mediolaterally oriented manner, and their knockdown or inhibition disrupts the F-actin and pMLC cables and apical constriction. The recruitment of anisotropic pMLC to the AJs by Dishevelled

2 and Celsr1 is mediated by the DAAM1-dependent activation of PDZ-RhoGEF. Similarly, in the *Xenopus* neural plate, dominant-negative mutants of Wnt/PCP components cause a reduction in the apical accumulation of Rho, an expansion of cell apices, and neurulation defects (Kinoshita et al. 2008). The suppression of DAAM1 activity also causes apical constriction to fail (Liu et al. 2011). These findings indicate that the Rho activity in the neural plate is anisotropically regulated by the Wnt/PCP pathway, to promote the polarized contraction of AJs and bending of the neural plate, and reveal that the Wnt/PCP pathway has dual functions in neural tube formation.

Other intracellular proteins that may modulate apical constriction are the Ena/VASP proteins, myristoylated alanine-rich C kinase substrate (MARCKS) proteins, and erythrocyte protein band 4.1-like 5 (Epb4.115/Lulu). The Ena/VASP family members are closely related, conserved actin-binding proteins. Vertebrates have three paralogous proteins, Mena (mammalian enabled), VASP (vasodilator stimulated phosphoprotein), and EVL (Ena/VASP like) (Krause et al. 2003). Ena/VASP proteins have a similar structural organization consisting of N- and C-terminal Ena/VASP homology domains (EVH1 and EVH2) and a proline-rich central region. EVH1 mediates the protein's subcellular localization by binding to the motif D/EFPPPP in binding partners, and EVH2 mediates its binding to G- and F-actin. In mice, triple (*Mena*^{-/-}; *VASP*^{-/-}; *EVL*^{-/-}) and double (*Mena*^{-/-}; *VASP*^{-/-}; *EVL*^{+/+}) mutant embryos exhibit neural tube closure defects, resulting in exencephaly (Menzies et al. 2004; Kwiatkowski et al. 2007). In *Xenopus*, an Ena orthologue (*Xena*) is highly expressed and localized to the cell cortex in the neural plate, whereas VASP and *Xevl* are relatively weakly expressed (Roffers-Agarwal et al. 2008). Inhibiting *Xena* causes failed neural tube closure, in association with defects in apical constriction and the apical accumulation of F-actin (Roffers-Agarwal et al. 2008). Mechanistically, the EVH1 domain in Ena/VASP functionally interacts with Shroom3 (Plageman et al. 2010). In MDCK cells, deletion of Shroom3's EVH1-binding site suppresses its activity in apical constriction. Moreover, a

dominant-negative mouse Mena consisting of only the EVH1 domain suppresses the Shroom3-induced apical constriction (Plageman et al. 2010). These findings suggest that Ena/VASP regulates apical constriction by facilitating the apical accumulation of F-actin and that the Ena/VASP-Shroom3 interaction is essential for the Shroom3-mediated apical constriction and apical recruitments of the Ena/VASP proteins themselves.

MARCKS and MacMARCKS (also called F52 and MRP) are closely related actin-binding, membrane-associated proteins (Arbuzova et al. 2002). MARCKS proteins are phosphorylated by PKC and interact with calmodulin, F-actin, and acidic phospholipids (Arbuzova et al. 2002). MARCKS-knockout mice display severe NTDs, manifesting as exencephaly and spina bifida (Stumpo et al. 1995; Chen et al. 1996; Wu et al. 1996). In the chick neural plate, MARCKS accumulates transiently at the apical side (Zolessi and Arruti 2001), whereas MacMARCKS localizes to the basolateral membrane and colocalizes with E-cadherin in MDCK cells (Myat et al. 1998).

Epb4.115/Lulu is a FERM domain-containing protein and an orthologue of the *Drosophila* FERM protein Yurt (Tepass 2009). Mutant mice with defects in this gene, named *limulus* (*lulu*) mice, exhibit failed neural tube closure (Lee et al. 2007b). In the *lulu* neuroepithelial cells, the apical F-actin and NMII extend to the basal side, causing ectopic actomyosin activity at basal positions. Together with the observation that the Lulu protein is concentrated at the apical side, these observations suggest that Epb4.115/Lulu functions to anchor the actomyosin machinery to the apical membrane, which is required for neural plate bending (Lee et al. 2007b). In cultured epithelial cells, ectopic Epb4.115/Lulu induces apical constriction, in a manner requiring the ROCK-mediated NMII's phosphorylation, but not Shroom3 (Nakajima and Tanoue 2010). As its paralogue Epb4.114b physically interacts with and activates p114RhoGEF (Terry et al. 2011), it is possible that Epb4.115/Lulu functions in apical constriction by activating specific RhoGEF(s).

In addition to intracellular proteins, cell adhesion proteins have also been implicated in neural tube closure, through their regulation of actomyosin dynamics. Cadherins are a large family of calcium-dependent cell-cell adhesion proteins, with more than 100 members (Suzuki and Takeichi 2008). Intracellularly, cadherins link the cortical actin through α -, β -, γ -, p120-catenins, and EPLIN, indicating that cadherins function in assembling actin in a manner depending on cell-cell contact (Abe and Takeichi 2008). Among the cadherins, N-cadherin is expressed in the neural plate, where it is concentrated in the apical cytoplasm (Detrick et al. 1990; Fujimori et al. 1990; Radice et al. 1997). The depletion of N-cadherin in *Xenopus* causes failed neural tube closure (Nandadasa et al. 2009). The N-cadherin-depleted cells show an expanded apical surface in association with reduced apical F-actin and pMLC, suggesting that N-cadherin is required for cell-surface tension and contractility (Nandadasa et al. 2009). In mice, although *N-cadherin*^{-/-} embryos have an almost normal neural tube (Radice et al. 1997), doubly heterozygous embryos with *Shroom3* (*Shroom3*^{+/-Gt}; *N-cadherin*^{+/-}) display exencephaly, suggesting that N-cadherin functions with Shroom3 to modulate apical constriction (Plageman et al. 2011b).

Another cell-adhesive molecule participating in apical constriction is nectin-2, a member of the immunoglobulin superfamily with a single-pass transmembrane domain (Takai et al. 2008). We recently reported that in *Xenopus*, nectin-2 is expressed preferentially in the neural plate and localized to AJs (Morita et al. 2010). The depletion of nectin-2 causes defects in apical constriction with reduced apical F-actin, and failed neural tube closure (Figure 9.7A). Conversely, ectopic nectin-2 induces apical constriction accompanied by increased apical F-actin in nonneural ectodermal cells. Nectin-2 and N-cadherin physically interact through their extracellular domains in a cis manner, and nectin-2 recruits N-cadherin to AJs. Furthermore, the coexpression of nectin-2 and N-cadherin induces apical constriction and F-actin accumulation more efficiently than either molecule alone, and their double knockdown synergistically exaggerates the failure of apical constriction. These

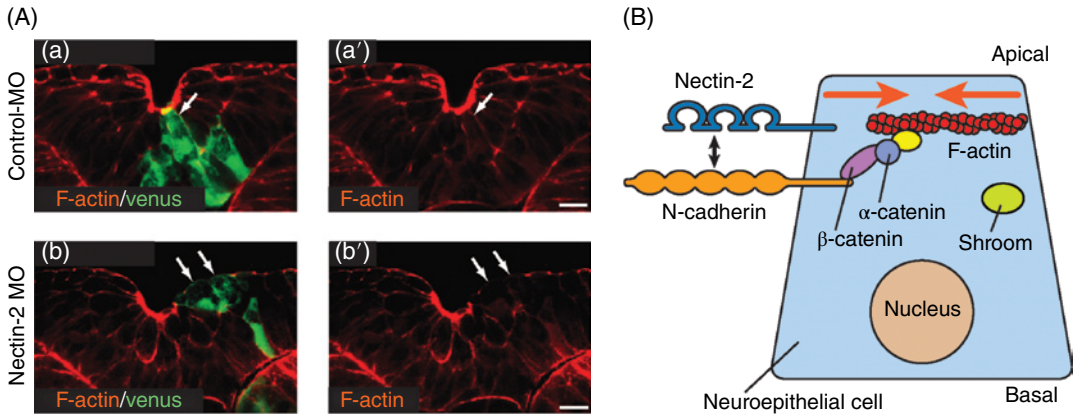


Figure 9.7 Mechanism of F-actin and N-cadherin recruitment to the apical side by nectin-2. (A) Nectin-2 knockdown in the neural plate suppressed the apical accumulation of F-actin and neural tube closure. Sections of the neural groove of embryos injected with control morpholino (MO) (a and a') or nectin-2 MO (b and b') show that the apical F-actin was reduced specifically in the venus-positive cells in the nectin-2 MO-injected embryo (b and b' arrows) compared with the control (a and a' arrows). Venus mRNA was used as a cell-lineage tracer. Scale bars indicate 20 μm . Modified from Morita et al. (2010). *Development*. (B) Schematic diagram of the nectin-2–N-cadherin interaction in apical constriction in the neuroepithelium. The extracellular domain of nectin-2 binds to that of N-cadherin, which indirectly interacts with F-actin via intracellular proteins, such as β - and α -catenins, to induce an apical accumulation of F-actin. Other intracellular components of the apical constriction machinery, including Shroom3, then contract the accumulated actin bundle to constrict the apex of the cell. Orange arrows indicate constriction of the apical surface. To see a color version of this figure, see Plate 22.

results suggest that nectin-2 functions in apical constriction by recruiting N-cadherin and F-actin to the apical region (Figure 9.7B) (Morita et al. 2010).

Functional interactions between growth factors and cell adhesion machineries are also of interest. Bone morphogenetic protein (BMP) was recently reported to control N-cadherin's function. In the chick neural plate, BMP blockade induces the endocytosis of N-cadherin through the regulation of apical–basal polarity, leading to apical constriction (Eom et al. 2011). An antagonizing role of BMP signaling in neural plate bending has also been shown in mice (Ybot-Gonzalez et al. 2002, 2007). In *Xenopus* (Lee and Harland 2010), disrupting endocytosis with dominant-negative dynamin causes inefficient apical constriction and defective neural tube closure. These findings raise the possibility that the BMP-dependent intracellular trafficking of N-cadherin affects apical constriction and neural plate bending. Together with the requirement for nectin-2, the necessity of N-cadherin's endocytosis for apical constriction may suggest that the fine-tuning of cell adhesion is essential for apical constriction.

Cell elongation and microtubules

While apical constriction is regulated by actomyosin, cell elongation – the other important cell morphogenetic process for neural tube closure – is mainly regulated by microtubules, cytoskeletal proteins composed of α - and β -tubulin. Microtubules nucleate from a minus-end anchoring protein γ -tubulin in centrosome or some noncentrosomal site (Job et al. 2003; Musch 2004; Bartolini and Gundersen 2006). In early neural cells, microtubules are distributed in the cortex and randomly oriented throughout the cell (Figure 9.6A). During cell elongation, however, microtubules polymerize and assemble apicobasally (Waddington and Perry 1966; Messier 1969; Schroeder 1970; Burnside 1971; Karfunkel 1971, 1972) (Figure 9.6B). Consistent with these findings, disrupting microtubules by vinblastine and colchicine inhibits both the initiation and maintenance of cell elongation, causing the neural cells to round up (Karfunkel 1971, 1972). Moreover, embryos treated with these inhibitors neither initiate nor maintain the elevation of the neural folds, resulting in failed neural tube closure (Karfunkel 1971,

1972). The mechanistic roles of microtubules in cell elongation are still not fully understood, but Burnside (1971) proposed that they transport cytoplasmic materials toward the extending ends of the cell. A recent study suggests that microtubules play an additional role in cell elongation as a positive regulator of cell–cell and cell–ECM adhesions (Suzuki et al. 2010).

To date, Shroom proteins and the MID1/MID2/Mig12 complex have been shown to regulate the microtubule organization in cells undergoing elongation. As in apical constriction, the disruption of Shroom3 also blocks cell elongation, and importantly, the assembly of the thick, apicobasally aligned microtubules in neural plate cells (Lee et al. 2007a, 2009). Strikingly, Shroom3 knockdown eliminates the apical accumulation of noncentrosomal γ -tubulin. Conversely, ectopic Shroom3 in animal cap cells is sufficient to induce the accumulation of γ -tubulin, apicobasally aligned microtubules, and cell elongation, but it does so without affecting the total level of γ -tubulin or physically interacting with it (Lee et al. 2007a). The other Shroom family proteins, Shroom1 and Shroom2, are expressed in the deep-layer cells, which only undergo elongation, and act to recruit γ -tubulin to the apical side (Fairbank et al. 2006; Lee et al. 2007a). Moreover, the knockdown of Shroom2 blocks cell elongation in deep neural cells, causing failed neural tube closure (Lee et al. 2009). These findings suggest that the Shroom family drives cell elongation by indirectly recruiting γ -tubulin to the apical side and inducing aligned microtubules along the apicobasal axis.

MID1 and its paralogue MID2 are RBCC/TRIM (N-terminal RING finger-B box-coiled coil/tripartite motif) proteins that associate with microtubules (Buchner et al. 1999; Cainarca et al. 1999; Short and Cox 2006) and physically interact with Mig12 (Mid1 interacting G12-like protein) (Berti et al. 2004). In humans, MID1 is responsible for X-linked Opitz G/BBB syndrome, which is characterized by hypertelorism, hypospadias, and other midline defects (Quaderi et al. 1997). Recently, Hayes et al. and we reported that the knockdown of both MID1 and MID2, or of Mig12, causes failed neural tube closure

(Hayes et al. 2007; Suzuki et al. 2010). The neuroepithelial cells in the knockdown embryos fail to undergo cell elongation, in association with destabilization and disorganization of the apicobasal microtubule arrays (Figure 9.8) (Suzuki et al. 2010), suggesting that a MID1/MID2/Mig12 complex-mediated stabilizing effect is required for microtubule reorganization, and hence for cell elongation.

These findings collectively show that cellular morphogenesis driven by cytoskeletal rearrangements is essential for the neural plate remodeling that forms the neural tube.

Complete tube closure assisted by nonneural ectoderm

As discussed earlier, the cellular morphogenesis consisting of apical constriction and elongation of the neural epithelial cells triggers the bending of the neural plate and is required for neural tube closure. However, whether both cellular morphogenesis and the planar rearrangement of neural cells that occur within the neural plate are sufficient for complete neural tube closure and how the nonneural tissues contribute, if any, to the event, have been matters of debate. In axolotl and chick, removal of the nonneural ectoderm that gives rise to epidermis perturbs neural tube closure (Alvarez and Schoenwolf 1992; Jacobson and Moury 1995; Hackett et al. 1997), and we confirmed that this is the case in *Xenopus laevis* as well, by isolating the neural ectoderm with or without the surrounding nonneural ectoderm. Based on these observations, it was speculated that the nonneural ectoderm plays a role in neural tube closure by pushing the neural folds toward the dorsal midline, and several other possible contributions of the nonneural ectoderm, including cell proliferation, cell-shape change, and cell rearrangements, have also been postulated (Karfunkel 1974) (Figure 9.9).

In the following sections, we will introduce our recent observations (Morita et al. 2012), discuss possible mechanisms, and propose a model for the mechanical contribution of the deep cells of the nonneural ectoderm in promoting complete neural tube closure in *Xenopus*.

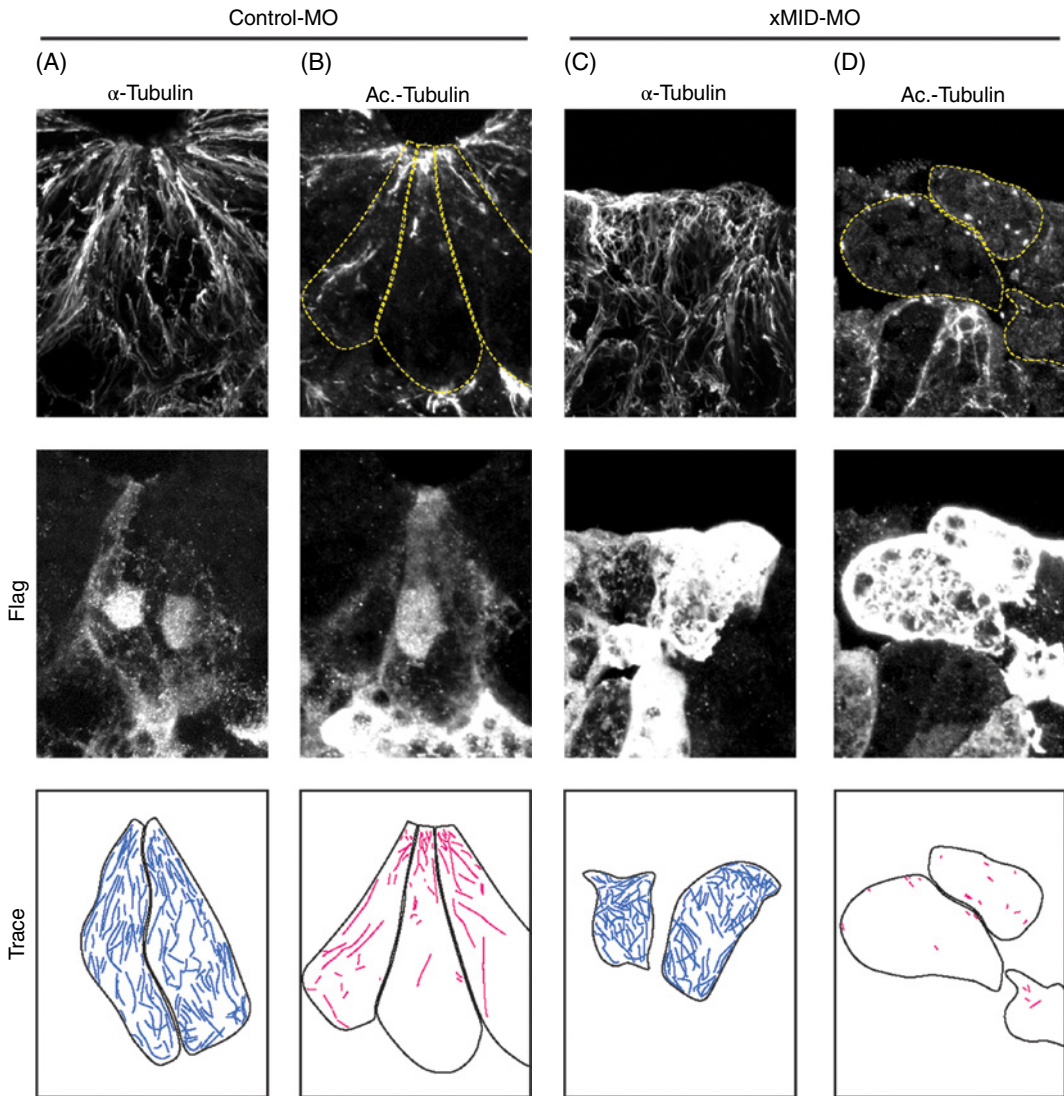


Figure 9.8 xMIDs associate with and regulate microtubules. Transverse sections through the neural plate of embryos unilaterally injected with control-MO (A and B) or xMID-MO (C and D), and stained for α -tubulin (A and C) or acetylated tubulin (Ac.-tubulin) (B and D) antibodies. *Flag- β -globin* mRNA was coinjected as a tracer and stained with an anti-Flag antibody (middle panels). Bottom panels show traced drawings of cells stained by α -tubulin and anti-acetylated tubulin antibodies. In the control columnar cells, the apicobasal arrays of microtubules were readily apparent (A). By contrast, in the xMID morphant cells, the arrays of microtubules were not polarized, and the cells were more rounded (C). To assess the stability of the polymerized microtubules, we analyzed their acetylation status. In the control cells, filamentous and continuous staining was detected, particularly in the apical region (B). By contrast, in the rounded xMID morphant cells, the acetylated tubulin staining was punctate (D).

Dispensability of cell division for neural tube closure in *Xenopus*

A possible contribution of oriented cell division to neural tube closure was proposed in chick embryo (Sausedo et al. 1997), in which it

was shown that the axis of cell division in the nonneural ectoderm was preferentially oriented along the DV axis. In *Xenopus*, however, it was previously shown that inhibiting cell division does not affect neural tube closure (Harris and Hartenstein 1991). When stage 10

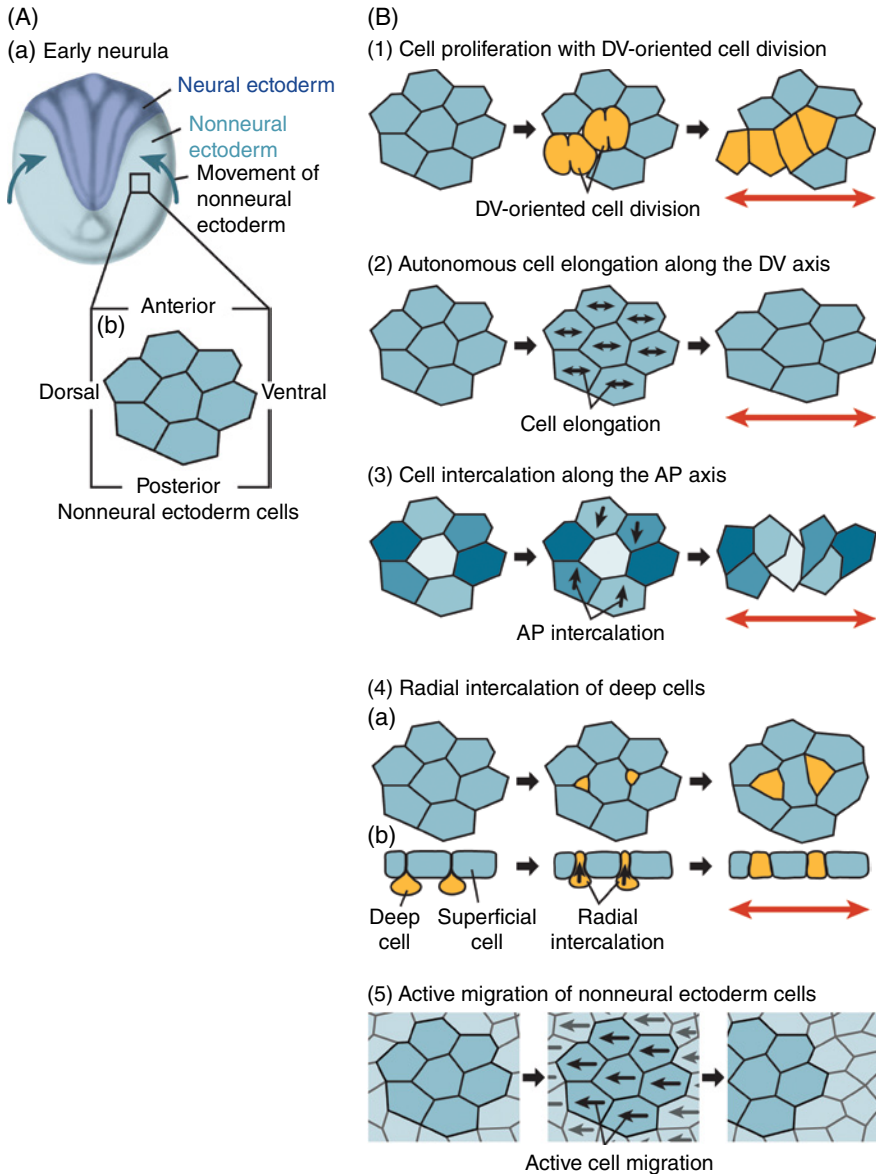


Figure 9.9 Schematic diagram of possible cellular morphogenetic events that may contribute to the nonneural cell movement. (A) Dorsal view of an early neurula embryo (a) and an illustration of magnified nonneural ectoderm cells (b). (B) Possible cellular morphogenetic events that could push the neural folds toward the dorsal midline via the movement of the nonneural ectoderm. (1) Cell proliferation with dorsoventrally oriented cell division. Cells in the nonneural ectoderm preferentially divide with the division plane perpendicular to the DV axis, increasing the number of cells along this axis, which could push surrounding cells dorsoventrally. (2) Autonomous cell elongation along the DV axis. Each of the nonneural ectoderm cells autonomously elongates along the DV axis, expanding the tissue dorsoventrally. (3) Cell intercalation along the AP axis. The nonneural ectoderm cells intercalate with each other along the AP axis, resulting in the extension of the tissue along the DV axis. (4) Radial intercalation of deep cells into the superficial layer. Cells beneath the superficial layer of the nonneural ectoderm (deep cells, indicated in yellow) intercalate radially into the surface tissue, wedging themselves between superficial cells. This could increase the surface area of the nonneural ectoderm and contribute to movement of the tissue. Views of the surface (a) and the cross section (b) are shown. (5) Active migration of nonneural ectoderm cells. Cells in the nonneural ectoderm themselves actively migrate toward the dorsal midline, causing movement of the tissue as a whole. To see a color version of this figure, see Plate 23.

embryos were treated with the DNA-synthesis inhibitors hydroxyurea and aphidicolin, the neural tube closed normally (Harris and Hartenstein 1991; Morita et al. 2012). The morphology of the closed neural tube in the embryos treated with these inhibitors was indistinguishable from that in normal embryos, indicating that neural tube closure proceeds without significant cell division in *Xenopus*.

Correlation of cell movement with tensile force in nonneural ectoderm

To address whether cell movement contributes to neural tube closure, we used digital scanned laser light-sheet fluorescence microscopy (DSLM) (Keller et al. 2008a), with which the entire surface of a living embryo can be observed. Using DSLM and a membrane-targeted EGFP (memEGFP) transgenic strain of *Xenopus laevis* (Takagi et al. 2013), which expresses memEGFP in all tissues, the displacement and shape change of ectoderm cells during neural tube closure were observed in whole embryos. Tracking cell displacement revealed that most of the nonneural ectoderm cells moved toward the dorsal side, as observed in previous studies (Keller 1976; Veldhuis et al. 2005). These cells moved faster in the medial region of the AP axis than did

those at the anterior and posterior ends. Furthermore, the cells in the region close to the dorsal side moved faster than those located more ventrally. These findings indicated that there are velocity gradients along both the DV and AP axes. The tracking data also indicated that most of the ectoderm cells moved in the same direction as their neighbors, rarely changing their relative position or intermingling along the AP axis (Figure 9.10), suggesting that cell rearrangement is unlikely to occur or that it has only a limited effect on nonneural cell movement. To understand the cellular effects at the morphological level, we analyzed the cell-shape changes in the nonneural ectoderm by measuring the aspect ratio of the cells and the angles of their longest axis. This analysis revealed that the cells in the medial region along the AP axis became elongated dorsoventrally during neural tube closure and that this tendency was greater in the cells in the dorsal side of the nonneural ectoderm than in those of the ventral side.

To test whether the cell-shape change, namely, elongation along the DV axis, occurs as a result of autonomous cell morphogenesis or an external force, we examined the tension of the nonneural ectoderm. To demonstrate the force on the nonneural ectoderm, we cut the superficial layer using laser ablation (Toyama et al. 2008). If a stretching force were exerted on the nonneural cells, the gap should

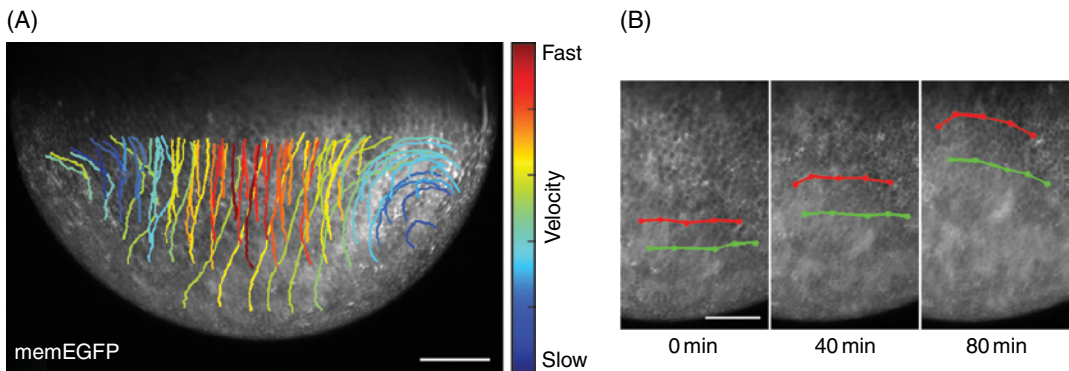


Figure 9.10 Movements of nonneural ectoderm cells toward the dorsal midline. (A) Trajectories and velocities of nonneural ectoderm cells in a DSLM image. Cells moved toward the dorsal midline, with the cells in the middle of the AP axis moving fastest. A lateral view of an early neurula embryo is shown. The upper side is dorsal and the anterior is to the left. (B) Tracking of the relative positions of nonneural cells. The positions of superficial cells in the lateral view of the DSLM images were connected by lines (red and green) and tracked during neural tube closure. Scale bars indicate 200 μm in A and 100 μm in B. To see a color version of this figure, see Plate 24.

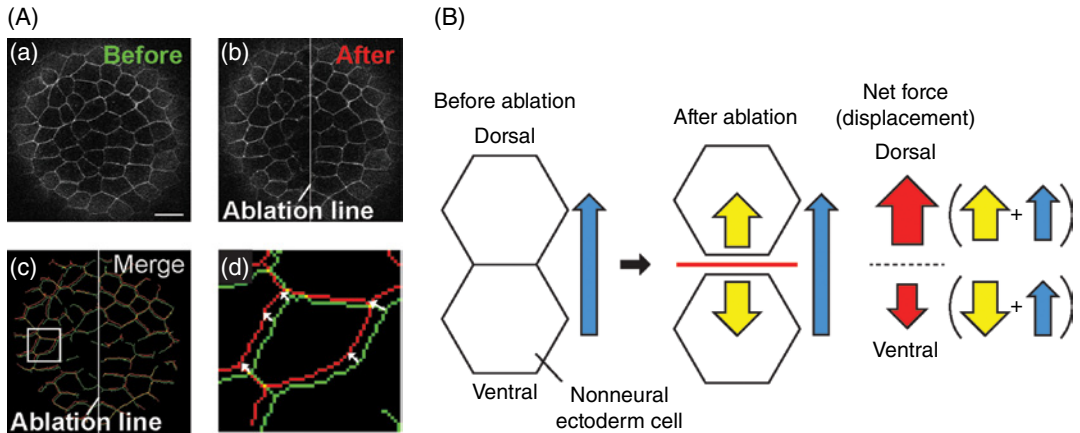


Figure 9.11 Laser ablation in the nonneural ectoderm. (A) Laser ablation on the lateral surface of the nonneural ectoderm along the AP axis. Fluorescent images of a memGFP-injected embryo taken just before (a) and immediately after (1.5 seconds; b) the incision. These images were merged after image processing, and the displacement of cell vertices between the two time points was measured (c). White boxed region in (c) is magnified in (d). White arrows in (d) indicate the displacement of the cell membrane. Upper side is the embryo's anterior, and dorsal is to the left. (B) Schematic diagram indicating the forces on the nonneural ectoderm cells (arrows) and their displacement by laser ablation. During neurulation, cells in the nonneural ectoderm move toward the dorsal side with a certain force (blue arrow; before ablation). Upon laser ablation (red line; after ablation), the cells separated in opposite directions according to the tensile force. As we assume that this tissue is in a state of equilibrium, based on the DSLM observations, the forces causing the separation may have the same magnitude (yellow arrows; after ablation). Therefore, the displacement observed after ablation can be interpreted as the result of the sum of the forces of tissue movement (blue) and tissue separation (yellow), with a higher value in the dorsal side and a lower one in the ventral side (red arrows). Scale bar indicates 20 μm . To see a color version of this figure, see Plate 25.

expand along the axis of the force. When a cut was made along the AP axis, the cells on the dorsal side of the ablation line shifted further than those on the ventral side, at all the neurula stages examined, and the angle was biased toward the anterior in the lateral area of the neurula embryos. In the DV axis cut, the cells at the anterior and posterior side of the cut shifted markedly toward the anterior and posterior ends, respectively (Figure 9.11A). We interpreted these results as follows (Figure 9.11B): during neurulation, cells in the nonneural ectoderm move toward the dorsal side with a certain force (blue arrow; before ablation). These cells are separated upon laser ablation according to the tensile force that is presumably equilibrated within the tissue (yellow arrows; after ablation). Taken together, the displacement observed after ablation can be interpreted as the sum of these forces, with a higher value in the dorsal side and a lower one in the ventral side (red arrows).

Function of deep cells to generate a motile force for the nonneural ectoderm

The nonneural ectoderm also consists of a superficial and a deep-cell layer. To analyze the motive force of the nonneural ectoderm, we focused on the movement of the deep-layer cells. Although these cells have long been known to exist in *Xenopus* (Schroeder 1970), their movement had not been observed in live embryos. By injecting the mRNA for membrane-targeted GFP (memGFP) into a slightly deeper part of eight-cell-stage embryos, we preferentially labeled the deep-layer cells. Interestingly, in contrast to the highly epithelialized cells of the superficial layer, which are polygonal with sharp edges that reflect well-developed cell-cell adhesion, the deep-layer cells have an amorphous shape with protrusions (Figure 9.12A), and they lack apically localized ZO-1 protein, a characteristic structure of epithelial cells. Time-lapse

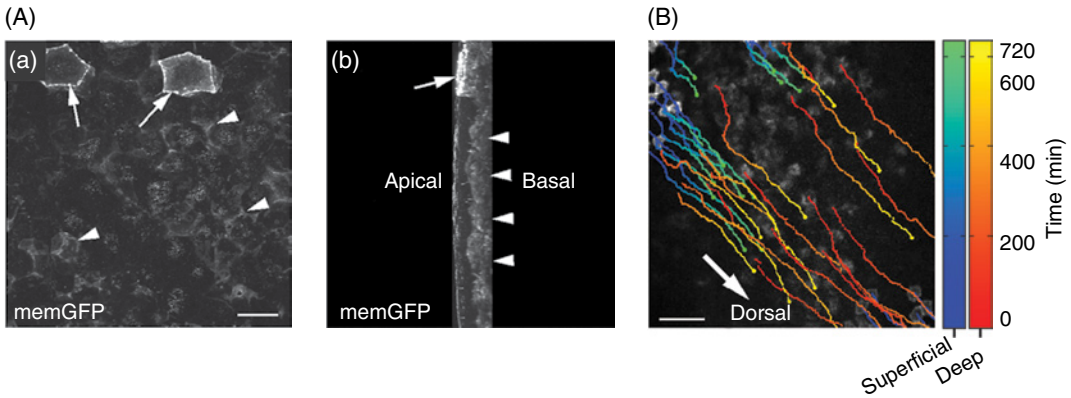


Figure 9.12 Migration of deep cells in the nonneural ectoderm toward the dorsal side. (A) Morphology and position of deep cells in the nonneural ectoderm. Nonneural ectoderm cells in an embryo injected with memGFP were viewed from the surface (a) and as a reconstructed Y–Z section (b, reconstruction of (a)). Deep cells had ambiguous boundaries (arrowheads) while superficial ones had sharp cell–cell boundaries, facing the outside of the embryo (arrows). (B) Trajectories of superficial (blue to green) and deep (orange to yellow) cell movements in the nonneural ectoderm of a wild-type embryo. The deep cells moved faster than the superficial ones (superficial, $0.667 \pm 0.020 \mu\text{m min}^{-1}$; deep, $0.813 \pm 0.027 \mu\text{m min}^{-1}$). Arrow points toward the dorsal side. Scale bars indicate $20 \mu\text{m}$ in A and $100 \mu\text{m}$ in B. To see a color version of this figure, see Plate 26.

observations showed that the deep cells are highly motile toward the dorsal side (Figure 9.12B). Quantitative analysis of the cell movements revealed that the deep cells move faster than the superficial ones, and the distance between closely positioned deep and superficial cells increases with time, although some cells in more ventral areas do not show marked displacement. These findings indicate that the deep-layer cells may play an active role and the superficial cells a passive one in bringing the two neural folds to the midline for neural tube closure.

Since it was previously suggested that the tissue movement in the nonneural ectoderm is secondary to the morphogenetic movements in the neural plate (Jacobson and Gordon 1976), we inhibited convergent extension and apical constriction, the two major morphogenetic movements in the neural plate, simultaneously, using a dominant-negative form of *Xdsh* (*Xdd1*) and a morpholino oligonucleotide (MO) against nectin-2 (*nec2*-MO), a cell adhesion molecule (Wallingford and Harland 2002; Morita et al. 2010). The inhibition of these molecules in the neural plate did not affect the cell movements in the nonneural ectoderm significantly, suggesting that the major morphogenetic movements in the neural plate play a limited role in the nonneu-

ral movement and that the nonneural tissue generates a significant force for its own morphogenesis.

To confirm that the dorsoanterior movement of the nonneural deep cells is the source of the tensile force on the superficial cells and that synchronized cell movements provide the force to complete the neural tube closure, we inhibited the cell movement in the nonneural ectoderm. During *Xenopus* neurulation, the three germ layers become clearly separated by extracellular matrix (ECM), which includes fibronectin (FN) (Davidson et al. 2004), and the cell–ECM adhesion molecule integrin- $\beta 1$ (Vicente-Manzanares et al. 2009) accumulates at high levels where the ectoderm and mesoderm make contact, suggesting that the deep ectoderm cells could attach to and migrate on the ECM via integrins (Figure 9.13A). Previous studies also demonstrated that FN and integrin play important roles in morphogenetic events in *Xenopus*, such as gastrulation and neural tube closure (Barreto et al. 2003; Davidson et al. 2006). Therefore, to inhibit deep-cell movement, we knocked down integrin- $\beta 1$ selectively in the nonneural ectoderm with a specific MO (*Itg $\beta 1$* -MO). The morphant embryos showed failed neural-fold fusion, indicating impaired neural tube closure. Time-lapse observation showed that the

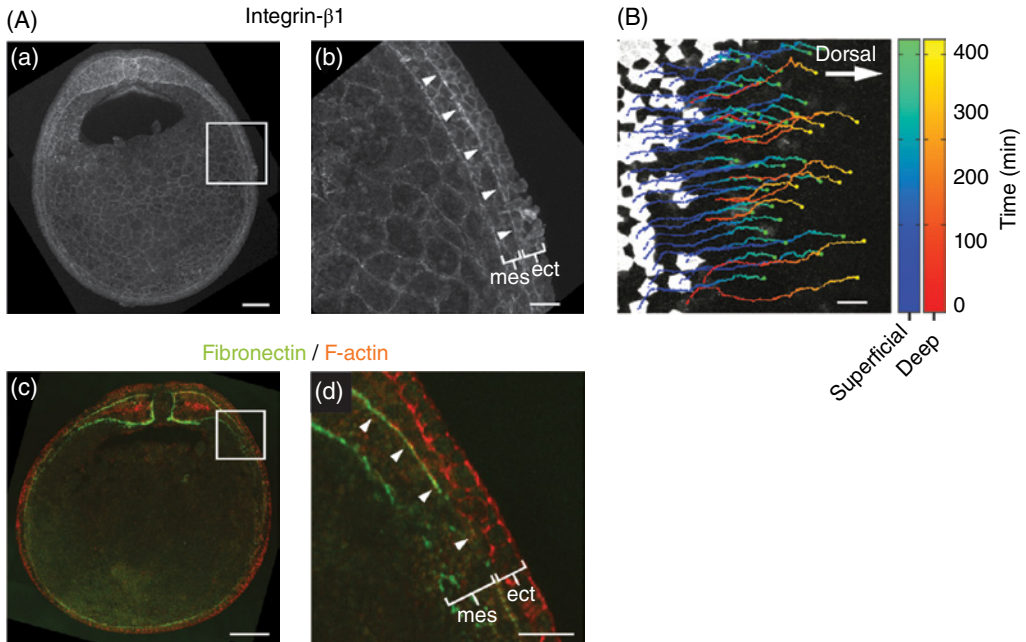


Figure 9.13 Localization of integrin- β 1 and its function in nonneural ectoderm movement. (A) Immunostaining of integrin- β 1 and fibronectin (FN). Integrin- β 1 (a and b) and FN (c and d) were localized to the border between the ectoderm and mesoderm with high density (arrowheads). **ect** indicates ectoderm, **mes** is mesoderm. (B) Trajectories of superficial (blue to green) and deep (orange to yellow) cell movements in the nonneural ectoderm of an *Itg β 1*-MO-injected embryo. Both superficial and deep cells moved significantly more slowly (superficial: $0.523 \pm 0.012 \mu\text{m min}^{-1}$; deep: $0.715 \pm 0.032 \mu\text{m min}^{-1}$) compared with wild-type embryos. Arrow points toward the dorsal side. Scale bars indicate $200 \mu\text{m}$ in Aa and Ac and $50 \mu\text{m}$ in Ab, Ad, and B. To see a color version of this figure, see Plate 27 .

integrin- β 1-depleted cells still moved toward the dorsal side. However, quantitative analysis showed that the movement of the nonneural cells was significantly compromised (Figure 9.13B).

We next analyzed the tensile force on the nonneural ectoderm of the integrin- β 1 morphants. Importantly, after laser ablation, the difference in expansion between the dorsal and ventral sides and the dorsally biased displacement were not observed in the morphants. In addition, these embryos showed a lower aspect ratio and relatively scattered angles of the major axis compared with the wild type, indicating that the tension on the superficial cells was reduced in them.

Since a change in epithelial cell thickness was suggested to drive epidermal cell movement in the salamander embryo (Brun and Garson 1983), we examined this possibility in the integrin- β 1 morphants of *Xenopus*. In wild-type embryos, the cell thickness of the

nonneural superficial layer decreased during neurulation, as reported in other amphibians (Burnside 1971; Brun and Garson 1983). The cell thickness in the morphants also decreased with a pattern similar to that of the wild type, indicating that the *Itg β 1*-MO did not affect the cell thinning of the nonneural superficial layer. Similarly, radial intercalation of nonneural deep cells into the superficial layer could contribute to the movement of this tissue. During neurulation in *Xenopus*, however, the radial intercalation is mostly observed from the late-neurula stages, when the neural tube has almost closed (Stubbs et al. 2006), suggesting that radial intercalation is unlikely to contribute to major movements of the nonneural ectoderm. Taken together, these results strongly suggest that active movement of the deep-layer cells is the primary source of tensile force on the superficial cells and that the coordinated movement of the nonneural ectoderm contributes to neural tube closure.

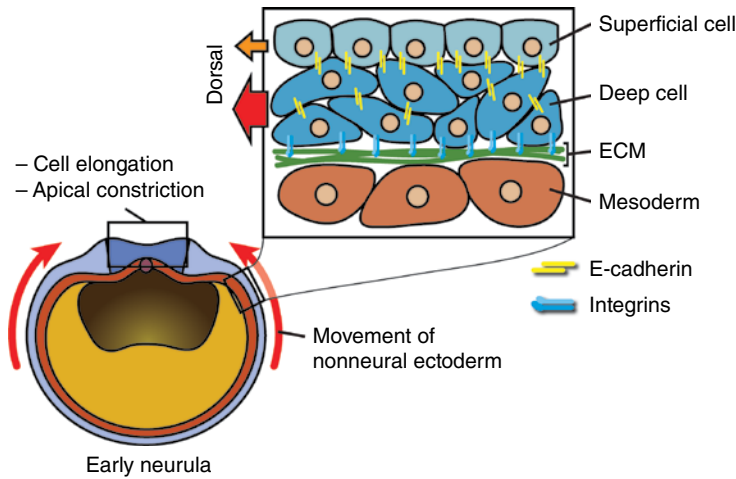


Figure 9.14 Mechanism of the dorsally directed movement of nonneural ectoderm. Schematic diagram of a mechanism for nonneural cell movement toward the dorsal midline. Deep cells in the nonneural ectoderm bind to ECM that accumulates between the ectoderm and mesoderm via integrin- β 1. These cells also adhere to the overlying superficial cells through E-cadherin. The deep cells migrate on the ECM toward the dorsal midline, pulling the superficial cells together. In collaboration with the cellular morphogenetic events in the neural ectoderm, this autonomous movement of the nonneural ectoderm contributes to the completion of neural tube closure. To see a color version of this figure, see Plate 28.

Connection between the deep and superficial cells by E-cadherin

Our findings regarding the nonneural ectoderm movement suggested that the deep cells pull the overlying superficial cells, bringing them toward the dorsal side. If this is the case, there should be an adhesive interaction between the layers. In fact, the cell-cell adhesion molecule E-cadherin is localized to the border between these layers and to the superficial apical junctions in *Xenopus* (Nandadasa et al. 2009). In addition, the knockdown of E-cadherin in the nonneural ectoderm results in a significant delay in neurulation (Nandadasa et al. 2009). We therefore examined whether E-cadherin-mediated cell adhesion is involved in the movement of the nonneural cells, using a specific MO (Ecad-MO). We found that, although Ecad-MO-injected nonneural cells moved dorsally, the absolute value of the velocity of the deep-layer cells and the relative horizontal distance of both layers were significantly larger than in the wild type. These results suggested that the attachment of the two layers was normally maintained by E-cadherin and support our

hypothesis that cell-cell interactions between the two layers of nonneural ectoderm enable the coordinated cell movement toward the dorsal side that is required for complete neural tube closure.

Collectively, the findings from other groups and ours have unveiled the following mechanism for the function of nonneural ectoderm during neural tube closure (Figure 9.14): deep cells of the nonneural ectoderm adhere to ECM that accumulates between the ectoderm and mesoderm, and this interaction enables the deep cells to migrate toward the dorsal side, guided by an as-yet-unidentified directional cue(s). The migration of the deep cells generates a pulling force on the superficial cells of the nonneural ectoderm through the E-cadherin-mediated adhesion between them, leading to the dorsally directed movement of this tissue.

In summary, in this chapter we explained how the proper formation of the neural tube of *Xenopus* is achieved by the coordination of autonomous cell morphogenetic events and cell rearrangements within the neural plate and by an external force from the lateral nonneural ectoderm that brings the neural folds to the dorsal midline.

References

- Abe, K. and Takeichi, M. 2008. EPLIN mediates linkage of the cadherin catenin complex to F-actin and stabilizes the circumferential actin belt. *Proc. Natl. Acad. Sci. USA* 105:13–19.
- Alvarez, I. S. and Schoenwolf, G. C. 1992. Expansion of surface epithelium provides the major extrinsic force for bending of the neural plate. *J. Exp. Zool.* 261:340–348.
- Arbuzova, A., Schmitz, A. A. and Vergeres, G. 2002. Cross-talk unfolded: MARCKS proteins. *Biochem. J.* 362:1–12.
- Baker, P. C. and Schroeder, T. E. 1967. Cytoplasmic filaments and morphogenetic movement in the amphibian neural tube. *Dev. Biol.* 15:432–450.
- Barreto, G., Reintsch, W., Kaufmann, C. and Dreyer, C. 2003. The function of *Xenopus* germ cell nuclear factor (xGCNF) in morphogenetic movements during neurulation. *Dev. Biol.* 257:329–342.
- Bartolini, F. and Gundersen, G. G. 2006. Generation of noncentrosomal microtubule arrays. *J. Cell Sci.* 119:4155–4163.
- Berti, C., Fontanella, B., Ferrentino, R. and Meroni, G. 2004. Mig12, a novel Opitz syndrome gene product partner, is expressed in the embryonic ventral midline and co-operates with Mid1 to bundle and stabilize microtubules. *BMC Cell Biol.* 5:9.
- Brodland, G. W. 2006. Do lamellipodia have the mechanical capacity to drive convergent extension? *Int. J. Dev. Biol.* 50:151–155.
- Brun, R. B. and Garson, J. A. 1983. Neurulation in the Mexican salamander (*Ambystoma mexicanum*): a drug study and cell shape analysis of the epidermis and the neural plate. *J. Embryol. Exp. Morphol.* 74:275–295.
- Buchner, G., Montini, E., Andolfi, G., et al. 1999. MID2, a homologue of the Opitz syndrome gene MID1: similarities in subcellular localization and differences in expression during development. *Hum. Mol. Genet.* 8:1397–1407.
- Burnside, B. 1971. Microtubules and microfilaments in newt neurulation. *Dev. Biol.* 26:416–441.
- Burnside, B. 1973. Microtubules and microfilaments in amphibian neurulation. *Am. Zool.* 13:989–1006.
- Cainarca, S., Messali, S., Ballabio, A. and Meroni, G. 1999. Functional characterization of the Opitz syndrome gene product (midin): evidence for homodimerization and association with microtubules throughout the cell cycle. *Hum. Mol. Genet.* 8:1387–1396.
- Chen, J., Chang, S., Duncan, S. A., Okano, H. J., Fishell, G. and Aderem, A. 1996. Disruption of the MacMARCKS gene prevents cranial neural tube closure and results in anencephaly. *Proc. Natl. Acad. Sci. USA* 93:6275–6279.
- Copp, A. J. and Bernfield, M. 1994. Etiology and pathogenesis of human neural tube defects: insights from mouse models. *Curr. Opin. Pediatr.* 6:624–631.
- Copp, A. J. and Greene, N. D. 2010. Genetics and development of neural tube defects. *J. Pathol.* 220:217–230.
- Davidson, L. A., Keller, R. and DeSimone, D. W. 2004. Assembly and remodeling of the fibrillar fibronectin extracellular matrix during gastrulation and neurulation in *Xenopus laevis*. *Dev. Dyn.* 231:888–895.
- Davidson, L. A., Marsden, M., Keller, R. and Desimone, D. W. 2006. Integrin alpha5beta1 and fibronectin regulate polarized cell protrusions required for *Xenopus* convergence and extension. *Curr. Biol.* 16:833–844.
- De Robertis, E. M. and Kuroda, H. 2004. Dorsal-ventral patterning and neural induction in *Xenopus* embryos. *Annu. Rev. Cell Dev. Biol.* 20:285–308.
- Detrick, R. J., Dickey, D. and Kintner, C. R. 1990. The effects of *N*-cadherin misexpression on morphogenesis in *Xenopus* embryos. *Neuron* 4:493–506.
- Domingo, C. and Keller, R. 1995. Induction of notochord cell intercalation behavior and differentiation by progressive signals in the gastrula of *Xenopus laevis*. *Development* 121:3311–3321.
- Eagleson, G. W. and Harris, W. A. 1990. Mapping of the presumptive brain regions in the neural plate of *Xenopus laevis*. *J. Neurobiol.* 21:427–440.
- Elul, T. and Keller, R. 2000. Monopolar protrusive activity: a new morphogenic cell behavior in the neural plate dependent on vertical interactions with the mesoderm in *Xenopus*. *Dev. Biol.* 224:3–19.
- Elul, T., Koehl, M. A. and Keller, R. 1997. Cellular mechanism underlying neural convergent extension in *Xenopus laevis* embryos. *Dev. Biol.* 191:243–258.
- Eom, D. S., Amarnath, S., Fogel, J. L. and Agarwala, S. 2011. Bone morphogenetic proteins regulate neural tube closure by interacting with the apicobasal polarity pathway. *Development* 138:3179–3188.
- Ezin, A. M., Skoglund, P. and Keller, R. 2003. The midline (notochord and notoplate) patterns the cell motility underlying convergence and extension of the *Xenopus* neural plate. *Dev. Biol.* 256:100–114.
- Fairbank, P. D., Lee, C., Ellis, A., Hildebrand, J. D., Gross, J. M. and Wallingford, J. B. 2006. Shroom2 (APXL) regulates melanosome biogenesis and localization in the retinal pigment epithelium. *Development* 133:4109–4118.

- Fujimori, T., Miyatani, S. and Takeichi, M. 1990. Ectopic expression of *N*-cadherin perturbs histogenesis in *Xenopus* embryos. *Development* 110:97–104.
- Glaser, O. C. 1914. On the mechanism of morphological differentiation in the nervous system. *Anat. Rec.* 8:525–551.
- Hackett, D. A., Smith, J. L. and Schoenwolf, G. C. 1997. Epidermal ectoderm is required for full elevation and for convergence during bending of the avian neural plate. *Dev. Dyn.* 210:397–406.
- Hagens, O., Ballabio, A., Kalscheuer, V., et al. 2006. A new standard nomenclature for proteins related to Apx and Shroom. *BMC Cell Biol.* 7:18.
- Haigo, S. L., Hildebrand, J. D., Harland, R. M. and Wallingford, J. B. 2003. Shroom induces apical constriction and is required for hinge point formation during neural tube closure. *Curr. Biol.* 13:2125–2137.
- Harris, W. A. and Hartenstein, V. 1991. Neuronal determination without cell division in *Xenopus* embryos. *Neuron* 6:499–515.
- Hayes, J. M., Kim, S. K., Abitua, P. B., et al. 2007. Identification of novel ciliogenesis factors using a new in vivo model for mucociliary epithelial development. *Dev. Biol.* 312:115–130.
- Hildebrand, J. D. 2005. Shroom regulates epithelial cell shape via the apical positioning of an actomyosin network. *J. Cell Sci.* 118:5191–5203.
- Hildebrand, J. D. and Soriano, P. 1999. Shroom, a PDZ domain-containing actin-binding protein, is required for neural tube morphogenesis in mice. *Cell* 99:485–497.
- Jacobson, A. G. and Gordon, R. 1976. Changes in the shape of the developing vertebrate nervous system analyzed experimentally, mathematically and by computer simulation. *J. Exp. Zool.* 197:191–246.
- Jacobson, A. G. and Moury, J. D. 1995. Tissue boundaries and cell behavior during neurulation. *Dev. Biol.* 171:98–110.
- Jaffe, A. B. and Hall, A. 2005. Rho GTPases: biochemistry and biology. *Annu. Rev. Cell Dev. Biol.* 21:247–269.
- Job, D., Valiron, O. and Oakley, B. 2003. Microtubule nucleation. *Curr. Opin. Cell Biol.* 15:111–117.
- Jones, C. and Chen, P. 2007. Planar cell polarity signaling in vertebrates. *Bioessays* 29:120–132.
- Juriloff, D. M. and Harris, M. J. 2012. A consideration of the evidence that genetic defects in planar cell polarity contribute to the etiology of human neural tube defects. *Birth Defects Res. A Clin. Mol. Teratol.* 94:824–840.
- Karfunkel, P. 1971. The role of microtubules and microfilaments in neurulation in *Xenopus*. *Dev. Biol.* 25:30–56.
- Karfunkel, P. 1972. The activity of microtubules and microfilaments in neurulation in the chick. *J. Exp. Zool.* 181:289–301.
- Karfunkel, P. 1974. The mechanisms of neural tube formation. *Int. Rev. Cytol.* 38:245–271.
- Keller, R. E. 1976. Vital dye mapping of the gastrula and neurula of *Xenopus laevis*. II. Prospective areas and morphogenetic movements of the deep layer. *Dev. Biol.* 51:118–137.
- Keller, R., Shih, J. and Sater, A. 1992. The cellular basis of the convergence and extension of the *Xenopus* neural plate. *Dev. Dyn.* 193:199–217.
- Keller, R., Davidson, L., Edlund, A., et al. 2000. Mechanisms of convergence and extension by cell intercalation. *Philos. Trans. R. Soc. Lond. B. Biol. Sci.* 355:897–922.
- Keller, P. J., Schmidt, A. D., Wittbrodt, J. and Stelzer, E. H. 2008a. Reconstruction of zebrafish early embryonic development by scanned light sheet microscopy. *Science* 322:1065–1069.
- Keller, R., Shook, D. and Skoglund, P. 2008b. The forces that shape embryos: physical aspects of convergent extension by cell intercalation. *Phys. Biol.* 5:015007.
- Kinoshita, N., Sasai, N., Misaki, K. and Yonemura, S. 2008. Apical accumulation of Rho in the neural plate is important for neural plate cell shape change and neural tube formation. *Mol. Biol. Cell* 19:2289–2299.
- Krause, M., Dent, E. W., Bear, J. E., Loureiro, J. J. and Gertler, F. B. 2003. Ena/VASP proteins: regulators of the actin cytoskeleton and cell migration. *Annu. Rev. Cell Dev. Biol.* 19:541–564.
- Kwiatkowski, A. V., Rubinson, D. A., Dent, E. W., et al. 2007. Ena/VASP is required for neurogenesis in the developing cortex. *Neuron* 56:441–455.
- Lee, H. Y. and Nagele, R. G. 1985. Studies on the mechanisms of neurulation in the chick: interrelationship of contractile proteins, microfilaments, and the shape of neuroepithelial cells. *J. Exp. Zool.* 235:205–215.
- Lee, J. Y. and Harland, R. M. 2010. Endocytosis is required for efficient apical constriction during *Xenopus* gastrulation. *Curr. Biol.* 20:253–258.
- Lee, C., Scherr, H. M. and Wallingford, J. B. 2007a. Shroom family proteins regulate gamma-tubulin distribution and microtubule architecture during epithelial cell shape change. *Development* 134:1431–1441.
- Lee, J. D., Silva-Gagliardi, N. F., Tepass, U., McGlade, C. J. and Anderson, K. V. 2007b. The FERM protein Epb4.115 is required for organization of the neural plate and for the epithelial-mesenchymal transition at the primitive streak of the mouse embryo. *Development* 134:2007b–2016.

- Lee, C., Le, M. P. and Wallingford, J. B. 2009. The shroom family proteins play broad roles in the morphogenesis of thickened epithelial sheets. *Dev. Dyn.* 238:1480–1491.
- Linville, G. P. and Shepard, T. H. 1972. Neural tube closure defects caused by cytochalasin B. *Nat. New Biol.* 236:246–247.
- Liu, W., Komiya, Y., Mezzacappa, C., Khadka, D. K., Runnels, L. and Habas, R. 2011. MIM regulates vertebrate neural tube closure. *Development* 138:2035–2047.
- MacDonald, B. T., Tamai, K. and He, X. 2009. Wnt/ beta-catenin signaling: components, mechanisms, and diseases. *Dev. Cell* 17:9–26.
- Menzies, A. S., Aszodi, A., Williams, S. E., et al. 2004. Mena and vasodilator-stimulated phosphoprotein are required for multiple actin-dependent processes that shape the vertebrate nervous system. *J. Neurosci.* 24:8029–8038.
- Messier, P. E. 1969. Effects of beta-mercaptoethanol on the fine structure of the neural plate cells of the chick embryo. *J. Embryol. Exp. Morphol.* 21:309–329.
- Morita, H., Nandadasa, S., Yamamoto, T. S., Terasaka-Iioka, C., Wylie, C. and Ueno, N. 2010. Nectin-2 and N-cadherin interact through extracellular domains and induce apical accumulation of F-actin in apical constriction of *Xenopus* neural tube morphogenesis. *Development* 137:1315–1325.
- Morita, H., Kajiura-Kobayashi, H., Takagi, C., Yamamoto, T. S., Nonaka, S. and Ueno, N. 2012. Cell movements of the deep layer of non-neural ectoderm underlie complete neural tube closure in *Xenopus*. *Development* 139:1417–1426.
- Musch, A. 2004. Microtubule organization and function in epithelial cells. *Traffic* 5:1–9.
- Myat, M. M., Chang, S., Rodriguez-Boulan, E. and Aderem, A. 1998. Identification of the basolateral targeting determinant of a peripheral membrane protein, MacMARCKS, in polarized cells. *Curr. Biol.* 8:677–683.
- Nakajima, H. and Tanoue, T. 2010. Epithelial cell shape is regulated by Lulu proteins via myosin-II. *J. Cell Sci.* 123:555–566.
- Nandadasa, S., Tao, Q., Menon, N. R., Heasman, J. and Wylie, C. 2009. N- and E-cadherins in *Xenopus* are specifically required in the neural and non-neural ectoderm, respectively, for F-actin assembly and morphogenetic movements. *Development* 136:1327–1338.
- Nishimura, T. and Takeichi, M. 2008. Shroom3-mediated recruitment of Rho kinases to the apical cell junctions regulates epithelial and neuroepithelial planar remodeling. *Development* 135:1493–1502.
- Nishimura, T., Honda, H. and Takeichi, M. 2012. Planar cell polarity links axes of spatial dynamics in neural-tube closure. *Cell* 149:1084–1097.
- Plageman, T. F., Jr., Chung, M. I., Lou, M., et al. 2010. Pax6-dependent Shroom3 expression regulates apical constriction during lens placode invagination. *Development* 137:405–415.
- Plageman, T. F., Jr., Chauhan, B. K., Yang, C., et al. 2011a. A Trio-RhoA-Shroom3 pathway is required for apical constriction and epithelial invagination. *Development* 138:5177–5188.
- Plageman, T. F., Jr., Zacharias, A. L., Gage, P. J. and Lang, R. A. 2011b. Shroom3 and a Pitx2-N-cadherin pathway function cooperatively to generate asymmetric cell shape changes during gut morphogenesis. *Dev. Biol.* 357:227–234.
- Quaderi, N. A., Schweiger, S., Gaudenz, K., et al. 1997. Opitz G/BBB syndrome, a defect of midline development, is due to mutations in a new RING finger gene on Xp22. *Nat. Genet.* 17:285–291.
- Quintin, S., Gally, C. and Labouesse, M. 2008. Epithelial morphogenesis in embryos: asymmetries, motors and brakes. *Trends Genet.* 24:221–230.
- Radice, G. L., Rayburn, H., Matsunami, H., Knudsen, K. A., Takeichi, M. and Hynes, R. O. 1997. Developmental defects in mouse embryos lacking N-cadherin. *Dev. Biol.* 181:64–78.
- Roffers-Agarwal, J., Xanthos, J. B., Kragtorp, K. A. and Miller, J. R. 2008. Enabled (Xena) regulates neural plate morphogenesis, apical constriction, and cellular adhesion required for neural tube closure in *Xenopus*. *Dev. Biol.* 314:393–403.
- Rolo, A., Skoglund, P. and Keller, R. 2009. Morphogenetic movements driving neural tube closure in *Xenopus* require myosin IIB. *Dev. Biol.* 327:327–338.
- Rothbacher, U., Laurent, M. N., Deardorff, M. A., Klein, P. S., Cho, K. W. and Fraser, S. E. 2000. Dishevelled phosphorylation, subcellular localization and multimerization regulate its role in early embryogenesis. *EMBO J.* 19:1010–1022.
- Sausedo, R. A., Smith, J. L. and Schoenwolf, G. C. 1997. Role of nonrandomly oriented cell division in shaping and bending of the neural plate. *J. Comp. Neurol.* 381:473–488.
- Schoenwolf, G. C. and Franks, M. V. 1984. Quantitative analyses of changes in cell shapes during bending of the avian neural plate. *Dev. Biol.* 105:257–272.
- Schroeder, T. E. 1970. Neurulation in *Xenopus laevis*. An analysis and model based upon light and electron microscopy. *J. Embryol. Exp. Morphol.* 23:427–462.
- Shih, J. and Keller, R. 1992. The epithelium of the dorsal marginal zone of *Xenopus* has organizer properties. *Development* 116:887–899.
- Short, K. M. and Cox, T. C. 2006. Subclassification of the RBCC/TRIM superfamily reveals a novel motif necessary for microtubule binding. *J. Biol. Chem.* 281:8970–8980.

- Sive, H. L., Grainger, R. M. and Harland, R. M. 2007. *Xenopus laevis* Keller Explants. *CSH Protoc* 2007:pdb prot4749.
- Smith, J. L. and Schoenwolf, G. C. 1997. Neurulation: coming to closure. *Trends Neurosci.* 20:510–517.
- Sokol, S. Y. 1996. Analysis of Dishevelled signalling pathways during *Xenopus* development. *Curr. Biol.* 6:1456–1467.
- Stubbs, J. L., Davidson, L., Keller, R. and Kintner, C. 2006. Radial intercalation of ciliated cells during *Xenopus* skin development. *Development* 133:2507–2515.
- Stumpo, D. J., Bock, C. B., Tuttle, J. S. and Blackshear, P. J. 1995. MARCKS deficiency in mice leads to abnormal brain development and perinatal death. *Proc. Natl. Acad. Sci. USA* 92:944–948.
- Suzuki, S. C. and Takeichi, M. 2008. Cadherins in neuronal morphogenesis and function. *Dev. Growth Differ.* 50 Suppl 1:S119–S130.
- Suzuki, M., Hara, Y., Takagi, C., Yamamoto, T. S. and Ueno, N. 2010. MID1 and MID2 are required for *Xenopus* neural tube closure through the regulation of microtubule organization. *Development* 137:2329–2339.
- Suzuki, M., Morita, H. and Ueno, N. 2012. Molecular mechanisms of cell shape changes that contribute to vertebrate neural tube closure. *Dev. Growth Differ.* 54:266–276.
- Takagi, C., Sakamaki, K., Morita, H., et al. 2013. Transgenic *Xenopus laevis* for live imaging in cell and developmental biology. *Dev. Growth Differ.* 55:422–433.
- Takai, Y., Ikeda, W., Ogita, H. and Rikitake, Y. 2008. The immunoglobulin-like cell adhesion molecule nectin and its associated protein afadin. *Annu. Rev. Cell Dev. Biol.* 24:309–327.
- Tepass, U. 2009. FERM proteins in animal morphogenesis. *Curr. Opin. Genet. Dev.* 19:357–367.
- Terry, S. J., Zihni, C., Elbediwy, A., et al. 2011. Spatially restricted activation of RhoA signalling at epithelial junctions by p114RhoGEF drives junction formation and morphogenesis. *Nat. Cell Biol.* 13:159–166.
- Toyama, Y., Peralta, X. G., Wells, A. R., Kiehart, D. P. and Edwards, G. S. 2008. Apoptotic force and tissue dynamics during *Drosophila* embryogenesis. *Science* 321:1683–1686.
- Ueno, N. and Greene, N. D. 2003. Planar cell polarity genes and neural tube closure. *Birth Defects Res. C Embryo Today* 69:318–324.
- Veldhuis, J. H., Brodland, G. W., Wiebe, C. J. and Bootsma, G. J. 2005. Multiview robotic microscope reveals the in-plane kinematics of amphibian neurulation. *Ann. Biomed. Eng.* 33:821–828.
- Vicente-Manzanares, M., Choi, C. K. and Horwitz, A. R. 2009. Integrins in cell migration—the actin connection. *J. Cell Sci.* 122:199–206.
- Waddington, C. H. and Perry, M. M. 1966. A note on the mechanisms of cell deformation in the neural folds of the Amphibia. *Exp. Cell Res.* 41:691–693.
- Wallingford, J. B. 2005. Neural tube closure and neural tube defects: studies in animal models reveal known knowns and known unknowns. *Am. J. Med. Genet. C Semin. Med. Genet.* 135C:59–68.
- Wallingford, J. B. 2010. Low-magnification live imaging of *Xenopus* embryos for cell and developmental biology. *Cold Spring Harb Protoc* 2010:pdb prot5425.
- Wallingford, J. B. 2012. Planar cell polarity and the developmental control of cell behavior in vertebrate embryos. *Annu. Rev. Cell Dev. Biol.* 28:627–653.
- Wallingford, J. B. and Harland, R. M. 2001. *Xenopus* Dishevelled signaling regulates both neural and mesodermal convergent extension: parallel forces elongating the body axis. *Development* 128:2581–2592.
- Wallingford, J. B. and Harland, R. M. 2002. Neural tube closure requires Dishevelled-dependent convergent extension of the midline. *Development* 129:5815–5825.
- Wallingford, J. B., Rowning, B. A., Vogeli, K. M., Rothbacher, U., Fraser, S. E. and Harland, R. M. 2000. Dishevelled controls cell polarity during *Xenopus* gastrulation. *Nature* 405:81–85.
- Wallingford, J. B., Fraser, S. E. and Harland, R. M. 2002. Convergent extension: the molecular control of polarized cell movement during embryonic development. *Dev. Cell* 2:695–706.
- Wei, L., Roberts, W., Wang, L., et al. 2001. Rho kinases play an obligatory role in vertebrate embryonic organogenesis. *Development* 128:2953–2962.
- Wu, M., Chen, D. F., Sasaoka, T. and Tonegawa, S. 1996. Neural tube defects and abnormal brain development in F52-deficient mice. *Proc. Natl. Acad. Sci. USA* 93:2110–2115.
- Ybot-Gonzalez, P. and Copp, A. J. 1999. Bending of the neural plate during mouse spinal neurulation is independent of actin microfilaments. *Dev. Dyn.* 215:273–283.
- Ybot-Gonzalez, P., Cogram, P., Gerrelli, D. and Copp, A. J. 2002. Sonic hedgehog and the molecular regulation of mouse neural tube closure. *Development* 129:2507–2517.
- Ybot-Gonzalez, P., Gaston-Massuet, C., Girdler, G., et al. 2007. Neural plate morphogenesis during mouse neurulation is regulated by antagonism of Bmp signalling. *Development* 134:3203–3211.
- Zolessi, F. R. and Arruti, C. 2001. Apical accumulation of MARCKS in neural plate cells during neurulation in the chick embryo. *BMC Dev. Biol.* 1:7.

Section III

Metamorphosis and Organogenesis

- Chapter 10 Primordial Germ Cell Migration
- Chapter 11 Development of Gonads, Sex Determination, and Sex Reversal in *Xenopus*
- Chapter 12 The *Xenopus* Pronephros: A Kidney Model Making Leaps toward Understanding Tubule Development
- Chapter 13 Development of Neural Tissues in *Xenopus laevis*
- Chapter 14 The Development of the Immune System in *Xenopus*
- Chapter 15 Neural Regeneration in *Xenopus* Tadpoles during Metamorphosis

10 Primordial Germ Cell Migration

Aliaksandr Dzementsei & Tomas Pieler

Institute for Developmental Biochemistry, Göttingen, Germany

Abstract: In many animal species primordial germ cells (PGCs) have to migrate during embryogenesis in a directional manner from the region of their specification to the site of gonad formation. Active migration of *Xenopus laevis* PGCs begins at the tailbud stage of embryonic development. They migrate first within the endoderm, and later through dorsal mesentery. In this chapter we summarize what is known about cellular and molecular mechanisms of PGC migration in *X. laevis*, and compare it to cell migration in other species.

Primordial germ cells (PGCs) are progenitors to the germ cells during early stages of embryogenesis in animal species including *Xenopus*. Specification of the PGCs occurs in a region distinct from the one where the formation of gonads will occur. Thus, during embryogenesis, PGCs have to migrate from the region of their specification to the territory of gonad formation. The ability of individual cells for directional migration in a complex environment is not unique to the PGCs, but certainly a fascinating phenomenon to study.

Over the years, a variety of different techniques have been employed for the identification and tracking of individual PGCs in *Xenopus* embryos. Initially, PGCs were distinguished from somatic cells via the presence of a microscopically identifiable cytoplasmic inclusions, referred to as germ plasm (Blackler

1965; Whittington and Dixon 1975). When methods to analyze the molecular composition of the germ plasm became available, whole mount *in situ* hybridization (WMISH) using antisense RNAs complementary to germ-cell-specific mRNAs, such as Xpat, was introduced in order to visualize PGCs in the fixed embryos (Hudson and Woodland 1998; Houston and King 2000a). Alternatively, antibodies for germ plasm-specific proteins, such as XVLG1 (*Xenopus* vasa-like gene), were employed (Komiya et al. 1994). With the availability of fluorescent microscopy techniques, *in vivo* observation of PGCs became possible. Due to the high amount of mitochondria in germ plasm, PGCs can be labeled by DiOC₆(3) (3,3'-dihexyloxacarbocyanine). If embryos at the early stages are treated with this fluorescent dye, it accumulates on

hyperpolarized membranes, such as mitochondria, and is translocated into the lipid bilayer (Venkataraman et al. 2004). The drawback of this method is potential toxicity and dilution of the dye during development, making it difficult to distinguish PGCs from the surrounding cells after neurula stages. Another approach was to inject chimeric mRNAs, containing ORFs encoding different fluorescent proteins fused to 3'-UTR of germ plasm-specific mRNAs. It was shown that such 3'-UTRs mediate PGC-specific stabilization by protection against miRNA-mediated RNA degradation after the MBT (Kataoka et al. 2006; Koebernick et al. 2010). Fusion of these 3'-UTRs to other ORFs developed into a very powerful tool in promoting PGC-specific overexpression of proteins for their functional analysis (Morichika et al. 2010; Takeuchi et al. 2010; Tarbashevich et al. 2011). More recently, using the same principal approach, a novel transgenic *Xenopus laevis* line with fluorescently labeled mitochondria was generated, which can now be used for germ plasm and PGC visualization *in vivo* (Taguchi et al. 2012).

In *Xenopus*, specification of PGCs occurs on the basis of the inheritance of maternally supplied regulatory activities. These factors, mostly constituents of the germ plasm, become enriched at the vegetal cortex during oogenesis; after fertilization, they become asymmetrically segregated between daughter blastomeres. Cells in the vegetal part of the embryo inheriting the germ plasm will become PGCs. At the blastula stage, the germ plasm is mostly found in three to seven cells located in between the vegetal pole and the floor of the blastocoel (Whittington and Dixon 1975; Houston and King 2000a).

During gastrulation, PGCs, together with the surrounding endodermal cells, involute inside of the embryo. At this stage, PGCs are in tight contact with their neighboring cells and thereby seem to undergo passive migration (Whittington and Dixon 1975; Houston and King 2000a). After gastrulation, PGCs are located centrally within the endodermal cell mass. They remain associated with surrounding cells up to stage 23 (Nishiumi et al. 2005; Terayama et al. 2013). From stage 24 onward, PGCs start active directional migration within the endoderm. They migrate within a cohort of cells as individual

cells in the context of endodermal somatic cells, first laterally, then dorsally and anteriorly until they reach the dorsal crest of the endoderm (Houston and King 2000a).

Migration of PGCs within the endoderm is coupled to changes of their locomotive activity (Terayama et al. 2013) (Figure 10.1). Prior to migration (stages 18 and 24), isolated PGCs show little protrusion formation and exhibit mainly a spherical round morphology, similar to somatic endodermal cells. Upon dispersal in the endoderm at stage 28, isolated PGCs acquire an elongated shape, correlating with the onset of migratory activity. At stage 33/34, PGCs exhibit a high level of cellular dynamics, which is characterized by the formation of numerous bleb-like protrusions and migratory activity. In these stages, PGCs alternate between locomotive and pausing phases. At stage 41, isolated PGCs exhibit a reduced tendency to form bleb-like protrusions and locomotive activity. Subsequent migration of the PGCs to the gonads takes place via the dorsal mesentery, a thin strip of connective tissue that links the dorsal body wall and the gut. The mesentery forms from two sheets of splanchnic mesoderm surrounding the gut. As these sheets converge at the dorsal crest of the endoderm, PGCs exit the endoderm and incorporate into the mesentery (stage 43/44). From the mesentery, PGCs then migrate laterally to the forming genital ridges, enter the gonads, and differentiate into germ line stem cells capable of forming the gametes (Wylie and Heasman 1976, 1993).

Migration of *Xenopus* PGCs within the endoderm happens via a blebbing-associated mechanism (Tarbashevich et al. 2011; Terayama et al. 2013). Blebs are pressure-driven plasma membrane protrusions formed by the cells. In majority of the animal cells, plasma membrane is tightly bound to the underlying actomyosin cortex. Myosin motors constantly keep the cortex under tension, applying a pressure on the cytoplasm. If disruption occurs either in the cortex or at the interface between cortex and plasma membrane, the internal pressure of the cell generated by actomyosin contraction drives the cytoplasm to flow into this space. As a result, spherical cellular bleb-like protrusion is formed (Charras and Paluch 2008; Fackler and Grosse 2008). In nonmigrating

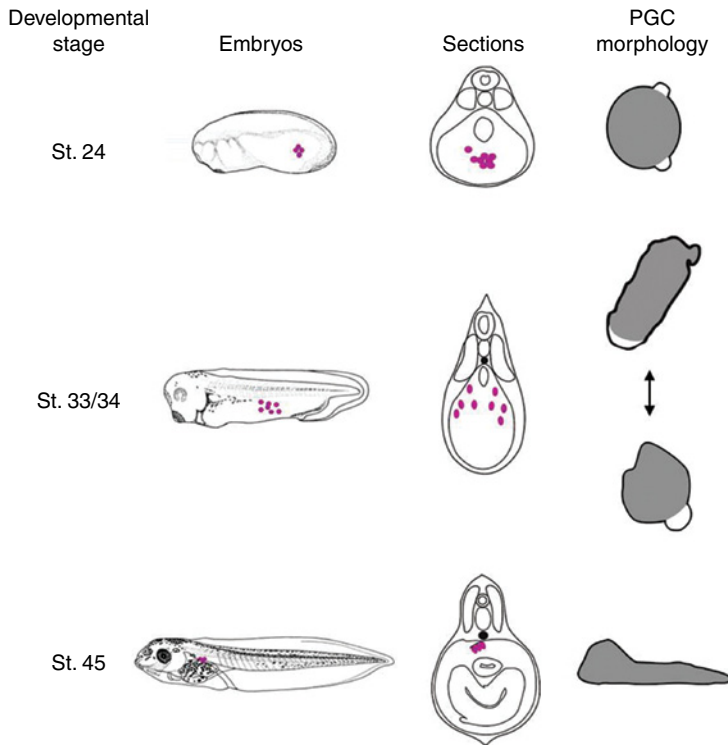


Figure 10.1 PGC motility and morphology during different developmental stages of *X. laevis* embryos. Embryos are drawn after Nieuwkoop and Faber (1994). Vertical sections perpendicular to the anterior–posterior with the positions of PGCs (“pink dots”) in the embryo are indicated. The morphology of isolated PGCs indicated according to Terayama et al. (2013); Heasman and Wylie (1978). (We thank Olena Steshenko for the help with the image preparation.) To see a color version of this figure, see Plate 29.

cells, the actomyosin cortex reassembles on the plasma membrane and the bleb retracts to the initial position. In migratory polarized cells, formation of the blebs occurs preferentially at the leading edge. In these cells, cortex repolymerization on the surface of the bleb is followed by a new disruption of cortex–plasma membrane interactions before the bleb is retracted. This results in the formation of a new bleb at the leading edge before the retraction of a former bleb occurs. The position of the bleb at the leading edge can also be stabilized by newly formed interactions with extracellular substrates. In both of these cases, the plasma membrane of the bleb is not retracted to the initial position, and the cell translocates to a new position with the help of actomyosin cortex contraction in the rear (Charras and Paluch 2008).

Actin polymerization and myosin activity are also required for the locomotion and protrusion formation of *Xenopus* PGCs. In nonmigrating

PGCs, actin filaments are localized to the periphery of the cell, forming a cortex underlying the plasma membrane, while in the migratory PGCs actin filaments can be found in the rear, but not at the leading edge of the cell (Terayama et al. 2013). Inhibition of actin polymerization and myosin activity by chemical inhibitors results in a loss of protrusion formation and cell locomotion. Similar results were obtained by inhibition of RhoA/ROCK signaling in *Xenopus* PGCs (Terayama et al. 2013). This signaling regulates bleb formation by phosphorylating myosin light chain (MLC) (Fackler and Grosse 2008).

In order to migrate directionally, blebs should form primarily on the leading edge of the cell. Most of the cells that migrate via bleb-associated mechanism are guided by chemoattractants. For the amoeba *Dictyostelium discoideum*, such attractants are nutrients and cAMP; for neutrophils – complement factor C5a, platelet-activating factor (PAF), and

formylated Met-Leu-Phe (fMLP). PGCs derived from zebrafish, chicken, and mouse are guided by a system consisting of the chemoattractant stem cell-derived factor 1 (SDF-1), also known as Chemokine C-X-C motif ligand 12 (CXCL12), and its receptor C-X-C chemokine receptor type 4 (CXCR4) (Doitsidou et al. 2002; Knaut et al. 2003; Molyneaux et al. 2003; Stebler et al. 2004). Guidance of zebrafish PGCs by SDF-1 was reported to be tightly regulated by dynamic expression of SDF-1 during embryogenesis. By modifying the position of the SDF-1 expression, PGCs can be attracted to intermediate positions before reaching the gonads. The beginning of SDF-1 expression in a new domain is coupled to a rapid degradation of *sdf-1* mRNA by miRNA-dependent mechanism (Staton et al. 2011). In addition, SDF-1 ligand is cleared by the somatic cells via CXCR7, an SDF-1 receptor that is involved in its degradation (Boldajipour et al. 2008).

In the case of *Xenopus* PGCs, cell migration is also guided by chemoattractants, originating from the dorsal part of the embryo. Isolated *X. laevis* PGCs can be polarized and migrate toward extracts prepared from stage 30 to 31 embryos lacking endoderm (Tarbashevich et al. 2011). Interestingly, expression of chemoattractant SDF-1 in *X. laevis* embryos at the tailbud stage can be observed in dorsal and anterior structures: the mid- and hindbrain, otic vesicles and eyes, dorsal fin, and posterior heart anlage (Braun et al. 2002). Expression of the receptor CXCR4 can also be observed in PGCs at tailbud stages 24–40 (Nishiumi et al. 2005). Overexpression of SDF-1 in the embryos upon knockdown of its repressor IRX5 leads to mislocalization of PGCs, due to a loss of directionality in their migration within the endodermal cell mass (Bonnard et al. 2012). In addition, interference with endogenous SDF-1 or CXCR4 expression results in a decreased number of PGCs arriving at the genital ridges (Takeuchi et al. 2010). Thus, even though it seems highly likely that this signaling system serves a role in PGC polarization and migration, an exact guidance mechanism for *Xenopus* PGCs remains to be determined.

CXCR4, as well as other receptors involved in chemotaxis, belongs to G-protein coupled receptor (GPCR) family. In the context of cell migration, activated heterotrimeric G-proteins

activate various downstream pathways, including calcium flux (Dutt et al. 1998; Blaser et al. 2006), Phospholipase C (PLC), and Phosphatidylinositol 3-kinase (PI3-kinase) (Wang et al. 2000). Activation of PI3-kinases was reported to be one of the major events for polarization of many migratory cells (Chung et al. 2001; Iijima et al. 2002). PI3-kinases generate inositol phospholipids, which bind to a subset of PH domain-containing molecules, thus recruiting them to the membrane. There are three classes of enzymes in PI3-kinase family (Katso et al. 2001). Class I PI3-kinases catalyze the phosphorylation of the 3' hydroxyl subunit of PIP2, converting it into PIP3. This class of enzymes was shown to be involved in the regulation of cellular polarization by the localization of PIP3 to the leading edge of the cell (Meili et al. 1999; Haugh et al. 2000; Servant et al. 2000; Merlot and Firtel 2003; Dumstrei et al. 2004). Asymmetrical localization of PIP2 and PIP3 in the cell facilitates the recruitment of PH domain-containing proteins, primary effectors of PI3-kinase signaling pathway, to the leading edge. The restriction of PIP3 to the leading edge of the cell is also influenced by the function of PI3K antagonist PTEN (phosphatase and tensin homolog), a phosphoinositide 3'-specific phosphatase that dephosphorylates PIP3 to PIP2 (Maehama and Dixon 1998). Studies in *Dictyostelium* have revealed that, in resting cells, PTEN is localized to the plasma membrane, uniformly distributed all over the cell (Funamoto et al. 2002; Iijima and Devreotes 2002). In chemotaxing cells, PTEN is down-regulated at the leading edge but persists at the sides and the back of the cell. Thus, PTEN prevents the accumulation of PIP3 exclusively at the sides and the rear of the cell, resulting in cellular polarization.

Polarization of *Xenopus* PGCs also correlates with asymmetries in respect to the intracellular PIP3 distribution (Tarbashevich et al. 2011). PIP3 is found to be enriched in the bleb-like protrusions formed by isolated PGCs at migratory stage. Downregulation of endogenous PIP3 levels leads to a decrease in PGC number and to abnormal PGC migration. Loss of endogenous PIP3 is also coupled to the loss of plasma membrane blebbing. One of the molecules involved in generating PIP3 asymmetries in *Xenopus* PGCs is the kinesin

KIF13B. The corresponding maternal mRNA localizes to the germ plasm and is later detected in PGCs up to tailbud stages of development. Knockdown of KIF13B leads to the loss of PIP3 enrichment and inhibits formation of bleb-like protrusions in PGCs isolated from stage 30 to 32 embryos. In contrast, KIF13B overexpression leads to increased plasma membrane blebbing and PIP3 enrichment throughout the plasma membrane (Tarbashevich et al. 2011). Thus, similar to what is observed upon reducing the cellular levels of PIP3, knockdown of KIF13B results in a decrease of PGC number and abnormal PGC migration. In good correlation, KIF13B was previously shown to be involved in the polarization of hippocampal neurons prior to axonal growth. It was suggested that KIF13B might contribute to the local enrichment of PIP3 at the tip of growing neurites by directional transport of PIP3-containing vesicles, mediated by the interaction with a PIP3-binding protein (PIP3BP or Centaurin- α 1) (Horiguchi et al. 2006). However, the exact molecular mechanism by which KIF13B influences the PIP3 distribution in *Xenopus* PGCs remains to be determined.

In vitro migration of murine PGCs was reported to be activated by the Kit ligand (KL) as a guiding cue, and also described to depend on the PI3-kinase pathway (Farini et al. 2007). In the zebrafish model system, the *in vivo* motility of PGCs depends on appropriate PIP3 levels, but a polarized distribution of PIP3 was not observed. It was proposed that PI3K activity might be linked to substrate adhesion, rather than to polarization (Dumstrei et al. 2004). Instead, a major role in the formation and stabilization of cellular bleb-like protrusions in zebrafish PGCs was assigned to calcium. Calcium levels are elevated at the leading edge of migrating cells, which leads to phosphorylation and activation of myosin by Myosin light-chain kinase (MLCK) (Blaser et al. 2006). Myosin-dependent contraction near the leading edge serves as a driving force for the motility of zebrafish PGCs (Kardash et al. 2010; Goudarzi et al. 2012).

As outlined earlier, PIP3 polarization was described to be relevant for a number of different cells migrating via a bleb-associated mechanism, including *Dictyostelium* amoeba

and vertebrate neutrophils (Franca-Koh et al. 2006, 2007; Yoo et al. 2010). In the case of *Dictyostelium*, however, multiple parallel pathways appear to be involved in chemotaxis, with each individual one, such as the PI3K pathway, being dispensable (Hoeller and Kay 2007; Van Haastert and Veltman 2007; King and Insall 2008). Several observations suggest that multiple pathways might also be involved in regulating the directional migration of *Xenopus* PGCs. One of these comes from experiments characterizing the *Xenopus* glutamate receptor interacting protein 2 (XGRIP2). Similar to KIF13B, XGRIP2 is also encoded by germ plasm-specific, maternal mRNA. GRIP multi-PDZ domain family proteins usually serve as adaptor proteins, and they are involved in various processes, including cell-matrix interactions during embryogenesis in mammals and control of directional migration of embryonic muscle cells in *Drosophila* (Swan et al. 2004; Takamiya et al. 2004). Knockdown of XGRIP2 resulted in decelerated PGC migration at tailbud stages and a decrease in the average number of PGCs. PGCs in XGRIP2 morphants were mislocalized to more posterior positions at stage 33/34 (Tarbashevich et al. 2007). These observations on PGC migration in XGRIP2 morphant embryos were confirmed in a second, independent study, revealing that the ability of the PGCs to enter dorsal mesentery was also significantly impaired (Kirilenko et al. 2008).

Another pathway involved in regulation of PGC migration in *Xenopus* is the one depending on Notch/Suppressor of Hairless [Su(H)]. The Notch receptor and its ligands Delta and Serrate are single-pass transmembrane proteins. When Notch binds to one of these ligands, the Notch intracellular domain (NICD) is released and translocates into the nucleus, where it forms a complex together with Su(H) and regulates gene expression (Lai 2004). Suppression or activation of this pathway in the endoderm of *Xenopus* embryos starting from stage 18, as well as PGC-specific activation, resulted in defects in PGC migration in the endoderm. In this case, PGCs failed to reach dorsal mesentery by stage 41 and were found ectopically in the endoderm. Similar results were observed upon knockdown of *X-Delta-2*, one of the ligands of Notch

(Morichika et al. 2010). Activation of the Notch pathway leads to the induction of the expression of HES and HES-related genes, which encode basic helix–loop–helix-type transcriptional repressors (Iso et al. 2003). Activation of such genes in the PGCs, as well as in somatic endodermal cells was observed upon activation of Notch signaling in the endoderm of *Xenopus* embryos. Altogether these data suggest that proper levels of Notch/Su(H) activity in the endoderm are required for normal PGC migration. Perturbation of this pathway may affect directionality, motility, and/or adhesion of PGCs (Morichika et al. 2010).

For the translocation of the cell body, directionally migrating cells need to interact with their environment. Unlike lamellipodia-based migration, where cells rely on adhesion to generate traction force (Giannone et al. 2007; Le Clainche and Carlier 2008), cells migrating via bleb-associated mechanism are usually characterized by a decrease in adhesive activity (Fackler and Grosse 2008). Interaction with a substrate can be achieved through weak adhesion to the surrounding cells or via the extracellular matrix. Conversely, blebbing cells can exert forces on the surrounding environment perpendicular to the direction of movement. In this latter case, a cell can squeeze itself forward without or with very little adhesion to the substrate (Charras and Paluch 2008). An important role in the motility of zebrafish PGCs has been attributed to cell–cell adhesion mediated by E-cadherin. Prior to migration, these cells express relatively high levels of E-cadherin, which is then reduced in the migratory PGCs (Blaser et al. 2005). A minimum level of this adhesion molecule is nevertheless still required, in order to generate a traction force. Zebrafish PGCs form Rac-dependent actin brushes coupled to E-cadherin at their leading edge. During blebbing, the cell appears to attach to neighboring cells by E-cadherin. Together with RhoA-dependent retrograde flow of the brushes, this generates traction force for cellular translocation. When the cell advances forward, brushes disassemble, while new ones appear at the newly formed leading edge (Kardash et al. 2010). Conversely, elevated levels of E-cadherin in the migratory cells decrease their motility (Goudarzi et al. 2012).

As mentioned earlier, active PGC migration in *Xenopus* starts after stage 24, when the cluster which these cells formed at earlier stages starts to disperse (see also Figure 10.1). In addition, PGCs also change their morphology, from a spherical and poorly blebbing to a motile elongated form (Nishiumi et al. 2005; Terayama et al. 2013). In normal *Xenopus* embryos, although PGCs migrate as a cohort, they do not form direct contacts with one another. Analysis of sectioned tailbud (stage 28–36) and early tadpole (stage 42–45) stage embryos showed that the area of contact between PGCs and somatic cells is relatively small, leaving gaps between these cells. In contrast, somatic cells surrounding PGCs, both *in vivo* and *in vitro*, exhibit a high-degree cell–cell contact formation (Kamimura et al. 1976, 1980; Heasman and Wylie 1978).

Independent observations coming from the analysis of different germ plasm-associated RNAs have suggested that regulation of cell adhesion is involved in PGC development in *Xenopus* embryos; *Xdazl* is encoded by one such maternal germ plasm mRNA. The *Xdazl* protein is a positive translational regulator which functions by direct recruitment of the poly(A)-binding protein on *Xdazl* target mRNAs (Collier et al. 2005). Maternal depletion of *Xdazl* mRNA results in a loss of PGCs at the late tailbud stages, as well as in abnormal PGC migration earlier on (Houston and King 2000b). In contrast to interference with endogenous KIF13B or XGRIP2 levels, where cells were migrating within the endoderm with aberrant direction, *Xdazl* knockdown resulted in clustering of PGCs at the early tailbud stages.

A similar phenotype was also observed upon knockdown of *Germes* and *XDeadEnd*, both encoded by the other germ plasm-associated mRNAs (Berekelya et al. 2003, 2007; Horvay et al. 2006). The predicted *Germes* protein contains two leucine zipper motifs and putative calcium-binding EF-hand domain, but does not show substantial homology to other known proteins (Berekelya et al. 2003). It colocalizes with two dynein light chains (*dlc8a* and *dlc8b*) and is suggested to regulate germ plasm formation and development. Overexpression of *Germes* results in a decrease of the average number of PGCs at the tailbud

stage (stage 33/34). Furthermore, the remaining PGCs failed to migrate laterally and were found deep in the endoderm. This phenotype might either be a direct result of *Germes*-mediated effect on cytoskeletal motor complexes in the PGCs, or an indirect one through alterations in germ plasm organization (Berekelya et al. 2007).

DeadEnd is an RNA-binding protein, shown to counteract miRNA-mediated mRNA degradation in zebrafish and *Xenopus* PGCs (Kedde et al. 2007; Kobernick et al. 2010). Knockdown of DeadEnd in *Xenopus* embryos revealed a phenotype very similar to the one observed with *Xdazl* morphants. PGCs at stages 24–25 failed to start active migration and remained clustered in the endoderm, which was followed by decrease of their number at stages 31–32 (Horvay et al. 2006). In the zebrafish, the onset of DeadEnd zygotic expression was found to correlate with the initiation of PGC blebbing and migration (Blaser et al. 2005); knockdown of this protein abolishes formation of bleb-like protrusions and PGC migration (Goudarzi et al. 2012). Interestingly, in the same study, this phenotype could be rescued by simultaneous induction of myosin contractility using MLCK, decrease of E-cadherin-mediated adhesion, and decrease of cortical rigidity, suggesting that proper regulation of these features is sufficient for restoring cell migration of PGCs in DeadEnd morphant zebrafish embryos. However, the molecular mechanisms which might link *Xdazl*, *Germes*, and *XdeadEnd* functions in the context of PGC migration in fish and frogs remain to be defined.

Similar to the cells migrating within the endoderm, PGCs isolated from *X. laevis* embryos at stages 42–45 show plasma membrane blebbing on artificial substrates (Wylie and Roos 1976; Heasman et al. 1977). Migration of PGCs at these embryonic stages *in vivo* occurs through the dorsal mesentery. When seeded on a monolayer of amphibian mesentery cells, such spherical PGCs attach to the substrate and form filopodia-like protrusions (see Figure 10.1). Similar to bleb-associated migration, translocation is mediated by the contraction of the cell body and cytoplasm being pushed forward, resulting in an elongation of the cell. Following detachment of the rear, cells return to a spherical shape upon

arrival in the new position. Similar cell shapes of PGCs were observed in sectioned embryos (Heasman et al. 1977; Heasman and Wylie 1978). Adhesion of PGCs to somatic mesentery cells was discovered to be mediated by fibronectin, a large extracellular protein which can bind to extracellular matrix components and membrane-spanning receptor proteins called integrins (Heasman et al. 1981; Pankov and Yamada 2002). Mesentery cells produce large amounts of fibronectin both *in vivo* and *in vitro*. Isolated PGCs, in contrast, do not secrete detectable quantities of fibronectin *in vitro*, but are able to adhere to fibronectin and also fibronectin-producing cells, regaining migratory and invasive ability (Heasman et al. 1981; Wylie and Heasman 1982; Brustis et al. 1984). Interestingly, fibrils of fibronectin formed by mesentery cells *in vitro* were demonstrated to be often colinear with microfilament bundles within the cells (Heasman et al. 1981; Wylie and Heasman 1982). As PGCs frequently formed filopodia-like protrusions and were elongated in the same direction as underlying cells, it was suggested that somatic cells might influence directionality of PGC migration through dorsal mesentery. For the future, it remains a major challenge to define the regulation of these events on a molecular level and to tie them to the function of the regulators of PGC development and migration in *Xenopus*, in particular the set of RNA-binding proteins that are already known to play a major role in this context.

References

- Berekelya L.A., Ponomarev M.B., Luchinskaya N.N., Belyavsky A.V. 2003. *Xenopus* *Germes* encodes a novel germ plasm-associated transcript. *Gene Expr Patterns*. 3(4):521–524.
- Berekelya L.A., Mikryukov A.A., Luchinskaya N.N., Ponomarev M.B., Woodland H.R., Belyavsky A.V. 2007. The protein encoded by the germ plasm RNA *Germes* associates with dynein light chains and functions in *Xenopus* germline development. *Differentiation*. 75(6):546–558.
- Blackler A.W. 1965. The continuity of the germline in amphibians and mammals. *Annee Biol*. 4:627–635.
- Blaser H., Eisenbeiss S., Neumann M., et al. 2005. Transition from non-motile behaviour to directed

- migration during early PGC development in zebrafish. *J Cell Sci.* 118(17):4027–4038.
- Blaser H., Reichman-Fried M., Castanon I., et al. 2006. Migration of zebrafish primordial germ cells: a role for myosin contraction and cytoplasmic flow. *Dev Cell.* 11(5):613–627.
- Boldajipour B., Mahabaleshwar H., Kardash E., et al. 2008. Control of chemokine-guided cell migration by ligand sequestration. *Cell.* 132(3):463–473.
- Bonnard C., Strobl A.C., Shboul M., et al. 2012. Mutations in IRX5 impair craniofacial development and germ cell migration via SDF1. *Nat Genet.* 44(6):709–713.
- Braun M., Wunderlin M., Spieth K., Knöchel W., Gierschik P., Moepps B. 2002. *Xenopus laevis* Stromal cell-derived factor 1: conservation of structure and function during vertebrate development. *J Immunol.* 168(5):2340–2347.
- Brustis J.J., Cathalot B., Peyret D., Gipouloux J.D. 1984. Evolution of *Xenopus* endodermal cells cultured on different extracellular matrix components. Identification of primordial germ cells. *Anat Embryol (Berl).* 170(2):187–196.
- Charras G., Paluch E. 2008. Blebs lead the way: how to migrate without lamellipodia. *Nat Rev Mol Cell Biol.* 9(9):730–736.
- Chung C.Y., Funamoto S., Firtel R.A. 2001. Signaling pathways controlling cell polarity and chemotaxis. *Trends Biochem Sci.* 26(9):557–566.
- Collier B., Gorgoni B., Loveridge C., Cooke H.J., Gray N.K. 2005. The DAZL family proteins are PABP-binding proteins that regulate translation in germ cells. *EMBO J.* 24(14):2656–2666.
- Doitsidou M., Reichman-Fried M., Stebler J., et al. 2002. Guidance of primordial germ cell migration by the chemokine SDF-1. *Cell* 111(5): 647–659.
- Dumstrei K., Mennecke R., Raz E. 2004. Signaling pathways controlling primordial germ cell migration in zebrafish. *J Cell Sci.* 117(20):4787–4795.
- Dutt P., Wang J.F., Groopman J.E. 1998. Stromal cell-derived factor-1 alpha and stem cell factor/kit ligand share signaling pathways in hemopoietic progenitors: a potential mechanism for cooperative induction of chemotaxis. *J Immunol.* 161(7):3652–3658.
- Fackler O.T., Grosse R. 2008. Cell motility through plasma membrane blebbing. *J Cell Biol.* 181(6):879–884.
- Farini D., La Sala G., Tedesco M., De Felici M. 2007. Chemoattractant action and molecular signaling pathways of Kit ligand on mouse primordial germ cells. *Dev Biol.* 306(2):572–583.
- Franca-Koh J., Kamimura Y., Devreotes P. 2006. Navigating signaling networks: chemotaxis in Dictyostelium discoideum. *Curr Opin Genet Dev.* 16(4):333–338.
- Franca-Koh J., Kamimura Y., Devreotes P.N. 2007. Leading-edge research: PtdIns(3,4,5)P3 and directed migration. *Nat Cell Biol.* 9(1):15–17.
- Funamoto S., Meili R., Lee S., Parry L., Firtel R.A. 2002. Spatial and temporal regulation of 3-phosphoinositides by PI 3-kinase and PTEN mediates chemotaxis. *Cell.* 109(5):611–623.
- Giannone G., Dubin-Thaler B.J., Rossier O., et al. 2007. Lamellipodial actin mechanically links myosin activity with adhesion-site formation. *Cell.* 128(3):561–575.
- Goudarzi M., Banisch T.U., Mobin M.B., et al. 2012. Identification and regulation of a molecular module for bleb-based cell motility. *Dev Cell.* 23(1):210–218.
- Haugh J.M., Codazzi F., Teruel M., Meyer T. 2000. Spatial sensing in fibroblasts mediated by 3' phosphoinositides. *J Cell Biol.* 151(6):1269–1280.
- Heasman J., Wylie C.C. 1978. Electron microscopic studies on the structure of motile primordial germ cells of *Xenopus laevis* in vitro. *J Embryol Exp Morphol.* 46:119–133.
- Heasman J., Mohun T., Wylie C.C. 1977. Studies on the locomotion of primordial germ cells from *Xenopus laevis* in vitro. *J Embryol Exp Morphol.* 42:149–161.
- Heasman J., Hynes R.O., Swan A.P., Thomas V., Wylie C.C. 1981. Primordial germ cells of *Xenopus* embryos: the role of fibronectin in their adhesion during migration. *Cell.* 27(3 Pt2):437–447.
- Hoeller O., Kay R.R. 2007. Chemotaxis in the absence of PIP3 gradients. *Curr Biol.* 17(9):813–817.
- Horiguchi K., Hanada T., Fukui Y., Chishti A.H. 2006. Transport of PIP3 by GAKIN, a kinesin-3 family protein, regulates neuronal cell polarity. *J Cell Biol.* 174(3):425–436.
- Horvay K., Claussen M., Katzer M., Landgrebe J., Pieler T. 2006. *Xenopus* Dead end mRNA is a localized maternal determinant that serves a conserved function in germ cell development. *Dev Biol.* 291(1):1–11.
- Houston D.W., King M.L. 2000a. Germ plasm and molecular determinants of germ cell fate. *Curr Top Dev Biol.* 50:155–181.
- Houston D.W., King M.L. 2000b. A critical role for Xdazl, a germ plasm-localized RNA, in the differentiation of primordial germ cells in *Xenopus*. *Development.* 127(3):447–456.
- Hudson C., Woodland H.R. 1998. Xpat, a gene expressed specifically in germ plasm and primordial germ cells of *Xenopus laevis*. *Mech Dev.* 73:159–168.
- Iijima M., Devreotes P. 2002. Tumor suppressor PTEN mediates sensing of chemoattractant gradients. *Cell.* 109(5):599–610.
- Iijima M., Huang Y. E., Devreotes P. 2002. Temporal and spatial regulation of chemotaxis. *Dev. Cell.* 3(4), 469–478.

- Iso T., Kedes L., Hamamori Y. 2003. HES and HERP families: multiple effectors of the Notch signaling pathway. *J Cell Physiol.* 194(3):237–255.
- Lai E.C. 2004. Notch signaling: control of cell communication and cell fate. *Development.* 131(5):965–973.
- Le Clainche C., Carlier M.F. 2008. Regulation of actin assembly associated with protrusion and adhesion in cell migration. *Physiol Rev.* 88(2):489–513.
- Kamimura M., Ikenishi K., Kotani M., Matsuno T. 1976. Observations on the migration and proliferation of gonocytes in *Xenopus laevis*. *J Embryol Exp Morphol.* 36(1):197–207.
- Kamimura M., Kotani M., Yamagata K. 1980. The migration of presumptive primordial germ cells through the endodermal cell mass in *Xenopus laevis*: a light and electron microscopic study. *J Embryol Exp Morphol.* 59:1–17.
- Kataoka K., Yamaguchi T., Orii H., Tazaki A., Watanabe K., Mochii M. 2006. Visualization of the *Xenopus* primordial germ cells using a green fluorescent protein controlled by cis elements of the 3' untranslated region of the DEADSouth gene. *Mech Dev.* 123(10):746–760.
- Katso R., Okkenhaug K., Ahmadi K., White S., Timms J., Waterfield M.D. 2001. Cellular function of phosphoinositide 3-kinases: implications for development, homeostasis, and cancer. *Annu Rev Cell Dev Biol.* 17:615–675.
- Kardash E., Reichman-Fried M., Maître J.L., et al. 2010. A role for Rho GTPases and cell-cell adhesion in single-cell motility in vivo. *Nat Cell Biol.* 12(1):47–53.
- Kedde M., Strasser M.J., Boldajipour B., et al. 2007. RNA-binding protein Dnd1 inhibits microRNA access to target mRNA. *Cell.* 131(7):1273–1286.
- King J.S., Insall R.H. 2008. Chemotaxis: TorC before you Akt. *Curr Biol.* 18(18):R864–R866.
- Kirilenko P., Weierud F.K., Zorn A.M., Woodland H.R. 2008. The efficiency of *Xenopus* primordial germ cell migration depends on the germplasm mRNA encoding the PDZ domain protein Grip2. *Differentiation.* 76(4):392–403.
- Knaut H., Werz C., Geisler R., Nüsslein-Volhard C., The Tübingen 2000 Screen Consortium. 2003. A zebrafish homologue of the chemokine receptor *Cxcr4* is a germ-cell guidance receptor. *Nature.* 421(6920):279–282.
- Koebornick K., Loeber J., Arthur P.K., Tarbashevich K., Pieler T. 2010. Elr-type proteins protect *Xenopus* Dead end mRNA from miR-18-mediated clearance in the soma. *Proc Natl Acad Sci USA.* 107(37):16148–16153.
- Komiya T., Itoh K., Ikenishi K., Furusawa M. 1994. Isolation and characterization of a novel gene of the DEAD box protein family which is specifically expressed in germ cells of *Xenopus laevis*. *Dev Biol.* 162(2):354–363.
- Maehama T., Dixon J.E. 1998. The tumor suppressor, PTEN/MMAC1, dephosphorylates the lipid second messenger, phosphatidylinositol 3,4,5-trisphosphate. *J Biol Chem.* 273(22):13375–133378.
- Meili R., Ellsworth C., Lee S., Reddy T.B., Ma H., Firtel R.A. 1999. Chemoattractant-mediated transient activation and membrane localization of Akt/PKB is required for efficient chemotaxis to cAMP in *Dictyostelium*. *EMBO J.* 18(8):2092–2105.
- Merlot S., Firtel R.A. 2003. Leading the way: directional sensing through phosphatidylinositol 3-kinase and other signaling pathways. *J Cell Sci.* 116(17):3471–3478.
- Molyneaux K.A., Zinszner H., Kunwar P.S., et al. 2003. The chemokine SDF1/CXCL12 and its receptor CXCR4 regulate mouse germ cell migration and survival. *Development.* 130(18):4279–4286.
- Morichika K., Kataoka K., Terayama K., et al. 2010. Perturbation of Notch/Suppressor of Hairless pathway disturbs migration of primordial germ cells in *Xenopus* embryo. *Dev Growth Differ.* 52(2):235–244.
- Nieuwkoop P.D., Faber J. 1994. *Normal Table of Xenopus laevis (Daudin)*. New York: Garland Publishing Inc.
- Nishiumi F., Komiya T., Ikenishi K. 2005. The mode and molecular mechanisms of the migration of presumptive PGC in the endoderm cell mass of *Xenopus* embryos. *Dev Growth Differ.* 47(1):37–48.
- Pankov R., Yamada K.M. 2002. Fibronectin at a glance. *J Cell Sci.* 115(Pt20):3861–3863.
- Servant G., Weiner O.D., Herzmark P., Balla T., Sedat J.W., Bourne H.R. 2000. Polarization of chemoattractant receptor signaling during neutrophil chemotaxis. *Science.* 287(5455):1037–1040.
- Staton A.A., Knaut H., Giraldez A.J. 2011. miRNA regulation of *Sdf1* chemokine signaling provides genetic robustness to germ cell migration. *Nat Genet.* 43(3):204–211.
- Stebler J., Spieler D., Slanchev K., et al. 2004. Primordial germ cell migration in the chick and mouse embryo: the role of the chemokine SDF-1/CXCL12. *Dev Biol.* 272(2):351–361.
- Swan L.E., Wichmann C., Prange U., et al. 2004. A glutamate receptor-interacting protein homolog organizes muscle guidance in *Drosophila*. *Genes Dev.* 18:223–237.
- Taguchi A., Takii M., Motoishi M., Orii H., Mochii M., Watanabe K. 2012. Analysis of localization and reorganization of germ plasm in *Xenopus* transgenic line with fluorescence-labeled mitochondria. *Dev Growth Differ.* 54(8):767–776.
- Takamiya K., Kostourou V., Adams S., et al. 2004. A direct functional link between the multi-PDZ domain protein GRIP1 and the Fraser syndrome protein Fras1. *Nat Genet.* 36:172–177.

- Takeuchi T., Tanigawa Y., Minamide R., Ikenishi K., Komiya T. 2010. Analysis of SDF-1/CXCR4 signaling in primordial germ cell migration and survival or differentiation in *Xenopus laevis*. *Mech Dev.* 127(1-2):146-158.
- Tarbashevich K., Koebornick K., Pieler T. 2007. XGRIP2.1 is encoded by a vegetally localizing, maternal mRNA and functions in germ cell development and anteroposterior PGC positioning in *Xenopus laevis*. *Dev Biol.* 311(2):554-565.
- Tarbashevich K., Dzementsei A., Pieler T. 2011. A novel function for KIF13B in germ cell migration. *Dev Biol.* 349(2):169-178.
- Terayama K., Kataoka K., Morichika K., Orii H., Watanabe K., Mochii M. 2013. Developmental regulation of locomotive activity in *Xenopus* primordial germ cells. *Dev Growth Differ.* 2013;55(2):217-228.
- Van Haastert P.J., Veltman D.M. 2007. Chemotaxis: navigating by multiple signaling pathways. *Sci STKE.* 346:pe40.
- Venkataraman T., Dancausse E., King M.L. 2004. PCR-based cloning and differential screening of RNAs from *Xenopus* primordial germ cells, cloning uniquely expressed RNAs from rare cells. In *Methods in Molecular Biology: Germ Cell Protocols (Molecular Embryo Analysis, Live Imaging, Transgenesis and Cloning)*, Vol. 2, edited by H. Schatten, pp. 67-78. Totowa: Humana Press.
- Wang J.F., Park I.W., Groopman J.E. 2000. Stromal cell-derived factor-1 α stimulates tyrosine phosphorylation of multiple focal adhesion proteins and induces migration of hematopoietic progenitor cells: roles of phosphoinositide-3 kinase and protein kinase C. *Blood.* 95(8):2505-2513.
- Whittington P.M., Dixon K.E. 1975. Quantitative studies of germ plasm and germ cells during early embryogenesis of *Xenopus laevis*. *J Embryol Exp Morphol.* 33(1):57-74.
- Wylie C.C., Heasman J. 1976. The formation of the gonadal ridge in *Xenopus laevis*. *J Embryol Exp Morphol.* 35(1):125-138.
- Wylie C.C., Roos T.B. 1976. The formation of the gonadal ridge in *Xenopus laevis*. III. The behaviour of isolated primordial germ cells in vitro. *J Embryol Exp Morphol.* 35(1):149-157.
- Wylie C.C., Heasman J. 1982. Effects of the substratum on the migration of primordial germ cells. *Philos Trans R Soc Lond B Biol Sci.* 299(1095):177-183.
- Wylie C.C., Heasman J. 1993. Migration, proliferation, and potency of primordial germ cells. *Semin Dev Biol.* 4(3):161-170.
- Yoo S.K., Deng Q., Cavnar P.J., Wu Y.I., Hahn K.M., Huttenlocher A. 2010. Differential regulation of protrusion and polarity by PI3K during neutrophil motility in live zebrafish. *Dev Cell.* 18(2):226-236.

11

Development of Gonads, Sex Determination, and Sex Reversal in *Xenopus*

Rafał P. Piprek¹ & Jacek Z. Kubiak²

¹Department of Comparative Anatomy, Institute of Zoology, Jagiellonian University, Kraków, Poland

²CNRS and University of Rennes 1, Institute of Genetics & Development of Rennes (IGDR), UMR 6290, Faculty of Medicine, Rennes, France

Abstract: In *Xenopus*, the gonadal ridges, i.e., presumptive gonads, appear at a feeding tadpole stage. Such undifferentiated gonads have a potential to form either testis or ovary. During the larval period of life, the molecular machinery driven by sex-determining genes establishes the gonadal sex of previously sexually undifferentiated anlagen and reinforces structural and functional changes resulting in the formation of sexually differentiated gonad. Here, we overview these processes focusing on *Xenopus laevis* but also referring to other anuran species.

Origin and structure of undifferentiated gonad

The studies of various anuran species – *Xenopus laevis*, *Rana sylvatica*, *Rana pipiens*, *Rana nigromaculata*, *Rhacophorus arboreus*, and *Bombina variegata* – show that frogs and toads have very similar general pattern of gonad development. However, there are also important interspecific differences in the timing of sexual differentiation, metamerization, and formation of the gonadal medulla (Merchant-Larios and Villalpando 1981; Iwasawa and Yamaguchi 1984; Tanimura and Iwasawa 1988, 1989; Piprek et al. 2010).

The gonads are composed of somatic and germ cells. The germ cells derive from the primordial germ cells (PGCs) that originate in

the endoderm. They migrate via dorsal mesentery toward the ventral surface of the mesonephroi where the genital ridges form. PGCs move by extruding a single filopodium. The contact guidance is important in this process. The orientation of extracellular matrix over which the PGCs migrate dictates the direction of migration (Wylie et al. 1979), and the interference (by using exogenous antibodies) with the function of the important component of the extracellular matrix, fibronectin, impairs both the adhesion and migration of PGCs (Heasman et al. 1985). This indicates that the contact with fibronectin is crucial for PGCs' migration. Moreover, chemokine SDF-1 (stromal cell-derived factor-1, CXCL12) and its receptor CXCR4 are involved in the migration guidance and survival as well as in the

differentiation of PGCs in *Xenopus*, zebrafish, chicken, and mouse (Takeuchi et al. 2010). SDF-1 protein is present on the cell surface of dorsal mesentery and the genital ridges, while its receptor CXCR4 is expressed on PGCs. The knockdown of CXCR4 results in decreased number of PGCs reaching the genital ridges, whereas the ectopic expression of SDF-1 in PGCs leads to their erroneous localization (Takeuchi et al. 2010). During the migration, PGCs undergo proliferation. They divide about three times, and approximately 30 PGCs colonize the forming genital ridge in *Xenopus* and other anuran species (Whittington and Dixon 1975; Wylie and Heasman 1993). The PGCs invade the genital ridges one by one (*Xenopus*) or in groups (*R. pipiens*) (Merchant-Larios and Villalpando 1981).

The genital ridges form when the PGCs migrating from the gut reach their target location at the ventral surface of the mesonephroi. In all species studied so far, the first morphologically recognizable sign of gonad formation is two longitudinal folds of coelomic epithelium (*mesothelium*) running under mesonephroi along both sides of the dorsal mesentery that suspends the gut (Figure 11.1A) (Witschi 1929; Wylie et al. 1976; Piprek et al. 2010). The formation of genital ridges takes place in the period when tadpoles begin feeding, i.e., at Nieuwkoop and Faber (NF) stage 46 in *Xenopus* (Whittington and Dixon 1975; Wylie et al. 1976; Houston et al. 1998; Houston and King 2000) and at Gosner stage 25 in other anuran species.

In the forming genital ridges, the PGCs undergo important transformation. They round up and lose the filopodia as well as the ability to migrate (Figure 11.1A). Subsequently, desmosomal connections form between the germ and epithelial cells that cover the genital ridges (Wylie et al. 1976). Concomitantly, the size of germ cell diminishes due to the loss of yolk. From the moment of the loss of yolk and the ability to migrate, the germ cells are termed gonia or gonial cells (Witschi 1929; Ogielska 2009). According to other authors, all germ cells until sexual differentiation of gonads into testes or ovaries are termed PGCs (Villalpando and Merchant-Larios 1990).

Germ cells of the genital ridge lie on the epithelial monolayer (gonadal superficial

epithelium) continuous with coelomic epithelium composed of squamous cells (*mesothelium*) (Wylie et al. 1976). Epithelial cells in the region of genital ridges undergo intense proliferation, become cuboidal and tightly packed. Concomitantly, the genital ridges grow and form the primordial gonads (Figure 11.1A). The somatic cells surrounding the primordial gonad together with enclosed germ cells constitute the gonadal cortex that is underlined by a basal lamina (Merchant-Larios and Villalpando 1981) (Figure 11.2). In the center of the primordial gonad the primary cavity forms. This cavity is invaded by somatic cells, which proliferate to form gonadal medulla. The medulla remains sterile because germ cells are located only in the cortex (Figure 11.1B). The medullar cells derive from the proliferating epithelium that covers the gonad. They cross through the interrupted basal lamina, gather, and form the medulla knots that are located metamerically along the gonad. The number of gonadal metameres (gonomeres) depends on the species; *X. laevis* gonad contains about 14 gonomeres (Chang and Witschi 1956). In genus *Bombina*, the medulla is absent within the undifferentiated gonads and form during the ovarian differentiation (Lopez 1989; Piprek et al. 2010). Earlier studies suggested that medullar cells originate from the mesonephros (Swingle 1926; Witschi 1929, 1956; Christensen 1930; Cheng 1932; Rugh 1951; Lopez 1989) or from the interrenal blastema, i.e., the presumptive interrenal glands (Vannini and Sabbadin 1954; Nieuwkoop and Faber 1967), but majority of later studies indicate that the gonadal medulla originates from proliferating coelomic epithelium surrounding the gonad (Merchant-Larios 1979; Merchant-Larios and Villalpando 1981; Iwasawa and Yamaguchi 1984; Tanimura and Iwasawa 1988, 1989; Falconi et al. 2004).

The processes of proliferation and cell migration result in the formation of the undifferentiated gonad composed of the peripherally located cortex containing germ cells and central medulla (Figure 11.2). The gonadal cortex and medulla are underlined by their own basal laminae. The cortex and medulla are separated by the stromal space, which becomes occupied by melanophores, blood vessels, and mesonephros-derived somatic

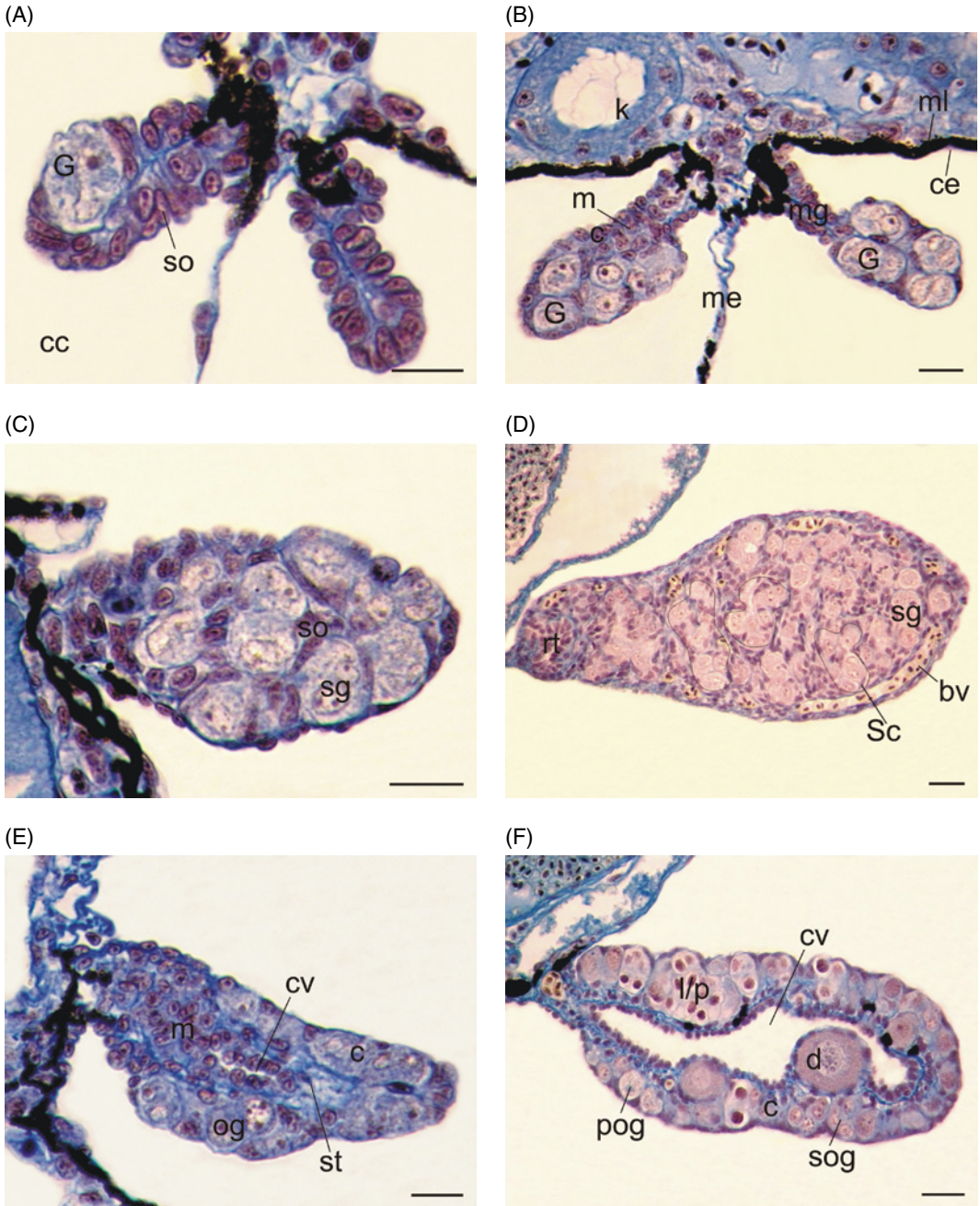


Figure 11.1 The development of gonads in *X. laevis*. (A) The genital ridges at NF stage 49. One germ cell (G) surrounded by small somatic cells (so) and coelomic cavity (cc) are visible on the cross section of the gonad. (B) The undifferentiated gonads at NF stage 50. The superficial epithelium of the gonad remains continuous with the coelomic epithelium (ce), and together with the germ cells forms the gonadal cortex (c). The dorsal mesentery (me) is located between the gonads and black melanophores (ml) form a layer at the ventral surface of the kidneys (k). The gonadal mesentery (mesogonium, mg), the gonadal medulla (m). (C) The early testis at NF stage 53. The spermatogonia (sg) are surrounded by flattened somatic cells (pre-Sertoli cells; so) with crescent-shaped nuclei. This is the beginning of the formation of testis cords. (D) The testis at NF stage 66. The testis is filled with numerous tubule-shaped testis cords (three of these cords are encircled) consisting of spermatogonia (sg) enclosed by Sertoli cells (Sc). Rete testis (rt) and blood vessels (bv) are visible. (E) The early ovary at NF stage 53. The germ cells (oogonia; og) are located in the cortex (c). The medulla (m) remains sterile and its cells disperse forming the secondary cavity (cv). Cells deriving from the mesonephroi immigrate to the stromal space (st) of the gonad, i.e., between the cortex and medulla. (F) In the NF stage 63 ovary, the cortex (c) is the dominant part of the gonad. The extensive secondary cavity (cv) lined with the somatic cells of the gonadal medulla is located in the center of the ovary. Primary and secondary oognia (pog, sog) as well as oocytes in prophase (leptotene and pachytene, l-p; diplotene, d) are visible. Picroaniline and Debreuil staining. Scale bar is equal to 20 μ m. To see a color version of this figure, see Plate 30.

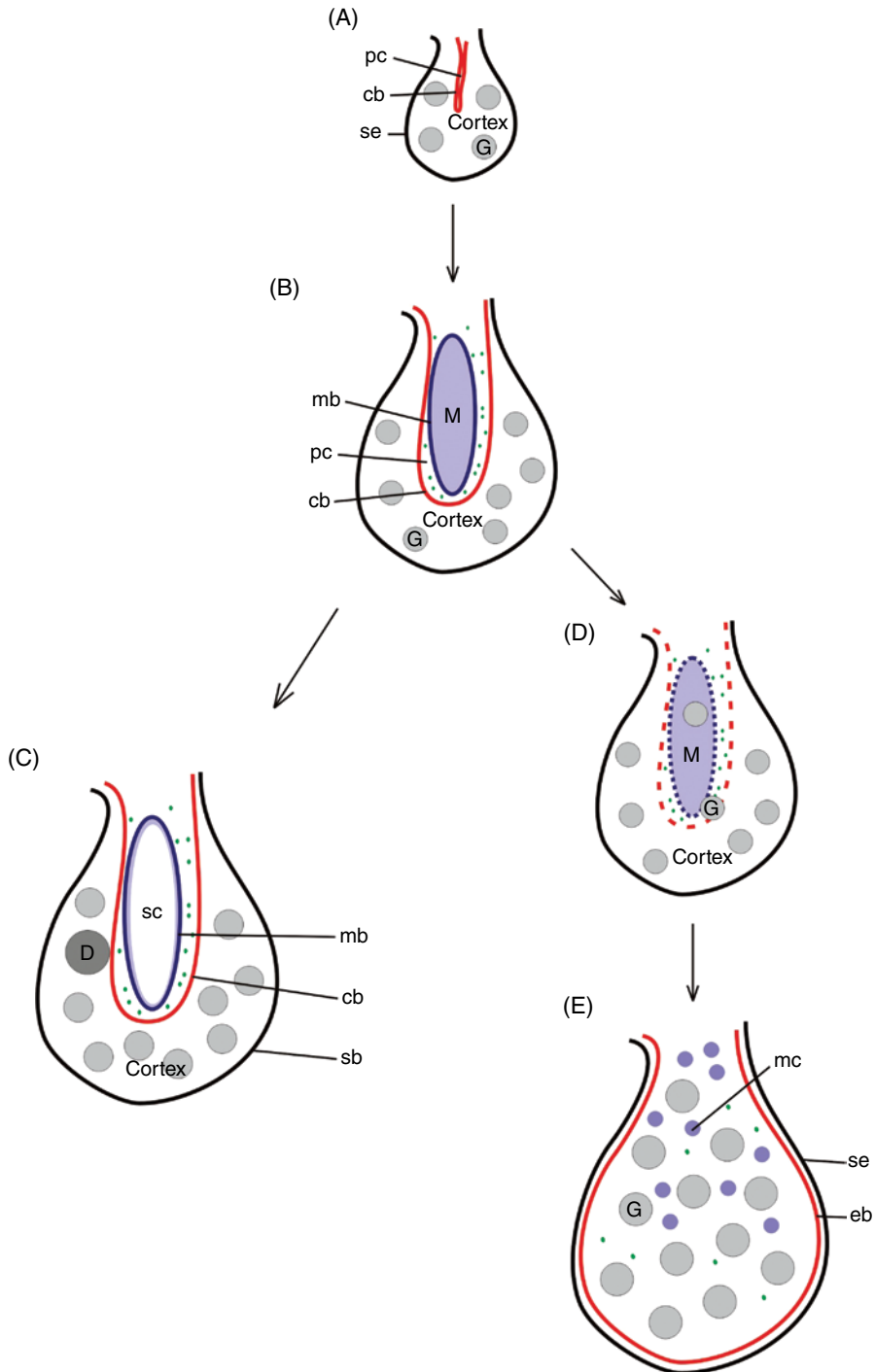


Figure 11.2 The gonadal development in anuran amphibians. (A) The genital ridge (NF stage 49 in *X. laevis*) is composed of germ cells (G) that together with superficial epithelium (se) form the cortex. The cortex is based on the basal lamina (cb) that encloses the gonadal primary cavity (pc). (B) In the undifferentiated gonad (NF stage 51), the germ cells (G) are located only within the cortex. The central region of the gonad is the medulla (M). The basal lamina of the medulla (mb) and the basal lamina of the cortex (cb) are also visible. (C) During the ovary differentiation (starting from NF stage 53 in *X. laevis*), the germ cells remain in the cortex, and the basal laminae between the cortex and medulla are maintained. The cells within medulla disperse and thus the ovarian secondary cavity (sc) forms in the medulla. (D) During the testicular differentiation (NF stage 52 in *X. laevis*), the basal laminae of the gonadal cortex and medulla disintegrate and the fusion of the cortex and medulla occurs; the germ cells disperse within the gonads. (E) In the testes the germ cells and somatic cells, including the medullar cells (mc), are evenly distributed; the basal lamina of the superficial epithelium (eb) is rebuilt and the epithelium is sterile. All germ cells in larval testes are spermatogonia.

cells, which give rise to the precursors of steroidogenic cells (Leydig and *theca* cells) and connective tissue of the gonads.

In the undifferentiated gonads in *Xenopus*, the germ cells gather in the medial (central) part, leaving the anterior and caudal regions of the undifferentiated gonad germ cell-less. As a result, the medial part forms the proper gonad, and the anterior part (progonad) grows and differentiates into the fingerlike fat body, whereas the posterior part (epigonad) forms a small and sterile appendage (Witschi 1929; Ogielska 2009). The absence of germ cells in the anterior part of the genital ridge plays a key role in the formation of the fat body; the total depletion of germ cells within the entire genital ridge in *X. laevis* results in the transdifferentiation of the sterile gonad into the adipose tissue (Piprek et al. 2012a). In *Xenopus*, the cells of the fat body, which is the main adipose frog tissue, express the adipose differentiation-related protein fatvg (Chan et al. 2001).

Sexual differentiation of the gonads

The sexual differentiation of the gonads is a process in which highly important differences in the gonadal structure appear allowing testes and ovaries to become distinguishable from each other (Figure 11.1C and E). The earliest studies showed that during the differentiation of the testis, the germ cells migrate from the cortex into the gonadal medulla, whereas in the ovaries, these cells remain in the cortex (Witschi 1929). Thus, the differentiation of the male gonads requires germ cell translocation across basal laminae that separate the cortex and medulla. The sex-specific distribution of germ cells within the gonads is regulated by sex determination pathways. Although mechanisms operating in these pathways remain unknown, we can hypothesize that the regulation of the cell-cell contacts, crossing through basal laminae, and possibly guidance by chemoattraction are involved in the sexual differentiation of the gonads.

The appearance of the very first signs of sexual differentiation of the gonad correlates with the differences in the distribution of laminins, which are the component of basal lamina. During the testicular differentiation, laminins

become distributed over the entire gonad and afterward gather around the forming testis cords (El Jamil et al. 2008a). In the ovaries, like in the undifferentiated gonad, laminins are maintained between the cortex and medulla. This shows that the distribution of laminins is sex specific and reflects the structural changes occurring during gonad differentiation. Thus, the pattern of laminin distribution can be used as an early marker of gonadal sex. There are several distinct modes of gonad differentiation in anurans:

- (1) The differentiated type – when undifferentiated gonad differentiates and transforms directly into either the testis or ovary (*Xenopus* and *Bombina*; Gramapurohit et al. 2000; Saidapur et al. 2001; Piprek et al. 2010).
- (2) The undifferentiated type – when undifferentiated gonad develops into the ovary or remains undifferentiated and then differentiates into testes (*Pelophylax esculentus*, *Rana ornativentris*, and *Bufo bufo*; Gramapurohit et al. 2000; Saidapur et al. 2001).
- (3) The semidifferentiated type – when gonads first differentiate into ovaries and then in the genetic males the ovaries transdifferentiate into the testis through degeneration of oocytes and formation of the seminiferous tubules (*R. ornativentris*, *Rana catesbeiana*, *Rana japonica*, *R. nigromaculata*, *Rhacophorus schlegelii*, and *Rana curtipes*; Iwasawa 1959, 1960; Hsu and Wang 1981; Gramapurohit et al. 2000; Ogielska 2009).

Studies on *Silurana tropicalis* (El Jamil et al. 2008a) and *Bombina variegata* (Piprek et al. 2010) showed that independently of the sex, the gonadal development progresses from the anterior to the posterior end of the gonad. The earliest signs of sexual differentiation of the gonad are first visible in its anterior part and subsequently in the central part. While gonadal sex is already visibly established in the anterior part, the posterior part of the gonad still remains undifferentiated.

In *X. laevis*, the gonadal sex becomes morphologically distinguishable between NF stages 52 and 53 (Villalpando and Merchant-Larios

1990). In *S. tropicalis*, the first signs of sexual differentiation of gonads are recognizable between NF stages 48 and 51 (El Jamil et al. 2008a). That shows allochronic differences in gonadal development among anuran species. Significant differences in the rate of the gonadal development among anuran amphibians underlie structural diversity of developing gonads.

Development of testis

The testicular differentiation begins when the basal laminae between the cortex and medulla disintegrate. This leads to the fusion of the cortex and medulla and dispersion of the germ cells within the differentiating male gonad (Figures 11.1C and 11.2). In *X. laevis*, the sexual differentiation of gonads takes place at about NF52 stage. In early testes, the germ cells are evenly distributed within the whole organ. After the dispersion of the germ cells, the superficial epithelium is sterile, does not contact with the germ cells, and transforms into the *tunica albuginea* that encloses the testes (Falconi et al. 2004; Piprek et al. 2010). Just after sexual differentiation of gonads, the whole testis loses metamorphosis, shortens, and becomes ovoid. The germ cells within the testis are surrounded by somatic cells. These supporting cells, termed pre-Sertoli cells, derive from the proliferating superficial epithelium of the gonad. The agglomerates of the pre-Sertoli and germ cells grow and elongate forming the testis cords (Figure 11.1C and D). Differentiating Sertoli cells create a microenvironment for enclosed spermatogonia regulating their proliferation and differentiation. During the completion of metamorphosis, the lumen appears in the center of the testis cords, and thus, they become the seminiferous tubules. The testis cords and later the seminiferous tubules elongate, and their diameter increases due to the proliferation of somatic and germ cell (Figure 11.1D). The seminiferous tubules become connected with the sterile tubules located in the center of the testis termed *rete testis* through which the sperm is transported to the kidney tubules.

The space between the seminiferous tubules is occupied by the interstitial tissue composed of steroidogenic Leydig cells, fibroblasts, and

blood vessels. It has been suggested that in juvenile frogs, the Leydig cells differentiate from mesonephric cells that immigrated to the differentiating gonad (Hsu and Wang 1981). The Leydig cells are responsible for the production of male sex hormones such as testosterone (T), 5 α -dihydrotestosterone (DHT), and androstenedione (A4) in differentiated gonad; however, the production of sex hormones starts before sexual differentiation of the gonad in the extragonadal locations. In *X. laevis* tadpole, androgens can be detected as early as NF stage 47 when the level of the steroidogenesis enzyme Δ 5-3 β -HSD is highest in the interrenal glands that are homologue of the cortex of mammalian adrenal glands. Thus, the steroid production in tadpoles begins before the sexual differentiation of the gonads; however, the massive steroidogenesis occurs in the gonads at NF stage 53 (Kang et al. 1995). Thus, the steroidogenesis in the gonads begins during the onset of sexual differentiation and continues in the differentiated testes and ovaries. The role of steroid hormones in sex-determining gene expression remains obscure.

Spermatogenesis

The earliest germ cells in the male gonads are primary spermatogonia that have lobular nuclei. In the developing testes, spermatogonia are enclosed by the pre-Sertoli cells and form the testis cords (Figure 11.1C and D). Primary spermatogonia are mitotically active, and after several rounds of mitosis, they divide by incomplete cytokinesis giving rise to the cyst of secondary spermatogonia connected by cytoplasmic bridges. In some anurans (*Pachymedusa dacnicolor*, *Rana lessonae*, *Rana ridibunda*, *Rana esculenta*, *Rana cyanophlyctis*), there are two types of primary spermatogonia distinguished on the basis of their staining with hematoxylin and eosin: the pale and the dark (Ogielska and Bartmanska 2009a). The pale spermatogonia have homogeneous chromatin in their nuclei and pale cytoplasm. They function as stem cells and serve as a permanent source of spermatogonia. Dark spermatogonia are smaller, have dark cytoplasm and heterochromatin-rich nuclei, and

are destined to become secondary spermatogonia. The first meiotic divisions and therefore the appearance of the earliest spermatocytes in *X. laevis* occur 2–3 months after metamorphosis (Witschi 1971). In *X. laevis*, there are approximately 256 (2^8) primary spermatocytes within one cyst, which implies that each secondary spermatogonium undergoes eight or sometimes six or seven mitotic divisions (Takamune et al. 1995). In *X. laevis*, the meiotic division (from the entry into prophase until the end of the second meiotic division) lasts 24 days, and the formation of spermatozoa (sperm; spermiogenesis) lasts 12 days (Kalt 1976). After the formation of spermatozoa, the wall of the cyst disrupts and the sperm are freed into the lumen of seminiferous tubules and are transported outside via tubules of *rete testis*, the kidney tubules and ureter.

First spermatozoa are usually encountered in 1-year-old frogs after the first hibernation, but in some species, especially in tropical anurans such as *Xenopus*, the first sperm may appear as early as 6 months after metamorphosis (Mikamo and Witschi 1963), while in *S. tropicalis*, the reproductive maturity and sperm were detected 39 weeks postfertilization, i.e., about 9 months after metamorphosis (Olmstead et al. 2009).

Development of ovary

The developing ovary is composed of the cortex and centrally located medulla (Witschi 1929). The germ cells are located within the cortex and the ovarian medulla is sterile (Figures 11.1E and 11.2). As in the undifferentiated gonads, the ovarian medulla is located within the primary cavity of the gonads. The cells within the medulla spread, resulting in the formation of the secondary ovarian cavity in the center of the ovary (Figure 11.1E and F). Because the ovarian cavity forms in each gonadal metamere (gonomere), the ovary becomes visibly metameric. The germ cells present in the ovarian cortex are surrounded by somatic cells derived from the superficial epithelium. The somatic cells surrounding germ cells flatten and differentiate into prefollicular cells. *Xenopus* ovary has thin cortex, which is characteristic for species with many

ovarian lobules (in *Xenopus* 14–15 lobules are present in the ovary). These ovarian lobules are well visible in juvenile females and are less distinct in adults (Ogielska and Bartmanska 2009b).

Mesenchymal cells deriving from the mesonephroi gather around the germ cells surrounded by follicular cells and form *theca interna*, the structure that synthesizes testosterone. *Theca interna* in the ovary shares the origin (mesonephroi) and function (testosterone synthesis) with the Leydig cells in the testes; thus, these two cell lineages are homologues. In the ovaries, the follicular cells produce aromatase enzyme that converts testosterone (T) to estradiol (E2 or 17 β E). The level of aromatase expression is low at the time of the genital ridge formation (i.e., NF stage 48) and increases starting from NF stage 50 to reach the peak at NF stage 52 (the sex-determining period). The level of aromatase decreases at NF stage 54 when the gonadal sex has been established (Iwabuchi et al. 2007). This pattern of aromatase expression indicates that a peak of estradiol production coincides with the period of sex determination suggesting an important role of sex steroids in sex determination.

Oogenesis

Primary oogonia are descendants of PGCs in the ovaries. Each primary oogonium (cystoblast) divides four times by incomplete cytokinesis giving rise to the cyst or nest of 16 secondary oogonia (cystocytes) connected by cytoplasmic bridges (Kloc et al. 2004). Each nest is surrounded by somatic (prefollicular) cells (Kloc et al. 2004) (Figure 11.1F). After entering into prophase of I meiotic division, the secondary oogonia become the oocytes and prefollicular cells invade the space between oocytes breaking cytoplasmic bridges and separating oocytes. At the end of this process, each oocyte becomes surrounded by the layer of follicular cells.

The oocytes appear already during tadpole development as early as NF stage 55. Oocytes of anurans proceed through the leptotene, zygotene, and pachytene of the first meiotic prophase and become arrested in long diplotene

phase until ovulation (Figure 11.1F). Diplotene oocyte growth phase (accumulation of yolk and size increase) is customarily divided into six stages: stages I and II (previtellogenesis) and stages III–VI (vitellogenesis) (Dumont 1972). The adult ovary is composed of asynchronously growing diplotene oocytes of various sizes (stage I to stage VI) (Dumont 1972).

The thickness of ovarian cortex depends on the size and number of oocytes and the age and annual cycle of the female (Ogielska and Bartmanska 2009b). Oogonia are restricted to the outermost part of the cortex. The oocytes are arranged in the gradient from the smallest in the external part of the cortex to the largest positioned next to the ovarian cavity.

Upon ovulation, the oocytes covered by follicular cells are freed into the coelomic cavity and then are caught by the ostia of the oviducts.

Sex determination

In *X. laevis*, the males are homogametic (ZZ), whereas the females are heterogametic (ZW). The ZZ/ZW sex-determining system in *X. laevis* was demonstrated by backcrossing sex-reversed and normal individuals (Chang and Witschi 1956) and showing that the ZZ neofemales mated with ZZ males gave 100% ZZ male progeny. However, the identity of genes driving gonadal development remained unknown for a long time. The quest for identification of sex-determining genes led to the discovery of several sex-linked markers. Malic enzyme (malate dehydrogenase) is a sex-related gene in *X. laevis* and some other anuran species such as *R. pipiens* and *Rana brevipedata* (Graf 1989; Sumida and Nishioka 1994; Eggert 2004). In addition, 17 sex-linked amplified fragment length polymorphisms (AFLPs) were identified in the genome of *S. tropicalis* (Olmstead et al. 2010).

The turning point in the understanding of the sex determination in *X. laevis* was the finding of the female sex-determining gene (Yoshimoto et al. 2008). This W-linked *DM-W* gene responsible for ovary development is a paralogue of *Dmrt1* autosomal gene that encodes a transcription factor key in male sex determination and/or testis development in

vertebrates (Ferguson-Smith 2007). In chicken, the Z-linked DMRT1 factor participates in male sex determination similarly to its Y-linked homologue *DMY/dmrt1bY* in the teleost fish medaka. In *X. laevis*, *DM-W* is expressed only transiently during sex determination period (NF stages 48–52) exclusively in ZW gonads (Yoshimoto et al. 2008). The onset of *DM-W* expression takes place at NF stage 48 (onset of the genital ridge formation), the peak of *DM-W* expression is observed at NF stage 50, and *DM-W* expression ceases at NF stage 53 (onset of sexual differentiation of gonads). At NF stage 53, there is upregulation of expression of another gene *Dmrt1* in both ZZ and ZW gonads with stronger expression in ZZ gonads, which may indicate initiation of testicular development (Figure 11.3). The gonads of transgenic ZZ tadpoles carrying exogenous *DM-W* developed an ovarian cavity and primary oocytes indicating sex reversal and stressing the role of *DM-W* as the primary female sex-determining gene in *X. laevis* (Yoshimoto et al. 2008).

The gonads of ZZ transgenic tadpoles carrying exogenous transgene *DM-W* showed not only ovarian structure and oogenesis but also ovarian-specific upregulation of two other genes, *Foxl2* and *Cyp19*, immediately after sex-determining period (Okada et al. 2009). *Cyp19* encodes P450 aromatase converting androgens into estrogens and thus is engaged in the female sex differentiation. A forkhead transcription factor, *Foxl2*, is involved in ovarian development and can also enhance expression of aromatase gene in teleosts and mammals (Pannetier et al. 2006; Wang et al. 2007; Yamaguchi et al. 2007). Thus, *DM-W* may initiate ovarian differentiation by inducing/enhancing *Foxl2*, which upregulates *Cyp19*, increases the level of estrogens, and orchestrates transformation of the undifferentiated gonads into the ovaries.

The *DM-W* and *DMRT1* proteins colocalize in the somatic cells surrounding germ cells (prefollicular cells) in ZW *X. laevis* gonads during sex determination period (Yoshimoto et al. 2010). Experiments with *Dmrt1*-driven luciferase reporter system revealed that *DM-W* dose-dependently antagonized the transcriptional activity of *DMRT1*. The knockdown of *DM-W* resulted in the formation of gonad with

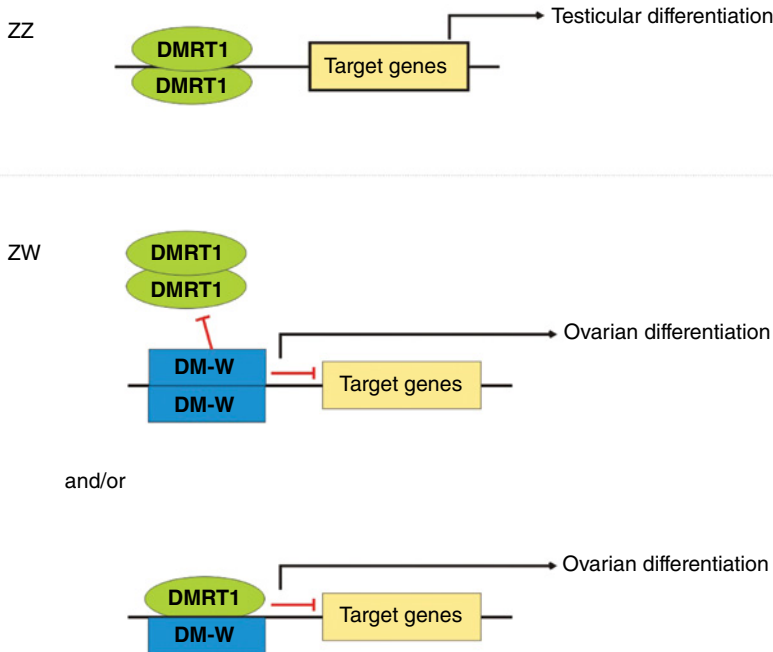


Figure 11.3 The molecular mechanism of sex determination that takes place in the supporting cells of undifferentiated gonads in *X. laevis*. In the ZZ gonads DMRT1 is expressed in the somatic cells of the developing gonads and as a homodimer induces the testicular differentiation. In the ZW gonads *DM-W* gene is expressed in the flattened somatic cells that enclose the germ cells. Hypothetically, the *DM-W* homodimerization or *DM-W*/DMRT1 heterodimerization leads to the repression of the testicular differentiation and development of the ovary.

testicular structure and development of few ZW frogs into males. However, ectopic *DMRT1* expression induced testicular differentiation in ZZ individuals (Yoshimoto et al. 2010). This indicates that antagonistic interactions between *DM-W* and *DMRT1* are responsible for development of opposite sexes in *X. laevis* (Figure 11.3). In ZZ gonads, *DMRT1* probably regulates the expression of the genes driving testicular differentiation, whereas in ZW gonads, *DM-W* interferes with the *DMRT1* action and enhances estrogen production. *DM-W* might compete with *DMRT1* for the target gene in ZW undifferentiated gonads during sex determination and induce ovary formation. Alternatively, a *DM-W*/*DMRT1* heterodimer may bind the *DMRT1* target sequence leading to its transcriptional repression.

It has been suggested that *DM-W* evolved from *Dmrt1* as a dominant-negative type gene for the ZZ/ZW-type system, which is an example of a “neofunctionalization” (Yoshimoto et al. 2010). DNA binding domains of *DM-W* and *DMRT1* proteins share high amino acid

sequence identity (89%); however, their transactivation regions show no significant sequence similarity (Yoshimoto et al. 2008).

Genomic analysis demonstrated that *DM-W* originated from *Dmrt1* after separation of *Xenopus* and *Silurana* lineages but before divergence of *X. laevis* and *X. clivii*, so this gene is not found in *S. tropicalis* (Bewick et al. 2011). The sex-determining system in *S. tropicalis* and other anurans remains unknown. In the frog *Rana rugosa*, *Dmrt1* is not expressed in the undifferentiated gonad or the ovary, but its expression was observed in the Sertoli and interstitial cells in the testes (Shibata et al. 2002, Aoyama et al. 2003). This indicates that *DMRT1* plays an important role in sex determination in other than *X. laevis* species and points to the diversity of molecular regulation mechanisms of sex determination in anurans. Interestingly, because of allotetraploidy, *X. laevis* has two *Dmrt* genes: *Dmrt1 α* and *Dmrt1 β* .

SOX9 is another key transcription factor crucial for the male sex determination in many vertebrates such as teleosts, reptiles, chicken,

and mammals (Piprek 2009). The sex-determining role of *Sox9* in amphibians has not been proven. In *X. laevis*, RT-PCR analysis showed that *Sox9* is expressed in the gonads of both sexes, which indicates that in *Xenopus*, in contrast to other vertebrates, *Sox9* expression is not male-specific (Takase et al. 2000). However, the immunolocalization study in *S. tropicalis* indicated the different localization of SOX9 in the cells of testes and ovaries: the SOX9 was found in both male and female gonads, in the nuclei of Sertoli cells in the developing testes, in the cytoplasm of previtellogenic oocytes, and in the nuclei of vitellogenic oocytes in the ovaries (El Jamil et al. 2008b). This suggests different roles for SOX9 in the developing testes and previtellogenic and vitellogenic oocytes.

Sex reversal

Numerous experiments have shown that epigenetic factors can override the genetic sex determination in amphibians (Table 11.1) (Eggert 2004). Estradiol may cause feminization and testosterone may cause masculinization of the gonad dependent on the species (Wallace et al. 1999; Piprek et al. 2012b). *X. laevis* tadpoles grown in the presence of 50 µg/L of estradiol from the onset of feeding until metamorphosis all become females. Estradiol leads to ovarian development and feminization by inhibition of cortex and medulla fusion and germ cell dispersion that are characteristic for testicular differentiation. Interestingly, there is a sensitivity period during which exogenous estradiol is able to alter sexual differentiation of gonads (Chang and Witschi 1956; Villalpando and Merchan-Larios 1990; Piprek et al. 2012b). This period is restricted to about 1 week in the middle of the larval period, about 3 weeks after the onset of tadpole feeding. In *X. laevis*, NF stage 50–52 gonads treated with estradiol undergo conversion from testicular to ovarian development. Complete feminization requires about 9 days of estradiol treatment (Miyata et al. 1999).

Estradiol causes complete sex reversal (one-sex progeny) in *X. laevis* when administered before sexual differentiation of the gonad

(Villalpando and Merchant-Larios 1990). However, when the hormones are applied during sexual differentiation (NF stages 52–54), they cause partial sex reversal, i.e., hermaphroditism (intersex gonads). Subsequent exposure to testosterone reverses the process of feminization. However, hormones have no impact when administered after sexual differentiation of the gonads.

Endogenous steroids are crucial for the gonadal development in *Xenopus*, which is corroborated by observation of animals exposed to atrazine – a potent endocrine disruptor and one of the most commonly used pesticides (Table 11.1). Atrazine depletes synthesis of testosterone and enhances estrogen production. Due to the disturbed balance between these hormones, atrazine exposure results in gonadal malformations including hermaphroditism, males with multiple testes (single-sex polygonadism, SSP), complete feminization, reduced testicular volume due to decreased number of germ and somatic cells, demasculinization (chemical castration), and testicular oogenesis (Hayes et al. 2006). The genetic males (ZZ) exposed to atrazine can develop into functional females that mate with unexposed males and produce viable eggs (Hayes et al. 2010). The effects occur at atrazine concentration as low as 0.1 ppb (µg/L), i.e., lower than normally encountered in unpolluted environment. Thus, the endocrine disruptor pollutants may influence sexual development of amphibians by androgen/estrogen balance disruption, which may contribute to the amphibian decline.

The effect of ethynylestradiol, a synthetic estrogen and another environment pollutant, on gonadal development of *S. tropicalis*, was described by Pettersson et al. (2006). The exposure to ethynylestradiol caused female-biased phenotypic sex ratios in juveniles and adults (Table 11.1). Among 9-month-old frogs, 97% had ovaries and were sexually matured. Other environmental pollutants are synthetic androgens such as trenbolone that is commonly used in the cattle industry. Exposure of *S. tropicalis* tadpoles to 17β-trenbolone at such low concentrations as 78 ng/L caused a significant shift of sex ratio toward males (Olmstead et al. 2012). The hermaphroditic

Table 11.1 Compounds disrupting sexual development in anurans.

Compound	Compound properties	Effect on gonadal sex	Species	References
17 β -Estradiol	Female sex hormone	Male-to-female sex reversal	<i>X. laevis</i> <i>S. tropicalis</i>	Chang and Witschi (1956); Villalpando and Merchant-Larios (1990); Piprek et al. (2012b)
Ethinylestradiol	Synthetic oestrogen	Male-to-female sex reversal	<i>S. tropicalis</i>	Pettersson et al. (2006)
17 β -Trenbolone	Synthetic androgen	Female-to-male sex reversal	<i>S. tropicalis</i>	Olmstead et al. (2012)
Atrazine	Sex steroid production disruptor	Male-to-female sex reversal, demasculinization	<i>X. laevis</i>	Hayes et al. (2006); Hayes et al. (2010)
Fadrozole	Aromatase inhibitor (decrease of oestrogens)	Female-to-male sex reversal	<i>S. tropicalis</i>	Olmstead et al. (2009)
Finasteride	5 α -reductase inhibitor (decrease of Dihydrotestosterone (DHT))	Male-to-female sex reversal	<i>S. tropicalis</i>	Duarte-Gúterman et al. (2009)
Ammonium perchlorate	Thyroid hormone disruptor	Female-to-male sex reversal	<i>X. laevis</i>	Goleman et al. (2002)
Triiodothyronine (T ₃)	Thyroid hormone	Increase of aromatase and 5 α -reductase expression, direct effects on gonad development was not analyzed	<i>S. tropicalis</i>	Duarte-Gúterman et al. (2010)

gonads were composed of the well-developed cortex and medulla, both containing germ cells. Olmstead et al. (2009) tested also the effect of fadrozole, i.e., the aromatase and thus estrogen synthesis inhibitor, at concentration of 1–64 µg/L on gonadal development in *S. tropicalis*. The highest concentrations (above 16 µg/L) caused complete masculinization of all tadpoles and all neomales had normal sperm number and were undistinguished from control males. Lower fadrozole concentrations caused bias in sex ratio toward males, intersex and female reproductive impairment. These results prove the role of estrogens in gonadal differentiation in this species. Duarte-Guterman et al. (2009) showed the influence of finasteride, i.e., the blocker of 5-reductase that transforms testosterone into very active form dihydrotestosterone (DHT), on gonad differentiation and gene expression in *S. tropicalis* (Table 11.1). The inhibition of DHT synthesis with finasteride caused bias of sex ratio toward females, intersex occurrence, and inhibition of ovarian gene expression such as reductase genes. This indicates that DHT is key androgen for male sex development in amphibians.

The exposure of *X. laevis* tadpoles to ammonium perchlorate, the inhibitor of thyroid hormones, skewed sex ratio toward females (Table 11.1) (Goleman et al. 2002). In *S. tropicalis*, the triiodothyronine (T_3) increases aromatase and reductase expression prior to the gonadal differentiation (Duarte-Guterman et al. 2010). This suggests that also thyroid hormones may play a role in testis development by a cross talk with sex steroids. The transplantation of the testes from metamorphosed male *X. laevis* to the tadpoles showed the masculinizing effect of the testis on the undifferentiated gonads. This suggests that so far unidentified testicular diffusing factor causes female-to-male sex reversal probably by inhibition of aromatization of androgens to estrogens (Mikamo and Witschi 1963, 1964; Kelley 1996). That hypothetical factor is not an androgen since a female-to-male sex reversal has never been mimicked in *X. laevis* by exposure of tadpoles to testosterone (Villalpando and Merchant-Larios 1990; Piprek et al. 2012b).

Temperature is another epigenetic factor influencing the sexual development in amphibians (reviewed by Eggert 2004). Witschi (1929) described sex reversal of all females in *Rana sylvatica* by breeding tadpoles at high temperature ($32^\circ\text{C} \pm 2^\circ\text{C}$). However, according to Piquet (1930), a 20°C temperature masculinizes some females in *Rana temporaria*. A feminizing effect of high temperature was also described for urodelan species *Pleurodeles poireti* (reviewed in Dournon et al. 1984). Although, no effect of temperature on sexual development in *X. laevis* has been observed, a temperature influenced sexual development of hybrid polyploid forms of *X. laevis* (Kobel et al. 1996). Low temperature (16°C) masculinized such *X. laevis* tadpoles, whereas high temperature (26°C) had feminizing effect; i.e., the effect was opposite to that observed for ranids and bufonids (reviewed by Eggert 2004).

Sex-reversed individuals are often fertile; testes of ZW *Xenopus* neomales are able to produce sperm and ovaries of ZZ neofemales produce eggs. This indicates that the differentiation of the germ cells into spermatogonial or oogonial lineage is dependent on the somatic part of the gonad rather than the sex chromosome status in the germ cells. Transplantation of PGCs also supports these observations (Blackler 1962). Germ cells develop into eggs or sperm depending on whether they are in the testis or ovary but not depending on the ZZ or ZW sex chromosome status of the germ cells (Mikamo and Witschi 1964).

Conclusions

Although the gonad development is similar among different amphibians, the existing interspecific differences reflect long evolution of amphibians. The shape of gonads, cortex and medulla, as well as the timing of sexual differentiation of gonads vary among anurans. The effect of steroid hormones on gonadal development shows that also the sex-determining systems are divergent. To date, *X. laevis* remains the only amphibian species in which the primary sex-determining gene *DM-W* has been discovered. Due to the

absence of this gene in *S. tropicalis*, the sex determination in this species remains to be discovered.

References

- Aoyama S., Shibata K., Tokunaga S., Takase M., Matsui K., Nakamura M. 2003. Expression of *Dmrt1* protein in developing and in sex-reversed gonads of amphibians. *Cytogenetic and Genome Research* 101:295–301.
- Bewick A.J., Anderson D.W., Evans B.J. 2011. Evolution of the closely related, sex-related genes DM-W and DMRT1 in African clawed frogs (*Xenopus*). *Evolution* 65(3):698–712.
- Blackler A.W. 1962. Transfer of primordial germ-cells between two subspecies of *Xenopus laevis*. *Journal of Embryology and Experimental Morphology* 10:641–651.
- Bowles J., Knight D., Smith C., et al. 2006. Sex-specific regulation of retinoic acid levels in developing mouse gonads determines germ cell fate. *Science* 312:596–600.
- Chan A.P., Kloc M., Bilinski S., Etkin L.D. 2001. The vegetally localized mRNA *fatvg* is associated with the germ plasm in the early embryo and is later expressed in the fat body. *Mechanisms of Development* 100(1):137–140.
- Chang C.Y., Witschi E. 1956. Genetic control and hormonal reversal of sex differentiation in *Xenopus*. *Proceedings of the Society for Experimental Biology and Medicine* 89:150–152.
- Cheng T.H. 1932. The germ cell history of *Rana cantabrigensis* (Baird): I. Germ cell origin and gonadal formation. *Zeitschrift für Mikroskopisch-Anatomische Forschung* 16:497–541.
- Christensen K. 1930. Sex differentiation and development of oviducts in *Rana pipiens*. *American Journal of Anatomy* 45:159–187.
- Dumont J.N. 1972. Oogenesis in *Xenopus laevis* (Daudin). I. Stages of oocyte development in laboratory maintained animals. *Journal of Morphology* 136:153–179.
- Dournon C., Guillet F., Boucher D., Lacroix J.C. 1984. Cytogenetic and genetic evidence of male sexual inversion by treatment in the newt *Pleurodeles poireti*. *Chromosoma* 90:261–264.
- Duarte-Guterman P., Langlois V.S., Hodgkinson K., et al. 2009. The aromatase inhibitor fadrozole and the 5-reductase inhibitor finasteride affect gonadal differentiation and gene expression in the frog *Silurana tropicalis*. *Sexual Development* 3(6):333–341.
- Duarte-Guterman P., Langlois V.S., Pauli B.D., Trudeau V.L. 2010. Expression and T3 regulation of thyroid hormone- and sex steroid-related genes during *Silurana (Xenopus) tropicalis* early development. *General and Comparative Endocrinology* 166(2):428–435.
- Eggert C. 2004. Sex determination: the amphibian models. *Reproduction Nutrition Development* 44(6):539–549.
- El Jamil A., Magre S., Mazabraud A., Penrad-Mobayed M. 2008a. Early aspects of gonadal sex differentiation in *Xenopus tropicalis* with reference to an antero-posterior gradient. *Journal of Experimental Zoology A* 309:127–137.
- El Jamil A., Kanhoush R., Magre S., Boizet-Bonhoure B., Penrad-Mobayed M. 2008b. Sex-specific expression of SOX9 during gonadogenesis in the amphibian *Xenopus tropicalis*. *Developmental Dynamics* 237(10):2996–3005.
- Falconi R., Dalpiaz D., Zaccanti F. 2004. Ultrastructural aspects of gonadal morphogenesis in *Bufo bufo* (Amphibia Anura) 1. Sex differentiation. *Journal of Experimental Zoology A* 301:378–388.
- Ferguson-Smith M. 2007. The evolution of sex chromosomes and sex determination in vertebrates and the key role of DMRT1. *Sexual Development* 1(1):2–11.
- Goleman W.L., Urquidí L.J., Anderson T.A., Smith E.E., Kendall R.J., Carr J.A. 2002. Environmentally relevant concentrations of ammonium perchlorate inhibit development and metamorphosis in *Xenopus laevis*. *Environmental Toxicology and Chemistry* 21:424–430.
- Graf J.D. 1989. Sex linkage of malic enzyme in *Xenopus laevis*. *Experientia* 45(2):194–196.
- Gramapurohit N.P., Shanbhag B.A., Saidapur S.K. 2000. Pattern of gonadal sex differentiation, development, and onset of steroidogenesis in the frog, *Rana curtipipes*. *General and Comparative Endocrinology* 119:256–264.
- Hayes T.B., Stuart A.A., Mendoza M., et al. 2006. Characterization of atrazine-induced gonadal malformations in African clawed frogs (*Xenopus laevis*) and comparisons with effects of an androgen antagonist (cyproterone acetate) and exogenous estrogen (17 β -estradiol): support for the demasculinization/feminization hypothesis. *Environmental Health Perspectives* 114(S-1):134–141.
- Hayes T.B., Khoury H., Narayan A., et al. 2010. Atrazine induces complete feminization and chemical castration in male African clawed frogs (*Xenopus laevis*). *Proceedings of the National Academy of Sciences USA* 107:4612–4617.
- Heasman J., Hynes R.O., Swan A.P., Thomas V., Wylie C.C. 1985. Primordial germ cells in *Xenopus* embryos: the role of fibronectin in their adhesion during migration. *Cell* 27:437–447.
- Houston D.W., King M.L. 2000. A critical role for Xdazl, a germ plasm-localized RNA, in the

- differentiation of primordial germ cells in *Xenopus*. *Development* 127(3):447–456.
- Houston D.W., Zhang J., Maines J.Z., Wasserman S.A., King M.L. 1998. A *Xenopus* DAZ-like gene encodes an RNA component of germ plasm and is a functional homologue of *Drosophila* boule. *Development* 125:171–180.
- Hsu C.Y., Wang H.J. 1981. Production of sterile gonads in tadpoles by 17 β -ureide steroid. *Proceedings of the National Science Council, China, B: Biological Science* 5:322–327.
- Iwabuchi J., Wako S., Tanaka T., Ishikawa A., Yoshida Y., Miyata S. 2007. Analysis of the p450 aromatase gene expression in the *Xenopus* brain and gonad. *Journal of Steroid Biochemistry and Molecular Biology* 107(3–5):149–155.
- Iwasawa H. 1959. Effects of thiourea on the gonadal development of *Rana temporaria ornativentris* larvae. *Zoological Magazine* 68:6–11.
- Iwasawa H. 1960. Inhibitory effect of *para*-hydroxypropionophenone on the development of gonad in thyroidectomized frog larvae. *Endocrinologia Japonica* 7:181–186.
- Iwasawa H., Yamaguchi K. 1984. Ultrastructural study of gonadal development in *Xenopus laevis*. *Zoological Science* 1:591–560.
- Kalt M.R. 1976. Morphology and kinetics of spermatogenesis in *Xenopus laevis*. *Journal of Experimental Zoology* 195(3):393–407.
- Kang L., Marin M., Kelley D. 1995. Androgen biosynthesis and secretion in developing *Xenopus laevis*. *General and Comparative Endocrinology* 100:293–307.
- Kelley D. 1996. Sexual differentiation in *Xenopus laevis*. In *The Biology of Xenopus*, R. Tinsley and H. Kobel (Eds.), pp. 143–176, Oxford University Press, Oxford.
- Kloc M., Bilinski S., Dougherty M.T., Brey E.M., Etkin L.D. 2004. Formation, architecture and polarity of female germline cyst in *Xenopus*. *Developmental Biology* 266(1):43–61.
- Kobel H.R., Loumont C., Tinsley R.C. 1996. The extant species. In *The Biology of Xenopus*. R. C. Tinsley and H. R. Kobel (Eds.), pp. 9–33, Clarendon Press for The Zoological Society of London, Oxford.
- Koubova J., Mencke D.B., Zhou Q., Capel B., Griswold M.D., Page D.C. 2006. Retinoic acid regulates sex-specific timing of meiotic initiation in mice. *Proceedings of the National Academy of Sciences USA* 103:2474–2479.
- Lopez K. 1989. Sex differentiation and early gonadal development in *Bombina orientalis* (Anura: Discoglossidae). *Journal of Morphology* 199:299–311.
- Merchant-Larios H. 1979. Origin of the somatic cells in the rat gonad: an autoradiographic approach. *Annales De Biologie Animale, Biochimie, Biophysique* 19:1219–1229.
- Merchant-Larios H., Villalpando I. 1981. Ultrastructural events during early gonadal development in *Rana pipiens* and *Xenopus laevis*. *Anatomical Record* 199:349–360.
- Mikamo K., Witschi E. 1963. Functional sex-reversal in genetic females of *Xenopus laevis*, induced by implanted testes. *Genetics* 48:1411–1421.
- Mikamo K., Witschi E. 1964. Masculinization and breeding of the WW *Xenopus*. *Experientia* 20: 622–623.
- Miyata S., Koike S., Kubo T. 1999. Hormonal reversal and the genetic control of sex differentiation in *Xenopus*. *Zoological Science* 16:335–340.
- Nieuwkoop P.D., Faber J. 1967. *Normal Table of Xenopus laevis (Daudin): A Systematical and Chronological Survey of the Development from the Fertilized Egg Till the End of Metamorphosis*. 2nd ed., North Holland, Amsterdam.
- Ogielska M. 2009. Undifferentiated amphibian gonad. In *Reproduction of Amphibians*. M. Ogielska (Ed.), pp. 1–33, Science Publishers, Enfield.
- Ogielska M., Bartmanska J. 2009a. Spermatogenesis and male reproductive system in Amphibia-Anura. In *Reproduction of Amphibians*. M. Ogielska (Ed.), pp. 34–99, Science Publishers, Enfield.
- Ogielska M., Bartmanska J. 2009b. Oogenesis and Female Reproductive System in Amphibia-Anura. In *Reproduction of Amphibians*. M. Ogielska (Ed.), pp. 153–272, Science Publishers, Enfield.
- Okada E., Yoshimoto S., Ikeda N., et al. 2009. *Xenopus* W-linked DM-W induces FoxL2 and Cyp19 expression during ovary formation. *Sexual Development* 3(1):38–42.
- Olmstead A.W., Kosian P.A., Korte J.J., Holcombe G.W., Woodis K.K., Degitz S.J. 2009. Sex reversal of the amphibian, *Xenopus tropicalis*, following larval exposure to an aromatase inhibitor. *Aquatic Toxicology* 91(2):143–150.
- Olmstead A.W., Lindberg-Livingston A., Degitz S.J. 2010. Genotyping sex in the amphibian, *Xenopus (Silurana) tropicalis*, for endocrine disruptor bioassays. *Aquatic Toxicology* 98(1):60–66.
- Olmstead A.W., Kosian P.A., Johnson R., et al. 2012. Trenbolone causes mortality and altered sexual differentiation in *Xenopus tropicalis* during larval development. *Environmental Toxicology and Chemistry* 31(10):2391–2398.
- Pannetier M., Fabre S., Batista F., et al. 2006. FOXL2 activates P450 aromatase gene transcription: towards a better characterization of the early steps of mammalian ovarian development. *Journal of Molecular Endocrinology* 36(3):399–413.
- Pettersson I., Arukwe A., Lundstedt-Enkel K., Mortensen A.S., Berg C. 2006. Persistent sex-reversal and oviducal agenesis in adult *Xenopus (Silurana) tropicalis* frogs following larval

- exposure to the environmental pollutant ethynylestradiol. *Aquatic Toxicology* 79(4):356–365.
- Piprek R.P. 2009. Genetic mechanisms underlying male sex determination in mammals. *Journal of Applied Genetics* 50:347–360.
- Piprek R.P., Pecio A., Szymura J.M. 2010. Differentiation and development of gonads in the Yellow-Bellied Toad, *Bombina variegata* L., 1758 (Amphibia: Anura: Bombinatoridae). *Zoological Science* 27:47–55.
- Piprek R.P., Pecio A., Kubiak J.Z., Szymura J.M. 2012a. Differential effects of busulfan on gonadal development in five divergent anuran species. *Reproductive Toxicology* 34(3):393–401.
- Piprek R.P., Pecio A., Kubiak J.Z., Szymura J.M. 2012b. Differential effects of testosterone and 17 β -estradiol on gonadal development in five anuran species. *Reproduction* 144(2):257–267.
- Piquet J. 1930. Détermination du sexe chez les Batraciens en fonction de la température. *Revue Suisse de Zoologie* 37:173–281.
- Rugh R. 1951. *The Frog: Its Reproduction and Development*. McGraw-Hill, New York.
- Saidapur S.K., Gramapurohit N.P., Shanbhag B.A. 2001. Effect of sex steroids on gonadal differentiation and sex reversal in the frog, *Rana curtipipes*. *General and Comparative Endocrinology* 124:115–123.
- Shibata K., Takase M., Nakamura M. 2002. The *Dmrt1* expression in sex-reversed gonads of amphibians. *General and Comparative Endocrinology* 127(3):232–241.
- Sumida M., Nishioka M. 1994. Geographic variability of sex-linked loci in the Japanese brown frog, *Rana japonica*. *Scientific Report of Laboratory for Amphibian Biology Hiroshima University* 3: 173–195.
- Swingle W.W. 1926. The germ cells of anurans. II. An embryological study of sex differentiation in *Rana catesbeiana*. *Journal of Morphology* 41: 441–546.
- Takamune K., Teshima K., Maeda M., Abé SI. 1995. Characteristic features of preleptotene spermatocytes in *Xenopus laevis*: increase in the nuclear volume and first appearance of flattened vesicles in these cells. *Journal of Experimental Zoology* 273:264–270.
- Takeuchi T., Tanigawa Y., Minamide R., Ikenishi K., Komiya T. 2010. Analysis of SDF-1/CXCR4 signaling in primordial germ cell migration and survival or differentiation in *Xenopus laevis*. *Mechanisms of Development* 127:146–158.
- Takase M., Noguchi S., Nakamura M. 2000. Two *Sox9* messenger RNA isoforms, isolation of cDNAs and their expression during gonadal development in the frog *Rana rugosa*. *FEBS Letters* 466:249–254.
- Tanimura A., Iwasawa H. 1988. Ultrastructural observations on the origin and differentiation of somatic cells during gonadal development in the frog *Rana nigromaculata*. *Development, Growth and Differentiation* 30:681–691.
- Tanimura A., Iwasawa H. 1989. Origin of somatic cells and histogenesis in the primordial gonad of the Japanese tree frog *Rhacophorus arboreus*. *Anatomy and Embryology* 180:165–173.
- Vannini E., Sabbadin A. 1954. The relation of the interrenal blastema to the origin of the somatic tissues of the gonad in frog tadpoles. *Journal of Embryology and Experimental Morphology* 2: 275–289.
- Villalpando I., Merchant-Larios H. 1990. Determination of the sensitive stages for gonadal sex-reversal in *Xenopus laevis* tadpoles. *International Journal of Developmental Biology* 34:281–285.
- Wallace H., Badawy G.M.I., Wallace B.M.N. 1999. Amphibian sex determination and sex reversal. *Cellular and Molecular Life Sciences* 55:901–909.
- Wang D.S., Kobayashi T., Zhou L.Y., et al. 2007. Foxl2 up-regulates aromatase gene transcription in a female-specific manner by binding to the promoter as well as interacting with ad4 binding protein/steroidogenic factor 1. *Molecular Endocrinology* 21(3):712–725.
- Whittington P.M., Dixon K.E. 1975. Quantitative studies of germ plasm and germ cells during early embryogenesis of *Xenopus laevis*. *Journal of Embryology and Experimental Morphology* 33(1):57–74.
- Witschi E. 1929. Studies on sex differentiation and determination in amphibians: I. Development and sexual differentiation of the gonads of *Rana sylvatica*. *Journal of Experimental Zoology* 52: 235–265.
- Witschi E. 1956. *Development of Vertebrates*. WB Saunders, Philadelphia.
- Witschi E. 1971. Mechanisms of sexual differentiation: Experiments with *Xenopus laevis*. In *Hormones and Development*. M. Hamburg, E. Barrington (Eds.), pp. 601–618, Meredith, New York.
- Wylie C.C., Heasman J. 1993. Migration, proliferation, and potency of primordial germ cells. *Seminars in Developmental Biology* 4:161–170.
- Wylie C.C., Bancroft M., Heasman J. 1976. The formation of the gonadal ridge in *Xenopus laevis*. II. A scanning electron microscope study. *Journal of Embryology and Experimental Morphology* 35:139–148.
- Wylie C.C., Heasman J., Swan A., Anderton B.H. 1979. Evidence for substrate guidance of primordial germ cells. *Experimental Cell Research* 121:315–324.
- Yamaguchi T., Yamaguchi S., Hirai T., Kitano T. 2007. Follicle-stimulating hormone signaling and

- Foxl2 are involved in transcriptional regulation of aromatase gene during gonadal sex differentiation in Japanese flounder, *Paralichthys olivaceus*. *Biochemical and Biophysical Research Communications* 359:935–940.
- Yoshimoto S., Okada E., Umemoto H., et al. 2008. A W-linked DM-domain gene, DM-W, participates in primary ovary development in *Xenopus laevis*. *Proceedings of the National Academy of Sciences USA* 105:2469–2474.
- Yoshimoto S., Ikeda N., Izutsu Y., Shiba T., Takamatsu N., Ito M. 2010. Opposite roles of DMRT1 and its W-linked paralogue, DM-W, in sexual dimorphism of *Xenopus laevis*: implications of a ZZ/ZW-type sex-determining system. *Development* 137:2519–2526.

12

The *Xenopus* Pronephros: A Kidney Model Making Leaps toward Understanding Tubule Development

Rachel K. Miller^{1,*}, Moonsup Lee,^{1,2} & Pierre D. McCrea,^{1,2}

¹Department of Biochemistry and Molecular Biology, The University of Texas MD Anderson Cancer Center, Houston, TX

²Program in Genes and Development, The University of Texas Graduate School of Biomedical Sciences at Houston, Houston, TX

*Current Affiliation: Department of Pediatrics, University of Texas Medical School at Houston, Houston, TX

Abstract: The *Xenopus* embryonic kidney, the pronephros, serves as a useful model for the study of nephron development as well as tubulogenesis in general. The history of embryological studies on pronephric development through transplantation, explant, and animal cap experiments provides a valuable body of knowledge on which to base current studies. Continued investigation of the molecular underpinnings of nephric formation and the sustained development of innovative techniques complement the fundamental embryological advantages of this system. Because the *Xenopus* pronephros is composed of a single functional nephron that lies just beneath the ectoderm through all stages of development, it can be easily manipulated via microdissection techniques and visualized both in living embryos and in fixed tissue. The ability to target molecular alterations specifically to the pronephric anlagen through the application of kidney-specific transgenic promoters along with cell fate-based microinjections of mRNAs or morpholinos provides the ability to manipulate gene expression in a spatially restricted manner. Recently, light-inducible morpholinos have provided a means to temporally regulate gene expression in *Xenopus*, as have transgenic promoters. Application of targeted nuclease technologies should also soon provide the ability to manipulate amphibian models at the level of genomic DNA. Because the *Xenopus* pronephros progresses into a functional nephron in 3–4 days within an embryo that develops outside the mother, it provides unique advantages for observations of nephrogenesis. Additionally, recent work suggests that the *Xenopus* kidney will facilitate studies on nephron regeneration. In this chapter, we will review key studies in *Xenopus* pronephric development and highlight current innovations that will accelerate our understanding of kidney formation and tubulogenesis in the near future.

Introduction

Our understanding of how the kidney develops and is maintained is relevant to ultimately addressing human disease. Through

investigation of the fundamental mechanisms of renal genesis, researchers are beginning to elucidate the mechanisms underlying kidney pathologies that originate during embryogenesis, including numerous cystic diseases

and Wilms tumor, a developmental cancer. Determining how the kidney is maintained is likewise a precursor to understanding why diseases develop later in life. For example, cellular signaling pathways involved in normal kidney homeostasis are often deregulated in kidney cancer (Clevers and Nusse 2012). Investigation of renal maintenance will support the generation of new therapies to treat later-onset diseases including cancers, cystic diseases, and chronic kidney disease (CKD). In this latter case, CKD resulting primarily from hypertension and diabetes is a growing health and financial burden worldwide. Remarkably, in the United States, CKD affected 13% of the population between 1999 and 2004 (Coresh et al. 2007). Globally, the cost of dialysis and transplants is expected to exceed one trillion U.S. dollars over the next decade (Lysaght 2002). Greater insight upon kidney development and homeostasis is thus a required step in progressing toward regenerative and stem cell therapies to repair damaged nephrons (Blitz et al. 2006).

In addition to providing valuable knowledge regarding kidney disease, the study of renal development employing various model organisms will help promote understanding of the kidney's evolutionary relationships and functional solutions. Animals have evolved physiological alterations necessary to cope with diverse environments, such as land and aqueous environments of varying salinity. The kidney of vertebrate amniotes passes through three defined and successive stages that have been indicated to reflect various conditions that confronted predecessors across evolutionary time (Vize and Smith 2004). In vertebrate amniotes, including reptiles, birds, and mammals, those distinct successive structures are, respectively, the pronephros, the mesonephros, and the metanephros (pro, anterior; meso, intermediate; meta, succeeding) (Beuchat and Braun 1988; Vize 2003b). Whereas fish and amphibians, including *Xenopus*, progress only through the first two kidney forms, resulting in a terminal functional mesonephros in adults (Rich et al. 2002; Jones 2005). Although each kidney form consecutively replaces its precursor, its establishment is structurally dependent on the preceding form (Saxén 1987). Similar inductive

events, signaling cascades, and gene products drive the development of the three successive stages, reflected in the fact that similar markers are expressed within the proximal tubules, distal tubules, and collecting ducts of these structures. While each consecutive organ is more complex than the previous, each is composed of the same basic unit of filtration, the nephron.

Several vertebrate experimental models are commonly used for the study of nephric development, including mouse, chick, frog, and fish (Dressler 2006). Each has experimental advantages and drawbacks. This chapter will focus on the established advantages as well as newly developed advances of the *Xenopus* model in the study of nephric development. Primary experimental advantages of *Xenopus* include the external development of large (>1 mm in diameter) embryos, the ability to control the expression of gene targets within the nephric primordium, and the simple structure and accessibility of the nephron. More recent advances have allowed for the temporal and spatial regulation of gene product expression, including the application of kidney-specific promoters and light-inducible morpholinos, and further, nuclease technologies are providing the opportunity to manipulate gene expression at the DNA level. Considering the significant body of knowledge already in hand, in conjunction with opportunities made available using new technologies, the *Xenopus* kidney will provide future insights upon renal genesis, homeostasis, and regeneration.

***Xenopus* embryonic kidney development**

The *Xenopus* embryonic kidney, the pronephros, while as functionally complex as later kidney forms, offers experimental simplicity because it is a single nephron, including tubules, a duct, and glomus (Figure 12.1B) (Vize et al. 1997; Carroll et al. 1999b; Rich et al. 2002). Each of these components is critical to the function of the nephron. The glomus serves to filter the blood as does the glomerulus of a metanephric nephron, but their structures differ slightly. While the blood filtrate from the

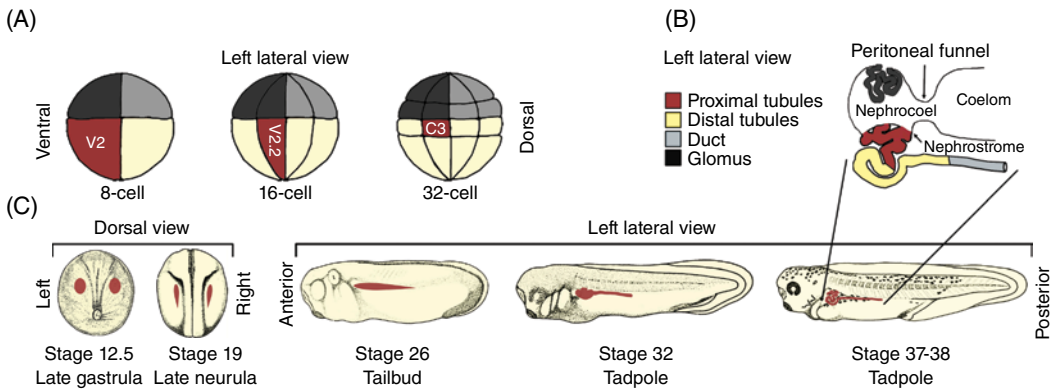


Figure 12.1 Kidney fate map and development. (A) Fate maps of early blastula stage embryos. Vegetal cells (on top of embryos) are marked to indicate dorsal (light gray) versus ventral (dark gray). The V2 (8-cell), V2.2 (16-cell), and C3 (32-cell) vegetal blastomeres (on bottom of embryos) are marked in dark red to show cells fated to contribute to the pronephros. (B) Diagram of the pronephros at stages 36–38. The glomus (dark gray), proximal tubules (dark red), distal tubules (light yellow), and collecting duct (light gray) are indicated (left lateral view). (C) Stages of pronephric development. Pronephric anlagen is depicted in dark red at each embryonic stage from early gastrula through tadpole stages. Specification and patterning occur through late gastrula and late neurula stages (dorsal views), while differentiation and morphogenesis occur through tailbud and tadpole stages (left lateral view). To see a color version of this figure, see Plate 31.

metanephric glomerulus enters the nephric tubules through a surrounding sac called the Bowman's capsule, the glomus does not have a Bowman's capsule. Rather, it is surrounded by the nephrocoel, which is connected with the coelom (Drummond and Majumdar 2003). The proximal tubules, distal tubules, and collecting duct serve conserved roles in actively resorbing components of the filtrate, like salts and amino acids, and transporting wastes for excretion through the cloaca. The embryonic kidney serves the function of osmoregulation and ensures that these freshwater *Xenopus* embryos do not accumulate fluid. Pronephric cells are specified from the intermediate mesoderm during gastrulation (Brennan et al. 1998), followed by segregation into the nephric components (Carroll et al. 1999b). Research within the field has sought to determine how the pronephros forms (Gibson et al. 2002; Jones 2005). This section will give an overview of *Xenopus* nephrogenesis, describing the processes of pronephric fate determination, specification, induction, differentiation and morphogenesis, followed by studies in *Xenopus* related to human disease. Throughout the chapter, fundamental experiments utilizing embryological and molecular techniques will be highlighted.

Pronephric fate

Embryological studies on pronephric development in amphibians have been performed since the early 1920s. Some of the earliest studies focused on determining which cells in early embryos are fated to give rise to the pronephros (Aghajanian et al. 2002; Dizon et al. 2002). Building upon the work of Nieuwkoop and Faber (NF) (Nieuwkoop and Faber 1956; Kornstein and Clayton 2002; Wark et al. 2002), more recent studies have utilized vital dyes in *Xenopus laevis* to define the fates of early cells (blastomeres) injected at embryonic blastocyst stages. The resulting findings have determined which cells predominantly contribute to the pronephric anlagen, namely, the V2 cell at the 8-cell stage, the V2.2 cell at the 16-cell stage, and the C3 cell at the 32-cell stage, with lesser inputs from several other cells (Figure 12.1A) (Moody 1987a, b; Bauer et al. 1994; Biegon et al. 2002). The *X. laevis* fate maps resulting from such studies have become invaluable to the research community and are readily accessible via Xenbase (Harms et al. 2002). The appropriate early blastomeres can be injected with mRNAs or morpholinos for fated delivery to the left-versus-right or both nephric fields (Moody 1987a; Moody 1987b; Saulnier et al. 2002).

Coinjected lineage tracers are often used to confirm successful targeting (Stewart et al. 2009).

Although the noted select blastomeres are fated to contribute to the pronephros, at early stages, they have not yet been induced to begin their developmental program. In other words, outside of their developmental context, they would not become part of the kidney lineage. The region just ventral to the anterior somites during gastrulation (NF stage 12.5) will be induced to become pronephric and will contribute to the nephric field (Figure 12.1C) (Vize et al. 2003). Classical studies on *X. laevis* performed by Holtfreter defined the nephric field as the region in which ectoderm transplanted into the embryo is induced to form pronephric tubules (Figure 12.2A) (Holtfreter 1933). This implies that a signal is received within the field instructing it to become the nephric tissue. Recent studies show that this signal is derived from anterior somites that lie just dorsal to the pronephric anlagen. This was demonstrated in *Xenopus* by preventing somites from forming through the experimental process of ultraviolet (UV) light-induced ventralization and observing that the pronephros does not form (Seufert et al. 1999).

Pronephric induction and specification

Elegant studies using embryo explants have further helped define the timing and the nature of the inductive signal. Such studies support the hypothesis that the inductive signal is derived from the anterior somites. Explanted uncommitted mesoderm is induced toward the nephric fate when cultured adjacent to explanted anterior somites between two animal caps (naïve ectoderm removed from the animal pole of the embryo at blastula stages) (Seufert et al. 1999) (Figure 12.2B). In this configuration, known as a Holtfreter sandwich, the mesoderm will only differentiate into nephric tissue (as assayed by immunostaining or RT-PCR) if it has been induced.

To determine when the tissue within the nephric field receives the inductive signal and is specified, explants of the presumptive

nephric primordium were cultured in Holtfreter sandwiches (Figure 12.2D). Using such techniques, experiments have shown that the tubule and glomus are specified in the late gastrula (NF stage 12.5), while the collecting duct is specified by the early neurula (NF stage 14) (Seufert et al. 1999) (Figure 12.1C).

More recent work combining classical embryological and loss-of-function molecular techniques shows that *Wnt11b* is required for pronephros formation. *Wnt11b* can also induce nephrogenesis *ex vivo* using Holtfreter sandwiches, suggesting that this ligand is a potential pronephric inducer (Tételin and Jones 2010). Chordin, which is expressed as a consequence of fibroblast growth factor (FGF) signaling within the Spemann organizer, directs the formation of the anterior somitic region required for induction of the nephric field, presumably through its extracellular antagonism of bone morphogenic proteins (BMPs) (Mitchell and Sheets 2001, 2002; Mitchell et al. 2007). The expression of *p27* (*Xic1*), a cyclin-dependent kinase inhibitor, within the somites is also required for pronephric induction, likely via cell cycle regulation. Contrary to prior hypotheses, somite segmentation does not appear necessary for kidney formation, indicating that somite patterning is not required for pronephric development (Naylor et al. 2009). A TGF-beta ligand, glial cell line-derived neurotrophic factor (GDNF), is expressed within the pronephros soon after nephron induction as well as within the anterior somites, but its requirement for pronephros formation has not been established (Kyuno and Jones 2007).

Animal cap explant techniques have also provided insights into the induction of the pronephric field (Hensley and Nurnberg 2002) (Figure 12.2B). Naïve animal cap ectoderm derived from late blastula stages cultured *in vitro* in the presence of the TGF-beta superfamily member, activin, and the nuclear hormone receptor ligand, retinoic acid (RA), expresses kidney-specific markers such as *pax8* and *pax2* and displays a histology that is indicative of nephric tubules, duct, and glomus (Ryffel 1995; Uochi and Asashima 1996; Brennan et al. 1999; Osafune et al. 2002). It is noteworthy that in these

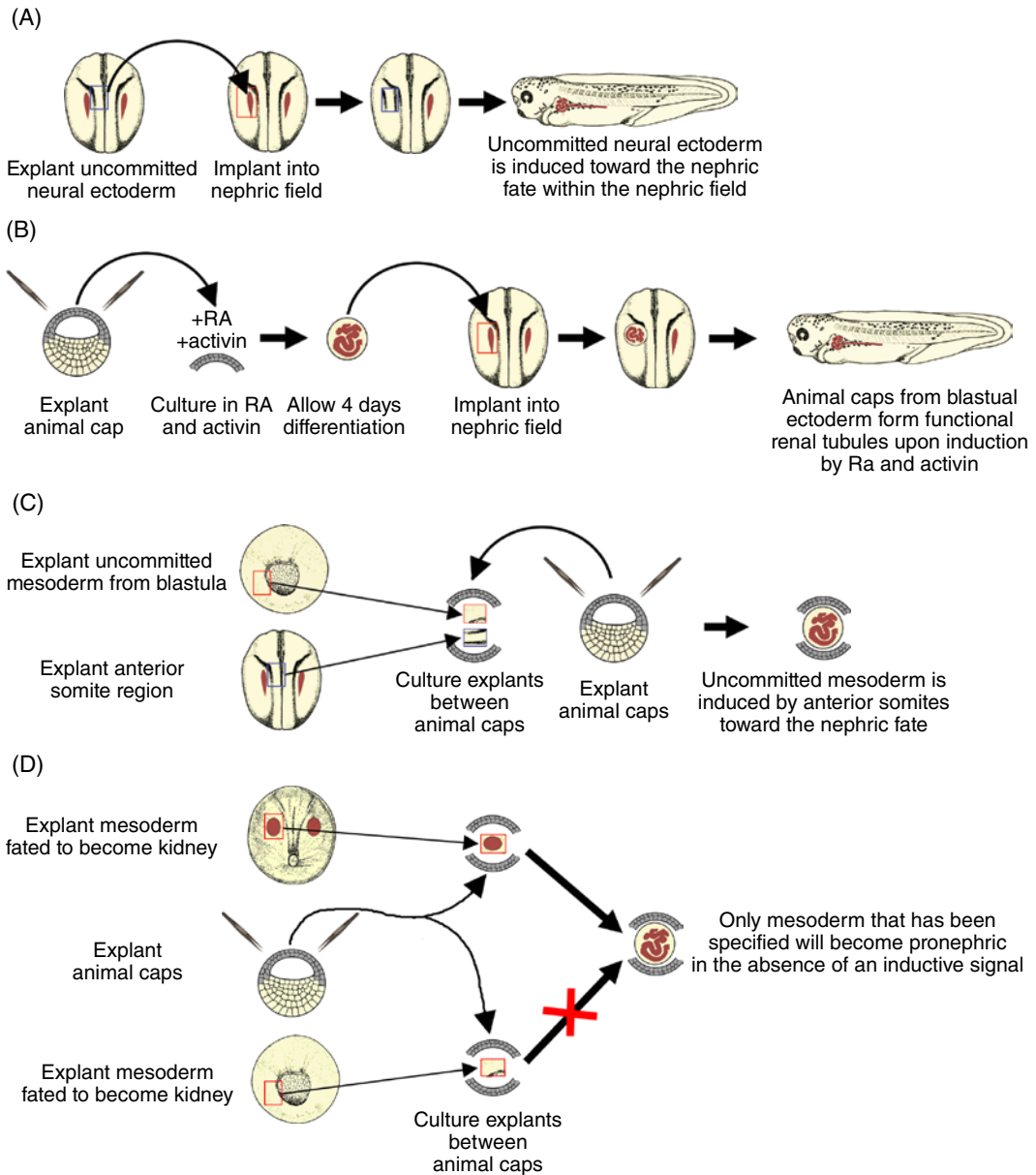


Figure 12.2 Explant and grafting experiments. (A) Identification of nephric field. When explanted uncommitted ectoderm is grafted into a region ventral to the anterior somites (the nephric field), it is induced toward the nephric fate. (B) Differentiation of naïve progenitors into nephric tubules. Naïve animal cap ectoderm isolated from the blastula stage is induced to form nephric tubules through 4 days of culture with RA and activin. When the tubules are transplanted back into the embryo at late neurula stages, they will form functional pronephroi. (C) Identification of inducing tissue. When uncommitted mesoderm from late blastula stage and the anterior somites from late neurula stage are explanted and cultured adjacent to one another between two blastula stage animal cap (naïve ectoderm) explants (Holtfreter sandwich), the mesoderm is induced to form nephric tubules. (D) Determining the timing of specification. Only mesoderm that is specified is competent to form nephric tubules when explanted and cultured in a Holtfreter sandwich (between two animal caps).

cases, immature ectoderm is being reprogrammed to form a tissue normally derived from the intermediate mesoderm, suggesting that the cells of the blastocyst are competent to become pronephric in the presence of appropriate inductive signals. Studies *in vivo* verify that RA is required for induction of the pronephros (Cartry et al. 2006). Together, this work indicates that the activin and RA signaling pathways are somehow involved in inducing pronephric specification, possibly via their respective regulation of the cell cycle and Hox genes. However, the broad relationships between *wnt11b*, chordin, and activin/RA signals have not yet been investigated. Additionally, calcium signaling may play a role in nephrogenesis downstream of RA (Leclerc et al. 2008).

From the perspective of regenerative biology, it is striking that pronephric tissues generated *ex vivo* from naïve ectoderm (see preceding text) continue to function when transplanted ventral to the anterior somites of a tailbud embryo whose endogenous pronephric anlagen has been explanted (Figure 12.2B). The implant's functionality is grossly reflected in its capacity to protect the embryo against edema (fluid accumulation) that would otherwise arise following nephrectomy (Chan et al. 1999). Such studies suggest a future promise in reprogramming tissue lineages for therapeutic and regenerative applications.

The earliest known molecular indicators of pronephric induction are the expression of the transcription factors *lim1* and *pax8*, which are each required for nephrogenesis (Carroll and Vize 1999) (Figure 12.4). Further, ectopic overexpression of *lim1* and *pax8* results in the formation of superfluous pronephroi, supporting their role in kidney induction (Carroll and Vize 1999). The hepatocyte nuclear factor 1-beta (*hnf1-beta*) transcription factor is further expressed at late gastrula stages (Demartis et al. 1994; Pogge yon Strandmann and Ryffel 1995; Weber et al. 1996). A dominant-active form of *hnf1-beta* rescues the induction of ectopic kidney formation by *lim1* and *pax8*, indicating an antagonizing role (Wu et al. 2004). An odd-skipped related transcription factor, *osr*, expressed during gastrulation, is further necessary and sufficient for induction of the pronephros, possibly through the

recruitment of Groucho-like corepressors (Tena et al. 2007). During late gastrulation, the paired-like homeobox genes *mix 1* and *2* support continued *lim1* and *pax8* expression as their knockdown results in the inhibition of *lim1* and *pax8* expression. The effects from *mix 1* and *2* knockdown cause expansion of *fgf4* and *8* expression and can be rescued through the inhibition of FGF during gastrulation. These studies suggest that early FGF signaling must be attenuated in late gastrula stages to prevent the inhibition of pronephric specification (Colas et al. 2008). Together, these molecular studies in conjunction with classical embryological experiments have provided a basic framework of the fate, specification, and induction of the pronephric tissue on which to build upon.

Pronephric patterning

Once the nephric field is induced, patterning of the pronephros begins (Stumpf et al. 1995; Gibson et al. 2002). Early expression of the transcription factor *lim1* during late gastrula stages defines the anterior and posterior boundaries on the anlagen, while *pax8* expression is thought to spatially restrict the *lim1* signal (Heller and Brandli 1997; Carroll and Vize 1999) (Figure 12.1C). These early molecular markers are expressed in distinct but overlapping domains that synergize to pattern the primordium on the anterior/posterior axis, ultimately giving rise to the pronephric tubules, duct, and glomus (Jones 2003). Pronephric patterning proceeds with the expression of *wnt4* within the pronephric precursors and *pax2* within the prospective tubules and duct at gastrula stages (Carroll et al. 1999a). Mediolateral patterning, which distinguishes the tubules from the glomus, begins at later neurula stages (NF 18) once *wt1* is expressed in the medial, glomar primordium. *wt1* expression restricts *lim1* and *pax8* expression to the lateral regions (Carroll and Vize 1996). Dorsoventral patterning begins with the restricted dorsal expression of *wnt4* and Notch pathway components at tailbud stages (NF 26–30), which follows their prior required expression at late neurula stages (NF 18–22) (Carroll et al. 1999a; Thomas et al. 2002) (Figure 12.1C).

Pronephric differentiation and morphogenesis

After pronephric patterning, the tissue begins to undergo the processes of differentiation and morphogenesis in tailbud and tadpole stages (Figure 12.1C). Condensing mesenchymal cells within the primordium begin to elongate as they prepare to transition into columnar tubular epithelia. Simultaneously, cells within the nephric mesoderm begin to segregate from the remaining intermediate mesoderm. These processes result in the formation of a cell mass called the nephrotome, which can be visualized externally at tailbud stages as a bulge positioned ventrally to the anterior somites. Finally, the cells begin to polarize to form a true columnar epithelium. FGF signaling is required for the condensation and epithelialization of the pronephric primordium (Urban et al. 2006). *wnt4* expression is coincident with the epithelialization of the pronephric tubules and is required for their formation (Saulnier et al. 2002). Recent studies suggest that *wt1* and *sox11*, whose expression patterns overlap with *wnt4*, are required to synergistically direct its expression (Murugan et al. 2012). Upon *wnt4* expression, canonical signaling becomes active, as marked by beta-catenin transcriptional readouts (Lyons et al. 2009). Numerous additional components of the canonical Wnt pathway are likewise present in the developing pronephros (Zhang et al. 2011). Supporting the importance of canonical signals is that their antagonism significantly decreases nephric primordium proliferation (McCoy et al. 2011). Other studies indicate that Notch signaling plays a role in determining whether cells will adopt a tubular or ductal cell fate (McLaughlin et al. 2000).

Recent work also suggests that the expression of pronephric genes is tightly regulated by microRNAs (miRNAs) (Wessely et al. 2010). The knockdown of *dicer* and *dgcr8*, which are required for the biogenesis of miRNAs, delays the differentiation of renal epithelium, resulting in abnormalities and edema (Agrawal et al. 2009). *miR-30*, which is expressed in the pronephros, regulates *lim1* and is required for its downregulation after early developmental stages. Further, the knockdown of *miR-30* leads to increased *lim1*

expression and delayed epithelial differentiation within the pronephros (Agrawal et al. 2009).

Several other factors also affect nephron differentiation and morphogenesis. *hnf1-beta* expression continues within the anlagen during neurula stages and is accompanied by overlapping expression of two transcription factors, *e4f1* and *zfp3611*, whose protein products directly interact with Hnf1-beta and modulate nephric morphogenesis (Dudziak et al. 2008). Dystroglycan (Dg), a laminin receptor, is required for the shaping of the nephron, indicating that basement membrane is involved in nephrogenesis and that Dg helps anchor pronephric cells to the basement membrane through laminin-1 (Bello et al. 2008).

Complementing gene expression that takes place within the anlagen itself, components of the mesodermal tissues surrounding the pronephros promote nephron differentiation. Morphological development of the pronephros is abrogated following both overexpression and knockdown of *xc3hH-3b*, whose protein product is a zinc-finger protein expressed during tailbud stages that modulates *tnf-alpha* mRNA stability (Kaneko et al. 2003) (Figure 12.1C). Interestingly, complement system components *c1qa* and *c3bc4b*, which are known for their role in innate immunity, are also expressed in the pronephros during morphogenic stages, suggesting an undefined developmental role (McLin et al. 2008). The pronephric primordium develops in an anterior-to-posterior sequence, with tubule precursors forming first, followed by the elongation of the duct during tailbud stages (NF 21–27).

Likewise, the pronephric duct itself segregates from the lateral mesoderm sequentially from the anterior to the posterior of the embryo at early tailbud stages (Drawbridge et al. 2003) (Figure 12.1C). Through studies using scanning electron microscopy, the development of the duct has been visualized (Poole and Steinberg 1984). Embryological techniques known as Holtfreter split-back experiments show that the duct does not elongate when the axial mesoderm is bisected through its projected trajectory, demonstrating that contiguous mesoderm is required for the duct's elongation caudally (toward the posterior) (Holtfreter 1944). Disruption of mesoderm just ventral to somites 4 through

9 inhibits the formation of the duct, suggesting that this region of mesoderm is required for duct formation (Lynch and Fraser 1990; Cornish and Etkin 1993). These studies together suggest that both the posterior migration of the duct and the segregation of the duct from axial mesoderm account for its development. As the pronephric duct extends toward the posterior, it meets and fuses with the anterior migrating duct precursors from the cloaca, the rectal diverticulum (Heller and Brandli 1997). Thus, at tadpole stages (NF 36), establishment of an intact duct through the connection of these convergently migrating tubes enables subsequent pronephric function (Schultheiss et al. 2003).

Morphogenesis of the tubule begins at tailbud stages forming three dorsal branches, which will connect with the nephrostomes, structures that serve to funnel the glomerular filtrate into the pronephros. Several signals are involved in nephron morphogenesis, including those of the BMP and Wnt pathways. When BMP, a TGF- β family member, is knocked down just prior to differentiation and morphogenesis of renal tissues, the pronephric duct and tubules are severely deformed, indicating the requirement of BMP signals for these processes (Bracken et al. 2008). Downstream of BMP signaling, the Tbx2 transcription factor is required for regulation of the pronephros size. Tbx2 participates in a negative feedback loop in which two of its gene targets, Gremlin (BMP antagonist) and Hey1 (transcription factor), each antagonize BMP activity (Cho et al. 2011). The Iroquois (*irx*) genes are also involved in maintaining the size of the pronephric territory through the positive regulation of BMP signaling (Alarcon et al. 2008). *X. laevis* annexin IV (*anx-4*) expression, specifically within the tubules, also moderates pronephros size (Seville et al. 2002). Annexins have wide-ranging cellular roles that include modulation of protein interactions at the cell cortex and in vesicle trafficking. Recent work on *Xenopus tropicalis* demonstrates that the transcription factor *yap*, which mediates organ size through the Hippo pathway, is highly expressed in the developing pronephros (Nejigane et al. 2011). Thus, the Hippo pathway may also help to

regulate the size of the pronephros, although a functional relationship is yet to be established.

The process of tubule formation also requires Wnt-mediated planar cell polarity (PCP) signaling through Frizzled 8, Inversin, Daam1, and other pathway components (Satow et al. 2004; Lienkamp et al. 2010; Miller et al. 2011). While canonical Wnt components (such as beta-catenin) are required for earlier stages of kidney development, noncanonical PCP signaling appears to be required for later morphogenic processes (Miller and McCrea 2010; Zhang et al. 2011). When noncanonical signals are inhibited, cell proliferation rates notably increase within the pronephros. This is consistent with evidence indicating that noncanonical and canonical Wnt signals have antagonistic effects during nephric development. Current studies using live imaging suggest that kidney tubule morphogenesis requires convergent extension and cell intercalation processes as characterized earlier in neural tube formation (see succeeding text) (Davidson and Keller 1999; Lienkamp et al. 2012). Additionally, *mlk2* (a MAP kinase kinase kinase) is expressed in the developing pronephric tubules as they epithelialize and is required for morphogenesis (Poitras et al. 2003). Finally, even the expression patterns of Clock genes, such as nocturnin, *xdmal1*, and *xper1*, have suggested their potential involvement in the differentiation or morphogenesis of the nephron (Curran et al. 2008). Overall, the studies indicate that the processes of differentiation and morphogenesis are complex and integrally linked.

Mediolateral patterning

While the anteroposterior axis of the kidney primordium allows for the tubule and duct to be distinguished, the mediolateral patterning of the kidney allows for the segregation of the tubules and glomerulus (Figure 12.1B). As mentioned previously, the amphibian glomerulus is enclosed by a nephrocoel that is fused with the coelom rather than a Bowman's capsule as is found in metanephric kidneys of amniotes (Drummond and Majumdar 2003). The glomerulus forms from tissue expressing *wt1* in the medial

region and, at late neurula stages (NF 18), restricts *lim1* and *pax8* expression to the lateral regions (Carroll and Vize 1996). The antagonistic expression of these markers appears to influence whether the tissue will form tubules or the glomus (Wallingford et al. 1998). The knockdown of *wt1* in combination with *foxc2* resulted in the loss of all glomus marker expression, suggesting that they are together required for its formation (White et al. 2010). Studies on the *lmx1b* transcription factor show that it regulates glomus size and lies upstream of *wt1*. Similar to *wt1*, its expression domain is complementary to that of *lim1*, indicating that *lmx1b* and *lim1* direct differentiation into glomus versus tubule fates, respectively (Haldin et al. 2008). To regulate cell fate, Notch acts initially in the medial regions to promote glomus and then acts through Hairy-related transcription factor (HRT) to upregulate *wnt4* and promote tubule fates (Taelman et al. 2006; Naylor and Jones 2009). At early tailbud stages, the formation of the coelom splits the intermediate mesoderm into the splanchnic and somatic mesoderm, distinguishing the progenitors that will give rise to the glomus versus the tubule/duct lineages. The vascular component of the glomus is derived from a branch from the dorsal aorta that invades the glomerular epithelium (Vize et al. 1997). The cardinal vein, which runs down the length of the duct, and the sinus, which surrounds the tubular epithelium, are derived from the condensing mesenchymal cells that are converted into the endothelial vasculature (Brandli 1999). Thus, within the anterior region of the pronephros, the tubules and glomus are distinguished via mediolateral patterning.

***Xenopus* as a model of disease and regeneration**

Xenopus has become an increasingly valued model to identify factors that may be dysfunctional in human renal diseases (Ryffel 2003). This can be attributed to both the conservation of signals driving induction, specification, patterning, differentiation, and morphogenesis among vertebrate nephrons (Brandli 1999; Raciti et al. 2008; Wingert and Davidson 2008) and the experimental advantages of

amphibians noted earlier. Clear links exist between human mutations that cause kidney developmental anomalies and disease, and defects observed in *Xenopus* when these genes are disrupted. Gene alterations known to promote cystic kidney diseases, renal malformations, renal cancers, and diabetes in humans have been investigated in *Xenopus*. Continued research on the frog is likely to uncover new causative genes in human renal diseases, possibly through screens focused on phenotypes that mimic human conditions.

Mutations in the transcription factor *hnf1-beta*, which is expressed after kidney induction in frogs, contribute to human maturity-onset diabetes (MODY5), as well as renal developmental defects including cysts. The expression of dominant-active human *hnf1-beta* in *Xenopus* embryos produces agenesis, while other mutations cause hypertrophy of the pronephros, paralleling the defects observed in human patients (Wild et al. 2000; Bohn et al. 2003). Through experiments on *Xenopus* embryos, HNF1-beta has been found to antagonize *lim1*, *pax8*, and subsequent marker expression, and its domains involved in nephrogenesis have been identified (Wu et al. 2004; Sauert et al. 2012). Together, these studies support the significance of investigating the effects of human mutations in the *Xenopus* developmental system.

Several cystic kidney diseases in humans result from mutations in proteins associated with primary cilia. These sensory signaling centers act as cellular "antennae". Autosomal dominant polycystic kidney disease (PKD) can arise from mutations in polycystin 2 (*pkd2*), a transmembrane channel associated with the primary cilia. Mouse mutations affecting the RNA-binding protein, bicaudal C (*bicc1*), result in fluid-filled nephric cysts analogous to those seen in some forms of PKD in humans. The work on *Xenopus* indicates that *bicc1* knockdown produces cyst-like morphologies within the nephron similar to PKD abnormalities (Tran et al. 2007). *Bicc1* modulates *pkd2* by antagonizing microRNA-17 (*miR-17*), which otherwise destabilizes the *pkd2* transcript. The knockdown of *bicc1* is rescued by reducing *miR-17* activity, validating these results *in vivo* (Tran et al. 2010). Another cilia-related gene, *inversin*, is mutated in the human developmental cystic kidney

disease, type II nephronophthisis. The knockdown of *inversin* or *frizzled 8*, components of the Wnt/PCP pathway, results in pronephric defects in the morphogenesis and differentiation of the tubule. *frizzled 8* depletion defects are rescued by *inversin* overexpression, consistent with *Inversin* acting downstream of *Frizzled 8* (Lienkamp et al. 2010).

The human transmembrane Golgi phosphoprotein 2 (GOLPH2) is upregulated in human renal cell carcinoma among other diseases. The expression of *golp2* in the *Xenopus* pronephros reduces the expression of tubule and duct differentiation markers, while knockdown correspondingly causes increased expression of glomus markers, such as *nephrin* and *wt1*. *golp2* thus appears to modulate decisions relevant to producing tubular versus glomerular structures (Li et al. 2012). *Evi1* and *MEL1*, zinc-finger transcription factors involved in myeloid leukemia, also help pattern the pronephros. Within the distal tubule and duct compartments, *evi1* and *mel1* transcripts are expressed prior to morphogenesis. Their expression, which is stimulated by retinoid signaling, promotes distal tubule and duct marker expression and inhibits proximal tubule and glomerular lineages (Van Campenhout et al. 2006).

Intriguing new data suggest that the *Xenopus* pronephros will provide a model of renal regeneration. Upon partial or total removal of the pronephros at NF stages 37–38, a fraction (~17%) of tadpoles regenerate pronephric tubules within 21 days (Caine and McLaughlin 2013). Within a few hours of nephrectomy, tadpoles displayed increased Caspase and MMP-9 activity, indicating that their activity may be necessary for the regenerative process (Caine and McLaughlin 2013). This pioneering study has established the pronephros as a model for studies of the regenerative capacity of the nephron. It has also opened the door for research aimed toward understanding which developmental signals may also be required for tissue regeneration.

Modulation of gene expression

The recent advances in molecular techniques have enabled modulation of gene expression in the *Xenopus* system (Khokha 2012). Progress

in the genetic manipulation of *Xenopus* has been primarily achieved through the use of *X. tropicalis* and improvements in nuclease technologies. These advances have been complemented by improvements in knockout as well as transgenic technologies. This section will concentrate on advances in such select promising techniques to probe *Xenopus* pronephric development.

Genetics in *Xenopus*

Although *X. laevis* has been the primary experimental model utilized, their complex, allotetraploid genome has prohibited the ability to perform forward genetic screens. Additionally, their generation time (~1 year to reach sexual maturity) impedes studies involving genetic crosses. However, the more recent use of a similar species, *X. tropicalis*, has promoted studies involving forward genetic screens as well as the ability to cross mutants. *X. tropicalis* has a diploid genome, its generation time is approximately 6 months, and its genome has been fully sequenced and assembled (Hirsch et al. 2002; Hellsten et al. 2010).

However, relative to *X. laevis*, *X. tropicalis* embryos are approximately two-thirds the size, making microinjection, microdissection, and imaging more difficult. Additionally, their embryos are typically fertilized via natural mating, reducing the developmental synchrony of the population. Given that *X. tropicalis* adults are maintained at 25°C rather than 18°C, they develop more rapidly, reducing the developmental windows for microinjection. Ultimately, the reduced size of the embryos also results in a smaller pronephros, countering one of the primary advantages of the *Xenopus* model.

Nonetheless, forward genetic screens have been carried out in *X. tropicalis* using a variety of strategies including the use of transposons, ionizing radiation, and ENU (*N*-ethyl-*N*-nitrosourea)-mediated mutagenesis (Goda et al. 2006; Abu-Daya et al. 2012; Del Viso et al. 2012; Yergeau et al. 2012). Numerous mutations have been identified and characterized; however, few have been examined in the context of kidney development. Studies utilizing genetic mutants in *X. tropicalis* are

expected to provide novel insight into kidney development. Recently, for example, the *ruby* mutation was characterized, resolved as a missense mutation in *pax8* that caused similar developmental kidney defects as those observed in *pax8* knockdowns (Del Viso et al. 2012). Although this study did not uncover novel genes affecting kidney formation, it confirms how forward genetic screens should prove useful in such studies. In the future, it will be beneficial to examine both new and existing *X. tropicalis* mutants to identify gene products with roles in renal pathologies and development.

Genome editing

Recent developments in nuclease technologies make it possible to edit the genome to generate loss-of-function mutations within *Xenopus*. Two techniques have been utilized in *X. tropicalis* to modify gene sequences with high efficiency (Young et al. 2011; Lei et al. 2012). Zinc-finger nucleases (ZFNs) and transcription activator-like effector nucleases (TALENs) induce DNA double-stranded breaks (DSB) within a desired genomic location. This initiates endogenous repair mechanisms including homologous recombination (HR) and nonhomologous end joining (NHEJ), resulting in deletions and insertions in the targeted gene locus. A third genome-editing tool, the CRISPR–Cas system, has thus far been utilized in the zebrafish system (Hwang et al. 2013) more recently in *Xenopus* (Nakayama et al. 2013). Each of these techniques is likely to permit the coordinate targeting of sequence regions shared among alleles of a chosen gene, saving considerable time in breeding to homozygosity. The ability to modify chosen genomic sequences using nuclease technologies will undoubtedly enable the targeted knockout of genes in the future studies.

Gene knockdown strategies

While whole-animal loss-of-function experiments have important uses, it is often more advantageous to target gene modifications to

a particular tissue to reduce confounding secondary effects from adjacent structures. In *Xenopus*, antisense morpholinos are commonly used to inhibit the production of gene products. Morpholinos are most often designed to inhibit mRNA translation, but they can also be directed to alter pre-RNA splicing, resulting in a codon frameshift and premature translational stop. Commonly, the knockdown of a targeted gene product within a desired embryonic region makes use of established *Xenopus* fate maps (Figure 12.1A). Primarily, such maps allow one to microinject an early embryonic cell (blastomere) at the blastula stage, whose daughter cells are known to contribute to the tissue of interest.

Morpholinos have thus far been the preferred means of knocking down gene function in *Xenopus* because RNAi techniques have not generally proven as effective. Recent work, however, indicates that providing exogenous catalytically active Argonaute, a component of the RNA-induced silencing complexes (RISCs), in combination with an siRNA, enables the knockdown of the corresponding targeted mRNA (Lund et al. 2011). Therefore, quite soon, siRNA-mediated knockdown of a targeted transcript may be accessible in the developing kidney and more broadly in *Xenopus*.

Targeted injections at early blastula stages roughly restrict the knockdown of gene expression spatially, but they do not allow temporal regulation, with the exception of using certain inducible constructs (Sive et al. 2000). Recently, the ability to selectively control morpholino activity through photocaging was developed, and it has proved effective in *Xenopus* (Deiters et al. 2010). The caged morpholino is not able to bind its intended mRNA target until UV light has uncaged it, allowing knockdown at a chosen developmental stage. Photocleavable morpholinos have also been developed (Shestopalov et al. 2007) and commercialized by Gene Tools. Although research utilizing photocleavable morpholinos in *Xenopus* has yet to be published, they have already been shown to be effective in zebrafish studies (Eisenhoffer et al. 2012; Tallafuss et al. 2012).

In the context of kidney development, photo-inducible morpholinos will be particularly

useful. By first targeting the morpholino microinjection to an early blastomere(s) whose daughter cells roughly contribute to the pronephros (see spatial targeting), the morpholino's activity can then be temporally regulated via light cleavage. This will allow for endogenous gene products to be manipulated at specific times in the nephric field, expanding the types of questions an investigator can address. As noted earlier, temporal control of gene knockdown will reduce potential complications arising from secondary effects upon tissues adjoining the kidney. For example, there are a proportion of daughter cells that arise from a blastomere(s) contributing to kidney that instead contribute to somites. Since somitic signals participate in kidney induction (Seufert et al. 1999), the ability to temporally control knockdown, via light-activated or light-inactivated morpholinos, will reduce unwanted secondary effects.

Transgenesis

Transgenesis has already become a useful tool for studies on *Xenopus* pronephric development, and the number of available lines continues to expand (Figure 12.3). As in mice, the generation of *Xenopus* transgenic animals can refine both spatial and temporal control of gene expression. Transgenesis permits the expression of native or mutant gene products, including dominant-active or dominant-negative constructs, as well as the targeting of fluorescent-fusion proteins to mark chosen subcellular compartments within cells of the forming kidney. *Xenopus* transgenics were first discovered with the observation of rare transmissions of microinjected DNA to progeny (Etkin et al. 1987). Since then, more efficient techniques have been developed for integration of transgenes into the *Xenopus* genome. This has included transposon, bacteriophage integrase, meganuclease, and restriction enzyme-mediated integration (Kroll and Amaya 1996; Zayed et al. 2004; Allen and Weeks 2005; Hamlet et al. 2006; Ogino et al. 2006a, 2006b). Given the promise of transgenic approaches, the research community has established resource centers to centrally house and generate transgenic lines,

specifically the National *Xenopus* Resource and the European *Xenopus* Resource Center (Pearl et al. 2012). This section will highlight the transgenic models that have and will continue to be useful in studies of pronephric development.

Several transgenic models have targeted fluorescent labels to the *Xenopus* pronephros. For example, green fluorescent protein (GFP) was expressed under the control of a 6kb fragment of the *hmf1-alpha* promoter, driving GFP within the pronephros (and certain other organs) of *X. laevis* (Ryffel and Lingott 2000). Similarly, the expression of GFP within the kidney and other tissues was achieved using the promoter of the thyroid hormone receptor beta A gene (Oofusa et al. 2001). Using Tol2-mediated insertion, a transgene encoding the *ef-1a* promoter, driving the expression of GFP, has been integrated into the jovan heat (*joh*) locus of *X. tropicalis* (Yergeau et al. 2010). This insertion, near the *hmf1-beta* gene, results in GFP expression within the pronephros. The use of embryos in which the pronephros has been labeled with GFP will assist in visualizing its development *in vivo*. This in turn will facilitate larger screens of kidney formation, as well as an investigator's ability to probe more discrete abnormalities (see succeeding text).

In addition to the previously noted GFP reporters of the *Xenopus* pronephros, we have shown that the zebrafish cadherin-17 promoter drives expression there as well (Naylor et al. 2013) (Figure 12.3). For this work, we used Tol2 transposon-mediated transgenesis within *X. laevis* embryos. A transgenic line expressing fluorescent labels under the control of the zebrafish cadherin-17 promoter will be generated and made available. Characterizing more precisely when and where varying kidney promoters are expressed will enable more sophisticated targeted expression of experimental constructs. Additionally, it will allow better *in vivo* visualization of pronephric development in the normal animal, including the resolution of chosen subcellular compartments or structures (e.g., GFP targeting to the nucleus, plasma membrane, or cytoskeleton).

Transgenics have also been utilized in the molecular analysis of pronephric development. Lines in which Wnt reporters have been integrated into *X. laevis* have enabled the

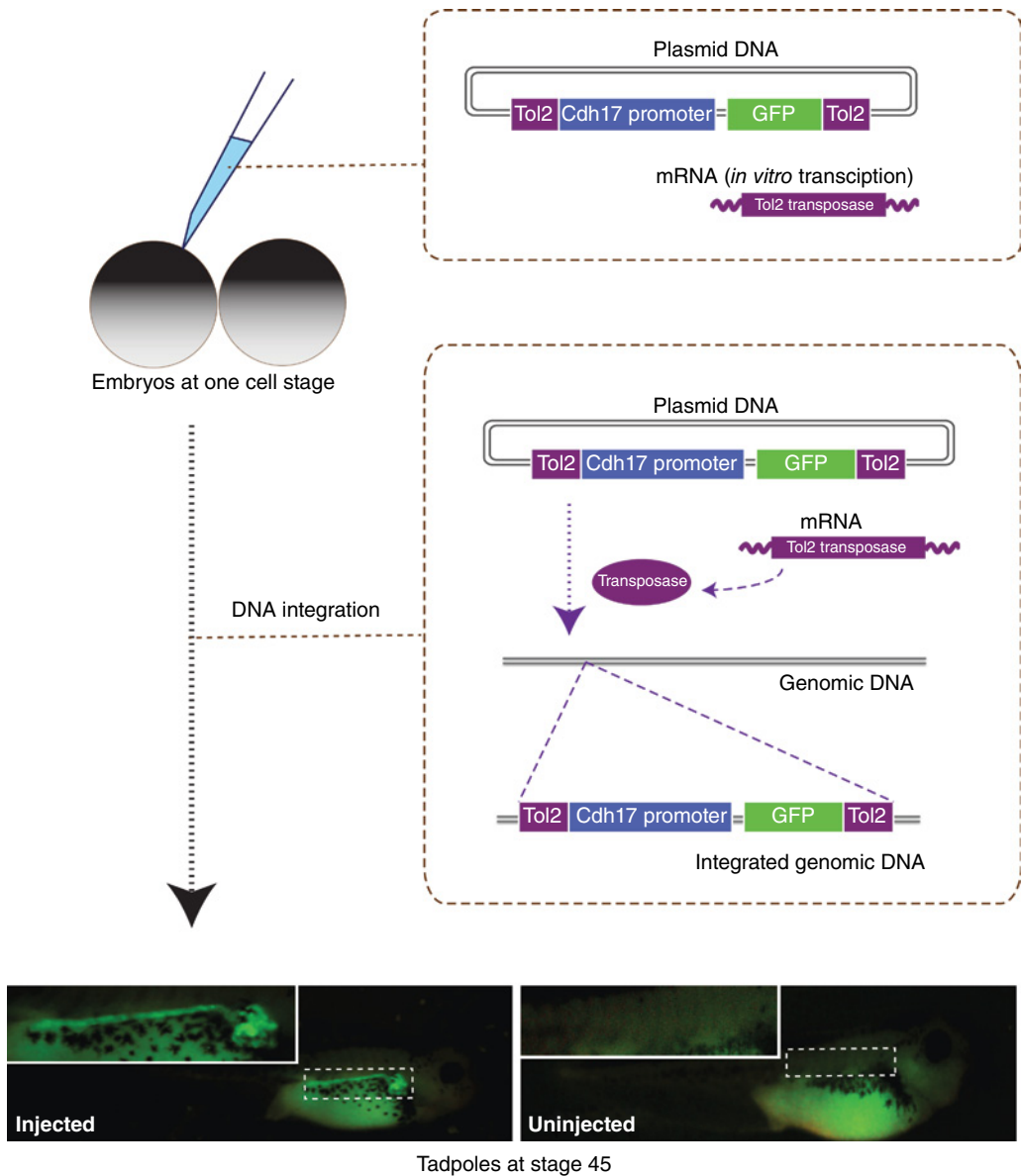


Figure 12.3 Transposon-mediated transgenesis. Tol2 transposon-mediated integration of the zebrafish cadherin-17 (Cdh17) promoter driving GFP in *X. laevis* embryos. Coinjection of a DNA plasmid containing *cdh17::gfp* flanked by Tol2 repeats with mRNA encoding the Tol2 transposase enzyme into single-cell embryos. Once translated in the embryo, the transposase will integrate the transgene into the *X. laevis* genome. Parental (F_0) tadpoles express GFP within their developing pronephros at stage 45.

visualization of the temporal and spatial regulation of beta-catenin-mediated Wnt signaling, both broadly during development and specifically within the pronephros (Denayer et al. 2006; Lyons et al. 2009). Transgenic integration of heat-shock-inducible Cre recombinase has been utilized to temporally overexpress a

mutated *hnf1-beta* transcription factor at the gastrula stage, resulting in malformation of the pronephros and edema among other phenotypes (Roose et al. 2009). This system has also been used to demonstrate that human patient mutations in *hnf1-beta*, which contribute to diabetes as well as defective kidney and liver

functions, and malformations of the pancreas and genital tract, result in malformation of proximal tubules and defects in pronephric size (Sauert et al. 2012). These pioneering studies in *Xenopus* transgenics have laid the groundwork for the spatial and temporal control of fluorescent markers, reporters, and other experimental constructs.

Imaging

Visualization of *Xenopus* pronephric development is facilitated by the external development of the embryo as well as the virtual transparency of the tadpole stage epidermis, with the exception of pigment cells. This allows for efficient whole-mount *in situ* and immunofluorescent staining of fixed tissue, as well as *in vivo* visualization of kidney in embryos expressing fluorophores under the control of kidney-specific promoters (as described previously). Following kidney development in *Xenopus* is enabled by the use of numerous established markers. They have allowed the evaluation of multiple

developmental processes, inclusive of specification, patterning, differentiation, and morphogenesis, as a function, for example, of knockdown or overexpression of a chosen gene product. Numerous subcellular markers are further available. This section will provide an overview of current developmental markers as well as subcellular markers to assess pronephric development.

Molecular markers

Over the past 20 years, the expression profiles of numerous genes have been characterized within the *Xenopus* pronephros, serving to mark developmental processes and phases. Through whole-mount *in situ* hybridization, the pronephric anlagen can be distinguished throughout development from induction to morphogenesis stages (Figures 12.4 and 12.5). While their number is growing, fewer antibodies exist that specifically mark the developing kidney at restricted developmental stages compared with the array of probes available to examine transcript expression.

(A)



(B)

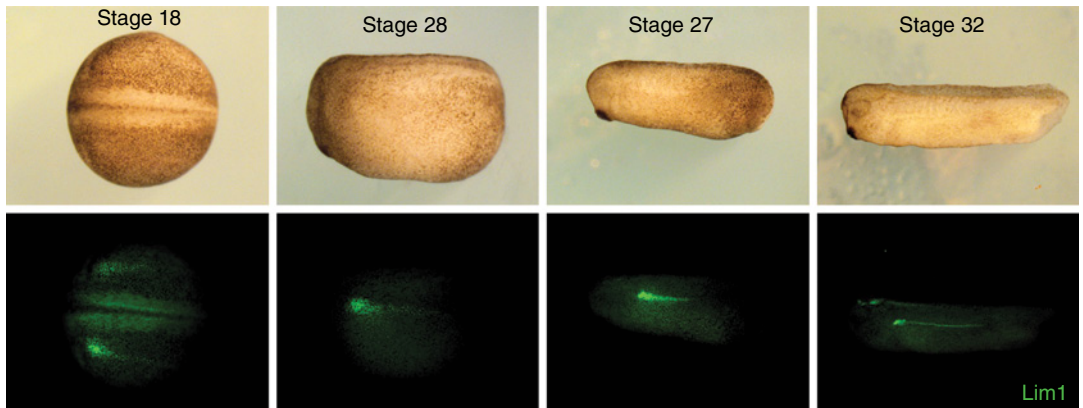


Figure 12.4 Early pronephric markers. A. *In situ* hybridization of early nephric markers. Whole-mount *in situ* hybridization patterns showing mRNA expression within the pronephros of *hnf1-beta* (*hnf1b*), *lim1*, and *pax8* in stage 28–32 embryos. (B) *Lim1* immunostaining through kidney development. Whole-mount immunofluorescence staining (bottom panels) of *Lim1* protein localization within the pronephros from neurula to tadpole stages (top panels).

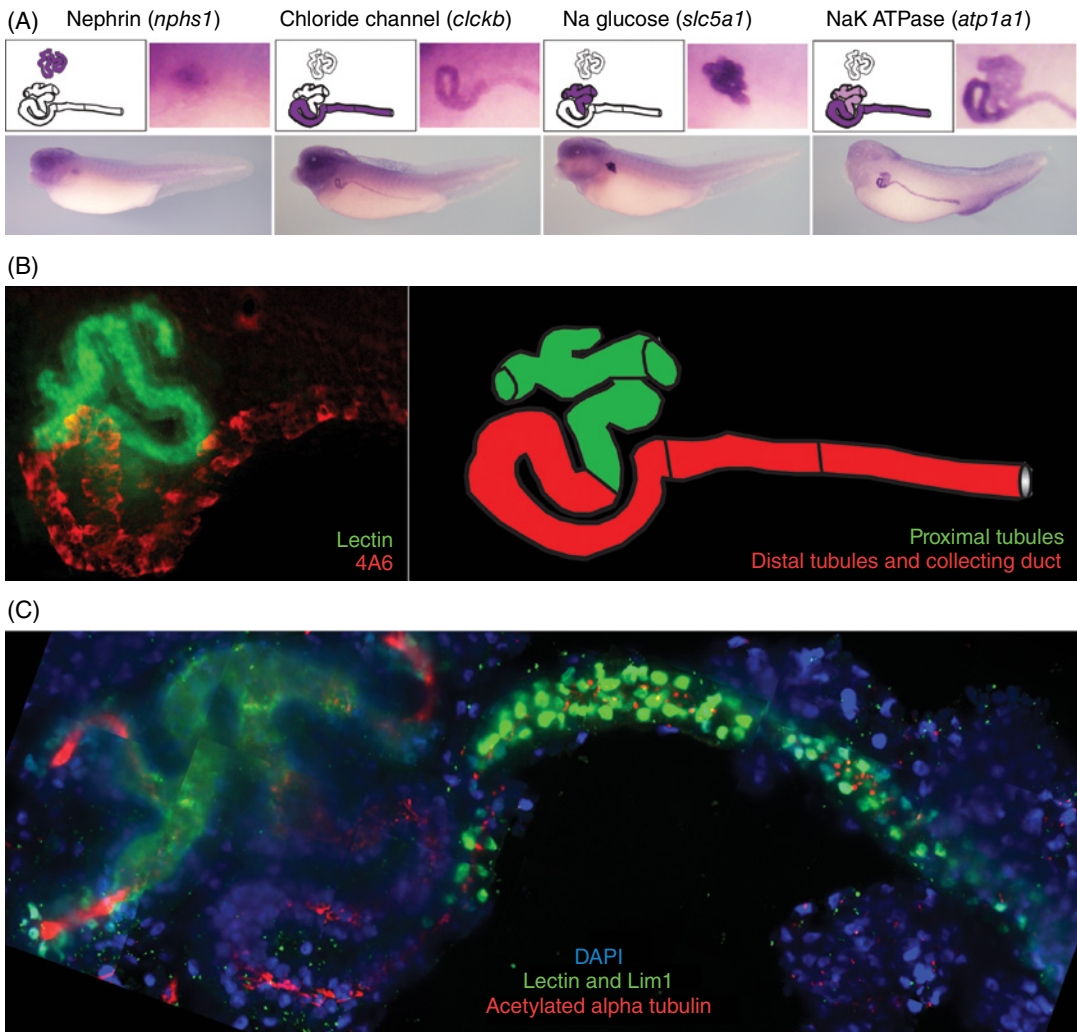


Figure 12.5 Late pronephric markers. (A) *In situ* hybridization of late pronephric markers. Whole-mount *in situ* hybridization showing mRNA expression of *nphs1*, *clckb*, *slc5a1*, and *atp1a1* within the developing glomerus, distal tubules and collecting duct, proximal tubules, and all tubular structures (respectively) at stages 38–40. (B) Immunostaining of pronephric tubules. Whole-mount fluorescent staining of the proximal tubules using a fluorescent lectin (green) and the distal tubules and collecting duct using the 4A6 antibody (red) at stage 38 imaged using stereomicroscopy. Fiji/ImageJ software was used to subtract background from the image. (C) Immunostaining of subcellular structures. Whole-mount fluorescent staining of the proximal tubules (fluorescent lectin – green), nuclei of the collecting duct (Lim1 antibody – green), pronephric cilia (acetylated alpha tubulin – red), and all nuclei (DAPI – blue) at stage 36 imaged using confocal microscopy. To see a color version of this figure, see Plate 32.

Transcripts that are expressed within the developing pronephros at various stages and within specific regions continue to be identified. The number of *in situ* markers available is too large to list in their entirety here, but many of the transcripts expressed in the pronephros are nicely presented in the XenMARK database (Gilchrist et al. 2009).

Several critical markers expressed at various stages of development will be highlighted, however. As discussed previously, *lim1*, *pax8*, and *hnf1-beta* are the first known transcripts to be expressed within the pronephric primordium around stage 12.5 and onward (Taira et al. 1994; Weber et al. 1996; Carroll and Vize 1999) (Figure 12.4A).

Shortly thereafter, *pax2* and *wnt4* begin to become visible at about stage 18 (Heller and Brandli 1997; Saulnier et al. 2002). Each of these early markers continues to be expressed within the developing tubules and duct through tadpole stages, except *wnt4*, which ceases expression in the ducts around stage 30. *wt1* is the earliest marker specific for glomerular lineages and begins to become visible at stage 20 (Carroll and Vize 1996).

As the pronephros begins to epithelialize, markers along the proximal and distal extent of the nephron begin to be distinguished. The glomerulus can be marked at later stages (~ stage 26) using probes against nephrin (*nphs1*) (Gerth et al. 2005) (Figure 12.5A). Within the developing proximal tubules, a sodium glucose cotransporter (*slc5a9*) begins to be expressed at stage 28 (Zhou and Vize 2004), while the distal tubule and collecting duct are marked by the chloride conductance channel (*clcnkb*) (Vize 2003a) (Figure 12.5A). A NaKATPase probe (*atp1a1*) can be utilized to visualize the entire nephric tube during differentiation and morphogenesis, including the proximal tubules, distal tubules, and collecting duct (Uochi et al. 1997) (Figure 12.5A). Together, the availability of numerous probes enables the visualization of kidney at various stages and positions during development.

Complementing the use of *in situ* hybridization, several antibodies are available that label different components of the kidney. Antibodies against Lim1 can be utilized to visualize the nuclei of cells that have been patterned during early nephrogenesis through morphogenesis of the tubules (Venegas-Ferrin et al. 2010) (Figures 12.4B and 12.5C). Immunostaining can be carried out to label the differentiated proximal tubules as well as the distal tubules and collecting duct using the 3G8 and 4A6 antibodies, respectively (Vize et al. 1995) (Figure 12.5B and C). Additionally, a fluorescently labeled *Erythrina cristagalli* lectin can also be utilized to label the proximal tubules (Miller et al. 2011) (Figure 12.5B and C). Cell division and apoptosis can be monitored throughout development using antibodies respectively directed against phosphorylated histone H3 and active caspase (Miller et al. 2011). Together, these

tools can be utilized in beginning to assess how the experimental manipulation of a gene product of interest might affect various stages of kidney development.

Live imaging

Fluorescent markers of certain subcellular components are available to visualize their corresponding cellular activities *in vivo*. For example, numerous cytoskeletal, membrane, nuclear, and other markers have enabled the imaging of cellular movements or other processes within living embryos (Skoglund et al. 2008; Kieserman and Wallingford 2009; Woolner et al. 2009; Brooks and Wallingford 2012). In the future, the full utilization of these tools within the developing pronephros will facilitate our understanding of cellular behaviors and movements during its morphogenesis. For example, pioneering studies have demonstrated that kidney tubules are formed by convergence extension movements similar to those utilized during gastrulation (Lienkamp et al. 2010; Lienkamp et al. 2012).

To this point, fluorescent subcellular markers have been expressed transiently by injection of transcripts into a blastomere contributing to the tissue of interest. However, with the improvement in transgenic technologies, and the use of tissue-specific promoters, it is becoming possible to drive the expression of fluorescent labels under temporal and spatial control. Promoters driving expression within specific tissues have already been utilized to visualize subcellular components within living tissues (Takagi et al. 2013). In the future, transgenic lines will help us to visualize subcellular processes relating to pronephric development in living developing embryos. Such models will allow more efficient analysis of the roles of particular gene products in nephrogenesis.

Screens

Xenopus embryos provide multiple avenues for the study of pronephric tubulogenesis. Embryos develop well suspended in an aqueous environment within multiwell plates,

and they are amenable to screens involving either microinjection strategies or the absorption of water-soluble drugs through their skin. Instead of intact embryos, an alternative model to follow kidney formation is to employ pronephric tubules induced from unspecified “stemlike” naïve ectoderm tissue (animal caps), isolated at late blastula stages (Ariizumi and Asashima 2001; Osafune et al. 2002). Either system could provide the basis for an unbiased screen aimed at identifying effects on nephric development. Most screens to date have used the whole-embryo system. However, the use of the animal cap system is likely to grow, such as to ascertain the function of genes relevant to kidney progenitor status (stemness) versus differentiation. Additionally, as the *Xenopus* pronephros has been recognized as a model of nephron regeneration (Caine and McLaughlin 2013), the screening strategies detailed here could additionally be applied in regeneration contexts.

Gain-of-function screens

The *X. tropicalis* full-length expression library allows for overexpression of genes in an unbiased manner (Gilchrist et al. 2004). A subset of the library has been used in a study to assess the consequence of overexpressing genes within the developing pronephros (Kyuno et al. 2008). This work suggested that 4% of the screened clones, whose transcripts are expressed in the developing kidney, play a role in nephrogenesis. The ability to easily overexpress transcripts within the developing pronephros (or animal cap) will facilitate the discovery of novel factors involved in vertebrate kidney development, as well as factors involved in programming kidney progenitors.

In silico screens

The wealth of information provided in databases continues to provide a broader understanding of diverse developmental processes. The European Renal Genome Project *Xenopus* Gene Expression Database provides images of gene expression patterns within the developing pronephros. This has facilitated an

unbiased screen of differentiation markers with regard to the segmentation patterns of the developing pronephros (Raciti et al. 2008). This study identified eight regions of the nephron with distinct gene expression, which can be divided into domains identified as the proximal tubule, intermediate tubule, distal tubule, and connecting tubule, similar to that of the human metanephric nephron. This study supports the functional relevance of studies on the *Xenopus* pronephros as related to human kidney disease.

Loss-of-function screens

In addition to genetic approaches, described previously, knockdown approaches are a viable means of performing loss-of-function screens in *Xenopus* embryos. To this point, it has been difficult and expensive to inhibit the individual functions of large numbers of genes because the most viable means for such screens has been through morpholino-mediated knockdown. However, a pilot study using this type of approach has proved useful in the context of studying head development (Kenwrick et al. 2004), suggesting it may be useful for the study of kidney. Especially with the continuing advances in RNAi technology in *Xenopus* (Lund et al. 2011), the application of large-scale loss-of-function screens in kidney may become practical.

Drug screens

Another means of performing a loss-of-function screen is to utilize characterized chemical libraries. A commercially available library of characterized bioactive compounds has been used successfully to screen for factors involved in vascular and lymphatic development (Kalin et al. 2009). Such a screen takes advantage of the growth of *Xenopus* embryos in liquid, allowing their relatively controlled exposure to drugs known to block developmental signaling pathways. Thus, screens can be carried out to block signaling activity at particular time points relevant to kidney development, bypassing effects upon earlier developmental processes. Such strategies will not only enable the study

of kidney specification, determination, differentiation, and morphogenesis but also enable studies of kidney maintenance and regeneration.

Transgenics in screens

Current screens largely rely on the use of *in situ* hybridization to characterize the effects of modifying gene expression or protein function (Kenwrick et al. 2004; Kalin et al. 2009; Kyuno et al. 2008; Raciti et al. 2008). However, screening technologies would be made more efficient through the use of transgenic embryos in which markers of interest within the pronephros were tagged fluorescently. This would enable faster visual screening of kidney phenotypes in living embryos. Transgenic embryos could be designed to express subcellular labels (described previously) under the control of promoters activated in specific cell lineages at developmental time points of interest. Such lines would facilitate kidney screens and allow visualization of developmental processes *in vivo*.

Conclusions

The development of embryological techniques, along with new technologies available to *Xenopus* researchers, has created new opportunities and approaches in the study of nephrogenesis. Prior work has demonstrated the structural and functional homology between the *Xenopus* pronephros and the mammalian metanephric nephron. Additionally, the classical approaches including microdissections and grafting complement current molecular approaches to provide a unique opportunity to explore nephron development, maintenance, and regeneration. New approaches to alter genetic sequences along with innovative imaging techniques will allow researchers to visualize nephrogenesis in living embryos. Such work is made more accessible because the *Xenopus* kidney forms beneath a semitransparent ectoderm. Additionally, through the manipulation of naïve ectoderm (animal caps), we will be able to address how progenitor cells are programmed toward kidney fates. Overall, the study of pronephric

development in *Xenopus* is likely to grow as a model to understand nephrogenesis in vertebrates generally.

Acknowledgments

We would like to thank Alan Davidson for graciously sharing the zebrafish cadherin-17 promoter driving *gfp* and for the Tol2 vector. We are also grateful to Norihiro Sudou and Masonari Taira for use of the Lim1 antibody they generated. We are thankful for our research support from an NIH NIGMS R01 grant (GM052112) (P.D.M.), a postdoctoral fellowship provided by the Odyssey Program and the Theodore N. Law Endowment for Scientific Achievement at the University of Texas MD Anderson Cancer Center (R.K.M.), a postdoctoral fellowship from the National Kidney Foundation (FLB1628) (R.K.M.), an NIH NIDDK K01 Career Development Award (1K01DK092320) (R.K.M.), and a Cancer Prevention Research Initiative of Texas (C.P.R.I.T.) Fellowship (M.L.), without which this work would not be possible.

References

- Abu-Daya, A., M. K. Khokha, and L. B. Zimmerman. 2012. The hitchhiker's guide to *Xenopus* genetics. *Genesis* 50(3): 164–175.
- Aghajanian, C., S. Soignet, D. S. Dizon, et al. 2002. A phase I trial of the novel proteasome inhibitor PS341 in advanced solid tumor malignancies. *Clin Cancer Res* 8(8): 2505–2511.
- Agrawal, R., U. Tran, and O. Wessely. 2009. The miR-30 miRNA family regulates *Xenopus* pronephros development and targets the transcription factor *Xlim1/Lhx1*. *Development* 136(23): 3927–3936.
- Alarcon, P., E. Rodriguez-Seguel, A. Fernandez-Gonzalez, R. Rubio, and J. L. Gomez-Skarmeta. 2008. A dual requirement for Iroquois genes during *Xenopus* kidney development. *Development* 135(19): 3197–3207.
- Allen, B. G. and D. L. Weeks. 2005. Transgenic *Xenopus laevis* embryos can be generated using phiC31 integrase. *Nat Methods* 2(12): 975–979.
- Ariizumi, T. and M. Asashima. 2001. In vitro induction systems for analyses of amphibian organogenesis and body patterning. *Int J Dev Biol* 45(1): 273–279.

- Bauer, D. V., S. Huang, and S. A. Moody. 1994. The cleavage stage origin of Spemann's Organizer: Analysis of the movements of blastomere clones before and during gastrulation in *Xenopus*. *Development* **120**(5): 1179–1189.
- Bello, V., C. Sirour, N. Moreau, E. Denker, and T. Darribere. 2008. A function for dystroglycan in pronephros development in *Xenopus laevis*. *Dev Biol* **317**(1): 106–120.
- Beuchat, C. A. and E. J. Braun. 1988. Allometry of the kidney: implications for the ontogeny of osmoregulation. *Am J Physiol* **255**(5 Pt 2): R760–767.
- Biegon, A., M. Alvarado, T. F. Budinger, et al. 2002. Region-selective effects of neuroinflammation and antioxidant treatment on peripheral benzodiazepine receptors and NMDA receptors in the rat brain. *J Neurochem* **82**(4): 924–934.
- Blitz, I. L., G. Andelfinger, and M. E. Horb. 2006. Germ layers to organs: using *Xenopus* to study "later" development. *Semin Cell Dev Biol* **17**(1): 133–145.
- Bohn, S., H. Thomas, G. Turan, S. Ellard, C. Bingham, A. T. Hattersley, and G. U. Ryffel. 2003. Distinct molecular and morphogenetic properties of mutations in the human HNF1beta gene that lead to defective kidney development. *J Am Soc Nephrol* **14**(8): 2033–2041.
- Bracken, C. M., K. Mizeracka, and K. A. McLaughlin. 2008. Patterning the embryonic kidney: BMP signaling mediates the differentiation of the pronephric tubules and duct in *Xenopus laevis*. *Dev Dyn* **237**(1): 132–144.
- Brandli, A. W. 1999. Towards a molecular anatomy of the *Xenopus* pronephric kidney. *Int J Dev Biol* **43**(5): 381–395.
- Brennan, H. C., S. Nijjar, and E. A. Jones. 1998. The specification of the pronephric tubules and duct in *Xenopus laevis*. *Mech Dev* **75**(1–2): 127–137.
- Brennan, H. C., S. Nijjar, and E. A. Jones. 1999. The specification and growth factor inducibility of the pronephric glomus in *Xenopus laevis*. *Development* **126**(24): 5847–5856.
- Brooks, E. R. and J. B. Wallingford. 2012. Control of vertebrate intraflagellar transport by the planar cell polarity effector Fuz. *J Cell Biol* **198**(1): 37–45.
- Caine, S. T. and K. A. McLaughlin. 2013. Regeneration of functional pronephric proximal tubules after partial nephrectomy in *Xenopus laevis*. *Dev Dyn* **242**(3): 219–229.
- Carroll, T. J. and P. D. Vize. 1996. Wilms' tumor suppressor gene is involved in the development of disparate kidney forms: evidence from expression in the *Xenopus* pronephros. *Dev Dyn* **206**(2): 131–138.
- Carroll, T. J. and P. D. Vize. 1999. Synergism between Pax-8 and lim-1 in embryonic kidney development. *Dev Biol* **214**(1): 46–59.
- Carroll, T. J., J. B. Wallingford, and P. D. Vize. 1999a. Dynamic patterns of gene expression in the developing pronephros of *Xenopus laevis*. *Dev Genet* **24**(3–4): 199–207.
- Carroll, T., J. Wallingford, D. Seufert, and P. D. Vize. 1999b. Molecular regulation of pronephric development. *Curr Top Dev Biol* **44**: 67–100.
- Cartry, J., M. Nichane, V. Ribes, et al. 2006. Retinoic acid signalling is required for specification of pronephric cell fate. *Dev Biol* **299**(1): 35–51.
- Chan, T. C., T. Ariizumi, and M. Asashima. 1999. A model system for organ engineering: transplantation of in vitro induced embryonic kidney. *Naturwissenschaften* **86**(5): 224–227.
- Cho, G. S., S. C. Choi, E. C. Park, and J. K. Han. 2011. Role of Tbx2 in defining the territory of the pronephric nephron. *Development* **138**(3): 465–474.
- Clevers, H. and R. Nusse. 2012. Wnt/beta-catenin signaling and disease. *Cell* **149**(6): 1192–1205.
- Colas, A., J. Cartry, I. Buisson, M. Umbhauer, J. C. Smith, and J. F. Riou. 2008. Mix.1/2-dependent control of FGF availability during gastrulation is essential for pronephros development in *Xenopus*. *Dev Biol* **320**(2): 351–365.
- Coresh, J., E. Selvin, L. A. Stevens, et al. 2007. Prevalence of chronic kidney disease in the United States. *JAMA* **298**(17): 2038–2047.
- Cornish, J. A. and L. D. Etkin. 1993. The formation of the pronephric duct in *Xenopus* involves recruitment of posterior cells by migrating pronephric duct cells. *Dev Biol* **159**(1): 338–345.
- Curran, K. L., S. LaRue, B. Bronson, et al. 2008. Circadian genes are expressed during early development in *Xenopus laevis*. *PLoS One* **3**(7): e2749.
- Davidson, L. A. and R. E. Keller. 1999. Neural tube closure in *Xenopus laevis* involves medial migration, directed protrusive activity, cell intercalation and convergent extension. *Development* **126**(20): 4547–4556.
- Deiters, A., R. A. Garner, H. Lusic, et al. 2010. Photocaged morpholino oligomers for the light-regulation of gene function in zebrafish and *Xenopus* embryos. *J Am Chem Soc* **132**(44): 15644–15650.
- Del Viso, F., D. Bhattacharya, Y. Kong, M. J. Gilchrist, and M. K. Khokha. 2012. Exon capture and bulk segregant analysis: rapid discovery of causative mutations using high-throughput sequencing. *BMC Genomics* **13**: 649.
- Demartis, A., M. Maffei, R. Vignali, G. Barsacchi, and V. De Simone. 1994. Cloning and developmental expression of LFB3/HNF1 beta transcription factor in *Xenopus laevis*. *Mech Dev* **47**(1): 19–28.
- Denayer, T., F. Van Roy, and K. Vleminckx. 2006. In vivo tracing of canonical Wnt signaling in

- Xenopus* tadpoles by means of an inducible transgenic reporter tool. *FEBS Lett* **580**(2): 393–398.
- Dizon, D. S., P. J. Sabbatini, C. Aghajanian, M. L. Hensley, and D. R. Spriggs. 2002. Analysis of patients with epithelial ovarian cancer or fallopian tube carcinoma retreated with cisplatin after the development of a carboplatin allergy. *Gynecol Oncol* **84**(3): 378–382.
- Drawbridge, J., C. M. Meighan, R. Lumpkins, and M. E. Kite. 2003. Pronephric duct extension in amphibian embryos: migration and other mechanisms. *Dev Dyn* **226**(1): 1–11.
- Dressler, G. R. 2006. The cellular basis of kidney development. *Annu Rev Cell Dev Biol* **22**: 509–529.
- Drummond, I. A. and A. Majumdar. 2003. Pronephric glomus and vasculature. *The Kidney: From Normal Development to Congenital Disease*. P. D. Vize, A. S. Woolf, and J. Bard, Academic Press, Amsterdam.
- Dudziak, K., N. Mottalebi, S. Senkel, et al. 2008. Transcription factor HNF1beta and novel partners affect nephrogenesis. *Kidney Int* **74**(2): 210–217.
- Eisenhoffer, G. T., P. D. Loftus, M. Yoshigi, et al. 2012. Crowding induces live cell extrusion to maintain homeostatic cell numbers in epithelia. *Nature* **484**(7395): 546–549.
- Etkin, L. D., B. Pearman, and R. Ansah-Yiadom. 1987. Replication of injected DNA templates in *Xenopus* embryos. *Exp Cell Res* **169**(2): 468–477.
- Gerth, V. E., X. Zhou, and P. D. Vize. 2005. Nephric expression and three-dimensional morphogenesis of the *Xenopus* pronephric glomus. *Dev Dyn* **233**(3): 1131–1139.
- Gibson, P. G., H. Powell, J. Coughlan, et al. 2002. Limited (information only) patient education programs for adults with asthma. *Cochrane Database Syst Rev* (2): CD001005.
- Gilchrist, M. J., A. M. Zorn, J. Voigt, J. C. Smith, N. Papalopulu, and E. Amaya. 2004. Defining a large set of full-length clones from a *Xenopus tropicalis* EST project. *Dev Biol* **271**(2): 498–516.
- Gilchrist, M. J., M. B. Christensen, O. Bronchain, et al. 2009. Database of queryable gene expression patterns for *Xenopus*. *Dev Dyn* **238**(6): 1379–1388.
- Goda, T., A. Abu-Daya, S. Carruthers, M. D. Clark, D. L. Stemple, and L. B. Zimmerman. 2006. Genetic screens for mutations affecting development of *Xenopus tropicalis*. *Plos Genet* **2**(6): e91.
- Haldin, C. E., K. L. Masse, S. Bhamra, S. Simrick, J. I. Kyuno, and E. A. Jones. 2008. The *lmx1b* gene is pivotal in glomus development in *Xenopus laevis*. *Dev Biol* **322**(1): 74–85.
- Hamlet, M. R., D. A. Yergeau, E. Kuliyeve, et al. 2006. Tol2 transposon-mediated transgenesis in *Xenopus tropicalis*. *Genesis* **44**(9): 438–445.
- Harms, W., P. Peschke, K. J. Weber, et al. 2002. Dose-dependent differential effects of low and pulsed dose-rate brachytherapy in a radioresistant syngenic rat prostate tumour model. *Int J Radiat Biol* **78**(7): 617–623.
- Heller, N. and A. W. Brandli. 1997. *Xenopus* Pax-2 displays multiple splice forms during embryogenesis and pronephric kidney development. *Mech Dev* **69**(1–2): 83–104.
- Hellsten, U., R. M. Harland, M. J. Gilchrist, et al. 2010. The genome of the Western clawed frog *Xenopus tropicalis*. *Science* **328**(5978): 633–636.
- Hensley, P. L. and H. G. Nurnberg. 2002. SSRI sexual dysfunction: a female perspective. *J Sex Marital Ther* **28**(Suppl 1): 143–153.
- Hirsch, N., L. B. Zimmerman, and R. M. Grainger. 2002. *Xenopus*, the next generation: *X. tropicalis* genetics and genomics. *Dev Dyn* **225**(4): 422–433.
- Holtfreter, J. 1933. The influence of host aging and the different organ zones on the differentiation of accumulated gastrula-ectoderm. *Wilhelm Roux Archiv* **127**(4): 619–775.
- Holtfreter, J. 1944. Experimental studies on the development of the pronephros. *Rev Can Biol* **3**: 220–250.
- Hwang, W. Y., Y. Fu, D. Reyon, et al. 2013. Efficient genome editing in zebrafish using a CRISPR–Cas system. *Nat Biotechnol* **31**(3): 227–229.
- Jones, E. A. 2003. Molecular control of pronephric development: an overview. *The Kidney: From Normal Development to Congenital Disease*. P. D. Vize, A. S. Woolf, and J. Bard, Academic Press, Amsterdam.
- Jones, E. A. 2005. *Xenopus*: a prince among models for pronephric kidney development. *J Am Soc Nephrol* **16**(2): 313–321.
- Kalin, R. E., N. E. Banziger-Tobler, M. Detmar, and A. W. Brandli. 2009. An in vivo chemical library screen in *Xenopus* tadpoles reveals novel pathways involved in angiogenesis and lymphangiogenesis. *Blood* **114**(5): 1110–1122.
- Kaneko, T., T. Chan, R. Satow, T. Fujita, and M. Asashima. 2003. The isolation and characterization of XC3H-3b: a CCCH zinc-finger protein required for pronephros development. *Biochem Biophys Res Commun* **308**(3): 566–572.
- Kenwrick, S., E. Amaya, and N. Papalopulu. 2004. Pilot morpholino screen in *Xenopus tropicalis* identifies a novel gene involved in head development. *Dev Dyn* **229**(2): 289–299.
- Khokha, M. K. 2012. *Xenopus* white papers and resources: folding functional genomics and genetics into the frog. *Genesis* **50**(3): 133–142.
- Kieserman, E. K. and J. B. Wallingford. 2009. In vivo imaging reveals a role for Cdc42 in spindle positioning and planar orientation of cell divisions during vertebrate neural tube closure. *J. Cell Sci.* **122**(Pt 14): 2481–2490.

- Kornstein, S. G. and A. H. Clayton. 2002. *Women's Mental Health: A Comprehensive Textbook*, New York, Guilford.
- Kroll, K. L. and E. Amaya. 1996. Transgenic *Xenopus* embryos from sperm nuclear transplantations reveal FGF signaling requirements during gastrulation. *Development* **122**: 3173–3183.
- Kyuno, J. and E. A. Jones. 2007. GDNF expression during *Xenopus* development. *Gene Expr Patterns* **7**(3): 313–317.
- Kyuno, J., K. Masse, and E. A. Jones. 2008. A functional screen for genes involved in *Xenopus* pronephros development. *Mech Dev* **125**(7): 571–586.
- Leclerc, C., S. E. Webb, A. L. Miller, and M. Moreau. 2008. An increase in intracellular Ca²⁺ is involved in pronephric tubule differentiation in the amphibian *Xenopus laevis*. *Dev Biol* **321**(2): 357–367.
- Lei, Y., X. Guo, Y. Liu, et al. 2012. Efficient targeted gene disruption in *Xenopus* embryos using engineered transcription activator-like effector nucleases (TALENs). *Proc Natl Acad Sci USA* **109**(43): 17484–17489.
- Li, L., L. Wen, Y. Gong, et al. 2012. *Xenopus* as a model system for the study of GOLPH2/GP73 function: *Xenopus* GOLPH2 is required for pronephros development. *PLoS One* **7**(6): e38939.
- Lienkamp, S., A. Ganner, C. Boehlke, et al. 2010. Inversin relays Frizzled-8 signals to promote proximal pronephros development. *Proc Natl Acad Sci USA* **107**(47): 20388–20393.
- Lienkamp, S. S., K. Liu, C. M. Karner, et al. 2012. Vertebrate kidney tubules elongate using a planar cell polarity-dependent, rosette-based mechanism of convergent extension. *Nat Genet* **44**(12): 1382–1387.
- Lund, E., M. D. Sheets, S. B. Imboden, and J. E. Dahlberg. 2011. Limiting Ago protein restricts RNAi and microRNA biogenesis during early development in *Xenopus laevis*. *Genes Dev* **25**(11): 1121–1131.
- Lynch, K. and S. E. Fraser. 1990. Cell migration in the formation of the pronephric duct in *Xenopus laevis*. *Dev Biol* **142**(2): 283–292.
- Lysaght MJ. 2002. Maintenance dialysis population dynamics: current trends and long term implications. *J Am Soc Nephrol* **13**: 37–40.
- Lyons, J. P., R. K. Miller, X. Zhou, et al. 2009. Requirement of Wnt/ β -catenin signaling in pronephric kidney development. *Mech Dev* **126**(3–4): 142–159.
- McCoy, K. E., X. Zhou, and P. D. Vize. 2011. Non-canonical wnt signals antagonize and canonical wnt signals promote cell proliferation in early kidney development. *Dev Dyn* **240**(6): 1558–1566.
- McLaughlin, K. A., M. S. Ronces, and M. Mercola. 2000. Notch regulates cell fate in the developing pronephros. *Dev Biol* **227**(2): 567–580.
- McLin, V. A., C. H. Hu, R. Shah, and M. Jamrich. 2008. Expression of complement components coincides with early patterning and organogenesis in *Xenopus laevis*. *Int J Dev Biol* **52**(8): 1123–1133.
- Miller, R. K. and P. D. McCrea. 2010. Wnt to build a tube: contributions of Wnt signaling to epithelial tubulogenesis. *Dev Dyn* **239**(1): 77–93.
- Miller, R. K., S. G. Canny, C. W. Jang, et al. 2011. Pronephric tubulogenesis requires Daam1-mediated planar cell polarity signaling. *J Am Soc Nephrol* **22**(9): 1654–1664.
- Mitchell, T. S. and M. D. Sheets. 2001. The FGFR pathway is required for the trunk-inducing functions of Spemann's organizer. *Dev Biol* **237**(2): 295–305.
- Mitchell, T. S. and M. D. Sheets. 2002. Chordin mediates pronephros induction by the trunk organizer. *Developmental Biology* **247**(2): 467–467.
- Mitchell, T., E. A. Jones, D. L. Weeks, and M. D. Sheets. 2007. Chordin affects pronephros development in *Xenopus* embryos by anteriorizing presomitic mesoderm. *Dev Dyn* **236**(1): 251–261.
- Moody, S. A. 1987a. Fates of the blastomeres of the 16-cell stage *Xenopus* embryo. *Dev Biol* **119**(2): 560–578.
- Moody, S. A. 1987b. Fates of the blastomeres of the 32-cell-stage *Xenopus* embryo. *Dev Biol* **122**(2): 300–319.
- Murugan, S., J. Shan, S. J. Kuhl, et al. 2012. WT1 and Sox11 regulate synergistically the promoter of the Wnt4 gene that encodes a critical signal for nephrogenesis. *Exp Cell Res* **318**(10): 1134–1145.
- Nakayama, T., M. B. Fish, M. Fisher, J. Oomen-Hajagos, G. H. Thomsen, and R. M. Grainger. 2013. Simple and efficient CRISPR/Cas9-mediated targeted mutagenesis in *Xenopus tropicalis*. *Genesis* **51**(12): 835–843.
- Naylor, R. W. and E. A. Jones. 2009. Notch activates Wnt-4 signalling to control medio-lateral patterning of the pronephros. *Development* **136**(21): 3585–3595.
- Naylor, R. W., R. J. Collins, A. Philpott, and E. A. Jones. 2009. Normal levels of p27 are necessary for somite segmentation and determining pronephric organ size. *Organogenesis* **5**(4): 119–128.
- Naylor, R. W., A. Przepiorski, Q. Ren, J. Yu, and A. J. Davidson. 2013. HNF1 β is essential for nephron segmentation during nephrogenesis. *J Am Soc Nephrol* **24**(1): 77–87.
- Nejigane, S., Y. Haramoto, M. Okuno, S. Takahashi, and M. Asashima. 2011. The transcriptional coactivators Yap and TAZ are expressed during early *Xenopus* development. *Int J Dev Biol* **55**(1): 121–126.
- Nieuwkoop, P. D. and J. Faber. 1956. *Normal Table of Xenopus laevis (Daudin): A Systematical and Chronological Survey of the Development from the Fertilized Egg Till the End of Metamorphosis*, North-Holland Publishing Company, Amsterdam.

- Ogino, H., W. B. McConnell, and R. M. Grainger. 2006a. High-throughput transgenesis in *Xenopus* using I-SceI meganuclease. *Nat Protoc* **1**(4): 1703–1710.
- Ogino, H., W. B. McConnell, and R. M. Grainger. 2006b. Highly efficient transgenesis in *Xenopus tropicalis* using I-SceI meganuclease. *Mech Dev* **123**(2): 103–113.
- Oofusa, K., O. Tooi, A. Kashiwagi, et al. 2001. Expression of thyroid hormone receptor betaA gene assayed by transgenic *Xenopus laevis* carrying its promoter sequences. *Mol Cell Endocrinol* **181**(1–2): 97–110.
- Osafune, K., R. Nishinakamura, S. Komazaki, and M. Asashima. 2002. In vitro induction of the pronephric duct in *Xenopus* explants. *Dev Growth Differ* **44**(2): 161–167.
- Pearl, E. J., R. M. Grainger, M. Guille, and M. E. Horb. 2012. Development of *Xenopus* resource centers: the National *Xenopus* Resource and the European *Xenopus* Resource Center. *Genesis* **50**(3): 155–163.
- Pogge von Strandmann, E. and G. U. Ryffel. 1995. Developmental expression of the maternal protein XDCoH, the dimerization cofactor of the homeoprotein LFB1 (HNF1). *Development* **121**(4): 1217–1226.
- Poitras, L., N. Bisson, N. Islam, and T. Moss. 2003. A tissue restricted role for the *Xenopus* Jun N-terminal kinase kinase MLK2 in cement gland and pronephric tubule differentiation. *Dev Biol* **254**(2): 200–214.
- Poole, T. J. and M. S. Steinberg. 1984. Different modes of pronephric duct origin among vertebrates. *Scan Electron Microsc* (Pt 1): 475–482.
- Raciti, D., L. Reggiani, L. Geffers, et al. 2008. Organization of the pronephric kidney revealed by large-scale gene expression mapping. *Genome Biol* **9**(5): R84.
- Rich, R. L., L. R. Hoth, K. F. Geoghegan, et al. 2002. Kinetic analysis of estrogen receptor–ligand interactions. *Proc Natl Acad Sci USA* **99**(13): 8562–8567.
- Roose, M., K. Sauert, G. Turan, et al. 2009. Heat-shock inducible Cre strains to study organogenesis in transgenic *Xenopus laevis*. *Transgenic Res* **18**(4): 595–605.
- Ryffel, B. 1995. Role of proinflammatory cytokines in a toxic response: application of cytokine knockout mice in toxicological research. *Toxicol Lett* **82–83**: 477–482.
- Ryffel, G. U. 2003. What can a frog tell us about human kidney development. *Nephron Exp Nephrol* **94**(2): e35–43.
- Ryffel, G. U. and A. Lingott. 2000. Distinct promoter elements mediate endodermal and mesodermal expression of the HNF1alpha promoter in transgenic *Xenopus*. *Mech Dev* **90**(1): 65–75.
- Satow, R., T. C. Chan, and M. Asashima. 2004. The role of *Xenopus* frizzled-8 in pronephric development. *Biochem Biophys Res Commun* **321**(2): 487–494.
- Sauert, K., S. Kahnert, M. Roose, et al. 2012. Heat-shock mediated overexpression of HNF1beta mutations has differential effects on gene expression in the *Xenopus* pronephric kidney. *PLoS One* **7**(3): e33522.
- Saulnier, D. M., H. Ghanbari, and A. W. Brandli. 2002. Essential function of Wnt-4 for tubulogenesis in the *Xenopus* pronephric kidney. *Dev Biol* **248**(1): 13–28.
- Saxén, L. 1987. *Organogenesis of the Kidney*, Cambridge; New York, Cambridge University Press.
- Schultheiss, T. M., R. G. James, A. Listopadova, and D. Herzlinger. 2003. Formation of the nephric duct. *The Kidney: From Normal Development to Congenital Disease*. P. D. Vize, A. S. Woolf and J. Bard, Academic Press, Amsterdam.
- Seufert, D. W., H. C. Brennan, J. DeGuire, E. A. Jones, and P. D. Vize. 1999. Developmental basis of pronephric defects in *Xenopus* body plan phenotypes. *Dev Biol* **215**(2): 233–242.
- Seville, R. A., S. Nijjar, M. W. Barnett, K. Masse, and E. A. Jones. 2002. Annexin IV (Xanx-4) has a functional role in the formation of pronephric tubules. *Development* **129**(7): 1693–1704.
- Shestopalov, I. A., S. Sinha, and J. K. Chen. 2007. Light-controlled gene silencing in zebrafish embryos. *Nat Chem Biol* **3**(10): 650–651.
- Sive, H. L., R. M. Grainger, and R. M. Harland. 2000. *Early Development of Xenopus laevis: A Laboratory Manual*, Cold Spring Harbor, Cold Spring Harbor Laboratory Press.
- Skoglund, P., A. Rolo, X. Chen, B. M. Gumbiner, and R. Keller. 2008. Convergence and extension at gastrulation require a myosin IIB-dependent cortical actin network. *Development* **135**(14): 2435–2444.
- Stewart, M. D., C. W. Jang, N. W. Hong, A. P. Austin, and R. R. Behringer. 2009. Dual fluorescent protein reporters for studying cell behaviors in vivo. *Genesis* **47**(10): 708–717.
- Stumpf, H., S. Senkel, H. M. Rabes, and G. U. Ryffel. 1995. The DNA binding activity of the liver transcription factors LFB1 (HNF1) and HNF4 varies coordinately in rat hepatocellular carcinoma. *Carcinogenesis* **16**(1): 143–145.
- Taelman, V., C. Van Campenhout, M. Solter, T. Pieler, and E. J. Bellefroid. 2006. The Notch-effector HRT1 gene plays a role in glomerular development and patterning of the *Xenopus* pronephros anlagen. *Development* **133**(15): 2961–2971.
- Taira, M., H. Otani, M. Jamrich, and I. B. Dawid. 1994. Expression of the LIM class homeobox

- gene Xlim-1 in pronephros and CNS cell lineages of *Xenopus* embryos is affected by retinoic acid and exogastrulation. *Development* **120**(6): 1525–1536.
- Takagi, C., K. Sakamaki, H. Morita, et al. 2013. Transgenic *Xenopus laevis* for live imaging in cell and developmental biology. *Dev Growth Differ* **55**(4): 422–433.
- Tallafuss, A., D. Gibson, P. Morcos, et al. 2012. Turning gene function ON and OFF using sense and antisense photo-morpholinos in zebrafish. *Development* **139**(9): 1691–1699.
- Tena, J. J., A. Neto, E. de la Calle-Mustienes, C. Bras-Pereira, F. Casares, and J. L. Gomez-Skarmeta. 2007. Odd-skipped genes encode repressors that control kidney development. *Dev Biol* **301**(2): 518–531.
- Tételin, S. and E. A. Jones. 2010. *Xenopus* Wnt11b is identified as a potential pronephric inducer. *Dev Dyn* **239**(1): 148–159.
- Thomas, H., B. Badenberg, M. Bulman, et al. 2002. Evidence for haploinsufficiency of the human HNF1alpha gene revealed by functional characterization of MODY3-associated mutations. *Biol Chem* **383**(11): 1691–1700.
- Tran, U., L. M. Pickney, B. D. Ozpolat, and O. Wessely. 2007. *Xenopus* Bicaudal-C is required for the differentiation of the amphibian pronephros. *Dev Biol* **307**(1): 152–164.
- Tran, U., L. Zakin, A. Schweickert, et al. 2010. The RNA-binding protein bicaudal C regulates polycystin 2 in the kidney by antagonizing miR-17 activity. *Development* **137**(7): 1107–1116.
- Uochi, T. and M. Asashima. 1996. Sequential gene expression during pronephric tubule formation in vitro in *Xenopus* ectoderm. *Dev. Growth Differ.* **38**: 625–634.
- Uochi, T., S. Takahashi, H. Ninomiya, A. Fukui, and M. Asashima. 1997. The Na⁺, K⁺-ATPase alpha subunit requires gastrulation in the *Xenopus* embryo. *Dev Growth Differ* **39**(5): 571–580.
- Urban, A. E., X. Zhou, J. M. Ungos, D. W. Raible, C. R. Altmann, and P. D. Vize. 2006. FGF is essential for both condensation and mesenchymal–epithelial transition stages of pronephric kidney tubule development. *Dev Biol* **297**(1): 103–117.
- Van Campenhout, C., M. Nichane, A. Antoniou, et al. 2006. Evil is specifically expressed in the distal tubule and duct of the *Xenopus* pronephros and plays a role in its formation. *Dev Biol* **294**(1): 203–219.
- Venegas-Ferrin, M., N. Sudou, M. Taira, and E. M. del Pino. 2010. Comparison of Lim1 expression in embryos of frogs with different modes of reproduction. *Int J Dev Biol* **54**(1): 195–202.
- Vize, P. D. 2003a. The chloride conductance channel ClC-K is a specific marker for the *Xenopus* pronephric distal tubule and duct. *Gene Expr Patterns* **3**(3): 347–350.
- Vize, P. D. 2003b. Embryonic kidneys and other nephrogenic models. *The Kidney: From Normal Development to Congenital Disease*. P. D. Vize, A. S. Woolf, and J. Bard, Academic Press, Amsterdam.
- Vize, P. D. and H. W. Smith. 2004. A homeric view of kidney evolution: a reprint of H.W. Smith's classic essay with a new introduction. Evolution of the kidney. 1943. *Anat Rec* **277**(2): 344–354.
- Vize, P. D., E. A. Jones, and R. Pfister. 1995. Development of the *Xenopus* pronephric system. *Dev Biol* **171**(2): 531–540.
- Vize, P. D., D. W. Seufert, T. J. Carroll, and J. B. Wallingford. 1997. Model systems for the study of kidney development: use of the pronephros in the analysis of organ induction and patterning. *Dev Biol* **188**(2): 189–204.
- Vize, P. D., T. J. Carroll, and J. B. Wallingford. 2003. Induction, development and physiology of the pronephric tubules. *The Kidney: From Normal Development to Congenital Disease*. P. D. Vize, A. S. Woolf, and J. Bard, Academic Press, Amsterdam.
- Wallingford, J. B., T. J. Carroll, and P. D. Vize. 1998. Precocious expression of the Wilms' tumor gene xWT1 inhibits embryonic kidney development in *Xenopus laevis*. *Dev Biol* **202**(1): 103–112.
- Wark, P. A., S. L. Johnston, J. L. Simpson, M. J. Hensley, and P. G. Gibson. 2002. Chlamydia pneumoniae immunoglobulin A reactivation and airway inflammation in acute asthma. *Eur Respir J* **20**(4): 834–840.
- Weber, H., E. P. Strandmann, B. Holewa, et al. 1996. Regulation and function of the tissue-specific transcription factor HNF1 alpha (LFB1) during *Xenopus* development. *Int J Dev Biol* **40**(1): 297–304.
- Wessely, O., R. Agrawal, and U. Tran. 2010. MicroRNAs in kidney development: lessons from the frog. *RNA Biol* **7**(3): 296–299.
- White, J. T., B. Zhang, D. M. Cerqueira, U. Tran and O. Wessely. 2010. Notch signaling, wt1 and foxc2 are key regulators of the podocyte gene regulatory network in *Xenopus*. *Development* **137**(11): 1863–1873.
- Wild, W., E. Pogge von Strandmann, A. Nastos, et al. 2000. The mutated human gene encoding hepatocyte nuclear factor 1beta inhibits kidney formation in developing *Xenopus* embryos. *Proc Natl Acad Sci USA* **97**(9): 4695–4700.
- Wingert, R. A. and A. J. Davidson. 2008. The zebrafish pronephros: a model to study nephron segmentation. *Kidney Int* **73**(10): 1120–1127.
- Woolner, S., A. L. Miller, and W. M. Bement. 2009. Imaging the cytoskeleton in live *Xenopus laevis* embryos. *Methods Mol Biol* **586**: 23–39.

- Wu, G., S. Bohn, and G. U. Ryffel. 2004. The HNF1beta transcription factor has several domains involved in nephrogenesis and partially rescues Pax8/lim1-induced kidney malformations. *Eur J Biochem* **271**(18): 3715–3728.
- Yergeau, D. A., C. M. Kelley, E. Kulyev, et al. 2010. Remobilization of Tol2 transposons in *Xenopus tropicalis*. *BMC Dev Biol* **10**: 11.
- Yergeau, D. A., C. M. Kelley, H. Zhu, E. Kulyev, and P. E. Mead. 2012. Forward genetic screens in *Xenopus* using transposon-mediated insertional mutagenesis. *Methods Mol Biol* **917**: 111–127.
- Young, J. J., J. M. Cherone, Y. Doyon, et al. 2011. Efficient targeted gene disruption in the soma and germ line of the frog *Xenopus tropicalis* using engineered zinc-finger nucleases. *Proc Natl Acad Sci USA* **108**(17): 7052–7057.
- Zayed, H., Z. Izsvak, O. Walisko, and Z. Ivics. 2004. Development of hyperactive sleeping beauty transposon vectors by mutational analysis. *Mol Ther* **9**(2): 292–304.
- Zhang, B., U. Tran, and O. Wessely. 2011. Expression of Wnt signaling components during *Xenopus* pronephros development. *PLoS One* **6**(10): e26533.
- Zhou, X. and P. D. Vize. 2004. Proximo-distal specialization of epithelial transport processes within the *Xenopus* pronephric kidney tubules. *Dev Biol* **271**(2): 322–338.

13

Development of Neural Tissues in *Xenopus laevis*

William A. Muñoz^{1,2}, Amy K. Sater⁴, & Pierre D. McCrea^{1,3}

¹Department of Biochemistry and Molecular Biology, The University of Texas MD Anderson Cancer Center, Houston, TX

²Stowers Institute for Medical Research, Kansas City, MO

³Program in Genes and Development, The University of Texas Graduate School of Biomedical Sciences at Houston, Houston, TX

⁴Department of Biology and Biochemistry, University of Houston, Houston, TX

Abstract: The *Xenopus* nervous system has contributed greatly to our understanding of the various signals that induce, specify and differentiate cells away from ectoderm and towards neural fates. Following the discovery of the Spemann organizer in 1924, much work has been undertaken to identify the fundamental signals that pattern the embryo, and in time, better tools to identify the molecules became available and began to provide answers. By applying such tools in *Xenopus*, researchers have revised dogmas to advance the field of neural development, for example, the arrival and experimental support in the 1990's for the "default model" of neural specification. This chapter presents an overview of the early processes and signals that form the central and peripheral nervous systems of *Xenopus laevis*, with attention made to select discoveries that promoted our understanding of these tremendously complex systems.

Introduction

The human nervous system is a tremendously complex system that has a role in much of what we do, from involuntary actions such as breathing and digestion to higher thought processes such as reaching toward an understanding of the nervous system itself. With such complexity, there are numerous opportunities for small defects to result in detrimental biological effects. With an estimated one billion people worldwide having a neurological disorder, understanding how the nervous system is formed, maintained, and repaired is

of prominent biomedical importance (World Health Organization. Dept. of Mental Health and Substance Abuse 2006). Due to the availability of numerous molecular and other markers (Gilchrist et al. 2009), and the ease of observing and manipulating *Xenopus* embryos, this model system is already well recognized for offering experimental advantages in studies of neural development.

In *Xenopus*, the nervous system is derived from the dorsal, lateral, and dorsolateral ectoderm (Bonstein et al. 1998; Sato et al. 2005). During early gastrulation, specification signals (also known as neural inducers) from the

involving dorsal mesoderm disposed affected cells toward neural fates, this process is known as neural specification (Sharpe and Gurdon 1990). These specified regions form the neural plate, which undergoes various morphogenetic processes at both the cellular and tissue levels to form the neural tube (see Chapter 9 by Naoto Ueno). The neural tube ultimately gives rise to the central nervous system (CNS) through various signaling cascades that regulate the neurogenic gene regulator network. In parallel to specification and formation of the neural tube, neural crest cells are also being formed. The neural crest is derived from the neural plate boundary and delaminates from the neural plate during neural tube closure (Milet and Monsoro-Burq 2012). Once separated, the neural crest cells undergo a rather drastic process, including an epithelial-to-mesenchymal transition (EMT), and migration away from the neural tube. Such migrations are first seen anteriorly (rostrally) in the cranial regions, where neural crest derivatives ultimately include cranial ganglia and much of the cartilage and bones of the head (Stuhlmiller and Garcia-Castro 2012; Theveneau and Mayor 2012). As such migrations of neural crest cell populations continue from more posterior (caudal) regions of the dorsal neural tube, contributions to many tissues are ultimately made, prominently including the peripheral nervous system.

In this chapter, while we do not discuss the mechanistic formation of the neural tube (see Chapter 9 by Naoto Ueno), we focus on the signals and early processes involved in forming both the central and peripheral nervous systems of *Xenopus laevis*. General models of neural development are available from other resources (Gilbert 2006; Sanes et al. 2012).

***Xenopus* as a model system of neural development**

Xenopus has been classically used as a model system for understanding neural development, providing significant insights relevant to other vertebrates. *Xenopus* provides numerous advantages including the ease of isolating explants or conducting transplantations, facilitated by the large embryo

size (>1 mm), and the rapid experimental manipulations of targeted gene products, such as via injection of a selected mRNA (overexpression) or the injection of a morpholino to block translation of an endogenous transcript (depletion) (Krieg and Melton 1987; Heasman et al. 2000). Additionally, as the early stages of *Xenopus* have been fate-mapped, injections can be spatially targeted to early embryonic regions that are fated to contribute largely if not exclusively to neural tissues, while more sophisticated transgenic approaches are now being devised (see Chapter 12 by Rachel Miller for transgenic approaches) (Moody 1987a, b; Sive et al. 2000).

There is a sizable number of proven *Xenopus* markers that report upon specific neural stages and tissues which are well represented in the XenMARK database (Table 13.1) (Gilchrist et al. 2009). These markers, when coupled with simple gross observation, allow for the ready evaluation of neural phenotypes.

Neural specification

Since the discovery of Spemann's organizer almost 90 years ago showed that the mesodermal dorsal lip of amphibian embryos induces surrounding cells towards the formation of a dorsoventral body axis (Spemann and Mangold 1924), developmental biologists have been in search of how this small region patterns so much of the embryo. In this pursuit, *Xenopus* has been instrumental not only in identifying various inductive signals that contribute to organizer activity but also how their distinctive roles pattern the embryo.

One of developmental biology's most influential experiments of the 20th century was conducted by Hans Spemann and Hilde Mangold in 1924 and relied upon tissue transplantation between newts. They removed the dorsal lip of an early gastrulating pigmented newt embryo and implanted it into the presumptive ventral epidermis of an early gastrulating nonpigmented newt embryo. The pigmented donor tissue went on to induce a secondary gastrulation site, involute properly, and differentiate into notochord and other mesodermal structures normally derived from the dorsal lip. Most interestingly, nonpigmented host cells

Table 13.1 Primers for quantitative RT-PCR of neural specification and differentiation genes.

Primer pairs and PCR cycling conditions			
Target gene	Sequence	Annealing temp (°C)	Reference
Xwnt8	U: 5'-TATCTGGAAGTTGCAGCATACA-3' D: 5'-GCAGGCACTCTCGTCCCTCTGT-3'	55	http://www.hhmi.ucla.edu/derobertis/
Krox20	U: 5'-CCGGCCATCCTCAGACCCAGAAA-3' D: 5'-CGCCACGCCGCTGTTGCCGAGTTC-3'	55	http://www.hhmi.ucla.edu/derobertis/
Chordin	U: 5'-GTTGTACATTTGGTGGGAA-3' D: 5'-ACTCAGATAAGAGCGATCA-3'	55	http://www.hhmi.ucla.edu/derobertis/
NCAM	U: 5'-GCGGGTACCTTCTAATAGTCAC-3' D: 5'-GGCTTGGCTGTGGTTCTGAAGG-3'	55	http://www.hhmi.ucla.edu/derobertis/
Nkx2.5	U: 5'-GAGCTACAGTTGGGTGTGTGGT-3' D: 5'-GTGAAGCGACTAGGTATGTGTCA-3'	55	http://www.hhmi.ucla.edu/derobertis/
N-tubulin	U: 5'-ATGCTGATCTACGCAAAC-3' D: 5'-AGATAGCAGCTACTGTGAG-3'	55	http://www.hhmi.ucla.edu/derobertis/
Otx2	U: 5'-GGATGGATTTGTTACATCCGTC-3' D: 5'-CACTCTCCGAGCTCACTTCCC-3'	55	http://www.hhmi.ucla.edu/derobertis/
Shh	U: 5'-AACACACCTGGGCACACCTC-3' D: 5'-TCCAAAAGCCAAGTCCCTAT-3'	55	http://www.hhmi.ucla.edu/derobertis/
Sox2	U: 5'-GAGGATGGACACTTATGCCAC-3' D: 5'-GGACATGCTGTAGGTAGGCGA-3'	55	http://www.hhmi.ucla.edu/derobertis/
Delta-1	U: 5'-GCACTACCAGAGCAACGTGT-3' D: 5'-GGAACAACGAAGGAGTTGGT-3'	54*	Seo et al. (2007)
Ash1	U: 5'-CCCCAACTATTTCCACGATA-3' D: 5'-TGCTACTCCGCATCTCAGAA-3'	54*	Seo et al. (2007)
Twist	U: 5'-GAGGCGATCTGCTAGGAAAA-3' D: 5'-CCTCTGACTCTGCAGCTCCT-3'	54*	Seo et al. (2007)
Iro3	U: 5'-GAGCCTTCTGCCCTACAG-3' D: 5'-GGGATAAAAGGCTGGGTGA-3'	54*	Seo et al. (2007)
Gadd45	U: 5'-TGACTGGGTTCCCACTATCA-3' D: 5'-GGACCTCAACCAGCGTAATC-3'	54*	Seo et al. (2007)
NeuroD	U: 5'-GAGCAGAGTCAGGACATCCA-3' D: 5'-GCTTGACGTGGAATACATGG-3'	54*	Seo et al. (2007)
Id3	U: 5'-GTTATTTGCCACCCCATCTG-3' D: 5'-TTACTAGCCAAGCCCCACAC-3'	54*	Lim et al. (2011)
Dlx3	U: 5'-GGTTCAGCGAAATGTTCCAT-3' D: 5'-ATGGAGTGGCACTGGATTTC-3'	54*	Lim et al. (2011)
Dlx5	U: 5'-GCGCTGAATGCGTATCAGTA-3' D: 5'-AGGGCTCCCATAGCCATAGT-3'	54*	Lim et al. (2011)
Foxd5a	U: 5'-CCAATCTGTGACCCTCCACT-3' D: 5'-CTTCCCGGACAACCTGTAA-3'	54*	Lim et al. (2011)
Fzd10	U: 5'-GACGCAAGACAAGTGCAAAA-3' D: 5'-CTGCTGGGATAGAGCTGGTC-3'	54*	Lim et al. (2011)
Cxcr4	U: 5'-ACTGCATTTGGGAGAACACC-3' D: 5'-CTGAGGTGAATGCGTTCTGA-3'	54*	Lim et al. (2011)
Msx1	U: 5'-TTATGCAACTGCCAGAGGAG-3' D: 5'-GGGCTTCTGTTGGTTTTGT-3'	54*	Lim et al. (2011)
Zic1	U: 5'-TCCGTACATGAGGCAGCC-3' D: 5'-TTGTTGCACGACTTTTTGGG-3'	54*	Lim et al. (2011)

*indicates predicted annealing temperature based on OligoCalc (Kibbe 2007).

from host ectoderm were induced to form a new dorsal axis at the site of transplantation, including a complete neural plate. Spemann

defined this donated region as the organizer, as it was capable of inducing nearby tissues to change their fates, organizing them into a

secondary axis. The work following this has shown that while this is not the earliest inductive process in the embryo, it is a central event, providing signals to specify the dorsal axis and the neural tube.

Spemann's organizer originates from two distinct signaling centers: the Nieuwkoop center and the blastula chordin- and noggin-expressing (BCNE) region (Nieuwkoop 1973; Gerhart et al. 1989; De Robertis and Kuroda 2004). The Nieuwkoop center, specified by beta-catenin signaling and VegT/Vg1 mRNA localization (Figure 13.1A) (Smith and Harland 1991; Zhang and King 1996; Tao et al. 2005; Cha et al. 2008), consists of the dorsal-most vegetal cells of the blastula and provides the dorsalizing (Wnt signaling components) and mesoderm induction signals (Xnr1, 2, 4, 5, and 6) to the organizer. The ectopic activation of the canonical Wnt pathway in ventral vegetal cells induces a secondary organizer and ultimately a duplicate axis, similar to organizer transplant experiments (Sokol et al. 1991).

One of the major targets of this induction in the organizer tissues is the activation of the *gooseoid* gene, which is specific to the organizer and can itself induce a duplicate axis when overexpressed in ventral cells (Cho et al. 1991). The *gooseoid* gene encodes a homeobox-containing protein with numerous gene targets whose products are needed by the organizer (Niehrs et al. 1993). Gooseoid expression indirectly results in response to upstream canonical Wnt signaling, as a consequence of intermediaries such as the homeobox genes *Twin* and *Siamois*, each direct Wnt/beta-catenin gene targets expressed in the Nieuwkoop center (Lemaire et al. 1995; Laurent et al. 1997). *Twin* and *Siamois* can either homodimerize or heterodimerize to bind a conserved P3 site within the Wnt-responsive proximal element of the *gooseoid* promoter. The knockdown of both transcription factors, simultaneously, results in a failure of organizer formation (Bae et al. 2011). Interestingly, *Twin* and *Siamois* are not sufficient for organizer induction.

TGF-beta signaling from the vegetal cells, together with the actions of *Twin* and *Siamois*, induces strong activation of *gooseoid* and other transcription factors important for organizer function. Two transcripts localized to the vegetal cortex of the embryo have been

implicated in the activation of the TGF-beta signaling pathway. One of these encodes a member of the TGF-beta superfamily, *Vg1*, while the other is a transcription factor, *VegT*, that instructs endoderm to produce and secrete several TGF-beta superfamily members (*activin*, *Derriere*, and *nodal* proteins). These TGF-beta signals induce the expression of the mesoderm-specifying factor *Brachyury* (*Xbra*) (Weeks and Melton 1987; Thomsen and Melton 1993; Zhang and King 1996; Zhang et al. 1998; Kofron et al. 1999; Sun et al. 1999; Agius et al. 2000).

The nodal-related proteins are expressed in the mesoderm in a gradient with strongest expression in the dorsal regions. This gradient is established through VegT-mediated signaling from the ventral cells and beta-catenin in the dorsal regions. The resulting gradient of TGF-beta signaling intersecting with beta-catenin signaling contributes to the specification of the Spemann's organizer, marked by strong expression of *gooseoid* (Figure 13.1B) (Agius et al. 2000).

Separate from the Nieuwkoop center, the BCNE region is established in the dorsal animal and marginal regions during early blastula stages. This region is specified via localized beta-catenin signaling and a low level of nodal signals, both a result of maternally deposited *xNorrin* protein in the animal cap (Wessely et al. 2001; Xu et al. 2012). The cells of the BCNE partially contribute to the organizer and much of the anterior CNS, providing early signaling antagonists, chordin and noggin, to the neuroectoderm for neural induction (Kuroda et al. 2004).

In *Xenopus*, the neural plate and its borders differentiate from a portion of the ectoderm that is neural competent. This region is termed the neuroectoderm. The neuroectoderm lies adjacent to the Spemann's organizer during late blastula stages, receiving various inductive signals from the organizer. As gastrulation begins, the organizer is involuted and begins to contribute to various endodermal tissues. During this involution, the organizer continues to signal to the overlying neuroectoderm, but now in a vertical manner further inducing neural specification (Sater et al. 1993).

The signals responsible for neuroectoderm specification have been the focus of extensive

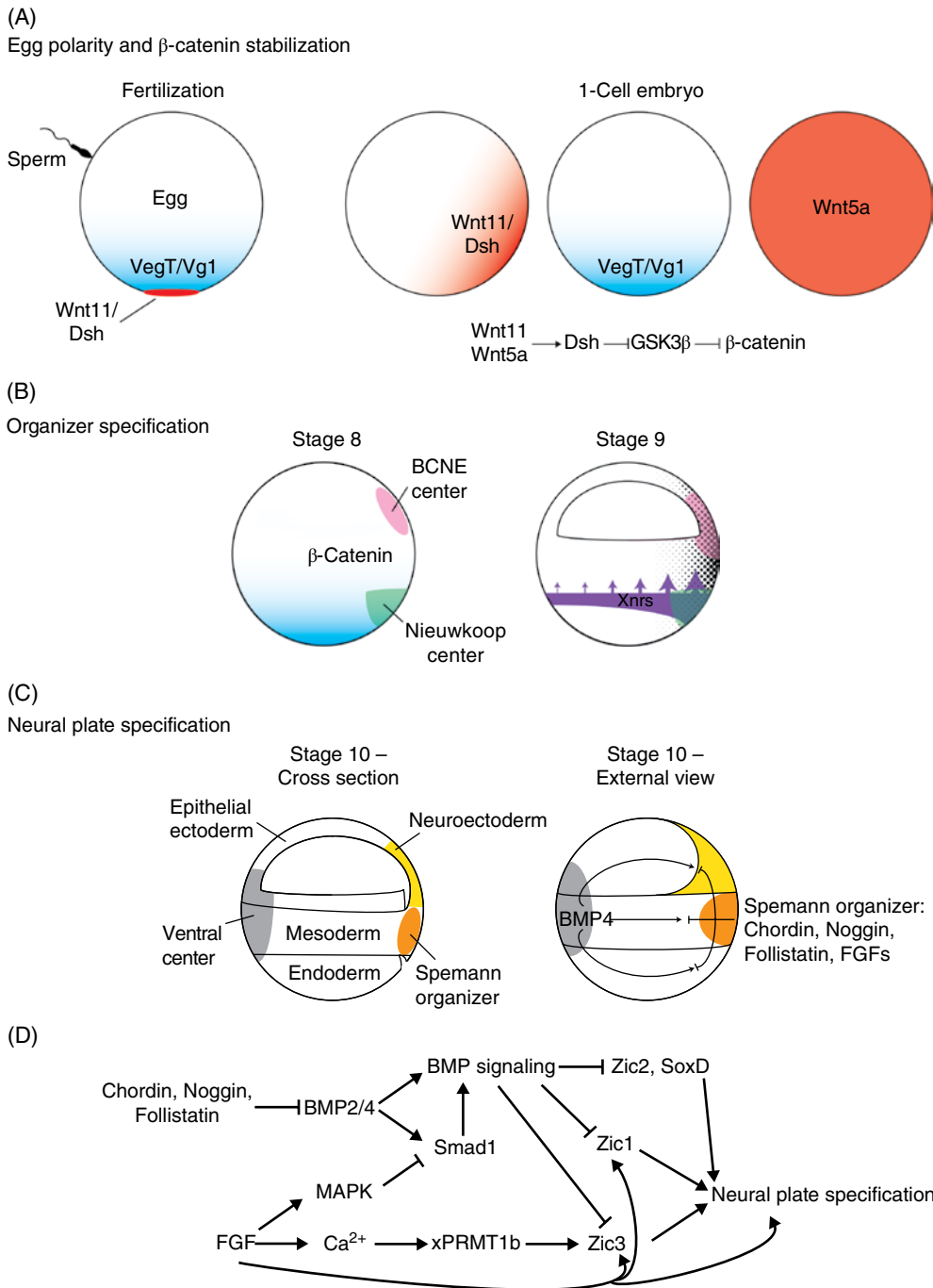


Figure 13.1 Summary of neural specification. (A) Wnt5a is ubiquitously expressed in the oocyte and embryo. Dishevelled (Dsh) and Wnt11 are relocalized from the vegetal pole of the egg during cortical rotation/fertilization to establish a dorsal gradient. Wnt5a and Wnt11 bind each other and in cooperation with Dsh inhibit GSK3 β -mediated degradation of β -catenin. A TGF- β signal inducing transcription factor, VegT, and a TGF- β family member, Vg1, are also localized in a vegetal gradient originating from maternal contributions. (B) At early blastula stages, VegT/Vg1 signals, and stabilized β -catenin, specify the Nieuwkoop center, while stabilized β -catenin and lesser levels of TGF- β signals specify the blastula chordin–noggin-expressing center (BCNE). At the later blastula stage, VegT/Vg1 and β -catenin signals induce a gradient of nodal-related proteins (Xnrs) in the endoderm, signaling to the overlying mesoderm. The strongest Xnr signals originate in the dorsal Nieuwkoop center. (C) At the start of gastrulation, the Spemann’s organizer has formed and has begun to express dorsalizing factors. The dorsalizing factors are important for specification of several regions, but here, we focus on the neuroectoderm. Neuroectoderm-specifying factors include chordin, noggin, follistatin, and FGFs. (D) Signals from the Spemann organizer (chordin, noggin, follistatin, and FGF) indirectly activate downstream transcription factors (Zic1, Zic2, Zic3, and SoxD) necessary for neural specification. To see a color version of this figure, see Plate 33.

research for decades with various dogmas overturned, resulting in what is now known as the “default” model. This model states that the ectoderm is fated to become neural tissue; however, bone morphogenetic proteins (BMPs) induce the ectoderm to become epidermal (Wilson and Hemmati-Brivanlou 1995; Suzuki et al. 1997). Neural tissue is induced upon the inhibition of the activities of BMPs, which when bound to their receptors lead to the activation of Smad1/5/8. Activated Smad1/5/8 proteins dimerize with Smad4 and then translocate to the nucleus where they alter gene expression. Targets of the Smads in the ectoderm induce epidermal differentiation, preventing neural specification (Nie et al. 2006). Inhibition occurs via sequestration of the BMPs by diffusible molecules (e.g., chordin and noggin, among others, discussed later) released from the organizer tissue (Smith and Slack 1983; Khokha et al. 2005). Noggin was the first direct neural-specifying gene identified. To determine if it was a neural-specifying gene product, two criteria had to be met. These criteria were as follows: (i) the specifier molecule must induce neural tissue from the animal cap ectoderm in the absence of dorsal mesoderm, and (ii) competent ectoderm can be induced at the gastrula stage to a neural lineage, when dorsal mesoderm can induce neural tissue. Additionally, it was expected that the specifier be expressed in a temporal and spatial manner coinciding with neural development. Finally, disruption of the specifier’s activity should block neural development. Noggin fulfilled all these requirements (Lamb et al. 1993). The other neural specifiers were confirmed in similar ways (Figure 13.1C) (Hemmati-Brivanlou et al. 1994; Piccolo et al. 1996).

Chordin and noggin physically interact with the BMPs, preventing the BMPs from binding their receptors (Sasai et al., 1995; Piccolo et al., 1996; Zimmerman et al., 1996; Groppe et al., 2002), and therefore block epithelial specification. Follistatin also contributes to BMP inhibition through weaker physical interactions with BMPs and activin (Hemmati-Brivanlou et al. 1994). Once BMPs are inhibited in the neuroectoderm, several transcription factors important for neuroectoderm differentiation are upregulated, including *Zic1*, *Zic2*, *Zic3*, and *SoxD* (Nakata et al. 1997; Mizuseki et al. 1998a, b).

Simply put, BMP signaling induces epidermal differentiation in the ectoderm, and the organizer blocks such signals to allow neural specification to proceed.

While the “default” model created a basis for studying neural specification, it does not account for many of the necessary signals in neuroectoderm differentiation. One such signal comes from FGF signaling. Contrary to other model organisms, in normal *Xenopus* neuroectoderm, inhibition of BMPs is sufficient for neuroectoderm differentiation. However, when FGF signaling is disrupted, neural specification triggered by BMP inhibition can be blocked, indicating that instructional signaling is also required (Slack and Tannahill 1992). One proposed mechanism is that MAPK is activated by FGF signaling. MAPK phosphorylates Smad1, inhibiting its activity as a downstream effector of BMP signaling (Uzgare et al., 1998; Pera et al. 2003; Sater et al. 2003). The dual repression of Smad1 activity through BMP inhibition and FGF effects on MAPK during neuroectoderm differentiation suggests that Smad1 activity must be strongly blocked to allow the expression of neural genes.

Data from other organisms indicates that BMP inhibition alone does not induce neuroectoderm differentiation and that FGF roles independent of BMP may be necessary. Independent of BMP activity, FGF upregulates several transcription factors necessary for neural specification, including *sox2/3* and *foxd5alpha* (Wills et al. 2009; Rogers et al. 2011). *Foxd5* itself regulates a gene network that controls induction of neural progenitors from immature neural ectoderm and later inhibits differentiation of the progenitors (Neilson et al. 2012).

Calcium signaling has also been implicated in neuroectoderm differentiation, potentially as a very early differentiation signal. Increases in intracellular calcium concentration induce neuroectoderm differentiation irrespective of BMP activity. During development, the increase is mediated by the dihydropyridine-sensitive Ca^{2+} channel (DSCC), which is localized at the plasma membrane, with antagonism of DSCC inhibiting neuroectoderm differentiation and agonists inducing neuroectoderm differentiation independent of BMP inhibition (experimentally, intracellular Ca^{2+} stores can contribute to

differentiation as well). Intracellular calcium is believed to regulate Zic3 through an arginine *N*-methyltransferase, xPRMT1b, that is transcriptionally upregulated when the calcium concentration is increased. Interestingly, increased intracellular calcium levels cannot induce neuroectoderm in animal cap explants, but can induce it in intact embryos through ectopic dorsal mesoderm formation (Palma et al., 2001; Aruga and Mikoshiba 2011). This suggests that the increased intracellular calcium is having two potential roles in neuroectoderm induction: dorsalizing the mesoderm and directly regulating pathways in the ectoderm (Figure 13.1D).

The blastula of the *Xenopus* embryo represents a large pluripotent population, and recent research on early specification has begun to focus on the regulation of pluripotency in these cells. The Gadd45 family, for example, has been a subject of such studies. Gadd45a and Gadd45g appear to regulate cell proliferation and mediate the exit of pluripotent cells into neural cell differentiation pathways (Kaufmann and Niehrs 2011). In the future, knowledge of how the gastrula cells know when to begin specification from their pluripotent state will be crucial in understanding neural specification.

This section has introduced ideas from the current field, such as that multiple signaling centers including the BCNE, Nieuwkoop center, and Spemann's organizer contribute to early neural specification (as reflected in the markers Sox2 and Sox3), and the markers associated with fated neurons (neural cell adhesion molecule (NCAM), nervous system-specific beta-tubulin and nervous system-specific ribonucleoprotein (NRP1)) (Richter et al. 1988; Richter et al. 1990; Wills et al., 2009). These signaling centers accomplish this through the regulation of numerous conserved signaling pathways that must be coordinated temporally and spatially to start shaping and connecting the most complex structure of the vertebrate body, the nervous system.

Formation of the anterior–posterior axis

While the inductive signals discussed in the section “Neural Specification” provide the basis for early neural specification, they do

not explain how the various neural structures are formed/induced and why different regions of the animal have distinctive structures. The neural tube differentiates into forebrain, midbrain, hindbrain, and spinocaudal structures and does so in an anterior to posterior orientation.

To test if differentiation occurs via signaling between tissues, and if so, what tissues were involved, Otto Mangold performed a classical experiment. He transplanted the dorsal lip from various stages of gastrulation into the early gastrula. He observed that as development progressed and different inductive cells were transplanted from the involuting dorsal lip, the tissue near the transplant would be ectopically induced into different tissues dependent on what stage the donor tissue was isolated. This implied that separate inducing activities may exist for the various tissues. Several molecules and pathways have been identified to control this regional specification and will now be described.

The first cells to involute at the dorsal lip are termed the leading-edge endomesoderm and go on to form the prechordal mesoderm and pharyngeal endoderm. These tissues induce the most anterior head structures, including the forebrain and midbrain from the neuroectoderm. In addition to BMP inhibition signals from the endomesoderm, the Wnt pathway must also be inhibited to induce the anterior head structures from the neuroectoderm. Wnt inhibitor signals from the endomesoderm include Cerberus, Frzb, and Dickkopf (Leyns et al. 1997; Wang et al. 1997; Glinka et al. 1998). Cerberus is a secreted protein that binds BMPs, nodal-related proteins, and Wnt8, preventing them from activating their targets in the neuroectoderm (Piccolo et al. 1999). Cerberus, Frzb, and Dickkopf are specific in their requirement for head specification, but not trunk–tail development (Bouwmeester et al. 1996). Frzb is a soluble form of the transmembrane Wnt receptor, Frizzled, and can bind/sequester Wnt ligands away from full-length Frizzleds to reduce their activity. Dickkopf interacts with the Wnt coreceptors, LRP-5/6, triggering their endocytosis and subsequent degradation (Niehrs 2006). This molecule is necessary for the formation of

both the head and prechordal plate (Glinka et al. 1998). The neural plate also contributes to the repression of BMP and Wnt signals through the expression of Noggin1 and Noggin2, respectively (Bayramov et al. 2011). Additionally, FGF signaling is suppressed in anterior structures, through regulatory mechanisms discussed later. Insulin-like growth factors have also been implicated in the formation of the anterior regions. The mechanism is thought to be through cross-interference with both the Wnt and BMP signaling pathways (Richard-Parpaillon et al. 2002; Pera et al. 2003). With BMP, FGF, and Wnt signaling repressed in the anterior region, *Otx2*, a major anterior head-specifying gene, is expressed. It is required to induce head formation from the midbrain/hindbrain border to the anteriormost part of the brain (Pannese et al. 1995). With expression complementary to that of *Otx2*, *Gbx2* specifies the brain regions posterior to the midbrain/hindbrain border (von Bubnoff et al. 1996).

The later cells to involute at the dorsal lip predominately contribute to the notochord and induce the hindbrain and trunk neuroectoderm. This specification is accomplished through Wnt and retinoic acid gradients. Both have the highest signaling in the posterior region of the neural plate and little to no signaling in the anterior neural regions (Lopez and Carrasco 1992; Chen et al. 1994; Kiecker and Niehrs 2001). The gradient of Wnt signaling is established through the expression of Wnt ligands and pathway components in the posterior region, and expression of Wnt inhibitors in the anterior (Wodarz and Nusse 1998; Zhang et al. 2012). A retinoic acid gradient appears to be the result of the expression of retinoic acid-synthesizing proteins in the posterior and retinoic acid-degrading proteins in the anterior embryo (Kolm and Sive 1997; Tanibe et al. 2008). Various members of the FGF family, including eFGF, FGF3, FGF8, and FGF9, are expressed in a gradient fashion (Tannahill et al. 1992; Kengaku and Okamoto 1995; Song and Slack 1996; Isaacs 1997; Fletcher et al. 2006). FGF mRNA is expressed in newly formed posterior tissues, with degradation of the transcript beginning shortly thereafter (Dubrulle and Pourquie 2004). Each of these gradients has been shown to affect

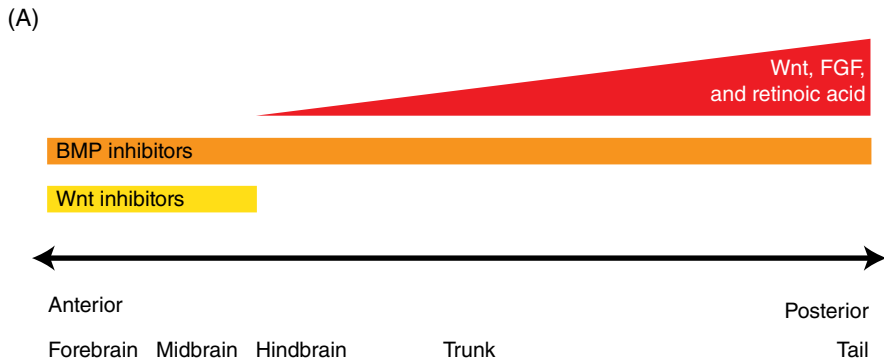
the expression of the Hox genes via the regulation of Cdx genes (Cho and De Robertis 1990; Kolm and Sive 1995; Pownall et al. 1996; Janssens et al. 2010). Ultimately, the powerful Hox genes specify anterior–posterior polarity, except in the most anterior regions, and this function is conserved across vertebrates and numerous invertebrates (Patel 1994).

As the Hox genes are only expressed from the hindbrain through posterior structures, it would be expected that other transcription factors regulate positional identity in more anterior structures. The best characterized of these transcription factors are the Pax genes, identified by their homeodomain region and paired box domain. Most members of the family are expressed in the developing nervous system, each localizing to specific regions of the cranial neural derivatives where they confer specific differentiation signals (Pieper et al. 2011). This section has aimed to show that numerous signaling pathways are coordinated throughout development to form neural plate-derived structures such as the neural tube, which spans much of the embryo's length and forms the CNS (Figure 13.2).

Neurulation and dorsal–ventral patterning

Following the neuralization of the neuroectoderm, the neural plate undergoes a dramatic morphogenetic process to form a hollow neural tube along the anterior–posterior axis of the embryo that exhibits dorsal–ventral polarity (see Chapter 9 by Naoto Ueno). Concurrently, the neural crest cells begin to migrate from the dorsal aspect of this tube. The dorsal–ventral polarity of the neural tube helps define the organization of the neural tube, for example, localizing the motor neurons to the ventral regions adjoining the floorplate and the sensory neurons to the dorsal regions adjoining the roofplate.

The polarity of the neural tube is mostly due to interactions with surrounding tissues. The notochord located ventrally to the floorplate is the main inducer of the neural tube's dorsal–ventral polarity. When the neural tube is dissected from surrounding tissue, it remains nonpolarized; however, if the neural



(B)

Proteins involved in neural induction	
Protein name	References
Wnt ligands	
Wnt8	Domingos et al. (2001); Kiecker and Niehrs (2001)
Wnt3a	Elkouby and Frank (2010)
Wnt inhibitors	
Cerberus	Bouwmeester et al. (1996)
Frzb	Wang et al. (1997)
Dickkopf	Glinka et al. (1998)
Noggin1/2	Bayramov et al. (2011)
BMPs	
BMP2	Suzuki et al. (1997)
BMP4	Wilson and Hemmati-Brivanlou (1995)
BMP inhibitors	
Chordin	Piccolo et al. (1996); Sasai et al. (1995)
Noggin	Lamb et al. (1993); Zimmerman et al. (1996)
Follistatin	Hemmati-Brivanlou et al. (1994)
RA synthesizing proteins	
Ra1DH2	Chen et al. (2001)
RA degrading proteins	
xCyp26	Tanibe et al. (2008)
FGFs	
eFGF	Pownall et al. (1996)
FGF3	Tannahill et al. (1992)
FGF8	Fletcher et al. (2006)
FGF9	Song and Slack (1992)

Figure 13.2 Model and table of some of the proteins involved in neural anterior–posterior axis specification. (A) Various signals from the mesendoderm and mesoderm specify the anterior–posterior axis. BMP inhibitors block the formation of nonneural ectoderm in the neuroectoderm. Wnt inhibitors induce anterior head structure formation (forebrain and hindbrain). Gradients of Wnts, FGFs, and retinoic acid posteriorize the embryo, regulating the HOX genes in a dose-dependent manner. (B) Table of some of the proteins involved in anterior–posterior axis specification, with select references.

tube is left in place and a secondary notochord is transplanted to a more dorsal region of the neural tube, a second floorplate is induced, indicating that the notochord is necessary and sufficient for the polarity of the neural tube (Holtfreter 1934).

With the development of molecular markers to help define this polarity several decades later, the polarity signal from the notochord was finally identified. This signal was shown to be sonic hedgehog (Shh), a secreted morphogen. Initially, it is expressed in the notochord, but soon after, its expression is induced in the floorplate of the neural tube as well (Figure 13.3A–D) (Roelink et al. 1994; Ekker et al. 1995). In the floorplate region where Shh activity is strongest, the cells express the ventral fate marker *Nkx2.2*. Moving dorsally, as the Shh activity decreases, the cells of the neural tube exhibit increased *Olig2* and then *Pax7* expression (Figure 13.3E) (Dessaud et al. 2008). While roofplate specification and formation has been characterized in both chick and mouse, it has not been well investigated in *Xenopus*, leaving many questions open. If the *Xenopus* roofplate is specified in a similar way as these other organisms, then it is induced by BMPs and other TGF-beta-like signals from the ectoderm. The dorsal–ventral polarity of the neural tube, established by the Shh gradient and other potential unidentified signals, is important for specifying which neurons are formed within the different regions of the neural tube (Figure 13.3F–H).

Neural plate border specification and neural crest induction

While we concentrated previously upon processes contributing to the neural tube/CNS, we here focus on neural crest cells, which are derived from cells at the boundary of the neural plate and prospective epidermis and give rise to the peripheral nervous system and various other tissues. For example, neural crest cells form the neurons and glia of the sensory, sympathetic, and parasympathetic nervous systems, pigment cells, smooth muscle cells, and most of the mesenchyme in the head. In the head, they contribute in large part to the skeletal structures, as well as

various ganglia structures not derived from cranial placodes. Beginning with the cranial neural crest in the prospective anterior or anterior region of the embryo, followed by crest in the prospective trunk and tail regions, crest cells are specified during gastrulation, with induction continuing into neurulation and using many of the same signals employed previously for the neural tube (summarized in Figure 13.4) (Gont et al. 1993; Villanueva et al. 2002; Klymkowsky et al. 2010). Once induced, and during neural tube formation, neural crest cells delaminate from the neuroectoderm and then migrate laterally and ventrally throughout much of the embryo to ultimately populate and contribute to numerous cell types and tissues listed previously (Steventon et al. 2009).

Grafting experiments in axolotl between pigmented and nonpigmented animals revealed that neural crest cells are induced by both the epidermis and the neural plate (Moury and Jacobson 1990). Later, these results were confirmed in *Xenopus* with the use of various markers for neural crest. Molecular identification of neural crest cells begins at early stages of neurulation, as often followed via the expression of zinc-finger or helix–loop–helix transcription factors such as *XSnail*, *XSlug*, and *XTwist* (Nieto et al. 1994; Mayor et al. 1995; Linker et al. 2000).

The neural crest precursors are derived from the border of the neural plate, where it is in contact with the nonneural ectoderm. In this region, various transcription factors are upregulated (e.g., *Zic1*, *Msx1*, *Msx2*, *Dlx3*, *Dlx5*, *Pax3*, and *Pax7*), specifying this region as the neural plate boundary. Their expression is a consequence of this region receiving a number of signals, described later (Milet and Monsoro-Burq 2012; Stuhlmiller and Garcia-Castro 2012). Such signals prepare these cells at the neural plate border, making them neural crest competent for yet further signals that will induce them to become neural crest, preplacodal ectoderm, or Rohon-Beard primary neuron cells.

After the neural plate border is made competent by the neural plate border specifiers, additional signals are then integrated to begin neural crest cell induction. These secondary signals induce the expression of neural crest

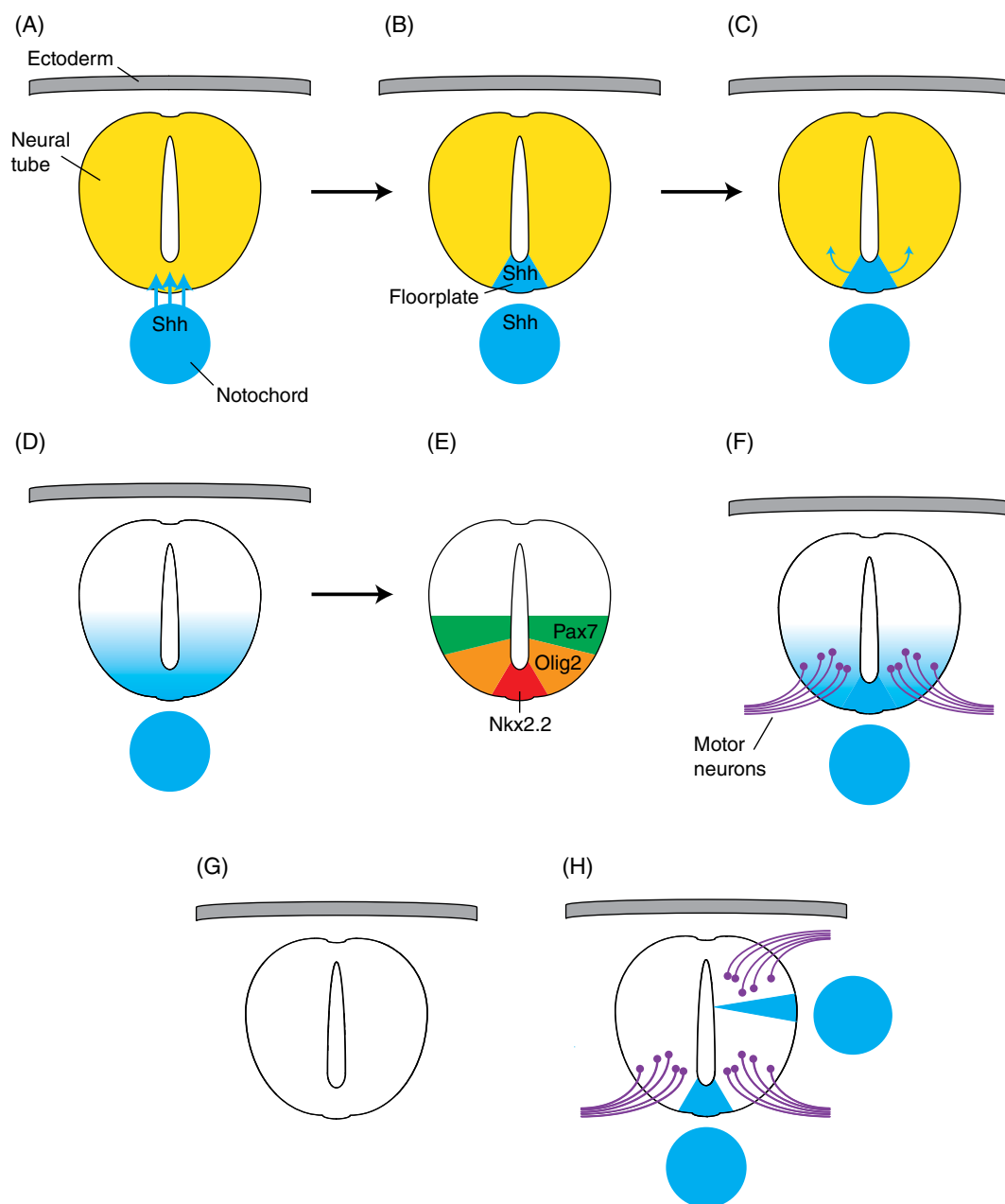


Figure 13.3 *Xenopus* neural tube dorsal-ventral specification and experimental manipulations. (A) The notochord secretes sonic hedgehog (Shh), which signals to the floor of the recently closed neural tube. (B) The floorplate begins to express Shh. (C) Shh diffuses dorsally, forming a gradient strongest in the floorplate. (D) Shh gradient is established in the neural tube. (E) Neural identifying transcription factors (Nkx2.2, Olig2, and Pax7) are expressed in a manner dependent on the levels of Shh present. (F) Dependent on transcriptional programs responsive to the Shh gradient, motor neurons are formed near the floorplate. (G) When the notochord is removed prior to neural tube closure, no Shh signal is presented to the floorplate. Therefore, no Shh gradient-dependent dorsal-ventral patterning occurs in the neural tube. (H) A second notochord is placed dorsally, adjacent to the neural tube. This secondary notochord is capable of inducing an ectopic floorplate and a secondary set of motor neurons.

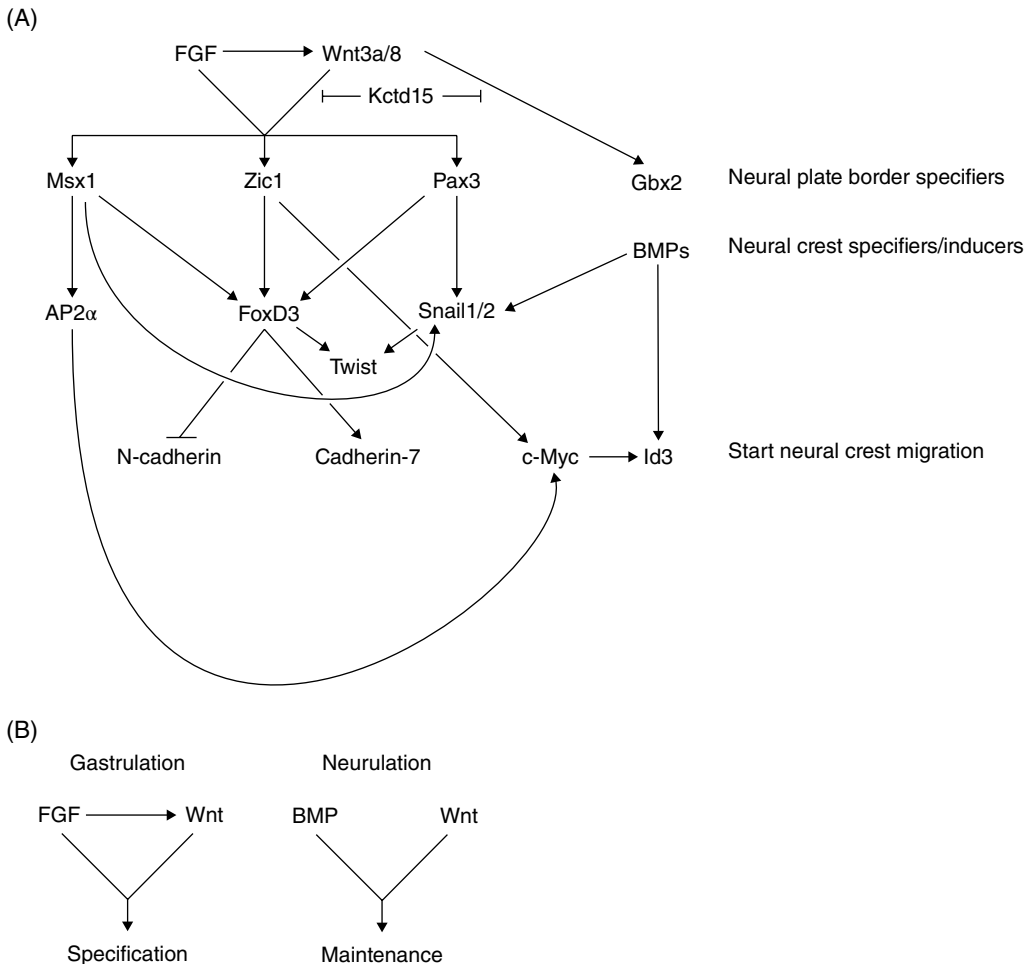


Figure 13.4 Putative regulatory network of neural crest specification, maintenance, and migration. (A) Wnt and FGF signals regulate the specification of the neural plate during gastrulation through induction of several transcription factors (Msx1, Zic1, Pax3, and Gbx2). These transcription factors then increase the expression of various neural crest specifiers (AP2alpha, FoxD3, Snail1/2, and Twist), which are further activated by intermediate BMP signals and additional Wnt signals. Continued expression of specifying molecules (Twist, FoxD3, Snail1/2, and AP2alpha) assists in stabilizing the neural crest population and allows downstream processes to promote neural crest delamination and migration (e.g., via the expression/actions of N-cadherin, cadherin-7, c-Myc, and Id3). (B) Simple model of the two phases of neural crest induction. FGF and Wnts signal the early specification neural crest in the neural plate border, while at later developmental stages, BMPs and Wnts provide signals to maintain the neural crest population.

inducers/additional transcription factors such as *snail1*, *slug/snail2*, *sox8*, *sox9*, *sox10*, *foxd3*, *ap-2*, *twist*, *c-myc*, and *id* family members along with other effector genes. During neurulation, these transcription factors collectively induce the cells to become neural crest and stabilize the neural crest population (neural crest cell maintenance). By the end of neurulation, these transcription factors have begun to assist in the terminal differentiation of neural crest.

This differential expression of the two groups of transcription factors described earlier suggested that neural crest is induced during gastrulation at the prospective neural plate border and then undergoes another round of signaling that maintains the neural crest cell population. This is supported by basic embryology experiments where neural crest explants (neural folds obtained from neurula stage embryos) were dissected from the embryo and cultured with or without the

intermediate mesoderm until stage 23 equivalent. When the explants were cultured alone, they lost expression of the neural crest marker *Snail2*, but explants cultured with intermediate mesoderm maintained expression of this marker (Steventon et al. 2009).

The pathways involved in inducing the neural crest cells have been the focus of research for many years and have been well described mechanistically despite a lack of direct regulatory studies at the gene level. Additionally, since the inducers regulate the transcriptional expression of each other, the hierarchy between them has remained difficult to discern. Future research of regulatory elements at the gene level will help in defining how each inducer is regulated by other inducers and, for example, if distinct or shared signaling pathways are employed.

The neural plate boundary itself results from the actions of several pathways converging to regulate the expression of boundary specifiers. Intermediate levels of BMP activity as well as Wnt signals have been shown to control the expression of *Msx1*, *Pax3*, and *Zic1*, boundary specifiers required for neural crest formation (Tribulo et al. 2003; Monsoro-Burq et al. 2005; Sato et al. 2005). As neural plate boundary specifiers downstream of Wnt signals, *Pax3* and *Zic1* in turn activate the neural crest inducers *Snail2/Slug* and *Foxd3* (Hong and Saint-Jeannet 2007).

The tissues surrounding the neural plate border provide the signals necessary for induction and maintenance of the neural crest. The paraxial mesoderm, nonneural ectoderm, and neural tissues all have been shown to participate in neural crest induction and maintenance (Mancilla and Mayor 1996; Bonstein et al. 1998; Pieper et al. 2012). However, recently, the role of the mesoderm in neural crest induction has been questioned. This was suggested because injection of an amino-terminally truncated form of *Cerberus* that inhibits nodal signaling and therefore mesoderm formation still allows the expression of *Snail2* and *Sox3* at neurula stages (Wu et al. 2011).

Classically, the first neural crest-inducing pathway was proposed to be an intermediate level of BMP signaling at the neural plate border region from where neural crest cells are derived. During gastrulation, this could be

accomplished via the expression of BMP ligands from the prospective ectoderm, as well as BMP inhibitors from the underlying paraxial mesoderm. As a result (in part) of the intermediate levels of BMP that arise, high-level expression of various genes required for neural crest induction ensues, including *Snail*, *Slug*, *AP-2*, and *Foxd3* (LaBonne and Bronner-Fraser 1998; Marchant et al. 1998; Sasai et al. 2001; Luo et al. 2003; Sauka-Spengler and Bronner-Fraser 2008). More recently, it has been shown that BMP signaling alone cannot induce neural crest cells, meaning that other pathways are involved. One such pathway is an indirect induction initiated via *Fgf8* that increases *Wnt8*-ligand expression to signal from the mesoderm to the prospective neural crest. This Wnt signal is thought to induce neural crest cells transiently, but then at later stages, intermediate levels of BMP signals along with the Wnt signals are required for long-term establishment of the neural crest cells (Mayor et al. 1995; Mayor et al. 1997; Saint-Jeannet et al. 1997; LaBonne and Bronner-Fraser 1998; Bang et al. 1999; Dewardorf et al. 2001; Monsoro-Burq et al. 2003; Monsoro-Burq et al. 2005; Wu et al. 2005; Hong et al. 2008; Steventon et al. 2009).

Wnt signaling induces the transcriptional expression of *Snail2* and *FoxD3* in an *Msx1*-dependent manner, as well as through *Pax3* and *Zic1* (Monsoro-Burq et al. 2005; Sato et al. 2005). The Wnt pathway also regulates the expression of two essential specifiers of the neural crest, namely, *AP-2*, and a posteriorizing homeobox transcription factor, *Gbx2* (Luo et al. 2002; Li et al. 2009). Given the spatial and temporal expression of *Wnt3a* and *Wnt8* (paraxial mesoderm, dorsolateral marginal zone, and posterior neural plate), as well as their knockdown effects, *Wnt3a* and *Wnt8* have been suggested as the primary canonical Wnt ligands contributing to neural crest formation (Hong et al. 2008; Steventon et al., 2009; Elkouby et al. 2010). Other studies have implicated additional components of the Wnt pathway in neural crest induction, including *Frizzled7*, *Lrp6*, *Dishevelled 1* and *2*, and a novel negative regulator of the canonical Wnt pathway, *Kctd15* (Tamai et al. 2000; Dewardorf et al. 2001; Abu-Elmagd et al. 2006; Gray et al. 2009; Dutta and Dawid 2010). Two other

potential modifiers of the Wnt pathway, *Kremen2* and *Kermit*, have also been shown to have effects on neural crest development (Tan et al. 2001; Hassler et al. 2007).

Interestingly, the canonical Wnt pathway machinery operating upon beta-catenin also regulates certain members/isoforms of the p120 and plakophilin–catenin subfamilies (e.g., p120 isoform1) (Park et al. 2006; Hong et al. 2010). A number of these catenins have also been found to modulate neural crest development (Ciesiolka et al. 2004; Gu et al. 2009; Tran et al. 2011; Munoz et al. 2012). Conceivably, therefore, canonical Wnt-mediated effects upon neural crest induction or maintenance could involve the coordinate Wnt-responsive actions of distinct catenins. Furthermore, there has been evidence implicating noncanonical Wnt signaling (defined as not being transduced via beta-catenin, such as via small GTPases) in neural crest induction (Ossipova and Sokol 2011). Whatever the mechanism, Wnt signaling has an impact upon neural crest induction and maintenance (Steventon et al. 2009).

Recently, Indian hedgehog signaling has been shown to be necessary for neural crest formation, maintenance, and migration. Loss of function of Indian hedgehog results in losses of both the neural plate border and neural crest specifiers, while neural and epidermal markers become expanded. As proliferation and apoptosis were not affected by these experimental changes in Indian hedgehog signaling, it is believed that these alterations are a result of changed cell fate decisions (Aguero et al. 2012).

While neural plate boundary specification and neural crest induction pathways have been extensively studied, very little is known about the direct regulation of the downstream transcription factors targeted by these pathways. Identification of the proteins responsible for direct regulation and their function has become a major focus of the field. One earlier study identified a required *Lef1* site in the *Snail2*/*Slug* promoter (Vallin et al. 2001). More recently, a LIM adaptor protein, *LMO4*, was shown to bind to promoter elements of the *Snail*/*Slug* family members and was found necessary for *Snail*/*Slug* family member's ability to induce neural crest (Ochoa et al. 2011).

In this section, we have outlined some of the induction processes involved in generating neural crest. This induction is believed to occur in a two-step process with FGF and Wnt signals providing the initial inductive signals during gastrulation, followed by BMP and Wnt signals during neurulation to further induce the neural crest cells and maintain the specified cells as neural crest (Figure 13.4B). Much work must still be done to show the mechanisms behind how the various signaling pathways regulate the expression of the various neural crest specifiers at either the transcriptional or posttranscriptional levels.

Neural crest delamination and migration

Once neural crest cells are specified during neurulation, the prior noted neural crest specifiers then induce delamination, EMT, and migration. *Snail1* and *Slug*/*Snail2* are prominent examples of specifiers controlling these later cellular activities (Carl et al. 1999; LaBonne and Bronner-Fraser 2000). Delamination is the process by which the neural crest cells separate themselves from the neuroectoderm. While the neural plate is still open, the neural crest cells from the cranial region delaminate simultaneously (Sadaghiani and Thiebaud 1987). The trunk neural crest behave differently, delaminating individually after neural tube closure, and at times vary dramatically along the anterior–posterior axis (Davidson and Keller 1999). The mechanisms regulating delamination in *Xenopus* have not been well worked out, but significant work has been done in mouse and chick. From the mouse and chick studies, various signals are at play during delamination and EMT, with their respective activities being dependent upon location along the anterior–posterior axis (reviewed in Theveneau and Mayor 2012). Following delamination and EMT, the neural crest cells begin to migrate toward their sites of terminal differentiation. Here, we will briefly discuss *Xenopus* delamination and how the neural crest begins to migrate away from the neural tube.

While little is known about the delamination process in *Xenopus*, it has been shown

that once the neural crest cells delaminate, they do not begin migration immediately (Sadaghiani and Thiebaud 1987). The delamination process is partially mediated by reducing the strength of cell–cell adhesion between the neural crest and neighboring tissues while maintaining strong interactions between neural crest cells themselves (Alfandari et al. 2010). Additional mechanisms of delamination have been well characterized in other model systems and are reviewed in Theveneau and Mayor (2012).

Following delamination, the neural crest cells undergo a dramatic cellular change, EMT, and begin to migrate away from the neural tube in streams toward their final sites of differentiation. While the EMT process has not been well studied in *Xenopus*, there have been significant contributions from *Xenopus* to understanding neural crest cell migration. The neural crest cells migrate in specific patterns that are based on various cues and early differentiation pathways (Krotoski et al. 1988; Collazo et al. 1993). For the cells to migrate, they must first weaken the interactions between themselves and the extracellular matrix, allowing greater mobility (Theveneau et al. 2010). To reduce cell–cell adhesion between neural crest cells, various metalloproteinases such as ADAM13 are expressed that have cadherin-cleaving capabilities (Alfandari et al. 1997; Alfandari et al. 2001; Harrison et al. 2004; Alfandari et al. 2010). Additionally, cadherin switching occurs when the neural crest cells begin to take on migratory behaviors (Vallin et al. 1998).

Regulatory mechanisms that contribute to neural crest migration include the actions of ephrins and their receptors. These proteins restrict the intermingling of the different regions of neural crest as they migrate, though how this is accomplished is unknown (Smith et al. 1997; Helbling et al. 1998; Kuriyama and Mayor 2008). In other vertebrate species, semaphorins have been shown to properly position neural crest cells during their migration, through effects on cell structure and cell–cell interactions (Tamagnone and Comoglio 2004). Together, such signals are thought to produce defined regions permissive to neural crest cell migration and others that are restrictive or repulsive.

Once the permissive and repulsive regions are established, the neural crest cells begin migrating in “streams” along the permissive regions. How the neural crest directionally migrates has not been studied thoroughly *in vivo*, but *in vitro* studies suggest it may be partially dependent on gradients of chemoattractants (Kuriyama and Mayor 2008). Further study of chemotaxis in these cells is still strongly warranted.

The neural crest cells are also highly polarized in their direction of migration. Noncanonical Wnt signaling/planar cell polarity signals (which by definition are not beta-catenin mediated) are instrumental in enabling this orientation, perhaps primarily through modulating the cytoskeleton and cell shape/migration–polarity. Noncanonical Wnt11 has been suggested as a ligand relevant to this pathway in neural crest cells, as it is expressed adjacent to premigratory neural crest, and mislocalization of this signal inhibits its function in promoting neural crest migration (De Calisto et al. 2005).

Complementing the inputs described earlier, a recent model has been described for neural crest directional migration based upon cell–cell contacts. In this model, neural crest cells migrate as groups, with dynamic cell–cell contacts being necessary for directional migration. Crest cells begin their migration at the neural plate as a sheet of cells, which then separate into smaller clusters and streams of cells. These smaller groups of cells follow the free edge of the cluster, migrating into regions where no neural crest cells are present. The migration into these regions provides directional migration to the cluster (Theveneau and Mayor 2012). This occurs through at least two distinct mechanisms termed contact inhibition of locomotion and coattraction. Contact inhibition of locomotion occurs when a migrating cell comes into contact with another cell and ceases to migrate, at least so long as the inhibitory signal (cell–cell contact) is maintained. When numerous migratory cells are in full contact with each other, it is the free cell edges that exhibit migratory behaviors away from the cluster. This free-edge movement promotes directional migration of the entire crest cluster, with cell–cell contacts cycling between being lessened and reforming

in the following cells (Carmona-Fontaine et al. 2008). In keeping with such a model, *in vitro* work has shown that chemotactic (directional) migratory responses are reduced when neural crest cells lose contact with each other (Thomas and Yamada 1992). Further, while the mechanism is still being defined, isolated neural crest cells that advance too rapidly or in an errant direction appear to rejoin the larger cluster or stream via a process termed coattraction (Theveneau et al. 2010). With the neural crest cells clustered (or reclustered), their migratory response to chemotactic signals, such as Sdf1, is significantly increased (Theveneau and Mayor 2012). Such chemoattraction allows for migration of the neural crest cells away from the neural tube and toward regions of terminal differentiation.

Contributing to the control of later neural crest processes are proteins regulating the cell cycle and differentiation. Some examples include the basic helix–loop–helix (bHLH) protein, Hairy2, and the helix–loop–helix protein, Id3, which are expressed starting at the neural plate border stage. Hairy2 or Id3 knockdowns result in loss of neural crest markers due to defects that arise in the cell cycle (Kee and Bronner-Fraser 2005; Nagatomo and Hashimoto 2007). c-Myc maintains the neural crest precursors in a multipotent state through the activity of Id3 (Bellmeyer et al. 2003; Light et al. 2005). Recently, Stat3 activity, regulated by Id3 and Hairy2, was reported to regulate cell proliferation and neural crest differentiation as well (Nichane et al. 2009). While the findings summarized in this section provide early evidence of how EMT and migration may be regulated, future research will be needed to more fully understand areas such as how *Xenopus* neural crest cells begin EMT and the mechanism(s) of how neural crest cells migrate.

Molecular regulation of neurogenesis

In both morphological and molecular terms, the early neural ectoderm is distinct from the presumptive epidermis by the midgastrula stage (st. 11): the neural plate adopts a columnar morphology and expresses a distinct set of genes, including many that are

either activated or upregulated by the inhibition of BMP signaling (Uzman et al. 1998). Initially, the neural plate includes a deep layer of columnar cells underlying a superficial layer; cells in both layers undergo a round of cell division soon after gastrulation is complete. As neurulation continues, the two cell layers of the neural plate intercalate, but cells from each layer retain distinct identities (Hartenstein 1989). Many cells originating in the deep layer will form the primary neurons, which differentiate during tailbud stages and establish the tadpole CNS (Hartenstein 1989). The process by which neurons differentiate is referred to as neurogenesis. Most cells derived from the superficial layer show a significantly greater capacity for proliferation and are responsible for secondary neurogenesis, which generates most of the adult CNS (Hartenstein 1989). Most cells responsible for primary neurogenesis will subsequently withdraw from the cell cycle following the post-gastrulation mitosis and initiate neuronal differentiation (Hartenstein 1989). Terminal differentiation of the primary neurons begins shortly after neural tube closure (Figure 13.5a). The newly specified midgastrula neural ectoderm is characterized by the expression of a set of transcription factors that act in concert to establish an immature neural state (reviewed in Rogers et al. 2009). Some of these genes are maternally expressed, while others are activated shortly after the onset of gastrulation. In these cases, neural specification leads to persistence or upregulation of expression, mostly in response to the inhibition of BMP signaling. While the regulatory relationships among these genes are still emerging, a central component of the newly specified neural gene regulatory network (GRN) is the forkhead family member *FoxD5*, which regulates transcription both positively and negatively to promote neural specification and expand the neural ectoderm (Yan et al. 2009). Continued expression of *FoxD5* has been shown to require FGF signaling, as well as inhibition of BMP (Rogers et al. 2011). A second maternally expressed gene, *geminin*, maintains the proliferative capacity of the newly specified neural ectoderm (Seo et al. 2005). *FoxD5* directly activates *geminin*, *Sox11*, and *Zic2*, which maintain the expression of

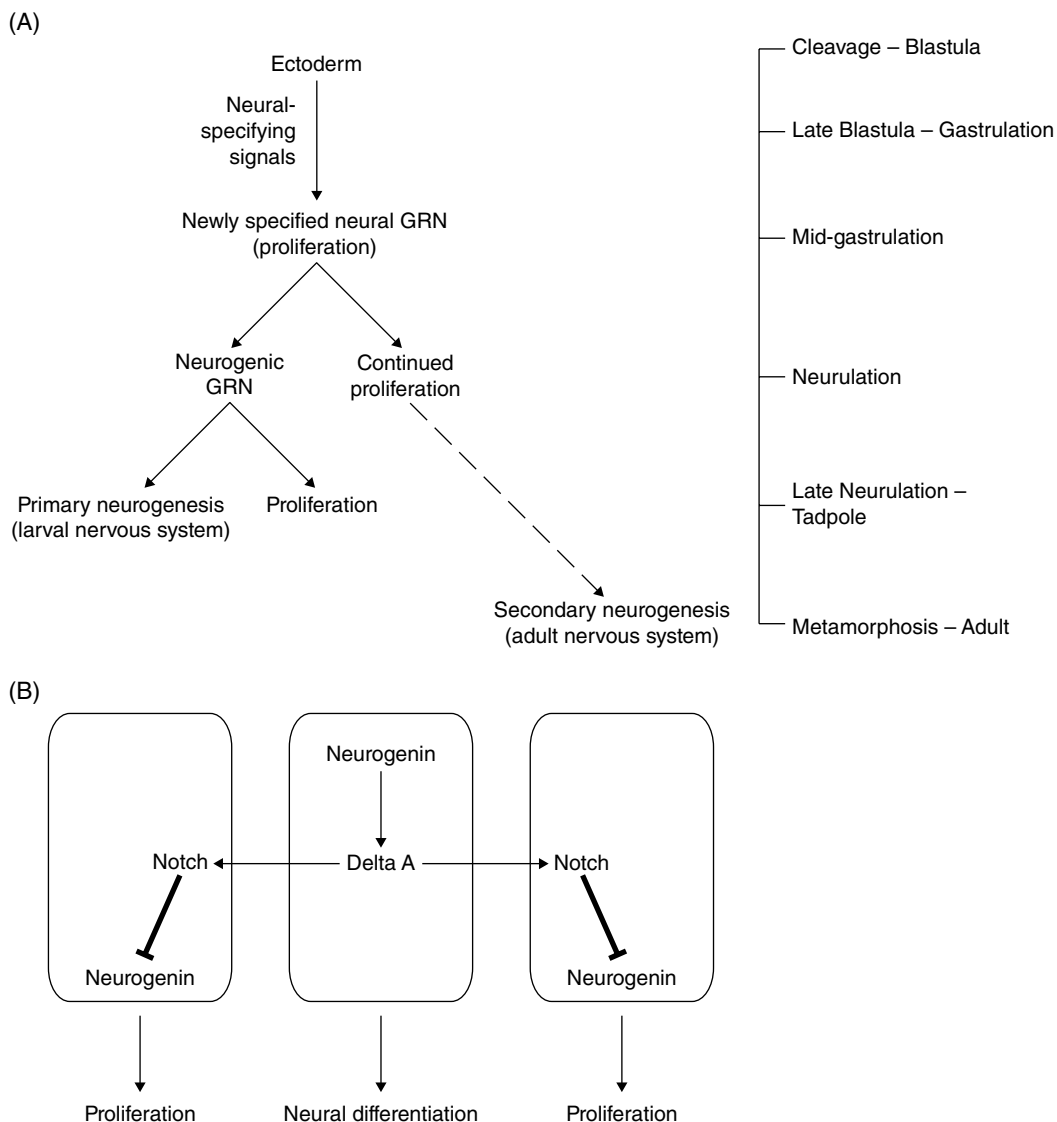


Figure 13.5 Neurogenic processes of *X. laevis*. (A) Progression of ectoderm cells from neural induction through primary neurogenesis. (B) Lateral inhibition of neuronal differentiation through DeltaA/Notch signaling. GRN = Gene Regulatory Network.

one another and also promote the expression of *Sox2* and *Sox3*; these six genes are the major components of the newly specified neural GRN (Rogers et al. 2009).

These six genes also negatively regulate members of the Iroquois family (*Irxf1*, 2, and 3, formerly known as *Xiro1–3*), which are transcription factors associated with the transition to the neurogenic GRN. The *Irxf* genes are initially expressed in the dorsal ectoderm of early gastrula embryos and may

function during gastrulation to define the region of the prospective neural ectoderm; they subsequently serve to delineate neurogenic regions within the posterior neural plate (reviewed in Cavodeassi et al. 2001). The upregulation of the *Irxf* genes after the end of gastrulation provides negative feedback to *FoxD5* (Yan et al. 2009), which declines in expression after early neurula (st. 14). Together with *Zic1* and *Zic3*, the *Irxf* genes regulate the expression of the neurogenic

bHLH factors, including *neurogenin1* and *neurogenin2*. Unlike *Irx1* and *Irx2*, *Irx3* promotes the expression of *Xenopus Achaete-Scute Homologue-3* (*XASH3*), which suppresses neuronal differentiation via a notch-independent mechanism (Bellefroid et al. 1998).

These regulatory interactions between the *Zic* and *Irx* genes result in three broad antero-posterior bands of *neurogenin* expression on either side of the midline; cells in the intervening regions maintain high levels of *Zic2* expression, which inhibits neurogenesis during neurulation (Brewster et al. 1998). High levels of neurogenin increase the expression of *DeltaA*, which signals through notch to downregulate the expression of neurogenin in adjacent cells (Ma et al. 1996). As a result, a subset of non-adjacent cells in each band will maintain high levels of neurogenin and express *NeuroD*, which activates genes associated with neuronal differentiation. Thus, the positioning of differentiated neurons is established via Notch-mediated lateral inhibition (Figure 13.5b). Notch signaling also promotes the expression of *Geminin* and *Zic2* in the nondifferentiating neural ectoderm, which maintains the proliferative capacity of these cells (Yan et al. 2009).

In *Xenopus*, as in mammals, the formation of the CNS involves a complex interplay between cell cycle regulation and the initiation of neuronal differentiation (reviewed in Hindley and Philpott 2012). Commitment to a neural fate is maintained, even while cells are held in an immature proliferative state and prevented from differentiating. At a fundamental level, the maintenance of the proliferative state is mediated by lateral inhibition via Notch signals, which inhibit the expression of both *neurogenin2* (*Ngn2*) and the cyclin-dependent kinase inhibitor (CDKi) *Xic1* (Vernon et al. 2006). *Geminin* has a twofold role: it represses transcriptional activation of neurogenic genes (Yellajoshiyula et al. 2011) and parallel studies of *geminin* function in embryonic mouse fore-brain have demonstrated that *geminin* establishes bivalent chromatin modifications at neurogenic genes; these activating (trimethylated H3K4) and repressive (trimethylated H3K27) modifications leave neurogenic genes in a reversibly repressed state (Yellajoshiyula et al. 2011). *Geminin* also promotes cell proliferation via interactions with the DNA replica-

tion machinery at origins of replication (reviewed in Seo and Kroll 2006). Additional regulation of proliferation and differentiation can occur via modifications in the length of the G1 phase: during a short G1 phase, active cyclin-dependent kinase (CDK) complexes accumulate more rapidly, and they inhibit differentiation by phosphorylating *Ngn2*, reducing its activity (Ali et al. 2011). Conversely, *Ngn2* remains hypophosphorylated, and thus able to promote neuronal differentiation, for a longer interval during a prolonged G1 phase.

While components and interactions within the neurogenic gene network are highly conserved among vertebrates (reviewed in Chitnis 1999), the newly specified neural GRN has comparatively fewer parallels with other vertebrates. Although *Sox* and *Zic* family members are expressed in response to neural specification, *FoxD5* has not been implicated in the initiation of neural development in other vertebrate model systems. Moreover, although other members of the *Fox* family participate in the regulation of later aspects of neural development (Hindley and Philpott 2012), none have been shown to play a role in neural specification in other vertebrates. Although *geminin* plays a significant role in mammalian neurogenesis, its functions in the earliest phases of mammalian neural development are less clear. Some differences in specific patterns of gene regulation in newly induced neural ectoderm between *Xenopus* and other vertebrates may reflect differences in the dependence on inhibition of BMP signaling (Rogers et al. 2011). The considerable redundancy at the level of molecular regulation, however, may render these initial differences insignificant while increasing the robustness of neural specification. In any event, as the newly specified neural ectoderm transitions to the neurogenic phase, the molecular regulation of neurogenesis proceeds along conserved pathways.

Although the process of neurogenesis begins with changes in gene expression during gastrulation, it continues throughout embryonic and larval development. The regulatory networks that initiate neuronal differentiation are activated in subsets of cells within the neural ectoderm, while other cells are restricted from differentiation and

continue to proliferate. While the genetic interactions responsible for primary neurogenesis have been studied extensively, the regulation of secondary neurogenesis is less well understood. Throughout neural development, however, the integrated control of proliferation and differentiation ensures the formation of an early functional CNS that can sustain larval activity as continuing proliferation establishes the foundation for secondary neurogenesis and the adult CNS.

Conclusions

With almost 90 years passing since the identification of the Spemann's organizer, numerous workers have contributed to identifying diverse signals, pathways, and tissues necessary for neural specification, induction, and differentiation of both the central and peripheral nervous systems. The complexity of the nervous system continues to present questions that will lead researchers down new paths, likely contradicting current dogmas. As such, the mechanisms relating to direct gene regulation during neural specification and differentiation and to how neural crest cells are induced to undergo EMT and begin migration are large, relatively open questions in *Xenopus* development. Studies in these areas should provide information useful in understanding human development and disease, as many of the pathways or their interrelationships are conserved across species. Further, given the variety and power of experimental tools currently available to *Xenopus* researchers, with more actively in the making, this model will continue to be among those at the center of providing insights upon key questions in neural biology.

Acknowledgments

This work was earlier supported by the NIH (RO1GM52112 to P.D.M.) and an NIH Research Supplement to Promote Diversity in Health-Related Research (W.A.M.). W.A.M. has also been supported from a Cancer Prevention and Research Institute of Texas Research Training Award (RP101502).

References

- Abu-Elmagd, M., Garcia-Morales, C., Wheeler, G. N., 2006. Frizzled7 mediates canonical Wnt signaling in neural crest induction. *Dev Biol.* 298, 285–98.
- Agius, E., Oelgeschlager, M., Wessely, O., Kemp, C., De Robertis, E. M., 2000. Endodermal Nodal-related signals and mesoderm induction in *Xenopus*. *Development.* 127, 1173–83.
- Aguero, T. H., Fernandez, J. P., Lopez, G. A., Tribulo, C., Aybar, M. J., 2012. Indian hedgehog signaling is required for proper formation, maintenance and migration of *Xenopus* neural crest. *Dev Biol.* 364, 99–113.
- Alfandari, D., Wolfsberg, T. G., White, J. M., DeSimone, D. W., 1997. ADAM 13: a novel ADAM expressed in somitic mesoderm and neural crest cells during *Xenopus laevis* development. *Dev Biol.* 182, 314–30.
- Alfandari, D., Cousin, H., Gaultier, A., et al, 2001. *Xenopus* ADAM 13 is a metalloprotease required for cranial neural crest-cell migration. *Curr Biol.* 11, 918–30.
- Alfandari, D., Cousin, H., Marsden, M., 2010. Mechanism of *Xenopus* cranial neural crest cell migration. *Cell Adh Migr.* 4, 553–60.
- Ali, F., Hindley, C., McDowell, G., et al, 2011. Cell cycle-regulated multi-site phosphorylation of Neurogenin 2 coordinates cell cycling with differentiation during neurogenesis. *Development.* 138, 4267–77.
- Aruga, J., Mikoshiba, K., 2011. Role of BMP, FGF, calcium signaling, and Zic proteins in vertebrate neuroectodermal differentiation. *Neurochem Res.* 36, 1286–92.
- Bae, S., Reid, C. D., Kessler, D. S., 2011. Siamois and Twin are redundant and essential in formation of the Spemann organizer. *Dev Biol.* 352, 367–81.
- Bang, A. G., Papalopulu, N., Goulding, M. D., Kintner, C., 1999. Expression of Pax-3 in the lateral neural plate is dependent on a Wnt-mediated signal from posterior nonaxial mesoderm. *Dev Biol.* 212, 366–80.
- Brewster, R., Lee, J., Ruiz i Altaba, A., 1998. Gli/Zic factors pattern the neural plate by defining domains of cell differentiation. *Nature*, 393(6685), 579–83.
- Bayramov, A. V., Eroshkin, F. M., Martynova, N. Y., Ermakova, G. V., Solovieva, E. A., Zaraisky, A. G., 2011. Novel functions of Noggin proteins: inhibition of Activin/Nodal and Wnt signaling. *Development.* 138, 5345–56.
- Bellefroid, E. J., Kobbe, A., Gruss, P., Pieler, T., Gurdon, J. B., Papalopulu, N., 1998. Xiro3 encodes a *Xenopus* homolog of the *Drosophila* Iroquois genes and functions in neural specification. *EMBO J.* 17, 191–203.

- Bellmeyer, A., Krase, J., Lindgren, J., LaBonne, C., 2003. The protooncogene c-myc is an essential regulator of neural crest formation in *xenopus*. *Dev Cell*. 4, 827–39.
- Bonstein, L., Elias, S., Frank, D., 1998. Paraxial-fated mesoderm is required for neural crest induction in *Xenopus* embryos. *Dev Biol*. 193, 156–68.
- Bouwmeester, T., Kim, S., Sasai, Y., Lu, B., De Robertis, E. M., 1996. Cerberus is a head-inducing secreted factor expressed in the anterior endoderm of Spemann's organizer. *Nature*. 382, 595–601.
- Carl, T. F., Dufton, C., Hanken, J., Klymkowsky, M. W., 1999. Inhibition of neural crest migration in *Xenopus* using antisense slug RNA. *Dev Biol*. 213, 101–15.
- Carmona-Fontaine, C., Matthews, H. K., Kuriyama, S., et al, 2008. Contact inhibition of locomotion in vivo controls neural crest directional migration. *Nature*. 456, 957–61.
- Cavodeassi, F., Modolell, J., Gomez-Skarmeta, J. L., 2001. The Iroquois family of genes: from body building to neural patterning. *Development*, 128(15), 2847–55.
- Cha, S. W., Tadjuidje, E., Tao, Q., Wylie, C., Heasman, J., 2008. Wnt5a and Wnt11 interact in a maternal Dkk1-regulated fashion to activate both canonical and non-canonical signaling in *Xenopus* axis formation. *Development*. 135, 3719–29.
- Chen, Y., Huang, L., Solursh, M., 1994. A concentration gradient of retinoids in the early *Xenopus laevis* embryo. *Dev Biol*. 161, 70–6.
- Chitnis, A. B., 1999. Control of neurogenesis – lessons from frogs, fish and flies. *Curr Opin Neurobiol*, 9(1), 18–25.
- Cho, K. W., De Robertis, E. M., 1990. Differential activation of *Xenopus* homeo box genes by mesoderm-inducing growth factors and retinoic acid. *Genes Dev*. 4, 1910–6.
- Cho, K. W., Blumberg, B., Steinbeisser, H., De Robertis, E. M., 1991. Molecular nature of Spemann's organizer: the role of the *Xenopus* homeobox gene gooseoid. *Cell*. 67, 1111–20.
- Ciesiolka, M., Delvaeye, M., Van Imschoot, G., et al, 2004. p120 catenin is required for morphogenetic movements involved in the formation of the eyes and the craniofacial skeleton in *Xenopus*. *J Cell Sci*. 117, 4325–39.
- Collazo, A., Bronner-Fraser, M., Fraser, S. E., 1993. Vital dye labelling of *Xenopus laevis* trunk neural crest reveals multipotency and novel pathways of migration. *Development*. 118, 363–76.
- Davidson, L. A., Keller, R. E., 1999. Neural tube closure in *Xenopus laevis* involves medial migration, directed protrusive activity, cell intercalation and convergent extension. *Development*. 126, 4547–56.
- De Calisto, J., Araya, C., Marchant, L., Riaz, C. F., Mayor, R., 2005. Essential role of non-canonical Wnt signalling in neural crest migration. *Development*. 132, 2587–97.
- De Robertis, E. M., Kuroda, H., 2004. Dorsal-ventral patterning and neural induction in *Xenopus* embryos. *Annu Rev Cell Dev Biol*. 20, 285–308.
- Deardorff, M. A., Tan, C., Saint-Jeannet, J. P., Klein, P. S., 2001. A role for frizzled 3 in neural crest development. *Development*. 128, 3655–63.
- Dessaud, E., McMahon, A. P., Briscoe, J., 2008. Pattern formation in the vertebrate neural tube: a sonic hedgehog morphogen-regulated transcriptional network. *Development*. 135, 2489–503.
- Domingos, P. M., Itasaki, N., Jones, C. M., et al., 2001. The Wnt/beta-catenin pathway posteriorizes neural tissue in *Xenopus* by an indirect mechanism requiring FGF signalling. *Dev Biol*, 239(1), 148–60.
- Dubrulle, J., Pourquie, O., 2004. fgf8 mRNA decay establishes a gradient that couples axial elongation to patterning in the vertebrate embryo. *Nature*. 427, 419–22.
- Dutta, S., Dawid, I. B., 2010. Kctd15 inhibits neural crest formation by attenuating Wnt/beta-catenin signaling output. *Development*. 137, 3013–8.
- Ekker, S. C., McGrew, L. L., Lai, C. J., et al., 1995. Distinct expression and shared activities of members of the hedgehog gene family of *Xenopus laevis*. *Development*. 121, 2337–47.
- Elkouby, Y. M., Frank, D., 2010. *Wnt/beta-catenin signaling in vertebrate posterior neural development*. Morgan & Claypool Life Sciences, San Rafael, CA.
- Elkouby, Y. M., Elias, S., Casey, E. S., et al., 2010. Mesodermal Wnt signaling organizes the neural plate via Meis3. *Development*. 137, 1531–41.
- Fletcher, R. B., Baker, J. C., Harland, R. M., 2006. FGF8 spliceforms mediate early mesoderm and posterior neural tissue formation in *Xenopus*. *Development*. 133, 1703–14.
- Gerhart, J., Danilchik, M., Doniach, T., Roberts, S., Rowing, B., Stewart, R., 1989. Cortical rotation of the *Xenopus* egg: consequences for the antero-posterior pattern of embryonic dorsal development. *Development*. 107 Suppl, 37–51.
- Gilbert, S. F., 2006. *Developmental biology*. Sinauer Associates, Inc. Publishers, Sunderland, MA.
- Gilchrist, M. J., Christensen, M. B., Bronchain, O., et al., 2009. Database of queryable gene expression patterns for *Xenopus*. *Dev Dyn*. 238, 1379–88.
- Glinka, A., Wu, W., Delius, H., Monaghan, A. P., Blumenstock, C., Niehrs, C., 1998. Dickkopf-1 is a member of a new family of secreted proteins and functions in head induction. *Nature*. 391, 357–62.
- Gont, L. K., Steinbeisser, H., Blumberg, B., de Robertis, E. M., 1993. Tail formation as a continuation of gastrulation: the multiple cell populations of the *Xenopus* tailbud derive from the late blastopore lip. *Development*. 119, 991–1004.
- Gray, R. S., Bayly, R. D., Green, S. A., Agarwala, S., Lowe, C. J., Wallingford, J. B., 2009. Diversification

- of the expression patterns and developmental functions of the dishevelled gene family during chordate evolution. *Dev Dyn.* 238, 2044–57.
- Groppe, J., Greenwald, J., Wiater, E., et al., 2002. Structural basis of BMP signalling inhibition by the cystine knot protein Noggin. *Nature.* 420, 636–42.
- Gu, D., Sater, A. K., Ji, H., et al., 2009. *Xenopus* delta-catenin is essential in early embryogenesis and is functionally linked to cadherins and small GTPases. *J Cell Sci.* 122, 4049–61.
- Harrison, M., Abu-Elmagd, M., Grocott, T., Yates, C., Gavrilovic, J., Wheeler, G. N., 2004. Matrix metalloproteinase genes in *Xenopus* development. *Dev Dyn.* 231, 214–20.
- Hartenstein, V., 1989. Early neurogenesis in *Xenopus*: the spatio-temporal pattern of proliferation and cell lineages in the embryonic spinal cord. *Neuron.* 3, 399–411.
- Hassler, C., Cruciat, C. M., Huang, Y. L., Kuriyama, S., Mayor, R., Niehrs, C., 2007. Kremen is required for neural crest induction in *Xenopus* and promotes LRP6-mediated Wnt signaling. *Development.* 134, 4255–63.
- Heasman, J., Kofron, M., Wylie, C., 2000. Beta-catenin signaling activity dissected in the early *Xenopus* embryo: a novel antisense approach. *Dev Biol.* 222, 124–34.
- Helbling, P. M., Tran, C. T., Brandli, A. W., 1998. Requirement for EphA receptor signaling in the segregation of *Xenopus* third and fourth arch neural crest cells. *Mech Dev.* 78, 63–79.
- Hemmati-Brivanlou, A., Kelly, O. G., Melton, D. A., 1994. Follistatin, an antagonist of activin, is expressed in the Spemann organizer and displays direct neuralizing activity. *Cell.* 77, 283–95.
- Hindley, C., Philpott, A., 2012. Co-ordination of cell cycle and differentiation in the developing nervous system. *Biochem J.* 444, 375–82.
- Holtfreter, J., 1934. Formative Reize in der Embryonalentwicklung der Amphibien dargestellt an Explantationsversuchen. *Arch exp. Zellforsch.* 15, 281–301.
- Hong, C. S., Saint-Jeannet, J. P., 2007. The activity of Pax3 and Zic1 regulates three distinct cell fates at the neural plate border. *Mol Biol Cell.* 18, 2192–202.
- Hong, C. S., Park, B. Y., Saint-Jeannet, J. P., 2008. Fgf8a induces neural crest indirectly through the activation of Wnt8 in the paraxial mesoderm. *Development.* 135, 3903–10.
- Hong, J. Y., Park, J. I., Cho, K., et al., 2010. Shared molecular mechanisms regulate multiple catenin proteins: canonical Wnt signals and components modulate p120-catenin isoform-1 and additional p120 subfamily members. *J Cell Sci.* 123, 4351–65.
- Isaacs, H. V., 1997. New perspectives on the role of the fibroblast growth factor family in amphibian development. *Cell Mol Life Sci.* 53, 350–61.
- Janssens, S., Denayer, T., Deroo, T., Van Roy, F., Vleminckx, K., 2010. Direct control of Hoxd1 and Irx3 expression by Wnt/beta-catenin signaling during anteroposterior patterning of the neural axis in *Xenopus*. *Int J Dev Biol.* 54, 1435–42.
- Kaufmann, L. T., Niehrs, C., 2011. Gadd45a and Gadd45g regulate neural development and exit from pluripotency in *Xenopus*. *Mech Dev.* 128, 401–11.
- Kee, Y., Bronner-Fraser, M., 2005. To proliferate or to die: role of Id3 in cell cycle progression and survival of neural crest progenitors. *Genes Dev.* 19, 744–55.
- Kengaku, M., Okamoto, H., 1995. bFGF as a possible morphogen for the anteroposterior axis of the central nervous system in *Xenopus*. *Development.* 121, 3121–30.
- Khokha, M. K., Yeh, J., Grammer, T. C., Harland, R. M., 2005. Depletion of three BMP antagonists from Spemann's organizer leads to a catastrophic loss of dorsal structures. *Dev Cell.* 8, 401–11.
- Kibbe, W. A., 2007. OligoCalc: an online oligonucleotide properties calculator. *Nucleic Acids Res.* 35, W43–6.
- Kiecker, C., Niehrs, C., 2001. A morphogen gradient of Wnt/beta-catenin signalling regulates anteroposterior neural patterning in *Xenopus*. *Development.* 128, 4189–201.
- Klymkowsky, M. W., Rossi, C. C., Artinger, K. B., 2010. Mechanisms driving neural crest induction and migration in the zebrafish and *Xenopus laevis*. *Cell Adh Migr.* 4, 595–608.
- Kofron, M., Demel, T., Xanthos, J., et al., 1999. Mesoderm induction in *Xenopus* is a zygotic event regulated by maternal VegT via TGFbeta growth factors. *Development.* 126, 5759–70.
- Kolm, P. J., Sive, H. L., 1995. Regulation of the *Xenopus* labial homeodomain genes, HoxA1 and HoxD1: activation by retinoids and peptide growth factors. *Dev Biol.* 167, 34–49.
- Kolm, P. J., Sive, H. L., 1997. Retinoids and posterior neural induction: a reevaluation of Nieuwkoop's two-step hypothesis. *Cold Spring Harb Symp Quant Biol.* 62, 511–21.
- Krieg, P. A., Melton, D. A., 1987. In vitro RNA synthesis with SP6 RNA polymerase. *Methods Enzymol.* 155, 397–415.
- Krotoski, D. M., Fraser, S. E., Bronner-Fraser, M., 1988. Mapping of neural crest pathways in *Xenopus laevis* using inter- and intra-specific cell markers. *Dev Biol.* 127, 119–32.
- Kuriyama, S., Mayor, R., 2008. Molecular analysis of neural crest migration. *Philos Trans R Soc Lond B Biol Sci.* 363, 1349–62.
- Kuroda, H., Wessely, O., De Robertis, E. M., 2004. Neural induction in *Xenopus*: requirement for ectodermal and endomesodermal signals via Chordin, Noggin, beta-Catenin, and Cerberus. *PLoS Biol.* 2, E92.

- LaBonne, C., Bronner-Fraser, M., 1998. Neural crest induction in *Xenopus*: evidence for a two-signal model. *Development*. 125, 2403–14.
- LaBonne, C., Bronner-Fraser, M., 2000. Snail-related transcriptional repressors are required in *Xenopus* for both the induction of the neural crest and its subsequent migration. *Dev Biol*. 221, 195–205.
- Lamb, T. M., Knecht, A. K., Smith, W. C., et al., 1993. Neural induction by the secreted polypeptide noggin. *Science*. 262, 713–8.
- Laurent, M. N., Blitz, I. L., Hashimoto, C., Rothbacher, U., Cho, K. W., 1997. The *Xenopus* homeobox gene twin mediates Wnt induction of goosecoid in establishment of Spemann's organizer. *Development*. 124, 4905–16.
- Lemaire, P., Garrett, N., Gurdon, J. B., 1995. Expression cloning of Siamois, a *Xenopus* homeobox gene expressed in dorsal-vegetal cells of blastulae and able to induce a complete secondary axis. *Cell*. 81, 85–94.
- Leyns, L., Bouwmeester, T., Kim, S. H., Piccolo, S., De Robertis, E. M., 1997. Frzb-1 is a secreted antagonist of Wnt signaling expressed in the Spemann organizer. *Cell*. 88, 747–56.
- Li, B., Kuriyama, S., Moreno, M., Mayor, R., 2009. The posteriorizing gene Gbx2 is a direct target of Wnt signalling and the earliest factor in neural crest induction. *Development*. 136, 3267–78.
- Light, W., Vernon, A. E., Lasorella, A., Iavarone, A., LaBonne, C., 2005. *Xenopus* Id3 is required downstream of Myc for the formation of multipotent neural crest progenitor cells. *Development*. 132, 1831–41.
- Lim, J. W., Hummert, P., Mills, J. C., Kroll, K. L., 2011. Geminin cooperates with Polycomb to restrain multi-lineage commitment in the early embryo. *Development*, 138(1), 33–44.
- Linker, C., Bronner-Fraser, M., Mayor, R., 2000. Relationship between gene expression domains of Xsnail, Xslug, and Xtwist and cell movement in the prospective neural crest of *Xenopus*. *Dev Biol*. 224, 215–25.
- Lopez, S. L., Carrasco, A. E., 1992. Retinoic acid induces changes in the localization of homeobox proteins in the antero-posterior axis of *Xenopus laevis* embryos. *Mech Dev*. 36, 153–64.
- Luo, T., Matsuo-Takasaki, M., Thomas, M. L., Weeks, D. L., Sargent, T. D., 2002. Transcription factor AP-2 is an essential and direct regulator of epidermal development in *Xenopus*. *Dev Biol*. 245, 136–44.
- Luo, T., Lee, Y. H., Saint-Jeannet, J. P., Sargent, T. D., 2003. Induction of neural crest in *Xenopus* by transcription factor AP2alpha. *Proc Natl Acad Sci U S A*. 100, 532–7.
- Ma, Q., Kintner, C., Anderson, D. J., 1996. Identification of neurogenin, a vertebrate neuronal determination gene. *Cell*, 87(1), 43–52.
- Mancilla, A., Mayor, R., 1996. Neural crest formation in *Xenopus laevis*: mechanisms of Xslug induction. *Dev Biol*. 177, 580–9.
- Marchant, L., Linker, C., Ruiz, P., Guerrero, N., Mayor, R., 1998. The inductive properties of mesoderm suggest that the neural crest cells are specified by a BMP gradient. *Dev Biol*. 198, 319–29.
- Mayor, R., Morgan, R., Sargent, M. G., 1995. Induction of the prospective neural crest of *Xenopus*. *Development*. 121, 767–77.
- Mayor, R., Guerrero, N., Martinez, C., 1997. Role of FGF and noggin in neural crest induction. *Dev Biol*. 189, 1–12.
- Milet, C., Monsoro-Burq, A. H., 2012. Neural crest induction at the neural plate border in vertebrates. *Dev Biol*. 366, 22–33.
- Mizuseki, K., Kishi, M., Matsui, M., Nakanishi, S., Sasai, Y., 1998a. *Xenopus* Zic-related-1 and Sox-2, two factors induced by chordin, have distinct activities in the initiation of neural induction. *Development*. 125, 579–87.
- Mizuseki, K., Kishi, M., Shiota, K., Nakanishi, S., Sasai, Y., 1998b. SoxD: an essential mediator of induction of anterior neural tissues in *Xenopus* embryos. *Neuron*. 21, 77–85.
- Monsoro-Burq, A. H., Fletcher, R. B., Harland, R. M., 2003. Neural crest induction by paraxial mesoderm in *Xenopus* embryos requires FGF signals. *Development*. 130, 3111–24.
- Monsoro-Burq, A. H., Wang, E., Harland, R., 2005. Msx1 and Pax3 cooperate to mediate FGF8 and WNT signals during *Xenopus* neural crest induction. *Dev Cell*. 8, 167–78.
- Moody, S. A., 1987a. Fates of the blastomeres of the 16-cell stage *Xenopus* embryo. *Dev Biol*. 119, 560–78.
- Moody, S. A., 1987b. Fates of the blastomeres of the 32-cell-stage *Xenopus* embryo. *Dev Biol*. 122, 300–19.
- Moury, J. D., Jacobson, A. G., 1990. The origins of neural crest cells in the axolotl. *Dev Biol*. 141, 243–53.
- Munoz, W. A., Kloc, M., Cho, K., et al., 2012. Plakophilin-3 is required for late embryonic amphibian development, exhibiting roles in ectodermal and neural tissues. *PLoS One*. 7, e34342.
- Nagatomo, K., Hashimoto, C., 2007. *Xenopus* hairy2 functions in neural crest formation by maintaining cells in a mitotic and undifferentiated state. *Dev Dyn*. 236, 1475–83.
- Nakata, K., Nagai, T., Aruga, J., Mikoshiba, K., 1997. *Xenopus* Zic3, a primary regulator both in neural and neural crest development. *Proc Natl Acad Sci U S A*. 94, 11980–5.
- Neilson, K. M., Klein, S. L., Mhaske, P., Mood, K., Daar, I. O., Moody, S. A., 2012. Specific domains of FoxD4/5 activate and repress neural transcription

- factor genes to control the progression of immature neural ectoderm to differentiating neural plate. *Dev Biol.* 365, 363–75.
- Nichane, M., Ren, X., Bellefroid, E. J., 2009. Self-regulation of Stat3 activity coordinates cell-cycle progression and neural crest specification. *EMBO J.* 29, 55–67.
- Nie, X., Luukko, K., Kettunen, P., 2006. BMP signaling in craniofacial development. *Int J Dev Biol.* 50, 511–21.
- Niehrs, C., 2006. Function and biological roles of the Dickkopf family of Wnt modulators. *Oncogene.* 25, 7469–81.
- Niehrs, C., Keller, R., Cho, K. W., De Robertis, E. M., 1993. The homeobox gene gooseoid controls cell migration in *Xenopus* embryos. *Cell.* 72, 491–503.
- Nieto, M. A., Sargent, M. G., Wilkinson, D. G., Cooke, J., 1994. Control of cell behavior during vertebrate development by Slug, a zinc finger gene. *Science.* 264, 835–9.
- Nieuwkoop, P. D., 1973. The organization center of the amphibian embryo: its origin, spatial organization, and morphogenetic action. *Adv Morphog.* 10, 1–39.
- Ochoa, S. D., Salvador, S., LaBonne, C., 2011. The LIM adaptor protein LMO4 is an essential regulator of neural crest development. *Dev Biol.* 361, 313–25.
- Ossipova, O., Sokol, S. Y., 2011. Neural crest specification by noncanonical Wnt signaling and PAR-1. *Development.* 138, 5441–50.
- Palma, V., Kukuljan, M., Mayor, R., 2001. Calcium mediates dorsoventral patterning of mesoderm in *Xenopus*. *Curr Biol.* 11, 1606–10.
- Pannese, M., Polo, C., Andreazzoli, M., et al., 1995. The *Xenopus* homologue of Otx2 is a maternal homeobox gene that demarcates and specifies anterior body regions. *Development.* 121, 707–20.
- Park, J. I., Ji, H., Jun, S., et al., 2006. Frodo links Dishevelled to the p120-catenin/Kaiso pathway: distinct catenin subfamilies promote Wnt signals. *Dev Cell.* 11, 683–95.
- Patel, N. H., 1994. Developmental evolution: insights from studies of insect segmentation. *Science.* 266, 581–90.
- Pera, E. M., Ikeda, A., Eivers, E., De Robertis, E. M., 2003. Integration of IGF, FGF, and anti-BMP signals via Smad1 phosphorylation in neural induction. *Genes Dev.* 17, 3023–8.
- Piccolo, S., Sasai, Y., Lu, B., De Robertis, E. M., 1996. Dorsoventral patterning in *Xenopus*: inhibition of ventral signals by direct binding of chordin to BMP-4. *Cell.* 86, 589–98.
- Piccolo, S., Agius, E., Leyns, L., et al., 1999. The head inducer Cerberus is a multifunctional antagonist of Nodal, BMP and Wnt signals. *Nature.* 397, 707–10.
- Pieper, M., Eagleson, G. W., Wosniok, W., Schlosser, G., 2011. Origin and segregation of cranial placodes in *Xenopus laevis*. *Dev Biol.* 360, 257–75.
- Pieper, M., Ahrens, K., Rink, E., Peter, A., Schlosser, G., 2012. Differential distribution of competence for panplacodal and neural crest induction to non-neural and neural ectoderm. *Development.* 139, 1175–87.
- Pownall, M. E., Tucker, A. S., Slack, J. M., Isaacs, H. V., 1996. eFGF, Xcad3 and Hox genes form a molecular pathway that establishes the antero-posterior axis in *Xenopus*. *Development.* 122, 3881–92.
- Richard-Parpaillon, L., Heligon, C., Chesnel, F., Boujard, D., Philpott, A., 2002. The IGF pathway regulates head formation by inhibiting Wnt signaling in *Xenopus*. *Dev Biol.* 244, 407–17.
- Richter, K., Grunz, H., Dawid, I. B., 1988. Gene expression in the embryonic nervous system of *Xenopus laevis*. *Proc Natl Acad Sci U S A.* 85, 8086–90.
- Richter, K., Good, P. J., Dawid, I. B., 1990. A developmentally regulated, nervous system-specific gene in *Xenopus* encodes a putative RNA-binding protein. *New Biol.* 2, 556–65.
- Roelink, H., Augsburger, A., Heemskerk, J., et al., 1994. Floor plate and motor neuron induction by vhh-1, a vertebrate homolog of hedgehog expressed by the notochord. *Cell.* 76, 761–75.
- Rogers, C. D., Moody, S. A., Casey, E. S., 2009. Neural induction and factors that stabilize a neural fate. *Birth Defects Res C Embryo Today.* 87(3), 249–62.
- Rogers, C. D., Ferzli, G. S., Casey, E. S., 2011. The response of early neural genes to FGF signaling or inhibition of BMP indicate the absence of a conserved neural induction module. *BMC Dev Biol.* 11, 74.
- Sadaghiani, B., Thiebaud, C. H., 1987. Neural crest development in the *Xenopus laevis* embryo, studied by interspecific transplantation and scanning electron microscopy. *Dev Biol.* 124, 91–110.
- Saint-Jeannet, J. P., He, X., Varmus, H. E., Dawid, I. B., 1997. Regulation of dorsal fate in the neuraxis by Wnt-1 and Wnt-3a. *Proc Natl Acad Sci U S A.* 94, 13713–8.
- Sanes, D. H., Reh, T. A., Harris, W. A., 2012. Development of the nervous system. Academic Press, Burlington, MA.
- Sasai, Y., Lu, B., Steinbeisser, H., De Robertis, E. M., 1995. Regulation of neural induction by the Chd and Bmp-4 antagonistic patterning signals in *Xenopus*. *Nature.* 376, 333–6.
- Sasai, N., Mizuseki, K., Sasai, Y., 2001. Requirement of FoxD3-class signaling for neural crest determination in *Xenopus*. *Development.* 128, 2525–36.

- Sater, A. K., Steinhardt, R. A., Keller, R., 1993. Induction of neuronal differentiation by planar signals in *Xenopus* embryos. *Dev Dyn.* 197, 268–80.
- Sater, A. K., El-Hodiri, H. M., Goswami, M., et al., 2003. Evidence for antagonism of BMP-4 signals by MAP kinase during *Xenopus* axis determination and neural specification. *Differentiation.* 71, 434–44.
- Sato, T., Sasai, N., Sasai, Y., 2005. Neural crest determination by co-activation of Pax3 and Zic1 genes in *Xenopus* ectoderm. *Development.* 132, 2355–63.
- Sauka-Spengler, T., Bronner-Fraser, M., 2008. A gene regulatory network orchestrates neural crest formation. *Nat Rev Mol Cell Biol.* 9, 557–68.
- Seo, S., Kroll, K. L., 2006. Geminin's double life: chromatin connections that regulate transcription at the transition from proliferation to differentiation. *Cell Cycle.* 5(4), 374–9.
- Seo, S., Herr, A., Lim, J. W., Richardson, G. A., Richardson, H., Kroll, K. L., 2005. Geminin regulates neuronal differentiation by antagonizing Brg1 activity. *Genes Dev.* 19(14), 1723–34.
- Seo, S., Lim, J. W., Yellajoshiyula, D., Chang, L. W., Kroll, K. L., 2007. Neurogenin and NeuroD direct transcriptional targets and their regulatory enhancers. *EMBO J.* 26(24), 5093–108.
- Sharpe, C. R., Gurdon, J. B., 1990. The induction of anterior and posterior neural genes in *Xenopus laevis*. *Development.* 109, 765–74.
- Sive, H. L., Grainger, R. M., Harland, R. M., 2000. Early development of *Xenopus laevis* – a laboratory manual. Cold Spring Harbor Laboratory Press, Cold Spring Harbor, NY.
- Slack, J. M., Tannahill, D., 1992. Mechanism of anteroposterior axis specification in vertebrates. Lessons from the amphibians. *Development.* 114, 285–302.
- Smith, J. C., Slack, J. M., 1983. Dorsalization and neural induction: properties of the organizer in *Xenopus laevis*. *J Embryol Exp Morphol.* 78, 299–317.
- Smith, W. C., Harland, R. M., 1991. Injected Xwnt-8 RNA acts early in *Xenopus* embryos to promote formation of a vegetal dorsalizing center. *Cell.* 67, 753–65.
- Smith, A., Robinson, V., Patel, K., Wilkinson, D. G., 1997. The EphA4 and EphB1 receptor tyrosine kinases and ephrin-B2 ligand regulate targeted migration of branchial neural crest cells. *Curr Biol.* 7, 561–70.
- Sokol, S., Christian, J. L., Moon, R. T., Melton, D. A., 1991. Injected Wnt RNA induces a complete body axis in *Xenopus* embryos. *Cell.* 67, 741–52.
- Song, J., Slack, J. M., 1996. XFGF-9: a new fibroblast growth factor from *Xenopus* embryos. *Dev Dyn.* 206, 427–36.
- Spemann, H., Mangold, H., 1924. Induction of embryonic primordia by implantation of organizers from a different species. *Roux's Arch Entw Mech.* 100, 599–638.
- Steventon, B., Araya, C., Linker, C., Kuriyama, S., Mayor, R., 2009. Differential requirements of BMP and Wnt signalling during gastrulation and neurulation define two steps in neural crest induction. *Development.* 136, 771–9.
- Stuhlmiller, T. J., Garcia-Castro, M. I., 2012. Current perspectives of the signaling pathways directing neural crest induction. *Cell Mol Life Sci.* 69, 3715–37.
- Sun, B. I., Bush, S. M., Collins-Racie, L. A., et al., 1999. derriere: a TGF-beta family member required for posterior development in *Xenopus*. *Development.* 126, 1467–82.
- Suzuki, A., Kaneko, E., Ueno, N., Hemmati-Brivanlou, A., 1997. Regulation of epidermal induction by BMP2 and BMP7 signaling. *Dev Biol.* 189, 112–22.
- Tamagnone, L., Comoglio, P. M., 2004. To move or not to move? Semaphorin signalling in cell migration. *EMBO Rep.* 5, 356–61.
- Tamai, K., Semenov, M., Kato, Y., et al., 2000. LDL-receptor-related proteins in Wnt signal transduction. *Nature.* 407, 530–5.
- Tan, C., Deardorff, M. A., Saint-Jeannet, J. P., Yang, J., Arzoumanian, A., Klein, P. S., 2001. Kermit, a frizzled interacting protein, regulates frizzled 3 signaling in neural crest development. *Development.* 128, 3665–74.
- Tanibe, M., Michiue, T., Yukita, A., et al., 2008. Retinoic acid metabolizing factor xCyp26c is specifically expressed in neuroectoderm and regulates anterior neural patterning in *Xenopus laevis*. *Int J Dev Biol.* 52, 893–901.
- Tannahill, D., Isaacs, H. V., Close, M. J., Peters, G., Slack, J. M., 1992. Developmental expression of the *Xenopus* int-2 (FGF-3) gene: activation by mesodermal and neural induction. *Development.* 115, 695–702.
- Tao, Q., Yokota, C., Puck, H., et al., 2005. Maternal wnt11 activates the canonical wnt signaling pathway required for axis formation in *Xenopus* embryos. *Cell.* 120, 857–71.
- Theveneau, E., Mayor, R., 2012. Neural crest delamination and migration: from epithelium-to-mesenchyme transition to collective cell migration. *Dev Biol.* 366, 34–54.
- Theveneau, E., Marchant, L., Kuriyama, S., et al., 2010. Collective chemotaxis requires contact-dependent cell polarity. *Dev Cell.* 19, 39–53.
- Thomas, L. A., Yamada, K. M., 1992. Contact stimulation of cell migration. *J Cell Sci.* 103, 1211–4.
- Thomsen, G. H., Melton, D. A., 1993. Processed Vg1 protein is an axial mesoderm inducer in *Xenopus*. *Cell.* 74, 433–41.
- Tran, H. T., Delvaeye, M., Verschuere, V., et al., 2011. ARVCF depletion cooperates with Tbx1

- deficiency in the development of 22q11.2DS-like phenotypes in *Xenopus*. *Dev Dyn.* 240, 2680–7.
- Tribulo, C., Aybar, M. J., Nguyen, V. H., Mullins, M. C., Mayor, R., 2003. Regulation of *Msx* genes by a Bmp gradient is essential for neural crest specification. *Development.* 130, 6441–52.
- Uzgare, A. R., Uzman, J. A., El-Hodiri, H. M., Sater, A. K., 1998. Mitogen-activated protein kinase and neural specification in *Xenopus*. *Proc Natl Acad Sci U S A.* 95, 14833–8.
- Uzman, J. A., Patil, S., Uzgare, A. R., Sater, A. K., 1998. The role of intracellular alkalization in the establishment of anterior neural fate in *Xenopus*. *Dev Biol.* 193(1), 10–20.
- Vallin, J., Girault, J. M., Thiery, J. P., Broders, F., 1998. *Xenopus* cadherin-11 is expressed in different populations of migrating neural crest cells. *Mech Dev.* 75, 171–4.
- Vallin, J., Thuret, R., Giacomello, E., Faraldo, M. M., Thiery, J. P., Broders, F., 2001. Cloning and characterization of three *Xenopus* slug promoters reveal direct regulation by Lef/beta-catenin signaling. *J Biol Chem.* 276, 30350–8.
- Vernon, A. E., Movassagh, M., Horan, I., Wise, H., Ohnuma, S., Philpott, A., 2006. Notch targets the Cdk inhibitor *Xic1* to regulate differentiation but not the cell cycle in neurons. *EMBO Rep.* 7, 643–8.
- Villanueva, S., Glavic, A., Ruiz, P., Mayor, R., 2002. Posteriorization by FGF, Wnt, and retinoic acid is required for neural crest induction. *Dev Biol.* 241, 289–301.
- von Bubnoff, A., Schmidt, J. E., Kimelman, D., 1996. The *Xenopus laevis* homeobox gene *Xgbx-2* is an early marker of anteroposterior patterning in the ectoderm. *Mech Dev.* 54, 149–60.
- Wang, S., Krinks, M., Lin, K., Luyten, F. P., Moos, M., Jr., 1997. *Frzb*, a secreted protein expressed in the Spemann organizer, binds and inhibits Wnt-8. *Cell.* 88, 757–66.
- Weeks, D. L., Melton, D. A., 1987. A maternal mRNA localized to the vegetal hemisphere in *Xenopus* eggs codes for a growth factor related to TGF-beta. *Cell.* 51, 861–7.
- Wessely, O., Agius, E., Oelgeschlager, M., Pera, E. M., De Robertis, E. M., 2001. Neural induction in the absence of mesoderm: beta-catenin-dependent expression of secreted BMP antagonists at the blastula stage in *Xenopus*. *Dev Biol.* 234, 161–73.
- Wills, A. E., Choi, V. M., Bennett, M. J., Khokha, M. K., Harland, R. M., 2009. BMP antagonists and FGF signaling contribute to different domains of the neural plate in *Xenopus*. *Dev Biol.* 337, 335–50.
- Wilson, P. A., Hemmati-Brivanlou, A., 1995. Induction of epidermis and inhibition of neural fate by Bmp-4. *Nature.* 376, 331–3.
- Wodarz, A., Nusse, R., 1998. Mechanisms of Wnt signaling in development. *Annu Rev Cell Dev Biol.* 14, 59–88.
- World Health Organization. Dept. of Mental Health and Substance Abuse., 2006. Neurological disorders: public health challenges. World Health Organization, Geneva.
- Wu, J., Yang, J., Klein, P. S., 2005. Neural crest induction by the canonical Wnt pathway can be dissociated from anterior-posterior neural patterning in *Xenopus*. *Dev Biol.* 279, 220–32.
- Wu, M. Y., Ramel, M. C., Howell, M., Hill, C. S., 2011. SNW1 is a critical regulator of spatial BMP activity, neural plate border formation, and neural crest specification in vertebrate embryos. *PLoS Biol.* 9, e1000593.
- Xu, S., Cheng, F., Liang, J., Wu, W., Zhang, J., 2012. Maternal *xNorrin*, a canonical Wnt signaling agonist and TGF-beta antagonist, controls early neuroectoderm specification in *Xenopus*. *PLoS Biol.* 10, e1001286.
- Yan, B., Neilson, K. M., Moody, S. A., 2009. *foxD5* plays a critical upstream role in regulating neural ectodermal fate and the onset of neural differentiation. *Dev Biol.* 329, 80–95.
- Yellajoshiyula, D., Patterson, E. S., Elitt, M. S., Kroll, K. L., 2011. Geminin promotes neural fate acquisition of embryonic stem cells by maintaining chromatin in an accessible and hyperacetylated state. *Proc Natl Acad Sci U S A.* 108, 3294–9.
- Zhang, J., King, M. L., 1996. *Xenopus* VegT RNA is localized to the vegetal cortex during oogenesis and encodes a novel T-box transcription factor involved in mesodermal patterning. *Development.* 122, 4119–29.
- Zhang, J., Houston, D. W., King, M. L., Payne, C., Wylie, C., Heasman, J., 1998. The role of maternal VegT in establishing the primary germ layers in *Xenopus* embryos. *Cell.* 94, 515–24.
- Zhang, X., Abreu, J. G., Yokota, C., et al., 2012. Tiki1 is required for head formation via Wnt cleavage-oxidation and inactivation. *Cell.* 149, 1565–77.
- Zimmerman, L. B., De Jesus-Escobar, J. M., Harland, R. M., 1996. The Spemann organizer signal noggin binds and inactivates bone morphogenetic protein 4. *Cell.* 86, 599–606.

14

The Development of the Immune System in *Xenopus*

Louis Du Pasquier

Zoology and Evolutionary Biology, University of Basel, Basel, Switzerland

Abstract: The immune system of *Xenopus* shows numerous variations on the theme of development when compared to mammals. These variations, that are as many natural experiments, help understanding what is essential and what is accessory for the development of an immune system. These are early hatching, absence of materno-fetal interaction, cellular simplicity at the onset of immune competence, simplicity of the lymphoid organs, and existence of a metamorphosis. To exploit these peculiarities *Xenopus* strains, clones, and species have been used in various sets of experiments at the molecular, biochemical, cellular, surgical, organismic, and immunogenetic levels, which contributed to better understand thymus education, somatic diversification of B cells, and the interplay between innate and adaptive arms of the immune system of vertebrates.

Introduction

Most of the elements of the *Xenopus* immune system have been analyzed in detail during the past five decades (Du Pasquier et al. 1989; Robert and Ohta 2009). Whether belonging to the innate or adaptive immunity arms, they are, with rare exceptions, homologous and very similar to those of warm-blooded vertebrates, in particular mammals. The *Xenopus* immune system is more mammalian-like than that of fish or even that of birds. All the elements and often their organization at the gene and protein levels show remarkable conservation with minor quantitative differ-

ences in gene numbers and organ complexity. This applies to innate immunity components such as complement, lectins, Toll-like receptors (TLRs), and their signaling cascades. It also applies to the adaptive immune system components such as the lymphomyeloid cell types, major histocompatibility complex (MHC), immunoglobulins, T cell receptors (TCR) and B cell receptors (BCR), and their way to somatically create antigen-specific repertoires. Yet, when compared to mammals, the expression of these elements during ontogeny is peppered with variations. These variations are therefore like natural informative experiments on the human immune system. So, it is

no wonder that *Xenopus* has reached the status of a model system for immunologists (Robert and Cohen 2011).

Among those variations, one can cite the following:

- *Xenopus* hatches 2 days after fertilization with an incomplete immune system.
- No materno-fetal interactions take place between larvae and mother.
- Unlike in mammals, the immune system of *Xenopus* develops early, under pressure to produce quickly a heterogeneous repertoire of immunoreceptors before lymphocyte numbers reach 5000, thereby imposing a limitation on repertoire size not seen in mammals.
- With the existence of a metamorphosis, the immune system is submitted to a new evaluation of self.
- In a more general definition of the word **development**, one could consider the existence of the many polyploid species of *Xenopus* as a model to study some aspects of the phylogenetic development of an immune system linked to whole-genome duplication, but this is beyond the scope of this chapter (Kobel and Du Pasquier 1986; Evans 2008).

The aforementioned features would be enough to make *Xenopus* an interesting model, but in addition, several aspects of *Xenopus* development and body plan make this genus a better model than mammals for the study of the early development of the adaptive immune system. They can be summarized as follows:

- *Xenopus* is easy to breed in the lab by injection of gonadotrophin hormones. Large progenies can be obtained (hundreds of sibs).
- The thymus is visible through the skin of the tadpole; therefore, thymectomy is easy to perform very early.
- The immune responses vary depending on the temperature, which provides a tool to modulate experimentally the responses.
- Grafting of hematopoietic precursors can be performed very early in development.
- Chimera construction is much easier than in warm-blooded vertebrates.

- *Xenopus* lives long (20–40 years) which allows long-term experiments.
- Tumor cell lines are available.
- Cellular markers such the *borealis* chromatin marker (Thiébaud 1983), the 1 nucleolus mutant (Elsdale et al. 1958), and ploidy gene mapping techniques allow sophisticated cell lineage tracking experiments (Chrétien et al. 1997).
- Partially inbred strains and several MHC-type clones of isogenic interspecies hybrids (Kobel and Du Pasquier 1975) as well as some transgenic strains are available (Chesneau et al. 2008 and http://www.unidue.de/home/fb/ifz/forschung/ae/de_Transgenic_Xenopus_strains.shtml).
- The genome of the Western clawed frog *Xenopus tropicalis* is accessible (Hellsten et al. 2010) and that of *Xenopus laevis* is under way (http://polaris.icmb.utexas.edu/index.php/Xenopus_Genome_Project).
- Expressed sequence tag (EST) libraries from various species exist, and several monoclonal antibodies recognizing surface receptors, immunoglobulins, and other immunity-relevant epitopes are available.

In this chapter, we shall summarize the knowledge concerning the development of the immune system with its innate and adaptive arms. First, we survey the differentiation of the immune system during *Xenopus* ontogeny, then describe its responses, and finally focus on immunological aspects of metamorphosis.

The establishment of innate immunity components during *Xenopus* ontogeny

Of all known innate immunity mediators, only a few seem to be expressed in tadpoles. TLR5 expression has been detected at tail bud stages (Pollet 2010) and perhaps plays a role in protection from pathogens. For other TLRs, a tissue distribution analysis suggests that all TLR mRNAs are ubiquitously expressed in all tissues of the adult frog and tadpole (no exact tadpole stage(s) was (were) given in this study). The results were obtained with 40 cycles of polymerase chain reaction (PCR) (Ishii et al. 2007) (Figure 14.1).

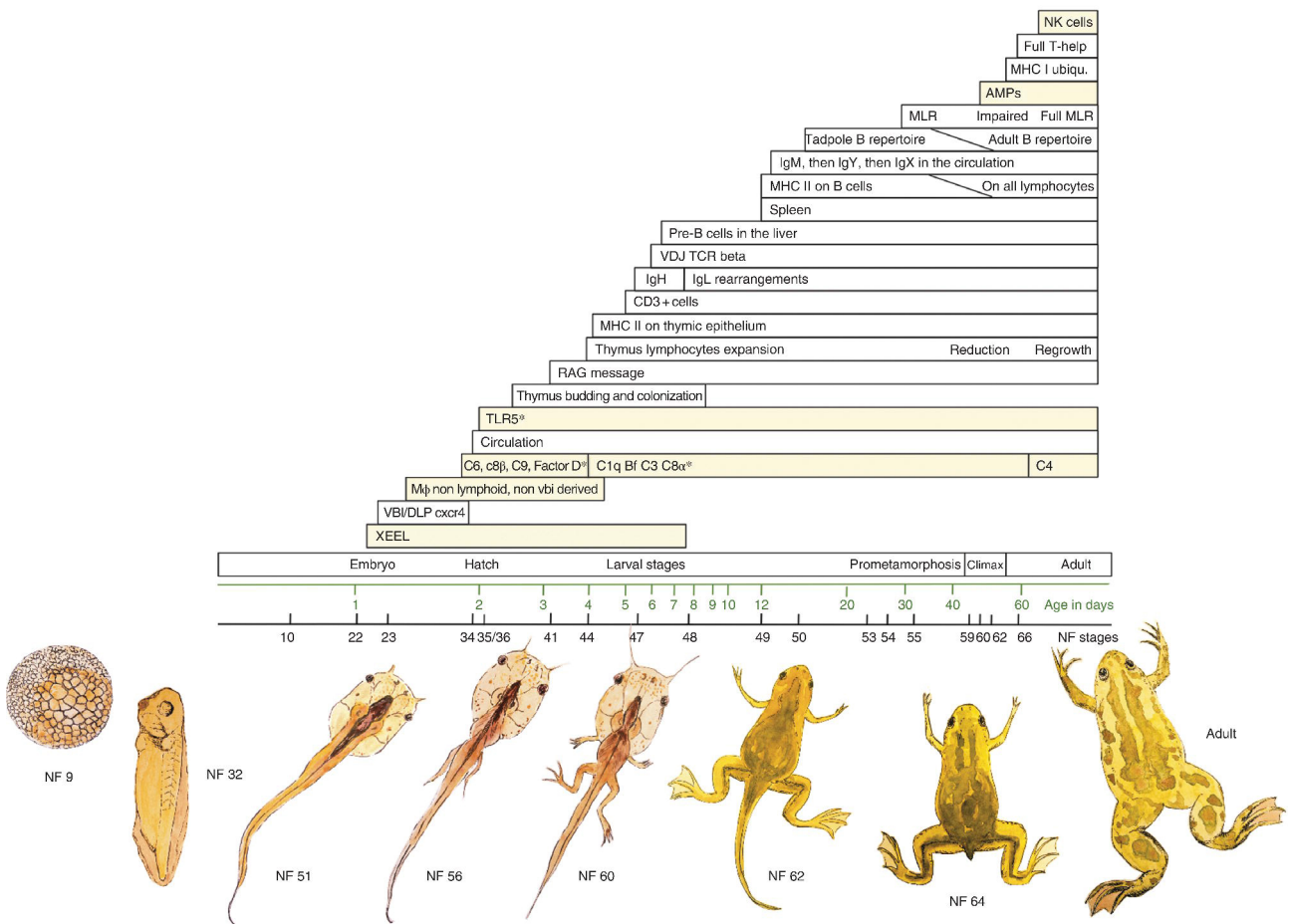


Figure 14.1 Sequential appearance of innate and adaptive immune system components during the ontogeny of *Xenopus*. Time scale has been represented on log scale to separate visually better the early events. AMP, antimicrobial peptides; C6, C8a C8β, factor D, C1q, Bf, C3, C4, components of the complement system; DLP, dorsolateral plate mesoderm; IgH, immunoglobulin heavy chain; IgL, immunoglobulin light chain; Mφ macrophage; MHC, major histocompatibility complex; MLR, mixed leukocyte reaction; NF, Nieuwkoop and Faber stages (1967); NK, natural killer; RAG, recombination activating gene; TCR, T cell receptor; TLR, toll-like receptor; VBI, ventral blood island; VDJ, variable, joining, and diversity segments of a functional variable region gene of immunoglobulin or T cell receptor; XEEL, *Xenopus laevis* embryonic epidermal lectin; In beige, components of the innate system; *, not necessarily involved in immunity. To see a color version of this figure, see Plate 34.

Among other early expressed innate immunity effectors, the *X. laevis* embryonic epidermal lectin, a calcium-dependent saccharide-binding lectin, increases from neurula/tail bud stages through hatching and then declines 1 week after fertilization. It may offer protection to the young larvae (Nagata 2005). One of *X. tropicalis* carbohydrate-recognizing receptors consists of a long type of peptidoglycan-recognizing protein (PGRP-L) similar to the *Drosophila* PGRP-Lb and is expressed from 72h after fertilization. Given that after LPS stimulation in adults the production of this molecule was upregulated significantly in the liver, intestine, and spleen, it has been proposed that it participates in immunity (Qi et al. 2011).

However, many immunity effectors do not show up before much later, i.e., around metamorphosis, including most antimicrobial peptides (Pollet 2010). Logically, their expression seems to be linked to the appearance in the adult skin at metamorphosis of the glands that secrete them. A poorly developed innate immunity might also be responsible for the susceptibility of tadpoles to certain viral infections. Larval susceptibility had been conventionally attributed to ineffective adaptive immunity, but in fact, the problem may be due to the innate compartment of the immune system (De Jesús Andino et al. 2012). In comparison to adults, when infected with frog virus 3, the leukocytes and tissues of tadpoles reacted 3 days later than adults and expressed 10–100 times less inflammation-associated TNF- α , IL-1 β and IFN- γ and antiviral *Mx1* genes.

The complement is another set of components well conserved in *Xenopus* and playing a role in innate immunity. Complement components that could contribute to the membrane attack complex (MAC) are expressed during gastrula/early neurula stages in *X. laevis* (McLin et al. 2008) that suggests an early role in eliminating bacteria. Interestingly, the comparison between *X. tropicalis* and *X. laevis* shows that in *X. tropicalis*, members of this complex are induced earlier and stronger than in *X. laevis* (i.e., maximum expression at stage 16 instead of 33). Further, the homologues of the MAC regulators protectin (CD59) and CPN1 also show the same divergence between the two species. Thus, the coordinated earlier

induction of multiple MAC genes in *X. tropicalis* might have been selected in response to microbial conditions specific to *X. tropicalis*, relative to *X. laevis* or perhaps also because *X. tropicalis* develops on the average at higher temperatures than *X. laevis* (Yanai et al. 2011).

On the other hand, some studies suggest that the complement molecules traditionally attributed to the innate immune system can actually serve more than one system and be used in developmental pathways (McLin et al. 2008). For instance, several complement component genes are expressed in an organ-specific manner during early organogenesis with a pattern of expression not typical of molecules involved in immunity or in immunity only. Properdin, C1qA, C3, and C9 are strongly expressed in the neural plate for instance. C1qR and C6 localize in the neural crest area, whereas C3aR and C1qA are predominantly expressed in the mesoderm. The early expressed C3a functions as chemo-attractant, in particular during the migration of neural crest cells (Carmona-Fontaine et al. 2011). Similarly, Ami, another homologue of the complement factor D (that cleaves factor B), is expressed from neurula onwards and could be involved in immunity via the alternative complement pathway, but it might be also involved in the triglyceride metabolism in fat cells (Inui and Asashima 2006). Finally, C4b is expressed later at tail bud stage in the pronephros together with C1qA and C3b (McLin et al. 2008).

Natural killer (NK) cells, effector cells of innate immunity, are not detected in tadpoles. They will be reviewed in the MHC section (Horton et al. 2003) since these cells monitor MHC expression on cells infected by viruses.

The establishment of the adaptive immune system components

Lymphomyeloid cell precursors

The adaptive immune system is centered on the usage of lymphoid (T and B cells) and of myeloid lineages (antigen-presenting cells and macrophages, granulocytes, and neutrophils), both lineages being produced in the hematopoietic organs. An atlas of *Xenopus*

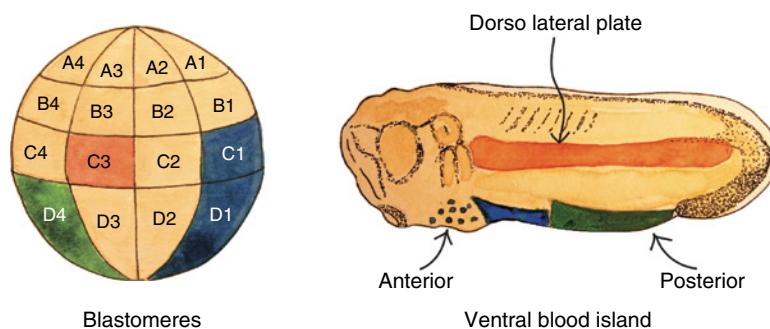


Figure 14.2 The mesoderm regions contributing to hematopoiesis in *Xenopus*. Reassembled and redrawn from Ciau-Uitz et al. (2010). To see a color version of this figure, see Plate 35.

hematology is helpful to recognize the morphology of the cells belonging to these different lineages (Hadj-Azimi et al. 1987). In *Xenopus* embryos, it is the lateral plate mesoderm that contributes to hematopoiesis (Figure 14.2). Its dorsal section, called dorsal lateral plate (DLP), and its more ventral one, called ventral blood island (VBI), give rise to erythrocytes, thymocytes, and B and T lymphocytes (Kau and Turpen 1983; Maéno et al. 1985). In very young larvae of *X. laevis*, the VBI is the main source of hematopoietic stem cells. In late larvae and adults, the contribution of VBI to hematopoiesis is minimal and DLP-derived cells are predominant (Maéno et al. 1985). At the gastrula stage, it is a high level of the bone morphogenic protein (BMP4) activity that specifies the VBI determination. BMP plays a major role by inducing numerous other genes involved in hematopoiesis such as GATA-1 and GATA-2, SCL, LMO, and the Wnt signaling molecules Xwnt 8. The expression of a dominant-negative BMP type 1 receptor inhibits the two forms of hematopoiesis (VBI and DLP dependent) proving the importance of the BMP4 signaling in both pathways (reviewed in Sadlon et al. 2004).

The myeloid lineage is generated early from the anterior part of the VBI. It is the earliest expressed lineage of hematopoietic cells. Distinct mechanisms are involved in the myeloid cell differentiation in the anterior and posterior VBI (Figure 14.2). The regulation of the Wnt signaling pathway is essential for the differentiation of myeloid cells in the anterior VBI but not for the differentiation of myeloid cells in the posterior VBI. Signaling through the vascular endothelial growth factor is

necessary for the differentiation of myeloid cells in the posterior but not those in the anterior VBI (Maéno et al. 2012).

The early **myelocytes** express Spib, an ETS transcription factor involved in the differentiation and migration of myeloid cells (Costa et al. 2008). They express also two other molecular markers that typify early myelocytes, a peroxidase family member (XPOX2) and Ly-6/uPAR-related protein (XLURP-1) (Smith et al. 2002; Tashiro et al. 2006). Based on morphology, other macrophage-like cells that stain for a *Xenopus* common leukocyte marker, XL-1, and that may not originate from the VBI (Ohinata et al. 1989; Ohinata et al. 1990) can be found in several locations of the mesenchyme in the stage 32 embryos, before the establishment of vascularization at stage 33/34 and long before the emergence of lymphocytes. Another panleukocyte marker, XL-2, is expressed even earlier at tail bud stage 24 on cells with amoeboid morphology and therefore looking like macrophages (Miyanaga et al. 1998).

The myeloid lineage participates early in function that may play a role in immune responses. They are the first active cells of the immune system (Smith et al. 2002; Costa et al. 2008). By migrating to wounds or local bacteria intrusions, they participate in immunity before the establishment of a vasculature (stage 35; Levine et al. 2003). But they may also contribute to morphogenesis early in development and at metamorphosis when they remove remnants of apoptotic cells (Ishizuya-Oka 1996). Myeloid cells that give rise to macrophages and antigen-presenting cells are important elements of the innate and

adaptive system. They have not been studied in detail with respect to the antigen presentation machinery in *Xenopus*. Larval peritoneal macrophages are morphologically distinct compared to adult; they do not express MHC classic class I molecules and respond differently to bacterial stimulation. In contrast to adults, they express CD91, the endocytic receptor for α 2-macroglobulin that mediates the internalization of certain heat shock proteins (Marr et al. 2005). Langerhans-like cells, i.e., epidermal dendritic cells of the myeloid lineage, have been noticed in early and late larval stages in the wound epithelia of regenerating hind limbs at both larval and adult stages (Mescher et al. 2007). In adults, they are conspicuous in the skin where they form a relatively tight network (Du Pasquier and Flajnik 1990).

The myeloid lineage cells can be encountered in the circulation, and they are present throughout the body (monocytes, peritoneal macrophages). They do not seem to require, in contrast to lymphoid cells, any specific organ for their maturation. In mammals, the bone marrow plays an important role in the segregation of the lymphoid and myeloid lineages (Kondo 2010), but *Xenopus* tadpoles do not have bone marrow and its equivalent is not known although the larval liver might be involved in the process.

The lymphoid organs and the lymphoid cells

In *X. laevis* larvae, the lymphocytes are found consistently in the thymus, the spleen, the ventral cavity bodies, the hematopoietic peripheral layer of the liver, and the intertubular tissue of pro- and mesonephros. A few small lymphoid aggregates are visible along the gut associated with the epithelium. However, the lymph glands found in other species are absent in *Xenopus* larvae (Manning and Horton 1969).

The thymus

The thymus (reviewed in Du Pasquier et al. 1989) arises through an invagination and a proliferation of the dorsal epithelium of the

second pharyngeal pouch around day 3 after fertilization (stage 40). Its development shows a number of differences when compared to other vertebrates. The expression of three transcription factors – *gcm2*, *hoxa3*, and *foxn1* – associated with pharyngeal gland development in vertebrates has been monitored, together with the neural crest contribution to thymus development. In most species, *Hoxa3* is expressed in the third pharyngeal pouch endoderm where it directs thymus formation. However, in *Xenopus*, the thymus primordium derives from the second pharyngeal pouch endoderm only, which is *hoxa3* negative, suggesting that a different mechanism regulates thymus formation in frogs. Similarly, *foxn1*, a transcription factor crucial for thymic development in mammals, is not detected in the epithelium of the pharyngeal pouch in *Xenopus*. Its expression is initiated when thymic epithelial cells start to differentiate and express MHC class II molecules (see MHC section). Finally, although there is a controversy regarding the role of neural crest in thymus differentiation, the *Xenopus* ablation/transplantation experiments seem to prove that the neural crest elements are not essential for the initial development of the thymus and T cell differentiation (Lee et al. 2013).

Detached from the branchial epithelium during stage 45, the thymus then takes a position between the eye and the ear. Free and large basophilic cells first appear migrating through the head mesenchyme from the VBI and DLP in the vicinity of the thymus at stage 43. These cells stain with the monoclonal antibody RC47 marker of early lymphoid lineage (<http://www.urmc.rochester.edu/mbi/resources/Xenopus/available-res.cfm>).

One day later, the thymic epithelium begins expressing class II molecules but not the classic MHC class Ia molecules (see MHC section; Du Pasquier and Flajnik 1990). By days 6–8, the cortex/medulla architecture becomes visible (Manning and Horton 1969). After entering the thymus, the basophilic cells proliferate, giving rise to a considerable number of lymphocytes at stage 48. By stage 51, the thymus is fully differentiated: the cortex contains mainly proliferating lymphocytes in the digitations of the epithelial cells. The medulla is made of epithelial cells with cytoplasmic granules

and rough endoplasmic reticulum. It contains macrophages from early stages onwards. Unlike in mammals, the cortex and medulla are separated by a distinct cellular barrier (Nagata 1977). Melanophores first appear at stage 48 mostly at interface of medulla and cortex. This area will be later rich in blood vessels and IgM-producing plasma cells (Flajnik et al. 1988). The thymus reaches its peak larval size (about $1-2 \times 10^6$ lymphocytes; Figure 14.6) at stage 58 (Sterba 1950; Du Pasquier and Weiss 1973; Rollins-Smith et al. 1984). It involutes losing up to 90% of its cells in the cortex during the metamorphic climax (Sterba 1952; Du Pasquier and Weiss 1973) during which more macrophages are seen in the shrinking cortex. At this time, the thymus is translocated towards the tympanum. A second histogenesis follows, with the appearance of myoepithelial cells, amine-containing cells, and larger cysts (Clothier and Balls 1985). After metamorphosis, a new type of macrophages, presumed by some authors to be an equivalent of nurse cells, appears. The thymus contains $1-3 \times 10^7$ cells about 2-3 months after metamorphosis. Then, it undergoes a regression at the time of sexual maturity, when it becomes more and more embedded in fatty tissue and its ratio of cortex/medulla decreases (Figure 14.6) (reviewed in Du Pasquier et al. 1989). This evolution of the thymus is under the control of endocrine factors such as glucocorticoids. Following a treatment of young tadpoles with dexamethasone (a cortisol receptor agonist) for 1 week, the thymus shrinks due to a loss of lymphocytes. The effect is reversible with the administration of the glucocorticoid receptor antagonist RU-486 (Schreiber 2011). The concentration of glucocorticoid receptors that are undetectable before metamorphosis increases during metamorphosis and declines in toadlets. The generation of a high number of receptors (that should confer enhanced glucocorticoid sensitivity particularly to the lymphoid compartment) could be responsible for the disappearance of a large lymphocyte population and for compromising T cell functions (Marx et al. 1987). *In vitro*, corticosteroids rather than triiodothyronine inhibit the PHA-induced proliferation of lymphocytes. Therefore, the loss of larval lymphocytes and

the changes of lymphocyte function at metamorphosis may be due to elevated concentrations of corticosteroids rather than to the direct action of thyroid hormones (TH) (Rollins-Smith and Blair 1993; Rollins-Smith et al. 1997).

The spleen

The spleen appears about 12-14 days after fertilization as a mesenchymal thickening in the mesogastrium. Both its red pulp and white pulp start to be distinguishable at stage 48. At stage 50, it has acquired its fundamental structure with delineated regions of red (hematopoietic) and white (lymphopoietic) pulp (reviewed in Manning and Horton 1982). The nodules of white pulp, with their central arteriola surrounded by lymphocytes, are lined by a boundary layer of cells. Scattered lymphocytes mainly of the T lineage are present in the perifollicular area. The larval spleen is minimally not at all hematopoietic and is therefore proportionally richer in B cells than that of an adult. During metamorphosis, the number of splenic lymphocytes reaches a plateau ($0.5-1 \times 10^6$) or may even decrease like in the thymus. Afterward, the organ grows steadily until it contains about 4×10^7 lymphocytes in 300g adults (Du Pasquier and Weiss 1973).

Using ploidy markers in histocompatible *Xenopus* strain combinations, it was found that the larval spleen contains stem cells for the adult hematopoietic erythroid and lymphoid lineages (details in succeeding text; Chrétien et al. 1997).

The ventral cavity bodies

In the anterior part of the tadpole body, the ventral and dorsal cavity bodies occupy the central part of the pharynx (Manning and Horton 1969; Tochinali 1975). It seems that they mainly consist of T cells because they are depleted of most of their lymphocytes after thymectomy (Manning 1971; Manning and Horton 1982). They disappear at metamorphosis.

The gut

Conspicuous lymphoid nodules are present in the adult but not the tadpole intestine. They

are rich in B cells. Numerous plasma cells producing IgM and IgX, but not IgY, are also visible in the mucosa (Mußmann et al. 1996). The gut T cell content has not been analyzed in detail. Gross examination of the isolated larval alimentary tract reveals no lymphoid accumulations. However, lymphocytes were seen in reasonable numbers (20% of recovered cells) by light and electron microscopy in the developing intestine of stage 48 tadpoles (Marshall and Dixon 1978). Histology reveals numerous lymphoid accumulations in close relationship with the epithelium of the gut from the pharyngoesophagus to the rectum (Tochinai 1975).

The liver

In the liver, lymphopoiesis is associated with the lymphomyeloid peripheral layer (Hadj-Azimi and Fischberg 1967), which persists throughout the life of *Xenopus*, but not in other anuran species where it disappears at metamorphosis. Pre-B cells can be detected in the liver by stage 48. It is possible that tadpole liver plays a role of fetal liver in mammals; such possibility is supported by the fact that similar to murine and human fetal liver, *Xenopus* tadpole liver expresses activation-induced cytidine deaminase (AID) (Kuraoka et al. 2009). Later, the subcapsular region of the liver can become an abundant source of antibody-forming cells, easily detectable by immunofluorescence (Mußmann et al. 1998).

Bone marrow

The bone marrow of *Xenopus* develops after metamorphosis. Little is known about its function. From studies with mitogens or from early cytological observations, it seems to be poorly lymphopoietic (Green and Cohen 1979). However, cells with blastoid morphology typical of lymphocyte precursors have been described, and recombination activating gene (RAG) is expressed. No consistent expression of another B cell-specific enzyme XI/AID, the homologue of mammalian AID (see succeeding text), is detected in the marrow of stimulated or unstimulated animals (Marr et al. 2007).

The kidneys

The DLP is so close to the pronephric tubules and duct that it is analogous to the mammalian aorta–gonad–mesonephros region that is a primary source of hematopoietic stem cells. In tadpoles, intertubular tissue is mainly granulocytopoietic with some erythropoiesis, whereas lymphopoiesis is minimal (Brändli 1999).

The adaptive immune system:
Expression of its essential receptors during ontogeny

MHC class I and class II modulation

Like in mammals, the MHC of *Xenopus* (Ohta et al. 2006) encodes class I (classic and non-classic) and class II molecules with different tissue distributions. Whereas classic class Ia is ubiquitously expressed in adults, class II shows some tissue specializations. These vary during ontogeny.

Class Ia

Originally, it was found that two different MHC-encoded antigens, recognized by alloantisera on peripheral blood cells, appear at different times during ontogeny. A lymphocyte antigen (later to be identified as class II) appears 15 days before the end of metamorphosis, and another antigen present on red cells and on lymphocytes (later identified as the polymorphic classic class Ia) appears 1.5 months after the end of metamorphosis (Du Pasquier et al. 1979). Thus, there is an unusual asynchrony in the expression of genes tightly linked in one MHC gene complex (Flajnik et al. 1986). Immunofluorescence on frozen sections from tadpoles and immunoprecipitation do not detect the classic class Ia molecule in tadpoles, but this molecule is present in all tissues at metamorphosis. Immunofluorescence detects an otherwise uncharacterized MHC-linked alloantigen (still undetermined biochemically) on tadpole thymic epithelium from the earliest stages of thymus differentiation.

The cellular changes associated with the modulation of MHC class Ia expression have been analyzed in the red cell population because of easy availability of cells and of reagents. Stage 55 larval and adult erythrocytes

have distinct volumes. This allows their separation by Percoll gradient centrifugation when they coexist in metamorphosing animals at the time of replacement of one cell type by another. With an alloantiserum produced against *Xenopus* MHC class Ia and other reagents, these different populations can be distinguished at metamorphosis. Tadpole cells have no MHC class Ia antigens on the cell surface. But both tadpole and adult erythrocytes express a **mature erythrocyte** marker, recognized by a specific monoclonal antibody (F1F6). During metamorphosis, immature erythrocytes (thus F1F6 negative), but already expressing adult levels of cell-surface MHC class Ia antigens, are found in the bloodstream by 12 days after tail resorption. These immature cells are biosynthetically active, produce adult hemoglobin, and mature gradually into fully F1F6-positive cells by 60 days after the completion of metamorphosis. All cells in the new erythrocyte series express adult levels of MHC antigens. Tadpole erythrocytes, which were biosynthetically active during larval stages, become metabolically inactive at the metamorphic climax. They are completely cleared from the circulation by 60 days after metamorphosis. The most abundant erythrocyte cell-surface proteins from tadpoles and adults, as judged by two-dimensional gel electrophoresis, are very different.

Erythrocytes from tadpoles arrested in their development by a metamorphosis blocker (sodium perchlorate) for long periods of time express intermediate levels of MHC class Ia antigens, suggesting a **leaky** expression of these molecules in the tadpole cells. This expression seems to be independent of other biochemical and morphological changes that occur at metamorphosis (Flajnik and Du Pasquier 1988; Flajnik et al. 1988).

The absence of class Ia on tadpole cell surfaces raises some questions about the NK cells whose function is to monitor class Ia expression. With a specific monoclonal antibody, NK cells are detected relatively late in larval life, at approximately 7 weeks post-fertilization. This is about 2 weeks after the time when surface MHC class Ia expression can first be detected. The number of NK cells is and remains small until 3–4 months, but by 1 year, there is a sizeable population of these

cells. Functionally, in agreement with the staining data, larval splenocytes (from either 5- or 7-week-old tadpoles) fail to kill MHC-deficient thymus-derived tumor cell targets. Killing is still poor in 3–4-month froglets, compared with high levels of tumor cell cytotoxicity mediated by splenocytes from older frogs. So, apparently, NK cells fail to develop prior to MHC class Ia protein expression and, therefore, do not contribute to the larval immune system, whereas they do provide an important backup for T cells in the adult frog by contributing to antitumor immunity (Horton et al. 2003; see also response to minor histocompatibility antigens on tumor and Figure 14.6).

Class Ia molecules are but one set among a larger family of class I molecules and the frog *X. laevis* possesses at least nine subfamilies of class Ib genes (*Xenopus* nonclassical MHC class I (XNC)). At least one of them, XNC10, besides being detected on the surface of thymic lymphoid tumors, is preferentially expressed by circulating T cells and thymocytes of the CD8 lineage both in adult and in larvae from the onset of thymus organogenesis (Goyos et al. 2009).

Class II

Using immunoprecipitation from radiolabeled spleen and thymus lysates with various alloantisera, xenoantisera, or monoclonal antibodies, and functional assays such as mixed lymphocyte reaction analysis, it was determined that although the same MHC class II molecules are expressed throughout ontogeny, the larvae and adult differ in their distribution. In tadpoles, class II epitopes can be detected only on B cells, macrophages (whatever their location), spleen reticulum, thymus epithelium, and the pharyngobuccal cavity. In addition, all adult T cells express class II on their surface. The modification of the class II expression pattern affecting lymphocytes occurs at metamorphosis. Around this time, other changes are visible: the skin is invaded by class II-positive dendritic cells that look like Langerhans cells, and the skin glands differentiate and also express class II. The gut, which expressed class II in discrete areas of the embryonic tissue, becomes invaded with B cells in many more places, and

its epithelium also becomes class II positive (Du Pasquier and Flajnik 1990). This second round of class II expression is accompanied by the ubiquitous expression of the class Ia.

It seems that the expression of class Ia and class II is under different developmental control in premetamorphosis larvae: class II expression is dependent on the morphological changes due to metamorphosis, whereas class Ia is not (see preceding text). The same perchlorate-blocked larvae mentioned in the previous section had relatively few class II+thymic lymphocytes throughout the 6-month period of study, and the proportion of class II+splenic lymphocytes was approximately equal to that of IgM+B lymphocytes. Thus, perchlorate-treated animals retained the larval pattern of class II expression (Rollins-Smith and Blair 1990). (This observation has to be kept in mind when reading the section on dependence of antibody response on metamorphosis.)

Lymphocyte receptors

T cells

RAG-1 expression, indicative of immunoglobulin superfamily (TCR and BCR) gene rearrangement activity, can be detected by PCR from whole larvae as early as 3 days after fertilization at stage 41/42 before any lymphoid organ architecture can be safely identified (Mußmann et al. 1998). Later, in juvenile frogs, the highest levels of RAG-1 and RAG-2 expression were observed in the thymus, with lower levels in the liver and spleen, and even lower levels in the kidneys. In adults, the thymus and bone marrow are the principal sites of expression of both genes. The RAG-2, but not RAG-1, is expressed in oocytes, a finding not surprising given the upregulation of virtually any message in the oocytes (Greenhalgh et al. 1995).

Rearrangements of TCR genes

A systematic survey of the expression of TCR α , β , γ , δ genes has not been performed yet. Full-length TCR β transcripts are already detectable in the thymus at 6 days following fertilization (stage 45/46). Full-length TCR β message can be isolated in the thymus only from day 6 to 8 (stage 47/48) onwards, amid

sterile transcripts of C γ and other incomplete products (e.g., J-C) – an observation also made in mammals and urodeles (Meier 2003; Robert and Ohta 2009). The expression of V β genes is progressive (Figure 14.3) and completes just before the apex of metamorphosis.

CD3, CD4, CD8, CD5, and CTX

The CD3 is a complex of several polypeptide chains associated with the TCR that gives it its signaling capacity. Among those chains, the CD3 ϵ is conserved among vertebrates and a reagent raised against human CD3 ϵ happened to cross-react with *Xenopus*. This allowed for monitoring T cells by sorting and immunohistology. The expression early in ontogeny is summarized in Figure 14.3, the CD3 ϵ being detected as early as day 6 after fertilization at the time of the aforementioned TCR γ and β rearrangements.

CD4 transcripts were detected by PCR 4 days after fertilization (stage 41/44) both in the thymus and intestine, whereas both CD8 α and β signal were detectable 1 day later at stage 43/46 and only in the thymus (Chida et al. 2011). Anti-CD8 Mab stains the inner part of the thymus cortex but does not stain the thin subcapsular region rich in mitosis and likely corresponding to mammalian zone containing the double-negative cells (Du Pasquier and Flajnik 1990).

The number of CD8+ cells in the spleen rises from nil at stage 52 to 20% in the 6-month-old adult, whereas a steady 75% is observed in the thymus (Gravenor et al. 1995).

In mammals, CD5 is a scavenger-like receptor expressed in association with the antigen-specific receptors on T and B-1a lymphocytes. In addition to its inhibitory function, CD5 seems to be a regulator of cell death and a receptor for pathogen-associated molecular patterns, which could bear on innate immunity functions (Soldevila et al. 2011). A homologue has been identified in *X. laevis* that behaves like a T cell antigen (*Xenopus* B cells acquire the CD5 homologue only when they are stimulated in the presence of T cells). This antigen is detectable as early as stage 49 in the spleen and thymus where it is present in about 35% of the cell. The percentage increases to 50% in both organs in the adult (Gravenor et al. 1995).

Another IgSF marker, the transmembrane protein CTX (cortical thymocyte-specific

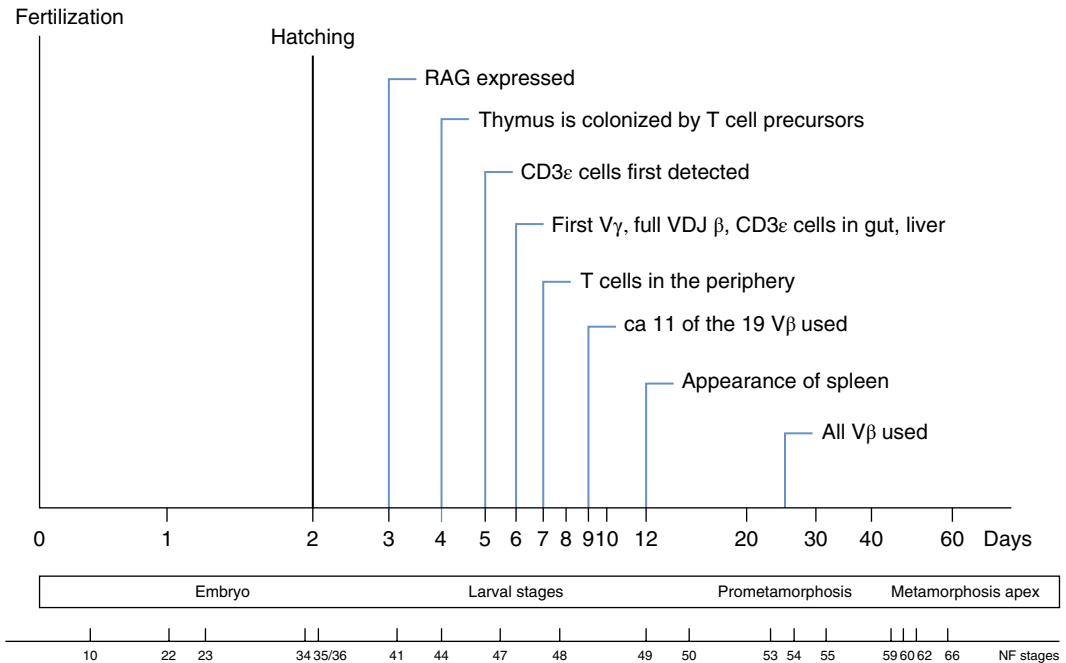


Figure 14.3 T cell differentiation during *Xenopus* ontogeny. RAG, recombination activating gene; VDJ, variable, joining, and diversity segments of T cell receptor.

antigen of *Xenopus*; Chrétien et al. 1996), the homologue of which in chicken tags the recent thymus emigrants (Kong et al. 1998), can first be detected by immunocytochemistry and flow cytometry at 8 days postfertilization (stage 48), about 1 day after CD8 $^{+}$ cells first appear. This CTX $^{+}$ population of lymphocytes corresponds to the murine immature double-positive (CD4 $^{+}$ CD8 $^{+}$ TCR $^{+}$) thymocyte subset. By 12 days postfertilization, T cells in the entire cortex except for the outermost layer are intensely CTX positive, whereas those in the medulla are negative. This pattern persists throughout larval and postmetamorphic life (Robert and Cohen 1998).

B cells

Xenopus and mammals have similar organization and usage of their BCR genes, i.e., their immunoglobulin gene loci, with combinatorial joining of V, D, and J elements (Schwager et al. 1988; Schwager et al. 1989; Schwager et al. 1991a). The differences in B cell development between mammals and *Xenopus* are due to major differences in developmental kinetics, cell number, and lymphoid organ architecture. *Xenopus* larvae hatch 2

days after fertilization and individuals are under pressure to develop an immune repertoire when the number of available cells is small (approximately 5 and 200 IgM-positive cells on days 5 and 11 after fertilization, respectively). As already mentioned in the T cell section, RAG-1 expression can be detected as early as 3 days after fertilization (Figure 14.4). The first immunoglobulin heavy chain (IgH) rearrangements are isolated by PCR from cDNA preparation of 5-day-old larvae (Du Pasquier et al. 2000). The earliest immunoglobulin light chain (IgL) rearrangements containing V ρ (homologous to κ) were isolated from 8- to 13-day-old larvae, respectively. The expression of the third light chain isotype homologous to mammalian λ has not been studied in detail during ontogeny.

In the liver (Figure 14.4), in a first phase of differentiation spanning days 5–12 after fertilization before immunological competence, the heavy (H) chain locus starts rearranging, which is followed, 3 days later, by the light (L) chain locus rearrangement. The first B cells expressing H and L chain are detectable by immunohistology on day 10.

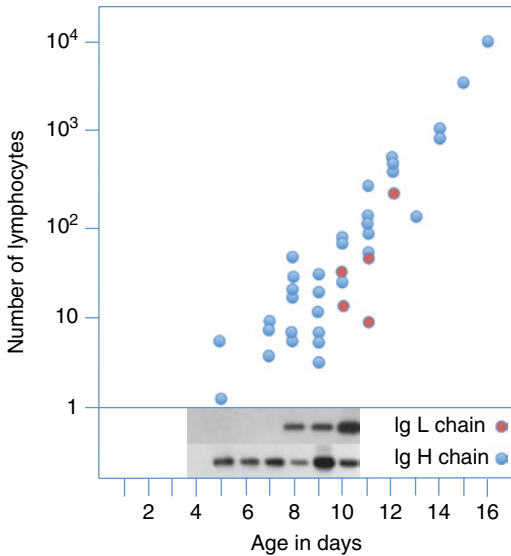


Figure 14.4 B cell development in the larval liver of *Xenopus*. Upper part, number of lymphocytes identified by immunofluorescence with anti-Ig heavy and anti-light chain antibodies. Lower part, results of PCR (gel electrophoresis of PCR fragments) with Ig heavy and light chain primers. Ig heavy chain message is detected on day 53 days before light chain message.

The cells detected earlier that stain with anti-heavy chain only correspond most probably to the pre-B cells. A doubt remains though, because the ontogeny of the third isotype of light chain has not been studied. Despite the small number of cells available and the lack of external antigen selection at these early stages, the repertoire of those early B cells is heterogeneous as judged from the sequences of the cDNA obtained from those stages. The 11 VH families are used consecutively, although their genes are interspersed in the genome. The earliest and most abundant family used (VH1) is homologous to the VH3 family of human and to the VH7183 of the mouse, which are also overrepresented in early mammalian development. In the second phase, from day 12 to 13 onwards, the spleen differentiates and the animal becomes immunologically competent. The V, D, and J usage of stage 56–58 tadpoles is similar to that of adults, although VDJ junctions lack N nucleotides until metamorphosis (Schwager et al. 1991b).

A preferential reading frame for D and one specific DJ junction are overrepresented during this second phase.

AID is another B cell-specific enzyme that plays no role in T cell differentiation of gnathostomes but plays a major role in diverse somatic events at the immunoglobulin gene level in B cells, i.e., somatic hypermutation, gene conversion, and IgH class switch.

During ontogeny, the expression of *Xenopus* AID homologue is detected as early as 5 days postfertilization in the liver before the first fully differentiated B cells appear (Marr et al. 2007). Concomitant with the appearance of mature B cells, the AID homologue is upregulated upon bacterial stimulation or viral infection at later larval stages (Marr et al. 2007). Because, as will be described later, somatic mutation plays a role in larval response, one can anticipate that AID functions early in ontogeny.

CD3ε on NK cells

As a logical consequence of the absence of classic class Ia epitopes in tadpoles, no NK cells have been detected with the anti-NK cell 1F8 monoclonal antibody until the time of metamorphosis 7–8 weeks postfertilization (stage 58), and no *in vitro* NK killing activity has been detected with stage 58 larval splenocytes (Horton et al. 2003). Yet, perhaps some of the CD3ε-expressing cells (Göbel et al. 2000; Meier 2003) found in various larval tissues correspond to larval NK cells because these cells express the epsilon and zeta chains of the CD3 complex.

Selection of T and B cell repertoires

Role of the thymus

The somatic, RAG-mediated, random generation of diverse TCRs with many specificities including potentially dangerous autoimmune ones requires selection for the establishment of a functional repertoire. This selection begins in the thymus and eventually produces a repertoire of CD4⁺ and CD8⁺ T cells that is both MHC restricted and able to react with non-self-epitopes. In mammals, selection takes place in the thymic cortex at the level of

the CD4+ CD8+ double-positive thymocytes. Low-affinity self-peptide–MHC ligands presented by cortical epithelial cells lead to positive selection of T cells. High-affinity self-ligands (the potentially dangerous ones) will trigger clonal deletion by induction of apoptosis. The lack of affinity results in **death by neglect**. Although many experiments on *Xenopus*, such as thymectomies, reconstitutions, and chimera constructions, have shown that the selection of repertoires in this species obeys the general **vertebrate** laws, the *Xenopus* ontogeny model provided important complementing information on the subject.

Complete thymectomy is easy to perform in *Xenopus*, unlike in mouse where the presence of second thymus might complicate experimental outcome. As Horton and Manning stated in 1972, the “early-thymectomized *Xenopus* may simply be closer to a completely athymic condition.” Indeed, early thymectomy in *Xenopus* completely abrogates allograft rejection, response to T cell mitogens, switch to IgY (the IgG *Xenopus* equivalent), but not IgM or IgX production. One can therefore anticipate that the thymus in frogs has the same effect on lymphocyte education as it has in warm-blooded vertebrates (Tochinai and Katagiri 1975; Du Pasquier and Horton 1976). With the discovery of the MHC restriction phenomenon, some new questions arose: would T cells that traverse an allogenic thymus during early and late life become restricted to interact, *in vivo*, with other leukocytes and target cells that display the MHC antigens of the thymus haplotype? *Xenopus* turned out to be a nearly ideal model to address this question (Flajnik et al. 1985). Chimeras were constructed with pairs of 24-hour-old *Xenopus* embryos such that the anterior region of an embryonic chimera contained the thymus anlagen and was of one MHC genotype, whereas the posterior region contained the anlagen of all hemopoietic cells and was of another genotype. The following assays were used to determine the MHC haplotype restriction specificity of T cells in chimeras that had been reared through metamorphosis: specific antibody responses (IgM and IgY)

to dinitrophenylated keyhole limpet hemocyanin known to be MHC restricted in adult normal *Xenopus* (Bernard et al. 1981) and rejection of minor H locus disparate skin grafts that expressed the MHC antigens of either the thymus donor or the lymphocyte donor and mixed leukocyte culture. A major observation was that MHC-mismatched chimeras displayed **split tolerance** since they accepted skin grafts of the thymus haplotype but had lymphocytes that proliferated *in vitro* (mixed leukocyte reaction (MLR)) in response to MHC antigens of the thymus donor strain as well as to MHC antigens of third-party donors. IgM responses of MHC-matched and MHC-mismatched chimeras and of nonchimeric controls did not differ. However, the T-dependent IgY responses of MHC-mismatched thymus/lymphocyte chimeras peaked later than those of MHC-matched chimeras and normal controls. Data from skin grafting protocols were consistent with the proposition that there may be *in vivo* selection of T cells reactive to minor H antigens presented in association with the MHC antigens of the thymus rather than that of the lymphocytes themselves. The split tolerance was confirmed later in the chicken model and suggested the importance of regulatory networks insuring peripheral tolerance.

In mammals, the selection of a complete repertoire in the thymus was a mystery with respect to the selection of the epitopes thought not to be present in the thymus. The mystery was solved when a transcription factor **autoimmune regulator** (Aire) was discovered. Aire is expressed in medullary thymic epithelial cells and its activity leads to exposing developing T cells to tissue-specific antigens other than those of the thymus itself, providing within the thymus new self-epitopes for repertoire selection. A homologue of Aire exists in both *X. tropicalis* and *X. laevis* (Saltis et al. 2008). Unexpectedly, frog Aire is quite divergent from human and mouse, both in sequence and domain/region composition. But despite this poor conservation, Aire expression is the highest in the thymus of *Xenopus* and the gene is thought to be involved in tolerance induction.

Acquisition of tolerance to self-antigens or the Triplett experiment controversy

An important aspect of the ontogenetic development of the immune system and repertoire establishment is the consequence of encounters between self-antigens and the incipient immune system. "Does the organism carry genetic information which allows its immune system to recognize the animal's own antigenic determinants, or is the ability to recognize self a property that is acquired during embryogenesis" (Triplett 1962).

If immunological tolerance to organ-specific self-antigens occurs at an early and fixed time period, then hosts that have been experimentally deprived of these antigens early in life, lacking the opportunity to become tolerant, would be expected to reject implants. This is what was apparently shown in the now classic **Triplett experiment**. In the tree frog *Hyla regilla*, Triplett removed the pituitary gland (hypophysis) from young larva and preserved it by transplantation in an intermediary host. The immune system of the hypophysectomized individual developed without contact with this organ. When grafted back later in life, the pituitary was rejected because no tolerance had been acquired.

There have been problems repeating this experiment perhaps because of immunogenetic reasons. Indeed, the Triplett experiment was not performed in genetically defined strains. This could explain why the results obtained in histocompatible or isogenic *Xenopus* submitted to the same protocol differed (Rollins-Smith and Cohen 1982; Maéno and Katagiri 1984; Rollins-Smith et al. 1990). These experiments showed that pituitary or eye self-implants were never rejected, whereas control allogenic implants were usually rejected by larval hosts and were always rejected by adult hosts. These results contrast with those reported by Triplett and suggest in fact that frogs and perhaps other higher vertebrates can become tolerant to self-organ-specific antigens throughout life.

However, more recently, this issue was addressed again by other groups, whose results agree with Triplett's conclusions but with different time margins (Enomoto and Tochinali 1999). When using lens antigens in

the histocompatible (but not fully isogenic) *jj Xenopus* strain, the results supported Triplett's hypothesis. Young adults whose eyes were removed during early larval life rejected syngenic lenses. This rejection did not occur in intact frogs or in those animals enucleated in later larval or adult life. When the lymphocytes were assayed in an *in vitro* test (never done before), the splenocytes from intact frogs did not proliferate in response to a cocultured syngenic lens, whereas those from frogs that had been enucleated at any of the larval stages, or even after metamorphosis (the time margin difference alluded to previously mentioned), proliferated intensely. Both of these responses were shown to be thymus dependent.

Is the tolerance induction submitted to different laws in function of the different self-antigens? Are there immunogenetic aspects responsible for the discrepancies? It seems that the cleanest experimental protocols are the one using fully isogenic strains and we tend to accept the conclusions from those. But perhaps the readouts in the different experimental setups have different sensitivities.

B cell repertoire selection in *Xenopus*

Like in many other species, B cell selection has received less attention than T cell selection and its modalities are unknown. The status of the pre-B cell is not known in *Xenopus*. Editing (Luning Prak et al. 2011) can certainly occur in *Xenopus* not only because the locus architecture with its cryptic splicing sites suggests it but also because typical rearrangement circles, which are the witnesses of this process, have been found in B cell libraries (Du Pasquier unpublished).

Immunity during ontogeny

The egg itself and the early embryonic stages can be passively protected by antibody molecules transferred from the mother and probably by some not yet studied intrinsic immunity mechanisms (Poorten and Kuhn 2009).

Xenopus tadpoles are **visibly** immunologically competent from the moment one can detect histologically the spleen and when

the total number of lymphocytes in the animal does not exceed one million. Upon injection with an antigen such as sheep red cells, hapten-carrier immunogens, bacteriophages, and various viruses, *Xenopus* tadpoles will make IgM antibodies and also, when injected with traditionally thymus-dependent antigens, will show limited T help (Kidder et al. 1973). They can reject xenografts and certain types of allografts (Horton 1969), which indicates the presence of T cell immunity, and their lymphocytes can proliferate in MLR, an *in vitro* test for class II recognition by T cell.

The ontogeny of the immune system is characterized by a rise in the number of lymphocytes with a few thousands cells at the onset of competence to adulthood with about 100 million lymphocytes for a 300 g *Xenopus* – about half of the lymphocyte number present in the spleen of a 25 g mouse. The protein concentration in body fluid also increases and some organs, such as the thymus, change their location. The ontogeny of *Xenopus* like that of all anurans is also marked by a very special moment, the metamorphosis. Metamorphosis is a critical period when increased concentrations of hormones, principally the TH and corticosteroid hormones (CH), lead to the loss and/or to the remodeling of many tissues and organs, including the immune system. Many new self-antigens, which were absent in the larvae, are expressed at this time. The possible expression of many new genes in an individual, whose immune system is functional, like that of a tadpole, raises several questions (Rollins-Smith 1998). How does the animal become tolerant to these new epitopes, and does it revise its repertoire? Does it generate suppressor cells? Reciprocally, how do adult lymphocytes sense the tadpoles' epitopes? Are lymphocytes involved in metamorphosis? An increased level of corticosteroids during metamorphosis appears to induce apoptosis of susceptible lymphocytes. How does this affect resistance to pathogens and tolerance induction? Later, we will discuss the results of observations and experiments, covering the first ca 12 weeks of *Xenopus* life, which partially answered these questions.

Antibody responses

Endogenously produced immunoglobulins of the IgM isotype are first detected, independently of any experimentally induced response, in the peritoneal fluid of larvae at stage 49 (about 12 days), which corresponds to the stage when the spleen appears. IgY, the IgG equivalent, can be detected 3 days later at stage 50. The ability to produce antibody following an injection of DNP-KLH immunogen increases during development from stage 50 to 59 (i.e., from 15 to 45 days postfertilization).

The tadpole B cell repertoire or rather the antibody diversity that results from it is less heterogeneous than that of the adult frog, certainly a reflection of the great difference in cell number between the larval and the adult systems. Yet tadpoles respond to all the antigens that have been tried so far – sheep red cells, tobacco mosaic virus, *Bordetella pertussis*, bacteriophages, skin grafts, hapten-carrier immunogens, and phosphorylcholine – by producing specific antibodies.

Specific IgY antibody synthesis is not obvious in larval primary response but is easily detectable in adults. Even though IgY is produced in very low amounts in larvae, isoelectric focusing (IEF) spectrotypes of the antibody can be monitored by IEF, provided the animals are well immunized and kept at high temperature (25°C). The heterogeneity of the response is somewhat lower in tadpoles (up to 12 antibody IEF bands) than in adults (up to 20 antibody IEF bands).

By measuring the relative affinity evolution of anti-DNP antibodies at different times after immunization, a maturation of the anti-DNP response has been observed in both adult and larval *X. laevis*. Still, the antibodies produced by larvae are of lower affinity and less heterogeneous than those produced by adults; therefore, their specificity might be broader, and this explains why with so few cells the larval immune system still covers the spectrum of antigens present in its environment (Hsu and Du Pasquier 1984a,b). These properties of tadpole response could be due to a lack of or a reduced rate of somatic hypermutation. Therefore, cDNA sequences utilizing VH1 elements were compared to

germ line counterparts in isogenic LG7 tadpoles during an immune response. Indeed, tadpole VH1 sequences contained somatic mutations, which is consistent with the early expression of XI AID mentioned earlier. There were 0–5 mutations per sequence, all single base-point mutations, with the high ratio of GC to AT base-pair alterations similar to that observed in adult frogs (Wilson et al. 1992, 1995).

Injection of isogenic primed adult T cell led to a greater production of antibodies with more IgY, but the specificity remained of the larval type. The larval antibody repertoire studied using IEF and affinity determination for DNP is unchanged after the addition of adult helper T cells. Thus, the expression of a larval repertoire is the result of a B cell pool peculiar to larvae and is not influenced, except in its quantity, by adult T cells. Helper T cells in tadpoles are what limit the response. Injection of adult T cells in isogenic animals makes them behave as adult in terms of switch capacity.

The immunized tadpoles metamorphose and can be reimmunized 1 year later as adult to check whether memory can cross metamorphosis. Larval spectrotypes can be seen reexpressed, whereas the response, like any mammalian memory response, is higher and faster (Du Pasquier et al. 1979). Although metamorphosis results in profound changes in the lymphoid system associated with the apparent acquisition of self-tolerance to new antigens, immunological memory of antigens injected during larval life persists after the metamorphosis period (Du Pasquier and Haimovich 1976). This indicates that some lymphoid cells must escape the changes at metamorphosis either because of their higher number at the moment of depletion or because of protection in a specific location or also perhaps because of a different sensitivity to the hormonal triggers.

Continuity between larval and postmetamorphosis stages can also be seen when stem cells are monitored using the ploidy markers. At least part of adult hematopoietic tissue

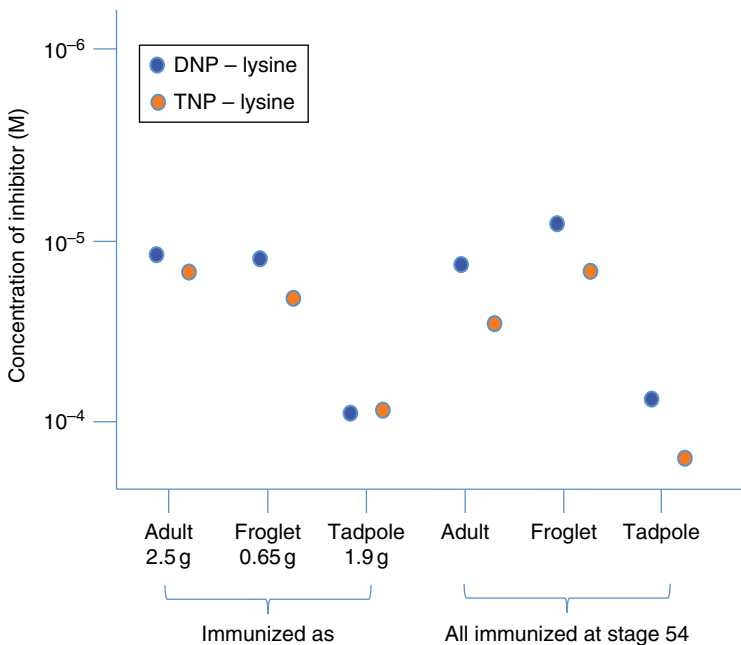


Figure 14.5 Anti-DNP antibody production in tadpoles, metamorphosing, and adult individuals. The test used to measure antibody relative affinities is an inhibition of inactivation of modified bacteriophage in the presence of decreasing molarities of inhibitor (DNP-lysine) (Hsu and Du Pasquier 1984a,b). The lowest the molarity of the inhibitor, the highest the affinity. The antibodies were raised against DNP-KLH and cross-react with TNP. To see a color version of this figure, see Plate 36.

(red cells, B and T cells) arises from precursors present in the tadpole spleen. Six months after metamorphosis, an adult thymus from an individual that received larval spleen cells shows about 1% of its thymocytes to be of donor origin. In the case of the T cell precursors, these splenic precursors contribute to the wave of T cell that colonizes the new thymus after metamorphosis for its second histogenesis (Chrétien et al. 1997).

The changes in lymphocyte repertoires correlate with the morphological changes linked to metamorphosis and not with age or cell numbers. The results of experiments in which tadpole and adult *Xenopus* were manipulated to be of comparable size with comparable cell numbers (giant tadpole, small adults; Figure 14.5) showed that they exhibited stage-specific antibody expression. The production of adult-type higher-affinity anti-DNP antibodies proved to be independent of the age and size of the individual and was concomitant with the completion of metamorphosis. The appearance of new antibody specificities at metamorphosis suggests that their expression occurs with the major cell turnover and renewal during this period of morphological changes (Hsu and Du Pasquier 1992), which are accompanied by qualitatively different selecting environments in which lymphocytes developed.

Response to polymorphic histocompatibility antigens during ontogeny

The MLR is an *in vitro* test monitoring the proliferative capacity of T cells triggered by polymorphic MHC class II epitopes. It has been used throughout ontogeny in *Xenopus*. Tadpole T cells stimulated by tadpole B cells that express class II of a different MHC genotype do respond in MLR according to the classic adult pathway showing the classic 1:4 segregation pathway in progenies from parents heterozygous at the MHC locus. During metamorphosis, their capacity to proliferate is temporarily obliterated in a way that suggests that only the two-haplotype differences are detected. Within a family derived from MHC disparate and heterozygous parents, instead of 25% nonreactive

combinations, 75% are detected and the normal percentage (25%) is regained progressively 5–6 weeks after the completion of metamorphosis (Figure 14.6). During the period of decline and regain of MLR capacity, graft rejection capacity is also modified and specific tolerance can be more readily induced, even more than in larval life, especially to minor H antigens (Bernardini et al. 1969; Bernardini et al. 1970; Chardonnes and Du Pasquier 1973; Du Pasquier and Chardonnes 1975).

Yet despite an apparent normal MLR capacity, the tadpole T cell compartment is not quite the same in its recognition or effector capacity as that of adults. For MHC-linked differences, whether the tadpole will reject one- or two-haplotype disparate donor skin depends on the nature of the alleles (DiMarzo and Cohen 1982). Tadpoles do not reject skin grafts differing at some minor H loci. In adults, all minor or major differences will lead to a more or less rapid rejection: 21 days for major and up to 75 days for minor. Graft rejection when it occurs in tadpoles suggests that cytotoxic CD8 T cells can be generated from tadpole T cells. We have seen earlier in this chapter that only few CD8 cells can be detected in tadpole.

But from the viewpoint of the target, the tadpole cells apparently lack the target epitope, the MHC class Ia molecule. Will tadpole cells be killable by CTL? According to Horton et al. (1989), they can be if the stimulus has been strong enough, i.e., multiple. The target molecules have still not been identified formally in this situation. It is reasonable to assume that class II, known to be expressed in tadpoles, could mediate the killing. However, considering the fact that tadpoles express several nonclassic class I molecules, one could also argue that the killing is triggered via those molecules. Their polymorphism is not known but they segregate on the same chromosome as class II and class Ia even though they are located at a great distance from each other on the chromosome (Courtet et al. 2001).

Responses to minor histocompatibility antigens on tumors

As we have just seen, recognition of minor H antigens is not perfect in tadpoles and this is

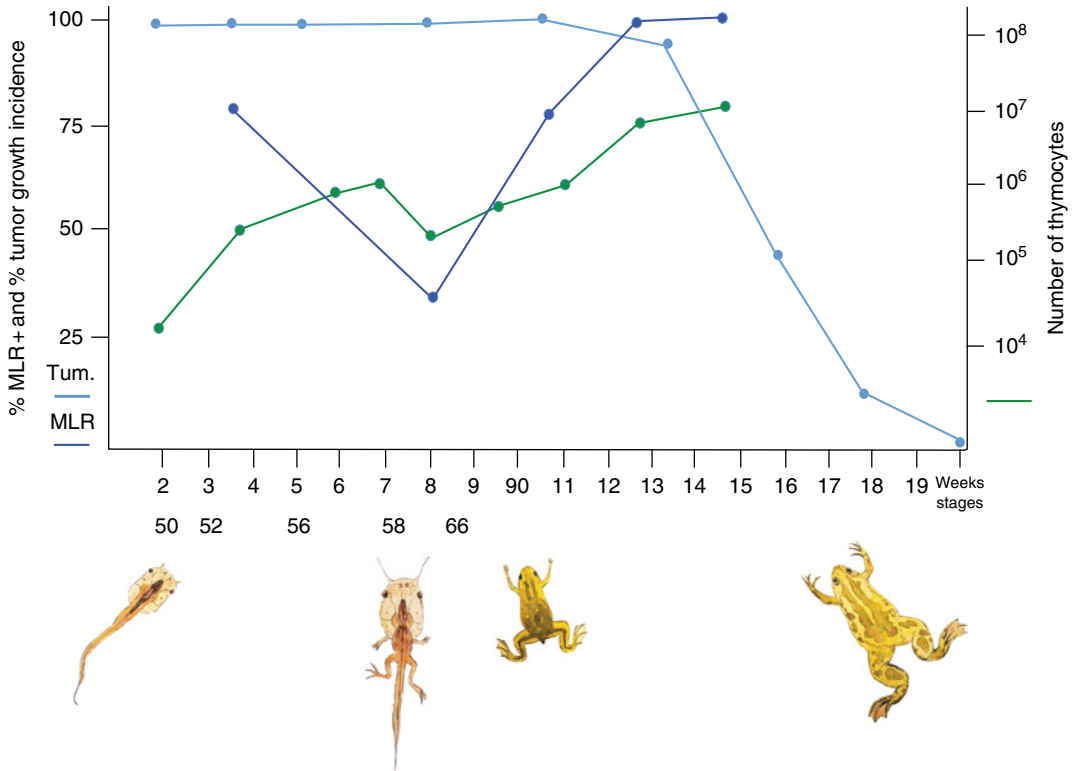


Figure 14.6 Antitumor immunity acquisition in function of mixed lymphocyte reaction and thymocyte number evolution. Source: Robert et al. (1995). To see a color version of this figure, see Plate 37.

further exemplified in the model of larval antitumor immunity. Cells of lymphoid tumor ff2 (of the ff MHC genotype) injected alive into ff tadpoles homozygous at the MHC level but differing at some minor H loci will be tolerated by tadpoles but not by adults. The curve of acquisition of immunity to these minor H loci is roughly similar to the curve of recovery mentioned before MLR activity. The kinetics of MLR decline and recovery match well the curve of the evolution of lymphocyte number in the thymus and spleen, and the end of recovery marks the final acquisition of complete responsiveness to minor H differences (Robert et al. 1995) (Figure 14.6). Therefore, the resistance of the host against transplanted tumor cells rises during the postmetamorphic development in parallel with the second histogenesis observed in the thymus, the expression of MHC class II by peripheral T cells, and the onset of expression of the classic class Ia molecules.

Yet tadpoles are not totally insensitive to minor H differences. Priming with irradiated ff2 cells at larval stages does interfere with tumor growth in transplanted young postmetamorphic adults, suggesting that long-lived memory has been generated and has been maintained through metamorphosis. Thus, the lack of tumor rejection by larvae might result from an incomplete effector function rather than from a total absence of recognition. Theoretically, the impaired tadpole response could be due to a lack of competent cells (due to the depletion seen in Figure 14.6) or to the regulatory activity of a cell population. Experiment involving passive transfer of cells from larval cells into a tumor cell recipient should answer this question. We might in fact be in a situation similar to that of split tolerance (see the education section). The notion of split tolerance comes recurrently during ontogeny in *Xenopus*. It was also suggested

by the experiments described by Horton et al. (1993):

[F]ollowing larval grafting of semiallogenic tissues, mixed leukocyte culture performed at the end of metamorphosis (6 weeks), and again at 6 months, reveals splenocyte reactivity toward donor-strain stimulators. Immunohistological findings extend this observation of anti-donor reactivity (suggesting incomplete tolerance) to the graft site. Thus despite excellent health when viewed externally, apparently tolerated second-set skin transplants display localized infiltration (especially into the epidermis) by CD8+ T cells and increased numbers of MHC class I and II-expressing cells by 3 weeks postgrafting.

Immunological issues at metamorphosis

Metamorphosis is a critical time of transition when increased concentrations of TH and CH under the control of a central hypothalamic mediator orchestrate the loss or reorganization of many tissues and organ systems, including the immune system. During this period (Figure 14.7), triiodothyronine (T3) and tetraiodothyronine (T4) control a complex hierarchical cascade of target genes via binding to specific receptors, TCR α and TCR β , ligand-activated transcription factors belonging to the nuclear receptor superfamily.

Upon metamorphosis into juvenile *Xenopus*, every organ undergoes extensive morphological and/or functional changes such as death and resorption of larval tissues, remodeling of larval tissues, and *de novo* growth and differentiation. This means that many new molecules which were not part of the larval environment appear, and one can wonder whether the larval and adult immune systems will recognize stage-specific epitopes, and if yes, what are they and what will be the consequences? In the immune system, an increased corticosteroid level seems to induce apoptosis of some susceptible lymphocytes. The reorganization that follows may indeed have fundamental consequences (Rollins-Smith 1998). It could serve to eliminate unnecessary lymphocytes that could be destructive if they recognized newly emerging adult-specific antigens. It could also serve to

eliminate larval-specific tissues bound to disappear at metamorphosis such as the tail.

Larval antiadult responses?

An observation made in *Rana* suggested that the larval immune system could consider the adult epitopes as foreign and respond to them. *Rana catesbeiana* tadpoles immunized with the main hemoglobin component of the adult frog of the same species produced precipitating and agglutinating antibodies against the immunogen. After natural metamorphosis, these immunized froglets had, as their only major hemoglobin, a protein immunologically and electrophoretically different from the major hemoglobin of control froglets (Maniatis et al. 1968).

These experiments were performed without genetically controlled strains, and allelic specificities might have been involved rather than developmentally regulated epitopes. It was also hard to explain how the antiglobulin antibodies would have an effect on an intracellular antigen. Therefore, it became necessary to repeat such experiments under the better-defined conditions offered by the *Xenopus* model. In fact, the result of one of the experiments on *Xenopus* agreed with the results of the *Rana's* experiment (Chardonnes 1976). Animals that had been submitted to grafting before metamorphosis with adult tissues have shown symptoms of hemorrhages in their own skin around the time of metamorphosis. Some animals had died and others recovered. This phenomenon was called the **red disease**. Knowing about the differences between adult and larval red cells (Flajnik and Du Pasquier 1988), these experiments were repeated using a different setup for the injection of erythrocytes into isogenic *Xenopus* (Figure 14.8). Isogenic tadpoles at 2 weeks of age were injected with adult red cells of the same genotype known to differ by MHC class I, hemoglobin, and other surface antigens.

The results were not clear-cut. At the time of the normal metamorphosis, a certain number of individuals, but never all of them, even within an isogenic clone, developed the red disease symptoms. Hemorrhages were seen in the skin and many of the affected animals died. This could have been interpreted as the occurrence of an autoimmune reaction counteracted

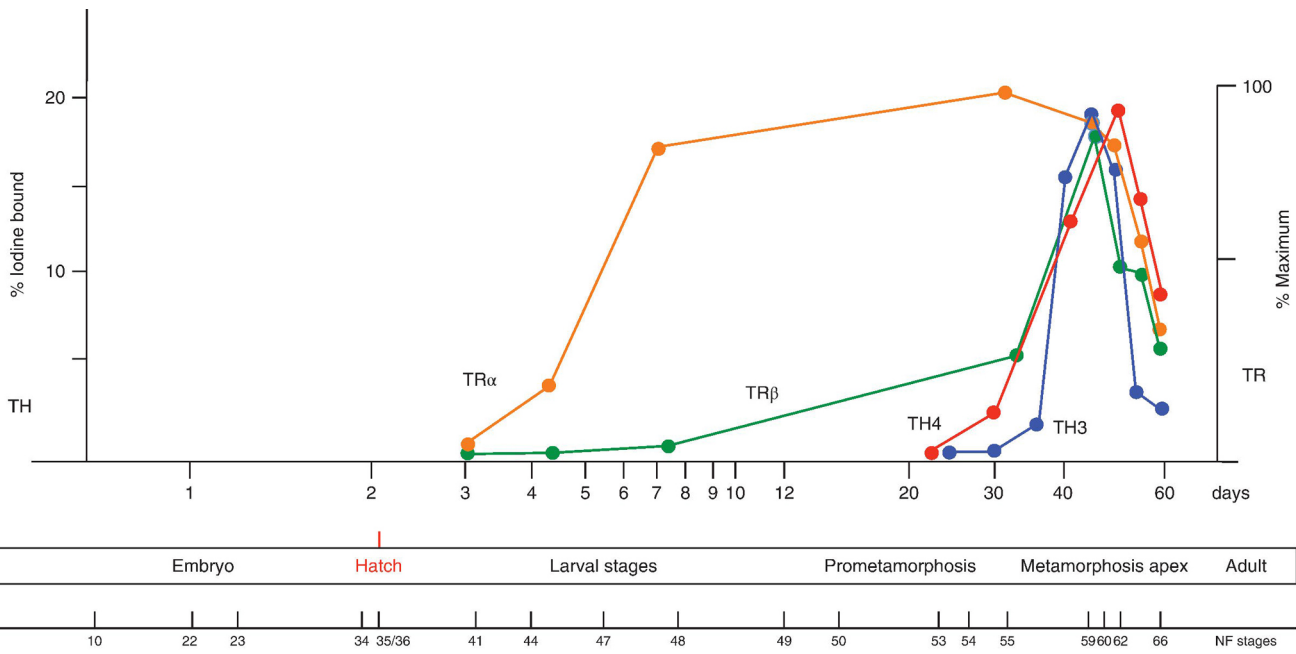


Figure 14.7 TH level evolution during *Xenopus* ontogeny. Source: Flajnik et al. (1987) and Morvan-Dubois et al. (2008).

naturally and efficiently in some cases. Because of a lack of the reagents at the time, this assumption could not be proven and those preliminary results were not published. More recently, several observations have been reported that larval lymphocytes could indeed be stimulated by adult cells of the very same genotype (i.e., isogenic). A summary of the MLR results is presented in the upper part of Table 14.1.

All these facts suggest that the larval immune system is able to recognize as foreign at least some of the adult-specific epitopes that appear all over the body at metamor-

phosis. This would be consistent with the possibility to launch an autoimmune reaction. In the experiment shown in Figure 14.8, the early deliberate immunization might have enriched the immune system in an antiadult lymphocyte population that normally would not have been amplified. The self-thymectomy and lymphoid depletion in the spleen occurring at metamorphosis might not have been sufficient to deplete the immune antiadult population, hence the reaction.

Since in the normal situation the animals do not die from autoimmune disease, one could

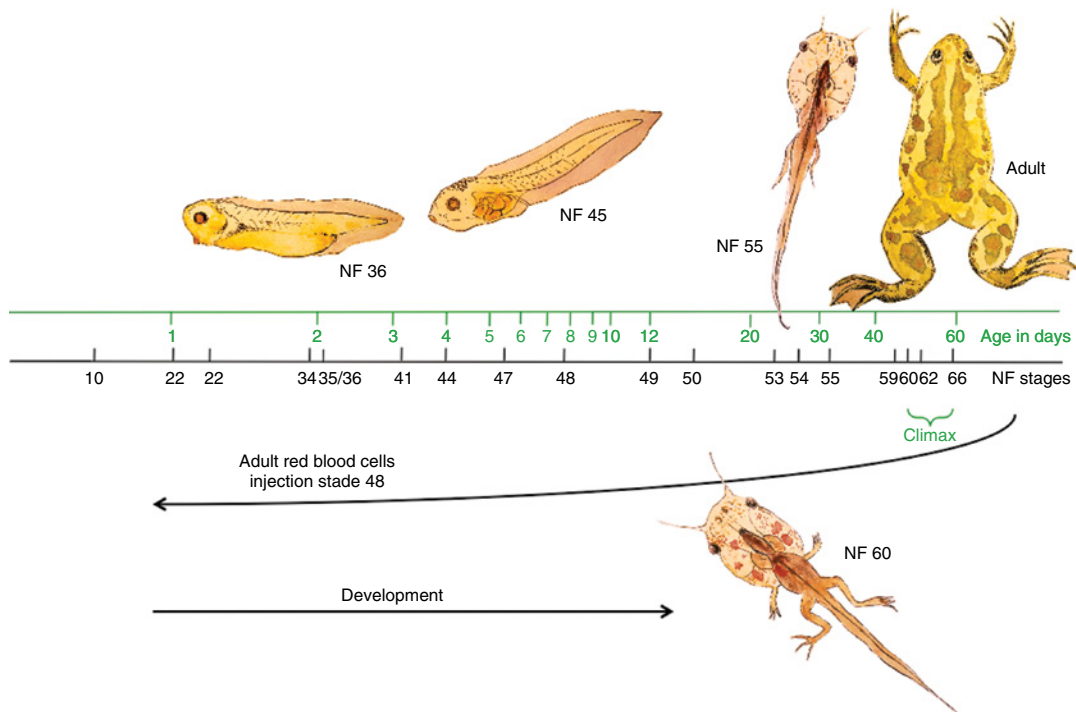


Figure 14.8 Protocol for the generation of red disease in *Xenopus* NF: Nieuwkoop and Faber stages.

Table 14.1 Age-related unidirectional MLR.

Responders	Irradiated stimulators			
	Larval thymus ac	Adult thymus ac	Adult PBL ac	Adult thymus xy
Larval thymus ac	1.0	3.4	5.8	2.3
		3.2	2.7	5.8
		1.3	4.9	
Adult thymus ac	2.5 2.1	1.0	0.8	3.3
				2.9

Stimulation indices measured on day 5 of the culture. a, c, x, y: MHC class II alleles.

Source: Summarized from Du Pasquier et al. (1979).

anticipate the existence of immunoregulatory events with some elimination or blockage of autoimmune effector mechanisms. We shall discuss them later.

Adult antilarval responses?

Is the reciprocal of the preceding situation true? Can the adult immune system recognize larval epitopes; in other words, does the adult immune system receive a new education when the larval determinants are no longer presented? Theoretically, the adult lymphocyte population, as it comes out of a new selection round through the regenerated thymus with a new repertoire of T cells, can perhaps recognize larval epitopes and become capable of recognizing and rejecting larval tissues. There are several reports that this is the case. Proliferation in MLR has indeed been observed when larval irradiated isogenic cells were used as stimulators of fully grown adult T cells. A summary of the results is presented in the lower part of Table 14.1. Given that both adults and larvae express apparently the same class II and knowing that MLR is in principle due to class II differences, we face here a very special case of MLR. In addition, within the inbred J strain, the young adults of *X. laevis* reject skin grafts (in principle a T cell-dependent phenomenon) from larvae of the same strain, which indicates that there is histoincompatibility between larval and adult skin tissues (Izutsu and Yoshizato 1993). Finally, adult and metamorphic climax splenocytes proliferate *in vitro* in response to contact with larval tail tissue. The larval cells of the epidermis are recognized and made apoptotic by splenocytes obtained from adults and/or metamorphosing individuals. With the help of a specific anti-T cell monoclonal antibody, the effector cells were characterized as T cells, even in the early thymectomized tadpoles. This suggests the presence of an unconventional thymus-independent pathway of generating certain types of T cells (Izutsu et al. 1996; Izutsu 2009).

More complex experiments have been designed to check what would be the tail target epitopes for the adult lymphocytes (Izutsu 2009; Mukaigasa et al. 2009).

Two tail skin keratin-related proteins (ouroboros) encoded by the genes *ouro1* and

ouro2 are expressed specifically at the climax of metamorphosis. They can be considered as antigens since they generate proliferative responses *in vitro* of naive adult T cells – a reaction that resembles the MLR of adult versus larval lymphocytes. They also elicit specific antibody production (Izutsu and Maéno 2005). When *ouro1* and *ouro2* expression is knocked down, tail skin tissue remains after metamorphosis. In summary, these authors, on the basis of results of immunohistochemical and T cell proliferation analyses, conclude that the adult frogs exhibit humoral and cell-mediated immune responses to some larva- or metamorphosis-specific antigen molecules present in epidermal cells. These observations highlight the possibility that the acquired immune system contributes to remodeling processes in *Xenopus* morphogenesis.

There is, however, a fundamental problem in the interpretation of all these experiments – the fact that thymectomized animals, known to be devoid of T cells, metamorphose perfectly well, without delay. If a mechanism implicating T cells really exists, then it cannot be the only or the essential one. The implication of T cells is far from being proven. Indeed, non-T cell events have been observed, and a combination of T-dependent and T-independent and nonimmune mechanisms may be at work during this period. After all, metamorphosis is complex enough to be under the dependence of multiple mechanisms. Most models propose that tail resorption during amphibian metamorphosis is controlled mainly by a cell-autonomous mechanism of programmed cell death triggered by TH (Ishizuya-Oka et al. 2010). In fact, autonomy seems to have been demonstrated in several cases for various tissues, especially tail muscles (reviewed in Furlow and Neff 2006). Immunocyte involvement is secondary with cells of the hemopoietic system, macrophages, getting involved in the resorption of larval tissue by phagocytosing apoptotic cells (Ishizuya-Oka 1996; Ishizuya-Oka 2011).

There is still much to do in this area and perhaps a more subtle analysis of the metamorphosis in thymectomized animals will be necessary.

Immunoregulation at metamorphosis

Tadpoles go through a period around the time of metamorphosis during which they can become tolerant to many new self-antigens. Obviously, a subtle regulation of immune mechanisms has to take place. In order to see if metamorphosing animal contained population of lymphocytes that would suppress the graft rejection of animals that were already beyond this period, the experiments of passive transfer of cells in isogenic strains of *Xenopus* were performed. Lymphocytes from normal metamorphosing animal were injected into 6-month-old adults when they were normally immunocompetent. Then, the animals were grafted with a minor H locus disparate skin fragment. As long as these injections were performed every 2–3 days, the grafts were not attacked at all or attacked weakly (Du Pasquier and Bernard 1980). A similar effect was obtained by injecting cells from animals made tolerant to semiallogenic graft or minor H different individuals (Ono and Tochinali 1995). Interestingly, in the case of the Ono experiment, the cells from the tolerated skin were able to suppress. Were they all skin cells or did they contain passenger leukocytes? The reciprocal experiment, preventing perimetamorphic tolerance induction by injecting tadpoles with normal adult cells, failed. However, passive transfer of antigraft immunity could be observed, provided the cells came from a specifically primed individual and were injected at the same time as the graft was applied. So, memory cells are not as sensitive to the suppression as are the cells responding in the first set. The situation is somehow similar to that of memory B cell mentioned earlier. Most probably, certain T cells escape the drastic remodeling happening at metamorphosis (Rollins-Smith et al. 1996). The cells responsible for the regulation were probably T cells because of immunohistology localization (Ono and Tochinali 1995) and because thymectomies performed during midlarval or late larval life did affect the induction of tolerance capacity hence the population of regulatory cells (Barlow and Cohen 1983). Thus, the efficacy with which thymectomy affected tolerance depended on the developmental stage at which it was performed, on the haplotype disparity between donor and host, and on the size of the transplant.

The assumption that the immune system could be dangerous at metamorphosis led to the hypothesis and to the demonstration of the existence of immunosuppression. But what about if one takes the opposite view, namely, that the immune system is useful at metamorphosis, as suggested by the ouroboros experiments? Do we see finally the result of a highly specific blockage of the dangerous larvae antiadult responses associated to the maintenance of the useful adult antiouroboros activity? A lot of issues need further study and clarification.

Conclusion

The early ontogeny of *Xenopus* and the larval period offer interesting variations on the theme of immune system differentiation.

The natural lack of class Ia classic MHC epitopes and the variations in expression of class II MHC encoded within the same complex is an equivalent of selective KO experiments and represents, to our knowledge, a unique case in experimental biology. The lack of class Ia epitopes in young tadpoles cannot be without some consequences on the repertoire of lymphocytes.

The necessity to acquire a minimal repertoire when the number of lymphocyte is limiting has raised several issues of fundamental interest. How does a randomly generated repertoire allow survival when the cell number is low (the E–T (elephant-tadpole) paradox; Langman and Cohn 1987)?

Selection of low-affinity antibodies in larvae with a broader spectrum of cross-reactivity seems to have been the solution selected during evolution.

Is the larval *Xenopus* thymus selection an exact equivalent of the selection process present in mammals? The phenotypes of the cells in the larval lymphoid organs suggest that there might be differences. Perhaps, in *Xenopus*, only the period of second histogenesis of the thymus is homologous to the period of thymus selection in mammals. It might be wise to reinvestigate the role of the thymus at a more refined level. The situation might be more complex than originally thought because of the existence of metamorphosis.

The transition at metamorphosis, probably the most fascinating and original aspect of the developing *Xenopus* immune system, implies remodeling of repertoires and regulatory immune networks. The roles of cytokines and neuroendocrine aspect in those events have so far not been studied.

Metamorphosis could be envisaged as an analogue of mammalian pregnancy with similar suppression events being necessary. After all, a tadpole is an immunologically competent individual pregnant with an adult self, with all the adult genes ready to be expressed at once or almost at the time of the apex of metamorphosis. Clearly, this situation implies a new set of selection among the lymphocytes.

The transfer of immunological memory across metamorphosis raises the interesting question of transdifferentiation or lineage reprogramming (Sisakhtnezhad and Matin 2012). Some larval cells (memory B cells generated during the larval response) with larval cell properties (lack of class Ia) go across metamorphosis but as adult B cells end up expressing class Ia). It looks as if we indeed see transdifferentiation of B cells with the onset of class Ia expression at metamorphosis. We still need an unequivocal demonstration of the presence of this process in *Xenopus*.

Regulatory cells, perimetamorphic immunosuppression, balances between central and peripheral tolerance, split tolerance, and possible involvement of the immune system in tissue resorption at metamorphosis are other domains that were touched upon. Although very interesting observations have been made in these areas, we still do not have satisfactory explanations. No doubt though that with the application of modern techniques such as transgenesis, gene silencing, better reagents and strains, and *in vitro* correlate systems, many of the aforementioned questions will be answered within the next 10 years.

Acknowledgments

I would like to thank Prof. Ivan Lefkovits for his comments on the manuscript.

References

- Barlow EH, Cohen N (1983). The thymus dependency of transplantation allotolerance in the metamorphosing frog *Xenopus laevis*. *Transplantation*. 35(6):612–619.
- Bernard CC, Bordmann G, Blomberg B, Du Pasquier L (1981). Genetic control of T helper cell function in the clawed toad *Xenopus laevis*. *Eur J Immunol*. 11(2):151–155.
- Bernardini N, Chardonnens X, Simon D (1969). Development after metamorphosis of immunologic competence between cutaneous homografts in *Xenopus laevis* Daudin. *C R Acad Sci Hebd Seances Acad Sci D*. 269(11):1011–1014.
- Bernardini N, Chardonnens X, Simon D (1970). Tolerance of cutaneous allografts in *Xenopus laevis*. Influence of the size and age of the graft. *C R Acad Sci Hebd Seances Acad Sci D*. 270(19):2351–2354.
- Brändli AW (1999). Towards a molecular anatomy of the *Xenopus* pronephric kidney. *Int J Dev Biol*. 43(5):381–395.
- Carmona-Fontaine C, Theveneau E, Tzekou A, et al. (2011). C3a controls mutual cell attraction during collective cell migration. *Complement fragment*. *Dev Cell*. 21(6):1026–1037.
- Chardonnens X (1976). La tolérance aux antigènes d'histocompatibilité pendant la métamorphose de l'amphibien anoure, *Xenopus laevis*: un modèle pour l'étude de la tolérance au self [dissertation]. Université de Genève.
- Chardonnens X, Du Pasquier L (1973). Induction of skin allograft tolerance during metamorphosis of the toad *Xenopus laevis*: a possible model for studying generation of self tolerance to histocompatibility antigens. *Eur J Immunol*. 3(9):569–573.
- Chesneau A, Sachs LM, Chai N, et al. (2008). Transgenesis procedures in *Xenopus*. *J Biol Cell*. 100(9):503–521.
- Chida AS, Goyos A, Robert J (2011). Phylogenetic and developmental study of CD4, CD8 α and β T cell co-receptor homologs in two amphibian species, *Xenopus tropicalis* and *Xenopus laevis*. *Dev Comp Immunol*. 35(3):366–377.
- Chrétien I, Robert J, Marcuz A, Garcia-Sanz JA, Courtet M, Du Pasquier L (1996). CTX, a novel molecule specifically expressed on the surface of cortical thymocytes in *Xenopus*. *Eur J Immunol*. 26(4):780–791.
- Chrétien I, Marcuz A, Du Pasquier L (1997). A ploidy marker to track lymphocytes after cell transfer between genetically identical or inbred *Xenopus*. In: Lefkovits I, editor. *Immunology Methods Manual*. San Diego: Academic Press, p. 2381–2394.

- Ciau-Uitz A, Liu F, Patient R (2010). Genetic control of hematopoietic development in *Xenopus* and zebrafish. *Int J Dev Biol.* 54(6–7):1139–1149.
- Clothier RJ, Balls M (1985). Structural changes in the thymus glands of *Xenopus laevis* during development. In: Balls M, Bownes M, editors. *Metamorphosis*. Oxford: Clarendon, p. 332–359.
- Costa RM, Soto X, Chen Y, Zorn AM, Amaya E (2008). spib is required for primitive myeloid development in *Xenopus*. *Blood.* 112(6):2287–2296.
- Courtet M, Flajnik M, Du Pasquier L (2001). Major histocompatibility complex and immunoglobulin loci visualized by in situ hybridization on *Xenopus* chromosomes. *Dev Comp Immunol.* 25:149–157.
- De Jesús Andino F, Chen G, Li Z, Grayfer L, Robert J (2012). Susceptibility of *Xenopus laevis* tadpoles to infection by the ranavirus Frog-Virus 3 correlates with a reduced and delayed innate immune response in comparison with adult frogs. *Virology.* 432(2):435–443.
- DiMarzo SJ, Cohen N (1982). An in vivo study of the ontogeny of alloreactivity in the frog, *Xenopus laevis*. *Immunology.* 45(1):39–48.
- Du Pasquier L, Weiss N (1973). The thymus during the ontogeny of the toad *Xenopus laevis*: growth, membrane bound immunoglobulins and mixed lymphocyte reaction. *Eur J Immunol.* 3:773–777.
- Du Pasquier L, Chardonnes X (1975). Genetic aspects of the tolerance to allografts induced at metamorphosis in the toad *Xenopus laevis*. *Immunogenetics.* 2:431–440.
- Du Pasquier L, Haimovich J (1976). The antibody response during amphibian ontogeny. *Immunogenetics.* 3:381–391.
- Du Pasquier L, Horton JD (1976). The effect of thymectomy on the mixed leukocyte reaction and phytohemagglutinin responsiveness in the clawed toad *Xenopus laevis*. *Immunogenetics.* 3:105–112.
- Du Pasquier L, Bernard CC (1980). Active suppression of the allogeneic histocompatibility reactions during the metamorphosis of the clawed toad *Xenopus*. *Differentiation.* 16(1):1–7.
- Du Pasquier L, Flajnik MF (1990). Expression of MHC class II antigens during *Xenopus* development. *Dev Immunol.* 1(2):85–95.
- Du Pasquier L, Blomberg B, Bernard CCA (1979). Ontogeny of immunity in amphibians: changes in antibody repertoires and appearance of adult major histocompatibility antigens in *Xenopus*. *Eur J Immunol.* 9(11):900–906.
- Du Pasquier L, Schwager J, Flajnik MF (1989). The immune system of *Xenopus*. *Annu Rev Immunol.* 7:251–275.
- Du Pasquier L, Robert J, Courtet M, Mußmann R (2000). B-cell development in the amphibian *Xenopus*. *Immunol Rev.* 175:201–213.
- Elsdale TR, Fischberg M, Smith S (1958). A mutation that reduces nucleolar number in *Xenopus laevis*. *Exp Cell Res.* 14(3):642–643.
- Enomoto T, Tochinali S (1999). Immune response to self lens in *Xenopus laevis* enucleated during larval life. *Dev Immunol.* 7(1):23–32.
- Evans BJ (2008). Genome evolution and speciation genetics of clawed frogs (*Xenopus* and *Silurana*). *Front Biosci.* 13:4687–4706.
- Flajnik MF, Du Pasquier L (1988). MHC class I antigens as surface markers of adult erythrocytes during the metamorphosis of *Xenopus*. *Dev Biol.* 128(1):198–206.
- Flajnik MF, Du Pasquier L, Cohen N (1985). Immune responses of thymus/lymphocyte embryonic chimeras: studies on tolerance and major histocompatibility complex restriction in *Xenopus*. *Eur J Immunol.* 15(6):540–547.
- Flajnik MF, Kaufman JF, Hsu E, Manes M, Parisot R, Du Pasquier L (1986). Major histocompatibility complex-encoded class I molecules are absent in immunologically competent *Xenopus* before metamorphosis. *J Immunol.* 137(12):3891–3899.
- Flajnik MF, Hsu E, Kaufman JF, Du Pasquier L (1987). Changes in the immune system during metamorphosis of *Xenopus*. *Immunol Today.* 8:58–64.
- Flajnik MF, Hsu E, Kaufman JF, Du Pasquier L (1988). Biochemistry, tissue distribution and ontogeny of surface molecules detected on *Xenopus* hemopoietic cells. In: Miyasaka M, Trnka Z, editors. *Differentiation Antigens in Lymphohemopoietic Tissues*. New York: M. Dekker, p. 387–419.
- Furlow JD, Neff ES (2006). A developmental switch induced by thyroid hormone: *Xenopus laevis* metamorphosis. *Trends Endocrinol Metab.* 17(2):40–47.
- Göbel TW, Meier EL, Du Pasquier L (2000). Biochemical analysis of the *Xenopus laevis* TCR/CD3 complex supports the “stepwise evolution” model. *Eur J Immunol.* 30(10):2775–2781.
- Goyos A, Ohta Y, Guselnikov S, Robert J (2009). Novel nonclassical MHC class Ib genes associated with CD8 T cell development and thymic tumors. *Mol Immunol.* 46(8–9):1775–1786.
- Gravenor I, Horton TL, Ritchie P, Flint E, Horton JD (1995). Ontogeny and thymus-dependence of T cell surface antigens in *Xenopus*: flow cytometric studies on monoclonal antibody-stained thymus and spleen. *Dev Comp Immunol.* 19(6):507–523.
- Green N, Cohen N (1979). Phylogeny of immunocompetent cells. III. Mitogen response characteristics of lymphocyte subpopulations from normal

- and thymectomized frogs (*Xenopus laevis*). Cell Immunol. 48:59–70.
- Greenhalgh P, Olesen CE, Steiner LA (1995). Characterization and expression of recombination activating genes (RAG-1 and RAG-2) in *Xenopus laevis*. J Immunol. 151(6):3100–3110.
- Hadji-Azimi I, Fischberg M (1967). Hématopoïèse périhépatique chez le batracien anoure *Xenopus laevis*. Comparaison entre les individus normaux et les porteurs de tumeurs lymphoïdes. Rev Suisse Zool. 74:641–645.
- Hadji-Azimi I, Cooseman V, Canicatti C, Perrenot N (1987). Atlas of adult *Xenopus laevis* hematology. Dev Comp Immunol. 11:807–874.
- Hellsten U, Harland RM, Gilchrist MJ, et al. (2010). The genome of the Western clawed frog *Xenopus tropicalis*. Science. 328(5978):633–636.
- Horton JD (1969). Ontogeny of the immune response to skin allografts in relation to lymphoid organ development in the amphibian *Xenopus laevis* Daudin. J Exp Zool. 170(4):449–465.
- Horton JD, Manning MJ (1972). The response to skin allografts in *Xenopus laevis* following thymectomy at early stages of lymphoid organ maturation. Transplantation. 14:141–154.
- Horton TL, Horton JD, Varley CA (1989). In vitro cytotoxicity in adult *Xenopus* generated against larval targets and minor histocompatibility antigens. Transplantation. 47(5):880–882.
- Horton JD, Horton TL, Ritchie P (1993). Incomplete tolerance induced in *Xenopus* by larval tissue allografting: evidence from immunohistology and mixed leucocyte culture. Dev Comp Immunol. 17(3):249–262.
- Horton TL, Stewart R, Cohen N, et al. (2003). Ontogeny of *Xenopus* NK cells in the absence of MHC class I antigens. Dev Comp Immunol. 27(8):715–726.
- Hsu E, Du Pasquier L (1984a). Ontogeny of the immune system in *Xenopus*. I. Larval immune response. Differentiation. 28:109–115.
- Hsu E, Du Pasquier L (1984b). Ontogeny of the immune system in *Xenopus* II. Antibody repertoire differences between larvae and adults. Differentiation. 28:116–122.
- Hsu E, Du Pasquier L (1992). Changes in the amphibian antibody repertoire are correlated with metamorphosis and not with age or size. Dev Immunol. 2(1):1–6.
- Inui M, Asashima M (2006). A novel gene, Ami is expressed in vascular tissue in *Xenopus laevis*. Gene Expr Patterns. 6(6):613–619.
- Ishii A, Kawasaki M, Matsumoto M, Tochinai S, Seya T (2007). Phylogenetic and expression analysis of amphibian *Xenopus* Toll-like receptors. Immunogenetics. 59(4):281–293.
- Ishizuya-Oka A (1996). Apoptosis of larval cells during amphibian metamorphosis. Microsc Res Tech. 34(3):228–235.
- Ishizuya-Oka A (2011). Amphibian organ remodeling during metamorphosis: insight into thyroid hormone-induced apoptosis. Dev Growth Differ. 53(2):202–212.
- Ishizuya-Oka A, Hasebe T, Shi YB (2010). Apoptosis in amphibian organs during metamorphosis. Apoptosis. 15(3):350–364.
- Izutsu Y (2009). The immune system is involved in *Xenopus* metamorphosis. Front Biosci. 14: 141–149.
- Izutsu Y, Yoshizato K (1993). Metamorphosis-dependent recognition of larval skin as non-self by inbred adult frogs (*Xenopus laevis*). J Exp Zool. 266(2):163–167.
- Izutsu Y, Maéno M (2005). Analyses of immune responses to ontogeny-specific antigens using an inbred strain of *Xenopus laevis* (J strain). Methods Mol Med. 105:149–158.
- Izutsu Y, Yoshizato K, Tochinai S (1996). Adult-type splenocytes of *Xenopus* induce apoptosis of histocompatible larval tail cells in vitro. Differentiation. 60(5):277–286.
- Kau CL, Turpen JB (1983). Dual contribution of embryonic ventral blood island and dorsal lateral plate mesoderm during ontogeny of hemopoietic cells in *Xenopus laevis*. J Immunol. 131(5):2262–2266.
- Kidder GM, Ruben LN, Stevens JM (1973). Cytodynamics and ontogeny of the immune response of *Xenopus laevis* against sheep erythrocytes. J Embryol Exp Morphol. 29(1):73–85.
- Kobel HR, Du Pasquier L (1975). Production of large clones of histocompatible fully identical clawed toads (*Xenopus*). Immunogenetics. 2:87–91.
- Kobel HR, Du Pasquier L (1986). Genetics of polyploid *Xenopus*. Trends Genet. 2:310–315.
- Kondo M (2010). Lymphoid and myeloid lineage commitment in multipotent hematopoietic progenitors. Immunol Rev. 238(1):37–46.
- Kong F, Chen CH, Cooper MD (1998). Thymic function can be accurately monitored by the level of recent T cell emigrants in the circulation. Immunity. 8(1):97–104.
- Kuraoka M, Liao D, Yang K, et al. (2009). Activation-induced cytidine deaminase expression and activity in the absence of germinal centers: insights into hyper-IgM syndrome. J Immunol. 183(5): 3237–3248.
- Langman RE, Cohn M (1987). The E-T (elephant-tadpole) paradox necessitates the concept of a unit of B-cell function: the protection. Mol Immunol. 24(7):675–697.
- Lee YH, Williams A, Hong CS, You Y, Senoo M, Saint-Jeannet JP (2013). Early development of the thymus in *Xenopus laevis*. Dev Dyn. 242(2):164–178.

- Levine AJ, Munoz-Sanjuan I, Bell E, North AJ, Brivanlou AH (2003). Fluorescent labeling of endothelial cells allows in vivo, continuous characterization of the vascular development of *Xenopus laevis*. *Dev Biol*. 254:50–67.
- Luning Prak ET, Monestier M, Eisenberg RA (2011). B cell receptor editing in tolerance and autoimmunity. *Ann N Y Acad Sci*. 1217:96–121.
- Maéno M, Katagiri C (1984). Elicitation of weak immune response in larval and adult *Xenopus laevis* by allografted pituitary. *Transplantation*. 38(3): 251–355.
- Maéno M, Tochinali S, Katagiri C (1985). Differential participation of ventral and dorsolateral mesoderms in the hemopoiesis of *Xenopus*, as revealed in diploid-triploid or interspecific chimeras. *Dev Biol*. 110(2):503–508.
- Maéno M, Komiyama K, Matsuzaki Y, et al. (2012). Distinct mechanisms control the timing of differentiation of two myeloid populations in *Xenopus* ventral blood islands. *Dev Growth Differ*. 54(2): 187–201.
- Maniatis GM, Steiner LA, Ingram VM (1968). Tadpole antibodies against frog hemoglobin and their effect on development. *Science*. 165(3888):67–69.
- Manning MJ (1971). The effect of early thymectomy on histogenesis of the lymphoid organs in *Xenopus laevis*. *J Embryol Exp Morphol*. 26:219–229.
- Manning MJ, Horton JD (1969). Histogenesis of lymphoid organs in larvae of the South African clawed toad, *Xenopus laevis* (Daudin). *J Embryol Exp Morphol*. 22(2):265–277.
- Manning M, Horton JD (1982). RES structure and function of the amphibia. In: Cohen N, Sigel MM, editors. *The Reticuloendothelial System*, Vol. 3, Phylogeny and Ontogeny. New York: Plenum, p. 424–459.
- Marr S, Goyos A, Gantress J, Maniero GD, Robert J (2005). CD91 up-regulates upon immune stimulation in *Xenopus* adult but not larval peritoneal leukocytes. *Immunogenetics*. 56(10):735–742.
- Marr S, Morales H, Bottaro A, Cooper M, Flajnik M, Robert J (2007). Localization and differential expression of activation-induced cytidine deaminase in the amphibian *Xenopus* upon antigen stimulation and during early development. *J Immunol*. 179(10):6783–6789.
- Marshall JA, Dixon KE (1978). Cell specialization in the epithelium of the small intestine of feeding *Xenopus laevis* tadpoles. *J Anat*. 126:133–144.
- Marx M, Ruben LN, Nobis C, Duffy D (1987). Compromised T-cell regulatory functions during anuran metamorphosis: the role of corticosteroids. *Prog Clin Biol Res*. 233:129–140.
- McLin VA, Hu CH, Shah R, Jamrich M (2008). Expression of complement components coincides with early patterning and organogenesis in *Xenopus laevis*. *Int J Dev Biol*. 52(8):1123–1133.
- Meier E (2003). T cell development and the diversification and selection of the *Xenopus* T cell receptor beta chain repertoire [dissertation]. Edmonton: University of Alberta.
- Mescher AL, Wolf WL, Moseman EA, et al. (2007). Cells of cutaneous immunity in *Xenopus*: studies during larval development and limb regeneration. *Dev Comp Immunol*. 31(4):383–393.
- Miyanaga Y, Shiurba R, Nagata S, Pfeiffer CJ, Asashima M (1998). Induction of blood cells in *Xenopus* embryo explants. *Dev Genes Evol*. 207(7): 417–426.
- Morvan-Dubois G, Demeneix BA, Sachs LM (2008). *Xenopus laevis* as a model for studying thyroid hormone signalling: from development to metamorphosis. *Mol Cell Endocrinol*. 293:71–79.
- Mußmann R, Du Pasquier L, Hsu E (1996). Is *Xenopus* IgX an analog of IgA? *Eur J Immunol*. 26(12):2823–2830.
- Mußmann R, Courtet M, Du Pasquier L (1998). Development of the early B cell population in *Xenopus*. *Eur J Immunol*. 28(9):2947–2959.
- Mukaigasa K, Hanasaki A, Maéno M, et al. (2009). The keratin-related Ouroboros proteins function as immune antigens mediating tail regression in *Xenopus* metamorphosis. *Proc Natl Acad Sci U S A*. 106(43):18309–18314.
- Nagata S (1977). Electron microscopic study on the early histogenesis of thymus in the toad, *Xenopus laevis*. *Cell Tissue Res*. 179(1):87–96.
- Nagata S (2005). Isolation, characterization, and extra-embryonic secretion of the *Xenopus laevis* embryonic epidermal lectin, XEEL. *Glycobiology*. 15(3):281–290.
- Nieuwkoop PD, Faber J (1967). *Normal Table of Xenopus laevis* (Daudin). Amsterdam: North Holland Publishing company.
- Ohinata H, Tochinali S, Katagiri C (1989). Ontogeny and tissue distribution of leukocyte-common antigen bearing cells during early development of *Xenopus laevis*. *Development*. 107(3):445–452.
- Ohinata H, Tochinali S, Katagiri C (1990). Occurrence of nonlymphoid leukocytes that are not derived from blood islands in *Xenopus laevis* larvae. *Dev Biol*. 141(1):123–129.
- Ohta Y, Goetz W, Hossain MZ, Nonaka M, Flajnik MF (2006). Ancestral organization of the MHC revealed in the amphibian *Xenopus*. *J Immunol*. 176(6):3674–3685.
- Ono M, Tochinali S (1995). Demonstration of cells possessing tolerance-inducing activity in *Xenopus*

- laevis* rendered tolerant perimetamorphically. *Transplantation*. 60(1):66–70.
- Pollet N (2010). Expression of immune genes during metamorphosis of *Xenopus*: a survey. *Front Biosci*. 15:348–358.
- Poorten TJ, Kuhn RE (2009). Maternal transfer of antibodies to eggs in *Xenopus laevis*. *Dev Comp Immunol*. 33(2):171–175.
- Qi ZT, Zhang QH, Wang ZS, et al. (2011). Cloning and expression analysis of a long type peptidoglycan recognition protein (PGRP-L) from *Xenopus tropicalis*. *Dongwuxue Yanjiu*. 32(4): 371–378.
- Robert J, Cohen N (1998). Ontogeny of CTX expression in *Xenopus*. *Dev Comp Immunol*. 22(5–6): 605–612.
- Robert J, Ohta Y (2009). Comparative and developmental study of the immune system in *Xenopus*. *Dev Dyn*. 238(6):1249–1270.
- Robert J, Cohen N (2011). The genus *Xenopus* as a multispecies model for evolutionary and comparative immunobiology of the 21st century. *Dev Comp Immunol*. 35(9):916–923.
- Robert J, Guét C, Du Pasquier L (1995). Ontogeny of the alloimmune response against a transplanted tumor in *Xenopus laevis*. *Differentiation*. 59(3):135–144.
- Rollins-Smith LA (1998). Metamorphosis and the amphibian immune system. *Immunol Rev*. 166:221–230.
- Rollins-Smith LA, Cohen N (1982). Self-pituitary grafts are not rejected by frogs deprived of their pituitary anlagen as embryos. *Nature*. 299(5886): 820–821.
- Rollins-Smith LA, Blair P (1990). Expression of class II major histocompatibility complex antigens on adult T cells in *Xenopus* is metamorphosis-dependent. *Dev Immunol*. 1(2): 97–104.
- Rollins-Smith LA, Blair PJ (1993). The effects of corticosteroid hormones and thyroid hormones on lymphocyte viability and proliferation during development and metamorphosis of *Xenopus laevis*. *Differentiation*. 54(3):155–160.
- Rollins-Smith LA, Parsons SCV, Cohen N (1984). During frog ontogeny, PHA and Con A responsiveness of splenocytes precedes that of thymocytes. *Immunology*. 52:491–500.
- Rollins-Smith LA, Parsons SC, Cohen N (1990). Immune responses of intact and embryonically enucleated frogs to self-lens antigens. *J Immunol*. 145(10):3262–3267.
- Rollins-Smith LA, Needham DA, Davis AT, Blair PJ (1996). Late thymectomy in *Xenopus* tadpoles reveals a population of T cells that persists through metamorphosis. *Dev Comp Immunol*. 20(3):165–174.
- Rollins-Smith LA, Barker KS, Davis AT (1997). Involvement of glucocorticoids in the reorganization of the amphibian immune system at metamorphosis. *Dev Immunol*. 5(2):145–152.
- Sadlon TJ, Lewis ID, D'Andrea RJ (2004). BMP4: its role in development of the hematopoietic system and potential as a hematopoietic growth factor. *Stem Cells*. 22(4):457–474.
- Saltis M, Criscitiello MF, Ohta Y, et al. (2008). Evolutionarily conserved and divergent regions of the autoimmune regulator (Aire) gene: a comparative analysis. *Immunogenetics*. 60(2): 105–114.
- Schreiber AM (2011). Visualizing and quantifying the suppressive effects of glucocorticoids on the tadpole immune system in vivo. *Adv Physiol Educ*. 35(4):445–453.
- Schwager J, Grossberger D, Du Pasquier L (1988). Organization and rearrangement of immunoglobulin M genes in the amphibian *Xenopus*. *EMBO J*. 7(8):2409–2415.
- Schwager J, Bürckert N, Courtet M, Du Pasquier L (1989). Genetic basis of the antibody repertoire in *Xenopus*: analysis of the Vh diversity. *EMBO J*. 8(10):2989–3001.
- Schwager J, Bürckert N, Schwager M, Wilson M (1991a). Evolution of immunoglobulin light chain genes: analysis of *Xenopus* IgL isotypes and their contribution to antibody diversity. *EMBO J*. 10(3):505–511.
- Schwager J, Bürckert N, Courtet M, Du Pasquier L (1991b). The ontogeny of diversification at the immunoglobulin heavy chain locus in *Xenopus*. *EMBO J*. 10(9):2461–2470.
- Sisakhtnezhad S, Matin MM (2012). Transdifferentiation: a cell and molecular reprogramming process. *Cell Tissue Res*. 348(3):379–396.
- Smith SJ, Kotecha S, Towers N, Latinkic BV, Mohun TJ (2002). XPOX2-peroxidase expression and the XLURP-1 promoter reveal the site of embryonic myeloid cell development in *Xenopus*. *Mech Dev*. 117(1–2):173–186.
- Soldevila G, Raman C, Lozano F (2011). The immunomodulatory properties of the CD5 lymphocyte receptor in health and disease. *Curr Opin Immunol*. 23(3):310–318.
- Sterba G (1950). Über die morphologischen und histogenetischen Thymus probleme bei *Xenopus laevis* nebst einigen Bemerkung über die Morphologie der Kaulquappen. *Abh Sachs Akad Wiss*. 44:1–54.
- Sterba G (1952). Mitteilung über die Altersinvolution des Amphibien Thymus. I. Volumetrische Bestimmungen am Thymus des Krallenfrosches *Xenopus laevis* Daud. *Anat Anz*. 99:106–114.
- Tashiro S, Sedohara A, Asashima M, Izutsu Y, Maeno M (2006). Characterization of myeloid

- cells derived from the anterior ventral mesoderm in the *Xenopus laevis* embryo. *Dev Growth Differ.* 48:499–512.
- Thiébaud CH (1983). A reliable new cell marker in *Xenopus*. *Dev Biol.* 98(1):245–249.
- Tochinai S (1975). Distribution of lympho-epithelial tissues in the larval African clawed toad *Xenopus laevis* (Daudin). *J Fac Sci Hokkaido Univ Sci.* 6:803–811.
- Tochinai S, Katagiri C (1975). Complete abrogation of immune response to skin allografts and rabbit erythrocytes in the early thymectomized *Xenopus*. *Devel Growth Diff.* 17: 383–394.
- Triplett EL (1962). On the mechanism of immunologic self recognition. *J Immunol.* 89:505–510.
- Wilson M, Hsu E, Marcuz A, Courtet M, Du Pasquier L, Steinberg C (1992). What limits affinity maturation of antibodies in *Xenopus*—the rate of somatic mutation or the ability to select mutants? *EMBO J.* 11(12):4337–4347.
- Wilson M, Marcuz A, du Pasquier L (1995). Somatic mutations during an immune response in *Xenopus* tadpoles. *Dev Immunol.* 4(3):227–234.
- Yanai I, Peshkin L, Jorgensen P, Kirschner MW (2011). Mapping gene expression in two *Xenopus* species: evolutionary constraints and developmental flexibility. *Dev Cell.* 20(4): 483–496.

15 Neural Regeneration in *Xenopus* Tadpoles during Metamorphosis

Mauricio Moreno, Karina Tapia, & Juan Larrain

Department of Cell and Molecular Biology, Centre for Aging and Regeneration, Millennium Nucleus in Regenerative Biology, Faculty of Biological Sciences, Pontificia Universidad Católica de Chile, Santiago, Chile

Abstract: The process of regeneration is quite common in many species. The main difference is each species' regenerative ability. *Xenopus laevis* is a good model to study regeneration, and throughout its lifespan this animal model has different regenerative capacities that vary depending on the tissue or organ. In general, the regenerative capacity of *Xenopus* inversely depends on metamorphosis progression, thus in larval stages the regenerative capabilities are extensive, while the closer to metamorphosis the lesser degree of regeneration is achieved. Nevertheless, there are organs or tissues that do not follow this rule and have the ability to regenerate over lifetime.

So far, several regenerating systems have been studied in *X. laevis* including the tail, limbs, spinal cord, lens, optic nerve, neural retina, and intestine. In this chapter, we focus on neural regeneration during metamorphosis, with emphasis on spinal cord, neural retina, lens and optic nerve. In addition, a brief description is made on telencephalon and mesencephalon regeneration in *Xenopus*. Finally, we also include two well-studied regeneration systems, as limb and tail regeneration after amputation. Although, they are not neural regenerative systems intrinsically, both show in their process of regeneration that they have to rearrange new nerve connections in the regenerates. We describe the relationship between regeneration and nervous connections in these regenerates.

For many years, humans have wondered why only certain species throughout the tree of life are able to regenerate body parts that have been damaged or amputated and other species are not. As early as the 1700s, Trembley, among others, performed pioneering work on Hydra studying its tremendous ability to regenerate (Lenhoff and Lenhoff 1991). One definition published in 2003 describes regeneration as the complete reestablishment, both structural

and functional, of a tissue or structure that has been lost or damaged in postembryonic stages through the reactivation of processes that previously occurred during embryonic development (Gilbert 2003).

Accordingly, the process of regeneration is quite common in many species, with several aspects being conserved, from early cell migration to the signaling pathways involved. The main difference is each species'

regenerative ability. Many mammalian species show limited tissue and organ regeneration while other organisms, such as amphibians, have the remarkable ability to regenerate different tissues and organs (Slack et al. 2008). One of these animals is *Xenopus laevis*, a carnivorous clawed frog originally found in southern Africa, which has the ability to regenerate various organs at certain periods during its lifespan. This property is a consequence of the metamorphosis where a massive transformation takes place involving structural, functional, and behavioral aspects that occur throughout the transition from the larval stage to the adult stage, during which the animal adapts its body to change from an aquatic environment to one with terrestrial features (Nieuwkoop and Faber 1967).

In general, during larval stages, the *Xenopus* tadpole's regenerative capabilities are extensive in several types of tissues. However, as metamorphosis proceeds, this regenerative capacity is lost (Nieuwkoop and Faber 1967; Beck et al. 2009). These very features make *X. laevis* a very good model to study regeneration and improve our understanding of the molecular and cellular mechanisms that allow regeneration, which are switched off during metamorphosis. *Xenopus* has many advantages that make it a powerful model to study regeneration at a cellular and molecular level. It is a standard model used in research, with the *ex utero* developing embryos and the possibility to obtain thousands of offspring throughout the year. The different stages used for regeneration studies are easily reared under established conditions (around 2 months after fertilization to get a juvenile frog) and are well described (Gaete et al. 2012).

In addition, a series of methodologies used in embryonic development can also be used to study regeneration in later stages. For example, the entire cell lineage made by Slack's group describing tail regeneration using embryo transplants from GFP donors to wild-type recipients established how the different tail tissues regenerate after amputation (Gargioli and Slack 2004). Moreover, functional experiments of gain and loss of function can be performed, together with transgenesis. Whole-mount or section *in situ* hybridization is possible with numerous probes available; morpholino oligonucleotide electroporation; there is a UniGene

collection of near to 30,000 *Xenopus* genes and an extensive collection of expressed sequence tags (ESTs); transcriptome analysis can be performed by microarray approaches using the commercially available chips for *X. laevis* and *Xenopus tropicalis*; next-generation sequencing technology is also available to perform transcriptome analysis; the *X. tropicalis* genome sequence has been launched, and the *X. laevis* genome sequencing is due to be released soon. Finally, as the tadpoles and juvenile frogs are raised in an aquatic habitat, it is possible to perform functional experiments using different drugs that could be involved in the regeneration process by direct addition of the drug to the rearing water (Harland and Grainger 2011).

Due to this account of technical reasons, and considering the dependence of its regeneration ability on metamorphosis progression, *X. laevis* currently appears to be a very appealing model to study regeneration. So far, several regenerating systems have been studied in *X. laevis* including the tail, limbs, spinal cord, lens, optic nerve, neural retina, and intestine, among others (see Table 15.1). Considering the topic of this chapter on neural regeneration during metamorphosis, we will be mainly focused on spinal cord, lens, neural retina, and optic nerve regeneration. However, a brief discussion on tail and limb regeneration will be included to understand how these organs are regenerated after amputation and what is the relationship, if any, between regeneration and nervous connections in the regenerates.

Spinal cord regeneration

Throughout the vertebrate subphylum, adult amniotes have lost their regenerative capacity in many tissues. On the contrary, anamniotes such as urodeles have maintained the regeneration capacity throughout their whole lifespan. Otherwise, anurans are an intermediate case, as regenerative capacity is exceptional in larval stages but is lost in adulthood.

The anuran spinal cord is a clear example of their regenerative capabilities. During larval stages before metamorphosis, these animals regenerate the spinal cord after damage and achieve complete functional recovery at a high rate. Nevertheless, after metamorphosis, either

Table 15.1 Regeneration ability of *X. laevis*.

Organ or tissue	Regeneration in larval stages	Regeneration after metamorphosis	Source of progenitor cells	References
Spinal cord	Yes	No	Sox2+ ependymal cells	Gaete et al. (2012)
Lens	Yes	Yes	Outer cornea cells (larvae) Unknown (adults)	Freeman (1963); Filoni et al. (1997), and Yoshii et al. (2007)
Neural retina	Yes	Yes	Retinal pigmented epithelial cells and CMZ cells	Sakaguchi et al. (1997); Vergara and Del Rio-Tsonis (2009); and Yoshii et al. (2007)
Optic nerve	Yes	Yes	Retinal ganglion cells	Zhao and Szaro (1997); Sedohara et al. (2003)
Tail	Yes	NA	Sox2+ cells (spinal cord) Pax7+ satellite cells (muscle) Unknown (notochord)	Gargioli and Slack (2004); Chen et al. (2006); Gaete et al. (2012)
Limb	Yes	No/partial	ND	Christen and Slack (1997); Endo et al. (2000); Yokoyama et al. (2001) Lin et al. (2013)
Telencephalon	Yes	No	ND	
Mesencephalon	Yes	No	Ventricular zone cells	Sharma and Cline (2010); Bestman et al. (2012); McKeown et al. (2013)

Summary of regeneration before or after metamorphosis in different organs or tissues. The fourth column shows the possible progenitor cells that allow regeneration according to the literature. NA, not applicable; ND, not determined.

in juvenile or adult stages they are not able to regenerate the spinal cord after injury, remaining irreversibly paraplegic. Regenerative abilities have been associated for many years to metamorphosis. As metamorphosis elapses, the ability to regenerate is lost in many tissues (Sims 1962; Filoni et al. 1984; Beattie et al. 1990; Gaete et al. 2012). Figure 15.1 depicts the different stages mentioned from premetamorphosis larval stages (46–54), along with prometamorphosis stages (54–58), to metamorphosis climax stages (58–66) according to Nieuwkoop and Faber (1967).

In 1962, it was described that spinal cord transection between the fifth and sixth neural arches in stage 56 tadpoles did not show any apparent change in the transection site, except

for an increase in the number of axons. At that time, this demonstrated that axonal regeneration is not limited by local changes. Moreover, it was observed that Mauthner axons and the main axons of primary motoneurons do not regenerate (Sims 1962). Mauthner cells are located in the hindbrain and activate fast-start response in most swimming vertebrates, particularly fish and amphibians, for escaping from predatory attacks. Each Mauthner cell has an axon running down the length of the spinal cord on the opposite site of the soma (Fetcho 1991; Eaton et al. 2001). Nevertheless, 20 years later, Lee demonstrated that *Xenopus* tadpoles ranging from stages 46 to 56 are indeed able to regenerate the Mauthner axons after spinal cord transection, suggesting that

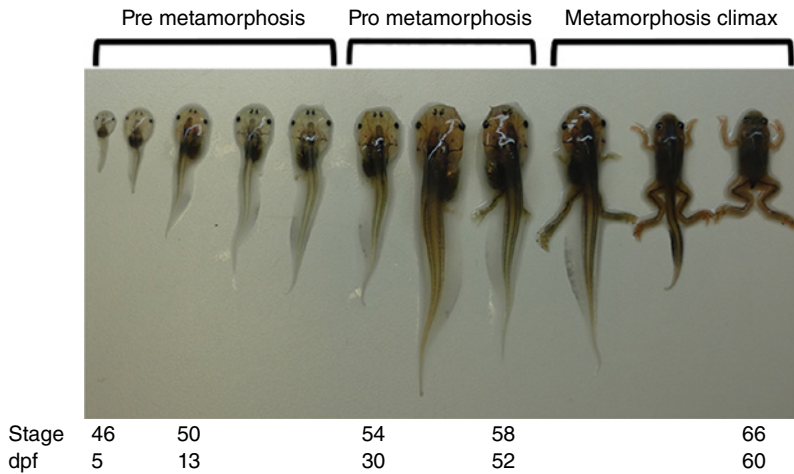


Figure 15.1 *X. laevis* metamorphosis stages. Schematic representation of *X. laevis* metamorphosis from premetamorphosis stages (46–54) where one of the main features is limb bud growth; prometamorphosis stages (54–58) where hind limb growth is observed; and metamorphosis climax stages (58–66) where tail reabsorption occurs among other changes. It is important to note that as metamorphosis proceeds, the regeneration ability is lost. Embryos are cultured at 22° for the indicated days postfertilization (dpf) to reach different stages until metamorphosis is completed.

the return to a normal function could be due to the reconnection of a regenerating neuron with its normal targets (Lee 1982).

By 1979, experiments performed using *X. laevis* tadpoles from stages 54 to 56 demonstrated that after a complete transection of the spinal cord between the seventh and ninth body segments, cell aggregates comprised of ependymal cells occupy the lesion space. It is also possible to observe neurite extensions and resettlement of longitudinal axons surrounded by glia (Michel and Reier 1979). Experiments show that after a complete transection of the spinal cord in *Xenopus* tadpoles' stages 51–53, the swimming activity is restored showing recovery 1 week after the spinal cord injury. Microscopy allowed observing the growth of serotonergic axons through the lesion, filling the gap between both spinal cord stumps (Filoni et al. 1984; Beattie et al. 1990; Gibbs et al. 2011; Gaete et al. 2012).

Due to this inverse correlation between regenerative capacity and ongoing metamorphosis, some experiments have been performed using compounds that alter metamorphosis to evaluate the tadpoles' regenerative capacity. Researchers have used triiodothyronine (T3), a thyroid hormone that stimulates metamorphosis, and methimazole,

an inhibitor of metamorphosis by inhibition of synthesis of thyroid hormones. The results showed that when metamorphosis is accelerated by T3, the capacity to regenerate the spinal cord after transection diminishes considerably. On the contrary, the animals that were transected and treated with methimazole were able to regenerate axons across the lesion and partially seal off the gap when metamorphosis was arrested (Gibbs et al. 2011).

Recent research suggests that after spinal cord transection at the level of the thoracic vertebrae region of stage 50 tadpoles, ependymal cells might be capable of migration to the lesion site allowing regeneration. The novelty here is that ependymal cells express Sox2, a transcription factor present in neural precursor cells. Sox2+ cells proliferate and might migrate to the gap forming cellular aggregates involved in the spinal cord regeneration process (see Figure 15.2). Transgenic animals bearing a predicted form of a dominant-negative Sox2 show a decreased proliferation of spinal cord cells and disrupted both spinal cord and tail regeneration after injury. Another important point is that Sox2 levels change as metamorphosis is occurring, which results in a decrease of Sox2+ cells in nonregenerative stages (stage 66 postmetamorphosis) (Gaete et al. 2012; see

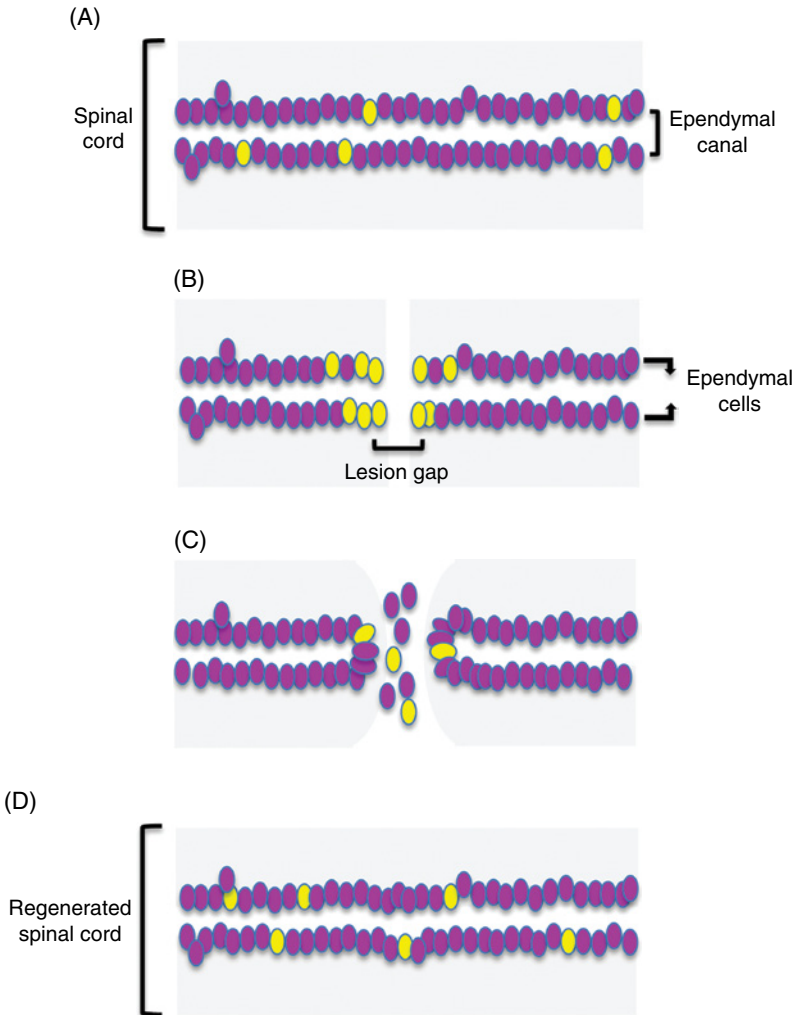


Figure 15.2 Spinal cord regeneration. This diagram shows the main events after spinal cord injury until regeneration is complete in *X. laevis* tadpoles (stage 50). (A) Longitudinal view of spinal cord highlighting the ependymal canal and the ependymal cells facing it. The black staining depicts Sox2+ cells and Sox2+ plus BrdU+ staining is shown in white. (B) Transection of the spinal cord. Two days after the lesion, there is a massive proliferation of cells and many of them are Sox2+ and BrdU+ and surround both stumps. (C) Rostral and caudal stump closure. The stumps begin to close from day 2 until day 10 after the injury. Different kinds of cells fill the gap, Sox2+ cells together with Sox2+/BrdU+ and others could migrate to the ablation gap. These cells form a substrate that allows the meeting of both stumps and the crossing of axons. (D) Regenerated spinal cord. The spinal cord is able to regenerate around 20–30 days after the injury. The drawing shows the restoration of the spinal cord containing a normal ependymal canal, ependymal cells, and Sox2 expression along the cord. Source: Based on Gaete et al. (2012) and unpublished results from our laboratory. To see a color version of this figure, see Plate 38.

Table 15.1). Accordingly, the downregulation of Sox2 is correlated with the decline of the regenerative capacity as *X. laevis* reaches metamorphosis. These results could suggest that these Sox2+ cells migrate to the lesion site to support axonal regeneration. In fact, Gibbs

and Szaro have demonstrated, by sequential retrograde double labeling using fluorescent dextran amines, that axonal regrowth contributes to functional recovery of stage 58/59 tadpoles hemisected between the fourth and fifth vertebrae (Gibbs and Szaro 2006).

Lens regeneration

One of the best-characterized models of lens regeneration is that of adult newts, in which the new lens is formed from pigmented dorsal iris cells – a well-known process called Wolffian regeneration after G. Wolff, who described this regeneration in 1895 (Tsonis et al. 2004; Tsonis 2006). This kind of regeneration does not occur in *Xenopus*. In 1963, Freeman described a different mechanism in *Xenopus* larvae where the new lens is formed by transdifferentiation of cells from the outer cornea (Freeman 1963). Much like *Xenopus*' general regenerative capabilities, regeneration of the lens is also dependent upon the developmental stage. Hence, only larvae are able to regenerate the lens after removal from the inner layer of the outer cornea (Freeman 1963; Filoni et al. 1997). This regenerative capacity decreases from stage 50 to juvenile frogs, when it completely disappears (Freeman 1963, Table 15.1). Regeneration occurs through transdifferentiation of the outer cornea epithelium to lens cells. The factor responsible for this is presumably produced by the neural retina and secreted to the vitreous chamber (Reeve and Wild 1981; Filoni et al. 1982; Bosco et al. 1997a) (see Figure 15.3). The decline in the *Xenopus* tad-

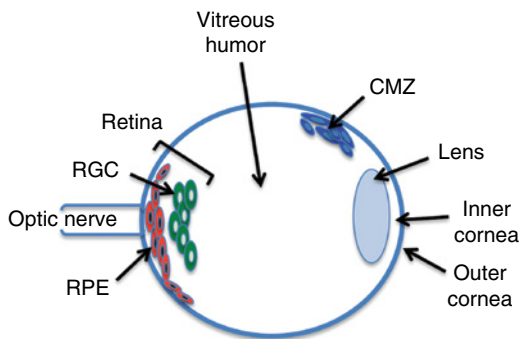


Figure 15.3 Representation of a *X. laevis* eye. This figure depicts a diagram of the different structures and type of cells important for the regeneration process in *X. laevis*. Some of the cells that belong to the layered retina are represented here: retinal pigment epithelium (RPE) and retinal ganglion cells (RGCs). The CMZ cells are shown almost adjacent to the lens. The inner and outer cornea is also shown, with the optic nerve to the left and the vitreous humor filling the white space. To see a color version of this figure, see Plate 39.

poles' regenerative capacity as animals reach metamorphosis could be a result of a rapid closure of the inner cornea. This was suggested by performing cornea grafts free of inner cornea from adult animals (postmetamorphosis) into larval eyes in which the implants were able to form lens fibers (Filoni et al. 1997).

It has been demonstrated that a related species, *X. tropicalis*, is able to regenerate the lens through transdifferentiation. Using a transgenic line expressing GFP under the $\gamma 1$ -*crystallin* promoter, Henry and colleagues showed that, unlike *X. laevis*, the process of transdifferentiation occurs at a lower frequency due to a much higher rate of inner cornea healing. This healing forms a barrier that prevents the signals secreted by the neural retina to reach the outer cornea (Henry and Elkins 2001). In fact, when the lens is replaced by a physical barrier (Millipore™ filter), the cornea transdifferentiation does not take place, showing that mechanical interference of the contact between the soluble vitreous factor and the outer cornea precludes regeneration (Cioni et al. 1982). The molecular nature of these signals has not been obtained, but it has been demonstrated *in vitro* that the outer cornea cultured in the presence of FGF-1 activates a transdifferentiation process in which lens fibers are obtained (Bosco et al. 1997a, b). Nevertheless, the FGF molecular mechanism has not been fully elucidated, although it has been shown to be independent of its mitogenic activity, as the presence of an inhibitor of DNA replication and cell proliferation does not prevent the activity of FGF over isolated outer cornea (Bosco et al. 1997b).

Aside from FGF, it has been demonstrated that conservation of gene expression between the process of transdifferentiation and embryonic lens formation exists. Analyzing the expression by *in situ* hybridization of genes known to be involved in embryo lens induction (Schaefer et al. 1999) or by making a subtraction cDNA library for genes involved in cornea-to-lens transdifferentiation (Henry et al. 2002), it has been established that some genes such as *pax6*, *otx2*, *sox3*, *prox1*, and $\gamma 6$ -*cry* are expressed during both embryonic lens formation and cornea-to-lens transdifferentiation. A few years ago, one study demonstrated

that the lens regeneration competence is specifically associated to a localized *pax6* expression in the lentogenic area and, importantly, a misexpression of *pax6* in flanking epidermis allows transdifferentiation of this noncompetent tissue into lens in response to the vitreous factor (Gargioli et al. 2008).

All of these genes have been described to participate in newts during both embryonic development and regeneration of the lens, including FGF ligands and receptors (Del Rio-Tsonis et al. 1997, 1999).

Finally, there is one important study that was performed in mature *X. laevis* (aged 3–9 months after metamorphosis). This analysis showed that regeneration of the lens after removal could be achieved in a mature animal instead of the previously established facts. Thus, 80% of the lens regenerated at a quicker rate and to a better quality when the neural retina was not removed. This suggested the involvement of a retinal factor for the lens to regenerate. In this way, the lens regeneration percentage is reduced to 50 when both the lens and neural retina are surgically removed. Additionally, 5 days following the operation, a lenslike structure was observed by immunocytochemical detection using a lens crystalline antibody. By day 30 after removal, the regenerated lens was almost identical to the intact lens (Yoshii et al. 2007). The authors do not have any evidence about the source of cells from which the regeneration occurs, but they suggest that remaining lens cells after surgery could proliferate and differentiate into lens fibers and reconstitute the whole structure. If this were the mechanism, there would not have been transdifferentiation but rather a repair mechanism similar to the one described in rabbits (Gwon et al. 1990; Gwon et al. 1993; Yoshii et al. 2007) (Table 15.1).

To date, no functional studies have been conducted to explore how transcriptional factors induced by lentectomy are modulated and how the transdifferentiation process is regulated. Additionally, the nature of the vitreous factor is unknown, and so, it is crucial to understand how this factor, together with *pax6*, first triggers the dedifferentiation process of corneal cells and then the proliferation and transdifferentiation. These steps are possibly modulated by the transcription factors

induced and/or other factors not described yet in order to finally regenerate the complete lens structure (Yoshii et al. 2007).

Neural retina regeneration

Regeneration of the retina in amphibians takes place by transdifferentiation of the retina pigmented epithelial (RPE) cells in a very limited period during early development. As adults, some urodeles (newts) are able to regenerate the retina by transdifferentiation (Mitashov 1997). Other adult amphibians regenerate the retina partially from precursors located in the ciliary marginal zone (CMZ), or other regions of the retina, or the Müller glia cells (Mitashov 1997; Reh and Levine 1998) (see Figure 15.3).

In the case of *X. laevis* tadpoles, it has been demonstrated that RPE cells cultured *in vitro* in the presence of FGF-2 transdifferentiate into neural retina. The RPE cells are able to originate new retina including neurons and photoreceptors and FGF-2 can stimulate the production of retinal glial cells from RPE (see Figure 15.3). These results are possible only if RPE cells are growing in suspension; any adhesion to the substrate prevents transdifferentiation. The transplant of these RPE cells into a lentectomized eye of *Xenopus* at larval stages demonstrated that RPE cells transdifferentiate to regenerate into neurons and glia. Conversely, when the transplant was performed into an empty eye or enucleated orbit, regeneration was prevented, indicating that transdifferentiation depended on the presence of certain factors secreted by the remaining retina (Sakaguchi et al. 1997). Evidence shows that FGF-2 acts through the activation of the MAPK signaling pathway during retina regeneration in *X. laevis* tadpoles. A heparin-coated bead soaked in FGF-2 transplanted into an eye where the neural retina was removed was able to induce neural retina regeneration *in vivo*, and when assessed, the regenerated tissue was positive for neural markers and was able to form an optic nerve (Vergara and Del Rio-Tsonis 2009).

On the other hand, it was well established that the only amphibians able to regenerate the neural retina at adult stages were the

urodele amphibians (as newts). Nevertheless, it has been demonstrated that even post-metamorphic *X. laevis* animals can regenerate the neural retina after removal. The neural retina regenerates by transdifferentiation from the RPE cells and by differentiation of stem cells from the CMZ (see Figure 15.3 and Table 15.1). In addition, RPE cells from adult animals are able to transdifferentiate to neural cells under *in vitro* culture conditions. These neural cells express specific neural markers such as acetylated tubulin and neurofilament, and this response is stimulated when the growth factors FGF-2 and IGF-1 are included in the culture media (Yoshii et al. 2007).

Optic nerve regeneration

Central nerve regeneration is an important issue in terms of recovery of function after damage. The optic nerve contains essentially one kind of axons that arise from a single neuronal population, the retinal ganglion cells (RGCs), and project via the optic nerve to the visual centers of the brain (see Figure 15.3). In the *X. laevis* optic nerve, axonal outgrowth is in synchrony with development. These features make the *X. laevis* optic nerve a very well-studied model since its regeneration capacity is maintained throughout life (Taylor et al. 1989). This is a distinctive feature compared to the regeneration of the spinal cord, lens, retina, tail, or limb in *X. laevis*, which are almost confined to the tadpole stages, and does not occur postmetamorphosis or in adult stages (Tanaka and Ferretti 2009) (see Table 15.1).

It has been shown *in vitro* that myelin and oligodendrocytes of the optic nerve of *X. laevis*, unlike the ones derived from the spinal cord, are permissive for axonal growth (Lang et al. 1995). Regeneration of the optic nerve requires the activation of specific genes involved in axonal growth. Gervasi and colleagues have found that the expression of different neurofilament (NF) mRNAs is increased after optic nerve damage (Gervasi et al. 2003). Two of these genes, GAP-43 and the medium neurofilament NF-M, have a role in facilitating regeneration. Decreasing the expression of NF decreases axon elongation in both developing and regenerating axons (Walker et al. 2001),

and the overexpression of GAP-43 induces axonal outgrowth and enhanced arborization (Leu et al. 2010). Recently, it has been demonstrated that the RNA binding protein heterogeneous nuclear ribonucleoprotein K (hnRNPK) is essential in *X. laevis* for optic axon regeneration and for efficient nuclear export and translation of growth-associated transcripts (Liu et al. 2012). Previously, it was shown that hnRNPK was able to bind both GAP-43 and NF-M mRNAs (Liu and Szaro 2011). On the other hand, it has been established that another filament protein, xefiltin, a *X. laevis* neuronal intermediate filament nIF protein, is highly expressed in RGCs and is important both during optic nerve development and during optic axon regeneration (Zhao and Szaro 1997).

A significant paper published by Sedohara and colleagues showed that they are able to induce eye formation *in vitro* using *X. laevis* early gastrula and late blastula embryo explants. Dorsal lip and lateral marginal zone (LMZ) isolated from early gastrulae were sandwiched between two sheets of animal caps from late blastulae and cultured until the control sibling embryos reached the stage 42. At this time, the explants observed directly under a stereomicroscope showed the lens and RPE structures visible in the *in vitro* obtained eye. Hematoxylin and eosin staining showed that lens, neuroretinal layer, and RPE were similar to a normal eye. Further characterization using RT-PCR showed that only the explants obtained in this form were able to express β -crystallin, a marker gene for mature lens. Furthermore, electron microscopy analysis of the *in vitro* obtained eye demonstrated the presence of differentiated cells such as rod photoreceptor and lens cells. The rod photoreceptor cells contained the inner and outer segments as a normal eye (Sedohara et al. 2003).

To trace the lineage of the graft into the recipient tadpole, Sedohara and colleagues injected two cell embryos with Texas Red dextran amine (TRDA), using the labeled explants to obtain an *in vitro* eye until the sibling embryos reached the stage 33. They then transplanted the *in vitro* obtained eye into a sibling recipient stage 33 tadpole where one normal eye was surgically removed, including the optic vesicle, the lens vesicle,

and the optic stalk. The TRDA signal was only observed in the grafted side. The following day, all the grafted eyes had rooted to the host tadpole. Fifteen days after the transplant, when the tadpole reached the stage 50, the grafted eye had connected properly to the recipient. Observation at high magnification showed that a structure similar to an optic nerve had originated from the transplanted eye. The TRDA signal was only present in the transplanted side and in the respective optic nerve, indicating that this structure was generated exclusively from the grafted eye. After that, electron microscopy confirmed that the fiber extending from the grafted eye was structurally an optic nerve.

One month after the graft, 60% of the transplanted eyes remained in the host tadpoles. Then, the animals reached metamorphosis and became juvenile frogs with the grafted eye settled in only 20% of the hosts. The grafted eyes strongly resembled the host's eye after metamorphosis (Sedohara et al. 2003).

To study the connection of the new optic nerve, Sedohara and colleagues used DiI labeling (a lipophilic fluorescent stain for cell membranes and other hydrophobic structures showing orange fluorescence) and demonstrated that the new optic nerve was able to make the right connections and reached the tectum of the host tadpole, showing a normal retinotectal projection. Finally, they investigated the functionality of the grafted eye and found that animals were also able to sense light variations, demonstrating that grafted eyes were functional (Sedohara et al. 2003).

Role of neural regeneration during tail regeneration

The *Xenopus* tadpole tail is derived from the embryonic tail bud and trunk tissue from the posterior part of neurula. It consists of different tissues that include muscle, notochord, skin, vertebrae, and spinal cord, among others (Tucker and Slack 1995). Each one of these structures is organized in a particular way and plays an important role during development and regeneration. The tail muscle is segmented and flanks the spinal cord and vertebral column (Gargioli and Slack 2004).

Tadpole tails can regenerate after amputation from stage 40 until stage 60 where the metamorphosis climax is reached and the tail is reabsorbed (Filoni and Bosco 1981). Nevertheless, a so-called refractory period from stages 46 to 47/48 is the exception to this continuous tail regeneration activity. In this refractory period, any tail tissue is unable to regenerate after amputation and the wound is only covered by skin (Beck et al. 2003).

After tail amputation, epidermal cells migrate to cover the wound with an epithelial layer; subsequently, the spinal cord stump closes to generate a neural ampulla (first described in 1957 by Stefanelli) (Slack et al. 2008), the notochord develops a bullet-shaped mass of cells, and the muscle fibers at the cut end tend to degenerate (Gargioli and Slack 2004; Slack et al. 2008). Undifferentiated mesenchyme-like cells accumulate around the neural ampulla and bullet-shaped notochord forming the regeneration blastema. In almost 20 days, the tadpole tail completely regenerates (Gargioli and Slack 2004).

Many molecular signaling pathways have been described in tail development, and similar pathways are activated back in the regeneration process. For example, Notch and Wnt pathways participate both in the development and regeneration of the tail and other tissues (Beck and Slack 1998; Beck and Slack 1999). But not all the developmental pathways are reactivated in tail regeneration. That is the case of *sonic hedgehog* (*shh*), which is not expressed in the tail blastema or tissue regenerates, although its function in the patterning of the developing neural tube is well known. Besides, *shh* is normally expressed in the floor plate of the ventral neural tube; thus, its absence in the tail regenerate might imply a deficient spinal cord patterning (Sugiura et al. 2004).

Fate mapping analysis of tail regeneration performed by Slack's group using transgenic animals expressing GFP established the origin of the three main axial structures in the regenerated tail. Results demonstrated that the spinal cord solely regenerates from the spinal cord stump, while the notochord does so from the notochord stump. For muscle it was demonstrated that regeneration occurs from satellite cells positive for *pax7* expression (Gargioli and Slack 2004; Chen et al. 2006).

Importantly, even though the mechanisms of regeneration are different for spinal cord/notochord and muscle, there is no transdifferentiation of any tissue or cell type into another, as seen in urodeles and the *Xenopus* lens and retina (Echeverri et al. 2001; Gargioli and Slack 2004; Chen et al. 2006; Slack et al. 2008).

In *Xenopus*, the regenerated tail is not a perfect copy of the original one. For example, the muscle tissue that regenerates from satellite cells is not as obviously segmented as it was before amputation (Lin et al. 2007; Slack et al. 2008; Rodrigues et al. 2012), and regeneration of neural crest cell derivatives after is also incomplete (Lin et al. 2007). Among the main neural crest derivatives are pigment cells, with melanophores being the most prominent. It has been established that after tail amputation these cells are formed from unpigmented precursors and not from the spinal cord or skin mesenchyme cells (Lin et al. 2007) (see Table 15.1).

The second derivative of the neural crest cells are the spinal ganglia or dorsal root ganglia that contain a condensation of cell bodies of sensory neurons entering the spinal cord on each spinal nerve with associated glia (An et al. 2002). The *Xenopus* spinal nerves follow the primitive pattern that is one pair of nerves per one myotome (Nishikawa and Wassersug 1988). After tail amputation, spinal ganglia are almost completely missing and the normal segmented pattern of spinal nerves is not established in the regenerated tail, although extramedullary sensory neurons may be present (Filoni and Bosco 1981; Lin et al. 2007; Slack et al. 2008). Nevertheless, the regenerated tail contains some sensory innervation because there are dorsally located neurons in the regenerated spinal cord. The authors performed *in situ* hybridization to analyze the expression of p75 neurotrophin receptor (p75NTR) and Brn3a, a transcriptional factor acting in sensory neurons. Both marker genes, p75NTR and Brn3a, are expressed in dorsal root ganglia in normal tails and in a lateral position in the regenerated spinal cord (Lin et al. 2007).

There is a network of innervation detected by antibody staining and retrograde labeling with DiI. To study the arrangement of fiber tracts and neuronal cell bodies, Lin and colleagues performed immunostaining for β -III-tubulin, which is specific for neurons.

The results showed in a lateral view that the segmental pattern of axons seen in a normal tail is not observed in the regenerated tail and that the axons innervating it arrive from areas more anterior to the amputation level. Transverse sections showed quite similar fiber tracts between the wild-type spinal cord and the regenerated one (Lin et al. 2007). Additionally, Lin and colleagues studied the expression of Hu, a neuron-specific protein belonging to the neuron-specific family of RNA binding proteins in vertebrates, to confirm the presence of neurons. Positive signal shows some neurons located dorsally which may be sensory neurons, and others that are located ventrally or laterally corresponding probably to motor neurons (Lin et al. 2007).

When the regenerated tadpoles are touched, they swim to escape, suggesting the presence in the regenerated tail of sensory innervation. They confirmed this fact by immunostaining against the 200 kDa neurofilament showing the presence of peripheral axons in the regenerated tail. Moreover, retrograde labeling with DiI injected directly under the skin indicated that the regenerated tail is innervated with sensory fibers (Lin et al. 2007).

All the previous studies show that, regardless of the great reduction in dorsal root ganglia, there is abundant sensory innervation in the regenerated tail. There are both sensory and motor neurons in the regenerated tail and probably the axons present in the regenerate come from neurons in the stump (Lin et al. 2007).

On the other hand, Gaete and colleagues have recently shown that the spinal cord has a very important role in tail regeneration in accordance with previous findings by Taniguchi and coworkers (2008). The overexpression of a dominant-negative Sox2 has a role on the complete tail regeneration, affecting all tail tissues including notochord and muscle, regardless of specific Sox2 expression in the spinal cord. In addition, it has been found that the induction of *sox2* transcript precedes the expression of *Xbra*, a notochord progenitor marker, and BrdU incorporation in spinal cord cells is upregulated before than notochord and mesenchyme cells. In addition, the down-regulation of Sox2 expression mainly affects the proliferation of spinal cord cells but also

has an effect on BrdU incorporation into notochord cells. Therefore, it appears that the regeneration of the spinal cord commands and is the initial step for the regeneration of the other tail tissues (Gaete et al. 2012) (see Figure 15.2).

Role of neural regeneration during limb regeneration

X. laevis is able to regenerate its limbs depending on the developmental stage. It is important to note that limb regeneration capacity is remarkable during early stages of development. However, this capacity is gradually lost while the animal enters metamorphosis (Dent 1962). This decline starts when the tadpoles reach the stage 53, determining that the tadpole is unable to regenerate the toes and postmetamorphic juvenile frogs only produce unsegmented cartilaginous spikes rather than a proper limb (Tschumi 1957; Dent 1962; Maden 1981) (see Table 15.1).

It has been demonstrated that hind limb amputation at stages 55/56/57 is correlated with the reexpression of xFGF-8 in the distal epidermis for successful limb regeneration (Christen and Slack 1997). Hind limb buds from stages competent for regeneration are formed of mostly undifferentiated mesenchyme cells surrounded by epidermis. Yokoyama and colleagues using recombinant limbs showed that the regenerative capacity resides in the mesenchyme by fusing mesenchyme to epidermis using both regenerative stage 52 and nonregenerative stage 56 limbs. Only the competent mesenchyme was able to induce the expression of FGF-8 in the nonregenerative stage epidermis allowing regeneration to proceed. In the opposite situation, the regenerative epidermis was not able to induce the nonregenerative mesenchyme, and as a consequence, these limbs could not regenerate. The authors demonstrated that mesenchyme regenerative capacity is related to the expression of FGF-10 (Yokoyama et al. 2000). Then, by successfully performing functional experiments, Yokoyama and colleagues showed that FGF-10 certainly is responsible for mesenchyme regenerative capacity. By inserting FGF-10 protein-soaked

beads into the stump of a nonregenerative limb (stage 56), some regeneration activity was shown. In addition, FGF-10 beads were able to induce the expression of *shh*, *msx1*, and endogenous *fgf-10* in nonregenerative mesenchyme, lengthening the period of regeneration competence to later stages (Yokoyama et al. 2001).

Amputated larval forelimbs tend to regenerate better than hind limbs (Endo et al. 2000). However, experiments performed in juvenile frogs (stage 60) demonstrated that after amputation of the forelimb, a fibroblast pseudoblastema is formed which is called a fibroblastema. The fibroblastema grows and differentiates asymmetrically increasing the number of cartilaginous cells and losing connective tissue and muscle (Korneluk and Liversage 1984). The regenerative capacity of forelimbs in juvenile frogs is much more limited generating a hypomorphic spike equivalent to the structures generated after amputation of hind limbs in postmetamorphic stages (Dent 1962).

Recently, Lin and colleagues demonstrated that limb regeneration could be induced in juvenile frogs. The authors transplanted larval progenitor cells obtained from stage 53 tadpoles, onto the cut limb surface, embedded in a fibrin matrix. By using transgenic animals bearing an inducible stabilized β -catenin, Lin and colleagues discovered that Wnt signaling is necessary for successful regeneration (Lin et al. 2013) (see Table 15.1).

Apart from Wnt/ β -catenin, additional factors required for growth, survival, and patterning information such as FGF-10, Shh, and thymosin β 4 were also used. With all these factors present, the larval limb graft was shown to allow regeneration of the postmetamorphic frog forelimb. Considering that host cells do not have endogenous regeneration competence, it is noteworthy that the regenerated limb was formed by cells derived from both graft and host. It is important to observe that neither the additional factors used nor β -catenin are sufficient to support partial regeneration when used separately, and that only larvae limb progenitor cells are able to promote this process. Importantly, other experiments show that regenerated limbs are segmented, express Gdf5 (a joint

marker), contain muscle tissue, and are ossified and innervated (Lin et al. 2013).

Nerve regeneration was demonstrated by immunofluorescence staining using a β -tubulin III antibody. This staining showed profuse innervation and nerve bundles in the limb regenerate. In the same way, these results were confirmed by histological analyses using hematoxylin and eosin staining. Moreover, transmission electron microscopy images of limb regenerate showed the presence of multiple small myelinated axons (2–5 μ m) and, when observed at a higher magnification, an axon with numerous closely packed myelin lamellae. These limbs are functional and animals are able to eat normally by grabbing food when compared to spike-bearing controls (Lin et al. 2013). Considering this important new data, the question of how a structurally and functionally normal regenerated limb in an adult individual can be connected or reconnected to the nervous system remains unanswered. Is there neurogenesis or axonogenesis or axonal regrowth in the amputation region? These important issues remain to be addressed.

As has been evidenced, almost all available data for limb regeneration in *Xenopus* lacks the information regarding neural regeneration, and it has been focused mostly on the appendage regeneration. It has been established that in urodeles limb regeneration is nerve dependent and the success of regeneration depends on some trophic factors released by the cut axons in the limb (Brockes 1984; Brockes 1987). In *Xenopus* regeneration-competent tadpoles, a nerve dependency for limb regeneration has not been found (Filoni and Paglialunga 1990; Cannata et al. 2001; Kumar and Brockes 2012). Nevertheless, the formation of a hypomorphic spike in postmetamorphic juvenile frogs seems to be nerve dependent. Actually, when the forelimbs of froglets are denervated, regeneration is obstructed and the expression of FGF-8 in epidermis and *msx-1* in the blastema both are nerve dependent (Endo et al. 2000; Suzuki et al. 2005).

Telencephalon and mesencephalon regeneration

Although not treated in detail in this chapter, it is important to mention two other brain

structures that have been studied in the context of regeneration in *X. laevis*: the telencephalon, a brain structure that processes olfactory information in frogs (Yoshino and Tochinali 2004), and the optic tectum of the mesencephalon (Endo et al. 2007).

First, it has been shown that the telencephalon regenerates only during larval stages, with *Xenopus* tadpoles from stages 47 to 53 having a high regenerative capacity when a massive part of the telencephalon is ablated, unlike the adults, which lose such ability. Regeneration of the telencephalon requires the reconnection with the olfactory nerves to reform the olfactory bulb, a process that takes around a month producing an almost normal structure in morphology, types of cells and their distribution, and connection between neurons (Yoshino and Tochinali 2004; Yoshino and Tochinali 2006) (see Table 15.1).

Second, the regeneration ability of the optic tectum in *X. laevis* is reduced as the tadpole reaches metamorphosis. As described for the telencephalon, it is likely that regeneration of the optic tectum also requires neural connection for regeneration. It has been shown that in the absence of optic nerve innervation the optic tectum regeneration is impaired (Endo et al. 2007). Neurogenesis in the optic tectum occurs in the ventricular zone during larval stages of *X. laevis*; additionally, the same ventricular zone is activated for proliferation after injury (Straznicki and Gaze 1972; Endo et al. 2007). It has been shown that these proliferative cells differentiate into neurons and are included into the retinal circuit (Gaze et al. 1979). Recently, Cline's laboratory demonstrated that cell proliferation and differentiation of progenitor cells in the optic tectum are regulated by visual system input to the tectum (Sharma and Cline 2010; Bestman et al. 2012).

Moreover, this group has demonstrated that after partial ablation of the optic tectum in stage 47 *X. laevis* tadpoles, new neurons are generated after injury, as proved by *N*- β -tubulin immunostaining. These neurons are generated from tectal progenitor cells that proliferate after the lesion and are recognized by a positive immunolabeling for phosphohistone H3 and Musashi, an RNA binding protein that is enriched in neural progenitor cells. Moreover, *in vivo* imaging

showed that Sox2+ neural progenitors differentiate into new neurons with complex dendritic arbors. Additionally, McKeown and colleagues demonstrated that inhibition of cell proliferation impairs recovery from injury and, more importantly, that behavioral recovery is enhanced by changes in visual experience that stimulates progenitor cell proliferation in the optic tectum (McKeown et al. 2013) (see Table 15.1).

Summary and future perspectives

As we have discussed throughout this review, the anuran amphibian *X. laevis* is a very interesting model for studying neural regeneration. This frog presents different developmental life stages and it is able to regenerate only in some of them. In fact, most larval stages before metamorphosis have the ability to regenerate the spinal cord, optic nerve, telencephalon, optic tectum, lens, neural retina, limbs, and tail. However, as these animals metamorphose, their regenerative abilities are completely lost except for a few organs/tissues listed earlier (see Table 15.1).

Therefore, this animal model appears as a unique model to perform comparative studies between regenerative and nonregenerative stages in the same species, rather than considering these differences as disadvantageous. This could lead us to finding a way to promote regeneration in the nonregenerative stages, for example.

It is needless to say that genetic, cell, and molecular mechanisms responsible for this *X. laevis* feature are far from being known. Thus, a deep understanding could lead us to stimulate regeneration in adult stages of *X. laevis* and extrapolate these studies to other mammal models such as mouse and ultimately be able to use this knowledge for treatment of human conditions, where severe central or peripheral nervous system injury has occurred.

In spite of knowing that *X. laevis* is able to regenerate during larval stages, many questions remain unanswered. How can we explain the lack of regeneration in adult stages? Two possible explanations could be the following: (i) the population of proliferative progenitor cells loses its ability to regen-

erate or disappears with metamorphosis, and (ii) even though adult stages do have proliferative progenitor cells, these are obstructed to regenerate due to an unknown factor or gene product that alters the milieu.

Which are the mechanisms of recovery in all the discussed examples of regeneration in *X. laevis*? Is the remnant tissue reorganized to recover, or do newly generated neurons reenter to the damaged circuitry, allowing the functional recovery?

This means that either neurogenesis is activated or regrowth of axons occurs. Regarding neurogenesis, one important issue is to determine the identity of the neural progenitor cells that give rise to regeneration. The identity of the neural progenitor cells is known in only a few of the presented paradigms of *X. laevis* regeneration (e.g., lens, neural retina, telencephalon), while in the others, it is still unknown. In the case of the spinal cord, it has been suggested that Sox2+ cells lining the ependymal canal might be the progenitor cells allowing the functional recovery of the spinal cord.

When the tissue or organ is restored, how do the growing axons get over such long distances to surpass the lesion site? Is there any axonal pathfinding or molecules that could act as chemoattractants or chemorepellents?

Additionally, it is very important to establish whether new synaptic connections are formed and how these behave both at an electrophysiological and functional outcome.

Finally, dissecting the molecular basis of adult neurogenesis will unquestionably allow us to understand adult or nonregenerative stages neurogenesis. Thus, we will eventually be able to differentiate the regeneration process in the context of a developmental program from that observed in an adult.

Acknowledgments

We want to thank Leonor Palma for kind help with Figure 15.1 and also Dasfne Lee-Liu and Gabriela Edwards for comments on the manuscript. This work was supported by ICM (P07/011-F, P09/016-F), BASAL (PFB12/2007), and FONDECYT (11100348).

References

- An M, Luo RS, Henion PD. 2002. Differentiation and maturation of zebrafish dorsal root and sympathetic ganglion neurons. *J Comp Neurol* 446: 267–275.
- Beattie MS, Bresnahan JC, Lopate G. 1990. Metamorphosis alters the response to spinal cord transection in *Xenopus laevis* frogs. *J Neurobiol* 21, 1108–1122.
- Beck CW, Slack JMW. 1998. Analysis of the developing *Xenopus* tail bud reveals separate phases of gene expression during determination and outgrowth. *Mech Dev* 72: 41–52.
- Beck CW, Slack JMW. 1999. A developmental pathway controlling outgrowth of the *Xenopus* tail bud. *Development* 126: 1611–1620.
- Beck CW, Christen B, Slack JMW. 2003. Molecular pathways needed for regeneration of spinal cord and muscle in a vertebrate. *Dev Cell* 5: 429–439.
- Beck CW, Izpisua Belmonte JC, Christen B. 2009. Beyond early development: *Xenopus* as an emerging model for the study of regenerative mechanisms. *Dev Dyn* 238: 1226–1248.
- Bestman JE, Lee-Osbourne J, Cline HT. 2012. In vivo time-lapse imaging of cell proliferation and differentiation in the optic tectum of *Xenopus laevis* tadpoles. *J Comp Neurol* 520: 401–433.
- Bosco L, Testa O, Venturini G, Willems D. 1997a. Lens fibre transdifferentiation in cultured larval *Xenopus laevis* outer cornea under the influence of neural retina-conditioned medium. *Cell Mol Life Sci* 53: 921–928.
- Bosco L, Venturini G, Willems D. 1997b. In vitro lens transdifferentiation of *Xenopus laevis* outer cornea induced by Fibroblast Growth Factor (FGF). *Development* 124: 421–428.
- Brockes JP. 1984. Mitogenic growth factors and nerve dependence of limb regeneration. *Science* 225: 1280–1287.
- Brockes JP. 1987. The nerve dependence of amphibian limb regeneration. *J Exp Biol* 132: 79–91.
- Cannata SM, Bagni C, Bernardini S, Christen B, Filoni S. 2001. Nerve-independence of limb regeneration in larval *Xenopus laevis* is correlated to the level of fgf-2 mRNA expression in limb tissues. *Dev Biol* 231: 436–446.
- Chen Y, Lin G, Slack JMW. 2006. Control of muscle regeneration in the *Xenopus* tadpole tail by Pax7. *Development* 133: 2303–2313.
- Christen B, Slack JMW. 1997. FGF-8 is associated with anteroposterior patterning and limb regeneration in *Xenopus*. *Dev Biol* 192: 455–466.
- Cioni C, Filoni S, Bosco L. 1982. Inhibition of lens regeneration in larval *Xenopus laevis*. *J Exp Zool* 220: 103–108.
- Del Rio-Tsonis K, Jung JC, Chiu IM, Tsonis PA. 1997. Conservation of fibroblast growth factor function in lens regeneration. *Proc Natl Acad Sci USA* 94: 13701–13706.
- Del Rio-Tsonis K, Tomarev SI, Tsonis PA. 1999. Regulation of prox-1 during lens regeneration. *Invest Ophthalmol Vis Sci* 40: 2039–2045.
- Dent JN. 1962. Limb regeneration in larvae and metamorphosing individuals of the south African clawed toad. *J Morphol* 110: 61–77.
- Eaton RC, Lee RK, Foreman MB. 2001. The Mauthner cell and other identified neurons of the brainstem escape network of fish. *Prog Neurobiol* 63: 467–485.
- Echeverri K, Clarke JD, Tanaka EM. 2001. In vivo imaging indicates muscle fibre dedifferentiation is a major contributor to the regenerating tail blastema. *Dev Biol* 236: 151–164.
- Endo T, Tamura K, Ide H. 2000. Analysis of gene expressions during *Xenopus* forelimb regeneration. *Dev Biol* 220: 296–306.
- Endo T, Yoshino J, Kado K, Tochikai S. 2007. Brain regeneration in anuran amphibians. *Dev Growth Differ* 49: 121–129.
- Fetcho JR. 1991. Spinal network of the Mauthner cell. *Brain Behav Evol* 37: 298–316.
- Filoni S, Bosco L. 1981. Comparative analysis of the regenerative capacity of caudal spinal cord in larvae of several anuran amphibian species. *Acta Embryol Morphol Exp* 2: 199–226.
- Filoni S, Paglialonga L. 1990. Effect of denervation on hindlimb regeneration in *Xenopus laevis* larvae. *Differentiation* 43: 10–19.
- Filoni S, Bosco L, Cioni C. 1982. The role of neural retina in lens regeneration from cornea in larval *Xenopus laevis*. *Acta Embryol Morphol Exp* 3: 15–28.
- Filoni S, Bosco L, Cioni C. 1984. Reconstitution of the spinal cord after ablation in larval *Xenopus laevis*. *Acta Embryol Morphol Exp* 5: 109–129.
- Filoni S, Bernardini S, Cannata SM, D'Alessio A. 1997. Lens regeneration in larval *Xenopus laevis*: experimental analysis of the decline in the regeneration capacity during development. *Dev Biol* 187: 13–24.
- Freeman G. 1963. Lens regeneration from the cornea in *Xenopus laevis*. *J Exp Zool* 154: 39–66.
- Gaete M, Muñoz R, Sánchez N, et al. 2012. Spinal cord regeneration in *Xenopus* tadpoles proceeds through activation of Sox2-positive cells. *Neural Dev* 7: 13–30.
- Gargioli C, Slack JMW. 2004. Cell lineage tracing during *Xenopus* tail regeneration. *Development* 131: 2669–2679.
- Gargioli C, Giambra V, Santoni S, et al. 2008. The lens regenerating competence in the outer cornea and epidermis of larval *Xenopus laevis* is related to pax6 expression. *J Anat* 212: 612–620.

- Gaze RM, Keating MJ, Ostberg A, Chung SH. 1979. The relationship between retinal and tectal growth in larval *Xenopus*: implications for the development of the retino-tectal projection. *J Embryol Exp Morphol* 53: 103–143.
- Gervasi C, Thyagarajan A, Szaro BG. 2003. Increased expression of multiple neurofilament mRNAs during regeneration of vertebrate central nervous system axons. *J Comp Neurol* 461: 262–275.
- Gibbs KM, Szaro BG. 2006. Regeneration of descending projections in *Xenopus laevis* tadpole spinal cord demonstrated by retrograde double labeling. *Brain Res* 1088: 68–72.
- Gibbs KM, Chittur SV, Szaro BG. 2011. Metamorphosis and the regenerative capacity of spinal cord axons in *Xenopus laevis*. *Eur J Neurosci* 33:9–25.
- Gilbert, S. 2003. Metamorphosis, regeneration and aging. In: *Developmental Biology*. Seventh Edition. Sinauer Associates, Publishers, Sunderland, MA, pp. 575–612.
- Gwon AE, Gruber LJ, Mundwiler KE. 1990. A histologic study of lens regeneration in aphakic rabbits. *Invest Ophthalmol Vis Sci* 31: 540–547.
- Gwon A, Gruber LJ, Mantras C, Cunanan C. 1993. Lens regeneration in New Zealand albino rabbits after endocapsular cataract extraction. *Invest Ophthalmol Vis Sci* 34: 2124–2129.
- Harland RM, Grainger RM. 2011. *Xenopus* research: metamorphosed by genetics and genomics. *Trends Genet* 27: 507–515.
- Henry JJ, Elkins MB. 2001. Cornea-lens transdifferentiation in the anuran, *Xenopus tropicalis*. *Dev Genes Evol* 211: 377–387.
- Henry JJ, Carinato ME, Schaefer JJ, et al. 2002. Characterizing gene expression during lens formation in *Xenopus laevis*: evaluating the model for embryonic lens induction. *Dev Dyn* 224: 168–185.
- Korneluk RG, Liversage RA. 1984. Effects of radius-ulna removal on forelimb regeneration in *Xenopus laevis* froglets. *J Embryol Exp Morphol* 82: 9–24.
- Kumar A, Brookes JP. 2012. Nerve dependence in tissue, organ, and appendage regeneration. *Trends Neurosci* 35: 691–699.
- Lang DM, Rubin BP, Schwab ME, Stuermer CAO. 1995. CNS myelin and oligodendrocytes of the *Xenopus* spinal cord-but not optic nerve are non-permissive for axon growth. *J Neurosci* 15: 99–109.
- Lee MT. 1982. Regeneration and functional reconnection of an identified vertebrate central neuron. *J Neurosci* 2: 1793–1811.
- Lenhoff HM, Lenhoff SG. 1991. Abraham Trembley and the origins of research on regeneration in animals. In: C.E. Dinsmore (Ed.), *A History of Regeneration Research*, Cambridge University Press, Cambridge, pp. 47–65.
- Leu B, Koch E, Schmidt JT. 2010. GAP43 phosphorylation is critical for growth and branching of retinotectal arbors in zebrafish. *Dev Neurobiol* 70: 897–911.
- Lin G, Chen Y, Slack JMW. 2007. Regeneration of neural crest derivatives in the *Xenopus* tadpole tail. *BMC Dev Biol* 7: 56–70.
- Lin G, Chen Y, Slack JMW. 2013. Imparting regenerative capacity to limbs by progenitor cell transplantation. *Dev Cell* 24: 1–11.
- Liu Y, Szaro BG. 2011. hnRNP K post-transcriptionally co-regulates multiple cytoskeletal genes needed for axonogenesis. *Development* 138: 3079–3090.
- Liu Y, Yu H, Deaton SK, Szaro BG. 2012. Heterogeneous nuclear ribonucleoprotein K, an RNA-binding protein, is required for optic axon regeneration in *Xenopus laevis*. *J Neurosci* 32: 3563–3574.
- Maden M. 1981. Experiments on anuran limb buds and their significance for principles of vertebrate limb development. *J Embryol Exp Morphol* 63: 243–265.
- McKeown CR, Sharma P, Sharipov HE, Shen W, Cline HT. 2013. Neurogenesis is required for behavioral recovery after injury in the visual system of *Xenopus laevis*. *J Comp Neurol* 521: 2262–2278.
- Michel ME, Reier PJ. 1979. Axonal-ependymal associations during early regeneration of the transected spinal cord in *Xenopus laevis* tadpoles. *J Neurocytol* 8: 529–548.
- Mitashov VI. 1997. Retinal regeneration in amphibians. *Int J Dev Biol* 41: 893–905.
- Nieuwkoop PD, Faber J. 1967. *Normal Table of Xenopus laevis (Daudin)*. North-Holland, Amsterdam.
- Nishikawa K, Wassersug R. 1988. Morphology of the caudal spinal cord in *Rana* (ranidae) and *Xenopus* (pipidae) tadpoles. *J Comp Neurol* 269: 193–202.
- Reeve JC, Wild AE. 1981. Secondary lens formation from the cornea following implantation of larval tissues between the inner and outer cornea of *Xenopus laevis* tadpoles. *J Embryol Exp Morphol* 63: 121–132.
- Reh TA, Levine EM. 1998. Multipotential stem cells and progenitors in the vertebrate retina. *J Neurobiol* 36: 206–220.
- Rodrigues AMC, Christen B, Martí M, Izpisua Belmonte JC. 2012. Skeletal muscle regeneration in *Xenopus* tadpoles and zebrafish larvae. *BMC Dev Biol* 12: 9–26.
- Sakaguchi DS, Janick LM, Reh TA. 1997. Basic fibroblast growth factor (FGF-2) induced transdifferentiation of retinal pigment epithelium: generation of retinal neurons and glia. *Dev Dyn* 209: 387–398.
- Schaefer JJ, Oliver G, Henry JJ. 1999. Conservation of gene expression during embryonic lens formation and cornea-lens transdifferentiation in *Xenopus laevis*. *Dev Dyn* 215: 308–318.
- Sedohara A, Komazaki S, Asashima M. 2003. *In vitro* induction and transplantation of eye during

- early *Xenopus* development. *Dev Growth Differ* 45: 463–471.
- Sharma P, Cline HT. 2010. Visual activity regulates neural progenitor cells in developing *Xenopus* CNS through musashi1. *Neuron* 68: 442–455.
- Sims RT. 1962. Transection of the spinal cord in developing *Xenopus laevis*. *J Embryol Exp Morphol* 10: 115–126.
- Slack JMW, Lin G, Chen Y. 2008. The *Xenopus* tadpole: a new model for regeneration research. *Cell Mol Life Sci* 65: 54–63.
- Straznicky K, Gaze RM. 1972. The development of the tectum in *Xenopus laevis*: an autoradiographic study. *J Embryol Exp Morphol* 28: 87–115.
- Sugiura T, Taniguchi Y, Tazaki A, Ueno N, Watanabe K, Mochii M. 2004. Differential gene expression between the embryonic tail bud and regenerating larval tail in *Xenopus laevis*. *Dev Growth Differ* 46: 97–105.
- Suzuki M, Satoh A, Ide H, Tamura K. 2005. Nerve-dependent and -independent events in blastema formation during *Xenopus* froglet limb regeneration. *Dev Biol* 286: 361–375.
- Tanaka EM, Ferretti P. 2009. Considering the evolution of regeneration in the central nervous system. *Nat Rev Neurosci* 10: 713–723.
- Taniguchi Y, Sugiura T, Tazaki A, Watanabe K, Mochii M. 2008. Spinal cord is required for proper regeneration of the tail in *Xenopus* tadpoles. *Dev Growth Differ* 50: 109–120.
- Taylor JSH, Jack JL, Easter Jr. SS. 1989. Is the capacity for optic nerve regeneration related to continued retinal ganglion cell production in the frog? A test of the hypothesis that neurogenesis and axon regeneration are obligatorily linked. *Eur J Neurosci* 1: 626–638.
- Tschumi PA. 1957. The growth of the hindlimb bud of *Xenopus laevis* and its dependence upon the epidermis. *J Anat* 91: 149–173.
- Tsonis PA. 2006. How to build and rebuild a lens. *J Anat* 209: 433–437.
- Tsonis PA, Madhavan M, Tancous EE, Del Rio-Tsonis K. 2004. A newt's eye view of lens regeneration. *Int J Dev Biol* 48: 975–980.
- Tucker AS, Slack JMW. 1995. The *Xenopus laevis* tail-forming region. *Development* 121: 249–262.
- Vergara MN, Del Rio-Tsonis K. 2009. Retinal regeneration in the *Xenopus laevis* tadpole: a new model system. *Mol Vis* 15: 1000–1013.
- Walker KL, Yoo HK, Undamatla J, Szaro BG. 2001. Loss of neurofilaments alters axonal growth dynamics. *J Neurosci* 21: 9655–9666.
- Yokoyama H, Yonei-Tamura S, Endo T, Izpisua Belmonte JC, Tamura K, Ide H. 2000. Mesenchyme with fgf-10 expression is responsible for regenerative capacity in *Xenopus* limb buds. *Dev Biol* 219: 18–29.
- Yokoyama H, Ide H, Tamura K. 2001. FGF-10 stimulates limb regeneration ability in *Xenopus laevis*. *Dev Biol* 233, 72–79.
- Yoshii C, Ueda Y, Okamoto M, Araki M. 2007. Neural retinal regeneration in the anuran amphibian *Xenopus laevis* post-metamorphosis: transdifferentiation of retinal pigmented epithelium regenerates the neural retina. *Dev Biol* 303: 45–56.
- Yoshino J, Tochinai S. 2004. Successful reconstitution of the non-regenerating adult telencephalon by cell transplantation in *Xenopus laevis*. *Dev Growth Differ* 46: 523–534.
- Yoshino J, Tochinai S. 2006. Functional regeneration of the olfactory bulb requires reconnection to the olfactory nerve in *Xenopus* larvae. *Dev Growth Differ* 48: 15–24.
- Zhao Y, Szaro BG. 1997. Xefiltin, a *Xenopus laevis* neuronal intermediate filament protein, is expressed in actively growing optic axons during development and regeneration. *J Neurobiol* 33: 811–824.

Section IV

Novel Techniques and Approaches

- Chapter 16 Atomic Force Microscopy Imaging of *Xenopus laevis* Oocyte Plasma Membrane
- Chapter 17 Size Scaling of Subcellular Organelles and Structures in *Xenopus laevis* and *Xenopus tropicalis*
- Chapter 18 A Model for Retinal Regeneration in *Xenopus*
- Chapter 19 The *Xenopus* Model for Regeneration Research
- Chapter 20 Genomics and Genome Engineering in *Xenopus*

16

Atomic Force Microscopy Imaging of *Xenopus laevis* Oocyte Plasma Membrane

Francesco Orsini

Physics Department, Università degli Studi di Milano, Milan, Italy

Abstract: This chapter describes the application of atomic force microscopy (AFM) to the study of the *Xenopus laevis* oocyte plasma membrane. Different sample preparation protocols developed and optimized to perform AFM investigation of both external and intracellular sides of the oocyte native plasma membrane are presented and discussed. AFM imaging allowed visualization and dimensional characterization of protein complexes observed on both sides of the oocyte plasma membrane. In addition, a methodological approach based on the purification of oocyte plasma membrane by ultracentrifugation on a discontinuous sucrose gradient allowed to image oocyte membrane in a physiological-like environment as well as to identify a membrane protein, the human aquaporin 4, expressed in the oocytes. Taken together, these results confirm the potential of AFM as an useful tool for the structural characterization of proteins in native eukaryotic membranes as well as its relevance for describing the organization of protein complexes in native biological membranes.

Introduction

Biological membranes are tiny and highly complex architectures, which constitute the main component both of the cellular envelope and of many intracellular organelles. The membranes are composed of a phospholipid bilayer with inserted and attached (glyco)-proteins, which are in constant motion and interacting with each other. Even if many insights are known about the integrated proteins and the physical properties of phospholipid membranes, the combined system

and, in particular, the interplay between the lipid bilayer and the proteins or the interaction of the proteins with each other are still poorly understood. Therefore, the possibility of visualizing these processes would be of great significance.

Atomic force microscopy (AFM) is a scanning probe microscopy (SPM) technique that allows visualizing such processes in their natural environment at a single-molecule level. Characterizing membrane proteins with single-molecule techniques provides structural and functional insights that cannot be

obtained with more conventional approaches (Bippes and Müller 2011; Casuso et al. 2011). In particular, AFM allows the protein surface to be contoured at nanometer resolution in a buffer solution, which mimics the physiological environment and offers the possibility of monitoring the function-related structural conformational changes, the oligomeric assembly, and the spatial organization of single-membrane proteins or protein clusters, directly on the plasma membrane (Müller and Engel 2008; Frederix et al. 2009).

Living, cultured cells were studied by AFM at an early stage of AFM technique development. However, because of the softness of the native membrane structure, cellular membranes are poorly accessible to the AFM probe. Moreover, the elastic properties of the membrane and the presence of microvilli, which interfere with the AFM probe, reduce the attainable resolution of the cell structures. More suited for high-resolution applications are membranes spread on ultrasoft supports such as freshly cleaved mica leaves. So far, the best resolution of native membrane proteins under physiological conditions has been obtained on 2D crystalline protein array structures supported on mica. Subnanometer resolution was obtained on 2D crystalline bacteriorhodopsin hexagonally packed intermediate layers (Müller et al. 1995a), and even the closing and opening of the central pore of this protein as well as AFM probe-induced conformational changes were visualized (Müller et al. 1995b; Müller et al. 1996). Using the same approach, high-resolution images of native cholera toxin B layers (Shao and Yang 1995), of gap junctions (John et al. 1997), and of aquaporin 1 (Walz et al. 1996) were obtained. More recent studies showed that AFM enables the measurement of multiple parameters of membrane proteins. In fact, AFM has been applied to probe the oligomeric states and the conformational changes of membrane protein assemblies in their native environment (Müller et al. 2002; Fotiadis et al. 2003; Liang et al. 2003; Bahatyrova et al. 2004; Scheuring et al. 2006). The ability to determine different properties at high spatial resolution facilitated the mapping of structural flexibilities, electrostatic potentials, and electric currents (Philippson

et al. 2002; Müller et al. 2006). Moreover, by using the AFM tip as a tweezer, it is possible to characterize the unfolding and refolding pathways of single proteins and the location of their molecular interactions. These interactions dictate the stability of the proteins and might be modulated by ligands that alter the protein's functional state (Oesterhelt et al. 2000; Kedrov et al. 2004; Kedrov et al. 2005).

Xenopus laevis oocytes are widely employed for the expression and functional study of heterologous membrane proteins which can be expressed with high efficiency on oocyte plasma membranes. Many integral membrane proteins, including receptors, ion channels, and transporters, cloned in *X. laevis* oocytes have been characterized by taking advantage of sensitive techniques such as electrophysiology and radiotracer uptake (Cucu et al. 2004; Mari et al. 2006; Musa-Aziz et al. 2010).

X. laevis oocytes therefore provide a convenient and versatile system for studying the structure of membrane proteins by AFM, which offers an excellent way to study their supramolecular assembly directly in native membranes as well as their quaternary structures at molecular resolution without the need for crystallization. Moreover, this methodological approach opens promising perspectives for studying heterologous membrane proteins of relevant biomedical/pharmacological interest cloned in *X. laevis* oocytes.

In this chapter, the application of AFM to the study of *X. laevis* oocyte plasma membranes aiming at obtaining a qualitative and quantitative characterization both of the plasma membrane and of the membrane proteins is described. The detailed characterization of both sides of the oocyte plasma membrane is an essential preliminary step for further investigations of specific, heterologous membrane proteins cloned in this system. Therefore, AFM imaging of the human aquaporin 4 expressed in *X. laevis* oocyte, as a model of heterologous membrane protein, is also reported.

Atomic force microscopy

Until recently, objects smaller than one half the wavelength of light radiation could only be observed in an invasive way by means of

techniques such as electron microscopy and X-ray diffraction. The introduction of SPM allowed to overcome this limitation. SPM is a branch of nonoptical microscopy that forms images of surfaces using a physical probe to scan the specimen. An image of the sample surface is obtained by mechanically moving the probe in a raster scan of the specimen, line by line, and recording the probe–surface interaction as a function of the probe position. Based on a very local probe or tip, a strongly distance-dependent interaction, and close proximity between probe and sample, SPM is capable of visualizing structures at the atomic scale.

Binnig and Rohrer of Zurich IBM laboratories invented the scanning tunneling microscope (STM) in 1982 (Binnig et al. 1982), the first microscope of the SPM family. STM uses the tunneling current between a metal tip and a conducting surface to measure the tip–sample distance and generate a topographic image of the sample surface. However, STM relies on the electrical conductivity of the sample and requires that at least a few features on the sample surface must be electrically conductive to some degree. Though very useful for a variety of surface sciences, the necessity of conductive samples prevented the biological applications of STM.

To broaden this type of microscopy to the study of nonconductive samples, AFM was developed in 1986 (Binnig et al. 1986). Due to its nanometer resolution and capability of *in situ* imaging in liquid, air, or vacuum, AFM is now the most versatile branch of SPM developed for nonconductive samples and is commonly used to study macromolecules and biological samples. The basic setup of an AFM is shown in Figure 16.1. A sharp tip mounted on a small very flexible spring, called cantilever, acts as a local and sensitive force sensor that can be operated as an STM probe. When the interacting force varies because of the sample surface topography, the cantilever will deflect; this deflection can be detected and transformed into an image of the surface relief.

Using forces rather than tunneling current, AFM is not limited to conductive samples, and high-resolution topographic images can be obtained even in aqueous solution.

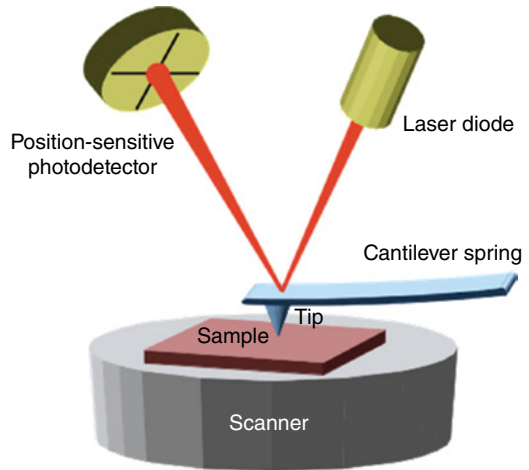


Figure 16.1 Schematic drawing of an AFM setup.

AFM can be used, for example, to characterize topographic details of surfaces from the submolecular to the cellular level, to monitor the dynamic processes of single molecules in physiologically relevant solutions, and to measure the forces between interacting molecules (Sturgis et al. 2009; Bippes and Müller 2011).

Not being restricted to conductive materials, AFM is a much more versatile technology than STM, and it is more suitable to study colloidal systems and soft matter such as biological systems. The number of publications related to AFM has increased constantly since its invention, and the instrument is now a fundamental tool in most research laboratories of the world. The materials being investigated are almost endless: thin and thick film coatings, ceramics, composites, synthetic and biological membranes, biological macromolecules like nucleic acids and proteins, cells and tissues, metals, polymers, and semiconductors. AFM is now applied in several fields of research, such as material science and engineering, biochemistry, and biology. In particular, in the last 10 years, a large number of biological applications of AFM have been reported, ranging from visualization of cells, membranes, and arrays of membrane proteins to individual proteins and DNAs (Sturgis et al. 2009; Casuso et al. 2011; Orsini et al. 2012). Besides imaging, AFM allows to measure the mechanical properties of biological samples

like elasticity and stiffness, and it has been used for the manipulation of individual biomolecules (Kienberger et al. 2006; Müller et al. 2006). AFM can be also used to measure interaction forces on the nanonewton scale. Recently, a whole new field of force measurements of notable interest to biology, which involves the interactions between ligand and receptor molecules, has been developed (Kedrov et al. 2005; Müller et al. 2006).

Sample preparation protocols for AFM imaging of *Xenopus laevis* oocyte plasma membrane

Sample preparation plays a fundamental role in AFM imaging of biological specimens which are often very soft and fragile. In particular, the interactions between the sample and the support surface, usually a freshly cleaved mica leaf or a cover slip, as well as the sample–AFM tip interactions, could induce artifacts and, in some cases, even damage the structural features of the visualized sample. Besides studying biological samples, it is also necessary to be able to perform AFM imaging in liquid, both to have reliable data operating in a physiological-like environment and to collect high-resolution AFM images reducing capillary forces between the AFM tip and the sample. AFM can work close to physiological conditions and give high-resolution images, the only requirement being that the sample is well flattened and adhered to a flat support.

For all these reasons, great efforts have been made both to develop protocols suitable for high-resolution AFM imaging of specific biological samples such as nucleic acids, proteins, and cells and to introduce new AFM imaging modes, optimizing imaging parameters and image analysis procedures, aiming at obtaining more information and minimizing the interaction forces.

Though AFM possesses features that render it an attractive tool for resolving the structural topography of membrane proteins, convenient sample preparation protocols have to be developed to utilize the full capabilities of this technique to image native membranes as well as membrane proteins. Because of these difficulties,

to date, only a few AFM investigations of endogenous membrane proteins on purified eukaryotic membranes have been performed (Fotiadis et al. 2003; Buzhynskyy et al. 2007), notwithstanding their relevant physiological and biomedical interest. The usefulness of developing preparation protocols that allow to reproducibly study native eukaryotic membrane proteins appears thus clear.

In AFM imaging of *X. laevis* oocyte plasma membrane, sample preparation represents one of the most crucial and challenging points to face. In fact, the extreme fragility of the oocyte plasma membrane and the force applied by the AFM tip to the sample surface during imaging, even operating under very soft measurement conditions, prevent the direct visualization of intact devitellinized oocytes. In addition, although oocytes are a very efficient system for the expression of heterologous membrane proteins, their large dimensions as well as the presence of a rich cytoplasmic content, with yolk and granules, make AFM imaging in liquid difficult thus that convenient preparation protocols have to be developed.

The main difficulties concern both the isolation from a very large cell (diameter of about 1 mm) of a clean fragment of plasma membrane, whose thickness is only 4–5 nm, and the deposition and adhesion of this thin isolated membrane layer on a flat surface. Several preparation protocols have been therefore developed and optimized to obtain well-flattened oocyte plasma membrane samples strongly attached to the support as required for AFM imaging (Orsini et al. 2006; Santacroce et al. 2006; Orsini et al. 2009; Orsini et al. 2010). Here, a detailed description of three different sample preparation protocols, developed and validated in our laboratory, to prepare *X. laevis* oocyte plasma membranes suitable for AFM imaging is reported. In particular, the protocols called Method A and Method B allow to perform AFM imaging of the external and the cytoplasmic sides of the oocyte plasma membrane, respectively. Both these methods have the advantage of an easy and a rapid preparation but require visualization of membranes in air. The sample exposure to air is necessary for allowing its adhesion to the mica support during the drying step. Though

some structural distortions induced by air-drying may occur, the arrangement and organization of membrane protein complexes are only minimally affected by air exposure as reported in previous works (Lau et al. 2002; Schillers et al. 2004).

More recently, to overcome this drawback we developed a novel preparation protocol, called Method C, based on the purification of oocyte plasma membrane by ultracentrifugation on a discontinuous sucrose gradient. The main advantages of this preparation in comparison to Methods A and B are the possibility both to purify membranes maintaining their integrity and functionality and to perform a high-resolution AFM imaging in liquid in a near-native environment because membrane samples well flattened and adhered to the mica support, often as a single-membrane bilayer, can be obtained. Method C, therefore, allowing both to prepare highly purified plasma membranes and to collect high-resolution AFM images in physiological-like conditions, appears to be very promising for studying heterologous membrane proteins expressed in *X. laevis* oocyte.

Method A: To visualize the external side of plasma membrane

Devitellinized *X. laevis* oocytes are placed in a Petri dish with Barth's solution (88mM NaCl, 1mM KCl, 0.82mM MgSO₄, 0.41mM CaCl₂, 0.33mM Ca(NO₃)₂, and 10mM Hepes/Tris, pH7.5) supplemented with 0.005% gentamycin sulfate and 2.5mM pyruvic acid and dissected with fine forceps to remove the cytoplasm and

nucleus. Patches of plasma membrane with adherent cytoplasmic material are deposited with the external side facing upward (easily recognizable on the basis of its color and surface features) on a freshly cleaved mica leaf placed in the same Petri dish as reported in Figure 16.2. When the solution is removed, air exposure flattens the membrane patch on the mica support, leading to a lateral outflow of the cytoplasmic material. The patch is then dried in air for approximately 20min to allow the adhesion to the mica support and rinsed with deionized water for 2min before AFM imaging.

Method B: To visualize the intracellular side of plasma membrane

This method is based on a protocol described elsewhere (Lau et al. 2002) with minor differences. Briefly, a devitellinized oocyte is placed on a freshly cleaved mica leaf in a Petri dish containing Barth's solution. Partial removal of the solution exposes the upper part of the oocyte membrane to air, which causes its laceration and the bursting of the oocyte, thus allowing a membrane fragment with remnants of cytoplasmic material to be exposed with the intracellular side facing upward. The subsequent gentle addition of Barth's solution (not directly on the membrane fragment) detaches the membrane fragment from the mica leaf, and leaves it floating on the solution surface with its intracellular side facing upward (the correct orientation of the membrane fragment is always verified by means of optical microscopy) as shown in Figure 16.3. After draining the cytosolic content,

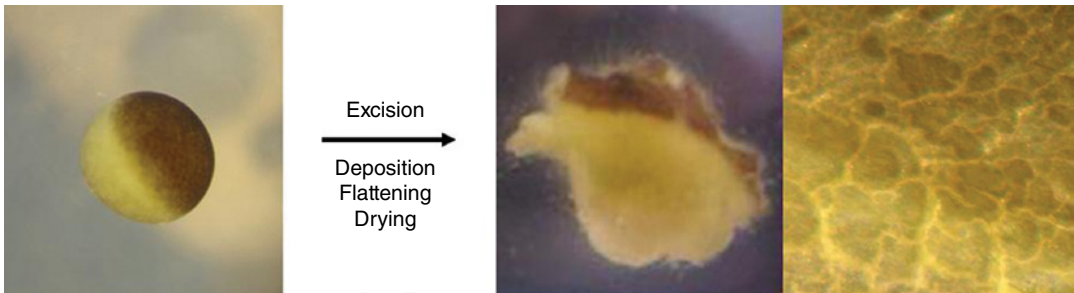


Figure 16.2 Patch of *X. laevis* oocyte plasma membrane with the external side facing upward obtained by excision (Method A).

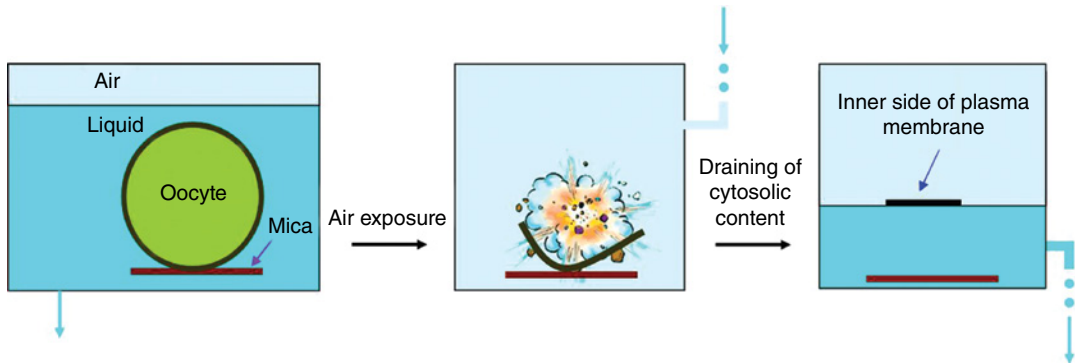


Figure 16.3 Cartoon of the preparation protocol to obtain an *X. laevis* oocyte plasma membrane patch with the intracellular side facing upward (Method B).

a clean plasma membrane fragment is left floating on the solution surface. The Barth's solution is then carefully removed, allowing the membrane fragment to adhere to the mica support. The sample is dried in air for about 20 min and then rinsed with deionized water for 2 min before AFM imaging.

Method C: To visualize the plasma membrane in liquid buffer

About 100–200 V- and VI-stage defolliculated *X. laevis* oocytes are homogenized in oocyte homogenization buffer (OHB) (250 mM sucrose, 5 mM $MgCl_2$, 10 mM HEPES/Tris, pH 7.5; 10 μ L per oocyte) by several cycles of pipetting. Homogenates are then centrifuged at 500 g for 5 min at 4°C. Lipids floating on the liquid surface are discarded, and the supernatant is recovered (about 1 mL). The pellet is resuspended in 1 mL of OHB and homogenized as in the preceding texts before centrifugation at 500 g for 5 min at 4°C. The supernatant is recovered (about 500 μ L) and combined with the first one. A volume of 1.5 mL of the supernatant is then loaded on the bottom of a discontinuous sucrose gradient composed of 80% sucrose in TNE buffer (10 mM Tris/HCl, 150 mM NaCl, pH 7.4) (1.5 mL), 35% sucrose in TNE (4 mL), and 10% sucrose in TNE (4 mL) and centrifuged at 30,000 g for 3 h at 4°C in a swinging bucket rotor. At the end of the ultracentrifugation, a major membrane band is clearly visible at the interface between 35% and 10% sucrose as reported in Figure 16.4. The band is then collected and stored at –20°C.

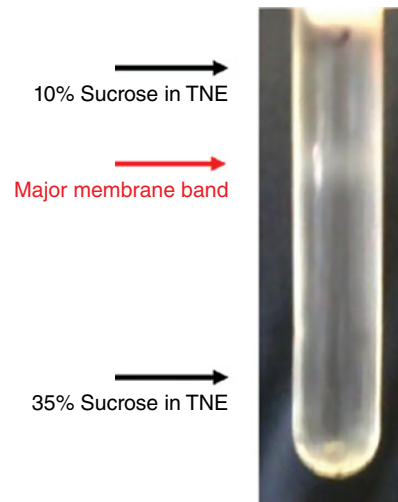


Figure 16.4 *X. laevis* oocyte plasma membrane band visible at the interface between 35% and 10% sucrose gradient (Method C).

For AFM imaging in liquid buffer, purified membranes are then diluted 1 : 20 in adsorption buffer (150 mM KCl, 250 mM $MgCl_2$, 10 mM Tris/HCl, pH 7.5). Before sample deposition, the mica support is immersed in 100 μ L of adsorption buffer for 1 min to facilitate the membrane adhesion. After buffer removal, 50 μ L of the membrane suspension is floated on the mica surface. After 10 min of adsorption, the sample is gently rinsed three times with 50 μ L of recording buffer (150 mM KCl, 10 mM HEPES/Tris, pH 7.5) to remove membranes that have not been adsorbed to the support. Finally, the

buffer is removed and a drop of 70 μ L of recording buffer is placed on the mica support before AFM imaging.

AFM imaging of *Xenopus laevis* oocyte plasma membrane

AFM imaging in air (Methods A and B)

AFM images reported in this section were collected in air operating in contact mode under constant force conditions. By operating in contact mode, it is possible to collect the topography and deflection mode signals simultaneously. Deflection mode images, although these do not give quantitative information of the visualized structure heights, are very useful in giving a direct imaging of the small corrugations on the sample surface and in analyzing the density and lateral dimension of the visualized structures.

AFM imaging was performed in air on oocyte plasma membrane samples prepared according to Methods A and B since air exposure of the sample was necessary both for obtaining flattened membrane patches on the mica support and for allowing their adhesion to the support. So, even if air is not a physiological environment and some structural distortions may occur, the assembly and the arrangement of the membrane protein complexes are expected to be only minimally affected as reported in literature (Le Grimmelc et al. 1995). Since *X. laevis* oocytes are a widely used model in the study of many development mechanisms and in the expression of heterologous proteins, the possibility offered by AFM to visualize and quantitatively investigate the oocyte plasma membrane in air appears nevertheless unique and interesting.

The presence of both plasma membrane and membrane proteins in samples prepared according to Methods A and B was confirmed by means of fluorescence microscopy (Orsini et al. 2006).

AFM imaging of oocyte plasma membrane samples showed differently arranged spherical-like protrusions on both sides of the plasma membrane. In particular, two different arrangements were clearly visualized: spherical-like protrusions arranged

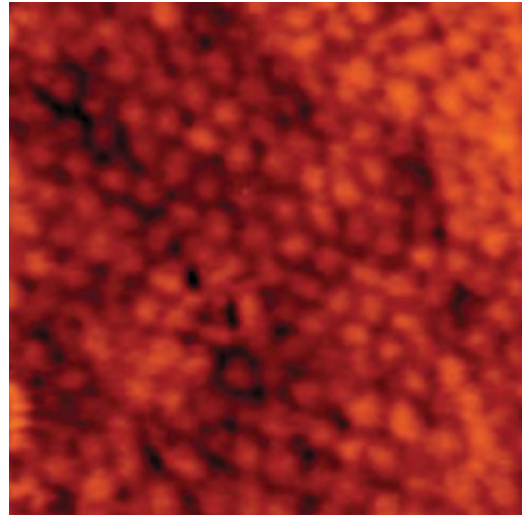


Figure 16.5 AFM deflection mode image of the external side of the *X. laevis* oocyte plasma membrane prepared according to Method A. An area covered by regular repeating and densely packed spherical-like protrusions is visualized. Scan area 400 \times 400 nm².

(i) heterogeneously and (ii) in a regular pattern as reported in Figure 16.5. In general terms, the most frequent surface pattern indicated a heterogeneous and disordered arrangement, although less frequent patterns showed regularly arranged and densely packed spherical-like structures which cover plasma membrane regions with lateral dimensions in the range of 400–700 nm (Orsini et al. 2006).

The spherical-like structures irregularly arranged were often located so close to each other that they overlapped or merged, thus making it difficult to perform a quantitative AFM analysis. On the contrary, the lateral dimension of the regular repeating and densely packed spherical-like protrusions visualized on the external side of the plasma membrane showed a normal distribution centered on 25.5 ± 0.3 nm (mean \pm SE, $n = 950$), while their height was in the range 2–5 nm. On the intracellular membrane side, the lateral dimension of the regularly arranged spherical-like protrusions showed a normal distribution centered on 30.2 ± 0.8 nm (mean \pm SE, $n = 845$) with a height of 1–3 nm. The observed difference between the lateral dimensions of the structures on the external

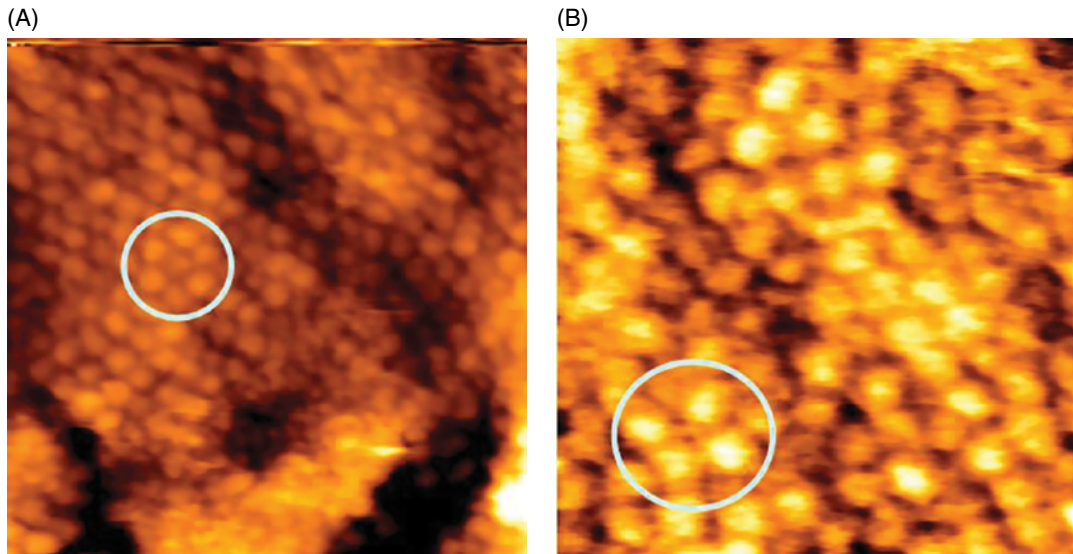


Figure 16.6 AFM deflection mode images of the external side of the *X. laevis* oocyte plasma membrane prepared according to Method A. Protein complexes disposed in two different arrangements – (A) hexagonal packing and (B) square packing – are visualized on plasma membrane. Scan area (A) $580 \times 580 \text{ nm}^2$; (B) $290 \times 290 \text{ nm}^2$.

and intracellular sides was statistically significant (*t*-Student's test: $P < 0.05$).

All the spherical-like structures were affected by proteolytic treatment, thus confirming their proteic nature as proved by the decreased size of their lateral dimensions measured in AFM deflection mode images collected on oocyte plasma membrane samples treated with trypsin (Orsini et al. 2006).

The apparent shape of the protein complexes was found to be spherical-like, possibly owing to the fact that lateral dimensions of the visualized structures are overestimated as a result of the convolution effect between the structure and the AFM tip. In fact, it must be pointed out that, when structures with lateral dimensions similar to the AFM tip radius are visualized, tip-sample convolution effects occur (Markiewicz and Goh 1995). The measurement of the protein height gives more reliable values since the vertical resolution of AFM is better than 0.5 nm and the tip-sample convolution effects are minimized.

The analysis of the ordered arrays displayed two well-defined types of identifiable arrangements of closely packed protein complexes. The first one is composed of a series of parallel rows of protein complexes arranged in a hexagonal packing, while the second one is

arranged in a square packing as shown in Figure 16.6.

The regular and densely packed pattern of the protein complexes were visualized on both sides of the plasma membrane and was observed in samples prepared by two different sample preparation protocols, thus suggesting that it is more likely due to a biological phenomenon than to an AFM artifact. The two arrangements visualized in AFM images represent two efficient ways to tessellate a plane with spherical structures. Thus, the hexagonal and square packings indicate that in the oocyte plasma membrane there are microdomains where the protein complexes are arranged in order to maximize their number on the membrane.

Experimental data show therefore that AFM imaging is a useful means of quantitatively describing the organization of protein complexes in native biological membranes.

In order to study in more detail the oligomeric assembly of membrane proteins, oocyte plasma membrane samples have to be investigated by AFM in a liquid buffer at higher resolution.

In fact, AFM imaging in buffer solution not only allows structural analysis of biological specimens to be carried out under native conditions but it also provides important pos-

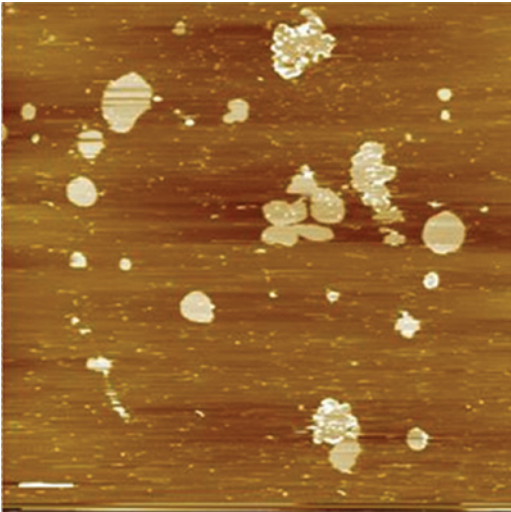


Figure 16.7 AFM topography image of the *X. laevis* oocyte plasma membrane samples prepared according to Method C and collected in a liquid buffer. Scan area $10 \times 10 \mu\text{m}^2$, vertical scale 23 nm, scale bar $1 \mu\text{m}$.

sibilities to control the tip–sample interactions and, eliminating the capillarity forces, to decrease the force induced on the sample by the AFM tip by 100 times (Müller et al. 1999), thus minimizing the tip–sample convolution effects which affect their lateral size.

At this aim, we have recently optimized a novel approach based on the purification of oocyte plasma membrane by ultracentrifugation on sucrose gradient (Method C), and the results are described in the following section.

AFM imaging in liquid buffer (Method C)

Figure 16.7 shows an AFM topography image of *X. laevis* oocyte plasma membrane purified by ultracentrifugation according to Method C and visualized in liquid buffer in contact mode.

AFM imaging showed large and planar membrane patches well adhered to the mica support, with lateral sizes of a few microns and heights of about 4–5 nm as expected for a lipid membrane bilayer. Moreover, on average, 4–5 membrane patches with lateral sizes larger than $1 \mu\text{m}$ were visible in a $10 \times 10 \mu\text{m}^2$ scan area, and the mica support surrounding the membrane patches was sufficiently clean to perform a

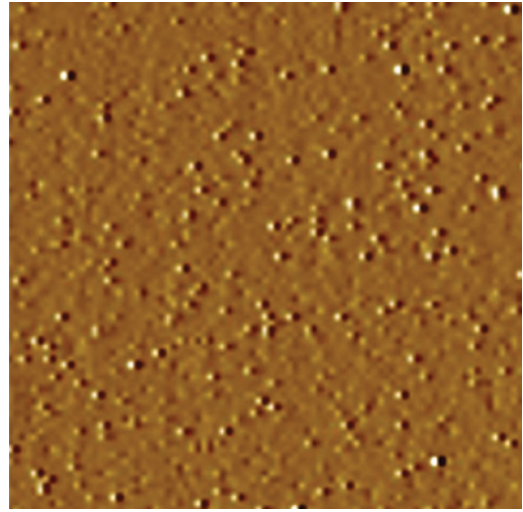


Figure 16.8 AFM deflection mode image of the *X. laevis* oocyte plasma membrane prepared according to Method C and collected in a liquid buffer. Spherical-like structures with heights lower than 1 nm are visible on the membrane surface. Scan area $300 \times 300 \text{ nm}^2$.

high-resolution AFM imaging. The analysis of AFM images allowed to quantitatively characterize the visualized membranes. In particular, the lateral dimension and the height of the membrane patches showed a normal distribution centered on $2.1 \pm 0.9 \mu\text{m}$ (mean \pm SD, $n=59$) and $4.4 \pm 0.6 \text{ nm}$ (mean \pm SD, $n=59$), respectively. More interestingly, a number of membrane patches showed a nanometer corrugation distributed on their whole surface. Root mean square roughness values of $0.32 \pm 0.03 \text{ nm}$ (mean \pm SD, $n=30$), measured on $100 \times 100 \text{ nm}^2$ areas, were calculated according to the equation

$$\text{rms}_{xy} = \sqrt{\sum_{x,y=1}^N \frac{(Z_{x,y} - Z_{\text{average}})^2}{N^2}}$$

where Z_{average} is the average Z value within the examined area, Z_{xy} is the local Z value, and N indicates the number of points within the area.

Biochemical analyses, namely, Bradford assay and fluorescence staining experiments, confirmed the presence of a high protein content in membrane samples prepared for AFM investigation.

High-resolution AFM imaging, performed by selecting small scan areas on membrane patches exhibiting a surface roughness, showed

spherical-like structures which resemble proteins in both size and shape as shown in Figure 16.8.

In particular, the height profile analysis pointed out structural features protruding from the membrane surface with heights lower than 1 nm and lateral size of 5.3 ± 0.8 nm (mean \pm SD, $n = 48$).

AFM data appear to be in good agreement with the known dimensions of some membrane proteins that show a great variety in shapes and dimensions, with some of them largely within the membrane lipid bilayer, while others have large extracellular regions.

Taken together, AFM imaging and biochemical assays suggest that the nanometer features visualized on the oocyte plasma membrane could be native membrane proteins, thus opening new perspectives for AFM investigation in liquid buffer of heterologous membrane proteins cloned in *X. laevis* oocytes.

To this aim, AFM imaging was applied to the study of human aquaporin 4, isoform M23 (AQP4-M23), expressed in *X. laevis* oocytes to prove, in a well-known model protein, that AFM recognition of spatial arrangement of heterologous membrane proteins expressed on the surface of plasma membrane could help their identification. In fact, AQP4-M23 was chosen because it forms orthogonal arrays of membrane-protruding particles when examined by freeze-fracture electron microscopy (Furman et al. 2003; Crane et al. 2009) corresponding to individual AQP4-M23 tetramers easily identifiable in AFM topography images.

In this study, complementary RNA (cRNA) was synthesized *in vitro* from cDNA clones of human AQP4-M23 and then microinjected into defolliculated *X. laevis* oocytes for expression. The functional expression of AQP4-M23 in the oocyte plasma membrane was verified, 3 days after the microinjection, by measuring the water permeability of oocytes from the rate of cell volume change produced by an osmotic gradient. The volumetric analysis showed that *X. laevis* oocytes have a low intrinsic water permeability and that AQP4-M23-expressing oocytes have a water permeability significantly higher than control oocytes, thus confirming the presence of AQP4-M23 on the plasma

membrane in the correct functional form. In addition, to better characterize the AQP4-M23 expression and to optimize protein overexpression conditions, the volumetric analysis was also performed on oocytes injected with different concentrations of cRNA. Experimental data indicated that the highest expression of functional AQP4-M23 was obtained by injecting oocytes with a cRNA concentration of about $0.3 \mu\text{g}/\mu\text{L}$ that was therefore used for the preparation of the membrane samples.

AFM imaging of *X. laevis* oocytes expressing AQP4-M23 was performed on plasma membrane purified according to Method C. The presence of AQP4-M23 in the purified oocyte plasma membrane was verified, before performing AFM imaging, by detecting the protein of interest by SDS-PAGE assay and Western blot analysis.

AFM imaging of purified oocyte plasma membrane expressing AQP4-M23 and obtained from oocytes injected with $0.3 \mu\text{g}/\mu\text{L}$ of AQP4-M23 cRNA was comparable to the one observed with untreated samples showing planar membrane patches with lateral sizes of a few microns and heights of about 5 nm.

High-resolution AFM imaging displayed intramembraneous particles (IMPs) of about 5 nm diameter protruding by about 1 nm from the membrane surface. Interestingly, some of these structures are arranged according to a square motif, thus suggesting that the component monomers, dimers, and tetramers of higher-order orthogonal arrays of AQP4-M23 tetramers were visualized as dispersed singlets. To support this hypothesis, it is worth noting that these structures were observed only in membrane samples prepared from transfected oocytes.

Finally, AFM topography image of a large square lattice of IMPs (Figure 16.9) confirms that AQP4-M23 proteins can be identified in the plasma membrane obtained by *X. laevis* oocytes injected with cRNA of AQP4-M23 isoform.

In particular, the inset of Figure 16.9 shows a square array with uniform lattice spacing of 6 nm containing more than 150 IMPs with 1–2 nm inter-IMP cross bridges. IMPs, whose dimensions range from 4 to 6 nm, appear to be arranged along two orthogonal axes of symmetry, giving them a checkerboard appearance.

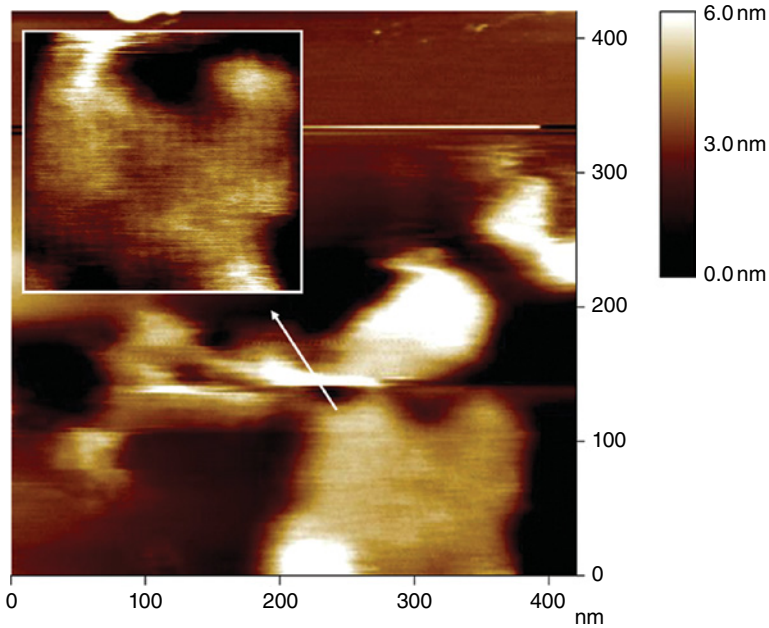


Figure 16.9 AFM topography image of the *X. laevis* oocyte plasma membrane expressing AQP4-M23, prepared according to Method C and collected in a liquid buffer. Scan area $425 \times 425 \text{ nm}^2$, vertical scale 6 nm. Inset: magnification of the surface corrugation visualized on top of the membrane. A square array of IMPs is visible. Scan area $150 \times 150 \text{ nm}^2$, vertical scale 2 nm. To see a color version of this figure, see Plate 40.

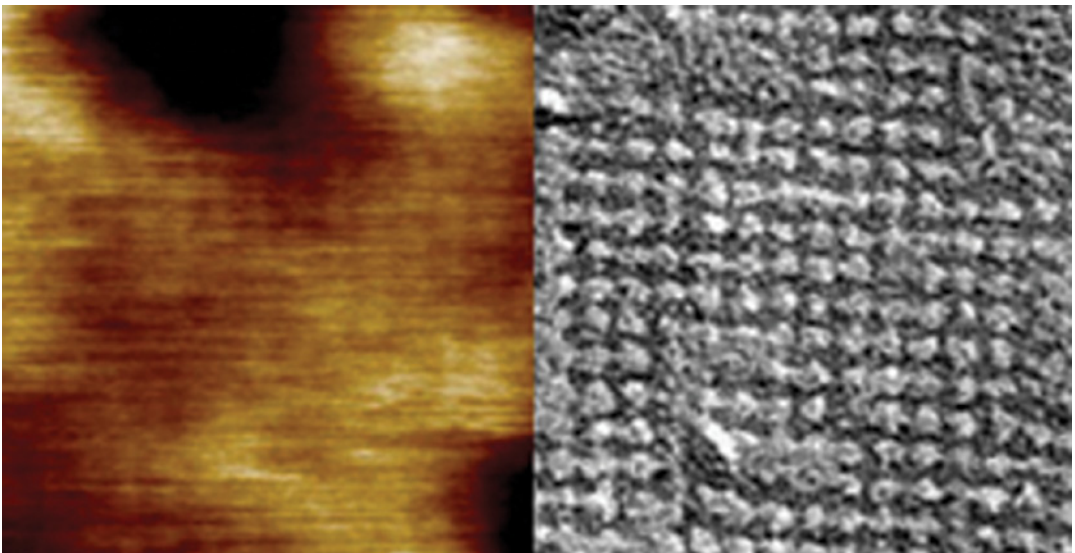


Figure 16.10 Square arrangement of AQP4-M23 tetramers, with a center-to-center distance of 6 nm as visualized in (left) an AFM topography image and (right) a TEM image. Scan areas: $100 \times 100 \text{ nm}^2$. From Furman et al. (2003). © 2003, National Academy of Sciences, U.S.A. To see a color version of this figure, see Plate 41.

AFM data as well as the comparison with the higher-order structures of AQP4-M23 which stand out as square arrays in freeze-fracture preparation (see Figure 16.10) and the fact that square arrays of IMPs were found only in AQP4-M23-transfected *X. laevis* oocytes allow to identify the IMPs visualized on the oocyte plasma membrane as individual AQP4-M23 tetramers.

These findings show the potential of AFM technique for studying the surface topography and the structure–function relationship of heterologous membrane proteins cloned in native eukaryotic membranes.

Conclusions and future perspectives

Biological membranes provide a unique example of highly integrated systems in which proteins and lipids arrange themselves in two dimensions to perform efficiently many different activities. The structure and dynamics of these self-organized assemblies are being increasingly studied both because of their biological importance and their interest to nanotechnology. To date, however, there is little direct information on the organization and self-assembly of native biological membranes and of the protein complexes within them. Understanding both the membrane protein function at a molecular level and the molecular origins of their folding, stabilization, and ligand binding and the interactions that fold and stabilize the spatial and structural formation of dynamic complexes of membrane proteins with signaling molecules poses an important challenge to modern biology, physiology, and pharmacology.

Here, AFM has been applied to the study of the plasma membrane of the *X. laevis* oocyte. Great attention has been dedicated to the development and the optimization of suitable sample preparation protocols in order to characterize qualitatively and quantitatively the structure of the native plasma membrane as well as membrane proteins of the *X. laevis* oocyte. In particular, two different approaches for membrane preparation, called Methods A and B, allowed to image in air both the external and intracellular sides of oocyte plasma membrane. Protein complexes whose dimensions

resulted statistically different between the external and the intracellular sides of the plasma membrane have been visualized and morphologically characterized. Besides, AFM imaging showed protein complexes disposed in a heterogeneous and disordered pattern along with less frequent plasma membrane regions with protein complexes densely packed and regularly arranged according to two different geometries, namely, hexagonal and square packings. Membrane protein clusters allow proteins to function in a way that is impossible if they were sparsely distributed (Ehrenhofer et al. 1997; Caldwell 2000). Recently, plasma membrane has been described on the basis of a dynamically structured mosaic model (Vereb et al. 2003), implying a nonrandom distribution of specific types of membrane proteins forming two levels of patterns: the first at a molecular and the second at a submicrometer level. Thus, our AFM images confirm that plasma membrane is not a homogeneous structure but is structured in domains with a particular biochemical composition that can be visualized as an ordered arrangement at the submicrometer level.

Finally, the use of purified plasma membrane from *X. laevis* oocytes opens new prospects in the AFM investigation of eukaryotic plasma membrane organization at highest and improved resolution. In particular, a novel protocol (Method C) based on the purification of functional oocyte membranes by ultracentrifugation on a sucrose gradient and in the subsequent AFM imaging in liquid buffer allowed to visualize and dimensionally characterize in physiological-like conditions native membrane proteins on *X. laevis* oocyte plasma membrane. In addition, this preparation protocol allowed to identify the isoform M23 of human aquaporin 4 (AQP4-M23) heterologously expressed in *X. laevis* oocytes. AFM topography images showed the characteristic square arrangement of AQP4-M23 tetramers, with a center-to-center distance of 6 nm. This well-recognizable spatial organization was seen only in AQP4-M23 cRNA-injected oocytes. AFM data, namely, the angles and spacing between tetramer subunits as well as the size of individual tetramers, are in agreement with both TEM

analyses reported in literature (Furman et al. 2003) and the current model of AQP4 (Ho et al. 2009).

In conclusion, the methodological approach described here demonstrates the potentiality of the AFM technique to study the expression of membrane proteins cloned in native eukaryotic membrane and their surface distribution and oligomeric assembly without the need of crystallization. In particular, these findings open appealing perspectives in the AFM investigation of heterologous membrane proteins of relevant biomedical interest cloned in a very efficient expression system such as the *X. laevis* oocytes and studied in physiological-like conditions.

References

- Bahatyrova, S., Frese, R.N., Siebert, C.A. et al. 2004. The native architecture of a photosynthetic membrane. *Nature*, 430:1058–1062.
- Binnig, G., Rohrer, H., Gerber, C., and Weibel, E. 1982. Surface studies by scanning tunneling microscopy. *Phys. Rev. Lett.*, 49:57–61.
- Binnig, G., Quate, C.F., and Gerber, C. 1986. Atomic force microscope. *Phys. Rev. Lett.*, 56:930–933.
- Bippes, C.A. and Müller, D.J. 2011. High-resolution atomic force microscopy and spectroscopy of native membrane proteins. *Rep. Prog. Phys.*, 74:086601.
- Buzhynskyy, N., Girmens, J.F., Faigle, W., and Scheuring, S. 2007. Human cataract lens membrane at subnanometer resolution. *J. Mol. Biol.*, 374:162–169.
- Caldwell, J.H. 2000. Clustering of sodium channels at the neuromuscular junction. *Microsc. Res. Tech.*, 49:84–89.
- Casuso, I., Rico, F., and Scheuring, S. 2011. Biological AFM: where we come from – where we are – where we may go. *J. Mol. Recognit.*, 24:406–413.
- Crane, J.M., Bennett, J.L., and Verkman, A.S. 2009. Live cell analysis of aquaporin-4 M1/M23 interactions and regulated orthogonal array assembly in glial cells. *J. Biol. Chem.*, 284:35850–35860.
- Cucu, D., Simaels, J., Jans, D., and Van Driessche, W. 2004. The transoocyte voltage clamp: a non-invasive technique for electrophysiological experiments with *Xenopus laevis* oocytes. *Pflügers Arch.*, 447:934–942.
- Ehrenhofer, U., Rakowska, A., Schneider, S.W., Schwab, A., and Oberleithner, H. 1997. The atomic force microscope detects ATP-sensitive protein clusters in the plasma membrane of transformed MDCK cells. *Cell Biol. Int.*, 21:737–746.
- Fotiadis, D., Liang, Y., Filipek, S., Saperstein, D.A., Engel, A., and Palczewski, K. 2003. Atomic-force microscopy: rhodopsin dimers in native disc membranes. *Nature*, 421:127–128.
- Frederix, P.L.T.M., Bosshart, P.D., and Engel A. 2009. Atomic force microscopy of biological membranes. *Biophysical J.*, 96:329–338.
- Furman, C.S., Gorelick-Feldman, D.A., Davidson, K.G.V. et al. 2003. Aquaporin-4 square array assembly: opposing actions of M1 and M23 isoforms. *Proc. Natl. Acad. Sci. U.S.A.*, 100:13609–13614.
- Ho, J.D., Yeh, R., Sandstrom, A. et al. 2009. Crystal structure of human aquaporin 4 at 1.8 Å and its mechanism of conduction. *Proc. Natl. Acad. Sci. U.S.A.*, 106:7437–7442.
- John, S.A., Saner, D., Pitts, J.D., Holzenburg, A., Finbow, M.E., and Lal, R. 1997. Atomic force microscopy of arthropod gap junctions. *J. Struct. Biol.*, 120:22–31.
- Kedrov, A., Ziegler, C., Janovjak, H., Kühlbrandt, W., and Müller, D.J. 2004. Controlled unfolding and refolding of a single sodium-proton antiporter using atomic force microscopy. *J. Mol. Biol.*, 340:1143–1152.
- Kedrov, A., Krieg, M., Ziegler, C., Kuhlbrandt, W., and Müller, D.J. 2005. Locating ligand binding and activation of a single antiporter. *EMBO Rep.*, 6:668–674.
- Kienberger, F., Ebner, A., Gruber, H.J., and Hinterdorfer, P. 2006. Molecular recognition imaging and force spectroscopy of single biomolecules. *Accounts Chem. Res.*, 39(1):29–36.
- Lau, J.M., You, H.X., and Yu, L. 2002. Lattice-like array particles on *Xenopus* oocyte plasma membrane. *Scanning*, 24:224–231.
- Le Grimmellec, C., Lesniewska, E., Giocondi, M.C., Cachia, C., Schreiber, J.P., and Goudonnet, J.P. 1995. Imaging of the cytoplasmic leaflet of the plasma membrane by atomic force microscopy. *Scanning Microsc.*, 9:401–411.
- Liang, Y., Fotiadis, D., Filipek, S., Saperstein, D.A., Palczewski, K., and Engel, A. 2003. Organization of the G protein-coupled receptors rhodopsin and opsin in native membranes. *J. Biol. Chem.*, 278:21655–21662.
- Mari, S.A., Soragna, A., Castagna, M. et al. 2006. Role of the conserved glutamine 291 in the γ -aminobutyric acid transporter rGAT-1. *Cell. Mol. Life Sci.*, 63:100–111.
- Markiewicz, P. and Goh, M.C. 1995. Atomic force microscope tip deconvolution using calibration arrays. *Rev. Sci. Instrum.*, 66:3186–3190.
- Müller, D.J. and Engel A. 2008. Strategies to prepare and characterize native membrane proteins and protein membranes by AFM. *Curr. Opin. Colloid Interface Sci.*, 13:338–350.

- Müller, D.J., Schabert, F.A., Buldt, G., and Engel, A. 1995a. Imaging purple membranes in aqueous solutions at sub-nanometer resolution by atomic force microscopy. *Biophysical J.*, 68:1681–1686.
- Müller, D.J., Buldt, G., and Engel, A. 1995b. Force-induced conformational change of bacteriorhodopsin. *J. Mol. Biol.*, 249:239–243.
- Müller, D.J., Schoenenberger, C.A., Büldt, G., and Engel, A. 1996. Immuno-atomic force microscopy of purple membrane. *Biophysical J.*, 70:1796–1802.
- Müller, D.J., Fotiadis, D., Scheuring, S., Müller, S.A., and Engel, A. 1999. Electrostatically balanced subnanometer imaging of biological specimens by atomic force microscopy. *Biophys. J.*, 76:1101–1111.
- Müller, D.J., Janovjak, H., Lehto, T., Kuerschner, L., and Anderson, K. 2002. Observing structure, function and assembly of single proteins by AFM. *Prog. Biophys. Mol. Biol.*, 79:1–43.
- Müller, D.J., Sapra, K.T., Scheuring, S. et al. 2006. Single-molecule studies of membrane proteins. *Curr. Opin. Struc. Biol.*, 16:489–495.
- Musa-Aziz, R., Boron, W.F., and Parker, M.D. 2010. Using fluorometry and ion-sensitive microelectrodes to study the functional expression of heterologously-expressed ion channels and transporters in *Xenopus* oocytes. *Methods*, 51:134–145.
- Oesterhelt, F., Oesterhelt, D., Pfeiffer, M., Engel, A., Gaub, H.E., and Müller, D.J. 2000. Unfolding pathways of individual bacteriorhodopsins. *Science*, 288:143–146.
- Orsini, F., Santacroce, M., Perego, C. et al. 2006. Atomic force microscopy characterization of *Xenopus laevis* oocyte plasma membrane. *Microsc. Res. Tech.*, 69:826–834.
- Orsini, F., Santacroce, M., Arosio, P. et al. 2009. Intermittent contact mode AFM investigation of native plasma membrane of *Xenopus laevis* oocyte. *Eur. Biophys. J.*, 38:903–910.
- Orsini, F., Santacroce, M., Arosio, P., and Sacchi, V.F. 2010. Observing *Xenopus laevis* oocyte plasma membrane by atomic force microscopy. *Methods*, 51:106–113.
- Orsini, F., Cremona, A., Arosio, P. et al. 2012. Atomic force microscopy imaging of lipid rafts of human breast cancer cells. *Biochim. Biophys. Acta – Biomembranes*, 1818:2943–2949.
- Philippesen, A., Im, W., Engel, A., Schirmer, T., Roux, B., and Müller, D.J. 2002. Imaging the electrostatic potential of transmembrane channels: atomic probe microscopy on OmpF porin. *Biophysical J.*, 82:1667–1676.
- Santacroce, M., Orsini, F., Perego, C. et al. 2006. Atomic force microscopy imaging of actin cortical cytoskeleton of *Xenopus laevis* oocyte. *J. Microsc.*, 223:57–65.
- Scheuring, S., Goncalves, R.P., Prima, V., and Sturgis, J.N. 2006. The photosynthetic apparatus of *Rhodospseudomonas palustris*: structures and organization. *J. Mol. Biol.*, 358:83–96.
- Schillers, H., Shahin, V., Albermann, L., Schafer, C., and Oberleithner, H. 2004. Imaging CFTR: A tail to tail dimer with a central pore. *Cell Physiol. Biochem.*, 14:1–10.
- Shao, Z. and Yang, J. 1995. Progress in high resolution atomic force microscopy in biology. *Quart. Rev. Biophys.*, 28:195–251.
- Sturgis, J.N., Tucker, J.D., Olsen, J.D., Hunter, C.N., and Niederman, R.A. 2009. Atomic force microscopy studies of native photosynthetic membranes. *Biochemistry*, 48:3679–3698.
- Vereb, G., Szölldosi, J., Matkò, J. et al. 2003. Dynamic, yet structured: the cell membrane three decades after the Singer-Nicolson model. *Proc. Natl. Acad. Sci. U.S.A.*, 100:8053–8058.
- Walz, T., Tittmann, P., Fuchs, K.H. et al. 1996. Surface topographics at subnanometer-resolution reveal asymmetry and sidedness of aquaporin-1. *J. Mol. Biol.*, 264:907–918.

17

Size Scaling of Subcellular Organelles and Structures in *Xenopus laevis* and *Xenopus tropicalis*

Lisa J. Edens & Daniel L. Levy

Department of Molecular Biology, University of Wyoming, Laramie, WY

Abstract: How organelle size is regulated is a fundamental question in cell biology. Cell sizes vary dramatically across different species and in different tissue types, and changes in cell size are especially dramatic during early development when cell division frequently occurs in the absence of cell growth. A largely unanswered question is how the sizes of organelles and subcellular structures are regulated relative to cell size, a phenomenon we refer to as scaling. In general, organelle size and/or number are proportionately greater in larger cells to accommodate increased metabolic or specific functional requirements of the cell. These correlations are not absolute and have not been investigated for some organelles, still the phenomenon of scaling provides a useful framework for understanding organelle size control. In this chapter, we review recent studies that have utilized different *Xenopus* systems to illuminate physiological mechanisms of organelle size regulation. The first half of the chapter discusses the characteristics of two related *Xenopus* species that exhibit size differences and describes how comparisons of *in vitro* egg extracts from these two species have contributed to our understanding of size regulation of the nucleus and mitotic spindle. In the second half of the chapter we focus on *Xenopus* developmental scaling when dramatic reductions in cell size occur and highlight how this system has informed size regulation of the nucleus, spindle, and mitotic chromosomes. We conclude with a discussion of the functional implications of organelle scaling and some future prospects about how these *Xenopus* systems might be used to elucidate size control of other organelles and subcellular structures.

Introduction to organelle scaling

Size impacts biological function at multiple levels, from ecosystems (Marquet et al. 2005) and organisms (Spence and Hutchinson 2012) to organs (Tumaneng et al. 2012) and cells (Chan and Marshall 2010). Because sizes are

regulated within defined regimes, there must be evolutionary constraints on this parameter. Consistent with this idea, altered size is associated with disease states (Zink et al. 2004; Webster et al. 2009), affects cell and organismal growth and development, and may contribute to speciation (Smith and Lyons 2011).

While our understanding of cell size determination is fairly advanced (Marshall et al. 2012), relatively little is known about size control of organelles and other subcellular structures. Importantly, size scaling at the subcellular level may determine how size is regulated at higher levels (Goehring and Hyman 2012).

Organelle size regulation is a fundamental problem in cell biology. Cell sizes vary dramatically across different species and in different tissue types. Changes in cell size are especially dramatic during early development when cell division frequently occurs in the absence of cell growth. A largely unanswered question is how the sizes of organelles and subcellular structures are regulated relative to cell size to ensure cell viability and proper function. Surface to volume ratios differ dramatically depending on cell size, placing variable demands on internal organelles and structures.

A variety of models have been proposed to describe how the size of an organelle might be determined. For example, the amount or size of organelle structural components might determine organelle size. Models invoking limiting pools of cytoplasmic components may be sufficient to account for organelle size, number, and scaling (Goehring and Hyman 2012). Alternatively, more dynamic mechanisms might be at play, such as feedback from the organelle that could regulate its own assembly or balancing of assembly and disassembly rates (Marshall 2008). Timing or physical constraints might also limit organelle growth. These types of models can explain length regulation of relatively simple structures like flagella and stereocilia. However, size-regulating mechanisms for organelles with more complex geometries have been difficult to elucidate.

Here we use the term scaling to refer to the phenomenon of size and/or number of organelles and other subcellular structures correlating positively with cell size. Larger cells have proportionately larger organelles to accommodate the increased metabolic or specific functional requirements of the cell. These correlations are not absolute and have not been investigated for some organelles, but the phenomenon of scaling provides a useful framework for understanding organelle size

control. As this chapter will focus on organelle size regulation in the context of scaling, it is important to distinguish size control from scaling. Organelle size can be impacted by many cellular manipulations, and while these can be informative, mechanisms used by the cell to actively control the size of its organelles are not necessarily revealed. Scaling is the normal regulation of organelle size by cells. By studying the scaling relationships between cell and organelle size, mechanisms of organelle size control are elucidated in a physiological context. General principles and properties of scaling have been discussed elsewhere (Marshall 2002; Marshall 2008; Spence 2009; Chan and Marshall 2010; Levy and Heald 2012).

In this chapter, we review recent studies that have utilized different *Xenopus* systems to illuminate physiological mechanisms of organelle size regulation. The first half of the chapter discusses the characteristics of two related *Xenopus* species that exhibit size differences and describes how comparisons of *in vitro* egg extracts from these two species have contributed to our understanding of size regulation of the nucleus and mitotic spindle. In the second half of the chapter, we focus on *Xenopus* developmental scaling when dramatic reductions in cell size occur and highlight how this system has informed size regulation of the nucleus, spindle, and chromosomes. We finish with some future prospects about how these *Xenopus* systems might be used to elucidate size control of other organelles and subcellular structures.

***Xenopus* interspecies scaling**

Organelle scaling has been investigated using two related *Xenopus* frog species: *Xenopus laevis* cells, eggs, and nuclei are larger than those of *Xenopus tropicalis* (Table 17.1 and Figure 17.1). *Xenopus* egg extracts contain all the cytoplasmic components necessary to assemble organelles and subcellular structures *in vitro* but lack the egg chromosomes, so assembly is initiated by addition of an exogenous chromatin source, usually demembrated *Xenopus* sperm. Cell cycle control during meiosis in *Xenopus* differs significantly

Table 17.1 Comparisons between *X. laevis* and *X. tropicalis*.

	<i>X. laevis</i>	<i>X. tropicalis</i>
Ploidy*	Pseudotetraploid	Diploid
Number of haploid chromosomes*	18	10
Genome size*	3.1×10^9 bp	1.7×10^9 bp
Optimal temperature*	16–22°C	25–30°C
Adult size*	10 cm	4–5 cm
Eggs/spawn*	300–1000	1000–3000
Generation time*	1–2 years	4 months
Egg diameter*	1–1.3 mm	0.7–0.8 mm
Erythrocyte cell volume [†]	$250 \mu\text{m}^3$	$122 \mu\text{m}^3$
Erythrocyte nuclear volume [†]	$10 \mu\text{m}^3$	$3 \mu\text{m}^3$

*Data from Bodart and Duesbery (2006) and <http://www.xenbase.org/anatomy/intro.do>.

[†]Data from Horner and Macgregor (1983).

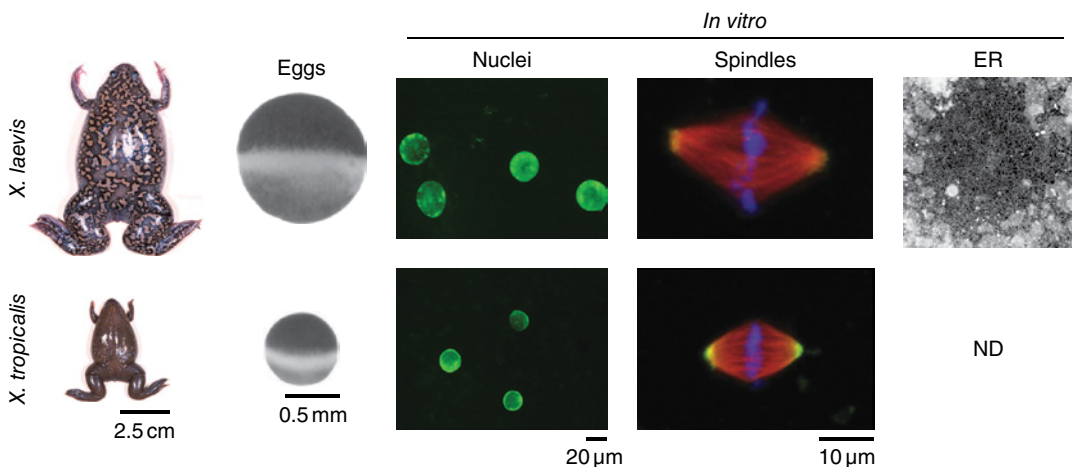


Figure 17.1 Examples of *Xenopus* interspecies organelle scaling. *X. laevis* frogs are larger than *X. tropicalis* frogs. *X. laevis* eggs are also larger than those from *X. tropicalis*, and extracts prepared from these eggs can be used to reconstitute nuclei, mitotic spindles, and ER. Nuclei were assembled in interphase egg extract from the two species using *X. laevis* sperm chromatin. The nuclei were visualized by immunofluorescence using an antibody against the nuclear pore complex (green). Image reprinted from Levy and Heald (2010). © 2010, with permission from Elsevier. Spindles were assembled in mitotic egg extract in the presence of fluorescently labeled tubulin (red). Also visualized are the DNA (blue) and katanin p60 (green). Image adapted with permission from Loughlin *et al.* (2011). ER was assembled in interphase *X. laevis* egg extract and visualized with a lipophilic membrane dye (DiI). This image is our unpublished data. The morphology of ER assembled in *X. tropicalis* egg extract is unknown. ND = not determined. To see a color version of this figure, see Plate 42.

from lower eukaryotes in that laid amphibian eggs are arrested in metaphase II of the meiotic cell cycle and are therefore easily manipulated to generate cell-free extracts to analyze interphase or mitotic organelles and structures. *X. tropicalis* egg extracts are capable of reconstituting the fundamental cell cycle events that have made *X. laevis* egg extracts so

useful in elucidating molecular mechanisms of development and cell biology in the absence of the cell. We use the term “interspecies scaling” to refer to comparisons between *X. laevis* and *X. tropicalis*.

Xenopus egg extracts are a powerful model system to investigate mechanisms and functions of organelle size regulation. These extracts

constitute an undiluted cytoplasm that is amenable to biochemical manipulation and have been extensively used to study various cellular activities including nuclear assembly and import (Chan and Forbes 2006), mitotic spindle regulation (Hannak and Heald 2006), and chromosome structure (Maresca et al. 2005). Since intact cells are not present, essential processes can be studied in an *in vitro* setting where proteins of interest are immunodepleted or inhibited with specific antibodies or compounds and recombinant proteins can be added. Subcellular structures are easily visualized by adding fluorescent membrane dyes or labeled organellar proteins, and live time-lapse microscopy enables functional and kinetic assays. Moreover, sufficient material can be obtained for biochemical experiments and protein purification.

Advantages of studying two closely related *Xenopus* species

X. laevis has many favorable characteristics as a model organism. Maintaining frogs in the laboratory is straightforward since they are aquatic, disease resistant, and easily fed. When injected with hormones, females produce many eggs that are large, sturdy, and easy to manipulate (Table 17.1). Development is external, so eggs can be fertilized *in vitro* and their large size facilitates visualization. Early development constitutes rapid synchronous cell divisions and embryos can be manipulated by mRNA, antibody, and antisense morpholino oligonucleotide microinjection. *X. laevis* is a well-studied vertebrate for which a large amount of information exists regarding both its cell and developmental biology. With a 4–6-month rest interval, individual female frogs can be repeatedly used for egg laying with no harm to the animal.

X. tropicalis has similarly favorable characteristics for laboratory use and for obtaining functional egg extracts and also has other qualities that make it uniquely suited for genetic studies of vertebrate development. Unlike the pseudotetraploid *X. laevis*, *X. tropicalis* is diploid with a smaller genome (Table 17.1), about half the size of the mouse genome. The Joint Genome Institute has sequenced

the *X. tropicalis* genome, providing a complete gene database (Hellsten et al. 2010). Such information will greatly accelerate efforts to identify specific proteins functioning in organelle scaling by proteomic analyses. Furthermore, the *X. tropicalis* generation time is much shorter than that of *X. laevis*, and the necessary rest period between ovulations is only 6–8 weeks. Additionally, given the close similarity between the two species, many resources and reagents developed for *X. laevis* can also be used with *X. tropicalis*, including antibodies and cDNA probes. Developmental progression is similar between the two species, and *X. tropicalis* embryos, which mature faster than *X. laevis* embryos, can also be manipulated by microinjection.

X. tropicalis holds great promise for use in systematic genetic studies since it is amenable to the generation of transgenic lines and mutagenesis owing to its relatively small diploid genome and short generation time (Carruthers and Stemple 2006). Microarrays have been developed for *X. laevis* and *X. tropicalis* and comprehensive comparative transcriptomics databases have been generated comparing changes in gene expression during development of the two species (Yanai et al. 2011). Thus, *X. tropicalis* offers prospects of genetic and genomic tools in addition to the great advantages of *X. laevis* as a model organism. Xenbase is an outstanding online resource (<http://www.xenbase.org/common/>).

Interspecies nuclear scaling

Understanding size control of the nucleus is particularly important because changes in nuclear size and shape are associated with aging and cancer (Prokocimer et al. 2009; Webster et al. 2009; Chow et al. 2012). Cancer cells with enlarged nuclei almost always represent more aggressive metastatic disease, thus nuclear size is measured by pathologists to stage and prognose many different cancers (Zink et al. 2004). Notably, nuclear size does not strictly correlate with ploidy in some cancers (Cremer et al. 2003), and oncogene activation in primary cultured cells is sufficient to cause nuclear enlargement, for instance by RET tyrosine kinase activation in

thyroid carcinoma (Fischer et al. 1998). Nuclear size changes have been reported in a variety of diverse systems, from assessment of physiological health in crayfish (Taylor et al. 2009) and evaluation of drought tolerance in desert plants (Granot et al. 2009), to cardiomyocyte response to induced hypothermia in rats (Meneghini et al. 2009) and estimation of hepatocellular aging (Nakajima et al. 2010).

Most eukaryotic cells contain a single nucleus responsible for storage and maintenance of the genomic DNA. Nuclear size scales with cell size over a wide range of species and cell types (Wilson 1925; Gregory 2011). Genome and cell size correlate; therefore, species with larger genomes generally have larger nuclei, and while this suggests that genome size or ploidy might determine nuclear size, these are only correlations and counterexamples exist. Diverse cell types within the same multicellular organism exhibit cell and nuclear size differences despite possessing the same nuclear DNA. Embryonic development and cell differentiation are also associated with dramatic cell and nuclear size changes that are independent of alterations in genome content (Butler et al. 2009). From a disease perspective, cancer cell nuclei are often enlarged independently of gross changes in ploidy (Tapon et al. 2001; Cremer et al. 2003; Zink et al. 2004).

It has long been observed that the karyoplasmic ratio, the ratio of nuclear to cytoplasmic volumes, is maintained at a constant value (Wilson 1925). Classic transplantation experiments support the idea that cytoplasmic volume and components regulate nuclear size. Heterokaryons formed by fusing hen erythrocytes with HeLa cells resulted in expansion of the erythrocyte nucleus, changes in its chromatin organization, and reactivation of DNA synthesis and transcription (Harris 1967). Similarly, somatic nuclei grew when injected into *X. laevis* eggs or oocytes (Gurdon 1976). Experimental manipulation of sea snail, *Crepidula plana*, embryos demonstrated that cytoplasmic volume, and not cell size per se, determined nuclear size (Conklin 1912). Recent *Xenopus* studies offer mechanistic insight into the cytoplasmic factors involved in nuclear scaling, further supporting the notion that cytoplasm is the

predominant determinant of nuclear size, with DNA bulk setting a minimum to the size of the nucleus.

Nuclear scaling was recapitulated using *X. laevis* and *X. tropicalis* egg extracts (Levy and Heald 2010). Addition of the same *X. laevis* chromatin to each extract formed nuclei that expanded more rapidly in *X. laevis* egg cytoplasm than in *X. tropicalis* cytoplasm, generating nuclei with over twice the nuclear envelope (NE) area (Figure 17.1). Mixing experiments using the two extracts produced a graded effect on nuclear size, demonstrating that titratable cytoplasmic factors determine the size of the nucleus in this system. Importantly, when nuclei were assembled with *X. tropicalis* sperm that have approximately half the DNA content of *X. laevis* sperm, nuclear size was only minimally smaller, demonstrating that cytoplasm has a greater effect on nuclear size than bulk DNA content (Levy and Heald 2010).

Nuclear import rates differed in the two extracts, with *X. laevis* nuclei exhibiting faster import than *X. tropicalis* nuclei. The levels of two nuclear import factors, importin α and Ntf2, differed between the two extracts. Modulating the levels of these two proteins was nearly sufficient to account for the differences in import and nuclear size between the two species. While importin α levels modulated bulk import rates, Ntf2 acted by reducing import of large cargo molecules. Lamin B was demonstrated to be one of the imported cargos mediating these nuclear size differences, consistent with nuclear growth depending on lamins (Dechat et al. 2010). The nuclear lamins are intermediate filament proteins that form a meshwork on the NE nucleoplasmic face and are important for chromatin organization and for providing mechanical strength to the nucleus (Misteli and Spector 2011). These experiments provided mechanistic insight into an example of interspecies nuclear scaling and highlighted a physiologically relevant role for nuclear import and components of nuclear structure like the lamina (Figure 17.2). These findings are consistent with what is known about nuclear size regulation in other systems that have been reviewed elsewhere (Edens et al. 2013; Levy and Heald 2012).

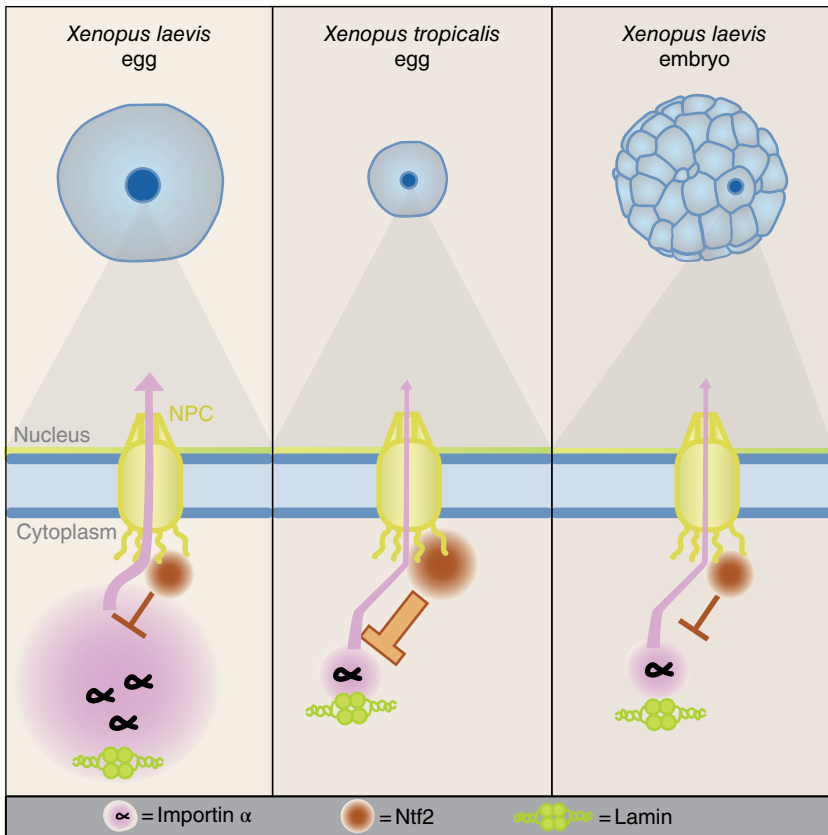


Figure 17.2 Interspecies and developmental nuclear scaling in *Xenopus*. Nuclei assembled in *X. laevis* egg extract are larger than nuclei assembled in *X. tropicalis* egg extract, correlating with differences in nuclear import between the two extracts. Importin α levels positively regulate nuclear size by controlling bulk import rates, while Ntf2 levels negatively regulate nuclear size by slowing large cargo translocation through the nuclear pore complex. These two factors are sufficient to account for interspecies nuclear scaling in *Xenopus*, and lamin B3 is one importin α cargo required for regulating nuclear size. During early *Xenopus* development, nuclear size scales smaller. Reductions in bulk import and importin α levels correlate with reductions in nuclear size up to the MBT, and ectopic expression of importin α by mRNA microinjection in the early embryo leads to increased nuclear size at the MBT. Image reprinted from Levy and Heald (2010). © 2010, with permission from Elsevier.

Interspecies mitotic spindle scaling

When sperm chromatin is added to *Xenopus* egg extract arrested in metaphase of meiosis II with cytostatic factor (CSF), half spindles form (Murray 1991). Addition of calcium releases the CSF arrest, leading to the formation of interphase nuclei and DNA replication. Subsequent addition of nondegradable cyclin B or CSF extract induces bipolar spindle formation and the extract is arrested in metaphase of mitosis (Tunquist and Maller 2003). Spindles can be visualized by the addition of fluorescently labeled tubulin as well as by immunofluores-

cence to visualize spindle poles (NuMA) and chromatin (Brown et al. 2007).

Though strictly speaking these egg extract spindles are meiotic, for simplicity we will refer to them as mitotic spindles because most findings in this system are consistent with mitotic spindle assembly (Cross and Powers 2009). The mitotic spindle is a dynamic bipolar microtubule array required for the staunch alignment and division of chromosomes into daughter cells during cell division. Investigations of *Xenopus* interspecies scaling take advantage of differences between *X. laevis* and *X. tropicalis* in organism, genome, and egg size (Table 17.1) to

expose mechanisms of spindle size, structure, and function regulation.

Spindles formed using *X. laevis* sperm chromatin in *X. tropicalis* egg extract were approximately 30% shorter than those assembled in *X. laevis* egg extract (Figure 17.1), while those assembled using *X. tropicalis* sperm nuclei were only 10% shorter in both *X. laevis* and *X. tropicalis* egg extracts (Brown et al. 2007). These data indicated that cytoplasmic factors rather than DNA amount primarily determine spindle length in this system. Extract titration experiments demonstrated that spindle length increased linearly with the proportion of *X. laevis* extract to *X. tropicalis* extract, further suggesting that cytoplasmic factors are responsible for interspecies spindle length scaling.

Mitotic spindles are dynamic structures *in vivo* as are those assembled *in vitro*. By adding preassembled spindles to egg extracts it was determined that spindle size is also dynamic. The size of the preassembled spindles changed only when extract of the other species was added and the size changed accordingly, i.e., *X. tropicalis* spindles grew when exposed to *X. laevis* extract and *X. laevis* spindles shrank when exposed to *X. tropicalis* extract (Brown et al. 2007).

In experiments designed to uncover regulatory mechanisms of spindle length scaling, microtubule dynamics were observed to differ between egg extracts from the two species. While microtubules grew approximately 20% slower in *X. tropicalis* egg extracts, frequencies of catastrophe (the switch from growth to shrinking) and rescue (renewed growth), steady-state microtubule length, and poleward flux rates were similar in both *Xenopus* extracts (Brown et al. 2007). Strikingly, when microtubule half-life was measured by adding extract to taxol-stabilized microtubules attached to a coverslip, it was observed that microtubules exposed to *X. laevis* extract were approximately 20-fold more stable than microtubules exposed to *X. tropicalis* extract. After a 3 min incubation, most microtubules exposed to *X. tropicalis* egg extract had depolymerized, while microtubules in *X. laevis* extract persisted, and mixing extracts resulted in intermediate microtubule stability (Loughlin et al. 2011). Collectively, these data

strongly suggested that soluble regulators of microtubule depolymerization were the primary determinants of interspecies spindle scaling in *Xenopus* extracts.

Antibody inhibition of candidate proteins known to be involved in microtubule depolymerization identified the catalytic subunit p60 of katanin as the critical component, as katanin inhibition increased microtubule half-life (Loughlin et al. 2011). Katanin is a heterodimeric AAA ATPase known to sever microtubules (McNally and Vale 1993). In *Caenorhabditis elegans*, katanin increases polymer number and shortens microtubule length during meiosis (Srayko et al. 2006), while in *Drosophila* katanin is known to localize to the kinetochore where it stimulates microtubule plus-end depolymerization (Zhang et al. 2007). Katanin protein levels were found to be similar in both *Xenopus* extracts. Nevertheless, purified *X. tropicalis* katanin protein sped up microtubule depolymerization in *X. laevis* extract while the addition of purified *X. laevis* katanin protein had no effect. These data indicated that the two katanins, despite 95% protein sequence identity and comparable microtubule affinity and severing activity, had altered activity in the two extracts (Loughlin et al. 2011).

The catalytic subunit p60 of *X. laevis* katanin was shown to be more highly phosphorylated than *X. tropicalis* katanin (Figure 17.3) (Loughlin et al. 2011). A predicted Aurora kinase consensus phosphorylation site was identified in the *X. laevis* katanin protein sequence at Serine 131 which is conserved in many vertebrate species (Whitehead et al. 2013), but not in the *X. tropicalis* katanin sequence. Mutation of S131 to alanine in the *X. laevis* katanin protein decreased phosphorylation to a similar extent as inhibition of Aurora kinase with VX680. Microtubule half-life also decreased three- to fourfold with the S131A mutant, while a phosphomimetic mutant of katanin did not affect microtubule-severing activity (Loughlin et al. 2011). Additionally, Aurora B kinase phosphorylated *X. laevis* katanin but not *X. tropicalis* katanin, and Aurora A only weakly phosphorylated either *in vitro* (Loughlin et al. 2011). These data suggested that *X. tropicalis* katanin lacks a phosphorylation site for Aurora B kinase that in *X. laevis* negatively regulates katanin activity resulting in increased microtubule stability.

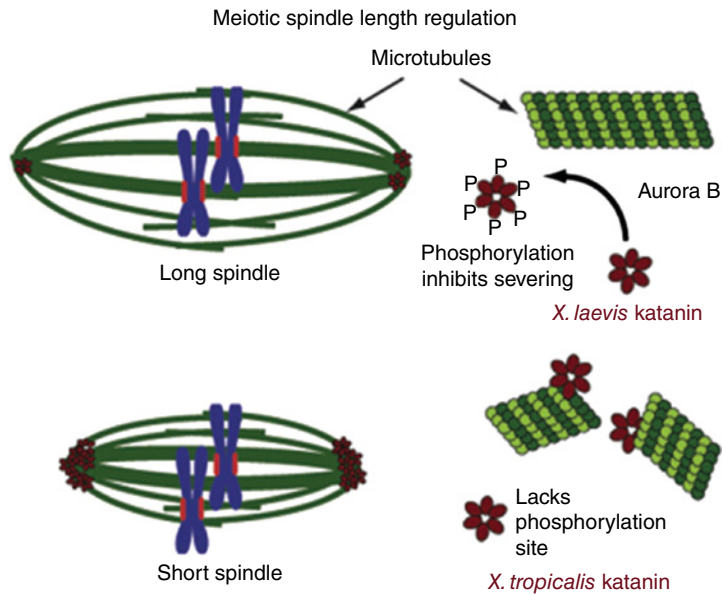


Figure 17.3 Interspecies mitotic spindle length scaling in *Xenopus*. Katanin is a microtubule-severing protein that in *X. laevis* contains an Aurora B kinase phosphorylation site that negatively regulates its activity, while *X. tropicalis* lacks this phosphorylation site. Therefore, increased activity of *X. tropicalis* katanin shortens spindles (bottom image), while phosphorylated inactive katanin in *X. laevis* results in longer spindles (top image). Image reprinted from Loughlin *et al.* (2011). © 2011, with permission from Elsevier.

A series of experiments was performed in order to correlate the katanin phosphorylation state with spindle length. Immunodepletion of p60 from *X. tropicalis* extract resulted in longer spindles and adding back *X. tropicalis* p60 or the S131A mutant of *X. laevis* p60 counteracted this effect. Additionally, Aurora B inhibition shortened *X. laevis* spindles, presumably through p60 activation, but not *X. tropicalis* spindles. Taken together, these data strongly suggest that the increased katanin activity displayed in *X. tropicalis* extracts can account for shorter spindles and increased microtubule depolymerization compared to *X. laevis* extracts in which katanin is negatively regulated by Aurora B kinase phosphorylation, ultimately contributing to spindle length scaling in *Xenopus* (Figure 17.3).

Interspecies mitotic chromosome scaling

Regulation of mitotic chromosome length is essential for faithful chromosome segregation during cell division. One might imagine

that mitotic errors could ensue if a mitotic chromosome was longer than half the length of the spindle at telophase. Indeed, artificially increasing the length of one chromosome arm in plants led to growth and developmental defects resulting from incomplete sister chromatid separation and the formation of chromatin bridges and micronuclei (Schubert and Oud 1997; Hudakova *et al.* 2002). In fly neuronal stem cells, long chromatid arms are counteracted by a cell elongation mechanism (Kotadia *et al.* 2012), and in yeast, increased chromosome compaction ensures faithful segregation of long chromosomes (Neurohr *et al.* 2011). Axial chromosome compaction is also important in animal cells to ensure complete chromatid separation (Lipp *et al.* 2007; Mora-Bermudez *et al.* 2007), and chromatin shape can impact the symmetry of assembled mitotic spindles and the number of poles that form (Dinarina *et al.* 2009). Important questions are: does mitotic chromosome scaling exist, and what mechanisms regulate mitotic chromosome structure and size?

Xenopus again provided a fruitful system to investigate mitotic chromosome scaling (Kieserman and Heald 2011). *Xenopus* sperm chromatin was added to egg extracts and cycled through interphase to induce DNA replication, followed by the isolation and quantification of metaphase chromosomes. Different from the interspecies scaling observed for nuclei and spindles, mitotic chromosomes in *X. laevis* and *X. tropicalis* egg extracts were of similar dimensions. The only statistically significant difference was that *X. tropicalis* mitotic chromosomes were slightly longer in *X. tropicalis* extract than in *X. laevis* extract. Thus, duplicated sperm chromosomes assembled in egg extracts do not exhibit interspecies scaling (Kieserman and Heald 2011).

Interestingly, mitotic sperm chromosomes assembled in egg extract were large relative to spindle length, frequently exceeding half the length of the metaphase spindle. A possible explanation is that anaphase B movements in the early embryo are fast and large, segregating chromosomes long distances on the order of hundreds of microns (Wuhr et al. 2008). In this scenario, chromosome length does not necessarily need to be scaled to spindle length because large cell size and unique anaphase B movements ensure that chromosomes are sufficiently segregated prior to cytokinesis (Kieserman and Heald 2011). This idea might also explain why mitotic chromosome size is not scaled between *X. laevis* and *X. tropicalis* eggs. Even though their cell sizes differ, chromosomes still must be segregated long distances during the first mitosis, thus necessitating large anaphase B movements in both species and avoiding the need to scale mitotic chromosome length. The situation is quite different as development proceeds and cells become smaller, and we will address this scenario later in the chapter.

Techniques: *X. tropicalis* egg extracts

Methods for the preparation and use of *X. laevis* egg extracts have been thoroughly reviewed elsewhere (Smythe and Newport 1991; Chan and Forbes 2006; Hannak and Heald 2006; Maresca and Heald 2006). *X. tropicalis* egg

extracts are prepared similarly to *X. laevis* egg extracts with some important differences, which we will summarize here. One excellent source for *X. tropicalis* husbandry is Mustafa Khokha's lab website (<http://khokha.medicine.yale.edu/index.html>). Two important differences between the species are the following: (i) while *X. laevis* are raised at 18–20°C, *X. tropicalis* are maintained at 27–28°C, and (ii) *X. laevis* frogs harbor pathogens that cause disease in *X. tropicalis*, so it is imperative that *X. laevis* water and equipment never come into contact with *X. tropicalis*.

Newly acquired *X. tropicalis* frogs should be injected with 50 units of human chorionic gonadotropin (hCG), using a 30 gauge needle, and allowed to rest 2 months prior to use to improve egg yield. To induce egg laying, frogs are first primed with a 10 unit hCG injection 16–24h prior to boosting with a 200 unit hCG injection. Frogs should be kept at room temperature and will have started laying eggs 5h after the boosting injection. Frogs should be kept in tank water for egg laying, not Marc's modified Ringer's (MMR). *X. tropicalis* are much more active than *X. laevis* and simply holding a frog in one's hand will encourage additional egg laying. New frogs generally provide the highest egg yield, which can suffer when successive ovulations are separated by long rest periods (more than 3 months).

Eggs are collected and extract prepared similarly to that of *X. laevis* with the following differences. Dejelling is performed with a fresh 3% L-cysteine solution prepared in water with the pH adjusted to 7.8–8.0 with concentrated potassium hydroxide. Because the smaller size of *X. tropicalis* eggs prevents assessment of complete dejelling by egg packing as with *X. laevis* eggs, dejelling is monitored by egg rotation so that the dark pigmented animal pole faces upward. One can expect approximately 200µL egg extract per frog. It is important to add cytochalasin D to the eggs prior to the crushing spin (e.g., 10µL of 10mg/mL cytochalasin D to 0.5mL egg lysis buffer). Once the extract is prepared, it must not be stored at a temperature below 16°C and never on ice. The extract should be used immediately in the same way one would use an *X. laevis* egg extract or held at 16°C or room temperature for up to 1–2h.

***Xenopus* developmental scaling**

Early embryo development represents a robust cellular scaling system because cell divisions are rapid with no overall growth in the size of the embryo itself. In *X. laevis*, the initially approximately 1 mm diameter fertilized egg undergoes 12 rapid, synchronous cell divisions (each ~30 min), to produce about four thousand 50 μm cells at the mid-blastula transition (MBT) (Nieuwkoop and Faber 1967). As the embryo proceeds through gastrulation, further reductions in cell size occur, reaching 12 μm in the tadpole. While *Xenopus* egg extracts represent the traditional model system, *Xenopus* embryo extracts can be manipulated and analyzed similarly to egg extracts (Levy and Heald 2010). Different-stage embryo extracts can be mixed and fractionated, and endogenous embryonic nuclei can be examined in their native cytoplasm. Changes in scaling factor abundance, localization, and activity can be monitored by protein immunoblot and immunofluorescence. A transcriptomics study comparing *X. laevis* and *X. tropicalis* development will undoubtedly facilitate analysis of embryo extract experiments (Yanai et al. 2011).

Furthermore, microinjected *Xenopus* embryos enable *in vivo* functional studies of organelle size regulation. Single-cell fertilized *X. laevis* embryos can be microinjected with mRNA to ectopically express proteins of interest, morpholino oligonucleotides to inhibit target mRNA expression, or inhibitory antibodies. As an example, microinjecting importin α mRNA at the one-cell stage increases nuclear size in the MBT embryo (Levy and Heald 2010). Embryos can also be injected to express fluorophores fused to a membrane-targeting sequence to visualize cells and organelles. To investigate functional consequences of altering organelle size, one blastomere of a two-cell embryo can be injected to alter organelle size in that half of the embryo, leaving the uninjected blastomere as a control. Live imaging of injected embryos can then be performed using Rhodamine-labeled dextran as an injection tracer.

Developmental nuclear scaling

Nuclear size decreases throughout early embryonic development in both *X. laevis* and *X. tropicalis* (Figure 17.4), providing another system to investigate nuclear scaling (Gerhart 1980; Montag et al. 1988; Levy and Heald 2010). Experimentally halving the DNA content in *X. laevis* embryonic nuclei only reduced NE surface area by 10%, demonstrating that, like egg cytoplasm, embryo cytoplasm determines nuclear size to a greater extent than ploidy (Levy and Heald 2010). Reductions in bulk import and cytoplasmic importin α levels correlated with reductions in nuclear size at the MBT, and nuclear size in the embryo was sensitive to importin α levels as its ectopic overexpression in MBT embryos increased nuclear size (Figure 17.2). In post-MBT embryos, ectopic expression of both importin α and lamin B was necessary to increase nuclear size. It is worth noting that lamins appear to become limiting at a time during development when total nuclear volume in the embryo plateaus (Gerhart 1980).

As with interspecies scaling, developmental nuclear scaling in *Xenopus* involves changes in nuclear import capacity and the lamins. However, this import pathway cannot fully account for nuclear size changes during development, leaving open questions about what roles nuclear export or membrane availability might play, as well as other novel scaling mechanisms (Edens et al. 2013). Potential functional implications for developmental nuclear scaling and regulation of the nucleocytoplasmic ratio are discussed later under “Functions of organelle scaling”.

Developmental mitotic spindle scaling

During the first seven cell divisions of *X. laevis* embryonic development, cell diameter decreases approximately fivefold, but the length of the mitotic spindle was observed to change very little, maintaining a maximum length of approximately 60 μm . Cell and spindle length are largely uncoupled during these early developmental stages, an example

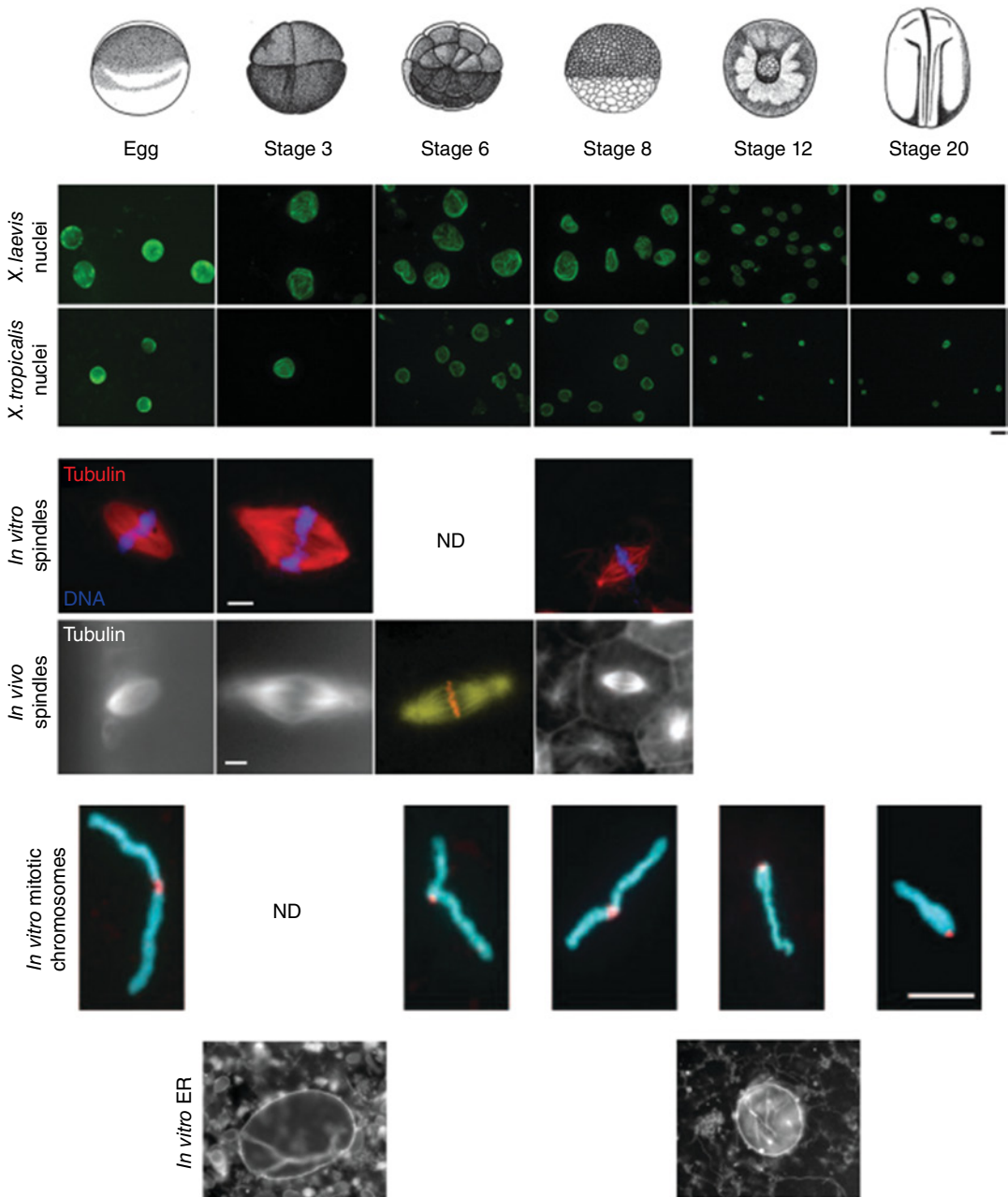


Figure 17.4 Examples of *Xenopus* developmental organelle scaling. The top of the figure depicts different-stage *X. laevis* embryos. Adapted from Nieuwkoop and Faber (1967). For images of nuclei, different-stage *Xenopus* embryos were arrested in late interphase with cycloheximide, to ensure complete fusion of karyomeres in pre-MBT embryos. Embryo extracts were prepared and endogenous nuclei were visualized by immunofluorescence using an antibody against the nuclear pore complex (green). The scale bar represents 20 μm . Nucleus images were adapted with permission from Levy and Heald (2010). *In vitro* spindles were assembled from *X. laevis* egg or embryo extracts and the microtubules (red) and DNA (blue) were visualized. *X. laevis in vivo* spindles were imaged in fixed hemisected eggs or embryos by tubulin immunofluorescence (grey). All spindle images were adapted from Wilbur and Heald (2013) made available using a Creative Commons Attribution License (<http://creativecommons.org/licenses/by/3.0/us/>), except for the stage 6 *in vivo* spindle image which was reprinted from Wuhr *et al.* (2008). © 2008, with permission from Elsevier, and depicts tubulin (yellow) and DNA (red) staining. The scale bars represent 10 μm . Mitotic chromosomes were obtained by isolating G_2 nuclei from different-stage *X. laevis* embryos and mitotically condensing the chromosomes in metaphase-arrested egg extract. Kinetochores (red) and DNA (blue) are visualized. The scale bar represents 5 μm . Images were adapted from Kieserman and Heald (2011) made available using a Creative Commons Attribution License (<http://creativecommons.org/licenses/by/3.0/us/>). ER was visualized in *X. laevis* embryo extracts using a lipophilic membrane dye (DiI). Depicted are embryonic nuclei with associated ER structures. These images are our unpublished data. ND = not determined. To see a color version of this figure, see Plate 43.

of negligible spindle scaling. However, a nearly twofold reduction in spindle length occurs between the seventh mitosis and the MBT (stage 8) when embryonic transcription begins (Figure 17.4). Furthermore, spindle length was observed to scale with cell size in stage 8 and 9 embryos (Wuhr et al. 2008). Before embryonic transcription begins, one can imagine three possible explanations for spindle shortening during development: (i) physical boundaries of the cell limit spindle length, (ii) a spindle lengthening factor is titrated as cells divide, and (iii) intrinsic properties of the spindle are sensitive to cytoplasmic volume. One of the major advantages of the *Xenopus* extract system is that the assembled spindles are exempt from both the physical barrier and limiting factor modes of regulation, as spindle length reached an upper limit of approximately 60 μm in extract that was unaltered when the spindle concentration was varied (Wuhr et al. 2008).

To assess the effect of DNA mass on spindle length, diploid and haploid embryos were compared early in development. Haploid embryos are generated by fertilizing eggs with UV-treated sperm. Upper spindle length was approximately 62 μm in diploid embryos and approximately 55 μm in haploid embryos, indicating DNA mass is not a major regulator of spindle size (Wuhr et al. 2008). Extracts prepared from embryos at various stages of development are capable of assembling mitotic spindles that are similar, but not identical, to spindles in intact embryos at the corresponding stage. While spindle length decreased by approximately 30 μm from stage 3 to stage 8 in the embryo, it decreased approximately 20 μm in extracts prepared from the same stages (Wilbur and Heald 2013) (Figure 17.4). Titrating stage 3 and stage 8 embryo extracts resulted in dose-dependent spindle length scaling (Wilbur and Heald 2013), thus suggesting that the length of the mitotic spindle is, like the meiotic spindle, primarily determined by cytosolic factors.

Assessment of global microtubule dynamics in both stage 3 and stage 8 mitotic spindles showed similar growth, severing, and poleward flux rates as well as a slight increase in microtubule nucleation in stage 3 spindles. Strikingly, the frequency of microtubule

catastrophe was threefold higher in stage 8 spindles (Wilbur and Heald 2013), suggesting that increased microtubule catastrophe influences developmental spindle length. Several candidate factors known to be involved in microtubule catastrophe and/or nucleation were screened for variability between stage 3 and stage 8 embryo extracts. The kinesin-13 catastrophe factor kif2a (Aizawa et al. 1992; Homma et al. 2003) weakly localized to stage 3 kinetochores and spindle poles, whereas stage 8 spindles exhibited greater amounts of kif2a localized homogeneously across the entire spindle with a slight enrichment at the poles (Figure 17.5). Additionally, antibody inhibition of kif2a had no effect on stage 3 spindles, while stage 8 spindles became longer with altered morphology, further indicating that kif2a is a developmental spindle size-determining factor (Wilbur and Heald 2013).

Further analysis of kif2a revealed a nuclear localization sequence and coimmunoprecipitation showed weak interaction between kif2a and importin α . kif2a disassembled taxol-stabilized microtubules; however, pretreatment of kif2a with importin α prevented microtubule depolymerization, suggesting that importin α directly regulates kif2a (Wilbur and Heald 2013). When kif2a levels were increased in stage 3 extracts, spindle size was reduced up to 22%, whereas increased importin α levels in stage 8 extracts lengthened spindles by 27% and this effect could be reversed by adding kif2a (Wilbur and Heald 2013). *In vivo* verification was performed by microinjecting importin α mRNA into embryos which resulted in a 20% increase in spindle length at stage 8 (Wilbur and Heald 2013).

While importin α levels in cytoplasmic extract decrease during development, analysis of whole embryo lysates revealed that in fact total importin α levels do not change, while its partitioning does. A modified form of importin α with reduced mobility on denaturing polyacrylamide gels was enriched in the lipid fraction of stage 8 extracts and completely absent from stage 3 extracts. In quantitative pull-down experiments, recombinant kif2a interacted with tenfold more importin α in stage 3 extracts than stage 8 extracts. Furthermore, importin α immunofluorescence was more intense at the cell edge than cytoplasm in stage

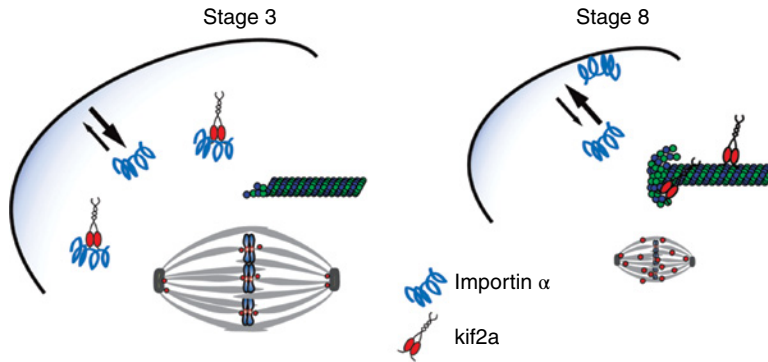


Figure 17.5 Developmental mitotic spindle length scaling in *X. laevis*. Importin α localizes to the cytosol where it forms an inhibitory complex with kif2a, a microtubule catastrophe protein, or to the cell periphery where it is unable to function as an inhibitor of kif2a. At stage 3 of development, importin α is primarily localized in the cytosol, thus inhibiting kif2a activity and promoting longer spindles. While at stage 8 of development, a likely posttranslational modification increases the partitioning of importin α to the cell periphery, thus increasing the concentration of active kif2a and shortening spindles. Image adapted from Wilbur and Heald (2013) made available using a Creative Commons Attribution License (<http://creativecommons.org/licenses/by/3.0/us/>).

8 embryos compared to stage 3 embryos (Wilbur and Heald 2013). Taken together, these data suggested that relocation of importin α to the cell periphery in stage 8 embryos leads to increased kif2a activity on microtubules and shorter spindles (Figure 17.5).

In order to determine kif2a functional effects on spindle assembly and structure, embryos were microinjected with kif2a recombinant protein immediately before the stage 3–4 cytokinesis. Although the mitotic spindle remained functional with no apparent timing, alignment, or segregation problems, spindle size was decreased and the orientation of metaphase spindles became randomized, indicating that there is a correlation between spindle size and orientation at metaphase in the early embryo (Wilbur and Heald 2013).

One major question that remains is how spindles segregate chromosomes in a cell 20 times their size. When embryos were fixed before, during, and after the 2-cell stage, it was observed that astral microtubules elongate at anaphase, form a hollow structure, eventually reach the cell cortex, and trigger cytokinesis (Wuhr et al. 2008). Thus, astral microtubules may facilitate chromatin separation during anaphase over long distances when the cells are large, such as in early development.

Regulation of microtubule depolymerization contributes to both interspecies and

developmental spindle length scaling. Early in development, importin α inhibits the microtubule depolymerizing protein kif2a, while in later stages importin α partitions to the cell periphery, resulting in increased kif2a activity and shorter spindles (Figure 17.5). Regulation of microtubule stability also contributes to interspecies scaling, in this case through differential phosphorylation and inhibition of the microtubule-severing protein katanin (Figure 17.3). Nevertheless, it is important to note that neither mechanism of spindle length regulation completely accounts for spindle size scaling during development or between species.

Developmental mitotic chromosome scaling

While differences in mitotic chromosome size were not observed between *X. laevis* and *X. tropicalis*, developmental mitotic chromosome scaling does occur. Measurements of chromosome length in fixed *X. laevis* embryos showed that mitotic chromosomes become shorter between the blastula and tail bud stages (Micheli et al. 1993). This is consistent with the notion that as cell size decreases during development, so too must mitotic chromosome size in order to ensure proper segregation. As visualization of chromosomes *in situ* in *Xenopus*

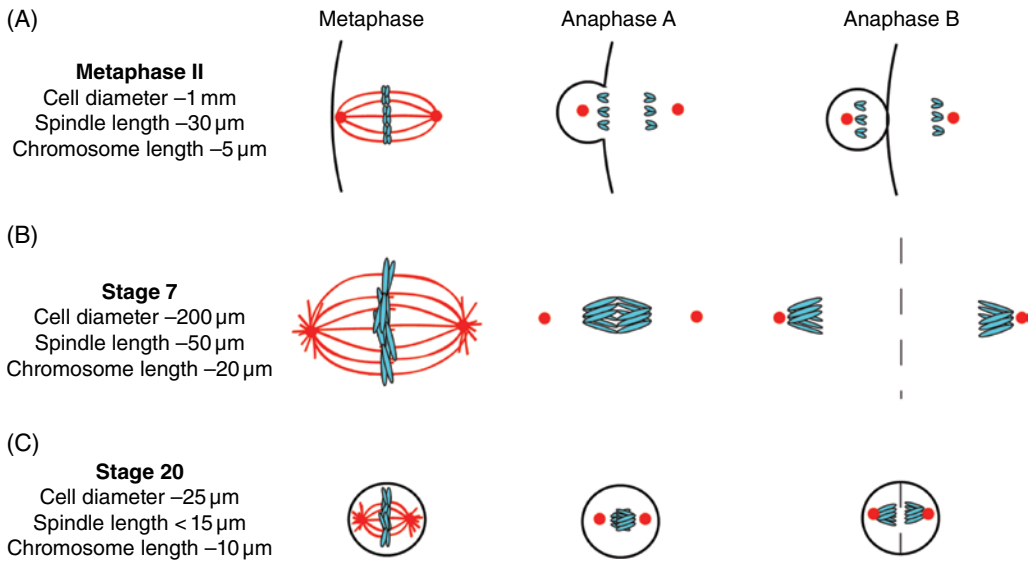


Figure 17.6 Models of coordinated spindle and chromosome scaling at different *Xenopus* developmental stages. Spindle microtubules are depicted as lines emanating from spindle poles (large dots) and contacting chromosomes aligned at the metaphase plate. The metaphase II-arrested egg is large relative to the meiotic spindle and small chromosomes. The spindle is positioned near the cell cortex, so anaphase movements need not be large. Asymmetric cell division produces one very small polar body and one very large egg, and small chromosomes ensure complete segregation. Cells in the pre-MBT stage 7 embryos are smaller than the egg but contain much larger chromosomes and spindles. During cell division, extended anaphase B movements promote the symmetric segregation of longer chromosomes to the center of daughter cells. In later stage 20 neurula embryos, cell, spindle, and chromosome sizes all scale smaller. Anaphase B movements are restricted by the small cell size, imposing a limit on chromosome and spindle length necessary to ensure complete chromosome segregation. Adapted from Kieserman and Heald (2011) made available using a Creative Commons Attribution License (<http://creativecommons.org/licenses/by/3.0/us/>). To see a color version of this figure, see Plate 44.

embryos is complicated by high background fluorescence and clustering of metaphase chromosomes, an alternate approach was taken whereby G_2 nuclei were isolated from different-stage embryos and incubated in metaphase-arrested egg extract (Kieserman and Heald 2011). G_2 embryo nuclei were expected to contain the factors responsible for regulating chromosome size and establishing higher-order chromatin architecture, and this approach successfully recapitulated changes in mitotic chromosome size during embryogenesis. While chromosome sizes were similar throughout early development prior to the MBT, progressive reductions in mitotic chromosome area were observed as embryos developed through blastula stages 9–11, with an approximate 50% decrease in chromosome area by neurula stage 20 (Kieserman and Heald 2011) (Figure 17.4).

Data support the idea that mitotic chromosome size is differentially regulated

throughout development, closely mirroring scaling of spindle length. In metaphase of meiosis II, the spindle and meiotic chromosomes are relatively small. This seems reasonable since the meiotic spindle is localized at the cortex of the egg so chromosomes only travel a short distance to form the polar body. Mitotic spindles in cleavage-stage pre-MBT embryos are approximately twice as long as the meiotic spindle, and mitotic chromosomes also tend to be quite long. Chromosome length scaling was not observed early in development when large anaphase B movements segregate chromosomes long distances across large cells. As anaphase B movements become constrained in the post-MBT embryo due to reductions in cell size, spindle and chromosome sizes scale smaller to ensure complete and faithful chromosome segregation (Figure 17.6). While these studies deal with chromosome scaling during mitosis, a completely unanswered question is how

interphase chromosome size and organization change with respect to nuclear and cell size.

As opposed to developmental scaling of the nucleus and spindle where cytoplasmic factors are the predominant regulators, developmental scaling of mitotic chromosomes appears to be intrinsically determined by chromosome architecture and depends on the embryonic stage of the nucleus. Developmentally regulated expression of specific DNA binding or nuclear proteins and/or modifications likely determines chromosome size. There are a number of candidate scaling factors, including core and linker histone isoforms, whose expression is known to change during development (Shechter et al. 2009a; Shechter et al. 2009b; Freedman and Heald 2010), and condensin I and II and topoisomerase II that regulate lower-order chromatin organization (Belmont 2006; Hudson et al. 2009; Tapia-Alveal et al. 2010). Changes in DNA and/or histone modifications may also play a role. One intriguing observation was that chromosomes in embryonic nuclei were refractory to remodeling by egg cytoplasm unless the nucleus was allowed to pass through the cell cycle (Kieserman and Heald 2011). This suggests that stable epigenetic mechanisms establish chromosome size and that these mechanisms can be reset by cell cycle progression, presumably DNA replication. The relevant chromosome scaling factors remain to be identified, as well as the effects of altering them *in vivo*.

Techniques: *Xenopus* embryo extracts

Xenopus embryo extracts have become increasingly common to elucidate mechanisms of organelle size regulation. To make embryo extract, one first fertilizes freshly laid eggs with macerated testes in a very small volume of water or physiological buffer for approximately 10 min; then, the eggs are flooded with 1/3× MMR. After 1 h, the eggs are dejellied in 2–3% L-cysteine (prepared in 1/3× MMR with pH adjusted to 7.8 with 10N potassium hydroxide) for 2–4 min and then rinsed 6–10 times in 1/3× MMR. Embryos are allowed to develop in 1/3× MMR to the desired stage. The first cleavage occurs approximately 1.5–2 h postfertilization followed by approximately 30 min cell cycles

up to the MBT. It is important for the survival of healthy embryos to remove unfertilized and dead embryos along the way. If embryonic nuclei will be isolated, embryos can be incubated in 0.54 mM cycloheximide at the desired developmental stage for approximately 1 h in order to synchronize nuclei at interphase. To make the extract, embryos are transferred to a microfuge tube and washed three times with 1 mL ELB+ (250 mM sucrose, 50 mM potassium chloride, 2.5 mM magnesium chloride, 10 mM HEPES pH 7.8, with 1/1000 volume of LPC mixture (21 mM leupeptin, 14.6 mM pepstatin, 16.5 mM chymostatin, or 10 mg/mL of each)), removing as much buffer as possible each time. 500 µL of ELB+ is then added to the embryos as well as 5 µL of 19.7 mM (10 mg/mL) cytochalasin D and 5 µL of 35.5 mM (10 mg/mL) cycloheximide. The embryos are packed by centrifuging at 200g for 1 min, as much buffer as possible is removed, and the embryos are crushed with a pestle (for later-stage embryos, it is important to effectively crush entire embryos with the pestle). The extract is centrifuged in a swinging bucket rotor at 10,000g for 10 min at 16°C. The upper lipid layer is pierced with a pipet tip and the middle cytoplasmic layer is then collected with a new pipet tip. To the cytoplasmic extract are added 1/50 volume of 50× energy mix (190 mM creatine phosphate disodium, 25 mM ATP disodium salt, 25 mM magnesium chloride), 1/100 volume of 35.5 mM cycloheximide, 1/500 volume of 19.7 mM cytochalasin D, and 1/1000 volume of LPC mixture. The extract should be gently mixed by inversion or with a wide-bore pipet tip (never pipet vigorously). Embryo extract containing nuclei can be stored at –80°C. In order to remove nuclei, the embryo extract is diluted 1 : 1 with ELB+ containing energy mix, cycloheximide, and cytochalasin D at the same concentrations as in the extract and then spun in a swinging bucket rotor at 17,000g for 15 min at 16°C. The embryo extract is then collected, making sure not to disturb the pellet of nuclei, and stored at –80°C.

Functions of organelle scaling

What is the functional significance of organelle scaling? Approaches to answering this question will depend on the particular organelle of

interest, so we will take the nucleus as an example (Edens et al. 2013). Nuclear volume might affect concentrations of macromolecules within the nucleus, kinetics of nuclear enzymes, chromosomal organization, and assembly of nuclear bodies. Much correlative data support the notion that proper nuclear size control is important for biological function. During early *C. elegans* development, NE surface area dictates centrosome attachment to the male pronucleus, likely by regulating the access of centrosome microtubules to dynein localized at the NE, and defects in this process disrupt normal development (Meyerzon et al. 2009). During *Drosophila* development, muscle cell size and muscle mass correlate with the number of nuclei per cell (Demontis and Perrimon 2009), and disrupting polyploidization in the large nuclei of *Drosophila* subperineurial glia leads to loss of the blood–brain barrier (Unhavaithaya and Orr-Weaver 2012). Nuclear import plays a central role in cell differentiation, for example, switching expression of importin α isoforms regulates differentiation of embryonic stem cells into disparate cell lineages (Yasuhara et al. 2009), and changes in nuclear pore complex composition contribute to cell differentiation and regulated gene expression (D’Angelo et al. 2012). In micropatterned endothelial cells, nuclear volume in the G₁ phase of the cell cycle was predictive of proliferative potential (Roca-Cusachs et al. 2008). Nesprins, outer nuclear membrane proteins that bind actin filaments, appear to control epithelial nuclear size and epidermal thickness in mice (Luke et al. 2008). An inner nuclear membrane protein in budding yeast, Mps3, functions in lipid and NE homeostasis (a mutant displays overproliferation of the NE) necessary for spindle pole body duplication and insertion (Friederichs et al. 2011).

Early developmental transitions can influence later differentiation and organogenesis in the embryo, so how nuclear size impacts timing and signaling in the early embryo is an important question. The MBT in *Xenopus* is characterized by longer cell cycles, cell division asynchrony, maternal mRNA transcript destabilization, and zygotic transcript upregulation. A critical ratio of total DNA content to cytoplasm determines MBT

timing in *Xenopus* (Newport and Kirschner 1982; Clute and Masui 1995). In rapid early developmental cell divisions, total cytoplasmic volume in the embryo remains the same while total DNA content increases through rounds of nuclear replication. Experimentally reducing cytoplasmic volume or increasing DNA amount resulted in a premature MBT. Conversely, reducing DNA content, by delaying nucleation in dividing embryos, resulted in a delayed MBT. While nuclei in early embryos are larger than nuclei at the MBT, total nuclear volume in the embryo increases continuously, reaching a maximum value at the MBT (Gerhart 1980; Levy and Heald 2010). It is tempting to speculate that nuclear size might determine MBT timing, something that can be directly tested by experimentally manipulating nuclear size in developing embryos.

Recent work has shown that chromosomes and genes are nonrandomly arranged in the nuclear space and gene expression profiles are influenced by chromatin three-dimensional arrangement and attachments to the nuclear envelope (Misteli and Spector 2011). In one illustrative example, nuclear import of the phosphatidic acid phosphatase lipin 1 caused nuclear shape changes that led to altered transcriptional output. Here, a nuclear shape change coordinates signaling from the nutrient-sensing mTOR complex with cholesterol and fatty acid biosynthesis by SREBP (Peterson et al. 2011). Spatial proximity of specific genes underlies the chromosomal translocations that give rise to many cancers, especially leukemias and lymphomas (Zhang et al. 2012). Changes in genome organization are likely critical during cellular differentiation as well.

How might nuclear size affect subnuclear organization and function? It will be possible to address this question by manipulating nuclear size *in vivo* and probing effects on nuclear organization with techniques such as chromosome conformation capture, fluorescence *in situ* hybridization, DNA adenine methyltransferase identification, and chromosome painting (Naumova and Dekker 2010), in conjunction with massive parallel sequencing to correlate changes in chromatin organization with gene expression patterns.

Future work will clarify the interplay between nuclear size, subnuclear organization, and cell and nuclear function and ultimately how breakdowns in these relationships contribute to disease. Approaches to understanding the functional relevance of scaling for other organelles will be unique to the organelle under study.

Future directions

In summary, *Xenopus* offers powerful *in vitro* and *in vivo* systems to decipher size control mechanisms for a variety of subcellular structures, including the nucleus, spindle, and mitotic chromosomes, and there is great potential to use these systems to investigate scaling of other organelles. Beyond elucidating scaling mechanisms, *Xenopus* provides insights into fundamental aspects of organelle biogenesis, structure, homeostasis, and regulation.

Scaling relationships between cell and organelle size have not been well documented in any system for many organelles, including the endoplasmic reticulum (ER), Golgi, and mitochondria. *Xenopus* egg and embryo extracts have the potential to inform scaling relationships and mechanisms for these other organelles. ER networks reconstituted using fractionated *X. laevis* egg extracts (Figure 17.1) facilitated the identification of ER morphogenic proteins (Dreier and Rapoport 2000; Voeltz et al. 2006). It has also been reported that varying the ratio of *Xenopus* egg extract cytosol/membrane can promote *in vitro* reconstitution of mitochondria and Golgi (Lu et al. 2006). In combination with these *in vitro* assays, new microscopy and computational techniques are being developed to quantify the sizes of organelles with complex morphologies, including plant ER (Bouchekhima et al. 2009) and yeast mitochondria (Rafelski et al. 2012). It is easy to imagine how these methods will prove useful for quantifying other organelles consisting of membrane networks.

By comparing size and morphology of these organelles in *X. laevis* and *X. tropicalis* egg extracts, as well as in *Xenopus* embryo extracts from different developmental stages, it may be possible to establish if these organelles exhibit size scaling. Our unpublished

data suggest that ER morphology does change during developmental progression in *X. laevis* (Figure 17.4). Similar approaches to those used to study scaling of the nucleus and spindle might then be applied to elucidate the mechanisms and factors responsible for scaling of these other organelles, such as extract-mixing experiments and candidate and fractionation approaches to identify relevant differences in scaling factor concentration, localization, isoform sequence and activity, and/or posttranslational modification. Obvious candidate scaling factors are organelle morphogenic components. Another important consideration is that many of these organelles are closely associated, for instance, the ER with the nucleus, mitochondria, Golgi, and plasma membrane (Anderson and Hetzer 2007; Friedman and Voeltz 2011). An area of interest will likely be how size scaling of one organelle is influenced by the sizes of other organelles, as it has already been demonstrated that altering ER morphology impacts nuclear size (Anderson and Hetzer 2008).

While extracts offer an excellent approach to investigate intrinsic molecular mechanisms of organelle scaling, ultimately one hopes to elucidate how organelle size influences cellular and organismal function. Toward that goal, it is important to validate and test extract findings using *in vivo* systems. We have already discussed how *Xenopus* embryos can be microinjected to investigate organelle scaling in an *in vivo* context, as well as the potential to produce transgenic *Xenopus*. Mammalian tissue culture systems represent another important *in vivo* approach. Factors that regulate organelle scaling in *Xenopus* can be investigated in cell culture to determine if mechanism is conserved and to decipher the function of proper organelle scaling. A fascinating and entirely unanswered question is how cell boundary confinement in different-size cells contributes to organelle scaling – answers await the development of microfluidic encapsulation approaches.

Exciting questions remain about how size scaling of other organelles is accomplished and what might be the functional significance (Levy and Heald 2012). The field of organelle scaling is wide open and varied *Xenopus* systems promise to provide many answers in the future.

Acknowledgments

We thank Karen White for critical reading of the manuscript. This work was supported by start-up funds from the University of Wyoming. L.J.E. is supported by a Wyoming IDeA Networks for Biomedical Research Excellence (INBRE) graduate assistantship.

References

- Aizawa, H., Sekine, Y., Takemura, R., Zhang, Z., Nangaku, M. and Hirokawa, N. 1992. Kinesin family in murine central nervous system. *J Cell Biol* 119:1287–1296.
- Anderson, D.J. and Hetzer, M.W. 2007. Nuclear envelope formation by chromatin-mediated reorganization of the endoplasmic reticulum. *Nat Cell Biol* 9:1160–1166.
- Anderson, D.J. and Hetzer, M.W. 2008. Reshaping of the endoplasmic reticulum limits the rate for nuclear envelope formation. *J Cell Biol* 182:911–924.
- Belmont, A.S. 2006. Mitotic chromosome structure and condensation. *Curr Opin Cell Biol* 18:632–638.
- Bodart, J.F. and Duesbery, N.S. 2006. *Xenopus tropicalis* oocytes: more than just a beautiful genome. *Methods Mol Biol* 322:43–53.
- Bouchekhima, A.N., Frigerio, L. and Kirkilionis, M. 2009. Geometric quantification of the plant endoplasmic reticulum. *J Microsc* 234:158–172.
- Brown, K.S., Blower, M.D., Maresca, T.J., Grammer, T.C., Harland, R.M. and Heald, R. 2007. *Xenopus tropicalis* egg extracts provide insight into scaling of the mitotic spindle. *J Cell Biol* 176:765–770.
- Butler, J.T., Hall, L.L., Smith, K.P. and Lawrence, J.B. 2009. Changing nuclear landscape and unique PML structures during early epigenetic transitions of human embryonic stem cells. *J Cell Biochem* 107:609–621.
- Carruthers, S. and Stemple, D.L. 2006. Genetic and genomic prospects for *Xenopus tropicalis* research. *Semin Cell Dev Biol* 17:146–153.
- Chan, R.C. and Forbes, D.I. 2006. In vitro study of nuclear assembly and nuclear import using *Xenopus* egg extracts. *Methods Mol Biol* 322:289–300.
- Chan, Y.H. and Marshall, W.F. 2010. Scaling properties of cell and organelle size. *Organogenesis* 6:88–96.
- Chow, K.H., Factor, R.E. and Ullman, K.S. 2012. The nuclear envelope environment and its cancer connections. *Nat Rev Cancer* 12:196–209.
- Clute, P. and Masui, Y. 1995. Regulation of the appearance of division asynchrony and microtubule-dependent chromosome cycles in *Xenopus laevis* embryos. *Dev Biol* 171:273–285.
- Conklin, E. 1912. Cell size and nuclear size. *J Exp Embryol* 12:1–98.
- Cremer, M., Kupper, K., Wagler, B. et al. 2003. Inheritance of gene density-related higher order chromatin arrangements in normal and tumor cell nuclei. *J Cell Biol* 162:809–820.
- Cross, M.K. and Powers, M.A. 2009. Learning about cancer from frogs: analysis of mitotic spindles in *Xenopus* egg extracts. *Dis Model Mech* 2:541–547.
- D'Angelo, M.A., Gomez-Cavazos, J.S., Mei, A., Lackner, D.H. and Hetzer, M.W. 2012. A change in nuclear pore complex composition regulates cell differentiation. *Dev Cell* 22:446–458.
- Dechat, T., Adam, S.A., Taimen, P., Shimi, T. and Goldman, R.D. 2010. Nuclear lamins. *Cold Spring Harb Perspect Biol* 2:a000547.
- Demontis, F. and Perrimon, N. 2009. Integration of Insulin receptor/Foxo signaling and dMyc activity during muscle growth regulates body size in *Drosophila*. *Development* 136:983–993.
- Dinarina, A., Pugieux, C., Corral, M.M. et al. 2009. Chromatin shapes the mitotic spindle. *Cell* 138:502–513.
- Dreier, L. and Rapoport, T.A. 2000. In vitro formation of the endoplasmic reticulum occurs independently of microtubules by a controlled fusion reaction. *J Cell Biol* 148:883–898.
- Edens, L.J., White, K.H., Jevtic, P., Li, X. and Levy, D.L. 2013. Nuclear size regulation: from single cells to development and disease. *Trends Cell Biol* 23(4):151–159.
- Fischer, A.H., Bond, J.A., Taysavang, P., Battles, O.E. and Wynford-Thomas, D. 1998. Papillary thyroid carcinoma oncogene (RET/PTC) alters the nuclear envelope and chromatin structure. *Am J Pathol* 153:1443–1450.
- Freedman, B.S. and Heald, R. 2010. Functional comparison of H1 histones in *Xenopus* reveals isoform-specific regulation by Cdk1 and RanGTP. *Curr Biol* 20:1048–1052.
- Friederichs, J.M., Ghosh, S., Smoyer, C.J. et al. 2011. The SUN protein Mps3 is required for spindle pole body insertion into the nuclear membrane and nuclear envelope homeostasis. *PLoS Genet* 7:e1002365.
- Friedman, J.R. and Voeltz, G.K. 2011. The ER in 3D: a multifunctional dynamic membrane network. *Trends Cell Biol* 21:709–717.
- Gerhart, J.C. 1980. Mechanisms regulating pattern formation in the amphibian egg and early embryo. In *Biological Regulation and Development*, edited by R. F. Goldberger, pp. 133–316. New York: Plenum.

- Goehring, N.W. and Hyman, A.A. 2012. Organelle growth control through limiting pools of cytoplasmic components. *Curr Biol* 22:R330–R339.
- Granot, G., Sikron-Persi, N., Gaspan, O. et al. 2009. Histone modifications associated with drought tolerance in the desert plant *Zygophyllum dumosum* Boiss. *Planta* 231:27–34.
- Gregory, T.R. 2011. Animal Genome Size Database. <http://www.genomesize.com> (accessed on November 08, 2013).
- Gurdon, J.B. 1976. Injected nuclei in frog oocytes: fate, enlargement, and chromatin dispersal. *J Embryol Exp Morphol* 36:523–540.
- Hannak, E. and Heald, R. 2006. Investigating mitotic spindle assembly and function in vitro using *Xenopus laevis* egg extracts. *Nat Protoc* 1:2305–2314.
- Harris, H. 1967. The reactivation of the red cell nucleus. *J Cell Sci* 2:23–32.
- Hellsten, U., Harland, R.M., Gilchrist, M.J. et al. 2010. The genome of the Western clawed frog *Xenopus tropicalis*. *Science* 328:633–636.
- Homma, N., Takei, Y., Tanaka, Y. et al. 2003. Kinesin superfamily protein 2A (KIF2A) functions in suppression of collateral branch extension. *Cell* 114:229–239.
- Horner, H.A. and Macgregor, H.C. 1983. C value and cell volume: their significance in the evolution and development of amphibians. *J Cell Sci* 63:135–146.
- Hudakova, S., Kunzel, G., Endo, T.R. and Schubert, I. 2002. Barley chromosome arms longer than half of the spindle axis interfere with nuclear divisions. *Cytogenet Genome Res* 98:101–107.
- Hudson, D.F., Marshall, K.M. and Earnshaw, W.C. 2009. Condensin: architect of mitotic chromosomes. *Chromosome Res* 17:131–144.
- Kieserman, E.K. and Heald, R. 2011. Mitotic chromosome size scaling in *Xenopus*. *Cell Cycle* 10:3863–3870.
- Kotadia, S., Montembault, E., Sullivan, W. and Royou, A. 2012. Cell elongation is an adaptive response for clearing long chromatid arms from the cleavage plane. *J Cell Biol* 199:745–753.
- Levy, D.L. and Heald, R. 2010. Nuclear size is regulated by importin alpha and Ntf2 in *Xenopus*. *Cell* 143:288–298.
- Levy, D.L. and Heald, R. 2012. Mechanisms of intracellular scaling. *Annu Rev Cell Dev Biol* 28:113–135.
- Lipp, J.J., Hirota, T., Poser, I. and Peters, J.M. 2007. Aurora B controls the association of condensin I but not condensin II with mitotic chromosomes. *J Cell Sci* 120:1245–1255.
- Loughlin, R., Wilbur, J.D., McNally, F.J., Nedelec, F.J. and Heald, R. 2011. Katanin contributes to interspecies spindle length scaling in *Xenopus*. *Cell* 147:1397–1407.
- Lu, P., Zheng, H. and Zhai, Z. 2006. In vitro reassembly of nuclear envelopes and organelles in *Xenopus* egg extracts. *Cell Res* 16:632–640.
- Luke, Y., Zaim, H., Karakesisoglou, I. et al. 2008. Nesprin-2 Giant (NUANCE) maintains nuclear envelope architecture and composition in skin. *J Cell Sci* 121:1887–1898.
- Maresca, T.J. and Heald, R. 2006. Methods for studying spindle assembly and chromosome condensation in *Xenopus* egg extracts. *Methods Mol Biol* 322:459–474.
- Maresca, T.J., Freedman, B.S. and Heald, R. 2005. Histone H1 is essential for mitotic chromosome architecture and segregation in *Xenopus laevis* egg extracts. *J Cell Biol* 169:859–869.
- Marquet, P.A., Quinones, R.A., Abades, S. et al. 2005. Scaling and power-laws in ecological systems. *J Exp Biol* 208:1749–1769.
- Marshall, W. 2002. Size control in dynamic organelles. *Trends Cell Biol* 12:414–419.
- Marshall, W.F. 2008. Engineering design principles for organelle size control systems. *Semin Cell Dev Biol* 19:520–524.
- Marshall, W.F., Young, K.D., Swaffer, M. et al. 2012. What determines cell size? *BMC Biol* 10:101.
- McNally, F.J. and Vale, R.D. 1993. Identification of katanin, an ATPase that severs and disassembles stable microtubules. *Cell* 75:419–429.
- Meneghini, A., Ferreira, C., Abreu, L.C., Valenti, V.E., Ferreira, M.C.F.F. and Murad, N. 2009. Memantine prevents cardiomyocytes nuclear size reduction in the left ventricle of rats exposed to cold stress. *Clinics (Sao Paulo)* 64:921–926.
- Meyerzon, M., Gao, Z., Liu, J., Wu, J.C., Malone, C.J. and Starr, D.A. 2009. Centrosome attachment to the *C. elegans* male pronucleus is dependent on the surface area of the nuclear envelope. *Dev Biol* 327:433–446.
- Micheli, G., Luzzatto, A.R., Carri, M.T., de Capoa, A. and Pelliccia, F. 1993. Chromosome length and DNA loop size during early embryonic development of *Xenopus laevis*. *Chromosoma* 102:478–483.
- Misteli, T. and Spector, D.L. 2011. *The Nucleus*. Cold Spring Harbor: Cold Spring Harbor Laboratory Press.
- Montag, M., Spring, H. and Trendelenburg, M.F. 1988. Structural analysis of the mitotic cycle in pre-gastrula *Xenopus* embryos. *Chromosoma* 96:187–196.
- Mora-Bermudez, F., Gerlich, D. and Ellenberg, J. 2007. Maximal chromosome compaction occurs by axial shortening in anaphase and depends on Aurora kinase. *Nat Cell Biol* 9:822–831.

- Murray, A.W. 1991. Cell cycle extracts. *Methods Cell Biol* 36:581–605.
- Nakajima, T., Nakashima, T., Okada, Y. et al. 2010. Nuclear size measurement is a simple method for the assessment of hepatocellular aging in non-alcoholic fatty liver disease: comparison with telomere-specific quantitative FISH and p21 immunohistochemistry. *Pathol Int* 60:175–183.
- Naumova, N. and Dekker, J. 2010. Integrating one-dimensional and three-dimensional maps of genomes. *J Cell Sci* 123:1979–1988.
- Neurohr, G., Naegeli, A., Titos, I. et al. 2011. A mid-zone-based ruler adjusts chromosome compaction to anaphase spindle length. *Science* 332:465–468.
- Newport, J. and Kirschner, M. 1982. A major developmental transition in early *Xenopus* embryos: I. characterization and timing of cellular changes at the midblastula stage. *Cell* 30:675–686.
- Nieuwkoop, P.D. and Faber, J. 1967. *Normal Table of Xenopus laevis (Daudin)*, 2nd ed. Amsterdam: North-Holland Publishing Company.
- Peterson, T.R., Sengupta, S.S., Harris, T.E. et al. 2011. mTOR complex 1 regulates lipin 1 localization to control the SREBP pathway. *Cell* 146:408–420.
- Prokocimer, M., Davidovich, M., Nissim-Rafinia, M. et al. 2009. Nuclear lamins: key regulators of nuclear structure and activities. *J Cell Mol Med* 13:1059–1085.
- Rafelski, S.M., Viana, M.P., Zhang, Y. et al. 2012. Mitochondrial network size scaling in budding yeast. *Science* 338:822–824.
- Roca-Cusachs, P., Alcaraz, J., Sunyer, R., Samitier, J., Farre, R. and Navajas, D. 2008. Micropatterning of single endothelial cell shape reveals a tight coupling between nuclear volume in G1 and proliferation. *Biophys J* 94:4984–4995.
- Schubert, I. and Oud, J.L. 1997. There is an upper limit of chromosome size for normal development of an organism. *Cell* 88:515–520.
- Shechter, D., Chitta, R.K., Xiao, A., Shabanowitz, J., Hunt, D.F. and Allis, C.D. 2009a. A distinct H2A.X isoform is enriched in *Xenopus laevis* eggs and early embryos and is phosphorylated in the absence of a checkpoint. *Proc Natl Acad Sci U S A* 106:749–754.
- Shechter, D., Nicklay, J.J., Chitta, R.K., Shabanowitz, J., Hunt, D.F. and Allis, C.D. 2009b. Analysis of histones in *Xenopus laevis*. I. A distinct index of enriched variants and modifications exists in each cell type and is remodeled during developmental transitions. *J Biol Chem* 284:1064–1074.
- Smith, F.A. and Lyons, S.K. 2011. How big should a mammal be? A macroecological look at mammalian body size over space and time. *Philos Trans R Soc Lond B Biol Sci* 366:2364–2378.
- Smythe, C. and Newport, J.W. 1991. Systems for the study of nuclear assembly, DNA replication, and nuclear breakdown in *Xenopus laevis* egg extracts. *Methods Cell Biol* 35:449–468.
- Spence, A.J. 2009. Scaling in biology. *Curr Biol* 19:R57–R61.
- Spence, A.J. and Hutchinson, J.R. 2012. A growing size synthesis. *Curr Biol* 22:R309–R314.
- Srayko, M., O'Toole E.T., Hyman, A.A. and Muller-Reichert, T. 2006. Katanin disrupts the microtubule lattice and increases polymer number in *C. elegans* meiosis. *Curr Biol* 16:1944–1949.
- Tapia-Alveal, C., Outwin, E.A., Trepolec, N., Dziadkowiec, D., Murray, J.M. and O'Connell, M.J. 2010. SMC complexes and topoisomerase II work together so that sister chromatids can work apart. *Cell Cycle* 9:2065–2070.
- Tapon, N., Ito, N., Dickson, B.J., Treisman, J.E. and Hariharan, I.K. 2001. The *Drosophila* tuberous sclerosis complex gene homologs restrict cell growth and cell proliferation. *Cell* 105:345–355.
- Taylor, S., Landman, M.J. and Ling, N. 2009. Flow cytometric characterization of freshwater crayfish hemocytes for the examination of physiological status in wild and captive animals. *J Aquat Anim Health* 21:195–203.
- Tumaneng, K., Russell, R.C. and Guan, K.L. 2012. Organ size control by Hippo and TOR pathways. *Curr Biol* 22:R368–R379.
- Tunquist, B.J. and Maller, J.L. 2003. Under arrest: cytotostatic factor (CSF)-mediated metaphase arrest in vertebrate eggs. *Genes Dev* 17:683–710.
- Unhavaithaya, Y. and Orr-Weaver, T.L. 2012. Polyploidization of glia in neural development links tissue growth to blood–brain barrier integrity. *Genes Dev* 26:31–36.
- Voeltz, G.K., Prinz, W.A., Shibata, Y., Rist, J.M. and Rapoport, T.A. 2006. A class of membrane proteins shaping the tubular endoplasmic reticulum. *Cell* 124:573–586.
- Webster, M., Witkin, K.L. and Cohen-Fix, O. 2009. Sizing up the nucleus: nuclear shape, size and nuclear-envelope assembly. *J Cell Sci* 122:1477–1486.
- Whitehead, E., Heald, R. and Wilbur, J.D. 2013. N-terminal phosphorylation of p60 katanin directly regulates microtubule severing. *J Mol Biol* 425:214–221.
- Wilbur, J.D. and Heald, R. 2013. Mitotic spindle scaling during *Xenopus* development by kif2a and importin alpha. *eLife* 2: e00290.
- Wilson, E.B. 1925. The karyoplasmic ratio. In *The Cell in Development and Heredity*, pp. 727–733. New York: The Macmillan Company.
- Wuhr, M., Chen, Y., Dumont, S. et al. 2008. Evidence for an upper limit to mitotic spindle length. *Curr Biol* 18:1256–1261.

- Yanai, I., Peshkin, L., Jorgensen, P. and Kirschner, M.W. 2011. Mapping gene expression in two *Xenopus* species: evolutionary constraints and developmental flexibility. *Dev Cell* 20:483–496.
- Yasuhara, N., Oka, M. and Yoneda, Y. 2009. The role of the nuclear transport system in cell differentiation. *Semin Cell Dev Biol* 20:590–599.
- Zhang, D., Rogers, G.C., Buster, D.W. and Sharp, D.J. 2007. Three microtubule severing enzymes contribute to the “Pacman-flux” machinery that moves chromosomes. *J Cell Biol* 177:231–242.
- Zhang, Y., McCord, R.P., Ho, Y.J. et al. 2012. Spatial organization of the mouse genome and its role in recurrent chromosomal translocations. *Cell* 148:908–921.
- Zink, D., Fischer, A.H. and Nickerson, J.A. 2004. Nuclear structure in cancer cells. *Nat Rev Cancer* 4:677–687.

18

A Model for Retinal Regeneration in *Xenopus*

Masasuke Araki

Department of Biological Sciences, Developmental Neurobiology Laboratory, Nara Women's University, Nara, Japan

Abstract: Complete retinal regeneration in adult animals occurs only in amphibians after surgical removal of the whole retina. This has been studied in adult *Xenopus laevis* both *in vivo* and *in vitro*, using transgenic animals and different tissue cultures. Two different regenerative cell sources are identified: one is the stem/progenitor cells of the ciliary marginal zone (CMZ) and the other is the retinal pigmented epithelial cells (RPE cells). The former regenerates the peripheral retina while the latter regenerates the central retina. The retinal vascular membrane (RVM), consisting of the inner limiting membrane of the retina and capillaries, plays a vital role for active regeneration. Both the CMZ cells and RPE cells migrate onto the RVM and start proliferation, indicating that cell niche alterations such as cell-substratum and cell-cell interactions trigger the regeneration process. The availability of several different types of culture models of RPE transdifferentiation is one of the advantages of amphibian retinal regeneration studies, because RPE cells can be controlled for the initiation of regeneration under the culture. Expression of *Rax* and *Pax6* genes, the earliest genes activated during retinal regeneration, is regulated by cell adhesion to the neighboring cells or extracellular matrices. We also introduced *Xenopus tropicalis* as a new animal model of *Xenopus* and found that the whole retina regenerates like *X. laevis*, and the regenerative cell source is solely the CMZ stem/progenitor cells. This is a novel mode of retinal regeneration, and the CMZ stem cell-based regeneration following whole retina removal is highly intriguing in the context of higher vertebrates such as mammals, which also have stem/progenitor cells in the ciliary epithelium. In summary, *Xenopus* model of retina regeneration provides powerful means for regeneration studies.

***Xenopus* as a model animal for the study of retinal regeneration**

Retinal regeneration in vertebrates

Retinal regeneration has been studied in a variety of vertebrates, including fish, amphibians, birds, and mammals, at many different stages

of development, from embryonic stages to adulthood. The origin of the stem/progenitor cells required for retinal regeneration differs from species to species. There are several different types of ocular tissues that contain retinal stem/progenitor cells, namely, the ciliary marginal zone (CMZ), the retina, the iris, and the retinal pigmented epithelium (RPE) (Del

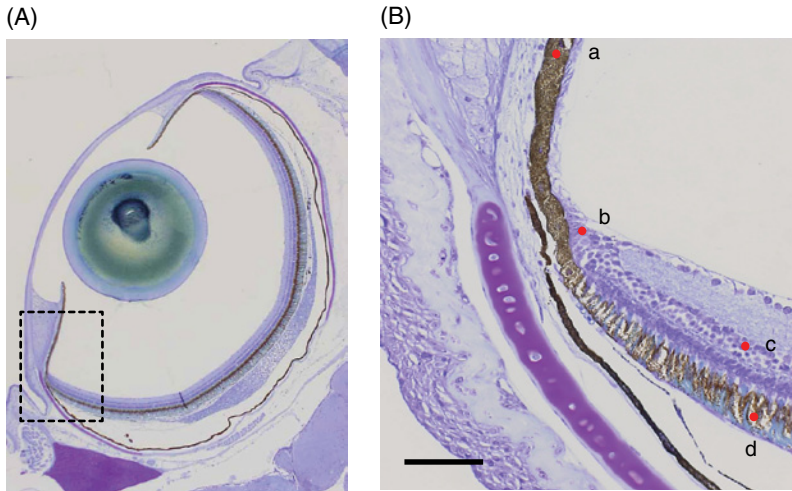


Figure 18.1 Retinal stem/progenitor cells in the vertebrate eye. Four distinct areas have been identified in the ocular tissues that contain retinal stem/progenitor cells: a, the iris pigmented epithelium; b, the CMZ or ciliary body epithelium; c, the intraretinal cells (this cell type changes depending on the animal species); and d, the RPE. The cell types recruited for retinal regeneration differ depending on species and depending on the extent to which the retina is injured. The area in the rectangle in A is shown in B at a higher magnification. The scale bar in B is 100 μm . *Medaka* eye stained by cresyl violet. To see a color version of this figure, see Plate 45.

Rio-Tsonis and Tsonis 2003; Hitchcock et al. 2004; Karl and Reh 2010) (Figure 18.1). The replacement of degenerating cells with proliferative stem-like cells has been reported in most vertebrates. Intraretinal glial cells (Müller cells) and rod precursors can both play a role in tissue repair, depending on the species, but only when the damage is limited to a small area (Hitchcock and Raymond 1992; Raymond and Hitchcock 1997; Reh and Fisher 2001). The ciliary marginal area also plays a critical role in retinal regeneration in fish, amphibians, and birds. In these animals, partial regeneration occurs with the use of progenitor cells in this area. One limitation of retinal regeneration is that it normally occurs only during a restricted period in development. However, amphibians retain the ability to regenerate throughout their lives (Hitchcock et al. 2004; Araki 2007a; Chiba and Mitashov 2007).

RPE is a potent source of retinal regeneration in amphibians. In other vertebrates, RPE is only active in retinal regeneration during early stages of embryonic development (Park and Hollenberg 1993; Reh and Fisher 2001). In more recent studies, pigmented epithelial cells in the ciliary margin and iris have been shown to be capable

of transdifferentiating into retinal neurons under certain culture conditions, indicating that ciliary pigmented epithelial cells are a potent source of regeneration in mammals (Ahmad et al. 2000; Sun et al. 2006; Ohta et al. 2008).

From these features, it is apparent that retinal regeneration can involve several different cell sources and mechanisms, depending on the animal species. The retina can be replaced or repaired by RPE cells via the transdifferentiation process or by stem-like cells in the CMZ and/or within the retina. Different animals use different strategies, and the ability to regenerate also depends on the age of the animal, although potent cells can be retained in a wide variety of animals. In the following section, I will focus on the transdifferentiation process of RPE cells, which are the main source of the regenerating retina of adult amphibians.

Retinal regeneration in amphibians

Amphibian retinal regeneration is unique in several ways (Del Rio-Tsonis and Tsonis 2003; Hitchcock et al. 2004; Araki 2007a; Filoni 2009). Remarkably, the complete regeneration of the

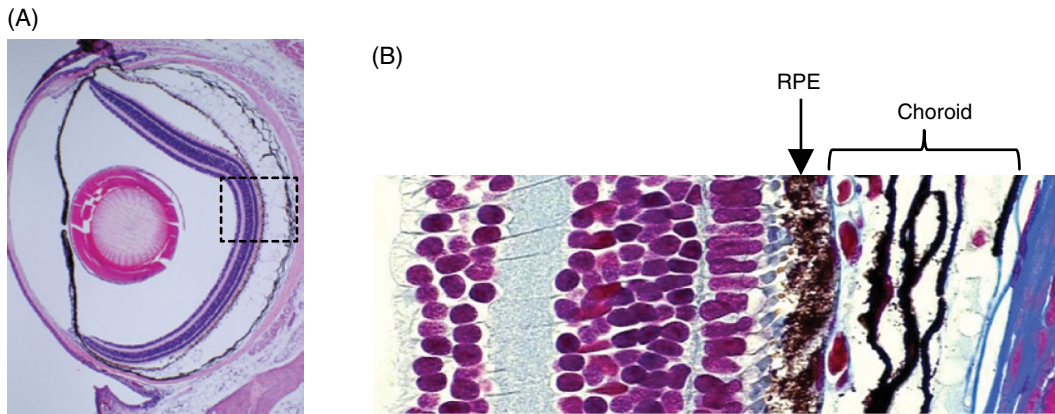


Figure 18.2 Newt eye and the retina. The rectangular area in A is shown in B at a higher magnification. In B, the structure of the neural retina and the RPE is shown at a higher magnification. Between the RPE and the choroid there is a basement membrane called Bruch's membrane. A is stained with hematoxylin and eosin and B is stained with Azan.

retina in adult animals after the removal of the whole retina occurs only in amphibians. This was once thought to occur only in urodele amphibians and has been best studied in the newt. Experimental studies of this phenomenon in the newt were initiated over a century ago at the end of the 19th century (see reviews by Okada 1991; Mitashov 1997; Hitchcock et al. 2004) (Figure 18.2). In contrast, it has long been believed that the regeneration ability of anurans is limited to the larval stage and is lost after metamorphosis, with some residual ability to repair partially damaged retinal tissues remaining in the adults (Lombardo 1969). Contrary to this generally accepted notion, however, we found that adult *Xenopus laevis* are able to regenerate their whole retina and lens after the surgical removal of these tissues (Araki 2007a; Yoshii et al. 2007). We observed this for the first time during a culture study of RPE tissues from the newt and *Xenopus*; similar to the newt RPE, the RPE cells from the adult *X. laevis* are also able to differentiate into neurons (Araki 2007b). This finding led us to reexamine whether the retina of adult *Xenopus* can regenerate. We found that regeneration takes place in mature animals following the surgical removal of the whole retina. This was the first demonstration that vertebrate species other than the urodele amphibians can retain regenerative capability in adulthood, allowing them to recover following the complete removal of the retina.

It is of importance to note that the retinal vascular membrane (RVM) is essential for this regeneration to occur as described in the following paragraphs (Yoshii et al. 2007). This may be why previous researchers were unable to observe this phenomenon, as no regeneration can occur in the absence of the RVM.

In *Xenopus*, two different regenerative retinal cell sources have been identified. One is the stem/progenitor cells of the CMZ, and the other is RPE cells. Because the newt retina regenerates mostly from the RPE cells through a process of transdifferentiation, we will focus on RPE cell transdifferentiation in *Xenopus*.

Many of the morphological features of newt retinal regeneration have been described previously (Stone 1950a, b; Hasegawa 1958; Reyer 1977), and the RPE cells are known to be the major source of the regenerating retina. Soon after the removal of the whole retina, the RPE cells become irregularly arranged and many begin to proliferate (allowing for BrdU labeling) to produce retinal stem/progenitor cells (Figure 18.3). Interestingly, the associated DNA synthesis (as indicated by BrdU labeling) occurs simultaneously in all of the RPE cells 3–4 days after retinal removal (Ikegami et al. 2002). This suggests that there is a latent period in the early phase of transdifferentiation. The proliferation of the original single epithelium results in the development of a stratified epithelium. The most basal layer of this epithelium faces Bruch's membrane

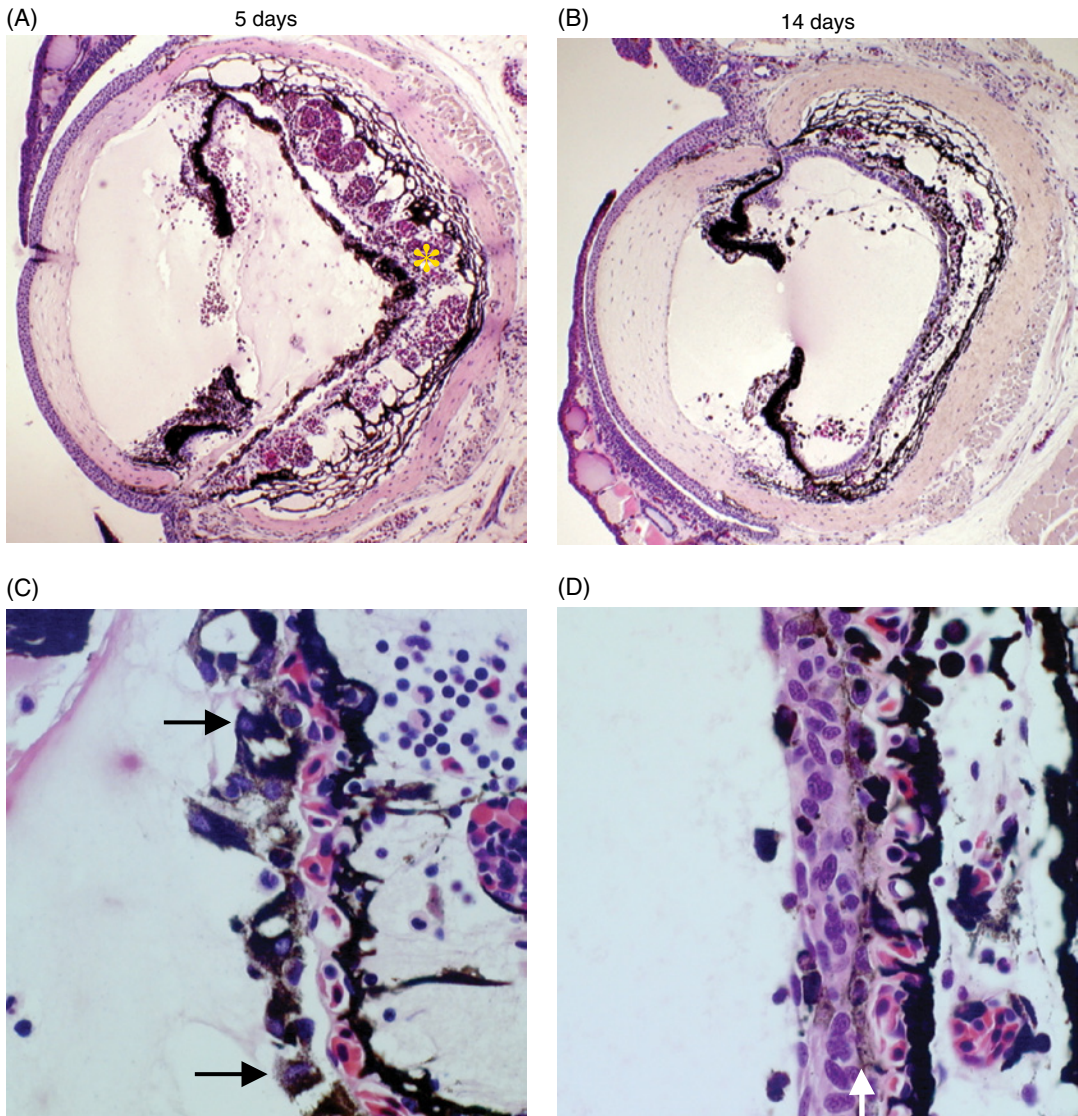


Figure 18.3 The early phase of transdifferentiation in newt retina regeneration. A and C show an eye at Day 5 and B and D show an eye at Day 14 (5 and 14 days after retinal removal). In A, the RPE cells are irregularly arranged (arrows in C). The choroid is swollen with blood cells stacking in the capillaries. This indicates that an inflammatory reaction is occurring in the choroid. At Day 14, a multistratified epithelium is formed, consisting of two layers, the neuroepithelium and the pigmented epithelium (white arrow in D). The latter is facing the choroid. Hematoxylin and eosin staining. Reprinted from Araki (2007a). © 2007, with permission from John Wiley & Sons, Inc. To see a color version of this figure, see Plate 46.

and redifferentiates into the RPE cells, while producing two layers; the inner layer (close to the lens) becomes a neuroepithelium, and the outer layer becomes the RPE layer. The basement membrane of the RPE (termed Bruch's membrane) appears to play a crucial role in RPE cell fate. During this process, the RPE cells first lose contact with Bruch's membrane (while they are irregu-

larly arranged), and then they reattach to the membrane (Figure 18.3). Cell-cell contact is also affected, as shown by the altered localization of cell adhesion molecules such as connexin 43 (Umino and Saito 2002). During this period, the RPE cells become stem-like cells, and their reattachment to Bruch's membrane fates them to become RPE cells again.

The behavior of *Xenopus* RPE cells in the early phase of the regeneration processes, which are considerably different from those of the newt, will be described in the following section. The most conspicuous difference is that in *Xenopus*, the RPE cells detach from Bruch's membrane and move to another basement membrane (the retinal basement membrane, referred to as the RVM in this chapter).

***X. laevis*: A new animal model of retinal regeneration**

As described in previous studies, anurans are believed to be unable to regenerate the retina after metamorphosis when the whole retina is injured. In tadpoles of several anuran species, regeneration does not occur (reviewed by Reyer 1977; Del Rio-Tsonis and Tsonis 2003; Hitchcock et al. 2004; Filoni 2009). However, retinal regeneration occurs through the stem/progenitor cells in the CMZ of *Xenopus* tadpoles (Ide et al. 1984). A recent intraocular transplantation study demonstrated that embryonic RPE tissues grafted in the posterior eye chamber can undergo transdifferentiation to regenerate new retinas in some species of *Rana* or *Xenopus* (Bosco 1988; Arresta et al. 2005). In some early studies, RPE tissues from adult frogs were shown to have the potential to transdifferentiate into a retina when the tissues were grafted into host larvae eyes (Lopashov and Sologub 1972; Sologub 1977). In *Rana* tadpoles, a new retina regenerated following devascularization-induced retina degeneration, which was accomplished with the complete removal of the eyeball before putting it back into the orbit (Reh and Nagy 1987). A more recent study showed that the retina regenerated after partial retinal resection in *Xenopus* embryos after the removal of one quadrant of the eyeball; however, this regeneration seemed to occur from the ciliary marginal cells rather than through RPE transdifferentiation (Martinez-De Luna et al. 2011).

We first observed retinal regeneration in adult *X. laevis* following complete retinectomy (Figures 18.4 and 18.5) (Yoshii et al. 2007). This occurs only when the RVM, consisting of the inner limiting membrane of the retina and capillaries, is left in the ocular chamber. The initial regeneration process is particularly

interesting because the microenvironments of the RPE cells are rapidly and drastically altered after retinal removal. This cell niche alteration is thought to trigger the cells to become retinal stem-like cells.

Soon after the retina is removed (within 24h), some RPE cells detach from Bruch's membrane and move toward the RVM. There, the cells adhere to the RVM and form a new single epithelium. The cells then become depigmented, proliferate, and finally differentiate into retinal tissues. By contrast, the RPE cells remaining on Bruch's membrane do not undergo any morphological changes. Such a conspicuous difference in the cell fates of the RPE cells at the RVM and those at Bruch's membrane suggests that the detachment of the RPE cells from Bruch's membrane and their subsequent adhesion to the RVM are prerequisites for transdifferentiation to occur. Bruch's membrane efficiently stabilizes the RPE differentiation state, while the RVM has a permissive role as a substratum for RPE cells to form a new epithelial layer. The epithelium then develops as a neuroepithelium. The molecular significance of these cellular behaviors is better understood in cultured tissues, as will be described in the following section. We presume that a similar mechanism also regulated RPE transdifferentiation in the newt. When we closely examined the morphological changes in the RPE cells in the initial phase of regeneration, the newt RPE cells were found to be detached from Bruch's membrane as soon as the retina was removed.

Very little is known about lens regeneration in the adult *Xenopus*. Therefore, it is worth mentioning that the lens also regenerates in *X. laevis* after metamorphosis (Yoshii et al. 2007). In tadpoles, the lens can regenerate from the outer cornea epithelium by transdifferentiation (Filoni et al. 1997). In our retinal regeneration study, the corneal tissues appeared to be intact and no morphological alterations were observed. In the retinal removal surgery, we normally remove the lens to keep the RVM in the posterior chamber and to increase the visibility of the surgical field. The lens is removed by sucking, leaving the lens capsule in the ocular chamber with some lens epithelial cells attached to the capsule. In our studies, a new lens regenerated over a period of 20–30 days. The retina appears to have an inducing effect

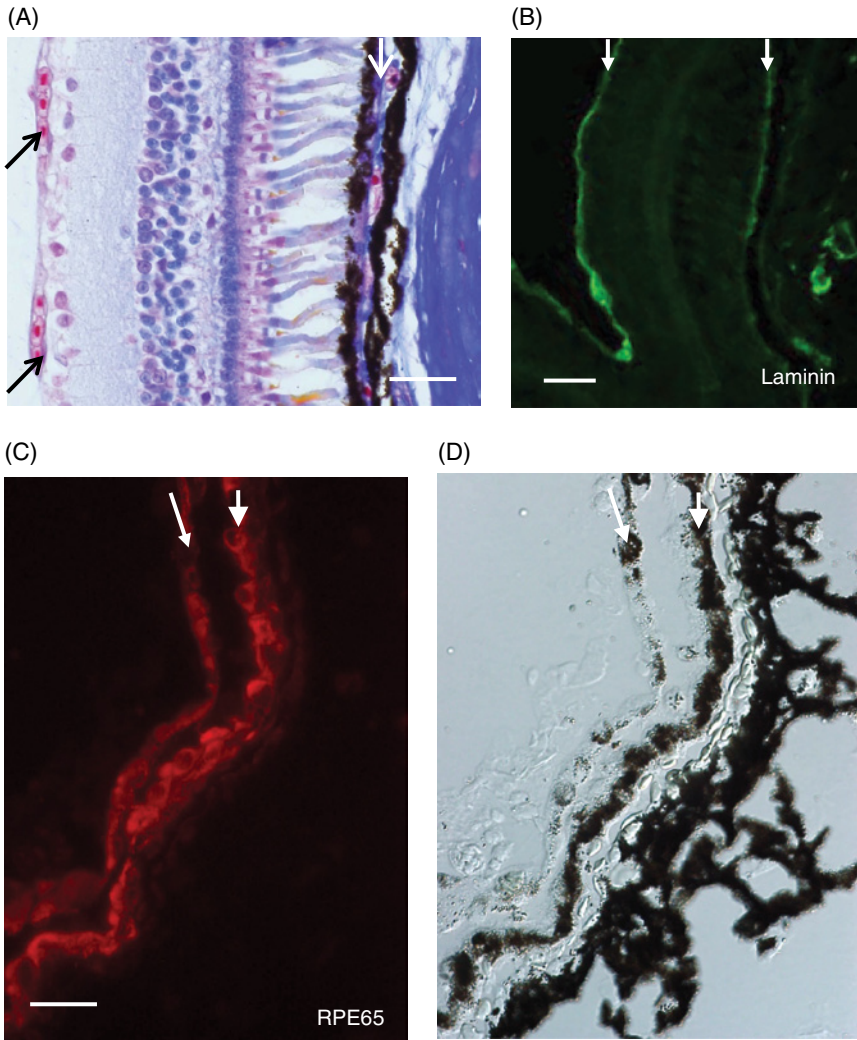


Figure 18.4 *X. laevis* retina and the early stages of retinal regeneration. A and B show a normal *X. laevis* retina. In A, the left arrows indicate the RVM, which consists of the inner limiting membrane and the retinal capillaries. The right white arrow points at Bruch's membrane. In B, laminin immunocytochemistry shows two positively stained membranes (arrows); one is the RVM and the other is Bruch's membrane. A is stained with Azan. The scale bars in A and B are 30 μm . C and D are taken from the same area and show an eye at Day 10 (10 days after retinectomy). The longer, thin arrows indicate the new RPE layer, which is formed by the migration of the RPE cell to the RVM. The shorter, thick arrows indicate the original RPE layers. RPE65 immunocytochemistry indicates that the pigmented cells on the vascular membrane are of RPE cell origin. The scale bar in C is 20 μm . B, C, and D are from Yoshii et al. (2007). © 2007, with permission from Elsevier. To see a color version of this figure, see Plate 47.

on lens regeneration, because the removal of both lens and retina delays lens regeneration, as reported in the anuran larva model (Coulombre and Coulombre 1970; Filoni et al. 1982; Schaefer et al. 1999). We speculate that a few lens epithelial cells adhering to the lens capsule are the source of the regenerating lens. This is therefore not a true transdifferen-

tiation process but is instead a healing process that occurs through the proliferation of lens epithelial cells. Some reports in the rabbit and cat have described lens regeneration after the anterior and posterior capsular bags have been left intact in the vitreous fluid (Gwon et al. 1993). Similar repair processes have been observed in *Xenopus*.

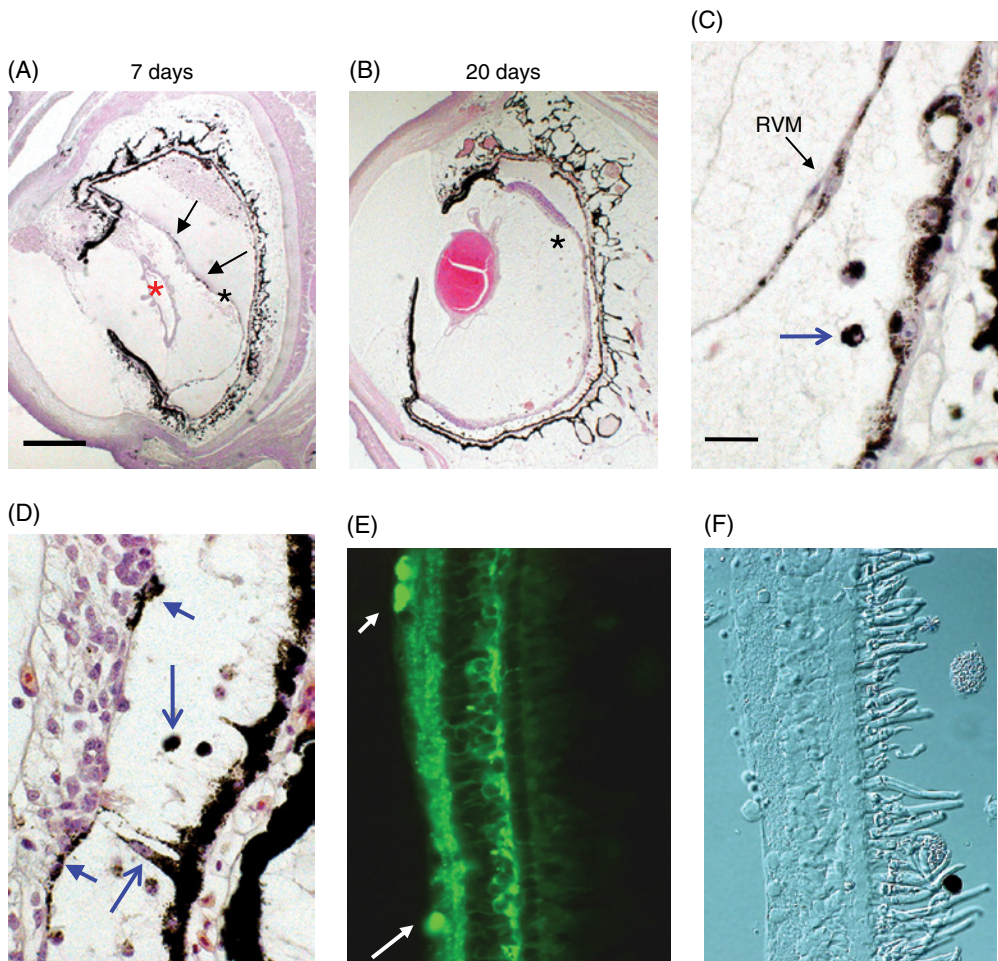


Figure 18.5 Retinal regeneration in *X. laevis*. (A and C) Day 7, (B and D) day 20, and (E and F) day 30. In A and C, a newly formed RPE layer (black arrows) is found on the RVM. The red asterisk in A is the remaining lens capsule. Between the RVM and the original RPE, isolated pigmented cells are often observed (blue arrows in C and D). These are considered to be migrating RPE cells. In B and D, a stratified epithelium has developed and some RPE cells attached to the epithelium at the luminal side (the shorter arrows in D). In E and F, a neural retina with a well-developed outer segment has regenerated by Day 30. Acetylated tubulin immunocytochemistry shows the different retinal layers. Arrows in E indicate the ganglion cells. Reprinted from Yoshii et al. (2007). © 2007, with permission from Elsevier. To see a color version of this figure, see Plate 48.

Culture models for the study of *X. laevis* retinal regeneration

One of the advantages of retinal regeneration studies in amphibians is that several culture models of RPE transdifferentiation have been established and well described, and the monitoring of the transdifferentiation process is possible. Although there have been a number of regeneration studies using tissue culture models, only a few amphibian

tissue culture studies have been reported to date. Neuronal differentiation of the RPE cells was shown to depend on the culture substratum, such as laminin, and on the presence of FGF2 in cultures of frog larva RPE cells (Reh and Nagy 1987; Sakaguchi et al. 1997). A dissociate culture model of the newt RPE cells showed that they exhibit L-type Ca channels in culture, suggesting that neuronal differentiation can occur under culture conditions (Sakai and Saito 1997).

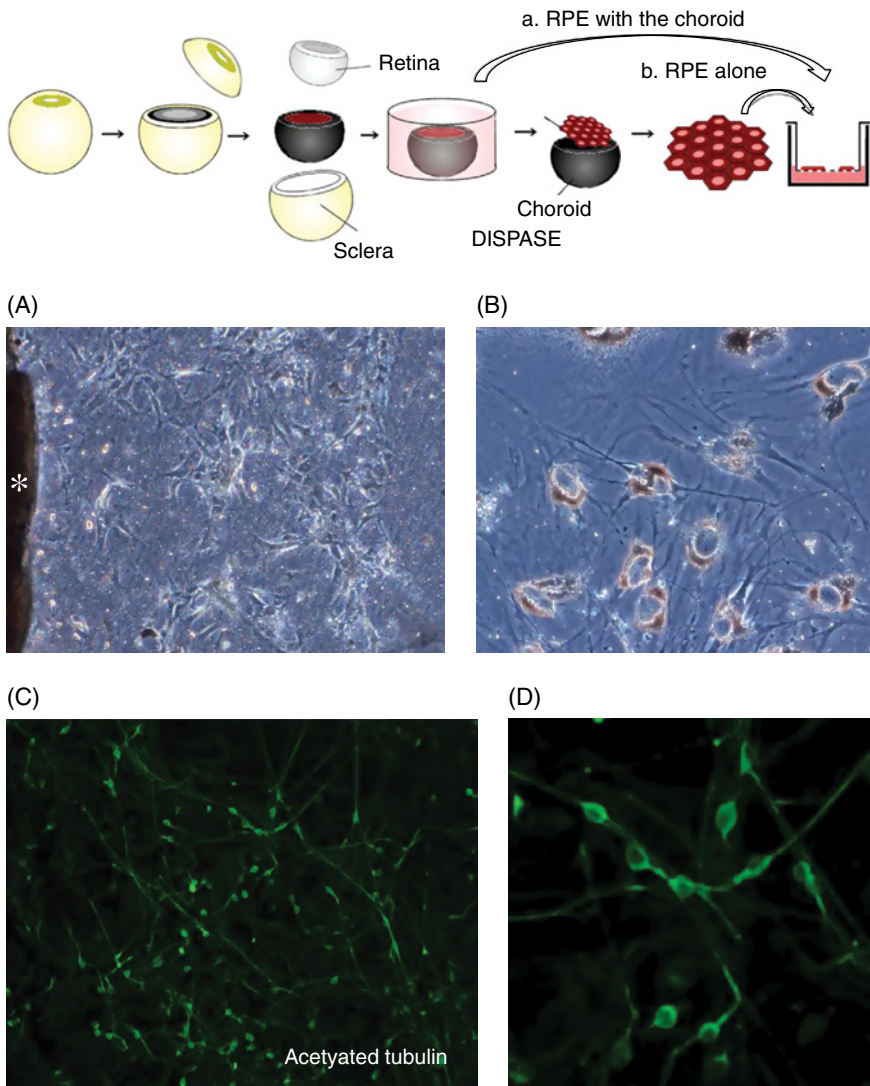


Figure 18.6 A flat tissue culture for the study of amphibian RPE cells. For the RPE tissue culture, the retina is removed from the posterior part of the eye, followed by removal of the sclera. The remaining tissue, consisting of the RPE and the choroid, is then placed on the membrane filter (a). Alternatively, the tissue can be incubated with Dispase, after which the RPE sheet can be mechanically isolated for culture on the filter cup (b). When the RPE with the choroid is cultured, neuronal differentiation is found, while no neuronal differentiation occurs when the RPE alone is cultured. However, the addition of FGF2 to the medium induces neuronal differentiation, suggesting the choroid is a source of FGF2 (see main text). (A–D) Tissue culture of newt RPE with the choroid on Day 30. In A, the asterisk shows the original explant. Here, the RPE cells have migrated out from the periphery of the explant and extended onto the filter. In B, numerous cells with pigment granules still in the cytoplasm show long branching neurite-like processes. (C and D) When the cultures are examined with antiacetylated tubulin, numerous positive cells are observed. Reprinted from Mitsuda et al. (2005). © 2005, with permission from Elsevier.

We attempted to build a new tissue culture model that reproduces all of the steps in newt RPE transdifferentiation (Figure 18.6) (Ikegami et al. 2002). In this method, referred

to as the flat membrane culture of RPE tissues, tissues consisting of the RPE and the choroid were cultured on a culture membrane filter (Falcon culture insert). This

method has the advantage that all of the processes of retinal cell differentiation can be traced under a phase-contrast microscope; the RPE cells of the explant migrate out at the periphery of the explant to the free membrane surface, where they gradually lose pigment granules and differentiate into neural cells. Transdifferentiation requires FGF2, which most likely is derived from the choroid (Mitsuda et al. 2005). This has been shown by culturing an RPE sheet with or without the addition of FGF2. The RPE associated with the choroid transdifferentiates into neural cells, while the RPE alone does not show retinal differentiation and its cells remain unchanged. Immunoblot analysis and RT-PCR show that the choroid is a rich source of FGF2 in the newt. It is interesting to note that there is a time window for FGF2 action between Day 5 and Day 10 *in vitro* and that FGF2 has no effect on RPE transdifferentiation when it is administered either before or after that period (Mitsuda et al. 2005). This indicates that FGF2 only affects RPE cells when they are in a certain physiological state. For instance, FGF2 does not induce RPE transdifferentiation when the tissues are not treated with Dispase (see section "An organ-based culture model for 3-D retinal tissue regeneration"). This cellular state is most likely attained a few days after the retina is removed, following a latent period. The molecular nature of this state is not well understood, but the expression of either *Rax* or *Pax6* is most likely involved in this process.

Newt RPE eyecup culture (a similar method to that described earlier) showed that an immediate-early activation of mitogen-activated protein kinase–extracellular signal-regulated kinases (MEK–ERK) signaling in the RPE cells is necessary for their entry into the cell cycle (Mizuno et al. 2012; Yoshikawa et al. 2012). The involvement of signaling molecules other than fibroblast growth factors (FGFs) is not well understood, but insulin or IGF1 appears to enhance neuronal differentiation when it is administered together with FGF2 (Fischer et al. 2002; Mitsuda et al. 2005). More recently, Wnt signaling has also been suggested to be involved in the regeneration of the zebrafish retina (Meyers et al. 2012).

A flat tissue culture model

As previously mentioned, the culture study of *Xenopus* RPE tissues allowed us to examine retinal regeneration in the adult *Xenopus*. Using the same culture conditions as were used for the newt, *Xenopus* RPE cells from adult animals were found to differentiate into retinal cells. This indicated that the *Xenopus* RPE has a transdifferentiation capacity in the adult stages, leading us to reexamine whether the RPE actually regenerates the retina *in vivo* in the adult *Xenopus* (Araki 2007b).

Xenopus RPE culture has been performed using the same method as for the newt (Figure 18.6); the RPE sheets combined with the choroid were obtained from the posterior eyecup and cultured on a membrane filter in a medium (L-15) supplemented with fetal bovine serum. After a few days, the RPE cells began to migrate out from the periphery of the explant and to form an epithelial sheet. This indicates that the RPE cells, originally facing the choroid interference with Bruch's membrane, actually moved onto the substratum (collagen-coated membrane filter). The cells then migrated even farther, eventually differentiating into neural cells in the outermost area of the culture. After approximately 10 days, this culture consisted of four different zones: the explant zone, the epithelial zone, the transition zone, and the differentiation zone (Figure 18.7) (Nabeshima et al. 2013). Such cell behaviors are comparable with those found *in vivo* during retinal regeneration, in which the RPE cells detach from Bruch's membrane and move to the RVM. There, the RPE cells form a new epithelium, proliferate, and differentiate into neural tissue.

Cell–cell and cell–matrix interactions, which are believed to play a role in RPE transdifferentiation, can also be studied using this culture model system. These studies have indicated that the presence of adhesion molecules such as N-cadherin and connexin 43 is related to the expression of the retinal stem/progenitor related genes *Rax* and *Pax6*. For example, intense *Pax6* expression has been found in the transition zone, where there is no connexin 43 expression (Nabeshima et al. 2013). Connexin

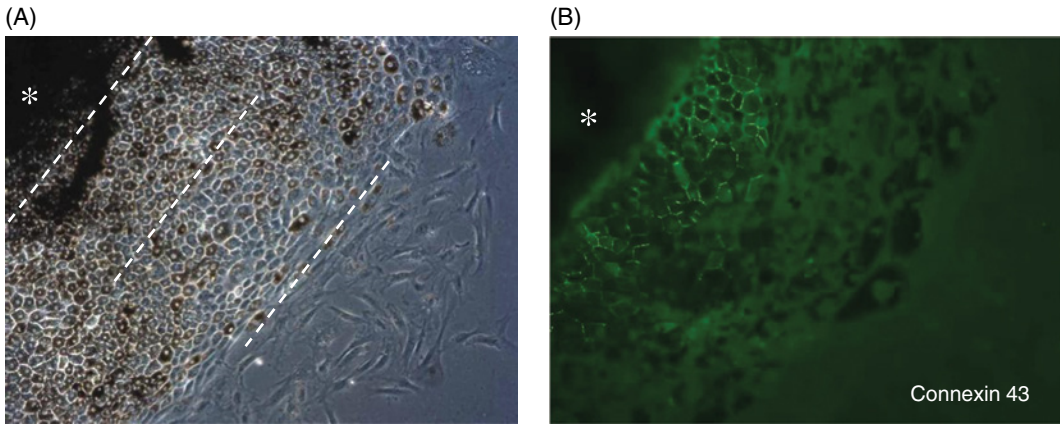


Figure 18.7 Tissue culture of *X. laevis* RPE with the choroid. (A) Phase-contrast micrograph of the tissue culture of the RPE and the choroid on Day 12 and (B) Connexin 43 immunocytochemistry. In A, four different zones can be distinguished from the left to the right: the explant zone (asterisk), the epithelial zone, the transition zone, and the differentiation zone. Connexin 43 localization was found in the epithelial zone, but not in the transition zone. Intense Pax6 localization was observed in the transition zone. Reprinted from Nabeshima et al. (2013). © 2013, Wiley Periodicals, Inc.

is a component of gap junctions, which allows the intercellular exchange of chemical or electrical signals (Mese et al. 2007). Recent studies have indicated that the ATP released via gap junction hemichannels from the RPE can trigger ocular development and regulates the proliferation of neural retinal progenitors during retinal development (Pearson et al. 2005; Massé et al. 2007). Whether *Pax6* gene regulation is under the direct control of the gap junctions in retinal regeneration must be examined further. We used a Rax promoter-EGFP transgenic *Xenopus* (see succeeding section) to trace Rax gene expression and thereby found that Rax is upregulated in the RPE cells that are deprived of cell-matrix interaction.

An organ-based culture model for 3-D retinal tissue regeneration

Two additional useful culture systems are the gel overlay culture and the gel embedding culture. We developed both of these systems to study *Xenopus* retinal regeneration, and the latter is a modification of the former. The most characteristic feature of this culture is that histogenesis of the 3-D retinal structures can be attained from the RPE tissues, and the whole-retinal regeneration process is reproduced under

culture conditions (Figure 18.8) (Araki 2007b; Kuriyama et al. 2009; Nabeshima et al. 2013).

For the Matrigel overlay culture, a *Xenopus* RPE sheet is isolated from the choroid and laid on a culture membrane filter cup. Matrigel is then overlaid on the RPE tissues. When the RPE sheets are not isolated from the choroid and are cultured together, the RPE cells proliferate while remaining pigmented instead of undergoing transdifferentiation (Kuriyama et al. 2009). This suggests that the RPE-choroid tissue interaction has a potential role in RPE transdifferentiation. To isolate a single RPE layer from the choroid, tissues consisting of both RPE and choroid were treated with Dispase, and then the RPE sheet was isolated mechanically using forceps to peel off the sheet. With this part of the procedure, it is often difficult to obtain the same size of RPE sheets, and sometimes only small fragments of RPE can be obtained. This problem was overcome using a new method, referred to as the Matrigel embedding culture method. This new method was developed recently in our laboratory (Nabeshima et al. 2013).

Using the Matrigel embedding method, tissues consisting of RPE and the choroid were treated with Dispase, a proteolytic enzyme for cell matrix components (Stenn et al. 1989). The resulting mixture was then embedded in the gel

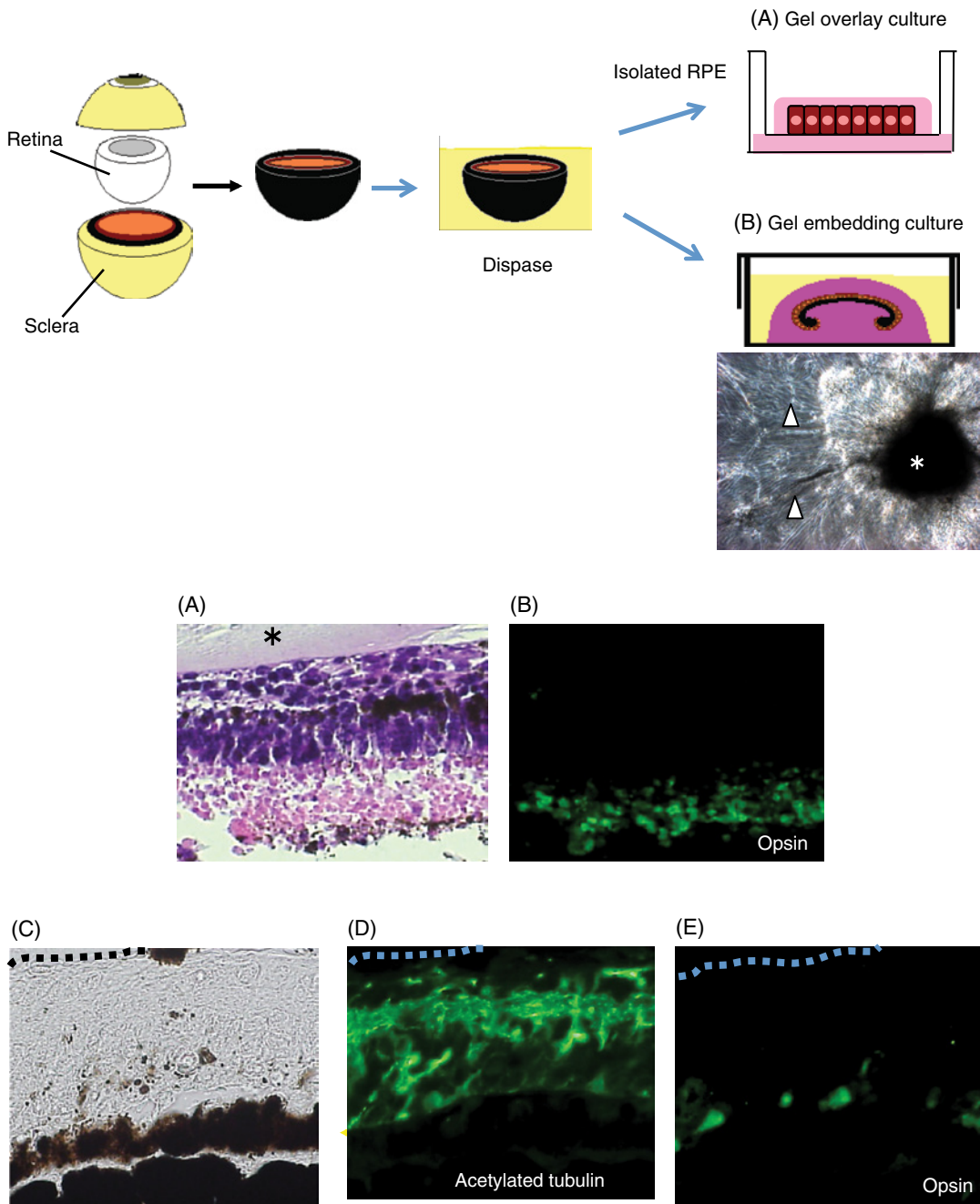


Figure 18.8 Organotypic culture for 3-D retinal tissue regeneration. The retina and sclera were removed from the posterior eye. After incubating the tissue (the RPE and the choroid) with Dispase, the tissue was either (a) placed on the culture membrane and overlaid with Matrigel or (b) inserted into the Matrigel. The phase-contrast micrograph shows well-elongated neuronal fibers (arrowheads) extending from the explant (asterisk). (A–E) By Day 30, retinal structures have regenerated. (A and B) and (C, D, and E) are the serial sections showing the formation of the outer segments (A) and the inner plexiform layer (D) (Nabeshima et al. 2013). Reprinted from Kuriyama et al. (2009). © 2013 Wiley Periodicals, Inc. To see a color version of this figure, see Plate 49.

without isolating the RPE sheet. This method has many advantages over the previous Matrigel overlay method for the reproduction of 3-D retinal structures. This method demonstrated that the RPE cells must be detached from the choroid before they can enter the regeneration pathway; when the RPE and choroid tissue are not treated with Dispase and are simply embedded in the gel immediately, no retinal tissues are regenerated, and the RPE remains a pigmented epithelium. This clearly shows that cell and extracellular matrix (ECM) interactions, which are mediated by collagen and other matrix proteins such as laminin and fibronectin, play a crucial role in the initial phase of regeneration. Dispase treatment appears not to affect the localization of N-cadherin in the RPE cells (our unpublished observation). Instead, Dispase may affect the turnover of the ECM component hyaluronan (HA), which has been shown to regulate cell migration, proliferation, and differentiation and activates intracellular signaling cascades during tissue injury and repair (Noble 2002; Jiang et al. 2007). It has been demonstrated that HA is an early component of the regenerative pathway and is required for cell proliferation during the early phases of *Xenopus* tail regeneration (Contreras et al. 2009). The data also suggest a possible crosstalk between HA and glycogen synthase kinase 3 beta (GSK3 β) signaling during tail regeneration. A similar turnover of ECM components may occur in the early phases of retinal regeneration, although it is unknown how this might relate to intracellular signaling processes.

Soon after the retina is removed from the *Xenopus* eye, the RPE cells quickly move to the RVM by leaving Bruch's membrane. Only those cells that have detached from the basement membrane and moved to the RVM can regenerate the retina. A key question thus arises: How do the cells become detached from Bruch's membrane when the retina is removed? Regeneration control by Dispase treatment in the culture model suggests that activation of certain proteases may occur after retinal removal. This disconnects RPE cells from the basement membrane. The upregulation of matrix metalloproteinases (MMPs) occurs soon after tissue injury and plays an important role in the initial phase of limb regeneration

(Vinarsky et al. 2005; Satoh et al. 2011). Whether this also occurs during retinal regeneration is an important question that is now being studied by a pharmacological method in our laboratory using the present culture model.

A transgenic approach to retinal regeneration

The development of transgenic animals is a powerful approach to the investigation of the genetic mechanisms involved in retinal regeneration. Although numerous studies have investigated *Xenopus* ocular development using transgenic animals, until recently, only a few studies have been performed on retinal regeneration. *In vivo Rax* silencing was accomplished with a shRNA-based transgenic *Xenopus* and provided information on *Rax* function during retinal regeneration (Pan et al. 2010; Martinez-De Luna et al. 2011). This study revealed that *Rax* actually functions during retinal regeneration in premetamorphic *X. laevis*, in which a partially resected retina was repaired by CMZ regeneration.

We recently produced two lines of transgenic *X. laevis* for genetic analysis of RPE trans-differentiation in postmetamorphic animals.

Transgenic *Xenopus* with an *efl- α* promoter-driven *EGFP*

We produced F1 and F2 lines of transgenic *X. laevis* containing an *EGFP* gene under the control of the *translation elongation factor 1- α* (*efl- α*) promoter and investigated how the gene is reactivated in RPE cells during retinal regeneration (Figure 18.9) (Ueda et al. 2012). *efl- α* promotes the GTP-dependent binding of aminoacyl-tRNA to ribosomes during peptide chain elongation and is a ubiquitous gene that is expressed in many tissues in the developing embryos. *efl- α* promoter-driven *EGFP* in transgenic animals has been widely used as a genetic marker because of ubiquitous expression of its reporter gene during development (Johnson and Krieg 1994; Ogino et al. 2006). The expression driven by this promoter, however, is progressively restricted during the late developmental stage for unknown reasons

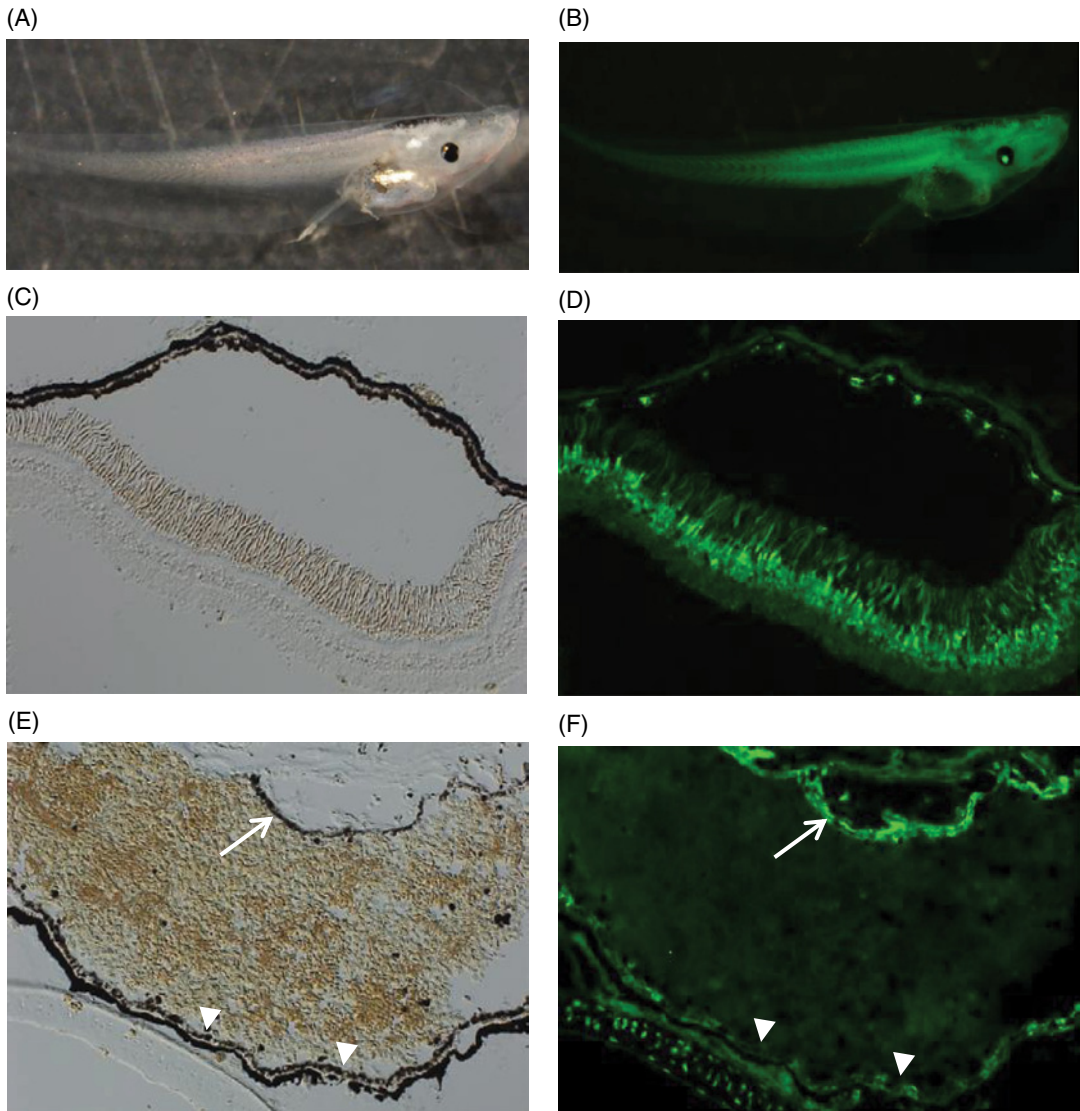


Figure 18.9 The generation of an EF-1 α promoter-EGFP transgenic *X. laevis*. (A and B) F1 tadpole at St. 50. A bright field image and a fluorescent image of the same animal. The F1 tadpole has a uniform expression of the *EGFP* transgene in its whole body. (C–F) The expression of *EGFP* in the neural retina and the RPE cells of adult F1 animal. (C and D) Nomarski differential image and EGFP staining of a normal eye. In D, only a few RPE cells stained positively for EGFP (arrowheads). In the neural retina, EGFP was detected in the inner nuclear layer and in the photoreceptor cell layer, although no EGFP expression was detected in the ganglion cell layer. The RPE and neural retina are artificially detached. (E and F) Nomarski differential image and expression of EGFP during retinal regeneration on Day 10. The arrows indicate the newly formed RPE layers on the RVM, while the arrowheads show the original RPE layers on Bruch's membrane. The RPE cells on the RVM stain much more intensely for EGFP than do those on Bruch's membrane. Reprinted from Ueda et al. (2012). © 2012, with permission from John Wiley & Sons, Inc.

and is dramatically reduced in several adult tissues. In transgenic zebrafish, the *Xenopus efl- α* promoter-driven *EGFP* expression is ubiquitously expressed in early development and is systematically silenced in adult tissues,

including the lens, NR, and RPE. *EGFP* expression, however, is temporarily renewed in Müller cells, which are the source of neuronal progenitors during zebrafish retinal regeneration (Thummel et al. 2006).

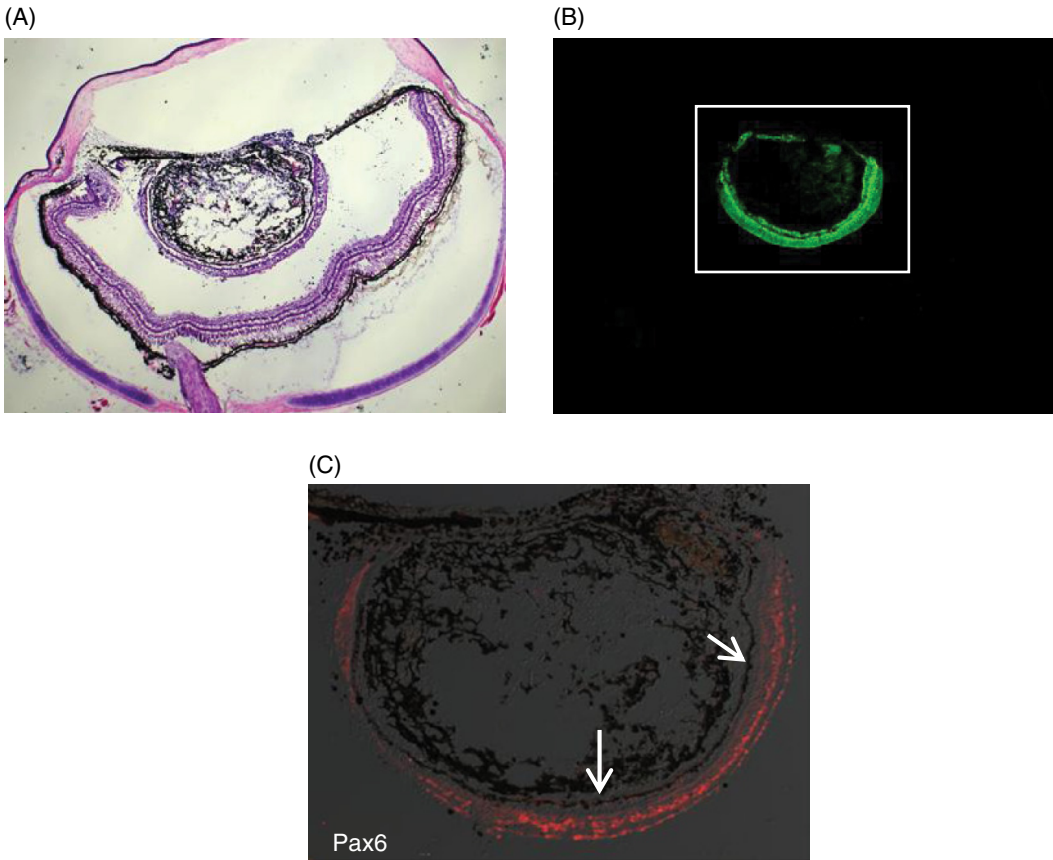


Figure 18.10 Intraocularly transplanted tissues from a transgenic animal at Day 35 post transplantation. The RPE with the choroid was isolated from the EF-1 α promoter–EGFP transgenic *X. laevis* and transplanted into the ocular chamber of a lenuctomized normal animal. (A and B) Identical sections stained with hematoxylin and eosin and EGFP, respectively. The explant is located near the pupil space. (C) Pax6 immunocytochemistry shows the laminar structure of the regenerating retina. Reprinted from Ueda et al. (2012). © 2012, with permission from John Wiley & Sons, Inc.

The use of the F1 and F2 lines for these experiments made our results very stable and reproducible (Ueda et al. 2012). EGFP expression was reduced in the adult ocular tissues of nonmanipulated transgenic *Xenopus*, and EGFP-expressing cells were occasionally found heterogeneously in the lens, NR, and RPE tissues. During retinal regeneration, the EGFP gene was found to be reactivated in the RPE and the ciliary marginal cells.

To determine if EGFP upregulation in the RPE cells during retinal regeneration is related to cell proliferation, immunocytochemistry for the proliferation marker proliferating cell nuclear antigen (PCNA) was performed on the eyes. In normal, nonmanipulated eyes, numerous RPE cells were

found to be positive for PCNA, and some were also found to be EGFP positive. When the eyes from a Day 20 postretinectomy were examined, the majority of the EGFP-positive cells were also stained for PCNA, suggesting that the reactivation of *efl- α* in the RPE cells is related to cell proliferation. *efl- α* transgenic animals were also used for a transplant study because of a genetic marker in the donor tissue. Intraocularly transplanted RPE tissues clearly transdifferentiate to regenerate the retina in the anterior ocular chamber (Figure 18.10). The preliminary results of our recent transplant study showed that when RPE tissues from *efl- α* transgenic are cultured under tissue culture conditions for 10 days followed by

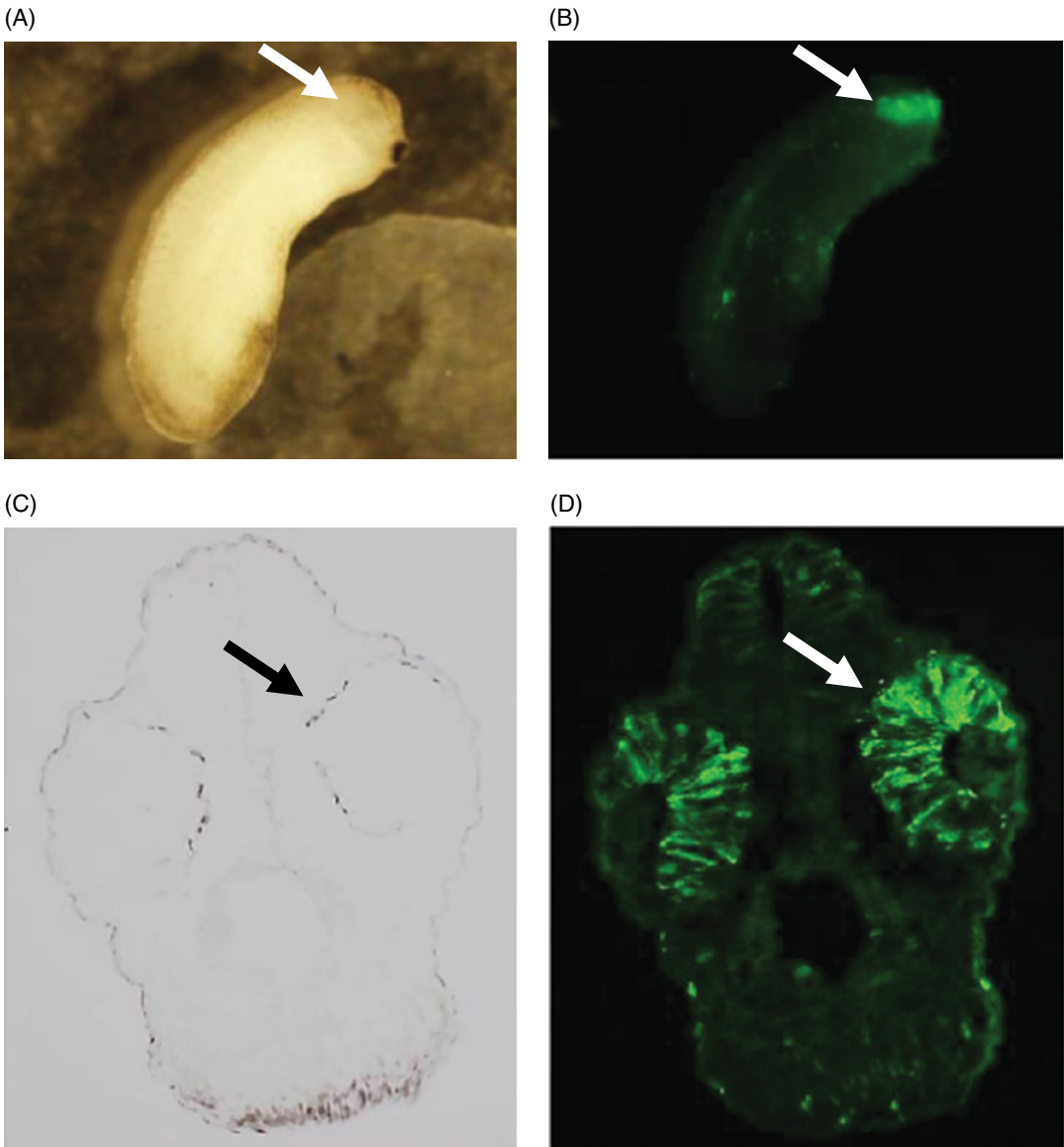


Figure 18.11 The generation of Rax promoter–EGFP transgenic *X. laevis*. EGFP expression in the transgenic animals at St. 27 (A and B) and St. 31 (C and D). EGFP is localized only in the ocular region. In D, the neural retina is intensely stained for EGFP (arrows) and the lens is devoid of staining. Reprinted from Nabeshima et al. (2013). © 2013, Wiley Periodicals, Inc.

intraocular transplantation into the RPE layer of the host eye, the transplants differentiate into the retinal layer and become continuous and integrated with the host retina (unpublished data). This suggests that the transplantation of cultured explant tissues can be a new approach for the functional recovery of damaged retinas.

Production of a Rax promoter–EGFP transgenic *Xenopus*

We next produced a transgenic animal line in which EGFP expression is under the control of the Rax promoter (Figure 18.11). The Rax gene is essential for ocular development and is one of the earliest genes to be expressed (Casarosa

et al. 1997; Zhang et al. 2000; Bailey et al. 2004). It is also an essential gene for retinal development (Zaghloul and Moody 2007) and is also one of the earliest genes activated during retinal regeneration (Martinez-De Luna et al. 2011). Transdifferentiation of RPE cells is believed to be accompanied by recapitulation of organogenesis during embryonic development, and the *Rax* promoter-EGFP transgenic animals are a useful model to analyze how the *Rax* gene is upregulated in the initial step of RPE transdifferentiation.

Using the F1 and F2 generations, we analyzed *Rax*-EGFP expression during retinal regeneration in a tissue culture model (Nabeshima et al. 2013). The transgenic animal was particularly useful for the flat tissue cultures because the real-time expression of

EGFP can be followed as RPE cells differentiate into neural cells.

As described earlier, four zones were clearly distinguished as the RPE cells migrating outwards from the periphery of the explant. The expression of transcription factors such as *Pax6* and *Rax*-EGFP was observed in different zones (Figure 18.12). *Rax*-EGFP expression preceded *Pax6* expression and was found in the RPE cells located in the explant and in the epithelial zone. EGFP expression was not uniform among cells in the same zone; in the epithelial zone, some cell clusters showed intense EGFP staining with neighboring EGFP-negative cells, possibly reflecting a cell-substratum interaction. The expression of both genes appears to occur in RPE cells that have lost contact with the basement membrane.

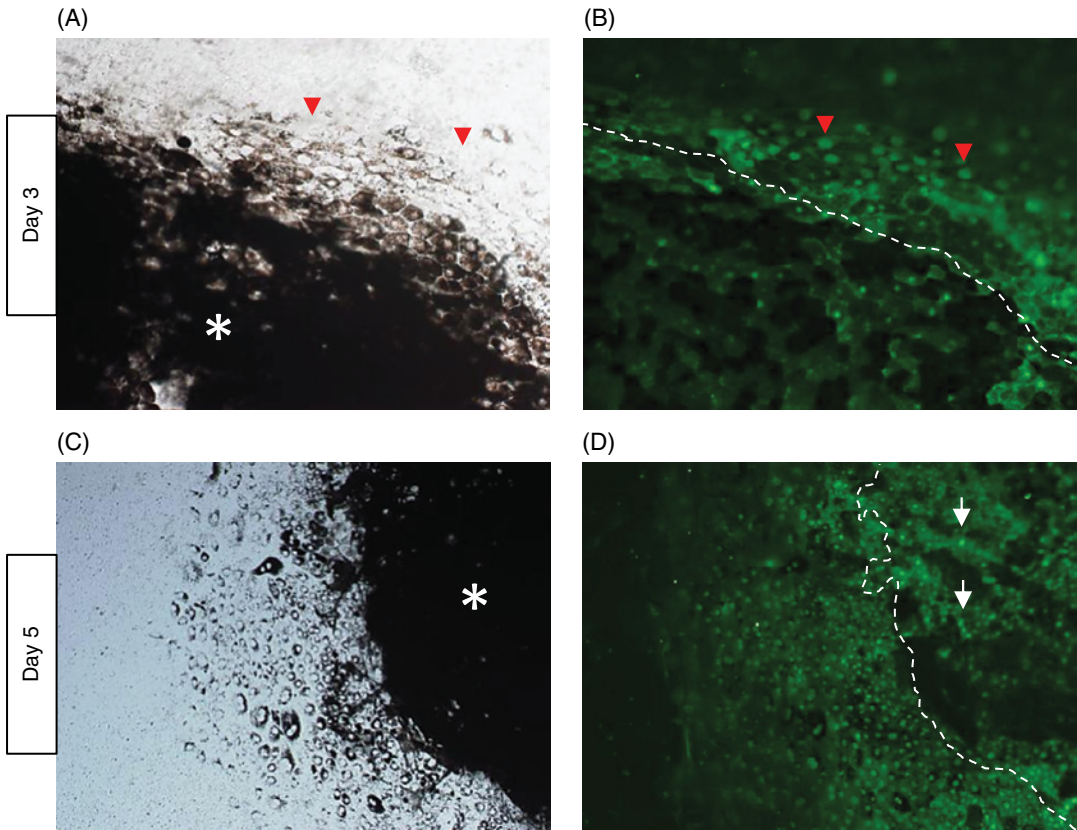


Figure 18.12 Real-time detection of EGFP fluorescence by *Rax*-promoter activity in the cultured RPE cells. (A and B) Day 3 and (C and D) Day 5. In A and B, only a few explant cells are positive for EGFP (asterisks), while many epithelial cells express EGFP (black & white arrowheads). The dotted line shows the boundary of the explant (asterisk) and the epithelial zone. In C and D, cells in the epithelial zone are positive for EGFP fluorescence, while those in the transition zone become mostly negative or less intensely fluorescent. Some cells in the explant have now become positive for EGFP (arrowheads). Reprinted from Nabeshima et al. (2013). © 2013, Wiley Periodicals, Inc.

***X. tropicalis*: A novel animal model for retinal regeneration**

An interesting feature of *Xenopus* as an animal model for retinal regeneration is that there are several closely related species of *Xenopus* available for experiments. *Xenopus tropicalis* has been particularly significant in multigenerational genetics research. *X. tropicalis* has been used for regeneration studies of the limbs, tail, jaw, cornea, and some ocular tissues (Henry and Elkins 2001; Lin et al. 2007; Kurosaka et al. 2008; Kashiwagi et al. 2010). These results indicate that there are some differences in its regeneration ability but that it is basically similar to that of *X. laevis*. We attempted to determine if *X. tropicalis* has a retinal regeneration ability similar to that of *X. laevis* and, if so, to confirm if it would be a more suitable animal model for genetic studies of retinal regeneration.

Although still preliminary, we observed that a complete new retina can regenerate by 30 days after the removal of the original retina. The regenerating retina is derived solely from the stem/progenitor cells of the CMZ, indicating that this is a novel mode of vertebrate retinal regeneration that has not been reported before (Miyake and Araki, 2014). Immediately following retinal removal, the RPE cells move to the RVM and reform a new epithelium, similar to that of *X. laevis*. In *X. tropicalis*, however, no sign of transdifferentiation was observed in the newly formed pigmented epithelium on the RVM. Under the two RPE tissue culture models, *X. tropicalis* RPE cells neither differentiated to neuronal cells nor formed a 3-D retinal structure but simply remained as RPE cells. This indicates that both *X. laevis* and *X. tropicalis* are excellent model animals for the study of cellular and molecular mechanisms of retinal regeneration because they have contrasting modes of regeneration: one mainly from RPE cells and the other from the stem/progenitor cells of the CMZ.

Two additional lines of research should be pursued. First, the RPE cells of *X. laevis* and *X. tropicalis* should be compared both *in vivo* and *in vitro* to explore the molecular mechanisms involved in RPE transdifferentiation, particularly in terms of the molecular function of early genes such as *Six3*, *Otx2*, *Rax*, and *Pax6*. Alterations in the microenvironments of the

RPE cells, such as changes in the cell–cell and cell–ECM interactions, must also be studied to see how they are related to the regulation of these genes. Secondly, a novel mode of retinal regeneration, namely, the CMZ stem cell-based regeneration following whole-retina removal, is highly intriguing in the context of higher vertebrates such as mammals, which also have stem/progenitor cells in the ciliary epithelium (see earlier section). A better understanding of the regeneration mechanisms of *X. tropicalis* may open new approaches for recruiting ciliary stem cells for *in vivo* retinal regeneration in other vertebrates.

A hypothetical model for retinal regeneration and future perspectives on retinal regeneration studies

The retina regenerates by RPE transdifferentiation in the adult *X. laevis* when the whole retina is removed. This process can be reproduced using two culture models (the flat method and the Matrigel embedding methods). *Rax* and *Pax6* are critical genes required for stem/progenitor cells to be expressed in RPE cells. From our *in vivo* and *in vitro* observations, we illustrate a hypothetical model of amphibian retinal regeneration (Figure 18.13).

RPE cells undergo transdifferentiation followed by subsequent retinal histogenesis in these culture models only when the RPE cells are freed from the choroid. The RPE cells remain densely pigmented when they are kept attached to the choroid and these features are very consistent with the *in vivo* observations that the RPE cells detach and move to the RVM where they form a new epithelium and regenerate the retina. The RPE cells that do not detach and that stay in Bruch's membrane do not undergo transdifferentiation. These results clearly indicate that the phenotypic expression of the RPE cells is largely dependent on cell–substratum (basement membrane) interactions. Cell–cell interactions are also likely to play a role. The flat culture model has an advantage in that it can trace the temporal and spatial expression patterns of regulating genes in the RPE cells. There is a distinct difference in the expression patterns

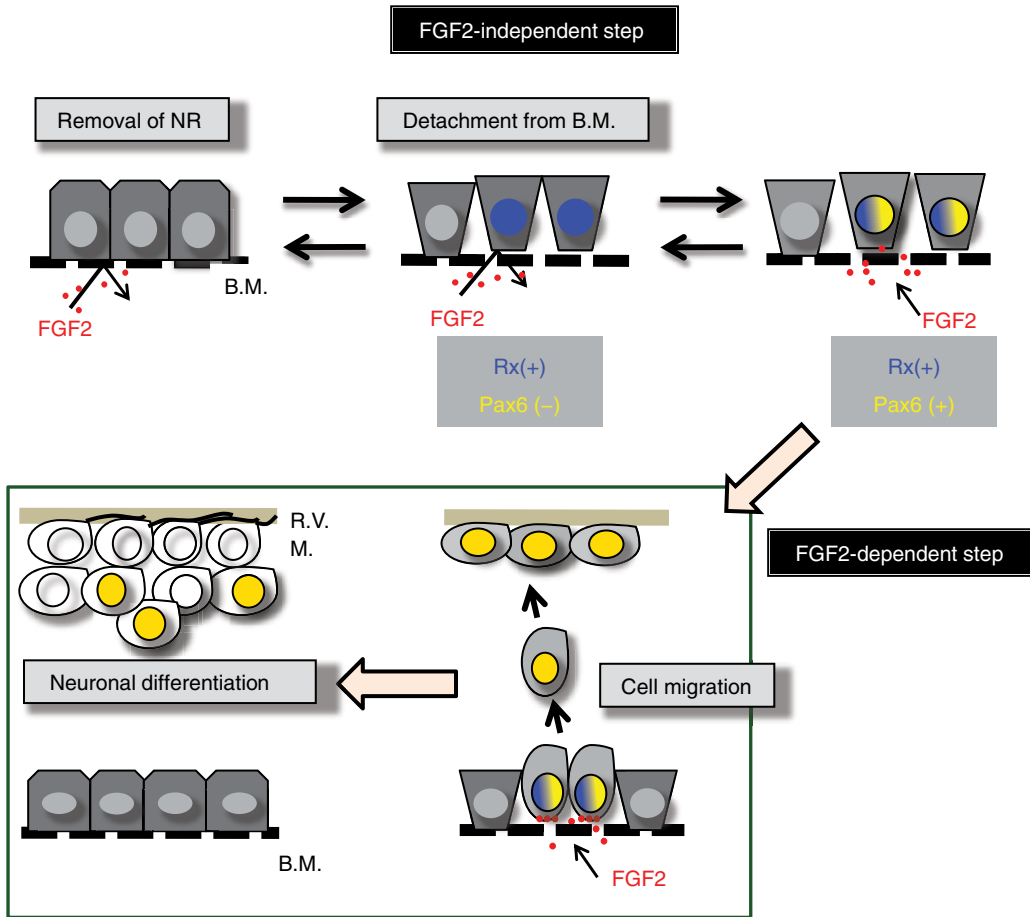


Figure 18.13 A hypothetical model for transdifferentiation begins in the RPE cells after retinal removal. In the normal eye, the RPE cells adhere to the basement membrane (Bruch's membrane). FGF2 appears to have no effect on the RPE cells in this situation. When the retina is removed, some of the RPE cells are detached from Bruch's membrane, most likely through an upregulation of MMP genes. The *Rax* gene also becomes upregulated in these cells. In the next step, which is FGF2 dependent, the RPE cells are detached from Bruch's membrane and begin to respond to FGF2 and peel off from the RPE layer. They then become positive for *Pax6* and move to the new basement membrane (the RVM) where they begin to proliferate and differentiate into retinal cells. The RPE cells left at Bruch's membrane can then readhere to the membrane and enter a stationary state (the normal state). The first step appears to be FGF2 independent and the second step appears to be FGF2 dependent. During the first step, the RPE cells return to the normal state, when not exposed to FGF2 for a period of time, indicating that this step is reversible. Reprinted from Kuriyama et al. (2009), with permission from John Wiley & Sons, Inc. To see a color version of this figure, see Plate 50.

of *Rax* and *Pax6*. *Rax* expression begins soon after the RPE cells lose contact with the matrix (Bruch's membrane) and seems to precede *Pax6* expression (Nabeshima et al. 2013). This finding suggests that *Rax* may regulate *Pax6* just as is observed during early neural development. FGF2 is another important environmental factor (Mitsuda et al. 2005; Susaki and Chiba 2007). This factor is required for RPE cells to undergo transdifferentiation *in vitro*

and is believed to be derived from the choroid (Mitsuda et al. 2005). Interestingly, FGF2 is not necessarily required for *Pax6* upregulation because RPE cells isolated from the choroid become *Pax6* positive in the presence of the FGF signaling inhibitors, SU5402 and U0126 (Kuriyama et al. 2009). Without FGF2 signaling, *Pax6* expression remains at a low level and is not prolonged, finally diminishing within a week. These observations indicate

that a loss of normal tissue interactions between RPE and the choroid has a central role in the onset of *Rax*, which is then followed by *Pax6*. FGF2 is needed for the intense and prolonged expression of *Pax6*, which finally triggers neuronal differentiation.

When ectopically induced, *Pax6* expression is sufficient to induce the transdifferentiation of RPE cells in the developing chick embryo (Azuma et al. 2005). However, *Pax6* expression is not sufficient for eye formation in *Xenopus* (Hirsch and Harris 1997). It has been speculated that *Pax6* is downstream of the FGF signaling pathway under the experimental conditions used for the chick embryos and that *Pax6* upregulation is necessary for FGF2-stimulated transdifferentiation (Spence et al. 2007). The present study implies that *Pax6* upregulation does not require FGF2 signaling and is brought about with *Rax* expression alone.

Our previous study showed that newt RPE cells can become unable to undergo transdifferentiation even in the presence of FGF2 when FGF2 is administered after a certain period of culturing (Mitsuda et al. 2005). This suggests that FGF2 effectively influences the RPE cells only when they are expressing *Pax6*. It has also been shown that the FGF signaling inhibitor, U0126, suppresses newt RPE cells, stopping them from migrating outside of the explant and thus preventing them from transdifferentiating (Mitsuda et al. 2005). Hence, it can be concluded that two steps occur in the initial phase of transdifferentiation (Figure 18.13). The first step is FGF2 independent. Altered tissue interactions and/or cell–cell interactions induce *Rax*, which promotes *Pax6* expression in the RPE cells. The cells then become susceptible to FGF2, and FGF2 drives the RPE cells into the second step. The second step involves the generation of retinal stem cells, most likely through the maintenance of *Pax6* expression at a certain level in RPE cells. The first step is reversible because the activated RPE cells (*Pax6*-positive form) return to the inactive form if FGF2 is not present.

The present study demonstrates that retinal regeneration is regulated by the combined control of intercellular communication, extracellular matrices, and cell growth factors.

These aspects will be the main issues in future studies on the molecular analysis of retinal regeneration. Although little is known about the molecular nature of the early phases of RPE transdifferentiation, the culture methods described here present an excellent experimental approach to investigate these issues.

Although still in the preliminary stage, we are developing a new animal model to study retinal regeneration: *X. tropicalis*. The comparison between this species and *X. laevis* will be an intriguing area for further study because RPE differentiation in these two species is conspicuously different. Two genetically similar animals with different modes of retinal regeneration are very powerful tools for use in regeneration studies, particularly when combined with culture models.

Acknowledgments

The author is grateful to all of his colleagues at the Developmental Neurobiology Laboratory, Nara Women's University. He also thanks the Institute for Amphibian Biology, Graduate School of Science, Hiroshima University, for providing *X. tropicalis* through the National BioResource Project of the MEXT, Japan. This work was supported in part by a Grant-in-Aid (Scientific Research on Innovative Area) and a Grant-in-Aid (Kiban-B and Kiban-C) from the Ministry of Education, Culture, Sports, Science and Technology of Japan and by a Nara Women's University Intramural Grant for Project Research.

References

- Ahmad I, Tang L, Pham H (2000) Identification of neural progenitors in the adult mammalian eye. *Biochem. Biophys. Res. Commun.* 270, 517–521.
- Araki M (2007a) Regeneration of the amphibian retina: Role of tissue interaction and related signaling molecules on RPE transdifferentiation. *Dev. Growth Differ.* 49: 109–120.
- Araki M (2007b) A comparative study of amphibian retinal regeneration by tissue culture technology – a review. In “Strategies for Retinal Tissue Repair and Regeneration in Vertebrates: From Fish to Human” (edited by Chiba) pp. 77–95. Research Signpost, Kerala.

- Arresta E, Bernardini S, Bernardini E, Filoni S, and Cannata SM (2005) Pigmented epithelium to retinal transdifferentiation and Pax6 expression in larval *Xenopus laevis*. *J. Exp. Zool.* 303A: 958–967.
- Azuma N, Tadokoro K, Asaka A, et al. (2005) Transdifferentiation of the retinal pigment epithelia to the neural retina by transfer of the Pax6 transcriptional factor. *Human Mol. Gene.* 14: 1059–1068.
- Bailey TJ, El-Hodiri H, and Zhang Li (2004) Regulation of vertebrate eye development of Rx gene. *Int. J. Dev. Biol.* 48: 761–770.
- Bosco L (1988) Transdifferentiation of ocular tissues in larval *Xenopus laevis*. *Differentiation* 39: 4–15.
- Casarosa S, Andreazzoli M, Simeone A, and Barsacchi G (1997) *Xrx1*, a novel *Xenopus* homeobox gene expressed during eye and pineal gland development. *Mech. Dev.* 61: 187–198.
- Chiba C and Mitashov VI (2007) Cellular and molecular events in the adult newt retinal regeneration. In “Strategies for Retinal Tissue Repair and Regeneration in Vertebrates: From Fish to Human” (edited by Chiba et al.) pp. 15–33. Research Signpost, Kerala.
- Contreras EG, Gaete M, Sánchez N, Carrasco H, and Larrain J (2009) Early requirement of hyaluronan for tail regeneration in *Xenopus* tadpoles. *Development* 136: 2987–2996.
- Coulombre JL and Coulombre AJ (1970) Influence of mouse neural retina on regeneration of chick neural retina from chick embryonic pigmented epithelium. *Nature* 228: 559–560.
- Del Rio-Tsonis K and Tsonis PA (2003) Eye regeneration at the molecular age. *Dev. Dyn.* 226: 211–224.
- Filoni S, Bosco L, and Cioni C (1982) The role of neural retina in lens regeneration from cornea in larval *Xenopus laevis*. *Acta Embryol. Morphol. Exp.* 3: 15–28.
- Filoni S, Bernardini S, Cannata SM, and D’Alessio A (1997) Lens regeneration in larval *Xenopus laevis*, experimental analysis of the decline in regeneration capacity during development. *Dev. Biol.* 187: 13–24.
- Filoni S (2009) Retina and lens regeneration in anuran amphibians. *Semin. Cell Dev. Biol.* 5: 528–534.
- Fischer AJ, McGuire CR, Dierks BD, and Reh TA (2002) Insulin and fibroblast growth factor 2 activate a neurogenic program in Müller glia of the chicken retina. *J. Neurosci.* 22: 9387–9398.
- Gwon A, Gruber LJ, Mantras C, and Cunanan C (1993) Lens regeneration in New Zealand albino rabbits after endocapsular cataract extraction. *Invest. Ophthalmol. Vis. Sci.* 34: 2124–2129.
- Hasegawa M (1958) Restitution of the eye after removal of the retina and lens in the newt, *Triturus pyrrhogaster*. *Embryologia.* 4: 1–32.
- Hirsch N and Harris WA (1997) *Xenopus* Pax-6 and retinal development. *J. Neurobiol.* 32: 45–61.
- Hitchcock P, Ochocinska M, Sieh A, and Otteson D (2004) Persistent and injury-induced neurogenesis in the vertebrate retina. *Prog. Ret. Eye Res.* 23: 183–194.
- Hitchcock PF and Raymond PA (1992) Retinal regeneration. *Trends Neurosci.* 15: 103–108.
- Henry JJ and Elkins MB (2001) Cornea-lens transdifferentiation in the anuran, *Xenopus tropicalis*. *Dev. Genes Evol.* 211: 377–387.
- Ide CF, Reynolds P, and Tompkins R (1984) Two healing patterns correlate with different adult neural connectivity patterns in regenerating embryonic *Xenopus* retina. *J. Exp. Zool.* 230: 71–80.
- Ikegami Y, Mitsuda S, and Araki M (2002) Neural cell differentiation from retinal pigment epithelial cells of the newt: An organ culture model for the urodele retinal regeneration. *J. Neurobiol.* 50: 209–220.
- Jiang D, Liang J, and Noble PW (2007) Hyaluronan in tissue injury and repair. *Annu. Rev. Cell Dev. Biol.* 23: 435–461.
- Johnson AD and Krieg PA (1994) pXex, a vector for efficient expression of cloned sequences in *Xenopus* embryos. *Gene* 147: 223–226.
- Karl MO and Reh TA (2010) Regenerative medicine for retinal diseases: Activating the endogenous repair mechanisms. *Trends Mol. Med.* 16(4): 193–202.
- Kashiwagi K, Kashiwagi A, Kurabayashi A, et al. (2010) *Xenopus tropicalis*: An ideal experimental animal in amphibia. *Exp. Anim.* 59: 395–405.
- Kurosaka H, Takano-yamamoto T, Yamashiro T, and Agata K (2008) Comparison of molecular and cellular events during lower jaw regeneration of newt (*Cynops pyrrhogaster*) and west African clawed frog (*Xenopus tropicalis*). *Dev. Dyn.* 237: 354–365.
- Kuriyama F, Ueda Y, and Araki M. (2009) Complete reconstruction of the retinal laminar structure from a cultured retinal pigment epithelium is triggered by altered tissue interaction and promoted by overlaid extracellular matrices. *Dev. Neurobiol.* 69: 950–958.
- Lin G, Chen Y, and Slack JMW (2007) Regeneration of neural crest derivatives in the *Xenopus* tadpole tail. *BMC Dev. Biol.* 7: 56.
- Lombardo F (1969) La rigenerazione della retina neurale negli adulti degli Anfibi anuri. *Arch. It. Anat. Embriol.* 74: 29–47.
- Lopashov GV and Sologub AA (1972) Artificial metaplasia of pigmented epithelium into retina in tadpoles and adult frogs. *J. Embryol. Exp. Morph.* 28: 521–546.
- Martinez-De Luna RI, Kelly LE, and El-Hodiri HM (2011) The retinal homeobox (Rx) gene is necessary for retinal regeneration. *Dev. Biol.* 353: 10–18.

- Massé K, Bhamra S, Eason R, Dale N, and Jones EA (2007) Purine-mediated signaling triggers eye development. *Nature* 449: 1058–1062.
- Mese G, Richard G, and White TW (2007) Gap junctions: Basic structure and function. *J. Invest. Dermatol.* 127: 2516–2524.
- Meyers JR, Hu L, Moses A, Kaboli K, Papandrea A, and Raymond PA (2012) β -catenin/Wnt signaling controls progenitor fate in the developing and regenerating zebrafish retina. *Neural Dev.* 7: 30.
- Mitashov VI (1997) Retinal regeneration in amphibians. *Int. J. Dev. Biol.* 41, 893–905.
- Mitsuda S, Yoshii C, Ikegami Y, and Araki M (2005) Tissue interaction between the retinal pigment epithelium and the choroid triggers retinal regeneration of the newt. *Cynops pyrrhogaster*. *Dev. Biol.* 280: 122–132.
- Miyake A and Araki M (2014) Retina stem/progenitor cells in the ciliary marginal zone complete retinal regeneration: *A study of retinal regeneration in a novel animal model*. *Dev. Neurobiol.* (in press).
- Mizuno A, Yasumuro H, Yoshikawa T, Inami W, and Chiba C (2012) MEK-ERK signaling in adult newt retinal pigment epithelium cells is strengthened immediately after surgical induction of retinal regeneration. *Neurosci. Lett.* 523: 39–44.
- Nabeshima A, Nishibayashi C, Ueda Y, Ogino H, and Araki M (2013) Loss of cell–extracellular matrix interaction triggers retinal regeneration accompanied by Rax and Pax6 activation. *Genesis* 51(6): 410–419.
- Noble PW (2002) Hyaluronan and its catabolic products in tissue injury and repair. *Matrix Biol.* 21: 25–29.
- Ogino H, McConnell WB, and Grainger RM (2006) Highly efficient transgenesis in *Xenopus tropicalis* using I-SceI meganuclease. *Mech. Dev.* 123: 103–113.
- Ohta K, Ito A, and Tanaka H (2008) Neuronal stem/progenitor cells in the vertebrate eye. *Dev. Growth Differ.* 50: 253–259.
- Okada TS (1991) *Transdifferentiation*. Oxford University Press, New York.
- Pan Y, Martinez-De Luna RI, Lou CH, et al. (2010) Regulation of photoreceptor gene expression by the retinal homeobox (Rx) gene product. *Dev. Biol.* 339: 494–506.
- Park CM and Hollenberg J (1993) Growth factor-induced retinal regeneration *in vivo*. *Int. Rev. Cytol.* 146: 49–74.
- Pearson RA, Dale N, Llaudet E, and Mobbs P (2005) ATP released via gap junction hemichannels from the pigment epithelium regulates neural retinal progenitor proliferation. *Neuron* 46: 731–744.
- Raymond PA and Hitchcock PF (1997) Retinal regeneration: Common principles but diversity of mechanism. *Adv. Neurol.* 72: 171–184.
- Reh TA and Nagy T (1987) A possible role for the vascular membrane in retinal regeneration in *Rana catesbeiana* tadpoles. *Dev. Biol.* 122: 471–482.
- Reh TA and Fisher AJ (2001) Stem cells in the vertebrate retina. *Brain Behav. Evol.* 58: 296–305.
- Reyer RW (1977) The amphibian eye: Development and regeneration. In “Hand Book of Sensory Physiology” (edited by F. Crescitelli), pp. 309–390. Springer-Verlag, Berlin and New York.
- Sakaguchi DS, Janick LM, and Reh TA (1997) Basic fibroblast growth factor (FGF-2) induced transdifferentiation of retinal pigment epithelium: Generation of neurons and glia. *Dev. Dyn.* 209: 387–398.
- Sakai H and Saito T. (1997) Na⁺ and Ca²⁺ channel expression in cultured newt retinal pigment epithelial cells: Comparison with neuronal types of ion channels. *J Neurobiol.* 32: 377–390.
- Satoh A, Makanae A, Hirata A, and Satou Y. (2011) Blastema induction in aneurogenic state and Prrx-1 regulation by MMPs and FGFs in *Ambystoma mexicanum* limb regeneration. *Dev. Biol.* 355: 263–274.
- Schaefer JJ, Oliver G, and Henry JJ (1999) Conservation of gene expression during embryonic lens formation and cornea-lens transdifferentiation in *Xenopus laevis*. *Dev. Dyn.* 215: 308–318.
- Sologub AA (1977) Mechanisms of repression and derepression of artificial transformation of pigment epithelium into retina in *Xenopus laevis*. *Roux’s Arch. Dev. Biol.* 182: 277–291.
- Spence JR, Madhavan M, Aycinena J-C, and Del Rio-Tsonis K (2007) Retina regeneration in the chick embryo is not induced by spontaneous Mitf downregulation but requires FGF/FGFR/MEK/Erk dependent upregulation of Pax6. *Mol. Vis.* 13: 57–65.
- Stone LS (1950a) Neural retina degeneration followed by regeneration from surviving retinal pigment cells in grafted adult salamander eyes. *Anat. Rec.* 106: 89–109.
- Stone LS (1950b) The role of retinal pigment cells in regenerating neural retinae of adult salamander eyes. *J. Exp. Zool.* 113: 9–32.
- Stenn KS, Stenn KS, Link R, Moellmann G, Madri J, and Kuklinska E (1989) Dispase, a neutral protease from *Bacillus Polymyxa*, is a powerful fibronectinase and type IV collagenase. *J. Invest. Dermatol.* 93: 287–290.
- Sun G, Asami M, Ohta H, Kosaka J, and Kosaka M (2006) Retinal stem/progenitor properties of iris pigment epithelial cells. *Dev. Biol.* 289: 243–252.
- Susaki K and Chiba C (2007) MEK mediates *in vitro* neural transdifferentiation of the adult newt retinal pigment epithelium cells: Is FGF2 an induction factor? *Pigment Cell Res.* 20(5): 364–379.

- Thummel R, Burket CT, and Hyde DR (2006) Two different transgenes to study gene silencing and re-expression during zebrafish caudal fin and retinal regeneration. *Scientific World Journal* 6: 65–81.
- Ueda Y, Mizuno N, and Araki M (2012) Transgenic *Xenopus laevis* with the *ef1-a* promoter as an experimental tool for amphibian retinal regeneration study. *Genesis* 50: 642–650.
- Umino Y and Saito T (2002) Spatial and temporal patterns of distribution of the gap junctional protein connexin-43 during retinal regeneration of adult newt. *J. Comp. Neurol.* 454: 255–262.
- Vinarsky V, Atkinson DL, Stevenson TJ, Keating MT, and Odelberg SJ. (2005) Normal newt limb regeneration requires matrix metalloproteinase function. *Dev. Biol.* 279: 86–98.
- Yoshii C, Ueda Y, Okamoto M, and Araki M (2007) Neural retinal regeneration in the anuran amphibian *Xenopus laevis* post-metamorphosis: Transdifferentiation of retinal pigmented epithelium regenerates the neural retina. *Dev. Biol.* 303: 45–56.
- Yoshikawa T, Mizuno A, Yasumuro H, et al. (2012) MEK-ERK and heparin-susceptible signaling pathways are involved in cell-cycle entry of the wound edge retinal pigment epithelium cells in the adult newt. *Pigment Cell Melanoma Res.* 25: 66–82.
- Zaghloul NA and Moody SA (2007) Alterations of *rx1* and *pax6* expression levels at neural plate stages differentially affect the production of retinal cell types and maintenance of retinal stem cell qualities. *Dev. Biol.* 306: 222–240.
- Zhang L, Mathers PH, and Jamrich M (2000) Function of *Rx*, but not *Pax6*, is essential for the formation of retinal progenitor cells in mice. *Genesis* 28: 135–142.

19

The *Xenopus* Model for Regeneration Research

Ying Chen¹ & Gufa Lin^{1,2}

¹Stem Cell Institute, University of Minnesota, Minneapolis, MN

²School of Life Science and Technology, Tongji University, Shanghai, China

Abstract: In recent years, *Xenopus* has become a favorable organism for regeneration research. This is largely due to the establishment of transgenic technologies that enable the investigation of gene functions in later developmental events, including organogenesis and regeneration. With micromanipulation techniques and inducible or tissue-specific promoters, it is also possible to manipulate gene expression in a time- and tissue-type-specific manner, allowing the investigation of gene function in the regeneration of specific tissues, such as the spinal cord in the tail. *Xenopus* can regenerate its tail, limb, and lens in the tadpole stage but regeneration capacity is gradually lost during metamorphosis, providing a ready-made model for understanding regeneration and investigating means for its promotion. In this chapter, we will use the tadpole tail as an example to discuss the cellular and molecular mechanisms underlying regeneration. Using the limb of the postmetamorphic frogs, we will explore the possibility of stimulating limb regeneration. In addition, we will also discuss lens regeneration. This chapter provides exciting examples of what *Xenopus* can offer for regeneration research, in addition to its role as a standard model organism for developmental and cell biology studies.

Introduction

Replacing lost organs or appendages after injury has long been an intriguing phenomenon in the animal kingdom. The underlying mechanisms of regeneration are currently being extensively investigated in a variety of model organisms (Brookes and Kumar 2008; Poss 2010; Tanaka and Reddien 2011). In vertebrates, appendage regeneration has been studied mostly in the urodele amphibians, newts, and salamanders. These urodele animals can

regenerate multiple tissues and organs, including the limb, tail, heart, jaw, brain, and retina, even as adults (Maden 2008). In recent years, The African clawed frog, *Xenopus laevis*, an anuran amphibian, has emerged as a new vertebrate regeneration model, mainly due to its unique regeneration behaviors (Slack et al. 2008; Tseng and Levin 2008; Beck et al. 2009).

Unlike urodele amphibians that maintain regenerative ability throughout their lifetime, *Xenopus* has a stage-dependent regenerative capacity. The tadpole limb bud has the ability

of complete regeneration at early developmental stages; then, this ability declines with the degree of differentiation and is eventually lost during metamorphosis (Dent 1962). Lens regeneration in *Xenopus* also undergoes an ontogenetic decline (Filoni 2009; Barbosa-Sabanero et al. 2012). Tadpoles of all ages will regenerate a lens, whereas postmetamorphic frogs will not. The tail of *Xenopus* tadpole regenerates nicely through larval life, with the exception of a refractory period, a short time period around stage 46/47, when the tadpoles start feeding (Beck et al. 2003). The regenerative capacity of the central nervous system, such as the axon regeneration after spinal cord transection, also declines along with development (Gibbs et al. 2011 and Chapter 15). The stage-dependent regenerative behaviors in *Xenopus* have attracted scientists to explore why the appendage regeneration ability is progressively lost and enabled investigation of methods to stimulate regeneration at regeneration-incompetent stages. So *Xenopus* provides a natural system that allows us to perform both gain- and loss-of-function studies to understand the underlying regenerative mechanisms.

Being a standard animal model in the field of developmental biology (Sive et al. 2000), *Xenopus* has a huge advantage for experimental work in regeneration studies. We already have a profound knowledge of the early developmental progress of *Xenopus* embryos. In this system, there is an inventory of cDNA and expression sequence tag (EST) libraries of different developmental stages and a pool of gene probes for gene function studies. We have a whole range of micromanipulation techniques for labeling tissues or changing their positions both in early-stage embryos and swimming tadpoles, allowing the tracing of their behavior during regeneration. This has been very useful for lineage analysis (Gargioli and Slack 2004) and for investigating tissue interactions during regeneration (Lin et al. 2012).

The establishment of transgenic techniques in 1996 has greatly advanced regeneration studies in *Xenopus* (Kroll and Amaya 1996). This gene transfer method is especially useful for gene function analysis at later developmental stages, as the transgene is integrated

into the genome, so unlike injected mRNA, it does not become diluted out at the tadpole and postmetamorphic stages. Earlier work has shown that mammalian promoters usually give good spatial and temporal control of transgene expression pattern in *Xenopus* transgenic embryos (Beck and Slack 1999a). So there are numerous “off-the-shelf” promoters available for use in *Xenopus*. In addition, to avoid possible developmental defects in early transgenic embryos, Beck et al. have utilized a heat shock promoter to induce transgene expression only during tail regeneration (Beck et al. 2003). Other inducible systems, such as the UAS-Gal4 and doxycycline-inducible systems, have also been adapted to *Xenopus* (Hartley et al. 2002; Ryffel et al. 2003; Das and Brown 2004; Gargioli and Slack 2004; Lin et al. 2012). This allows us to activate a transgene in a spatial and temporal context during regeneration. Today, there are plenty of *Xenopus* transgenic lines available and stocked (e.g., in the US National *Xenopus* Resource and the European *Xenopus* Resource Center, Portsmouth, UK). These transgenic lines will be valuable resources for deciphering regeneration mechanisms.

***Xenopus* tadpole tail regeneration**

After amputation, the *Xenopus* tadpole tail will regenerate within 2 weeks (Figure 19.1A). Tadpole tail regeneration proceeds in three phases. The first phase, within 24h after tail amputation, is a wound healing process in which the amputated surface is covered by a specialized wound epithelium that lacks an underlying dermis and basement membrane (Figure 19.1B) (Neufeld and Day 1996). Following wound healing, cell proliferation and migration dominate in the second phase of tail regeneration. As a result of the cell divisions and continuous cell migration to the wound site, a regeneration bud is noticeable growing from the amputated surface. The regeneration bud contains the expanded end of the spinal cord (spinal ampulla), the bullet-shaped mass of dividing notochord cells, and surrounding mesenchyme (Figure 19.1C) (Gargioli and Slack 2004). This is different from a “regeneration blastema”, which normally

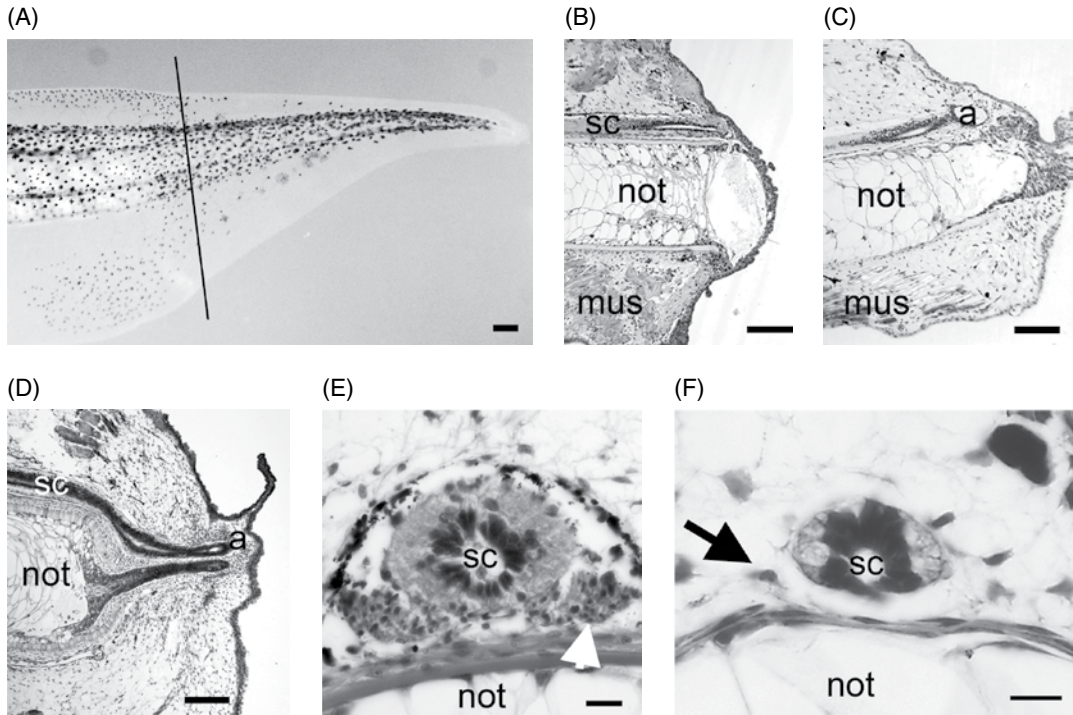


Figure 19.1 Regeneration of the tadpole tail. (A) A tadpole tail at 7 days post amputation (dpa). Black line indicates amputation level. (B–D) Hematoxylin and eosin (HE) staining on sagittal sections of tail regenerate (B) 1 dpa, (C) 2 dpa, and (D) 3 dpa, showing the phases of tail regeneration (B, wound healing; C, bud formation; D, outgrowth). (E and F) Cross sections of tails showing the presence (white arrow in E) and absence (black arrow in F) of the spinal ganglion in the (E) original and (F) regenerated tail. not, notochord; mus, muscle; sc, spinal cord; a, spinal ampulla. Scale bars in A–D, 100 μ m; scale bars in E–F, 20 μ m. C is reprinted with permission from Figure 1b in Slack et al. (2008).

refers to a region of undifferentiated cells typically present in limb regeneration. The final phase is the outgrowth of the regeneration bud (Figure 19.1D). At this stage, the new tail grows much faster than the normal growth rate and then forms a well-structured tail.

The regenerated tail is very similar to the original tail but is not an identical replica. The regenerated nervous system is not the same as the original. There are no spinal ganglia in the new tail and the axons innervating the new tail come from neurons in the tail stump, rather than from new neurons (Figure 19.1E and F). In addition, the new muscle is not segmented (reviewed in Slack et al. 2008).

Cellular origin in tail regeneration

Identifying the cellular origins of regenerated appendage is of particular interest for scientists

to develop cell-based therapies for organ replacement. To analyze cell origins in tadpole tail regeneration, Gargioli and Slack (2004) labeled three main types of axial tissues (the spinal cord, the notochord, and the muscle) within the tail by grafting explants of neural plate, notochord, and presomitic mesoderm, respectively, from *CMVGFP* transgenic neurulae into the presumptive tail region of wild-type host embryos. The resulting host tail has just one tissue type labeled with GFP. The *CMV* promoter remains active in all the tissue types of tails, so after the tail is amputated through the graft, a labeled cell should still express GFP even if it dedifferentiates or redifferentiates into the same or a different tissue type. The cell lineage during tail regeneration can then be traced (Figure 19.2A).

Studies in urodele have shown evidence of cell dedifferentiation and metaplasia during regeneration. This means that one differentiated

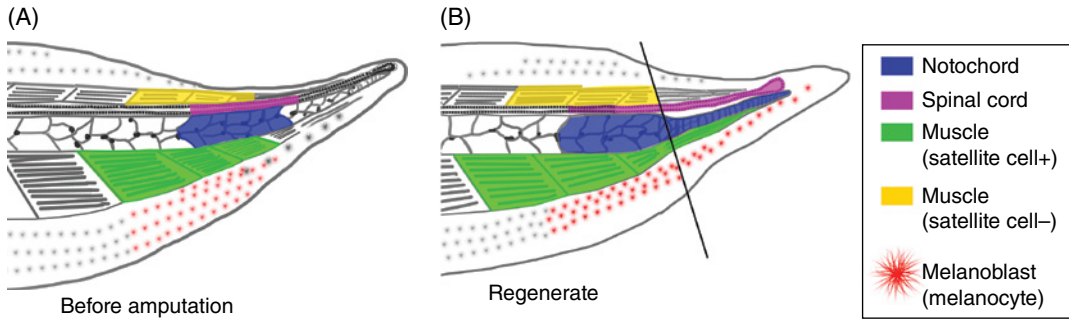


Figure 19.2 Diagram of origins of tissues in tail regeneration. (A) Specific tissue type in the tadpole tail (such as the spinal cord) can be labeled by transplantation of explant expressing fluorescence protein in early neurula stage (with a piece of neural plate) or tadpole stage (with a piece of whole spinal cord). (B) The labeling experiments show that the spinal cord regenerates from the spinal cord (magenta), the notochord regenerates from the notochord (blue), and the melanocyte regenerates from melanoblast (red). If satellite cells are labeled before amputation, the new muscle in tail regenerate will be labeled (green), but if satellite cells are not labeled, muscle in tail regenerate will not be labeled (yellow). The diagram is a summary of several labeling experiments (Gargioli and Slack 2004; Lin et al. 2007) and is also reproduced from Figure 2 in Beck et al. (2009). © 2009, John Wiley & Sons, Inc. To see a color version of this figure, see Plate 51.

cell type is converted to another, regardless of pathway or mechanism (Tosh and Slack 2002). Several examples have been reported in urodele regeneration (Brockes and Kumar 2002).

However, in *Xenopus*, neither dedifferentiation nor metaplasia was found during tail regeneration (Gargioli and Slack 2004; Lin et al. 2007). GFP expression was observed solely within the reforming spinal cord and notochord in neural plate and notochord graft experiments. Since the standard neural plate graft only labels the ventral part of the spinal cord, Slack's group further conducted graft of a whole piece of spinal cord at tadpole stage to find out what happens to all the cells of the spinal cord, especially cells on the dorsal side where cell emigration could occur, during regeneration. The result shows that about 0.5 mm of the GFP-labeled spinal cord populates the entire regenerating spinal cord. No labeled cells exit the spinal cord and contribute to other tissue types. Thus, this evidence clearly demonstrates that the two major tissues of the tail, the spinal cord and the notochord, regenerate from their own tissue types. Other tissue types in the regenerating tail, such as the pigment cells, are also derived from their corresponding tissue types in the stump (Lin et al. 2007) (Figure 19.2B).

To label the myofibers in tadpole tails, a piece of presomitic mesoderm was grafted in

both early and late neurula, and the resulting tadpole tail was subjected to GFP analysis during regeneration. Unlike the situations in the spinal cord and notochord regeneration, myofibers in the regenerates were rarely labeled with GFP from early neurulae grafts. But if the grafts were taken from a more lateral region of the presomitic mesoderm or from late-stage neurulae in which the lateral tissue has moved more dorsally, the regenerating tails contained a significant number of GFP-labeled myofibers (Gargioli and Slack 2004). This experiment firstly suggests that no dedifferentiation takes place in *Xenopus* tail muscle regeneration; GFP expression would be found in newly formed myofibers from amputations through regions containing labeled myofibers. Secondly, it indicates that some other type of cells rather than myofibers must be the precursor cells for the regenerated muscle in the tadpole tail. Further investigation shows that, as in mammalian muscle regeneration, *pax7*-expressing muscle satellite cells are the source of new muscles in *Xenopus* tadpole tails (Gargioli and Slack 2004; Chen et al. 2006). A recent study indicates that muscle dedifferentiation does occur after *Xenopus* tadpole tail amputation, but dedifferentiated muscle cells do not enter the cell cycle and will never contribute to new muscle, which excludes transdifferentiation of muscle cells (Ryffel et al. 2003; Rodrigues et al. 2012).

The aforementioned cell lineage tracing analysis in tail regeneration clearly shows that tissues in the tail (the spinal cord, the notochord, and the myofibers) behave independently, which means they regenerate from their respective specialized precursors (Figure 19.2B). This is highly similar to the mammalian digit tip regeneration, in which lineage-restricted progenitor cells are the cellular source to replace lost tissue (Rinkevich et al. 2011). This lineage restriction phenomenon during regeneration was also found in axolotl limb regeneration and zebrafish fin regeneration (Kragl et al. 2009; Tu and Johnson 2011), indicating a widely adopted cellular mechanism in appendage regeneration.

Molecular mechanisms in tail regeneration

Tools for molecular analysis

The tadpole tail has been extensively used as a model for studying the molecular mechanism for regeneration. This is in part due to the availability of a versatile toolbox for dissecting the molecular mechanism. First of all, there exists a set of techniques to manipulate gene expression. Despite that there is no homologous recombination technology to make knockouts, constitutive active and dominant negative forms of genes can be used to effectively obtain gain-of-function or loss-of-function activities (Table 19.1). For example, to stimulate bone morphogenetic protein (BMP) signaling pathways, Beck et al. used *Alk3*, a mutated, constitutively active form of the type I BMP receptor, which phosphorylates its targets in the absence of BMP ligand. To inhibit BMP signaling, they used *tBR*, a truncated BMP receptor that acts as a dominant negative form (Beck et al. 2003). Similarly, a dominant negative fibroblast growth factor (FGF) receptor *XFD* is used to inhibit FGF, and *Dickkopf-1* (*Dkk1*) is used to antagonize Wnt ligands (Amaya et al. 1991; Glinka et al. 1998; Lin and Slack 2008). Secondly, chemical genetics, which uses bioactive small molecules to manipulate protein function, is widely used in *Xenopus* regeneration studies. Several important pathways have been successfully

investigated using small molecules (Table 19.1). The beauty of using small molecule is that they can be added or washed away as needed, thus allowing the investigation of precise temporal requirement of the mechanisms under examination. For example, in the investigation of the action of histone deacetylase (HDAC) inhibitor valproic acid (VPA) during tail regeneration, Taylor and Beck (2012) limited the exposure of VPA to an hour. This would be very difficult by manipulating transgene expression in whole animals. Of course, in many cases, a combination of different approaches has been fruitful in epistasis analysis of signaling pathways during regeneration.

Global studies of gene expression in tail regeneration are limited in *X. laevis*, which is pseudotetraploid (Tazaki et al. 2005). But with the rapid adoption of *Xenopus tropicalis* in regeneration study, we anticipate that more genome-wide analysis will identify new components in *Xenopus* regeneration. Such an example is from Amaya's lab, in which they have identified potential new players in tail regeneration, such as metabolic processes involving the generation of hydrogen peroxide and NADPH (Love et al. 2011).

Signaling pathways in tail regeneration

Investigation of molecular pathways underlying tail regeneration has benefited from our understanding of the tail bud development. Important signaling pathways, including BMP, Notch, Wnt, and FGF, were first shown to be required in tail bud development (Beck and Slack 1999b) and subsequently demonstrated to be necessary for tail regeneration. Inhibition of BMP and Notch signaling blocks tail regeneration, and induction of BMP signaling activator *Alk3* or Notch signaling activator *NICD* restores tail regeneration in the refractory period (Beck et al. 2003). Members of the FGF family are well known for their role in anteroposterior patterning (AP) (Isaacs et al. 1994). Lin and Slack (2008) showed that FGF is also required for regeneration as tail regeneration is inhibited when FGF signaling is perturbed, either by the dominant negative FGF receptor *XFD* or the FGF receptor antagonist *SU5402*.

Table 19.1 Signaling pathways in *Xenopus* tail regeneration.

Pathway	Reagents (target)	Effects on regeneration	Phase affected	References
Epigenetics modification	TSA, VPA (HDAC)	Inhibitory	Wound healing, bud formation	Taylor and Beck (2012)
	Butyrate (HDAC)	Inhibitory	Wound healing, bud formation	Tseng et al. (2011) Tseng et al. (2011)
TGF β	SB 431542, SB 505124, LY 364947 (TGF β receptor)	Inhibitory	Wound healing, bud formation, bud outgrowth	Ho and Whitman (2008)
Apoptosis	M50054 (caspase-3), NS3694 (caspase)	Inhibitory	Bud formation	Tseng et al. (2007)
H ⁺ pump	Palytoxin (Na ⁺ /K ⁺ transporter)	Inhibitory	Bud formation	Adams et al. (2007)
	PMA (H ⁺ pump) Concanamycin, YCHE78 (V-ATPase)	Activating Inhibitory		
Sodium transporter	MS222 (sodium channel)	Inhibitory	Bud formation	Tseng et al. (2010)
	Na _v 1.5, SIK, monensin (sodium channel)	Activating		
BMP	Alk3 (BMP receptor)	Activating	Bud formation, bud outgrowth	Beck et al. (2003)
	tBR (BMP receptor) Noggin (BMP)	Inhibitory Inhibitory		
Notch	NICD (Notch)	Activating	Bud formation and outgrowth, spinal cord and notochord	Beck et al. (2003)
Wnt	MG132 (proteasome) β Cat* (beta-catenin)	Inhibitory Activating	Bud formation and outgrowth	Lin and Slack (2008)
	Dkk1 (Wnt) BIO (GSK3 β)	Inhibitory Activating		
FGF	FGF20 (ligand)	Activating	Bud formation and outgrowth	Lin and Slack (2008)
	XFD (FGFR) SU5402 (FGFR)	Inhibitory		
Chloride channel	Ivermectin + Cl ⁻ (GlyCL)	Inhibitory or activating	Unclear	Tseng and Levin (2012)
Hyaluronan (HA)	Methylumbelliferone (HA synthesis)	Inhibitory	Bud outgrowth	Contreras et al. (2009)
	HAS2 (HA synthesis)	Inhibitory	Bud outgrowth	

HDAC, histone deacetylases; TSA, trichostatin A; VPA, valproic acid; TGF β , transforming growth factor beta; BMP, bone morphogenetic protein; FGF, fibroblast growth factor; Alk3, constitutive active BMP receptor; tBR, truncated BMP receptor; β Cat*, constitutive active form of beta-catenin; GSK3 β , glycogen synthase kinase 3 beta; XFD, dominant negative FGF receptor; HAS, hyaluronan synthases.

As in limb bud development, the Wnt/beta-catenin signaling pathway is shown to be required for cell proliferation in tail regeneration. If the Wnt/beta-catenin pathway is inhibited, tail regeneration does not occur; if the pathway is activated, cell proliferation in

the regeneration bud is increased and outgrowth of the tail is expedited (Lin and Slack 2008). These studies indicate that the tail indeed utilizes similar developmental mechanisms in regeneration as in development (Stocum 2004).

The transforming growth factor β (TGF β) pathway is also required for tail regeneration. This was identified by chemical treatment of the amputated tail with SB 431542, an inhibitor of TGF β type I receptor (Ho and Whitman 2008). Interestingly, while BMP, Notch, Wnt/ β -catenin, and FGF pathways do not seem to interfere with the wound healing of the amputated tail, the TGF β signaling pathway is necessary for wound epithelium formation. SB 431542 treatment also inhibits formation of the regeneration bud and activation of the BMP pathway targets (Ho and Whitman 2008). Thus, TGF β plays multiple roles in different phases during tail regeneration.

In addition, several groups have identified the requirement for other biological events in tail regeneration, such as turnover of extracellular matrix and apoptosis. These events all seem to be related to the initiation of regeneration. The Larrain lab showed that the hyaluronan (HA) pathway is involved in the early stage of tail regeneration. HA synthesis is upregulated in the mesenchyme of the regeneration bud and inhibition of HA synthesis impairs the proliferation of mesenchymal cells in the regeneration bud, and hence inhibits tail regeneration (Contreras et al. 2009). This analysis reinforces the importance of turnover of extracellular matrix in tissue repair and regeneration. Levin's group has discovered an unexpected role of apoptosis during tail regeneration. Inhibiting caspase-3-mediated apoptosis in the early 24h period after amputation inhibits regeneration and reduces the number of mitotic cells, suggesting that the dying cells secrete some proproliferation signals (Tseng et al. 2007). This signal could be members of the Wnt family, as in the case of head regeneration in hydra, where it has been shown that apoptosis induces Wnt3a secretion in head regeneration (Chera et al. 2009). Intriguingly, an expanded region of apoptosis is observed in the nonregenerating tail stump of tadpoles amputated during the refractory period, suggesting that an intermediate amount of cell death is needed for regeneration to proceed (Tseng et al. 2007). How the tadpole tail achieves this is not clear.

More recently, the Levin group has demonstrated the important role of bioelectric signals in tail regeneration. After tail amputation,

cells in the tail stump are depolarized, and large outward currents leave the stump. But around 12–24h post amputation, the current direction is reversed and the cells in the stumps become repolarized again. This reversal of electric current at the tail stump has been suggested to correlate with whether tails regenerate or not (Reid et al. 2009). Levin's group has identified that the proton pump V-ATPase and the sodium transporters are both involved in the bioelectric regulation of tail regeneration (Adams et al. 2007; Tseng et al. 2010). But neither of these two signals is required for wound healing nor embryonic development of the tail, suggesting that they are regeneration specific. So far, it remains unclear how the bioelectric signal is transduced into transcriptional responses, but epigenetic modification (chromatin remodeling) mediated by sodium/butyrate transporters could be involved (Tseng and Levin 2012).

Epigenetic modification has recently been shown to be a critical element in the regulation of regenerative states (reviewed in Barrero and Izpisua Belmonte 2011). For example, the promoter of *shh* is highly methylated in postmetamorphic *Xenopus*, which may explain the low level of expression of *shh* (Yakushiji et al. 2007). In zebrafish, reduced expression of *dnmt-1* leads to increased regeneration capacity of the pancreatic beta cells (Anderson et al. 2009). Histone deacetylation has also been shown to regulate regeneration ability. Both Levin and Beck labs showed that HDAC inhibitors block tail regeneration (Tseng et al. 2011; Taylor and Beck 2012). The most potent inhibition of regeneration by HDAC inhibitors occurs during wound healing and prebud stages, indicating an early requirement for epigenetic modification in appendage regeneration (Taylor and Beck 2012).

Spatial and temporal aspects of signaling pathways

Interestingly, the temporal requirement for these signaling pathways in regeneration is different. For example, while a brief exposure (0–8h post amputation) to the small molecule SB 431542 (TGF β R antagonist) inhibits tail regeneration irreversibly, a continuous exposure to SU5402 (FGFR antagonist) for several days

is needed in order to inhibit tail regeneration (Ho and Whitman 2008; Lin and Slack 2008). Inhibition of BMP, Wnt, and FGF signaling pathways does not affect wound closure, but inhibits the formation of the regeneration bud and the outgrowth of the bud (Beck et al. 2003, 2006; Lin and Slack 2008). Thus, these temporal studies indicate that there is an order for the requirement of these signaling pathways during tadpole tail regeneration. And, indeed, epistasis analysis using a combination of transgenesis and chemical treatment has established at least one linear pathway during tail regeneration: the $TGF\beta \rightarrow BMP \rightarrow Wnt \rightarrow FGF$ linear pathway.

This has been done by activating one pathway and inhibiting another with combinations of gain- or loss-of-function transgenesis and chemical treatment (Table 19.1). When BMP is inhibited but Notch is activated, tail regeneration proceeds, though with defect in muscle regeneration. On the other hand, inhibition of the Notch pathway by MG132 will inhibit regeneration induced by BMP activation, suggesting that BMP acts upstream of Notch during tail regeneration (Beck et al. 2003). When Wnt signaling is inhibited with *Dkk1* and meanwhile FGF signaling is activated with overexpression of *Fgf20* ligand, tail regeneration is restored. However, when FGF is inhibited (with XFD transgenesis) and Wnt signaling is activated (with BIO treatment), tadpole tail fails to regenerate. These observations show that FGF signaling lies downstream of Wnt signaling during tail regeneration. Furthermore, both Wnt and FGF signaling lie downstream of BMP, as BMP inhibition leads to the failure of expression of genes in Wnt and FGF pathways (Lin and Slack 2008). On the other hand, activation of the BMP pathway is prevented by $TGF\beta$ inhibition (Ho and Whitman 2008), so it is very likely that $TGF\beta$ acts upstream of the remaining signaling pathways.

Whether the order of $TGF\beta \rightarrow BMP \rightarrow Wnt \rightarrow FGF$ pathways is also true during regeneration of other systems, such as the lens and limb, is not clear. Nevertheless, the tadpole tail is a good model for analyzing the relationship between pathways.

As the tail has quite well-defined tissue types, it is also possible to dissect the tissue

interactions between the spinal cord and muscle during regeneration. For example, if Wnt signaling is inhibited in the spinal cord, not only the spinal cord regeneration is inhibited, but also muscle regeneration is impaired. However, inhibiting Wnt signaling in muscle tissue does not disrupt spinal cord regeneration, suggesting that there is a dependence of spinal cord-produced signals for muscle regeneration, but not vice versa (Lin et al. 2012).

***Xenopus* limb as a model for stimulating regeneration**

Unlike the situation of the tail, where *Xenopus* is a leading model both for development and regeneration, the limb in *Xenopus* is not a traditional model either for development or regeneration. The limb bud in *Xenopus* appears rather late during development and takes much longer than mouse and chick to differentiate (Nieuwkoop and Faber 1994). However, the limb of *Xenopus* has an interesting regenerative behavior that makes it an ideal ready-made gain-of-function model for measures that can stimulate limb regeneration.

The tadpole normally regenerates its limbs at early developmental stages up to stage 53, when the limb bud is a flattened paddled shape, and then gradually loses the ability in late tadpole stages as the limb bud differentiates. After metamorphosis, the frog limbs can only produce an unsegmented cartilaginous spike after amputation (Dent 1962) (Figure 19.3A).

Over the past years, many methods have been attempted to stimulate limb regeneration in *Xenopus*. Some approaches were designed based on the results from normal limb regeneration in urodele amphibians. For example, early researchers were aware of the importance of dedifferentiation in the early phases of urodele limb regeneration. So, tissue trauma was made to increase the amount of dedifferentiation of mesodermal cells by repeatedly pricking the amputated hind limbs of metamorphosing tadpoles. Nerve supply was commonly thought to be an important factor in limb regeneration. So, early researchers tried to increase the amount of nerve at the amputation site by deviating the

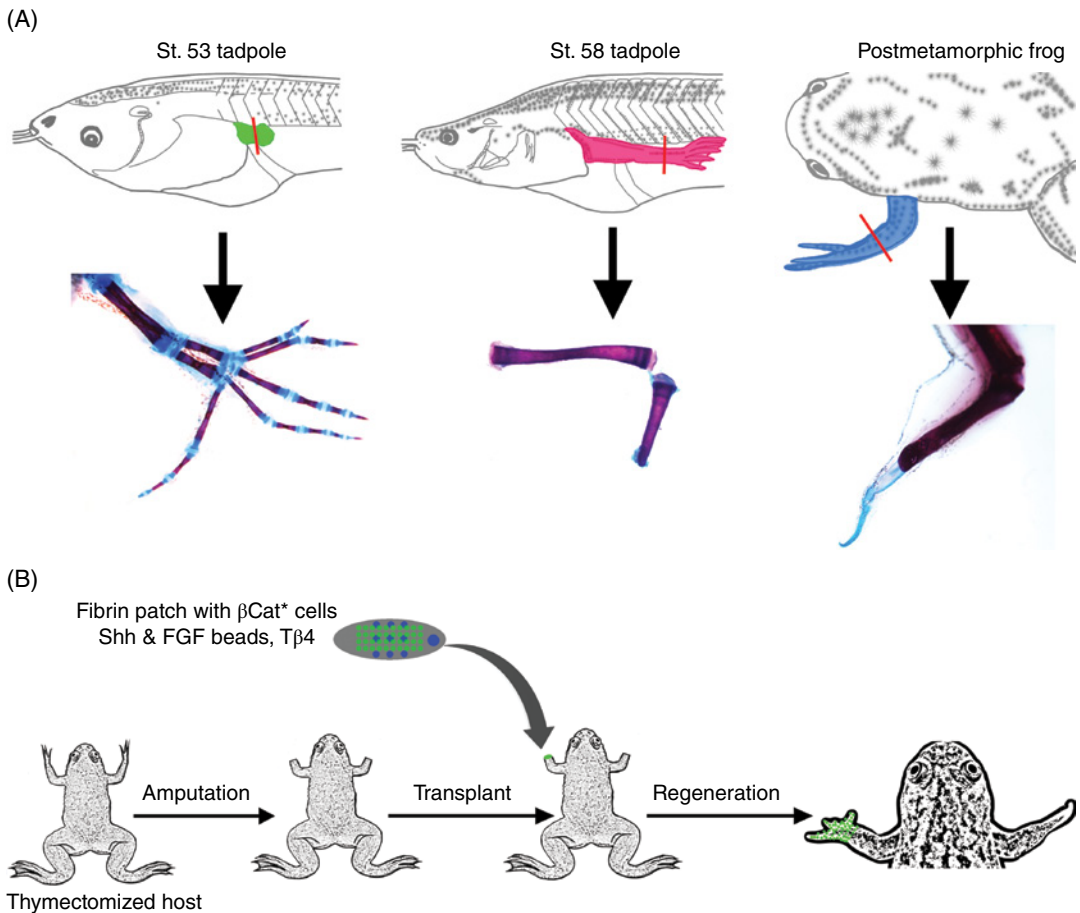


Figure 19.3 Limb regeneration in *Xenopus*. (A) Early tadpole limb (green, left) can fully regenerate, but late tadpole limb cannot (red, middle). Postmetamorphic frog can only regrow an unsegmented cartilaginous spark (blue, right). (B) Stimulation of limb regeneration in postmetamorphic frogs. Limb progenitor cells expressing high level of active beta-catenin, when delivered to the limb stump of a thymectomized frog in the presence of FGF10+Shh beads and thymosin beta 4 (T β 4), can stimulate multiple digit regeneration. Drawings of tadpole stages in A are after Nieuwkoop and Faber (1994). B is reprinted from the online graphic abstract in Lin et al. (2013). © 2012, with permission from Elsevier. To see a color version of this figure, see Plate 52.

sciatic nerve from the hind limb into the forelimb in frogs. Other strategies to stimulate limb regeneration have involved addition or removal of various extrinsic factors, such as putting tissue extracts or explants at the amputated limb sites. However, all reports of stimulating regeneration in postmetamorphic frog limbs have proved irreproducible, although some may have worked in tadpole limbs (Muller et al. 1999; Carlson 2007).

In recent decades, experiments to promote limb regeneration were mostly done at the molecular level. Many signaling pathways,

such as FGF, Wnt, and BMP pathways, have been identified to regulate limb regeneration in *Xenopus* tadpoles. Following limb amputation at regeneration-competent stage, migrating epidermal cells from the stump cover the wound surface, and a couple of days later, a multilayered apical epithelial cap (AEC) is formed. At this stage, *fgf8* is reexpressed in the AEC and *fgf10* is expressed in the underlying mesenchyme. Ide's group did a series of recombinant limb experiments and demonstrated that the regenerative capacity of *Xenopus* limbs is the property of

the mesenchyme and is correlated with the reexpression of *fgf10* (Yokoyama et al. 2000). Later, they showed that application of Fgf10 protein alone close to the amputated knee site could stimulate limb regeneration when the regenerative capacity falls (Yokoyama et al. 2001). However, the Slack group could not reproduce this result (Slack et al. 2004). This discrepancy could be due to variations in regenerative behaviors between batches of tadpoles. Or the variation may result from the amputation plane since regeneration in *Xenopus* tadpole is better if the amputation plane is through a joint region containing mostly fibroblastic cells, than through a cartilage condensation containing mainly differentiating chondrocytes (Wolfe et al. 2000; Nye and Cameron 2005). So for gain-of-function assays, limb amputation at tadpole stages should be performed carefully to avoid artifact.

Kawakami et al. (2006) found that Wnt/beta-catenin signaling is able to promote limb regeneration at stage 54, when the limb bud regeneration potential declines but is not completely lost. The requirement of the Wnt/beta-catenin pathway was further investigated in postmetamorphic frogs using a heat shock-inducible *Dkk1* (a Wnt antagonist) transgenic line. It was observed that Wnt/beta-catenin is not absolutely essential to initiate limb regeneration of young adults, possibly due to redundant roles from the nerve-derived signals (Yokoyama et al. 2011).

The BMP signaling pathway, which regulates *Xenopus* tadpole tail development and regeneration, is also required for limb regeneration in *Xenopus* tadpoles (Beck et al. 2006). Using a heat shock-inducible *noggin* transgenic line, Beck et al. demonstrated the temporal requirement of BMP signaling for blastema expansion during tadpole limb regeneration. *Msx1*, a direct target of BMP signaling, is expressed in mesenchymal cells of the limb blastema after limb amputation at regeneration-competent stage. The mesenchymal expression of *msx1* is thought to correlate with the dedifferentiation of blastema cells, and is considered as a readout of successful regeneration in urodele and mammalian appendage regeneration (Odelberg et al. 2000; Kumar et al. 2004). However,

overexpression of *msx1* is unable to rescue *Xenopus* limb regeneration, which suggests that addition of a single factor is not sufficient to regenerate a well-patterned limb (Barker and Beck 2009).

In fact, we have tested a set of single growth factors or their combinations, such as BMP2, BMP4, FGF8, FGF10, Wnt3a, and Shh, to activate signal transduction pathways either by applying protein or overexpressing transgenes in the limb stump. These factors have been shown to be essential in limb bud initiation, pattern formation, and tadpole hind limb regeneration. However, none of these factors or combinations displayed predicted power to induce frog forelimb regeneration (Lin et al. 2013). For these gain-of-function tests, we chose the *Xenopus* postmetamorphic frog forelimb as a regeneration model to avoid artifacts, since it has been documented that limb amputation through the radius and ulna level in postmetamorphic frog results in 100% simple spike formation (Tassava 2004). The limbs are already well developed, so the amputation plane can be easily controlled to normalize results.

Progenitor cell-based therapies have promise for tissue replacement. Early studies on *Xenopus* limb regeneration demonstrated that regeneration capacity is an intrinsic property of the developing limb rather than depending on the physiological state of the host (Muneoka et al. 1986; Sessions and Bryant 1988). This suggests that using regenerative competent limb bud cells may improve limb regeneration. Lin et al. tested this idea by grafting dissociated limb bud cells from limb regeneration-competent tadpoles to the amputated frog forelimb. They found that larval limb progenitor cells, with active Wnt/beta-catenin signaling, indeed could stimulate limb regeneration (Figure 19.3B). In addition, the success requires that the cells be delivered in a manner enabling good cell survival and supplemented with extracellular factors necessary for normal limb development. Although the regenerated digits are far from normal, they are segmented, innervated, express the joint marker *gdf5* in some cases, have substantial muscle tissue, and may show ossification. Remarkably, the host cells also make a substantial contribution in the

regenerated limbs despite their lack of regeneration competence (Lin et al. 2013).

This method to stimulate limb regeneration has potential clinical interest, since we can anticipate a procedure using iPS-derived progenitor cells to restore missing tissues in mammals. In fact, a similar approach involving transplanting neural progenitor cells in fibrin matrices containing growth factor cocktails has been reported to successfully repair severe spinal cord injury in rats (Lu et al. 2012). The stimulated limb regeneration in postmetamorphic frogs can be a useful platform for further exploring measurements to increase the quality of regeneration.

Lens regeneration

X. laevis tadpoles can regenerate a new lens through a process of transdifferentiation, in which the central region of the inner layer cells of the outer cornea dedifferentiates and redifferentiates to form a lens (Freeman 1963). Lens regeneration in *X. laevis* differs significantly from that of the well-known Wolffian lens regeneration in urodele amphibians, in which lens regeneration occurs at all developmental stages and involves transdifferentiation of the pigmented epithelial cells of the dorsal iris (reviewed in Beck et al. 2009; Henry and Tsonis 2010).

Unlike most other components of the eye, cornea development in *Xenopus* continues up to metamorphosis. In the larval tadpoles, the cornea consists of two separate layers. The outer layer is a squamous stratified epithelium, continuous with the epidermis and later becomes the postmetamorphic corneal epithelium. The inner layer is a thin sheet of loose mesenchymal cells, continuous with the sclera and later becomes the postmetamorphic substantia propria. Freeman (1963) documented the lens regeneration process in tadpoles in five distinct stages. In brief, after lentectomy, the inner layer cells change from squamous to cuboidal (stage 1), form a cell cluster by aggregation (stage 2), and become an epithelial vesicle that grows and expands into the space occupied by the original lens (stage 3). Then, the cells in the epithelial vesicle transdifferentiate to lens cells, with the formation

of primary lens fiber (stage 4) and the formation of secondary lens fiber (stage 5) (Figure 19.4).

The regenerated lens in *Xenopus* tadpoles is normally derived from the outer cornea that lies directly over the pupillary opening. The pericorneal epidermis also has lentogenic potential. Pieces of outer cornea or pericorneal epidermis implanted into the vitreous chamber will transdifferentiate into lens (Freeman 1963; Reeve and Wild 1978). Hence, this region together is termed the lentogenic area. Epidermal cells outside this region will not form a new lens when implanted into the vitreous chamber (Freeman 1963). Recently, it is shown that the lens-forming competence is closely related to the expression of *pax6*, a paired box transcription factor specifically expressed in the lentogenic area. Misexpression of *pax6* in flank epidermis is sufficient to induce a lens after implantation into the vitreous chamber, suggesting that *pax6* may confer regeneration competence to the lentogenic area (Gargioli et al. 2008).

The cornea to lens transdifferentiation is triggered by factors produced by neural retina and stored in the vitreous chamber. Removal of neural retina prevents lens regeneration from the outer cornea (Filoni et al. 1982). Cornea to lens transdifferentiation will take place in coculture of cornea epithelial and retinal tissues or in retinal conditioned medium (Bosco et al. 1997a, b). These studies suggest that the neural retina produces diffusible factors to support lens regeneration.

Though the factor(s) has not been identified, functional analysis of signaling pathways required for lens regeneration has recently begun to emerge (Henry et al. 2013). These include retinoic acid and hedgehog pathways in newt lens regeneration (Tsonis et al. 2000; Tsonis et al. 2004). In *Xenopus*, both FGF and BMP pathways are shown to be required for lens regeneration (Day and Beck 2011; Fukui and Henry 2011). Whether other signaling pathways important for tail and limb regeneration also regulate lens regeneration in the same manner is not yet known. The availability of transgenic *Xenopus* lines will provide a better understanding of the molecular mechanism of lens regeneration.

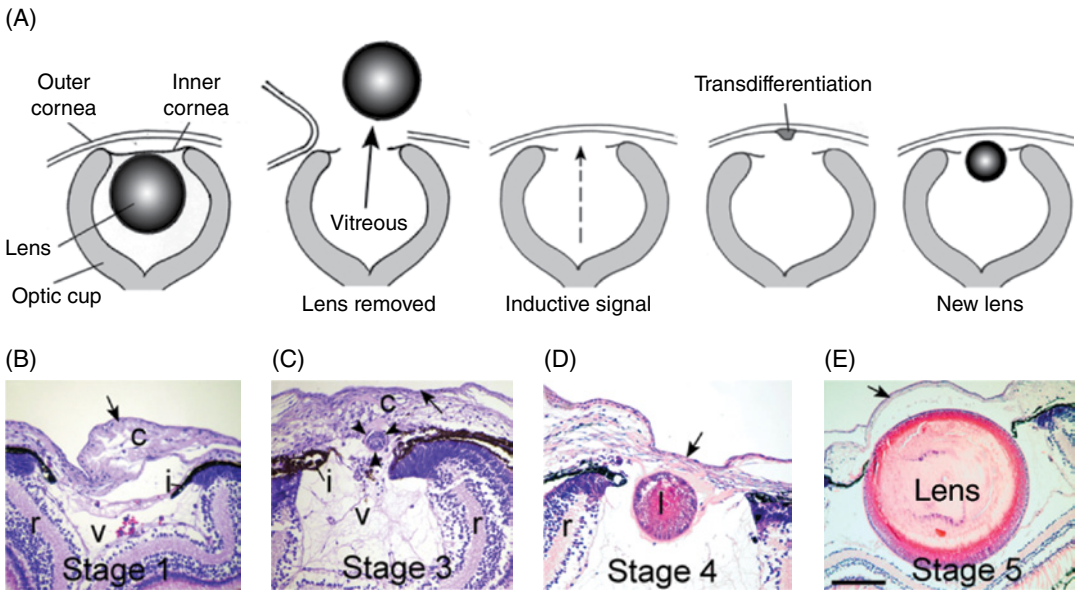


Figure 19.4 Progress of lens regeneration in tadpoles. (A) Schematic diagram showing the process of lentectomy in *Xenopus* tadpoles and regeneration of the lens from the outer cornea. The outer cornea is cut and flipped back, and the lens is extracted through the inner cornea and the outer cornea is replaced. (B–E) Histological sections of the eye after lentectomy at stage 50, stained with hematoxylin and eosin. Freeman's (1963) regeneration stages are used, but B = 24 h after lentectomy, C = 2 days, D = 3 days, and E = 8 days. c, cornea; r, retina; i, iris; v, vitreous; l, lentoid. Arrows denote the outermost layer of the cornea. Arrowheads in C mark aggregation of transdifferentiating cells. Reprinted from Figure 5A, B, C, D, E in Beck et al. (2009). © 2009, John Wiley & Sons, Inc.

Conclusions

The development of transgenic protocols provides an opportunity for *Xenopus* research labs to investigate later developmental events, including those of regeneration. Work in the last decades has shown that *Xenopus* is an excellent model for regeneration research. Various aspects of regeneration in *Xenopus*, such as the regeneration of new muscle from muscle satellite cells, have suggested that regeneration mechanisms in *Xenopus* are more akin to tissue repair in mammals than to regeneration in urodele amphibians in which dedifferentiation is more prominent. In this regard, *Xenopus* is not only a good model for solving some biological problem but is also useful for the development of more practical technologies for regenerative medicine, as evidenced by the possibility to stimulate limb regeneration in the nonregenerating frogs using progenitor cells. With the wider use of *X. tropicalis*, which is diploid and often has the

similar regeneration capacity to *X. laevis*, *Xenopus* will have much to offer for regeneration researches in the future.

Acknowledgments

The authors thank Dr. Jonathan Slack for critical reading of the manuscript and acknowledge support from the National Institute of Health.

References

- Adams, D. S., Masi, A., and Levin, M. 2007. H⁺ pump dependent changes in membrane voltage are an early mechanism necessary and sufficient to induce *Xenopus* tail regeneration. *Development* 134(7): 1323–35.
- Amaya, E., Musci, T. J., and Kirschner, M. W. 1991. Expression of a dominant negative mutant of the FGF receptor disrupts mesoderm formation in *Xenopus* embryos. *Cell* 66(2): 257–70.

- Anderson, R. M., Bosch, J. A., Goll, M. G., et al. 2009. Loss of Dnmt1 catalytic activity reveals multiple roles for DNA methylation during pancreas development and regeneration. *Developmental Biology* 334(1): 213–23.
- Barbosa-Sabanero, K., Hoffmann, A., Judge, C., Lightcap, N., Tsonis, P. A., and Del Rio-Tsonis, K. 2012. Lens and retina regeneration: new perspectives from model organisms. *The Biochemical Journal* 447(3): 321–34.
- Barker, D. M. and Beck, C. W. 2009. Overexpression of the transcription factor Msx1 is insufficient to drive complete regeneration of refractory stage *Xenopus laevis* hindlimbs. *Developmental Dynamics* 238(6): 1366–78.
- Barrero, M. J. and Izpisua Belmonte, J. C. 2011. Regenerating the epigenome. *EMBO Reports* 12(3): 208–15.
- Beck, C. W. and Slack, J. M. 1999a. Gut specific expression using mammalian promoters in transgenic *Xenopus laevis*. *Mechanisms of Development* 88(2): 221–7.
- Beck, C. W. and Slack, J. M. 1999b. A developmental pathway controlling outgrowth of the *Xenopus* tail bud. *Development* 126(8): 1611–20.
- Beck, C. W., Christen, B., and Slack, J. M. 2003. Molecular pathways needed for regeneration of spinal cord and muscle in a vertebrate. *Developmental Cell* 5(3): 429–39.
- Beck, C. W., Christen, B., Barker, D., and Slack, J. M. 2006. Temporal requirement for bone morphogenetic proteins in regeneration of the tail and limb of *Xenopus* tadpoles. *Mechanisms of Development* 123(9): 674–88.
- Beck, C. W., Izpisua Belmonte, J. C., and Christen, B. 2009. Beyond early development: *Xenopus* as an emerging model for the study of regenerative mechanisms. *Developmental Dynamics* 238(6): 1226–48.
- Bosco, L., Testa, O., Venturini, G., and Willems, D. 1997a. Lens fibre transdifferentiation in cultured larval *Xenopus laevis* outer cornea under the influence of neural retina-conditioned medium. *Cellular and Molecular Life Sciences* 53(11–12): 921–8.
- Bosco, L., Venturini, G., and Willems, D. 1997b. In vitro lens transdifferentiation of *Xenopus laevis* outer cornea induced by Fibroblast Growth Factor (FGF). *Development* 124(2): 421–8.
- Brockes, J. P. and Kumar, A. 2002. Plasticity and reprogramming of differentiated cells in amphibian regeneration. *Nature Reviews. Molecular Cell Biology* 3(8): 566–74.
- Brockes, J. P. and Kumar, A. 2008. Comparative aspects of animal regeneration. *Annual Review Cell Developmental Biology* 24(1): 525–549.
- Carlson, B. M. 2007. Principles of Regenerative Biology, Burlington, MA: Academic Press.
- Chen, Y., Lin, G., and Slack, J. M. 2006. Control of muscle regeneration in the *Xenopus* tadpole tail by Pax7. *Development* 133(12): 2303–13.
- Chera, S., Ghila, L., Dobretz, K., et al. 2009. Apoptotic cells provide an unexpected source of Wnt3 signaling to drive hydra head regeneration. *Developmental Cell* 17(2): 279–89.
- Contreras, E. G., Gaete, M., Sanchez, N., Carrasco, H., and Larrain, J. 2009. Early requirement of hyaluronan for tail regeneration in *Xenopus* tadpoles. *Development* 136(17): 2987–96.
- Das, B. and Brown, D. D. 2004. Controlling transgene expression to study *Xenopus laevis* metamorphosis. *Proceedings of the National Academy of Sciences of the United States of America* 101(14): 4839–42.
- Day, R. C. and Beck, C. W. 2011. Transdifferentiation from cornea to lens in *Xenopus laevis* depends on BMP signalling and involves upregulation of Wnt signalling. *BMC Developmental Biology* 11: 54.
- Dent, J. N. 1962. Limb regeneration in larvae and metamorphosing individuals of the South African clawed toad. *Journal of Morphology* 110: 61–77.
- Filoni, S. 2009. Retina and lens regeneration in anuran amphibians. *Seminars in Cell & Developmental Biology* 20(5): 528–34.
- Filoni, S., Bosco, L., and Cioni, C. 1982. The role of neural retina in lens regeneration from cornea in larval *Xenopus laevis*. *Acta Embryologiae et Morphologiae Experimentalis* 3(1): 15–28.
- Freeman, G. 1963. Lens regeneration from the cornea in *Xenopus laevis*. *The Journal of Experimental Zoology* 154: 39–65.
- Fukui, L. and Henry, J. J. 2011. FGF signaling is required for lens regeneration in *Xenopus laevis*. *The Biological Bulletin* 221(1): 137–45.
- Gargioli, C., Giambra, V., Santoni, S., et al. 2008. The lens-regenerating competence in the outer cornea and epidermis of larval *Xenopus laevis* is related to pax6 expression. *Journal of Anatomy* 212(5): 612–20.
- Gargioli, C. and Slack, J. M. 2004. Cell lineage tracing during *Xenopus* tail regeneration. *Development* 131(11): 2669–79.
- Gibbs, K. M., Chittur, S. V., and Szaro, B. G. 2011. Metamorphosis and the regenerative capacity of spinal cord axons in *Xenopus laevis*. *The European Journal of Neuroscience* 33(1): 9–25.
- Glinka, A., Wu, W., Delius, H., Monaghan, A. P., Blumenstock, C., and Niehrs, C. 1998. Dickkopf-1 is a member of a new family of secreted proteins and functions in head induction. *Nature* 391(6665): 357–62.
- Hartley, K. O., Nutt, S. L., and Amaya, E. 2002. Targeted gene expression in transgenic *Xenopus* using the binary Gal4-UAS system. *Proceedings of the National Academy of Sciences of the United States of America* 99(3): 1377–82.

- Henry, J. J. and Tsonis, P. A. 2010. Molecular and cellular aspects of amphibian lens regeneration. *Progress in Retinal and Eye Research* 29(6): 543–55.
- Henry, J. J., Thomas, A. G., Hamilton, P. W., Moore, L., and Perry, K. J. 2013. Cell signaling pathways in vertebrate lens regeneration. *Current Topics in Microbiology and Immunology* (367): 75–98.
- Ho, D. M. and Whitman, M. 2008. TGF-beta signaling is required for multiple processes during *Xenopus* tail regeneration. *Developmental Biology* 315(1): 203–16.
- Isaacs, H. V., Pownall, M. E., and Slack, J. M. 1994. eFGF regulates Xbra expression during *Xenopus* gastrulation. *The EMBO Journal* 13(19): 4469–81.
- Kawakami, Y., Esteban, C. R., Raya, M., et al. 2006. Wnt/beta-catenin signaling regulates vertebrate limb regeneration. *Genes & Development* 20(23): 3232–7.
- Kragl, M., Knapp, D., Nacu, E., et al. 2009. Cells keep a memory of their tissue origin during axolotl limb regeneration. *Nature* 460(7251): 60–5.
- Kroll, K. L. and Amaya, E. 1996. Transgenic *Xenopus* embryos from sperm nuclear transplantations reveal FGF signaling requirements during gastrulation. *Development* 122(10): 3173–83.
- Kumar, A., Velloso, C. P., Imokawa, Y., and Brookes, J. P. 2004. The regenerative plasticity of isolated urodele myofibers and its dependence on MSX1. *PLoS Biology* 2(8): E218.
- Lin, G. and Slack, J. M. 2008. Requirement for Wnt and FGF signaling in *Xenopus* tadpole tail regeneration. *Developmental Biology* 316(2): 323–35.
- Lin, G., Chen, Y., and Slack, J. M. 2007. Regeneration of neural crest derivatives in the *Xenopus* tadpole tail. *BMC Developmental Biology* 7: 56.
- Lin, G., Chen, Y., and Slack, J. M. 2012. Transgenic analysis of signaling pathways required for *Xenopus* tadpole spinal cord and muscle regeneration. *Anatomical Record* 295(10): 1532–40.
- Lin, G., Chen, Y., and Slack, J. M. 2013. Imparting regenerative capacity to limbs by progenitor cell transplantation. *Developmental Cell* 24(1): 41–51.
- Love, N. R., Chen, Y., Bonev, B., et al. 2011. Genome-wide analysis of gene expression during *Xenopus tropicalis* tadpole tail regeneration. *BMC Developmental Biology* 11: 70.
- Lu, P., Wang, Y., Graham, L., et al. 2012. Long-distance growth and connectivity of neural stem cells after severe spinal cord injury. *Cell* 150(6): 1264–73.
- Maden, M. 2008. Axolotl/newt. *Methods in Molecular Biology* 461: 467–80.
- Muller, T. L., Ngo-Muller, V., Reginelli, A., Taylor, G., Anderson, R., and Muneoka, K. 1999. Regeneration in higher vertebrates: limb buds and digit tips. *Seminars in Cell and Developmental Biology*. 10(4): 405–13.
- Muneoka, K., Hollerdinsmore, G., and Bryant, S. V. 1986. Intrinsic control of regenerative loss in *Xenopus laevis* limbs. *Journal of Experimental Zoology*. 240(1): 47–54.
- Neufeld, D. A. and Day, F. A. 1996. Perspective: a suggested role for basement membrane structures during newt limb regeneration. *The Anatomical Record* 246(2): 155–61.
- Nieuwkoop, P. D. and Faber, J. 1994. Normal Table of *Xenopus laevis* (Daudin), New York and London: Garland Publishing, Inc.
- Nye, H. L. D. and Cameron, J. A. 2005. Strategies to reduce variation in *Xenopus* regeneration studies. *Developmental Dynamics* 234(1): 151–8.
- Odelberg, S. J., Kollhoff, A., and Keating, M. T. 2000. Dedifferentiation of mammalian myotubes induced by msx1. *Cell* 103(7): 1099–109.
- Poss, K. D. 2010. Advances in understanding tissue regenerative capacity and mechanisms in animals. *Nature Review Genetics* 11(10): 710–22.
- Reeve, J. G. and Wild, A. E. 1978. Lens regeneration from cornea of larval *Xenopus laevis* in the presence of the lens. *Journal of Embryology and Experimental Morphology* 48: 205–14.
- Reid, B., Song, B., and Zhao, M. 2009. Electric currents in *Xenopus* tadpole tail regeneration. *Developmental Biology* 335(1): 198–207.
- Rinkevich, Y., Lindau, P., Ueno, H., Longaker, M. T., and Weissman, I. L. 2011. Germ-layer and lineage-restricted stem/progenitors regenerate the mouse digit tip. *Nature* 476(7361): 409–13.
- Rodrigues, A. M., Christen, B., Marti, M., and Izpisua Belmonte, J. C. 2012. Skeletal muscle regeneration in *Xenopus* tadpoles and zebrafish larvae. *BMC Developmental Biology* 12: 9.
- Ryffel, G. U., Werdien, D., Turan, G., Gerhards, A., Goosses, S., and Senkel, S. 2003. Tagging muscle cell lineages in development and tail regeneration using Cre recombinase in transgenic *Xenopus*. *Nucleic Acids Research* 31: 1044–51.
- Sessions, S. K. and Bryant, S. V. 1988. Evidence that regenerative ability is an intrinsic property of limb cells in *Xenopus*. *Journal of Experimental Zoology*. 247: 39–44.
- Sive, H. L., Grainger, R. M., and Harland, R. M. 2000. Early Development of *Xenopus laevis*: A Laboratory Manual, Cold Spring Harbor, NY: Cold Spring Harbor Laboratory Press.
- Slack, J. M., Beck, C. W., Gargioli, C., and Christen, B. 2004. Cellular and molecular mechanisms of regeneration in *Xenopus*. *Philosophical Transactions of the Royal Society of London Series B: Biological Sciences* 359(1445): 745–51.
- Slack, J. M., Lin, G., and Chen, Y. 2008. The *Xenopus* tadpole: a new model for regeneration research. *Cellular and Molecular Life Sciences* 65(1): 54–63.

- Stocum, D. L. 2004. Tissue restoration through regenerative biology and medicine. *Advances in Anatomy, Embryology, and Cell Biology* 176: III–VIII, 1–101.
- Tanaka, E. M. and Reddien, P. W. 2011. The cellular basis for animal regeneration. *Developmental Cell* 21(1): 172–85.
- Tassava, R. A. 2004. Forelimb spike regeneration in *Xenopus laevis*: testing for adaptiveness. *Journal of Experimental Zoology* 301(2): 150–9.
- Taylor, A. J. and Beck, C. W. 2012. Histone deacetylases are required for amphibian tail and limb regeneration but not development. *Mechanisms of Development* 129(9–12): 208–18.
- Tazaki, A., Kitayama, A., Terasaka, C., Watanabe, K., Ueno, N., and Mochii, M. 2005. Macroarray-based analysis of tail regeneration in *Xenopus laevis* larvae. *Developmental Dynamics* 233(4): 1394–1404.
- Tosh, D. and Slack, J. M. 2002. How cells change their phenotype. *Nature Reviews. Molecular Cell Biology* 3(3): 187–94.
- Tseng, A. S. and Levin, M. 2008. Tail regeneration in *Xenopus laevis* as a model for understanding tissue repair. *Journal of Dental Research* 87(9): 806–16.
- Tseng, A. S. and Levin, M. 2012. Transducing bioelectric signals into epigenetic pathways during tadpole tail regeneration. *Anatomical Record* 295(10): 1541–51.
- Tseng, A. S., Adams, D. S., Qiu, D., Koustubhan, P., and Levin, M. 2007. Apoptosis is required during early stages of tail regeneration in *Xenopus laevis*. *Developmental Biology* 301(1): 62–9.
- Tseng, A. S., Beane, W. S., Lemire, J. M., Masi, A., and Levin, M. 2010. Induction of vertebrate regeneration by a transient sodium current. *The Journal of Neuroscience* 30(39): 13192–200.
- Tseng, A. S., Carneiro, K., Lemire, J. M., and Levin, M. 2011. HDAC activity is required during *Xenopus* tail regeneration. *PLoS One* 6(10): e26382.
- Tsonis, P. A., Trombley, M. T., Rowland, T., Chandraratna, R. A., and del Rio-Tsonis, K. 2000. Role of retinoic acid in lens regeneration. *Developmental Dynamics* 219(4): 588–93.
- Tsonis, P. A., Vergara, M. N., Spence, J. R., et al. 2004. A novel role of the hedgehog pathway in lens regeneration. *Developmental Biology* 267(2): 450–61.
- Tu, S. and Johnson, S. L. 2011. Fate restriction in the growing and regenerating zebrafish fin. *Developmental Cell* 20(5): 725–32.
- Wolfe, A. D., Nye, H. L. D., and Cameron, J. A. 2000. Extent of ossification at the amputation plane is correlated with the decline of blastema formation and regeneration in *Xenopus laevis* hindlimbs. *Developmental Dynamics* 218(4): 681–697.
- Yakushiji, N., Suzuki, M., Satoh, A., et al. 2007. Correlation between Shh expression and DNA methylation status of the limb-specific Shh enhancer region during limb regeneration in amphibians. *Developmental Biology* 312(1): 171–82.
- Yokoyama, H., Tamura, S. Y., Endo, J. C., Izpisua-Belmonte, J. C., Tamura, K., and Ide, H. 2000. Mesenchyme with FGF10 expression is responsible for regenerative capacity in *Xenopus* limb buds. *Developmental Biology* 219: 18–29.
- Yokoyama, H., Ide, H., and Tamura, K. 2001. FGF-10 stimulates limb regeneration ability in *Xenopus laevis*. *Developmental Biology* 233(1): 72–9.
- Yokoyama, H., Maruoka, T., Ochi, H., et al. 2011. Different requirement for Wnt/beta-catenin signaling in limb regeneration of larval and adult *Xenopus*. *PLoS One* 6(7): e21721.

20

Genomics and Genome Engineering in *Xenopus*

Léna Vouillot¹, Aurore Thélie¹, Thibault Scalvenzi¹,
& Nicolas Pollet^{1,2}

¹CNRS, Institute of Systems and Synthetic Biology, Université d'Evry-Val-d'Essonne, Evry, France

²Genopole, Centre d'Exploration et de Recherche Fonctionnelle Amphibiens Poissons, Evry, France

Abstract: We are now at the golden age of *Xenopus* genetics and genomics. The enormous progresses in *Xenopus* genomics, transgenesis, and targeted genome modifications have completely changed the ways of thinking experimental approaches using this model. We report here a comprehensive overview of the current knowledge and recent developments on genomics and genome engineering in *Xenopus*. In the first part, we focus on genomics: *Xenopus laevis* and *Xenopus tropicalis* genome sequencing projects, bioinformatics and genomic resources, and *Xenopus* repetitive elements (the “mobilome”), functional genomics, and genetics. In the second part, we deal with *Xenopus* genome engineering: mutagenesis project, transgenesis, and genome engineering using targeted nucleases. While much has been learned, there is still a need to push forward genomics and genetics studies in *Xenopus*.

Introduction

Xenopus are much more than simply the product of a genome, but they are nonetheless characterized to a large extent by their genome. Therefore, the sequencing and analysis of *Xenopus* genomes fundamentally advances our knowledge of amphibian biology. At the same time, our ability to modify this genome will enable us to learn more concerning vertebrate developmental genetics.

Amphibians such as *Xenopus* have a long history of being a powerful system for the analysis of vertebrate gene functions during

development (Harland and Grainger 2011). Their physiology shares a remarkable degree of similarity with their mammalian counterpart, making it highly likely that data gained from genomic approaches in *Xenopus* will accurately predict human gene functions and biology. The genetic and physiological proximity between humans and *Xenopus* is particularly well established and recognized for endocrine regulation for which *Xenopus* is a reference model.

In addition, there is a growing interest in manipulating the *Xenopus* genome because the use of this amphibian model in place of

the mammalian animal models fulfills the “Replacement Reduction and Refinement” principle that applies to all current research funding agencies. Studies on small model organisms derived from amphibians, such as prefeeding tadpoles, correspond with efforts towards reducing animal experimentation. Such small model organisms exploit the physiological pertinence of whole-organism approaches with the advantages of accelerated testing in microvolumes such as via use of 96-well plates or flow through readings (Fini et al. 2007, 2009; Blackiston et al. 2010). Tadpoles from mutant or transgenic lines are developed to express reporter genes in a tissue-specific manner to image organogenesis under normal and pathologic conditions and employed as low-cost animal models for whole-organism drug discovery screens (Wheeler and Liu 2012). Moreover, transgenic tadpoles are powerful tools to explore the interaction of specific genes with the environment and/or toxins and to understand the relationship between biochemical and metabolic pathways and toxic effects.

Xenopus genomics

Xenopus laevis and *Xenopus tropicalis* genome sequencing projects

Many advantages of the *Xenopus* model rely on the knowledge of its genome and on the comprehensiveness and quality of its genomic sequence. The *X. tropicalis* genome sequence has been published in 2005 and stands as the reference amphibian genome (Hellsten et al. 2010). In addition, several groups are currently sequencing the *X. laevis* genome. As it stands now, biologists interested in mining the *Xenopus* genome have access to two and even three genomes if one considers the allotetraploid nature of the *X. laevis* genome.

The genome of *X. tropicalis* is 1.7 Gbp large and spread over 10 chromosomes; it is the only diploid species of the *Xenopodinae* (Pollet and Mazabraud 2006). The data generated in the framework of the *X. tropicalis* genome sequencing project represent the genome of a single seventh-generation inbred Nigerian frog (Hellsten et al. 2010). The published genome

assembly was the version JGI 4.1 (August 2005), also known as xenTro2. It has been slightly updated to a version JGI 4.2 (November 2009, xenTro3, GenBank Assembly ID GCA_000004195.1). At the time of writing, this version JGI 4.2 is available through the Ensembl portal (*Xenopus* release 70), the UCSC browser, and the NCBI Assembly database. A more recent update led to version 7 (GenBank Assembly ID GCA_000004195.2), available through Xenbase. To improve the long-range organization of the assembly, a happy mapping project was recently initiated (Jiang et al. 2011); a new genetic map based on Illumina sampling was constructed (Mitros, Lyon et al., unpublished), and dense bacterial artificial chromosome (BAC) end sequencing was performed (Pollet et al., unpublished). To further advance genome sequence completeness and contiguity, additional data using exome sequencing and shotgun sequencing (via Illumina technology) are being integrated into the existing assembly (Viso et al. 2012) (Mitros, Lyon et al., unpublished). Moreover, a revised and an improved chromosome-scale assembly is in progress and should be available in the near future (Jenkins et al., unpublished).

Even as the genome sequence quality can and should be improved, we can already discuss some parameters of the *X. tropicalis* genome computed from the published assembly (Li 2011). These parameters are presented in Table 20.1. The C value measure for *X. tropicalis* is 1.74 pg (Thiébaud and Fischberg 1977), which corresponds to a nuclear DNA content of 1.70 Gbp. With a total assembled sequence length of 1.51 Gbp, we can deduce that around 190 million base pairs (Mbp) of sequence may fall in heterochromatic and highly repetitive regions. There remains an additional predicted 153 Mbp of gaps in the assembly that may correspond to interspersed repeated sequences. In conclusion, we are still missing some pieces of the frog genome puzzle.

The number of *X. tropicalis* gene loci can be estimated from the annotations. There are 18,429 protein-coding genes annotated in assembly 4.2 and 28,165 protein-coding genes in assembly 7.1, but cloned cDNAs are available for only half of them. Moreover, the gene models can be inaccurate in terms of coding sequence prediction because they do not take

Table 20.1 Parameters of the *X. tropicalis* genome.

Genome assembly	Version 4.2 (GCA_000004195.1, November 2009)
Gene build	Ensembl, February 2011
Database version	70.42
Golden path length	1,511,717,716
Base pairs	1,358,329,334
%GC	40,07
Gene transcripts	24,160
Coding genes	18,429
Orthologous to human genes	14,224 (77%)
With gene ontology accession	14,941 (81%)
Noncoding genes	1,282
Pseudogenes	173
Genescan gene predictions	43,859
Gene exons	244,166
Largest gene	Protein tyrosine phosphatase receptor D (ptprd) 898,498 bp
5' UTR*	70 nt ($N=8949$)
3' UTR*	451 nt ($N=7875$)
Exon size	119 bp ($N=244,166$)
Exon number	9
Genomic extant	11,118
Coding sequence	1,227 (408 aa)
Transcript size [†]	1,592
18429 protein-coding genes	

All computed values are medians.

*Considered only if >10 nt

[†]From the data of Tan et al. (2012)

into account the cDNA sequences available in databases. Indeed, less than half of the protein sequences predicted from gene models correspond to complete ORFs (Gilchrist 2012). A better proteome dataset will be defined based on the recent RNAseq data (see section “*Xenopus* functional genomics”). However, it is unclear how RNAseq data will be represented in the sequence databases. A typical *Xenopus* gene is much like a human gene in terms of exon number and coding sequence size. The genomic span of a typical *Xenopus* gene appears a bit small compared to other vertebrate genomes, and this may be due to the current status of the assembly. The estimated sizes of 5' and 3' untranslated regions (UTR) are significantly smaller than what is known in other vertebrates. The simplest explanation is that this difference arose due to

a problem of annotation. The annotation of 5' and 3' UTR needs improvement because it is required for promoter identification and the prediction of miRNA target sites.

The genome of *X. laevis* is 3.1 Gbp and spread over 18 chromosomes (Thiébaud and Fischberg 1977). The allotetraploid genome of *X. laevis* has and is being sequenced by the Wallingford and Marcotte labs along with Scott Hunicke-Smith at the University of Texas at Austin (USA), in conjunction with the Harland and Rokhsar groups at UC Berkeley (USA), and with Taira and collaborators at the University of Tokyo (Japan). A draft assembly is already available via *Xenbase* thanks to the investigators of this project. A whole-genome shotgun sequencing approach using massively parallel sequencing technologies is occurring on DNA extracted from the inbred J strain. The sequences are derived from standard Illumina fragments of 225bp, 450bp, and 750bp and provide 75× coverage. In addition, mate-pair sequencing on libraries of 1.5 kilobase pair (kbp), 4 kbp, and 10 kbp is used to increase the genome coverage across repeats. Finally, fosmid and BAC end sequences are used to build scaffolds. The current assembly (*X. laevis* v6.1) spans 3.64 Gbp in scaffolds larger than 1000 base pairs. The typical sequence contigs in this assembly are about 18.5 kbp long, while they are 70 kbp long in the *X. tropicalis* assembly. Overall, around 98% of the single-copy sequences are represented, and 87% of protein-coding genes are contained in a single scaffold. Therefore, this assembly is already extremely useful. There are 34,000 protein-coding genes predicted, and 62% of the *X. tropicalis* genes are present in the form of two homeologs in *X. laevis*. The conservation of synteny between these two genomes is strong and will be useful to study genome rearrangements. The future developments on this assembly are to improve the long-range coverage of the current assembly using genetic mapping and BAC end sequencing and to improve the annotation using RNAseq data (see section “*Xenopus* functional genomics”). In the future, shallow sequencing from various species of *Xenopus* should enable insightful comparative studies.

The availability of the *X. tropicalis* genome sequence will have an impact upon many

studies of tetrapod gene and genome evolution. This is nicely illustrated by the conservation of synteny over large chromosomal regions between man and frog genomes (Figure 20.1). For example, Macha and colleagues analyzed the evolutionary origin of the mammalian X chromosome and clarified the natural history of X chromosome evolution in tetrapods (Mácha et al. 2012). The integration of cytogenetics landmarks into the *X. tropicalis* draft genome sequence proved to be a decisive piece of data to analyze tetrapod chromosome evolution (Khokha et al. 2009;

Krylov et al. 2010; Voss et al. 2011; Wells et al. 2011). In another example, Bossuyt and collaborators discovered the convergent evolution of a gene encoding the caerulein amphibian skin toxin in *Xenopus* and *Litoria* frogs (Roelants et al. 2010). In the future, many other studies will benefit from the availability of *X. tropicalis* and *X. laevis* genome sequences. Other *Xenopus* and amphibian genomes will be available and should enable insightful studies of the complex and large genomes found in amphibians and the evolution of tetrapods and vertebrates.

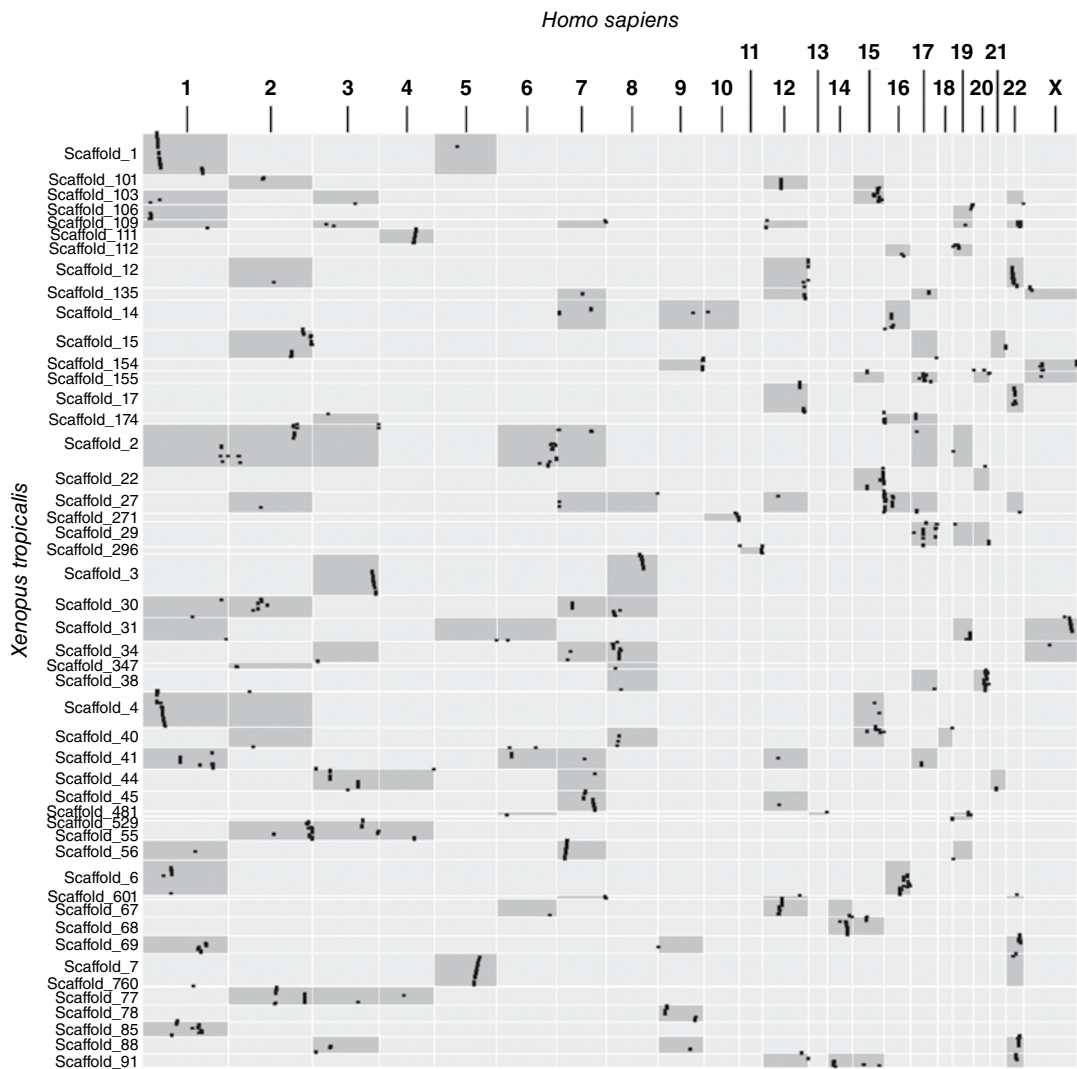


Figure 20.1 Oxford grid view of the synteny between *Homo sapiens* and *X. tropicalis* genomes. Each column represents one human chromosome, and each line represents one frog scaffold. Each orthologous gene is plotted in the relevant cell according to its chromosomal position. Data from homology tables of *compara_mart*, version 49 of the ensembl database identified 1825 one-to-one mapped orthologs (<http://oxgrid.angis.org.au>).

Bioinformatics and resources

A wide variety of online resources provide access to the ever expanding wealth of data available for the study of *Xenopus* biology (Gilchrist and Pollet 2012). The first principle to follow when we use these resources is to use the official *Xenopus* gene nomenclature described in Xenbase (Table 20.2). This is even more important for data providers because it increases the added value of bioinformatics resources. These resources support many forms of biological experimentation and are listed in Table 20.3. The central information provider is Xenbase: it is a tremendous tool for day-to-day research, and it is an effective vector for the dissemination of knowledge

Table 20.2 Nomenclature conventions for *Xenopus* genes and proteins.

Species	Gene	Protein
<i>Xenopus</i>	<i>lin28a</i>	Lin28a
<i>X. tropicalis</i> specific paralogs	<i>hes5.1</i> and <i>hes5.2</i>	Hes5.1 and Hes5.2
<i>X. laevis</i> homeologs	<i>hes9.1a</i> and <i>hes9.1b</i>	Hes9.1a and Hes9.1b
Zebrafish	<i>lin28a</i>	Lin28a
Human	<i>LIN28A</i>	LIN28A
Mouse	<i>Lin28a</i>	LIN28A
Generic	<i>Lin28a</i>	Lin28a

and the promotion of *Xenopus* as a model organism (Bowes et al. 2008, 2010; James-Zorn et al. 2013).

The *Xenopus* mobilome

Repetitive elements including transposable elements (TEs) span more than 30% of the *Xenopus* genome sequence (Hellsten et al. 2010). In this amphibian genome and unlike the mammalian genomes, DNA transposons predominate over retrotransposons (Figure 20.2). All these transposons are present in intergenic regions, in introns, and even in untranslated regions, such as the last exons corresponding to the 3' UTR of mRNAs. The transposon world in the *Xenopus* genome is a complex mixture of numerous different families of DNA transposons and retrotransposons. These transposons have an effect upon transcription and mRNA stability, and they can fulfill specific roles when they are "domesticated" (Sinzelle et al. 2009). While our knowledge of transposons in *Xenopus* is fragmentary, it is progressing slowly.

Although DNA transposons are the most abundant repetitive element in *Xenopus*, some retrotransposons have been characterized. The endogenous retrovirus XTERV1 was identified serendipitously from a survey of cDNA sequences (Sinzelle et al. 2011). XTERV1 is present in many copies in the *Xenopus* genome

Table 20.3 Web resources for *Xenopus* genome data mining.

Web resources	URLs
NCBI <i>Xenopus</i> Genome Resources	www.ncbi.nlm.nih.gov/genome/guide/frog
Xenbase	www.xenbase.org
<i>Xenopus</i> Nomenclature Guidelines	www.xenbase.org/gene/static/geneNomenclature.jsp
<i>Xenopus</i> Gene Collection (XGC)	xgc.nci.nih.gov
<i>X. laevis</i> genome project	polaris.icmb.utexas.edu/index.php/Xenopus_Genome_Project
<i>Xenopus</i> mutation project	www.sanger.ac.uk/Projects/D_rerio/xmp/
Xenmark	genomics.nimr.mrc.ac.uk/apps/XenMARK/
Gurdon Institute <i>X. tropicalis</i> Full-Length Database	genomics.nimr.mrc.ac.uk/online/xt-fl-db.html
<i>X. laevis</i> research resource for immunobiology	www.urmc.rochester.edu/mbi/resources/Xenopus/
Transcriptome of <i>Xenopus tropicalis</i>	jason.chuang.ca/research/xenopus/
Metazome	www.metazome.net/
<i>Xenopus</i> Ensembl	www.ensembl.org/Xenopus_tropicalis/Info/Index
<i>Xenopus</i> genomes at NIMR	genomes.nimr.mrc.ac.uk/cgi-bin/hgGateway
<i>X. tropicalis</i> superfamily protein database	supfam.cs.bris.ac.uk/SUPERFAMILY/cgi-bin/gen_list.cgi?genome=Xt

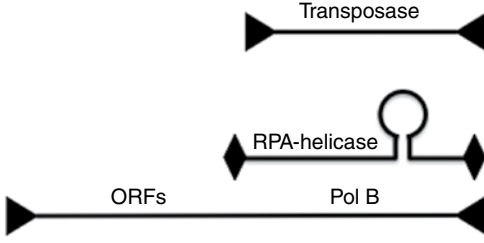
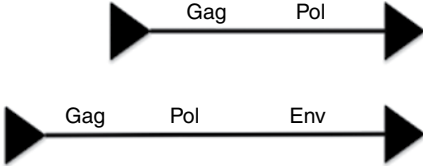
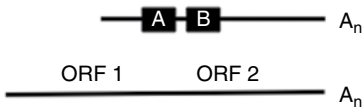
	Family	% Genome fraction
	<i>hAT</i>	6.10
	<i>Kolobok</i>	5.80
	<i>Harbinger</i>	4.70
	<i>Tc1/Mariner</i>	4.70
	<i>PiggyBac</i>	1.30
	<i>Helitrons</i>	0.60
	<i>Polintons</i>	0.01
	Unclassified	1.79
	Total	25.00
		BEL
DIRS		1.00
Copia		0.30
ERV III		0.10
ERV I		0.02
Unclassified		0.88
Total		3.60
	SINES	3.80
	Penelope	1.20
	L1 (L1, Tx1 clades)	0.40
	Total	5.40
Others		0.50

Figure 20.2 Transposon composition of the *X. tropicalis* genome. The percentage of base pairs occupied by the different transposons in the *X. tropicalis* genome is derived from Hellsten et al. (2010).

with a single full-length element and less than 10 full-length defective elements. This endogenous retrovirus of the *Epsilonretrovirus* family has infected its host around 41 million years ago and is now domesticated. XTERV1 is transcribed and its expression is regulated by various stress signals. However, we do not know if it can produce viral particles and if it affects its host physiology.

Some DNA transposons like the piggyBac families Uribo 1 and Uribo2 seem to be active in the *Xenopus* genome. There is evidence of recent excision events for these two families. For other piggyBac transposon families like Kobuta, there is evidence of domestication by the host genome (Hikosaka et al. 2007). The activity of these piggyBAC transposons can be linked to a particular class of miniature inverted-repeat transposable elements (MITEs). MITEs are nonautonomous DNA transposons known to be very numerous in

large genomes. In the *X. tropicalis* genome, there is a family of MITEs named T2 present in 21,000 copies. These T2 MITEs belong to the family of piggyBAC transposons and some copies seem to be recently active while others seem to have lost their capacity to transpose a long time ago (Hikosaka and Kawahara 2010).

The observation of active and domesticated transposons reveals the existence of regulatory systems. Indeed, the levels of transcripts derived from some DNA transposons are regulated during *Xenopus* development. Some Tc1-mariner transposons are upregulated at gastrula stage in the Spemann organizer and later in neural tissues (TXr and TXz) (Sinzelle et al. 2005; Faunes et al. 2011). Importantly, both sense and antisense transcripts of these transposons were observed. In addition, small piwi RNAs derived from these sense and antisense transcripts are frequently observed. Therefore,

these transposons are under the regulation of the Piwi machinery during early development.

Most TEs are inherited by vertical transmission but horizontal transfer can also be the mode of transmission. A member of the hAT type of DNA transposon named Space Invader (SPIN) has been observed in five mammalian species and two tetrapods including *X. tropicalis* (Pace et al. 2008). The simplest explanation for the patchy distribution of this transposon between species is horizontal transfer. It may well be that other examples of horizontal transfer can be found by analyzing the genomes of *Xenopus*. The availability of both *X. tropicalis* and *X. laevis* genomes represents a gold mine for studying TEs' evolution and regulation.

Xenopus functional genomics

The genome sequence of *X. tropicalis* is a fundamental resource facilitating rapid progress in applying transcriptomic, genomic, proteomic, and systems biological approaches for which the *Xenopus* system is well suited. In addition, metabolomics has been recently applied to *Xenopus* embryos to uncover the activity of metabolic pathways (Vastag et al. 2011). We will present here the recent development of functional genomics resources and reagents and the study of transcriptomes and of the epigenome. We will not cover proteomics since we are not experts in this field.

Transcriptomics

The expressed sequence tags (EST) method of gene identification has led to the fast discovery of *Xenopus* genes thanks to several international initiatives. A strategic panel of cDNA libraries has been constructed and tag-sequenced for both *X. tropicalis* and *X. laevis*. As a consequence, we can estimate the expression profiles through development and across adult tissues for most mRNAs. In addition, we have full-length cDNA clones for 8380 *X. laevis* genes and 6620 *X. tropicalis* genes. A new ORFeome project has been undertaken to produce a nonredundant collection of *Xenopus* ORF and thereby extend the collection of physically manipulable genes (Gilchrist 2012).

As a follow-up of the EST projects, microarray experiments have been widely used by the *Xenopus* community. In microarray experiments, the expression levels of thousands of transcripts can be quantified in parallel. Even if the microarray technology has its shortcomings, its efficiency to compare the transcriptomes between two or more samples is well proven. Several studies have been realized in *Xenopus* to identify target genes of transcription factors or of signaling pathways, of RNA targets of RNA-binding proteins, or to identify genes associated with metamorphosis or regeneration (Graindorge et al. 2006, 2008; Love et al. 2011a). In more elaborate experiments, microarrays have been used to compare the repertoire of expression in the same tissues but in different species (Malone et al. 2007; Malone and Michalak 2008; Chan et al. 2009). Among the most notable results obtained using microarrays, we would like to mention the recent work of Yanai and colleagues (Yanai et al. 2011). In this study, the transcriptome of *X. laevis* and *X. tropicalis* embryos was compared, and the expression profiles of 11,000 orthologous genes were made available in Xenbase and in a specialized website (kirschner.med.harvard.edu/Xenopus_Transcriptomics.html). Importantly, the conservation in gene expression between the two species proved to be very strong, although differences in the timing of expression revealed genes associated with the heterochrony between these two frog species. Everyone can find *Xenopus* microarray studies and associated gene expression data in the GEO database at the NCBI and in the ArrayExpress database at the EBI. However, microarray data from different studies are difficult to integrate because they have been produced using different technological platforms (Agilent, Affymetrix, NimbleGen, custom design). Thus, it requires specific bioinformatics skills to fetch and comparatively analyze datasets which may provide informative data to a given research area.

The recent advent of massively parallel RNA sequencing has shed additional light on the RNA composition of eggs and embryos. RNA sequencing enables the quantification and the precise identification, at the nucleotide level, of the RNA molecules present in the cell.

Moreover, this method can be used downstream of various biochemical procedures such as cell fractionation and immunoprecipitation. *Xenopus* oocytes and embryos are perfectly suited to such approaches because of their accessibility. As a consequence, we already have several RNA sequencing datasets available. The pervasive transcription that occurs in oocytes has been the focus of two studies. The oocyte equipped with its lampbrush chromosomes is able to produce an amazing transcriptome in which germ and somatic cell type-specific transcripts are produced in equally large quantities (Simeoni et al. 2012). All these transcripts are correctly spliced and very stable in the cytoplasm. Moreover, intronic RNAs are unusually stable in the nucleus and persist up to the early embryonic stages of development (Gardner et al. 2012).

A glimpse of the complexity of the transcriptome in the embryo and the tadpole has been obtained by a deep RNAseq survey covering 23 developmental time points, from just after fertilization to tadpoles at feeding stages (Tan et al. 2012). Thus, all tadpole cell types have been included, and all developmental and differentiation processes have been represented. This is the first RNAseq transcriptome survey of this scope for a vertebrate model organism. The dataset is excellent thanks to the use of paired-end reads and large sample sizes, and it can be browsed on the web (<http://jason.chuang.ca/research/xenopus/>). This amazing resource is likely to increase considerably our knowledge of the embryonic proteome.

To underscore the enormous potential of discoveries that RNAseq holds in the future, we would like to cite the comparative study of alternative splicing between vertebrate species from frog to man (Barbosa-Morais et al. 2012). The nucleotide resolution and the genome scale of RNAseq enabled the comparison of alternative splicing in six adult tissues between nine species. This study showed that alternative splicing in frog is less frequent than in mammals, and paves the way for the evolutionary analysis of transcriptomes in tetrapods.

RNAseq is also the method of choice to study the small RNA component of transcriptomes. miRNAs, piRNAs, and other noncod-

ing small RNAs were found in the oocyte and in the egg with the first studies being focused upon small RNA sequencing in *Xenopus* (Armisen et al. 2009; Lau et al. 2009; Robine et al. 2009). The majority of small RNA reads found in oocytes and eggs are derived from TEs. By itself, this underscores the need to increase our knowledge of the *Xenopus* mobilome and the quality of the genome annotation. The size of the small RNAs identified in the oocyte and their coimmunoprecipitation with diverse Piwi proteins identifies them as piwi RNAs (Lau et al. 2009; Robine et al. 2009). Unfortunately, one-quarter of sequence reads cannot be mapped to the genome sequence. More recently, the small RNA component of the transcriptome was analyzed in gastrula-stage embryos (Faunes et al. 2012). Like in oocytes and eggs, piwi RNA predominate the small RNA transcriptome of gastrula. It may very well be that the small RNAs present in the eggs are stable enough to be present even after gastrulation. In addition, piwi RNA can be generated *de novo* from the 3' UTR of maternal mRNA after fertilization.

miRNAs were found to constitute the majority of small RNAs in somatic cells of the adult (Armisen et al. 2009). Moreover, miRNAs were identified in ectoderm explants at stage 11.5 (gastrula), at stage 26 (tail bud), and in retinal ganglion cells where they play active roles in cell differentiation (Marcet et al. 2011; Baudet et al. 2012).

A profusion of transcriptomics data have been generated from studies using the *Xenopus* model. However, all these data are not yet integrated with the genome sequence. We should expect a much better annotation of genes, transcripts, and proteins derived from the *Xenopus* genome in the near future.

Epigenomics

Many studies have been performed to analyze the dynamics of the chromatin during early development in *Xenopus*, in particular by the laboratory of Gert Jan Veenstra (Bogdanović et al. 2012). As a consequence, we have now a map of the methylation state of the *X. tropicalis* genome, a map of histone H3 methylation (H3K4me3, H3K9ac, H3K27me3), a map of RNA polymerase II and

TBP occupancy, and the possibility to integrate these maps with gene expression profiles. We know that there are between 72,000 and 104,000 methylated regions in both intergenic and intragenic regions in late blastula and gastrula stages of embryos. However, there is no relationship yet worked out between transcriptional activity and DNA methylation status in these early embryos in contrast to the situation in oocytes and tadpoles (Bogdanovic et al. 2011). The mapping of promoters and transcribed regions in gastrula using RNA polymerase II in conjunction with open and closed chromatin marks revealed genomic regions associated with localized gene expression (Akkers et al. 2010). The transcription start sites and TBP binding sites were also identified by massively parallel sequencing, and used to define promoters active in the oocyte and in gastrulae (Van Heeringen et al. 2011). Other studies are ongoing to reference chromatin state maps at multiple stages of early embryonic development and to identify interactions between promoters and enhancers. All of these efforts will be crucial to help interpret the genome sequence and to discover the roles of the functional elements identified by the ENCODE consortium (Dunham et al. 2012).

Xenopus genetics

Many *X. tropicalis* strains available commercially or through stock centers are inbred but they are not pure (Pearl et al. 2012). *X. laevis* strains in animal facilities are likewise not inbred with the notable exception of the J strain. Thus, the design of experiments involving genetic perturbations using morpholino oligonucleotides (MOs) or genome editing using chimeric nucleases must take into account the genetic polymorphism. There are at least two other reasons to take into consideration genetic polymorphisms: one concerning genetic mapping and the other concerning the discrimination of induced mutations versus natural polymorphisms. Genetic mapping is required for long-range genome assembly and for positional cloning. The discrimination of induced mutations is required in mutagenesis

screens, or in genome editing when one must characterize mutants.

However, only few surveys of genetic polymorphism have been performed on *X. tropicalis* and even less on *X. laevis*. For use in gene mapping, one effort was to identify microsatellite polymorphisms between Nigerian frogs and one of two strains originating from the Ivory Coast (Fierro et al. 2007; Xu et al. 2008; Wells et al. 2011). In the framework of a cDNA sequencing project, Fierro et al. identified eight single-nucleotide polymorphisms derived from mitochondrial genes, three of which (snp1A, snp2A, snp6G) are specific to the Adiopodoume strain (Fierro et al. 2007). A set of 225 novel polymorphism markers made of di-, tri-, tetra-, and pentanucleotide sequence repeats were found in cDNA clusters. To generate a genetic map, Xu and collaborators studied the distribution of microsatellites in the genome of *X. tropicalis* (Xu et al. 2008; Wells et al. 2011). They analyzed sequences representing about one-fourth of the genome and identified di-, tri-, and tetranucleotide repeats. They found on average 161 dinucleotide, 27 trinucleotide, and 17 tetranucleotide repeats per Mbp. Two-thirds of the microsatellites are motifs made of AT, AAT, and AGAT. Like in other vertebrate genomes, trinucleotide repeats are more prevalent in coding regions. However, the predominance of the AT repeats in the *X. tropicalis* genome differs from observations made in other vertebrates where the AC repeats are most common. The polymorphism rate of 5128 nonredundant microsatellites was determined by genotyping Ivory Coast and Nigerian strain individuals and used to build a genetic map (Wells et al. 2011). This genetic map was built from genotyping data obtained after scoring 2979 microsatellite markers on 380 informative meioses. The F2 mapping panel was obtained from parents of Ivory Coast (F5) and Nigerian (F7) strains. Linkage analysis enabled the identification of 10 major and 4 minor linkage groups with an effective size of 1658 cM. FISH to metaphasic chromosomes was used to map the linkage groups to the 10 chromosomes. This enabled the integration of the genetic map with cytogenetics and the genome sequence. A notable observation was that the short arm of chromosome 2

was not covered by this genetic map. The correspondence between the sequence and the genetic distances varied over three orders of magnitude from about 4 kb/cM to over 3000 kb/cM. The average correspondence is 581 kb/cM, comparable to the value of 625 kb/cM for zebrafish. This map proved its usefulness to improve the long-range coverage of the *X. tropicalis* genome sequence and to map genes identified by mutations.

Another effort was to study genetic polymorphism in laboratory strains of *X. tropicalis* (Showell et al. 2011). Showell and colleagues noticed an unexpectedly high frequency of polymorphism in their laboratory-bred frogs in the framework of a mutagenesis project. They sequenced 23 amplicons derived from 17 gene loci, including coding and noncoding regions. Showell and colleagues obtained these genotypes from tadpoles derived from two matings between Nigerian F5 frogs maintained in their facility. They observed a frequency of polymorphism of about 0.001, meaning one polymorphism per kbp. This frequency was 0.00082 for coding regions and 0.00270 for noncoding regions. In parallel, they genotyped frogs of the Ivory Coast F8 ($N=29$) and Nigerian F5 ($N=22$) strains obtained from Nasco. As expected, they observed a higher frequency of polymorphism of 0.0023, with values of 0.0012 for coding regions and 0.0034 for noncoding regions. These values are coherent with the theoretical expectations derived from the inbreeding coefficients. These polymorphisms will enable investigators to trace the origins of *X. tropicalis* frogs using phylogeny.

***Xenopus* genome engineering**

Mutants

Forward genetics in *Xenopus* was seriously considered with the launch of the *X. tropicalis* diploid model. Today, after a decade of efforts by talented groups of scientists, approximately a dozen mutants have been identified (Grammer et al. 2005; Noramly et al. 2005; Goda et al. 2006). It has been difficult to discover the causative mutations by positional cloning at a time when genetics and genomics

resources were just being developed. But with our current resources, some mutants have been completely characterized (Abu-Daya et al. 2009, 2011; Geach and Zimmerman 2010; Viso et al. 2012).

In a recent published study, del Viso and collaborators used exon capture high-throughput sequencing to discover mutations (Viso et al. 2012). In this approach, exons and nearby flanking sequence are deciphered after hybridization of a given DNA sample on a microarray containing a set of exons. This set of exons was designed based on gene annotation and cDNA sequences. In the case of *X. tropicalis*, many exons can be identified thanks to cDNA sequencing projects, but they are still missing in the last genome assembly available (v7.1). The sequences obtained from nonmutant animals can be used to improve the genome assembly, either locally or globally.

Transgenesis procedures: Updates and novel strategies

Xenopus transgenesis has been used for many years to study gene expression and regulation *in vivo*. In parallel with these applications, several research groups have driven the improvement of the transgenesis technology in *Xenopus* (Chesneau et al. 2008). New and useful transgenesis applications have been developed such as a wnt signaling pathway reporter lines (Deroo et al. 2004; Denayer et al. 2006), cell and tissue lineage reporters for imaging (Roose et al. 2009; Suzuki et al. 2010; Love et al. 2011b; Rankin et al. 2011; Kerney et al. 2012), or biochemical analysis (Watson et al. 2012). More recently, these applications have expanded to include the development of human disease models (Kaya et al. 2012). All transgenic techniques are applicable to both *X. laevis* and *X. tropicalis*. However, the restriction enzyme-mediated integration (REMI) method is difficult to use in *X. tropicalis* due to the large volume of material to be injected into its smaller unfertilized eggs. Strategies have been developed to address these species specificities through the use of transposon technology or meganuclease approaches (Pan et al. 2006; Sinzelle et al. 2006; Shibano et al. 2007).

What's new in transgenesis?

REMI and I-SceI combination

The REMI method has been used in *X. laevis* since the late 1990s to generate nonmosaic F0 founders. However, in many cases, the integration occurs in more than one site in the genome and the transgene is present as multimers (Kroll and Amaya 1996). The I-SceI meganuclease method has been developed to bypass the drawbacks of the REMI method and to integrate a single copy of the transgene. However, the mosaicism in F0 embryos is higher (Pan et al. 2006; Chesneau et al. 2008). L'hostis-Guidet and collaborators combined the existing REMI and I-SceI protocols to obtain an optimized transgenesis method and to reduce the problems associated with both techniques (L'hostis-Guidet et al. 2009). In their protocol, the sperm nuclei are incubated with an I-SceI digested plasmid and then injected in unfertilized eggs. This technique has given good results with respect to the specific expression of N β Tub-EGFP transgene in the central nervous system for 29% of injected embryos, a limited number of transgenes integrated, and a transmission rate to the next generations close to the Mendelian ratio. Moreover, L'hostis-Guidet and coworkers added a WPRE, a posttranscriptional regulatory element from the woodchuck hepatitis virus, to the 3' end of the transgene sequence. This WPRE is known to increase reporter gene expression when using a weak promoter. They demonstrated the efficiency of the WPRE to significantly increase the expression level of GFP under the control of the neuroD low-activity promoter. This work opens the way to the study of weak promoters by transgenesis in *Xenopus*.

Transposon-mediated transgenesis

We know that transposons can be used to produce transgenic frogs (Hamlet et al. 2006; Sinzelle et al. 2006). The Sleeping Beauty system can be used to produce transgenic *X. tropicalis* and *X. laevis* (Sinzelle et al. 2006; Yergeau et al. 2009, 2010a, 2011). However, the transgene is not integrated by a transposition event but by an illegitimate recombination activated by the Sleeping Beauty

transposase (Sinzelle et al. 2006; Yergeau et al. 2009). An interesting feature provided by transposons concerns the possibility of remobilization after genome integration. Yergeau and collaborators have worked on this subject with Tol2 and Sleeping Beauty (Yergeau et al. 2010b, 2011). They demonstrated that a single copy of Tol2 or Sleeping Beauty can move and generate novel integration events. They also show that remobilized transposons are transmitted through the germ line. These lines of transgenic animals are extremely interesting tools to identify novel regulatory elements in the genome.

Novel transgenesis tools

Novel strategies and tools are needed to produce transgenic animals easier and faster and with a higher level of genetic engineering. Love and collaborators have developed a molecular cloning toolbox for transgenesis named pTransgenesis (Love et al. 2011b). This toolbox enables the assembly of promoters, reporters (fluorescent proteins), transgenesis markers (crystallin RFP), insulators, and integration devices (I-SceI, Tol2). They generated a collection of donor plasmids using the Gateway system. These donor plasmids can be combined into more complex constructs based on site-specific recombination using the L/R clonase. This modular library of genetic devices offers the possibility to make transgenesis in different species such as frogs, fishes, and flies. pTransgenesis may become a wonderful resource in the future if it is used by a large community.

The site-specific integration of transgenes is a very much sought-after technique of genome engineering. It has been achieved in different organisms such as mouse, fish, or plant using the well-known CRE/LOX system (Feil 2007). Zuber et al. (2012) developed a method named FRT recombinase-mediated transgenesis for *Xenopus*. In the first step of this method, a transgene flanked by FRT sites is integrated in transgenic animals. In the second step, the FLP recombinase is used in F1 embryos to exchange the integrated FRT cassette with another cassette of interest. This allows a site-specific integration in the host transgene. This technique

seems to be a good alternative to avoid problems in expression levels as a consequence of position-dependent integration.

The reason to integrate a transgene in chromosomes for functional studies was driven because the injection of plasmid or linear DNA leads to transient and nonreproducible expression. Moreover, plasmids do not allow the insertion of large DNA fragments, with several vertebrate promoters being 10–100 kbp long. The advent of BAC cloning vectors and BAC genomic library resources changed this landscape (Ishii et al. 2004; Kelly et al. 2005). Since BACs can contain large DNA inserts of 50–300 kbp, they can contain more regulatory sequences required for driving tissue-specific expression. Recently, Fish and collaborators reported the use of BAC DNA injection to generate transgenic animals (Fish et al. 2012). They showed that fluorescent reporter expression in embryos recapitulate the endogenous expression of a gene after injection of a recombiner BAC into fertilized eggs. They also reported that the regulated expression of the reporter lasts longer than plasmid injection because BACs are replicated. This technique should allow large-scale promoter studies until metamorphosis stage, and without integration in the host genome.

The BAC injection technique to generate transgenic *Xenopus* is a very attractive method. It can be easily implemented due to the availability of BAC resources covering the entire *X. tropicalis* genome (Pollet et al., unpublished). BAC recombineering constitutes the bottleneck but it is a proven technology used in mice (Johansson et al. 2010). Nevertheless, there are technical drawbacks such as expression variegation and low efficiency of integration (Beil et al. 2012). The development of chimeric nuclease technologies with zinc finger nucleases (ZFNs) and transcription activator-like effector nucleases (TALENs) offers the possibility to improve transgenesis procedures (Le Provost et al. 2010). In *Xenopus*, these nuclease technologies have been used to induce mutations, but they have not yet been used for site-specific insertion. This could well be the next challenge for transgenesis in *Xenopus*.

Targeted genome editing

Gene knockout by homologous recombination in embryonic stem (ES) cells allowed the study of gene function by the characterization of altered mutants. While ES cell lines exist for the mouse and more recently for the rat, the study of gene function using homologous recombination was limited to other vertebrate species. For precise genome editing in species such as *Xenopus*, it is now possible to use chimeric proteins composed of a nuclease domain associated to an engineered DNA recognition domain. These chimeric proteins are named ZFNs and TALENs. More recently, the CRISPR/Cas system joined ZFNs and TALENs to form a collection of tools enabling high-precision genome editing.

Zinc finger nucleases

ZFNs are engineered proteins made of two modules. The first module is a zinc finger DNA-binding domain engineered to recognize a targeted DNA sequence. The zinc finger domain is composed of four to six zinc finger motifs. Each zinc finger motif is able to recognize three base pairs. This DNA-binding module allows the targeting of a specific 12–18 base pair sequence within a DNA molecule. The second module is a catalytic nuclease domain derived from the restriction endonuclease *FokI*. This domain is able to cleave the double strand of DNA after dimerization with a second nuclease domain. Accordingly, ZFNs work as pairs of proteins, and the two DNA-binding sites must be separated by 5–7 base pairs to allow the dimerization and DNA cleavage. ZFNs were initially injected as DNA and their effects were observed by integration events. Afterwards, ZFNs mRNAs were injected into embryos, and the efficiency of this method was excellent (Beumer et al. 2008). Thus, the most frequently used delivery method for ZFNs requires their mRNAs. Once delivered to the cells, ZFNs induce the cleavage of the targeted sequence. Two mechanisms can be triggered by this cleavage: a natural DNA-repair process using the nonhomologous end joining (NHEJ) pathway and homologous recombination. NHEJ is an imperfect repair process and it will lead to mutations such as

insertions or deletions. Homologous recombination might allow a targeted integration if a donor DNA is provided.

In the next paragraph, we will see that ZFNs are one of the best engineering tools for genome editing. But critics highlighted an interesting problem with ZFNs: the off-target effect. Indeed, the main problem was the cleavage of other sequences due to the non-specific dimerization of ZFNs. In the first experiments using ZFNs in *Xenopus*, this effect led to a significant fraction of embryos with developmental defects (Young et al. 2011). The solution was the design of new proteins containing mutant nuclease domains (Miller et al. 2007). This improved architecture allows a 40-fold reduction of nonspecific dimerization and thus significantly reduces and minimizes off-target effects.

Use of ZFNs

ZFNs have been successfully used in a wide variety of organisms: plants and animals including mammals. The efficiency of ZFNs in living cells was first tested in *Xenopus* oocytes (Bibikova et al. 2001). Both engineered DNA substrates and the nucleases were injected into *X. laevis* oocyte nuclei. DNA cleavage and homologous recombination were observed. These experiments proved that ZFNs were able to recognize and cleave their targets *in vivo*. The next step was the design of ZFN pairs able to recognize a gene sequence in an organism (Bibikova et al. 2002). Targeted chromosomal cleavage and mutagenesis were demonstrated in both somatic and germ cells. One year later, the same team demonstrated that targeted gene replacement by homologous recombination was also possible in *Drosophila* (Bibikova et al. 2003). The use of ZFNs in other animals such as zebrafish, sea urchin, rat, and mouse led to the same success (Doyon et al. 2008; Meng et al. 2008; Geurts et al. 2009; Carbery et al. 2010; Mashimo et al. 2010; Meyer et al. 2010; Ochiai et al. 2012). In 2011, the journal *Nature Methods* cited ZFNs as the "Method of the Year" for cell engineering. Indeed, these nucleases proved their efficiency in biological and biomedical applications. A famous example was the increase of HIV-1 resistance in CD4+ T cells by genome editing using ZFNs (Perez et al. 2008).

Xenopus is infamously known for the possibility to perform gain-of-function experiments, while reverse genetics experiments are limited to the use of antisense MOs that allow only transient knockdowns (Ymlahi-Ouazzani et al. 2010). Young et al. provided the first proof of principle that ZFNs induce mutations in the genome of the diploid *X. tropicalis* (Young et al. 2011). To develop conditions for gene disruption in *X. tropicalis*, they used transgenic animals with a single-copy eGFP transgene. The embryos were injected with ZFNs mRNA targeting the eGFP coding region and a subsequent loss of fluorescence was observed. At higher doses, the number of cells without fluorescence increased. Sequencing the tadpole's DNA showed multiple distinct indels ranging from 5 to 20bp. Therefore, they targeted the disruption of the endogenous gene *noggin* (Smith and Harland 1992). Six pairs of ZFNs targeting the *noggin* locus were designed and injected in two-cell embryos. The sequencing of the *noggin* locus from injected tadpole's DNA showed a frequency of mutant amplicons from 10% to 47% with a wide panel of insertions and deletions from 5 to 195bp. Selected mutant embryos were raised to sexual maturity and outcrossed to wild-type animals (Figure 20.3). The rate of germ-line mutagenesis was computed after sequencing the *noggin* locus from the offspring DNA. For three males, this rate varies between 12% and 24%. This study proved that ZFN-induced mutant alleles can be transmitted through the germ line. In conclusion, this first work allowed the development of a protocol for gene disruption with ZFNs in *Xenopus*.

In a second study, the tyrosinase gene of *X. tropicalis* was mutated to produce an albino line (Nakajima et al. 2012). Tyrosinase plays an essential role in the first step of melanin biosynthesis. Without this enzyme, pigment cells are devoid of melanin. Mutants for tyrosinase genes are precious to facilitate research techniques like fluorescent reporter imaging, *in situ* hybridization analysis, or transplantation experiments. While an albino mutant of *X. laevis* is naturally available, there is no such strain for *X. tropicalis*. Three pairs of ZFNs were designed to target the conserved region of the tyrosinase gene. The induction of

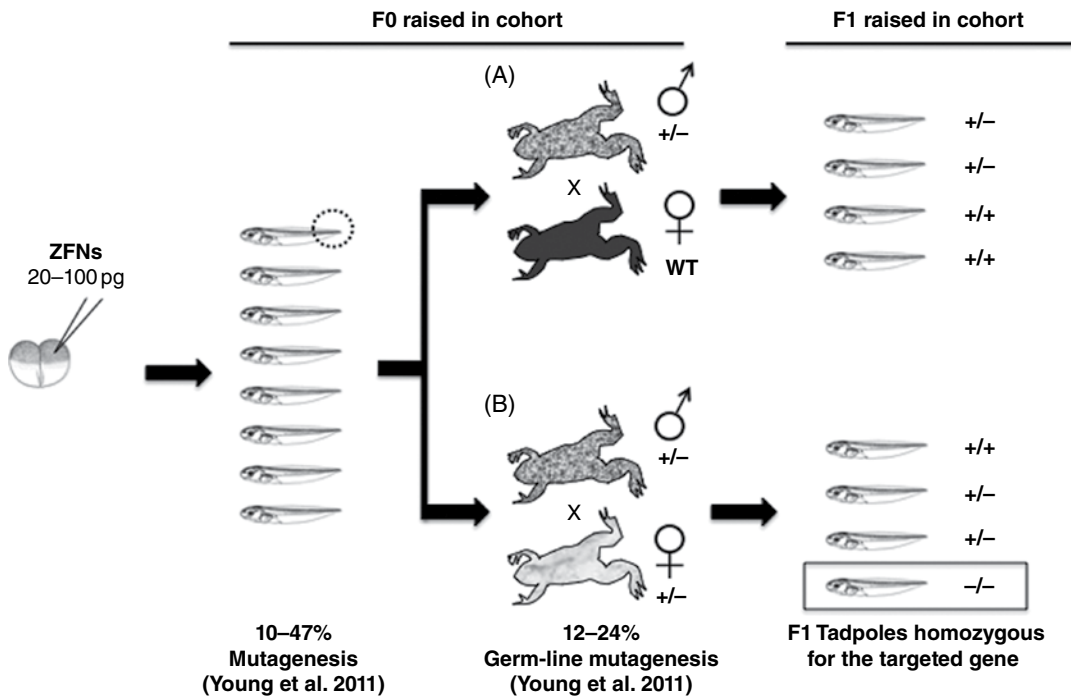


Figure 20.3 Crossing schemes to analyze ZFN- or TALEN-induced mutations. The cross A allows the identification of carriers of the mutations and to evaluate the germ-line mosaicism. The cross B allows the obtention of homozygous tadpoles.

biallelic mutations of the tyrosinase gene in pigment cells should be revealed by a lack of pigmentation. Indeed, areas of skin without pigmentation were observed in 41 froglets from 574 injected embryos. These froglets were raised to sexual maturity and crosses made between them. Only 10 albinos out of 3256 tadpoles were obtained from nine crosses. Nevertheless, the genotyping of six founder frogs showed different types of mutations on both chromosomes: a one- or two-base deletion/substitution and a 367-base deletion. The low transmission rate of mutations is possibly due to the low number of mutated germ cells in the F0 founder frogs. By crossing these founder frogs to wild-type animals, the percentage of mutated germ cells was evaluated as 10%. This percentage is comparable to the mutation rate calculated by Young et al. with *noggin* mutant frogs. The authors concluded that the observation of vitiligo patches on the skin of F0 frogs injected with ZFN mRNAs proved the efficiency of ZFNs. However, the high level of mosaicism in these F0 animals does not ensure a high level of

mutated germ cells. This new albino *X. tropicalis* line will extend the panel of available *Xenopus* mutants.

These first experiments in *Xenopus* using ZFNs proved their efficiency to disrupt endogenous genes. However, the cost of ZFNs needs to be considered, since these custom-engineered tools are expensive. The prices are fixed by Sangamo BioSciences that obtained the exclusive rights for genetic engineering and gene modification using ZFNs. The number of zinc finger protein-related patents granted in the United States increased from 1997 (Chandrasekharan et al. 2009). In 2001, Sangamo BioSciences already owned 42 patents, 8 of them on rules and libraries for constructing sets of zinc finger domains. However, researchers can find open-science alternatives. The Zinc Finger Consortium founded by J. Keith Joung and Dan Voytas was created to facilitate access to Sangamo's proprietary databases (Wright et al. 2006). Zinc Finger Tools created by Carlos Barbas and his team provides free tools to locate potential zinc finger protein target sites in

DNA sequences (Mandell and Barbas 2006). The Consortium offers via Addgene a library of plasmids encoding 140 zinc finger modules that recognize and specifically bind triplets of nucleotide. To bend ZFNs rules, Laura DeFrancesco praised the virtues of another technology for genome editing, the TAL nucleases (DeFrancesco 2011).

TAL nucleases

TAL effectors are less known than ZFNs because they were discovered in 2007. The access, cost, and availability of TAL effectors seem to be less problematic for the academic research community. TALENs are made of two modules. The first corresponds to an assembled DNA-binding domain and the second is a FokI domain exactly like in ZFNs (Boch and Bonas 2010). The DNA-binding domain comes from proteins secreted by plant pathogens in the bacterial genus *Xanthomonas*. The DNA-binding motifs of TAL effectors consist of a tandem repeat of 34 amino acids. Each repeat is able to bind a single base pair according to a code deciphered by Boch et al. in 2009. TALENs were tested in *C. elegans*, zebrafish, and rat (Sander et al. 2011; Tesson et al. 2011; Wood et al. 2011).

In *Xenopus*, Lei et al. tested the injection of TALEN assembled using the Golden Gate method (Cermak et al. 2011). Eight pairs of TALENs were created to recognize and disrupt eight *Xenopus* genes, including the *noggin* gene as addressed by Young et al. with ZFNs. Indeed, the goal of this work was to compare the efficiency of TALENs and ZFNs. The first observation was that *Xenopus* embryos were more tolerant to high doses of TALEN mRNA than ZFN mRNA. Sequencing the targeted genes from F0 DNA showed a large panel of indel mutations, and the analysis of F1 progeny indicated that these mutations were inherited (Lei et al. 2012).

In 2012, Ishibashi et al. produced albino *X. tropicalis* frogs as had Nakajima et al. but using TALENs. They showed that 68% of the injected embryos display an albino phenotype at tadpole stages, with biallelic mutations in pigmented cells. These mutations were transmitted to the offspring but with a significant mosaicism of the germ line since only 16 eggs

out of 423 were unpigmented. We can thus wonder how to compare nuclease-mediated mutagenesis and antisense MOs in the framework of loss-of-function experiments. Indeed, antisense MOs result in transient loss of functions contrary to TALENs or ZFNs, which allows the permanent disruption of gene function. However, the mosaicism of mono- and biallelic mutations is so high that it may prove difficult to interpret phenotypes induced by TALENs or ZFNs in F0 individuals. We believe that the possibility to establish mutant lines is really the key point of this technology. These lines will facilitate the study of disrupted gene function at all stages of development unlike MOs. Another advantage of TALENs is that it can be driven under the control of a specific promoter. Thus, we can decide to disrupt a gene at a given stage in a specific tissue.

Since 2011, four publications demonstrated the use of ZFNs and TALENs in *X. tropicalis*. Indeed, this *Xenopus* species is diploid and its genome is well known. Thus *X. tropicalis* was the perfect amphibian model to test these new technologies. However, *X. laevis* is a more widespread model, so we may question the use of ZFNs and TALENs to engineer its genome. We believe that the complexity of *X. laevis* allotetraploid genome constitutes a first barrier. In all instances where two homeologs exists, it will be necessary to inactivate the two duplicated genes, i.e., four DNA targets instead of two. A second barrier is made by the Mendelian transmission of the mutant alleles since the theory predicts a 50% chance of producing a gamete with the two homeologs mutated when all germ cells are carriers of the mutations. Thus, the production and maintenance of *X. laevis* mutant lines would be difficult. An application that may prove to be of interest is if ZFNs or TALENs can be used for site-specific integration.

ZFNs and TALENs are challenged by a novel technology for genome editing (Cong et al. 2013; Mali et al. 2013). This technique is based on the association between an engineered RNA sequence and bacterial Cas proteins that can trigger double-stranded DNA breaks. The RNA sequence endows Cas proteins with the capability to recognize a targeted DNA sequence and to cleave it. The

first results show targeting rates of 2–25% according to the type of human cells (Mali et al. 2013). The beauty of this system is its simplicity: there is no need to design a DNA-binding protein domain since a small 20-nucleotide RNA fragment drives the specificity of DNA binding. A single Cas protein loads a guide RNA and cleaves the DNA. Wonderful! We can envision complex combinations of gene knockdown and DNA engineering in *Xenopus* for the coming years.

Acknowledgments

We are grateful for personal communications from Richard Harland, Jerry Jenkins, Dan Rokhsar, Jeremy Schmutz, and Shengqiang Shu on the *X. laevis* genome sequencing project. We would like to thank all members of the *Xenopus* Genome Steering Committee for sharing their information and in particular Mustafa Khokha for the coordination. Work in the laboratory is supported by the Association Française Contre les Myopathies (AFM project Amphigenetools).

References

- Abu-Daya, A., Sater, A.K., Wells, D.E., Mohun, T.J., and Zimmerman, L.B. (2009). Absence of heart-beat in the *Xenopus tropicalis* mutation muzak is caused by a nonsense mutation in cardiac myosin myh6. *Developmental Biology* 336, 20–29.
- Abu-Daya, A., Nishimoto, S., Fairclough, L., Mohun, T.J., Logan, M.P.O., and Zimmerman, L.B. (2011). The secreted integrin ligand nephronectin is necessary for forelimb formation in *Xenopus tropicalis*. *Developmental Biology* 349, 204–212.
- Akkers, R.C., Van Heeringen, S.J., Manak, J.R., Green, R.D., Stunnenberg, H.G., and Veenstra, G.J.C. (2010). ChIP-chip designs to interrogate the genome of *Xenopus* embryos for transcription factor binding and epigenetic regulation. *PLoS One* 5, e8820.
- Armisen, J., Gilchrist, M.J., Wilczynska, A., Standart, N., and Miska, E.A. (2009). Abundant and dynamically expressed miRNAs, piRNAs, and other small RNAs in the vertebrate *Xenopus tropicalis*. *Genome Research* 19, 1766–1775.
- Barbosa-Morais, N.L., Irimia, M., Pan, Q., et al. (2012). The evolutionary landscape of alternative splicing in vertebrate species. *Science* 338, 1587–1593.
- Baudet, M.-L., Zivraj, K.H., Abreu-Goodger, C., et al. (2012). miR-124 acts through CoREST to control onset of *Sema3A* sensitivity in navigating retinal growth cones. *Nature Neuroscience* 15, 29–38.
- Beil, J., Fairbairn, L., Pelczar, P., and Buch, T. (2012). Is BAC transgenesis obsolete? State of the art in the era of designer nucleases. *Journal of Biomedicine & Biotechnology* 2012, 308414.
- Beumer, K.J., Trautman, J.K., Bozas, A., et al. (2008). Efficient gene targeting in *Drosophila* by direct embryo injection with zinc-finger nucleases. *Proceedings of the National Academy of Sciences of the United States of America* 105, 19821–19826.
- Bibikova, M., Carroll, D., Segal, D.J., et al. (2001). Stimulation of homologous recombination through targeted cleavage by chimeric nucleases. *Molecular and Cellular Biology* 21, 289–297.
- Bibikova, M., Golic, M., Golic, K.G., and Carroll, D. (2002). Targeted chromosomal cleavage and mutagenesis in *Drosophila* using zinc-finger nucleases. *Genetics* 161, 1169–1175.
- Bibikova, M., Beumer, K., Trautman, J.K., and Carroll, D. (2003). Enhancing gene targeting with designed zinc finger nucleases. *Science* 300, 764.
- Blackiston, D., Shomrat, T., Nicolas, C.L., Granata, C., and Levin, M. (2010). A second-generation device for automated training and quantitative behavior analyses of molecularly-tractable model organisms. *PLoS One* 5, e14370.
- Boch, J. and Bonas, U. (2010). Xanthomonas AvrBs3 family-type III effectors: discovery and function. *Annual Review of Phytopathology* 48, 419–436.
- Boch, J., Scholze, H., Schornack, S., et al. (2009). Breaking the code of DNA binding specificity of TAL-type III effectors. *Science* 326, 1509–1512.
- Bogdanovic, O., Long, S.W., Van Heeringen, S.J., et al. (2011). Temporal uncoupling of the DNA methylome and transcriptional repression during embryogenesis. *Genome Research* 21, 1313–1327.
- Bogdanović, O., Van Heeringen, S.J., and Veenstra, G.J.C. (2012). The epigenome in early vertebrate development. *Genesis* 50, 192–206.
- Bowes, J.B., Snyder, K.A., Segerdell, E., et al. (2008). Xenbase: a *Xenopus* biology and genomics resource. *Nucleic Acids Research* 36, D761–D767.
- Bowes, J.B., Snyder, K.A., Segerdell, E., et al. (2010). Xenbase: gene expression and improved integration. *Nucleic Acids Research* 38, D607–D612.
- Carbery, I.D., Ji, D., Harrington, A., et al. (2010). Targeted genome modification in mice using zinc-finger nucleases. *Genetics* 186, 451–459.
- Cermak, T., Doyle, E.L., Christian, M., et al. (2011). Efficient design and assembly of custom TALEN

- and other TAL effector-based constructs for DNA targeting. *Nucleic Acids Research* 39, e82.
- Chan, E.T., Quon, G.T., Chua, G., et al. (2009). Conservation of core gene expression in vertebrate tissues. *Journal of Biology* 8, 33.
- Chandrasekharan, S., Kumar, S., Valley, C.M., and Rai, A. (2009). Proprietary science, open science and the role of patent disclosure: the case of zinc-finger proteins. *Nature Biotechnology* 27, 140–144.
- Chesneau, A., Sachs, L.M., Chai, N., et al. (2008). Transgenesis procedures in *Xenopus*. *Biology of the Cell* 100, 503–521.
- Cong, L., Ran, F.A., Cox, D., et al. (2013). Multiplex genome engineering using CRISPR/Cas systems. *Science* 339(6121): 819–823.
- DeFrancesco, L. (2011). Move over ZFNs. *Nature Biotechnology* 29, 681–684.
- Denayer, T., Van Roy, F., and Vlemminckx, K. (2006). In vivo tracing of canonical Wnt signaling in *Xenopus* tadpoles by means of an inducible transgenic reporter tool. *FEBS Letters* 580, 393–398.
- Deroo, T., Denayer, T., Van Roy, F., and Vlemminckx, K. (2004). Global inhibition of Lef1/Tcf-dependent Wnt signaling at its nuclear end point abrogates development in transgenic *Xenopus* embryos. *The Journal of Biological Chemistry* 279, 50670–50675.
- Doyon, Y., McCammon, J.M., Miller, J.C., et al. (2008). Heritable targeted gene disruption in zebrafish using designed zinc-finger nucleases. *Nature Biotechnology* 26, 702–708.
- Dunham, I., Kundaje, A., Aldred, S.F., et al. (2012). An integrated encyclopedia of DNA elements in the human genome. *Nature* 489, 57–74.
- Faunes, F., Sanchez, N., Moreno, M., et al. (2011). Expression of transposable elements in neural tissues during *Xenopus* development. *PLoS One* 6, e22569.
- Faunes, F., Almonacid, L.I., Melo, F., and Larrain, J. (2012). Characterization of small RNAs in *Xenopus tropicalis* gastrulae. *Genesis* 50, 260–270.
- Feil, R. (2007). Conditional somatic mutagenesis in the mouse using site-specific recombinases. *Handbook of Experimental Pharmacology* 178, 3–28.
- Fierro, A.C., Thuret, R., Coen, L., et al. (2007). Exploring nervous system transcriptomes during embryogenesis and metamorphosis in *Xenopus tropicalis* using EST analysis. *BMC Genomics* 8, 118.
- Fini, J.-B., Le Mevel, S., Turque, N., et al. (2007). An in vivo multiwell-based fluorescent screen for monitoring vertebrate thyroid hormone disruption. *Environmental Science & Technology* 41, 5908–5914.
- Fini, J.-B., Pallud-Mothré, S., Le Mével, S., et al. (2009). An innovative continuous flow system for monitoring heavy metal pollution in water using transgenic *Xenopus laevis* tadpoles. *Environmental Science & Technology* 43, 8895–8900.
- Fish, M.B., Nakayama, T., and Grainger, R.M. (2012). Simple, fast, tissue-specific bacterial artificial chromosome transgenesis in *Xenopus*. *Genesis* 50, 307–315.
- Gardner, E.J., Nizami, Z.F., Talbot, C.C., and Gall, J.G. (2012). Stable intronic sequence RNA (sisRNA), a new class of noncoding RNA from the oocyte nucleus of *Xenopus tropicalis*. *Genes & Development* 26, 2550–2559.
- Geach, T.J. and Zimmerman, L.B. (2010). Paralysis and delayed Z-disc formation in the *Xenopus tropicalis* unc45b mutant dicky ticker. *BMC Developmental Biology* 10, 75.
- Geurts, A.M., Cost, G.J., Freyvert, Y., et al. (2009). Knockout rats via embryo microinjection of zinc-finger nucleases. *Science* 325, 433.
- Gilchrist, M.J. (2012). From expression cloning to gene modeling: the development of *Xenopus* gene sequence resources. *Genesis* 50, 143–154.
- Gilchrist, M.J. and Pollet, N. (2012). Databases of gene expression in *Xenopus* development. *Methods in Molecular Biology* 917, 319–345.
- Goda, T., Abu-Day, A., Carruthers, S., Clark, M.D., Stemple, D.L., and Zimmerman, L.B. (2006). Genetic screens for mutations affecting development of *Xenopus tropicalis*. *PLoS Genetics* 2, e91.
- Graindorge, A., Thuret, R., Pollet, N., Osborne, H.B., and Audic, Y. (2006). Identification of post-transcriptionally regulated *Xenopus tropicalis* maternal mRNAs by microarray. *Nucleic Acids Research* 34, 986–995.
- Graindorge, A., Le Tonquèze, O., Thuret, R., Pollet, N., Osborne, H.B., and Audic, Y. (2008). Identification of CUG-BP1/EDEN-BP target mRNAs in *Xenopus tropicalis*. *Nucleic Acids Research* 36, 1861–1870.
- Grammer, T.C., Khokha, M.K., Lane, M.A., Lam, K., and Harland, R.M. (2005). Identification of mutants in inbred *Xenopus tropicalis*. *Mechanisms of Development* 122, 263–272.
- Hamlet, M.R., Yergeau, D.A., Kuliyeve, E., et al. (2006). Tol2 transposon-mediated transgenesis in *Xenopus tropicalis*. *Genesis* 44, 438–445.
- Harland, R.M. and Grainger, R.M. (2011). *Xenopus* research: metamorphosed by genetics and genomics. *Trends in Genetics* 27, 507–515.
- Hellsten, U., Harland, R.M., Gilchrist, M.J., et al. (2010). The genome of the Western clawed frog *Xenopus tropicalis*. *Science* 328, 633–636.
- Hikosaka, A. and Kawahara, A. (2010). A systematic search and classification of T2 family miniature inverted-repeat transposable elements (MITEs) in *Xenopus tropicalis* suggests the existence of recently active MITE subfamilies. *Molecular Genetics and Genomics* 283, 49–62.
- Hikosaka, A., Kobayashi, T., Saito, Y., and Kawahara, A. (2007). Evolution of the *Xenopus* piggyBac

- transposon family TxpB: domesticated and untamed strategies of transposon subfamilies. *Molecular Biology and Evolution* 24, 2648–2656.
- Ishii, Y., Asakawa, S., Taguchi, Y., Ishibashi, S., Yagi, T., and Shimizu, N. (2004). Construction of BAC library for the amphibian *Xenopus tropicalis*. *Genes & Genetic Systems* 79, 49–51.
- James-Zorn, C., Ponferrada, V.G., Jarabek, C.J., et al. (2013). Xenbase: expansion and updates of the *Xenopus* model organism database. *Nucleic Acids Research* 41, D865–D870.
- Jiang, Z., Michal, J.J., Beckman, K.B., et al. (2011). Development and initial characterization of a HAPPY panel for mapping the *X. tropicalis* genome. *International Journal of Biological Sciences* 7, 1037–1044.
- Johansson, T., Broll, I., Frenz, T., et al. (2010). Building a zoo of mice for genetic analyses: a comprehensive protocol for the rapid generation of BAC transgenic mice. *Genesis* 48, 264–280.
- Kaya, F., Mannioui, A., Chesneau, A., et al. (2012). Live imaging of targeted cell ablation in *Xenopus*: a new model to study demyelination and repair. *The Journal of Neuroscience* 32, 12885–12895.
- Kelly, L.E., Davy, B.E., Berbari, N.F., Robinson, M.L., and El-Hodiri, H.M. (2005). Recombineered *Xenopus tropicalis* BAC expresses a GFP reporter under the control of Arx transcriptional regulatory elements in transgenic *Xenopus laevis* embryos. *Genesis* 41, 185–191.
- Kerney, R.R., Brittain, A.L., Hall, B.K., and Buchholz, D.R. (2012). Cartilage on the move: cartilage lineage tracing during tadpole metamorphosis. *Development, Growth & Differentiation* 54, 739–752.
- Khokha, M.K., Krylov, V., Reilly, M.J., et al. (2009). Rapid gynogenetic mapping of *Xenopus tropicalis* mutations to chromosomes. *Developmental Dynamics* 238, 1398–1346.
- Kroll, K.L. and Amaya, E. (1996). Transgenic *Xenopus* embryos from sperm nuclear transplantations reveal FGF signaling requirements during gastrulation. *Development* 122, 3173–3183.
- Krylov, V., Kubickova, S., Rubes, J., et al. (2010). Preparation of *Xenopus tropicalis* whole chromosome painting probes using laser microdissection and reconstruction of *X. laevis* tetraploid karyotype by Zoo-FISH. *Chromosome Research* 18, 431–439.
- Lau, N.C., Ohsumi, T., Borowsky, M., Kingston, R.E., and Blower, M.D. (2009). Systematic and single cell analysis of *Xenopus* Piwi-interacting RNAs and Kiwi. *The EMBO Journal* 28, 2945–2958.
- Le Provost, F., Lillico, S., Passet, B., Young, R., Whitelaw, B., and Vilotte, J.L. (2010). Zinc finger nuclease technology heralds a new era in mammalian transgenesis. *Trends in Biotechnology* 28, 134–141.
- Lei, Y., Guo, X., Liu, Y., et al. (2012). Efficient targeted gene disruption in *Xenopus* embryos using engineered transcription activator-like effector nucleases (TALENs). *Proceedings of the National Academy of Sciences of the United States of America* 109, 17484–17489.
- L’hostis-Guidet, A., Recher, G., Guillet, B., et al. (2009). Generation of stable *Xenopus laevis* transgenic lines expressing a transgene controlled by weak promoters. *Transgenic Research* 18, 815–827.
- Li, W. (2011). On parameters of the human genome. *Journal of Theoretical Biology* 288, 92–104.
- Love, N.R., Chen, Y., Bonev, B., et al. (2011a). Genome-wide analysis of gene expression during *Xenopus tropicalis* tadpole tail regeneration. *BMC Developmental Biology* 11, 70.
- Love, N.R., Thuret, R., Chen, Y., et al. (2011b). pTransgenesis: a cross-species, modular transgenesis resource. *Development* 138, 5451–5458.
- Mali, P., Yang, L., Esvelt, K.M., et al. (2013). RNA-guided human genome engineering via Cas9. *Science* 339(6121): 823–826.
- Malone, J.H. and Michalak, P. (2008). Gene expression analysis of the ovary of hybrid females of *Xenopus laevis* and *X. muelleri*. *BMC Evolutionary Biology* 8, 82.
- Malone, J.H., Chrzanowski, T.H., and Michalak, P. (2007). Sterility and gene expression in hybrid males of *Xenopus laevis* and *X. muelleri*. *PloS One* 2, e781.
- Mandell, J.G. and Barbas, C.F. (2006). Zinc finger tools: custom DNA-binding domains for transcription factors and nucleases. *Nucleic Acids Research* 34, W516–W523.
- Marcet, B., Chevalier, B., Luxardi, G., et al. (2011). Control of vertebrate multiciliogenesis by miR-449 through direct repression of the Delta/Notch pathway. *Nature Cell Biology* 13, 693–699.
- Mashimo, T., Takizawa, A., Voigt, B., et al. (2010). Generation of knockout rats with X-linked severe combined immunodeficiency (X-SCID) using zinc-finger nucleases. *PloS One* 5, e8870.
- Meng, X., Noyes, M.B., Zhu, L.J., Lawson, N.D., and Wolfe, S.A. (2008). Targeted gene inactivation in zebrafish using engineered zinc-finger nucleases. *Nature Biotechnology* 26, 695–701.
- Meyer, M., De Angelis, M.H., Wurst, W., and Kühn, R. (2010). Gene targeting by homologous recombination in mouse zygotes mediated by zinc-finger nucleases. *Proceedings of the National Academy of Sciences of the United States of America* 107, 15022–15026.
- Miller, J.C., Holmes, M.C., Wang, J., et al. (2007). An improved zinc-finger nuclease architecture for highly specific genome editing. *Nature Biotechnology* 25, 778–785.

- Mácha, J., Teichmanová, R., Sater, A.K., et al. (2012). Deep ancestry of mammalian X chromosome revealed by comparison with the basal tetrapod *Xenopus tropicalis*. *BMC Genomics* 13, 315.
- Nakajima, K., Nakajima, T., Takase, M., and Yaoita, Y. (2012). Generation of albino *Xenopus tropicalis* using zinc-finger nucleases. *Development, Growth & Differentiation* 54, 777–784.
- Noramly, S., Zimmerman, L., Cox, A., Aloise, R., Fisher, M., and Grainger, R.M. (2005). A gynogenetic screen to isolate naturally occurring recessive mutations in *Xenopus tropicalis*. *Mechanisms of Development* 122, 273–287.
- Ochiai, H., Sakamoto, N., Fujita, K., et al. (2012). Zinc-finger nuclease-mediated targeted insertion of reporter genes for quantitative imaging of gene expression in sea urchin embryos. *Proceedings of the National Academy of Sciences of the United States of America* 109, 10915–10920.
- Pace, J.K., Gilbert, C., Clark, M.S., and Feschotte, C. (2008). Repeated horizontal transfer of a DNA transposon in mammals and other tetrapods. *Proceedings of the National Academy of Sciences of the United States of America* 105, 17023–17028.
- Pan, F.C., Chen, Y., Loeber, J., Henningfeld, K., and Pieler, T. (2006). I-SceI meganuclease-mediated transgenesis in *Xenopus*. *Developmental Dynamics* 235, 247–252.
- Pearl, E.J., Grainger, R.M., Guille, M., and Horb, M.E. (2012). Development of *Xenopus* resource centers: the National *Xenopus* Resource and the European *Xenopus* Resource Center. *Genesis* 50, 155–163.
- Perez, E.E., Wang, J., Miller, J.C., et al. (2008). Establishment of HIV-1 resistance in CD4+ T cells by genome editing using zinc-finger nucleases. *Nature Biotechnology* 26, 808–816.
- Pollet, N. and Mazabraud, A. (2006). Insights from *Xenopus* genomes. *Genome Dynamics* 2, 138–153.
- Rankin, S.A., Zorn, A.M., and Buchholz, D.R. (2011). New doxycycline-inducible transgenic lines in *Xenopus*. *Developmental Dynamics* 240, 1467–1474.
- Robine, N., Lau, N.C., Balla, S., et al. (2009). A broadly conserved pathway generates 3'UTR-directed primary piRNAs. *Current Biology* 19, 2066–2076.
- Roelants, K., Fry, B.G., Norman, J.A., Clynen, E., Schoofs, L., and Bossuyt, F. (2010). Identical skin toxins by convergent molecular adaptation in frogs. *Current Biology* 20, 125–130.
- Roose, M., Sauert, K., Turan, G., et al. (2009). Heat-shock inducible Cre strains to study organogenesis in transgenic *Xenopus laevis*. *Transgenic Research* 18, 595–605.
- Sander, J.D., Cade, L., Khayter, C., et al. (2011). Targeted gene disruption in somatic zebrafish cells using engineered TALENs. *Nature Biotechnology* 29, 697–698.
- Shibano, T., Takeda, M., Suetake, I., et al. (2007). Recombinant Tol2 transposase with activity in *Xenopus* embryos. *FEBS Letters* 581, 4333–4336.
- Showell, C., Carruthers, S., Hall, A., Pardo-Manuel de Villena, F., Stemple, D., and Conlon, F.L. (2011). A comparative survey of the frequency and distribution of polymorphism in the genome of *Xenopus tropicalis*. *PLoS One* 6, e22392.
- Simeoni, I., Gilchrist, M.J., Garrett, N., Armisen, J., and Gurdon, J.B. (2012). Widespread transcription in an amphibian oocyte relates to its reprogramming activity on transplanted somatic nuclei. *Stem Cells and Development* 21, 181–190.
- Sinzelle, L., Pollet, N., Bigot, Y., and Mazabraud, A. (2005). Characterization of multiple lineages of Tc1-like elements within the genome of the amphibian *Xenopus tropicalis*. *Gene* 349, 187–196.
- Sinzelle, L., Vallin, J., Coen, L., et al. (2006). Generation of transgenic *Xenopus laevis* using the Sleeping Beauty transposon system. *Transgenic Research* 15, 751–760.
- Sinzelle, L., Izsvák, Z., and Ivics, Z. (2009). Molecular domestication of transposable elements: from detrimental parasites to useful host genes. *Cellular and Molecular Life Sciences* 66, 1073–1093.
- Sinzelle, L., Carradec, Q., Paillard, E., Bronchain, O.J., and Pollet, N. (2011). Characterization of a *Xenopus tropicalis* endogenous retrovirus with developmental and stress-dependent expression. *Journal of Virology* 85, 2167–2179.
- Smith, W.C. and Harland, R.M. (1992). Expression cloning of noggin, a new dorsalizing factor localized to the Spemann organizer in *Xenopus* embryos. *Cell* 70, 829–840.
- Suzuki, K.T., Kashiwagi, K., Ujihara, M., et al. (2010). Characterization of a novel type I keratin gene and generation of transgenic lines with fluorescent reporter genes driven by its promoter/enhancer in *Xenopus laevis*. *Developmental Dynamics* 239, 3172–3181.
- Tan, M.H., Au, K.F., Yablonovitch, A., et al. (2012). RNA sequencing reveals diverse and dynamic repertoire of the *Xenopus tropicalis* transcriptome over development. *Genome Research* 23, 201–216.
- Tesson, L., Usal, C., Ménoiret, S., et al. (2011). Knockout rats generated by embryo microinjection of TALENs. *Nature Biotechnology* 29, 695–696.
- Thiébaud, C.H. and Fischberg, M. (1977). DNA content in the genus *Xenopus*. *Chromosoma* 59, 253–257.
- Van Heeringen, S.J., Akhtar, W., Jacobi, U.G., Akkers, R.C., Suzuki, Y., and Veenstra, G.J.C. (2011). Nucleotide composition-linked divergence of vertebrate core promoter architecture. *Genome Research* 21, 410–421.

- Vastag, L., Jorgensen, P., Peshkin, L., Wei, R., Rabinowitz, J.D., and Kirschner, M.W. (2011). Remodeling of the metabolome during early frog development. *PLoS One* 6, e16881.
- Viso, F., Bhattacharya, D., Kong, Y., Gilchrist, M.J., and Khokha, M.K. (2012). Exon capture and bulk segregant analysis: rapid discovery of causative mutations using high-throughput sequencing. *BMC Genomics* 13, 649.
- Voss, S.R., Kump, D.K., Putta, S., et al. (2011). Origin of amphibian and avian chromosomes by fission, fusion, and retention of ancestral chromosomes. *Genome Research* 21, 1306–1312.
- Watson, F.L., Mills, E.A., Wang, X., Guo, C., Chen, D.F., and Marsh-Armstrong, N. (2012). Cell type-specific translational profiling in the *Xenopus laevis* retina. *Developmental Dynamics* 241, 1960–1972.
- Wells, D.E., Gutierrez, L., Xu, Z., et al. (2011). A genetic map of *Xenopus tropicalis*. *Developmental Biology* 354, 1–8.
- Wheeler, G.N. and Liu, K.J. (2012). *Xenopus*: an ideal system for chemical genetics. *Genesis* 50, 207–218.
- Wood, A.J., Lo, T.-W., Zeitler, B., et al. (2011). Targeted genome editing across species using ZFNs and TALENs. *Science* 333, 307.
- Wright, D. A., Thibodeau-Beganny, S., Sander, J.D., et al. (2006). Standardized reagents and protocols for engineering zinc finger nucleases by modular assembly. *Nature Protocols* 1, 1637–1652.
- Xu, Z., Gutierrez, L., Hitchens, M., Scherer, S., Sater, A.K., and Wells, D.E. (2008). Distribution of polymorphic and non-polymorphic microsatellite repeats in *Xenopus tropicalis*. *Bioinformatics and Biology Insights* 2, 157–169.
- Yanai, I., Peshkin, L., Jorgensen, P., and Kirschner, M.W. (2011). Mapping gene expression in two *Xenopus* species: evolutionary constraints and developmental flexibility. *Developmental Cell* 20, 483–496.
- Yergeau, D.A., Johnson Hamlet, M.R., Kuliyeve, E., et al. (2009). Transgenesis in *Xenopus* using the Sleeping Beauty transposon system. *Developmental Dynamics* 238, 1727–1743.
- Yergeau, D.A., Kelley, C.M., Zhu, H., Kuliyeve, E., and Mead, P.E. (2010a). Transposon transgenesis in *Xenopus*. *Methods* 51, 92–100.
- Yergeau, D.A., Kelley, C.M., Kuliyeve, E., et al. (2010b). Remobilization of Tol2 transposons in *Xenopus tropicalis*. *BMC Developmental Biology* 10, 11.
- Yergeau, D.A., Kelley, C.M., Kuliyeve, E., et al. (2011). Remobilization of Sleeping Beauty transposons in the germline of *Xenopus tropicalis*. *Mobile DNA* 2, 15.
- Ymlahi-Ouazzani, Q., J Bronchain, O., Paillard, E., et al. (2010). Reduced levels of survival motor neuron protein leads to aberrant motoneuron growth in a *Xenopus* model of muscular atrophy. *Neurogenetics* 11, 27–40.
- Young, J.J., Cherone, J.M., Doyon, Y., et al. (2011). Efficient targeted gene disruption in the soma and germ line of the frog *Xenopus tropicalis* using engineered zinc-finger nucleases. *Proceedings of the National Academy of Sciences of the United States of America* 108, 7052–7057.
- Zuber, M.E., Nihart, H.S., Zhuo, X., Babu, S., and Knox, B.E. (2012). Site-specific transgenesis in *Xenopus*. *Genesis* 50, 325–332.

Index

- Acetabularia*, 4
Actin, 27, 105, 106, 169–74, 180, 191, 193, 194
 microfilaments, 27
Activin, 242, 244
Actomyosin cortex, 190, 191
ADAM13, 253
ADAR1, 7, 12
Adherens junctions, 168, 170
Adhesion, 193–5
AEC, 376
Affinity, 276, 278–80, 286
AFM, 311–23
 imaging, 311, 312, 314–20, 322
 topography image, 319–22
AJs, 168, 170–172
Albino, 395–7
Algorithm, 16, 23, 24, 34
Allograft, 276, 278
Allotetraploid, 384, 385, 397
5 α -dihydrotestosterone, 204, 209, 210
Anillin, 105–7
Animal, 17, 18, 29, 30, 32–4, 215, 218, 219, 231, 232
 cap, 215, 218, 219, 231, 232
 hemisphere, 17, 18
 -vegetal axis, 17, 29, 30, 32–4
Animally localized transcripts, 67
Anterior-posterior axis, 245–7, 252
Antibody diversity, 278
Antigen presentation, 267–9, 271
ap-2, 250, 251
Aphidicolin, 177
Apical, 105, 107–9, 163, 164, 168–74, 179, 181
 constriction, 163, 164, 168–74, 179, 181
 junctional complexes, 105, 107, 108
aPKC, 68, 117, 118
Aplysia, 34
Apoptosis, 276, 278, 282
Apoptotic, 268, 285
Aromatase, 205, 206, 209, 210
Ascidian embryo, 106, 107, 109
Assembly, 384, 385, 391–3
Asymmetric, 103, 104, 106–9
 cell division, 103, 106, 117, 118
 furrowing, 103, 104, 106–9
Asymmetry, 67–9
ATP, 33
Atrazine, 208, 209
Atypical PKC, 68, 117
AU-rich element, 48
Aurora kinase, 331, 332
Autoimmune, 275, 276, 282, 284, 285
Axin complex, 140, 142, 143
Axis determination, 134, 140
BAC, 384, 385, 394
 DNA injection, 394
 genomic library, 394
Bacterial artificial chromosome, 384

- Balbani body, 17, 18, 61, 76
- Basal, 118, 200, 202–4
bodies, 118
lamina, 200, 202–4
- Basement membrane, 348–50, 357, 361, 363
- Basic setup, 313
- Basolateral, 61, 68, 104, 106–9
polarity, 61, 68
- BBs, 118, 119, 121, 122, 124
- BCR, 264, 273, 274
- β -catenin, 130–132, 134–6, 138–51, 153, 154, 242, 243, 252, 253, 373, 374, 376, 377
- β -tubulin, 170–175
- Bicoid, 20–23
- Bilateral, 108
- Bioinformatics, 383, 387, 389
- Biphasic induction, 108
- Blastema, 301, 303, 304
- Blastomeres, 106, 109, 217, 218, 225, 226, 230
- Blastula, 104–6, 109, 139, 142–4, 146, 148, 153, 154
- Bleb, 190, 193–5
-associated mechanism, 193–5
-like protrusions, 190, 193, 195
- Blebbistatin, 170
- Bone morphogenetic protein (BMP), 144–6, 173, 218, 222, 243–8, 250–252, 254, 256, 372–8
- Border of the neural plate, 248
- Boundary specifiers, 251
- Brachyury*, 242
- BrdU, 348
- Bruch's membrane, 348–351, 354, 357, 358, 362, 363
- CAC-rich RNA, 21, 22, 24
- Cadherins, 172, 173, 181
- Cadherin switching, 253
- Caenorhabditis elegans*, 106, 108
- Calcium signaling, 244
- Calmodulin, 172
- Canonical, 130–132, 134, 135, 138, 140, 149, 242, 251, 252
pathway, 130–132, 134, 135, 138, 140, 149
Wnt pathway, 242, 251, 252
- Caspase-3, 373, 374
- Cas proteins, 397
- CDK, 256
- CDKi, 256
- Cdx, 246
- Cell, 103–6, 108, 109, 164–71, 173, 174, 176, 181, 253–355
-cell adhesion, 253
division, 103–6, 108, 109
elongation, 164, 168–70, 173, 174, 176, 181
intercalation, 165–7, 171, 176
-matrix interactions, 354, 355
plasma membrane, 103
polarity, 105
size, 325, 326, 329, 333, 334, 336–9
- Cellular, 18, 34, 190, 192
differentiation, 34
dynamics, 190
extracts, 18
polarization, 192
- Central, 106, 163
mitotic spindle, 106
nervous system, 163
- Centrioles, 61, 62, 69, 118, 119, 122–3, 125
- Centroid*, 81, 86
- Cerberus, 245, 247, 251
- Chemoattractants, 191, 192
- Chemokine C-X-C motif ligand, 12, 192
- Chemotaxis, 192, 193
- Chiasmata, 4
- Chimera, 265, 276
- Chimeric, 391, 394
nucleases, 391
proteins, 394
- Choroid, 348, 349, 353–7, 359, 362–4
- Chromatids, 4–9
- Chromatin, 326, 327, 329–33, 337–40
- Chromomeres, 4–7
- Chromosome(s), 325–7, 330, 332, 333, 335, 337–41
segregation, 332, 338
scaling, 332, 333, 337–9
- Ciliary marginal zone, 299, 346
- Ciliogenesis, 112, 118, 119, 121–3
- cis* dominance, 49
- cis*-inhibition, 119, 124
- Cleaving embryo, 104
- Climax of metamorphosis, 285
- Cluster, 61
- c-Myc, 250, 254
- CMZ, 295, 298–300, 346–8, 350, 357, 362
- Competence, 264, 274, 278
- Complement, 264, 266, 267
- Condensin, 339
- Connexin, 43, 349, 354, 355
- Contact inhibition, 253
- Convergence-extension, 131, 134, 140, 148, 149, 154
- Convergent extension, 164–8, 171, 179
- Cornea, 295, 298, 299
- Cortex, 200–206, 210
- Cortical rotation, 60, 61, 65, 68, 69, 139–42
- CPE, 41, 43–51
-combinatorial code, 49
- CPEB, 84, 85
- CPEB1, 41, 43–6, 48–52
- CPEB4, 41, 44, 45, 49–51
- CPSE, 41, 46, 49
- Cranial, 240, 248
ganglia, 240
placodes, 248

- CRE/LOX system, 393
 CRISPR/Cas system, 394
 Cross-talk, 131, 132, 143, 146
 CstF-77, 45, 46
 C-X-C chemokine receptor type 4, 192
 CXCL12, 192
 CXCR4, 192, 199, 200
Cyp19, 206
 Cyst, 61–3
 Cystoblast, 77–9
 Cystocytes, 79
 Cytochalasin, 170
 Cytokeratin filaments, 64, 66
 Cytokinesis, 105–9, 333, 337
 Cytokinetic furrow, 103–5, 107, 109
 Cytoplasm, 17–18, 23, 28, 30–33, 328–30, 334, 336, 339, 340
 Cytoplasmic bridges, 61, 69
 Cytoskeletal proteins, 25
 Cytoskeleton, 26, 27
- DAAM1, 171
 DAPI, 4, 5
 DDX5/p68, 30
 DDX6, 40–42, 45, 46
Dead-end, 80, 81, 83, 86, 92
 Deadenylase, 45
DeadSouth, 80–82, 85, 86
 Dedifferentiation, 370, 371, 375, 377, 379
 Default model, 239, 244
 Delamination, 250, 252, 253
 Deletion, 395, 396
 DeltaA, 255, 256
 /Notch signaling, 255
 Dendritic cells, 269, 272
 Dephosphorylation, 104
 Derriere, 242
 Determination, 217, 232
 Deuterosomes, 119, 121–3
 Developmental, 60, 325, 326, 334, 339
 fate, 60
 scaling, 325, 326, 334, 339
 DHT, 204, 209, 210
 Dickkopf, 245, 247
Dictyostelium discoideum, 191–3
 Differentiation, 217, 219, 221–4, 228, 230–232
 Digital scanned laser light-sheet fluorescence microscopy, 177
 Dihydropyridine-sensitive Ca²⁺ channel, 244
 Dimerization domains, 21, 22, 31
 Diploid, 384, 392, 395, 397
 Directional migration, 190, 193
 Dishevelled, 131, 142, 154, 166, 168, 171
 Dispase, 353–7
 Dkk1, 372, 373, 375, 377
 dlb, 7
- Dlx, 241, 248
Dmrt1, 206, 207
 DM-W, 206, 207
 Dnd1 86, 87, 92
 Dorsal, 164, 166–8, 302
 mesoderm, 164, 166–8
 root ganglia, 302
 Dorsalizing center, 140–143, 146
 Dorsal-ventral polarity, 246, 248
 Dorsoventral, 146, 147, 149, 154
 patterning, 146, 147, 149, 154
 polarization, 146
 Double, 7, 273, 274, 276
 -loop bridges, 7
 -negative cells, 273
 -positive, 274, 276
Drosophila, 4, 17, 18, 20–22, 26, 29, 34, 75, 79, 80, 82, 86, 88–91, 131, 134, 145, 148, 149
 melanogaster, 17, 21
 pseudoobscura, 21
 DSCC, 244
 DSLM, 177, 178
 Ducts, 216–18, 220–224, 229, 230
 Dynamamin, 173
 Dynein, 27, 30, 31, 33
- Early, 17, 18, 27–9, 46–51, 64, 69, 131, 143–6
 class, 46–51
 gene regulation, 143
 mesoderm induction, 146
 pathway, 17, 19, 27–9, 64, 69
 patterning, 131, 143–6
 4E-BP, 39, 45
 E-cadherin, 172, 181, 194, 195
 ECM, 174, 179, 181
 Ectoderm, 113–17, 119, 120, 123, 149
 -mesoderm separation, 149
 Ectopic axis, 134
 Edema, 220, 221, 227
efl-α promoter, 357, 358
 eFGF, 246, 247
 EGFP, 355, 357
 Egg, 61, 68, 69, 325–7, 329–31, 333–5, 338, 341
 cortex, 61, 68, 69
 extract, 325–7, 329–31, 333–5, 338, 341
 eIF2, 39, 40
 eIF4E1b, 41, 45, 46
 eIF4F, 38, 39
 Electric current, 374
 Elongation, 164–71, 173, 174, 176, 177, 181
 Elr-type protein, 25
 Embryo extract, 334–6, 339, 341
 Embryonic axis, 61
 EMT, 240, 252–4, 257
 Ena/VASP, 170–172
 ENCODE consortium, 391

- Endoderm, 76–8, 80, 81, 85, 86, 88–91, 189, 190, 192–5
Endomesoderm, 245
Endoplasmic reticulum, 25, 28, 341
Engrailed, 136, 149, 154
ePAB, 41, 48
Ependymal, 295–303
 canal, 297, 305
 cells, 295–7
Ephirins, 253
Epidermis, 112, 113, 117, 119, 123–5
Epigenomics, 390
Epigonad, 203
Epithelial, 103, 106, 108, 109, 240
 cell, 103, 106, 108, 109
 -to mesenchymal transition, 240
Epithelium, 103, 104, 107, 109
 integrity, 104
EPLIN, 172
EST, 389, 392
Estradiol, 205, 208, 209
Ethinylestradiol, 208, 209
Evolution, 386, 389, 390
Exencephaly, 171, 172
Explant, 215, 218–20
Expressed sequence tag, 389
Extracellular matrix, 179, 194, 195

F-actin, 169–74, 180
Fadrozole, 209, 210
Fate, 215, 217–21, 223, 225, 232
 -based, 215, 217–21, 223, 225, 232
 maps, 217, 225
Fatvg, 203
Feulgen, 4
FGF, 139, 140, 144–6, 218, 220, 221, 243, 244, 246, 247, 250–252, 254, 363, 364, 372–8
 signaling inhibitors, 363, 364
FGF2, 352–4, 363, 364
FGF3, 246, 247
FGF8, 246, 247, 251
FGF9, 246, 247
FGF20, 373, 375
Fibroblastema, 303
Fibronectin, 179, 180, 199
Finasteride, 209, 210
Flamingo, 134, 137, 148
Floorplate, 246, 248, 249
Fluid flow, 123, 124
FN, 179, 180
FokI, 394, 397
Follicular cells, 205, 206
Follistatin, 243, 244, 247
Forebrain, 245, 247, 256
Forelimbs, 303, 304
Foxd, 241, 244, 250, 251, 254–6
Foxile, 115, 116, 119, 123
Foxl2, 206
Frizzled, 131, 132, 147, 148, 245, 251
Froglet, 304
FRT recombinase, 393
FRYG2, 40–42
Frzb, 245, 247
Furrow ingression, 104, 108
Fz, 131, 132, 135, 137–9, 142, 143, 147–9, 151–4

Gadd45, 241, 245
Gametes, 190
Gap junctions, 355
Gastrula, 103, 104, 106, 107, 109, 133–5, 141, 145–7, 153, 154, 217, 218, 220, 227
Gastrulation, 217, 218, 220, 230
Gateway, 387, 393
Gbx2, 246, 250, 251
gdf5, 377
GDNF, 218
Gel embedding culture, 355, 356–61
geminin, 254, 256
Gene, 387, 395
 disruption, 395
 nomenclature, 387
Genetics, 224, 384, 385, 391, 392
 distance, 392
 map, 384, 391, 392
 mapping, 385, 391
Genital ridges, 199–203, 205, 206
Genome, 225, 382, 392–5, 397
 editing, 225, 391, 394, 395, 397
 engineering, 382, 392, 393
 integration, 393
 sequencing, 383, 384, 398
Genomics, 383–5, 387, 389, 392
Germ, 64, 65, 75–7, 79–89, 91, 114–16, 189, 190, 193–5, 199–207, 210
 cells, 199–207, 210
 -cell-specific mRNAs, 189
 layer, 114–16
 plasm, 64, 65, 75–7, 79–89, 91, 189, 190, 193–5
Germes, 80, 81, 194, 195
Germinal, 3, 61, 63–6, 69, 76
 granules, 61, 63–6, 69, 76
 vesicle, 3
Germline cells, 75, 89
GFM, 76, 79, 80
GFP, 370, 371
GG, 76, 79–86
GLD2, 45, 46, 50, 51
Glia, 248
Glomerus, 216, 217
Glomus, 216–18, 220, 222–4, 229, 230
Glucocorticoids, 270
Golden Gate method, 397

- Goosecoid, 242
 Gonad, 199–210
 Gonadal, 199–202
 cortex, 200–202
 medulla, 199–201, 203
 ridges, 199
 Gonia, 200, 201
 Gonomers, 200
 G-protein coupled receptor (GPCR), 192
 gpt11, 81
 Grip2, 81
 GRN, 254–6
 Growth, 17
 Guanylyl 5' cap, 39
- Hairpin, 21
 Hairy2, 254
 Hermaphroditism, 208
Hermes, 80, 81, 83–5
 HES, 194
 -related genes, 194
 Heterotrimeric G-proteins, 192
 H1 histone, 91
 Higher-order RNA structures, 20, 25, 34
 Hind limb, 296, 303
 Hippo pathway, 222
 Histocompatibility, 264, 266, 270, 280
 Histone, 339, 390
 H3 methylation, 390
 hnRNP, 25, 30–32
 Holtfreter sandwich, 218, 219
 Homeostasis, 109
 Homologous recombination, 393–5
 Horizontal transfer, 389
 Hox, 246, 247
 Hyaluronan, 373, 374
 Hydroxurea, 177
 Hypophysectomized individual, 277
- Id3, 241, 250, 254
 IGF1, 354
 IgM, 270, 271, 273, 274, 276, 278
 IgX, 266, 271, 276
 IgY, 271, 276, 278, 279
 Imaging, 222, 224, 228, 230, 232, 313, 314–17,
 319, 322
 in air, 317
 in liquid, 313, 314–16, 319, 322
 iMELK, 105
 Immune responses, 265, 268, 285
 Immunization, 278, 284
 Immunofluorescence, 271, 275
 Immunoglobulins, 264, 265, 278
 Immunological competence, 274
 Immunostaining, 218, 228–30
 Importin, 329, 330, 334–7, 340
- Indian hedgehog, 252
 Induced mutations, 391, 396
 Inducer, 218
 Induction, 217–20, 223, 226, 228
 Inductive signal, 218–20
 Initiation, 38–41, 46
 Innate immunity, 264–6, 273
 Inositol phospholipids, 192
 Insertion, 394, 395
In situ, 10, 11, 29, 228–30, 232
 hybridization, 10, 11, 29
 Insulin-like growth factors, 246
 Integrin, 179–81
 Intercalation, 118, 120–122, 125
 Intergenic regions, 387
 Intermediate mesoderm, 217, 220, 221, 223
 Intermitochondrial, 61
 Intermolecular RNA base pairing, 21, 23
 Interrenal glands, 200, 204
 Intersex gonads, 208
 Interspecies scaling, 326, 327, 330, 333, 334, 337
 Intron, 387, 390
 Ionocytes, 113, 116, 117, 119, 120
 Iris, 346, 347
 Iroquois family, 255
 I-SceI meganuclease, 393
 Isogenic, 265, 277, 279, 282, 284–6
 interspecies hybrids, 265
- Katanin, 327, 331, 332, 337
 Kctd15, 250, 251
 Kermit, 252
 Kidney, 215–232
 Kif2a, 336, 337
 KIF13B, 193, 194
 Kinesin, 192
 Kinesin I, 27
 Kinesin II, 19, 23, 27, 29, 30
 Knockdown, 220, 221, 223–226, 228, 231
 Kremen2, 252
- Lamellipodia, 166, 167, 194
 Lamina, 329
 Lamin B, 329, 330, 334
 Laminin, 203, 351, 352, 357
 Lampbrush chromosomes, 3, 4, 6, 7, 12, 13
 Larval stages, 293–5, 299, 304, 305
 Laser ablation, 177, 178, 180
 Late, 17–20, 29, 47–50, 64, 65, 69
 class, 47–50
 pathway, 17–20, 29, 64, 65, 69
 Lateral, 117, 119, 266, 268
 inhibition, 117, 119
 plate mesoderm, 266, 268
 LBCs, 4–11
 LE, 19

- Leading edge, 191–4, 245
Lectins, 264
Lef1, 252
Lens, 293–5, 298–300, 350, 351, 368, 369, 378, 379
 regeneration, 350, 351, 368, 369, 378, 379
Lentectomy, 299, 378, 379
Lentogenic area, 378
Lesion gap, 297
Leyding cells, 203–5
lim1, 220, 221, 223, 228–30
Limb, 294, 303, 304, 368, 370, 372, 373, 375–9
 bud, 368, 373, 375, 377
 regeneration, 294, 303, 304, 368, 370, 372,
 375–9
limulus, 172
Lineage, 75–7, 89, 218, 220, 223, 224, 230, 232
Linkage group, 391
LMO4, 252
Localization signals, 67
Localized synthesis of proteins, 16
Locomotive activity, 190
LRP5/6, 131, 132, 135, 137, 245
Lulu, 170–172
- Macrophages, 267–70, 272, 285
MAPK, 139, 143, 144, 146, 243, 244
MAP kinase, 47, 51
Mapping, 384, 385, 391
MARCKS, 171, 172
Markers, 216, 218, 220, 223, 224, 228–32
Maskin, 45, 46
Maternal, 104, 114–16, 118
 determinant, 114–16, 118
 embryonic leucine zipper kinase, 104
 mRNA, 104
 Wnt11, 134
Mauthner axons, 295
MBE, 51
MBT, 106, 109, 190, 330, 334–336, 338–340
MCCs, 112, 113, 118, 119, 121–125
MDCK, 108, 170, 171
Medulla, 199–205, 208, 210
Meganuclease, 392, 393
Meiotic prophase, 205
MEK-ERK, 354
MELK, 104–7
Membrane-targeted EGFP, 177
memEGFP, 177
Memory, 279, 281, 286
Mesencephalon, 293, 295, 304
Mesoderm, 217–23
Mesonephros, 216
Mesentery, 195
Mesoderm, 17
Mesonephros, 199–201, 204, 205
Messenger transport organizer, 64
Metalloproteinases, 253, 357
Metamorphosis, 293–305
Metamorphic climax, 270, 272, 285
Metanephros, 216
Metasynchronous, 109
Methylation, 390, 391
METRO, 63–5, 76
MFOLD, 21–33
MHC, 105, 106, 264–7, 269, 271, 272, 275, 276,
 280–282, 284, 286
Microarray, 389, 392
Microinjection, 328, 330
microRNA, 119, 122
Microsatellite, 391
Microtubule depolymerization, 141
Microtubules, 27, 29, 30, 32, 169, 170, 173–5,
 330–332, 335–8, 340
MID1, 170, 174
MID2, 170, 174
Midblastula transition, 106, 109, 334
Midbrain, 149, 2–7
 -hindbrain boundary, 149
Midzone, 103, 106
Mig12, 170, 174
Migrate, 248, 252–4
Migratory activity, 190, 195
Miller spreads, 7
miRNA, 195, 221, 385, 390
MITES, 388
Mitochondrial, 17–19, 27, 29–33, 61, 63, 69, 76–83
 cloud, 17–19, 27, 29–33, 61, 63, 69, 76–83
 cement, 61, 69
Mitotic spindle, 325–8, 330–334, 336–8
 scaling, 330–334
MLC, 169–172
MLCK, 193, 195
MLR, 266, 276, 278, 280, 281, 284, 285
MMPs, 357, 363
Mobilome, 383, 387, 390
Molecular, 18, 27, 29, 30, 32, 33, 66
 beacons, 66
 motors, 18, 27, 29, 30, 32, 33
Morphogen, 69
Morphogenesis, 217, 221–4, 228, 230, 232
Morpholino oligonucleotide, 179, 215–17, 225, 226,
 231, 391
Mos, 41, 46–51
Motor neurons, 246, 249
mRNA, 16–18, 23–5, 28, 34, 38, 40–43
 localization, 16–18, 24, 25, 28, 34, 41, 42
 element, 18
 poly[A] tails, 43
 trafficking, 23
 translation, 38, 40–42
mRNPs, 40–42, 45
Msx, 241, 248, 250, 251, 377

- Mucociliary epithelium, 113, 114, 117, 121, 123
 Mucus-secreting goblet cells, 113, 117
 Müller cells, 347–58
 Multiciliated cells, 112, 113, 122
 Musashi1, 43, 44, 47, 50, 51
 Musashi2, 44, 45
 Muscle regeneration, 371, 375
 Mutagenesis, 224
 Mutant, 384, 391, 392, 394, 395–397
 Mutation, 387, 391, 392, 394–7
 Myelocytes, 268
 Myosin, 105, 106, 190, 191, 193, 195
 heavy chain, 105, 106
 light-chain kinase, 193
 Myristoylated alanine-rich C kinase
 substrate, 171
- Nanos, 18, 33, 80, 81, 83–90
 Nanos1, 42, 43
 Narrowing, 164–6, 168, 171
 N-cadherin, 172, 173, 354, 357
 NCAM, 241, 245
 Nectrin-2, 170, 172, 173, 179, 180
 Nephrogenesis, 215, 217, 218, 220, 221, 223,
 230–232
 Nephron, 215–18, 220–224, 230–232
 regeneration, 215, 216, 223, 224, 231, 232
 Nephrostomes, 222
 Nerve regeneration, 294, 300, 304
 Nest, 61, 69
 Neural, 116, 117, 163–81, 239–57, 267, 269, 301
 ampulla, 301
 cell adhesion molecule, 245
 crest, 267, 269
 cells, 240, 248, 251–4, 257
 induction, 248
 GRN, 255, 256
 inducers, 164, 239
 induction, 116, 117, 242, 247, 255
 plate, 240–243, 246, 248, 250–255, 257
 border specifiers, 248
 regeneration, 293, 294, 301, 303–305
 retina, 293–295, 298–300, 305
 specification, 239–41, 243–5, 254, 256, 257
 tube, 163–81, 240, 242, 245, 246, 248, 249, 252–4
 defects, 163
 Neurepithelium, 349
 NeuroD, 241, 256
 Neuroectoderm, 242–8, 252
 Neurogenin, 255, 256
 Neuronal, 16, 254–6
 differentiation, 254–6
 synapses, 16
 Neurons, 245, 246, 248, 249, 254, 256, 295, 296, 299,
 300, 302, 304, 305
 Neurula, 133, 149, 150, 217–21, 223, 228
- Newt, 348–350, 352–4, 364
 NFkB/Rel signaling, 139, 140, 143–6
 NHEJ, 394
 Nieuwkoop center, 242, 243, 245
 Nigerian frog, 384, 391, 392
 Nkx2.2, 248, 249
 NMII, 169, 170, 172
 Nodal, 69, 141, 144, 242, 243, 245, 251
 flow, 69
 related proteins, 141, 144
 Noggin, 242–4, 246, 247, 373, 377
 Noggin1, 246, 247
 Noggin2, 246, 247
 Noncanonical pathway, 130–132, 134, 135, 138, 140,
 148, 149
 Noncoding RNA, 65, 66, 390
 Nonhomologous end joining, 394
 Nonmuscle myosin II, 169, 170
 Nonneural ectoderm, 163, 164, 172, 174–81
 Nonregenerative stages, 296, 303, 305
 Notch, 193, 194, 255, 256, 372–5
 Notochord, 166–9, 240, 246, 248, 249
Notophthalmus, 5, 8, 9, 11
 Notoplate, 166, 167
 NRPI, 245
 NTDs, 163
 Ntf2, 329, 330
 Nuclear, 139, 142–4, 146, 147, 150, 328–30, 334
 β-catenin, 139, 142–4, 146, 147, 150
 import, 329, 330, 334
 scaling, 328–30, 334
 Nuclease domain, 394, 395
 Nucleus, 16–18, 30–32, 325, 326, 328, 329, 331, 335,
 339–41
 Number of lymphocytes, 269, 275, 278, 286
 Nurse cells, 3, 4
- Oct4, 91
 Oct91, 91, 92, 114, 115
 Off-target, 395
 Olfactory nerve, 304
 Olig2, 248, 249
 Oocyte, 3–11, 134, 201, 203, 205, 206, 311, 312,
 314–17, 320, 322, 323
 Nucleus, 3
 transfer method, 134
 Oogenesis, 17, 18, 30, 60–62, 66, 69, 70, 190
 Oogonia, 61, 69, 201, 205, 206, 210
 Oolemma, 108
 Optic nerve, 293–5, 298–301, 304, 305
 Organ-based culture, 354, 355
 Organelle, 325–8, 334, 335, 339, 341
 scaling, 325–8, 334, 335, 339, 341
 size, 325–6, 334, 339, 341
 Organizer, 130, 131, 141, 145
 Organogenesis, 133, 138, 149

- Oscar, 20
Otx2, 241, 246, 362
Ovary, 199, 201–3, 205–7, 210
- p120-catenins, 172
Pachytene, 79
Pancreas, 107, 109
Parasympathetic, 248
PARN, 45, 46
Passive migration, 190
Pat1, 45, 46
Patterning, 131, 146, 217, 218, 220–223, 228
 of the gastrula, 146
 network, 131
Pax, 246, 248–51
Pax6, 346, 354, 355, 359, 361–4, 378
Pax7, 248, 249, 371
pax8, 218, 220, 223, 225, 228, 229
PCNA, 359
PCP, 119, 122–4, 131, 132, 134, 138, 140, 148, 149,
 167, 168, 171
Perchlorate, 272, 273
PGCs, 75–92, 189–95, 199, 200, 205, 210
Pharyngeal endoderm, 245
Phosphatase and tensin homolog, 192
Phosphatidylinositol 3-kinase, 192
Phospholipase C, 192
Phosphorylation, 104
Photoactivation, 31, 32
Photobleaching, 33
Phylogenetic comparisons, 21
piggyback, 388
Pigment, 17, 18, 248
 cells, 248
 granules, 17
PI3-kinase, 192, 193
PIP2, 192
piRNA, 82, 92, 390
Piwi, 83–5
Piwi RNA, 388–90
PKC, 131, 132, 135, 140, 149, 154, 172
Placophilin, 252
Planar polarity, 61, 68, 122, 131, 132, 148, 167
Plasma membrane, 311, 312, 314–22
PLC, 192
Ploidy, 265, 270, 279
Pluripotency, 114–16
Polarity, 16, 17, 29, 32, 34, 112, 117, 121–4
Polarized, 16–18, 27, 29, 34, 107–9
 cells, 107–9
pol III transcription, 5, 9, 12, 13
Polyadenylation factors, 30
Poly[A] polymerase, 45
Polymorphic, 271, 280
 histocompatibility, 280
Polymorphism, 280, 391, 392
 Positional cloning, 391, 392
 Posteriorizing activity, 148
 Prechordal mesoderm, 245
 Preplacodal ectoderm, 248
 Prickle, 134, 137, 148
 Primary oogonia, 78, 79
 Primordial germ cells, 195, 199, 200, 205, 210
 Progonad, 203
 Promoter, 215, 216, 226–8, 230, 232
 Pronephric, 215, 217, 218, 220, 228
 anlagen, 215, 217, 218, 220, 228
 field, 218
 Pronephros, 215–32
 Prrp, 26, 30–32
 Pseudoblastema, 303
 PTEN, 192
 pTransgenesis, 393
 Pum1, 47
 Pum2, 47, 48
- RA, 218–20
Rab, 32
Rac, 194
Radial intercalation, 176, 180
RAG, 266, 271, 273–5
RAP55, 41, 42, 45, 46
Rax, 346, 354, 355, 357, 360–364
 promoter, 355, 360, 361
Recognition domain, 394
Refractory period, 301
Regeneration, 294–6, 304, 369, 370, 373–5
 ability, 294–6, 304
 bud, 369, 370, 373–5
Regulatory, 388, 393
 elements, 393
 system, 388
REMI, 392, 393
Remodeling, 278, 282, 285, 286
Renal, 215, 216
 genesis, 215, 216
 maintenance, 216
REPFIND, 23, 24
Resources, 383, 387, 389, 392, 394
Rete testis, 204, 205
Reticulon, 81, 82
Retina, 299, 346–64
 pigmented epithelial cells, 299
Retinal, 295, 298, 300, 346–64
 ganglion cells, 295, 298, 300
 pigmented epithelium, 346
 regeneration, 346–64
 stem/progenitor cells, 346–8
 vascular membrane, 346, 348
Retinoic acid, 218, 246, 247
Retrotransposon, 387, 388
Retrovirus XTERV1, 387, 388

- Reverse genetics, 395
RhoA, 191, 194
Rho family, 170
Ribonucleoprotein, 5, 8, 11, 19, 25–34
Ribosomal RNA, 9, 11
 genes, 17
Ringo, 41, 47, 48, 50, 51
RNA, 6, 8, 18–23, 25–7, 29, 31, 32, 390, 391
 binding domains, 25
 binding proteins, 18–20, 23, 25–7, 29, 31, 32
 folding programs, 21
 kissing, 22
 polymerase II, 6, 8, 390, 391
 -RNA interactions, 22
RNase H-dependent mRNA degradation, 26
RNP, 5, 8, 11, 25, 26, 29, 31, 84
 -associated proteins, 25, 26, 29, 31
 -like material, 84
ROCK1, 170, 171
ROCK2, 170
Rod precursors, 347
Rohon-Beard primary neuron cells, 248
Roofplate, 246, 248
RPE, 298–300, 346–64
RRM, 42
rtn3.1, 81, 83
RT-PCR, 9
RVM, 346, 348, 350–352, 354, 357, 358, 362, 363
Ryk/Ror2, 131
- Salamander, 11
Satellite cells, 371, 379
Sdf1, 254
SDF-1, 192, 199, 200
SDF-1/CXCR4, 76
Sec1, 32
Secreted Wnt inhibitors, 146, 147
Seminiferous tubules, 203–5
Sensory neurons, 246
Septin, 106
Sequence repeats, 391
Sequestration, 40
Sertoli cells, 201, 204, 207, 208
Sex, 204, 206, 208–10
 hormones, 204, 209
 -linked markers, 206
 reversal, 206, 208–10
Sexual differentiation, 199, 200, 203, 204, 206, 208, 210
Shh, 241, 248, 249, 374, 376, 377
Shroom3, 170–174
Siamois, 139, 140, 143–6, 242
Signaling, 112, 115–17, 119, 120, 122, 124
siRNA, 225
sisRNA, 10
Site-specific insertion, 394
Six3, 362
Sleeping Beauty system, 393
Smad1, 243, 244
Small, 108, 109, 390
 intestine, 108, 109
 RNA, 390
Small RhoA GTPase, 105, 106
Smooth muscle cells, 248
Snail, 250–252
Somitic mesoderm, 167
Sonic hedgehog, 248, 249
Sox, 241, 243–5, 250, 251, 254–6
Sox2, 2957, 302, 305
SOX9, 207, 208
Space invader, 389
Specification, 217–20, 223, 228, 232
Spemann's organizer, 240, 242, 243, 245, 257
Sperm, 75, 82, 326, 327, 329–31, 333, 336
Spermatocytes, 205
Spermatogenesis, 204
Spermatogonia, 204, 205, 210
Spermatozoa, 205
Spikes, 303, 304
SPIN, 389
Spinal, 293–7, 300–303, 305, 369, 370
 ampulla, 369, 370
 cord, 293–7, 300–303, 305
 ganglia, 302
Splenocytes, 272, 275, 277, 285
Splicing factors, 30,
Split tolerance, 276, 281, 282,
43S preinitiation complex, 38–40
Stable intronic sequences, 10
Stat3, 254
Staufen, 20, 21, 23, 25–7, 30–32
Stem cell-derived factor 1, 192
Stem cells, 75, 77–9, 87, 91, 92, 268, 270, 271, 279
Stem/progenitor cells, 346–8, 350, 362
Steroidogenesis, 204
Strabismus/VanGogh, 134, 137, 140, 148
Strain, 391, 392
Stretching force, 177
Structural, 42, 43, 66, 67
 element, 42, 43
 function, 66
 role, 66, 67
Stump, 296, 297, 301–3
Su(H), 193, 194
Superficial epithelial cells, 164
Sympathetic, 248
Synapses, 34
Synaptic, 17, 34
 plasticity, 17
 transcriptome, 34
Syntaxin1B2, 21, 22
Synteny, 385, 386

- T3, 282
T4, 282
Tadpole, 217, 221, 222, 224, 227, 228, 230, 293–305
Tail, 293, 294, 296, 301, 302, 369–375
 amputation, 301, 302
 regeneration, 293, 294, 296, 301, 302, 369–375
Tailbud, 217, 220–223
TALENs, 394, 396, 397
Targeted genome editing, 393
TBP occupancy, 391
Tc1-mariner transposons, 388
TCR, 264, 266, 273–5, 282
TCS, 41, 43–5, 47, 48, 50, 51
TE, 387, 389, 390
Tectum, 301, 304, 305
Telencephalon, 293, 295, 304, 305
Temporal regulation, 48, 49
Tensile force, 177–180
Ternary complex, 38–40
Testis, 199, 201, 203–6, 210
 cord, 201, 203, 204
Testosterone, 204, 205, 208, 210
Tetraiodothyronine, 282
Tetrapod, 386, 389, 390
TGF β , 141, 144, 242, 243, 373–5
Thin-to-thick regions, 11
Thymectomy, 265, 268, 279, 285
Thymocytes, 268, 272, 276, 280, 281
Thyroid hormone, 296
Tissue, 131, 137, 140, 149, 346, 352–5, 359, 361, 362
 cultures, 346, 352–5, 359, 361, 362
 separation, 131, 137, 140, 149
TLRs, 264, 265
Tol2, 393
Tolerance induction, 276–8, 286
Toll-like receptors, 264, 266
Topoisomerase, 339
Transcription, 3, 4, 6–9, 220–224, 227
 factor, 220–224, 227
 units, 4, 6–9
Transcriptome, 387, 389, 390
Transcriptomic, 389, 390
Transdifferentiation, 122, 125, 298–300, 301, 346–55, 357, 3614, 371, 378, 379
Transection, 295–7
Transfer of cells, 281, 286
Transgenesis, 383, 392–394
 tools, 393
Transgenic, 215, 224, 226–8, 230, 232, 346, 355, 357–61
Translational regulator, 194
Transposable element, 387, 388
Transposase, 388, 393
Transposon, 387–90, 393
Trenbolone, 208, 209
Triiodothyronine, 270, 282
trim36, 81, 83, 86, 88
Trimethylated H3K4, 256
Triturus cristatus, 6, 11
Tub β 4, 24
Tubule, 215–24, 228–31
Tubulogenesis, 215, 230
Tumor cell lines, 265
Tunica albuginea, 204
Twin, 242
Tyrosinase, 395, 396

Ultracentrifugation, 311, 315, 316, 319, 322
Undifferentiated gonad, 199–203, 205–7, 210
Unilateral, 103, 108
Unineme hypothesis, 7
Untranslated exons, 387
UTR, 19–21, 24
UV-irradiation, 141

Vangl2, 68
Vasa, 82, 83, 85–7
V-ATPase, 373, 374
VBI, 266, 268, 269
Vegetal, 17–20, 23, 24–33, 60, 61, 63, 64, 67, 69, 190
 cortex, 17–20, 23, 25–33, 190
 hemisphere, 17, 27, 60, 61, 63, 64, 67, 69
 localization pathway, 32
 pole, 17–19, 24, 25, 33, 190
Vegetally localized RNA, 64–7, 69, 140, 141
VegT, 17, 19, 27, 33, 65, 66, 68, 88–90, 114–16, 141, 144, 145
VegT/Veg1, 242, 243
Ventral blood islands, 266, 268
Vera/Vg1RBP, 20, 25, 26, 28–32
Vertical transmission, 389
Vg1, 17–22, 25–30, 32, 33, 41, 42
VgRBP60, 25, 26
VH families, 275
Vitellogenesis, 206
VM1, 25, 26

Wnt, 130–154, 168, 171, 218, 220–224, 226, 227, 230, 354, 372–7
 expression, 130, 133, 134
 signal activities, 130
 -Fz-Daam-RhoGTPase/JNK pathway, 131
 /PCP pathway, 168, 171
 -receptor specificity, 134, 135
Wnt5a, 131–4, 137–140, 143, 147–51
Wnt11, 131–5, 137–9, 142, 143, 145, 147–9, 151, 152, 154
WPRE, 393

XASH3, 256
Xcat-2, 17, 19–23, 27, 29, 33

- Xdazl*, 80, 81–3, 85, 87, 89, 194, 195
XDeadEnd, 194, 195
X-Delta-2, 193
Xdsh, 168, 179
Xenopus borealis, 21
Xenopus glutamate receptor interacting protein 2, 193
XGRIP2, 193, 194
Xic1, 256
Xiwi, 84, 85
X-linked Opitz G/BBB syndrome, 174
Xlsirt, 19, 22, 27, 29, 33, 65, 66, 81
xNorrin, 242
Xnr1, 242
Xnr3, 140, 143, 144, 146
Xpat, 23, 24, 80–83, 85, 189
xPRMT1b, 243, 245
XSlug, 248
XSnail, 248
XStau, 26, 27
XTwist, 248
Xwnt-11, 29
Yolk, 10, 17, 200, 206
 formation, 10
 protein, 17
Zar2, 41, 44, 45, 47, 52
Zebrafish, 192–5
ZFNs, 394–7
Zic, 241, 243, 244, 248, 250, 251, 254–6
Zinc finger, 394–7
ZO-1, 170, 178
Zygotic *Wnt8*, 145, 146

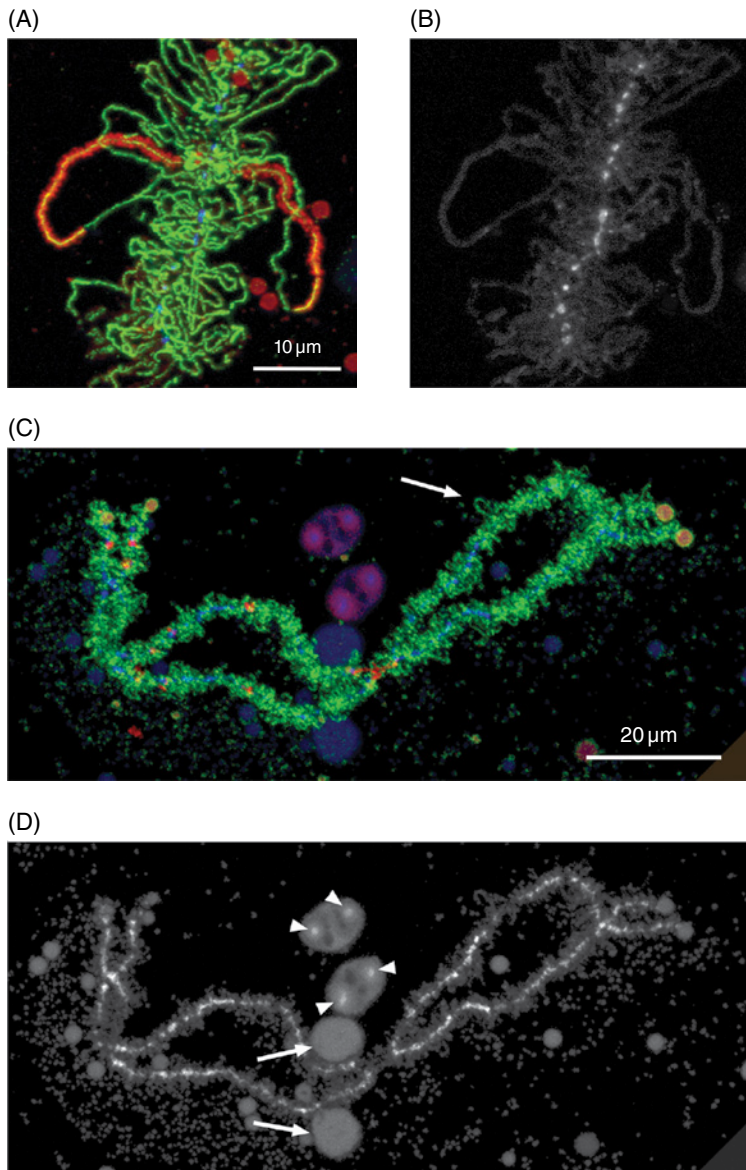


Plate 1 LBCs of the newt *Notophthalmus viridescens* (A and B) and *X. tropicalis* (C and D). (A) A short segment of an LBC stained with antibodies against pol II (green) and the RNA-binding protein CELF1 (red) (Morgan 2007). The axes of all loops appear as diffraction-limited green lines, because they are covered with closely spaced pol II molecules. One pair of sister chromatids is preferentially stained with CELF1, revealing the prominent thin-to-thick orientation of the associated loop matrix (RNP transcripts). (B) The same segment of LBC stained with the DNA-specific dye DAPI reveals the axis of transcriptionally inactive chromomeres. (C) Bivalent No. 2 of *X. tropicalis* stained with antibodies against pol II (green) and pol III (red). The vast majority of loops are transcribed by pol II. The loops of *X. tropicalis* are much shorter than those of the newt, and only a few are recognizable as loops in this image (arrow). (D) The same bivalent showing strong staining of the chromomere axes with DAPI. DAPI also reveals two amplified rDNA cores (arrowheads) in each of two extrachromosomal nucleoli. Regions of high protein concentration in the nucleoli also bind DAPI to a lesser extent. The same is true of two moderately stained structures near the middle of this bivalent (arrows), which represent loop pairs whose matrix has fused into a single large mass (lumpy loops).

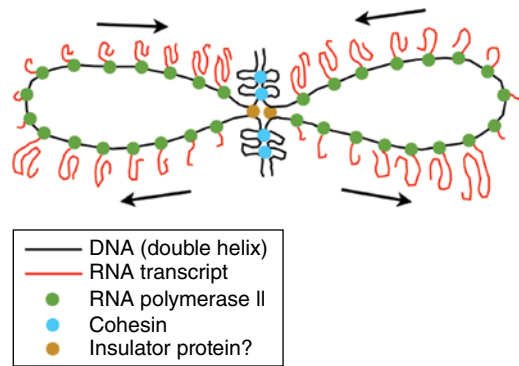


Plate 2 Highly stylized diagram of LBC structure. Transcriptionally active sister chromatids extend laterally from the main axis of the chromosome, which consists of regions where transcriptionally inactive sisters are closely paired and associated with cohesins (Austin et al. 2009). Loops can consist of one or more TUs, which may have either the same or opposite polarities on the same loop. RNA polymerase II molecules are packed closely along the DNA axis of each loop and elongating RNA transcripts are attached to them. The transcripts are associated with various proteins, including splicing factors (not shown here). It is not known what holds the bases of the loops together. One possibility is that insulators or similar molecules that define transcriptionally active regions of chromatin are involved.

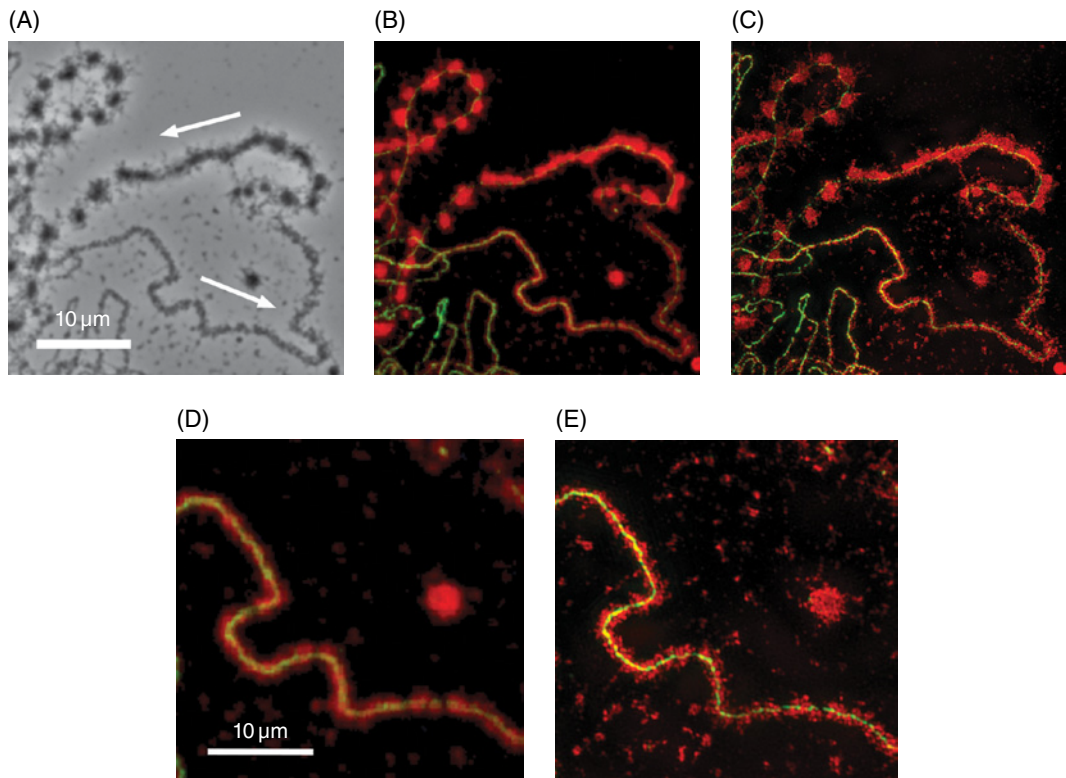


Plate 3 Images of a loop from the newt *N. viridescens*. (A) The entire loop imaged by phase contrast microscopy. The pronounced thin-to-thick polarity of the RNP matrix signifies the direction of transcription (arrows). (B) A confocal image of the same loop after immunostaining with mAb H14 against phosphorylated pol II (green) and mAb Y12 against symmetrical dimethylarginine, an epitope found on several splicing snRNPs (red). Green pol II stain is evident at the thin end of the loop but is obscured by the heavy mAb Y12 stain along most of the loop. (C) Image of the same loop taken by structured illumination superresolution microscopy. (D) Confocal image of the thin end of the loop at higher magnification. (E) The same loop imaged by structured illumination microscopy. Pol II now appears as a green line of nearly uniform width along the length of the loop. The red RNP matrix is resolved into a series of small particles about 50 nm in diameter. The superresolution images were taken on a DeltaVision OMX structured illumination microscope by Sidney Shaw and James Powers, Department of Biology, Indiana University.

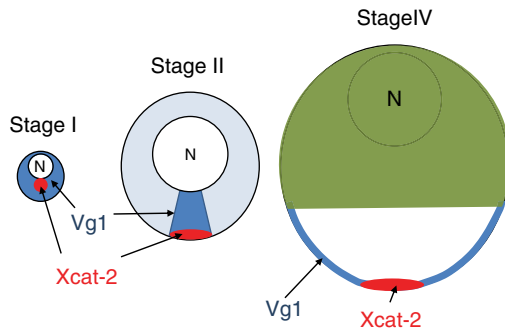


Plate 4 Distribution of early- and late-pathway RNAs in stage I-IV oocytes. On the left is a stage I oocyte showing the nucleus (N), the Vg1 mRNA distributed throughout the cytoplasm (blue), and the Xcat-2 localized to the Balbiani body or mitochondrial cloud adjacent to the nucleus (red). By stage II, the mitochondrial cloud and early-pathway RNAs have moved to the vegetal cortex, whereas late-pathway RNAs, such as Vg1 (blue), begin to localize to a wedge-shaped structure between the nucleus (N) and the early-pathway RNAs at the vegetal pole. A stage IV oocyte is shown on the right with a pigmented animal hemisphere at the top and Vg1 (blue) distributed through most of the vegetal cortex. Xcat-2 (red) and other early RNAs remain in the vegetal cortex but mostly at the vegetal pole. The oocytes are drawn to relative scale with the stage I oocyte being approximately 100 μM in diameter. The process of growing from a stage I to stage IV oocyte takes months in an adult female. For a comprehensive book of protocols and high-quality photos of different-staged oocytes, the reader is referred to volume 36 of *Methods in Cell Biology* (O'Keefe et al. 1991).

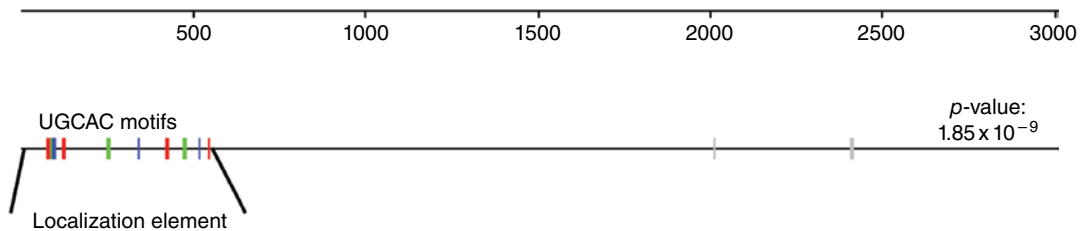


Plate 5 REPFIND output of the Xpat 3'-UTR. REPFIND was used to identify the most significant cluster of any repeat greater than 5 nt in length. The scale bar at the top represents the length of the 3'-UTR in nt. The colored bars represent UGCAC motifs (different colors are used to help visual counting only) considered in the calculated p -value shown at the right. The two grey bars to the right represent UGCAC motifs that were not included in the calculation. The p -value is the probability of finding this particular cluster. The first approximately 550-nt fragment localizes when injected into oocytes, whereas the remaining approximately 2.5-kb fragment does not (Betley et al. 2002).

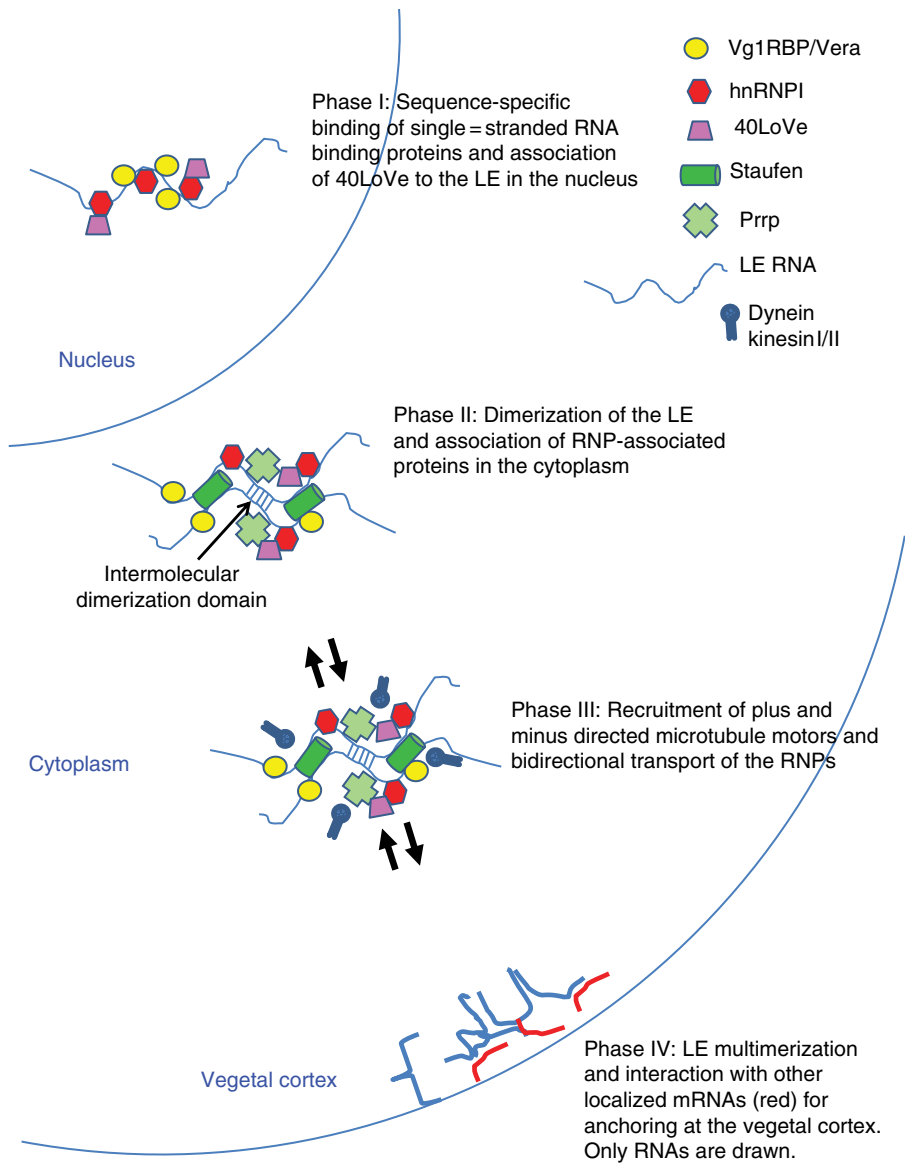


Plate 6 Four hypothetical phases to RNA localization in *Xenopus* oocytes. Features of the *cis*-elements that specify vegetal localization and the proteins involved in the localization process are described in the text. In this figure, sequence-specific RNA binding proteins and RNP-associated proteins, including the double-stranded RNA binding protein Staufen, are depicted as the indicated symbols at the upper right of the figure. A generic RNA LE that directs a particular mRNA to the vegetal cortex is shown as a squiggly line. During the first phase, the RNA is mostly single-stranded in the nucleus. Phases II and II occur throughout the cytoplasm, while the fourth phase, anchoring, occurs in the mitochondrial cloud of stage I oocytes (not depicted) or the vegetal cortex of stage II–IV oocytes.

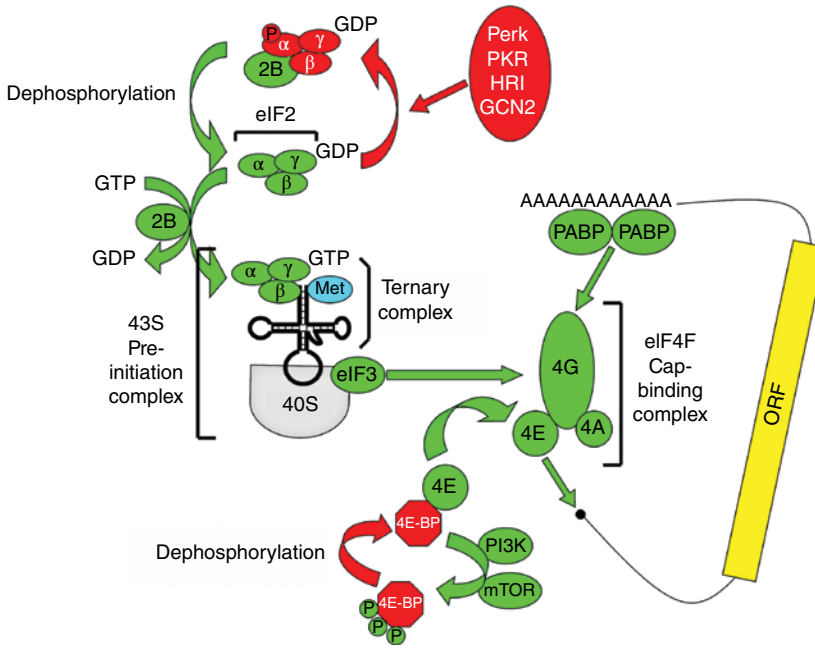


Plate 7 Translation initiation. Translation initiation in eukaryotes is a complex, multistep process. Of central importance is the formation of two major complexes: the 43S preinitiation complex and the eIF4F cap-binding complex. Formation of both complexes can be regulated to control gene expression. ORF, open reading frame; PABP, poly[A] binding protein; eIF, eukaryotic initiation factor; Met, methionine; PI3K, phosphoinositide 3-kinase; mTOR, mammalian target of rapamycin; 4E-BP, eIF4E binding protein; GTP, guanine triphosphate; GDP, guanine diphosphate; PERK, PRK-like ER kinase; PKR, protein kinase double-stranded RNA dependent; GCN2, general control nonderepressible-2; HRI, heme-regulated inhibitor.

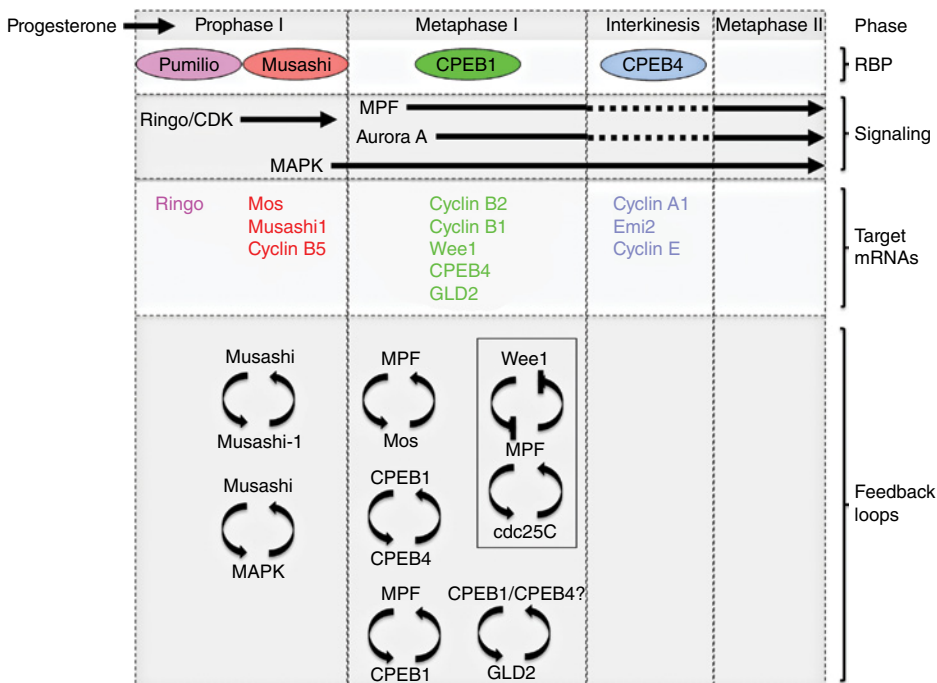


Plate 8 A series of positive feedback loops mediate amplification of a weak progesterone "trigger" signal to trigger activation of MPF. The sequential action of specific RBP regulates the ordered activation of signal transduction pathways and temporal recruitment of maternal mRNAs during meiotic cell cycle progression. A number of nested positive feedback loops contribute to the amplification of the initial progesterone stimulus and all-or-none transition through the cell cycle. For the purposes of focus on mRNA translational control and clarity, a number of negative feedback loops have been omitted. See text for details.

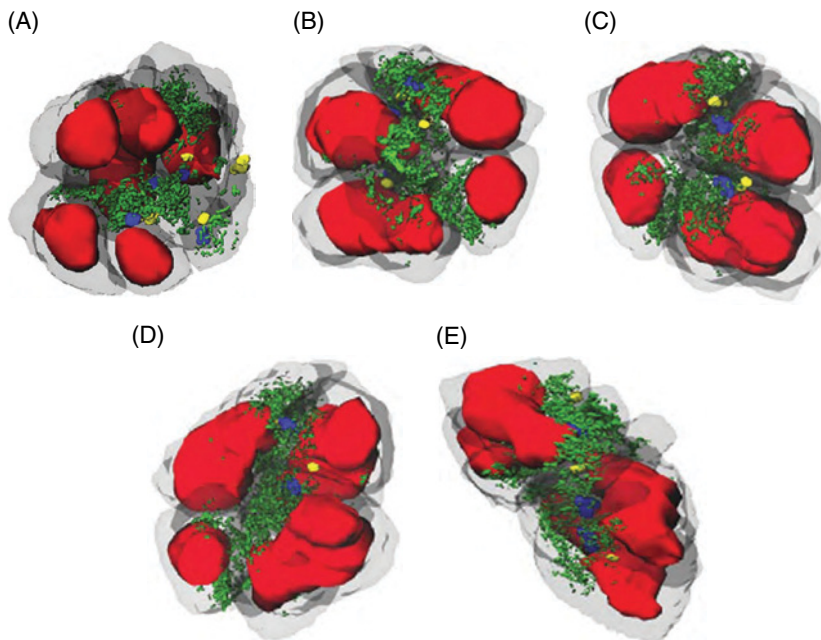


Plate 9 Three-dimensional reconstruction of interphase cysts. Two different eight-cell cysts with six nuclei visible. Cyst 1 (A) and four different views of cyst 2 (B–E). Cytoplasm is gray, nuclei are red, mitochondria of PMC are green, centrioles are blue, and ring canals are yellow. In cyst 1, five ring canals and four centrioles near the PMC and ring canals are visible. Spatial relationships between mitochondria, centrioles, and ring canals are visible in all reconstructions. Also note the constant distance (2 μm) between the centrioles and ring canals in all cystocytes (see text). PMC, ring canals, and centrioles face each other and are located centripetally in “the rosette” conformation (see text). These reconstructions were from 38 serial ultrathin sections similar to the section shown in Figure 1B in Kloc et al. (2004a). Reprinted from Kloc et al. (2002) © with permission from Elsevier.

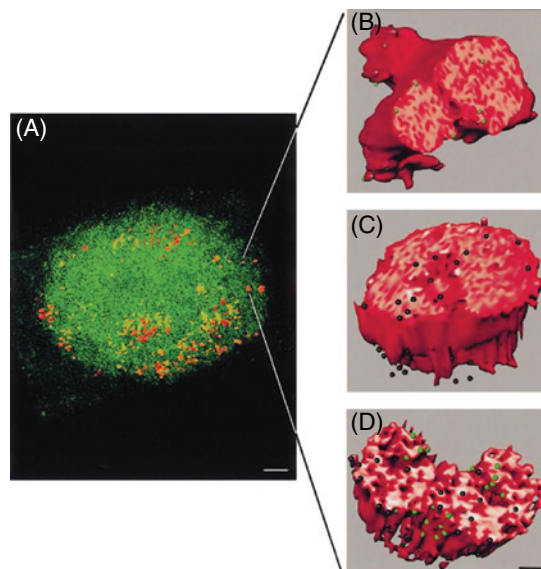


Plate 10 Three-dimensional ultrastructural reconstruction of mitochondrial cloud and germinal granules in stage I oocyte. (A) The mitochondrial cloud was reconstructed from 21 serial electron microscopy (EM) sections. The cloud is a sphere composed of thousands of mitochondria (green speckles) and germinal granules (red spheres). Germinal granules are concentrated in the form of a ring in the METRO region that is the part of the cloud facing the vegetal pole and are excluded from the center of the cloud. The oocyte nucleus, not visible in the picture, is above, and the vegetal pole of the oocyte is below the plane of the picture. (B and D) The half sections of three germinal granules from a mitochondrial cloud similar to the one shown in A. The images were reconstructed from four serial sections of oocytes hybridized *in situ* with Xpat (B and D) and Xcat2 (C and D) antisense RNA probes. The Xpat RNA (green dots) is predominantly on the granule periphery with a small portion localized internally, while the majority of Xcat2 (black dots) is sequestered internally in the granule. For better clarity of the image, the original silver-enhanced gold label was replaced (using proper logarithm and computational programs; see Materials and Methods in Kloc et al. 2002) with uniform-sized dots. The bar is equal to 4.5 μm in A and 250 nm in B–D. Reprinted from Kloc et al. (2004) © with permission from Elsevier.

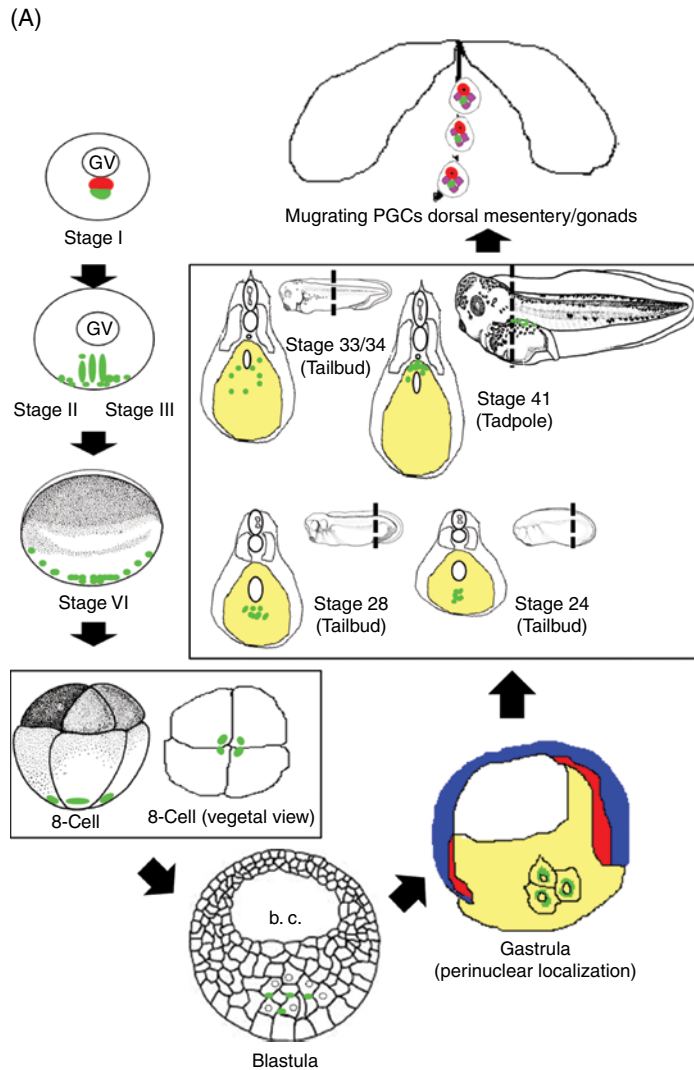


Plate 11 Schematic of germline formation in *Xenopus laevis*. (A) Stage I oocyte: germ plasm (green) assembles in MC (red) in close association with the germinal vesicle (GV). Stage II/III oocyte: MC fragments and moves toward the vegetal cortex. Stage VI: germ plasm within the vegetal cortical area. Eight-cell embryo: germ plasm is inherited by vegetal blastomeres shown from the lateral and vegetal pole perspective. Blastula: germ plasm lies near the plasma membrane of four to six cells, the pPGCs. Gastrulation: germ plasm translocates by a microtubule-based mechanism to a perinuclear position. The germline (PGCs) is now segregated from endoderm lineage (yellow, endoderm; red, mesoderm; blue, ectoderm). Tail bud stages 24–34: PGCs begin migration steps clustering, dispersing laterally, directionally migrating dorsally, and, at tadpole 41, reaggregating at the dorsal tip of the endoderm (adapted from Figure 1e'–h' in Terayama K, Kataoka K, Morichika K, Orii H, Watanabe K, Mochii M. Developmental regulation of locomotive activity in *Xenopus* primordial germ cells. *Dev Growth Differ* 2013;55(2):217–228.) Tadpole: PGCs migrate along the dorsal mesentery to reach the presumptive gonads.

(B)

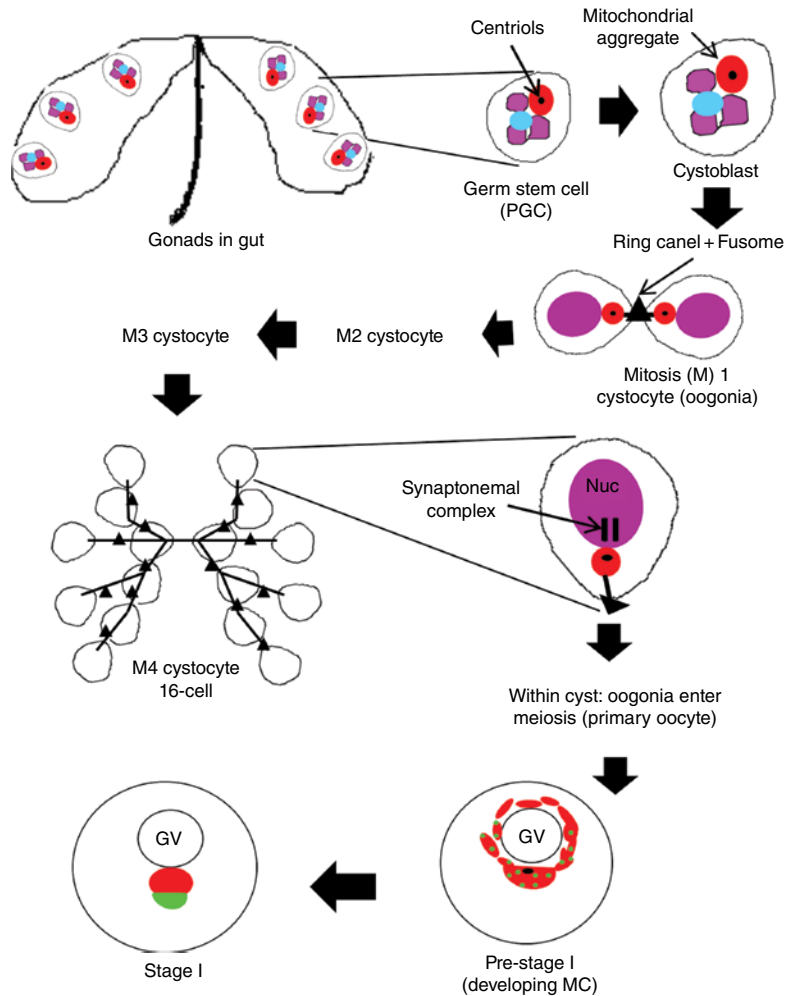


Plate 11 (continued) (B) Tadpole: PGCs enter somatic gonads where they pass through a mitotic proliferative stage (germ stem cell, cystoblast). Female germline cyst formation: at some point, cystoblast will undergo incomplete cytokinesis, remaining connected through four divisions (M1–M4) by cytoplasmic bridges (ring canals) to form the germline cyst. Note the polarity that is maintained throughout the divisions. Mitochondrial aggregate, the synaptonemal complex, the centriole, the ring canal, and the fusome that likely indicate the future vegetal pole of the oocyte. Primary oocyte: oogonia enter meiosis and transition into primary oocyte within cyst. During prophase, follicle cells move between oocytes and the interconnections are lost. Pre-stage I oocyte: mitochondria aggregates surround the nucleus (GV) with the aggregate containing the centriole becoming the major site of germ plasm formation. Stage I oocyte: mature MC with germ plasm assembled toward the vegetal pole. Germ plasm or PGCs (green), mitochondria (red), centriole (black dot), nucleus (purple), nuage (light blue), synaptonemal complex (black bars), ring canal (black line), and fusome (black triangle). (Adapted from Figs. 8 and 10 in Kloc M, Bilinski S, Dougherty MT, Brey EM, Etkin LD. Formation, architecture and polarity of female germline cyst in *Xenopus*. *Dev Biol* 2004a;266(1):43–61.) (All staging is according to the Normal Table of *Xenopus laevis* (Nieuwkoop and Faber 1967) (Daudin), Amsterdam: North-Holland Publishing Co.)

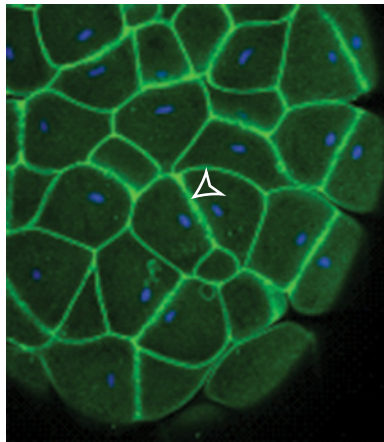


Plate 12 Localization of MELK in a *Xenopus* blastula stage embryo. MELK (green) is localized at cell–cell contacts. In dividing cells, MELK is also concentrated at the division site (empty arrowhead) between mitotic chromosomes. DNA is in blue.

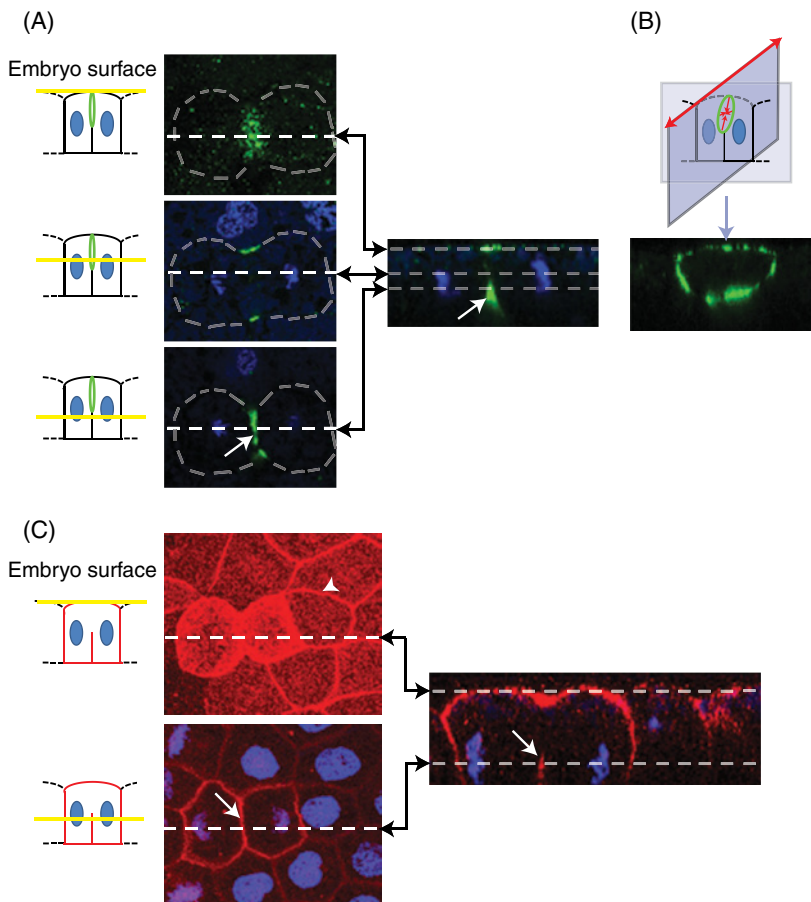


Plate 13 Localization of anillin and MELK in dividing gastrula stage embryo. (A) Localization of anillin (green) in the epithelium of a gastrula stage embryo. Diagrams on the left: yellow lines mark the confocal planes relative to the embryo surface. Grey dashed lines were drawn to indicate the limits of the dividing cell. White dashed line symbolizes the plane used for orthogonal projection of the confocal planes shown on the right. The green circle corresponds to the closing cytokinetic furrow. The arrow points to the asymmetric cytokinetic furrow. (B) Anillin localizes as a ring between the two daughter cells as shown on the orthogonal projection of the confocal planes. (C) Localization of MELK (red) in the epithelium of a gastrula stage embryo. Diagrams on the left: yellow lines mark the confocal planes relative to the embryo surface. White dashed line symbolizes the plane used for orthogonal projection of the confocal planes shown on the right. In interphase cells, MELK is localized at the apical junctional complexes (white arrow). In cells undergoing cytokinesis, MELK is localized all around the cell cortex as shown by the orthogonal projection.

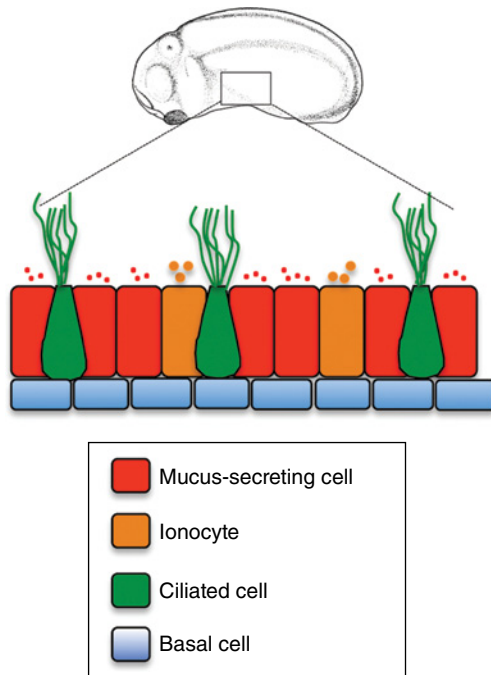


Plate 14 Cellular composition of the mature *Xenopus* embryonic epidermis. At the tail bud stage, the epidermis exhibits its final aspect. MCCs (green) and ionocytes (brown) are inserted in the superficial epithelial layer among mucus-secreting cells (red). Cells in the inner layer (blue) display a flattened morphology and rest on a basal lamina (not represented). Note the production of small secretory vesicles by mucus-secreting cells and of larger vesicles by ionocytes.

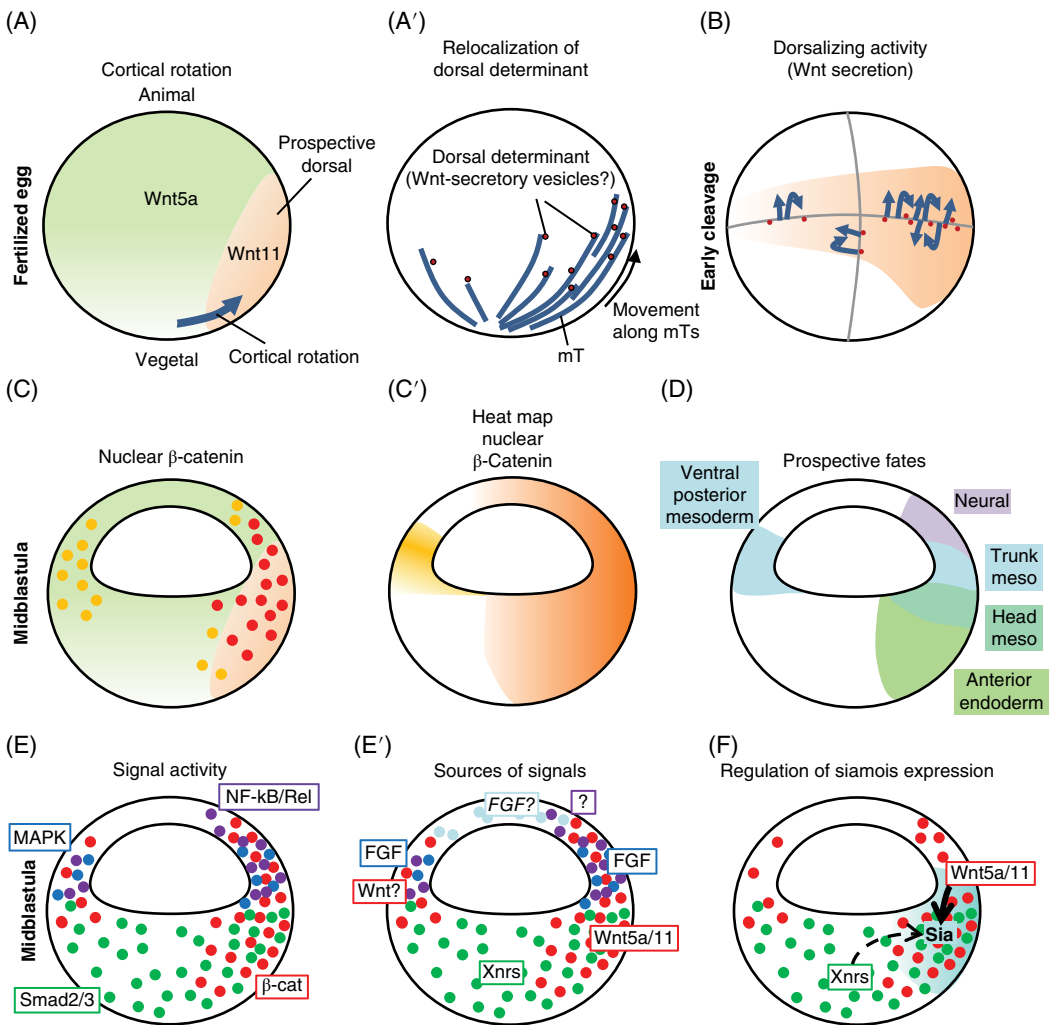


Plate 15 Maternal Wnt- β -catenin. (A) Distribution of Wnt ligands in the fertilized embryo. Two major maternal ligands are present in the *Xenopus* egg: Wnt11 mRNA is vegetally localized in the oocyte. After fertilization, Wnt11 protein is relocalized to the side opposite to sperm entry, due to a movement of the egg cortex called cortical rotation (Schroeder et al. 1999). Wnt5a mRNA is not localized. The shallow gradient represents the default distribution common to most *Xenopus* transcripts, with lower levels in the yolk-rich vegetal pole. (A') Cortical rotation of maternal dorsal determinant. Relocalization of the dorsal determinant has been shown to depend on microtubules. A subpopulation of microtubules is organized in parallel arrays on the prospective dorsal side, and vesicles have been observed to move toward the equator (Houlston 1994). These vesicles most likely transport Wnt11, either ready to be secreted, or possibly already interacting with its receptors Fz7 and LRP6. Note that the global microtubule distribution has not yet been established. The sparser tracks of microtubules on the ventral side represent a hypothetical broader gradient of upward relocalization yielding to a graded Wnt11 distribution around the equator (panel B), which would explain the presence of nuclear β -catenin all around the equator in the blastula (panel C, see Schohl and Fagotto 2002, 2003). (B) Hypothetical activation of the early maternal Wnt pathway. The β -catenin-activating determinant is here assumed to consist of Wnt11-containing secretory vesicles. Several lines of evidence indicate that the pathway is already activated at early cleavage stages, presumably through both paracrine and autocrine signaling (arrows). (C) Nuclear β -catenin localization (dots) in the early blastula. The diagram compares Wnt5a/Wnt11 distribution (after cortical rotation) and nuclear β -catenin localization in the blastula, is based on Schohl and Fagotto (2002). (C') Corresponding heat map of predicted β -catenin signaling activity. (D) Prospective regions under the influence of maternal Wnt- β -catenin signaling. Maternal β -catenin takes part in the determination of several different regions that correspond to the future neuroderm, trunk and head mesoderm, and anterior mesoderm. (E) Distribution of the four major inducing signals in the *Xenopus* blastula. Nuclear activated MAPK, Smad2 and β -catenin distributions have been established by Schohl and Fagotto (2002). NF κ B/Rel activity has been detected using a reporter gene (Armstrong et al. 2012). (E') Correspondence between nuclear signals and soluble ligands. A maternal FGF contribution has been suspected but not demonstrated (light blue). However, most of the FGF activity is probably due to early zygotic FGF ligands induced by maternal β -catenin and Xnrs (dark blue). Indirect evidence argues that the NF κ B/Rel pathway is controlled by maternal extracellular ligands (Armstrong et al. 1998). (F-F'') Interplay between the four signaling pathways. (F) Siamois (and closely related Twin) account for the transcriptional dorsalizing activity. They are direct targets of maternal β -catenin, with also a contribution from Xnr/Smad2 signaling.

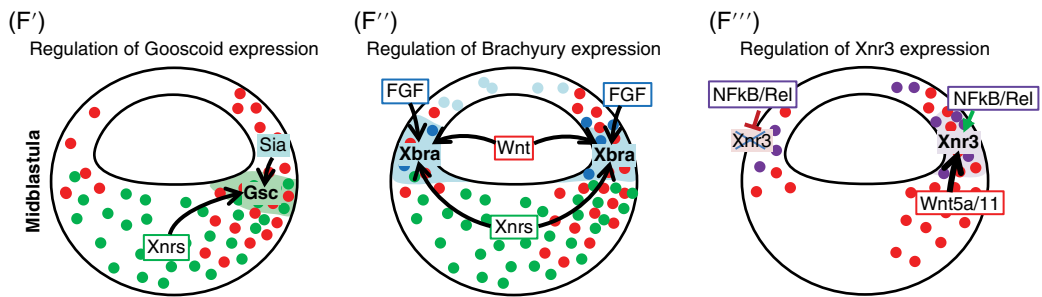


Plate 15 (continued) (F') Head mesoderm transcription factor Goosecoid (Gsc) is activated by the joined activities of Siamois and Xnrs. (F'') Posterior and ventral mesoderm induction (Xbra) requires cooperation of Wnt, Xnr and FGF signaling. Note that the animal and vegetal boundaries of Xbra expression are further constrained by additional mechanisms (reviewed in Heasman 2006) (F''') Xnr3 is an active component of the dorsalizing center, required in particular for formation of the neuroderm. Xnr3 is a direct target of Wnt- β -catenin and NFkB/Rel pathways. Note the repressive action of ventral NFkB/Rel (Armstrong et al. 1998).

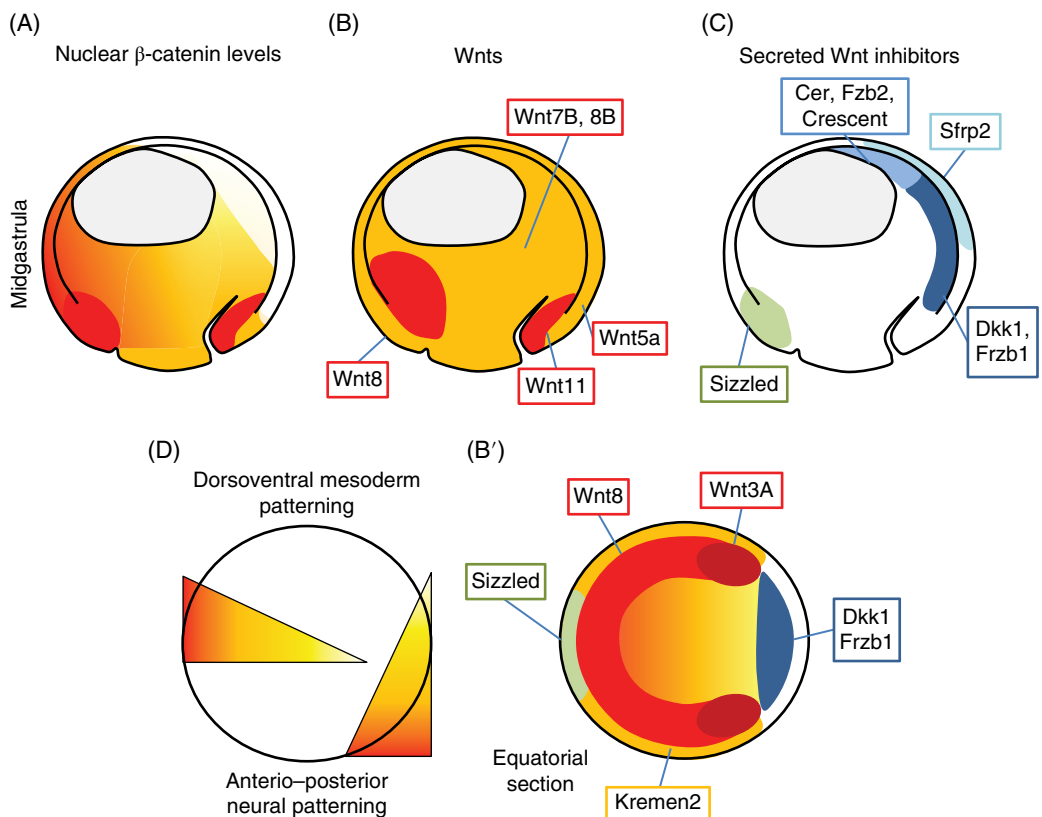


Plate 16 Wnt- β -catenin signaling in the *Xenopus* gastrula. The diagrams depict β -catenin signaling (A) (Schohl and Fagotto 2002) and the contribution of various Wnts (B, B', red-orange) and Wnt secreted inhibitors (C, B', blue-green), inferred from published *in situ* hybridization (summarized in Table 1, see Xenbase; Bouwmeester et al. 1996; Salic et al. 1997; Wang et al. 1997; Bradley et al. 2000; Pera and De Robertis 2000; Mao and Niehrs 2003; Hassler et al. 2007). (D) Two major sources of Wnts control β -catenin signaling during gastrulation (Heasman 2006; Hikasa and Sokol 2013): (A) ventro-lateral Wnt8 in involved in mesoderm patterning and is required in particular for expression of the myogenic MyoD in the paraxial mesoderm. A dorsal posterior source, probably due to a combination of Wnt3A, expressed in the paraxial mesoderm, and Wnt5a/Wnt11, expressed in the blastopore lip, provides a posteriorizing signal that patterns the neuroderm. A large number of soluble antagonists are secreted in the dorsal side, mostly by the anterior and trunk mesoderm. Their function is required for development of head and dorsal structures. An additional Wnt inhibitor, Sizzled, is expressed in the most ventral side and moderated there the action of Wnt8. Wnt8 activity is reinforced on the lateral sides by the agonist Kremen2.

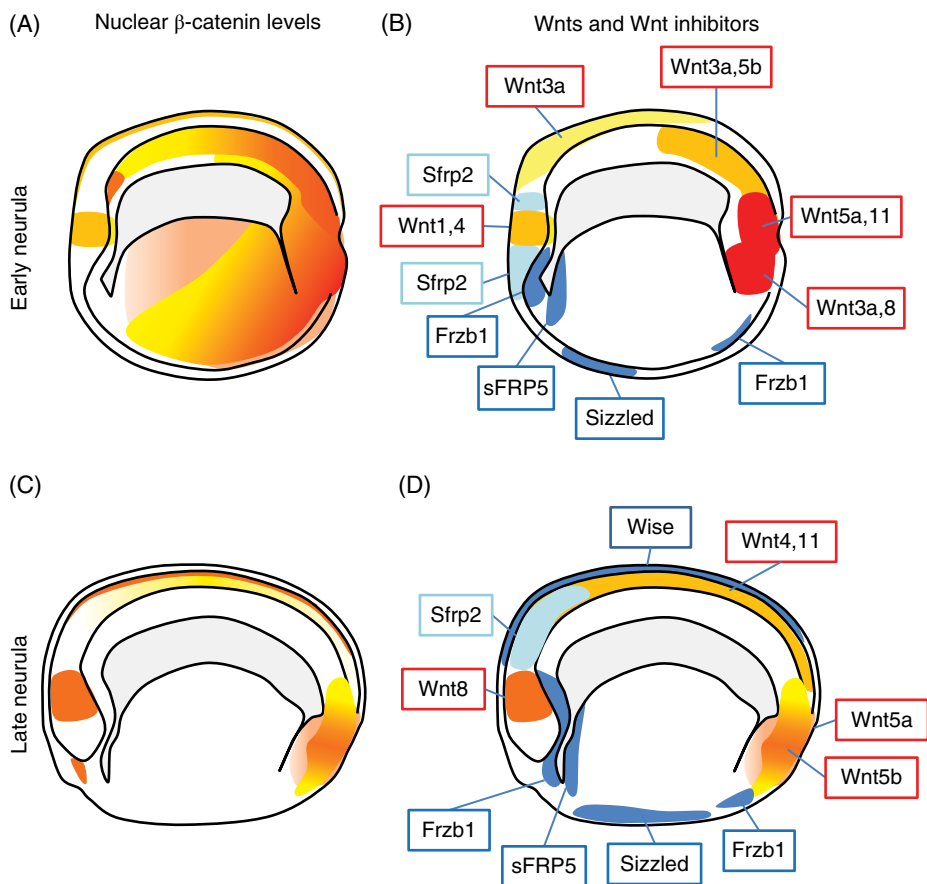


Plate 17 Wnt- β -catenin signaling in the *Xenopus* neurula. β -Catenin nuclear localization (A and C) and Wnt and Wnt inhibitor expression (B and D). Most of the β -catenin activity seems to be explainable by the published Wnts and Wnt inhibitors (summarized in Table 1, see Xenbase; Wang et al. 1997; Bradley et al. 2000; Pera and De Robertis 2000; Pilcher and Krieg 2002; Bell et al. 2003; Itasaki et al. 2003; Mao and Niehrs 2003), although direct systematic studies are lacking for most of the cases.

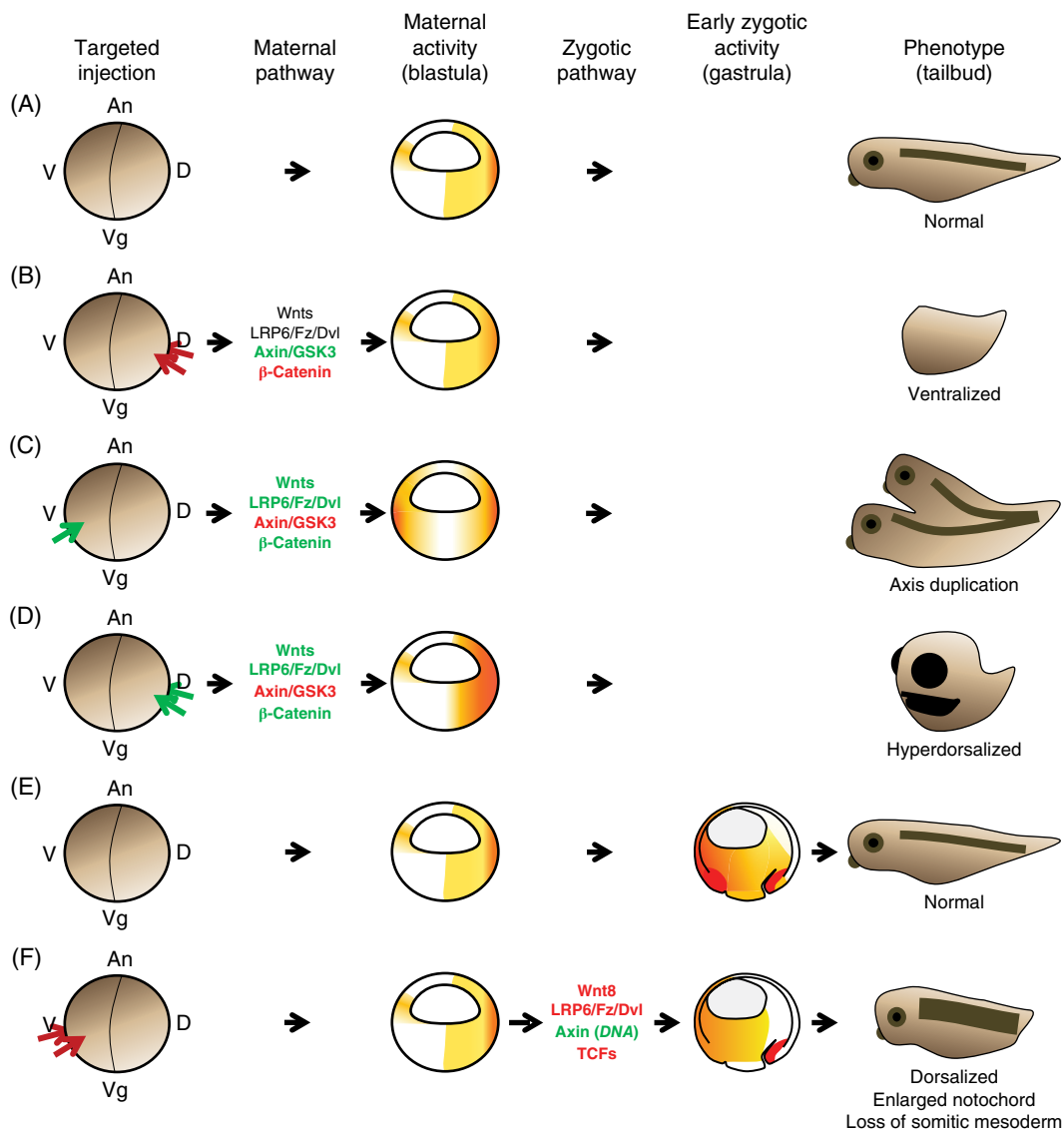


Plate 18 Major experimental interference strategies and corresponding phenotypes. (A) Normal maternal β -catenin signaling. (B) Endogenous maternal Wnt- β -catenin signaling can be blocked by dorsal injection of inhibitory reagents (red, e.g., β -catenin MO, Heasman et al. 2000, or dominant negative TCF3, Molenaar et al. 1996), or overexpression of negative regulators (green, such as Axin, Zeng et al. 1997). The resulting phenotype is a ventralized embryo. The severity of the phenotype ranges from reduction of anterior structures (cement gland, eyes) to complete loss of anterior and dorsal structures. The pathway cannot be inhibited by targeting upstream components of the pathway (black, e.g., Dsh). Interference with these upstream steps requires manipulations (depletion) in the oocytes (Tao et al. 2005; Kofron et al. 2007; Tadjuidje et al. 2011). (C) Ectopic activation in the ventral side produces embryos with duplicated anterior/dorsal structures (siamese twins). Manipulations include expression/overexpression of any positive regulator (green, e.g., Wnts, Smith and Harland 1991), or interference with negative regulators (red, e.g., dominant negative GSK3, Pierce and Kimelman 1995). Note that while dominant negative Axin forms injected as mRNA readily block maternal signaling (Fagotto et al. 1999), Axin MO fail to do so, presumably because maternal Axin is sufficiently stable (Schneider et al. 2012). (D) Similar manipulations on the dorsal side produce hyperdorsalized embryos, with large heads and reduced tail. (E) Normal maternal and zygotic β -catenin signaling. (F–G) Injections of reagents interfering with upstream components, such as Wnt inhibitors (Glinka et al. 1998) or dominant negative Wnt constructs (Hoppler et al. 1996) do not interfere with the maternal dorsalizing signal, but affect zygotic signals. (F) Ventral injections perturb mesoderm patterning, leading to axial defects (enlarged notochord and reduced or absent somites).

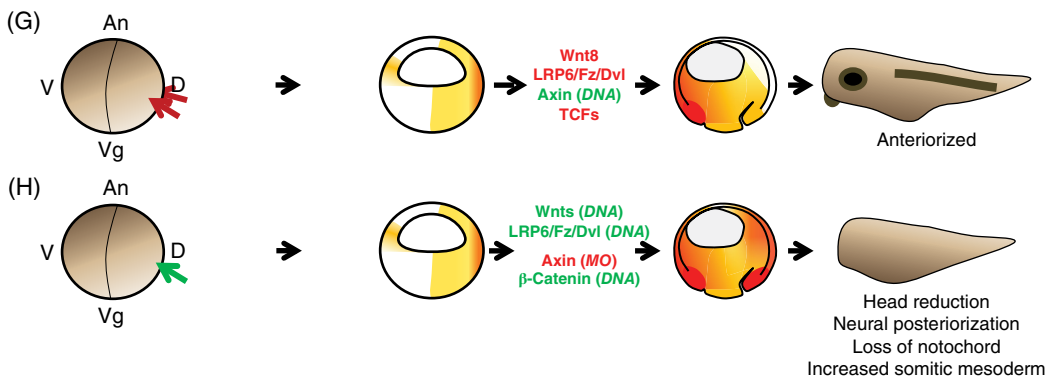


Plate 18 (continued) (G) Dorsal manipulations affect neural patterning (anteriorization). The same phenotypes are observed when with a positive components (e.g., β -catenin-Engrailed repressor, Montross et al. 2000) by injection of plasmid DNA. Because zygotically transcribed constructs only reach significant levels of expression in the late blastula/early gastrula, they do not affect maternal patterning. (H) Zygotic activation of the pathway can be similarly achieved by injection of plasmid DNA coding for example for Wnts, Wnt receptors, Dsh or β -catenin. The phenotypes include reduction in head structures and general posteriorization of the neural tube, decrease or loss of notochord and expansion of the somitic mesoderm. Axin depletion by morpholino injections is another example leading to the same phenotype (Schneider et al. 2012).

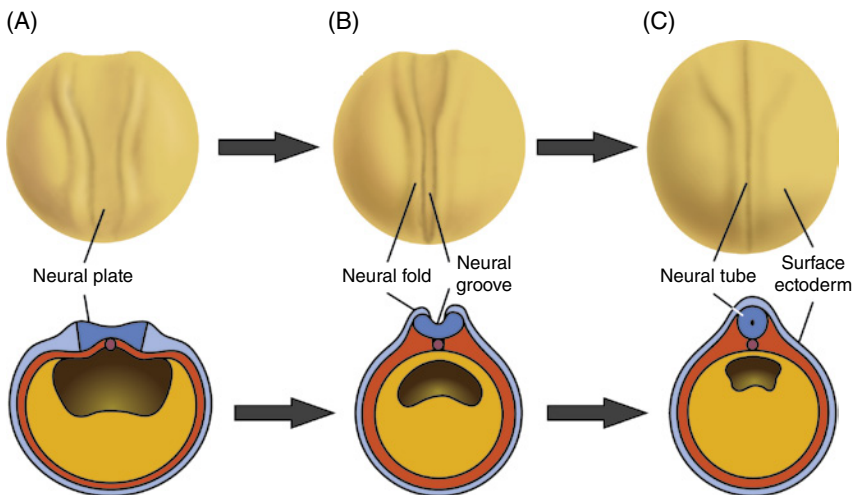


Plate 19 *Xenopus* neural tube formation. Dorsal views (Top) and transverse sections (Bottom) of generalized amphibian embryos in early (A), middle (B), and late (C) neurulae. (A) By the end of gastrulation, a flat neural plate (blue) is formed as a thickening of the ectoderm on the dorsal surface of the embryo. (B) The lateral borders of the neural plate rise to form the neural folds. As development proceeds, the neural folds continue to rise, and the neural plate bends to form the neural groove. (C) The edges of the neural folds eventually meet at the dorsal midline, where they fuse to form a hollow structure, the neural tube, positioned beneath the overlying surface ectoderm (light blue).

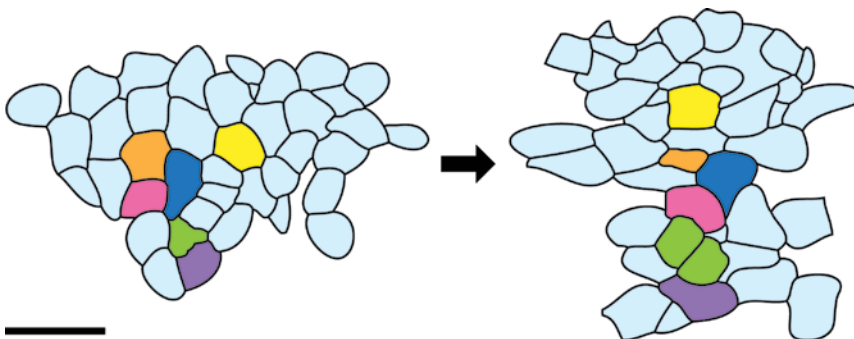


Plate 20 Cell rearrangement during convergent extension. Illustration based on video recordings showing that cell rearrangements occur as a result of mediolateral cell intercalation during convergent extension from stage 11.5 (left) to 17 (right). Modified from Elul, T. and Keller, R. 2000. Monopolar protrusive activity: a new morphogenic cell behavior in the neural plate dependent on vertical interactions with the mesoderm in *Xenopus*. *Dev. Biol.* 224:3–19. Scale bar indicate 40 μ m.

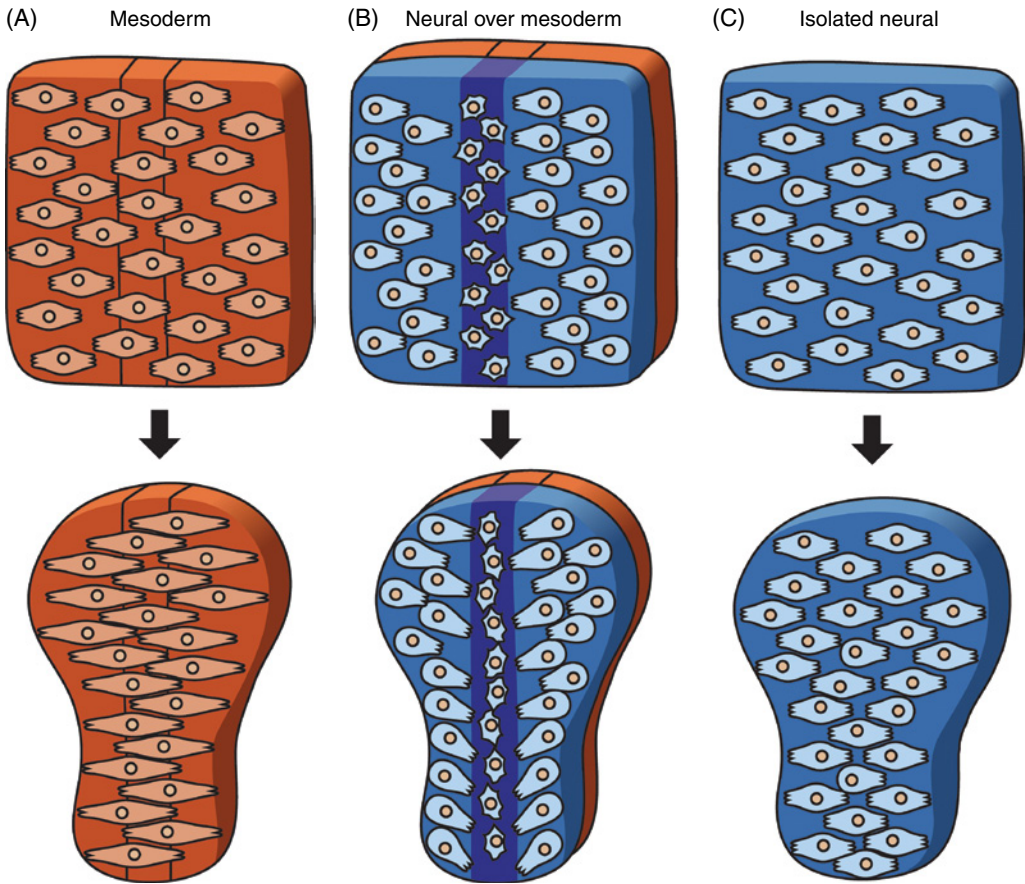


Plate 21 Convergent extension in mesoderm and neural explants. Cell morphology and polarity in isolated dorsal mesoderm (Shih and Keller, 1992) (A), neural-over-mesoderm (Elul and Keller, 2000) (B), and posterior neural ectoderm (Elul et al., 1997) explants (C). Red, mesoderm; blue, posterior neural tissue. In B, dark blue indicates the notochord. Modified from Wallingford, J. B. and Harland, R. M. 2001. *Xenopus* Dishevelled signaling regulates both neural and mesodermal convergent extension: parallel forces elongating the body axis. *Development* 128:2581–2592.

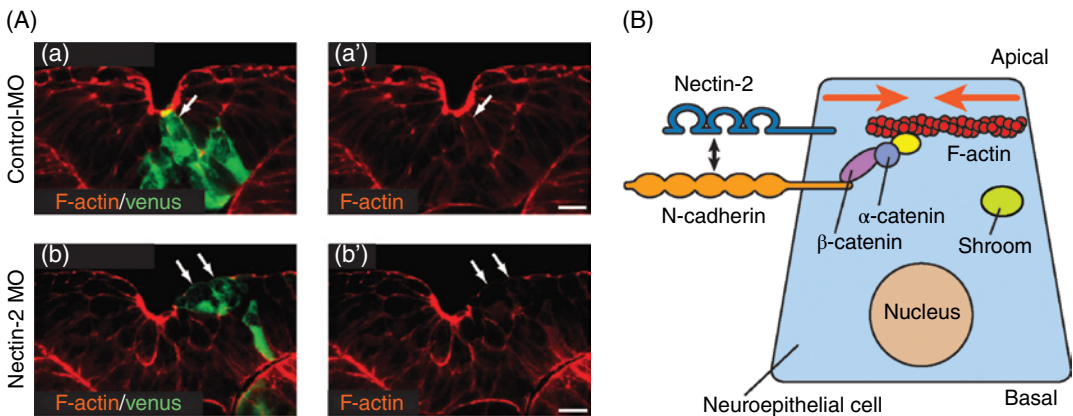


Plate 22 Mechanism of F-actin and N-cadherin recruitment to the apical side by nectin-2. (A) Nectin-2 knockdown in the neural plate suppressed the apical accumulation of F-actin and neural tube closure. Sections of the neural groove of embryos injected with control morpholino (MO) (a and a') or nectin-2 MO (b and b') show that the apical F-actin was reduced specifically in the venus-positive cells in the nectin-2 MO-injected embryo (b and b' arrows) compared with the control (a and a' arrows). Venus mRNA was used as a cell-lineage tracer. Scale bars indicate 20 μm . Modified from Morita et al. (2010). *Development*. (B) Schematic diagram of the nectin-2–N-cadherin interaction in apical constriction in the neuroepithelium. The extracellular domain of nectin-2 binds to that of N-cadherin, which indirectly interacts with F-actin via intracellular proteins, such as β - and α -catenins, to induce an apical accumulation of F-actin. Other intracellular components of the apical constriction machinery, including Shroom3, then contract the accumulated actin bundle to constrict the apex of the cell. Orange arrows indicate constriction of the apical surface.

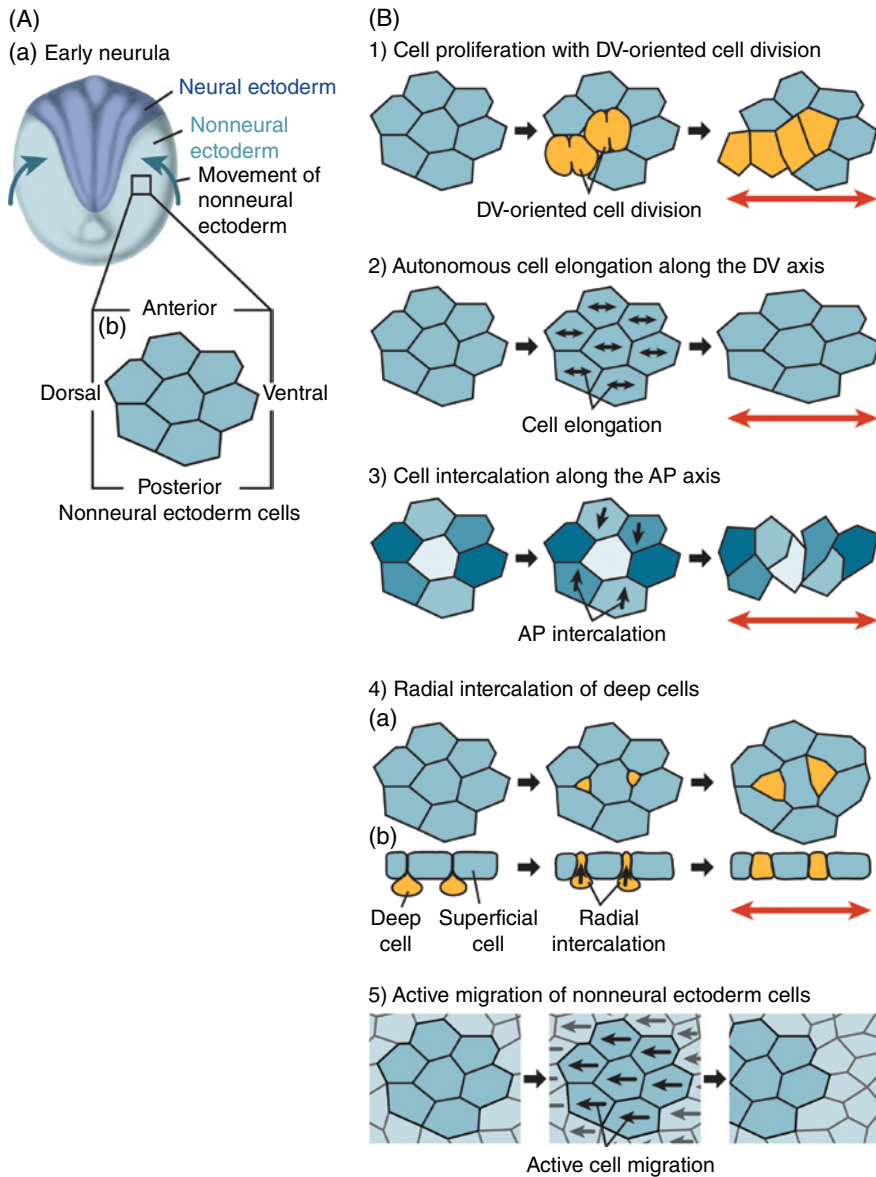


Plate 23 Schematic diagram of possible cellular morphogenetic events that may contribute to the nonneural cell movement. (A) Dorsal view of an early neurula embryo (a) and an illustration of magnified nonneural ectoderm cells (b). (B) Possible cellular morphogenetic events that could push the neural folds toward the dorsal midline via the movement of the nonneural ectoderm. (1) Cell proliferation with dorsoventrally oriented cell division. Cells in the nonneural ectoderm preferentially divide with the division plane perpendicular to the DV axis, increasing the number of cells along this axis, which could push surrounding cells dorsoventrally. (2) Autonomous cell elongation along the DV axis. Each of the nonneural ectoderm cells autonomously elongates along the DV axis, expanding the tissue dorsoventrally. (3) Cell intercalation along the AP axis. The nonneural ectoderm cells intercalate with each other along the AP axis, resulting in the extension of the tissue along the DV axis. (4) Radial intercalation of deep cells into the superficial layer. Cells beneath the superficial layer of the nonneural ectoderm (deep cells, indicated in yellow) intercalate radially into the surface tissue, wedging themselves between superficial cells. This could increase the surface area of the nonneural ectoderm and contribute to movement of the tissue. Views of the surface (a) and the cross section (b) are shown. (5) Active migration of nonneural ectoderm cells. Cells in the nonneural ectoderm themselves actively migrate toward the dorsal midline, causing movement of the tissue as a whole.

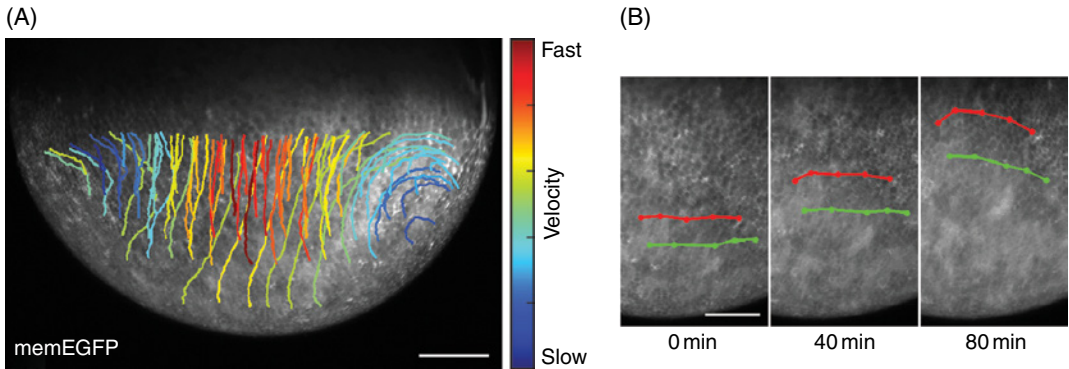


Plate 24 Movements of nonneural ectoderm cells toward the dorsal midline. (A) Trajectories and velocities of nonneural ectoderm cells in a DSLM image. Cells moved toward the dorsal midline, with the cells in the middle of the AP axis moving fastest. A lateral view of an early neurula embryo is shown. The upper side is dorsal and the anterior is to the left. (B) Tracking of the relative positions of nonneural cells. The positions of superficial cells in the lateral view of the DSLM images were connected by lines (red and green) and tracked during neural tube closure. Scale bars indicate 200 μm in A and 100 μm in B.

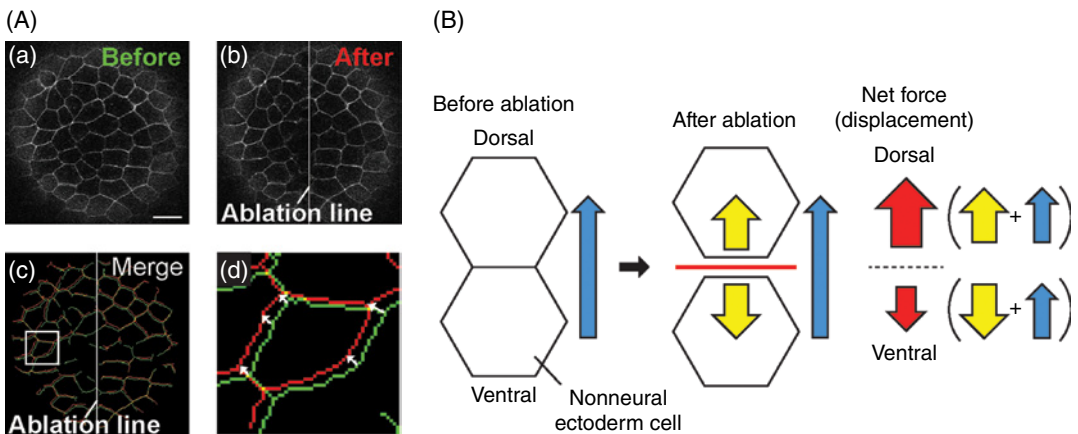


Plate 25 Laser ablation in the nonneural ectoderm. (A) Laser ablation on the lateral surface of the nonneural ectoderm along the AP axis. Fluorescent images of a memEGFP-injected embryo taken just before (a) and immediately after (1.5 seconds; b) the incision. These images were merged after image processing, and the displacement of cell vertices between the two time points was measured (c). White boxed region in (c) is magnified in (d). White arrows in (d) indicate the displacement of the cell membrane. Upper side is the embryo's anterior, and dorsal is to the left. (B) Schematic diagram indicating the forces on the nonneural ectoderm cells (arrows) and their displacement by laser ablation. During neurulation, cells in the nonneural ectoderm move toward the dorsal side with a certain force (blue arrow; before ablation). Upon laser ablation (red line; after ablation), the cells separated in opposite directions according to the tensile force. As we assume that this tissue is in a state of equilibrium, based on the DSLM observations, the forces causing the separation may have the same magnitude (yellow arrows; after ablation). Therefore, the displacement observed after ablation can be interpreted as the result of the sum of the forces of tissue movement (blue) and tissue separation (yellow), with a higher value in the dorsal side and a lower one in the ventral side (red arrows). Scale bar indicates 20 μm .

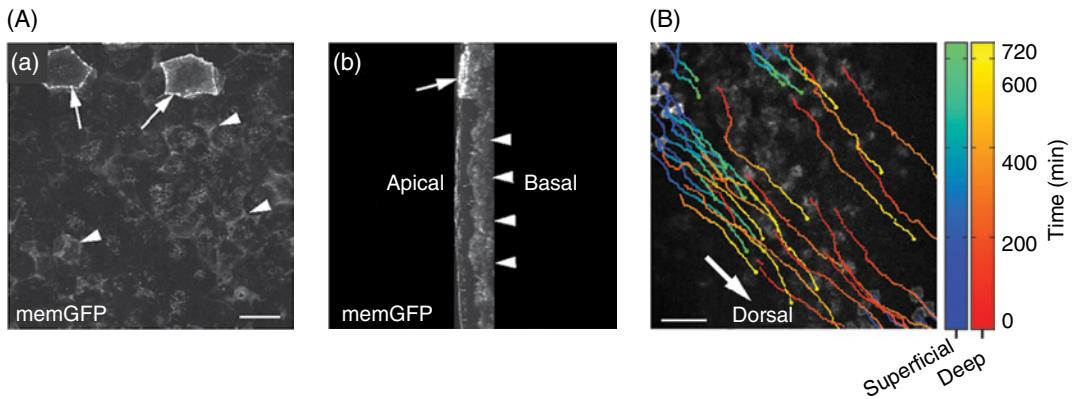


Plate 26 Migration of deep cells in the nonneural ectoderm toward the dorsal side. (A) Morphology and position of deep cells in the nonneural ectoderm. Nonneural ectoderm cells in an embryo injected with memGFP were viewed from the surface (a) and as a reconstructed Y-Z section (b, reconstruction of (a)). Deep cells had ambiguous boundaries (arrowheads) while superficial ones had sharp cell-cell boundaries, facing the outside of the embryo (arrows). (B) Trajectories of superficial (blue to green) and deep (orange to yellow) cell movements in the nonneural ectoderm of a wild-type embryo. The deep cells moved faster than the superficial ones (superficial, $0.667 \pm 0.020 \mu\text{m min}^{-1}$; deep, $0.813 \pm 0.027 \mu\text{m min}^{-1}$). Arrow points toward the dorsal side. Scale bars indicate $20 \mu\text{m}$ in A and $100 \mu\text{m}$ in B.

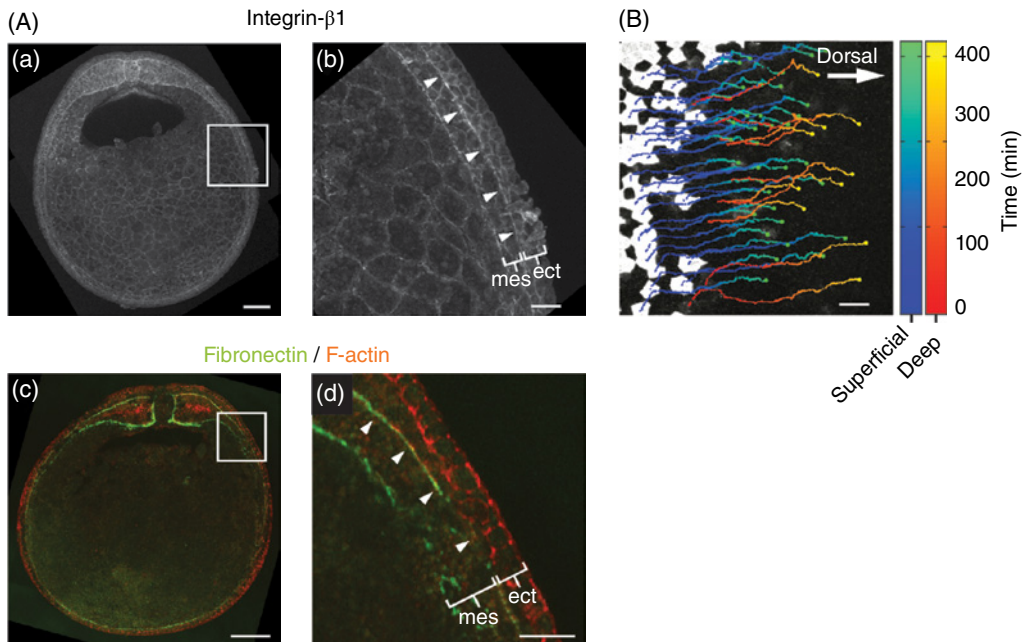


Plate 27 Localization of integrin- $\beta 1$ and its function in nonneural ectoderm movement. (A) Immunostaining of integrin- $\beta 1$ and fibronectin (FN). Integrin- $\beta 1$ (a and b) and FN (c and d) were localized to the border between the ectoderm and mesoderm with high density (arrowheads). **ect** indicates ectoderm, **mes** is mesoderm. (B) Trajectories of superficial (blue to green) and deep (orange to yellow) cell movements in the nonneural ectoderm of an Itg $\beta 1$ -MO-injected embryo. Both superficial and deep cells moved significantly more slowly (superficial: $0.523 \pm 0.012 \mu\text{m min}^{-1}$; deep: $0.715 \pm 0.032 \mu\text{m min}^{-1}$) compared with wild-type embryos. Arrow points toward the dorsal side. Scale bars indicate $200 \mu\text{m}$ in Aa and Ac and $50 \mu\text{m}$ in Ab, Ad, and B.

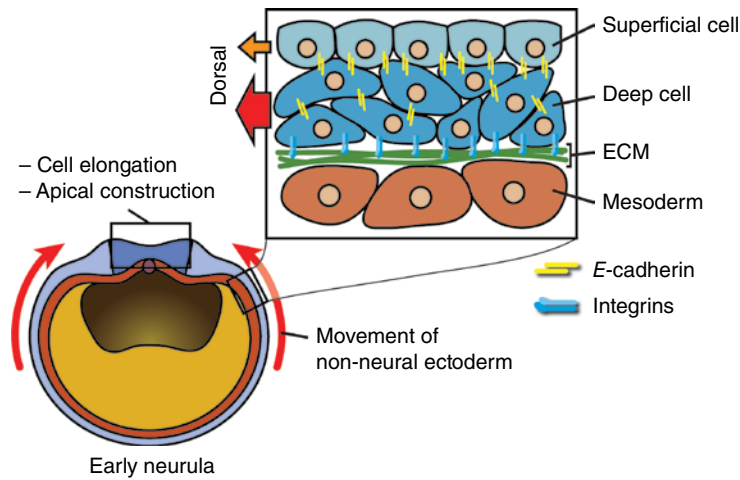


Plate 28 Mechanism of the dorsally directed movement of nonneural ectoderm. Schematic diagram of a mechanism for nonneural cell movement toward the dorsal midline. Deep cells in the nonneural ectoderm bind to ECM that accumulates between the ectoderm and mesoderm via integrin- β 1. These cells also adhere to the overlying superficial cells through E-cadherin. The deep cells migrate on the ECM toward the dorsal midline, pulling the superficial cells together. In collaboration with the cellular morphogenetic events in the neural ectoderm, this autonomous movement of the nonneural ectoderm contributes to the completion of neural tube closure.

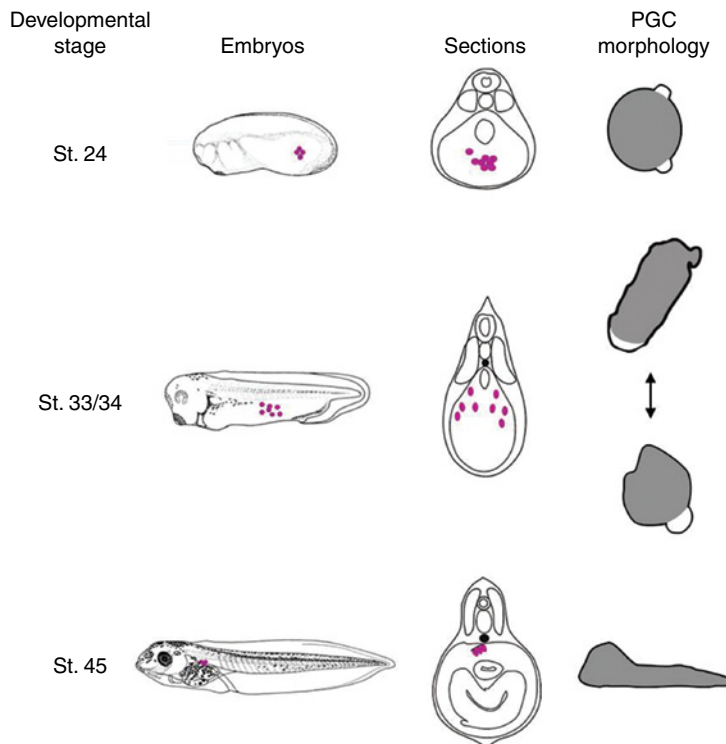


Plate 29 PGC motility and morphology during different developmental stages of *X. laevis* embryos. Embryos are drawn after Nieuwkoop and Faber (1994). Vertical sections perpendicular to the anterior–posterior with the positions of PGCs (“pink dots”) in the embryo are indicated. The morphology of isolated PGCs indicated according to Terayama et al. (2012); Heasman and Wylie (1978). (We thank Olena Steshenko for the help with the image preparation.)

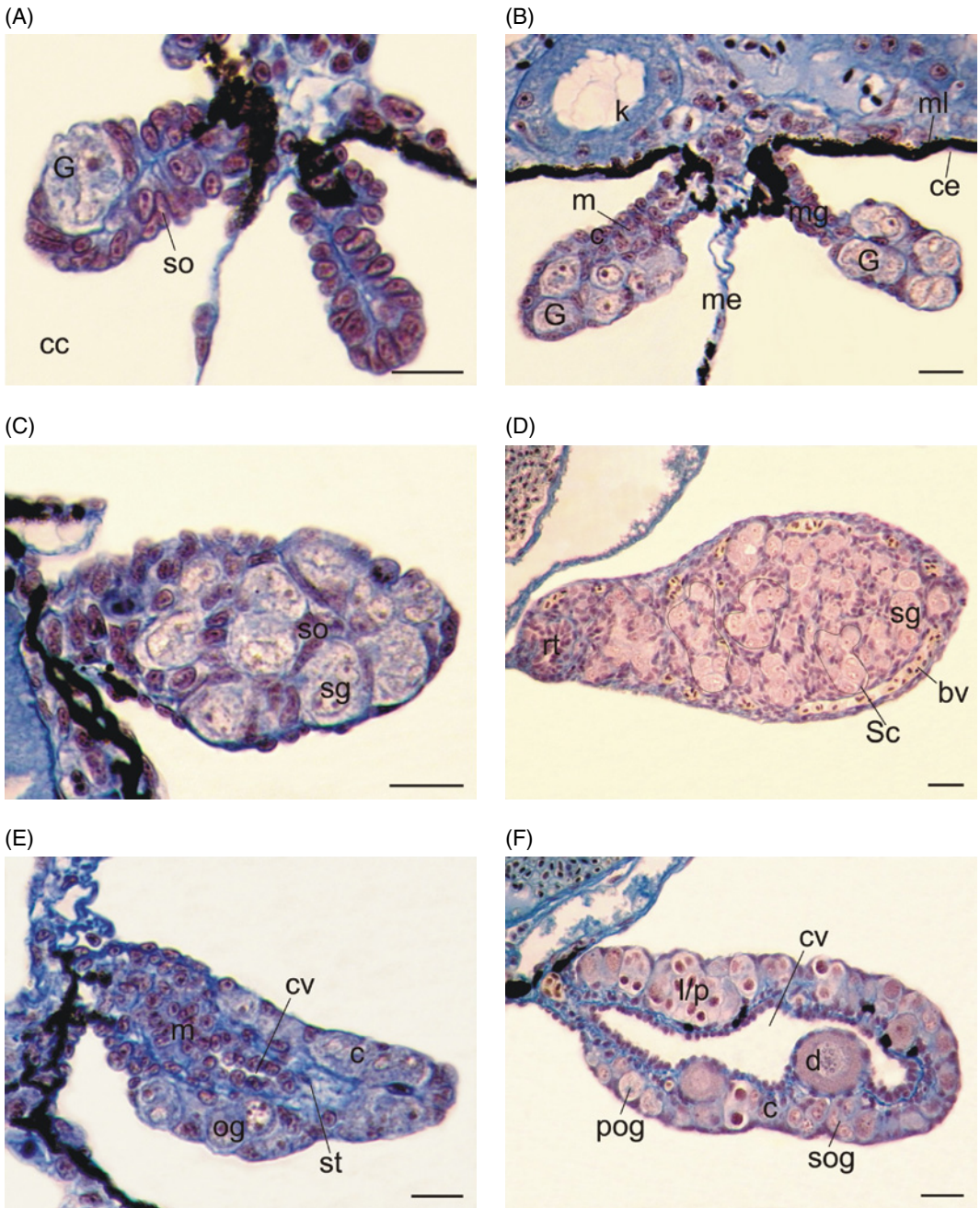


Plate 30 The development of gonads in *X. laevis*. (A) The genital ridges at NF stage 49. One germ cell (G) surrounded by small somatic cells (so) and coelomic cavity (cc) are visible on the cross section of the gonad. (B) The undifferentiated gonads at NF stage 50. The superficial epithelium of the gonad remains continuous with the coelomic epithelium (ce), and together with the germ cells forms the gonadal cortex (c). The dorsal mesentery (me) is located between the gonads and black melanophores (ml) form a layer at the ventral surface of the kidneys (k). The gonadal mesentery (mesogonium, mg), the gonadal medulla (m). (C) The early testis at NF stage 53. The spermatogonia (sg) are surrounded by flattened somatic cells (pre-Sertoli cells; so) with crescent-shaped nuclei. This is the beginning of the formation of testis cords. (D) The testis at NF stage 66. The testis is filled with numerous tubule-shaped testis cords (three of these cords are encircled) consisting of spermatogonia (sg) enclosed by Sertoli cells (Sc). Rete testis (rt) and blood vessels (bv) are visible. (E) The early ovary at NF stage 53. The germ cells (oogonia; og) are located in the cortex (c). The medulla (m) remains sterile and its cells disperse forming the secondary cavity (cv). Cells deriving from the mesonephroi immigrate to the stromal space (st) of the gonad, i.e., between the cortex and medulla. (F) In the NF stage 63 ovary, the cortex (c) is the dominant part of the gonad. The extensive secondary cavity (cv) lined with the somatic cells of the gonadal medulla is located in the center of the ovary. Primary and secondary oognia (pog, sog) as well as oocytes in prophase (leptotene and pachytene, l-p; diplotene, d) are visible. Picroaniline and Debreuil staining. Scale bar is equal to 20 μ m.

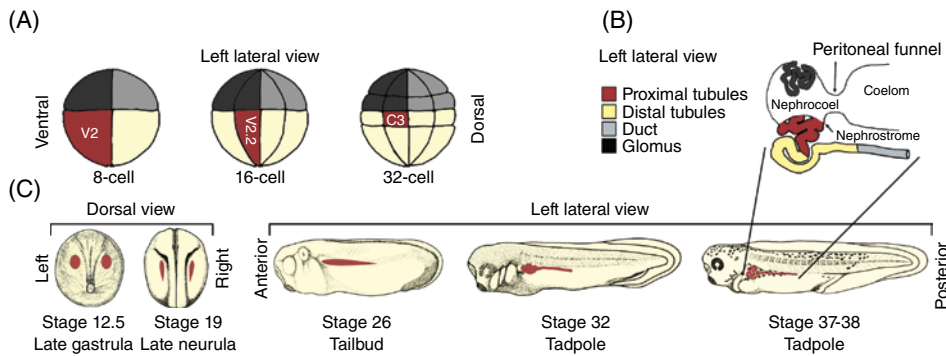


Plate 31 Kidney fate map and development. (A) Fate maps of early blastula stage embryos. Vegetal cells (on top of embryos) are marked to indicate dorsal (light gray) versus ventral (dark gray). The V2 (8-cell), V2.2 (16-cell), and C3 (32-cell) vegetal blastomeres (on bottom of embryos) are marked in dark red to show cells fated to contribute to the pronephros. (B) Diagram of the pronephros at stages 36–38. The glomus (dark gray), proximal tubules (dark red), distal tubules (light yellow), and collecting duct (light gray) are indicated (left lateral view). (C) Stages of pronephric development. Pronephric anlagen is depicted in dark red at each embryonic stage from early gastrula through tadpole stages. Specification and patterning occur through late gastrula and late neurula stages (dorsal views), while differentiation and morphogenesis occur through tailbud and tadpole stages (left lateral view).

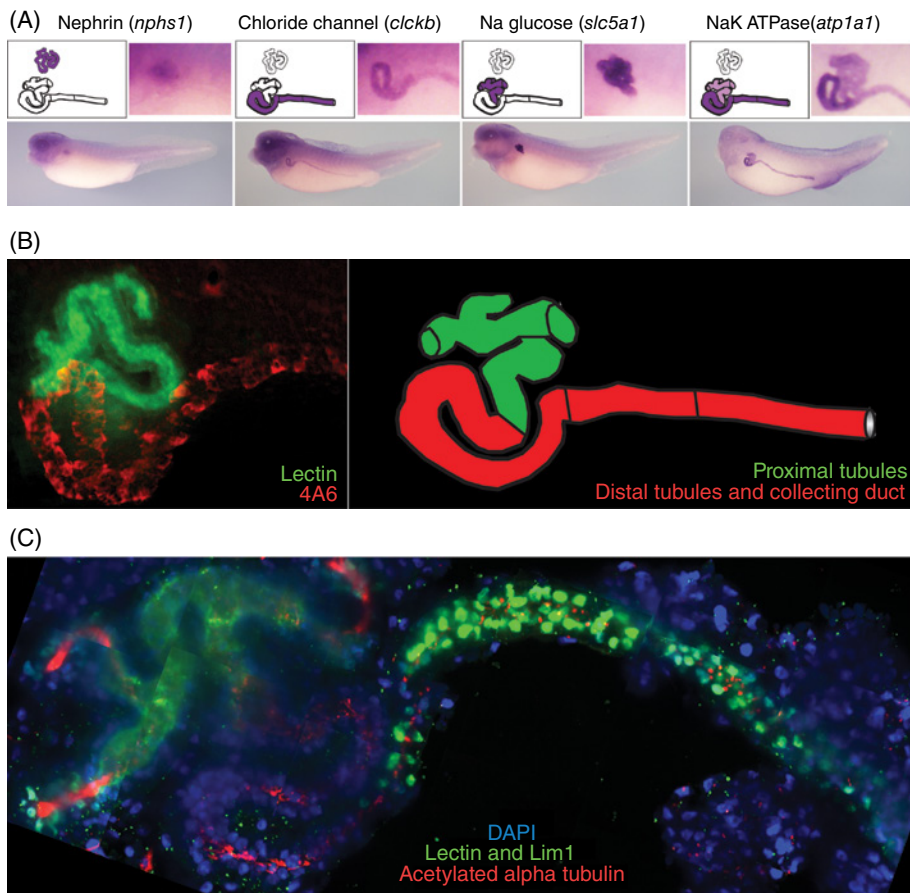


Plate 32 Late pronephric markers. (A) *In situ* hybridization of late pronephric markers. Whole-mount *in situ* hybridization showing mRNA expression of *nphs1*, *clckb*, *slc5a1*, and *atp1a1* within the developing glomus, distal tubules and collecting duct, proximal tubules, and all tubular structures (respectively) at stages 38–40. (B) Immunostaining of pronephric tubules. Whole-mount fluorescent staining of the proximal tubules using a fluorescent lectin (green) and the distal tubules and collecting duct using the 4A6 antibody (red) at stage 38 imaged using stereomicroscopy. Fiji/ImageJ software was used to subtract background from the image. (C) Immunostaining of subcellular structures. Whole-mount fluorescent staining of the proximal tubules (fluorescent lectin – green), nuclei of the collecting duct (Lim1 antibody – green), pronephric cilia (acetylated alpha tubulin – red), and all nuclei (DAPI – blue) at stage 36 imaged using confocal microscopy.

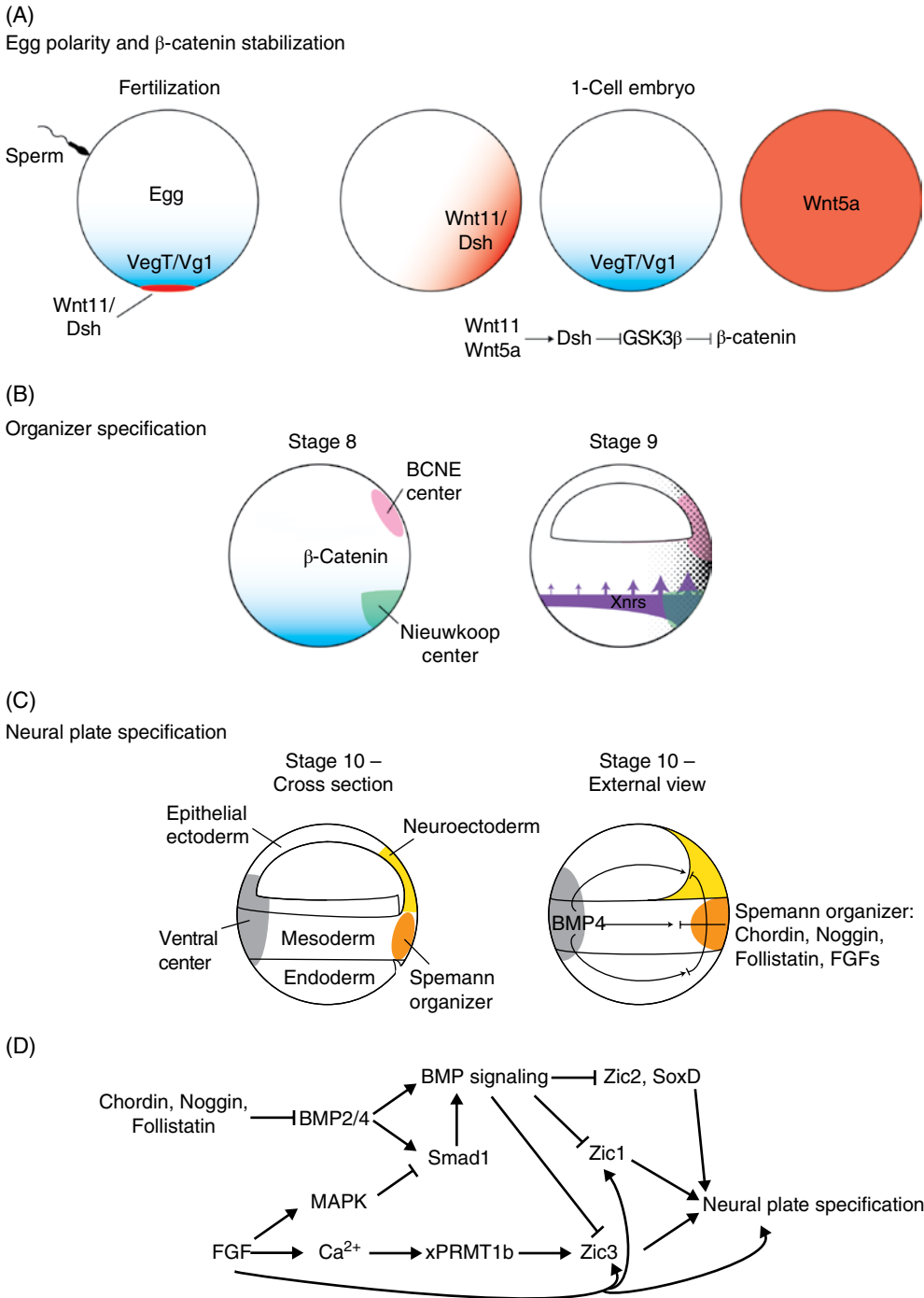


Plate 33 Summary of neural specification. (A) Wnt5a is ubiquitously expressed in the oocyte and embryo. Dishevelled (Dsh) and Wnt11 are relocated from the vegetal pole of the egg during cortical rotation/fertilization to establish a dorsal gradient. Wnt5a and Wnt11 bind each other and in cooperation with Dsh inhibit GSK3 β -mediated degradation of beta-catenin. A TGF- β signal inducing transcription factor, VegT, and a TGF- β family member, Vg1, are also localized in a vegetal gradient originating from maternal contributions. (B) At early blastula stages, VegT/Vg1 signals, and stabilized beta-catenin, specify the Nieuwkoop center, while stabilized beta-catenin and lesser levels of TGF- β signals specify the blastula chordin–noggin-expressing center (BCNE). At the later blastula stage, VegT/Vg1 and beta-catenin signals induce a gradient of nodal-related proteins (Xnrs) in the endoderm, signaling to the overlying mesoderm. The strongest Xnr signals originate in the dorsal Nieuwkoop center. (C) At the start of gastrulation, the Spemann’s organizer has formed and has begun to express dorsalizing factors. The dorsalizing factors are important for specification of several regions, but here, we focus on the neuroectoderm. Neuroectoderm-specifying factors include chordin, noggin, follistatin, and FGFs. (D) Signals from the Spemann organizer (chordin, noggin, follistatin, and FGF) indirectly activate downstream transcription factors (Zic1, Zic2, Zic3, and SoxD) necessary for neural specification.

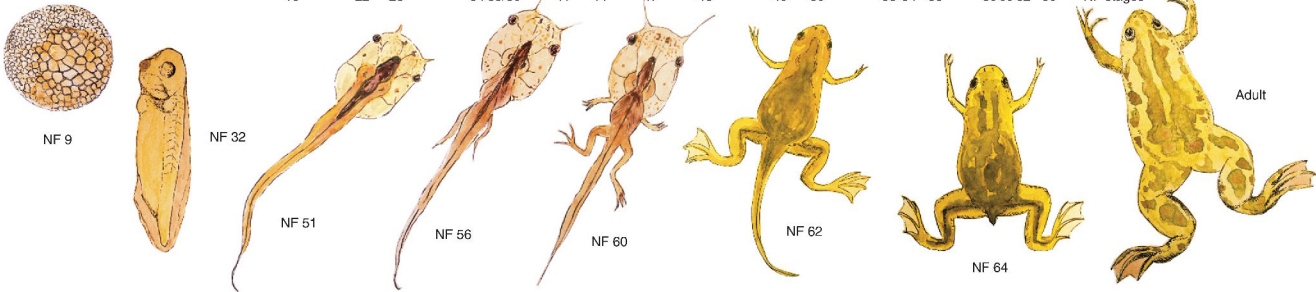
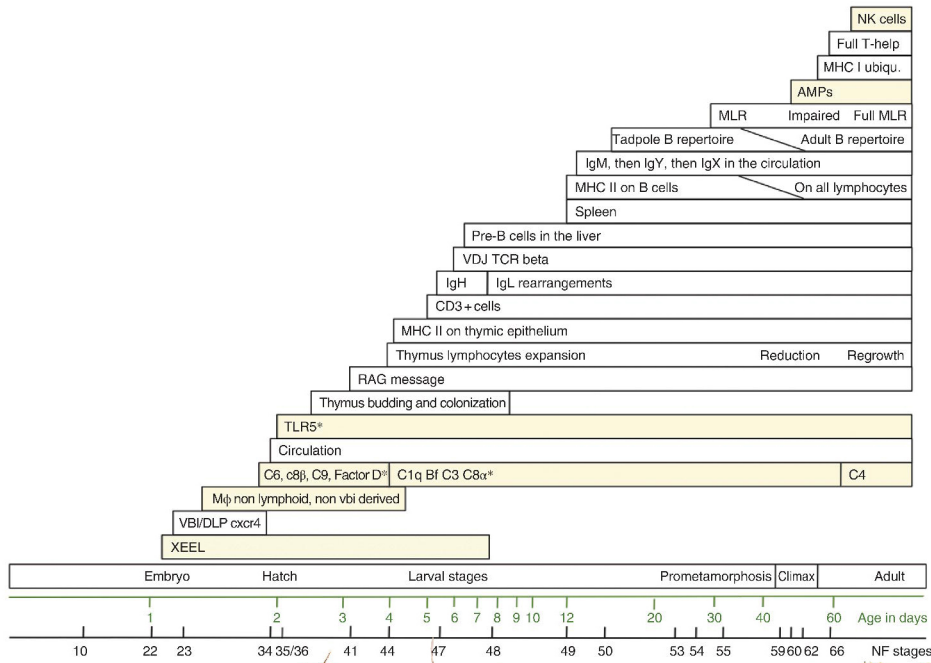


Plate 34 Sequential appearance of innate and adaptive immune system components during the ontogeny of *Xenopus*. Time scale has been represented on log scale to separate visually better the early events. AMP, antimicrobial peptides; C6, C8a C8β, factor D, C1q, Bf, C3, C4, components of the complement system; DLP, dorsolateral plate mesoderm; IgH, immunoglobulin heavy chain; IgL, immunoglobulin light chain; Mφ, macrophage; MHC, major histocompatibility complex; MLR, mixed leukocyte reaction; NF, Nieuwkoop and Faber stages (1967); NK, natural killer; RAG, recombination activating gene; TCR, T cell receptor; TLR, toll-like receptor; VBI, ventral blood island; VDJ, variable, joining, and diversity segments of a functional variable region gene of immunoglobulin or T cell receptor; XEEL, *Xenopus laevis* embryonic epidermal lectin; In beige, components of the innate system; *, not necessarily involved in immunity.

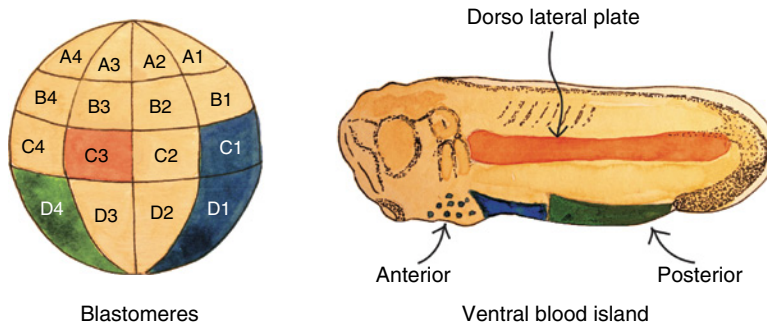


Plate 35 The mesoderm regions contributing to hematopoiesis in *Xenopus*. Reassembled and redrawn from Ciau-Uitz et al. (2010).

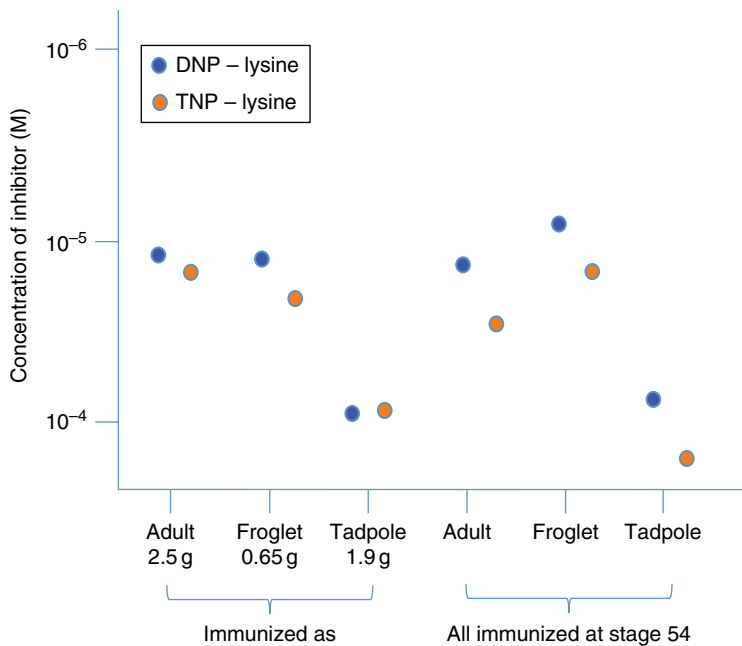


Plate 36 Anti-DNP antibody production in tadpoles, metamorphosing, and adult individuals. The test used to measure antibody relative affinities is an inhibition of inactivation of modified bacteriophage in the presence of decreasing molarities of inhibitor (DNP-lysine) (Hsu and Du Pasquier 1984a, b). The lowest the molarity of the inhibitor, the highest the affinity. The antibodies were raised against DNP-KLH and cross-react with TNP.

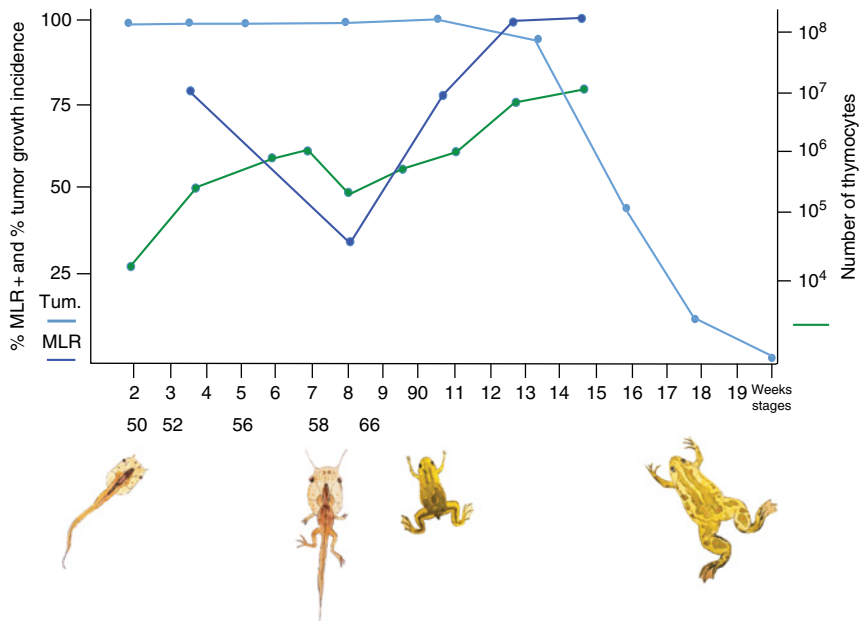


Plate 37 Antitumor immunity acquisition in function of mixed lymphocyte reaction and thymocyte number evolution. Source: Robert et al. (1995).

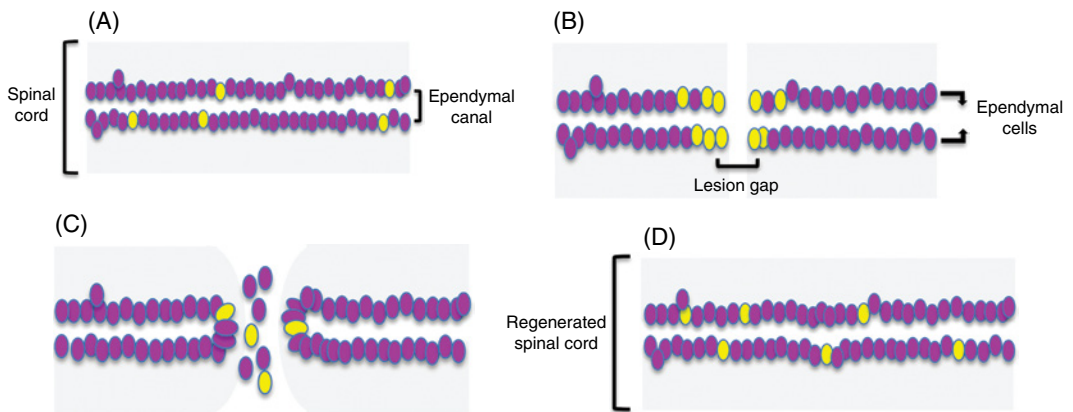


Plate 38 Spinal cord regeneration. This diagram shows the main events after spinal cord injury until regeneration is complete in *X. laevis* tadpoles (stage 50). (A) Longitudinal view of spinal cord highlighting the ependymal canal and the ependymal cells facing it. The black staining depicts Sox2+ cells and Sox2+ plus BrdU+ staining is shown in white. (B) Transection of the spinal cord. Two days after the lesion, there is a massive proliferation of cells and many of them are Sox2+ and BrdU+ and surround both stumps. (C) Rostral and caudal stump closure. The stumps begin to close from day 2 until day 10 after the injury. Different kinds of cells fill the gap, Sox2+ cells together with Sox2+/BrdU+ and others could migrate to the ablation gap. These cells form a substrate that allows the meeting of both stumps and the crossing of axons. (D) Regenerated spinal cord. The spinal cord is able to regenerate around 20–30 days after the injury. The drawing shows the restoration of the spinal cord containing a normal ependymal canal, ependymal cells, and Sox2 expression along the cord. Source: Based on Gaete et al. (2012) and unpublished results from our laboratory.

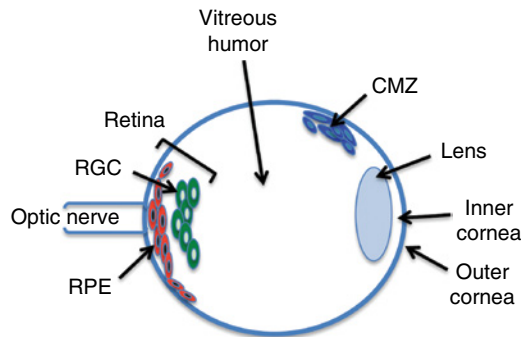


Plate 39 Representation of a *X. laevis* eye. This figure depicts a diagram of the different structures and type of cells important for the regeneration process in *X. laevis*. Some of the cells that belong to the layered retina are represented here: retinal pigment epithelium (RPE) and retinal ganglion cells (RGCs). The CMZ cells are shown almost adjacent to the lens. The inner and outer cornea is also shown, with the optic nerve to the left and the vitreous humor filling the white space.

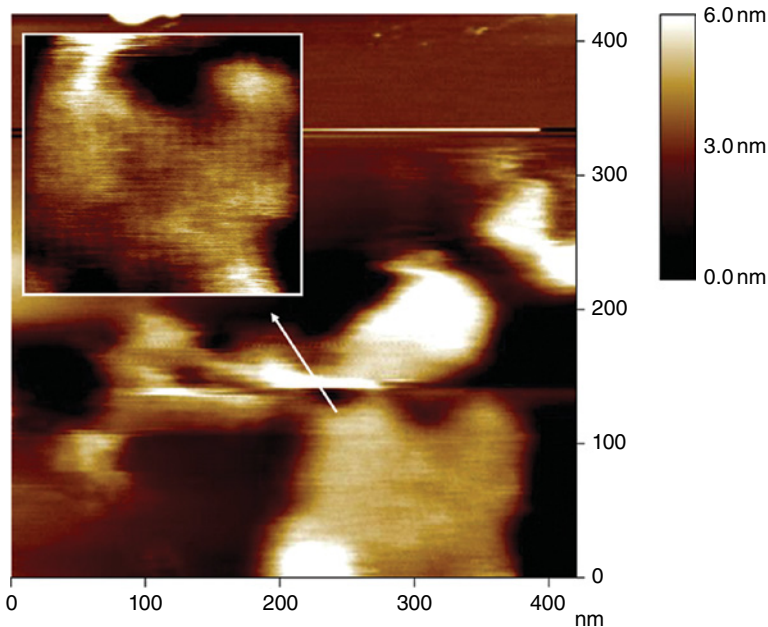


Plate 40 AFM topography image of the *X. laevis* oocyte plasma membrane expressing AQP4-M23, prepared according to Method C and collected in a liquid buffer. Scan area $425 \times 425 \text{ nm}^2$, vertical scale 6 nm. Inset: magnification of the surface corrugation visualized on top of the membrane. A square array of IMPs is visible. Scan area $150 \times 150 \text{ nm}^2$, vertical scale 2 nm.

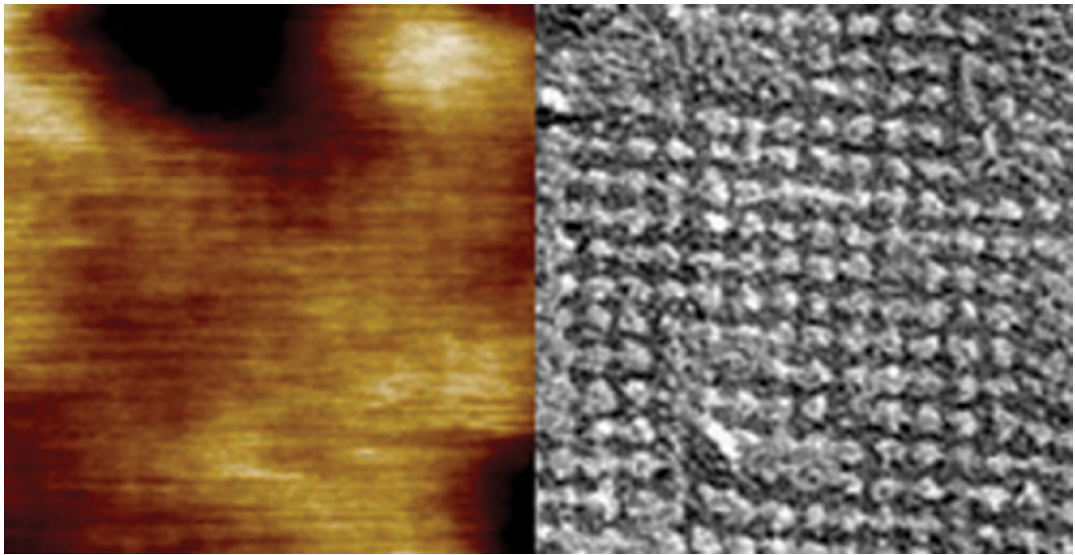


Plate 41 Square arrangement of AQP4-M23 tetramers, with a center-to-center distance of 6 nm as visualized in (left) an AFM topography image and (right) a TEM image. Scan areas: $100 \times 100 \text{ nm}^2$. From Furman et al. (2003). © 2003, National Academy of Sciences, U.S.A.

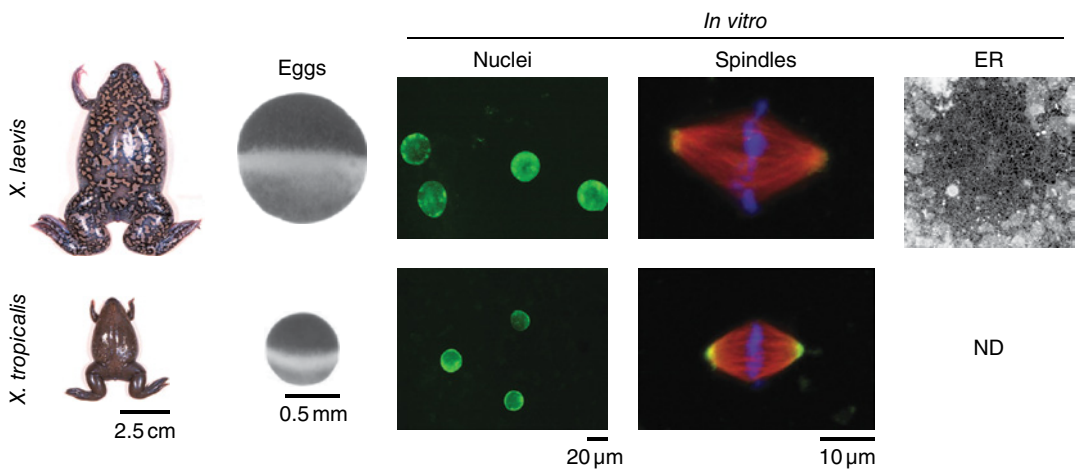


Plate 42 Examples of *Xenopus* interspecies organelle scaling. *X. laevis* frogs are larger than *X. tropicalis* frogs. *X. laevis* eggs are also larger than those from *X. tropicalis*, and extracts prepared from these eggs can be used to reconstitute nuclei, mitotic spindles, and ER. Nuclei were assembled in interphase egg extract from the two species using *X. laevis* sperm chromatin. The nuclei were visualized by immunofluorescence using an antibody against the nuclear pore complex (green). Image reprinted from Levy and Heald (2010). © 2010, with permission from Elsevier. Spindles were assembled in mitotic egg extract in the presence of fluorescently labeled tubulin (red). Also visualized are the DNA (blue) and katanin p60 (green). Image adapted with permission from Loughlin et al. (2011). ER was assembled in interphase *X. laevis* egg extract and visualized with a lipophilic membrane dye (DiI). This image is our unpublished data. The morphology of ER assembled in *X. tropicalis* egg extract is unknown. ND=not determined.

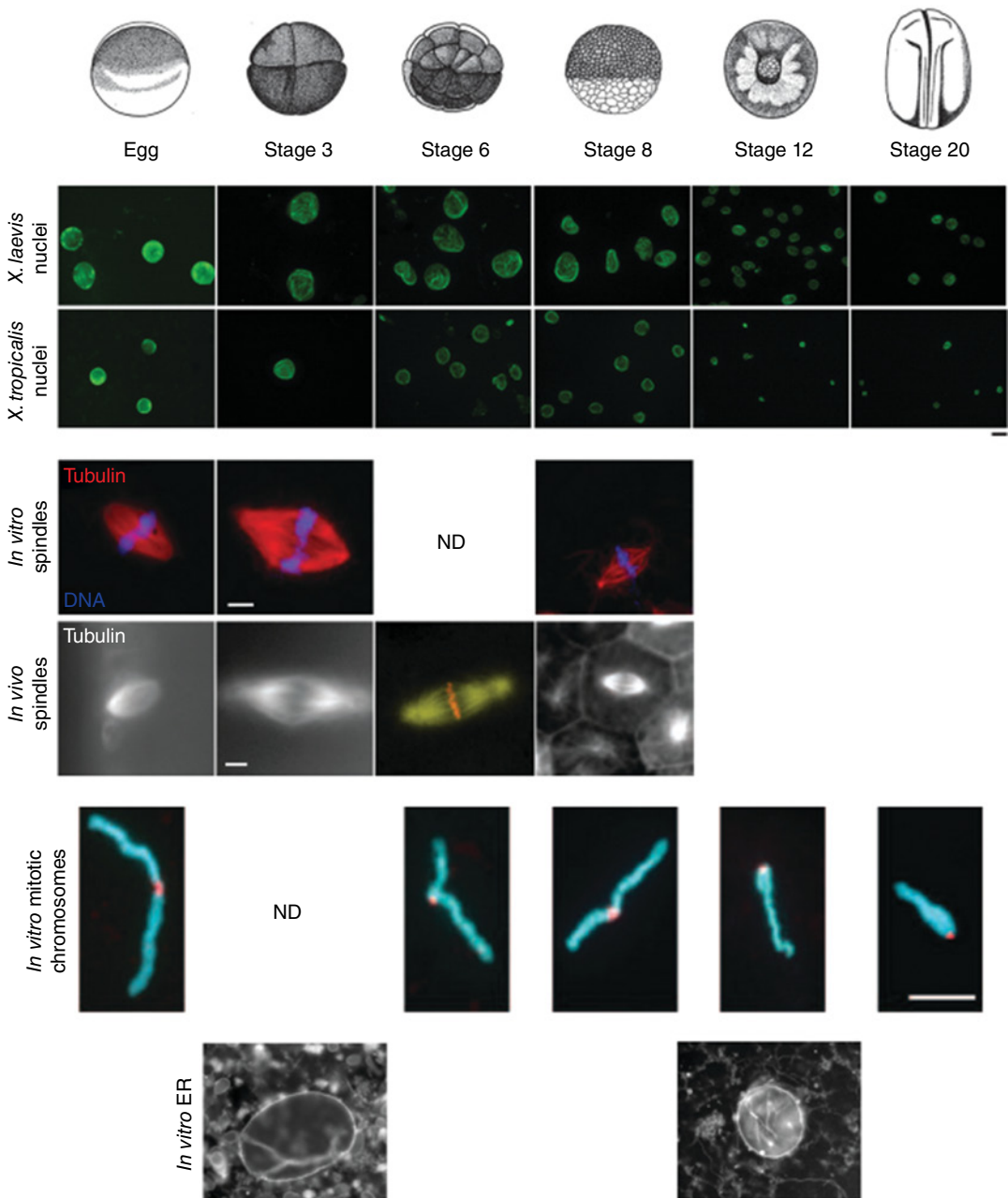


Plate 43 Examples of *Xenopus* developmental organelle scaling. The top of the figure depicts different-stage *X. laevis* embryos. Adapted from Nieuwkoop and Faber (1967). For images of nuclei, different-stage *Xenopus* embryos were arrested in late interphase with cycloheximide, to ensure complete fusion of karyomeres in pre-MBT embryos. Embryo extracts were prepared and endogenous nuclei were visualized by immunofluorescence using an antibody against the nuclear pore complex (green). The scale bar represents 20 μm . Nucleus images were adapted with permission from Levy and Heald (2010). *In vitro* spindles were assembled from *X. laevis* egg or embryo extracts and the microtubules (red) and DNA (blue) were visualized. *X. laevis in vivo* spindles were imaged in fixed hemisected eggs or embryos by tubulin immunofluorescence (grey). All spindle images were adapted from Wilbur and Heald (2013) made available using a Creative Commons Attribution License (<http://creativecommons.org/licenses/by/3.0/us/>), except for the stage 6 *in vivo* spindle image which was reprinted from Wuhr *et al.* (2008). © 2008, with permission from Elsevier, and depicts tubulin (yellow) and DNA (red) staining. The scale bars represent 10 μm . Mitotic chromosomes were obtained by isolating G_2 nuclei from different-stage *X. laevis* embryos and mitotically condensing the chromosomes in metaphase-arrested egg extract. Kinetochores (red) and DNA (blue) are visualized. The scale bar represents 5 μm . Images were adapted from Kieserman and Heald (2011) made available using a Creative Commons Attribution License (<http://creativecommons.org/licenses/by/3.0/us/>). ER was visualized in *X. laevis* embryo extracts using a lipophilic membrane dye (DiI). Depicted are embryonic nuclei with associated ER structures. These images are our unpublished data. ND=not determined.

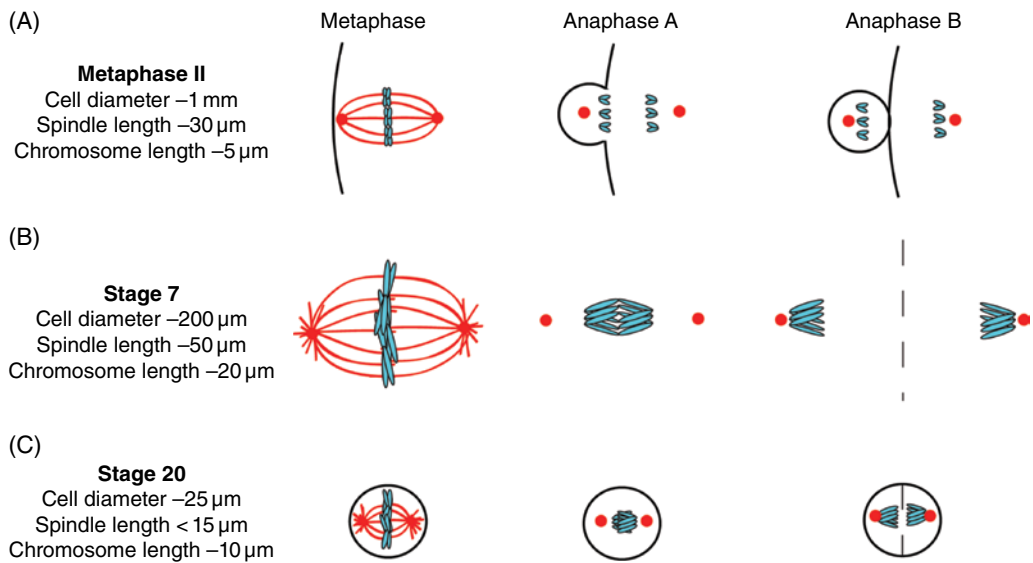


Plate 44 Models of coordinated spindle and chromosome scaling at different *Xenopus* developmental stages. Spindle microtubules are depicted as lines emanating from spindle poles (large dots) and contacting chromosomes aligned at the metaphase plate. The metaphase II-arrested egg is large relative to the meiotic spindle and small chromosomes. The spindle is positioned near the cell cortex, so anaphase movements need not be large. Asymmetric cell division produces one very small polar body and one very large egg, and small chromosomes ensure complete segregation. Cells in the pre-MBT stage 7 embryos are smaller than the egg but contain much larger chromosomes and spindles. During cell division, extended anaphase B movements promote the symmetric segregation of longer chromosomes to the center of daughter cells. In later stage 20 neurula embryos, cell, spindle, and chromosome sizes all scale smaller. Anaphase B movements are restricted by the small cell size, imposing a limit on chromosome and spindle length necessary to ensure complete chromosome segregation. Adapted from Kieserman and Heald (2011) made available using a Creative Commons Attribution License (<http://creativecommons.org/licenses/by/3.0/us/>).

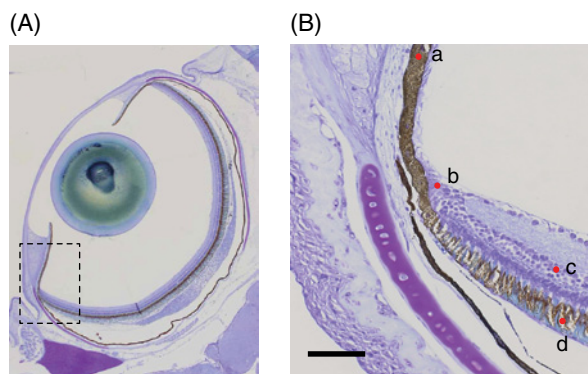


Plate 45 Retinal stem/progenitor cells in the vertebrate eye. Four distinct areas have been identified in the ocular tissues that contain retinal stem/progenitor cells: a, the iris pigmented epithelium; b, the CMZ or ciliary body epithelium; c, the intraretinal cells (this cell type changes depending on the animal species); and d, the RPE. The cell types recruited for retinal regeneration differ depending on species and depending on the extent to which the retina is injured. The area in the rectangle in A is shown in B at a higher magnification. The scale bar in B is 100 μ m. *Medaka* eye stained by cresyl violet.

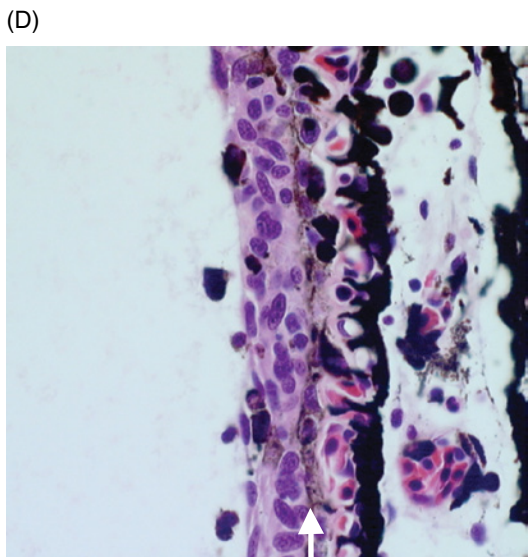
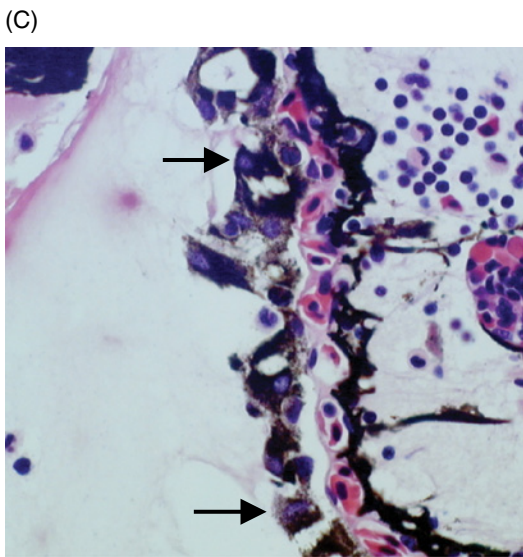
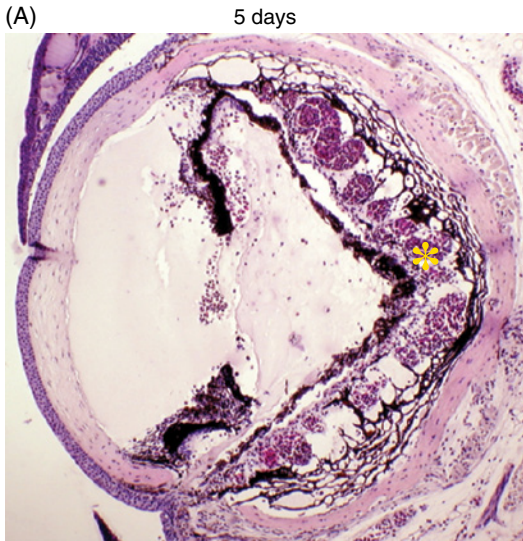


Plate 46 The early phase of transdifferentiation in newt retina regeneration. A and C show an eye at Day 5 and B and D show an eye at Day 14 (5 and 14 days after retinal removal). In A, the RPE cells are irregularly arranged (arrows in C). The choroid is swollen with blood cells stacking in the capillaries. This indicates that an inflammatory reaction is occurring in the choroid. At Day 14, a multistratified epithelium is formed, consisting of two layers, the neuroepithelium and the pigmented epithelium (white arrow in D). The latter is facing the choroid. Hematoxylin and eosin staining. Reprinted from Araki (2007a). © 2007, with permission from John Wiley & Sons, Inc.

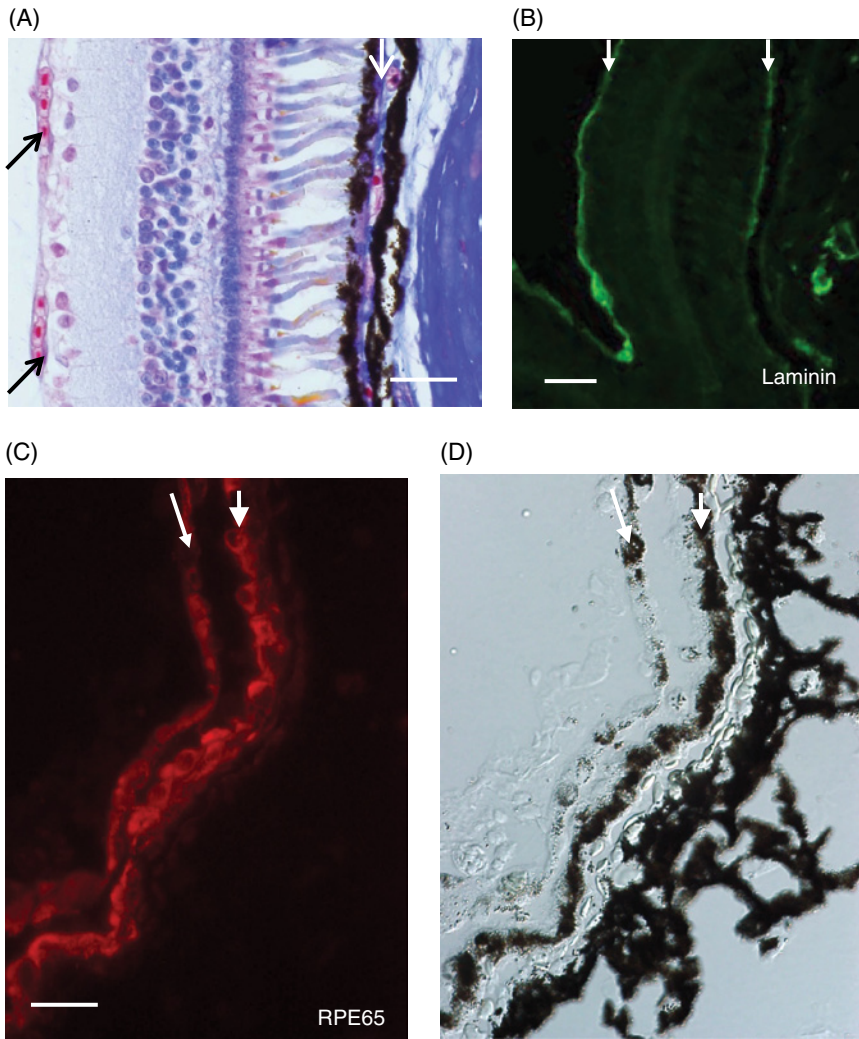


Plate 47 *X. laevis* retina and the early stages of retinal regeneration. A and B show a normal *X. laevis* retina. In A, the left arrows indicate the RVM, which consists of the inner limiting membrane and the retinal capillaries. The right white arrow points at Bruch's membrane. In B, laminin immunocytochemistry shows two positively stained membranes (arrows); one is the RVM and the other is Bruch's membrane. A is stained with Azan. The scale bars in A and B are 30 μm . C and D are taken from the same area and show an eye at Day 10 (10 days after retinectomy). The longer, thin arrows indicate the new RPE layer, which is formed by the migration of the RPE cell to the RVM. The shorter, thick arrows indicate the original RPE layers. RPE65 immunocytochemistry indicates that the pigmented cells on the vascular membrane are of RPE cell origin. The scale bar in C is 20 μm . B, C, and D are from Yoshii et al. (2007). © 2007, with permission from Elsevier.

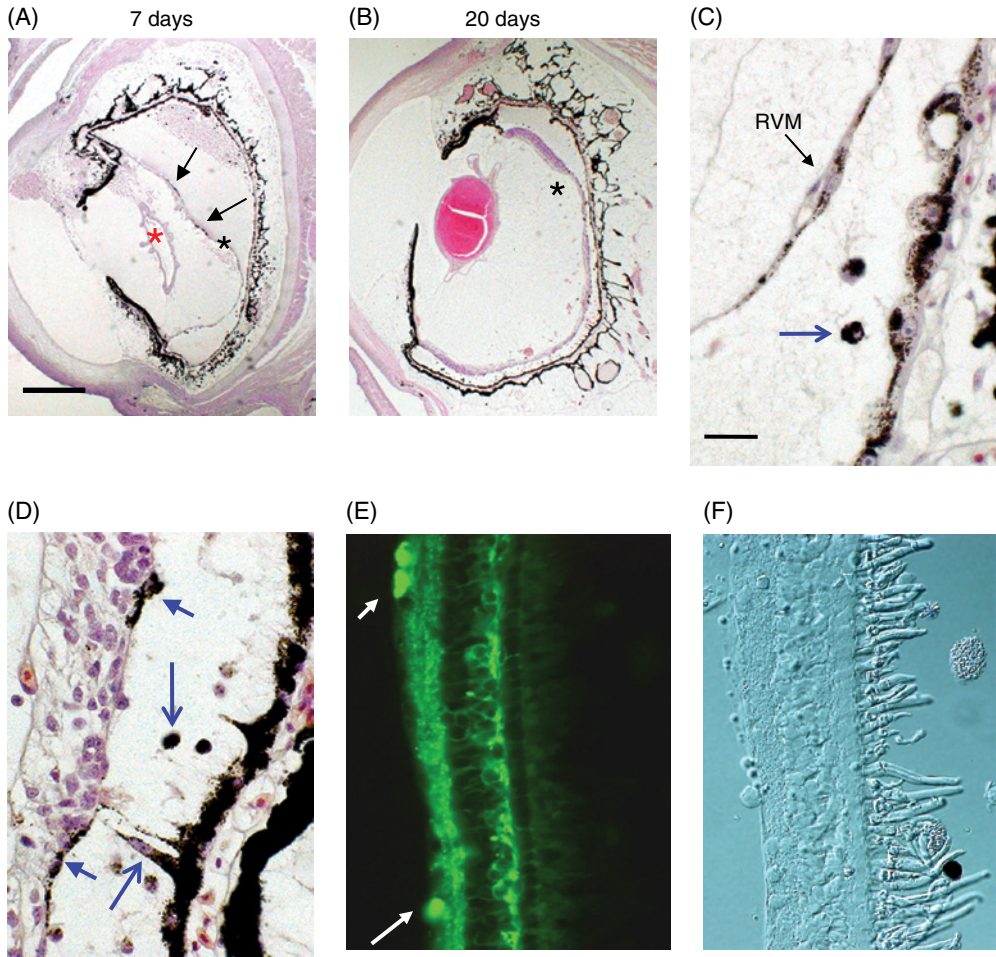


Plate 48 Retinal regeneration in *X. laevis*. (A and C) Day 7, (B and D) day 20, and (E and F) day 30. In A and C, a newly formed RPE layer (black arrows) is found on the RVM. The red asterisk in A is the remaining lens capsule. Between the RVM and the original RPE, isolated pigmented cells are often observed (blue arrows in C and D). These are considered to be migrating RPE cells. In B and D, a stratified epithelium has developed and some RPE cells attached to the epithelium at the luminal side (the shorter arrows in D). In E and F, a neural retina with a well-developed outer segment has regenerated by Day 30. Acetylated tubulin immunocytochemistry shows the different retinal layers. Arrows in E indicate the ganglion cells. Reprinted from Yoshii et al. (2007). © 2007, with permission from Elsevier.

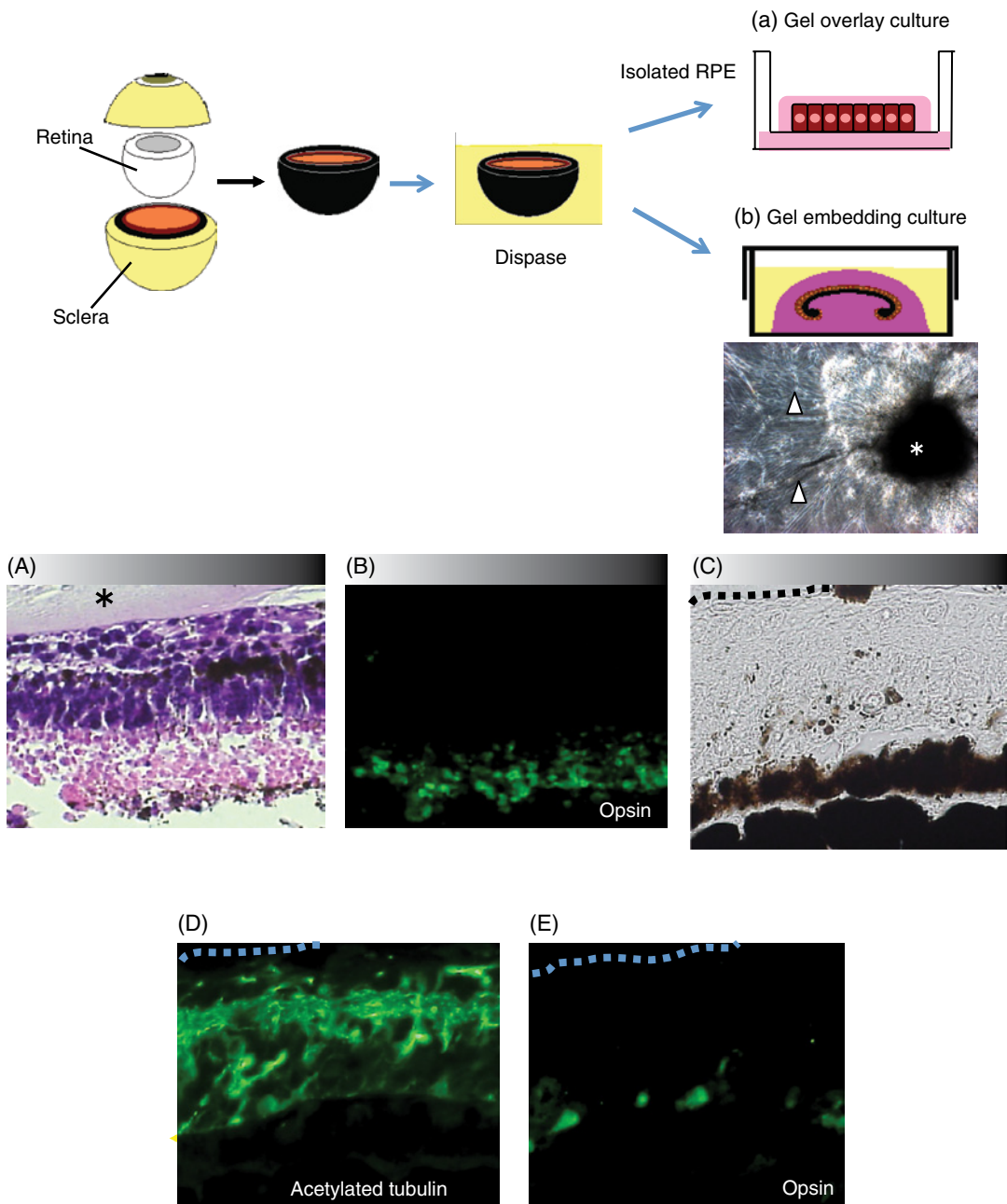


Plate 49 Organotypic culture for 3-D retinal tissue regeneration. The retina and sclera were removed from the posterior eye. After incubating the tissue (the RPE and the choroid) with Dispase, the tissue was either (a) placed on the culture membrane and overlaid with Matrigel or (b) inserted into the Matrigel. The phase-contrast micrograph shows well-elongated neuronal fibers (arrowheads) extending from the explant (asterisk). (A–E) By Day 30, retinal structures have regenerated. (A and B) and (C, D, and E) are the serial sections showing the formation of the outer segments (A) and the inner plexiform layer (D) (Nabeshima et al. 2013). Reprinted from Kuriyama et al. (2009). © 2013 Wiley Periodicals, Inc.

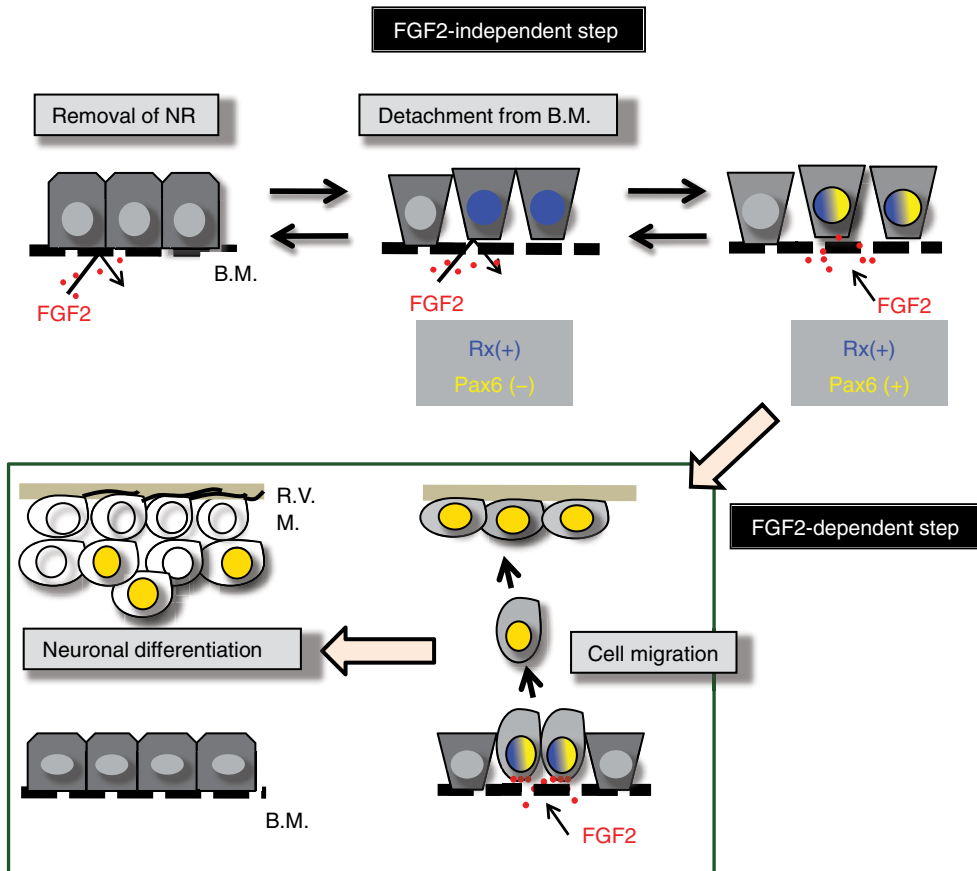


Plate 50 A hypothetical model for transdifferentiation begins in the RPE cells after retinal removal. In the normal eye, the RPE cells adhere to the basement membrane (Bruch's membrane). FGF2 appears to have no effect on the RPE cells in this situation. When the retina is removed, some of the RPE cells are detached from Bruch's membrane, most likely through an upregulation of MMP genes. The Rax gene also becomes upregulated in these cells. In the next step, which is FGF2 dependent, the RPE cells are detached from Bruch's membrane and begin to respond to FGF2 and peel off from the RPE layer. They then become positive for Pax6 and move to the new basement membrane (the RVM) where they begin to proliferate and differentiate into retinal cells. The RPE cells left at Bruch's membrane can then readhere to the membrane and enter a stationary state (the normal state). The first step appears to be FGF2 independent and the second step appears to be FGF2 dependent. During the first step, the RPE cells return to the normal state, when not exposed to FGF2 for a period of time, indicating that this step is reversible. Reprinted from Kuriyama et al. (2009), with permission from John Wiley & Sons, Inc.

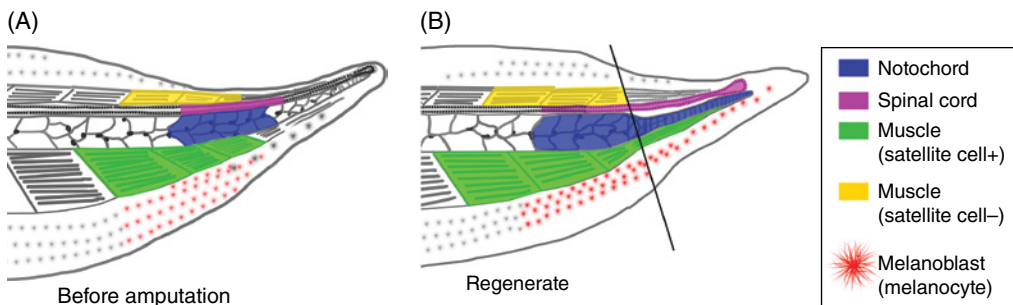


Plate 51 Diagram of origins of tissues in tail regeneration. (A) Specific tissue type in the tadpole tail (such as the spinal cord) can be labeled by transplantation of explant expressing fluorescence protein in early neurula stage (with a piece of neural plate) or tadpole stage (with a piece of whole spinal cord). (B) The labeling experiments show that the spinal cord regenerates from the spinal cord (magenta), the notochord regenerates from the notochord (blue), and the melanocyte regenerates from melanoblast (red). If satellite cells are labeled before amputation, the new muscle in tail regenerate will be labeled (green), but if satellite cells are not labeled, muscle in tail regenerate will not be labeled (yellow). The diagram is a summary of several labeling experiments (Gargioli and Slack 2004; Lin et al. 2007) and is also reproduced from Figure 2 in Beck et al. (2009). © 2009, John Wiley & Sons, Inc.

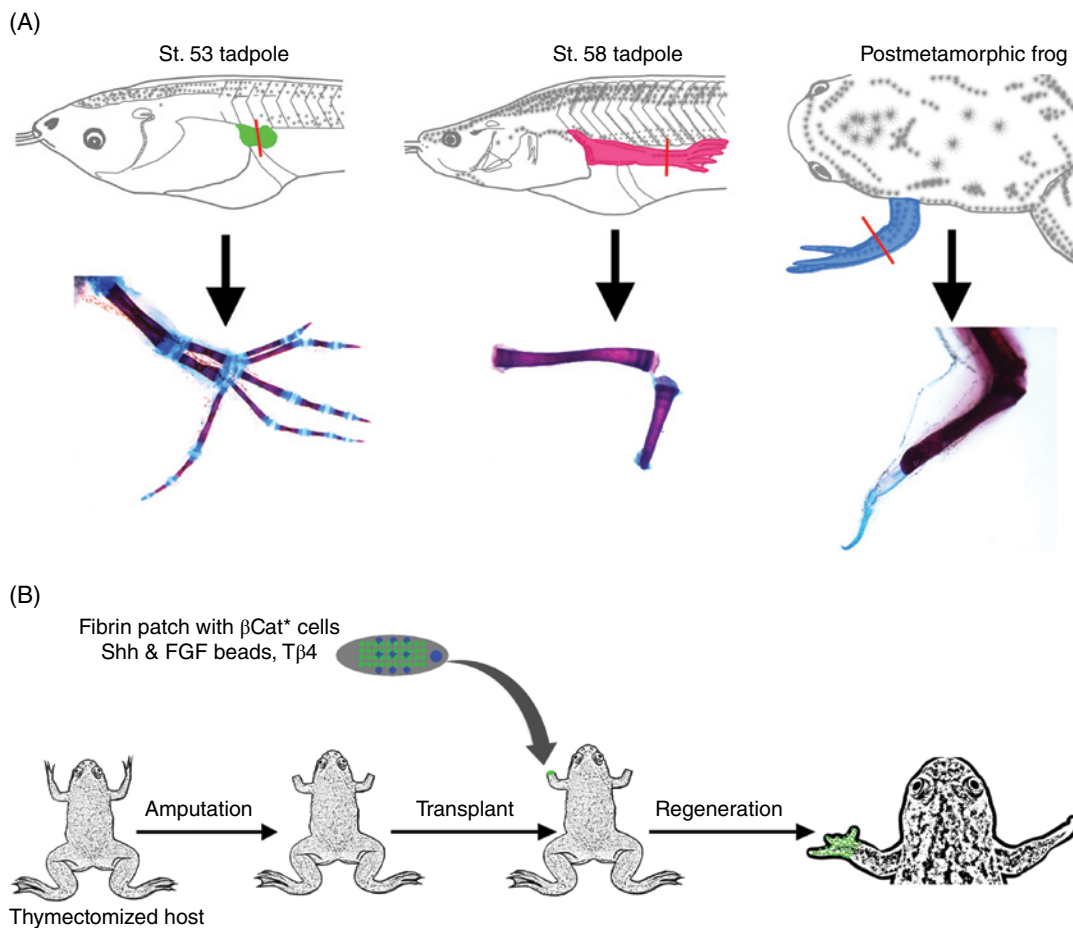


Plate 52 Limb regeneration in *Xenopus*. (A) Early tadpole limb (green, left) can fully regenerate, but late tadpole limb cannot (red, middle). Postmetamorphic frog can only regrow an unsegmented cartilaginous spark (blue, right). (B) Stimulation of limb regeneration in postmetamorphic frogs. Limb progenitor cells expressing high level of active beta-catenin when delivered to the limb stump of a thymectomized frog in the presence of FGF10 + Shh beads and thymosin beta 4 (T β 4) can stimulate multiple digit regeneration. Drawings of tadpole stages in A are after Nieuwkoop and Faber (1994). B is reprinted from the online graphic abstract in Lin et al. (2013). © 2012, with permission from Elsevier.